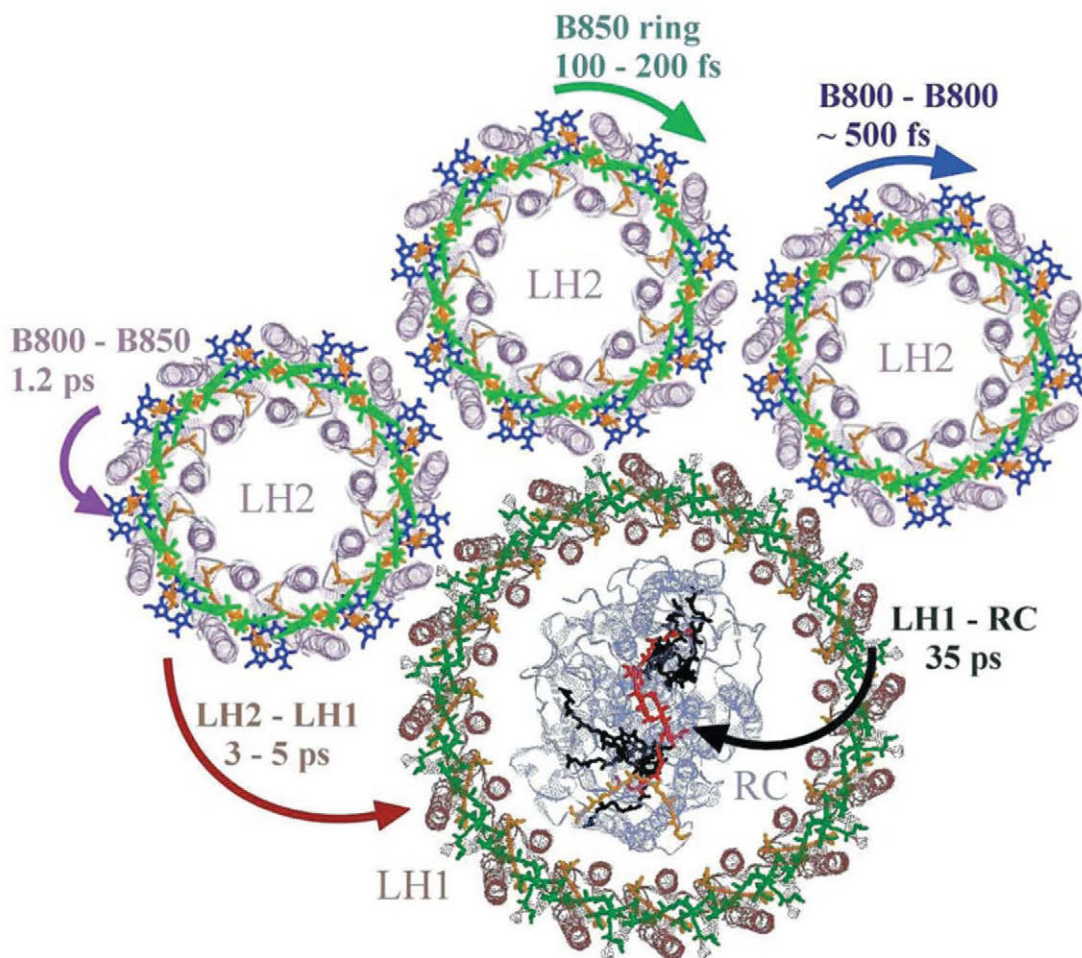


# Light-Harvesting Antennas in Photosynthesis



Beverley R. Green and William W. Parson (Eds.)

# Light-Harvesting Antennas in Photosynthesis



# Advances in Photosynthesis and Respiration

---

VOLUME 13

---

*Series Editor:*

**GOVINDJEE**

*University of Illinois, Urbana, Illinois, U.S.A.*

*Consulting Editors:*

Christine FOYER, *Harpending, U.K.*

Elisabeth GANTT, *College Park, Maryland, U.S.A.*

John H. GOLBECK, *University Park, Pennsylvania, U.S.A.*

Susan S. GOLDEN, *College Station, Texas, U.S.A.*

Wolfgang JUNGE, *Osnabrück, Germany*

Hartmut MICHEL, *Frankfurt am Main, Germany*

Kirmiyuki SATOH, *Okayama, Japan*

James Siedow, *Durham, North Carolina, U.S.A.*

The scope of our series, beginning with volume 11, reflects the concept that photosynthesis and respiration are intertwined with respect to both the protein complexes involved and to the entire bioenergetic machinery of all life. *Advances in Photosynthesis and Respiration* is a book series that provides a comprehensive and state-of-the-art account of research in photosynthesis and respiration. Photosynthesis is the process by which higher plants, algae, and certain species of bacteria transform and store solar energy in the form of energy-rich organic molecules. These compounds are in turn used as the energy source for all growth and reproduction in these and almost all other organisms. As such, virtually all life on the planet ultimately depends on photosynthetic energy conversion. Respiration, which occurs in mitochondrial and bacterial membranes, utilizes energy present in organic molecules to fuel a wide range of metabolic reactions critical for cell growth and development. In addition, many photosynthetic organisms engage in energetically wasteful photorespiration that begins in the chloroplast with an oxygenation reaction catalyzed by the same enzyme responsible for capturing carbon dioxide in photosynthesis. This series of books spans topics from physics to agronomy and medicine, from femtosecond processes to season long production, from the photophysics of reaction centers, through the electrochemistry of intermediate electron transfer, to the physiology of whole organisms, and from X-ray crystallography of proteins to the morphology of organelles and intact organisms. The goal of the series is to offer beginning researchers, advanced undergraduate students, graduate students, and even research specialists, a comprehensive, up-to-date picture of the remarkable advances across the full scope of research on photosynthesis, respiration and related processes.

*The titles published in this series are listed at the end of this volume and those of forthcoming volumes on the back cover.*

# Light-Harvesting Antennas in Photosynthesis

*Edited by*

**Beverley R. Green**

*University of British Columbia,  
Vancouver, Canada*

and

**William W. Parson**

*University of Washington,  
Seattle, U.S.A.*



SPRINGER-SCIENCE+BUSINESS MEDIA, B.V.

A C.I.P. Catalogue record for this book is available from the Library of Congress.

ISBN 978-90-481-5468-5      ISBN 978-94-017-2087-8 (eBook)  
DOI 10.1007/978-94-017-2087-8

---

The camera ready text was prepared by  
Lawrence A. Orr, Center for the Study of Early Events in Photosynthesis,  
Arizona State University, Tempe, Arizona 85287-1604, U.S.A.

*Printed on acid-free paper*

All Rights Reserved

© 2003 Springer Science+Business Media Dordrecht  
Originally published by Kluwer Academic Publishers in 2003

No part of this work may be reproduced, stored in a retrieval system, or transmitted  
in any form or by any means, electronic, mechanical, photocopying, microfilming, recording  
or otherwise, without written permission from the Publisher, with the exception  
of any material supplied specifically for the purpose of being entered  
and executed on a computer system, for exclusive use by the purchaser of the work.

This book is dedicated to our parents:

Mary Green (1911–2002), who supported all her daughter's professional endeavors and was a constant presence during the writing of this book.

Rowland Green (1902–1971), who taught her to look at things with a critical eye and ask pointed questions.

William Parson (1913–2002), who showed his son the excitement of science.

Buffy Parson (1912– ), who reminds him that art is important too.

# Editorial

## ***Advances in Photosynthesis and Respiration***

I am delighted to announce the publication of the long-awaited *Light-Harvesting Antennas*, Volume 13, edited by Beverley R. Green and William W. Parson in our Series *Advances in Photosynthesis and Respiration*.

The present volume is a sequel to the following twelve volumes in the *Advances in Photosynthesis and Respiration* (AIPH) series.

### **Published Volumes**

- (1) *Molecular Biology of Cyanobacteria* (Donald R. Bryant, editor, 1994);
- (2) *Anoxygenic Photosynthetic Bacteria* (Robert E. Blankenship, Michael T. Madigan and Carl E. Bauer, editors, 1995);
- (3) *Biophysical Techniques in Photosynthesis* (Jan Amesz\* and Arnold J. Hoff\*, editors, 1996);
- (4) *Oxygenic Photosynthesis: The Light Reactions* (Donald R. Ort and Charles F. Yocum, editors, 1996);
- (5) *Photosynthesis and the Environment* (Niel R. Baker, editor, 1996);
- (6) *Lipids in Photosynthesis: Structure, Function and Genetics* (Paul-André Siegenthaler and Norio Murata, editors, 1998);
- (7) *The Molecular Biology of Chloroplasts and Mitochondria in Chlamydomonas* (Jean David Rochaix, Michel Goldschmidt-Clermont and Sabeeha Merchant, editors, 1998);
- (8) *The Photochemistry of Carotenoids* (Harry A. Frank, Andrew J. Young, George Britton and Richard J. Cogdell, editors, 1999);
- (9) *Photosynthesis: Physiology and Metabolism* (Richard C. Leegood, Thomas D. Sharkey and Susanne von Caemmerer, editors, 2000);
- (10) *Photosynthesis: Photobiochemistry and Photo-biophysics* (Bacon Ke, author, 2001);

---

\*deceased

- (11) *Regulation of Photosynthesis* (Eva-Mari Aro and Bertil Andersson, editors, 2001); and
- (12) *Photosynthetic Nitrogen Assimilation and Associated Carbon and Respiratory Metabolism* (Christine Foyer and Graham Noctor, editors, 2002).

See <http://www.wkap.nl/series.htm/AIPH/> for further information and to order these books. Please note that the members of the International Society of Photosynthesis Research, ISPR (<http://www.photosynthesisresearch.org/>) receive special discounts.

### **Light-Harvesting Antennas**

In 1932, at the California Institute of Technology, Pasadena, Assistant Professor of Biophysics Robert (Bob) Emerson (1903-1959) and his undergraduate student William (Bill) Arnold (1904- 2001) did the most remarkable experiment. Using brief saturating light flashes, spaced at optimum dark periods, they measured O<sub>2</sub> evolution in the green alga *Chlorella* by manometry, a technique that had been perfected earlier by Otto Warburg. The results were surprising: a maximum of only one O<sub>2</sub> molecule was evolved per 2,400 chlorophyll molecules present. The concept that hundreds of chlorophyll molecules were associated with each 'photoenzyme' was born. Since the quantum yield of O<sub>2</sub> evolution was high, Hans Gaffron (1902-1979) and K. Wohl implied, in 1936, that light energy absorbed by the bulk chlorophyll molecules is transferred among these molecules until it reaches the 'photoenzyme.' Now, we know that the bulk chlorophyll molecules, bound to proteins, serve as the 'antenna,' and the photoenzyme is the 'reaction center.'

Volume 13 (*Light-Harvesting Antennas*), edited by Beverley Green and William Parson, exposes before our very own eyes the structure and function



of this intricate and marvelous machinery. The book is unique in the degree to which it emphasizes the integration of molecular biological, biochemical and biophysical approaches. The collaboration of these two editors with very different areas of expertise shows the advantages of such an approach: Beverley Green, whose photograph and a brief biography appears in this volume, is a biochemist who was one of the major players in untangling the light-harvesting pigment-protein complexes of higher plants and chromophyte algae; Bill Parson, whose photograph and a brief biography also appears in this volume, is a 'very fast' biophysicist who is well-known for his studies of the sub-picosecond events in which light energy is absorbed by antenna systems and transferred to photosynthetic reaction centers. The two editors have assembled an outstanding team of authors, all of international repute, representing a broad spectrum of interests, and coordinated the contributions to make a well-organized, understandable and comprehensive volume. This book treats all aspects of photosynthetic light-harvesting antennas, from the biophysical mechanisms of light absorption and energy transfer to the structure, biosynthesis and regulation of antenna systems in whole organisms. It sets the great variety of antenna pigment-protein complexes in their evolutionary context and at the same time brings in the latest hi-tech developments. Throughout, there is a consistent attempt to deal with both biophysical and molecular biological information as it relates to different sides of the same question. It is 'a real book with chapters,' not a compilation of review articles.

### The Scope of the Series

*Advances in Photosynthesis and Respiration* is a book series that provides, at regular intervals, a comprehensive and state-of-the-art account of research in various areas of photosynthesis and respiration. Photosynthesis is the process by which higher plants, algae, and certain species of bacteria transform and store solar energy in the form of energy-rich organic molecules. These compounds are in turn used as the energy source for all growth and reproduction in these and almost all other organisms. Virtually all life on the planet thus ultimately depends on photosynthetic energy conversion. Respiration, which occurs in mitochondria and in bacterial membranes, utilizes energy

present in organic molecules to fuel a wide range of metabolic reactions critical for cell growth and development. In addition, many photosynthetic organisms engage in energetically wasteful *photorespiration* that begins in the chloroplast with an oxygenation reaction catalyzed by the same enzyme responsible for capturing carbon dioxide in photosynthesis. This series of books spans topics from physics to agronomy and medicine, from femtosecond ( $10^{-15}$  s) processes to season-long production, from the photophysics of reaction centers, through the electrochemistry of intermediate electron transfer, to the physiology of whole organisms, and from X-ray crystallography of proteins to the morphology of organelles and intact organisms. The intent of the series is to offer beginning researchers, advanced undergraduate students, graduate students, and even research specialists, a comprehensive, up-to-date picture of the remarkable advances across the full scope of research on bioenergetics and carbon metabolism.

### Future Books

The readers of the current series are encouraged to watch for the publication of the forthcoming books:

- (1) *Photosynthesis in Algae* (Editors: Anthony W.D. Larkum, Susan Douglas, and John A. Raven);
- (2) *Chlorophylls and Bacteriochlorophylls: Biochemistry, Biophysics and Biological Function* (Editors: Bernhard Grimm, Robert J. Porra, Wolfhart Rüdiger and Hugo Scheer);
- (3) *Respiration in Archae and Bacteria*. 2 volumes (Editor: Davide Zannoni );
- (4) *Chlorophyll a Fluorescence: A signature of Photosynthesis* (Editors: George Papageorgiou and Govindjee);
- (5) *Plant Respiration* (Editors: Miquel Ribas-Carbo and Hans Lambers);
- (6) *Photosystem II: The Water/Plastoquinone Oxido-reductase in Photosynthesis* (Editors: Thomas J. Wydrzynski and Kimiyuki Satoh);
- (7) *Photosystem I: The NADP<sup>+</sup>/Ferredoxin Oxidoreductase in Oxygenic Photosynthesis* (Editor: John Golbeck);
- (8) *Photosynthesis: A Comprehensive Treatise; Biochemistry, Biophysics and Molecular*

*Biology*, 2 volumes (Editors: Julian Eaton-Rye and Baishnab Tripathy)

- (9) *Photoprotection, Photoinhibition, Gene Regulation and Environment* (Editors: Barbara Demmig-Adams, William W. Adams III and Autar Mattoo);
- (10) *The Structure and Function of Plastids* (Editors: Kenneth Hooper and Robert Wise); and
- (11) *History of Photosynthesis Research* (Editor: Govindjee)

In addition to these contracted books, we are interested in publishing several other books. Topics planned are: Global Aspects of Photosynthesis and Respiration; Protein Complexes of Photosynthesis and Respiration; Biochemistry and Biophysics of Respiration; Protonation and ATP Synthesis; Functional Genomics; Proteonomics, The Cytochromes; Molecular Biology of Cyanobacteria; Laboratory Methods for Studying Leaves and Whole

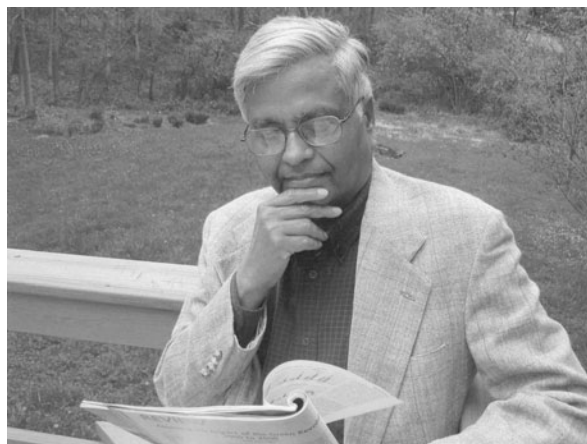
Plants; and C-3 and C-4 Plants.

Readers are requested to send their suggestions for these and future volumes (topics, names of future editors, and of future authors) to me by E-mail (gov@uiuc.edu) or fax (1-217-244-7246).

In view of the interdisciplinary character of research in photosynthesis and respiration, it is my earnest hope that this series of books will be used in educating students and researchers not only in Plant Sciences, Molecular and Cell Biology, Integrative Biology, Biotechnology, Agricultural Sciences, Microbiology, Biochemistry, and Biophysics, but also in Bioengineering, Chemistry, and Physics.

I take this opportunity to thank Beverley Green; William Parson; all the authors of Volume 13; Larry Orr; Jacco Flipsen, Noeline Gibson; Evan Delucia, and my wife Rajni Govindjee for their valuable help and support that made the publication of *Light-Harvesting Antennas* possible.

Govindjee  
Series Editor  
*Advances in Photosynthesis and Respiration*  
University of Illinois at Urbana-Champaign  
Department of Plant Biology  
265 Morrill Hall, 505 South Goodwin Avenue  
Urbana, IL 61801-3707, U.S.A.  
E-mail: gov@uiuc.edu;  
URL: <http://www.life.uiuc.edu/govindjee>



### Govindjee

*The story of the Series editor's name and a bit of his personal background.*

Govindjee, who uses one name only, grew up in Allahabad (India). He was born in 1932 to (Mrs) Savitri Devi Asthana and (Mr) Vishveshwar Prasad Asthana. His father was a college teacher, and then a representative of the Oxford University Press in the then United Provinces (UP) of India. His family name, Asthana, was dropped by his father in response to the 'Arya Samaj Movement' that was against the 'Caste System,' and believed in the ideals of the Vedic times. After his father's death in 1943, his older brother Krishnaji (Professor of Physics, University of Allahabad) was responsible for bringing him up and served as his role model. Shri Ranjan, who had been a graduate student of Felix Frost Blackman, trained him in Plant Physiology.

Govindjee came to Urbana, Illinois, U.S.A., as a Fulbright Scholar, and a Fellow of 'Physico-Chemical Biology' in 1956, with his name written as 'Govind Jee.' He was not happy to be called 'G. Jee,' and, thus, began to use 'Govindjee' as his one and only name. This has caused problems in citations, and in many formal settings. He has been called by many names: N.F.N. Govindjee (where N.F.N. stands for No First Name); I. Govindjee (where I stands for Illini); Mister Govindjee; and once A.V.P. Govindjee (where A. stands for Allahabad, and V.P. are the initials of his father). Quite often, his name has appeared with the

initials of his doctoral students: the longest being J.C.M. Govindjee, Jr (where J.C.M. stood for John Clingman Munday). Govindjee received his training in the area of 'Photosynthesis' first from Robert Emerson, and then from Eugene Rabinowitch. Govindjee obtained his Ph.D. in Biophysics at the University of Illinois, in 1960. He has been on its faculty since 1961. Since July, 1999 he has been Professor Emeritus of Biochemistry, Biophysics and Plant Biology at the University of Illinois at Urbana-Champaign. A brief formal biography of Govindjee is available in Foyer CH and Noctor G (eds) (2003) *Photosynthetic Nitrogen Assimilation and Associated Carbon and Respiratory Metabolism*, Advances in Photosynthesis and Respiration, Volume 12, Kluwer Academic Publishers, Dordrecht, The Netherlands.

He was married to Rajni Verma in 1957 at Urbana, Illinois. They have two children: Sanjay Govindjee (his wife is Marilyn) and Anita Govindjee (her husband is Morten Christiansen) and three grand children (Sunita Christiansen; Arjun Govindjee and Rajiv Govindjee).

Currently, Govindjee focuses his attention on two topics: (1) Chlorophyll *a* Fluorescence: A Probe of Photosynthesis; and (2) History of Photosynthesis Research; he is equally concerned with photosynthesis education (see his web site: <http://www.life.uiuc.edu/govindjee>).

# Contents

<b>Editorial</b>	<b>vii</b>
<b>Contents</b>	<b>xi</b>
<b>Preface</b>	<b>xvii</b>
<b>Color Plates</b>	<b>CP-1</b>

## ***Part I. Introduction to Light-Harvesting***

---

<b>1</b>	<b>Photosynthetic Membranes and Their Light-Harvesting Antennas</b>	<b>1–28</b>
	<i>Beverley R. Green, Jan M. Anderson and William W. Parson</i>	
	Summary	2
	I. Introduction	2
	II. Photosynthetic Prokaryotes	6
	III. Chloroplasts of Photosynthetic Eukaryotes	14
	To be Continued...	23
	Acknowledgments	23
	References	23
<b>2</b>	<b>The Pigments</b>	<b>29–81</b>
	<i>Hugo Scheer</i>	
	Summary	29
	I. Introduction	30
	II. Functions: A Short Overview	30
	III. The Pigments	34
	IV. Analytics	67
	V. Pigment Substitution Methods	69
	References	71
<b>3</b>	<b>Optical Spectroscopy in Photosynthetic Antennas</b>	<b>83–127</b>
	<i>William W. Parson and V. Nagarajan</i>	
	Summary	84
	I. Introduction	84
	II. Absorption Coefficient	85
	III. Charge-Transfer Transitions	86
	IV. Circular Dichroism	86
	V. Configuration Interactions	90
	VI. Dipole Strength	92
	VII. Electromagnetic Radiation	92
	VIII. Excitons	95
	IX. Fluorescence Yield and Lifetime	100

X.	Infrared Spectroscopy	101
XI.	Internal Conversion	103
XII.	Linear Dichroism and Fluorescence Anisotropy	103
XIII.	Mathematical Tools	106
XIV.	Raman Scattering	107
XV.	Resonance Energy Transfer	108
XVI.	Singlet and Triplet States	111
XVII.	Spectral Bandshapes and Dynamics	113
XVIII.	Spontaneous Fluorescence	116
XIX.	Time-Resolved Spectroscopy	118
XX.	Transition Dipoles	120
XXI.	Wavefunctions	123
	Acknowledgement	125
	References	125

#### **4 The Evolution of Light-harvesting Antennas 129–168**

*Beverley R. Green*

	Summary	130
I.	Introduction	130
II.	Origins	131
III.	How Proteins and Their Genes Evolve	136
IV.	Pigment Biosynthesis Genes	142
V.	Photosynthetic Reaction Centers and the Core Antenna Family	145
VI.	Phycobiliproteins	148
VII.	LHC Superfamily	150
VIII.	Single Membrane Helix Antennas of Purple and Green Filamentous Bacteria	155
IX.	Antenna Proteins Unique to Certain Groups	156
X.	The Big Picture: The Five Divisions of Photosynthetic Bacteria	157
	References	160

### ***Part II. Structure and Function in Light-Harvesting***

---

#### **5 The Light-Harvesting System of Purple Bacteria 169–194**

*Bruno Robert, Richard J. Cogdell and Rienk van Grondelle*

	Summary	170
I.	Introduction	170
II.	Components of the Light-Harvesting System of Purple Bacteria	171
III.	Structure-Function Relationships in Bacterial Antennas	176
IV.	Energy Transfer in Light-Harvesting Proteins from Purple Bacteria	181
V.	Conclusion	188
	Acknowledgments	188
	References	188

#### **6 Antenna Complexes from Green Photosynthetic Bacteria 195–217**

*Robert E. Blankenship and Katsumi Matsuura*

	Summary	195
--	---------	-----



	I. Introduction	196
	II. Chlorosome Structure, Pigment Stoichiometry and Protein Content	201
	III. Redox-Dependent Regulation of Energy Transfer in Chlorosomes	204
	IV. Fenna-Matthews-Olson Protein	207
	V. Kinetics and Pathways of Energy Transfer in Chlorosomes and Membranes of Green Bacteria	209
	VI. Conclusions and Future Work	210
	Acknowledgment	211
	References	211
<b>7</b>	<b>Light-Harvesting in Photosystem II</b>	<b>219–251</b>
	<i>Herbert van Amerongen and Jan P. Dekker</i>	
	Summary	220
	I. Introduction	220
	II. The Photosystem II Genes and Proteins	221
	III. Individual Photosystem II Antenna Complexes	222
	IV. Reaction Center Containing Photosystem II Complexes	235
	V. Overall Trapping of Excitation Energy	242
	References	245
<b>8</b>	<b>Structure and Function of the Antenna System in Photosystem I</b>	<b>253–279</b>
	<i>Petra Fromme, Eberhard Schlodder and Stefan Jansson</i>	
	Summary	254
	I. Introduction	254
	II. The Architecture of Cyanobacterial Photosystem I	255
	III. Structural Organization of the Core Antenna System	261
	IV. Plant Photosystem I	266
	V. Excitation Energy Transfer and Trapping in PS I	270
	Acknowledgment	275
	References	275
<b>9</b>	<b>Antenna Systems and Energy Transfer in Cyanophyta and Rhodophyta</b>	<b>281–306</b>
	<i>Mamoru Mimuro and Hiroto Kikuchi</i>	
	Summary	282
	I. Introduction	282
	II. Molecular Architecture of Antenna Systems in Cyanobacteria and Red Algae	282
	III. Energy Flow in Antenna Systems of Cyanobacteria	291
	IV. Three-Dimensional Structures of Phycobiliproteins	292
	V. Electronic States of Chromophores in Phycobiliproteins	298
	VI. Energy Transfer	301
	VII. Concluding Remarks	302
	Acknowledgments	302
	References	302

**10 Antenna Systems of Red Algae: Phycobilisomes with Photosystem II and Chlorophyll Complexes with Photosystem I 307–322**

*Elisabeth Gantt, Beatrice Grabowski and Francis X. Cunningham, Jr.*

Summary	307
I. Introduction	308
II. Structure and Composition of the Antenna Systems	308
III. Phylogenetic Implications of LHC Structure and Function	315
IV. Light Acclimation Responses	315
V. Energy Distribution	318
VI. Future Problems to be Addressed	319
Acknowledgments	319
References	319

**11 Light-Harvesting Systems in Chlorophyll c-Containing Algae 323–352**

*Alisdair N. Macpherson and Roger G. Hiller*

Summary	324
I. Introduction	324
II. Groups Having One Main Light Harvesting System	328
III. Groups Having Two Distinct Light Harvesting Systems	333
IV. Concluding Remarks	347
Acknowledgments	348
References	348

***Part III. Biogenesis, Regulation and Adaptation***

---

**12 Biogenesis of Green Plant Thylakoid Membranes 353–372**

*Kenneth Cline*

Summary	353
I. Introduction	354
II. Methodologies for Higher Plant Chloroplasts	354
III. Overview of Localization Processes	356
IV. Different Mechanisms Address Different Translocation Problems	359
V. The In Vivo Site of Thylakoid Protein Transport and Insertion	364
VI. Chlorophyll Synthesis And The Insertion Of Antenna Proteins	364
VII. Future Prospects	367
References	368

**13 Pulse Amplitude Modulated Chlorophyll Fluorometry and its Application in Plant Science 373–399**

*G. Heinrich Krause and Peter Jahns*

Summary	373
I. Introduction	374
II. The Measuring Principle of the Pulse Amplitude Modulation Fluorometer	374
III. Initial and Variable Fluorescence	375
IV. Ratio of Maximum Variable to Maximum Total Fluorescence, $F_v/F_m$	378
V. Fluorescence Quenching	379

VI. Photosynthetic Yield and Rate of Linear Electron Transport Determined by Fluorescence Analysis	388
VII. Application of Chlorophyll Fluorescence in the Study of Mutants	391
VIII. Conclusion and Perspectives	392
Acknowledgment	393
References	393
<b>14 Photostasis in Plants, Green Algae and Cyanobacteria: The Role of Light Harvesting Antenna Complexes</b>	<b>401–421</b>
<i>Norman P. A. Huner, Gunnar Öquist and Anastasios Melis</i>	
Summary	402
I. Introduction	402
II. Stress and Photostasis	404
III. Acclimation And Photostasis	409
IV. Chloroplast Biogenesis and Photostasis	415
V. Sensing Mechanisms Involved in Photostasis	416
Acknowledgments	416
References	417
<b>15 Photoacclimation of Light Harvesting Systems in Eukaryotic Algae</b>	<b>423–447</b>
<i>Paul G. Falkowski and Yi-Bu Chen</i>	
Summary	424
I. Introduction	424
II. Photoacclimation	425
III. Light in aquatic environments	425
IV. Physiological Responses to Changes in Spectral Irradiance	429
V. Light Harvesting Systems and the Effective Absorption Cross Section of Photosystem II	432
VII. Light Harvesting Complexes	438
VIII. The 'Nested Signal' Hypothesis	442
Acknowledgments	443
References	443
<b>16 Multi-level Regulation of Purple Bacterial Light-harvesting Complexes</b>	<b>449–470</b>
<i>Conan S. Young and J. Thomas Beatty</i>	
Summary	450
I. Introduction	450
II. Gene Organization and Expression	452
III. Assembly of LH Complexes	459
IV. Other genes and proteins relevant to LH complex assembly or structure	462
V. Concluding Remarks and Future Prospects	464
Acknowledgments	465
References	465

**17 Environmental Regulation of Phycobilisome Biosynthesis 471–493**

*Arthur R. Grossman, Lorraine G. van Waasbergen and David Kehoe*

Summary	471
I. Introduction	472
II. Phycobilisome Structure	472
III. Complementary Chromatic Adaptation	473
IV. Model for the Control of Complementary Chromatic Adaptation	481
V. Control of Phycobilisome Biosynthesis During Nutrient Limitation	482
VI. Concluding Remarks	488
Acknowledgments	488
References	488

**Index 495**

# Preface

Why a book on light-harvesting antennas? Light-harvesting antennas are the pigment-protein complexes that absorb light and transfer energy to the photosynthetic reaction centers, where the photochemical electron-transfer reactions occur. In any photosynthetic membrane, only a small fraction of the pigment molecules participates directly in the reactions that lead to charge separation and electron flow. For each reaction center chlorophyll or bacteriochlorophyll, there are many pigment molecules that collect the light. The antenna complexes include a wide variety of chlorophylls, carotenoids and phycobilins, which are attached to an even more varied collection of proteins. This molecular variety reflects the evolutionary diversity of photosynthetic organisms.

Our objective in bringing together the chapters of this book was to provide a comprehensive review of current knowledge about light-harvesting antennas of plants, algae and photosynthetic bacteria in a framework that integrates the biochemical and structural picture with what can be learned from modern biophysical approaches. Because of the range of experimental techniques used to study problems related to light harvesting, it is difficult to acquire a comprehensive picture of an antenna system and its function by reading only the primary literature. This book attempts to provide some of these pictures by taking an integrative approach. As Govindjee so nicely expressed it, this is 'a real book with chapters', not just a compilation of review articles.

The four chapters of Part I deal with topics that apply to all photosynthetic organisms. Chapter 1 (Green, Anderson and Parson) introduces the light-harvesting antennas and places them in context in their photosynthetic membranes. Photosynthetic pigments and their biosynthesis are the subject of Chapter 2 (Scheer). Chapter 3 (Parson and Nagarajan) explains biophysical aspects of photosynthesis and the experimental and theoretical approaches used to study energy transfer in antenna systems. This chapter is uniquely organized in modules that can be read independently for information on particular topics. Chapter 4 (Green) discusses the molecular evolution of light-harvesting antenna families, pigment

biosynthesis enzymes and the photosynthetic prokaryotes.

Most of the chapters of Part II deal with specific groups of photosynthetic organisms: purple bacteria in Chapter 5 (Robert, Cogdell and van Grondelle), green sulfur and green filamentous bacteria in Chapter 6 (Blankenship and Matsuura), cyanobacteria in Chapter 9 (Mimuro and Kikuchi), red algae in Chapter 10 (Gantt, Grabowski and Cunningham) and all the algae with chlorophyll *c* in Chapter 11 (Macpherson and Hiller). This is an unusual but logical approach, since each group of organisms has several types of antenna that operate in conjunction with one another. Much of the biophysical data can be understood only by considering all the participants in the context of the overall molecular structure.

Two exceptions to this organismal approach are the chapters that emphasize the core Chl *a* antennas of Photosystem I and Photosystem II. Chapter 7 on Photosystem II (van Amerongen and Dekker) and Chapter 8 on Photosystem I (Fromme, Schlodder and Jansson) are focused treatments of the individual photosystems, drawing on the recently-determined high resolution structures of the cyanobacterial photosystems, and on our growing biochemical knowledge of the chlorophyll *a/b* antennas (light harvesting complexes, LHCs) of green plant chloroplasts.

Part III considers the interrelated aspects of biosynthesis and assembly of photosynthetic membranes and their acclimation in response to environmental conditions. Chapter 12 (Cline) focuses on the assembly of the higher plant photosynthetic membrane. It is followed by chapters on the role of antennas in photostasis (Chapter 14, Huner, Öquist and Huner) and on photoacclimation in eukaryotic algae (Chapter 15, Falkowski and Chen). These are complemented by a chapter on pulse-amplitude modulated (PAM) fluorimetry that provides a comprehensive explanation of this much used (and sometimes abused) technique (Chapter 13, Krause and Jahns). The last two chapters are concerned with regulation at the molecular level of purple bacterial antennas (Chapter 16, Young and Beatty) and cyanobacterial phycobilisomes (Chapter 17, Grossman, van Waasbergen and Kehoe).



We are living in the golden age of photosynthesis research. Energy transfer can now be studied by very powerful biophysical techniques. High-resolution three-dimensional structures have been determined for a number of photosynthetic complexes, making it possible to design experiments that test the relationships between structure and function. Modern molecular biological approaches are also beginning to clarify the biosynthesis of the photosynthetic apparatus and its adaptation to changing conditions. None of these approaches can work effectively in isolation. We hope that our book will help to build bridges that span the gaps and encourage researchers to study the mysteries of light-harvesting antennas in an integrative fashion. At the same time, we have tried to provide clear explanations of basic concepts suitable for beginning graduate students and advanced undergraduates, in the hope of enticing some of them into this fascinating field of research.

We have many people to thank. First of all our authors, without whom there would be no book. They were willing to look beyond their research specialties to give the reader a more encompassing view of light-harvesting, and they cheerfully put up with requests for extensive editorial changes, as well as the inevitable delays in publication. We also thank the editors of several earlier books in this series — Bob Blankenship, Harry Frank and Don Bryant— for their very helpful advice on editing and book publishing. Larry Orr is a very special person: his patience, good humor and professional competence in typesetting and assembling this book (and others in the series) have helped us immensely. Last but not least Govindjee, without whom there would be no series. He has provided generous measures of advice and encouragement to all the editors and authors over the years.

Beverley R. Green,  
Botany Department,  
University of British Columbia, Canada  
brgreen@interchange.ubc.ca

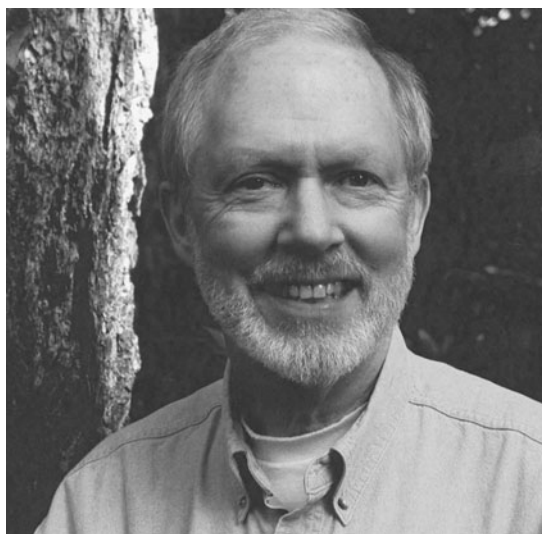
William W. Parson,  
Biochemistry Department,  
University of Washington, U.S.A.  
parsonb@u.washington.edu



**Beverley R. Green**

Beverley Green is Professor of Botany at the University of British Columbia. Although she is a native of that province and has spent much of her life there, her scientific career has been much more wide-ranging. She obtained her B.Sc. in chemistry (Hons.) from the University of B.C. in 1960, and her Ph.D. in Biochemistry from the University of Washington in 1965. She then spent two years as a NATO Post-doctoral Fellow in the laboratories of René Thomas and Jean Brachet at the Université Libre de Bruxelles, working on the genetics of bacteriophage lambda and the chloroplast DNA of the giant green alga *Acetabularia*. Because of her interest in photosynthetic organisms in general and chloroplasts in particular, she accepted a faculty position in the Department of Botany at the University of British Columbia in 1967. While trying to identify the proteins that could be synthesized by isolated chloroplasts in vitro (and therefore likely encoded on chloroplast DNA), she discovered that most of them were unidentified thylakoid membrane proteins, some of which retained chlorophyll when separated on

non-denaturing gels. This somewhat unconventional entry into the photosynthesis field led to the characterization of a number of novel chlorophyll-proteins from higher plants and algae, most of which turned out to be light-harvesting antennas. Their gene sequences showed that they were members of a large protein family, now called the Light-harvesting complex (LHC) Superfamily, which includes light stress-response proteins as well as light-harvesting proteins. Members of this family feature prominently in many chapters of this book. Her research is now oriented toward the molecular evolution of chloroplasts, particularly the secondary endosymbiosis(es) that gave rise to the algae with chlorophyll *c*, and the problem of protein import into chloroplasts surrounded by four membranes. As a member of the Diatom Genome Consortium, she is involved in the analysis of the first algal genome sequenced. Her research has now come full circle, with the discovery of single-gene minicircles in dinoflagellate chloroplasts!

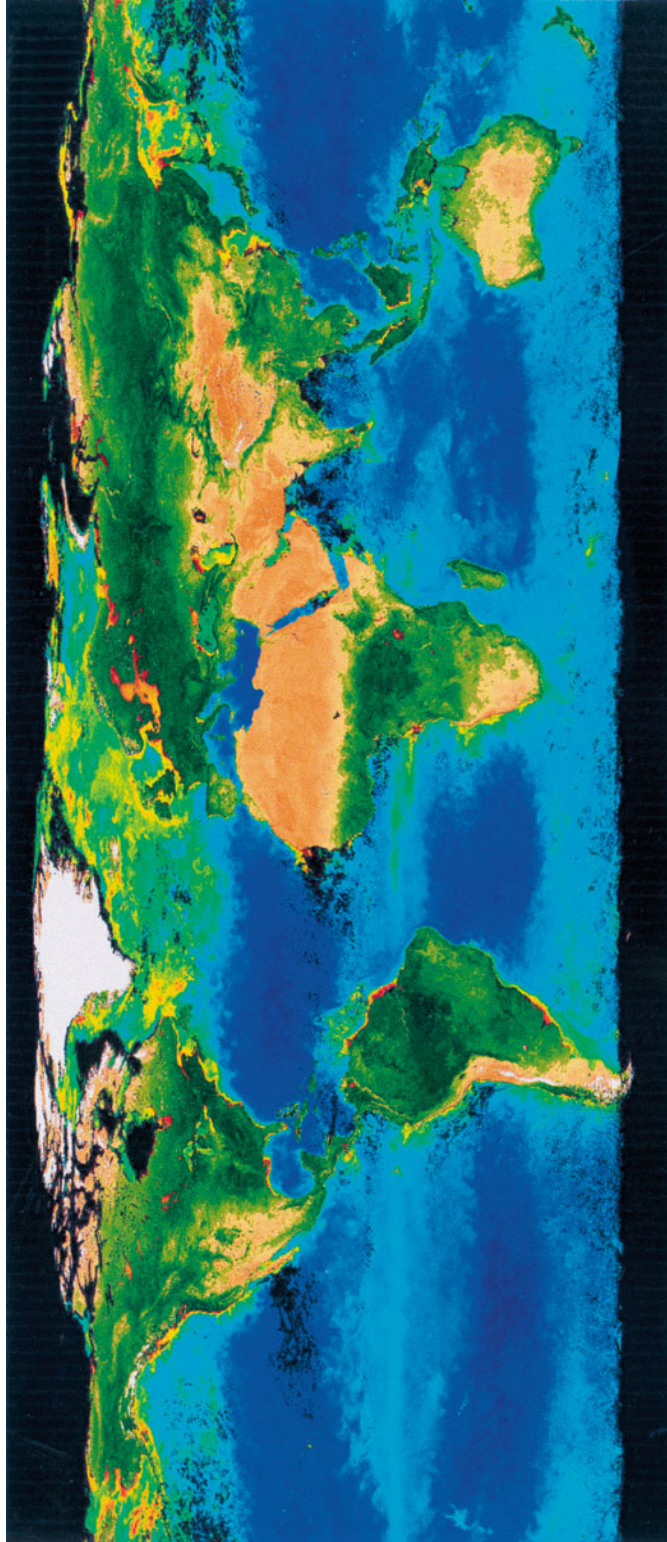


**William W. Parson**

William Parson is Professor of Biochemistry and Adjunct Professor of Chemistry at the University of Washington, Seattle, Washington. He received his undergraduate degree from Harvard University, Cambridge, Massachusetts, in 1961 and his Ph.D. with Harry Rudney in Biochemistry from Case Western Reserve University, Cleveland, Ohio, in 1965. Predoctoral studies of the biosynthesis of ubiquinone led to an interest in the role of ubiquinone in photosynthesis, which he pursued as a postdoctoral fellow in the laboratories of Britton Chance and Don DeVault at the University of Pennsylvania. While at Pennsylvania, he used pulsed laser techniques to show that the initial photochemical reaction in purple photosynthetic bacteria is the oxidation of a bacteriochlorophyll complex (P) and that the oxidized bacteriochlorophyll ( $P^+$ ) then draws an electron from a *c*-type cytochrome. After moving to the University of Washington in 1967, he showed that each  $P^+$  can oxidize multiple cytochrome hemes, measured the kinetics of electron transfer between the primary and

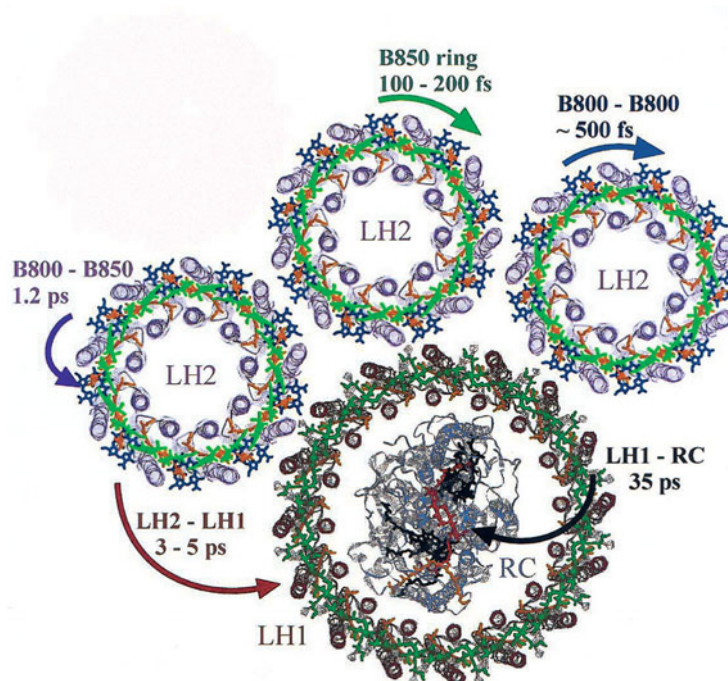
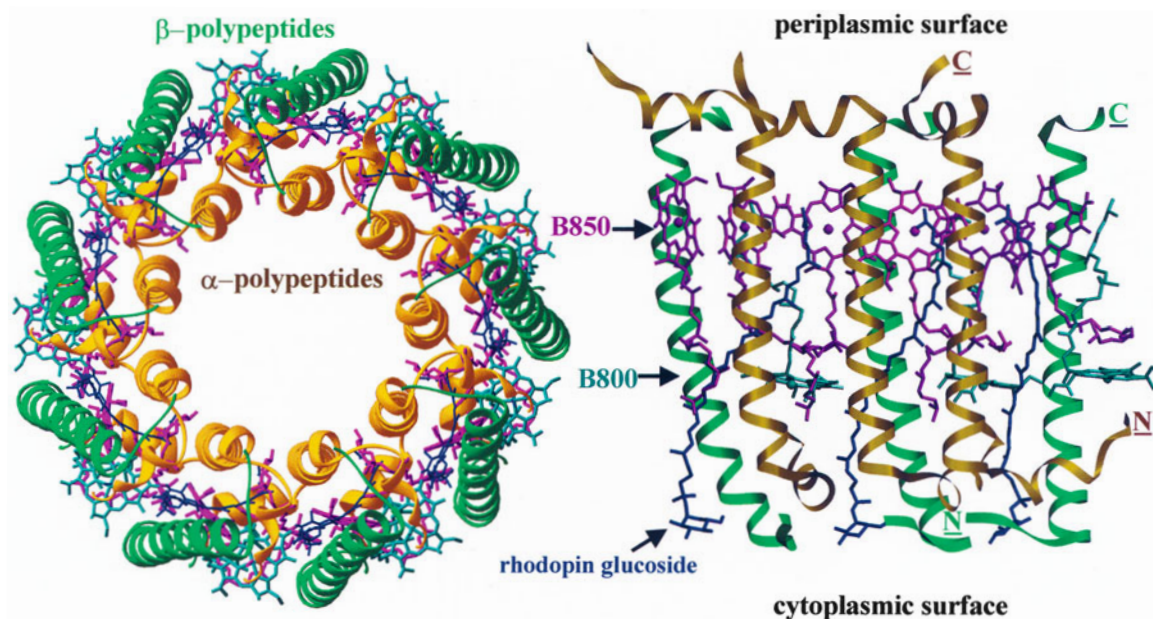
secondary electron acceptors, identified ubiquinone to be the secondary acceptor, and found that bacteriopheophytin (BPh) served as an intermediate between the excited bacteriochlorophyll ( $P^*$ ) and the primary quinone. In pioneering measurements on picosecond and sub-picosecond time scales, Parson and his coworkers explored the dynamics and temperature dependence of electron transfer from  $P^*$  to the BPh and the quinone in wild-type and mutant reaction centers, and studied rapid relaxations and energy-transfer processes in bacterial antenna complexes. They also introduced measurements of photoacoustic signals and delayed fluorescence for determining the energies of transient intermediates in the charge-separation reactions. Branching into computational chemistry, they have explored the pigment-pigment interactions that underlie the spectroscopic properties of photosynthetic bacterial reaction centers and antenna complexes, and the pigment-protein interactions that determine the energies of transient electron-transfer states.

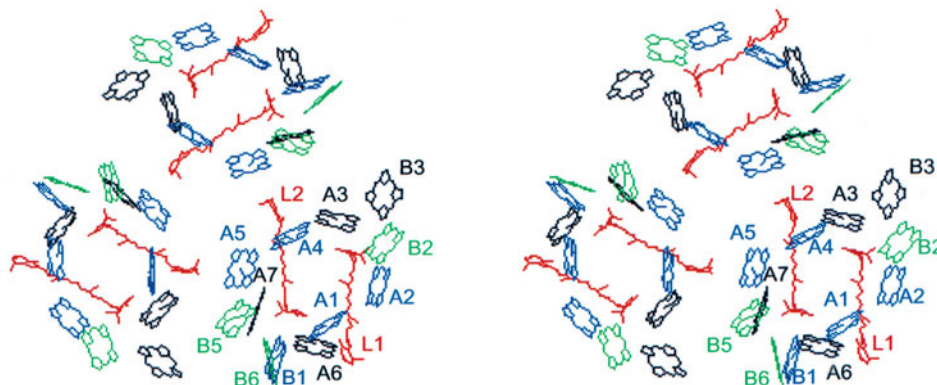
# Color Plates



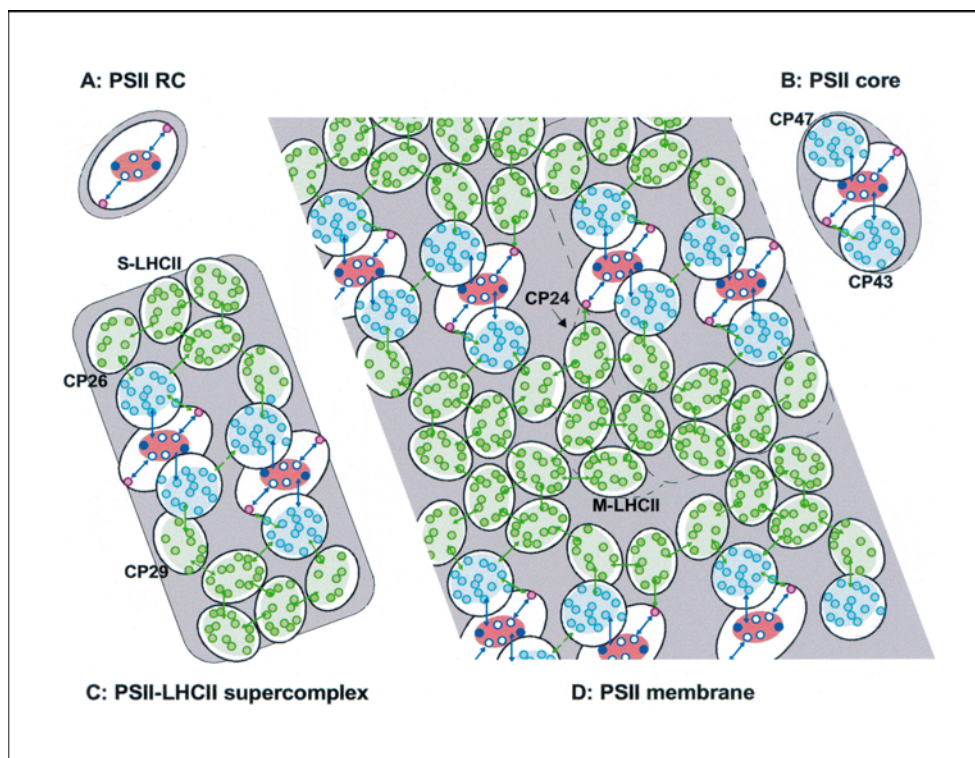
*Color Plate 1.* The global distribution of chlorophyll in marine and terrestrial ecosystems in the summer, as derived from SeaWiFS satellite data. Almost all the chlorophyll is in light-harvesting antenna complexes. Chlorophyll concentrations range from red (very high) through dark and light green to yellow (low) on land, and from blue-green to light blue to dark blue in the oceans. Yellow-brown areas are deserts. See also Chapter 15, p 427.





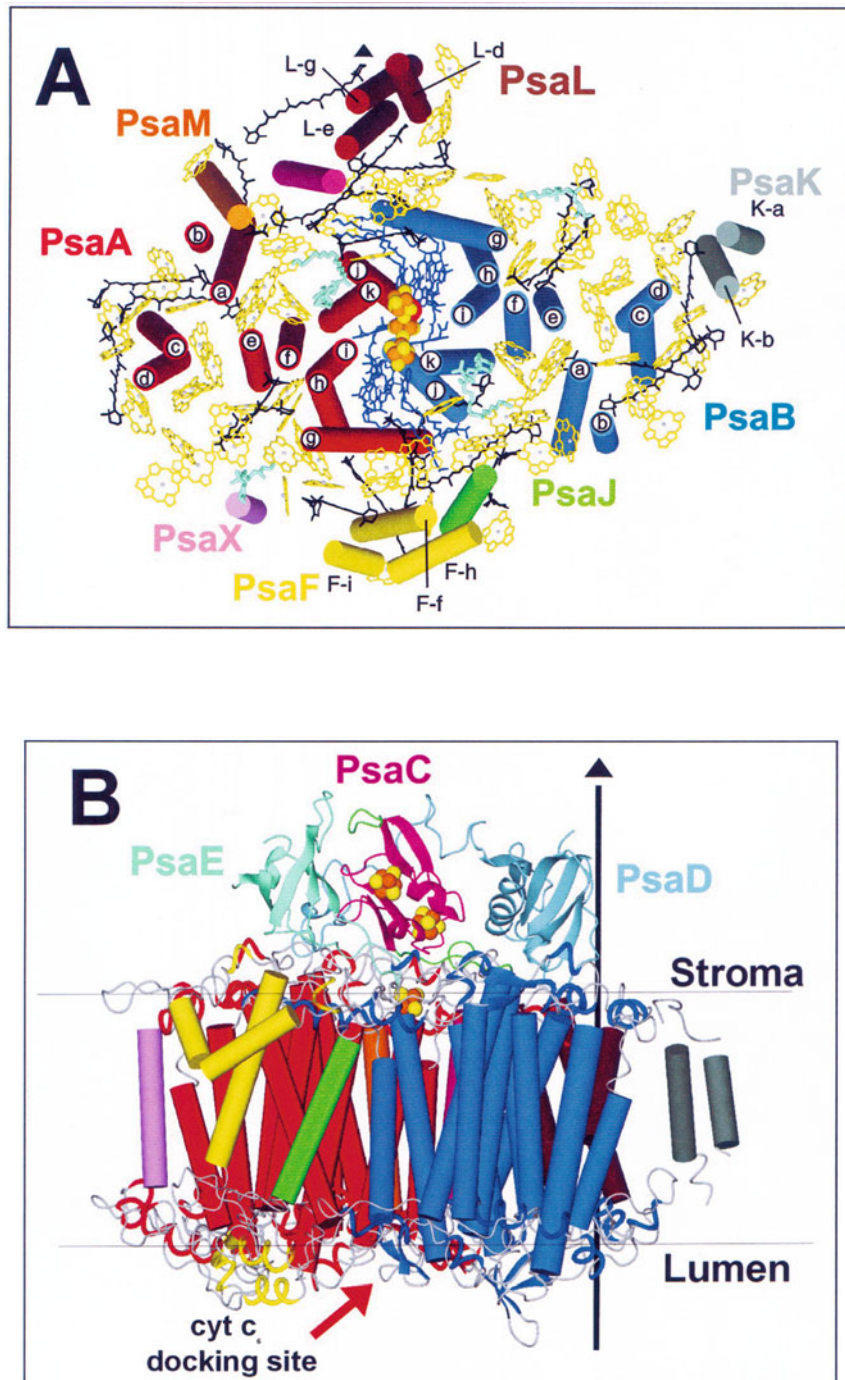


*Color Plate 4.* Stereo top view of the chromophores resolved in the 3.4 Å crystal structure of LHCII (Kühlbrandt et al., 1994). L1 and L2 indicate the positions of the structurally resolved xanthophylls, while A1–B6 indicate the sites of the Chls, numbered according to Kühlbrandt et al. (1994). The chlorophylls in blue and green have been shown to be Chl *a* and Chl *b*, respectively, while those in black have been proposed to have a mixed character. See Chapter 7, pp 223–227 and Table 4.

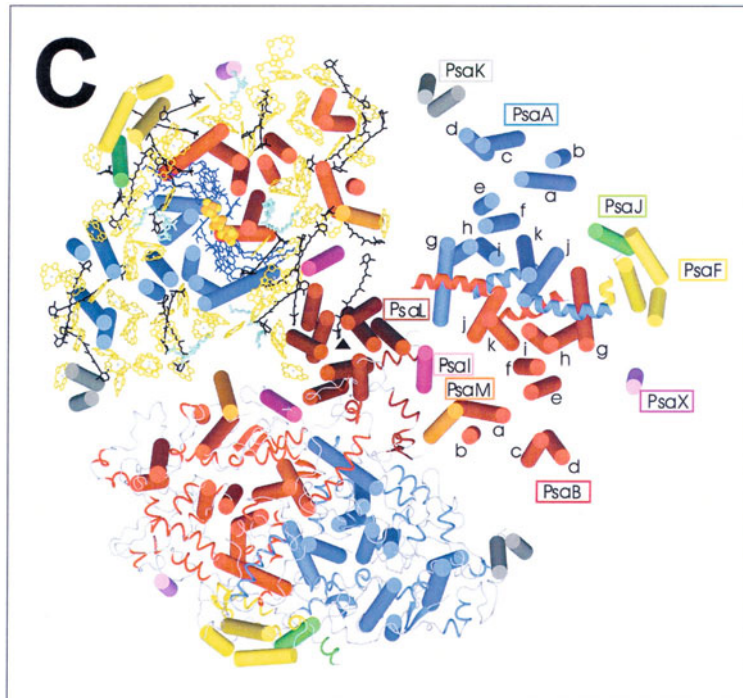


*Color Plate 5.* Schematic representation of energy transfer and trapping processes in (A) PS II RC complex, (B) monomeric PS II core complex, (C)  $C_2S_2$  PSII-LHCII supercomplex and (D) part of a membrane with a regular array of  $C_2S_2M$  PSII-LHCII supercomplexes. In (D) the supercomplexes are contoured by dashed lines and are darker gray than the surrounding membrane. The pigments (circles) are placed at *approximate* positions according to the various crystal structures. Four central Chls of PS II RC, white with blue rim; Phe, dark blue; peripheral Chl of PS II RC, magenta; core antenna, light blue; peripheral antenna Chl *a*, light green; Chl *b*, dark green. The trapping process ( $\tau_{\text{trap}}$ , red area in the PS II RC) is relatively important in the PS II RC complex, the delivery of the excitation energy ( $\tau_{\text{del}}$ , dark blue arrows) is important in the PS II core complex, the migration processes ( $\tau_{\text{mig}}$ , green arrows) are significant in PSII-LHCII supercomplexes and PS II membranes. The light blue and green areas represent areas in which ultrafast energy transfer among groups of chlorophylls is expected in core and peripheral antenna proteins, respectively; light blue arrows represent a few less likely (relatively slow) energy transfer routes. See Chapter 7, p 241.

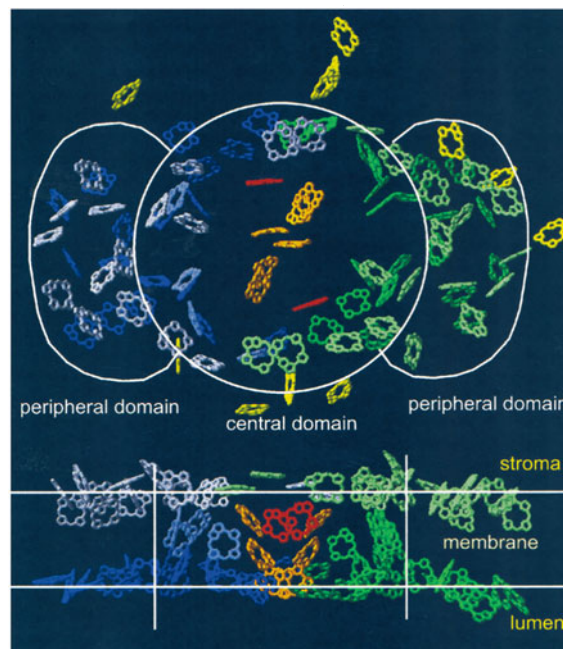




*Color Plate 6.* (A) and (B): Arrangement of protein subunits and cofactors in one monomeric unit of Photosystem I. Transmembrane helices are shown as columns. Chlorophylls (yellow) are represented by their head-groups, with the ring substituents omitted for clarity. RC chromophores, dark blue; carotenoids, black; lipids, azure. The Fe/S atoms of the [4Fe-4S] clusters are represented by small spheres. (A) View from the stromal side onto the membrane plane, showing only the transmembrane part of Photosystem I; (B) view along the membrane plane, with the organic cofactors omitted for clarity. The arrow indicates the threefold symmetry axis of the trimeric structure. (Continued on next page). See Chapter 8, p 256.

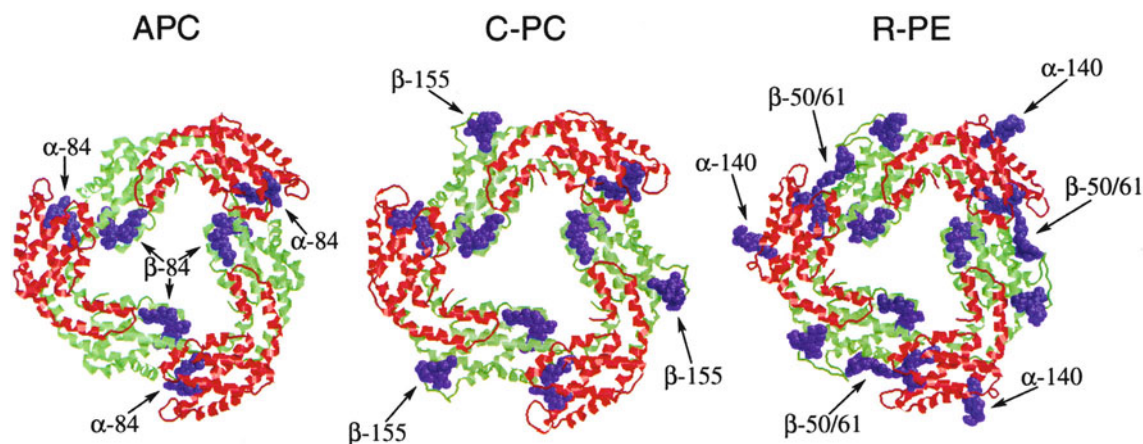


*Color Plate 6, continued. (C) Organization of the PS I trimer. View from the stromal side onto the membrane plane, with the stromal subunits omitted for clarity. Different structural elements are shown in each of the three monomers. In the top right monomer the transmembrane helices are shown as columns and the subunits are labeled. The top left monomer shows the complete set of cofactors along with the transmembrane helices. In the lower monomer, the  $\alpha$ -helices of the stromal and luminal loop regions are shown as ribbons. (1JB0.pdb file, Jordan et al., 2001). See Chapter 8, p 256–259.*

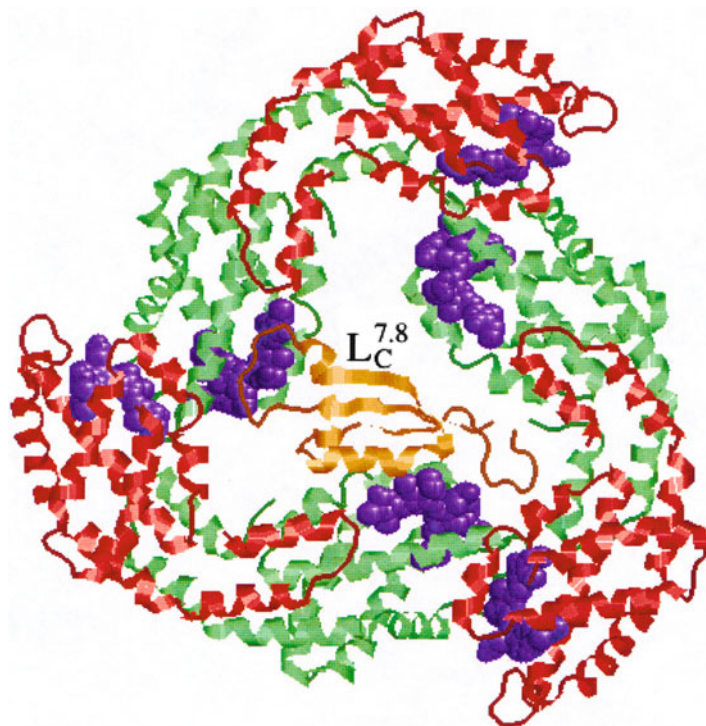


*Color Plate 7. The arrangement of the Chls in one monomer of Photosystem I. Only the Chls rings are shown for clarity. Top: view from the stromal side onto the membrane plane. Bottom: view along the membrane plane. See Chapter 8, p 261.*

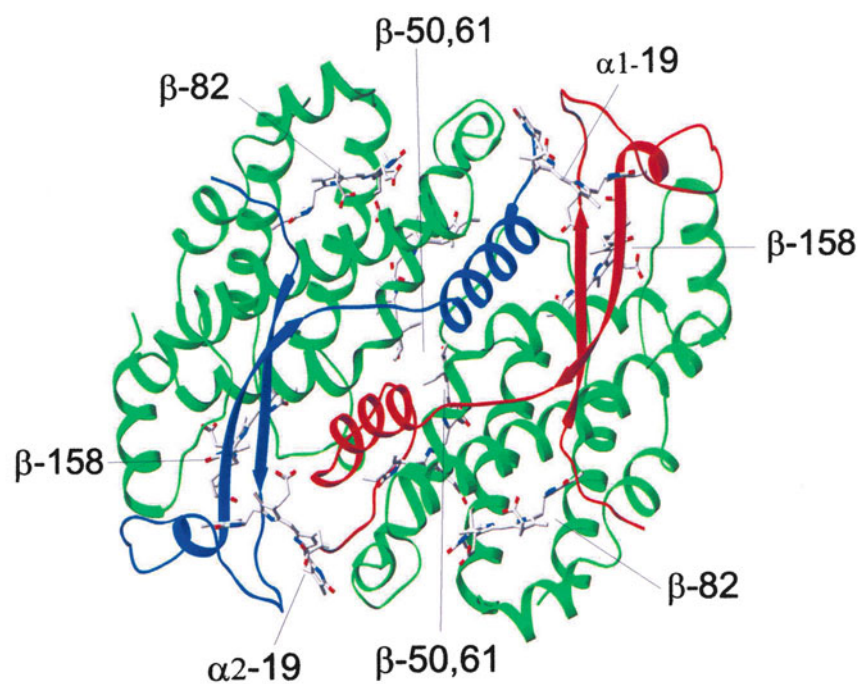




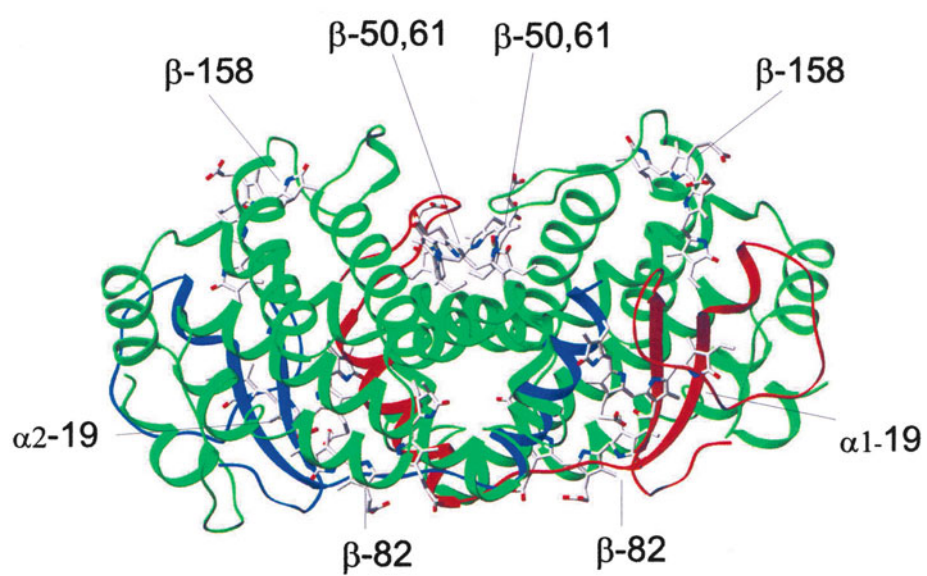
*Color Plate 8.* Crystal structures of three phycobiliproteins (APC, C-PC, and R-PE). These  $(\alpha\beta)_3$  trimers are drawn on the basis of the structure of APC (Brejc et al., 1995; 1ALL.PDB), C-PC (Düring et al., 1991; 1CPC.PDB), and R-PE (Chang et al., 1996; 1LIA.PDB). Each basic block, the  $(\alpha\beta)_3$  trimer, is shown from a viewpoint along the symmetry axis, and chromophores are shown in blue colored space-filling representation. APC has one  $\alpha$ -84 chromophore in each  $\alpha$ -subunit (red) and one  $\beta$ -84 chromophore in each  $\beta$ -subunit (green). In C-PC,  $\beta$ -155 chromophores are added compared to APC. In R-PE,  $\alpha$ -140 chromophores and  $\beta$ -50/ $\beta$ -61 chromophores are added compared to C-PC. See Chapter 9, pp 288, 293–297.



*Color Plate 9.* APC  $(\alpha\beta)_3$  including the linker polypeptide  $L_C^{7.8}$  (gold) in the cavity of the trimer. From PDB structure file 1B33.PDB (Reuter et al., 1999). The  $\alpha$ -subunits or the  $\beta$ -subunits of APC are shown as red or green ribbons, respectively, and the chromophores ( $\alpha$ -84 and  $\beta$ -84) as space-filling models (blue). The  $L_C^{7.8}$  linker polypeptide interacts directly with the two of the three  $\beta$ -84 chromophores (Reuter et al., 1999). See Chapter 9, pp 293–295.

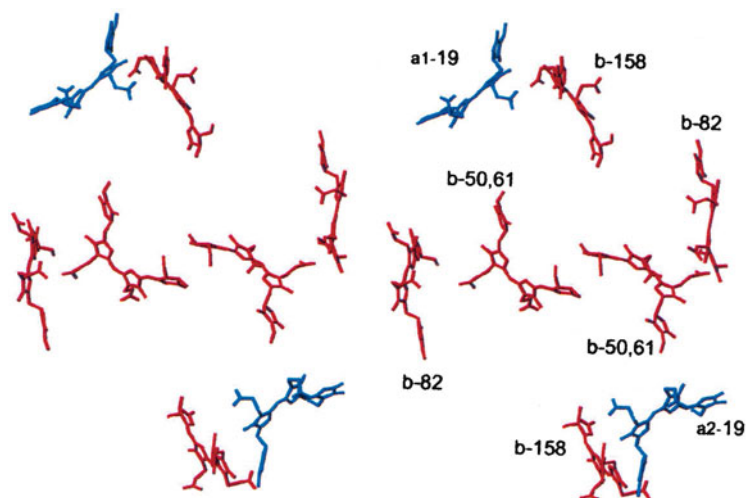


A

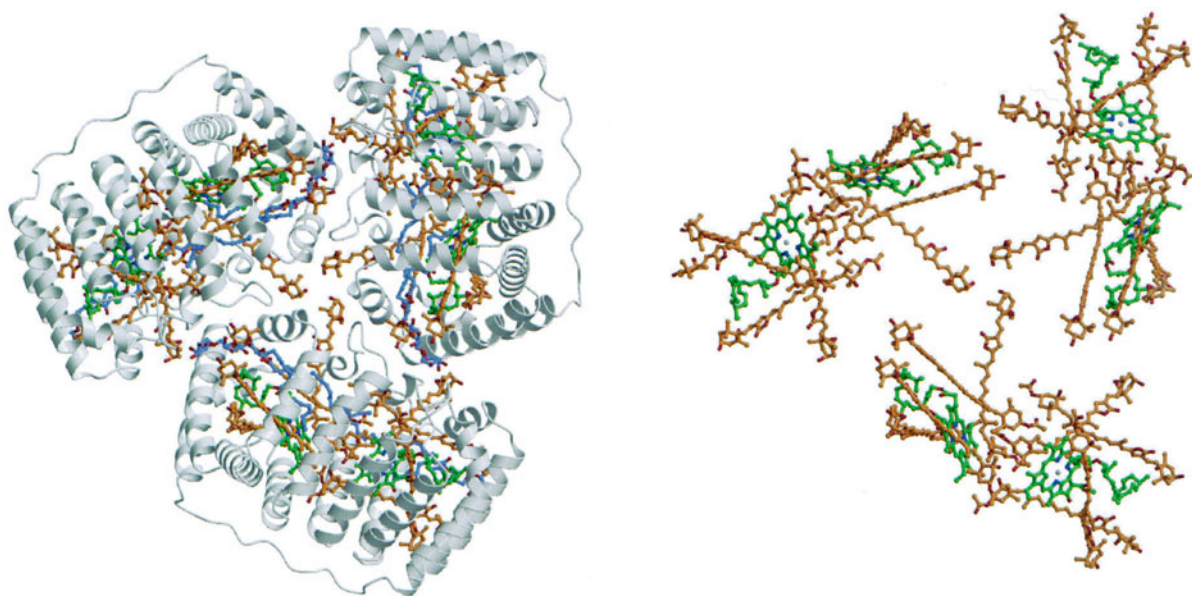


B

Color Plate 10. Ribbon diagrams of PE545 from *Rhodomonas* sp. A, from below; B, from the side. Green,  $\beta$ -subunits; red,  $\alpha$ -1 subunit; blue,  $\alpha$ -2 subunit. Numbers, chromophore-binding residues; white stick models, chromophores. See Chapter 11, pp. 334–336.



*Color Plate 11.* Stereogram of PE545 chromophores. a1–19, a2–19 (blue) are bound to the  $\alpha$ -subunits (see Color Plate 10); b, bound to  $\beta$ -subunits. . See Chapter 11, pp. 334–343.



*Color Plate 12.* Trimer of peridinin-Chl *a* protein (PCP). Left, protein shown as gray ribbons, enclosing chromophores. Right, chromophores only. Green, Chl *a*; orange, peridinin; blue, digalactosyl diglyceride. See Chapter 11, pp. 340–343.

# Chapter 1

## Photosynthetic Membranes and Their Light-Harvesting Antennas

Beverley R. Green\*

*Botany Dept., University of British Columbia, Vancouver, B.C. Canada V6T 1Z4*

Jan M. Anderson

*Photobioenergetics, Research School of Biological Sciences,  
Australian National University, GPO Box 475, Canberra ACT 2601, Australia*

William W. Parson

*Biochemistry Dept., Box 357350, University of Washington, Seattle, WA 98195-7350, U.S.A.*

Summary .....	2
I. Introduction .....	2
A. How Antennas Work .....	2
B. Molecular Environment .....	6
II. Photosynthetic Prokaryotes .....	6
A. The Five Groups of Photosynthetic Prokaryotes and Their Electron Transport Chains .....	6
B. Types of Antenna .....	8
C. The Prokaryotic Core Antennas and Reaction Centers .....	9
D. Green Bacteria: Distal and Extrinsic Antennas .....	9
1. The Chlorosome .....	9
2. The Fenna-Matthews-Olson (FMO) Protein .....	10
3. Photosynthetic Membrane Organization .....	10
E. Purple Bacteria: Core and Distal Antennas .....	11
1. LH1, LH2 and LH3: An Antenna Family .....	11
2. Membrane Organization .....	11
F. Cyanobacteria .....	11
1. Core Antennas and Phycobilisomes .....	12
2. Photosynthetic Membrane Organization .....	12
3. Exceptions to the Rule: Chl <i>b</i> in Prochlorophytes and Chl <i>d</i> in <i>Acaryochloris</i> .....	13
III. Chloroplasts of Photosynthetic Eukaryotes .....	14
A. Evolutionary Origin of Chloroplasts .....	14
1. Primary Endosymbiosis .....	14
2. Secondary Endosymbioses .....	16
B. Thylakoid Membrane Structure: Algae and Their LHCs .....	18
1. Rhodophyte Algae .....	19
2. Cryptophyte Algae .....	20
3. Heterokonts and Haptophytes .....	20
4. Dinoflagellates .....	20
5. Green Algae .....	20

---

\*Author for correspondence, email: brgreen@interchange.ubc.ca



C. Higher Plant Chloroplasts and Their Antennas .....	21
1. Granal Structure and Lateral Segregation .....	21
2. The LHC Superfamily .....	22
3. Acclimation and Grana .....	22
To be Continued.....	23
Acknowledgments .....	23
References .....	23

## Summary

Light-harvesting antennas are pigment-proteins that absorb light energy and transfer it to photosynthetic reaction centers. This chapter starts with a brief non-technical explanation of how antennas harvest light. The antennas of the five divisions of photosynthetic bacteria (including cyanobacteria) are introduced; the antennas are placed in the context of their photosynthetic membranes. The evolutionary origin of chloroplasts by primary and secondary endosymbiosis is explained. A brief description of the various algal groups is followed by a more detailed discussion of the higher plant chloroplast and the roles of the LHC superfamily antennas. Throughout, readers are directed to the relevant chapters in the book where detailed information can be found.

## I. Introduction

Photosynthetic organisms contain several distinct types of pigment-protein complexes that cooperate to achieve efficient capture of solar energy. The reaction centers provide specialized sites where an excited chlorophyll (Chl) or bacteriochlorophyll (BChl) dimer transfers an electron to a neighboring molecule, launching a series of secondary electron-transfer reactions that ultimately drive the reduction of CO<sub>2</sub> to carbohydrates. The movement of electrons is coupled to the generation of a H<sup>+</sup> electrochemical gradient across the photosynthetic membrane, and this gradient provides the energy to drive ATP synthesis and maintain other ionic gradients. Reaction centers (RCs) are remarkably efficient: at low light intensities, they transfer one electron to the acceptor and remove one electron from a secondary donor virtually every time they are excited (Wraight and Clayton, 1973). But even in bright sunlight the reactive

pair of Chls or BChls in an isolated reaction center would absorb a photon only a few times per second (Blankenship, 2002), and this rate would drop off severely in the dense shade of a rain forest or in the mud of a tidal salt flat. The primary role of the light-harvesting antenna complexes is to increase the rate of photosynthesis by absorbing light and transferring the excitation energy to the reaction centers.

A light-harvesting antenna consists of one or more chromophores, small molecules that absorb light, and the protein or proteins to which the chromophores are bound. Photosynthetic organisms use only three classes of chromophore: the chlorophylls and bacteriochlorophylls, the phycobilins, and the carotenoids (Fig. 1, Table 1). Their structures and biosynthetic pathways are described in Chapter 2 (Scheer). The chromophores are bound to specific proteins, most of which are members of seven major protein families: the core complex family, the protobacterial antenna complexes (LH1, LH2 and LH3), chlorosomes, the FMO protein, phycobilisomes, the LHC superfamily, and the preidinin-Chl *a* protein (Table 1).

### A. How Antennas Work

Although a variety of pigment-protein complexes serve as antennas in photosynthetic organisms, they all must meet several basic requirements. They must absorb visible or near infrared light strongly, and the excited states generated by this absorption must be

*Abbreviations:* BChl, Chl – bacteriochlorophyll, chlorophyll; CP43, CP47 – core antennas of PS II; D1, D2 – reaction center proteins of PS II; ER – endoplasmic reticulum; EST – expressed sequence tag, a cDNA sequence; FCP – fucoxanthin Chl *a/c* protein; FMO protein – Fenna-Matthews-Olson BChl *a* protein of green sulfur bacteria; IsiA – Chl *a* protein induced by Fe limitation, product of *isiA* gene, also called CP43'; LH1, LH2, LH3 – proteobacterial antennas; LHC – member of light-harvesting complex superfamily; NPQ – non-photochemical quenching; Pcb – prochlorophyte Chl *a/b* protein; PsaA, PsaB – PS I reaction center-core antenna proteins; PS I, PS II – Photosystem I, Photosystem II; RC – reaction center

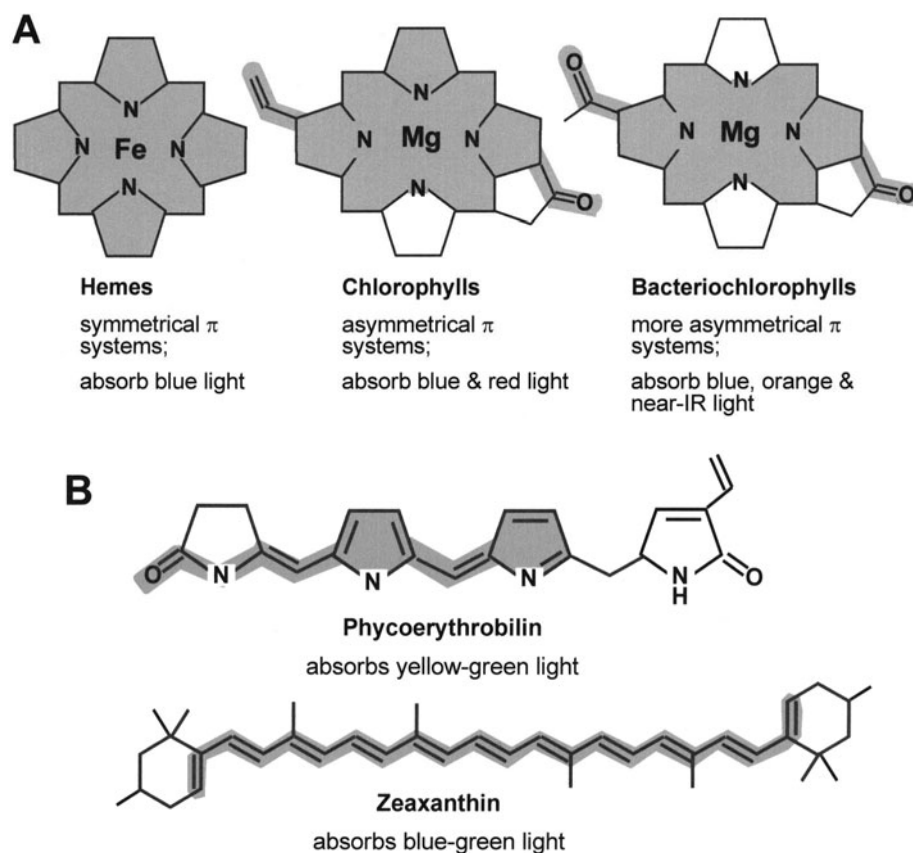


*Fig. 1.* Electronic structure of photosynthetic pigments. A. Hemes, chlorophylls and bacteriochlorophylls. The long-wavelength (Qy) absorption bands of chlorophylls and bacteriochlorophylls are shifted to longer wavelengths and increased in strength relative to the corresponding bands of symmetric porphyrins such as heme. The shading in the structural diagrams indicates the regions covered by  $\pi$ -electron systems. B. Phycobilins and carotenoids have extended, quasi-linear  $\pi$ -electron systems (shaded). These molecules absorb in the regions of the visible spectrum between the strong absorption bands of chlorophylls and bacteriochlorophylls, and are used as accessory antenna pigments. Carotenoids also play important roles in protecting against excessively strong light.

sufficiently long lived. They must be relatively stable molecules that can be packed together in a way that provides paths for excitations to migrate to the reaction centers. They also should have ways of deactivating potentially destructive sideproducts such as triplet states and singlet  $O_2$ . Some antennas also undergo structural modification to optimize their operation in response to large variations in the intensity or wavelength of the incident light.

Chlorophylls, bacteriochlorophylls and phycobilins lend themselves particularly well to being antennas. First, they absorb sunlight strongly. Chlorophyll *a* in solution has intense absorption bands in both the blue (430 nm) and red (660 nm) regions of the spectrum, chlorophyll *b* has corresponding bands peaking near 460 and 650 nm, and bacteriochlorophyll *a* has bands near 380 and 780 nm (Fig. 2). The

strengths of these bands can be expressed qualitatively in terms of the peak molar absorption coefficients ( $\epsilon$ ), which range from about  $5 \times 10^4 \text{ M}^{-1}\text{cm}^{-1}$  for the 650 nm band of chlorophyll *b* to almost  $10^5 \text{ M}^{-1}\text{cm}^{-1}$  for the 780 nm band of bacteriochlorophyll *a* (see Table 1 in Chapter 2, Scheer). For example, a 0.1 mM solution of bacteriochlorophyll *a* in a 1-cm cuvette would absorb about 99% of the energy in a beam of 770 nm light. A more meaningful analysis should consider the integrated area under the absorption band rather than just the height of the peak (Fig. 2), but these molecules are strong absorbers by almost any measure. In addition, because their excited states lie at relatively low energies, chlorophylls and bacteriochlorophylls can serve as acceptors for energy transferred from molecules that absorb at shorter wavelengths, such as carotenoids and phycobilins.

Table 1. Light-harvesting Antennas and Pigment Classes

Antenna Type	Pigment Class	Anoxygenic Prokaryotes	Oxygenic Prokaryotes	Eukaryotes (chloroplasts)
Core Complex family	BChl, Chl, carotenoids	Chlorobiaceae, Heliobacteriaceae	Cyanobacteria: PS I core complex PS II: CP47, CP43, IsiA Chl <i>a/b</i> antenna (prochlorophytes)	All photosynthetic eukaryotes: PS I core complex PS II: CP47, CP43
LH1, LH2, LH3	BChl, carotenoids	Purple proteobacteria, Chloroflexaceae		
Chlorosomes	BChl, carotenoids	Chlorobiaceae, Chloroflexaceae		
FMO (Fenna-Matthews-Olson BChl <i>a</i> protein)	BChl only	Chlorobiaceae		
Phycobilisomes	phycobilins only		Cyanobacteria: (except some prochlorophytes)	Rhodophytes, Cryptophytes
LHC superfamily	Chl, carotenoids		Cyanobacteria: one-helix proteins probably involved in photoprotection	Chlorophytes, plants: Chl <i>a/b</i> proteins Rhodophytes: Chl <i>a</i> proteins Heterokonts, Haptophytes, Cryptophytes, Dinoflagellates: Chl <i>a/c</i> proteins
Peridinin-Chl <i>a</i> protein	Chl, carotenoids			Dinoflagellates only

It is instructive to contrast the spectroscopic properties of chlorophyll and bacteriochlorophyll with those of symmetric porphyrins such as the heme derivatives of protoporphyrin IX that are found in hemoglobin, myoglobin and *c*-type cytochromes (Fig. 1). The long-wavelength absorption bands of the symmetric porphyrins are much weaker; porphyrins absorb blue light well but are essentially transparent to orange or red light. This qualitative difference in spectroscopic properties stems from the different shapes of the  $\pi$ -electron systems of the molecules (Gouterman, 1961). As shown in Fig. 1A, reduction of one or more of the pyrrole rings and addition of conjugated keto or vinyl groups makes the  $\pi$ -system progressively less symmetrical in the chlorophylls and bacteriochlorophylls. Though hemes are used extensively as electron carriers in both photosynthetic and nonphotosynthetic organisms, they do not form the basis of any known antenna system.

Along with having an unsuitable absorption spectrum, an antenna system built with hemes would have another serious problem. The excited states of hemes decay on picosecond or sub-picosecond time scales by internal processes involving the iron atom. An excited heme thus has little opportunity to transfer its energy to another molecule, and an excitation in a

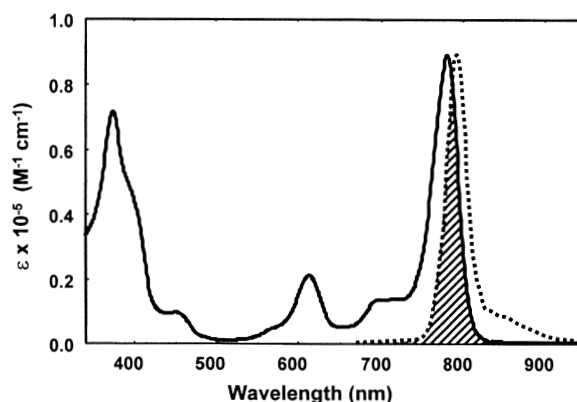


Fig. 2. Absorption (—) and fluorescence emission (---) spectra of bacteriochlorophyll *a* in pyridine (adapted from Becker et al. 1991). Cross-hatching indicates the region where the two spectra overlap.

cluster of hemes would be degraded rapidly to heat. Replacing the Fe by Mg greatly extends the lifetime of the excited state. An excited molecule of chlorophyll or bacteriochlorophyll can remain in the excited state for 10 ns or longer (a very long time in terms of energy transfer) before it relaxes back to its resting ('ground') state by emitting light as fluorescence or dissipating the energy in intra-molecular nuclear motions (heat). Energy transfer to



a neighboring molecule can compete easily with these relatively slow processes.

Although chlorophyll and bacteriochlorophyll absorb blue and red light well, they absorb green and yellow light only weakly (Fig. 2). Photosynthetic organisms use carotenoids or phycobilins to fill this gap. As illustrated in Fig. 1B, these molecules resemble chlorophylls and bacteriochlorophylls in having extended  $\pi$ -electron systems, but differ in having quasi-linear rather than cyclic structures. Their absorption spectra can be tuned over wide ranges by changing the number of conjugated double bonds: increasing the length of the  $\pi$ -electron system shifts the absorption to longer wavelengths. Depending on the length of the  $\pi$ -system, carotenoids can act either as antennas, transferring energy to other molecules, or as energy quenchers, accepting excess excitation energy and converting it harmlessly into heat. This flexibility of function allows carotenoids to play important photoprotective roles in both antennas and reaction centers. Protecting the photosynthetic apparatus from excess light energy appears to be a major function of some members of the LHC superfamily (Chapter 13, Krause and Jahns; Chapter 14, Huner et al.).

Transfer of energy from one molecule to another in photosynthetic antenna systems can occur by several different physical mechanisms depending on the arrangement of the donor and acceptor. In some cases, the pigments are so close together that they can reasonably be described as a single 'super-molecule' in which the excitation energy spreads almost instantaneously over the entire complex. When the pigments are farther apart, the excitation tends to be more localized at any given time and can be viewed as hopping randomly from site to site. The mechanism of energy transfer in this domain, termed resonance energy transfer or inductive resonance, was explained by T. Förster (1951, 1965), who showed how its rate depends on the intermolecular distance and orientation of the energy donor and acceptor. If the distance ( $r$ ) is large relative to the dimensions of the molecules themselves, the rate varies inversely with the sixth power of  $r$ . For two bacteriochlorophyll molecules with similar absorption spectra, the efficiency of energy transfer over a distance of 20 Å would be about 99.99%.

For molecules separated by a fixed distance, the rate of resonance energy transfer increases with the molar absorption coefficient of the energy acceptor. The strong absorption bands of bacteriochlorophyll and chlorophyll at long wavelengths thus are well

suited to rapid energy transfer. The rate also depends on the overlap of the fluorescence emission spectrum of the energy donor with the absorption spectrum of the acceptor (cross-hatched area in Fig. 2). This is partly a matter of conserving energy. The energy lost as the donor decays to the ground state must match the energy gained as the acceptor is excited. The requirement for energy matching does not mean that the donor actually fluoresces; energy transfer by actual emission and reabsorption would have a different dependence on the intermolecular distance and generally would be much less efficient. Rather, resonance energy transfer represents a quantum mechanical resonance between two states with the same energy, analogous to the resonance between the two valence-bond structures of benzene. In one state the energy donor is excited and the acceptor is in its ground state; in the other state the acceptor is excited and the donor has relaxed. Transitions between these two states are driven by interactions between the oscillating electron clouds on the two molecules, and it is these interactions that give rise to the characteristic dependence of the rate on  $r^{-6}$ . Chapter 3 (Parson and Nagarajan) discusses the physical basis of the phenomenon in more detail.

Because a portion of the electronic excitation energy can be degraded to heat as each excited molecule equilibrates with its surroundings, excitations tend to move to complexes whose excited states lie at progressively lower energies. Early studies by L. N. M. Duysens (1952) showed that when cell suspensions of the purple bacteria *Chromatium vinosum* or *Rhodospirillum rubrum* were excited by light of various wavelengths, the energy was used for photosynthesis only to the extent that it was transferred to bacteriochlorophyll-protein complexes that absorbed at the longest wavelengths. The 'action' spectrum for photosynthesis (a plot of the rate of photosynthesis as a function of the wavelength of the incident light) was essentially the same as the excitation spectrum for fluorescence from these complexes. In some organisms, the excited states of the reaction centers lie lower in energy than those of the antenna complexes and thus act as traps for the excitation energy. However, the electron-transfer reactions that occur in the reaction center may be so rapid that they trap the energy kinetically even if the excited state of the reaction center is somewhat higher in energy. Migration of excitons to the reaction centers often occurs on roughly the same time scale as the initial electron-transfer reactions, so that both processes influence the overall kinetics of trapping.

### B. Molecular Environment

All the antenna chromophores are bound to specific proteins that are either embedded in the photosynthetic membrane or associated with the membrane surface. Reaction center proteins are very hydrophobic and are always embedded in the lipid bilayer, which makes possible both the spatial separation of charges within the membrane and the development of an electrochemical potential across the membrane. The spatial organization of pigment-protein complexes within the bilayer plane affects the efficiency of energy transfer among antenna complexes, and between them and the reaction centers. We therefore need to consider membrane structure as well as the structure of the individual antennas in order to understand how photosynthetic systems work. The rest of this chapter will introduce the different antenna classes and discuss their arrangements in the photosynthetic membranes. How organisms respond to varying illumination conditions by regulating their antenna systems is discussed in the chapters of Part III.

Understanding of photosynthetic antenna systems has advanced dramatically on multiple fronts in the last few years. High-resolution crystal structures have been obtained for several major antenna

complexes, and studies by cryoelectron microscopy have yielded medium-level structures of additional complexes. Complexes from many different species of photosynthetic organisms have been purified and characterized biochemically, and a rapidly expanding body of information on their DNA sequences, protein structure and pigment compositions has provided insight into the relationships among the antenna systems of various species. New experimental techniques using short pulses from lasers have allowed kinetic studies with femtosecond ( $10^{-15}$  s) time resolution, and new techniques for site-directed mutagenesis have made it possible to explore how subtle changes in protein structure affect the energetics and dynamics of energy transfer. The chapters of Part II will discuss these topics in detail.

## II. Photosynthetic Prokaryotes

### A. The Five Groups of Photosynthetic Prokaryotes and Their Electron Transport Chains

Photosynthetic prokaryotes (including the cyanobacteria) belong to five distinct taxonomic groups that are not closely related to each other by any

Table 2. Divisions of photosynthetic prokaryotes

Group	Life-style	RC Type	Core Antenna (pigments)	Distal Antenna (pigments)	Extrinsic Antenna (pigments)
Heliobacteria	Obligate anaerobe	FeS	RC core (30 BChl <i>g</i> )	–	–
Green sulfur bacteria (Chlorobiaceae)	Obligate anaerobe	FeS	RC core (16 BChl <i>a</i> )	–	Chlorosomes (BChl <i>c,d,e</i> ) FMO (BChl <i>a</i> )
Green filamentous bacteria (Chloroflexaceae)	Facultative anaerobic phototroph	Q	LH1 (BChl <i>a</i> )	–	Chlorosomes (BChl <i>c</i> )
Purple bacteria (Proteobacteria)	Facultative anaerobic phototroph	Q	LH1 (36–38 BChl <i>a</i> or BChl <i>b</i> )	LH2, LH3 (BChl <i>a</i> or BChl <i>b</i> )	–
Cyanobacteria	Oxygenic photoautotroph	FeS (PS I)	PS I-RC core (80 Chl <i>a</i> )	–	Phycobilisomes (phycobilins)
		Q (PS II)	PS II:CP47, CP43 (30–40 Chl <i>a</i> ) <sup>†</sup>	Pcbs (Chl <i>a/b</i> ) (only in prochlorophytes)	(No phycobilisomes but phycoerythrin in some prochlorophytes)

Data for heliobacteria from Neerken and Ames (2001); for green sulfur bacteria from Hauska et al. (2001). See also Chapters 5 (Robert et al.), 7 (van Amerongen and Dekker) and 8 (Fromme et al.) <sup>†</sup>*Acaryochloris* has mostly Chl *d* instead of Chl *a*.

criterion (Stackebrandt et al. 1996, Gupta et al., 1999). The heliobacteria and green sulfur bacteria are obligate anaerobes with a single photosynthetic RC of the FeS-type, like the PS I RC of cyanobacteria and chloroplasts (Table 2, Fig. 3). However, the heliobacteria (e.g. *Heliobacterium*, *Heliobacillus*) belong to the 'low G+C' group of Gram positive bacteria (Madigan and Ormerod, 1995) whereas the green sulfur bacteria (Chlorobiaceae) are Gram negative and somewhat related to the Chlamydia-Cytophaga group (Stackebrandt et al., 1996). The green sulfur bacteria can use hydrogen sulfide or thiosulfate as an electron donor with  $\text{NADP}^+$  as the ultimate electron acceptor (Fig. 3), whereas the heliobacteria use only reduced carbon compounds as donors.

The purple bacteria and green filamentous bacteria (Chloroflexaceae) have a single RC of the quinone-type like Photosystem II (PS II). Light-driven electron flow is predominantly cyclic in the purple bacteria (Fig. 3). The electrochemical gradient produced in this process is used to drive electrons uphill from a variety of exogenous electron donors (e.g.  $\text{H}_2$ ,  $\text{H}_2\text{S}$ ,  $\text{S}_2\text{O}_3^{2-}$ , or reduced carbon compounds, depending on

the species) to reduce co-enzymes for biosynthesis. Members of both groups synthesize BChl and many of them photosynthesize only under anaerobic conditions. They can all grow heterotrophically in the presence of a suitable reduced carbon source and  $\text{O}_2$ . However, these two groups are not closely related to each other either. The purple bacteria belong to the Proteobacteria (a widespread and metabolically diverse group), whereas the green filamentous bacteria are an early branching lineage on 16S and 23S rRNA trees (Ludwig and Schleifer, 1994; Stackebrandt et al., 1996; Pace, 1997).

The fifth division of photosynthetic prokaryotes, the aerobic cyanobacteria, are unique among the prokaryotes in having a linear electron transport chain with both FeS (PS I) and Q (PS II) types of RC. Water is the initial electron donor, with the result that molecular oxygen is produced, so this process is referred to as oxygenic photosynthesis. The many similarities between cyanobacterial and chloroplast photosynthetic electron transport chains provide strong support for the endosymbiotic origin of all chloroplasts from a cyanobacterial ancestor (see below). Much of the information we have about

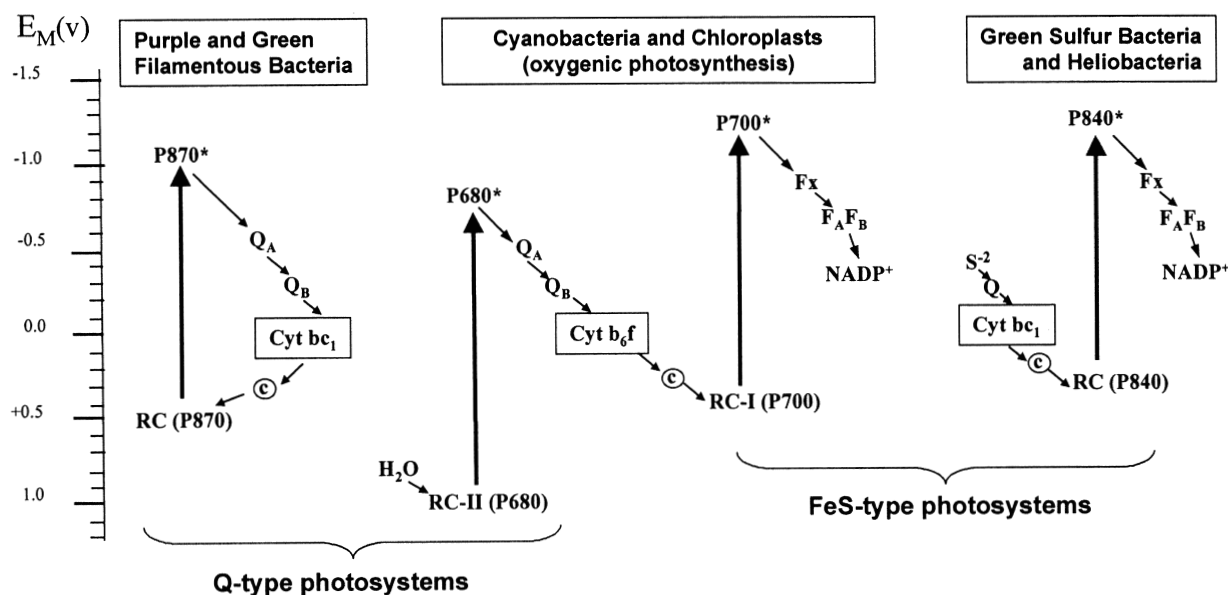


Fig. 3. Photosynthetic electron transport chains of photosynthetic bacteria and chloroplasts. RC, reaction center; Fx,  $F_A F_B$ , Fe-S centers of FeS-type photosystems,  $Q_A$ ,  $Q_B$ , primary and secondary quinones of Q-type photosystems,  $E_M$ , standard redox potential, ©, mobile electron carrier, usually *c*-type cytochrome or small copper protein. Note that no cytochrome  $bc_1$  complex has been found in green filamentous bacteria and cyclic electron flow has not been demonstrated. Heliobacteria use reduced organics rather than reduced sulfur as electron donors, and their terminal electron acceptors are not well understood.

eukaryotic photosynthesis comes from studies on cyanobacteria, as can be seen in the chapters on Photosystem II (Chapter 7, Dekker and van Amerongen) and Photosystem I (Chapter 8, Fromme et al.). The cyanobacteria are clearly very separate from the four divisions of anoxygenic bacteria on the basis of their light-harvesting antennas (Table 2). The Core Complex family is the only one found in both groups, since it is part of the PS I RC in cyanobacteria/chloroplasts and the PS I-like RC of the Chlorobiaceae and the Heliobacteria (Fig. 4).

All photosynthetic electron transport chains, with the exception of the Chloroflexaceae, have a large membrane-intrinsic cytochrome complex consisting of a two-heme cytochrome *b*, a Rieske Fe-S protein, a *c*-type cytochrome and several minor proteins. This complex receives electrons from a reaction center via quinones, which diffuse in the lipid bilayer. The passage of electrons through the intrinsic cytochrome complex is coupled to the transport of protons across the membrane, generating a proton-motive force. The cytochrome complexes are similar to those found in mitochondria and in non-photosynthetic eubacteria and archaebacteria. Because of their widespread distribution, it has been proposed that the cytochrome complex originated prior to the evolution of

photosynthetic reaction centers (Schütz et al., 2000). In many photosynthetic prokaryotes, the respiratory and photosynthetic electron transport chains share components and may co-exist in the same region of the membrane bilayer.

### B. Types of Antenna

Antennas are divided into three categories in Table 2. Core antennas are those associated very closely with the reaction centers. The FeS-type reaction center proteins are larger than the Q-type RC proteins and bind antenna Chls or BChls as well as the pigments involved in charge separation. In contrast, the Q-type RC proteins bind only the chromophores involved in charge separation; their core antenna B(Chl)s are bound by separate polypeptides (Fig. 4). The purple and green filamentous bacteria have rings of small single-helix polypeptides, with each polypeptide binding one or two BChls (LH1). Cyanobacterial PS II has a completely different core antenna: two relatively large Chl *a*-binding proteins, CP47 and CP43, associated with each RC.

The other membrane-intrinsic antennas, LH2 and LH3 in purple bacteria and the unique Chl *a/b* antennas of the prochlorophytes (cyanobacteria), are

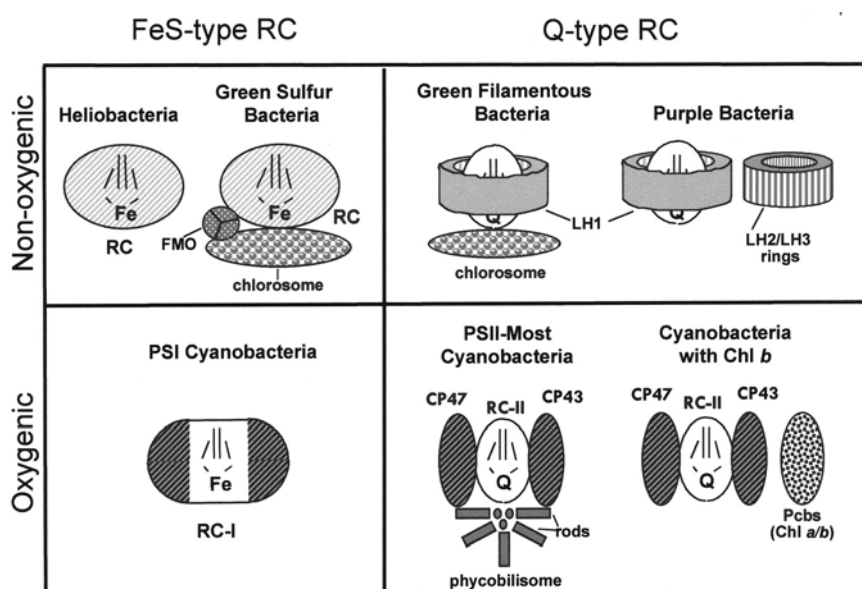


Fig. 4. Prokaryotic light-harvesting antennas. RC-antenna complexes of heliobacteria and green sulfur bacteria are hatched more lightly than cyanobacterial PS I to indicate that they bind fewer pigment molecules (Table 2). PS I is oversimplified: some Chl *a* are bound by the RC part of the core complex (Schubert et al., 1998). LH1, LH2 and LH3 of the purple bacteria are rings of 8 to 16 dimeric subunits; it is assumed that LH1 of green filamentous bacteria also forms a ring around the RC. The figures are oriented with the cytoplasmic surface on the lower side and periplasmic or luminal surface on the upper side.

referred to as distal antennas. Their proteins belong to the same families as the core antennas of their respective groups, which indicates that they are the result of ancient gene duplications. The many Chl *a/b* and Chl *a/c* proteins of eukaryote chloroplasts (Table 1) would be considered distal antennas, and are discussed in Section IV. In most species, the ratio of distal antennas to RCs is under environmental control. The distal antennas are more highly expressed under low-light conditions than under high-light conditions, in contrast to the core antennas, which generally occur in a fixed ratio to RCs.

The extrinsic antennas are those associated with the surface of the photosynthetic membrane (Fig. 4, Table 2). The Fenna-Mathews-Olson protein (FMO) is unique to the green sulfur bacteria, whereas chlorosomes are found in both groups of 'green' bacteria. These components are discussed in detail in Chapter 6 (Blankenship and Matsuura). The phycobilisomes are found in cyanobacteria and some of their eukaryotic descendants (chloroplasts). They will be introduced below and discussed in more detail in Chapter 9 (Mimuro and Kikuchi) and Chapter 10 (Gantt et al.). Their regulation in response to light conditions and nutritional status is covered in Chapter 17 (Grossman et al.).

### *C. The Prokaryotic Core Antennas and Reaction Centers*

The reaction center core complexes of green sulfur bacteria and heliobacteria have long been known to resemble PS I of cyanobacteria and chloroplast (Nitschke and Rutherford, 1991). The PS I core complex has two related proteins (PsaA and PsaB), each of which has 11 transmembrane helices. The inner five helices of each polypeptide provide the 'cage' for the RC chromophores, while the outer six helices bind 79 antenna Chls (Chapter 8, Fromme et al.). The FeS-type RCs of the heliobacteria and green sulfur bacteria are likely to be organized the same way (Chapter 6, Blankenship and Matsuura; Hauschka et al., 2001; Fyfe et al., 2002). However, only one gene encodes the RC polypeptide in these two photosystems, so the RC core complex is a homodimer rather than a heterodimer. Furthermore, a much smaller number of BChls is associated with heliobacterial and green sulfur photosystems than with PS I (Table 2).

The heliobacteria are unique in having only a core antenna. They do not have their own chapter in this

volume, but several excellent reviews are available elsewhere (Amesz, 1995a,b; Madigan and Ormerod, 1995; Neerken and Amesz, 2001). Earlier work including descriptions of their membrane structure can be found in Sprague and Varga (1986) and Fuller et al. (1985).

In cyanobacterial (and chloroplast) PS II, each of the 11-helix core proteins (PsaA and PsaB) appears to have split into a 5-helix protein (D1 and D2, respectively) and a 6-helix protein (PsbB, PsbC). D1 and D2 form the 'cage' around the RC chromophores and do not bind any additional antenna Chls, whereas PsbB and PsbC bind approximately 14 Chl *a* each to form the Chl-protein complexes CP47 and CP43 (Fig. 4). Approximately 14 Chl *a* are associated with each complex. Although there is minimal sequence similarity between CP47/CP43 and the N-terminal halves of PsaA/PsaB, the number of transmembrane helices and the structural similarities suggest that the two 11-helix proteins PsaA and PsaB that make up the Chl-protein complex CPI are evolutionarily related to the 5-helix D1/D2 plus the 6-helix PsbB/PsbC. (Chapter 4, Green; Chapter 8, Fromme et al.). There is no similarity of sequence or structure between the LH1 antenna proteins of anoxygenic prokaryotes and the PS II proteins CP47 and CP43.

### *D. Green Bacteria: Distal and Extrinsic Antennas*

#### *1. The Chlorosome*

Two unrelated groups of prokaryotes, the green sulfur bacteria (Chlorobiaceae) and the green filamentous bacteria (Chloroflexaceae, also called 'green non-sulfur' bacteria), have large cigar-shaped antenna complexes (chlorosomes) appressed to the inner surface of the plasma membrane (Chapter 6, Blankenship and Matsuura). This is the distinguishing feature of the two kinds of green bacteria and the only thing that unites them. The fact that chlorosomes are found in two such unrelated groups of bacteria suggests that one group must have acquired them from the other by lateral gene transfer (Olson, 1998). The chlorosome's structure is still incompletely understood, probably because it is largely made up of BChl, with a relatively small contribution from protein. In both groups, the BChls (BChls *c*, *d* or *e*) appear to be organized in rod-shaped aggregates surrounded by a lipid monolayer that forms the chlorosome envelope (Staehelin et al., 1978; 1980; Sprague and Varga, 1986; Olson, 1998; Chapter 6,

Blankenship and Matsuura). In contrast to all the other types of light-harvesting antenna, most of the proteins are not involved in binding BChl but rather are components of the chlorosome envelope (Vassilieva et al., 2000, 2002). The size and BChl content of chlorosomes is regulated by light and oxygen in the Chloroflexaceae, and to a lesser extent by light in the Chlorobiaceae (Oelze and Golecki, 1995). It appears that the chlorosome envelope is present even when *Chloroflexus* is growing under non-photosynthetic (aerobic) conditions, and fills with BChl under conditions that induce the photosynthetic apparatus (Oelze and Golecki, 1995; Foidl et al., 1998). Some recent work suggests that *Chlorobium* chlorosomes also act as bags that can be filled with variable amounts of BChl *c* (Vassilieva, 2002).

Chlorosomes of both groups of green photosynthetic bacteria can vary considerably in size and BChl content depending on the particular species (Sprague and Varga, 1986; Oelze and Golecki, 1995; Martinez-Planells et al., 2002). The chlorosomes of Chloroflexaceae are generally smaller than those of the Chlorobiaceae: roughly  $100 \times 30 \times 15$  nm, versus  $150 \times 60 \times 25$  nm (Sprague and Varga, 1986; Oelze and Golecki, 1995; Olson, 1998). However, measurements by atomic force microscopy suggest these measurements are underestimates (Martinez-Planells et al., 2002). Olson (1998) estimated 100–200 chlorosome BChls/RC in *Chloroflexus* and 1000–2000 BChls/RC in green sulfur bacteria. Although the exact number of BChls per chlorosome is debatable (Martinez-Planells et al., 2002), it is clear that the chlorosomes increase the total size of the light-harvesting antenna system by several orders of magnitude in both divisions of green bacteria.

The chlorosome has a baseplate that appears as an ordered array of small, tightly packed particles (Staehelin et al., 1978, 1980; Oelze and Golecki, 1995). The baseplate binds the small amount of BChl *a* found in chlorosomes, and has a characteristic absorption maximum at 795 nm (Blankenship et al., 1995). It is believed to act as intermediate in transfer of excitation energy from the BChl rods to the RCs (Olson, 1998; Chapter 6, Blankenship and Matsuura).

## 2. The Fenna-Matthews-Olson (FMO) Protein

The Fenna-Matthews-Olson protein is found only in the green sulfur bacteria. It consists of trimeric units, each composed of 7 BChls wrapped in a polypeptide

beta barrel. There is no carotenoid associated with this complex. Because it is a soluble protein, it was the first chlorophyll-protein to be crystallized and have its structure determined to high resolution (Matthews et al., 1979). However, the structure of the FMO protein turned out to be unique, so it did not provide any insights into the structures of other Chl-proteins. Scanning transmission electron microscopy of FMO-RC complexes suggests that two FMO trimers are attached to each RC core (Rémigy et al., 2002). It is still not clear how much of the energy absorbed by the chlorosome pigments is transferred to the RC via the FMO protein (Chapter 6, Blankenship and Matsuura).

## 3. Photosynthetic Membrane Organization

The photosynthetic electron transport chains of Chlorobiaceae, Chloroflexaceae and heliobacteria are located in the cell membranes, which lack the elaborate invaginations seen in purple bacteria. This means that there is no lateral segregation of photosynthetic complexes from other membrane-bound enzymes such as dehydrogenases. The cell membranes of *Heliobacterium chlorum* are packed with particles, consistent with the high (70%) protein content of the membranes (Fuller et al., 1985; Sprague and Varga, 1986).

Ultrastructural studies on the green bacteria have concentrated on the chlorosomes and their mode of attachment to the membrane. Readers are referred to the excellent review by Oelze and Golecki (1995) for both scanning and transmission electron micrographs; earlier work was reviewed by Sprague and Varga (1986). There is still some uncertainty about the location of the FMO protein in green sulfur bacteria. Trimers of the FMO protein are frequently modeled as forming a layer between the chlorosome baseplate and the RC (Olson, 1998; Vassilieva et al., 2000), or partly embedded in the lipid bilayer beside the RC with chlorosomes attached (Li et al., 1997; Chapter 6, Blankenship and Matsuura). The fact that FMO-RC complexes can be isolated in an active state supports the idea that they are in direct contact in vivo (Rémigy et al., 2002). The spatial relationship of baseplate, chlorosome and FMO protein to the cell membrane should be re-examined with samples prepared by the new high-pressure freezing technology.

The Chloroflexaceae do not have the FMO protein, and each of their chlorosomes appears to be in direct contact with a number of RCs. In addition, each RC



is accompanied by a membrane-intrinsic light-harvesting complex that is believed to be similar to LH1 of purple bacteria based on protein sequence similarity, although there is no direct evidence that it forms a ring around the RC (Chapter 6, Blankenship and Matsuura). Spectroscopically, this complex is more similar to purple bacterial LH2 in having two absorption maxima (at 808 and 865 nm), which implies that it probably contains three BChls per polypeptide dimer (see below). The spatial relationship between the chlorosomes and the LH1/2 complexes in green filamentous bacteria is unknown.

### *E. Purple Bacteria: Core and Distal Antennas*

#### *1. LH1, LH2 and LH3: An Antenna Family*

The antennas of purple bacteria are the best understood of all the light-harvesting antennas. The purple bacteria are easy to cultivate and are facultatively photosynthetic, which means that the development of the photosynthetic apparatus under anaerobic conditions can be studied and mutant strains can be preserved. A new era in the study of membrane proteins began with the first successful X-ray crystal structure of a membrane protein complex, that of the *Rhodospseudomonas viridis* RC (Deisenhofer et al., 1985). High-resolution structures were later obtained for several of the antenna complexes (McDermott et al., 1995; Koepke et al., 1996; McLuskey et al., 2001). This information has made it possible to undertake sophisticated structure-function studies employing targeted mutagenesis and in vitro reconstitution (Chapter 5, Robert et al.).

The repeating unit of the LH1 core antenna is a dimer of two small polypeptides,  $\alpha$  and  $\beta$ , each having one membrane-spanning helix and binding one BChl. Each pair has an associated carotenoid molecule that participates in energy transfer. The antenna complex probably consists of a ring of 12 to 16  $\alpha/\beta$  pairs that partly or completely surrounds the RC. The 24 to 32 BChls are oriented in a very regular array with their planes perpendicular to the membrane plane and close enough to their neighbors to make energy transfer among them very efficient (Chapter 5, Robert et al.).

The distal antennas (LH2, LH3) are composed of rings of  $\alpha$  and  $\beta$  polypeptides whose sequences are related to those of the LH1  $\alpha$  and  $\beta$  polypeptides. In contrast to LH1, however, the  $\alpha/\beta$  dimer binds a third BChl, oriented parallel rather than perpendicular to

the membrane plane. These complexes form rings of 8 or 9 dimers containing a total of 24 to 27 BChls. Their absorption maxima are at shorter wavelengths than those of LH1, facilitating a 'funnel' type of excitation transfer. LH2 (B800–850) has absorption peaks at 800 and 850 nm, and LH3 (B800–820) at 800 and 820 nm. The LH2 and LH3 rings are believed to abut the RC-LH1 complex and transfer energy to the RC via LH1 (Color Plate 3; Chapter 5, Robert et al.).

#### *2. Membrane Organization*

In contrast to the green bacteria and heliobacteria, purple bacteria grown in the light under anaerobic conditions develop extensive intracellular membranes derived from and continuous with the cell membrane (reviewed in Drews and Golecki, 1995). These membranes can be isolated as sealed vesicles (chromatophores). Depending on the species and the growth conditions, freeze-fracture studies show several size classes of intramembrane particles. In earlier studies it was suggested that particles of about 9 nm were RCs without associated antennas and particles of 10–12 nm were RCs surrounded by a ring of LH1; the acquisition of LH2 was correlated with an increase in slightly larger particles, which were interpreted as RC-LH1 surrounded by an LH2 ring. However, it now seems clear that LH2 consists of rings that are separate from the RC-LH1 complex (Chapter 5, Robert et al.).

There is still lively debate over the supramolecular organization of LH1-RC and how this complex might be associated with the cytochrome  $bc_1$  complex (Vermeiglio and Joliot, 1999, 2002; Crofts, 2000; Frese et al., 2000). To complicate the situation, there appear to be significant inter-specific differences. It would be instructive to re-evaluate the older electron microscopic data in the light of current ideas about the structure of these macrocomplexes.

### *F. Cyanobacteria*

There is now convincing evidence that all chloroplasts are the descendants of a primitive cyanobacterium that established a permanent endosymbiotic relationship with a non-photosynthetic eukaryotic host (see Section III). This concept drives and illuminates much of the current research on cyanobacterial photosynthesis. Many aspects of this research were covered in the first volume of this



series, *Molecular Biology of Cyanobacteria* (Bryant, 1995). The contributions of cyanobacteria to the structural elucidation of photosystems I and II are covered in Chapters 7 (van Amerongen and Dekker) and 8 (Fromme et al.) of this book; cyanobacterial phycobilisomes are discussed in detail in Chapter 9 (Mimuro and Kikuchi).

### 1. Core Antennas and Phycobilisomes

Cyanobacteria are the only obligately aerobic group of photosynthetic prokaryotes. They are unique in having two photosystems organized in a linear electron transport chain, where electrons are extracted from water by PS II and donated to ferredoxin, NADP<sup>+</sup> or other acceptors after a second excitation by PS I (Fig. 3). They are also distinguished by the fact that they do not make BChls. Instead, they use mainly Chl *a*, with the exception of *Acaryochloris marina*, which utilizes Chl *d* (reviewed by Akiyama et al., 2002). The core antennas of PS I carry a larger number of light-harvesting pigments than the FeS-type RC-antennas of the anaerobic bacteria (Table 2). The core antennas of PS II (CP47, CP43) appear to be structurally (and probably evolutionarily) related to the 'built-in' antenna part of the PS I RC proteins PsaA and PsaB (Schubert et al., 1998; Zouni et al., 2001; Kamiya and Shen, 2003).

In addition to the core antennas, cyanobacteria have complex macromolecular structures called phycobilisomes attached to the cytoplasmic surface of the photosynthetic membranes (Fig. 4). The phycobilisome is the only light-harvesting antenna to utilize linear tetrapyrroles, the phycobilins, as chromophores. The phycobilin-binding proteins are assembled into hexameric rings, which are stacked on each other to form cylindrical rods (Fig. 4; Chapter 9, Mimuro and Kikuchi). The rods, made up of phycocyanin and phycoerythrin, are linked to core cylinders of allophycocyanin. These cylinders are in turn associated with the photosynthetic membrane, where they are bound to PS II and transfer most of their energy to it. Because the energy of the excited chromophores decreases in the order phycoerythrin > phycocyanin > allophycocyanin > PS II reaction center, a cascade of energy flows from the outermost phycoerythrin units into the PS II reaction centers. The structure and function of cyanobacterial phycobilisomes are discussed in detail in Chapter 9 (Mamoru and Kikuchi), and in earlier reviews by Sidler (1995), Gantt (1995) and MacColl (1998).

Regulation of phycobilisome structure and pigment content at the molecular level is covered in Chapter 17 (Grossman et al.).

Phycobilisomes and the FMO protein of green sulfur bacteria are the only antennas that do not contain carotenoids. It is generally accepted that carotenoids are essential for protecting other light-absorbing molecules from the deleterious side-effects of radiation. Whether the lack of carotenoids in these two types of antenna has something to do with their being extrinsic to the membrane is an open question. The only other 'soluble' antenna is the peridinin-Chl *a* protein of dinoflagellates. In this antenna, which is located in the thylakoid lumen, the carotenoids are the main antenna molecules and the Chl serves to transfer energy to other antennas or to the reaction centers (Chapter 14, Macpherson and Hiller).

### 2. Photosynthetic Membrane Organization

The photosynthetic membranes of cyanobacteria are usually visualized as single flattened membrane sacs (thylakoid membranes) lying in the cytoplasm of the cell. The membranes are not appressed to each other because their outside surfaces are covered with phycobilisomes. The number and arrangement of the membranes are species-specific and dependent on physiological conditions (Staehelin, 1986; Olive et al., 1997). In contrast to the chromatophores of purple bacteria, cyanobacterial thylakoids may not be physically connected to the plasma membrane, or connections may be rare. This question is not settled (Gantt, 1995; Mullineaux, 1999; Zak et al., 2001). Some but not all of the core proteins of the photosystems are found in purified plasma membranes of *Synechocystis* sp. PCC 6803, suggesting that initial stages of assembly occur in the plasma membrane, not the thylakoid membranes (Zak et al., 2001). This could be explained if there are dynamic (temporary) connections between the two membrane systems, or if there is vesicular transport between them, something that has not yet been reported in prokaryotes.

Whereas completely assembled photosystems are found only in the thylakoid membranes, functioning respiratory complexes are found in both cytoplasmic and thylakoid membranes (Gantt, 1995). This means that there is no segregation of O<sub>2</sub>-producing and O<sub>2</sub>-utilizing reactions in the thylakoid membranes. The 'primitive' cyanobacterium *Gloeobacter* does not have thylakoids, but carries out both photosynthesis

and respiration in the plasma membrane (Guglielmi et al., 1981).

Since there is no surface contact between thylakoids in cyanobacteria, they do not form grana as do higher plant thylakoids, and there is no lateral segregation of the two photosystems. However, there does appear to be a mechanism for regulating the relative amount of excitation energy delivered to PS II versus PS I (reviewed by Fujita et al., 1995; van Thor et al., 1998; Mullineaux, 1999; Li et al., 2001). PS I units, with 80–90 antenna Chls each, greatly outnumber PS II units. Phycobilisomes, with many more chromophores, appear to transfer most of their absorbed energy to PS II. However, there is evidence that some of this energy is transferred to PS I, and that the amount transferred is increased in a ‘state transition’ after illumination by light preferentially absorbed by PS II. Just how this transfer occurs is unclear (Fujita et al., 1995; Olive et al., 1997; Mullineaux, 1999; Li et al., 2001). It could involve direct transfer from PS II to PS I (requiring that the distance between the two photosystems can change) or movement of the phycobilisome itself from PS II to PS I. Alternatively, if the phycobilisome detached from PS II without movement to PS I, it would decrease the efficiency of energy transfer to PS II and give the appearance of a relative increase in the amount of energy reaching PS I. Phycobilisomes evidently are attached to PS II in some way, but the nature of the attachment is not clear (Gantt, 1995; Bald et al., 1996; Mullineaux, 1999; Sarcina et al., 2001). Measurements of fluorescence recovery after photobleaching showed that phycobilisomes diffuse in the plane of the membrane at an unexpectedly high rate, whereas PS II is stationary on the same time scale (Sarcina et al., 2001). This would be consistent with either detachment or movement of the PBS. However, freeze-fracture studies support movement of PS II units in the plane of the membrane (Olive et al., 1997).

### 3. Exceptions to the Rule: Chl *b* in *Prochlorophytes* and Chl *d* in *Acaryochloris*

The prochlorophytes are a heterogeneous group of cyanobacteria distinguished from other cyanobacteria by having a Chl *a/b* light-harvesting antenna and no phycobilisomes, although some strains do have small amounts of phycobiliproteins (Matthijs et al., 1995; Partensky et al., 1999; Ting et al., 2002). The three known genera of prochlorophytes, *Prochloron*,

*Prochlorothrix* and *Prochlorococcus*, occupy very different habitats, have different pigment ratios, and are not related to each other on 16S rRNA or protein trees (Turner, 1997; Urbach et al., 1998; Turner et al., 1999). However, the genes encoding chlorophyllide *a* oxygenase, the enzyme that converts chlorophyllide *a* to chlorophyllide *b*, do appear to be related, suggesting either common descent or lateral gene transfer (Tomitani et al., 1999; Chapter 4, Green).

The prochlorophyte Chl *a/b* polypeptides (Pcbs) are not related to the Chl *a/b* proteins of plants and green algae, but are part of the PS II Core Complex family (Table 1); i.e., they are related to CP43, and more distantly to CP47 (LaRoche et al., 1996; van der Staay et al., 1998; Chapter 4, Green). The *Prochlorococcus* antenna binds divinyl Chl *a* (Chl *a*<sub>2</sub>) and divinyl Chl *b* (Chl *b*<sub>2</sub>) rather than Chl *a* and *b*, and pigment ratios depend on the ecotype (Partensky et al., 1999). In a low-light-adapted strain of *Prochlorococcus*, 18 Pcb antenna proteins form a ring around PS I, approximately doubling the antenna size (Bibby et al., 2001a). The Pcb icon in Fig. 4 is placed next to CP43 to show its relationship with CP43, but whether Pcbs can be associated with both PS II and PS I, and whether their location depends on light and nutrient conditions remain to be determined.

The prochlorophyte Pcb proteins are closely related to another member of the Core Complex family, the Chl *a*-binding IsiA protein (sometimes referred to as CP43'), which is synthesized in all cyanobacteria in response to Fe deprivation and the subsequent down-regulation of phycobilisomes and Chl *a*. CP43' was originally believed to be associated with PS II and a number of possible roles were proposed (reviewed in Burnap et al., 1993; Falk et al., 1995), including acting as a nonradiative energy dissipater (Park et al., 1999; Sandström et al., 2002). However, it has recently been shown to form a ring with 18-fold rotational symmetry around PS I (Bibby et al., 2001b,c; Boekema et al., 2001a) and to increase the PS I antenna size by a factor of two (Andrizhiyevskaya et al., 2002). The IsiA-PS I trimer complex is the source of the increased 685 nm fluorescence emission usually attributed to the PS II antenna (Sandström et al., 2001, 2002). The evolution of this family is discussed in more detail in Chapter 4 (Green).

*Acaryochloris marina* is an unusual cyanobacterium that contains mostly Chl *d*, with only about 3% Chl *a* (Miyashita et al., 1996; Boichenko et al., 2000; Akiyama et al., 2002). Photosystem I appears to contain only Chl *d*, and its special pair

absorbs at 740 rather than 700 nm (Hu et al., 1998; Boichenko et al., 2000). Four Chl *a* and two pheophytin *a* molecules probably are part of the PS II reaction center (Boichenko et al., 2000; Akiyama et al., 2002). *A. marina* has a membrane-intrinsic light-harvesting antenna with a polypeptide of 34–35 kDa that may bind some Chl *a* as well as Chl *d* (Chen et al., 2002). Like the prochlorophytes, it does not have phycobilisomes but instead has short rods made of phycocyanin or a mixture of phycocyanin and allophycocyanin, which transfer energy to PS II (Marquardt et al., 1997; Hu et al., 1999).

### III. Chloroplasts of Photosynthetic Eukaryotes

#### A. Evolutionary Origin of Chloroplasts

##### 1. Primary Endosymbiosis

Many lines of evidence support the idea that the chloroplast originated from a cyanobacterium that

was engulfed by (or invaded) a non-photosynthetic eukaryote that already had a mitochondrion (Gray, 1992, 1999; Douglas, 1998; McFadden, 1999, 2001; Cavalier-Smith, 2000). This ancestral cyanobacterium established a stable endosymbiotic relationship with its host and eventually became an integral part of the host cell (Fig. 5A). The photosynthetic membranes of chloroplasts and cyanobacteria have many structural and functional similarities, which include strong similarities between the phycobilisomes of cyanobacteria and those of red and glaucophyte algae (Chapter 9, Mimuro and Kikuchi; Chapter 10, Gantt et al.). Furthermore, chloroplast genomes contain 100–200 genes, which consistently group with their cyanobacterial homologs on phylogenetic trees (Delwiche et al., 1995; Martin et al., 1998, 2002; Adachi et al., 2000). However, within the cyanobacteria-chloroplast clade, the chloroplast sequences are on a unique branch, so that it has not been possible to determine which group of cyanobacteria might have been the ancestor of the chloroplast (Turner, 1997; Turner et al., 1999). This is hardly surprising, considering that the primary endo-

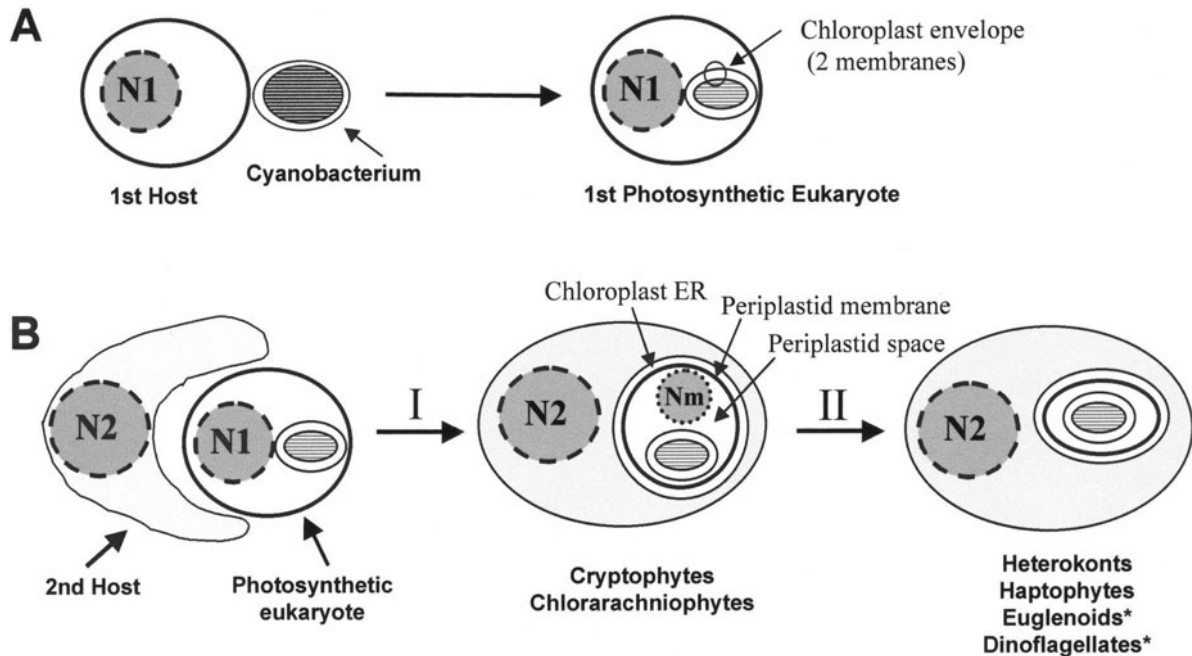


Fig. 5. Origin of chloroplasts by endosymbiosis. A. Primary endosymbiosis gave rise to the common ancestor of red, green and glaucophyte algae. B. Secondary endosymbioses gave rise to the other algal groups. It is still not clear how many different secondary endosymbiogenic events there were. N1, N2—nuclei of first host and second host, respectively; Nm—nucleomorph (relict of N1). \*—euglenoids and dinoflagellates have only three membranes surrounding the chloroplast. Chloroplast ER may or may not have ribosomes on its cytoplasmic surface, but in both cases it is continuous with the rough endoplasmic reticulum (ER) (Ishida et al., 2000). Compare Figs. 8 and 9.

symbiosis that gave rise to the chloroplast may have occurred as long as 1.2 billion years ago (Chapter 4, Green). The ancestral cyanobacterial line may now be extinct, or the gene sequences may have diverged so much that the relationships are unrecognizable.

The establishment of the primary endosymbiosis required many steps (Table 3). The endosymbiont would probably have used existing mechanisms that allowed bacterial cells to invade and multiply in eukaryotic cells, such as the systems that allow rhizobial infection of root cells by nitrogen-fixing bacteria, or those of the intracellular bacterial parasites of animals (Hueck, 1998; Marie et al., 2001; Büttner and Bonas, 2002)). The metabolic systems of the two cells would have gradually become coordinated, probably adapting existing transporters to transfer ions and small molecules between host and endosymbiont. Copies of endosymbiont genes were transferred to the host nucleus, by mechanisms that are still not well understood but which are in use today (reviewed by Millen et al., 2001). Some genes acquired suitable promoters, possibly by insertion next to a host promoter; these allowed them to be expressed and the encoded proteins synthesized on cytoplasmic ribosomes. Some of the proteins provided functions the host did not have, or functioned more efficiently than the host homolog and eventually replaced it. For example, it appears that a number of

plant glycolytic genes were acquired from the chloroplast and are not related to nuclear genes of non-photosynthetic eukaryotes (Martin and Schnarrenberger, 1997; Martin and Hermann, 1998).

Some of the transferred genes acquired sequences that allowed their products to be imported back into the chloroplast. These included genes for most of the enzymes of carbon fixation, lipid metabolism (including galactolipid synthesis), and pigment and isoprenoid biosynthesis (Martin et al., 2002). An essential step was therefore the co-evolution of protein import systems (Cavalier-Smith, 2000). As the endosymbiont became more integrated into the host cell, regulatory systems to coordinate metabolic pathways had to evolve. Eventually most endosymbiont genes were lost because their functions were no longer needed, or they were rendered redundant by nuclear-encoded genes of either host or endosymbiont origin.

Similarity of gene content and gene order, as well as phylogenetic analysis, supports the idea that a single successful primary endosymbiogenesis gave rise to the ancestor of all chloroplasts (Martin et al., 1998, 2002; Stoebe and Kowallik, 1999; Palmer, 2000). Given the complicated nature of this process, it is hardly surprising that the successful reduction of the cyanobacterial ancestor to a completely integrated part of the eukaryotic cell happened only once. This

Table 3. Steps involved in primary endosymbiosis

1. Mechanisms to avoid destruction by host defenses. May have involved a host with defective phagosomal membranes, or an endosymbiont with an invasive system similar to those possessed by modern bacterial intracellular pathogens such as *Listeria* and *Legionella*.
2. Adaptation of small-molecule transport systems to allow passage of photosynthate from endosymbiont to host, and other nutrients from host to endosymbiont.
3. Transfer of copies of endosymbiont genes to host nucleus.
  - a. Successful copy transfer involved the acquisition of promoters, allowing them to be expressed, and their products synthesized on cytoplasmic ribosomes. Some of them eventually replaced or augmented host genes and functions.
  - b. Some genes also acquired presequences that enabled the proteins to be taken up by the endosymbiont.
  - c. Some host genes also acquired presequences allowing their products to be imported into the endosymbiont.
4. Co-evolution of protein import systems in the chloroplast envelope.
5. Coordination of carbohydrate, isoprenoid and lipid biosynthesis pathways as well as ion and small-molecule transport systems.
6. Loss of genes from chloroplast genome:
  - a. Some functions were no longer needed (e.g. cell wall synthesis) or were redundant (provided by host cell).
  - b. Nuclear copies of transferred genes worked more efficiently, or were under better control.
  - c. Eventual reduction to current number of 100–200 genes.

does not mean that it was the only endosymbiotic relationship between cyanobacteria and non-photosynthetic eukaryotes to have developed over the hundreds of millions of years of existence of eukaryotes. As mentioned above, there are a number of extant examples of intracellular bacterial endosymbionts, which have lost some genes but have not progressed to the stage of complete integration within their host's cell (Hueck, 1998).

The descendants of the first photosynthetic eukaryote gave rise to three algal lineages: the green line (green algae and plants), the red line (rhodophyte algae) and the glaucophyte algae (Fig. 6). All of these have chloroplasts surrounded by two envelope membranes, which are believed to have originated from the two cell membranes of the gram negative cyanobacterial ancestor. In fact, glaucophytes retain a residual peptidoglycan layer between the two membranes, analogous to that of the cyanobacteria. Molecular phylogenetic analysis suggests that the glaucophyte line branched off first, followed by the divergence of the red and green algae from a common ancestor (Martin et al., 1998, 2002; Stoebe and Kowallik, 1999; Moreira et al., 2000; Palmer, 2000).

The glaucophytes make only Chl *a* and use phycobilisomes as their antenna system (in addition to the Core Complex antennas). They are the only group of photosynthetic eukaryotes that do not have members of the LHC (light-harvesting complex) superfamily (see below). Red algae also use phycobilisomes and make only Chl *a*, but they have a PS I-associated LHC antenna that binds only Chl *a* (Chapter 10, Gantt et al.). The green algae have lost phycobilisomes but are able to make Chl *b*, which is bound along with Chl *a* to members of an expanded LHC protein family associated with both photosystems.

This raises the question of where Chl *b* synthesis arose. It has been suggested that all cyanobacteria originally made Chl *b*, but that the gene was lost in all lines except those that gave rise to the chloroplast ancestor and the three prochlorophytes (Bryant, 1992). This scenario is supported by the sequence relatedness of cyanobacterial, plant and green algal chlorophyllide *a* oxygenases (Tomitani et al., 1999). However, the possibility that the enzyme arose in one of the four cyanobacterial groups and was passed to the others by lateral gene transfer should also be considered (Raymond et al., 2002; Chapter 4, Green).

## 2. Secondary Endosymbioses

Not all chloroplasts are descended directly from the primary endosymbiont. There are a number of algal groups whose chloroplasts are surrounded by three or four bounding membranes (Fig. 5B, Fig. 6). These include the euglenoids and chlorarachniophytes, which have Chl *b*, and all the algae with Chls *c*: heterokonts, haptophytes, cryptophytes and dinoflagellates. It was first suggested by S. P. Gibbs (1981) that these algae were the product of secondary endosymbiosis, where non-photosynthetic eukaryotes engulfed and enslaved either green or red algae, got rid of most of the engulfed cell, and domesticated the chloroplast (Palmer and Delwiche, 1996; Douglas, 1998; Cavalier-Smith, 2000; MacFadden 1999, 2001). Of the four membranes now surrounding the chloroplast, the inner two originate from the original plastid envelope and the next one (periplastid membrane) from the endosymbiont's cell membrane (Fig. 5). The outermost membrane appears to be part of the host's endomembrane system and was probably derived from fusion of the food vacuole membrane with the host's endoplasmic reticulum (ER) (Cavalier-Smith, 2000). As a result, the chloroplast can now be considered to be in the lumen of the ER. The periplastid membrane would have been lost in the euglenoid and dinoflagellate lines, which have only three membranes around their chloroplasts.

The best evidence in favor of secondary endosymbiosis is the continued existence in two algal groups of a remnant of the endosymbiont's old nucleus called the nucleomorph. The cryptophyte nucleomorph has three miniature chromosomes that retain about 400 protein-coding genes, only about 30 of which are targeted to the chloroplast. Most of the genes are required just for maintenance of the nucleomorph (Zauner et al., 2000; Douglas et al., 2001). The *Chlorarachnion* nucleomorph also has three minichromosomes that are similar to the cryptophyte nucleomorph chromosomes in being very compact, having overlapping genes, and having rRNA gene clusters at the ends of the chromosomes (Gilson and McFadden, 1996; 2002).

It appears that many genes were transferred from the nucleus of the endosymbiont to the nucleus of the host during the establishment of the secondary endosymbiosis, and that there has been relatively little gene transfer from the chloroplast to the nucleus of the second host. In order for the endosymbiosis to

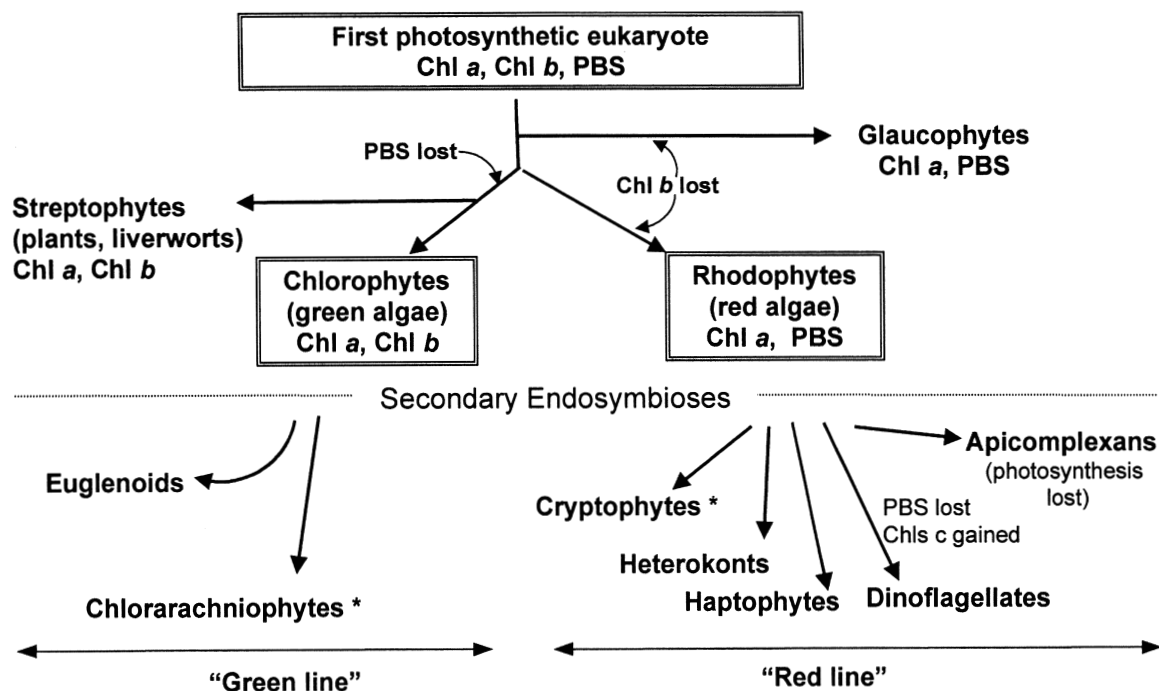


Fig. 6. Schematic evolutionary tree of all groups known to have chloroplasts and their photosynthetic pigments. \* indicates that chlorarachniophytes and cryptophytes still retain a nucleomorph. PBS, phycobilisomes. Cryptophytes have phycobiliproteins in the thylakoid lumen, but do not have phycobilisomes (Chapter 11, Macpherson and Hiller).

be successful, the host had to develop a mechanism for transporting chloroplast-targeted proteins across four membranes. It was suggested by Gibbs (1979) and later shown experimentally that the first step is translation of these proteins on ribosomes bound to the ER membrane and their insertion into the lumen of the ER (Bhaya and Grossman, 1991; Lang et al., 1998; Ishida et al., 2000; Apt et al., 2002). Nothing is known about how the proteins traverse the periplastidal membrane, but it is assumed that once they do, they engage the normal chloroplast envelope translocon (Apt et al., 2002).

Molecular evidence as well as pigment composition suggests that green algal endosymbionts provided the chloroplasts of both euglenoids and chlorarachniophytes but that the host cells were different, i.e. they are the result of two independent secondary endosymbioses (McFadden, 2001). There is considerably more debate about the number of endosymbioses in the 'red line' (Douglas, 1998; Cavalier-Smith 2000; McFadden, 2001). Most nuclear gene trees put haptophytes, heterokonts and cryptophytes on completely separate branches (Ben Ali et al., 2001), suggesting that they may be the result of three secondary endosymbioses, but a recent analysis of concatenated chloroplast genes supports their origin

from a single secondary endosymbiosis (Yoon et al., 2002).

Dinoflagellates are a more complicated story. According to nuclear rRNA gene phylogenies, their closest relatives are the apicomplexans, which include parasites such as *Plasmodium* and *Toxoplasma*. Many of the apicomplexa have a relict non-photosynthetic plastid with a small genome (reviewed by Wilson, 2002). These genomes carry no photosynthetic genes, but do have rRNA and some ribosomal protein genes as well as four other open reading frames that are highly conserved among all chloroplasts. The rRNA sequences of dinoflagellate and apicomplexan plastids are so divergent that it is not possible to tell if the plastids had a common ancestor (Zhang et al., 2000). Other genes are equally divergent, and there is considerable debate about whether the apicomplexans had a red algal or a green algal ancestor (Köhler et al., 1997; Fast et al., 2001; Funes et al., 2002). However, conserved plastid genes encoding photosynthetic membrane proteins (Zhang et al., 1999) and a number of nuclear genes including those encoding the major Chl *a/c* light-harvest complex proteins (Durnford et al., 1999; Deane et al., 2000) support the red algal origin of the dinoflagellate plastid.



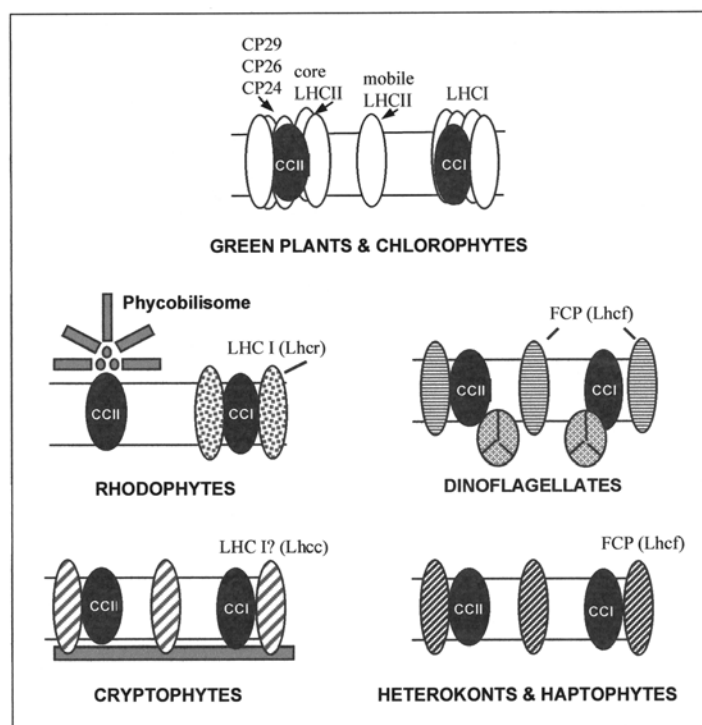


Fig. 7. Eukaryotic light-harvesting antennas. CCI, CCII – core complexes of PS I and PS II, respectively. Elongated ovals, members of the LHC superfamily: spotted, red algal LHCI (Chl *a* only); white, various members of Chl *a/b* clade; striped or hatched, fucoxanthin Chl *a/c* proteins. Cryptophytes have phycobiliproteins in thylakoid lumen (dark gray bar) but no phycobilisomes. Trimeric structures in dinoflagellate lumen are peridinin Chl *a* protein. Chloroplast stroma is at top of figures. For abbreviations, see text and Table 4.

### B. Thylakoid Membrane Structure: Algae and Their LHCs

The thylakoid membranes of all chloroplasts appear as flattened membrane sacs, which may or may not be appressed to each other. The chloroplasts of different algal groups differ in the particular light-harvesting antennas they employ (Fig. 7), and in the arrangement of the thylakoids (Figs. 8, 9). There are differences not only in the way light is absorbed and transmitted to the core complexes, but also in the way excitation energy transfer is modified to deal with changing environmental conditions. The latter aspect is discussed extensively in the chapters of Part III.

Chloroplasts are distinguished from cyanobacteria in having membrane-intrinsic antenna complexes of the LHC superfamily. Even though this family may have originated from small one-helix proteins found in cyanobacteria (Green, Chapter 4; Green and Kühlbrandt, 1995), the three-helix members that bind both Chl and carotenoids and have a demon-

strated light-harvesting function are found only in eukaryotes (Fig. 7). Members of the LHC superfamily function not only to harvest light, but also to protect the photosynthetic apparatus against too much light. The family is particularly diversified in the green algae and plants, where its members are involved in a bewildering array of mechanisms for dealing with excitation energy. This is particularly important for land plants, which are exposed to a great range of light intensities coupled with the threats of desiccation stress and extreme temperature (Chapter 13, Krause and Jahns; Chapter 14, Huner et al.).

The structure of the major LHC (LHCII) of pea has been determined by electron crystallography (Kühlbrandt et al., 1994). The LHCs of other eukaryotes share enough sequence similarity, especially in the membrane domains, that they can be modeled on the LHCII structure. Cartoons showing predicted shape and conserved Chl binding residues in the LHCs of different groups can be found in Chapter 7 (van Amerongen and Dekker), Chapter 10 (Gantt et al.) and Chapter 11 (Macpherson and Hiller).



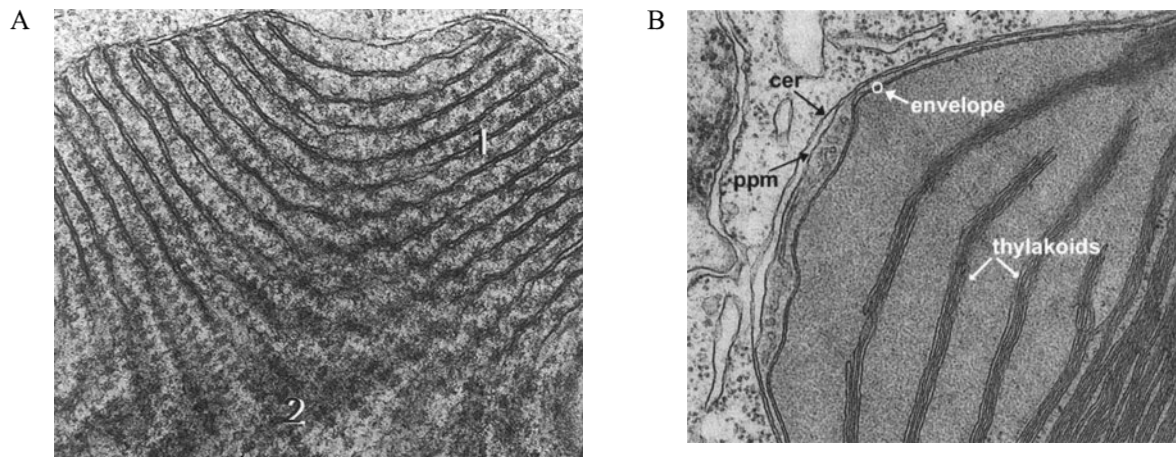


Fig. 8. Algal chloroplast ultrastructure. A. Red alga *Porphyridium cruentum*, showing the two envelope membranes and single thylakoids with phycobilisomes attached. 1, cross section, 2, grazing section over thylakoid face. Phycobilisome dimensions are about  $50 \times 32$  nm. B. Heterokont alga *Heterosigma akashiwo*, showing thylakoids in groups of three, appressed along most of their length. cer, chloroplast ER; ppm, periplastid membrane; white circle shows inner and outer envelope membranes. A, courtesy of E. Gantt, B, courtesy of K Ishida.

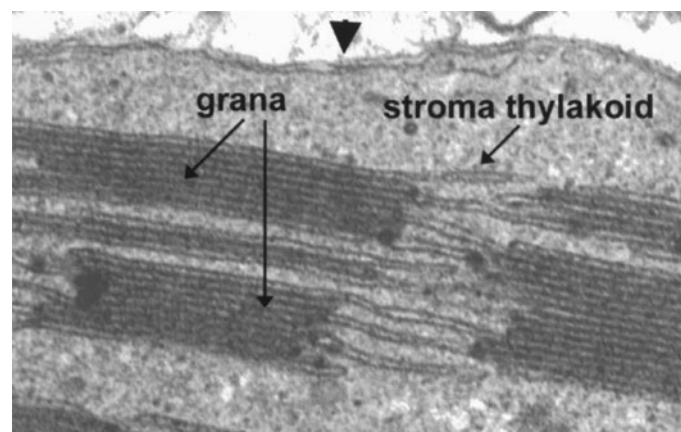


Fig. 9. Higher plant chloroplast ultrastructure (cucumber fruit). Note grana and stroma thylakoids, and two envelope membranes (arrowhead). Courtesy of A. L. Samuels.

The LHCs of all algal groups were reviewed by Green and Durnford (1996), and will be discussed very briefly along with thylakoid membrane structure in the rest of this section. Higher plant chloroplasts and their Chl *a/b* protein complexes have been extensively studied; they are covered in section IIIC.

### 1. Rhodophyte Algae

The thylakoids of red algae are single, mostly parallel but not appressed to each other because their surfaces are covered with phycobilisomes (Fig. 8A). The

phycobilisomes appear to transfer energy preferentially to PS II, like those of cyanobacteria (Gantt, 1995). In addition, red algae have a LHCI antenna (i.e. associated only with PS I) consisting of a number of proteins that bind only Chl *a* and carotenoids (Wolfe et al., 1994; Tan et al., 1997; Table 4). Fast responses to changes in light intensity or quality (state transitions) appear to be controlled via the trans-thylakoid pH gradient, while acclimation involves changes in the PS II/PS I ratio and antenna size (Chapter 10, Gantt et al.).

## 2. Cryptophyte Algae

Thylakoids of the cryptophyte algae are only loosely appressed in pairs. They do not have phycobilisomes, but have unique phycobiliprotein dimers located in the thylakoid lumen (Chapter 11, Macpherson and Hiller). The cryptophyte bilin pigments are also distinctive (Chapter 2, Scheer; Chapter 9, Mimuro and Kikuchi; Glazer and Wedemeyer, 1995). Cryptophytes also have a Chl *a/c* LHC antenna (Table 4). The three available protein sequences cluster with the red algal LHCI proteins (Deane et al., 2000; Chapter 4, Green; Chapter 11, Macpherson and Hiller). There is some evidence supporting the preferential association of this antenna with PS I (Chapter 11, Macpherson and Hiller). Immunocytochemistry showed no evidence for lateral heterogeneity of the photosystems in the plane of the membrane (Lichtlé et al., 1992a).

## 3. Heterokonts and Haptophytes

The thylakoids of these algae are arranged in groups of three appressed along most of their length (Fig. 8B). They have Chl *a/c* antennas that bind large amounts of the carotenoid fucoxanthin; the 19-acyloxy derivatives of fucoxanthin are a distinguishing characteristic of haptophytes. Most of the gene sequences are highly related to each other within the same organism, and are in the same branch of the phylogenetic tree (Durnford et al., 1999; Deane et al., 2000). However, a few sequences fall into the same clade as the red algal LHCI and the cryptophyte LHCs (Eppard and Rhiel, 1998; Eppard et al., 2000; Chapter 4, Green). With one possible exception, there is little evidence for association of any particular antenna protein with one photosystem or the other (Chapter 11, Macpherson and Hiller).

Immuno-electron microscopy showed no evidence of lateral segregation of PS I from PS II or the major fucoxanthin Chl *a/c* protein in the plane of the membrane in brown algae (Lichtlé et al., 1992b) or diatoms (Pysznik and Gibbs, 1992). Rather, there appears to be a greater concentration of both PS II and PS I complexes in stacked membrane domains compared to unstacked areas, although only a limited number of species have been examined. There may be varying and distinct microdomain organization of the photosystems within these stacked membrane domains. Excitation energy regulation may not involve state transitions or phosphorylation but does

involve a modified xanthophyll cycle (Lohr and Wilhelm, 1999).

## 4. Dinoflagellates

Dinoflagellates have peridinin Chl *a/c* antennas whose sequences place them at the base of the major fucoxanthin Chl *a/c* clade (Durnford et al., 1999; Deane et al., 2000). There is no information about how the antenna proteins are organized with respect to the two photosystems or whether they are evenly distributed along the membrane (Chapter 11, Macpherson and Hiller). However, 'normal' peridinin-containing dinoflagellates have a soluble antenna, the unique peridinin-Chl *a* complex, which is located in the thylakoid lumen. Its structure has been determined to high resolution and it is now the subject of many on-going biophysical investigations (Chapter 11, Macpherson and Hiller).

## 5. Green Algae

All green algal thylakoids have both stacked (appressed) and unstacked (non-appressed) regions. Often, e.g. in *Chlamydomonas*, membrane stacking occurs over quite long and irregular regions that rarely involve more than two or three thylakoids. The space between stacked thylakoids is wider in most green algae than in higher plants. *Euglena* thylakoids have irregular stacked and unstacked regions, consistent with their origin from a secondary green algal symbiont. Land plants are believed to have evolved from one class of green algae, the Charophyta (Bhattacharya and Medlin, 1998), and only in this group (e.g. *Nitella*) is the membrane organization virtually indistinguishable from that of plant chloroplasts, with regularly-aligned, appressed thylakoids. The thylakoids of these algae form grana stacks with more than two or three thylakoids per granum, interconnected through single stroma thylakoids.

It was widely assumed that the lateral heterogeneity of PS II and PS I distribution between appressed and non-appressed membranes of higher plant thylakoids (see below) would also be found in most green algae. However, studies with antisera to PS II and PS I components showed that a prasinophyte, *Tetraselmis subcordiformis* (Song and Gibbs, 1995) and *Chlamydomonas reinhardtii* (Bertos and Gibbs, 1998) have the same ratios of PS II/PS I in both stacked and unstacked areas, with a greater concentration of both

Table 4. LHC antennas, membrane structure and energy regulation

Group	LHC Antenna			Other Antennas	Thylakoid Organization	Energy regulation mechanisms
	Major Pigments	Protein Names	Photo-system			
Rhodophytes	Chl <i>a</i> , zeaxanthin, <i>b</i> -carotene	Lhcr, LhcaR	PS I	Phycobilisomes	Single, unappressed	State transitions ( $\Delta$ pH), PSI/PSII ratio
Cryptophytes	Chl <i>a</i> , Chls <i>c</i> Alloxanthin	Lhcc	PS I?	Phycobilins	Pairs, appressed. Electron-dense lumen	?
Heterokonts and Haptophytes	Chl <i>a</i> , Chls <i>c</i> , fucoxanthin	Lhcf	?	–	Threes, appressed. No lateral segregation of PS I from PSII or major FCP	Xanthophyll cycle
Dinoflagellates	Chl <i>a</i> , Chl <i>c</i> <sub>2</sub> , peridinin	Lhcd	?	Peridinin-Chl <i>a</i> protein	Triplets, appressed. No lateral segregation?	?
Chlorophyte algae and green plants	Chl <i>a</i> , Chl <i>b</i> , lutein	Lhca Lhcb	PS I PS II	–	Stacked (grana) and single (stroma) thylakoids. Lateral segregation of PS II and PS I	State transitions (LHCII movement), xanthophyll cycle, $\Delta$ pH, phosphorylation

photosystems in the stacked membrane domain, consistent with the distribution of freeze-fracture-particles (Staehelin, 1986). In contrast, earlier freeze fracture results (Olive and Wollman, 1988) suggested that PS I was present only in unstacked regions.

Confocal microscopy has been used elegantly by Gunning and Schwartz (1999) to demonstrate whether or not the photosystems are mainly segregated from each other in the green algae. Some members of the Charophyta showed bright areas of PS II fluorescence, indistinguishable from the grana of higher plants, suggesting lateral segregation of PS II from PS I. Other algae, including *Chlamydomonas*, revealed uniform fluorescence indicative of more uniform mixing of PS II and PS I in both stacked and unstacked membrane domains.

### C. Higher Plant Chloroplasts and Their Antennas

#### 1. Granal Structure and Lateral Segregation

In plant chloroplasts, the single continuous thylakoid membrane network is structurally differentiated into regular domains of closely appressed membranes in granal stacks (diameter 400–500 nm) (Staehelin and van der Staay, 1996), which are interconnected by single, non-stacked stroma thylakoids (Fig. 9). Only the outer surface of stroma thylakoids and the margins

and end membranes of grana stacks have direct contact with the chloroplast stroma and constitute the nonappressed membrane domains.

The striking structural differentiation of vascular plant thylakoids is accompanied by a functional differentiation involving lateral heterogeneity in the distribution of thylakoid membrane complexes. ATP synthase with its bulky head group and the PS I complex with bulky stroma-facing proteins are located exclusively in nonappressed membrane domains (Andersson and Anderson, 1980). Most PS II complexes with large antennas are located as PS II dimers in the appressed membrane regions, while fewer PS IIs with smaller antennas are located in the non-appressed domains. Linear electron transport and noncyclic photophosphorylation are confined to the grana, while cyclic photophosphorylation occurs in stroma thylakoids and end grana membranes (Albertsson, 1995, 2001). The cytochrome *b<sub>6</sub>f* complex occurs in both membrane domains, and its distribution between these two regions is highly dynamic.

Appressed granal formation depends on the interplay of van der Waals' attraction (largely conferred by LHCII), electrostatic repulsion and short-range hydration repulsion between thylakoid membranes, with the ordering of certain thylakoid protein complexes in appressed domains being driven by an increase in the overall entropy of the system

(Chow, 1999). If isolated plant thylakoid membranes are suspended in low-salt zwitterionic buffers such as tricine, membrane appression is gradually lost and the membranes became completely unstacked. Fractionation of unstacked membranes by detergents results in submembrane fractions with similar Chl *a/b* ratios and both PS II and PS I activities, demonstrating a uniform distribution of the photosystems (Izawa and Good, 1966).

Although not essential for photosynthesis, grana stacking confers advantages for photosynthetic function and its dynamic regulation (Anderson, 1999). The segregation of most PS II dimers in appressed granal domains limits excessive spillover of excitation energy from PS II to PS I (Anderson 1981). It also separates 'kinetically slow' PS II from 'fast' PS I (Trissl and Wilhelm, 1993). Grana stacking also allows maximum connectivity of LHCII both along and across the stacked granal domains and aids in the regulation of photosynthesis by balancing energy utilization with energy dissipation (Anderson 1999). Under high light, non-functional PS II units accumulate, thereby delaying the degradation of D1 protein and PS II disassembly: this is a major photoprotective strategy for plants (Anderson and Aro, 1994).

## 2. The LHC Superfamily

The ten distinct chlorophyll *a/b* proteins encoded by different *Lhc* nuclear-encoded genes bind varying amounts of Chl *a*, Chl *b* and the xanthophylls lutein, neoxanthin, violaxanthin, antheraxanthin and zeaxanthin. The PS II antenna consists of minor peripheral antenna complexes CP29 (Lhcb4), CP26 (Lhcb5) and CP24 (Lhcb6) and the major outer LHCII antenna with the lowest Chl *a/b* ratio, which comprises Lhcb1/Lhcb2 and Lhcb1/Lhcb3 heterotrimers and Lhcb1 homotrimers (Chapter 7, van Amerongen and Dekker). The PS I antenna (LHCI), comprising four Lhca proteins, Lhca1 through to Lhca4, is exclusively associated with PS I as Lhca2 and Lhca3 dimers and Lhca1/Lhca4 heterodimers (Fromme et al., Chapter 8). A variable amount of phosphorylated LHCII trimers may also be attached to PS I during state transitions (Chapter 13, Krause and Jahns; Chapter 15, Falkowski and Chen). Angiosperms and gymnosperms, which diverged about 350 million years ago, contain the same set of ten Lhc proteins. This strongly indicates that each protein complex has a specific function. The

chlorophyte alga *Chlamydomonas* has identifiable CP26 and CP29 complexes in the PS II core, but its major LHC antenna (LHC II) is not differentiated into distinct Lhcb1, Lhcb2, and Lhcb3 sub-types (Teramoto et al., 2001). This supports the idea that the unique molecular configuration of higher plant LHC II plays an important role in the formation of grana stacks.

The antenna composition of PS II and PS I is not only heterogeneous with respect to their position in different thylakoid regions (Jansson et al., 1997) but also in the supramolecular organization of PS II (van Amerongen and Dekker, Chapter 7). It is now clear that different native PS II-LHCII supercomplexes consisting of the dimeric PS II core complex surrounded by variable numbers of trimeric and monomeric Lhcb proteins can exist within a particular granal domain (Chapter 7, van Amerongen and Dekker). Less is known about the supramolecular structure of monomeric plant PS I, but it appears that the Lhca protein dimers are attached to one side of the RC+core antenna particle (Boekema et al., 2001), while the phosphorylated Lhcb trimers (if present) are associated with the other side (Fromme et al., Chapter 8).

## 3. Acclimation and Grana

As will be seen in a number of chapters of this book, the molecular mechanisms for both light harvesting and energy dissipation in varying light environments have been achieved in part by the evolution of different classes of LHC antenna throughout the plant kingdom. The ever-varying natural light environment, both light quality and quantity, is a crucial factor in the arrangement of the photosystems and the dynamic reversible movement of some LHCs. As shading occurs through the tree and leaf canopy (Björkman and Ludlow, 1972) or across a leaf, red and blue light are attenuated, and far-red light is enhanced. Alternatively, the aquatic light environment is severely attenuated as water depth increases, with far-red, then red, then blue being progressively depleted (Chapter 15, Falkowski and Chen). Hence shaded land environments favor excitation of PS I interspersed with direct sunflecks, while aquatic ecosystems effectively have no far-red light.

There are several rapid responses to changes in light quality. Within minutes, both state transitions promoted at lower light intensities, and the xanthophyll cycle promoted under high light, change

the effective absorption cross section of PS II in algae (Chapter 15, Falkowski and Chen) and plants (Chapter 13, Krause and Jahns; Horton et al., 1996; Niyogi, 1999). Furthermore, both plants and algae have developed multiple strategies to dissipate excess excitation energy as heat, which may be measured as non-photochemical quenching (NPQ) (Chapter 13, Krause and Jahns). NPQ involves acidification of the lumen, protonation of specific components of the PS II antenna within seconds, and operation of the xanthophyll cycle within minutes. Recently there has been debate about which specific Lhcb proteins are critical for thermal dissipation (Lhcb trimers, CP26, CP29 or PsbS (Li et al., 2000) or perhaps small linking peptides in the PS II antenna, e.g. PsbZ (Swiatek et al., 2001). Although PsbS has been shown to be essential for development of NPQ in *Arabidopsis*, it appears to be unique to the streptophyte (plant) line. No PsbS homologs have been detected in more than 30,000 ESTs from *Chlamydomonas reinhardtii* (Elrad et al., 2002), in more than 10,000 ESTs from the red alga *Porphyra purpurea* (Nikaido et al., 2000) or in the draft genome of the diatom *Thalassiosira pseudonana* (E. V. Armbrust et al., unpublished).

A short-term fine-tuning mechanism to regulate balanced light excitation between PS II and PS I depends on reversible phosphorylation of some outer LHCII units (Allen and Forsberg, 2001). When PS II is over-excited relative to PS I, a LHCII kinase regulated by the redox state of plastoquinone phosphorylates LHCII, and the phospho-LHCII migrates to PS I (Lunde et al., 2000). When PS I is over-excited relative to PS II, a specific phosphatase dephosphorylates LHCII, which then detaches from PS I and returns to PS II.

The degree of grana formation is regulated by light acclimation, in response to both light quality and quantity. The chloroplasts of shade and low-light plants have more and larger granal stacks, attributable to increased amounts of LHCII per P680, compared to those of sun and high-light plants (Anderson et al., 1995). Significantly, land plants always have more PS II than PS I, the reverse situation to cyanobacteria (Fujita 1997) and most algae. Shade and low-light plants not only have larger antenna for both photosystems, but also lower PS II/PS I ratios (1.2–1.8) compared to sun and high-light plants (PS II/PS I ratios >2.0) which have more PS IIs, each with smaller light-harvesting antenna, relative to PS I. Grana stacking aids in the conflicting demands of

efficient use of low light by PS II and protection of nonfunctional PS II in appressed membrane domains under high light.

### To be Continued...

This has been a brief introduction to the basic principles of light-harvesting and the great variety of light-harvesting antenna complexes employed by photosynthetic organisms. It is hoped the reader will be inspired to continue reading in the following chapters of this book, where a wealth of fascinating information can be found.

### Acknowledgments

We are grateful to Drs. R. Blankenship and D. A. Bryant for educating us about green bacteria and heliobacteria.

### References

- Adachi J, Waddell PJ, Martin W and Hasegawa (2000) Plastid genome phylogeny and a model of amino acid substitution for proteins encoded by chloroplast DNA. *J Mol Evol* 50: 348–358
- Akiyama M, Miyashita H, Kise H, Watanabe T, Mimuro M, Miyachi S and Kobayashi M (2002) Quest for minor but key chlorophyll molecules in photosynthetic reaction centers—unusual pigment composition in the reaction centers of the chlorophyll *d*-dominated cyanobacterium *Acaryochloris marina*. *Photosynth Res* 74: 97–107
- Albertsson P-A (1995) The structure and function of the chloroplast photosynthetic membrane—a model for the domain organisation. *Photosynth Res* 46: 141–149
- Albertsson P-A (2001) A qualitative model of the domain structure of the photosynthetic membrane. *Trends Plant Sci* 6: 349–354
- Allen JF and Forsberg J (2001) Molecular recognition in thylakoid structure and function. *Trends Plant Sci* 6: 317–326
- Amesz J (1995a) The heliobacteria, a new group of photosynthetic bacteria. *J Photochem Photobiol b* 30: 89–96
- Amesz J (1995b) The antenna-reaction center complex of heliobacteria. In: Blankenship RE, Madigan MT and Bauer CE (eds) *Anoxygenic Photosynthetic Bacteria*, pp 687–697. Kluwer Academic Publishers, Dordrecht
- Anderson JM (1981) Consequences of spatial separation of photosystems 1 and 2 in thylakoid membranes in higher plant chloroplasts. *FEBS Lett* 124: 1–10
- Anderson JM (1999) Insights into the consequences of grana stacking of thylakoid membranes of vascular plants: a personal perspective. *Aust J Plant Physiol* 26: 625–639
- Anderson JM and Aro E-M (1994) Grana stacking and protection of Photosystem II in thylakoid membranes of higher plants

- under sustained high irradiance: An hypothesis. *Photosynth Res* 41: 315–316
- Anderson JM, Chow WS and Park Y-L (1995) The grand design of photosynthesis: Acclimation of the photosynthetic apparatus to environmental cues. *Photosynth Res* 46: 129–139
- Andersson B and Anderson JM (1980) Lateral heterogeneity in the distribution of chlorophyll-protein complexes of the thylakoid membranes of spinach chloroplasts. *Biochim Biophys Acta* 593: 427–440
- Andrizhiyevskaya EG, Schwabe TME, Germano M, D'Haene S, Kruip J, van Grondelle R and Dekker JP (2002) Spectroscopic properties of PS I-IsiA supercomplexes from the cyanobacterium *Synechococcus* PCC 7942. *Biochim Biophys Acta* 1556: 265–272
- Apt KE, Zaslavskaya L, Lippmeier JC, Lang M, Kilian O, Wetherbee R, Grossman AR and Kroth PG (2002) In vivo characterization of diatom multipartite plastid targeting signals. *J Cell* 115: 4061–4069
- Bald D, Kruip J and Rögner M (1996) Supramolecular architecture of cyanobacterial thylakoid membranes: How is the phycobilisome connected with the photosystems? *Photosynth Res* 49: 103–118
- Becker M, Nagarajan V, and Parson WW (1991) Properties of the excited singlet states of bacteriochlorophyll-*a* and bacteriopheophytin-*a* in polar solvents. *J Am Chem Soc* 113: 6840–6848
- Ben Ali A, De Baere R, Van der Auwera G, De Wachter R and Van de Peer (2001) Phylogenetic relationships among algae based on complete large-subunit rRNA sequences. *Int J Syst Evol Microbiol* 51: 737–749
- Bertos NR and Gibbs SP (1998) Evidence for a lack of photosystem segregation in *Chlamydomonas reinhardtii* (Chlorophyceae). *J Phycol* 34: 1009–1016
- Bhattacharya D and Medlin L (1998) Algal phylogeny and the origin of land plants. *Plant Physiol* 116: 9–15
- Bhaya D and Grossman AR (1991) Targeting proteins to diatom plastids involves transport through an endoplasmic reticulum. *Mol Gen Genet* 229: 400–404
- Bibby TS, Nield J, Partensky F and Barber J (2001a) Antenna ring around Photosystem I. *Nature* 413: 590
- Bibby TS, Nield J and Barber J (2001b) A Photosystem II-like protein, induced under iron-stress, forms an antenna ring around the Photosystem I trimer in cyanobacteria. *Nature* 412: 743–745
- Bibby TS, Nield J and Barber J (2001c) Three-dimensional model and characterization of the iron stress-induced CP43'-Photosystem I supercomplex isolated from the cyanobacterium *Synechocystis* PCC 6803. *J Biol Chem* 276: 43246–43252
- Björkman O and Ludlow MM (1972) Characterization of the light climate on the floor of a Queensland forest. *Carn Instit Wash Year Bk* 71: 85–94
- Blankenship R E (2002) *Molecular Mechanisms of Photosynthesis*. Blackwell Science, Oxford
- Blankenship RE, Olson JM and Miller M (1995) Antenna complexes from green photosynthetic bacteria. In: Blankenship RE, Madigan MT and Bauer CE (eds) *Anoxygenic Photosynthetic Bacteria*, pp 399–435. Kluwer Academic Publishers, Dordrecht
- Boekema EJ, Hifney A, Yakushevskaya AE, Piotrowski M, Keegstra W, Berry S, Michel K-P, Pistorius EK and Kruip J (2001a) A giant chlorophyll-protein complex induced by iron deficiency in cyanobacteria. *Nature* 412: 745–748
- Boekema EJ, Jensen PE, Schlodder E, van Breemen JFL, van Roon H, Scheller HV and Dekker JP (2001b) Green plant Photosystem I binds light-harvesting complex I on one side of the complex. *Biochemistry* 40: 1029–1036
- Boichenko VA, Klimov VV, Miyashita H and Miyachi S (2000) Functional characteristics of chlorophyll *d*-predominating photosynthetic apparatus in intact cells of *Acaryochloris marina*. *Photosynth Res* 65: 269–277
- Bryant DA (1992) Puzzles of chloroplast ancestry. *Curr Biol* 2: 240–242.
- Bryant DA (ed) (1995) *The Molecular Biology of Cyanobacteria*. Kluwer Academic Publishers, Dordrecht
- Burnap RL, Troyan T and Sherman LA (1993) The highly abundant chlorophyll-protein complex of iron-deficient *Synechococcus* sp. PCC7942 (CP43') is encoded by the *isiA* gene. *Plant Physiol* 103: 893–902
- Büttner D and Bonas U (2002) Port of entry-the type III secretion translocon. *Trends Microbiol* 10: 186–192
- Cavalier-Smith T (2000) Membrane heredity and early chloroplast evolution. *Trends Plant Sci* 5: 174–182
- Cavalier-Smith T (2002a) Chloroplast evolution: Secondary symbiogenesis and multiple losses. *Curr Biol* 12: 62–64
- Cavalier-Smith T (2002b) Nucleomorphs: Enslaved algal nuclei. *Curr Opin Microbiol* 5: 612–619
- Chen M, Quinell RG and Larkum AWD (2002) The major light-harvesting pigment protein of *Acaryochloris marina*. *FEBS Lett* 514: 149–152
- Chow WS (1999) Grana formation: Entropy-assisted local order in chloroplasts? *Aust J Plant Physiol* 26: 641–647
- Crofts AR (2000) Response from Crofts. *Trends Microbiol* 8: 107–108
- Deane JA, Fraunholz M, Su V, Maier U-G, Martin W, Durnford DG and McFadden GI (2000) Evidence for nucleomorph to host nucleus gene transfer: Light-harvesting complex proteins from cryptomonads and chlorarachniophytes. *Protist* 151: 239–252
- Deisenhofer J, Epp O, Miki K, Huber R and Michel H (1985) Structure of the protein subunits in the photosynthetic reaction center of *Rhodospseudomonas viridis* at 3 Å resolution. *Nature* 318: 618–624
- Delwiche CF, Kuhsel M and Palmer JD (1995) Phylogenetic analysis of *tufA* sequences indicates a cyanobacterial origin of all plastids. *Mol Phylogenet Evol* 4: 110–128
- Douglas SE (1998) Plastid evolution: origins, diversity, trends. *Curr Opin Genet Devel* 8: 655–661
- Douglas SE and Penny SL (1999) The plastid genome of the cryptophyte alga *Guillardia theta*: Complete sequence and conserved syntenic groups confirm its common ancestry with red algae. *J Mol Evol* 48: 236–244
- Douglas S, Zauner S, Fraunholz M, Beaton M, Penny S, Deng L-T, Wu X, Reith M, Cavalier-Smith R and Maier U-G (2001) The highly reduced genome of an enslaved algal nucleus. *Nature* 410: 1091–1096
- Drews G and Golecki JR (1995) Structure, molecular organization and biosynthesis of membranes of purple bacteria. In: Blankenship RE, Madigan MT and Bauer CE (eds) *Anoxygenic Photosynthetic Bacteria*, pp 231–257. Kluwer Academic Publishers, Dordrecht
- Durnford DG, Deane JA, Tan S, McFadden GI, Gannt E and Green BR (1999) A phylogenetic assessment of the eukaryotic



- light-harvesting antenna proteins, with implications for plastid evolution. *J Mol Evol* 48: 59–68
- Duysens LNM (1952) Transfer of excitation energy in photosynthesis. Thesis, Univ. of Utrecht
- Elrad D, Niyogi KK and Grossman AR (2002) A major light-harvesting polypeptide of Photosystem II functions in thermal dissipation. *Plant Cell* 14: 1801–1816
- Eppard M and Rhiel E (1998) The genes encoding light-harvesting subunits of *Cyclotella cryptica* (Bacillariophyceae) constitute a complex and heterogeneous family. *Mol Gen Genet* 260: 335–345
- Eppard M, Krumbein WE, von Haeseler A and Rhiel E (2000) Characterization of *fcp4* and *fcp12*, two additional genes encoding light harvesting proteins of *Cyclotella cryptica* (Bacillariophyceae) and phylogenetic analysis of this complex gene family. *Plant Biol* 2: 283–289
- Falk S, Samson G, Bruce D, Huner NPA and Laudenbach DE (1995) Functional analysis of the iron-stress induced CP43' polypeptide of PS II in the cyanobacterium *Synechococcus* sp. PCC 7942. *Photosynth Res* 45: 51–60
- Fast NM, Kissinger JC, Roos DS and Keeling PJ (2001) Nuclear-encoded, plastid-targeted genes suggest a single common origin for apicomplexan and dinoflagellate plastids. *Mol Biol Evol* 18: 418–426
- Foidl M, Golecki JR and Oelze J (1998) Chlorophyll organization and function in green photosynthetic bacteria. *Photosynth Res* 55: 109–114
- Förster T (1951) Fluoreszenz Organischer Verbindungen. Vendenhoeck and Ruprecht, Göttingen
- Förster T (1965) Delocalized excitation and excitation transfer. In: Sinanoglu O (ed) *Modern Quantum Chemistry, Part III*, pp 93–137. Academic Press, New York
- Frese RN, Olsen JD, Branvall R, Westerhuis WHJ, Hunter CN and van Grondelle R (2000) The long-range supraorganization of the bacterial photosynthetic unit: A key role for PufX. *Proc Natl Acad Sci USA* 97: 5197–5202
- Fujita Y (1997) A study of the dynamic features of photosystem stoichiometry: Accomplishments and problems for future studies. *Photosynth Res* 53: 83–89
- Fujita Y, Murakami A, Aizawa K and Ohki K (1995) Short-term and long-term adaptation of the photosynthetic apparatus: Homeostatic properties of thylakoids. In: Bryant DA (ed) *The Molecular Biology of Cyanobacteria*, pp 677–692. Kluwer Academic Publishers, Dordrecht
- Fuller RC, Sprague SG, Gest H, Blankenship RE (1985) A unique photosynthetic reaction center from *Helio bacterium chlorum*. *FEBS Lett* 182: 345–349
- Funes S, Davidson E, Reyes-Prieto A, Magallón S, Herion P, King MP and González-Halphen D (2002) A green algal apicoplast ancestor. *Science* 298: 2155
- Fyfe PK, Jones MR and Heathcote P (2002) Insights into the evolution of the antenna domains of Type-I and Type-II photosynthetic reaction centres through homology modelling. *FEBS Lett* 530: 117–123
- Gantt E (1995) Supramolecular membrane organization. In: Bryant DA (ed) *The Molecular Biology of Cyanobacteria*, pp 119–138. Kluwer Academic Publishers, Dordrecht
- Gibbs SP (1979) The route of entry of cytoplasmically synthesized proteins into chloroplasts of algae possessing chloroplast ER. *J Cell Sci* 35: 253–266
- Gibbs SP (1981) The chloroplasts of some algal groups may have evolved from endosymbiotic eukaryotic algae. *Ann NY Acad Sci* 361: 193–208
- Gilson PR and McFadden GI (1996) The miniaturized nuclear genome of a eukaryotic endosymbiont contains genes that overlap, genes that are cotranscribed, and the smallest known spliceosomal introns. *Proc Natl Acad Sci USA* 93: 7737–7742
- Gilson PR and McFadden GI (2002) Jam packed genomes—a preliminary, comparative analysis of nucleomorphs. *Genetica* 115: 13–28
- Glazer AN and Wedemayer GJ (1995) Cryptomonad biliproteins—an evolutionary perspective. *Photosynth Res* 46: 93–105
- Gouterman MP (1961) Spectra of porphyrins. *J Mol Spectrosc* 6: 138–163
- Gray MW (1992) The endosymbiont hypothesis revisited. *Int Rev Cytol* 141: 233–357
- Gray MW (1999) Evolution of organellar genomes. *Curr Opin Genet Devel* 9: 678–687
- Green BR and Durnford DG (1996) The chlorophyll-carotenoid proteins of oxygenic photosynthesis. *Annu Rev Plant Physiol Plant Mol Biol* 47: 685–714
- Green BR and Kühlbrandt W (1995) Sequence conservation of light-harvesting and stress-response proteins in relation to the three-dimensional molecular structure of LHCII. *Photosynth Res* 44: 139–148
- Guglielmi G, Cohen-Bazire G and Bryant DA (1981) The structure of *Gloeobacter violaceus* and its phycobilisomes. *Arch Microbiol* 129: 181–189
- Gunning BES and Schwartz OM (1999) Confocal microscopy of thylakoid autofluorescence in relation to origin of grana and phylogeny in the green algae. *Aust J Plant Physiol* 26: 695–708
- Gupta RS, Mukhtar T and Singh B (1999) Evolutionary relationships among photosynthetic prokaryotes (*Helio bacterium chlorum*, *Chloroflexus aurantiacus*, cyanobacteria, *Chlorobium tepidum* and proteobacteria): Implications regarding the origin of photosynthesis. *Mol Microbiol* 32: 893–906
- Hauska G, Schoedl T, Rémygy H and Tsiotis G (2001) The reaction center of green sulfur bacteria. *Biochim Biophys Acta* 1507: 260–277
- Horton P, Ruban AV, and Walters RG (1996) Regulation of light harvesting in green plants. *Annu Rev Plant Physiol Mol Biol* 47: 655–684
- Hu Q, Miyashita H, Iwasaki I, Kurano N, Miyachi S, Iwaki M and Itoh S (1998) A Photosystem I reaction center driven by chlorophyll *d* in oxygenic photosynthesis. *Proc Natl Acad Sci USA* 95: 13319–13323
- Hu Q, Marquardt J, Iwasaki I, Miyashita H, Kurano N, Mörschel E and Miyachi S (1999) Molecular structure, localization and function of biliproteins in the chlorophyll *a/d* containing oxygenic photosynthetic procaryote *Acaryochloris marina*. *Biochim Biophys Acta* 1412: 250–261
- Hueck CJ (1998) Type III protein secretion systems in bacterial pathogens of animals and plants. *Microbiol Molec Biol Rev* 62: 379–433
- Ishida K, Cavalier-Smith T and Green BR (2000) Endomembrane structure and the chloroplast protein-targeting pathway in *Heterosigma akashiwo* (Raphidophyceae, Chromista). *J Phycol* 36: 1135–1144
- Izawa S and Good NE (1966) Effects of salt and electron transport on the conformation of isolated chloroplasts. II. Electron



- microscopy. *Plant Physiol* 41: 544–552
- Jansson S, Stefánsson H, Nyström U, Gustafsson P and Albertsson P-Å (1997) Antenna protein composition of PS I and PS II in thylakoid sub-domains. *Biochim Biophys Acta* 1320: 297–309
- Kamiya N and Shen J-R (2003) Crystal structure of oxygen-evolving Photosystem II from *Thermosynechococcus vulcanus* at 3.7 Å resolution. *Proc Natl Acad Sci USA* 100: 98–103
- Koepeke J, Hu X, Muenke C, Schulten K and Michel H (1996) The crystal structure of the light-harvesting complex II (B800–850) from *Rhodospirillum rubrum*. *Structure* 4: 581–597
- Köhler S, Delwiche CF, Denny PW, Tilney LG, Webster P, Wilson RJM, Palmer JD and Roos DS (1997) A plastid of probably green algal origin in apicomplexan parasites. *Science* 275: 1485–1488
- Kühlbrandt W, Wang DN, Fujiyoshi Y (1994) Atomic model of plant light-harvesting complex by electron crystallography. *Nature* 367: 614–621
- Lang M, Apt KE and Kroth PG (1998) Protein transport into 'complex' diatom plastids utilizes two different targeting signals. *J Biol Chem* 273: 30973–30978
- LaRoche J, van der Staay GWM, Partensky F, Ducret A, Aebersold R, Li R, Golden SS, Hiller RG, Wrench PM, Larkum AWD and Green BR (1996) Independent evolution of the prochlorophyte and green plant chlorophyll *a/b* light-harvesting proteins. *Proc Natl Acad Sci USA* 93: 15244–15248
- Li XI, Björkman O, Shih C, Grossman AR, Rosenquist M, Jansson S and Noyori KK (2000) A pigment-binding protein essential for the regulation of light-harvesting. *Nature* 403: 391–395
- Li Y, Zhang J, Zhao J and Jiang L (2001) Regulation mechanism of excitation energy transfer in phycobilisome-thylakoid membrane complexes. *Photosynthetica* 39: 227–232
- Li Y-F, Zhou W, Blankenship RE and Allen JP (1997) Crystal structure of the bacteriochlorophyll *a* protein from *Chlorobium tepidum*. *J Mol Biol* 271: 456–471
- Lichtlé C, McKay RML and Gibbs SP (1992a) Immunogold localization of Photosystem I and Photosystem II light-harvesting complexes in cryptomonad chloroplasts. *Biol. Cell* 74: 187–194
- Lichtlé C, Spilar A and Duval JC (1992b) Immunogold localization of light-harvesting and Photosystem I complexes in the thylakoids of *Fucus serratus* (Phaeophyceae). *Protoplasma* 166: 99–106
- Lohr M and Wilhelm C (1999) Algae displaying the diadinoxanthin cycle also possess the violaxanthin cycle. *Proc Natl Acad Sci USA* 96: 8784–8789
- Ludwig M and Gibbs SP (1989) Localization of phycoerythrin at the lumenal surface of the thylakoid membrane in *Rhodomonas lens*. *J Cell Biol* 108: 875–884
- Ludwig W and Schleifer KH (1994) Bacterial phylogeny based on 16S and 23S rRNA sequence analysis. *FEMS Microbiol Rev* 15: 155–173
- Lunde C, Jensen PE, Haldrup A, Knoetzel J and Scheller HV (2001) The PS I-H subunit of Photosystem I is essential for state transitions in plant photosynthesis. *Nature* 408: 613–615
- MacColl R (1998) Cyanobacterial phycobilisomes. *J Struct Biol* 124: 311–334
- Madigan MT and Ormerod JG (1995) Taxonomy, physiology and ecology of heliobacteria. In: Blankenship RE, Madigan MT and Bauer CE (eds) *Anoxygenic Photosynthetic Bacteria*, pp 17–30. Kluwer Academic Publishers, Dordrecht
- Marie C, Broughton WJ and Deakin WJ (2001) *Rhizobium* type III secretion systems: Legume charmers or alarmers? *Curr Opin Plant Biol* 4: 336–342
- Marquardt J, Senger H, Miyashita H, Miyachi S and Mörschel E (1997) Isolation and characterization of biliprotein aggregates from *Acaryochloris marina*, a *Prochloron*-like prokaryote containing mainly chlorophyll *d*. *FEBS Lett* 410: 428–432
- Martin W and Herrmann RG (1998) Gene transfer from organelles to the nucleus: How much, what happens, and why? *Plant Physiol* 118: 9–17
- Martin W and Schnarrenberger C (1997) The evolution of the Calvin cycle from prokaryotic to eukaryotic chromosomes: A case study of functional redundancy in ancient pathways through endosymbiosis. *Curr Genet* 32: 1–18
- Martin W, Stoebe B, Goremykin V, Hansmann S, Hasegawa M and Kowallik KV (1998) Gene transfer to the nucleus and the evolution of chloroplasts. *Nature* 393: 162–165
- Martin W, Rujan T, Richly E, Hansen A, Cornelsen, Lins T, Leister D, Stoebe B, Hasegawa M and Penny D (2002) Evolutionary analysis of *Arabidopsis*, cyanobacterial, and chloroplast genomes reveals plastid phylogeny and thousands of cyanobacterial genes in the nucleus. *Proc Natl Acad Sci USA* 99: 12246–12251
- Martinez-Planells, Arellano JB, Borrego CM, López-Iglesias C, Gich F and Garcia-Gil J (2002) Determination of the topography and biometry of chlorosomes by atomic force microscopy. *Photosynth Res* 71: 83–90
- Matthews BW, Fenna RE, Bolognesi MC, Schmid MR and Olson JM (1979) Structure of a bacteriochlorophyll *a*-protein from the green photosynthetic bacterium *Prosthecochloris aestuarii*. *J Mol Biol* 131: 259–285
- Matthijs HCP, van der Staay GWM and Mur LR (1995) Prochlorophytes: The 'other' cyanobacteria? In: Bryant DA (ed) *The Molecular Biology of Cyanobacteria*, pp 49–64. Kluwer Academic Publishers, Dordrecht
- McDermott G, Prince SM, Freer AA, Hawthornthwaite-Lawless AM, Papiz MZ, Cogdell RJ and Isaacs NW (1995) Crystal structure of an integral membrane light-harvesting complex from photosynthetic bacteria. *Nature* 374: 517–521
- McFadden GI (1999) Endosymbiosis and evolution of the plant cell. *Curr Opin Plant Biol* 2: 513–519
- McFadden GI (2001) Primary and secondary endosymbiosis and the origin of plastids. *J Phycol* 37: 951–959
- McLuskey K, Prince SM, Cogdell RJ and Isaacs NW (2001) The crystallographic structure of the B800–820 LH3 light-harvesting complex from the purple bacteria *Rhodospseudomonas acidophila* Strain 7050. *Biochemistry* 40: 8783–8789
- Millen RS, Olmstead RG, Adams KL, Palmer JD, Lao NT, Heddle L, Kavanagh TA, Hibberd JM, Gray JC, Morden CW, Calie PJ, Jermin LS and Wolfe KH (2001) Many parallel losses of *infA* from chloroplast DNA during angiosperm evolution with multiple independent transfers to the nucleus. *Plant Cell* 13: 645–658
- Miyashita H, Ikemoto H, Kurano N, Adachi K, Chihara M and Miyachi S (1996) Chlorophyll *d* as a major pigment. *Nature* 383: 402
- Moreira D, Le Guyader H and Phillippe H (2000) The origin of red algae and the evolution of chloroplasts. *Nature* 405: 69–72

- Mullineaux CW (1999) The thylakoid membranes of cyanobacteria: Structure, dynamics and function. *Aust J Plant Physiol* 26: 671–677.
- Neerken S and Ames J (2001) The antenna reaction center complex of heliobacteria: Composition, energy conversion and electron transfer. *Biochim Biophys Acta* 1507: 278–290.
- Nikaido I, Asamizu E, Nakajima M, Nakamura Y, Saga N and Tabata S (2000) Generation of 10,154 expressed sequence tags from a leafy gametophyte of a marine red alga, *Porphyra yezoensis*. *DNA Res* 7: 223–227
- Nitschke W and Rutherford AW (1991) Are all of the different types of photosynthetic reaction center variations on a common structural theme? *Trends Biochem Sci* 16: 241–243
- Niyogi KK (1999) Photoprotection revisited: Genetic and molecular approaches. *Annu Rev Plant Physiol Mol Biol* 50: 333–359
- Oelze J and Golecki JR (1995) Membranes and chlorosomes of green bacteria: Structure, composition and development. In: Blankenship RE, Madigan MT and Bauer CE (eds) *Anoxygenic Photosynthetic Bacteria*, pp 259–278. Kluwer Academic Publishers, Dordrecht.
- Olive J and Wellburn (1988) Supramolecular organization of the chloroplast and of the thylakoid membranes. In: Rochaix J-D, Goldschmidt-Clermont M and Merchant S (eds) *The Molecular Biology of Chloroplasts and Mitochondria in Chlamydomonas*, pp 233–254. Kluwer Academic Publishers, Dordrecht
- Olive J, Ajlani G, Astier C, Recouvreur M and Vernotte C (1997) Ultrastructure and light adaptation of phycobilisome mutants of *Synechocystis* PCC 6803. *Biochim Biophys Acta* 1319: 275–282
- Olson JM (1998) Chlorophyll organization and function in green photosynthetic bacteria. *Photochem Photobiol* 67: 61–75
- Pace NR (1997) A molecular view of microbial diversity and the biosphere. *Science* 276: 732–740
- Palmer JD (2000) A single birth of all plastids? *Nature* 405: 32–33
- Palmer JD and Delwiche CF (1996) Second-hand chloroplasts and the case of the disappearing nucleus. *Proc Natl Acad Sci USA* 93: 7432–7435
- Park YI, Sandström S, Gustafsson P and Öquist (1999) Expression of the *isiA* gene is essential for the survival of the cyanobacterium *Synechococcus* sp. PCC 7942 by protecting Photosystem II from excess light under iron limitation. *Molec Microbiol* 32: 123–129
- Partensky F, Hess WR and Vault D (1999) *Prochlorococcus*, a marine photosynthetic prokaryote of global significance. *Microbiol Mol Biol Rev* 63: 106–127
- Pysznik AM and Gibbs SP (1992) Immunochemical localization of Photosystem I and the fucoxanthin-chlorophyll *a/c* light-harvesting complex in the diatom, *Phaeodactylum tricornutum*. *Protoplasma* 189: 208–217
- Raymond J, Zhaxybayeva O, Gogarten JP, Gerdes SY and Blankenship RE (2002) Whole-genome analysis of photosynthetic prokaryotes. *Science* 298: 1616–1620
- Rémigy H-W, Hauska G, Müller SA and Tsiotis G (2002) The reaction centre from green sulphur bacteria: Progress towards structural elucidation. *Photosynth Res* 71: 91–98
- Sandström S, Park Y-I, Öquist G and Gustafsson P (2001) CP43', the *isiA* gene product, functions as an excitation energy dissipator in the cyanobacterium *Synechococcus* sp. PCC 7942. *Photochem Photobiol* 74: 431–437
- Sandström S, Ivanov AG, Park Y-I, Öquist G and Gustafsson P (2002) Iron stress responses in the cyanobacterium *Synechococcus* sp. PCC 7942. *Physiol Plant* 116: 255–263
- Sarcina M, Tobin MJ and Mullineaux CW (2001) Diffusion of phycobilisomes on the thylakoid membranes of the cyanobacterium *Synechococcus* 7942. *J Biol Chem* 276: 46830–46834
- Schubert W-D, Klukas O, Saenger W, Witt HT, Fromme P and Krauss N (1998) A common ancestor for oxygenic and anoxygenic photosynthetic systems: A comparison based on the structural model of Photosystem I. *J Mol Biol* 280: 297–314
- Schütz M, Brugna M, Lebrun E, Baymann F, Huber R, Stetter K-O, Hauska G, Toci R, Lemesle-Meunier D, Tron P, Schmidt C and Nitschke W (2000) Early evolution of cytochrome *bc* complexes. *J Mol Biol* 300: 663–675
- Sidler WA (1995) Phycobilisome and phycobiliprotein structures. In: Bryant DA (ed) *The Molecular Biology of Cyanobacteria*, pp 140–216. Kluwer Academic Publishers, Dordrecht
- Song X-Z and Gibbs S P (1995) Photosystem I is not segregated from Photosystem II in the green alga *Tetraselmis subcordiformis*. An immunogold and cytochemical study. *Protoplasma* 189: 267–280
- Sprague SG and Varga AR (1986) Membrane architecture of anoxygenic photosynthetic bacteria. In: Staehelin LA and Arntzen CJ (eds) *Photosynthesis III. Encyclopedia of Plant Physiology New Series, Vol 19*, pp 603–619. Springer-Verlag, Berlin
- Stackebrandt E, Rainey FA and Ward-Rainey N (1996) Anoxygenic phototrophy across the phylogenetic spectrum: Current understanding and future perspectives. *Arch Microbiol* 166: 211–223
- Staehelin LA (1986) Chloroplast structure and supramolecular organization of photosynthetic membranes. In: Staehelin LA and Arntzen CJ (eds) *Photosynthesis III. Encyclopedia of Plant Physiology New Series, Vol. 19*, pp 1–84. Springer-Verlag, Berlin
- Staehelin LA and van der Staay GWM (1996) Structure, composition, functional organization and dynamic properties of thylakoid membranes. In: Ort DR and Yocum CF (eds) *Oxygenic Photosynthesis: The Light Reactions*, pp 11–30. Kluwer Academic Publishers, Dordrecht
- Staehelin LA, Golecki JR, Fuller RC and Drews G (1978) Visualization of the supramolecular architecture of chlorosomes (Chlorobium type vesicles) in freeze-fractured cells of *Chloroflexus aurantiacus*. *Arch Microbiol* 119: 269–277
- Staehelin LA, Golecki JR and Drews G (1980) Supramolecular organization of chlorosomes (Chlorobium vesicles) and of their membrane attachment sites in *Chlorobium limicola*. *Biochim Biophys Acta* 589: 30–45
- Stoebe B and Kowallik KV (1999) Gene-cluster analysis in chloroplast genomics. *Trends Genet* 15: 344–347
- Swiatek M, Kuras R, Sokolenko A, Higgs D, Olive J, Cinque G, Müller B, Eichacker LA, Stern DB, Bassi R, Herrman RG and Wollman F-A (2001) The chloroplast gene *ycf9* encodes a Photosystem II (PS II) core subunit, PsbZ, that participates in PS II supramolecular architecture. *Plant Cell* 13: 1347–1367
- Tan S, Ducret A, Aebersold R and Gantt (1997) Red algal LHCI genes have similarities with both Chl *a/b* and *a/c*-binding proteins: A 21 kDa polypeptide encoded by *LhcaR2* is one of the six LHCI polypeptides. *Photosynth Res* 53: 129–140

- Teramoto H, Ono T and Minagawa J (2001) Identification of *Lhcb* gene family encoding the light-harvesting chlorophyll-*a/b* proteins of Photosystem II in *Chlamydomonas reinhardtii*. *Plant Cell Physiol* 42:849–856
- Ting CS, Rocap G, King J and Chisholm SW (2002) Cyanobacterial photosynthesis in the oceans: The origins and significance of divergent light-harvesting strategies. *Trends Microbiol* 10: 134–142
- Tomitani A, Okada K, Miyashita H, Matthijs HCP, Ohno T and Tanaka A (1999) Chlorophyll *b* and phycobilins in the common ancestor of cyanobacteria and chloroplasts. *Nature* 400: 159–162
- Trissl H-W and Wilhelm C (1993) Why do thylakoid membranes from higher plants form grana stacks? *Trends Biochem Sci* 18: 415–419
- Turner S (1997) Molecular systematics of oxygenic photosynthetic bacteria. *Pl Syst Evol (Suppl)* 11:13–52
- Turner S, Pryer KM, Miao VPW and Palmer JD (1999) Investigating deep phylogenetic relationships among cyanobacteria and plastids by small subunit rRNA sequence analysis. *J Eukaryot Microbiol* 46: 327–338
- Urbach E, Scanlon DJ, Distel DL, Waterbury JB and Chisholm SW (1998) Rapid diversification of marine picophytoplankton with dissimilar light-harvesting structures inferred from sequences of *Prochlorococcus* and *Synechococcus* (cyanobacteria). *J Mol Evol* 46: 188–201
- van der Staay GWM, Yurkova N and Green BR (1998) The 38 kDa chlorophyll *a/b* protein of the prokaryote *Prochlorothrix hollandica* is encoded by a divergent *pcb* gene. *Plant Mol Biol* 36: 709–716
- van Thor JJ, Mullineaux CW, Matthijs HCP and Hellingwerf KJ (1998) Light-harvesting and state transitions in cyanobacteria. *Botanica Acta* 111: 430–443
- Vassilieva EV, Frigaard N-U and Bryant DA (2000) Chlorosomes: The light-harvesting complexes of the green bacteria. *The Spectrum* 13: 7–13
- Vassilieva EV, Stirewalt VL, Jakobs CU, Frigaard N-U, Baker MA, Sotak AM and Bryant DA (2002) Subcellular localization of chlorosome proteins in *Chlorobium tepidum* and characterization of three new chlorosome proteins: CsmF, CsmH and CsmX. *Biochemistry* 41: 4358–4370
- Verméglio A and Joliot P (1999) The photosynthetic apparatus of *Rhodobacter sphaeroides*. *Trends in Microbiol* 7: 435–440
- Verméglio A and Joliot P (2002) Supramolecular organisation of the photosynthetic chain in anoxygenic bacteria. *Biochim Biophys Acta* 1555: 60–64
- Wilson RJM (2002) Progress with parasite plastids. *J Mol Biol* 319: 257–274
- Wolfe GR, Cunningham FX Jr, Durnford DG, Green BR and Gantt E (1994) Evidence for a common origin of chloroplasts with light-harvesting complexes of different pigmentation. *Nature* 367: 566–568
- Wraight CA and Clayton RK (1973) The absolute quantum efficiency of bacteriochlorophyll photooxidation in reaction centres of *Rhodospseudomonas sphaeroides*. *Biochim Biophys Acta* 333: 246–260
- Yoon HS, Hackett JD, Pinto G and Bhattacharya D (2002) The single, ancient origin of chromist plastids. *Proc Natl Acad Sci USA* 99: 15507–15512
- Zak E, Norling B, Maitra R, Huang F, Andersson B and Pakrasi HB (2001) The initial steps of biogenesis of cyanobacterial photosystems occur in plasma membranes. *Proc Natl Acad Sci USA* 98: 13443–13448
- Zauner S, Fraunholz M, Wastl J, Penny S, Beaton B, Cavalier-Smith T, Maier U-G and Douglas S (2000) Chloroplast protein and centrosomal genes, a tRNA intron, and odd telomeres in an unusually compact eukaryotic genome, the cryptomonad nucleomorph. *Proc Natl Acad Sci USA* 97: 200–205
- Zhang Z, Green BR and Cavalier-Smith T (1999) Single gene circles in dinoflagellate chloroplast genomes. *Nature* 400: 155–159
- Zhang Z, Green BR and Cavalier-Smith T (2000) Phylogeny of ultra-rapidly evolving dinoflagellate chloroplast genes: A possible common origin for sporozoan and dinoflagellate plastids. *J Mol Evol* 51: 26–40
- Zouni A, Will H-T, Kern J, Fromme P, Krauss N, Saenger W and Orth P (2001) Crystal structure of Photosystem II from *Synechococcus elongatus* at 3.8 Å resolution. *Nature* 409: 739–743

# Chapter 2

## The Pigments

Hugo Scheer\*

München Botanisches Institut der Universität Menzinger Str. 67, D-80638 München, Germany

Summary .....	29
I. Introduction .....	30
II. Functions: A Short Overview .....	30
A. Light Absorption .....	30
B. Energy Transfer to Reaction Centers .....	30
C. Protection (of the Photosynthetic Apparatus) Against Light-Induced Damage .....	31
D. Structure Stabilization .....	33
III. The Pigments .....	34
A. Chlorophylls .....	34
1. Structures and Distribution .....	34
a. 'Green' Chlorophylls: Chls <i>a</i> , <i>b</i> , <i>d</i> .....	34
b. Chlorophylls of the Porphyrin Type: The Chlorophylls <i>c</i> .....	35
c. Bacterial Chlorophylls: Bacteriochlorin-Type Pigments .....	35
d. Bacterial Chlorophylls of the Chlorin Type .....	36
e. Transmetalated Chlorophylls .....	37
f. 'Minor' Chlorophylls .....	42
2. Biosynthesis .....	42
3. Spectroscopy .....	46
B. Phycobiliproteins .....	48
1. Structures .....	48
2. Biosynthesis .....	50
3. Spectroscopy .....	53
C. Carotenoids .....	56
1. Structures .....	56
2. Biosynthesis .....	60
3. Spectroscopy .....	63
a. The $S_0 \rightarrow S_2$ Transition .....	65
b. The $S_0 \rightarrow S_1$ Transition .....	66
c. Triplet State .....	67
IV. Analytics .....	67
A. Extraction .....	68
B. Spectroscopic Analysis .....	68
C. Chromatography .....	69
V. Pigment Substitution Methods .....	69
References .....	71

### Summary

The pigments of antenna systems have several functions. 1: they absorb light efficiently, 2: they transfer the excitation energy with minimum losses to the reaction centers, 3: they degrade excess energy to heat, and 4: they contribute to the stabilization and regulation of the photosynthetic apparatus. The pigments used to fulfill these functions are chlorophylls, phycobilins and carotenoids. This chapter gives the structures, biosynthetic pathways and spectroscopic properties for each pigment type. Examples are given of strategies to study excitation energy transfer by selective introduction of specifically modified chromophores.

---

\*Email: [scheer-h@botanik.biologie.uni-muenchen.de](mailto:scheer-h@botanik.biologie.uni-muenchen.de)

## I. Introduction

Photosynthetic antennas have to perform three functions. 1: they absorb light efficiently, 2: they transfer the required excitation energy with minimum losses to the reaction centers, 3: they degrade excess energy with minimum damage to the photosynthetic apparatus. The pigments used to fulfill these functions are chlorophylls, phycobilins and carotenoids. The first two are mainly involved in light-harvesting, the absorption of photons and the efficient transfer of excitation energy, but there is evidence that they also can be modified to quench it, in a yet poorly understood fashion. The carotenoids contribute, too, to light-harvesting, but they are indispensable in light protection for degrading potentially damaging excess excitation energy or reactive oxygen species to (mostly) harmless heat. Other cofactors may be involved in this process, most notably the chloroquinone of green bacteria (Frigaard et al., 1998); these are not treated here, and the reader is referred to the specialized chapters.

The antenna chromophores, which are almost always bound to proteins, also contribute to the stabilization and regulation of the photosynthetic complexes. This chapter will focus on the occurrence, structures, biosyntheses and spectroscopic properties of the pigments in monodisperse solution and aggregates, and will give a general survey on their properties in the native environment. The detailed properties of the pigments in the protein environment of the native complexes will be dealt with in Chapters 5–11, and the general principles of excitation by light, excited state reactivity and dynamics are treated in chapter 3.

*Abbreviations:*  $\lambda$  – wavelength [nm];  $\epsilon$  – molar extinction coefficient [ $M^{-1} cm^{-1}$ ]; APC – allophycocyanin; BChl – bacteriochlorophyll;  $B_x, B_y$  – higher-energy absorption bands of tetrapyrroles in Vis/UV; Chl – chlorophyll; GGPP – geranylgeranyl pyrophosphate; Glc – glucose; HMB – hydroxymethylbilan; IC – internal conversion; ISC – intersystem crossing; Lac – lactose; NIR – near infra-red spectral range (700–1200 nm); NMR – nuclear magnetic resonance; Nomenclature – IUPAC numbering is used throughout; PΦB – phytochromobilin; PBG – porphobilinogen; PC – phycocyanin; PCB – phycocyanobilin; PE – phycoerythrin; PEB – phycoerythrobilin; PEC – phycoerythrocyanin; Phy – phytochrome; PP – pyrophosphate; protogen – protoporphyrinogen; PVB – phycoviolobilin;  $Q_x, Q_y$  – low-energy absorption bands of tetrapyrroles in Vis/NIR; RC – reaction center (type I and type II relate to the homologies with PS I and PS II, respectively); uro'gen – uroporphyrinogen; UV – ultra spectral range (200–400 nm); Vis – visible spectral range (400–700 nm)

## II. Functions: A Short Overview

The chromophores of photosynthetic light-harvesting systems have several functions. These are covered in detail in other chapters and books (Frank et al., 1999; Scheer, 1991a, 1994) and will be summarized here only in the context of the properties of the pigments detailed further in this chapter.

### A. Light Absorption

Antennas serve to increase the absorption cross-section of reaction centers. Consequently, the chromophores have, in their native environment (see spectroscopy of biliproteins) very intense absorptions ( $\epsilon \approx 10^5 M^{-1} cm^{-1}$ ), which in combination cover the entire range of the photosynthetically useful spectrum (330–900 and 1000–1100 nm). The gap results from the absorption of water at 960 nm, where no light-harvesting system has evolved. Chlorophyll (Chl) *a*, *b*, *d* and the bacteriochlorophylls (BChl) cover the wings of this range efficiently, with strong absorptions in the 330–480 nm and 630–1050 nm ranges. Filling the remaining 'green gap' is of particular importance in aquatic environments, where green light often prevails and the overall intensity is reduced. The 'green gap' is filled by the absorptions of the *c*-chlorophylls, the carotenoids and the biliproteins. Higher plants lack *c*-chlorophylls and biliproteins, and their carotenoids are quite inefficient in light-harvesting. Plants appear to have evolved a different strategy by investing more heavily in structure in the competition for light, on both macroscopic (growth towards the light) and microscopic scales (leaf structure, internal reflection).

### B. Energy Transfer to Reaction Centers

From the site of excitation to the reaction center where the energy *transduction* takes place, excitation energy has to be *transported* over considerable distances (e.g.  $\leq 50$  nm in the phycobilisome). This is only possible by *radiationless* transfer, for which three basic mechanisms are discussed (Chapter 3, Parson and Nagarajan): at long distances (theoretically up to 10 nm), only *Förster* transfer can operate, by which the energy hops in discrete steps from one pigment to the other. At shorter distances ( $\leq 2$  nm), exciton coupling can occur, by which two or more pigments are excited simultaneously and the excitation is consequently delocalized over the entire

‘unit’. Both mechanisms arise from dipolar coupling and are strongly distance-dependent, but also depend on the relative orientation and spectral properties of the pigments. At very short (contact) distances, an electron exchange mechanism (Dexter mechanism) can operate. Electron exchange has been proposed in particular for energy transfer from carotenoids to chlorophylls, in order to compete with their very rapid internal conversion (Section C.3). The close contact between the donor (carotenoid) and acceptor is clearly seen in all sufficiently resolved structures of light-harvesting chlorophyll-carotenoid-proteins (Kühlbrandt et al., 1994; Freer et al., 1996; Hofmann et al., 1996; Koepke et al., 1996). Since electron exchange, like electron transfer, requires orbital overlap, it is expected to be critically dependent on very small geometric changes. Electron exchange is also the major mechanism of triplet transfer (see ‘protection’).

When discussing *energy transfer efficiency*, two figures have to be considered separately. The first is the *quantum efficiency*  $\Phi_q$ , which describes the number  $n_{RC}$  of excitation quanta reaching the reaction centers (RC) relative to the number  $n_{abs}$  of quanta absorbed:

$$\Phi_q = n_{RC} / n_{abs} \quad (1)$$

The quantum efficiency  $\Phi_q$  can reach 100% with biliproteins and chlorophylls, it is more variable with the carotenoids, depending on whether their main functions are light-harvesting or light-protection (see below). The second factor is the *energetic efficiency*  $\Phi_e$ , which is defined by the energy  $e_{RC}$  used by the RC for charge separation relative to the energy  $e_{abs}$  of a photon absorbed by the light-harvesting apparatus.

$$\Phi_e = e_{RC} / e_{abs} \quad (2)$$

$\Phi_e$  relates to the energy gap between a light-quantum absorbed by the antenna and the  $S_1$  excitation energy of the RC, or more precisely of the primary donor in the RC. In extreme cases  $\Phi_e$  can be quite low; examples are the absorption by a carotenoid ( $\lambda_{max} \approx 500$  nm) or by an antenna BChl in the Soret band ( $\lambda_{max} \approx 350$  nm) in *Blastochloris* (*Rhodospseudomonas*) *viridis* and transfer to the RC ( $\lambda_{max} \approx 1000$  nm), where  $\Phi_e \approx 50\%$  and  $\approx 35\%$ , respectively. These losses are a consequence of the differentiation of the photosynthetic apparatus into antennas and reaction centers and the evolution of only a few types of

reaction centers, all absorbing in the low-energy region of the spectrum. This energy gap can, however, be used in part to funnel the excitation along an energy gradient towards the RC, with the phycobiosome as the prime example (Chapters 9 (Mimuro and Kikuchi) and 17 (Grossman et al.)). It should be noted that, curiously,  $\Phi_e$  can also be  $>100\%$ . A classical example is again *Blastochloris viridis*, where the antenna absorption peaks at 1025 nm, the RC at 980 nm ( $\Phi_e \approx 105\%$ ). Another example is the antenna of *Ostreobium* with Chl *a* populations extending their absorption maxima in the NIR to  $\lambda_{max} = 740$  nm, which feed PS I ( $\lambda_{max} 700$  nm), resulting in  $\Phi_e \approx 106\%$  (Fork and Larkum, 1989). Very recently the extreme case of an antenna absorbing at 963 nm has been reported for a BChl-*a* containing purple bacterium with an apparently conventional reaction center ( $\lambda_{max} 870$  nm), resulting in  $\Phi_e = 111\%$  (Permentier et al., 2001). The gained energy is principally of thermal origin. The common mechanism is the establishment of a Boltzmann equilibrium, and it is presently not clear if homogenous band broadening is involved in some cases (Chapter 3, Parson and Nagarajan) and the discussion by Trissl, 1993).

### C. Protection (of the Photosynthetic Apparatus) Against Light-Induced Damage

The pigments involved most intimately in photo-protection are the carotenoids, which act by a variety of protecting mechanisms against damage by light, directly and indirectly, in case the system becomes over-excited. These protective mechanisms are essential to photosynthesis in a varying light environment, but they also decrease the efficiency of photosynthesis and therefore have to be tightly controlled and/or set up in a way so that they only take action as ‘emergency valves’ (Chapters 7, 13–15)

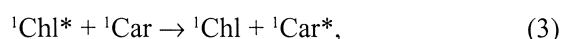
Most of the protective mechanisms rely on the very rapid internal conversion (IC) in carotenoids, which in turn is (mainly?) due to the high density of vibrational states in these rather flexible molecules in combination with the strongly forbidden  $S_0 > S_1$  excitation (see below). A second important factor is the very low energy of carotenoid triplets, which in many carotenoids is below that of chlorophylls and also below that of singlet oxygen (1274 nm, 7849  $\text{cm}^{-1}$  or 93.9 kJ/mole).

In the first protection mechanism, carotenoids simply act as filters that reduce the amount of blue and near-UV light reaching the photosynthetic



apparatus, a function they also perform in non-photosynthetic organisms or tissue. Examples are the aerobic bacteriochlorophyll-producing bacteria, where many carotenoids do not appear in the fraction of bacteriochlorophyll proteins (Takaichi, 1999; Shimada, 1995), and the algae, *Hematococcus pluvialis* (astaxanthin, Kobayashi et al., 1991a) and *Dunaliella bardawil* (9-*cis* and all-*trans*- $\beta,\beta'$ -carotenes, Ben-Amotz et al., 1989), where the majority of carotenoids are deposited in 'oleosome' type organelles. These organisms produce carotenoids in such amounts that they are used as a commercial sources for natural astaxanthin and  $\beta,\beta$ -carotene, respectively (Ben-Amotz et al., 1989; Kobayashi et al., 1991a).

Secondly, carotenoids can act as quenchers of chlorophyll excited singlet states (excited states are marked by asterisks in the following):

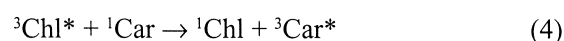


provided that the lowest energy of their singlet excited state is below that of the chlorophyll (see below). Since this energy can be tuned by the addition or removal of double bonds, the function of carotenoids can be switched between those of energy donors (= antenna pigment) and acceptors (= 'lightning rods'). The switching between light-harvesting and energy dissipation has been studied in considerable detail in the violaxanthin/zeaxanthin cycle of plants, where in particular the minor LHCII complexes have been implicated (Crimi et al., 2000; Chapters 3, 7, 13–15). The light-harvesting pigment violaxanthin, containing seven conjugated double bonds, is reversibly doubly de-epoxidized to zeaxanthin, containing nine conjugated double bonds (see Fig. 7B for structures), leading to an extension of the conjugation chain by two double bonds ( $\Delta 5$  and  $\Delta 5'$ ). Similar epoxidation-deepoxidation cycles, acting as a line of defense against light-induced damage, have been identified in algae, where they involve e.g. diadinoxanthin and diatoxanthin (Fig. 7B). The irreversible oxidation of  $\beta,\beta$ -carotene to zeaxanthin in the PS II-RC has recently been discussed as a potential signal for light-stress (Jahns et al., 2000).

The *non-photochemical quenching* mechanism of carotenoids is not understood at present. The most straightforward rationalization is that  $S_1$  of violaxanthin is above that of (neighboring) Chl *a* molecules, that of zeaxanthin below; the former

would then be a singlet energy donor, the latter an acceptor (and therefore quencher). One crucial problem is the determination of the singlet state energies of zeaxanthin and violaxanthin in situ, with recent data indicating that these are similar and below the energy of Chl *a* (Frank et al. 2000b). A thermally activated mechanism (see above and Chapters 3, 7, 13–15) could be operative, but it is possible that the carotenoids play yet another role. As a result of their generally very short-lived excited states, energy transfer from and to carotenoids is efficient only at very short distances between donor and acceptor (Chapter 3, Parson). Small structural changes can therefore result in large variations of energy-transfer efficiency, in particular for the Dexter mechanism.

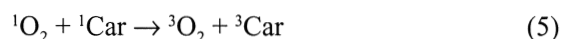
Thirdly, due their unusually low-lying triplet states, carotenoids can act as energy acceptors (quenchers) of chlorophyll triplets, even if their singlet states are above those of the chlorophylls. This reaction proceeds by the spin-allowed reaction:



Again, a close contact is required, because this transfer probably occurs by the electron exchange mechanism. While the formation of chlorophyll triplets by intersystem crossing is generally a slow process ( $\mu\text{s}$ ), it can be several orders of magnitude faster in photosynthetic organisms, as shown in detail in RCs of purple bacteria. Here, triplets of the primary donor  $^1\text{P870}$  are produced by radical-pair recombination when the quinone(s) are over-reduced (Hoff, 1993; Volk et al., 1995). Only this triplet state of the primary donor, not the singlet state, is quenched by the nearby carotenoids via an energy transfer chain involving an 'accessory' chlorophyll (BChl  $B_B$  in bacterial RC) as an intermediate (Frank et al., 1996; Angerhofer et al., 1998). It should be noted, however, that the mechanism has been studied in detail in only few cases, and that e.g. the RC of *Bl. viridis* contains a carotenoid (1,2-dihydroneurosporene) whose triplet energy is above that of the primary donor, a pair of BChl *b* molecules. This may be a reason for the low oxygen tolerance of this species (Laußermair and Oesterheld, 1992). Triplets can also be produced in antenna complexes, where the mechanism is unclear but may also involve radical recombination reactions (Law and Cogdell, 1998).

Last but not least, carotenoids are quenchers of

reactive oxygen species ( $^1\text{O}_2$ ,  $\text{OH}^-$ ) in case the aforementioned first defense lines become saturated or inefficient. Since the reaction



is spin-allowed, carotenoids with sufficiently low-lying triplet states can rapidly quench singlet oxygen. Their triplets are so low in energy that damaging effects can probably be neglected. They are also localized and comparably short-lived as a result of their conformational flexibility, charge transfer states and/or phytoisomerization. The abundant  $\beta,\beta$ -carotene and violaxanthin are, in solution, excellent quenchers of singlet oxygen (Edge and Truscott, 1999). The major quenching is believed to be photophysical with a recovery of the carotenoid *via* ISC-relaxation of  $^3\text{Car}$  to  $^1\text{Car}_0$ . However, a *non-productive photochemical quenching* with a concomitant oxygenation of the carotenoid should also be considered (Young, 1993a). A multitude of oxygenated carotenoids is produced if aerobic solutions of chlorophylls and  $\beta,\beta'$ -carotene are irradiated, and there is evidence that at least some of them are strong oxidants (Tregub et al., 1996; Edge and Truscott, 1999; Fiedor et al., 1999). Oxygenated carotenoids have also been identified in plant caroteno-chlorophyll proteins such as LHCII upon irradiation, but their importance and quantitation *in vivo* are unclear (R. Jennings, personal communication). Since epoxides are among the primary oxidation products of carotenoids, it can be speculated that the violaxanthin-zeaxanthin cycle is an adaptive utilization of such oxidations arising with the increasing amounts of oxygen during evolution.

Relatively little is known about the molecular mechanisms of quenching of other reactive oxygen species ( $\text{O}_2^-$ ,  $\text{OH}^-$ , peroxides). The formation of carotenoid peroxides (Young, 1993a) and of radical pairs by electron transfer (Frank et al., 1999) are among these processes. In non-photosynthetic organisms, the concept of terminating lipid peroxidation by the more expendable carotenoid molecules (Burton, 1990) has been advanced, but this may also apply to photosynthetic organisms.

Compared to the carotenoids, much less is known about the protective role, if any, of chlorophylls and biliproteins. It should be noted that the phycobiosomes conspicuously lack carotenoids, which distinguishes them from all other antennas. Biliprotein

triplets have been implicated in the generation of reactive oxygen species by biliproteins (He et al., 1996), but to the best of this author's knowledge they have never been positively identified, and several checks by ODMR have failed (A. Angerhofer and H. Scheer, unpublished). Chl cation radicals, which can be generated in antennas under saturating conditions, are good quenchers of Chl excited states (Law and Cogdell, 1998).

#### D. Structure Stabilization

As products of a co-evolution, all chromophores are integral components of the light-harvesting systems. As such, they are also integral to the systems' stabilities. This role is most obvious for the chlorophylls, which as free pigments show a remarkable potential for self-organization in both hydrophobic (Katz et al., 1978; van Rossum et al., 1998) and hydrophilic-aqueous media (Gottstein and Scheer, 1983; Katz et al., 1991; Scherz et al., 1991; Agostiano et al., 2000). Before the identification of chlorophyll proteins, speculations on the organization of light-harvesting complexes had focused on the self-aggregation of chlorophylls as a driving force. This model has been revived in two directions more recently. Firstly, X-ray structures have shown that chlorophylls are often so close to each other that considerable chlorophyll-chlorophyll interactions can be expected (Tronrud and Matthews, 1993; Kühlbrandt et al., 1994; Freer et al., 1996; Koepke et al., 1996; Klukas et al., 1999), with the pigments arranged in geometries that are very similar to those found in chlorophyll aggregates in mixed organic-aqueous media (Scherz et al., 1991). Strong interactions among the chlorophylls have been substantiated in particular in bacterial antennas (van Rossum et al., 1998; Leupold et al., 1999; Fiedor et al., 2000). Assembly problems are frequently observed if amino acids that bind to the central Mg are modified (Olsen et al., 1997). Together with the lack of formation of apoprotein complexes in the absence of chlorophylls (Kim et al., 1994), this points to a considerable contribution of chlorophylls to the formation and stability of the light-harvesting pigment-protein complexes. The thermodynamics of the influence of the central metal in the association of bacterial LH1 has been studied by Lapouge et al. (2000). Secondly, the presence of only very small amounts of protein in the chlorosomes of green bacteria (Chapter 6,

Blankenship and Matsuura) has revived the ideas of chlorophyll-only aggregates (Hirota et al., 1992; van Rossum et al., 1998; but see Niedermeier et al., 1992).

The contributions of carotenoids to the stability of complexes have been studied in some detail. Photosynthetic organisms treated with herbicides inhibiting carotenoid biosynthesis (Bramley, 1993), or mutations leading to the loss of carotenoids, do not form certain light-harvesting complexes, including the Chl *b*-containing complexes of green plants (Chapter 7, van Amerongen and Dekker), or these complexes are less stable. They often lack other components such as BChl *a*-B800 in the B800-850 complex of purple bacteria, or their assembly is modified (Lang and Hunter, 1994; Loach and Parkes-Loach, 1995) or inhibited (Paulsen, 1999) (Chapter 5, Cogdell et al.). For a more detailed discussion of the structural role of carotenoids, the reader is referred to a recent book in the same series (Frank et al., 1999).

Much less is known about the structural role of bilin chromophores. Since they are present in an energetically unfavorable configuration, it has been suggested that part of the folding energy of the protein is consumed for the 'stretching' of the chromophore (Scheer, 1982). Inhibition of the PCB- $\alpha$ -cys84 lyase in cyanobacteria leads to the expression of phycocyanin lacking this—and only this—chromophore, albeit at reduced levels. On the other hand, the aggregation of apo-biliproteins is considerably weaker than that of the holoproteins, which points to a contribution of the chromophores in increasing protein-protein interactions. It should be noted that, in particular, the  $\alpha$ -84 chromophores of cyanobacterial and rhodophytan biliproteins are located at the boundary between monomers ( $\alpha\beta$ ) in the native trimeric ( $\alpha\beta$ )<sub>3</sub> building blocs of the phycobilisome, and participate in the intermonomer interactions (Schirmer et al., 1987; Duerring et al., 1990; Ficner and Huber, 1993; Brejc et al., 1995; Reuter et al., 1999). Inactivation of phycobilin-cys- $\alpha$ 84 lyases and/or other mutations inhibiting the attachment of the  $\alpha$ -84 chromophore result generally in decreased levels of the corresponding biliprotein (Beguín et al., 1985; Swanson et al., 1992; Jung et al., 1995; Kahn et al., 1997), but it is currently not clear if this results from protein destabilization, feedback inhibition, or both.

### III. The Pigments

#### A. Chlorophylls

##### 1. Structures and Distribution

Chlorophylls are cyclic tetrapyrroles carrying a characteristic isocyclic five-membered ring, which is biosynthetically derived from the C-13 propionic acid side-chain of the common precursor, protoporphyrin IX (see IUPAC-IUB Joint commission biochemical nomenclature (1979, 1988) for nomenclature). They generally contain a central magnesium ion ( $Mg^{++}$ ), but one group of purple bacteria contains bacteriochlorophylls (BChl) in which  $Mg^{++}$  is replaced by  $Zn^{++}$ . Reaction centers of type II also contain the metal-free pheophytins, which participate in charge separation. Chemically, the chlorophylls can be characterized by the degree of unsaturation of the macrocycle: 1.) the fully unsaturated porphyrin system is present in the *c*-type chlorophylls of chromophyte algae and some prokaryotes (Fig. 1c), 2.) the 17,18-dihydroporphyrin (chlorin) system is present in the Chls *a*, *b* and *d* of oxygenic organisms (Fig. 1a), and also in the BChls *c*, *d* and *e* of green anoxygenic bacteria (Fig. 1b), and 3.) the 7,8,17,18-tetrahydroporphyrin (=bacteriochlorin) system is present in the bacteriochlorophylls *a*, *b* and *g* of anoxygenic bacteria (Fig. 1d). The three chlorophyll types have distinct spectroscopic properties: The *c*-type chlorophylls absorb moderately in the 620 nm region and strongly in the 400–450 nm region, the chlorin-type chlorophylls are characterized by two intense absorptions at the edges of the visible spectral region (Vis) at 400–470 and 640–700 nm, and the bacteriochlorin-type chlorophylls absorb only weakly in the Vis, but have two intense absorptions outside, in the near ultraviolet (UV) and the near infrared (NIR).

##### a. 'Green' Chlorophylls: Chls *a*, *b*, *d*

The most abundant chlorophyll is chlorophyll *a* (Chl *a*, Fig. 1a), which is present in the reaction centers of all and the light-harvesting systems of almost all oxygenic organisms, as well as in the RC of some anoxygenic bacteria (Kobayashi et al., 2000) (Tables 1, 2). Its absorption is intense ( $\epsilon \approx 10^5 \text{ M}^{-1}\text{cm}^{-1}$ ), but restricted to two narrow bands at the edges of the visible spectrum ( $\approx 430$  and  $\approx 680$  nm); it is therefore almost always accompanied by other pigments. These

are mainly chlorophylls, too, in the prochlorophytes, in the modern 'green line' of photosynthetic organisms (green algae, higher plants), and in the chromophytes. The prochlorophytes contain generally chlorophyll *b* (Chl *b*, Fig. 1a). With absorption bands at 460 and 650 nm, Chl *b* reduces the 'green gap,' the absorption gap in the spectral region from 500 to 600 nm. Another, relatively rare chlorophyll of the chlorin-type is Chl *d*, which has distinctly red-shifted absorptions compared to Chl *a*. While frequently found in small amounts in red algae (Allen, 1966), Chl *d* has been identified as the major pigment in a Chl *c*-containing prochlorophyte, *Acaryochloris marina* (Miyashita et al., 1997).

#### *b. Chlorophylls of the Porphyrin Type: The Chlorophylls c*

The chromophytes and some procaryotes contain members of the chlorophyll *c* family (Stauber and Jeffrey, 1988; Jeffrey et al., 1997; Miyashita et al., 1997). They absorb in the 'green gap,' the spectral region where Chl *a* and *b* absorb only weakly. However, their maximum absorption in the visible spectral range is several times less than that of Chl *a* or *b* (Table 2), so more chromophores are needed to achieve the same rate of excitation. All *c*-type chlorophylls are porphyrins, and most of them contain an acrylic side chain at C-17 (Fig. 1c). An important structural feature of most (but not all, see Fig. 1b) *c*-type chlorophylls is the free acrylic or propionic acid side-chain at C-17; they are not esterified like the other Chls and therefore are much more polar compounds.

The diversity of known *c*-type chlorophylls has recently increased considerably, and several new *c*-type chlorophylls have been identified over the past decade. [8-vinyl]-protochlorophyllide *a* (3,8-divinyl-pheoporphyrin *a*-Mg-monomethylester), which in green plants is a precursor to Chls *a* and *b*, has been shown a true antenna pigment in symbiotic prokaryotes (Helfrich et al., 1999). Furthermore, while the 'classical' *c*-type chlorophylls carry a free C-17 acrylic acid side chain, less polar pigments of this type have been known for more than ten years (Stauber and Jeffrey, 1988). For several of these new pigments, neither the structures nor the functional roles are presently established. Based on improved chromatographic systems, Zapata et al. have begun to identify several of them (Jeffrey et al., 1999; Zapata et al., 2000). The fascinating structure shown

in Fig. 1c has recently been suggested for one of them, in which Chl *c* is covalently linked to a galactolipid (Garrido et al., 2000). In view of the variety of (particularly marine) photosynthetic organisms, more surprises can be anticipated (Jeffrey et al., 1997; Jeffrey and Anderson, 2000). In this context, the presence of (non-covalently bound) lipid molecules in the vicinity of chlorophyll should also be mentioned; these have been found in the water-soluble PCP complex from *Amphidinium carterae* (Hofmann et al., 1996) and in the PS I core complex (Jordan et al., 2001).

#### *c. Bacterial Chlorophylls: Bacteriochlorin-Type Pigments*

All pigments of anoxygenic photosynthetic bacteria are denoted as bacteriochlorophylls. Many of them are true bacteriochlorins (=7,8,17,18-tetrahydroporphyrins), characterized by a partly saturated ring B in addition to ring D. The major spectral consequence is a considerable red-shift of the  $Q_y$ -absorption band to 750–800 nm in solution, and even more to 800–1020 nm in situ, and a blue-shifted Soret-band (<400 nm). Thereby, the absorptions are extended in both regions beyond those of all other chlorophylls. The most widely distributed bacteriochlorophyll, bacteriochlorophyll *a* (BChl *a*, Fig. 1d), is present in RCs and the core-antennas of most anoxygenic bacteria, as well as in the peripheral antennas of the purple bacteria (Scheer, 1991b). In some bacteria, it is replaced by the structurally related BChl *b*, which carries an ethylidene substituent at C-8 (instead of the ethyl group of BChl *a*) (Scheer et al., 1974; Steiner et al., 1981). The major pigment of the strictly anaerobic Gram-positive heliobacteria is BChl  $g_F$  (Fig 1d, the subscript refers to the esterifying alcohol, farnesol, see below), which is involved in light-harvesting as well as in electron transport in the functionally integrated type I-RC complex (Michalski et al., 1987).

The BChls *a*, *b* and *g* show distinct variations in their C-17<sup>3</sup>-esterifying alcohols. In certain purple bacteria, pigments with more highly unsaturated terpenoid alcohols can replace the BChl  $a_p$  (Katz et al., 1972) or BChl  $b_p$  (Steiner et al., 1981) (the subscript 'p' denotes phytol as esterifying alcohol). These modified pigments are often functional, but the role of the modified alcohols remains unclear. They have no influence on the absorption in monodisperse solution, but do affect aggregation of

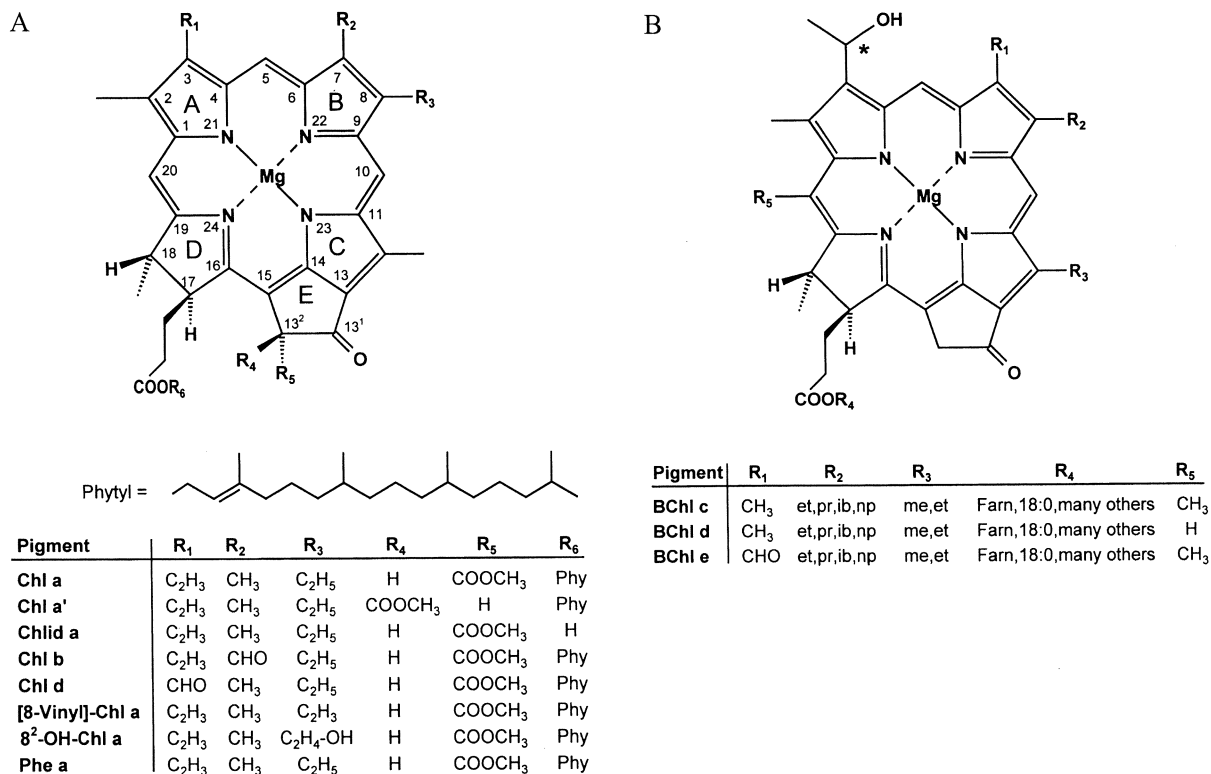


Fig. 1. Structures of chlorophylls (Chl) and bacteriochlorophylls (BChl). A: Plant chlorophylls (chlorins) with a single bond between C-17 and C-18. Only phytol is shown, the most abundant esterifying alcohol at the C-17 propionic acid side-chain. Note that Phe *a* lacks the central Mg. Numbering according to IUPAC-IUB Joint commission biochemical nomenclature, 1979, 1988). B: Bacterial chlorophylls of the chlorin type, with a single bond between C-17 and C-18: Bacteriochlorophylls *c*, *d*, *e*. (The putative BChl *f* is not shown.) These pigments, which occur in chlorosomes, are also referred to as Chlorobium chlorophylls in the older literature. Abbreviations: 18:0 = stearyl, et = ethyl, ib = isobutyl, np = neopentyl, pr = propyl. C-3<sup>1</sup> (marked by an asterisk) can occur in two epimeric configurations; the 3<sup>1</sup>R-to-3<sup>1</sup>S epimer ratio varies with the size of the C-8 substituent. (Continued on next page.)

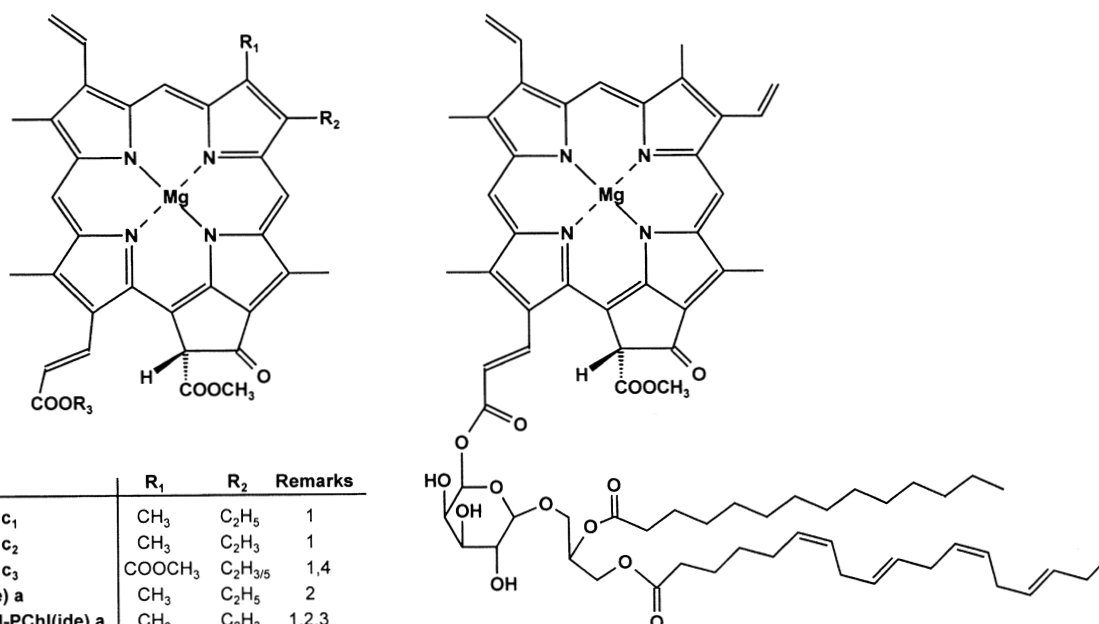
the pigments (Scheer et al., 1985). In the LH2 structure of *Rhodospseudomonas acidophila*, the 'phytyl-tails' show remarkable interactions among each other and with the carotenoids (Freer et al., 1996). It should also be noted that in *Rhodospirillum rubrum*, the bacteriochlorophylls of the RC are esterified with phytol, and those in the antennas with geranylgeraniol (Walter et al., 1979).

#### d. Bacterial Chlorophylls of the Chlorin Type

The variations among the structures are much larger and characteristic of the second group of bacteriochlorophylls, the BChls *c*, *d*, *e* and *f* (Fig. 1b). These BChls are abundant in green bacteria, where they are the main constituents of the peripheral antenna, the extra-membraneous chlorosomes (Chapter 6, Blankenship and Matsuura). Chemically, and in spite

of their names, the BChls *c*, *d* and *e* are not bacteriochlorins but rather chlorins. In addition, they show a number of unusual features and, based on a remarkable structural diversity, an exceptional number of structures whose significance is hardly understood at present (Blankenship et al., 1995b, Oelze and Golecki, 1995). Unifying features of these pigments are the lack of the 13<sup>2</sup>-COOCH<sub>3</sub> substituent of the isocyclic ring, and the presence of a CHOH-CH<sub>3</sub> substituent at C-3. The *c*- and *e*-type BChls are characterized by a 20-CH<sub>3</sub> substituent and, the *e*- (as well as putative *f*-) type BChls also carry a 7-CHO substituent, as does Chl *b*. They show large variations in the esterifying alcohols (Caple et al., 1978), they can be singly (C-12) and even multiply methylated (C-8<sup>2</sup>, C-12, C-20), and they can be epimers at C-3<sup>1</sup> (Fig. 1c) (Smith and Simpson, 1986; Tamiaki et al., 1994). Not all theoretically possible combinations of

C



D

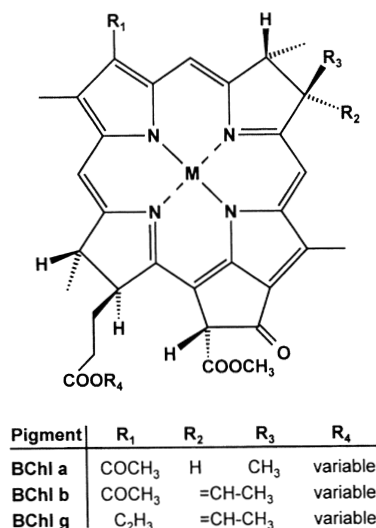


Fig. 1. (Continued from previous page) C: Chlorophylls of the porphyrin-type. Note the distinction between chlorophylls (Chl, esterified at C-17<sup>3</sup>, R<sub>3</sub> = esterifying alcohol) and chlorophyllides (Chlide, free C-17<sup>3</sup> acid group, R<sub>3</sub> = H), which is often blurred in the literature. Left: chlorophyll *c*-group and protochlorophyllides (no double bond between C-17<sup>1</sup> and C-17<sup>2</sup>); right: a novel hydrophobic chlorophyll *c* from *Emiliana huxleyi*. Remarks: 1) Stereochemistry at C-13<sup>2</sup> unknown, 2) No double-bond in the C-17 side-chain, 3) This pigment is also referred to as 'divinyl-PChlide *a*', 4) Mixture according to Garrido et al., 2000. D: Bacterial chlorophylls of the bacteriochlorin-type, with single bonds between C-7/C-8 and C-17/C-18: bacteriochlorophylls *a*, *b* and *g*.

these features have been found, but the BChls *c*, *d* and *e* still provide more than 50% of the currently known chlorophyll structures, in spite of the limited contribution of green bacteria to total photosynthesis. The role of these variations in the build-up and function of the chlorosome core, which appears to be largely devoid of proteins, is currently a major challenge in chlorophyll research.

#### e. Transmetalated Chlorophylls

Several closely related strains of photosynthetic bacteria (*Acidiphilium rubrum*) isolated from acidic mine ponds contain, besides the common Mg-complex large amounts (up to 90%) of [Zn]-BChl (Wakao et al., 1996; Kobayashi et al., 1999). As evidenced by the analysis of isolated antennas and



Table 1. Occurrence of photosynthetic light-harvesting pigments (mass pigments bold X, minor pigments in brackets). a: Tetrapyrrole pigments

Pigment	Organism <sup>a</sup>	Chloroflexaceae	Chlorobiaceae	Heliobacteria	Purple bacteria	Cyanophyta I <sup>b</sup>	Cyanophyta II <sup>b</sup>	Glaucoophyta (Cyanelles)	Rhodophyta	Chrysophyceae	Raphidophyceae	Pheophyceae	Xanthophyceae	Eustigmatophyceae	Bacillariophyceae (Diatoms)	Haptophyta	Cryptophyta	Dinophyta (Dinoflagellates) <sup>h</sup>	Euglenophyta	Chlorarachniophyta	Prasinophyceae	Chlorophyceae	Green plant plastids	
<b>Chlorophylls</b>																								
Chlorophyll a					X	X	X	X	X	X	X	X	X	X	X	X	X	X	X	X	X	X	X	X
[8-Vinyl]-Chlorophyll a						X																		
Chlorophyll b						X												(x) <sup>c</sup>	X	X	X	X	X	X
[8-Vinyl]-Chlorophyll b						X																		
Chlorophyll c <sub>1</sub>							x			X	X	(x)			X	X		(x) <sup>c</sup>						
Chlorophyll c <sub>2</sub>										X	X	X	(x)		X	X	X	X						
Chlorophyll c <sub>3</sub>										X						X								
Esterified Chlorophyll c																X								
Mg-[8-Vinyl]-Protochlorophyllid a							(x)														X <sup>d</sup>			
Chlorophyll d						X <sup>e</sup>		(x)																
Bacteriochlorophyll a		X	X		X																			
Bacteriochlorophyll b					X																			
Bacteriochlorophyll c		X	X																					
Bacteriochlorophyll d		X	X																					
Bacteriochlorophyll e			X																					
Bacteriochlorophyll f			X																					
Bacteriochlorophyll g				X																				
<b>Phycobilins</b>																								
Allophycocyanin					X		X																	
Phycocyanins (Phycobilisomes)					X		X																	
Phycocerythrins (Phycobilisomes)					X	X <sup>f</sup>	X																	
Cryptophyte-Phycocyanin (no Phycobilisome)																	X	X <sup>g</sup>						
Cryptophyte-Phycocerythrin (no Phycobilisome)																	X	X <sup>g</sup>						

a) See chapter 1 (Green and Anderson) for taxonomy of algae, in particular of the Heterokonts (Chrysophyceae, Raphidophyceae, Pheophyceae, Xanthophyceae, Eustigmatophyceae, Haptophyta). b) Cyanophyta I have the classical pigmentation (Chl *a* plus phycobilins). Cyanophyta II contain Chl *b* in addition to Chl *a*, and few or no phycobilins. c) Green-bacterial symbionts. d) Plus other chlorophyll *c*-type pigments. e) Identified only in few species, but here the major pigment. *Acaryochloris marina* (cyanophyta) contains mainly Chl *d*, traces of Chl *a*, and also Chl *c* and biliproteins (Marquardt et al., 1997). f) Only a C-type phycoerythrin has been found, not PC or APC, and no phycobilisomes. g) Endosymbiotic cryptophytes. h) Pigmentation depends on endosymbiotic photosynthetic organisms. Besides dinophytes, cryptophytes, green algae or various heterokonts are known. The pigments can be useful as phylogenetic markers.

reaction centers, this pigment is functional and partially replaces BChl *a* in all pigment proteins, and at all sites including the primary donor, P870 (Akiyami et al., 1998). Chlorophylls and precursors containing Zn as central metal, chemical and photophysical properties similar to those of the respective Mg-complexes (Hartwich et al., 1998; Noy et al., 1998b; Kobayashi et al., 1999). Most enzymes accept both as substrates (see e.g. Schoch et al., 1995), and the Zn-pigments can replace the

chlorophylls in all sites accessible to exchange or reconstitution (see below). A notable chemical difference is the increased stability of the Zn-chlorophylls towards acid: the acidity of the mine-ponds is therefore the likely evolutionary pressure responsible for a change of the central metal. The Zn-contents of the ponds are not unusually high, and Zn is incorporated under growth in media containing only traces of this metal. It is currently not clear whether the Zn is introduced by a specialized

Table 1. (Continued) Occurrence of photosynthetic light-harvesting pigments (mass pigments bold X, minor pigments in brackets). b: Carotenoids

Pigment (end groups, see Fig. 7a)	Organism <sup>a</sup>																
	Chloroflexaceae	Chlorobiaceae	Heliobacteria	Purple bacteria	Cyanophyta I <sup>b</sup>	Cyanophyta II <sup>b</sup>	Glaucoophyta (Cyanelles)	Rhodophyta	Chrysophyceae	Raphidophyceae	Pheophyceae	Xanthophyceae	Eustigmatophyceae	Bacillariophyceae (Diatoms)	Haptophyta	Cryptophyta	Dinophyta (Dinoflagellates) <sup>k</sup>
Alloxanthin											(x)					<b>X</b>	<b>X</b>
Antheraxanthin							(x)	(x)		(x)							<b>X</b> <b>X</b> <b>X</b>
Astaxanthin																(x)	(x)
Bacteriorubixanthinal				<b>X<sup>c</sup></b>													(x) <sub>i)</sub>
Caloxanthin (partly sulphate)				<b>X<sup>c</sup></b>	<b>X</b>										(x)		(x) <sub>i)</sub>
Canthaxanthin					<b>X</b>							(x)	(x)	(x)	(x)	(x)	(x)
α-Carotene (β,ε)						<b>X<sup>d</sup></b>	<b>X</b>	(x)							(x)	<b>X</b>	(x) <sub>i)</sub>
β-Carotene (β,β')	<b>X</b>	<b>X</b>		(x)	<b>X</b>	<b>X<sup>e</sup></b>	<b>X</b>	<b>X</b>	<b>X</b>	<b>X</b>	<b>X</b>	<b>X</b>	<b>X</b>	<b>X</b>	<b>X</b>	(x)	<b>X</b> <b>X</b> <b>X</b>
β-Caroten-2R-ol																	(x)
γ-Carotene (β,ψ)	<b>X<sup>f</sup></b>	<b>X<sup>f</sup></b>			<b>X</b>			(x)		(x)				(x)	(x)	(x)	(x)
γ-Carotene, hydroxy, (-acyl-glucosyl)	<b>X</b>	<b>X</b>								(x)						(x)	(x)
γ-Carotene, 4-keto	<b>X</b>																
ε-Carotene (ε,ε')								(x)		(x)		(x)	(x)	(x)			(x)
ζ-carotene (ψ, ψ)		(x)															
ζ-carotene, dihydroxy				<b>X</b>													
Chlorobactene, 1'-hydroxy, (-acyl-glucosyl)		<b>X</b>															
Crocoxanthin																(x)	
Cryptoxanthin (α, β)				<b>X</b>	(x)	(x)	(x)	(x)				<b>X</b>	(x)		(x)		(x) (x)
Diadinoxanthin									<b>X</b>	<b>X</b>	(x)	<b>X</b>	<b>X</b>	<b>X</b>	<b>X</b>	<b>X</b>	<b>X</b>
Diapocarotenoate, di-(acylglucosyl)-				<b>X<sup>c)</sup></b>													
Diapo-neurosporene				<b>X</b>													
Diatoxanthin								(x)	(x)	(x)	<b>X</b>	<b>X</b>	<b>X</b>	<b>X</b>		<b>X</b>	<b>X</b>
1,2-Dihydroneurosporene				<b>X</b>	<b>X</b>												
Dinoxanthin									(x)					(x)	(x)		<b>X</b>
Echinenone	<b>X</b>				<b>X<sup>g</sup></b>	(x)							(x)	(x)	(x)		(x) (x)
Erythroxanthin sulphate and related pigments				<b>X<sup>c)</sup></b>													<b>X</b>
Fucoxanthin							(x)	<b>X</b>	<b>X<sup>h</sup></b>	<b>X</b>				<b>X</b>	<b>X</b>		<b>X</b>
Fucoxanthin, 19'-butanoyloxy (+ homologues)															<b>X</b>		<b>X</b>
Fucoxanthin, 4-keto-19'-hexanoyloxy															<b>X</b>		
Heteroxanthin									<b>x</b>		<b>X</b>	(x)					<b>X</b>
Isorenieratene		<b>X</b>															
β-Isorenieratene		<b>X</b>															

a) See chapter 1 (Green and Anderson) for taxonomy of algae, in particular of the Heterokonts (Chrysophyceae, Raphidophyceae, Pheophyceae, Xanthophyceae, Eustigmatophyceae, Haptophyta). b) Cyanophyta I have the classical pigmentation (Chl *a* plus phycobilins). Cyanophyta II have phycobilins and other chlorophylls in place of, or in addition to Chl *a*. c) Only aerobic 'purple' bacteria. d) Unicellular species. e) Endosymbiotic species. f) Plus Hydroxyderivative, partly glucosylated, partly additionally acylated with fatty acid. g) Fresh water species. h) Marine species. i) Not in chloroplast. j) Scattered. k) Pigmentation depends on endosymbiotic photosynthetic organisms. Besides dinophytes, cryptophytes, green algae or various heterokonts are known. The pigments can be useful as phylogenetic markers.

chelatase, or by replacing an originally inserted Mg at a later biosynthetic stage. These organisms must either maintain a large intracellular store of Zn<sup>++</sup> that leads to incorporation by mass action, or have chetalases with modified specificities. There were

earlier reports on Zn-Proto IX in another acidophilic organism, the rhodophyte *Cyanidium caldarium* (*Galdieria sulphuraria*), which at that time was discussed as a precursor of biliproteins (Csatorday et al., 1981). It is now clear that biliproteins are formed

Table 1. b: Carotenoids. (Continued) Occurrence of photosynthetic light-harvesting pigments (mass pigments bold X, minor pigments in brackets).

Pigment (end groups, see Fig. 7a)	Organism <sup>a</sup>															
	Chloroflexaceae	Chlorobiaceae	Heliobacteria	Purple bacteria	Cyanophyta I <sup>b</sup>	Cyanophyta II <sup>b</sup>	Glaucochyta (Cyanelles)	Rhodophyta	Chrysophyceae	Raphidophyceae	Pheophyceae	Xanthophyceae	Eustigmatophyceae	Bacillariophyceae (Diatoms)	Haptophyta	Cryptophyta
Lutein								X								
Lycopene ( $\psi$ , $\psi$ )		X		X (x)												X
Monadoxanthin																x
Myxobactone	X															
Myxoxanthophyll					X											
Neoxanthin (9- <i>cis</i> -)									(x)	(x)	(x)	(x)		(x)		
Neurosporene		X														
Nostoxanthin				X <sup>c</sup>	X											
Okenone				X												
Oscillatoxanthin					X											
P-457																(x)
Peridinin (and derivatives)																X
Phytoene	X	X		X	X	X	X	X	X	X	X	X	X	X	X	X
Phytofluene	X	X		X	X	X	X	X	X	X	X	X	X	X	X	X
Prasinolaxanthin																
R.g.-keto III				X												
Rhodopin-glucoside		X		X												
Rhodopin, 1'-hydroxy (partly glucosylated)				X												
Rhodopinal (13- <i>cis</i> , partly glucosylated)				X												
Rhodovibrin				X												
Siphonaxanthin																X <sup>h</sup>
Siphonein																X <sup>h</sup>
Spheroidene				X												
Spheroidenone				X												
Spirilloxanthin				X												
Thioestece 460																
Vaucheriaxanthin (ester)									x			X	X			
Violaxanthin								(x)	x	(x) <sup>j</sup>	X		X			
Zeaxanthin (partly glycosylated)				X <sup>c</sup>	X	X	X	X	X <sup>h</sup>		(x)	X	(x)	(x)		x

a) See chapter 1 (Green and Anderson) for taxonomy of algae, in particular of the Heterokonts (Chrysophyceae, Raphidophyceae, Pheophyceae, Xanthophyceae, Eustigmatophyceae, Haptophyta). b) Cyanophyta I have the classical pigmentation (Chl *a* plus phycobilins). Cyanophyta II have phycobilins and other chlorophylls in place of, or in addition to Chl *a*. c) Only aerobic 'purple' bacteria. d) Unicellular species. e) Endosymbiotic species. f) Plus Hydroxyderivative, partly glucosylated, partly additionally acylated with fatty acid. g) Fresh water species. h) Marine species. i) Not in chloroplast. j) Scattered. k) Pigmentation depends on endosymbiotic photosynthetic organisms. Besides dinophytes, cryptophytes, green algae or various heterokonts are known. The pigments can be useful as phylogenetic markers.

via Fe-protoporphyrin, and to the author's knowledge the function of the Zn-porphyrin has never been established.

Transmetalated chlorophylls, with Hg, Cd, Ni, Cu, La, or Pb replacing Mg, have been isolated from lichens, microalgae and more recently from water plants grown on media enriched in the respective

metals (Küpper et al., 1996, 1998, 2000; Tao et al., 2001). In these organisms, photosynthesis is strongly impaired (Caspi et al., 1999). If judged from experiments with isolated light-harvesting complexes, the aforementioned metals (which bind much more strongly than Mg to the tetrapyrrole) can replace Mg spontaneously at concentrations likely to exist within

Table 2. location, functions and basic spectroscopic properties of photosynthetic pigments

Pigments	Location	Function(s)	Absorption <sup>c)</sup> $\lambda_{\max}$ (e) [solvent]	Emission <sup>c,d)</sup> $\lambda_{\max}$ [solvent]	I <sub>F</sub> <sup>k)</sup>	Refs <sup>e)</sup>
Chl <i>a</i>	All antennas (except billiproteins) Reaction centers	Light harvesting, electron transfer	$\approx 440$ , $\approx 670$ 430, 662(78.8) [A] 430,660(90.2)[D]	680–730 668, 713[A] 666[D]	++	1
Chl <i>b</i>	Peripheral antennas	Light harvesting	$\approx 460$ , $\approx 650$ 457,646(46.6)[90A] 454,643(56.3)[D]	$\approx 660$ 652, 710[A] 646[D]	++	1
Chl <i>c</i> , <sup>g)</sup>	Peripheral antennas	Light harvesting	$\approx 400$ , (500–600) 446,578,629(23.9)[AP] 446,579,628[D]	$\approx 620$ 633, 694[A]	++	1
Chl <i>c</i> , <sup>h)</sup>	Peripheral antenna	Light harvesting	453(218),586,626[AP] <sup>a)</sup> 438, 575, 625[A] <sup>a)</sup>	635,690[A] 627[D]	++	1
[8-Vinyl]-Pchl <i>a</i> , <sup>b,i)</sup>	a) Peripheral antenna b) Intermediate in (B)Chl biosynthesis	a) Light harvesting b) Biosynthesis intermediate			++	1
Chl <i>d</i> , <sup>f)</sup>	Antennas, reaction center	Light harvesting, electron transfer	$\approx 440$ , $\approx 690$	$\approx 700$	++	2
BChl <i>a</i>	Core and peripheral antennas, reaction centers	Light harvesting, electron transfer	<400, 800–880 357,391,573,772(91)[D] 365,608,772(60)[M]	820–920	++	2
BChl <i>b</i> , <sup>f)</sup>	Core and peripheral antennas, reaction centers	Light harvesting, electron transfer	<400, 800–1020 368,408,578,794(106)[D] 368,407,582,795 [A]	840–1040	++	2
BChl <i>c</i>	Peripheral antenna (chlorosomes)	Light harvesting	$\approx 440$ , 640–760 432,622,660 (92.7) [D] 435,620,670 (70.9) [M]	730–780	++	2 <sup>b)</sup>
BChl <i>d</i>	Peripheral antenna (chlorosomes)	Light harvesting	425,612,650 (87.9) [D] 427,612,659 (64) [M]		++	2 <sup>b)</sup>
BChl <i>e</i>	Peripheral antenna (chlorosomes)	Light harvesting	338,456,594,649(48.9) [A] 476, 660(41)[M]		++	6
BChl <i>g</i>	Antenna/reaction center unit	Light harvesting, electron transfer	<400, 780–850 408,418,575,763 [DO] 375,660(35.4) [UH <sup>+</sup> ]		++	2
Phycocyanobilin	Peripheral antenna, phycobilisomes	Light harvesting	371,550(53.7) [UH <sup>+</sup> ]	–	–	3
Phycocerythrobilin	Peripheral antenna, phycobilisomes	Light harvesting	15Z: 329,593(38.6) [UH <sup>+</sup> ] 15E: 331,533(35.6) [UH <sup>+</sup> ] 368, 495(94) [UH <sup>+</sup> ]	–	–	4,5
Phycoviolobilin	Peripheral antenna, phycobilisomes	Light harvesting, sensing (?)		–	–	3
Phycourobilin	Peripheral antenna, phycobilisomes	Light harvesting		–	–	4,5

a) In Chl *c*,<sub>1,2</sub> and [8-Vinyl]-Pchl *a* the band at  $\approx 625$  is more intense than that at  $\approx 580$  nm; in Chl *c*,<sub>3</sub> and Chl *c*,<sub>CS-170</sub> it is much less intense. b) Also termed Divinyl-protoclorophyllide *a* (DV-Pchl *a*) or Mg-2,4-divinyl pheophytin *a*, monomethyl ester. c)  $\lambda_{\max}$  in nm,  $\epsilon$  in  $\text{cm}^{-1}\text{M}^{-1}$ , solvent abbreviations: A = acetone, AP = acetone/1% pyridine, D = diethylether, DO = dioxane, H = hexane, UH<sup>+</sup> = 8 M urea, pH 1.9 d) Main peak underlined. e) 1=Jeffrey et al., 1997; 2=Oelze, 1985; 3=Bishop and Hixson, 1975; 5=Klotz and Glazer, 1985; 6=Borrego et al., 1999; 7=Smith and Benitez, 1955. f) Only in few species, but here main pigment. g) Spectra of Chl *c*,<sub>2</sub> and several other *c*-chlorophylls are similar. h) Spectra of Chl *c*,<sub>CS-170</sub> are similar. i) Spectra of Pchl *a* are similar. j) Extinction coefficients calculated from specific extinction coefficients using the 8-ethyl-11-methyl-17<sup>4</sup>-farnesyl structures. k) The fluorescence yield of the pigments varies with their environment.

the cells. It is interesting in this context that prospecting for Cu has been attempted via Chl fluorescence (Lanaras et al., 1993).

The rapid internal conversion of metals with unfilled *d*-shells explains the impaired photosynthetic capacity of plants that are stressed with heavy metals (Küpper et al., 1998). [Ni]-BChl *a* shows internal conversion (IC) on a time-scale <100fs; if it is incorporated in bacterial LH1 complexes, it can compete efficiently with energy transfer at time-scales down to 50 fs (Musewald et al., 1998, 1999; Noy et al., 1998a). It acts as a 'black hole': any exciton that passes by is degraded to heat. In vitro, this can be used to study unit-sizes and exciton delocalization (Fiedor et al., 2000, 2001, see below).

#### f. 'Minor' Chlorophylls

The number of recognized chlorophylls is constantly increasing. Structural variants are found in most photosynthetic organisms, often only in small amounts, and their functions are not always known. Some such pigments have been established as biosynthetic precursors or products of (bio)degradation, including Chl *a* esterified with terpenoid esters other than phytol (phytadi-, -tri-, or tetraene alcohols (Schoch et al., 1978; Shioi, 1991; but see also below), and pigments bearing a C-8 vinyl instead of an ethyl substituent (Rebeiz et al., 1994). However, many of these minor (and sometimes not so minor) chlorophylls are functional in photosynthesis. They are often localized in the reaction centers. An example is the metal-free pheophytin *a* (Phe) found in the PS II-RC. Its redox-potential being  $\approx 200$  mV more positive than that of Chl *a*, Phe serves as an early electron acceptor from P680 and transfers an electron on to the quinone,  $Q_A$  (Evans and Nugent, 1993). In bacterial RCs of type II, e.g. those of purple bacteria, Phe is structurally and functionally replaced by BPhe *a*, which has been shown to be very rapidly ( $\approx 1$ ps) reduced by the primary acceptor, BChl- $B_A$  (Schmidt et al., 1995), and to donate its electron subsequently to  $Q_A$  (reviewed by Dimagno and Norris, 1993).

The minor chlorophylls of type I-RCs are the  $13^2(S)$ -epimers of the respective major chlorophylls, the so-called prime-chlorophylls. Photosystem I of most oxygenic organisms contains Chl *a'* (Kobayashi et al., 1988), the  $13^2(S)$ -epimer of Chl *a*, the Chl *d*-containing *Acaryochloris marina* contains Chl *d'* instead (Kobayashi et al., 1999), and heliobacteria

contain BChl *g'* (Kobayashi et al., 1991b). At least for Chl *a'*, its location as one of the pigments of the special pair has recently been verified by the X-ray structure of a cyanobacterial PS I (Klukas et al., 1999; Jordan et al., 2001). By contrast, RCs from green bacteria, which are also likely to be of the type I, do not contain a prime-chlorophyll but rather Chl  $a_{\Delta 2,6}$ , viz. the 'normal' Chl *a* macrocycle esterified with  $\Delta 2,6$ -phytadienol (Kobayashi, 1996; Kobayashi et al., 2001). Chl *a* bearing an hydroxyethyl substituent at C-8 and esterified with farnesol (8<sup>2</sup>-hydroxy-Chl  $a_F$ ) has been identified in *Heliobacterium chlorum*, where it is believed to function as primary acceptor  $A_0$  (Van de Meent et al., 1991). Finally, the Chl  $a_{\Delta 13^1,13^2}$ -enol shows some of the spectral features of P700 in PS I-RCs (Wasielowski et al., 1981). A recent 3.8Å X-ray structure is still inconclusive in this respect because the second Chl of P700 is strongly distorted.

Antenna complexes also can contain modified pigments. Probably the most striking example is the presence of [8-vinyl]-Chls *a* and *b* as the most abundant pigments in *Prochlorococcus* species living in considerable depth ( $\approx 100$ m) (Goerick and Repeta, 1992). Since they absorb only slightly differently from the corresponding Chls *a* and *b* bearing an 8-ethyl-group instead, the functional significance of this substituent change is currently unclear.

#### 2. Biosynthesis

The biosynthesis of tetrapyrroles begins with the dedicated aminoacid 5-aminolevulinate (ALA), which can be formed by two different pathways (Fig. 2a). In the  $C_{4+1}$  or Shemin-pathway, it is formed by condensation of glycine with succinyl-CoA with ALA synthase. This reaction was elucidated half a century ago, by D. Shemin's group in a remarkable 'Selbstversuch' involving one of the first uses of radioactive tracers (Wittenberg and Shemin, 1950). After a long, unsuccessful search for ALA synthase in plants, Beale et al., 1975 demonstrated the direct conversion of the glutamate  $C_5$ -skeleton to that of ALA. The more roundabout sequence of this  $C_5$ -pathway involves, remarkably, activation of Glu by t-RNA<sup>Glu</sup> in a non-proteinogenic synthesis (Kannan-gara et al., 1994).

The distribution of the  $C_{4+1}$  and  $C_5$  pathways in higher plants and various classes of algae and photosynthetic bacteria has been discussed in considerable detail (Avissar et al. 1989; Avissar and

Moberg, 1995). The  $C_5$  pathway, which is probably the more ubiquitous, operates in green algae (Oh-hama et al., 1982, 1985a) and green plants, and several anoxygenic photosynthetic bacteria including *Chromatium* and *Prosthecochloris* (Oh-hama et al., 1986a,b), while animals and purple bacteria such as *Rhodobacter spheroides* use the  $C_{4+1}$  pathway (Oh-hama et al., 1985b).

Following ALA synthesis, two molecules of ALA condense to the pyrrole, porphobilinogen (PBG) (see Fig. 2a). The ensuing tetramerization of PBG to uroporphyrinogen (uro'gen) III has received considerable attention for more than 30 years (reviewed by Battersby and Leeper (1990), Jordan (1991, 1994), Leeper (1994) and Beale (1999)). The action of the two enzymes involved, PBG-deaminase and uro'gen III cosynthase, was clarified by a combination of NMR, synthesis of specifically labelled intermediates, model studies, and the preparation of enzyme-bound intermediate complexes of the PBG-deaminase. The latter catalyses the formation of a linear hexapyrrole. A dipyrrole binds to the enzyme, while the tetrapyrrole product, hydroxymethylbilane I (HMB), is released. HMB is very reactive and would cyclize non-enzymically to form uro'gen I in the absence of uro'gen III cosynthase. The cosynthase catalyses the cyclization of HMB, with a regular distribution of acetate and propionate side chains, to uro'gen III, an asymmetric series III tetrapyrrole, via a remarkable flip of ring D most likely involving a spiro-intermediate (Leeper, 1994).

Uro'gen III is a branching point: the Co and Ni branches lead to several rare, but biologically very important tetrapyrroles (F430, vitamin  $B_{12}$  and the Fe-containing siroheme); the other branch leads to the more abundant and ubiquitous Fe- and Mg-tetrapyrroles as well as to the bilins. In the latter pathways, urogen III is first decarboxylated six times to yield the still colorless (and photodynamically safe) protoporphyrinogen IX (protopogen). Only at this point, after the proper modifications of the side chains, is the tetrapyrrole macrocycle oxidized to form the aromatic  $\pi$ -system of protoporphyrin IX. The first half of this reaction is tightly controlled to ensure that the highly phototoxic porphyrins are formed only in manageable quantities and in the correct cell compartments (Beale, 1999). Since all porphyrinogens preceding protogen IX can oxidize spontaneously to porphyrins that are not metabolized further, they are kept at low concentrations by

feedback-inhibition of ALA synthesis by the late products, heme and protochlorophyllide (Pchlde).

Protoporphyrin IX is the second branching point in chlorophyll biosynthesis. The Fe-branch leads to hemes and bilins (Fig. 2a), and the Mg-branch to the chlorophylls (Fig. 2b). Both start with the insertion of the central metal into the macrocycle. In the case of Fe, the enzyme, ferrochelatase, is a single protein that requires neither energy nor specific cofactors besides  $Fe^{2+}$ . The insertion of Mg is considerably more complex, which parallels the difficulties in inserting this metal chemically and the thermodynamic instability of Mg-porphyrins in aqueous environments. Three gene-products cooperate in the Mg-insertion, which also requires ATP. The individual functions have been suggested from experiments with overexpressed proteins from purple bacteria (Jensen et al., 1998). The resulting Mg-protoporphyrin or its monomethyl-ester have been implicated in the feedback regulation of chlorophyll biosynthesis and nucleus-plastid communication (Kropat et al., 2000; La Rocca et al., 2001). After regiospecific methylation at C-13<sup>3</sup> (using  $CH_3$  derived from S-adenosyl-methionine (Porra et al., 1983)), ring E is formed. Formally, this reaction sequence requires the abstraction of six electrons (four at C-13<sup>1</sup>, one each at C-13<sup>2</sup> and C-15 for the ring closure) and the introduction of one oxygen. In the anaerobic purple bacteria, the reaction depends on vitamin  $B_{12}$ , which has been suggested to be involved in at least two of the oxidation steps (Gough et al., 2000). Here, the oxygens originate from water (Porra et al., 1995). In cyanobacteria, green plants, and in purple bacteria under aerobic conditions, an oxygenase is involved in the process (see Porra and Scheer, 1999). The resulting PChlid *a* is the last common precursor of the chlorophylls. It comes in two forms: the form carrying an 8-vinyl substituent ([8-vinyl]-Pchlde *a*, often termed 'Divinyl-PChlide *a*') is the main product in purple bacteria and marine *Prochlorococcus*, but also is present in many plants; the form carrying an 8-ethyl group (Pchlde *a* proper), is ubiquitous in oxygenic organisms. In addition, PChl(ide) *b* has been reported as a minor component (Kotzabasis and Senger, 1989), but this has been disputed (Scheumann et al., 1999). For green plants, a complex network has been shown for the reaction sequence from protoporphyrin IX to PChlide *a*, which involves not only parallel 8-ethyl and 8-vinyl-branches, but also branches with free and esterified C-17 propanoic acid side chains, with connections between the parallel



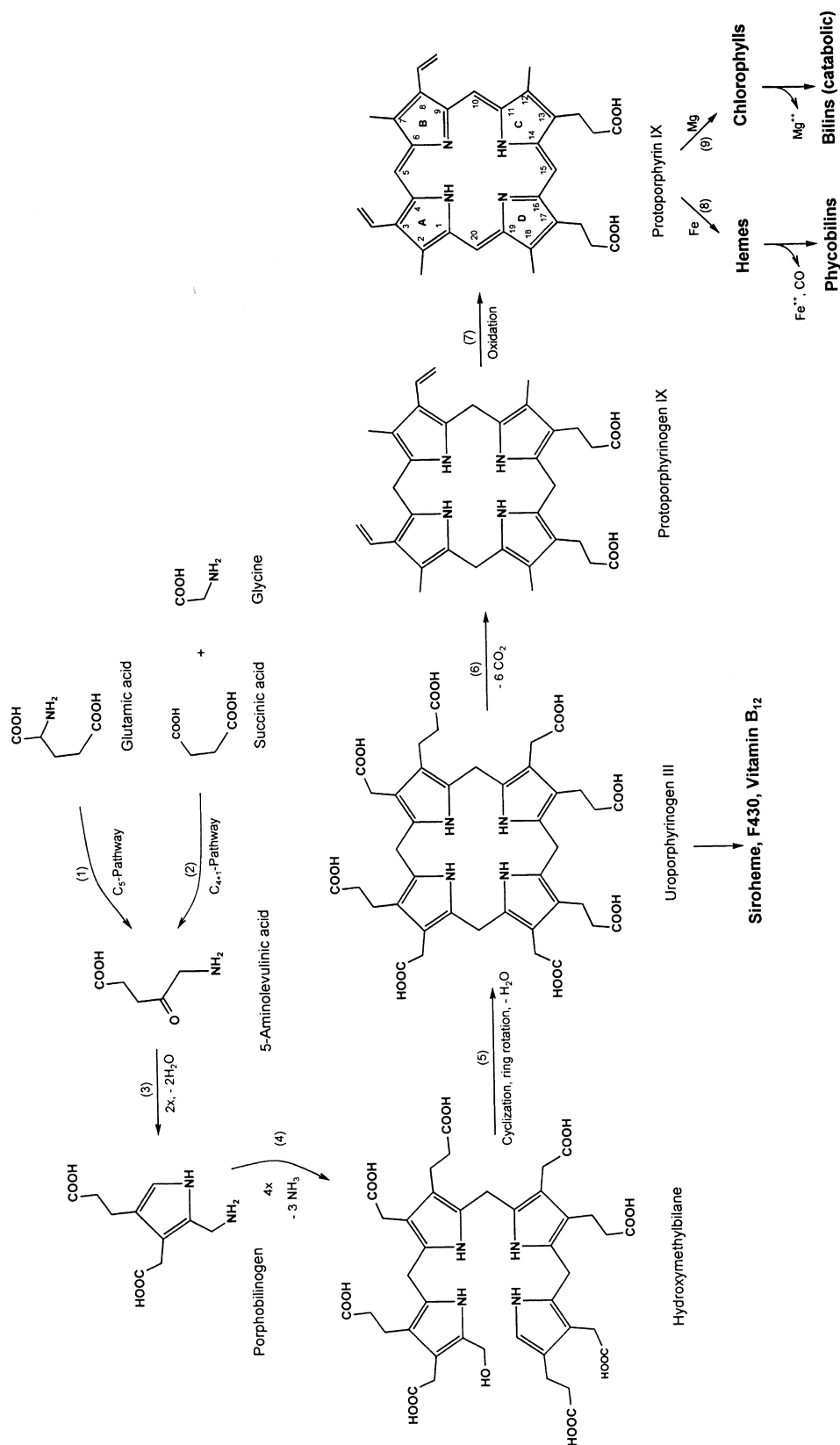
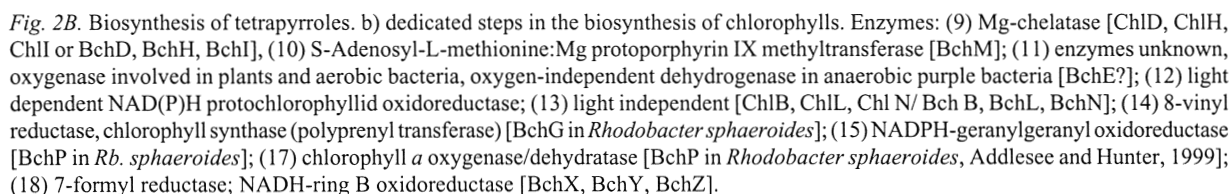


Fig. 2.4. Biosynthesis of tetrapyrroles. a) Early steps to protoporphyrin and general survey of entry into other tetrapyrrole pathways. Enzymes: (1) glutamyl-tRNA-synthetase, glutamyl-tRNA reductase and glutamate-1-semialdehyde aminotransferase; (2) ALA synthase; (3) porphobilinogen synthase (ALA dehydratase); (4) hydroxymethyl-bilane synthase (PBG deaminase); (5) uroporphyrinogen III synthase (urogen III cosynthase); (6) uroporphyrinogen III decarboxylase and coproporphyrinogen III oxidative decarboxylase; (7) protoporphyrinogen oxidase; (8) ferrochelatase; (9) Mg-chelatase [ChlD, ChlH, ChlI or BehD, BehH, BehI]. (Continued on next page)



the author's knowledge.

Two different classes of enzymes are responsible for the regio- and stereoselective reduction of the peripheral double bonds to yield the chlorin and bacteriochlorin type chlorophylls. A light-independent protochlorophyllide-NAD(P)H-oxidoreductase ('dark' POR) appears to be ubiquitous in all photosynthetic organisms, but in angiosperms is largely replaced by light-dependent enzymes ('light' PORA, or PORB) (Walmsley and Adamson, 1990).

PORA is one of the most intensely studied enzymes; it forms a stable enzyme-substrate complex (PChlide-holochrome), which accumulates to substantial amounts in dark-grown seedlings and is activated by light (Griffiths, 1991). In these plants, the complex accumulating in the dark inhibits PChlide formation by feedback of ALA synthesis (Beale, 1999), and the Chlide *a* formed as a product in the light is an activator for the formation of chlorophyll proteins (Eichacker et al., 1992). Both PChlide *a* and [8-vinyl]-PChlide *a* are substrates to the 'light' POR. Much less is known about the widely distributed 'dark' POR. The tetrapyrrole substrate specificity and product structures are similar, but the two enzymes appear quite unrelated. Recent sequence and enzymatic data of the three-subunit complex indicate a relation to nitrogenase, including the requirement of ferredoxin as reducing agent (Fujita and Bauer, 2000). In green plants, the final steps are the esterification and the hydrogenation of three of the four double-bonds of geranyl-geraniol, the esterifying alcohol. Again, a network of parallel reactions with multiple connections seems to exist (Rudiger, 1993). In *Rhodobacter sphaeroides*, BChG catalyses the esterification reaction (Addlesee et al., 2000).

Chl *b* is formed from Chl *a* by an oxygenase (Schneegurt and Beale, 1992; Porra et al., 1993; Oster et al., 2000), and can be converted back to Chl *a* (Scheumann et al., 1996; Ito et al., 1996), the latter reaction also occurs in higher plants before ring-opening during chlorophyll degradation (Folly and Engel, 1999). Nothing is known about the introduction of oxygenic functions at the same position into BChl *e* (7-formyl) and into Chl *c*<sub>3</sub> (8-COOCH<sub>3</sub>), or at position 8<sup>2</sup> in the RC pigment found in green bacteria (8-CH<sub>2</sub>CH<sub>2</sub>OH).

In anoxygenic bacteria, hydrogenation of ring D is followed by hydrogenation of ring B, by a variant of the 'dark' POR. The final steps of esterification and alcohol hydrogenation appear to be basically similar to the corresponding reactions in green plants and cyanobacteria (Naylor et al., 2000), in spite of different specificities leading to variations in hydrogenation (and length) of the alcohols (Biel, 1995; Senge and Smith, 1995). Very little is known about the biosynthesis of the other bacteriochlorophylls. BChl *g* is formally, and possibly biosynthetically, an isomer of Chl *a*, and the unsaturation of ring B in BChl *b* could as well be the result of a double-bond isomerization rather than a hydrogenation-dehydrogenation sequence, but the

enzymes have not been identified to the author's knowledge. Likewise, little is known about the biosynthesis of BChl *c*, *d* and *e*. In one species of green bacteria the genome has been sequenced. A number of candidate methyl-transferases has been annotated based on the presence of tetrapyrrole binding sites (D. Bryant, personal communication), but most of the reactions are unique for this type of pigment and require the isolated enzymes for confirmation. The extra methyl groups are derived from S-adenosylmethionine and the 7-CHO group is likely to be introduced by an oxygen-independent enzyme in view of the sensitivity of most green bacteria to oxygen.

### 3. Spectroscopy

The visible spectra of cyclic tetrapyrroles were first rationalized by the four-orbital model of Gouterman (Weiss, 1972, 1978). Excitations from the two highest occupied molecular orbitals (HOMO) to the two lowest unoccupied molecular orbitals (LUMO) result in four transitions in or near the visible region (300–800 nm), each of which usually is accompanied by one major vibronic band. In metalloporphyrins like Mg-protoporphyrin IX (Fig. 2b) with (nearly) four-fold symmetry ( $D_{4h}$ ), the transitions are pairwise degenerate. They give rise to the low-energy  $Q_{0-0}$  band with a vibronic side-band ( $Q_{0-1}$ ) in the 500–600 nm region, and to the high-energy Soret or B-bands ( $B_{0-0}$ ,  $B_{0-1}$ ) at the vis-uv border (Fig. 3 and Chapter 3, Parson). The B-bands are strongly allowed and intense ( $\epsilon \approx 10^5 \text{ cm}^{-1}\text{M}^{-1}$ ), while the Q-bands are only weakly allowed and an order of magnitude less intense ( $\epsilon \approx 10^4 \text{ cm}^{-1}\text{M}^{-1}$ ). Most synthetic metalloporphyrins are of this type and therefore have only moderate absorption in the visible spectral region.

Any lowering of the symmetry renders the visible bands less forbidden and increases their intensities. Even the introduction of the isocyclic ring E in PChlide and *c*-type Chlides increases the low-energy transitions ( $Q_y$ -band) two- to three- fold, which could be a major factor for the evolution of this characteristic feature of the chlorophylls. It is introduced early in the biosynthesis subsequent to the introduction of Mg, at a stage common to all chlorophylls, and takes place at the macrocyclic unsaturation level of the porphyrin. However, the *c*-type chlorophylls, which are pheoporphyrin Mg-complexes, still have relatively weak absorptions in the visible region (Table 2, Fig. 3), because the substituents perturb the symmetry of the conjugated  $\pi$ -system only slightly. This situation

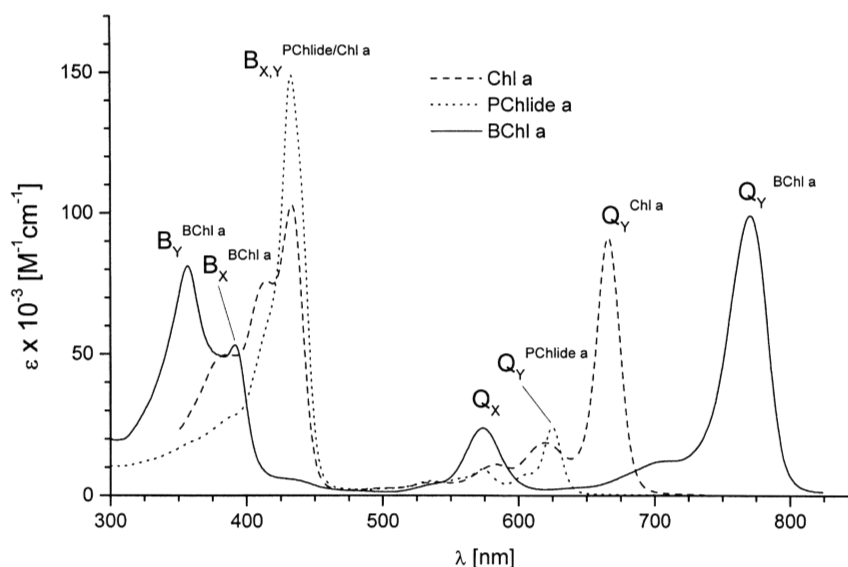


Fig. 3. Absorption spectra of cyclic conjugated tetrapyrroles in monodisperse solutions: Influence of conjugation system on spectra. Shown are the spectra of the porphyrin type (PChlide *a* = protochlorophyllide *a*), the chlorin type (Chl *a* = chlorophyll *a*) and the bacteriochlorin type (BChl *a* = bacteriochlorophyll *a*) and the assignments of the major absorption bands according to the four-orbital model.

is dramatically changed by the reduction of the porphyrin-macrocycle at C-17,18 to the chlorins, and additionally at C-7,8 to the bacteriochlorins. The symmetry of the  $\pi$ -system now is decreased so much that the intensities of the Q- and B-bands become comparable, thus increasing substantially light-harvesting in the Vis or NIR region, respectively. At the same time, the pairwise degeneracy also is removed, and the lowest-energy absorption band is red shifted (in organic solvents) to 650–680 nm (chlorins) or even 750–800 nm (bacteriochlorins). This lowest-energy transition is always polarized along the molecular Y-axis<sup>1</sup> connecting rings A and C, and this band is therefore termed Q<sub>Y</sub>. The higher-energy transition in the Vis region, which has less intensity, is polarized along the X-axis (rings B/D) and is therefore termed Q<sub>X</sub>. The corresponding B-bands (B<sub>X</sub>, B<sub>Y</sub>) still overlap in the chlorins (e.g. Chl *a*) but also split in the bacteriochlorins, so the latter show, well separated, all the bands predicted by Gouterman. There is, nonetheless, considerable mixing among the pure transitions which has been analyzed by Scherz et al. (1991) for BChl *a* and subsequently for BChls in which the native Mg is replaced by other metals (Noy et al., 1998b).

The polarization<sup>1</sup> of the transition dipole moments

is of two-fold importance in photosynthetic systems. Because natural light usually is only weakly polarized, and is further depolarized in water or within a leaf, a preferential, ordered orientation of the chlorophylls probably is of little importance for light absorption. However, the second function of antennas is the transfer of excitation energy to the RC, and this is strongly dependent on the relative orientations, and therefore transition dipole moments, of the pigments involved (Chapter 3, Parson). The polarization of the transition dipole moments is also of considerable importance in photosynthesis research. In ordered structures, such as are found in crystals and in part also in the photosynthetic membrane, knowing the orientation of the transition dipole moments with respect to the molecular coordinates allows one (at least in principle) to determine the orientation of the pigments in these structures. For this purpose, light with different polarizations (e.g. parallel and perpendicular to the plane of an oriented membrane) is used for absorption or fluorescence spectroscopy, from which the anisotropy (*r*) is determined:

$$r_{\text{absorption}} = \frac{A_{\parallel} - A_{\perp}}{A_{\parallel} + 2A_{\perp}} \quad (6)$$

In favorable cases, this allows the determination of

<sup>1</sup> Light is characterized by magnetic and electric vectors, which are perpendicular to each other. When defining the polarization of light in optical spectroscopy, reference usually is made to the electric vector (Chapter 3, Parson and Nagarajan).

the direction of a transition dipole moment with a precision of  $\approx 5^\circ$ . In the absence of excitonic coupling, this provides the orientations of the pigments (Boxer et al., 1982). Structural information can even be obtained for dimers if the conformational space is scanned appropriately (Gazit et al., 1996). Conversely, if an X-ray structure is known, information can be obtained on details of the excitonic coupling among the pigments, which changes the size and direction of the transition dipole moments. Using photo-selection experiments, similar information can be obtained even for systems in isotropic solution (Cantor and Schimmel, 1980; Michl and Thulstrup, 1986).

## B. Phycobiliproteins

### 1. Structures

Biliproteins (Apt et al., 1995; MacColl and Guard-Friar, 1987; Chapters 9, 10, 11, 17) are characteristic of the cyanobacteria, including some prochlorophytes and the conspicuously pigmented *Acaryochloris marina* (Marquardt et al., 1997). Among the eukaryotes, biliproteins occur in the plastids of red algae, glaucophytes like *Cyanophora paradoxa*, of the phylogenetically complex cryptophytes (who probably obtained their plastids from red algae by secondary endosymbiosis), and cryptophyte-

containing dinoflagellates (probably tertiary endosymbionts) (Chapters 1 and 9–11). Phycobilins are extra-membranous antenna pigments, and in most organisms they are organized in supramolecular complexes, the phycobilisomes (PBS; Chapters 9, 10). An exception are the cryptophyte biliproteins, whose supramolecular organization is unclear (Chapter 11, Hiller and Macpherson). The widespread phytochromes are biliproteins, too. Many of the chromophore-protein interactions are similar, but are involved in the different function of light sensing.

The chromophores of phycobiliproteins, the phycobilins, are tetrapyrroles, too. However, the four pyrrole rings do not form a macrocycle but are rather arranged in an open-chain fashion, and they also do not contain a central metal ligand. The name 'bilin' for such open chain tetrapyrroles is derived from their occurrence in bile liquid (see biosynthesis). Note the different numbering for the cyclic and linear tetrapyrroles (Figs. 1 and 4 and IUPAC-IUB Joint commission biochemical nomenclature, 1979, 1999).

The photosynthetic bilins comprise a family of structurally closely related chromophores (Fig. 4) (Beale, 1993; Schluchter and Glazer, 1999), which in the isolated state absorb only moderately ( $\epsilon \approx 17,000 \text{ M}^{-1}\text{cm}^{-1}$  for PCB, Fig. 6a) in the 500–600 nm region. The three most abundant are phycocyanobilin (PCB), phycoerythrobilin (PEB) and phycourobilin

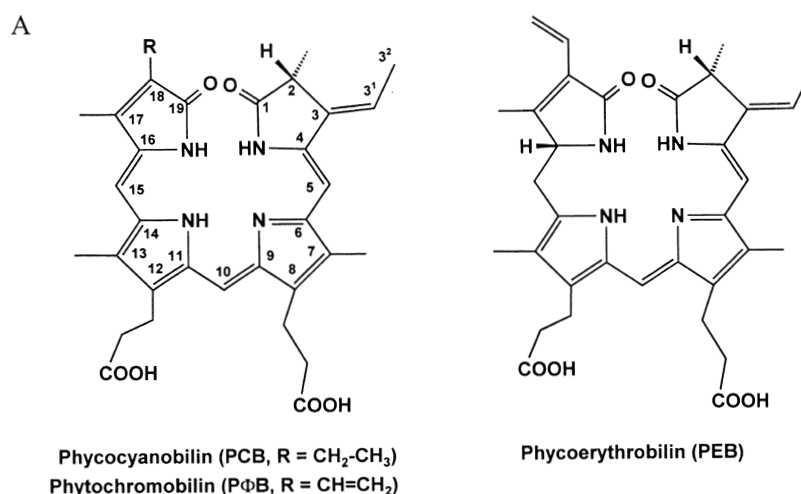
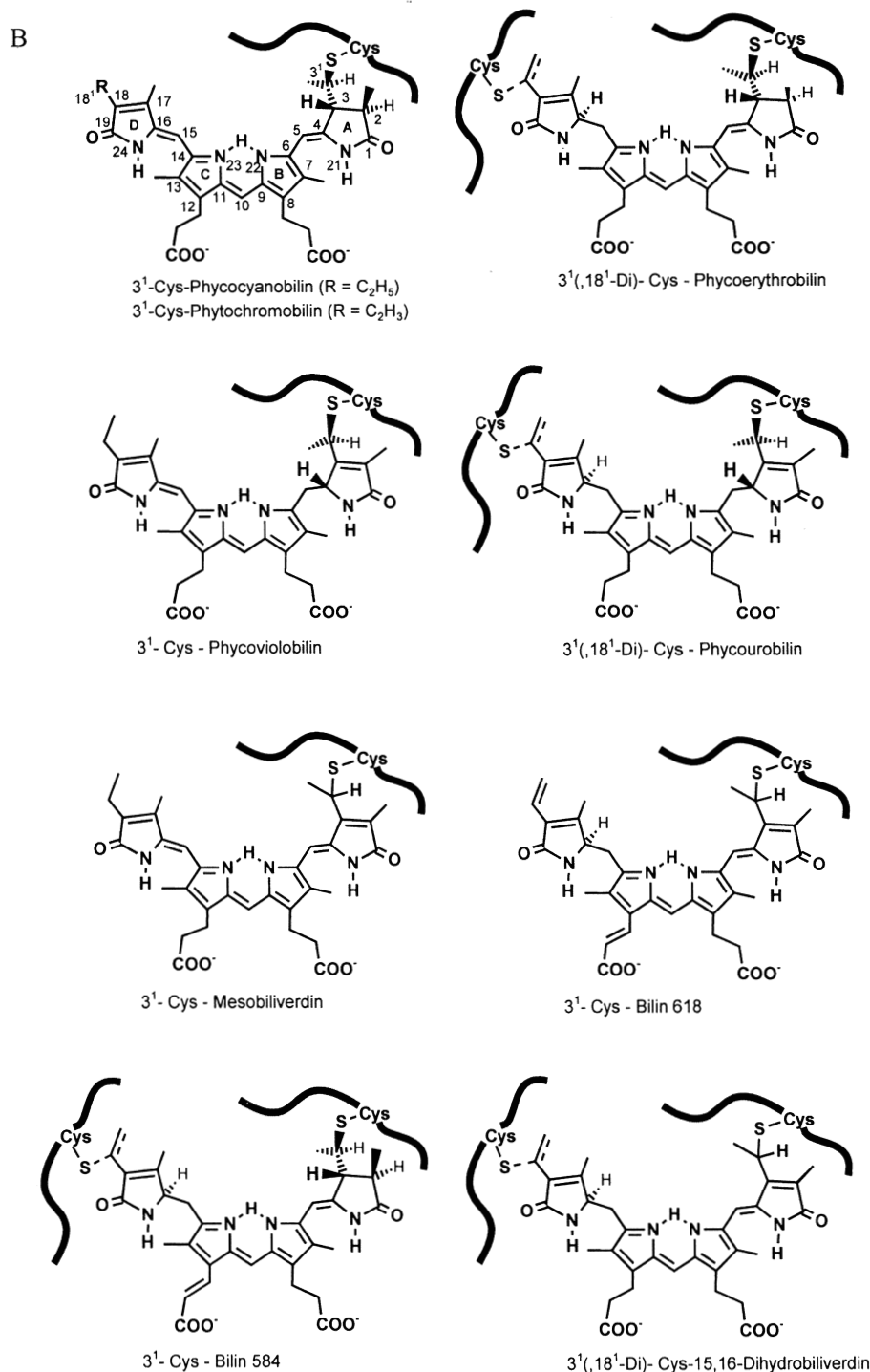


Fig. 4A. Structures of selected free phycobilins. The 3-ethylidene bilins (PCB = phycocyanobilin and PEB = phycoerythrobilin) are the only two free phycobilins found as biosynthetic precursors to the bound chromophores (Fig. 4b). Also shown is PΦB, the chromophore of most phytochromes, which differs from PCB only by having a vinyl instead of an ethyl group at C-18. The numbering is shown for phycocyanobilin; note that it differs from that of the cyclic tetrapyrroles (compare Figs. 1a and 4a). The bilins are shown (schematically) in their cyclic conformations, which are prevalent in solution, in denatured biliproteins, and in bilipeptides. They are shown in the uncharged form of the tetrapyrrole, but can be protonated (see spectra Fig. 6) and deprotonated at the central nitrogens (Scheer, 1982; Braslavsky et al., 1983; Falk, 1989). Numbering according to IUPAC-IUB Joint commission biochemical nomenclature, 1979, 1988).



*Fig. 4B.* Schematic structures of bound phycobilins in biliproteins. The top four chromophores are widespread among biliprotein containing organisms (Table 1a); the bottom four are unique for the cryptophyte phycobilins, which are not organized in phycobilisomes. The nomenclature is adapted from Beale, 1993b), and is based on the free chromophores. The bound chromophores are treated as cysteine addition products to the free molecules (see text). The numbering is shown for 3<sup>1</sup>-Cys-phycocyanobilin. Note that it differs from that of the cyclic tetrapyrroles (compare Figs. 1a and 4a). Chromophores with the prefix '3<sup>1</sup>(, 18<sup>1</sup>-Di)' are linked to some proteins at C-18<sup>1</sup> in addition to C-3<sup>1</sup>. All chromophores are shown in a schematic (semi-) extended conformation characteristic for the native biliproteins, including the phytochromes (Scheer, 1982; Braslavsky et al., 1983; Falk, 1989; Schirmer et al., 1987; Duerring et al., 1990; Brejc et al., 1995; Chang et al., 1996; Reuter et al., 1999; Wilk et al., 1999; Ficner and Huber, 1993). Numbering according to IUPAC-IUB Joint commission biochemical nomenclature (1979, 1988).



(PUB) (Fig. 4). The rare cyanobacterial biliprotein, phycoerythrocyanin, contains yet a fourth chromophore, which has been termed phycoviolobilin (PVB) or phycobiliviolin (Bishop et al., 1987). These four chromophores occur in phycobilisome-containing organisms. Cryptophytes, which do not form phycobilisomes (Chapter 11, Hiller and Macpherson), produce a variety of additional chromophores, some of them with an additional double-bond at the C-12 side-chain of the bilin. Interestingly, this position corresponds biosynthetically to C-17 in the chlorophylls, which in cases like Chl  $c_2$  also carries an acrylic acid side-chain; they may therefore have common ancestors and/or enzymes. Phytochromobilin, the chromophore of most phytochromes, is a close relative of PCB, differing from it only by the C-18 substituent (Fig. 4).

All phycobilin-chromophores are covalently linked to their apoproteins via thioether-bonds to cysteines<sup>2</sup>. The linkage to ring A at position 3<sup>1</sup> is present in all chromophores, and in some cases there is an additional link to ring D at position 18<sup>1</sup> (Fig. 4b). The bilins, from which they are formally derived, are mostly isomers containing nine C=C double-bonds, which is two less than in the animal pigment, biliverdin. Bilin 618, mesobiliverdin and 15,6-dihydrobiliverdin contain ten conjugated double-bonds, not counting that of the C-12 acrylic side chain of ring C in bilins 618 and 584. For the nomenclature of free bilins, see IUPAC-IUB Joint commission biochemical nomenclature (1979, 1988).

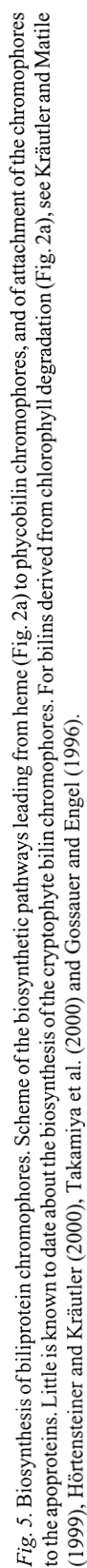
The nomenclature of biliprotein chromophores is mostly generic, and is ambiguous in several respects. The most confusing aspect is the frequent use of the same term, e.g. phycocyanobilin, for both the free chromophore (Fig. 4a) and for a chromophore covalently attached to the apoprotein (Fig. 4b). Due to its mode of attachment, the latter lacks one (in some cases even two) double bonds and therefore has a different molecular structure. In Fig. 4, the more specific nomenclature of Beale has been adopted to circumvent this ambiguity. It reserves the bilin name, e.g. phycocyanobilin (PCB) in the chosen example, to the free chromophore carrying the 3-ethylidene group, and the bound chromophores are characterized as cysteine addition products (Beale, 1993). Adding to this the position of the covalent linkage, the bound chromophore is 3<sup>1</sup>-Cys-phycocyanobilin. It can be

further specified by identifying the position of this cysteine, e.g. 3<sup>1</sup>-(Cys- $\alpha$ 84)-phycocyanobilin for the chromophore at Cys-84 of the  $\alpha$ -subunit. Finally, the complete description also requires the inclusion of the stereochemistry at the asymmetric centers and the methine bridges, and the state of protonation, which however is known only in a few cases (see below).

## 2. Biosynthesis

Most bilins (with the notable exception of those derived from chlorophyll) are synthesized via Fe-porphyrins, hemes. In animals, they mainly arise from hemoglobin in the catabolic turnover of red blood cells. In a complex reaction requiring three molecules each of NAD(P)H and O<sub>2</sub>, the macrocycle is opened at position 5 (note the different numbering in cyclic and open-chain tetrapyrroles, Figs. 1a and 4a,b) to yield biliverdin (biliverdin IX $\alpha$  in the older literature), and the C-5 of the cyclic tetrapyrrole is released as carbon monoxide. The anabolic reaction leading to phycobilins in cyanobacteria, rhodophytes and cryptophytes is similar, but their heme-oxygenases are soluble three-subunit systems in which ferredoxin instead of NAD(P)H functions as the immediate electron donor to the substrate (reviewed in Beale, 1993). The subsequent transformations of the product, biliverdin, have been studied in detail for only two of the phycobilin chromophores, phycocyanobilin (PCB) and phycoerythrobilin (PEB), in addition to the plant sensory chromophore phytochromobilin (P $\Phi$ B) (reviewed by Beale, 1993; Hirschberg and Chamovitz, 1994; Cornejo and Beale, 1997; Schluchter and Glazer, 1999; Frankenberg et al., 2001). Biliverdin is transformed into the phycobilin chromophores in a series of reactions that involve two reductive steps and several subsequent isomerizations, eventually yielding bilins carrying a 3E-ethylidene side chain, phycocyano- and phycoerythrobilin (Fig. 4a). Several different reaction sequences have been identified. The one shown in Fig. 5 has been studied in detail in the red alga *Cyanidium caldarium* (*Galdieria sulphuraria*) and probably also operates in cyanobacteria. Biliverdin is reduced first in a ferredoxin-dependent reaction to 15,16-dihydrobiliverdin, and then further by a different enzyme to  $\Delta$ 3,3<sup>1</sup>Z-PEB. The latter is a precursor to the isomeric  $\Delta$ 3,3<sup>1</sup>Z-PCB, even in cyanobacteria devoid of phycoerythrin. Both pigments are synthesized first with the 3-ethylidene

<sup>2</sup> A free chromophore has recently been suggested in a bacterial phytochrome (Davis et al., 1999).



side-chain in the Z-configuration. Before the attachment to the apoproteins, they are isomerized in a glutathione dependent reaction to the  $\Delta 3,3^1\text{E}$ -isomers, which are the substrates proper for the ligation reaction. The other pathway proceeds first to  $\Delta 3,3\text{Z}$ -P $\Phi$ B in a 1,4-hydrogenation reaction, which probably also occurs during the biosynthesis of P $\Phi$ B in plants (Frankenberg et al., 2001). The 18-vinyl group is subsequently reduced to yield PCB. Vinyl reductions are common in the cyclic tetrapyrroles (see section 3.A.2). It has been demonstrated in the green alga *Mesotaenium caldariorum*, which uses PCB (and not P $\Phi$ B) for its phytochrome (Wu et al., 1997). Note, however, that C-18 in bilins is biosynthetically equivalent to the ring A vinyl group of cyclic tetrapyrroles. Recently, bilirubin has been demonstrated as another reduction product, but its role is presently unclear (Schluchter and Glazer, 1999; Frankenberg et al., 2001).

The last step for the two phycobilins (as well as generally for P $\Phi$ B) is the attachment of the chromophores to their apoproteins. This reaction is currently only partly understood. In the biliproteins, up to four chromophores are bound regio- and stereospecifically to cysteines of a single apoprotein. A minimum of 7 ( $\alpha$ - and  $\beta$ -APC,  $\alpha$ -APB,  $\beta$ -AP<sub>16,2</sub>,  $\alpha$ - and  $\beta$ -PC, L<sub>cm</sub>) and often more (e.g. 13 in *Calothrix* PCC7601 (Kahn et al., 1997)) chromophorylated proteins are present in phycobilisomes, and some of the chromophores are even doubly linked (Fig 4b). This raises the question of how these chromophores become attached to specific positions (Schluchter and Glazer, 1999). In vitro, thiols can be added (reversibly, see below) to the free chromophores carrying a 3-ethylidene side chain, PCB and PEB (Köst et al., 1975 as well as P $\Phi$ B (Thümmel et al., 1981). In the phyto- and cyanochromes (phytochrome-like chromoproteins from cyanobacteria), the chromophore addition in vitro is an autocatalytic process that has been used to introduce non-natural chromophores (Kidd and Lagarias, 1990; Lamparter et al., 1997; Murphey and Lagarias, 1997; Wu et al., 1997; Lindner et al., 1998). The situation is more complex in the phycobiliproteins. In phycocyanin, which has been studied in some detail, two binding sites ( $\alpha$ -84,  $\beta$ -84) show autocatalytic binding. The third chromophore, which incidentally also has another stereochemistry (Schirmer et al., 1987), does not reconstitute in vitro (Arciero et al., 1988a). However, even for the former two sites the attachment is unspecific, and the PCB chromophore becomes

partly oxidized to a mesobiliverdin in the process (Arciero et al., 1988b). Proper binding to at least one of the sites ( $\alpha$ -84) has, however, been shown for the PCB chromophore in the presence of a lyase encoded by *cpcE* and *cpcF*, two genes that are located 3' of the phycocyanin genes on the *cpc*-operon (Fairchild et al., 1992; Swanson et al., 1992; Zhou et al., 1992; Fairchild and Glazer, 1994). This lyase ensures the proper stereochemistry at C-3 and C-3<sup>1</sup>, and also inhibits a concomitant oxidation of the chromophore. Homologous genes have been found in other biliprotein operons including that for PEC (Kufer et al., 1991; Jung et al., 1995) as well as in non-contiguous regions (Kahn et al., 1997; Schluchter and Glazer, 1999). Their mode of action is unclear, and their numbers are insufficient if a specific pair of lyase proteins is needed for each bilin binding site. Knockouts of the respective genes have produced different responses (see Steiger et al., 1999). While lack of the PC- $\alpha$ -84 lyase generally resulted in the formation of PC lacking the chromophore on the  $\alpha$ -subunit (Swanson et al., 1992), inactivation of *pecYZ* coding for a putative PE-lyase resulted in decreased levels of the fully chromophorylated protein (Kahn et al., 1997), and inactivation of *pecEF* coding for the PEC- $\alpha$ -84 lyase (Zhao et al., 2000) resulted in reduced PEC levels carrying a PCB instead of a PVB chromophore at Cys- $\alpha$ -84 (Jung et al., 1995). These data indicate that other lyases can replace the dedicated ones, or that more selective spontaneous (autocatalytic?) ligations may take place in vivo.

Analogous additions of PCB have been studied in other biliproteins (allophycocyanin,  $\beta$ -phycoerythrocyanin), and with other 3-ethylidene chromophores (PEB, P $\Phi$ B, modified PCB). The addition reaction of thiols to these chromophores is reversible, including the addition to the protein. The three chromophores, PCB, PEB and P $\Phi$ B, can be cleaved from PC and APC, PE, and phytochromes, respectively, by heating with alcohols or treatment with HBr in trifluoroacetic acid (Chapman et al., 1968; Schram and Kroes, 1971; Scheer, 1985). However, neither the addition nor the elimination reaction has been observed with a second group of chromophores, which as a common structural feature have an unsaturated ring A with a  $\Delta 2,3$  double bond. Of the eight chromophores shown in Fig. 4b, no less than five belong to this group. The elimination here does not form an ethylidene-group, but rather a vinyl group and the attachment could occur by addition of the cysteine thiol to the vinyl-group of the putative

free chromophore. Corresponding products are known for the heme chromophores in the *c*-type cytochromes, where this addition and its reversion have been well studied (Fuhrhop and Smith, 1975). It is even possible to cleave heme while still bound to the apocytochrome to yield an 'artificial' biliprotein (Rice et al., 1999). It also can be speculated that the second linkage to ring D in the doubly linked chromophores arises from such a reaction. However, there are no reports on the direct addition of an apobiliprotein to the 3-vinyl-group of any of this second type of phycobilins, nor on cleavage of the chromophore to yield a vinyl-bilin. In fact, only one of the second type of chromophores, 15,16-dihydrobiliverdin, has hitherto been identified as a free pigment in cyanobacteria, where it is a biosynthetic precursor of PEB and PCB.

An alternative mode of attachment has recently been reported for one chromophore of this group, phycoviolobilin, from binding studies with PCB to  $\alpha$ -apo-PEC. As in the PC operon, the PEC operon has two homologous genes coding for a lyase, *pecE* and *pecF*. In the absence of PecE/F, PC is added spontaneously to the apoprotein to yield a 3<sup>1</sup>-Cys- $\alpha$ -84-PCB adduct. In their presence, the corresponding PVB adduct is formed, which has an isomeric chromophore (Fig. 4b) (Zhao et al., 2000). The suggestion from these data is that the substrate of the reaction with PecE/F *in vivo* is not the hypothetical PVB carrying a 3-vinyl group, but instead PCB carrying a 3-ethylidene group, which is isomerized during the addition to yield the PVB-3<sup>1</sup>-Cys adduct. Similar lyase-catalyzed isomerizations might be envisioned for other chromophores of the second type, but the apparent lack of additional lyase proteins remains puzzling.

### 3. Spectroscopy

Biliproteins provide an advantage to their parent organisms by absorbing precisely in the 'green-gap' of the Chls *a* and *b*. This advantage is balanced, however, by the high protein content and the correspondingly high biosynthetic costs for phycobilin-containing antennas (Table 3). The reason for this investment probably is the unfavorable biophysical properties of free bilin-chromophores, which are remarkably unsuited for light-harvesting (Scheer, 1982; Braslavsky et al., 1983; Falk, 1989). Free phycocyanobilin has only moderate absorption in the visible range ( $\epsilon_{600\text{ nm}} \approx 17,000\text{ cm}^{-1}\text{M}^{-1}$ ), much

less than that of any other antenna chromophore (Fig. 6c). The extinction coefficient increases in PEB and PUB, the chromophore absorbing at shortest wavelengths (Fig. 6a), but even the latter is a much poorer absorber than, e.g. Chl *a*. Free bilins (as well as denatured phycobilins) also have short radiative lifetimes and correspondingly low fluorescence yields ( $<10^{-4}$ ), and are therefore rather efficient quenchers of excited states. Furthermore, they are chemically and photochemically very labile. Obviously, these properties need to be improved, because such chromophores are efficient degraders of excitation energy rather than collectors. Their only advantage is that they do not pose photodynamic problems. Free bilins are, nonetheless, found only in traces in photosynthetic tissue, mainly as degradation intermediates of chlorophylls (Kräutler and Matile, 1999; Gossauer and Engel, 1996).

The required improvements of the excited state properties are done admirably by the apoproteins, albeit at a considerable cost in the form of protein synthesis. In the native biliproteins, the photophysical properties of the chromophores are changed so profoundly that at first glance there is hardly any relation among the two states: the chromophore absorptions are increased more than five-fold ( $\epsilon \approx 10^5$ ) (Fig. 6c), the fluorescence lifetimes and thereby the yield increase by four orders of magnitude to nearly 100% (see Scheer, 1982). At the same time, the chromophores become quite stable, e.g. to oxygen. The reason for these dramatic changes is, however, not the formation of the covalent linkage to the apoprotein. Binding to the protein in fact hardly changes the properties of the chromophores. This is evidenced most clearly by the denatured phycobiliproteins, which show exactly the same 'undesirable' properties as the free chromophores. As an example, denatured phycocyanin (8 M urea, pH 1.9, heavy line in Fig. 6c) has practically the same spectrum as the derived chromopeptide or a cysteine-adduct of PCB, and is only slightly blue shifted but otherwise similar to that of free PCB. The dramatic changes in the properties of the biliprotein chromophores are brought about only in the native biliproteins. Here, the bilin chromophores render the phycobilins excellent antenna pigments, which absorb light efficiently and transfer it to the RC with quantum yields approaching 100% (Scheer, 1986). Variations of the proteins and in particular the association with linker-proteins allow in addition for a considerable tuning (up to 100 nm for e.g. PCB) of the absorption maxima (Reuter et

Table 3. Investment into chromophores in different antennas

Antenna	Esterifying alcohol investment into tetrapyrrole <sup>a)</sup>	Protein investment (kDa protein/chromophore)	Protein investment (kDa protein/tetrapyrrole)
Chlorosome (green bacteria)	3	<1	≈ 1
LHCII (green plants)	4	1.7	2.25
LHCII (heterokonts, dinophytes)	4 (Chl <i>a</i> ), 0 (Chls <i>c</i> )	1.7	2.25
LH1 (purple bacteria)	4	4.3	6.5
LH2 (purple bacteria)	4	2.6	4.3
PS I (type I RC with integrated antenna)	4	3.5	4
Allophycocyanin	—	16	16
C-Phycocyanin	—	11	11
C-Phycocerythrin	—	7.5	7.5

<sup>a)</sup> Number of isopentenylpyrophosphate units

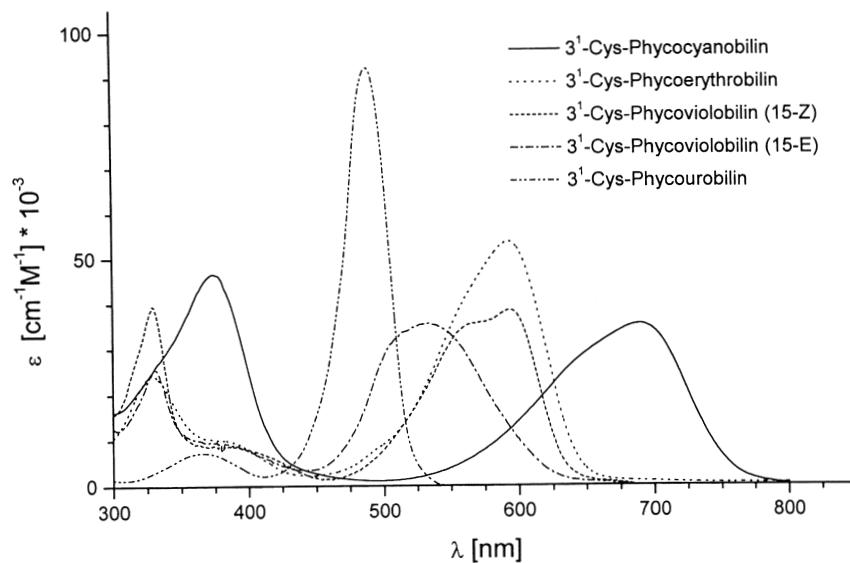


Fig. 6. Absorption spectra of open-chain tetrapyrroles in the free state and in native biliproteins: a: Spectra of the four phycobilin chromophores (top structures in Fig. 4b) from cyanobacterial and rhodophyte biliproteins in their protonated state. For 3<sup>1</sup>-Cys-PVB, the spectra of the 15Z- and 15E-isomers are shown. These isomers are photochemically interconvertible in the native protein, PEC. See Fig. 4b for the nomenclature. I thank K.-H. Zhao for the spectra of PVB, and M. Storf for the spectra of PCB and PEB. The spectrum of PUB has been redrawn from Klotz and Glazer (1985). The scaling of the ordinate is based on the extinction coefficients of Klotz and Glazer (1985), Glazer and Hixson (1975) and Bishop et al. (1987). Spectra of denatured biliproteins or of chromopeptides are very similar to the spectra of the free chromophores, while those of the native biliproteins are quite different (see Fig. 6c and text).

al., 1999) (Fig. 6c). Two molecular mechanisms have been considered for the optimized properties of the chromophores in native biliproteins: The first is a conformational change of the chromophores; the second, a restriction of their conformational mobility. Free bilins have a preferred cyclic conformation, with the four pyrrole rings arranged in a geometry similar to that in the cyclic tetrapyrroles (Braslavsky et al., 1983; Falk et al., 1984). The absorption spectrum is therefore of the porphyrin type, albeit with broader bands (see below), with a weak visible and a moderately intense near-uv band. The bands

are broader, however, due to the conformational flexibility. In the native biliproteins, they are brought into an energetically less favorable extended polyene-type conformation (Schirmer et al., 1987; Duerring et al., 1990; Ficner and Huber, 1993; Brejc et al., 1995), in which the long-wavelength transition is no longer forbidden (Scheer et al., 1982). This conformational change can explain the strongly increased absorption in the Vis well, but is of little consequence to the excited-state lifetime. This has been shown with free bilins having a similarly extended conformation, which still have quite low

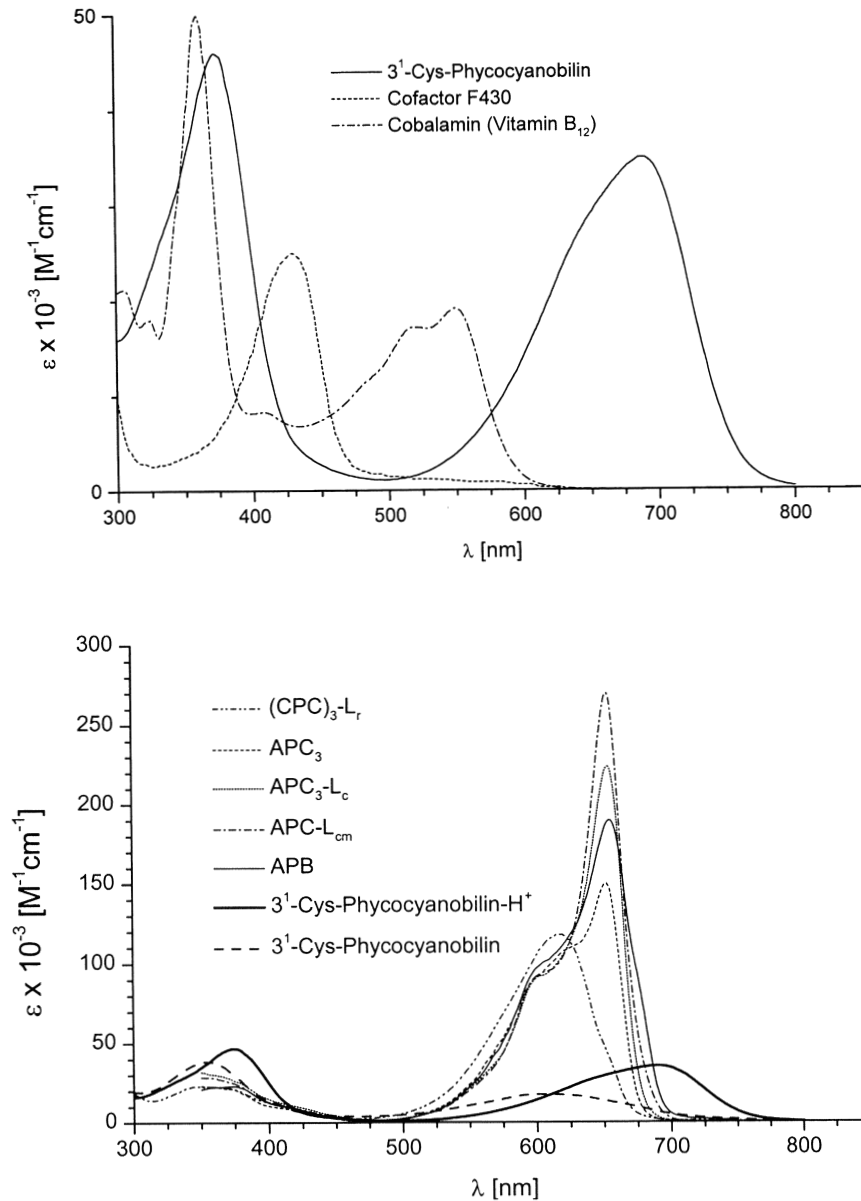


Fig. 6. (Continued) Absorption spectra of open-chain tetrapyrroles in the free state and in native biliproteins: b: Comparison of the spectra of an open-chain chromophore, protonated  $3^1\text{-Cys-PCB}$  in a cyclic conformation (C-phycocyanin in 8M urea, pH 1.9, spectrum provided by M. Storf; the spectroscopic properties of  $3^1\text{-Cys-PCB}$  chromopeptides are practically identical) and of two cyclic tetrapyrroles in which the conjugation chain is interrupted, cobalamin (vitamin B<sub>12</sub>) and cofactor F430 (spectra taken from Scheer, 2000). c: Environmental effects (conformation, protonation, type and state of the protein) on the spectra of a phycobilin chromophore,  $3^1\text{-Cys-PCB}$ . Shown is the same chromophore in its isolated, neutral ( $3^1\text{-Cys-PCB}$ , cyclic conformation) and protonated state ( $3^1\text{-Cys-PCB}$ , protonated, cyclic conformation, spectra from M. Storf), of C-phycocyanin in the native trimeric state with a bound rod-linker ( $(\text{CPC})_3\text{-L}_r$ ), of allophycocyanin in the native trimeric state ( $\text{APC}_3$ ), of its complexes with the core and the core-membrane linker ( $\text{APC}_3\text{-L}_{cm}$ ), and of allophycocyanin B (APB). In all known native biliproteins, the chromophores are present in slightly varying extended conformations (Brejc et al., 1995; Schirmer et al., 1987; Reuter et al., 1999). The allophycocyanin spectra were kindly provided by W. Reuter. The ordinates correspond to the extinction coefficients of single chromophores, averaged over all binding sites (see Gottschalk et al., 1993; Gottschalk et al., 1994). Note the large increase in absorption in the native biliproteins.

fluorescence yield ( $\sim 10^{-3}$ ) (Petrier et al., 1981). Two reasons have been suggested for this rapid deexcitation. One is intramolecular H-transfer; the other, the shallow conformational 'energy-landscape' of these flexible pigments. The latter leads to a high density of states as evidenced by the broad absorptions, which render high vibronic levels of the electronic ground state ( $S_0 v_x$ ) iso-energetic to excited state ( $S_1$ ) levels. This favors radiationless transitions from  $S_1$  to  $S_0$  and 'thermalization' (thermal equilibration) of the excited state energy, by which it becomes unavailable for photosynthesis. A restriction of the conformational freedom is therefore expected to slow down this process. This has indeed been verified with model chromophores, where the introduction of extra bonds between the rings strongly enhances fluorescence (De Groot et al., 1982; Kufer et al., 1983). A similar mechanism is likely to operate in the biliproteins, where the fluorescence lifetime is increased to 2–3 ns.

Protonation of free bilin chromophores approximately doubles their absorbance in the visible region (Fig. 6c). Since in the biliproteins an aspartate residue is close to the two central nitrogens, protonation is a potential additional source for the very strong absorption of these chromophores in the native phycobiliproteins (Chapter 9, Mimuro and Kikuchi; Kikuchi et al., 1997). However, this aspartate is flanked by the guanidine-group of an arginine residue, and it is therefore not clear from the structure if protonation takes place. Additional support to this idea has come from vibrational spectra (Siebert et al., 1990).

While all chlorophyll proteins also contain carotenoids, the biliproteins are devoid of them. In contrast to the high phototoxicity of chlorophyll, there is currently no good evidence that biliproteins can generate singlet oxygen, either in their free state, or integrated into the native protein (Section II).

## C. Carotenoids

### 1. Structures

Carotenoids are the structurally and functionally most diverse group of photosynthetic pigments. The term 'carotenoid' is used here in a general sense, encompassing both the 'carotenes' proper, which have hydrocarbon structures, and their oxygenated derivatives, which are often termed 'carotenoids' or 'xanthophylls.' Covering part of the 'green gap' ( $\lambda_{\max} = 450\text{--}550\text{ nm}$ ), the contribution of carotenoids to light-harvesting varies considerably. It is particularly large in purple photosynthetic bacteria, some heterokont and dinophyte algae (see e.g. the fucoxanthin and peridinin-chlorophyll proteins, Chapters 1 (Green and Anderson), 11 (Hiller and Macpherson)), while only about  $1/3$  of the light quanta absorbed by carotenoids in green plants are transferred to the reaction centers. However, while light-harvesting by carotenoids can largely be substituted by other pigments absorbing in the same spectral range, carotenoids are indispensable for photosynthesis as protective pigments against direct and indirect damage by light. With photosynthesis requiring a finely tuned and dynamic balance between the beneficial and deleterious effects of light, the central role of carotenoids is protection. Due to their protective function, carotenoids also are present in varying quantities in non-phototrophic organisms, as well as in non-photosynthetic organs (such as flowers), tissues or organelles of photosynthetic organisms.

There are currently more than 800 known carotenoids, each of which can form several *cis-trans* isomers and be further modified. Only a fraction of them is involved in photosynthesis. However, this fraction is already impressive with, e.g. about hundred carotenoids having been identified just in the

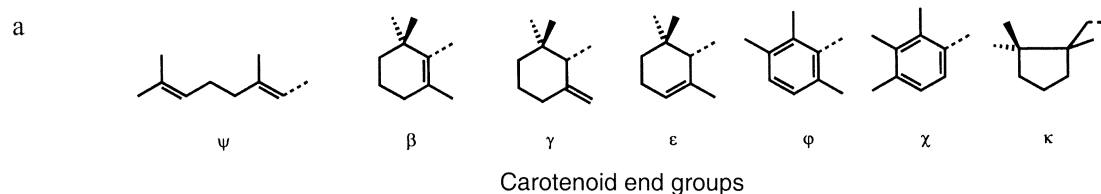


Fig. 7. Structures and absorption properties of carotenoids: a: The various end-groups of carotenoids are denoted by greek letters. Note that the Greek letters are used in somewhat confusing ways in the carotenoid literature. Besides referring to the end groups, they may also refer to isomers. In the first case, two Greek letters are given, corresponding to both ends of the linear structure; in the latter a single Greek letter is used. Two examples illustrate this:  $\beta$ -carotene carries two  $\beta$  end-groups, and is therefore systematically termed  $\beta,\beta$ -carotene.  $\alpha$ -carotene carries two  $\epsilon$  groups, and  $\gamma$ -carotene one  $\beta$  and one  $\psi$  end-group; they are therefore systematically termed  $\epsilon,\epsilon$ -carotene and  $\beta,\psi$ -carotene, respectively (Weedon and Moss, 1995; Fig. 7b).



Pigment $\lambda_{\text{max}}$ ( $\epsilon \cdot 10^{-3}$ [solvent])	Formula (if not specified, the all- <i>trans</i> -structure is shown)
<b>Alloxanthin</b> 423, 450, 479 [P]	
<b>Antheraxanthin</b> 422, 446 (137.2), 472 [E]	
<b>Astaxanthin</b> 470 (125.1) [H]	
<b>Bacteriorubixanthin</b>	
<b>Caloxanthin</b> 426, 449, 475 [E]	
<b>Canthaxanthin</b> 466 (124.1) [P]	
<b><math>\beta,\beta'</math>-Carotene</b> 425, 450 (138.9) [P]	
<b><math>\beta,\epsilon</math>-Carotene</b> 422, 444 (150.1), 473 [P]	
<b><math>\beta,\psi</math>-Carotene</b> 437, 462 (166.2), 494 [P]	
<b><math>\gamma</math>-Carotene, 1'-hydroxy, acyl-glucosyl</b>	

<b><math>\gamma</math>-Carotene, 4-keto</b> 465, 490(sh) [P] Hertzberg and Liaaen-Jensen, 1966	
<b><math>\epsilon,\epsilon'</math>-Carotene</b> 416, 440 (167.2), 470 [P]	
<b><math>\zeta</math>-Carotene</b> 377, 399 (138 [H]), 425 [E]	
<b><math>\zeta</math>-Carotene, dihydroxy</b>	
<b><math>\beta,\beta'</math>-Carotene-2R-ol</b> 430(sh), 452(126.4), 479 [A] Kjosen et al., 1972	
<b>Chlorobactene, 1'-hydroxy, acyl-glucosyl</b>	
<b>Crocoxanthin</b> 422, 445, 475 [H]	
<b>Diadinoxchrome</b> 410, 428/431(146), 458 [A]	
<b>Diadinoxanthin</b> 421, 445/7 (122.8), 475 [H]	
<b>Diapo-carotene-dioate, di-(acyl-glucosyl)</b> R = C <sub>12:0</sub> , C <sub>14:0</sub> , C <sub>14:1</sub> , C <sub>16:0</sub> at C <sub>6</sub> of Glc	
<b>Diapo-neurosporene</b>	

Fig. 7. (Continued) Structures and absorption properties of carotenoids: b. Selected carotenoids of photosynthetic organisms. The pigments are arranged in the same (alphabetic) order as in Table 1b. The list is incomplete, and the number of carotenoids is still growing rapidly. The numbering of the typical C<sub>40</sub>-skeleton is shown in the structure of  $\beta,\beta$ -carotene (IUPAC and IUB, 1971, 1975; Weedon and Moss, 1995). The carotenoid nomenclature used is mostly generic, often referring to the organism the carotenoid is first isolated from, or in which it is prominent. The greek letters ( $\beta$ ,  $\gamma$ ,  $\epsilon$ ,  $\phi$ ,  $\zeta$ ,  $\psi$ ) refer to the 'ends' of the structures (see Fig. 7a). Unless specifically noted, only the all-*trans* structures are shown; isomers may be present in vivo. Most of the structures are of the C<sub>40</sub> type; exceptions are the apo-carotenes and the di-glycosylated C<sub>30</sub> carotenoid thiothec 560. Glc = glucose, Lac = lactose.

<b>Diatoxanthin</b> 448, 476 [H]	
<b>1,2-Dihydro-neurosporene</b>	
<b>Dinoxanthin</b> 418, 442 (135), 471 [A]	
<b>Echinonone</b> 458 (118.7), 482 [P]	
<b>Erythroxanthin-sulfate</b>	
<b>Fucoxanthin</b> 425, 446/9 (105.3), 473	
<b>Fucoxanthin, 19'-butanoyloxy</b> (also hexanoyloxy) 418, 445 (109), 470 [A]	
<b>Fucoxanthin, 4-keto-19'-hexanoyloxy-</b>	
<b>Heteroxanthin</b>	
<b>Isorenieratene</b> 426, 448 (109.8), 475 [P]	
<b>Lutein</b> 432, 458 (127), 487 [B]	
<b>Lycopene</b> 444, 470 (184.9), 502 [P]	
<b>Monadoxanthin</b> 446 (142) [D]	
<b>Myxobactone</b>	
<b>Myxoxanthophyll</b> 450, 478 (185), 510 [A]	
<b>Neoxanthin, 9-cis</b> 415, 438(136 in [E]), 467 [A]	
<b>Notoxanthin</b> 428, 450, 478 [E]	
<b>Okenone</b> 460, 484(134.1), 516 [P]	
<b>Oscillaxanthin</b> 468, 492, 526 [E]	

Fig. 7b (Continued)

<b>P-457</b> 426(sh), 450 (154 at 457 in [A]), 485(sh) [M]	
<b>Pertidin</b> 467 (81.3) [B]	
<b>Phytoene</b> 276, 286 (68), 297 [P]	
<b>Phytofluene</b> 331, 348(73.2), 367 [P]	
<b>Prasinoxanthin</b> 450, 466 [E]	
<b>R.g. -keto III</b>	
<b>Rhodopin -β-D-glucoside</b>	
<b>Rhodopin, 1'-hydroxy</b>	
<b>Rhodopinal, 13-cis-</b>	
<b>Siphonaxanthin</b> 446, 468 [P]	
<b>Siphonoin</b>	
<b>Spheridene</b> 441, 468 (158.2), 502 [B]	
<b>Spheridenone</b> 460, 483, 515 [P]	
<b>Spirilloxanthin</b> 479, 510 (147.2), 546 [B]	
<b>Thioeste 460</b>	
<b>Vaucheriaxanthin</b> 420, 441, 467 [A]	
<b>Violaxanthin</b> 427, 453(4)(134.4), 483 [B]	
<b>Zeaxanthin (diglucoside)</b> R = H (= Glc)	

Fig. 7b (Continued)

anoxygenic bacteria. An incomplete display of carotenoids from photosynthetic organisms is shown in Fig. 7b, and their distribution among the phyla listed in Table 1b. More systematic surveys can be found in specialized reviews on photosynthetic bacteria (Takaichi, 1999), algae (Jeffrey et al., 1997), cyanobacteria (Hirschberg and Chamovitz, 1994) and plants and algae (Young, 1993b; DellaPenna, 1999). Some of the carotenoids can be used as taxonomic markers, in particular among the algae and, to a lesser degree, the phototrophic bacteria (Blankenship et al., 1995a).

Carotenoids are classically defined as diterpenes: two  $C_{20}$ -units (originally geranyl-geraniol) are joined tail-to-tail to a chain of 32 carbon atoms bearing eight methyl side-chains. The symmetry of the C-skeleton is also reflected in the nomenclature (see  $\beta$ , $\beta$ -carotene in Fig. 7b and IUPAC and IUB, 1971, 1975; Weedon and Moss, 1995): it counts from either end to the center. Note, however, that the first C-atom on either side is treated as an additional substituent. Generally, this basic carbon  $C_{40}$ -skeleton is either retained, or only slightly modified, e.g. by cyclization at one or both ends (Fig. 7a). However, much more extensive modifications are possible, and these seem to be particularly far-reaching in carotenoids dedicated to light harvesting. Common modifications involve the degree of unsaturation, *cis-trans* (E/Z) isomers, double-bond rearrangements including allenic and acetylenic units, the introduction of oxygen-containing functional groups, and glycosylation/acylation of these groups. More extensive modifications involve shortening of the carbon skeleton (usually in  $C_1$  or  $C_5$ -units, see e.g. thiotece 460 in Fig. 7b), extension of the skeleton to form, e.g.  $C_{50}$ -carotenoids, or the formation of  $C_{30}$ -carotenoids (diapo-carotenes) from condensation of two farnesyl- instead of geranylgeranyl-units (Fig. 8). One of the most widespread carotenes, peridinin, is a  $C_{37}$  pigment.

The structural variety of carotenoids is particularly large among the anoxygenic photosynthetic bacteria and the algae. In the former, it is (again, see chlorophyll section) most pronounced among the green bacteria (Chlorobiaceae) and in the phylogenetically complex group of aerobic purple bacteria, which synthesize BChl *a* and photosynthetically competent pigment-protein complexes under aerobic conditions. In the algae, the diversity is less complex, but the basic structures are sometimes extensively modified. As an example, the abundant bacillario-

phyte carotenoid peridinin is not only considerably functionalized, but has also three carbon atoms excised from the central part of the molecule. A recent book on phytoplankton (Jeffrey et al., 1997) lists 29 carotenoids as markers in oceanography. The variations are less in the photosynthetic apparatus of green plants, while derived tissues (flowers, fruits) have a variety of carotenoids that are generally located in the chromoplasts.

## 2. Biosynthesis

As terpenoids, carotenoids are products of isopentenyl-pyrophosphate metabolism. This intermediate can be synthesized either by the 'classical' pathway *via* mevalonate (Britton, 1993), or via the more recently discovered deoxyxylulose pathway (Lichtenhaler et al., 1997; Boucher and Doolittle, 2000) (Fig. 8). The phylogenetic distribution of the latter pathway is still under study, but it seems to be the pathway leading to carotenoids in most photosynthetic organisms. One  $C_5$ -unit (dimethylallyl-pyrophosphate) is condensed sequentially by prenyl transferases in a head-to-tail fashion with three isomeric  $C_5$ -units (isopentenyl-pyrophosphate) to yield geranylgeranyl-pyrophosphate (GGPP), an important branching point in terpenoid metabolism. GGPP is, directly or indirectly, the substrate for esterifying the C-17 propionic acid side chain of most chlorophylls (see above), linking the tetrapyrrole- and terpenoid pathways. The carotenoid branch (Fig. 8) begins with a tail-to-tail condensation of two molecules of GGPP by the dedicated enzyme phytoene synthase, which is the target of several herbicides that act by depriving the plants of the photoprotective carotenoids. Having only three conjugated double-bonds, the resulting phytoene is still uncolored. Dehydrogenation by phytoene-desaturase *via* phytofluene to lycopene is common to most of the photosynthetic carotenoids currently known (only few carotenoids derive from intermediates like neurosporene or from the  $C_{30}$  (diapocarotene) branch). Many pathways branch at lycopene (Fig. 8) and render some of the enzymes and products phylogenetic markers, in particular among the photosynthetic bacteria and algae (Blankenship et al., 1995a; Jeffrey et al., 1997). The  $C_{30}$  or diapocarotenoids of the heliobacteria and some other organisms are probably synthesized in a similar way, except that the pathway begins with the condensation of two  $C_{15}$ -units (farnesyl-pyrophosphate) to yield diapophytoene as the

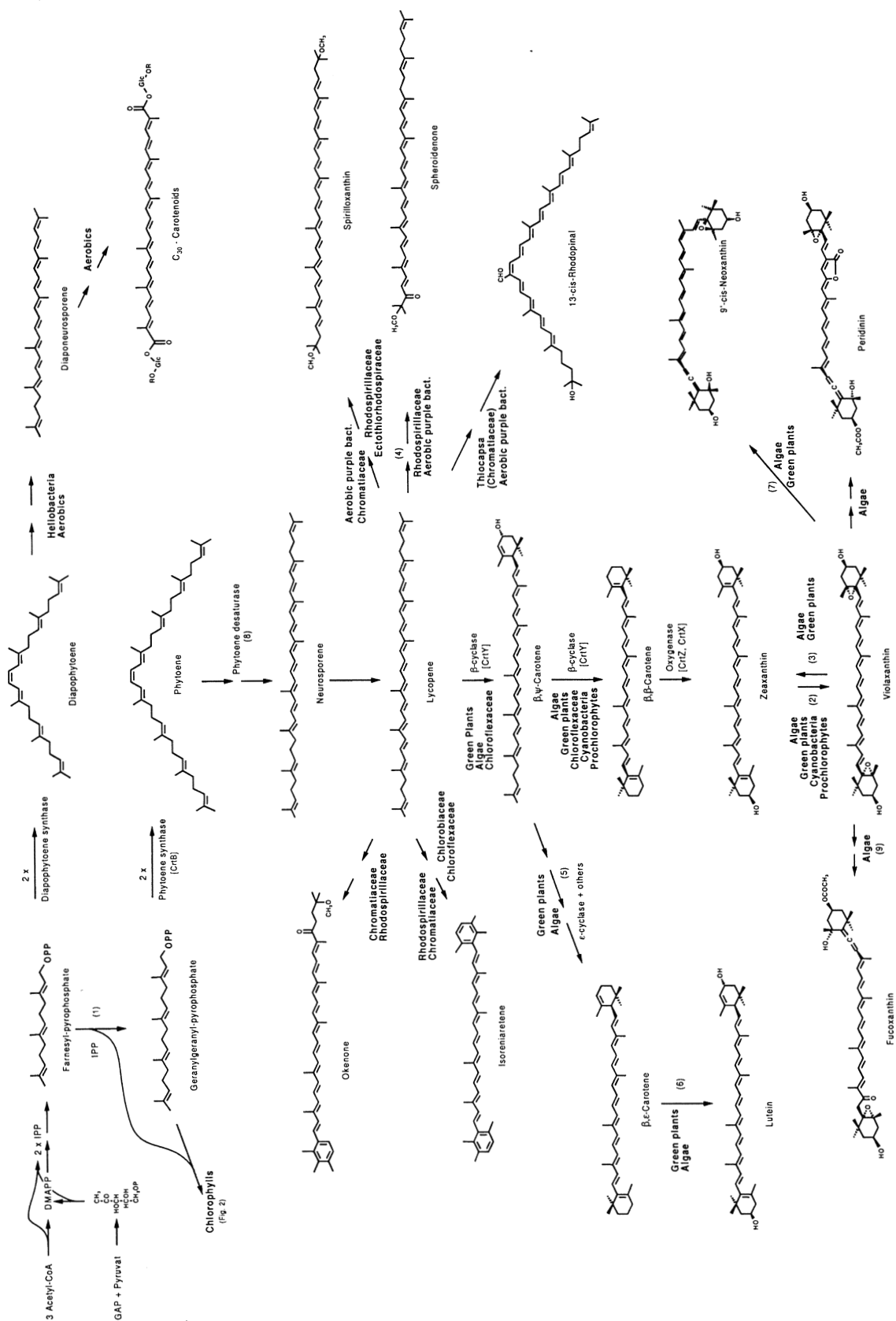
dedicated product, which is then further transformed (Fig. 8; Takaichi, 1999).

In this introductory overview, only the major branches of the carotenoid metabolism will be sketched. It should be pointed out that the genetic, regulatory and enzymic details are presently known only in few cases. For details, the reader is referred to specialized reviews on carotenoid biosynthesis (Hirschberg and Chamovitz, 1994; Alberti et al., 1995; Sandmann and Scheer, 1998; DellaPenna, 1999; Takaichi, 1999). Several pathways can be distinguished by the type(s) of transformation encountered. They are listed in Fig. 8 together with their distribution in the different photosynthetic organisms. It is likely that similar reactions in different branches are carried out by related enzymes, but this has not been established yet in most cases.

In the spheroidene pathway, one of the end-groups is oxygenated (or methoxylated) and can be further oxygenated as in spheroidenone. In the spirilloxanthin pathway, which is most widely distributed among the anoxygenic bacteria, both ends are oxygenated (or methoxylated) to yield spirilloxanthin. In a series of pigments derived from either pathway, a cross-conjugated aldehyde group is introduced at C-13 by oxidation of carbon C-20, which is linked to an E > Z isomerization of the  $\Delta_{13,14}$ -double bond yielding e.g. 13-*cis*-rhodopinal. While the aforementioned pathways lead to open-chain carotenoids, others begin with the cyclization of one or both of the end-groups. In anoxygenic bacteria, aromatic end rings are frequent among the *Chlorobiaceae* and *Chromatiaceae*, leading to pigments of the okenone (one end group cyclized) and isorenieretene type (two end groups cyclized). Aromatization requires a rearrangement of the C-skeleton by a shift of at least one methyl group, and the two branches differ by the methylation pattern of the end rings (see Figs. 7a, 8). In higher plants, algae cyanobacteria and the *Chloroflexaceae* (Fujita and Bauer, 2000; Chapter 1, Green and Anderson), pigments carrying aliphatic rings at the ends of the molecule are common in photosynthetic complexes. Here, two major branches can be distinguished. The common intermediate is  $\beta,\psi$ -carotene ( $\gamma$ -carotene, see the legend to Fig. 7a for the use of greek prefixes in carotenoid nomenclature), which results from  $\beta$ -cyclization at one end. In the most ubiquitous branch (plants, algae, cyanobacteria, *Chloroflexaceae*), the other end is cyclized in a similar fashion and probably by the same  $\beta$ -cyclase to yield  $\beta,\beta$ -carotene. This  $\beta,\beta'$ -

branch is traveled only a few steps in the *Chloroflexaceae*, while in plants it leads to zeaxanthin, antheraxanthin, violaxanthin, and neoxanthin. The more heavily modified carotenoids from algae and cyanobacteria are probably products of even further modifications down this pathway. As an example, it has been proposed that the most abundant carotenoid, fucoxanthin, is synthesized via violaxanthin (Lohr and Wilhelm, 1999). In the second branch ( $\beta,\epsilon$ ), which in plants and some algae is used together with the first one, the second cyclization (at the opposite end) is carried out by a different enzyme,  $\epsilon$ -cyclase, yielding the isomeric  $\alpha,\epsilon$ -carotene ( $\alpha$ -carotene). The main end-product of this branch is lutein. The biosynthesis of carotenoids has been studied in considerable detail in plants, cyanobacteria and purple bacteria. One practical reason for this is that many herbicides act by blocking carotenoid biosynthesis and thus impeding light protection. Some of the carotenoids are also commercially valuable products as natural food dyes, protectants or provitamins.

While it can be speculated that the plethora of structural modifications all play a role in optimizing carotenoids for the diverse functions they perform, their significance is only slowly emerging. One important factor is certainly the length of the conjugation system. By proper adjustment, the absorption maximum can be shifted considerably, which is critical for light-harvesting as well as energy transfer. Since the energies of other excited states (e.g. the triplet) parallel this energy change, the length of the conjugation system also is important for the protective functions. A minimum of seven conjugated double bonds is considered necessary to quench Chl *a* triplets, and nine double bonds to quench singlet oxygen, with both processes involving energy transfer to produce carotenoid triplets. A second important aspect is the introduction of functional side chains. These can optimize interactions with the environment, e.g. the protein, in order to position the pigments properly. However, they can also lead to more subtle changes that critically affect the complex excited-state dynamics of carotenoids, as has been shown recently with some highly modified pigments like peridinin and fucoxanthin (Frank et al., 2000a). Koyama et al. have suggested that the carotenoid bands also shift differently in response to the polarity of the environment, by which overlap can further be optimized (Fujii et al., 2001b). The accessibility and lifetime of the forbidden  $S_1$ -state (see below) depends



on the symmetry of the molecule, which is considerably reduced in these pigments. Modification of the side-chains can also change the solubility. While most carotenoids are hydrophobic molecules, there are many known modifications that render them more polar. A rare but extreme example is sulfonation (e.g. to erythroxanthin in the aerobic *Erythrobacter* sp.); another is the much more frequent glycosylation (e.g. by UDP-glucose in *Erwinia herbicola*). In some bacteria, up to 70% of the carotenoids are modified this way (Takaichi, 1999), and often the sugar group is modified further by acylation at C-6.

Little is known about the transformation of carotenoids once they are incorporated into pigment protein complexes. A notable exception is zeaxanthin (Fig. 7b). In plants, zeaxanthin is localized mainly in specialized antenna complexes such as CP29. In a tightly regulated reaction sequence, it can be reversibly epoxidized to violaxanthin; this violaxanthin-cycle provides an important (but poorly understood, Frank et al., 2000b) switch between efficient energy transfer (light harvesting) and non-photochemical quenching (energy dissipation as heat), with important consequences for light-protection of the photosynthetic apparatus (Chapters 13 (Krause and Jahns); 14 (Huner et al.)). The zeaxanthin/violaxanthin balance is controlled by physiological factors including the redox state of the plastoquinone pool. The irreversible oxidation of  $\beta,\beta$ -carotene to zeaxanthin in PS II-RCs also has been implicated as a means to increase the violaxanthin/antheraxanthin/zeaxanthin pool (Jahns et al., 2000). The violaxanthin cycle is also operative in green and some brown algae, and may even be more widespread (Lohr and Wilhelm, 1999). Other epoxidized carotenoids are frequent in all algae, and at least one of them (diadinoxanthin) has been shown to be involved in a similar, albeit only one-step, reversible deepoxidation cycle.

### 3. Spectroscopy

Two books have summarized the current state of the art in carotenoid spectroscopy with respect to structure, stereochemistry, analytical applications, and using carotenoids as probes for their environment (Britton et al., 1995; Frank et al., 1999). Analytical data and practical aspects of carotenoids from marine phytoplankton are nicely compiled by Jeffrey et al., (1997). As in the previous sections, only the basic features of the electronic spectra (absorption, emission) will be discussed here, and the reader is referred to the aforementioned sources as leading references.

The rod-shaped carotenoids show the typical absorption spectra of linear polyenes, which are characterized by some unusual features (see Britton, 1995a; Christensen, 1999; Koyama and Fujii, 1999; Robert, 1999 for recent reviews):

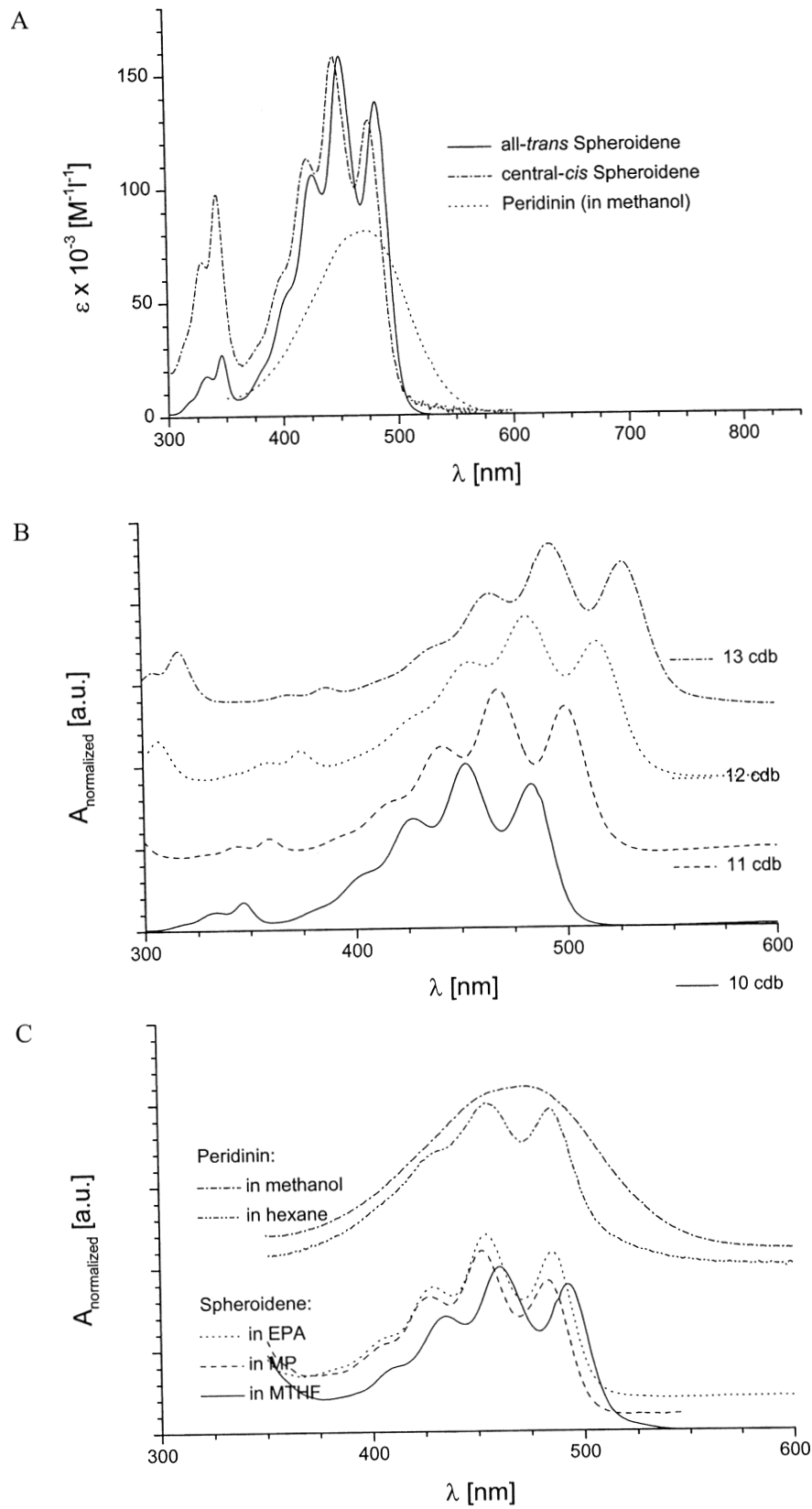
1: The  $S_0 \rightarrow S_1$  transition from the  $1A_g^-$  ground state to the  $2A_g^-$  lowest electronic excited state is optically forbidden<sup>3</sup>. While this is, strictly speaking, true only for  $C_2$ -symmetric carotenoids like  $\beta,\beta$ -carotene, this rule applies to most carotenoids and is only partially released in some of the most unsymmetric carotenoids such as peridinin.

2: The major optical absorption arises from the allowed  $S_0 \rightarrow S_2$  transition from the  $1A_g^-$  ground state to the  $1B_u^+$  state. It is generally split into several vibronic transitions, resulting in a series of three closely spaced absorption bands (Fig. 9A,B). These generally are well resolved, but can be broadened to a degree that they appear only as a major band with a poorly resolved shoulder on either side (Fig. 9C).

<sup>3</sup> The term 'forbidden' is used in spectroscopy a bit like the rules of the road in common life, meaning that a forbidden transition is unlikely, and that the likelihood decreases with the strictness of its 'forbiddenness.'

Fig. 8. Biosynthesis of carotenoids. Scheme of the biosynthetic pathways leading to different types of carotenoids in various classes of photosynthetic organisms. The end product shown for a given branch is only an example of the type of structures formed, and may not actually be present in all cases. The term 'aerobics' refers to the phylogenetically diverse group of aerobic bacteria producing BChl. IPP = isopentenyl-pyrophosphate, DMAPP = dimethylallyl-pyrophosphate, PP = pyrophosphate. Carotenoid biosynthesis enzymes (if no organism is mentioned, genes are named from the annotation in *Rhodobacter capsulatus*, *Rhodobacter sphaeroides* or *Erwinia herbicola*): (1) = prenyl transferase (geranyl-geranyl-pyrophosphate synthase [CrtE]); (2) zeaxanthin epoxidase [Aba1 in *Arabidopsis*], (3) violaxanthin deepoxidase [vde in tobacco], (4) chloroxanthin synthase (C-1 hydroxylase) [Crt C], chloroxanthin dehydrogenase [CrtD], methyl transferase [CrtF], C-2 oxygenase [CrtA], (5)  $\epsilon$ -cyclase [Lut2 in *Arabidopsis*], (6)  $\beta$ -oxygenase ( $\beta$ -ring hydroxylase) [CrtX, CrtZ] and  $\epsilon$ -oxygenase ( $\epsilon$ -ring hydroxylase) [Lut1 in *Arabidopsis*], (7) neoxanthin forming enzyme; (8) phytoene desaturase [CrtI] catalyses both steps in purple bacteria, while phytoene desaturase [CrtP] and  $\zeta$ -carotene desaturase [CrtQ] act sequentially in cyanobacteria; (9) via diadinoxanthin, proposed by Lohr and Wilhelm (1999).





3: Recent data indicate that yet another (forbidden) excited state,  $1B_u^-$ , lies between the 'classical'  $S_1$  ( $2A_g^-$ ) and  $S_2$  ( $1B_u^+$ ) states (Nagae et al., 2000; Fujii et al., 2001b). Strictly speaking, the latter would then be an  $S_3$  state, but the widely used term  $S_2$  for the  $1B_u^+$  state has been maintained for simplicity in this review.

4: All-*trans*-carotenoids show no further strong absorptions in the Vis and near UV spectral range, while the less symmetric *cis*-carotenoids show a typical '*cis*-band' 100–150 nm to the blue of the main absorption, whose intensity depends on the degree to which the symmetry is broken (Fig. 9A).

5: Most carotenoids show extremely rapid internal conversion (IC) and hence negligible fluorescence, with lifetimes in the range of only a few picoseconds. Since excitation transfer has to compete with IC, light-harvesting carotenoids need to be in close proximity to their energy acceptors, which are mostly chlorophylls.

6: Carotenoids have unusually low-lying triplet states. The triplet states of some are even slightly below the energy of singlet oxygen (1270 nm), which renders them efficient quenchers of this species. This is the case for  $\beta,\beta$ -carotene, whose  $T_1$  state (1270 nm = 7900 cm<sup>-1</sup>) contains only about 35% of the  $S_2$  excitation energy, which is the main absorption, and even only 55% of the energy of the optically forbidden  $S_1$  state (Christensen, 1999). By comparison, the  $T_1$  state of BChl has 65 % of the main absorption ( $S_1$ ) energy (Takiff and Boxer, 1988).

#### a. The $S_0 \rightarrow S_2$ Transition

The excited-state energies of carotenoids decrease progressively with an extension of the conjugation length (Fig. 9B). The majority of data concern the  $S_0 \rightarrow S_2$  absorptions ( $1A_g^- \rightarrow 1B_u^+$ ). The lowest-energy

band of this manifold shifts to the red from 297 nm in phytoene (three conjugated double-bonds) to 502 nm in lycopene (11 conjugated double bonds), 526 nm in spirilloxanthin (13 conjugated double bonds) and even 540 nm in the non-natural 3,4,3',4'-tetrahydrolycopene (15 conjugated double bonds). Although the red-shift frequently is said to occur continuously with increasing conjugation length, these data clearly indicate a progressively smaller increase. The excitation energy is expected to reach a limiting value even with conjugated chains of infinite length, and extrapolations have been used by several authors to estimate the position of the forbidden  $S_1$ -band (see Christensen, 1999 for a discussion).

Substituent effects in carotenoids have been treated in some detail (Britton, 1995a). Only few examples will be mentioned here. Of special interest is the presence of a high-energy band approximately 150 nm below the major  $S_2$ -absorption in *cis*-carotenoids (Fig. 9A). This so-called *cis*-peak is particularly strong ( $\epsilon \approx 25,000 \text{ M}^{-1} \text{ cm}^{-1}$ ) in the 13,14- and 15,15'-*cis*-isomers. Another point of interest is that, like many other pigments, carotenoids show a distinct red-shift upon distortion of the conjugated system. Such distortions can be caused by steric hindrance among the substituents. This effect is observed only for small to moderate twists of double bonds. If the molecule is distorted more strongly, as in allenic carotenoids, which carry two adjacent double bonds that are perpendicular to each other, the conjugation is effectively interrupted at the allenic (central) C-atom. While -OH or -OCH<sub>3</sub>-substituents have little effect on the spectra, unless they distort the system, conjugated carbonyl groups and the cross-conjugated CHO-group in rhodopinal-like pigments give red-shifts equivalent to a C=C bond. However, due to their polarizability and possibilities for specific interactions, such groups can give rise to much larger red-shifts in anisotropic environments like a protein. An extreme case is the blue lobster pigment,  $\alpha$ -crustacyanin, in which the astaxanthin chromophore is red-shifted by up to 150 nm from the absorption in

Fig. 9. Absorption spectra of carotenoids. A: Spectral types: The well resolved, three-banded absorption spectra of the all-*trans* and 15,15'-*cis* isomers of spheroidene, and the broad, poorly resolved one of peridinin (in methanol, see Fig. 9C). The *cis* isomer is characterized by an intense '*cis*-band' at ~340 nm. B: Effect of conjugation length: Spectra of spheroidene (10 conjugated double bonds (cdb)), 5',6'-dihydro-7',8'-dehydro-spheroidene (11 cdb), 7',8'-dehydro-spheroidene (12 cdb) and 1',2'-dihydro-3',4'-dehydro-spheroidene (13 cdb). Spectra modified from Fig. 4 of Desamero et al. (1998). The molecules were synthesized by the group of J. Lugtenburg, Univ. of Leiden. C: Solvent effects: Spectra of spheroidene in 2-methyl-tetrahydrofuran (MTHF), in 3-methyl pentane (MP), and in ethanol:petrolether-diethylether (EPA), and of peridinin in hexane and methanol. Spectra modified from Figure 2E of Frank et al. (2000a). I thank H. Frank, Univ. of CT, for providing all the data files for this figure.

organic solvents (Britton, 1995a). The presence of conjugated carbonyl groups has recently been recognized as an important factor for two particular spectroscopic features (Frank et al., 2000a). These are a broadening of the  $S_0 \rightarrow S_2$  absorption band, which is particularly pronounced in polar environments, and an increased lifetime of the  $S_1$  excited state (see below).

The absorption maximum also depends considerably on the solvent (Fig. 9C). The shift of the  $S_2$ -absorption band has been quantitatively related to the refractive index (high-frequency dielectric constant) of the solvent (Kuki et al., 1994; Andersson et al., 1991). The electrochromic shift of carotenoids in membranes can be considered a special case of the solvent dependence: if the pigments are oriented perpendicular to the membrane plane, they show distinct spectral shifts with changes in the membrane potential (Witt, 1975). Another special case is the effect of water, which in carotenoids leads to a considerable blue-shift of the major absorption. As in chlorophylls, this has been related to excitonic coupling in the aggregates formed by the poorly water-soluble carotenoids, but here the arrangement is such that most of the oscillator strength is transferred to the high-energy band. Excitonic coupling of carotenoids is not well documented in photosynthetic complexes, with the notable exception of the peridinin-chlorophyll protein (Koka and Song, 1977; Hofmann et al., 1996; see also chapter 11).

### *b. The $S_0 \rightarrow S_1$ Transition*

The position of the forbidden  $S_1$  state ( $2A_g^-$ ) and the involvement of this state in excited-state dynamics are of considerable interest in the photobiology of carotenoids and have been reviewed recently by Christensen (1999). Connecting two molecular orbitals of similar symmetry is forbidden for one-photon excitation, but allowed for (simultaneous) two-photon excitation, as was recognized some 30 years ago by Hudson and Kohler (1972), Schulten and Karplus (1972) and Granville et al. (1970) for short-chain conjugated polyenes. Due to experimental difficulties with the longer-chain carotenoids, most current estimates of the position and properties of the forbidden  $S_1$ -state rely on extrapolations from fluorescence studies on shorter carotenoids (see for example Gillbro et al., 1993). Direct observations by Raman excitation and fluorescence spectroscopy (Fujii et al., 1998, 2001b), and even by conventional

single-photon absorption spectroscopy (Mimuro et al., 1993; Fujii, 2001b; Polivka et al., 2001) have been reported more recently. These studies place the  $S_1$ -energy of  $\beta,\beta$ -carotene, for example, at 690 nm, which is very close to the  $S_1$ -energy of chlorophyll *a*. Energy transfer between carotenoids and chlorophylls is therefore possible in either direction, particularly if one considers possible energetic shifts of the chromophores in response to their environment, and the possibility of limited uphill energy transfer utilizing thermal energy. However, energy transfer also relies on selection rules, which inhibit dipolar energy-transfer mechanisms like Förster transfer for weak transitions (Chapter 3, Parson). For this reason, and because of the short lifetimes of carotenoid excited states, electron exchange has been discussed as the major energy transfer mechanism. This assumption may need reconsideration in view of mixing between the excited states. Moderate transition dipole moments (10–30% of that of the allowed  $S_0 \rightarrow S_2$  transition) have recently been determined for the  $S_0 \rightarrow S_1$  ( $1A_g^- \rightarrow 2A_g^-$ ) transition and the newly discovered  $1A_g^- \rightarrow 1B_u^-$  transition (Fujii et al., 2001b). Together with a careful balancing of a favorable transition overlap among the various carotenoid and chlorophyll excited states, this could provide efficient energy-transfer pathways by dipolar coupling. The structural diversity of carotenoids also could be used to optimize this process.

The situation is complicated further by the extremely rapid radiationless deexcitation of most carotenoids, not only from  $S_2$  to  $S_1$ , but also from  $S_1$  to  $S_0$ . As in the biliproteins, the reason for this rapid deexcitation is most likely the conformational flexibility of carotenoids. Koyama and coworkers have evaluated vibronic coupling between C=C stretching modes quantitatively as a major deexcitation pathway (Nagae et al., 2000). The rapid decay from  $S_1$  to the ground state combines with the forbidden nature of the radiative  $S_1 \rightarrow S_0$  transition to make fluorescence from  $S_1$  very weak.  $S_1 \rightarrow S_0$  fluorescence can be obscured by  $S_2 \rightarrow S_0$  fluorescence, by Raman lines of the solvent, and by the emission of impurities. Positive identification of carotenoid  $S_1$  fluorescence therefore requires very sensitive, time resolved techniques and careful controls. Moderately long-lived  $S_1$  excited states have been found recently in carotenoids with conjugated carbonyl groups, particularly in unpolar to moderately polar environments (Frank et al., 2000a). This might account for the selection of two such pigments, fucoxanthin

( $\tau_f \leq 70$  ps) and peridinin ( $\tau_f \leq 165$  ps), as the most abundant and ecophysiologically important light-harvesting carotenoids. However, even carotenoids that have very short  $S_1$  lifetimes in solution can transfer energy efficiently in some settings. For example, lycopene, spheroidene and neurosporene all transfer energy from their  $S_1$  states rapidly to BChl when they are reconstituted in LH2 complexes, apparently because mixing of the  $2A_g^-$  and  $1B_u^+$  configurations in the  $S_1$  state gives the  $S_1 \rightarrow S_0$  transition a significant dipole strength (Zhang et al., 2000).

The configurational space of carotenoids is further increased by the formation of double-bond ( $Z/E = cis/trans$ ) isomers. In solution, isomerization is a light-induced reaction, and a common triplet state has been identified for several of the isomers of  $\beta,\beta$ -carotene (Kuki et al., 1991; see Koyama and Fujii, 1999 for a recent review). The conformational space is somewhat restricted in carotenoproteins. Here, the all-*trans*-isomers are by far the most abundant in antennas, and most of the *cis*-isomers found upon extraction are likely artifacts. However, some *cis*-isomers are of particular importance: i) the biosynthesis of all  $C_{40}$ -carotenoids proceeds via *cis*-phytoene, which is isomerized on the way to carotene. ii) 9-*cis*-neoxanthin is a widespread antenna pigment in eukaryotes and an indispensable component of LHCII. iii) 15,15'-*cis* isomers have been identified in type II RCs from purple bacteria (DeGroot et al., 1992; Lancaster et al., 1995; Ohashi et al., 1996), and five *cis*-carotenoids have been identified recently in a high-resolution structure of PS I, including even di-*cis*-isomers (Jordan et al., 2000). Other isomers seem unrelated to photosynthetic pigment-protein complexes: *Dunaliella*, a halotolerant green alga, produces under stress large amounts of 9-*cis*- $\beta,\beta$ -carotene, which probably act as an absorption shield (Ben-Amotz et al., 1988), and the II- and 13-*cis*-isomers of the carotenoid derived retinal are found in dark-adapted rhodopsins and bacteriorhodopsins, respectively, as well as in intermediates of the pump-cycle of the latter. Transient *cis/trans* isomerizations probably also play a role in the rapid deexcitation of carotenoid triplet states (see below).

### c. Triplet State

An excited state of particular importance is the lowest triplet state ( $T_1$  or more correctly  $T_0$ ) of carotenoids. The direct excitation ( $S_0 \rightarrow T_1$ ) is forbidden and

therefore too weak to observe, and the equally forbidden  $S_1 \rightarrow T_1$  relaxation is negligible due to the short  $S_1$  lifetime. Optical studies of the carotenoid  $T_1$  state therefore rely on energy transfer from a sensitizer such as BChl, or on an extrapolation from shorter polyenes. Such studies place the  $T_1$  energy of  $\beta,\beta$ -carotene at 1380 nm or  $7250 \text{ cm}^{-1}$ , which is consistent with estimates from oxygen-quenching experiments (1266 nm,  $7900 \text{ cm}^{-1}$ ) (reviewed in Christensen, 1999). This energy is close to and slightly below that of singlet oxygen (1274 nm,  $7849 \text{ cm}^{-1}$ ), allowing for triplet energy transfer from the latter to  $\beta,\beta$ -carotene and other carotenoids with comparably low excitation energy. Since the radiationless  $T_1 \rightarrow S_0$  transition by ISC and IC occurs rapidly as a result of the conformational flexibility of carotenoids, this provides a safe means to deposit excess excitation energy as heat.

## IV. Analytics

Photosynthesis is a basic metabolic process, and the qualitative and quantitative analysis of photosynthetic pigments is used for many purposes. On a global scale, chlorophyll is frequently used to estimate and characterize the productivity of biotopes or photosynthetic communities. In mixed populations, specific marker pigments allow for an analysis of the composition on a genus basis. In homogenous cultures, the pigment composition is an important parameter to characterize the physiological status of the organism. Chl *a* often is used as one reference (besides, e.g. dry weight or leaf area) for other metabolic parameters, and its fluorescence can even be measured on a single-cell basis. Last but not least, the analysis of pigment/protein ratios is important for characterizing isolated pigment/protein complexes. High-resolution structures are currently available only for small, uniform units (except for PS I, Jordan et al., 2000), and the numbers and types of subunits present in more complex assemblies are the subjects of much study. Although medium- to low-resolution structures are available for some additional light-harvesting complexes, the number of bound pigments often is not well known (see, e.g. the discussion of the size of the purple bacterial LH1 complex; Loach et al., 1970; Ueda et al., 1985; Karrasch et al., 1995; Zuber and Cogdell, 1995; Francia et al., 1999; Jungas et al., 2000; Fiedor et al., 2000, 2001; Qian et al., 2000; Chapter 5, Cogdell et al.).

### A. Extraction

With few exceptions, notably of remote sensing, the first step in quantitative analyses of photosynthetic pigments is their extraction from the tissue or the isolated complexes. This is necessary because their properties can be profoundly changed by interactions with the apoproteins and/or neighboring pigments. Debatably, the extraction is probably the most critical step in the analysis. Only a few complications will be mentioned here.

While most chlorophylls and carotenoids are hydrophobic pigments and are soluble in nonpolar solvents, extracting them from biological materials requires solvents that are miscible with water to avoid inclusion of the pigments in protein precipitates and/or at the solvent-water interface. Some of the very nonpolar pigments can be extracted only after a preceding dehydration with a more polar solvent, or by repeated extraction. However, there is also an increasing number of chlorophylls (most of the *c*-type, Section II.A.1.a) and carotenoids (e.g. the glycosidic or sulfonated ones, Section II.C.3.a) that are quite polar and are only poorly soluble in nonpolar solvents.

Some organisms require extraction conditions that alter the pigments. In this case it may be best to ensure the complete and uniform conversion to a desired product. Examples are the conversion to rhodochlorins for the analysis of recalcitrant algae (Porra, 1990), and the pheophytinization of chlorophylls (removal of Mg) with acid. The pheophytins are less susceptible to degradation; it should be noted, however, that epoxidized carotenoids can be hydrolyzed under these conditions.

Obviously, the choice of solvent depends on the material to be extracted and the pigments to be analyzed. Jeffrey et al (1997) have listed the following criteria for solvents to be used under field conditions including on-board analysis on ships: 1: completeness of extraction, 2: absence of degradation and artifact production, 3: compatibility with the subsequent analysis (spectroscopy or chromatography), 4: precision (and dynamic range), 5: simplicity of the protocol, and 6: safety of the operator and the environment. The last two criteria are somewhat less stringent in laboratory as compared to field conditions. For marine phytoplankton, which contains many different pigments and some recalcitrant organisms, Wright et al. (1997) recommend sonication in dimethylformamide as meeting all these criteria except safety. Acetone, methanol or mixtures thereof are sufficient

for many purposes but are highly flammable, and methanol is not only toxic by itself, but renders the skin penetrable for many other materials including toxins.

Once the pigments are extracted, they should be analyzed immediately thereafter, and at least (after careful checks to ensure stability) on the same day. Two major methods are available for this analysis, spectroscopy (absorption or, in the case of chlorophylls, fluorescence) and chromatography. Spectroscopy is more rapid, but it requires knowledge of all pigments present in the sample and absorbing (or fluorescing) in the pertinent wavelength range, while chromatography is the more demanding but also more powerful technique. HPLC with modern diode-array detectors combines the advantages of both techniques.

### B. Spectroscopic Analysis

Formulas for quantitation of the pigments in a given solvent system often are developed in connection with a specific extraction protocol, and can be selected for diverse purposes. All spectroscopic methods have in common that they require the knowledge of *all* pigments present. Any contamination by pigments absorbing (or fluorescing) in the same spectral range will lead to more or less severe errors. These can be pigments from contaminating organisms, or artifactual products that arise during extraction and handling of the pigments to be analyzed. Leading references can be found for the analysis of bacteriochlorophylls in a review by Oelze (1985), for the analysis of phytoplankton pigments in a book by Jeffrey et al. (1997) and a review by Porra (1991), and for the analysis of plant chlorophylls in reviews by Strain and Svec (1966), Svec (1991) and Scheer (1988). Some of the spectroscopic methods include carotenoids, but their analysis is much more complicated, due to their large number and their wide distribution, including non-photosynthetic organisms. Important factors to consider are:

1. Most of the chlorophylls have major absorptions in spectral regions where few other pigments absorb. In these cases there is little interference from contaminants. However, many of the degradation products that can arise during storage or improper work-up also absorb in this region (Hyvärinen, 2000) gives a good compilation of these degradation products. Some of the degra-

dation products that are readily formed from chlorophyll have absorption spectra very similar to those of the parent pigments, and they can not be distinguished satisfactorily by spectroscopy using only a small number of wavelengths (Svec, 1991). Attention also has to be paid to precursors (Rüdiger and Schoch, 1991; Shioi and Beale, 1987).

2. While the number of photosynthetic pigments in healthy plants is relatively limited, it has recently been shown that heavy metals can be incorporated into the chlorophyll macrocycle in polluted areas, and also during extraction and workup (Küpper et al., 1996, 1998). A fairly flexible spectral deconvolution method has been developed for the analysis of such pigments based on defining a set of Gaussians that describe the spectra of the individual pigments (Küpper et al., 2000).

3. In principle, spectroscopic analysis of heterogeneous materials will fail if unaccounted pigments are present. This is particularly critical for non-axenic or symbiotic cultures, and in physiological studies of complex exosystems.

The analysis of biliprotein chromophores by spectroscopy alone is impractical because of the extreme spectral changes brought about by the apoproteins (Fig. 6c), and the chameleon-like spectral changes of bilins with the environmental conditions. However, the chromophore analysis of cyanobacteria, rhodophytes and glaucophytes is simplified by the small number of known chromophore structures, provided that interactions with the apoprotein are removed by denaturation under carefully controlled conditions prior to the analysis. Glazer and coworkers have determined the extinction coefficients of the four cyanobacterial chromophores (PCB, PEB, PVB and PUB) in 8M urea at pH 1.9 (Glazer and Hixson, 1975; Klotz and Glazer, 1985; Bishop et al., 1987; Table 2), from which Schluchter and Bryant (2001) have derived a matrix that can be used for simultaneous assessment of these four phycobilins. The acid conditions stabilize the chromophores because many bilins are very labile and are rapidly oxidized under neutral and alkaline conditions, particularly in the presence of traces of heavy metals (Scheer and Krauss, 1977; Krauss and Scheer, 1979). At the same time, the protonated chromophores have higher extinction coefficients and narrower spectra than the free bases (Fig. 6c).

### C. Chromatography

Whenever there is doubt about the components present, or whenever verification of the spectroscopic results is required, the method of choice is HPLC in combination with a multi-channel detection system such as a diode-array. A large variety of chromatographic systems is available for chlorophylls (Scheer, 1988; Jeffrey et al., 1997, 1999; Shioi, 1991; Zapata et al., 2000) and carotenoids (Davies and Köst, 1988; Bernhard, 1995; Britton, 1995b; Britton and Riesen, 1995; Haugan et al., 1995; Liaaen-Jensen and Hertzberg, 1995; Meyer et al., 1995; Pfander, 1995; Pfander and Niggli, 1995; Pfander and Riesen, 1995; Schiedt, 1995; Schierle et al., 1995; Takaichi, 2000). An HPLC method also has been developed for biliproteins (Swanson and Glazer, 1990).

Reverse-phases have for a long time been the HPLC material of choice. They give best resolution with most carotenoids. They also have been widely used for chlorophylls, in spite of an unfavorable resolving power as compared to silica, because they are less prone to artifact formation. Kobayashi et al. (1988) have shown, however, that HPLC on silica is suitable for chlorophylls including the 13<sup>2</sup>-epimers under appropriate conditions. For chlorophylls differing in their esterifying alcohols at C-17<sup>3</sup>, reverse phase materials are still the method of choice (Caple et al., 1978; Schoch et al., 1978; Steiner et al., 1981; Shioi and Beale, 1987). Polyethylene also has proven suitable for the separation of chlorophylls containing free acids, such as Chls c<sub>1</sub> and c<sub>2</sub>, which differ only by a double bond in the C-8 substituent (Fig. 1c) (Jeffrey et al., 1999). All the aforementioned precautions to prevent artifactual modifications have to be maintained throughout the workup, storage and chromatography. In the author's hands, storage is very critical and it is advisable, whenever possible, to perform the chromatography immediately after the extraction.

### V. Pigment Substitution Methods

The structural characterization of many photosynthetic pigment-protein complexes has set the stage for functional characterization on a molecular basis. These functions, light absorption, energy transfer, charge separation, electron transfer, and dissipation of excess energy, occur on time scales that are more

Table 4. Examples of the incorporation of modified pigments into pigment-protein complexes

Complex	Exchangeable pigments	Leading references
<b>Anoxygenic bacteria</b>		
Reaction center	BChl-B <sub>A</sub> , BChl-B <sub>B</sub> , BPhc-H <sub>A</sub> , BPhc-H <sub>A</sub> , carotenoids	Scheer and Struck, 1993; Struck and Scheer, 1990; Scheer and Hartwich, 1995; Shkuropatov and Shuvalov, 1993; Frank, 1999
LH1-antenna	BChl-B870	Ghosh et al., 1988; Miller et al., 1987; Loach and Parkes-Loach, 1995; Lapouge et al., 2000; Fiedor et al., 2001
LH2-antenna	BChl-B800	Clayton and Clayton, 1981; Bandilla et al., 1998; Desamero et al., 1998; Fraser et al., 1999; Frank et al., 1996; Frank, 1999
LH2-antenna	BChl-B850, B800	Fiedor and Scheer, unpublished
<b>Oxygenic photosynthesis</b>		
PS II-RC	Chl <i>a</i> , Phe <i>a</i>	Gall et al., 1998; Shkuropatov et al., in press, Kennis et al., 1997
Green LHCII-antenna	Chl <i>a</i> , Chl <i>b</i> , Carotenoids	Plumley and Schmidt, 1987; Paulsen, 1999; Paulsen, 1995; Croce et al., 2000
Rhodophytan LHC	Chl <i>a</i> , zeaxanthin	Grabowski et al., 2001
LHCI-antenna	Chl <i>a</i> , Carotenoids	Schmid et al., 1997
Peridinin-Chl-Protein	Chl <i>a</i> , Peridinin	Hiller et al., unpublished
Cytochrome <i>b<sub>6</sub>f</i>	Chl <i>a</i>	Pierre et al., 1997
Biliproteins	PCB, PEB, PVB, P <sub>B</sub>	Fairchild et al., 1992; Arciero et al., 1988a, Schluchter and Glazer, 1999; Zhao et al., 2000; Elich and Lagarias, 1989; Remberg et al., 1998

rapid than fast enzymatic reactions and reach the lower end of the timescale of molecular vibrations. They therefore have to be studied by rapid time-resolved or high-resolution spectroscopic methods supplemented by biochemical methods.

Parametric changes of certain chromophore redox potentials or absorption energies are particularly valuable tools for such an analysis. They can be brought about by a variety of methods, by which either the chromophores or the protein environments are modified so as to change only the target property with relatively little effect on the structure or other properties that could interfere with the analysis. Over the past 15 years, three such methods have proven particularly useful. Modifications of the chromophores' biosynthetic pathways have been most useful for the carotenoids (see Hunter et al. (1994) and Sandmann and Scheer (1998) for leading references). Site-directed mutagenesis of the chromophore binding pocket has been used to exchange pheophytins for chlorophylls or vice versa by removing or introducing amino acids capable of ligating the central Mg or allowing it to carry into the pocket a small ligand like water (Coleman and Youvan, 1990; Frank et al., 1993). Mutations of amino acids interacting with the peripheral groups have proven

particularly valuable for changing the redox potential of chlorophylls and their absorption spectra (Fowler et al., 1994; Ivancich et al., 1998; Nabedryk et al., 1998).

An alternative approach is the introduction of chemically modified chromophores, either by reconstitution or by exchange of chromophores. Methods are available for all three chromophore classes, although most work has been done with carotenoids and chlorophylls (Table 4). The work on chlorophylls (Scheer and Struck, 1993; Scheer and Hartwich, 1995) and carotenoids (Frank, 1999) has been reviewed.

Modified pigments can be either of natural origin, or obtained by chemical modification of natural pigments (Fig. 10). Total syntheses have been used with bilin chromophores (Foerstendorf et al., 2000; Inomata et al., 2000), while chlorophylls have mainly been obtained by chemical modifications (Scheer and Struck, 1993; Scheer and Hartwich, 1995; Schoch et al., 1995), and carotenoids usually are obtained from the large number of biological sources, or by inhibition of defined biosynthesis steps.

Photosynthetic complexes with modified chromophores have found widespread applications. Leading examples are given in Table 5 and the aforementioned



Table 5. Adjustable properties of chromophores, and examples of their use in studying photosynthetic pigment-protein complexes

Adjustable property	As probe for:	References
Excited state energy	Energy transfer (singlet and triplet) Excitonic coupling of chromophores Band assignments	Herek et al., 2000; Farhoosh et al., 1997 Struck et al., 1990 Hartwich et al., 1995
Redox potentials	Electron transfer Creation of trapping sites	Spörlein et al., 2000; Frieese et al., 1995
Excited state dynamics	Energy transfer Creation of unusual excited states	Fiedor et al., 2000; Fiedor et al., 2001; Fiedor et al., 2001
Functional groups	Interactions (pigment-pigment and pigment-protein) Redox potentials	Spörlein et al., 2000
Isotope composition	Labeling Assignments (NMR, vibrational and X-ray spectra, neutron scattering) Biosynthesis	Egorova-Zachernyuk et al., 1997 Porra et al., 1998

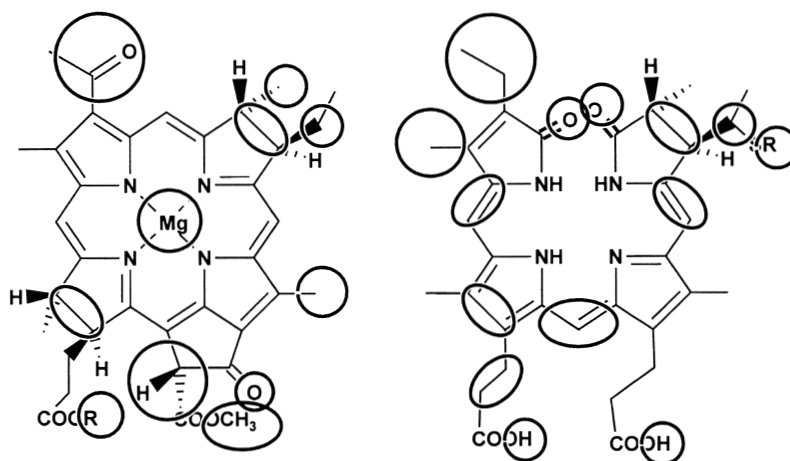


Fig. 10. Useful modifications of chlorophylls and phycobilin chromophores. The accessible functional groups are circled. Variations of these groups are found among the various natural pigments, or can be obtained by chemical or biosynthetic modification.

reviews. In addition, the native chromophores have been used as probes, either intrinsic or extrinsic, for many purposes. Thus, the phycobiliproteins have been used as convenient markers in the development of many separation techniques and for cell-sorting and surface mapping.

## References

- Addlesee HA and Hunter CN (1999) Physical mapping and functional assignment of the geranylgeranyl-bacteriochlorophyll reductase gene, *bchP*, of *Rhodobacter sphaeroides*. *J Bacteriol* 181: 7248–7255
- Addlesee HA, Fiedor L and Hunter CN (2000) Physical mapping of *bchG*, *orf427*, and *orf177* in the photosynthesis gene cluster of *Rhodobacter sphaeroides*: Functional assignment of the bacteriochlorophyll synthetase gene. *J Bacteriol* 182: 3175–3182
- Agostiano A, Catucci L, Colafemmina G, della Monica M and Scheer H (2000) Relevance of the phytyl chain of the chlorophylls on the lamellar phase formation and organization. *Biophys J* 84: 189–194
- Akiyama M, Kobayashi M, Kise H, Hara M, Wakao N and Shimada K (1998) Pigment composition of the reaction center complex isolated from an acidophilic bacterium *Acidiphilium rubrum* grown at pH3.5. *Photomed Photobiol* 20: 85–87
- Alberti M, Burke DH and Hearst JE (1995) Structure and sequence of the photosynthesis gene cluster. In: Blankenship R, Madigan MT and Bauer CE (eds) *Anoxygenic Photosynthetic Bacteria*, pp 1083–1106. Kluwer Academic Publishers, Dordrecht
- Allen MB (1966) Distribution of the chlorophylls. In: Vernon LP and Seely GR (eds) *The Chlorophylls*, pp 511–519. Academic press, New York

- Andersson PO, Gillbro T, Ferguson L. and Cogdell R.J. (1991) Absorption spectral shifts of carotenoids related to medium polarizability. *Photochem Photobiol* 54: 353–360
- Angerhofer A, Bornhäuser F, Aust V, Hartwich G and Scheer H (1998) Triplet energy transfer in bacterial photosynthetic reaction centers. *Biochim Biophys Acta* 1365: 404–420
- Apt KE, Collier JL and Grossman AR (1995) Evolution of phycobiliproteins. *J Mol Biol* 248: 79–96
- Arciero DM, Bryant DA and Glazer AN (1988a) In vitro attachment of bilins to apophycocyanin. 1. specific covalent adduct formation at cysteinyl residues involved in phycocyanobilin binding in C-phycocyanin. *J Biol Chem* 263: 18343–18349
- Arciero DM, Dallas JL and Glazer AN (1988b) In vitro attachment of bilins to apophycocyanin. 2. determination of the structures of tryptic bilin peptides derived from the phycocyanobilin adduct. *J Biol Chem* 263: 18350–18357
- Bandilla M, Ücker B, Ram M, Simonin I, Gelhaye E, McDermott G, Cogdell R and Scheer H (1998) Reconstitution of the B800 bacteriochlorophylls in the peripheral light harvesting complex B800-850 of *Rhodobacter sphaeroides* 2.4.1. with BChl *a* and modified (Bacterio)-chlorophyll. *Biochim Biophys Acta* 1364: 390–402
- Battersby AR and Leeper FJ (1990) Biosynthesis of the pigments of life: Mechanistic studies on the conversion of porphobilinogen to uroporphyrinogen III. *Chem Rev* 90: 1261–1274
- Beale SI (1993) Biosynthesis of Phycobilins. *Chem Rev* 93: 785–802
- Beale SI (1999) Enzymes of chlorophyll biosynthesis. *Photosynth Res* 60: 43–73
- Beale SI, Castelfranco PA and Granick S (1975) The biosynthesis of  $\delta$ -aminolevulinic acid from the intact carbon skeleton of glutamate in greening barley. *Proc Natl Acad Sci USA* 72: 2719–2723
- Beguin S, Guglielmo G, Rippka R and Cohen-Bazire G (1985) Chromatic adaptation in a mutant of *Fremyella-displiphon* incapable of phycoerythrin synthesis. *Biochimie* 67: 109–117
- Ben-Amotz A, Lers A and Avron M (1988) Stereo-isomers of  $\beta$ -carotene and phytoene in the algae *Dunaliella bardawil*. *Plant Physiol* 86: 1286–1291
- Ben-Amotz A, Shaish A and Avron M (1989) Mode of action of the massively accumulated  $\beta$ -carotene of *Dunaliella bardawil* in protecting the alga against damage by excess irradiation. *Plant Physiol* 91: 1040–1043
- Bensasson R, Land EJ and Truscott TG (1993) Excited States and Free Radicals in Biology and Medicine. Oxford University Press, Oxford
- Bernhard K (1995) Chromatography: Part II. Column chromatography. In: Britton G, Liaaen-Jensen S, and Pfander H (eds) Carotenoids: Isolation and Analysis, pp 117–130. Birkhäuser, Basel
- Biel AJ (1995) Genetic analysis and regulation of bacteriochlorophyll biosynthesis. In: Blankenship R, Madigan MT and Bauer CE (eds) Anoxygenic Photosynthetic Bacteria, pp 1125–1134. Kluwer Academic Publishers, Dordrecht
- Bishop JE, Rapoport H, Klotz AV, Chan CF, Glazer AN, Füglistaller P and Zuber H (1987) Chromopeptides from phycoerythrocyanin. Structure and linkage of the three bilin groups. *J Am Chem Soc* 109: 875–881
- Blankenship R, Madigan MT and Bauer CE (eds) (1995a) Anoxygenic Photosynthetic Bacteria. Kluwer Academic Publishers, Dordrecht
- Blankenship RE, Olson JM and Miller M (1995b) Antenna complexes from green photosynthetic bacteria. In: Blankenship R, Madigan MT and Bauer CE (eds) Anoxygenic Photosynthetic Bacteria, pp 399–435. Kluwer Academic Publishers, Dordrecht
- Borrego CM, Arellano JB, Abella CA, Gillbro T and Garcia-Gil J (1999) The molar extinction coefficient of bacteriochlorophyll *e* and the pigment stoichiometry in *Chlorobium phaeobacteroides*. *Photosynth Res* 60: 257–264
- Boucher Y and Doolittle WF (2000) The role of lateral gene transfer in the evolution of isoprenoid biosynthesis pathways. *Mol Microbiol* 37: 703–716
- Boxer SG, Kuki A, Wright KA, Katz BA and Xuong N (1982) Oriented properties of the chlorophylls—electronic absorption-spectroscopy of orthorhombic pyrochlorophyllide  $\alpha$ -apomyoglobin single-crystals. *Proc Natl Acad Sci USA* 79: 1121–1125
- Bramley PM (1993) Inhibition of carotenoid biosynthesis. In: Young AJ and Britton G (eds) Carotenoids in photosynthesis, pp 127–160. Chapman and Hall, London
- Braslavsky SE, Holzwarth AR and Schaffner K (1983) Solution confirmations, photophysics, and photochemistry of bilipigments—bilirubin and biliverdin daimethyl esters and related linear tetrapyrroles. *Angew Chem* 22: 656–674
- Brejč K, Ficner R, Huber R and Steinbacher S (1995) Isolation, crystallization, crystal structure analysis and refinement of allophycocyanin from the cyanobacterium *Spirulina platensis* at 2.3 Å resolution. *J Mol Biol* 249: 424–440
- Britton G (1993) Biosynthesis of carotenoids. In: Young AJ and Britton G (eds) Carotenoids in photosynthesis, pp 96–126. Chapman and Hall, London
- Britton G (1995a) UV/Visible spectroscopy. In: Britton G, Liaaen-Jensen S, and Pfander H (eds) Carotenoids, pp 13–62. Birkhäuser, Basel
- Britton G (1995b) Worked examples of Isolation and analysis: Example 1. Higher plants. In: Britton G, Liaaen-Jensen S, and Pfander H (eds) Carotenoids: Isolation and analysis, pp 201–214. Birkhäuser, Basel
- Britton G and Riesen R (1995) Worked examples of Isolation and analysis: Example 3. Bacteria. In: Britton G, Liaaen-Jensen S, and Pfander H (eds) Carotenoids: Isolation and Analysis, pp 228–238. Birkhäuser, Basel
- Britton G, Liaaen-Jensen S and Pfander H (1995) Carotenoids, Vol. 1B: Spectroscopy. Birkhäuser, Basel
- Bryant DA (ed) (1994) The Molecular Biology of Cyanobacteria. Kluwer Academic Publishers, Dordrecht
- Burton GW (1990) Antioxidant properties of carotenoids. *J Nutr* 119: 109–111
- Cantor CR and Schimmel PR (1980) Biophysical Chemistry Part II: Techniques for the Study of Biological Structure and Function. W. H. Freeman and Company, New York
- Caple MB, Chow H-C and Strouse CE (1978) Photosynthetic pigments of green sulfur bacteria (The esterifying alcohols of Bacteriochlorophylls *c* from *Chlorobium limicola*). *J Biol Chem* 253: 6730–6737
- Caspi V, Droppa M, Horvath G, Malkin S, Marder JB and Raskin VI (1999) The effect of copper on chlorophyll organization during greening of barley leaves. *Photosynth Res* 62: 165–174
- Chang WR, Jiang T, Wan ZL, Zhang JP, Yang ZX and Liang DC (1996) Crystal structure of R-phycoerythrin from *Polysiphonia urceolata* at 2.8 angstrom resolution. *J Mol Biol* 262: 721–731

- Chapman DJ, Cole WJ and Siegelman HW (1968) Cleavage of phycocyanobilin from C-phycocyanin. *Biochim Biophys Acta* 153: 692–698
- Christensen RL (1999) The electronic states of carotenoids. In: Frank HA, Young AJ, Britton G, and Cogdell RJ (eds) *The Photochemistry of Carotenoids*, pp 137–157. Kluwer Academic Publishers, Dordrecht
- Clayton RK and Clayton BJ (1981) B 850 pigment-protein complex of *Rhodospseudomonas sphaeroides*—extinction coefficients, circular dichroism and the reversible binding of Bacteriochlorophyll. *Proc Natl Acad Sci USA* 78: 5583–5587
- Coleman WJ and Youvan DC (1990) Spectroscopic analysis of genetically modified photosynthetic reaction centers. *Ann Rev Biophys Biophys Chem* 19: 333–367
- Cornejo J and Beale SI (1997) Phycobilin biosynthetic reactions in extracts of cyanobacteria. *Photosynth Res* 51: 223–230
- Crimi M, Dorra D, Börsinger CS, Giuffra E, Holzwarth AR and Bassi R (2001) Time-resolved fluorescence analysis of the recombinant Photosystem II antenna complex CP29. Effects of zeaxanthin, pH and phosphorylation. *Eur J Biochem* 268: 260–267
- Croce R, Cinque G, Holzwarth AR and Bassi R (2000) The Soret absorption properties of carotenoids and chlorophylls in antenna complexes of higher plants. *Photosyn. Res.* 64: 221–231
- Csatorday K, MacColl R and Berns DS (1981) Accumulation of protoporphyrin IX and zinc protoporphyrin IX in *Cyanidium caldarium*. *Proc Natl Acad Sci USA* 94: 1700–1702
- Davies BH and Köst H-P (1988) Carotenoids. In: Köst H-P (ed) *Chromatography of Plant Pigments*, Vol I: Fat-Soluble Pigments, pp 3–188. CRC-Press, Boca Raton
- Davis SJ, Vener AV and Vierstra RD (1999) Bacteriophytochromes: Phytochrome-like photoreceptors from nonphotosynthetic eubacteria. *Science* 286: 2517–2520
- De Groot HJM, Gebhard R, Vanderhoef I, Hoff AJ, Lugtenburg J, Violette CA and Frank HA (1992) C-13 magic angle spinning NMR evidence for a 15,15'-*cis* Configuration of the spheroidene in the *Rhodobacter sphaeroides* photosynthetic reaction center. *Biochemistry* 31: 12446–12450
- De Groot JA, Vandersteent R and Lugtenburg J (1982) Synthesis and reactivity of 22,23-methylene-2,3,17,18-tetramethyl-23-hydro-1,19-(21H,24H)-bilindion-10-enium trifluoroacetate. *Rec Trav Chim* 101: 263
- DellaPenna D (1999) Biosynthetic pathways and the distribution of carotenoids in photosynthetic organisms. In: Frank HA, Young AJ, Britton G, and Cogdell RJ (eds) *The Photochemistry of Carotenoids*, pp 21–37. Kluwer Academic Publishers, Dordrecht
- Desamero RZB, Chynwat V, van der Hoef I, Jansen FJ, Lugtenburg J, Gosztola D, Wasielewski MR, Cua A, Bocian DF and Frank HA (1998) Mechanism of energy transfer from carotenoids to bacteriochlorophyll: Light-harvesting by carotenoids having different extents of  $\pi$ -electron conjugation incorporated into the B850 antenna complex from the carotenoidless bacterium *Rhodobacter sphaeroides* R-26.1. *J Phys Chem B* 102: 8151–8162
- Dimagno TJ and Norris JR (1993) Initial electron transfer events in photosynthetic bacteria. In: Deisenhofer J and Norris JR (eds) *The Photosynthetic Reaction Center*, pp 105–132. Academic Press, New York
- Duerrig M, Huber R, Bode W, Ruembeli R and Zuber H (1990) Refined three-dimensional structure of phycoerythrocyanin from the cyanobacterium *Mastigocladus laminosus* at 2.7 Å. *J Mol Biol* 211: 633–644
- Edge R and Truscott TG (1999) Carotenoid radicals and the interaction of carotenoids with active oxygen species. In: Frank HA, Young AJ, Britton G, and Cogdell RJ (eds) *The Photochemistry of Carotenoids*, pp 223–234. Kluwer Academic Publishers, Dordrecht
- Egorova-Zachernyuk TA, van Rossum B, Boender GJ, Franken E, Ashurst J, Raap J, Gast P, Hoff AJ, Oschkinat H and De Groot HJM (1997) Characterization of pheophytin ground states in *Rhodobacter sphaeroides* R26 photosynthetic reaction centers from multispin pheophytin enrichment an 2D C13 MAS NMR dipolar correlation spectroscopy. *Biochemistry* 36: 7513–7519.
- Eichacker LA, Paulsen H and Rüdiger W (1992) Synthesis of chlorophyll *a* regulates translation of chlorophyll *a* apoprotein-P700, apoprotein-CP47, apoprotein-CP43 and apoprotein-D2 in barley etioplasts. *Eur J Biochem* 205: 17–24
- Elich TD and Lagarias JC (1989) Formation of a photoreversible phycocyanobilin-apophytochrome adduct in vitro. *J Biol Chem* 264: 12902–12908
- Evans MCW and Nugent HA (1993) Structure and function of the reaction center cofactors in oxygenic organisms. In: Deisenhofer J and Norris JR (eds) *The Photosynthetic Reaction Center*, pp 391–416. Academic Press, New York
- Fairchild CD and Glazer AN (1994) Nonenzymatic bilin addition to the gamma subunit of an apophytoerythrin. *J Biol Chem* 269: 28988–28996
- Fairchild CD, Zhao J, Zhou J, Colson SE, Bryant DA and Glazer AN (1992) Phycocyanin alpha-subunit phycocyanobilin lyase. *Proc Natl Acad Sci USA* 89: 7017–21
- Falk H (1989) *The chemistry of linear oligopyrroles and bile pigments*. Wien, Springer
- Falk H, Kapl G, Müller N and Zrunek U (1984) Phytochrommodellstudien: Konformationsanalytische Untersuchungen an 2,3-Dihydrobilatrien abc-Derivaten. *Monatsh Chem* 115: 1443–1451
- Farhoosh R, Chynwat V, Gebhard R, Lugtenburg J and Frank HA (1997) Triplet energy transfer between the primary donor and carotenoids in *Rhodobacter sphaeroides* R-26-1 reaction centers incorporated with spheroidene analogs having different extents of pi-electron conjugation. *Photochem Photobiol* 66: 97–104
- Ficner R and Huber R (1993) Refined crystal structure of phycoerythrin from *Porphyridium cruentum* at 2.3 Ångström resolution and localization of the gamma subunit. *Eur J Biochem* 218: 103–106
- Fiedor J, Fiedor L, Kammhuber N, and Scheer H (1999) Photoprotection by carotenoids? Photosensitized degradation of beta-carotene in organic solvent. In: Gülen D, Naqvi R, Robert B, and van Amerongen H (eds) *Interactions Between Chlorophylls and Carotenoids in Photosynthesis*, Book of Abstracts. European Science Foundation and Tübitak, Kemer-Antalya
- Fiedor L, Scheer H, Hunter NC, Tschirschwitz F, Voigt B, Ehlert J, Nibbering E, Leupold D and Elsässer T (2000) Introduction of a 60 fs deactivation channel in the photosynthetic antenna LH1 by Ni-bacteriopheophytin *a*. *Chem Phys Lett* 319: 145–152
- Fiedor L, Leupold D, Teuchner K, Voigt B, Hunter CN, Scherz A and Scheer H (2001) Excitation trap approach to analyze size and pigment-pigment coupling: Reconstitution of LH1 antenna

- of *Rhodobacter sphaeroides* with Ni-substituted bacteriochlorophyll. *Biochemistry* 40: 3737–3747
- Foerstendorf H, Benda C, Gärtner W, Storf, M, Scheer H and Siebert F (2001) FTIR studies of phytochrome photoreactions reveal the C=O bands of the chromophore: Consequences for its protonation states, conformation, and protein interaction. *Biochemistry* 40: 14952–14959
- Folly P and Engel N (1999) Chlorophyll *b* to chlorophyll *a* conversion precedes chlorophyll degradation in *Hordeum vulgare* L. *J Biol Chem* 274: 21811–21816
- Fork DC and Larkum AWD (1989) Light harvesting in the green alga *Ostreobium* sp, a coral symbiont adapted to extreme shade. *Marine Biol* 103, 381–385
- Fowler GJS, Sockalingum GD, Robert B and Hunter CN (1994) Blue shifts in bacteriochlorophyll absorbance correlate with changed hydrogen bonding patterns in light-harvesting 2 mutants of *Rhodobacter sphaeroides* with alterations at alpha-Tyr-44 and alpha-Tyr-45. *Biochem J* 299: 695–700
- Francia F, Wang J, Venturoli G, Melandri BA, Barz WP and Oesterhelt D (1999) The reaction center-LH1 antenna complex of *Rhodobacter sphaeroides* contains one PufX molecule which is involved in dimerization of this complex. *Biochemistry* 38: 6834–6845
- Frank HA (1999) Incorporation of carotenoids into reaction centers and light-harvesting pigment-protein complexes. In: Frank HA, Young AJ, Britton G, and Cogdell RJ (eds) *The Photochemistry of Carotenoids*, pp 235–244. Kluwer Academic Publishers, Dordrecht
- Frank HA, Innes J, Aldema M, Neumann R and Schenck CC (1993) Triplet State EPR of Reaction Centers from the His(L173) → Leu(L173) Mutant of *Rhodobacter sphaeroides* which contains a heterodimer primary donor. *Photosynth Res* 38: 99–109
- Frank HA, Chynwat V, Posteraro A, Hartwich G, Meyer M, Simonin I and Scheer H (1996) Triplet state energy transfer between the primary donor and the carotenoid in *Rhodobacter sphaeroides* R26.1 reaction centers exchanged with modified Bacteriochlorophyll pigments and reconstituted with spheroidene. *Photochem Photobiol* 64: 823–831
- Frank HA, Young AJ, Britton G and Cogdell RJ (1999) *The photochemistry of carotenoids*. Kluwer Academic Publishers, Dordrecht
- Frank HA, Bautista JA, Josue J, Pendon Z, Hiller R, Sharpless FP, Gosztola D and Wasielewski MR (2000a) Effect of solvent environment on the spectroscopic properties and dynamics of the lowest excited state of carotenoids. *J Phys Chem B* 104: 4569–4577
- Frank HA, Bautista JA, Josue JS and Young AJ (2000b) Mechanism of nonphotochemical quenching in green plants: Energies of the lowest excited singlet states of violaxanthin and Zeaxanthin. *Biochemistry* 39: 2831–2837
- Frankenberg N, Mukougawa K, Kohchi T and Lagarias JC (2001) Functional genomic analysis of the Hy2 family of ferredoxin-dependent bilin reductases from oxygenic photosynthetic organisms. *Plant Cell* 13, 965–978
- Fraser NJ, Dominy PJ, Ücker B, Simonin I, Scheer H and Cogdell R (1999) Selective release, removal and reconstitution of BChl *a* molecules into the B800 sites of LH2 complexes from *Rhodospseudomonas acidophila* 10050. *Biochemistry* 38: 9684–9692
- Freer A, Prince S, Sauer K, Papiz M, Hawthornthwaite-Lawless A, McDermott G, Cogdell R and Isaacs NW (1996) Pigment-pigment interactions and energy transfer in the antenna complex of the photosynthetic bacterium *Rhodospseudomonas acidophila*. *Structure* 4: 449–462
- Friese M, Hartwich G, Ogorodnik A, Scheer H and Michel-Beyerle ME (1995) No change of primary charge separation rate on lowering the energy of P<sup>+</sup>B<sup>-</sup> by exchanging 13<sup>2</sup>-OH-Ni-BChl *a* for the accessory BChl *a*. *Biophys J* 68: A367
- Frigaard NU, Matsuura K, Hirota M, Miller M and Cox RP (1998) Studies of the localization and function of isoprenoid quinones from green sulfur bacteria. *Photosynth Res* 58: 81–90
- Fuhrhop J-H and Smith KM (1975) Laboratory Methods in Porphyrin and Metalloporphyrin research. In: Smith, KM (ed) *Porphyrins and Metalloporphyrins*, pp 757–870. Elsevier, Amsterdam
- Fujii R, Onaka K, Kuki M, Koyama Y and Watanabe Y (1998) The 2A<sub>g</sub><sup>-</sup> energies of all-trans neurosporene and spheroidene as determined by fluorescence spectroscopy. *Chem Phys Lett* 288: 847–853
- Fujii R, Onaka K, Nagae H, Koyama Y and Watanabe Y (2001a) Fluorescence spectroscopy of all-trans-lycopene: comparison of the energy and the potential displacement of its 2A<sub>g</sub><sup>-</sup> state with those of neurosporene and spheroidene. *J. Luminesc.* 92: 213–222
- Fujii R, Ishikawa T, Koyama Y, Taguchi M, Isobe Y, Nagae H and Watanabe Y (2001b) Fluorescence spectroscopy of all-trans-anhydrosphorobilin and spirilloxanthin: detection of the 1B<sub>u</sub><sup>-</sup> fluorescence. *J Phys Chem A* 105: 5348–5355
- Fujita Y and Bauer CE (2000) Reconstitution of light-independent protochlorophyllide reductase from purified BchL and BchN-BchB subunits. *J Biol Chem* 275: 23583–23588
- Gall B, Zehetner A, Scherz A and Scheer H (1998) Modification of pigment composition in the isolated reaction center of Photosystem II. *FEBS Lett* 434: 88–92
- Garrido JL, Otero J, Maestro MA and Zapata M (2000) The main nonpolar chlorophyll *c* from *Emiliana huxleyi* (Prymnesiophyceae) is a chlorophyll *c*<sub>2</sub>-monogalactosyldiacylglyceride ester: A mass spectrometry study. *J Phycol* 36: 497–505
- Ghosh R, Hauser H and Bachofen R (1988) Reversible dissociation of the B873 light-harvesting complex from *Rhodospirillum rubrum* G9<sup>+</sup>. *Biochemistry* 27: 1004–1014
- Gillbro T, Andersson PO, Liu RSH, Asato AE, Takaishi S and Cogdell RJ (1993) Location of the Carotenoid 2A<sub>g</sub><sup>-</sup>-state and its role in photosynthesis. *Photochem Photobiol* 57: 44–48
- Glazer AN and Hixson CS (1975) Characterization of R-phycoerythrin. *Chromophore content of R-phycoerythrin and C-phycoerythrin*. *J Biol Chem* 250: 5487–5495
- Goericke R and Repeta D (1992) The pigments of *Prochlorococcus marinus*: The presence of divinyl-chlorophyll *a* and *b* in a marine procaryote. *Limnol Oceanogr* 37: 425–433
- Gossauer A and Engel N (1996) Chlorophyll catabolism—structures, mechanisms, conversions. *J Photochem Photobiol B*. 32: 141–151
- Gottschalk L, Lottspeich F and Scheer H (1993) Reconstitution of allophycocyanin from *Mastigocladus laminosus* with isolated linker polypeptide. *Photochem Photobiol* 58: 761–767
- Gottschalk L, Lottspeich F and Scheer H (1994) Reconstitution of an allophycocyanin trimer complex containing the c-terminal 21–23 kDa domain of the core-membrane linker polypeptide L<sub>cm</sub>. *Z Naturforsch* 49: 331–336
- Gottstein J and Scheer H. (1983) Long-wavelength-absorbing forms of bacteriochlorophyll *a* in solutions of Triton X100.

- Proc Natl Acad Sci 80: 2231–2234
- Gough SP, Petersen BO and Duus JO (2000) Anaerobic chlorophyll isocyclic ring formation in *Rhodobacter capsulatus* requires a cobalamine cofactor. Proc Natl Acad Sci USA 97: 6908–6913
- Grabowski B, Cunningham FX and Gantt E (2001) Chlorophyll and carotenoid binding in a simple red algal LHC crosses phylogenetic lines. Proc Natl Acad Sci USA 98: 2911–2916
- Granville MF, Holtom GR, Kohler BE, Christensen RL and d'Amico KL (1970) Experimental confirmation of the dipole forbidden character of the lowest excited singlet state in 1,3,5,7-octatetraene. J Chem Phys 70: 593–594
- Griffiths WT (1991) Protochlorophyllide photoreduction. In: Scheer H (ed) Chlorophylls, pp 433–450. CRC Press, Boca Raton
- Hartwich G, Scheer H, Aust V and Angerhofer A (1995) Absorption and ADMR studies on bacterial photosynthetic reaction centres with modified pigments. Biochim Biophys Acta. 1230: 97–113
- Hartwich G, Fiedor L, Simonin I, Cmiel E, Schäfer W, Noy D, Scherz A and Scheer H (1998) Metal-substituted Bacteriochlorophylls: I. Preparation and influence of metal and coordination on spectra. J Amer Chem Soc 120: 3675–3683
- Haugan JA, Aakermann T and Liaaen-Jensen S (1995) Worked examples of Isolation and analysis: Example 2. Macroalgae and microalgae. In: Britton G, Liaaen-Jensen S, and Pfander H (eds) Carotenoids: Isolation and Analysis, pp 215–227. Birkhäuser, Basel
- He J, Hu Y and Jiang L (1996) Photochemistry of Phycobiliproteins: First observation of reactive oxygen species generated from phycobiliproteins on photosensitization. J Amer Chem Soc 118: 8957–8958
- Helfrich M, Ross A, King GC, Turner AG and Larkum AWD (1999) Identification of 8-[vinyl]-protochlorophyllide *a* in phototrophic procaryotes and algae: Chemical and spectroscopic properties. Biochim Biophys Acta 1410: 262–272
- Herek JL, Fraser NJ, Pullerits T, Martinsson P, Polvika T, Scheer H, Cogdell RJ and Sundström V (2000) Mechanism of B800 → B850 energy transfer mechanism in bacterial LH2 complexes investigated by B800 pigment exchange. Biophys J 78: 2590–2596
- Hertzberg S and Liaaen-Jensen S (1966) The carotenoids of *Mycobacterium phlei* strain Vera. 1. The structures of the minor carotenoids. Acta Chem Scand 20: 1187–1194
- Hirota M, Moriyama T, Shimada K, Miller M, Olson JM and Matsuura K (1992) High degree of organization of Bacteriochlorophyll *c* in chlorosome-like aggregates spontaneously assembled in aqueous solution. Biochim Biophys Acta 1099: 271
- Hirschberg J and Chamovitz D (1994) Carotenoids in Cyanobacteria. In: Bryant DA (ed) The Molecular Biology of Cyanobacteria, pp 559–579. Kluwer Academic Publishers, Dordrecht
- Hoff AJ (1993) Magnetic resonance of bacterial photosynthetic reaction centers. In: Deisenhofer J and Norris JR (eds) The Photosynthetic Reaction Center, pp 332–386. Academic Press, New York
- Hofmann E, Wrench PM, Sharples FP, Hiller RG, Welte W and Diederichs K (1996) Structural basis of light-harvesting by carotenoids: Peridinin-chlorophyll-protein from *Ampidinium carterae*. Science 272: 1788–1791
- Hörtensteiner S and Kräutler B (2000) Chlorophyll breakdown in oilseed rape. Photosynth Res 64: 137–146
- Hudson BS and Kohler BE (1972) A low-lying weak transition in the polyene  $\omega,\omega'$ -diphenyloctatetraene. Chem Phys Lett 14: 299–304
- Hunter CN, Hundle BS, Hearst JE, Lang HP, Gardiner AT, Takaichi S and Cogdell RJ (1994) Introduction of new carotenoids into the bacterial photosynthetic apparatus by combining the carotenoid biosynthetic pathways of *Erwinia herbicola* and *Rhodobacter sphaeroides*. J Bacteriol 176: 3692–3697
- Hyvärinen K (2000) The Willstätter allomerization of Chlorophylls *a* and *b*. PhD. thesis, University of Helsinki, Finland
- Inomata K, Hanzawa H, Kinoshita H, Uchida K, Wada K, and Furuya M (2000) Contribution of organic chemistry to analysis of chromophore function in phytochromes. In: Gasparro F, Oleinick NL, Urbach F, and Hearst JE (eds) 13th International Congress on Photobiology, Abstract 446, p 147. American Society of Photobiology, San Francisco
- Ito H, Ohtsuka T and Tanaka A (1996) Conversion of chlorophyll *b* to chlorophyll *a* via 7-hydroxymethyl chlorophyll. J Biol Chem 271: 1475–1479
- IUPAC and IUB (1971) Tentative rules for the nomenclature of carotenoids. Biochemistry 10: 4827–4837
- IUPAC and IUB (1975) Nomenclature of Carotenoids (Recommendation 1974). Biochemistry 14: 1803–1804
- IUPAC-IUB Joint commission biochemical nomenclature (1979) Tetrapyrroles. Pur Appl Chem 51: 2251
- IUPAC-IUB Joint commission biochemical nomenclature (1988) Nomenclature of Tetrapyrroles. Eur J Biochem 178: 277–328
- Ivancich A, Artz K, Williams JC, Allen JP and Mattioli TA (1998) Effects of hydrogen bonds on the redox potential and electronic structure of the bacterial primary electron donor. Biochemistry 37: 11812–11820
- Jahns P, Depka B and Trebst A (2000) Xanthophyll cycle mutants from *Chlamydomonas reinhardtii* indicate a role of zeaxanthin in the D1 protein turnover. Plant Physiol Biochem. 28: 124–129
- Jeffrey SW and Anderson J (2000) *Emiliana huxleyi* (Haptophyta) holds promising insights for photosynthesis. J Phycol 36: 449–452
- Jeffrey SW, Mantoura RFC and Wright SWE (1997) Phytoplankton pigments in oceanography. UNESCO Publications, Paris
- Jeffrey SW, Wright SW and Zapata M (1999) Recent advances in HPLC pigment analysis of phytoplankton. Mar Freshwater Res 50: 879–896
- Jensen PE, Gibson LCD and Hunter CN (1998) Determinants of catalytic activity with the use of purified I, D and H subunits of the magnesium protoporphyrin IX chelatase from *Synechocystis* PCC 6803. Biochem J 334: 335–3344
- Jordan PM (1991) The biosynthesis of 5-aminolevulinic acid and its transformation into uroporphyrinogen III. In: Jordan PM (ed) Biosynthesis of Tetrapyrroles, pp 1–66. Elsevier, Amsterdam
- Jordan PM (1994) Biosynthesis of uroporphyrinogen III. Mechanism of action of porphobilinogen deaminase. In: Chadwick DJ and Ackrill K (eds) The Biosynthesis of Tetrapyrrole Pigments, pp 70–89. John Wiley and Sons, Chichester
- Jordan P, Fromme P, Witt HT, Klukas O, Saenger W and Krauß

- N (2001) Three-dimensional structure of cyanobacterial Photosystem I at 2.5 Å resolution. *Nature* 411: 909–917
- Jung LJ, Chan CF and Glazer AN (1995) Candidate genes for the phycoerythrocyanin alpha subunit lyase. Biochemical analysis of *pecE* and *pecF* interposon mutants. *J Biol Chem* 270: 12877–84
- Jungas C, Ranck J, Rigaud J, Joliot P and Vermeglio A (2000) Supramolecular organization of the photosynthetic apparatus of *Rhodobacter sphaeroides*. *EMBO J* 18: 534–542
- Kahn K, Mazel D, Houmard J, Tandeau de Marsac N and Schaefer MR (1997) A role for *cpeYZ* in cyanobacterial phycoerythrin biosynthesis. *J Bacteriol* 179: 998–1006
- Kannangara CG, Andersen RV, Pontoppidan B, Willows R and von Wettstein D (1994) Enzymic and mechanistic studies on the conversion of Glutamate to 5-Aminolaevulinate. In: Ciba Foundation Symposium 180 (ed) The Biosynthesis of the Tetrapyrrole Pigments, pp 3–25. Wiley, Chichester
- Karrasch S, Bullough PA and Ghosh R (1995) The 8.5 Å projection map of the light-harvesting complex I from *Rhodospirillum rubrum* reveals a ring composed of 16 subunits. *EMBO J* 14: 631–638
- Katz JJ, Strain HH, Harkness AC, Studier MH, Svec WA, Janson TR and Cope B. T. (1972) Esterifying alcohols in the Chlorophylls of purple photosynthetic bacteria. A new chlorophyll, bacteriochlorophyll (*gg*), all-*trans* geranylgeranyl bacteriochlorophyllide *a*. *J Amer Chem Soc* 94: 7938–7939
- Katz JJ, Shipman LL, Cotton TM and Janson TR (1978) Chlorophyll aggregation: Coordination interactions in Chlorophyll monomers, dimers and oligomers. In: Dolphin D (ed) The Porphyrins, Vol V, pp 402–458. Academic Press, New York
- Katz JJ, Bowman MK, Michalski TJ and Worcester DL (1991) Chlorophyll aggregation: Chlorophyll-water micelles as models for in vivo long-wavelength Chlorophyll. In: Scheer H (ed) Chlorophylls, pp 211–236. CRC-Press, Boca Raton
- Kennis JTM, Shkuropatov AY, vanStokkum IHM, Gast P, Hoff AJ, Shuvalov VA and Aartsma TJ (1997) Formation of a long-lived  $P^+B_A^-$  state in plant pheophytin-exchanged reaction centers of *Rhodobacter sphaeroides* R26 at low temperature. *Biochemistry* 36: 16231–16238
- Kidd DG and Lagarias JC (1990) Phytochrome from the green alga *Mesothaenium caldarium*: Purification and preliminary characterization. *J Biol Chem* 265: 7029–7033
- Kikuchi H, Sugimoto T, and Mimuro M. (1997) An electronic state of the chromophore, phycocyanobilin, and its interaction with the protein moiety in C-phycocyanin: Protonation of the chromophore. *Chem Phys Lett* 274: 460–465.
- Kim J, Eichacker LA, Rudiger W and Mullet JE (1994) Chlorophyll regulates accumulation of the plastid-encoded chlorophyll proteins P700 and D1 by increasing apoprotein stability. *Plant Physiol* 104: 907–916
- Kjösen H, Arpin N and Liaaen-Jensen S (1972) The carotenoids of *Trentepohlia iolithus* Isolation of  $\beta,\beta'$ -carotene-2-ol,  $\beta$ ,  $\epsilon$ -carotene-2-ol and  $\beta,\beta'$ -carotene-2,2'-diol. *Acta Chem Scand* 26: 3053–3067
- Klotz AV and Glazer AN (1985) Characterization of the bilin attachment sites in R-phycoerythrin. *J Biol Chem* 260: 4856–4863
- Klukas O, Schubert W-D, Jordan P, Krauß N, Fromme P, Witt HT and Saenger W (1999) Localization of two phyloquinones, QK and QK', in an improved electron density map of Photosystem I at 4 Å resolution. *J Biol Chem* 274: 7361–7367
- Kobayashi M (1996) Study of precise pigment composition of Photosystem I-type reaction centers by means of normal-phase HPLC. *J Plant Res* 109: 223–230
- Kobayashi M, Watanabe T, Nakazato M, Ikegami I, Hiyama T and Matsunaga T (1988) Chlorophyll *a*/P700 and Pheophytin *a*/P680 stoichiometries in higher plants and cyanobacteria determined by HPLC analysis. *Biochim Biophys Acta* 936: 81–89
- Kobayashi M, Kakizano T and Nagai S (1991a) Astaxanthin production by a green alga, *Haematococcus pluvialis* accompanied with morphological changes in Acetate media. *J Ferment. Bioeng* 71: 335–339
- Kobayashi M, Watanabe T, Ikegami I, vande Meent EJ and Ames J (1991b) Enrichment of bacteriochlorophyll *g*' in membranes of *Heliobacterium chlorum* by ether extraction. Unequivocal evidence for its existence in vivo. *FEBS Lett* 284: 129–131
- Kobayashi M, Akiyama M, Watanabe T and Kano H (1999) Exotic chlorophylls as key components of photosynthesis. *Curr Topics Plant Biol* 1: 17–35
- Kobayashi M, Oh-oka H, Akutsu S, Akiyama M, Tominaga K, Kise H, Nishida F, Watanabe T, Ames J, Koizumi M, Ashida N and Kano H (2000) The primary electron acceptor of green sulfur bacteria, bacteriochlorophyll 663, is chlorophyll *a* esterified with [Delta UC]2,6-phytyadienol. *Photosynth Res* 63: 269–280
- Koepeke J, Hu X, Muenke C, Schulten K and Michel H (1996) The crystal structure of the light-harvesting complex II (B800–850) from *Rhodospirillum rubrum*. *Structure* 4: 581–597
- Koka P and Song PS (1977) The chromophore topography and binding environment of peridinin-chlorophyll *a* protein complexes from marine dinoflagellate algae. *Biochim Biophys Acta* 495: 220–231
- Köst H-P, Rüdiger W and Chapman DJ (1975) Über die Bindung zwischen Chromophor und Protein in Biliproteiden. 1. Abbaueversuche und Spektraluntersuchungen. *Liebigs Ann Chem* 1975: 1582–1593
- Kotzabasis K and Senger H (1989) Evidence for the presence of chlorophyllide *b* in the green alga *Scenedesmus obliquus* in vivo. *Botan Acta* 102: 173–177
- Koyama Y and Fujii R (1999) *Cis-trans* carotenoids in photosynthesis: Configurations, excited state properties and physiological functions. In: Frank HA, Young AJ, Britton G, and Cogdell RJ (eds) The Photochemistry of Carotenoids, pp 161–188. Kluwer Academic Publishers, Dordrecht
- Krauss C and Scheer H (1979) Long-lived pi-cation radicals of bilindionato zinc complexes. *Tetrahedron Lett* 1979: 3553–3556
- Kräutler B and Matile P (1999) Solving the riddle of chlorophyll breakdown. *Acc Chem Res* 32: 35–43
- Kropat A, Oster U, Rüdiger W and Beck CF (2000) Chloroplast signalling in the light-induction of nuclear HSP70 genes requires the accumulation of chlorophyll precursors and their accessibility to cytoplasm/nucleus. *Plant J* 24: 523–531
- Kufer W, Scheer H and Holzwarth AR (1983) Isophorcarubin—a conformationally restricted and highly fluorescent bilirubin. *Isr J Chem* 23: 233–240
- Kufer W, Högner A, Eberlein M, Mayer K, Buchner A and



- Gottschalk Lu (1991) Gene bank M75599
- Kühlbrandt W, Wang DN and Fujiyoshi Y (1994) Atomic Model of Plant Light-Harvesting Complex by Electron Crystallography. *Nature* 367: 614–621
- Kuki M, Koyama Y and Nagae H (1991) Triplet-sensitized and thermal isomerization of all-*trans*, 7-*cis*, 9-*cis*, 13-*cis*, and 15-*cis* isomers of  $\beta$ -carotene: Configurational dependence of the quantum yield of isomerization via the T1 state. *J Phys Chem* 95: 7171–7180
- Kuki M, Nagae H, Cogdell RJ, Shimada K and Koyama Y (1994) Solvent effect on spheroidene in nonpolar and polar solutions and the environment of spheroidene in the light-harvesting complexes of *Rhodobacter sphaeroides* 2.4.1 as revealed by the energy of the  $1A_g^- \rightarrow 1B_u^+$  absorption and the frequencies of the vibronically coupled C=C stretching Raman lines in the  $1A_g^-$  and  $2A_g^-$  states. *Photochem Photobiol* 59: 116–124
- Küpper H, Küpper F and Spiller M (1996) Environmental relevance of heavy metal substituted chlorophylls using the example of water plants. *J Exp Bot* 47: 259–266
- Küpper H, Küpper F and Spiller M (1998) In situ detection of heavy metal substituted chlorophylls in water plants. *Photosynth Res* 58: 123–133
- Küpper H, Spiller M and Küpper FC (2000) Photometric method for the quantification of chlorophylls and their derivatives in complex mixtures: Fitting with Gauss-peak spectra. *Anal Biochem* 286: 247–256
- La Rocca N, Rascio N, Oster U and Rüdiger W (2001) Amitrole treatment of etiolated barley seedlings leads to deregulation of tetrapyrrole synthesis and to reduced expression of *Lhc* and *RbcC* genes. *Planta* 213: 101–108
- Lamparter T, Mittmann F, Gärtner W, Börner T, Hartmann E and Hughes J (1997) Characterization of recombinant phytochrome from the cyanobacterium *Synechocystis*. *Proc Natl Acad Sci USA* 94: 11792–11797
- Lanaras T, Moustakas M, Simeonides L, Diamantoglou S and Karataglis S (1993) Plant metal content, growth responses and some photosynthetic measurements of field-cultivated wheat growing on ore bodies enriched in Cu. *Physiol Planta* 88: 307–314
- Lancaster CRD, Ermler U and Michel H (1995) The structures of photosynthetic reaction centers from purple bacteria as revealed by X-ray crystallography. In: Blankenship R, Madigan MT and Bauer CE (eds) *Anoxygenic Photosynthetic Bacteria*, pp 503–526. Kluwer Academic Publishers, Dordrecht
- Lang HP and Hunter CN (1994) The relationship between carotenoid biosynthesis and the assembly of the light-harvesting LH2 complex in *Rhodobacter sphaeroides*. *Biochem J* 298: 197–205
- Lapouge K, Näveke A, Robert B, Scheer H and Sturgis JN (2000) Exchanging cofactors in the core antennae from purple bacteria: Structure and properties of Zn-bacteriopheophytin containing LH1. *Biochemistry* 39: 1091–1099
- Lauffermair E and Oesterheld D (1992) A system for site-specific mutagenesis of the photosynthetic reaction center in *Rhodospseudomonas viridis*. *EMBO J* 11: 777–783
- Law CJ and Cogdell RJ (1998) The effect of chemical oxidation on the fluorescence of the LH1 (B880) complex from the purple bacterium *Rhodobium marinum*. *FEBS Lett* 432: 1–2
- Leeper FJ (1994) The evidence for a spirocyclic intermediate in the formation of uroporphyrinogen III by cosynthesis. In: Chadwick DJ and Ackrill K (eds) *The Biosynthesis of Tetrapyrrole Pigments*, pp 111–123. John Wiley and Sons, Chichester
- Leupold D, Stiel H, Ehler J, Nowak F, Teuchner K, Bandilla M, Ücker B and Scheer H (1999) Photophysical characterization of the B800-depleted light harvesting complex B800  $\rightarrow$  850nm. *Chem Phys Lett* 301: 537–545
- Liaaen-Jensen S and Hertzberg S (1995) Worked examples of Isolation and analysis: Example 10. Carotenoid sulphates. In: Britton G, Liaaen-Jensen S, and Pfander H (eds) *Carotenoids: Isolation and Analysis*, pp 283–286. Birkhäuser, Basel
- Lichtenthaler HK, Schwender J, Disch A and Rohmer M (1997) Biosynthesis of isoprenoids in higher plant chloroplasts proceeds via a mevalonate-independent pathway. *FEBS Lett* 400: 271–274
- Lindner I, Knipp B, Braslavsky SE, Gärtner W and Schaffner K (1998) *Angew Chem Intl Ed Engl* 37: 1843–1846
- Loach PA and Parkes-Loach PS (1995) Structure-function relationships in core light-harvesting complexes (LHI) as determined by characterization of the structural subunit and by reconstitution experiments. In: Blankenship R, Madigan MT and Bauer CE (eds) *Anoxygenic Photosynthetic Bacteria*, pp 437–471. Kluwer Academic Publishers, Dordrecht
- Loach PA, Sekura DL, Hadsell RM and Stemer A (1970) Quantitative dissolution of the membrane and preparation of photoreceptor subunits from *Rhodospseudomonas sphaeroides*. *Biochemistry* 9: 724–733
- Lohr M and Wilhelm C (1999) Algae displaying then diadinoxanthin cycle also possess the violaxanthin cycle. *Proc Natl Acad Sci USA* 96: 8784–8789
- MacColl R and Guard-Friar D (1987) *Phycobiliproteins*, CRC Press, Boca Raton
- Marquardt J, Senger H, Miyashita H, Miyachi S and Morschel E (1997) Isolation and characterization of biliprotein aggregates from *Acaryochloris marina*, a Prochloron-like prokaryote containing mainly chlorophyll *d*. *FEBS Lett* 410: 428–432
- Meyer P, Riesen R and Pfander H (1995) Worked examples of Isolation and analysis: Example 9. Carotenoid glycosides and glycosyl esters. In: Britton G, Liaaen-Jensen S, and Pfander H (eds) *Carotenoids: Isolation and Analysis*, pp 277–282. Birkhäuser, Basel
- Michalski TJ, Hunt JE, Bowman MK, Smith U, Bardeen K, Gest H, Norris JR and Katz JJ (1987) Bacteriopheophytin *g*—Properties and some speculations on a possible primary role for bacteriochlorophyll *b* and *g* in the biosynthesis of chlorophylls. *Proc Natl Acad Sci USA* 84: 2570–2574
- Michl J and Thulstrup EW (1986) Spectroscopy with Polarized Light—Solute Alignment by Photoselection, in *Liquid Crystals, Polymers and Membranes*. VCH, New York
- Miller JF, Hinchigeri SB, Parkes-Loach PS, Callahan PM, Sprinkle JR, Riccobono JR and Loach PA (1987) Isolation and characterization of a subunit form of the light-harvesting complex of *Rhodospirillum rubrum*. *Biochemistry* 26: 5055–5062
- Mimuro M, Nagashima U, Nagaoka S, Takaichi S, Yamazaki I, Nishimura Y and Katoh T (1993) Direct measurement of the low-lying singlet excited ( $2/1 A_g$ ) state of a linear carotenoid, neurosporene, in solution. *Chem Phys Lett* 204: 101–105
- Miyashita H, Adachi K, Kurano N, Ikemoto H, Chihara M and Miyachi S (1997) Pigment composition of a novel oxygenic photosynthetic prokaryote containing chlorophyll *d* as the major chlorophyll, *Plant Cell Physiol* 38: 274–281.



- Murphy JT and Lagarias JC (1997) Purification and characterization of recombinant affinity peptide tagged oat phytochrome A. *Photochem Photobiol* 65: 750–758.
- Musewald C, Hartwich G, Pöllinger-Dammer F, Lossau H, Scheer H and Michel-Beyerle ME (1998) Time resolved spectral investigation of bacteriochlorophyll *a* and its transmetalated derivatives Zn-bacteriochlorophyll *a* and Pd-bacteriochlorophyll *a*. *J Phys Chem* 102: 8336–8342.
- Musewald C, Gilch P and Hartwich G (1999) Magnetic field dependence of ultrafast intersystem-crossing. A triplet mechanism on the picosecond timescale? *J Amer Chem Soc* 121: 8876–8881.
- Nabedryk E, Breton J, Williams JC, Allen JP, Kuhn M and Lubitz W (1998) FTIR characterization of the primary electron donor in double mutants combining the heterodimer HL(M202) with the LH(L131), HF(L168), FH(M197), or LH(M160) mutations. *Spectrochim. Acta A* 54: 1219–1230.
- Nagae H, Kuki M, Zhang J-P, Sashima T, Mukai Y and Koyama Y (2000) Vibronic coupling through the in-phase C=C stretching mode plays a major role in the  $2A_g^-$  to  $1A_g^-$  internal conversion of all-*trans*- $\beta$ -carotene. *J Phys Chem A* 104: 4155–4166.
- Naylor GW, Adlense HA, Gebson LCD and Hunter CN (2000) The photosynthesis gene cluster of *Rhodobacter sphaeroides*. *Photosynth Res* 62: 121–139.
- Niedermeier G, Scheer H and Feick R (1992) The functional role of protein in the organization of bacteriochlorophyll *c* in chlorosomes of *Chloroflexus aurantiacus*. *Eur J Biochem* 204: 685–692.
- Noy D, Brumfeld V, Ashur I, Yerushalmi R and Scheer H (1998a) Axial ligand coordination and photodissociation of nickel substituted bacteriochlorophyll *a*. In: Garab. G. (ed) *Photosynthesis: Mechanisms and Effects*, pp 4225–4228. Kluwer Academic Publishers, Dordrecht.
- Noy D, Fiedor L, Hartwich G, Scheer H and Scherz A (1998b) Metal-substituted bacteriochlorophylls. 2. Changes in redox potentials and electronic transition energies are dominated by intramolecular electrostatic interactions. *J Am Chem Soc* 120: 3684–3693.
- Oelze J (1985) Analysis in bacteriochlorophylls. *Meth Microbiol* 18: 257–284.
- Oelze J and Golecki JR (1995) Membranes and chlorosomes of green bacteria: Structure, composition and development. In: Blankenship R, Madigan MT and Bauer CE (eds) *Anoxygenic Photosynthetic Bacteria*, pp 259–278. Kluwer Academic Publishers, Dordrecht.
- Ohashi N, Ko-Chi N, Kuki M, Shimamura T, Cogdell RJ and Koyama Y (1996) The structures of  $S_0$  spheroidene in the light-harvesting (LH2) complex and  $S_0$  and  $T_1$  spheroidene in the reaction center of *Rhodobacter sphaeroides* 2.4.1 as revealed by Raman spectroscopy. *Biospectroscopy* 2: 59–69.
- Olsen JD, Sturgis JN, Westerhuis WHJ, Fowler GJS, Hunter CN and Robert B (1997) Site directed modification of the ligands to the bacteriochlorophylls of the light-harvesting LH1 and LH2 complexes of *Rhodobacter sphaeroides*. *Biochemistry* 36: 12625–12632.
- Oster U, Tanaka R, Tanaka A and Rüdiger W (2000) Cloning and functional expression of the gene encoding the key enzyme for chlorophyll *b* biosynthesis (CAO) from *Arabidopsis thaliana*. *Plant J* 21: 305–310.
- Paulsen H (1995) Chlorophyll *a/b*-binding proteins. *Photochem Photobiol* 62: 367–382.
- Paulsen H (1999) Carotenoids and the assembly of light-harvesting complexes. In: Frank HA, Young AJ, Britton G, and Cogdell RJ (eds) *The Photochemistry of Carotenoids*, pp 123–135. Kluwer Academic Publishers, Dordrecht.
- Permentier HP, Neerken S, Overmann J and Ames J (2001) A bacteriochlorophyll *a* antenna complex from purple bacteria absorbing at 963 nm, *Biochemistry* 40, 5573–5578.
- Petrier C, Jardon P, Dupuy C and Gautron R (1981) Spectroscopic study of tetrapyrrolic compounds as phytochrome models—biliverdin IX- $\gamma$ , phorbacilin and isophorbacilin dimethyl esters. *J Chim Phys* 78: 519–525.
- Pfander H (1995) Chromatography: Part I. General aspects. In: Britton G, Liaaen-Jensen S, and Pfander H (eds) *Carotenoids: Isolation and Analysis*, pp 109–116. Birkhäuser, Basel.
- Pfander H and Niggli U (1995) Chromatography: Part V. Supercritical fluid chromatography. In: Britton G, Liaaen-Jensen S, and Pfander H (eds) *Carotenoids: Isolation and Analysis*, pp 191–198. Birkhäuser, Basel.
- Pfander H and Riesen R (1995) Chromatography: Part IV. High-performance liquid chromatography. In: Britton G, Liaaen-Jensen S, and Pfander H (eds) *Carotenoids: Isolation and Analysis*, pp 145–190. Birkhäuser, Basel.
- Pierre Y, Breyton C, Lemoine Y, Robert B, Vernotte C, Popot JL (1997) On the presence and role of a molecule of chlorophyll *a* in the cytochrome *b<sub>6</sub>f* complex. *J Biol Chem* 272, 21901–21908.
- Plumley FG and Schmidt GW (1987) Reconstitution of chlorophyll *a/b* light-harvesting complexes—xanthophyll-dependent assembly and energy-transfer. *Biochim Biophys Acta* 84: 146–150.
- Polivka T, Zigmantas D, Frank HA, Bautista HA, Herek JL, Koyama Y, Fujii R and Sundström V (2001) Near infrared time-resolved study of the S-1 state dynamics of the carotenoid spheroidene. *J Phys Chem B* 105: 1072–1080.
- Porra RJ (1990) The assay of Chlorophylls *a* and *b* converted to their respective Magnesium-Rhodochlorin derivatives by extraction from recalcitrant algal cells with aqueous alkaline Methanol: Prevention of allomerization with reductants. *Biochim Biophys Acta* 1015: 493–502.
- Porra RJ (1991) Recent advances and re-assessments in Chlorophyll extraction and assay procedures for terrestrial, aquatic, and marine organisms, including recalcitrant algae. In: Scheer H (ed) *Chlorophylls*, pp 31–58. CRC-Press, Boca Raton.
- Porra RJ and Scheer H (1999) The origin of the oxygen atoms of chlorophyll molecules: A study of chlorophyll biosynthesis using mass spectrometry and  $^{18}\text{O}$  labelling. *Photosynth Res* 66: 159–172.
- Porra RJ, Klein O and Wright PE (1983) The proof by  $^{13}\text{C}$ -nuclear magnetic resonance spectroscopy of the predominance of the  $\text{C}_5$ -pathway over the Shemin pathway in chlorophyll biosynthesis and the formation of the methyl ester group of chlorophyll from glycine. *Eur J Biochem* 130: 509–516.
- Porra RJ, Schäfer W, Cmiel E, Katheder I and Scheer H (1993) Derivation of the formyl-group oxygen of chlorophyll *b* from molecular oxygen in greening leaves of a higher plant (*Zea mays*). *FEBS Lett* 323: 31–34.
- Porra RJ, Schäfer W, Katheder I and Scheer H (1995) The derivation of the oxygen atoms of the  $13^1$ -oxo- and 3-acetyl groups of bacteriochlorophyll *a* from water in *Rhodobacter*

- sphaeroides* cells adapting from respiratory to photosynthetic conditions: Evidence for an anaerobic pathway for the formation of isocyclic ring E. *FEBS Lett* 371: 21–24
- Porra RJ, Urzinger M, Winkler H, Bubenzer C and Scheer H (1998) Biosynthesis of the 3-acetyl and 13<sup>1</sup>-oxo groups of bacteriochlorophyll *a* in the facultative aerobic bacterium, *Rhodovulum sulfidophilum*: The presence of both oxygenase and hydratase pathways for isocyclic ring formation. *Eur J Biochem* 257: 185–191
- Qian P, Yagura T, Koyama Y and Cogdell RJ (2000) Isolation and purification of the reaction center (RC) and the core (RC-LH1) complex from *Rhodobium marinum*: the LH1 ring of the detergent-solubilized core complex contains 32 bacteriochlorophylls. *Plant Cell Physiol* 41: 1347–1353
- Rebeiz CA, Wu SM, Kuhadja M, Daniell H and Perkins EJ (1983) Chlorophyll *a* biosynthetic routes and chlorophyll *a* chemical heterogeneity in plants. *Mol Cell Biochem* 57: 97–125
- Rebeiz CA, Parham R, Fasoula DA and Ioannides IM (1994) Chlorophyll *a* biosynthetic heterogeneity. In: Chadwick DJ and Ackrill K (eds) *Biosynthesis of the Tetrapyrroles*, pp 177–189. Wiley Ltd, Chichester
- Remberg A, Ruddat A, Braslavsky SE, Gärtner W and Schaffner K (1998) Chromophore incorporation, Pr to Pfr kinetics, and Pfr thermal reversion of recombinant N-terminal fragments of phytochrome A and B chromoproteins. *Biochemistry* 37: 9983–9990
- Reuter W, Wiegand G, Huber R and Than ME (1999) Structural analysis at 2.2 Å of orthorhombic crystals presents the asymmetry of the allophycocyanin-linker complex, AP Lc(7,8), from phycobilisomes of *Mastigocladus laminosus*. *Proc Natl Acad Sci USA* 96: 1363–1368
- Rice JK, Fearnley IM and Barker PD (1999) Coupled oxidation of heme covalently attached to cytochrome b562 yields a novel biliprotein. *Biochemistry* 38: 16847–16855
- Robert B (1999) The electronic structure, stereochemistry and resonance Raman spectroscopy of carotenoids. In: Frank HA, Young AJ, Britton G, and Cogdell RJ (eds) *The Photochemistry of Carotenoids*, pp 189–201. Kluwer Academic Publishers, Dordrecht
- Rüdiger W (1993) Biosynthesis of tetrapyrroles in plants. *Naturwiss* 80: 353–360
- Rüdiger W and Schoch S (1991) The last steps of chlorophyll biosynthesis. In: Scheer H (ed) *Chlorophylls*, pp 451–464. CRC-Press, Boca Raton
- Sandmann G and Scheer H (1998) Chloroplast pigments: Chlorophylls and Carotenoids. In: Raghavendra AS (ed) *Photosynthesis—A Comprehensive Treatise*, pp 44–57. Cambridge University Press, Cambridge
- Scheer H (1982) Phycobiliproteins: Molecular aspects of photosynthetic antenna systems. In: Fong FK (ed) *Light Reaction Path of Photosynthesis*. pp 7–45. Springer Verlag, Berlin
- Scheer H (1985) Model compounds for the phytochrome chromophore. In: Smith H (ed) *Photomorphogenesis*, pp 227–256. Academic Press, London
- Scheer H (1986) Excitation transfer in Phycobiliproteins. In: Staehelin LA and Arntzen CJ (eds) *Photosynthesis III: Photosynthetic Membranes and Light-Harvesting Systems*, pp 327–337. Springer, Berlin
- Scheer H (1988) Chlorophylls: Chromatographic methods for the separation of chlorophylls. In: H.-P. Köst (ed) *Handbook of Chromatography: Plant Pigments Vol. 1*, pp 235–307. CRC press, Boca Raton
- Scheer H (ed) (1991a) *Chlorophylls*. Boca Raton, CRC-Press
- Scheer H (1991b) Structure and occurrence of Chlorophylls. In: Scheer H (ed) *Chlorophylls* pp 3–30. CRC-Press, Boca Raton
- Scheer H (2000) *Enzyklopädie Naturwissenschaft und Technik*. Ecomed, Landsberg
- Scheer H and Hartwich G (1995) Bacterial reaction centers with modified tetrapyrrole chromophores. In: Blankenship R, Madigan MT and Bauer CE (eds) *Anoxygenic Photosynthetic Bacteria*, pp 649–663. Kluwer Academic Publishers, Dordrecht
- Scheer H and Krauss C (1977) Studies on Plant Bile Pigments 3: Oxidative Photodimerization of a Phytochrome Pr Model Pigment, and its thermal Reversion. *Photochem Photobiol* 25: 311
- Scheer H and Struck A (1993) Bacterial reaction centers with modified tetrapyrrole chromophores. In: Deisenhofer J and Norris JR (eds) *The Photosynthetic Reaction Center*, pp 157–193. Academic Press, New York
- Scheer H, Svec WA, Cope BT, Studier MH, Scott RG and Katz JJ (1974) Structure of Bacteriochlorophyll *b*. *J Amer Chem Soc* 96: 3714
- Scheer H, Formanek H and Schneider S (1982) Theoretical studies of biliprotein chromophores and related bilepigments by molecular orbital and Ramachandran type calculation. *Photochem Photobiol* 36: 259–272
- Scheer H, Paulke B and Gottstein J (1985) Long-wavelength absorbing forms of bacteriochlorophylls. II. Structural requirements for formation in Triton X100 micelles and in aqueous methanol and acetone. In: Blauer G and Sund H (eds) *Optical properties and Structure of Tetrapyrroles*, pp 507–521. De Gruyter, London
- Scherz A, Rosenbach-Belkin V, Michalski TJ and Worcester DL (1991) Chlorophyll aggregates in aqueous solutions. In: Scheer H. (ed) *Chlorophylls*, pp 237–268. CRC Press, Boca Raton
- Scheumann V, Ito H, Tanaka A, Schoch S and Rüdiger W (1996) Substrate specificity of chlorophyll(ide) *b* reductase in etioplasts of barley (*Hordeum vulgare* L.). *Eur J Biochem* 242: 163–170
- Scheumann V, Klement H, Helfrich M, Oster U, Schoch S and Rüdiger W (1999) Protochlorophyllide *b* does not occur in barley etioplasts. *FEBS Lett* 445: 445–448
- Schiedt K (1995) Chromatography: Part III. Thin-layer chromatography. In: Britton G, Liaen-Jensen S, and Pfander H (eds) *Carotenoids: Isolation and Analysis*, pp 131–144. Birkhäuser, Basel
- Schierle J, Härdi W, Faccin N, Bühler I and Schüep W (1995) Worked examples of Isolation and analysis: Example 8: Geometrical isomers of  $\beta,\beta'$ -carotene. In: Britton G, Liaen-Jensen S, and Pfander H (eds) *Carotenoids: Isolation and Analysis*, pp 265–272. Birkhäuser, Basel
- Schirmer T, Bode W and Huber R (1987) Refined three-dimensional structures of two cyanobacterial C-phycocyanins at 2.1 and 2.5 Å resolution—a common principle of phycobilin-protein interaction. *J Mol Biol* 196: 677–695
- Schluchter WM and Bryant DA (2002) Analysis and reconstitution of phycobiliproteins: Methods for the characterization of bilin attachment reactions. In: Smith AG and Witty M (eds) *Heme, Chlorophyll and Bilins*, pp 311–334. Humana Press, Totowa, NJ
- Schluchter WM and Glazer AN (1999) Biosynthesis of

- Phycobiliproteins in Cyanobacteria. In: Peschek GA, Löffelhardt W and Schmetterer G (eds) *The Phototrophic Prokaryotes*, pp 83–95. Kluwer Academic Publishers, Dordrecht
- Schmid VHR, Cammarata KV, Bruns BU and Schmidt GW (1997) In vitro reconstitution of the Photosystem I light-harvesting complex LHCl-730: Heterodimerization is required for antenna pigment organization. *Proc Natl Acad Sci U. S. A.* 94: 7667–7672
- Schmidt S, Arlt T, Hamm P, Huber H, Nägele T, Wachtveitl J, Zinth W, Meyer M and Scheer H (1995) Primary electron-transfer dynamics in modified bacterial reaction centers containing pheophytin *a* instead of bacteriopheophytin *a*. *Spectrochim. Acta A* 51: 1565–1578
- Schneegurt MA and Beale SI (1992) Origin of the chlorophyll-*b* formyl oxygen in *Chlorella-vulgaris*. *Biochemistry* 31: 11677–11683
- Schoch S, Lempert U, Wieschhoff H and Scheer H (1978) High-performance liquid-chromatography of tetrapyrrole pigments. pheophytin esterified with different diterpene alcohols, isomeric biliverdins and synthetic bilins. *J Chromatogr* 157: 357–364
- Schoch S, Helfrich M, Wiktorsson B, Sundqvist C, Rüdiger W and Ryberg M (1995) Photoreduction of Zinc-protopheophorbide *b* with NADPH-protopheophyllide oxidoreductase from etiolated wheat (*Triticum aestivum* L.). *Eur J Biochem* 229: 291–298
- Schoch S, Lempert U, Wieschhoff H and Scheer H (1978) High-performance liquid-chromatography of tetrapyrrole pigments. pheophytin esterified with different diterpene alcohols, isomeric biliverdins and synthetic bilins. *J Chromatogr* 157: 357–364
- Schram BL and Kroes HH (1971) Structure of phycocyanobilin. *Eur J Biochem* 19: 581–594
- Schulten K and Karplus M (1972) On the origin of a low-lying forbidden transition in polyenes and related molecules. *Chem Phys Lett* 14: 305–309
- Senge MO and Smith KM (1995) Biosynthesis and structures of the bacteriochlorophylls. In: Blankenship R, Madigan MT and Bauer CE (eds) *Anoxygenic Photosynthetic Bacteria*, pp 137–151. Kluwer Academic Publishers, Dordrecht
- Shimada K (1995) Aerobic anoxygenic phototrophs. In: Blankenship R, Madigan MT and Bauer CE (eds) *Anoxygenic Photosynthetic Bacteria*, pp 105–122. Kluwer Academic Publishers, Dordrecht
- Shioi Y (1991) Analytical chromatography of Chlorophylls. In: Scheer H (ed) pp 59–88. CRC-Press, Boca Raton
- Shioi Y and Beale SI (1987) Polyethylene-based high-performance liquid chromatography of chloroplast pigments—resolution of mono- and divinyl-chlorophyllides and other pigment mixtures. *Anal Biochem* 162: 493–499
- Shkuropatov AY and Shuvalov VA (1993) Electron Transfer in pheophytin *a*-modified reaction centers from *Rhodobacter sphaeroides* (R-26). *FEBS Lett* 322: 168–172
- Shkuropatov AY, Khatypov RA, Shkuropatova VA, Zvereva MG, Owens TG and Shuvalov VA (1999) Reaction centers of Photosystem II with chemically modified pigment composition: exchange of pheophytins with 13<sup>1</sup>-deoxy-13<sup>1</sup>-hydroxy-pheophytin *a*. *FEBS Lett* 450: 163–167
- Siebert F, Grimm R, Rüdiger W, Schmidt G and Scheer H (1990) Infrared spectroscopy of phytochrome and model pigments. *Eur J Biochem* 194: 921–928
- Smith JHC and Benitez A (1955) Chlorophylls: Analysis in plant materials. In: Paech K and Tracey M (eds) *Methods of Plant Analysis*, pp. 142–196, Springer, Berlin
- Smith KM and Simpson DJ (1986) Stereochemistry of the bacteriochlorophyll *e* homologues. *J Chem Soc Chem Comm* 1986: 1682–1684
- Spörlein S, Zinth W, Meyer M, Scheer H and Wachtveitl J (2000) Primary electron transfer in modified bacterial reaction centers: Optimization of the first events in photosynthesis. *Chem Phys Lett* 322: 454–464
- Stauber JL and Jeffrey SW (1988) Photosynthetic pigments in 51 species of marine diatoms. *J Phycol* 24: 158–172
- Steiger S, Schafer L and Sandmann G (1999) High-light-dependent upregulation of carotenoids and their antioxidative properties in the cyanobacterium *Synechocystis* PCC 6803. *J. Photochem Photobiol B* 52: 14–18
- Steiner R, Schäfer W, Blos I, Wieschhoff H and Scheer H (1981) Delta 2,10-phytodienol as esterifying alcohol of bacteriochlorophyll *b* from *Ectothiorhodospira halochloris*. *Z Naturforsch* 36 c: 417–420
- Strain HH and Svec WA (1966) Extraction, separation, estimation and isolation of the Chlorophylls. In: Vernon LP and Seely GR (eds) *The Chlorophylls*, pp 21–66. Academic Press, New York
- Struck A and Scheer H (1990) Modified reaction centers from *Rhodobacter sphaeroides* R26. 1. Exchange of monomeric Bacteriochlorophyll with 13\*2-hydroxy-bacteriochlorophyll. *FEBS Lett* 261: 385–388
- Struck A, Cmiel E, Katheder I and Scheer H (1990) Modified reaction centers from *Rhodobacter sphaeroides* R26. 2. Bacteriochlorophylls with modified C-3 substituents at sites B<sub>A</sub> and B<sub>B</sub> *FEBS Lett* 268: 180–184
- Svec WA (1991) The distribution and extraction of the chlorophylls. In: Scheer H (ed) *Chlorophylls*, pp 89–102. CRC-Press, Boca Raton
- Swanson RV and Glazer AN (1990) Separation of phycobiliprotein subunits by reverse-phase high-pressure liquid chromatography. *Anal Biochem* 188: 295–299
- Swanson RV, Zhou J, Leary JA, Williams T, de Lorimier R, Bryant DA and Glazer AN (1992) Characterization of phycocyanin produced by *cpcE* and *cpcF* mutants and identification of an intergenic suppressor of the defect in bilin attachment. *J Biol Chem* 267: 16146–54
- Takaichi S (1999) Carotenoids and carotenogenesis in anoxygenic photosynthetic bacteria. In: Frank HA, Young AJ, Britton G, and Cogdell RJ (eds) *The Photochemistry of Carotenoids*, pp 39–69. Kluwer Academic Publishers, Dordrecht
- Takaichi S (2000) Characterization of carotenoids in a combination of a C18 HPLC column with isocratic elution and absorption spectra with a photodiode-array detector. *Photosynth Res* 65: 93–99
- Takamiya K-I, Tsuchiya T and Ohta H (2000) Degradation pathway(s) of chlorophyll: What has gene cloning revealed? *Trends Plant Sci* 5: 426–431
- Takiff L and Boxer SG (1988) Phosphorescence spectra of bacteriochlorophylls. *J Amer Chem Soc* 110: 4425–4426
- Tamiaki H, Takeuchi S, Tanikaga R, Balaban S, Holzwarth A and Schaffner K (1994) Diastereoselective control of aggregation of 3<sup>1</sup>-epimeric zinc methyl bacteriopheophorbides *d* in apolar solvents. *Chem Lett* 1994: 401–402
- Tao Y, Zhao G, Yang J, Ikeda S, Jiang J, Hu t, Chen W, Wei Z and Hong F (2001) Determination of double decker sandwich

- structured La-substituted chlorophyll by EXAFS. *J Synchrotron Rad* 8: 996–997
- Thümmel F, Brandlmeier T and Rüdiger W (1981) Preparations and properties of chromopeptides from the  $P_{fr}$  form of phytochrome. *Z Naturforsch* 36 c: 440–449
- Tregub I, Schoch S, Erazo S and Scheer H (1996) Red-light induced photoreactions of chlorophyll *a* mixtures with all-*trans* or 9-*cis*- $\beta$ -carotene. *J Photochem Photobiol C* 98: 51–58
- Trissl HW (1993) Long-wavelength absorbing antenna pigments and heterogeneous absorption bands concentrate excitons and increase absorption cross section. *Photosynth Res* 35: 247–263
- Tronrud DE and Matthews BW (1993) Refinement of the structure of a water-soluble antenna complex from green photosynthetic bacteria by incorporation of the chemically determined amino acid sequence. In: Deisenhofer J and Norris JR (eds) *The Photosynthetic Reaction Center*, pp 13–22. Academic Press, New York
- Ueda T, Morimoto Y, Sato M, Kakuno T, Yamashita J and Horio T (1985) Isolation, characterization, and comparison of a ubiquitous pigment-protein complex consisting of a reaction center and light-harvesting bacteriochlorophyll proteins present in purple photosynthetic bacteria. *J Biochem* 98: 1487–1498
- Van de Meent EJ, Kobayashi M, Erkelens C, van Veelen PA, Amesz J and Watanabe T (1991) Identification of 8<sup>2</sup>-hydroxychlorophyll *a* as a functional reaction center pigment in heliobacteria. *Biochim Biophys Acta* 1058: 356–362
- van Rossum B-J, Boender GJ, Mulder FM, Balaban TS, Holzwarth A, Schaffner K, Prytulla S, Oschkinat H and de Groot HJM (1998) Multidimensional CP-MAS <sup>13</sup>C NMR of uniformly enriched chlorophyll. *Spectrochim. Acta* 54: 1167–1176
- Volk M, Ogrodnik A and Michel-Beyerle ME (1995) The recombination dynamics of the radical pair  $P^+H^-$  in external magnetic and electric fields. In: Blankenship R, Madigan MT and Bauer CE (eds) *Anoxygenic Photosynthetic Bacteria*, pp 595–626. Kluwer Academic Publishers, Dordrecht
- Wakao, N, Yokoi N, Ioyama N, Hiraishi A, Shimada K, Konayashi M, Kise H, Iwaki M, Itoh S, Takaichi S and Sakurai Y (1996) Discovery of natural photosynthesis using Zn containing bacteriochlorophyll in an aerobic bacterium, *Acidiphilium rubrum*. *Plant Cell Physiol.* 37: 889–893
- Walmsley J and Adamson H (1990) Gabaculine inhibition of chlorophyll synthesis in light and darkness in intact barley (*Hordeum vulgare*) seedlings. *Plant Sci* 68: 65–70
- Walter E, Schreiber J, Zass E and Eschenmoser A (1979) Bacteriochlorophyll  $a_{GG}$  und Bakteriophäophytin  $a_P$  in den photosynthetischen Reaktionszentren von *Rhodospirillum rubrum* G9. *Helv Chim Acta* 62: 899–920
- Wasielowski MR, Norris JR, Shipman LL, Lin CP and Svec WA (1981) Monomeric chlorophyll *a* enol—evidence for its possible role as the primary electron donor in Photosystem I of plant photosynthesis. *Proc Natl Acad Sci USA* 78: 2957–2961
- Weedon BCL and Moss GP (1995) Structure and nomenclature. In: Britton G, Liaaen-Jensen S, and Pfander H (eds) *Carotenoids: Isolation and Analysis*, pp 27–70. Birkhäuser, Basel
- Weiss C (1978) Optical spectra of Chlorophylls. In: Dolphin D (ed) *The Porphyrins*, Vol III, pp 211–224. Academic Press, New York
- Weiss C Jr (1972) The pi-electron structure and absorption spectra of Chlorophylls in solution. *J Mol Spec* 44: 37–80
- Wilk KE, Harrop SJ, Jankova L, Edler D, Keenan G, Sharples F, Hiller RG and Curmi PMG (1999) Evolution of a light-harvesting protein by addition of new subunits and rearrangement of conserved elements: Crystal structure of a cryptophyte phycoerythrin at 1.63 Å resolution. *Proc Natl Acad Sci USA* 96: 8901–8906
- Witt HT (1975) Energy conservation in the functional membrane. In: Govindjee (ed) *Bioenergetics of Photosynthesis*, pp 493–455. Academic Press, New York
- Wittenberg J and Shemin D (1950) The location in protoporphyrin of the carbon atoms derived from the  $\alpha$ -carbon of glycine. *J Biol Chem* 185: 103–116
- Wright SW, Jeffrey SW and Mantoura RFC (1997) Evaluation of methods and solvents for pigment extraction. In: Jeffrey SW, Mantoura RFC, and Wright SW (eds) *Phytoplankton pigments in oceanography*, pp 261–305. UNESCO Publications, Paris
- Wu SH, McDowell MT and Lagarias JC (1997) Phycocyanobilin is the natural precursor of the phytochrome chromophore in the green alga *Mesotaenium caldariorum*. *J Biol Chem* 272: 25700–25705
- Young AJ (1993a) Factors that affect carotenoid composition in higher plants and algae. In: Young AJ and Britton G (eds) *Carotenoids in photosynthesis*, pp 161–205. Chapman and Hall, London
- Young AJ (1993b) Occurrence and distribution of carotenoids in photosynthetic systems. In: Young AJ and Britton G (eds) *Carotenoids in Photosynthesis*, pp 16–71. Chapman and Hall, London
- Zapata M, Rodriguez F and Garrido JL (2000) Separation of chlorophylls and carotenoids from marine phytoplankton: A new HPLC method using reversed phase C<sub>8</sub> column and pyridine-containing mobile phases. *Mar Ecol Prog Ser* 195: 29–45
- Zhang J-P, Fujii R, Qian P, Inaba T, Mizoguchi T, Koyama Y, Onaka K, Watanabe Y and Nagae H (2000) Mechanism of the carotenoid-to-bacteriochlorophyll energy transfer via the S<sub>1</sub> state in LH2 complexes from purple bacteria. *J Phys Chem B* 104: 3683–3691
- Zhao K-H, Deng M-G, Zheng M, Zhou M, Parbel A, Storf M, Meyer M, Strohmam B and Scheer H (2000) Novel activity of a phycobiliprotein lyase: Both the attachment of phycocyanobilin and the isomerization to phycoviolobilin are catalyzed by PecE and PecF. *FEBS Lett* 469: 9–13
- Zhou J, Gasparich GE, Stirewalt VL, de Lorimier R and Bryant DA (1992) The *cpcE* and *cpcF* genes of *Synechococcus* sp. PCC 7002. Construction and phenotypic characterization of interposon mutants. *J Biol Chem* 267: 16138–45
- Zuber H and Cogdell RJ (1995) Structure and organization of purple bacterial antenna complexes. In: Blankenship R, Madigan MT and Bauer CE (eds) *Anoxygenic Photosynthetic Bacteria*, pp 315–348. Kluwer Academic Publishers, Dordrecht

# Chapter 3

## Optical Spectroscopy in Photosynthetic Antennas

William W. Parson\* and V. Nagarajan

*Department of Biochemistry Box 357350, University of Washington,  
Seattle, WA 98195-7350 U.S.A.*

Summary .....	84
I. Introduction .....	84
II. Absorption Coefficient .....	85
III. Charge-Transfer Transitions .....	86
IV. Circular Dichroism .....	86
V. Configuration Interactions .....	90
VI. Dipole Strength .....	92
VII. Electromagnetic Radiation .....	92
VIII. Excitons .....	95
IX. Fluorescence Yield and Lifetime .....	100
X. Infrared Spectroscopy .....	101
XI. Internal Conversion .....	103
XII. Linear Dichroism and Fluorescence Anisotropy .....	103
XIII. Mathematical Tools .....	106
A. Vectors .....	106
B. Operators .....	106
C. Eigenfunctions and Eigenvalues .....	106
D. Complex Functions .....	106
E. Bra-ket Notation .....	106
XIV. Raman Scattering .....	107
XV. Resonance Energy Transfer .....	108
A. Dipole-Dipole Coupling .....	108
B. Exchange Coupling .....	110
C. Singlet-Singlet Annihilation .....	111
XVI. Singlet and Triplet States .....	111
XVII. Spectral Bandshapes and Dynamics .....	113
A. Vibronic Transitions .....	113
B. Homogeneous and Inhomogeneous Broadening .....	114
C. Spectral Hole Burning .....	115
XVIII. Spontaneous Fluorescence .....	116
A. The Einstein A and B Coefficients .....	116
B. The Strickler-Berg Equation .....	117
C. Stokes Shifts .....	117
XIX. Time-Resolved Spectroscopy .....	118
A. Time-Resolved Fluorescence .....	118
B. Time-Resolved Absorbance Changes .....	119
XX. Transition Dipoles .....	120
A. Definition and Interpretation .....	120

---

\*Author for correspondence, email: parsonb@u.washington.edu

B. Theoretical Evaluations of Transition Dipoles .....	122
XXI. Wavefunctions .....	123
A. Wavefunctions, Operators and Expectation Values .....	123
B. The Schrödinger Equation .....	124
Acknowledgement .....	125
References .....	125

## Summary

This chapter describes the main techniques of optical spectroscopy that are used to study the structure and operation of photosynthetic antenna systems. We outline the physical basis of optical absorption, fluorescence, linear and circular dichroism, exciton interactions and resonance energy transfer, and indicate the types of information that measurements of these phenomena can provide.

## I. Introduction

This chapter provides an introduction to the basic concepts of optical spectroscopy, with an emphasis on applications to photosynthetic antenna systems. Our goal is to fill in the physical background for the many spectroscopic experiments that are described in the other chapters of this book. To help the reader extract information on a particular topic as efficiently as possible, we have arranged the topics alphabetically in independent modules rather than in a pedagogical sequence. Cross-references to other modules are indicated with special type, as in ‘Dipole Strength.’

Readers who would like to follow a more orderly path might begin by reading the sections on Absorption Coefficient, Electromagnetic Radiation, and Fluorescence Yield and Lifetime, which describe the basic phenomena of optical absorption and emission. These sections could be followed by Dipole Strength, Transition Dipoles, Linear Dichroism and Fluorescence Anisotropy, Spectral Bandshapes and Dynamics, and Infrared Spectroscopy for more detailed discussions of absorption, and by Spontaneous Fluorescence for more on fluorescence. The sections on Excitons and Resonance Energy Transfer describe how inter-molecular interactions affect the absorption spectra

of dimers and higher oligomers and allow energy to move from one molecule to another. The discussions of Wavefunctions, Charge-Transfer Transitions, Configuration Interactions, Internal Conversion, and Singlet and Triplet States fill in additional details. Finally, Circular Dichroism, Time-resolved Spectroscopy and Raman Scattering describe specialized types of optical spectroscopy that are particularly useful for studying antenna complexes.

The spectroscopic phenomena of absorption and emission of light are rooted firmly in quantum mechanics, and because the language of quantum mechanics is mathematical, explanations of these phenomena can look intimidating to readers who have only a passing interest in math. We have tried to make our descriptions accessible to such readers. We assume that the reader is familiar with the general notions of derivatives, integrals and complex numbers, but is not (at least for the moment) interested in the details of solving differential or integral equations. We therefore present some of the important results with only brief explanations of their origins. Detailed information on most of these topics is available in several books on spectroscopy (Mataga and Kubota, 1970; Struve, 1989; Lippert and Macomber, 1995; Sauer, 1995; Ames and Hoff, 1996; McHale, 1999) and general texts on molecular quantum mechanics (Atkins, 1993; Schatz and Ratner, 1993; Levine, 1999).

Table 1 lists the commonly used symbols for physical constants and parameters. Section XIII pro-

---

*Abbreviations:* B<sub>x</sub>, B<sub>y</sub>, Q<sub>x</sub>, Q<sub>y</sub> – characteristic absorption bands of chlorophylls and pheophytins; CD – circular dichroism; CT – charge-transfer; FTIR – Fourier transform infrared; HOMO – highest occupied molecular orbital; IR – infrared; LD – linear dichroism; LUMO – lowest unoccupied molecular orbital

Table 1. Common Physical Constants and Parameters

Constant	Symbol	Value
Avogadro's number	$\mathcal{N}_A$	$6.022 \times 10^{23} \text{ mol}^{-1}$
Boltzmann's constant	$k_B$	$1.381 \times 10^{-23} \text{ joule K}^{-1}$
Planck's constant	$h$	$6.63 \times 10^{-34} \text{ joule s}$
$h/2\pi$	$\hbar$	$1.05 \times 10^{-34} \text{ joule s}$
Speed of light in a vacuum	$c$	$3 \times 10^8 \text{ m s}^{-1}$
Parameter	Symbol	Common Units
Frequency	$\nu$	$\text{s}^{-1} \text{ (Hz)}$
Refractive index	$n$	dimensionless
Temperature	$T$	K
Wavelength	$\lambda$	cm
Wavenumber ( $1/\lambda$ )	$\bar{\nu}$	$\text{cm}^{-1}$
Electric field	$\vec{E}$	volt $\text{cm}^{-1}$ or dyne $\text{esu}^{-1}$
Magnetic field	$\vec{B}$	gauss (oersted)

vides some mathematical background on vectors, operators and eigenfunctions, and explains the nomenclature that is used throughout the chapter.

## II. Absorption Coefficient

The strength of light passing through a sample decreases progressively because of absorption. The decrease in light intensity, or *irradiance*, over the course of a small volume element of the solution is proportional to the irradiance of the light entering the element ( $I$ ), the concentration of absorbing molecules ( $C$ ), and the thickness of the element ( $dl$ ):

$$dI \propto -I C dl$$

By integrating this expression, we find that if light with irradiance  $I_o$  is incident on a cell of length  $l$ , the irradiance of the transmitted light will be

$$I = I_o 10^{-\epsilon C l} \equiv I_o 10^{-A},$$

where  $A$  is the *absorbance* or *optical density* of the sample ( $A = \epsilon C l$ ) and  $\epsilon$  is a molecular property called the *molar extinction coefficient* or *molar absorption coefficient*. This is a statement of the *Beer-Lambert law*. The absorbance is a dimensionless quantity, so if  $C$  is given in units of molarity (M) and  $l$  is in cm,  $\epsilon$  has units of  $\text{M}^{-1} \cdot \text{cm}^{-1}$ . The absorption

coefficient ( $\epsilon$ ) depends strongly on the wavelength of the light, making  $A$  also a function of wavelength.

The percent of the incident light that is absorbed by the sample is  $100 \cdot (I_o - I)/I_o = 100 \cdot (1 - 10^{-A})$ , which is proportional to  $A$  if  $A \ll 1$ . A sample with an absorbance of 2 at a particular wavelength thus absorbs 99% of the incident light at that wavelength.

When a molecule absorbs light, it removes energy from the radiation field. The basic rule for absorption is that the difference between the energy of the excited state ( $E_e$ ) and the energy of the resting, or *ground*, state ( $E_g$ ) must equal the product of Planck's constant ( $h$ ) and the frequency of the light ( $\nu$ ):

$$\Delta E = E_e - E_g = h \nu$$

Given an excited state with an appropriate energy,  $\epsilon$  is proportional to the dipole strength of the transition, which depends on the shapes of the molecular wavefunctions for the ground and excited states. The absorption spectrum of a molecule thus can provide information on the molecular structure, as well as on the energies of the molecule's excited states.

Absorption sometimes is expressed as the *absorption cross-section*  $\sigma$ , which is given by:

$$\sigma = 3.817 \times 10^{-21} \epsilon \text{ cm}^2/(\text{M}^{-1} \text{ cm}^{-1}).$$

If the irradiance  $I_o$  incident on a thin sample is



given in  $\text{photons}\cdot\text{cm}^{-2}\cdot\text{s}^{-1}$ , a molecule with an absorption cross section  $\sigma\text{ cm}^2$  will be excited  $I_0\sigma$  times per second. The rate of excitation is independent of the concentration of absorbing molecules in the sample, as long as the sample is sufficiently thin or dilute so that  $I/I_0 \approx 1$  (i.e.,  $A \ll 1$ ).

If a sample contains a mixture of different pigments, the absorbance of each component is independent of the nature and concentrations of the other components and the total absorbance is the sum of the absorbances of the individual components:  $A = A_1 + A_2 + \dots$ . This is important because it allows us to use changes in the total absorbance to measure changes in the concentration of an individual component in a complex system.

The absorbance of proteins in the near-ultraviolet region of the spectrum is due mainly to tyrosine, tryptophan and phenylalanine residues. An individual absorbing moiety such as the macrocyclic ring of a chlorophyll molecule or the side chain of a tryptophan residue is referred to as a *chromophore*.

### III. Charge-Transfer Transitions

Charge-transfer (CT) absorption bands represent transitions in which an electron moves from one molecule to another. Because transfer of an electron requires overlap of the two molecular orbitals, CT bands usually are much weaker than the absorption bands associated with intramolecular excitations. Their dipole strengths typically are less than one debye<sup>2</sup>. CT bands also tend to be very broad, because the energy of the polar CT state can vary widely for molecules with slightly different configurations or environments. However, some CT absorption bands provide useful measures of macromolecular structure. Cytochrome *c*, for example, has a broad CT band near 700 nm that represents movement of an electron to the heme Fe from the methionine axial ligand; structural changes that separate the methionine from the heme cause the CT band to disappear.

CT transitions can mix with intramolecular excitations in photosynthetic reaction centers, and probably do so in some antenna complexes. The

lowest excited singlet state of a closely spaced bacteriochlorophyll or chlorophyll dimer such as the special pair of bacteriochlorophylls in the reaction center of purple bacteria thus can consist of a mixture of CT and intramolecular transitions. If the 'pure' CT lies above the intramolecular excited state in energy, this mixing will lower the energy of the mixed state (Parson and Warshel, 1987; Warshel and Parson, 1987; Zhou and Boxer, 1998).

Because a CT transition can result in a substantial change in the dipole moment of a molecule, the energy difference between the ground and excited states depends on the local electric fields acting on the molecule. An external electric field can shift the absorption band to higher or lower energies, depending on how the molecule is oriented with respect to the field. This is the *Stark effect*. If the molecules in a sample are randomly oriented with respect to the external field, the field will shift the transitions of some of the molecules to higher energies, and those of other molecules to lower energies. The result will be a broadening of the absorption band. Stark effects are seen with other types of absorption bands as well, and sometimes reflect changes in polarizability rather than changes in dipole moment, but they can be particularly strong in transitions that include large CT components (Bublitz and Boxer, 1997). In addition to photosynthetic reaction centers (Zhou and Boxer, 1998a,b), the bacterial LH1 complex and some of the components of Photosystem I show strong Stark effects (Beekman et al., 1997; Hayes et al., 2000; Ratsep et al., 2000).

### IV. Circular Dichroism

Many natural materials exhibit differences between their absorbance of left- and right-circularly polarized light. (See Electromagnetic Radiation for an explanation of circularly polarized light.) Such molecules are said to be *optically active*, and the difference between their absorbance of light with left- and right-circular polarization is called *circular dichroism* (CD). Circular dichroism provides information on

the asymmetry of the chromophore. It is widely used as a measure of secondary structure in macromolecules and for investigating the architecture of multimolecular complexes (Nakanishi et al., 1994; Ramsay and Eftink, 1994; Sosnick et al., 2000). Because the effect is relatively small (typically about 1 part in  $10^4$ ), CD usually is measured with a spectrometer that includes an electro-optic modulator for switching the measuring beam rapidly back and forth between right- and left-circular polarization. A phase- and frequency-sensitive amplifier is used to extract the small oscillatory component of the transmitted light.

The difference between a molecule's dipole strengths for left- and right-circularly polarized light is characterized by the *rotational strength*  $\mathcal{R}$  of an absorption band:

$$\mathcal{R} = \frac{3000 \ln 10 f_{\text{inc}}}{8\pi^3 \mathcal{N}} \int \frac{\Delta\epsilon}{\nu} d\nu$$

$$\approx 2.48n \int \frac{\Delta\epsilon}{\nu} d\nu \text{ (debye Bohr magnetons)/(M}^{-1} \text{ cm}^{-1}\text{)},$$

where  $\mathcal{N}$  is Avogadro's number,  $\Delta\epsilon$  is the difference between the molar extinction coefficients for left and right circularly polarized light ( $\epsilon_l - \epsilon_r$ ) in units of  $\text{M}^{-1} \text{ cm}^{-1}$ ,  $\nu$  is the frequency and  $n$  is the refractive index. Unlike the dipole strength,  $\mathcal{R}$  can be either positive or negative. Rotational strengths commonly are expressed in debye-Bohr magnetons per unit molarity and path length. A debye is a unit of electrical dipole and is  $10^{-18}$  esu-cm (see Dipole Strength). A Bohr-magneton ( $-e\hbar/2m$ ) is a unit of magnetic dipole and is  $9.274 \times 10^{-21}$  esu-cm. One debye-Bohr magneton therefore is  $9.274 \times 10^{-39}$  esu<sup>2</sup>·cm<sup>2</sup>.

Another technique for measuring CD makes use of the fact that linear polarization consists of a coherent superposition of left- and right-circular polarization (see Electromagnetic Radiation). If a beam of linearly polarized light passes through a sample that has different absorbances for left- and right-circularly polarized light, the balance of the two

polarizations will be upset and the transmitted beam will emerge with elliptical polarization. Early CD spectrometers measured this effect. Although most modern instruments use the polarization-modulation technique described above, CD still is sometimes reported in terms of the *molar ellipticity*,  $\theta_M$ , in units of degrees· $\text{M}^{-1} \text{ cm}^{-1}$  or degrees· $\text{mol}^{-1} \cdot \text{cm}^2$ . The relationship between  $\theta_M$  and  $\epsilon_l - \epsilon_r$  is

$$\theta_M = (180^\circ \times 100 \ln 10 / 4\pi) \Delta\epsilon = 3300^\circ \Delta\epsilon.$$

Circular dichroism results from coupled interactions of electrons with the electric and magnetic fields of light. The interactions with the electric field are discussed in several sections of this chapter (see Transition Dipole, Linear Dichroism and Fluorescence Anisotropy, and Fluorescence Yield and Lifetime). They depend on the dot product of the oscillating electric field ( $\vec{E}$ ) with the molecule's electric transition dipole ( $\vec{\mu}$ ). Interactions with the magnetic field depend similarly on the dot product of the oscillating magnetic field ( $\vec{B}$ ) with a molecule's *magnetic transition dipole* ( $\vec{m}$ ). Orbital motions of electrons in a molecule can give rise to a magnetic field just as an electric current passing through a coil of wire generates a magnetic field parallel to the axis of the coil, and the magnetic transition dipole reflects such induced magnetic fields. The magnetic transition dipole of a molecule can be calculated theoretically from the molecular orbitals (Warshel and Parson, 1987) or can be calculated from  $\vec{\mu}$  as described below. For a molecule with a planar  $\pi$ -electron system, motions of the electrons in this plane generate a magnetic dipole normal to the plane.

The interaction of  $\vec{m}$  with the magnetic field of light ( $-\vec{m} \cdot \vec{B}$ ) usually is much weaker than the interaction of  $\vec{\mu}$  with the electric field ( $-\vec{\mu} \cdot \vec{E}$ ). There are, however, situations in which the molecular symmetry makes  $-\vec{\mu} \cdot \vec{E}$  zero but allows weak absorption due to  $-\vec{m} \cdot \vec{B}$ . This is the case for the ' $n \rightarrow \pi^*$ ' transition of a carbonyl group, in which an electron moves from a nonbonding ( $n$ ) orbital of the oxygen atom to a  $\pi^*$  (antibonding) molecular orbital. In other cases, a small contribution from  $-\vec{m} \cdot \vec{B}$  to the absorption can either augment or oppose the

contribution from  $-\vec{\mu} \cdot \vec{E}$ , depending on whether the light has left- or right-circular polarization. The molecule then will exhibit CD.

For a molecule to absorb left- and right- circularly polarized light differently, it must be chiral, which means that the molecule has no plane of symmetry or center of inversion and so cannot be superimposed on its mirror image. Mathematically, what is necessary in order for a chromophore to exhibit CD is for  $\vec{m} \cdot \vec{\mu}$ , the dot product of  $\vec{m}$  and  $\vec{\mu}$ , to be nonzero. The rotational strength is given by

$$\mathfrak{R} = -\text{Im}\{\vec{m} \cdot \vec{\mu}\},$$

where  $\text{Im}\{\dots\}$  means the imaginary part of the quantity in braces. (For a complex number  $a = b + ic$ ,  $\text{Im}\{a\} = c$ .) In the expression for  $\mathfrak{R}$ ,  $\vec{\mu}$  is real but  $\vec{m}$  is imaginary; the product  $\vec{m} \cdot \vec{\mu}$  therefore is imaginary.  $\text{Im}\{\vec{m} \cdot \vec{\mu}\}$  is a real quantity, as it must be if  $\mathfrak{R}$  is measurable.

CD measurements can provide information on the arrangement and interactions of the individual chromophores in dimers or higher oligomers. Consider a complex of two similar molecules with ground-state wavefunctions  $^0\psi_a$  and  $^0\psi_b$  and excited-state wavefunctions  $^1\psi_a$  and  $^1\psi_b$ . As discussed in Excitons, the dimer will have two excited singlet states that can be described by linear combinations of the individual excitations:

$$\Psi_+ = C_1 {}^1\psi_a {}^0\psi_b + C_2 {}^0\psi_a {}^1\psi_b$$

$$\Psi_- = C_2 {}^1\psi_a {}^0\psi_b - C_1 {}^0\psi_a {}^1\psi_b.$$

The coefficients ( $C_i$ ) depend on the nature of the individual molecules and the geometry of the complex. In this representation, the electric and magnetic transition dipoles for the absorption bands of the dimer ( $\vec{\mu}_\pm$  and  $\vec{m}_\pm$ ) are linear combinations of the transition dipoles for the individual molecules ( $\vec{\mu}_a$ ,  $\vec{\mu}_b$ ,  $\vec{m}_a$  and  $\vec{m}_b$ ):

$$\vec{\mu}_\pm = C_1 \vec{\mu}_a \pm C_2 \vec{\mu}_b$$

$$\vec{m}_\pm = C_1 \vec{m}_a \pm C_2 \vec{m}_b.$$

To evaluate the rotational strengths of the absorption bands of the dimer, we need the dot products of the magnetic and electronic transition dipoles. For excitation to  $\Psi_+$ , we have

$$\begin{aligned} \mathfrak{R}_+ &= -\text{Im}\{(C_1 \vec{m}_a + C_2 \vec{m}_b) \cdot (C_1 \vec{\mu}_a + C_2 \vec{\mu}_b)\} \\ &= C_1^2 \text{Im}\{\vec{m}_a \cdot \vec{\mu}_a\} - C_2^2 \text{Im}\{\vec{m}_b \cdot \vec{\mu}_b\} \\ &\quad - C_1 C_2 \text{Im}\{\vec{m}_a \cdot \vec{\mu}_b\} - C_1 C_2 \text{Im}\{\vec{m}_b \cdot \vec{\mu}_a\} \\ &= C_1^2 \mathfrak{R}_a^0 + C_2^2 \mathfrak{R}_b^0 - C_1 C_2 \text{Im}\{\vec{m}_a \cdot \vec{\mu}_b + \vec{m}_b \cdot \vec{\mu}_a\}. \end{aligned}$$

The first two terms in this expression are just the intrinsic rotational strengths of the individual molecules ( $\mathfrak{R}_a^0$  and  $\mathfrak{R}_b^0$ ), weighted by the relative contributions that these molecules make to the excitation ( $C_1^2$  and  $C_2^2$ ). The third term represents coupled interactions of the two molecules with the magnetic and electric fields.

Similarly, the rotational strength for excitation of the dimer to its other excited state ( $\Psi_-$ ) is

$$\mathfrak{R}_- = C_2^2 \mathfrak{R}_a^0 + C_1^2 \mathfrak{R}_b^0 + C_1 C_2 \text{Im}\{\vec{m}_a \cdot \vec{\mu}_b + \vec{m}_b \cdot \vec{\mu}_a\}.$$

Again, the first two terms represent the intrinsic rotational strengths of the individual molecules, while the third term comes from coupled interactions of the dimer with the magnetic and electric fields.

In some cases,  $|\vec{m}_a \cdot \vec{\mu}_b|$  or  $|\vec{m}_b \cdot \vec{\mu}_a|$  can be much larger than  $|\vec{m}_a \cdot \vec{\mu}_a|$  or  $|\vec{m}_b \cdot \vec{\mu}_b|$ , so that the dimer's absorption bands have much larger rotational strengths than the corresponding bands of the individual molecules. This is particularly true for planar molecules. As we noted above, the magnetic transition dipole of such a molecule is normal to the molecular plane; the electric transition dipole, however, must lie in this plane. The magnetic and transition dipoles of a planar molecule thus are perpendicular to each other, making their dot product zero. This is in accord with the fact that a molecule with a plane of symmetry cannot be chiral. In a dimer, by contrast,  $\vec{\mu}_b$  could have almost any orientation with respect to  $\vec{m}_a$ , and  $\vec{\mu}_a$  could have almost any orientation with respect to  $\vec{m}_b$ , so the dot products  $|\vec{m}_a \cdot \vec{\mu}_b|$  and  $|\vec{m}_b \cdot \vec{\mu}_a|$  generally will not be zero.

Note that the term  $C_1 C_2 \text{Im}\{\vec{m}_a \cdot \vec{\mu}_b + \vec{m}_b \cdot \vec{\mu}_a\}$  enters with opposite sign in the expressions for  $\mathfrak{R}_+$  and  $\mathfrak{R}_-$ . If this term makes the dominant contributions to the rotational strengths,  $\mathfrak{R}_-$  and  $\mathfrak{R}_+$  will, accordingly, be equal in magnitude but opposite in sign. The resulting CD spectrum is said to be *conservative* (Fig. 1). Many photosynthetic bacterial antenna complexes have nearly conservative CD spectra in the long-wavelength region associated with the  $Q_y$  transitions of the bacteriochlorophylls. However, the spectra can be complicated by mixing with the higher-energy  $Q_x$  and Soret transitions (see Configuration Interactions and Scherz and Parson, 1984). This mixing can shift either positive or negative rotational strength from the higher-energy region to the  $Q_y$  region or vice versa.

The rotational strength of an oligomer's absorption band can be related to the geometry of the complex and the dipole strengths of the individual molecules. For this purpose, it is not necessary to calculate the magnetic transition dipoles from the molecular orbitals. Instead, we can obtain them from the electric dipoles by using the expression

$$\vec{m}_a = \vec{m}_a^0 - \frac{i\pi}{\lambda_a} \vec{R}_a \times \vec{\mu}_a.$$

Here  $\vec{m}_a^0$  is an intrinsic magnetic transition dipole of molecule  $a$ , which is independent of the location and orientation of the molecule,  $\vec{R}_a$  is the vector from the origin of the coordinate system to the center of the molecule,  $\lambda_a$  is the wavelength of the absorption band,  $\vec{\mu}_a$  again is the electric transition dipole, and  $\times$  indicates a cross product. (See Mathematical Tools for a definition of the vector cross product.) This expression rests on basic quantum mechanical equivalences and is, in principle, exact. A similar expression holds for molecule  $b$ :

$$\vec{m}_b = \vec{m}_b^0 - \frac{i\pi}{\lambda_b} \vec{R}_b \times \vec{\mu}_b.$$

By expanding the term:

$$\mp C_1 C_2 \text{Im}\{\vec{m}_a \cdot \vec{\mu}_b + \vec{m}_b \cdot \vec{\mu}_a\}$$

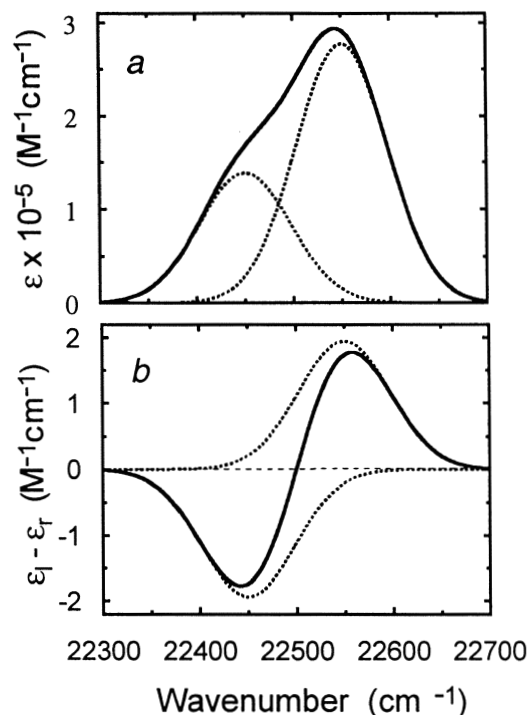


Fig. 1. Calculated absorption (a) and circular dichroism (b) of a dimer of identical molecules. The dotted lines show the molar extinction coefficients ( $\epsilon$ ) for the dimer's two absorption bands (a) and the difference between the extinction coefficients for left- and right-handed circularly polarized light ( $\epsilon_l - \epsilon_r$ ) (b). The solid lines show the overall absorption and CD spectra obtained by summing the contributions from the two bands. The absorption bands of the individual molecules were assumed to have no rotational strength and were given a Gaussian shape with an arbitrary width for illustration.

in the expression for  $\mathfrak{R}_+$  or  $\mathfrak{R}_-$  and using some vector algebra, we find that the coupled interactions of the dimer with the magnetic and electric fields make  $\mathfrak{R}_+$  and  $\mathfrak{R}_-$  dependent on the relative positions of the two molecules. Here are the results for the case that  $\lambda_a = \lambda_b = \lambda$ :

$$\mathfrak{R}_+ = C_1^2 \mathfrak{R}_a^0 + C_2^2 \mathfrak{R}_b^0 - C_1 C_2 \text{Im}\{\vec{m}_a^0 \cdot \vec{\mu}_b + \vec{m}_b^0 \cdot \vec{\mu}_a\} + (C_1 C_2 \pi / \lambda) \vec{R}_{ba} \cdot \vec{\mu}_b \times \vec{\mu}_a$$

$$\mathfrak{R}_- = C_2^2 \mathfrak{R}_a^0 + C_1^2 \mathfrak{R}_b^0 + C_1 C_2 \text{Im}\{\vec{m}_a^0 \cdot \vec{\mu}_b + \vec{m}_b^0 \cdot \vec{\mu}_a\} - (C_1 C_2 \pi / \lambda) \vec{R}_{ba} \cdot \vec{\mu}_b \times \vec{\mu}_a,$$

where  $\vec{R}_{ba}$  is the vector from the center of molecule  $a$  to the center of  $b$  ( $\vec{R}_{ba} = \vec{R}_b - \vec{R}_a$ ). In these expressions, the first two terms on the right again are

the weighted rotational strengths of the individual molecules. The next term,

$$\mp C_1 C_2 \text{Im}\{\vec{m}_a^0 \cdot \vec{\mu}_b + \vec{m}_b^0 \cdot \vec{\mu}_a\},$$

represents interactions of the electric transition dipole of one molecule with the intrinsic magnetic transition dipole of the other molecule ( $\vec{m}_a^0$  or  $\vec{m}_b^0$ ). This term, like the first two, is relatively small in most of the cases of interest here. This leaves the final term,  $\pm(C_1 C_2 \pi / \lambda) \vec{R}_{ba} \cdot \vec{\mu}_b \times \vec{\mu}_a$ , which is the most pertinent to photosynthetic antenna complexes because it depends strongly on the relative positions and orientations of the molecules that make up the complex. We'll call this the 'exciton contribution,'  $\Re_{\pm}^{\text{ex}}$ .

For a dimer of identical molecules, the coefficients  $C_1$  and  $C_2$  are both  $1/\sqrt{2}$  (see Excitons). If  $|\vec{R}_{ba}|$  and  $\lambda$  are given in the same units (*e.g.*, Å), then for such a dimer,

$$\Re_{\text{ex}} \approx (171 / \lambda) \vec{R}_{ba} \cdot \vec{\mu}_b \times \vec{\mu}_a \\ (\text{debye Bohr magnetons}) / \text{debye}^2.$$

Although we have developed the theory only for a dimer, the extension to larger systems is straightforward. The magnetic and transition dipoles for an absorption band of an oligomer are obtained by summing the contributions of all the subunits as explained under Excitons, and the rotational strength is evaluated as the imaginary part of their dot product.

Several qualitative results emerge from the expression for  $\Re_{\pm}^{\text{ex}}$ . First, note again that to the extent that  $\Re_{\pm}^{\text{ex}}$  dominates over the intrinsic rotational strengths of the individual molecules, the CD of the two exciton bands will be equal in magnitude and opposite in sign:  $\Re_{-}^{\text{ex}} = -\Re_{+}^{\text{ex}}$ . This is in contrast to the *dipole* strengths of the two bands, which are always positive but can differ substantially in magnitude (see Excitons). Second, because of the general properties of vector triple products such as  $\vec{R}_{ba} \cdot \vec{\mu}_b \times \vec{\mu}_a$ , both  $\Re_{+}^{\text{ex}}$  and  $\Re_{-}^{\text{ex}}$  will be zero if  $\vec{R}_{ba}$ ,  $\vec{\mu}_b$  and  $\vec{\mu}_a$  all lie in a plane, or if any two of these vectors are parallel to each other. This can make the CD of a dimer highly sensitive to changes in structure.

Note that  $|\Re_{\pm}^{\text{ex}}|$  increases linearly with  $|\vec{R}_{ba}|$ . This may seem counter to intuition. We would expect any measurable effects of interactions between the molecules to disappear when the molecules are far apart. Indeed, the observed strengths of the CD bands do disappear at large values of  $|\vec{R}_{ba}|$  because, although  $|\Re_{\pm}^{\text{ex}}|$  then is large, the rotational strengths of the two exciton absorption bands have opposite signs and the separation between the bands *decreases* as  $|\vec{R}_{ba}|^{-3}$  (see Excitons). When the two molecules are far apart the opposite rotational strengths of the overlapping bands cancel so that the measured signal goes to zero.

When the two exciton bands overlap strongly, the positions of the positive and negative CD peaks depend mainly on the shape of the underlying bands and are relatively insensitive to  $|\vec{R}_{ba}|$ . This points out a difficulty in interpreting experimental CD spectra: although the CD spectrum can be predicted unambiguously for a complex with known structure, oligomers with different structures can give similar spectra. Actually, even predicting the CD spectrum for a complex with known structure can be problematic because the spectrum can be complicated by mixing with higher excited states, such as states in which more than one of the monomeric units are excited, and by uncertainties in calculations of exciton-interaction matrix elements (see Excitons). Attempts to deduce the structure of an oligomer based on a CD spectrum therefore must be viewed critically. However, measurements of both the CD and absorption spectra in the region of several absorption bands may provide enough information to rule out some possible structures with good confidence.

## V. Configuration Interactions

Many spectroscopic transitions can be described approximately as the promotion of a single electron from the highest occupied molecular orbital (HOMO) to the lowest unoccupied molecular orbital (LUMO) with the absorption of light, or a transition in the opposite direction with the emission of light (see

Fig. 2a). However, this description assumes that the movement of the electron from one orbital to another has no effect on the other electrons in the molecule, which is a very simplistic assumption. A transition that involves complex perturbations of the electronic structure often can be described more accurately as a linear combination of transitions between various occupied orbitals and unoccupied orbitals. Thus, we can write an excitation from the ground state ( $^0\Psi$ ) to an excited singlet state ( $^1\Psi$ ) as

$$^0\Psi \rightarrow ^1\Psi = \sum_j \sum_k C_j^k \{ ^0\psi_j \rightarrow ^1\psi_k \},$$

where  $\{ ^0\psi_j \rightarrow ^1\psi_k \}$  means excitation of an electron from orbital  $j$  to orbital  $k$ . Each such combination of orbitals is termed an electron *configuration*, and the mixing of different configurations to give the overall transition is called *configuration interaction*. Itoh and I'Haya (1964) and Mataga and Kubota (1970) give general expressions for calculating the mixing coefficients ( $C_j^k$ ), which depend on the symmetry and energies of the individual orbitals.

In the case of porphyrins, chlorins and bacteriochlorins, transitions involving the orbitals one step below the HOMO and one step above the LUMO make small but significant contributions to the absorption bands in the visible and near-UV regions. Combining these orbitals with the HOMO and LUMO, we have four pertinent orbitals, which customarily are labeled  $a_{2u}$ ,  $a_{1u}$ ,  $e_{gx}$  and  $e_{gy}$  following Gouterman (1961). As shown in Fig. 2b, the four orbitals allow four possible configurations:  $a_{2u} \rightarrow e_{gy}$ ,  $a_{2u} \rightarrow e_{gx}$ ,  $a_{1u} \rightarrow e_{gy}$  and  $a_{1u} \rightarrow e_{gx}$ .

The relative energies of the  $a_{2u}$ ,  $a_{1u}$ ,  $e_{gx}$  and  $e_{gy}$  orbitals depend on the detailed structure of the molecule. In symmetrical metalloporphyrins,  $e_{gy}$  and  $e_{gx}$  are degenerate (*i.e.*, have identical energies) and  $a_{1u}$  and  $a_{2u}$  are very close together; in bacteriochlorophyll, the orbitals are well separated, increasing in energy in the order  $a_{2u} < a_{1u} < e_{gx} < e_{gy}$ . The strong, 'Q<sub>y</sub>' absorption band of bacteriochlorophyll near 780 nm (see Fig. 3 in Chapter 2, Scheer) represents mainly the configuration  $a_{1u} \rightarrow e_{gx}$  (HOMO  $\rightarrow$  LUMO) with a smaller contribution from  $a_{2u} \rightarrow e_{gy}$  (HOMO-1  $\rightarrow$  LUMO+1) (see Fig. 2c). The 'Q<sub>x</sub>' band

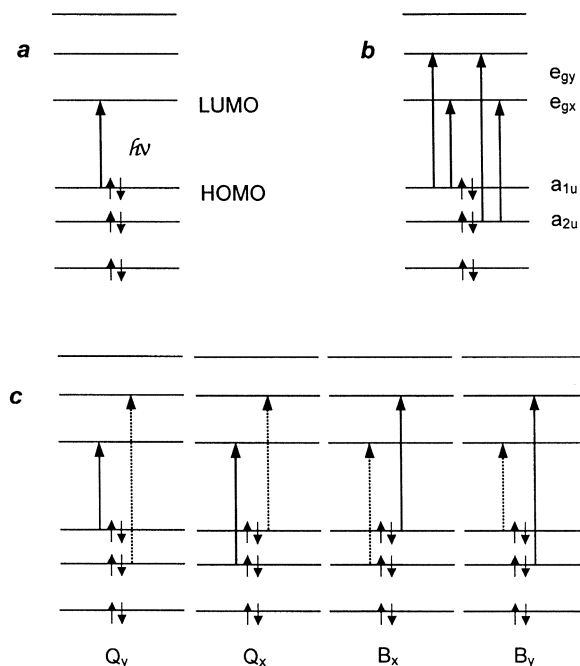


Fig. 2. (a) A spectroscopic transition in which an electron is excited from the highest occupied molecular orbital (HOMO) to the lowest unoccupied molecular orbital (LUMO). The horizontal bars represent molecular orbitals, with the vertical position indicating the orbital energy. Small arrows indicate electrons with spin up or down (see Singlet and Triplet States). (b) The main spectroscopic transitions of porphyrins, chlorins and bacteriochlorins involve various combinations of excitations from one of the two highest occupied orbitals ( $a_{2u}$  and  $a_{1u}$ ) to one of the two lowest unoccupied orbitals ( $e_{gx}$  and  $e_{gy}$ ). (c) The dominant contributions to the Q<sub>y</sub>, Q<sub>x</sub>, B<sub>x</sub> and B<sub>y</sub> absorption bands of bacteriochlorophyll are indicated with solid arrows; secondary contributions are shown with dotted arrows.

in the region of 600 nm represents mainly  $a_{2u} \rightarrow e_{gx}$  with a smaller amount of  $a_{1u} \rightarrow e_{gy}$ . The B<sub>y</sub> absorption band near 360 nm (the higher of the two 'Soret' bands) is made up mainly of the  $a_{2u} \rightarrow e_{gy}$  configuration, while the B<sub>x</sub> Soret band near 380 nm is mainly  $a_{1u} \rightarrow e_{gy}$ . The Q<sub>y</sub> and B<sub>y</sub> transition dipoles are oriented approximately along the axis connecting the nitrogen atoms in rings A and C; the Q<sub>x</sub> and B<sub>x</sub> transition dipoles, along the axis of the nitrogen atoms in rings B and D.

For additional information on the spectroscopic properties and molecular orbitals of chlorophylls and bacteriochlorophylls, see Chapter 2 (Scheer) and Hanson (1991).

## VI. Dipole Strength

The dipole strength  $D$  is a measure of the overall strength of an absorption band. It is given by the square of the magnitude of the transition dipole ( $\vec{\mu}$ ):

$$D = |\vec{\mu}|^2.$$

The dipole strength can be calculated theoretically from the molecular orbitals of the ground and excited states as discussed under Transition Dipole.

Experimentally, the dipole strength is related to the molar absorption coefficient ( $\epsilon$ ) by the integral

$$\begin{aligned} D &= \left( \frac{3000 \ln 10 \hbar c}{8\pi^3 \mathcal{N}_A} \right) \int \frac{n\epsilon}{\nu} d\nu \\ &= 9.186 \times 10^{-3} \int \frac{n\epsilon}{\nu} d\nu \frac{\text{debye}^2}{\text{M}^{-1}\text{cm}^{-1}} \\ &\approx 9.186 \times 10^{-3} n \int \frac{\epsilon}{\nu} d\nu \text{debye}^2/(\text{M}^{-1}\text{cm}^{-1}), \end{aligned}$$

where  $n$  is the refractive index, and one debye =  $10^{-18}$  esu·cm =  $3.336 \times 10^{-30}$  C·m. This expression assumes that the sample is isotropic (*i.e.*, that the absorbing molecules are oriented randomly). It also neglects the so-called local-field correction for the difference between the electric fields of light impinging on the sample and sensed at the molecule. See Alden et al. (1997) for a discussion of the local-field correction.

The strength of an absorption band sometimes is expressed in terms of the *oscillator strength*, a dimensionless quantity defined as

$$f = \frac{8\pi^2 m \nu}{3e^2 \hbar} D \approx \frac{2.303 \times 10^3 m c n}{\pi e^2 \mathcal{N}_A} \int \epsilon d\nu,$$

where  $m$  is the electron mass. If  $\nu$  is given in  $\text{s}^{-1}$  and  $\epsilon$  in  $\text{M}^{-1}\text{cm}^{-1}$ , then  $f \approx 1.44 \times 10^{-19} \int \epsilon d\nu$ . The oscillator strength has a value on the order of 1.0 for the strongest possible absorption band of a single chromophore.

## VII. Electromagnetic Radiation

Charged particles exert measurable forces on each other, and these forces conventionally are expressed in terms of *electric and magnetic fields*. Suppose a particle with charge  $Q_1$  is fixed in position at the origin of a coordinate system in a vacuum and a second particle with charge  $Q_2$  is located at position  $\vec{r}_2$ . The distance between the two charges then is  $|\vec{r}_2|$ . By Coulomb's law, the magnitude of the force acting on particle 2 ( $\vec{F}_2$ ) is

$$|\vec{F}_2| = Q_1 Q_2 |\vec{r}_2|^{-2}.$$

The force points toward particle 1 if  $Q_1$  and  $Q_2$  have opposite signs, and away from 1 if the charges have the same sign. The *electric field* ( $\vec{E}_2$ ) at the position of particle 2 is defined as the force that would act on an infinitesimally small, positive charge at this position. The amplitude (strength) of the field is simply

$$\vec{E}_2 = Q_1 |\vec{r}_2|^{-2}.$$

Moving charges create magnetic fields, and the magnetic field ( $\vec{B}_2$ ) acting on a magnetic pole  $m_2$  is defined analogously to the electric field.

The electric field generated by a pair of closely spaced positive and negative charges (an *electric dipole*) is simply the sum of the fields from the individual charges. If the distance between the positive and negative charges (the length of the dipole) oscillates with time, the electric and magnetic fields in the vicinity will oscillate at the same frequency. The oscillating electric and magnetic fields ( $\vec{E}$  and  $\vec{B}$ ) created by such a dipole spread out in a wave-like manner as shown in Fig. 3.  $\vec{E}$  and  $\vec{B}$  are everywhere perpendicular to each other and also to the direction of propagation of the wave. The two oscillating fields together constitute an *electromagnetic radiation field*. The term 'light' is used broadly to describe such radiation fields with oscillation frequencies in the range of  $10^{13}$  to  $10^{15}$  Hz (oscillations per second).

The waves associated with electromagnetic radiation fields propagate at a fixed velocity ( $c$ ) of



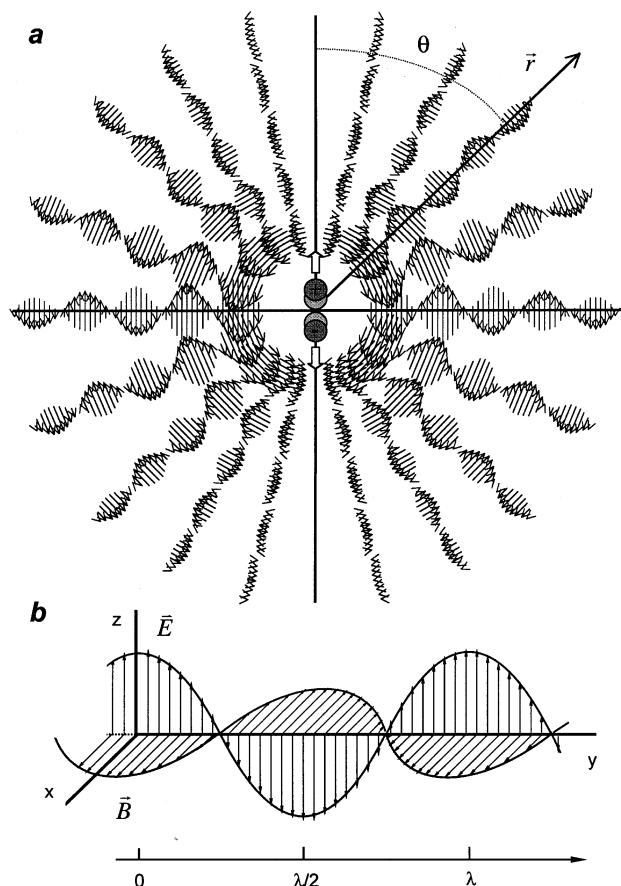


Fig. 3. (a) An oscillating dipole creates oscillating electric and magnetic fields that spread out in spherical waves. The circles with positive or negative charges represent an electric dipole that oscillates in length along the vertical axis. The thin arrows indicate the oscillating components of the electric field from the dipole at various positions at a given time. At large distances from the dipole, the electric and magnetic fields propagating along any given axis ( $\vec{r}$ ) are perpendicular to that axis. The amplitude of the field depends on the distance from the dipole and the sine of the angle ( $\theta$ ) between the dipole axis and the propagation axis. (b) The electric and magnetic fields in a plane wave of light at a given time as functions of position along the propagation axis. The scale at the bottom indicates the wavelength of the oscillations ( $\lambda$ ).

$3 \times 10^{10} \text{ cm} \cdot \text{s}^{-1}$  in a vacuum. In a dense medium with refractive index  $n$ , the velocity decreases to  $c/n$ . The oscillation frequency ( $\nu$ ) is independent of the medium, but the wavelength ( $\lambda$ ) depends on  $n$  and is given by

$$\lambda = c/n\nu.$$

The *wavenumber* ( $\bar{\nu}$ ) of the radiation is the reciprocal of the wavelength.

Just as an oscillating electric dipole generates an electromagnetic radiation field, the forces associated with an oscillating electromagnetic field will cause a

dipole to oscillate. This can result in transfer of energy from the radiation field to the dipole (*absorption* of light), transfer of energy from the dipole to the radiation field (*fluorescence* or *stimulated emission*), or a change in the propagation direction of the radiation (*light scattering*).

Light is said to be *plane polarized* or *linearly polarized* if the oscillating electric field vector remains parallel to a fixed vector as the wave propagates, as shown in Fig. 3b. It is *circularly polarized* if  $\vec{E}$  traces a corkscrew as illustrated in Fig. 4. Plane polarized light is used in measurements of linear

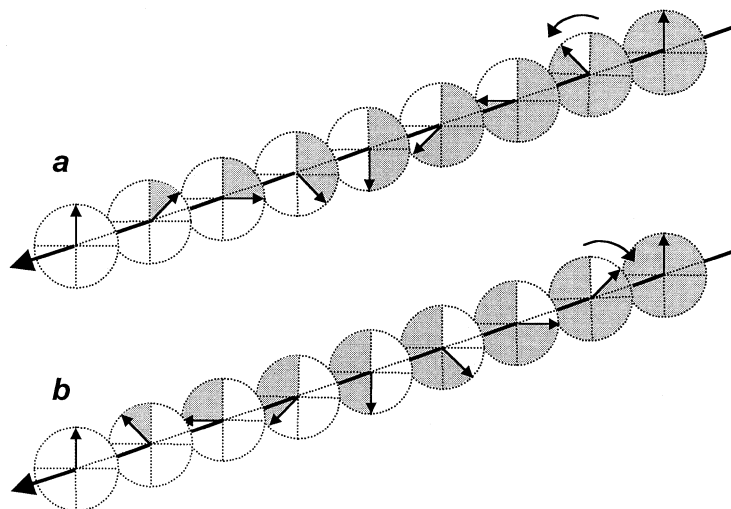


Fig. 4. Left (a) and right (b) circularly polarized light. In this illustration, both waves propagate from right to left in the direction indicated by the long arrows. The short arrows indicate the orientations of the electric field ( $\vec{E}$ ) at various positions at a particular time. An observer looking into the oncoming light sees the field rotating clockwise for right circular polarization and counterclockwise for left circular polarization (curved arrows). The magnetic field (not shown) rotates in phase with  $\vec{E}$ . Note that the components of  $\vec{E}$  and  $\vec{B}$  parallel to any given axis normal to the propagation direction oscillate sinusoidally as shown in Figure 3b.

dichroism and circularly polarized light in measurements of circular dichroism.

In Fig. 4, note that the electric field vector  $\vec{E}$  has a constant length but rotates either clockwise or counterclockwise with time and position along the propagation axis. One complete rotation corresponds to the classical oscillation period and wavelength of the field. The magnetic field ( $\vec{B}$ , not shown in the figure) is always perpendicular to  $\vec{E}$  and rotates in phase with it. Light is said to have 'left' circular polarization if the fields rotate counterclockwise from the perspective of someone looking into the oncoming light beam (Fig. 4a), and 'right' circular polarization if they rotate clockwise (Fig. 4b).

Plane polarized light can be described as a superposition of two circularly polarized beams rotating at the same frequency but in opposite directions. The components of the electromagnetic fields parallel to a fixed plane add constructively, while the components perpendicular to this plane cancel.

The *intensity* ( $I$ ) of a light beam, also called the *irradiance* or *fluence*, is the flux of radiant energy per unit cross-sectional area of the beam and has dimensions of  $\text{joules} \cdot \text{s}^{-1} \cdot \text{cm}^{-2}$  ( $\text{watts} \cdot \text{cm}^{-2}$ ). The

irradiance is proportional to the square of the electric field strength. For many spectroscopic applications, the relevant quantity is the *spectral density* ( $I(\nu)/\Delta\nu$ ), which is the irradiance per unit frequency interval ( $\Delta\nu$ ) and has units of  $\text{joules} \cdot \text{cm}^{-2}$ . The amplitude of the signal that would be recorded by a photomultiplier or other detector is proportional to  $I(\nu)S\Delta\nu$  or  $I(\lambda)S\Delta\lambda$ , where  $S$  is the cross-sectional area of the beam.

The *energy density* of a light beam,  $\rho(\nu)$ , is defined so that  $\rho(\nu)\Delta\nu$  is the amount of energy per unit volume in the spectral region with frequencies between  $\nu$  and  $\nu+\Delta\nu$ . Since light moves with a velocity  $c \cdot n^{-1}$ ,  $\rho(\nu) = (n/c)I$ .

In the quantum theory of light, an electromagnetic radiation field has quantized states similar to the states of the harmonic oscillator we discuss in *Infrared Spectroscopy*. The energies of these states are given by  $E_j = (j+1/2)\hbar\nu$ , where  $j$  can be zero or any positive integer. If the radiation interacts with matter and is absorbed,  $j$  usually decreases by 1, the energy of the radiation field decreases by  $\hbar\nu$  the matter gains the same amount of energy. When matter emits light,  $j$  usually increases by 1 and the energy of the radiation field increases by  $\hbar\nu$ . Such transactions can be

described as the absorption or emission of a *photon*, which is a particle with energy  $h\nu$  and a definite momentum but no mass. The value of  $j$  is interpreted as the number of *photons* in the radiation field. In addition to its characteristic frequency  $\nu$ , a photon has an intrinsic angular momentum or 'spin' that can be either right- or left-handed, corresponding to right- or left-circular polarization of the electromagnetic field.

### VIII. Excitons

If one molecule in a group of similar, closely packed molecules is excited, the excitation may hop from molecule to molecule in the manner of a moving particle. Such a mobile excitation is called an *exciton*. *Frenkel* excitons are those in which an excited electron and a vacancy or 'hole' in an otherwise filled molecular orbital migrate together from one molecule to another. *Wannier* excitons consist of more loosely associated electrons and holes. In photosynthetic antennas, we are concerned mainly with Frenkel excitons.

In the section on resonance energy transfer, we discuss relatively slow, stochastic hopping of excitations between widely spaced molecules. Here we are concerned with molecules that are closer together and interact more strongly, so that it may not be possible to say with certainty which molecule is excited at any given time. The molecular interactions that cause excitations to spread over several molecules are fundamentally the same in both cases, and can loosely be called *exciton interactions* or *exciton coupling*. They just are stronger in the situation of interest here because the molecules are closer together. As a result, the absorption, fluorescence and circular dichroism spectra of a dimer or higher oligomer can be significantly different from the spectra of the individual molecules. But we are not yet in the region of extremely strong interactions, where overlap of the molecular orbitals allows new bonds to form and the definition of the molecules themselves becomes blurred.

The effects of exciton interactions on spectroscopic properties provide a rich source of information on

photosynthetic antenna complexes. They are used widely to probe the structures of these complexes and to follow structural changes such as those that occur when large complexes are dissociated with detergents.

Consider a dimer comprised of two similar molecules,  $a$  and  $b$ . Suppose the molecules have ground states with wavefunctions  ${}^0\psi_a$  and  ${}^0\psi_b$ , respectively, and excited singlet states with wavefunctions  ${}^1\psi_a$  and  ${}^1\psi_b$ , and let the transition energies for exciting molecule  $a$  or  $b$  individually be  $E_a$  and  $E_b$ . As long as the molecules retain their individual identities, the ground-state wavefunction of the dimer can be written as the product  ${}^0\psi_a {}^0\psi_b$  to a reasonable approximation, and the energy of the ground state is just the sum of the molecular energies. If the molecules did not interact, we could write wavefunctions for the excited states of the dimer similarly as  ${}^1\psi_a {}^0\psi_b$  and  ${}^0\psi_a {}^1\psi_b$ . These are eigenfunctions of the combined Hamiltonian (energy operator) of the individual molecules ( $\tilde{H}_a + \tilde{H}_b$ ). (See Wavefunctions for an introduction to the Hamiltonian and eigenfunctions.) However, they are not eigenfunctions of the total Hamiltonian that includes the exciton interactions ( $\tilde{H}_a + \tilde{H}_b + \tilde{H}_{ab}$ ). This more complete formulation is needed if the excitation can move back and forth rapidly between the two molecules.

Let's denote the correct excited-state eigenfunctions as  $\Psi_+$  and  $\Psi_-$ , and express them as linear combinations of the old eigenfunctions:

$$\Psi_+ = C_1 {}^1\psi_a {}^0\psi_b + C_2 {}^0\psi_a {}^1\psi_b$$

$$\Psi_- = C_2 {}^1\psi_a {}^0\psi_b - C_1 {}^0\psi_a {}^1\psi_b.$$

The squares of the coefficients ( $C_i$ ) in these expressions then can be interpreted as the relative probabilities of finding the excitation on one molecule or the other, and can be normalized so that  $|C_1|^2 + |C_2|^2 = 1$ . Thus, if  $C_1 = \pm 1$  and  $C_2 = 0$ , only molecule  $a$  is excited in  $\Psi_+$  and only molecule  $b$  is excited in  $\Psi_-$ . For intermediate values of the coefficients, the excitation could be on either molecule.

In this formulation,  ${}^1\psi_a {}^0\psi_b$  and  ${}^0\psi_a {}^1\psi_b$  are referred to as the *basis states*, or simply *the basis*. We have assumed that these two states make the only significant contributions to the excited states of the dimer, but additional states could be included in the basis if necessary.

We can solve for the coefficients  $C_1$  and  $C_2$  by writing out the eigenvalue equations as matrix equations and using a mathematical procedure termed *diagonalizing* the Hamiltonian matrix. The same procedure can be used for complexes containing any number of molecules, but here we'll just give the results for a dimer:

$$C_1 = \sqrt{(1+s)/2}$$

$$C_2 = \sqrt{(1-s)/2},$$

with

$$s = \delta / \sqrt{\delta^2 + 4V^2}.$$

In these expressions,  $\delta$  is the difference between the energies of the states in which only molecule *a* or molecule *b* is excited ( $\delta = E_a - E_b$ ).  $V$  is the interaction energy or *coupling strength* that arises from the interaction term in the Hamiltonian,  $\tilde{H}_{ab}$ . The energies of the two excited states of the dimer are given by:

$$E_+ = \frac{E_a + E_b}{2} + \frac{1}{2}\sqrt{\delta^2 + 4V^2} \quad (1)$$

$$E_- = \frac{E_a + E_b}{2} - \frac{1}{2}\sqrt{\delta^2 + 4V^2}. \quad (2)$$

Before we discuss the relationship between  $V$  and the structure of the dimer, let's look at how the coefficients and energies of the excited states depend on the values of  $\delta$  and  $V$ . Figure 5 shows the coefficients as functions of the ratio of  $\delta$  to  $V$ . If  $|\delta| \gg |V|$ , then  $s \approx 1$  and the coefficients  $C_1$  and  $C_2$  approach 1.0 and zero, respectively.  $\Psi_+$  then approaches  ${}^1\psi_a {}^0\psi_b$  while  $\Psi_-$  approaches  ${}^0\psi_a {}^1\psi_b$ , and the energies of these states go to  $E_a$  and  $E_b$ , respectively, as shown in Fig. 6.

In the opposite limit, when the basis states are close together in energy relative to  $V$ ,  $s \approx 0$  and the coefficients become  $C_1 = C_2 = 1/\sqrt{2}$ . In this case, the two excited states  $\Psi_+$  and  $\Psi_-$  are *symmetric* and *antisymmetric combinations* of  ${}^1\psi_a {}^0\psi_b$  and  ${}^0\psi_a {}^1\psi_b$ :

$$\Psi_{\pm} = \frac{1}{\sqrt{2}} \left( {}^1\psi_a {}^0\psi_b \pm {}^0\psi_a {}^1\psi_b \right).$$

As Fig. 6 shows, the energies of  $\Psi_+$  and  $\Psi_-$  do not become identical when  $E_a = E_b$ . They maintain a minimum separation of  $2V$ . This *resonance splitting* is a purely quantum mechanical effect that results from mixing the two basis states and distributing the

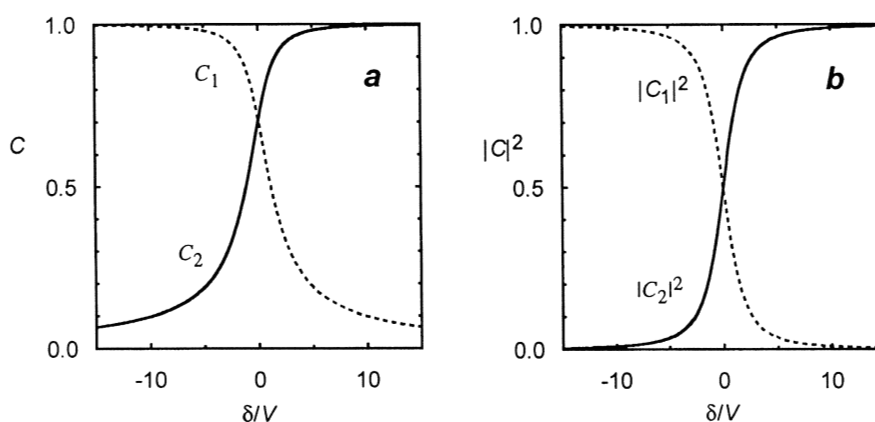


Fig. 5. The coefficients  $C_1$  and  $C_2$  (a) and their squares  $|C_1|^2$  and  $|C_2|^2$  (b) for one of the excited states of a dimer, as a function of  $\delta/V$ .  $\delta$  is the energy difference between the two basis states ( $E_a - E_b$ ) and  $V$  is the interaction energy.

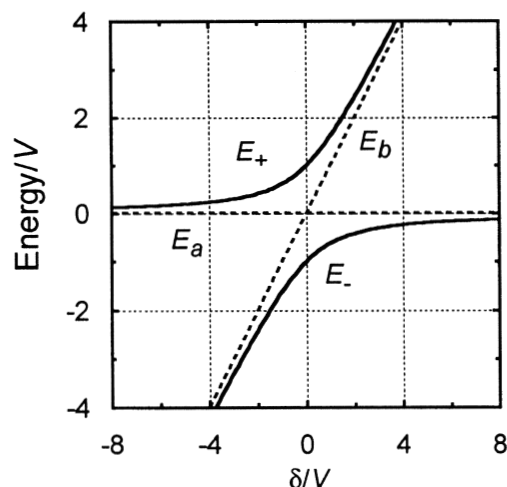


Fig. 6. Energies of the two excited states of a dimer ( $E_{\pm}$ , solid curves) as functions of the energy difference ( $\delta$ ) between the basis states. The energy scales are in units of the interaction energy  $V$ , which is held constant. The energy of  $^1\psi_a$  ( $E_a$ ) is fixed at zero while that of  $^1\psi_b$  ( $E_b$ ) is varied (dotted lines). At the point where  $E_a$  and  $E_b$  intersect,  $E_+$  and  $E_-$  are separated by  $2V$ .

excitation over the two molecules. A related phenomenon is the resonance stabilization of an aromatic molecule such as benzene in the ground state, where mixing of wavefunctions corresponding to different electronic structures gives rise to a mixed state that is more stable than the pure states.

Once the coefficients  $C_1$  and  $C_2$  are known, the spectroscopic properties of a dimer can be related straightforwardly to the properties of the individual molecules. The transition dipole for excitation of the dimer to  $\Psi_+$  or  $\Psi_-$  ( $\vec{\mu}_+$  or  $\vec{\mu}_-$ ) is simply a linear combination of the molecular transition dipoles ( $\vec{\mu}_a$  and  $\vec{\mu}_b$ ) with the same coefficients:

$$\vec{\mu}_+ = C_1\vec{\mu}_a + C_2\vec{\mu}_b$$

$$\vec{\mu}_- = C_2\vec{\mu}_a - C_1\vec{\mu}_b.$$

And the corresponding dipole strengths are:

$$D_+ = |\vec{\mu}_+|^2 = |C_1|^2 D_a + |C_2|^2 D_b + 2C_1C_2\vec{\mu}_a \bullet \vec{\mu}_b$$

$$D_- = |\vec{\mu}_-|^2 = |C_2|^2 D_a + |C_1|^2 D_b - 2C_1C_2\vec{\mu}_a \bullet \vec{\mu}_b,$$

where  $D_a$  and  $D_b$  are the dipole strengths of the

monomer transitions. The relative dipole strengths of the two absorption bands of the dimer can vary widely, depending on the coefficients  $C_1$  and  $C_2$ . But since  $|C_1|^2 + |C_2|^2 = 1$ , the sum of the dipole strengths is always  $D_a + D_b$ :

$$|\vec{\mu}_+|^2 + |\vec{\mu}_-|^2 = D_a + D_b.$$

If  $|\delta| \ll |V|$ , so that  $C_1 = C_2 = 1/\sqrt{2}$ , then the transition dipoles and dipole strengths of the dimer's bands are

$$\vec{\mu}_{\pm} = \frac{1}{\sqrt{2}}(\vec{\mu}_a \pm \vec{\mu}_b)$$

$$|\vec{\mu}_{\pm}|^2 = \frac{D_a + D_b}{2} \pm \sqrt{D_a D_b} \cos \theta,$$

where  $\theta$  is the angle between  $\vec{\mu}_a$  and  $\vec{\mu}_b$ . In this situation,  $\vec{\mu}_+$  and  $\vec{\mu}_-$  are simply symmetric and antisymmetric combinations of  $\vec{\mu}_a$  and  $\vec{\mu}_b$ , and are perpendicular to each other (see Linear Dichroism).

Now let's consider the interaction energy ( $V$ ). This energy reflects the charge-charge interactions between electrons on the two molecules. Using the bra-ket nomenclature (see Mathematical Tools) and neglecting dielectric screening by the intervening medium, we can write  $V$  formally as

$$V = \left\langle ^1\psi_b {}^0\psi_a \left| \frac{e^2}{r} \right| {}^0\psi_a {}^1\psi_b \right\rangle = \left\langle ^1\psi_b {}^0\psi_a \left| \frac{e^2}{r} \right| {}^0\psi_a {}^1\psi_b \right\rangle,$$

where  $e$  is the charge of an electron,  $r$  is the distance between electron positions on molecules  $a$  and  $b$ , and the brackets indicate an integral over all space.

To evaluate the integral in this expression for  $V$ , we need to know the molecular orbitals  ${}^0\psi_a$ ,  ${}^1\psi_a$ ,  ${}^0\psi_b$  and  ${}^1\psi_b$ . Suitable orbitals for chromophores with  $\pi$  electrons often can be written as linear combinations of atomic  $p$  orbitals. But a useful approximate expression for  $V$  can be obtained even without an explicit description of the molecular orbitals. This is done by writing out the intermolecular electrostatic

interactions as a sum of terms, using a *multipole expansion*. In general, the interactions of any two groups of 'point' charges at known positions can be written in this way. If the net charges of the individual molecules are not zero, then the leading term is the monopole-monopole (charge-charge) interaction energy,  $Q_a Q_b / R_{ab}$ , where  $Q_a$  and  $Q_b$  are the net charges and  $R_{ab}$  is the distance between the molecular centers, or more precisely, the centers of charge. However, this term does not contribute to  $V$  because, assuming that the basis wavefunctions are orthogonal,

$$\begin{aligned} & \left\langle {}^1\psi_b {}^0\psi_a \left| \frac{Q_a Q_b}{R_{ab}} \right| {}^0\psi_a {}^1\psi_b \right\rangle \\ &= \frac{Q_a Q_b}{R_{ab}} \left\langle {}^1\psi_b {}^0\psi_a \left| {}^0\psi_a {}^1\psi_b \right\rangle = 0. \end{aligned}$$

The first pertinent term in the multipole expansion usually is the *dipole-dipole* term, which corresponds to the classical energy of interaction of two electric dipoles located at the molecular centers. (See Transition Dipoles for a definition of electric dipoles.) Evaluating this term gives

$$V \approx \left\{ (\vec{\mu}_a \cdot \vec{\mu}_b) |\vec{R}_{ab}|^{-3} - 3(\vec{\mu}_a \cdot \vec{R}_{ab})(\vec{\mu}_b \cdot \vec{R}_{ab}) |\vec{R}_{ab}|^{-5} \right\} s^{-1}.$$

Here  $\vec{\mu}_a$  and  $\vec{\mu}_b$  are the transition dipoles of the two molecules,  $\vec{R}_{ab}$  is the vector from the center of molecule  $a$  to the center of  $b$  and the factor  $s^{-1}$  represents the dielectric screening by the intervening medium. This expression for  $V$ , in which the length of each dipole is assumed to be arbitrarily small, is called the *point-dipole approximation*. In a homogeneous medium with refractive index  $n$ , the screening factor  $s$  is approximately  $n^2$ .

Evaluating the dot products in the point-dipole expression and replacing  $s$  by  $n^2$  gives, for a dimer of identical molecules,

$$\begin{aligned} V &\approx D n^{-2} (\cos \theta - 3 \cos \alpha \cos \beta) |\vec{R}_{ab}|^{-3} \\ &= D n^{-2} \kappa |\vec{R}_{ab}|^{-3}, \end{aligned}$$

where  $D = D_a = D_b$  (the dipole strength of the

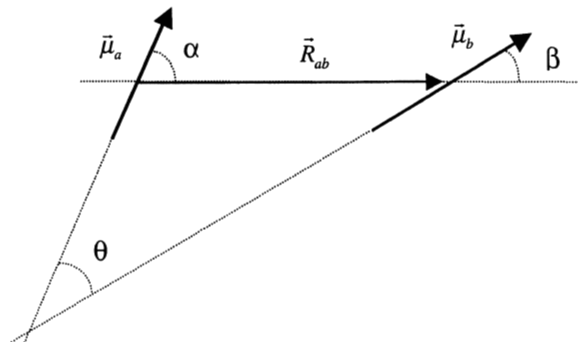


Fig. 7. In the point-dipole approximation, the energy of interaction of two dipoles ( $\vec{\mu}_a$  and  $\vec{\mu}_b$ ) depends on the magnitudes of the dipoles ( $|\vec{\mu}_a|$  and  $|\vec{\mu}_b|$ ), the center-to-center distance ( $|\vec{R}_{ab}|$ ), the angle between the dipoles ( $\theta$ ), and the angles of the dipoles with respect to  $\vec{R}_{ab}$  ( $\alpha$  and  $\beta$ ). This approximation usually is acceptable if  $|\vec{R}_{ab}|$  is much greater than  $|\vec{\mu}_a|/e$  and  $|\vec{\mu}_b|/e$ , where  $e$  is the charge of an electron.

monomer),  $\theta$  is the angle between the two transition dipoles,  $\alpha$  is the angle between  $\vec{\mu}_a$  and  $\vec{R}_{ab}$ , and  $\beta$  is the angle between  $\vec{\mu}_b$  and  $\vec{R}_{ab}$  (see Fig. 7). The last equation collects the dependences on the three angles into a geometrical factor  $\kappa$  that can vary between  $-2$  and  $+2$ :

$$\kappa = \cos \theta - 3 \cos \alpha \cos \beta.$$

Since  $D$  and  $|\vec{R}_{ab}|$  are positive quantities, the sign of  $V$  depends only on  $\kappa$ .

Figure 8 illustrates the application of these results to dimers of identical molecules in various arrangements. If the transition dipoles of the monomers are parallel and are aligned along the intermolecular axis as shown in Fig. 8a ( $\theta$ ,  $\alpha$  and  $\beta$  all  $0^\circ$ ),  $V$  is negative.  $\Psi_+$  then lies lower in energy than  $\Psi_-$ . All the dipole strength is associated with excitation of the dimer to  $\Psi_+$ , since  $D_+ = D(1 + \cos \theta) = 2D$  while  $D_- = D(1 - \cos \theta) = 0$ . The transition dipoles of the monomers thus add in  $D_+$  but cancel in  $D_-$ . Figure 8 does not show it, but the absorption spectrum of the dimer would be just the same if one of the monomers were turned around by  $180^\circ$ . In that case,  $V$  would be positive and  $\Psi_-$  would be lower in energy than  $\Psi_+$  but all the dipole strength still would go to the lower-energy transition.

If the transition dipoles of the monomers are perpendicular, as in Fig. 8b,  $V$  is zero; the two excited

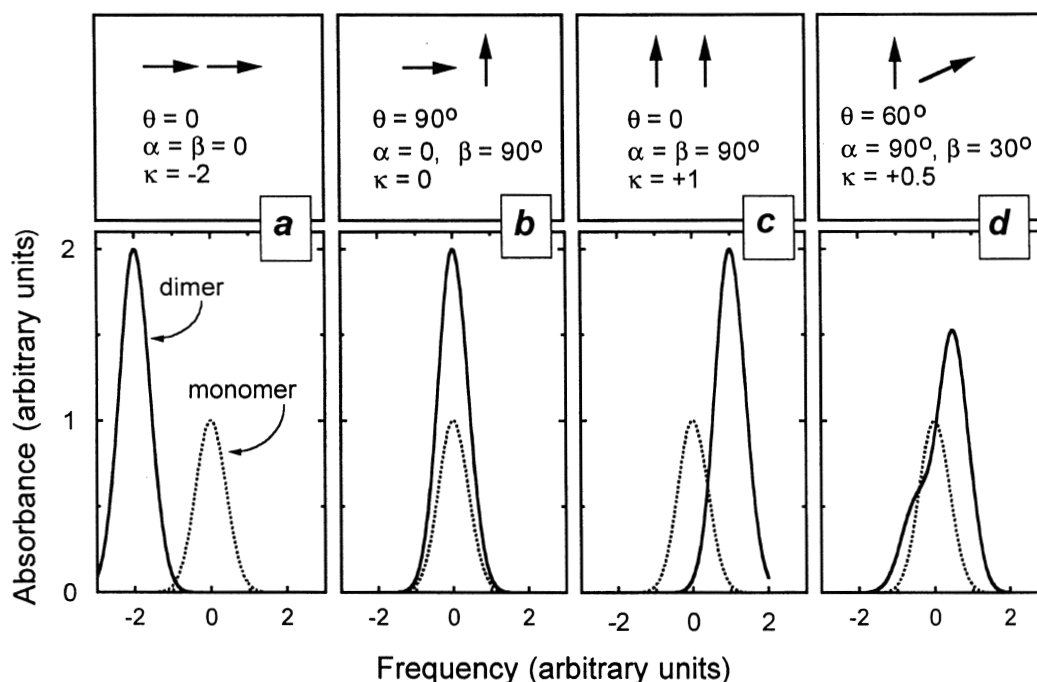


Fig. 8. Transition frequencies and dipole strengths of exciton bands of dimers with four different geometries. The orientations of the transition dipoles and the geometrical factor  $\kappa$  are indicated above each spectrum. The absorption spectrum of the monomer is shown with a dotted line and the spectrum of the dimer with a solid line. From left to right, the relative dipole strengths of the dimer's two bands ( $\Psi_-/\Psi_+$ ) are 0:2, 1:1, 0:2 and 0.5:1.5. ( $\Psi_-$  is the higher-energy transition in *a* and the lower-energy transition in *c* and *d*.) The exciton bands were given Gaussian shapes with the same width.

states of the dimer have the same energy, and transitions to  $\Psi_+$  and  $\Psi_-$  have the same dipole strength and are indistinguishable. If the monomer transition dipoles are parallel to each other but perpendicular to the intermolecular axis, as in Fig. 8c, then  $V$  is positive. In this case,  $\Psi_+$  is the higher-energy state and all of the dimer's dipole strength goes to the higher-energy excitation. Again, rotating one of the dipoles by  $180^\circ$  would change the sign of  $V$  and interchange the assignments of the transitions but would leave the spectrum unchanged. Finally, Fig. 8d shows an arrangement in which both of the dimer's absorption bands have significant dipole strengths.

These illustrations show that the absorption spectrum of a dimer depends strongly on the geometry of the complex. Although the absorption spectrum alone does not provide enough information to determine an unknown structure uniquely, it may be sufficient to rule out many otherwise plausible models. The circular dichroism spectrum can yield

additional information that further narrows the possibilities.

The concepts discussed above also apply to oligomers larger than dimers. The transition dipoles of the oligomer's absorption bands are written simply as sums of the transition dipoles of the individual molecules, and the coefficients are found by diagonalizing the interaction Hamiltonian. Analyses along these lines have helped to clarify the spectroscopic properties and excited-state dynamics of a variety of photosynthetic antenna complexes such as the bacterial LH2 complex (Nagarajan et al., 1999).

The point-dipole approximation for  $V$  becomes unreliable when the interacting molecules are too close together. The distance at which this occurs depends on the molecular structures and orientations, but as a rule of thumb for chlorophyll or bacteriochlorophyll, the approximation probably should not be trusted if the center-to-center distance is less than



about 10 Å. Several theoretical treatments that may be more reliable at short distances are available (Warshel and Parson, 1987; Scholes et al., 2001).

### IX. Fluorescence Yield and Lifetime

A molecule that has been excited by light can fall back to the ground state by spontaneously emitting light as fluorescence (see Spontaneous Fluorescence). But there are other 'nonradiative' paths by which the excited molecule can relax without fluorescing. These routes are often collected in a scheme like that shown in Fig. 9, which is called a *Jablonski diagram*.

*Intersystem crossing* is a transition between electronic states with different spins (see Singlet and Triplet States). Internal conversion is a relaxation between different electronic states with the same

spin. Molecules that are raised to higher excited states usually relax rapidly to the lowest excited singlet state by internal conversion before they fluoresce or undergo intersystem crossing to a triplet state. An excited molecule also may transfer the excitation energy to a neighboring molecule by resonance energy transfer, or enter into a photochemical process such as an electron-transfer reaction.

The overall rate constant for decay of an excited state ( $k_{tot}$ ) is the sum of the rate constants for fluorescence ( $k_r$ ), intersystem crossing ( $k_{isc}$ ), internal conversion to the ground state ( $k_{ic}$ ), resonance energy transfer ( $k_{ret}$ ), electron transfer ( $k_{et}$ ) and any other reactions:

$$k_{tot} = k_r + k_{isc} + k_{ic} + k_{ret} + k_{et} + \dots$$

The observed lifetime of the excited state ( $t_{tot} = 1/$

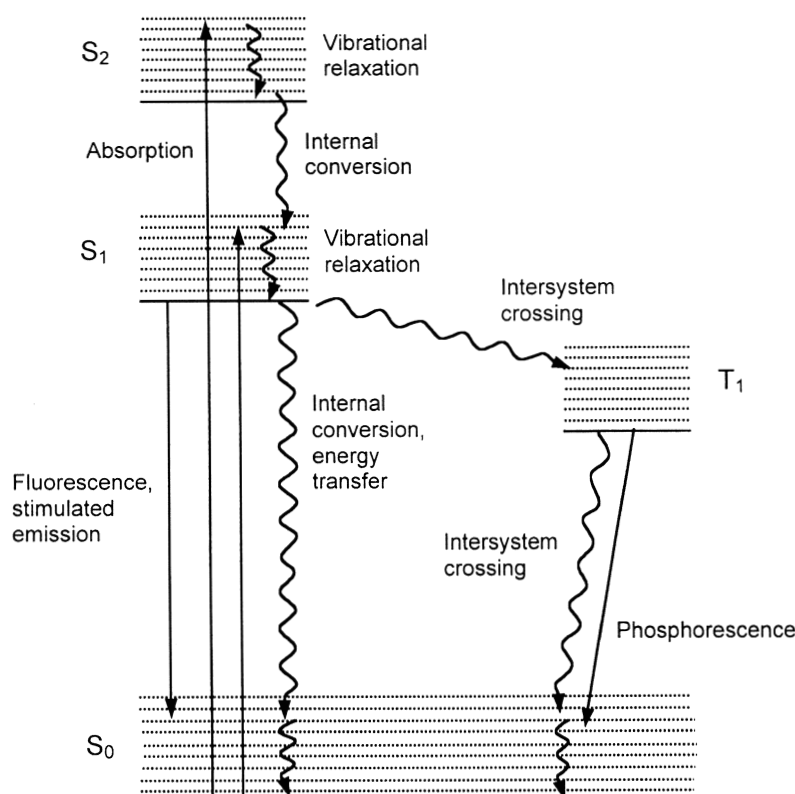


Fig. 9. A Jablonski diagram of pathways for formation and decay of excited states. Singlet states are labeled S and triplet states T, with subscripts 0, 1, 2... to denote the ground state and excited states of increasing energy. The dotted lines represent vibrational levels. Radiative processes are indicated with solid arrows; nonradiative processes, with wavy arrows. Upward arrows represent excitation by light.

$k_{tot}$ ), as measured by the time required for the fluorescence to decrease to  $1/e$  of its initial amplitude, thus is shorter than the radiative time constant,  $1/k_r$ . The *quantum yield* of fluorescence (the fraction of the excited molecules that decay by fluorescence) is given by the ratio of  $k_r$  to  $k_{tot}$ :

$$\phi = k_r / k_{tot}.$$

For molecules in solution, the rate constants  $k_{ret}$  and  $k_{et}$  for energy and electron transfer are pseudofirst-order rate constants that depend on the concentration of the reaction partner or energy acceptor. If we introduce an additional decay pathway by adding an electron acceptor, or in general any *quencher* (Q), the fluorescence quantum yield will decrease in a concentration-dependent manner:

$$\phi_f^Q = k_r / (k_{tot}^0 + k_Q[Q]),$$

where  $k_{tot}^0$  is the decay rate constant of the fluorescence in the absence of the quencher (the sum of the rate constants for all the decay mechanisms that do not involve the quencher). Rearranging the last two equations gives

$$\frac{\phi_f}{\phi_f^Q} = 1 + \frac{k_Q[Q]}{k_{tot}^0},$$

where  $\phi_f$  and  $\phi_f^Q$  are the quantum yields in the absence and presence of the quencher. The reciprocal of the fluorescence quantum yield ( $1/\phi_f^Q$ ) thus should increase linearly with the concentration of the quencher. This is known as the *Stern-Volmer equation*.

The sensitivity of the fluorescence yield and lifetime to a variety of quenchers makes fluorescence a versatile probe of macromolecular structure (Lakowicz, 1999). For instance, the fluorescence of tryptophan residues in proteins usually is quenched when these residues are exposed to water. This quenching can be used to study the folding or unfolding of a protein as a function of denaturant concentration, time or other variables. Exposure to oxygen also quenches the excited singlet states of

many molecules. This fact can be used to determine if a fluorophore is exposed to or shielded from oxygen dissolved in the solvent.

In photosynthetic antennas, energy transfer from one type of complex to another (for example from the B800 to the B850 complex of LH2) decreases the excited-state lifetime of the donor complex (see Resonance Energy Transfer).

## X. Infrared Spectroscopy

The length of the bond in a diatomic molecule such as CO tends to oscillate at a characteristic frequency that increases with the strength of the bond. The molecule's vibrational *mode* is associated with a set of quantum mechanical nuclear wavefunctions similar to those of a *harmonic oscillator*, which is a system that experiences a restoring force proportional to the displacement from the system's resting position. The energies of harmonic oscillator wavefunctions are given by

$$E_j = \left( j + \frac{1}{2} \right) \hbar \nu,$$

where  $\nu$  is the classical vibrational frequency of the mode and  $j = 0, 1, 2, \dots$ . Note that the lowest energy is not zero, as it would be in classical physics, but  $\hbar \nu / 2$ ; this is called the *zero-point energy*. Although actual nuclear wavefunctions depart from harmonic oscillator wavefunctions as a bond is stretched or compressed, the mathematical simplicity of harmonic oscillator wavefunctions makes them extremely useful for theoretical discussions.

A vibrational mode of a complex molecule typically involves simultaneous motions of many nuclei and cannot be described simply as the stretching or bending of an individual bond. But it usually is possible to assign such a vibrational mode to a particular combination of stretching, bending or twisting motions, and to describe these motions by a linear combination of displacements of the individual atomic coordinates. These collective vibrational

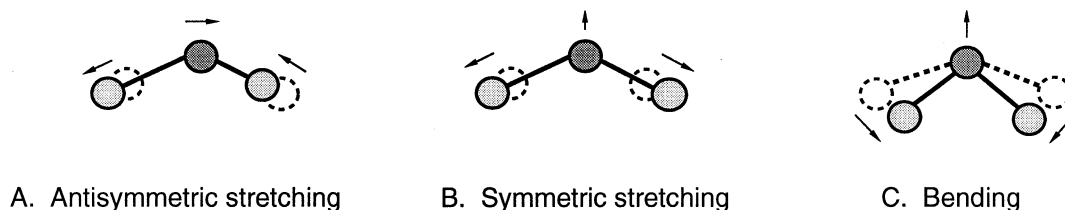


Fig. 10. The vibrational normal modes of a triatomic molecule. The *open and stippled circles* indicate positions of the terminal atoms at two times, and the *arrows* indicate directions of motion at an arbitrary time. The molecule's center of mass is stationary.

modes are the *normal modes* of the system and the associated combinations of coordinates are called the *normal coordinates*. Figure 10 illustrates the three normal modes of a triatomic molecule. Procedures for finding the compositions and frequencies of vibrational normal modes are described by Wilson et al. (1955). The vibrational energy of a molecule with multiple normal modes is the sum of the energies associated with all the individual modes.

Excitations of molecules to higher vibrational levels typically occur in the infrared (IR) region of the spectrum, with wavenumbers between 200 and 5,000  $\text{cm}^{-1}$  ( $\nu = 6 \times 10^{12}$  to  $1.5 \times 10^{14}$  Hz, or  $\lambda = 50$   $\mu\text{m}$  to 2  $\mu\text{m}$ ). The strength of the IR absorption band for such an excitation depends on several *selection rules*. First, strong bands usually involve transitions in which the integer  $j$  in the above equation increases by 1. Since the resting molecule usually will be in the lowest levels of all the vibrational modes with energies greater than the thermal energy, transitions from  $j = 0$  to  $j = 1$  usually dominate the absorption spectrum. The energy of the transition is  $\Delta E = E_1 - E_0 = \hbar\nu$ .

The second selection rule for IR absorption is that the vibration must change the molecule's dipole moment. The pertinent dipole moment here is the 'permanent' dipole moment of the molecule in its ground electronic state, not the transition dipole that determines the strength and linear dichroism of an electronic absorption band. The requirement for a change in the dipole moment rules out IR absorption for homonuclear diatomic molecules such as  $\text{O}_2$ , which have no dipole moment. The C=O bond of a carbonyl group, on the other hand, has a permanent dipole with the negative end on the O atom and the positive end on the C, and this dipole oscillates in

magnitude as the bond stretches and compresses.

Infrared spectroscopic studies of macromolecules have become increasingly common and powerful with the development of Fourier-transform IR (FTIR) spectroscopy (Griffiths and deHaseth, 1986; Braiman and Rothschild, 1988; Mäntele, 1993; Siebert, 1995). In a conventional IR spectrometer, a beam of IR light passes through the sample and then is dispersed by a monochromator so that the intensity of the transmitted light can be measured as a function of wavelength. FTIR spectrometers dispense with the monochromator. Light from a lamp is split into two beams that travel different paths but then both pass through the sample and proceed to the same detector. The length of one of the light paths is modulated by a moving mirror. When the beams recombine, light of a given wavelength interferes either constructively or destructively, depending on the wavelength and the difference between the path lengths. The moving mirror thus causes the signal at a given wavelength to oscillate with time. The absorption spectrum of the sample can be determined from the spectrum of the oscillatory components of the transmitted light. Because the wavelength scale can be calibrated very accurately, this technique allows one to measure small shifts in the spectrum caused by isotopic substitutions or other modifications of the sample.

In photosynthetic reaction centers and antenna complexes, IR measurements combined with site-directed mutagenesis and isotopic substitutions have been used to identify residues that interact with the pigments or that bind a proton when one of the electron carriers is reduced (Breton et al., 1997). For references to closely related studies, see Raman Spectroscopy.

## XI. Internal Conversion

*Internal conversion* is a non-radiative transition between two electronic states with the same electron spin multiplicity, such as a transition between two excited singlet states or two triplet states (see Singlet and Triplet States). (A transition between states with different spin is termed *intersystem crossing*.) The transitions that are most pertinent to photosynthetic antenna systems are relaxations from higher singlet states ( $S_n$ ) to the lowest ('first') excited singlet state ( $S_1$ ), or from  $S_1$  to the ground state ( $S_0$ ).

Internal conversion from  $S_1$  to  $S_0$  is one of the processes that compete with fluorescence (see Fluorescence Yield and Lifetime). Internal conversion from higher excited states to  $S_1$  usually occurs much more rapidly than internal conversion from  $S_1$  to  $S_0$ , and for this reason excited molecules usually emit fluorescence mainly from  $S_1$ . This observation is sometimes called *Kasha's rule*. As an example, if bacteriochlorophyll is excited in the Soret (360–400 nm) or  $Q_x$  (600 nm) absorption band, the molecule relaxes to its lowest excited singlet state ( $Q_y$ ) in less than  $10^{-13}$  s. In the absence of electron transfer or other quenching processes, the  $Q_y$  state then decays with a time constant of about  $10^{-8}$  s. If the rate constants for other processes are similar in the different states, the integrated fluorescence from  $S_1$  will be on the order of  $10^5$  times that from the higher excited states.

Within a related series of molecules, the rate of internal conversion from  $S_1$  to  $S_0$  decreases approximately exponentially with the energy gap between the two states ( $\Delta E_{00}$ ):

$$k \approx k_0 e^{-a\Delta E_{00}},$$

where the constants  $k_0$  and  $a$  depend on the type of molecule. The important energy difference here is the '0–0' difference between the lowest vibrational levels of the two electronic states (see Spectral Bandshapes). This exponential relationship is known as the *energy-gap law* (Siebrand, 1967a,b; Bixon and Jortner, 1968; Gelbart et al., 1970). The energy-gap law can be rationalized as follows: Since the total energy must be conserved during the transition,

internal conversion from  $S_1$  to  $S_0$  must create a vibrationally excited level of the electronic ground state. The larger the electronic energy gap, the more the amount of energy converted into vibrations. For a vibrational mode whose normal coordinates are only slightly displaced between the two electronic states, the lowest vibrational wavefunction of  $S_1$  has little spatial overlap with highly excited vibrational wavefunctions of  $S_0$ , making transitions between these vibrational states unlikely. (See Infrared Spectroscopy for more on normal coordinates and vibrational modes, and Spectral Bandshapes for vibrational overlap integrals.)

Measurements of the rates of internal conversion in carotenoids have been used with the energy-gap law to estimate the energies of transient excited states (Chynwat and Frank, 1995). However, more direct methods have given different results in some cases and may be preferable (Polívka et al., 1999, 2001; Frank et al., 2000).

## XII. Linear Dichroism and Fluorescence Anisotropy

A dependence of the absorption of linearly polarized light on the orientation of the polarization axis relative to the sample is called *linear dichroism* (LD). As discussed in Electromagnetic Radiation, the polarization axis of linearly polarized light refers to the orientation of the oscillating electric field ( $\vec{E}$ ). Linear dichroism reflects the fact that the interaction of this field with the transition dipole ( $\vec{\mu}$ ) varies if  $\vec{E}$  is rotated relative to the molecular orientation.

The strength of an optical transition is proportional to  $(\vec{\mu} \cdot \vec{E})^2$ , or  $|\vec{\mu}|^2 |\vec{E}|^2 \cos^2 \theta$ , where  $\theta$  is the angle between  $\vec{E}$  and  $\vec{\mu}$  for an individual absorbing molecule, and the bars denote averages over the orientations of all the molecules in the sample. For an isotropic sample, in which the molecules have random orientations, the average of  $\cos^2 \theta$  is simply 1/3, so

$$\overline{(\vec{\mu} \cdot \vec{E})^2} = \frac{1}{3} |\vec{\mu}|^2 |\vec{E}|^2.$$

The standard expression relating the molar absorption coefficient to the dipole strength ( $|\vec{\mu}|^2$ ) assumes that the sample is isotropic and includes this factor of 1/3. Rotating the polarization of the light does not affect the absorbance of an isotropic sample. For an anisotropic sample, on the other hand, the value of  $\cos^2 \theta$  depends on the extent to which the sample is ordered and on the polarization of the light relative to the orientation axis of the sample. In this case, the absorbance generally changes as the polarization axis is rotated. The results of such measurements often are expressed in terms of  $\epsilon_{\perp} - \epsilon_{\parallel}$ , where  $\epsilon_{\parallel}(\lambda)$  and  $\epsilon_{\perp}(\lambda)$  are the molar absorption coefficients for light polarized parallel and perpendicular to the orientation axis.

Measurements of LD can be used to explore the orientations of pigment molecules with respect to a macroscopic axis, or with respect to each other in a system containing multiple pigments. For example, if membranes containing the photosynthetic bacterial LH1 antenna system are ordered by drying on a flat surface, the long-wavelength ( $Q_y$ ) absorption band of bacteriochlorophyll is found to be maximal for light polarized parallel to the plane of the surface (Breton et al., 1981). This indicates that the  $Q_y$  transition dipoles, which are approximately parallel to the line connecting nitrogen atoms N1 and N3 of the bacteriochlorophyll molecules, lie more or less in the plane of the membrane. If purified pigment-protein complexes are oriented by stretching or compressing samples embedded in polyvinylalcohol or polyacrylamide, some of the absorption bands typically are maximal for light polarized parallel to the orientation axis, while others are strongest with orthogonally polarized light. Crystalline materials typically have very strong linear dichroism with respect to the crystal axes.

Linear dichroism also can be helpful for analyzing exciton interactions. A dimer formed from two identical molecules, each of which has one excited state, will have two absorption bands whose transition dipoles are proportional to the sum and difference of the transition dipoles of the individual molecules. Because the sum and difference of any two vectors are perpendicular to each other, the two absorption

bands necessarily have orthogonal LD. The absorption bands of larger oligomers also represent combinations of transitions of the individual molecules and can show strong LD. This can be particularly informative when some of the exciton bands are not well resolved in the isotropic absorption spectrum, because these may split into components with opposite signs in the LD spectrum. However, the analysis of the LD spectrum of an oligomer larger than a dimer is not necessarily straightforward, because each band can contain contributions from more than two molecules. The same is true even for a homodimer if the individual molecules have more than one excited state. The long-wavelength absorption band of a bacteriochlorophyll dimer, for example, may have contributions from both the  $Q_y$  and  $B_y$  transitions (see Configuration Interactions). Structural or environmental differences between the two chromophores of a dimer also can distort the symmetry of the LD spectrum by altering the relative contributions of the two molecules to the exciton bands.

As mentioned above, the magnitude of the LD manifested by a sample depends partly on how well the individual molecules are oriented. The failure to observe LD in a pigment-protein complex thus could reflect poor alignment of the complexes with respect to the laboratory axes, and say nothing about the orientations of the chromophores within the individual complexes.

Linear dichroism can be created in an isotropic sample by excitation with polarized light. If the light excites only a small fraction of the molecules in the sample, it will selectively pick out molecules that are oriented with their transition dipoles approximately parallel to  $\vec{E}$  ( $\theta \approx 0$ ). The excitation of molecules with other orientations falls off as  $\cos^2 \theta$ . This is termed *photoselection*. Spectra of absorbance changes caused by photoselective excitation will differ, depending on whether the measuring light is polarized parallel or perpendicular to the excitation. Such spectral differences are called *induced dichroism*. They commonly are expressed in terms of the absorption *anisotropy* ( $r$ ),

$$r = \{\Delta A_{\parallel} - \Delta A_{\perp}\} / \{\Delta A_{\parallel} + 2\Delta A_{\perp}\},$$

where  $\Delta A_{\parallel}$  and  $\Delta A_{\perp}$  are the absorbance changes measured with light polarized parallel and perpendicular to the excitation polarization. The anisotropy will decay with time if the excited molecules rotate or transfer the excitation energy to neighboring molecules with different orientations.

The same phenomenon underlies measurements of *fluorescence anisotropy*, in which one excites a sample selectively with polarized light and measures the fluorescence emission through polarizers parallel and perpendicular to the excitation. The fluorescence anisotropy is

$$r = \{F_{\parallel} - F_{\perp}\} / \{F_{\parallel} + 2F_{\perp}\},$$

where  $F_{\parallel}$  and  $F_{\perp}$  are the fluorescence intensities with parallel and perpendicular polarizations.

The denominator in the definition of anisotropy ( $F_{\parallel} + 2F_{\perp}$ ) is proportional to the total fluorescence,  $F_T$ , which includes components polarized along all three Cartesian axes:  $F_T = F_x + F_y + F_z$ . Suppose the excitation light is polarized parallel to the  $z$ -axis and we measure the fluorescence with polarizers parallel to the  $z$  and  $x$  axes, so that  $F_{\parallel} = F_z$  and  $F_{\perp} = F_x$ . The emission must be symmetrical in the plane normal to the excitation polarization, so  $F_y = F_x$ . Thus  $F_T = F_z + 2F_x = F_{\parallel} + 2F_{\perp}$ . The total fluorescence also can be obtained by measuring the fluorescence through a polarizer set at the 'magic angle'  $54.7^\circ$  from the  $z$ -axis. This is equivalent to combining  $z$ - and  $x$ -polarized measurements with weighting factors of  $\cos^2(54.7^\circ)$  and  $\sin^2(54.7^\circ)$ , which have the ratio 1:2. Fluorescence measured through a polarizer at the magic angle with respect to the excitation polarization is not affected by rotation of the chromophore. The same is true of absorbance changes induced by photoselection, and of the absorbance of a sample that is oriented with respect to a single axis: rotation of the chromophore will not change the absorbance measured through a polarizer set at  $54.7^\circ$  with respect to the orientation axis. The orientational averaging achieved by measuring at the magic angle also is used in NMR spectroscopy to sharpen bands that would otherwise be smeared out by anisotropic interactions.

The decay of absorption or fluorescence anisotropy

is commonly used to measure the rotational dynamics of molecules. Measurements of anisotropy decay are particularly useful for macromolecules, since the reorientation kinetics can be related to the size and shape of the molecule.

Measurements of fluorescence anisotropy also provide a convenient way of probing the relative orientations of the pigments in an antenna complex. Here the molecules are stationary and the orientation of the transition dipole of the emitting molecule changes because of resonance energy transfer. Neglecting coherence effects (see below), the expected value of  $r$  at short times after excitation is 0.4. If the excitation can migrate among molecules with completely random orientations,  $r$  will decrease to zero at long times, whereas if the migration is constrained to molecules that lie in a common plane, the limiting value at long times is 0.1. (These values are derived by integrating over all orientations of the molecules with respect to both the detection and excitation polarizations.) The dynamics of the anisotropy decay provide a measure of the rate at which excitations hop from pigment to pigment.

Another common situation is for a molecule to have two or more absorption bands with non-parallel transition dipoles. If a molecule is excited in one band and then emits fluorescence by a transition with a perpendicular transition dipole, the expected value of the anisotropy at short times is  $-0.2$ . This is the case when bacteriochlorophyll is excited in its  $Q_x$  absorption band near 600 nm and fluoresces in the  $Q_y$  band near 780 nm (Ebrey and Clayton, 1969).

Analysis of fluorescence or absorption anisotropy at very short times after an excitation pulse can be more complicated in systems that have multiple, closely spaced absorption bands. In such systems, a short pulse can excite multiple transitions, creating a coherent superposition of quantum states (Knox and Gulen, 1993; Wynne and Hochstrasser, 1993; Kühn and Sundström, 1997; Nagarajan et al., 1999). Superposition states can have absorption and emission anisotropies that exceed the classical upper limit of 0.4. The extra anisotropy typically decays within about 0.1 ps because of random fluctuations of the energies of the excited states.

### XIII. Mathematical Tools

#### A. Vectors

A vector is a quantity that has both a direction and a magnitude, whereas a *scalar* has only a magnitude. Length and mass are examples of scalars; displacement and velocity are vectors. To see the distinction, consider a walk around a square city block. If you return to the starting position after one loop, the length of your trip has been four times the length of the block, whereas your displacement, obtained by summing the vectors along four streets, is zero.

Any vector in a three-dimensional coordinate system can be written as the sum of its vector components in the  $x$ ,  $y$  and  $z$  directions. We indicate a vector either by a letter with an arrow on top or by specifying its Cartesian components:  $\vec{a} \equiv (a_x, a_y, a_z)$ . The length or *magnitude* of a vector  $(a_x, a_y, a_z)$  is  $|\vec{a}| = (a_x^2 + a_y^2 + a_z^2)^{1/2}$ . The *dot product* of two vectors  $\vec{a}$  and  $\vec{e}$  is a scalar defined by  $\vec{a} \cdot \vec{e} = a_x e_x + a_y e_y + a_z e_z$ , or  $|\vec{a}||\vec{e}|\cos(\theta)$ , where  $\theta$  is the angle between  $\vec{a}$  and  $\vec{e}$ . The *cross product* of  $\vec{a}$  and  $\vec{e}$ , denoted  $\vec{a} \times \vec{e}$ , is a vector with magnitude  $|\vec{a}||\vec{e}|\sin(\theta)$ , pointing in a direction perpendicular to both  $\vec{a}$  and  $\vec{e}$ .

#### B. Operators

An operator, denoted in this chapter by a character with a tilde on top, acts on and modifies the function or parameter that follows it. Consider, for example, the one-dimensional derivative operator  $\tilde{\nabla}_x = d/dx$  acting on the function  $f(x) = 3x^2$ . The operation is  $\tilde{\nabla}_x f(x) = \frac{d}{dx}\{3x^2\} = 6x$ . In quantum mechanics, every observable physical property that depends on position and time has a corresponding operator. This operator can be used to calculate the expected value of the property, as described later in this section.

#### C. Eigenfunctions and Eigenvalues

A function is said to be an *eigenfunction* of an operator if the function is unmodified in the operation except for multiplication by a constant. For example,

$e^x$  is an eigenfunction of the derivative operator because  $d\{e^x\}/dx = e^x$ . The *eigenvalue* of an operator is the multiplicative factor, which is 1 in this example.

#### D. Complex Functions

A complex function is a sum of real and imaginary functions, where an imaginary quantity means a quantity that is proportional to  $\sqrt{-1}$  ( $i$ ). The *complex conjugate* of a function (denoted by an asterisk following the function) is obtained by changing the sign of  $i$  everywhere in the function. For the complex function  $\vartheta(x) = e^{ix} = \cos(x) + i \sin(x)$ , the complex conjugate is  $\vartheta^*(x) = \cos(x) - i \sin(x) = e^{-ix}$ . The product of any complex function and its complex conjugate is real. Thus, for example,  $e^{ix} e^{-ix} = e^0 = 1$ . Complex functions abound in wave theory and quantum mechanics.

#### E. Bra-ket Notation

In the *bra-ket* notation for quantum mechanical integrals,  $\langle \psi_2 | \psi_1 \rangle$  means an integral of  $\psi_2^* \psi_1$  over all space (the total area under the product of  $\psi_2^*$  and  $\psi_1$ ). Here  $\psi_1$  and  $\psi_2$  could be any functions of position and time, and  $\psi_2^*$  is the complex conjugate of  $\psi_2$ . In ordinary calculus notation, this integral would be written  $\iiint \psi_2^* \psi_1 dx dy dz$ . Similarly,  $\langle \psi_2 | \tilde{A} | \psi_1 \rangle$  means an integral over all space of  $\psi_2^* \tilde{A} \psi_1$  (the area under the product of  $\psi_2^*$  and  $\tilde{A} \psi_1$ ), which is the same as  $\iiint \psi_2^* \tilde{A} \psi_1 dx dy dz$ .

Integrals of both these types arise frequently in quantum mechanics. For example,  $\langle \psi | \psi \rangle$  is interpreted as the probability of finding a system in a state with wavefunction  $\psi$ . And if we know that a system has wavefunction  $\psi$ , then  $\langle \psi | \tilde{A} | \psi \rangle$  gives the most probable value, or *expectation value* of the observable physical property corresponding to operator  $\tilde{A}$ . This integral takes the place of the classical physical equation describing how the observable property depends on position, time and other parameters. Thus, for the energy operator  $\tilde{\mathcal{H}}$  (the *Hamiltonian*),  $\langle \psi | \tilde{\mathcal{H}} | \psi \rangle$  is the most likely energy of a system with wavefunction  $\psi$ .



## XIV. Raman Scattering

When an electromagnetic wave impinges on a molecule, the oscillating electric field distorts the molecule's electron cloud and the distortion is modulated at the same frequency as the incident field. The motion of the electrons relative to the nucleus thus creates a dipole that oscillates at the frequency of the incident wave. As discussed in Electromagnetic radiation, such a dipole can radiate light in various directions at the same frequency. This is a classical description of light scattering. When the incident and emitted light have the same frequency, as just described, no net transfer of energy occurs and the process is called *Raleigh scattering*.

It also is possible, though less probable, for the frequency of the scattered light to be higher or lower than the incident light frequency, so that there is a net transfer of energy between the molecule and the electromagnetic field. This energy difference is transferred to, or extracted from a molecular vibrational mode. The molecule thus is either promoted to a higher vibrational level of the ground electronic state or demoted to a lower level. This process is termed *Raman scattering*. Figure 11

illustrates the main possibilities. Upward Raman transitions, called *Stokes Raman scattering*, usually predominate over downward transitions (*anti-Stokes Raman scattering*) because resting molecules reside mainly in the lowest levels of their vibrational modes (see IR Spectroscopy). A transition from this level to the next higher level often gives relatively strong scattering. The strength of anti-Stokes scattering increases with temperature, because an increasing number of molecules start out in higher vibrational levels. Anti-Stokes Raman scattering thus provides a way to measure the effective temperature of a molecule.

If the frequency of the incident light matches a transition frequency of the molecule, the modulation of the molecular dipole increases greatly in amplitude, resulting in the enhancement of scattering intensity by as much as a million-fold. The scattering then is called *resonance Raman scattering*.

Raman scattering usually is measured by irradiating a sample with a narrow line from a continuous laser, but time-resolved measurements also can be made by using a pulsed laser as the light source. Typically, light scattered at 90° from the axis of incidence is collected through a monochromator, and the

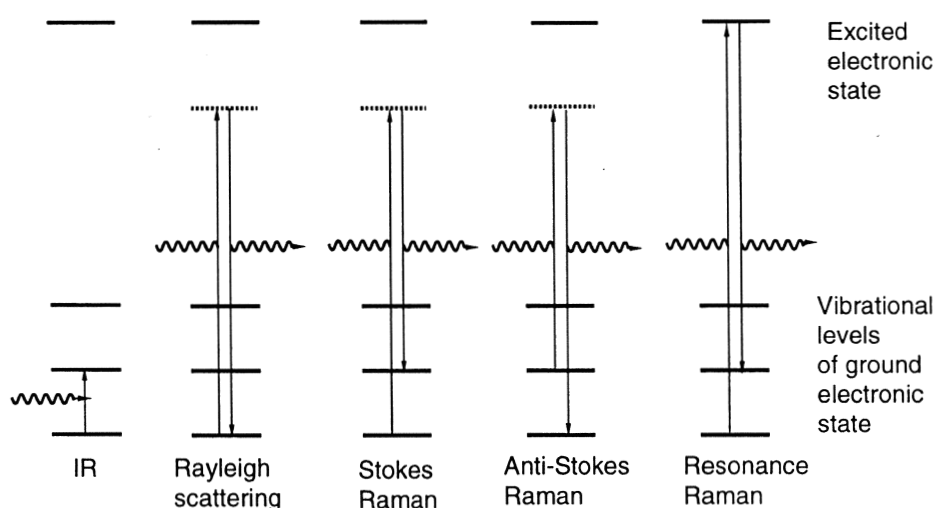


Fig. 11. Vibrational transitions in IR absorption and several types of light scattering. In IR spectroscopy, absorption of light (wavy horizontal line) excites a molecule directly to a higher vibrational level of the ground electronic state. In Rayleigh scattering, the molecule absorbs and emits light with the same energy, so that its energy remains constant. In Raman scattering, light with a different energy is emitted, leaving the molecule in either a higher or lower vibrational level (Stokes and anti-Stokes scattering, respectively). The dashed horizontal lines represent the total energy of the molecule plus the incident radiation. Resonance Raman scattering occurs if the energy of the incident light matches the transition energy to a higher electronic state.

irradiance of the signal is plotted as a function of the difference in wavenumber between the scattered and incident light ( $\bar{\nu}_s - \bar{\nu}_e$ ). The spectrum resembles an IR spectrum (see Infrared Spectroscopy). However, the relative intensities of the Raman and IR lines corresponding to various vibrational modes generally differ. Whereas IR absorption is seen for vibrations that modulate the dipole moment of a molecule, non-resonance Raman scattering is seen for vibrations that affect the electronic polarizability. Resonance Raman spectra of proteins differ from IR spectra in that signals from bound chromophores can dominate the weak, non-resonant signals from the protein. Raman scattering is distinguishable from fluorescence by the narrow widths of Raman lines and by their dependence on the frequency of the excitation light. Whereas fluorescence emission spectra measured with continuous light usually are more or less independent of the excitation frequency, a Raman line shifts linearly with  $\bar{\nu}_e$ , maintaining a constant value of  $(\bar{\nu}_s - \bar{\nu}_e)$ .

The sharp lines of a Raman spectrum usually are superimposed on a broad fluorescence background. The background signal can be removed by shifting the excitation frequency by a known amount (typically 1 to 10  $\text{cm}^{-1}$ ), which shifts all the Raman lines by the same amount but has negligible effect on the broad fluorescence signal. When the shifted spectrum is subtracted from the unshifted, the background mostly disappears, leaving a difference spectrum that includes only the sharp bands. Since the amount of shift is known, the Raman spectrum can be reconstructed from the difference spectrum.

Raman spectroscopy has been used extensively to study the ligation states and environments of hemes in proteins and to examine the ligands and hydrogen bonding of the protein to the pigments in photosynthetic reaction centers and antenna complexes (Mattioli et al., 1995; Olsen et al., 1997; Ivancich et al., 1998; Stewart et al., 1998; Czarnecki et al., 1999; Lapouge et al., 1999). Hydrogen bonding to the acetyl or keto oxygen atom shifts the C=O stretching mode to lower frequency, and the magnitude of this shift depends on the strength of the H-bond (Mattioli,

1995; Ivancich et al., 1998). Other vibrational modes can report on distortions of the bacteriochlorophyll from planarity (Olsen et al., 1997; Lapouge et al., 1999). Measurement of the resonance Raman spectrum is advantageous in such studies because the incident light can be tuned to the absorption band of a particular subset of the pigments. Changes in the strengths of Raman lines usually are more difficult to interpret than shifts in the vibrational frequencies because the strength is sensitive to many different factors.

New techniques for obtaining laser light in the near-UV have opened the door to resonance Raman studies of tyrosine, phenylalanine and tryptophan residues in proteins (Hu and Spiro, 1997; Deng and Callender, 1999).

## XV. Resonance Energy Transfer

### A. Dipole-Dipole Coupling

*Resonance energy transfer* plays a central role in photosynthetic antenna systems because it is the process by which excitations migrate from molecule to molecule and eventually reach the reaction centers. Because the rate of resonance energy transfer depends on the distance between the energy donor and acceptor, it also can be used experimentally to probe distances between sites in macromolecules.

Resonance energy transfer requires coupled downward and upward transitions of the two molecules, so that the total energy of the system remains constant. The energy lost by the donor must match the energy gained by the acceptor. The process is commonly called 'fluorescence resonance energy transfer' (FRET), which is a misnomer since the energy donor does not actually fluoresce. Instead, resonance energy transfer represents a quantum mechanical resonance between two super-molecular states of equal energy, and is driven, in most cases, by weak interactions of the electrons on the two molecules. However, resonance energy transfer resembles a combination of fluorescence and absorption in that the upward and downward

transitions must be able to occur with little nuclear motion. More formally, both transitions must have nonzero Franck-Condon factors (see Spectral Bandshapes).

The electronic interaction energy that most commonly drives resonance energy transfer is the same as the dipole-dipole interaction energy ( $V$ ) that underlies exciton interactions. As we discuss in Excitons, for molecules that are sufficiently far apart relative to the molecular dimensions,  $V$  is given approximately by the point-dipole expression:

$$V \approx \left\{ (\vec{\mu}_a \cdot \vec{\mu}_b) |\vec{R}_{ab}|^{-3} - 3(\vec{\mu}_a \cdot \vec{R}_{ab})(\vec{\mu}_b \cdot \vec{R}_{ab}) |\vec{R}_{ab}|^{-5} \right\} n^{-2}.$$

In this expression,  $\vec{\mu}_a$  and  $\vec{\mu}_b$  are the transition dipoles of the two molecules,  $\vec{R}_{ab}$  is the vector from the center of molecule  $a$  to the center of  $b$ , and  $n$  is the refractive index of the intervening medium. The factor  $n^{-2}$  expresses dielectric screening by the medium.

Relatively simple quantum mechanical considerations show that the rate of resonance energy transfer should be proportional to  $V^2$ , which in the point-dipole approximation is:

$$V^2 \approx D_a D_b \kappa^2 n^{-4} |\vec{R}_{ab}|^{-6}.$$

$D_a$  here is the dipole strength for absorption and stimulated emission by molecule  $a$  ( $D_a = |\vec{\mu}_a|^2$ ),  $D_b$  is the same for molecule  $b$ , and  $\kappa$  is a geometrical factor that depends on the orientations of the two transition dipoles. ( $\kappa = \cos \theta - 3 \cos \alpha \cos \beta$ , where  $\theta$  is the angle between  $\vec{\mu}_a$  and  $\vec{\mu}_b$  and  $\alpha$  and  $\beta$  are the angles that  $\vec{\mu}_a$  and  $\vec{\mu}_b$  make with  $\vec{R}_{ab}$ .) According to this expression for  $V^2$ , the rate of energy transfer will fall off with the sixth power of  $|\vec{R}_{ab}|$ .

Following the reasoning outlined above, T. Förster (1965) showed that the rate of resonance energy transfer between well-separated molecules can be related to the overlap of the fluorescence spectrum of the donor with the absorption spectrum of the acceptor, which is an easily measurable quantity. The quantity that is needed is an integral,  $\bar{J}$ , that includes a frequency-dependent weighting factor to convert the acceptor's dipole strength into a molar extinction

coefficient and convert the donor's dipole strength into a radiative rate constant (see Spontaneous Fluorescence):

$$\bar{J} = \int F_a \epsilon_b \bar{\nu}^{-4} d\bar{\nu} / \int F_a d\bar{\nu}.$$

In this expression,  $F_a$  is the fluorescence amplitude of the donor and  $\epsilon_b$  is the molar extinction coefficient of the acceptor, both of which are functions of the wavenumber ( $\bar{\nu} = 1/\lambda$ ). Integrating the weighted product of  $F_a$  and  $\epsilon_b$  over all wavenumbers incorporates the requirements that the coupled upward and downward transitions of the two molecules must conserve energy and must have nonzero Franck-Condon factors. The product of separate integrals of the fluorescence and absorption spectra would miss these requirements even though it could capture the dependence of the rate on the two dipole strengths.

The integral in the denominator of the expression for  $\bar{J}$  normalizes the fluorescence amplitude so that  $F_a$  can be in any convenient units. If  $\epsilon_b$  has the usual units of  $\text{M}^{-1}\text{cm}^{-1}$  and  $\bar{\nu}$  has units of  $\text{cm}^{-1}$ , the overlap integral  $\bar{J}$  will have units of  $\text{M}^{-1}\text{cm}^3$ . The rate constant for resonance energy transfer then is given by

$$k_{rt} = \left( \frac{8.78 \times 10^{23} \kappa^2 \phi_f^o}{n^4 \tau_f^o} \right) |\vec{R}_{ab}|^{-6} \bar{J} \text{ s}^{-1} / (\text{\AA}^{-6} \text{M}^{-1} \text{cm}^3),$$

where  $\phi_f^o$  and  $\tau_f^o$  are the quantum yield and lifetime of fluorescence from molecule  $a$  in the absence of energy transfer, and  $|\vec{R}_{ab}|$  is in  $\text{\AA}$ . The ratio  $\phi_f^o / \tau_f^o$  that appears in this expression is the donor's intrinsic rate constant for fluorescence ( $k_r$  in Fluorescence Yield and Lifetime).

To focus on the effect of the intermolecular distance ( $|\vec{R}_{ab}|$ ), the rate constant for resonance energy transfer often is written as

$$k_{rt} = \frac{1}{\tau_f^o} \left( |\vec{R}_{ab}| / R_o \right)^{-6}.$$

Here  $R_o$  is the intermolecular distance at which  $k_{rt}$  is equal to the overall rate constant for the decay of the excited state by all other mechanisms ( $1/\tau_f^o$ ), so that 50% of the decay occurs by energy transfer.  $R_o$  is

called the *Förster radius*. For energy transfer between two bacteriochlorophyll molecules,  $R_o$  is on the order of 100 Å. Using the above expression for  $k_{tr}$ ,  $R_o$  is given by

$$R_o = 9.80 \times 10^3 (\kappa^2 \phi_f^o n^{-4} \bar{J})^{1/6} \text{ Å}/(\text{M}^{-1} \text{ cm}^3)^{1/6}.$$

Stryer and Haugland (1967) verified the dependence of the energy-transfer rate on the inverse sixth power of the distance by using polypyrrole scaffolds to position energy donors and acceptors at distances ranging from 12 to 46 Å. They found the rate to vary as  $R^{-5.9 \pm 0.3}$ , in good agreement with the theory. Haugland et al. (1969) demonstrated that the rate was proportional to  $\bar{J}$  over a 40-fold range of this parameter.

Several additional points about the Förster theory warrant mentioning here. First, as discussed in Spectral Bandshapes and Dynamics, absorption and emission spectra can be broadened inhomogeneously by interactions of the chromophores with their surroundings. In principle, the spectra that enter into the overlap integral  $\bar{J}$  should not be the inhomogeneously broadened spectra of a large population of molecules, but rather the spectra for an individual donor-acceptor pair. The intermolecular distance  $|\vec{R}_{ab}|$  and the geometric factor  $\kappa^2$  also refer to an individual donor-acceptor pair. Averaging over an ensemble of donor-acceptor pairs with varying spectra or structures should be done at the level of  $k_{tr}$ , not  $\bar{J}$ ,  $|\vec{R}_{ab}|$ , or  $\kappa^2$ . However, the distinction fades if the structures and spectra fluctuate rapidly on the time scale of energy transfer, and the correction may be negligible in many cases even if the fluctuations are slower. A second point to note is that the refractive index  $n$  that appears in the expressions for  $k_{tr}$  and  $R_o$  refers to the medium surrounding the energy donor and acceptor, not to the medium in which the absorption and emission spectra are measured for the calculation of  $\bar{J}$ .

Finally, it is important to remember that the Förster treatment assumes that the donor and acceptor are sufficiently far apart for the point-dipole approximation to be valid. (See Excitons for discussion of this point.) The Förster theory thus cannot necessarily

be applied quantitatively to the closely packed pigments in photosynthetic reaction centers and antenna complexes, although it may provide considerable insight into how changing the absorption or emission spectrum or the arrangement of the chromophores would affect the transfer rate. For recent work on energy transfer in these systems, see Krueger et al. (1998), Scholes et al. (1999, 2001), Sumi (1999), Scholes and Fleming (2000) and Jordanides et al. (2001).

### B. Exchange Coupling

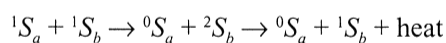
Förster's theory does not account for energy-transfer processes in which the donor and acceptor undergo changes of electron spin. Such changes of spin must occur in order for a molecule in an excited triplet state to transfer its excitation energy to an acceptor and decay to the ground singlet state, raising the acceptor from a singlet to an excited triplet state (see Singlet and Triplet States). These processes can occur by a mechanism known as *exchange coupling*, which was elucidated by D. L. Dexter (1953). In exchange coupling, the donor and acceptor exchange electrons. The donor transfers an electron (with fixed spin  $\alpha$  or  $\beta$ ) to the acceptor, while the acceptor transfers an electron (also with fixed spin) to the donor. If the two electrons have the same spin, the donor and acceptor retain their original spin states. If the electrons have different spins, the result is an exchange of the spin states of the donor and acceptor, singlet for triplet and vice versa, along with a transfer of energy.

In addition to allowing an exchange of spin between the two molecules, exchange coupling allows energy transfer to occur even when the transitions of the individual molecules are formally forbidden because they have very small dipole strengths. Whereas dipole-dipole coupling depends on the product of the two dipole strengths  $D_a$  and  $D_b$  as explained above, exchange coupling is independent of these parameters. However, because the electron-transfer processes that drive exchange coupling require orbital overlap of the electron donor and acceptor, exchange coupling is significant only for molecules that are essentially in contact. For more widely separated

molecules, it is much slower than the Förster mechanism except possibly in cases when  $D_a$  and  $D_b$  are extremely small. Its main importance in photosynthetic systems probably lies in the quenching of excited triplet states of chlorophylls and bacteriochlorophylls by carotenoids. It also underlies reactions of  $O_2$  with chlorophylls or bacteriochlorophylls in excited triplet states, which raise  $O_2$  to an excited singlet state (see Singlet and Triplet States).

### C. Singlet-Singlet Annihilation

Resonance energy transfer can occur between two molecules even if the acceptor, like the donor, is already in an excited singlet state ( $^1S$ ). In this case, the transfer promotes the acceptor to a higher excited state (e.g.,  $^2S$ ), which then usually decays quickly back to the lowest excited singlet state by internal conversion. The overall result of this sequence is degradation of one of the original electronic excitations into heat:



This is called *singlet-singlet annihilation*. Analogous triplet-triplet and singlet-triplet annihilation processes also occur.

The hallmark of singlet-singlet annihilation is a very rapid component in the decay of fluorescence that increases in amplitude quadratically with the excitation irradiance. Because the two excited molecules must be in close proximity in order to interact, the probability of singlet-singlet annihilation depends on the size of the domain over which excitations can migrate by ordinary resonance energy transfer. Measurements of this effect have been used to probe the sizes and organization of photosynthetic antennas. For recent examples, see Westerhuis et al. (1998), Barzda et al. (2001) and Trinkunas et al. (2001). Measurements of singlet-triplet annihilation have been used similarly (Monger and Parson, 1977).

## XVI. Singlet and Triplet States

Many experimental observations can be rationalized

well by treating electrons and protons as point masses with no internal structure. However, observations on the effects of magnetic fields indicate that these particles have an intrinsic angular momentum or 'spin' and an associated magnetic moment. If an electron is placed in an external magnetic field, the projection of its spin angular momentum on the axis of the field always takes on the value of  $\pm \hbar/2$ . The positive and negative values can be described formally by two spin wavefunctions,  $\alpha$  and  $\beta$ , or more loosely as 'spin up' and 'spin down.'

For most organic molecules in their ground state, the highest occupied molecular orbital (HOMO) has two electrons with antiparallel spins. Because we cannot tell which of these electrons has spin  $\alpha$  and which has  $\beta$ , the wavefunction for the ground state is written as a combination of the two possible assignments:

$$\Psi_g = \{\psi_g(1)\psi_g(2)\} \left\{ \frac{1}{\sqrt{2}} \alpha(1)\beta(2) - \frac{1}{\sqrt{2}} \alpha(2)\beta(1) \right\}$$

Here  $\psi_g$  is a wavefunction that depends on position, but not on spin, and the numbers in parentheses are labels for the electrons. The product  $\psi_g(1)\psi_g(2)$  means that both electrons have spatial wavefunction  $\psi_g$ ; and  $\alpha(j)\beta(k)$  means that electron  $j$  has spin wavefunction  $\alpha$  while electron  $k$  has  $\beta$ . The factors of  $1/\sqrt{2}$  normalize the overall wavefunction. For simplicity we have omitted the time-dependent factor  $\exp(-iE_g t/\hbar)$ , where  $E_g$  is the energy of the ground state.

Note that  $\Psi_g$  as written above changes sign if the labels of the two electrons are interchanged. Wolfgang Pauli noted that the wavefunctions of all multi-electronic systems have this property. In other words, the overall wavefunction invariably is 'antisymmetric' for an interchange of the coordinates (both positional and spin) of any two electrons. This principle rests on experimental measurements of atomic and molecular absorption spectra: absorption bands predicted on the basis of antisymmetric electronic wavefunctions are seen, whereas absorption bands predicted on the basis of symmetric electronic wavefunctions are never observed. Its most important ramification is that a

given spatial wavefunction can hold no more than two electrons, which follows because electrons have only two possible spin wavefunctions ( $\alpha$  and  $\beta$ ) and an electron can be described completely by specifying its spatial and spin wavefunctions.

Suppose that a molecule with wavefunction  $\Psi_g$  is excited by light, so that an electron is promoted from the HOMO to the lowest unoccupied orbital (LUMO). If there is no change in the net spin of the system during the excitation, as is usually the case, the spin part of the wavefunction remains the same as for the ground state. But the complete wavefunction for the excited state must represent the two possible ways that electrons 1 and 2 can be assigned to the HOMO and LUMO, and again the wavefunction must change sign if the labels of the electrons are interchanged. A suitable expression is:

$${}^1\Psi_e = \left\{ \frac{1}{\sqrt{2}} \psi_g(1)\psi_e(2) + \frac{1}{\sqrt{2}} \psi_g(2)\psi_e(1) \right\} \left\{ \frac{1}{\sqrt{2}} \alpha(1)\beta(2) - \frac{1}{\sqrt{2}} \alpha(2)\beta(1) \right\},$$

where  $\psi_e$  is the spatial wavefunction for the LUMO. The choice of a + sign for the combination of the spatial terms in the first brackets insures that the overall wavefunction is antisymmetric for an exchange of the two electrons, since a negative sign is used in the second brackets. The state described by such a wavefunction is referred to as a *singlet* state because when the spatial wavefunction is symmetric there is only one possible combination of spin wavefunctions (the one written above) that makes the overall wavefunction antisymmetric. Singlet states often are indicated by a superscript '1' as in  ${}^1\Psi_e$ .

If, instead, we choose the antisymmetric combination

$$\frac{1}{\sqrt{2}} \psi_g(1)\psi_e(2) - \frac{1}{\sqrt{2}} \psi_g(2)\psi_e(1)$$

for the spatial part of the wavefunction for the excited state, then there are three possible symmetric combinations of spin wavefunctions that make the

overall wavefunction antisymmetric:

$${}^3\Psi_e^{+1} = \left\{ \frac{1}{\sqrt{2}} \psi_g(1)\psi_e(2) - \frac{1}{\sqrt{2}} \psi_g(2)\psi_e(1) \right\} \left\{ \alpha(1)\alpha(2) \right\},$$

$${}^3\Psi_e^0 = \left\{ \frac{1}{\sqrt{2}} \psi_g(1)\psi_e(2) - \frac{1}{\sqrt{2}} \psi_g(2)\psi_e(1) \right\} \left\{ \frac{1}{\sqrt{2}} \alpha(1)\beta(2) + \frac{1}{\sqrt{2}} \alpha(2)\beta(1) \right\},$$

and

$${}^3\Psi_e^{-1} = \left\{ \frac{1}{\sqrt{2}} \psi_g(1)\psi_e(2) - \frac{1}{\sqrt{2}} \psi_g(2)\psi_e(1) \right\} \left\{ \beta(1)\beta(2) \right\}.$$

${}^3\Psi_e^{+1}$ ,  ${}^3\Psi_e^0$  and  ${}^3\Psi_e^{-1}$  are the three excited *triplet* states corresponding to excited singlet state  ${}^1\Psi_e$ . The triplet states usually have lower energies than the corresponding singlet state. This is a consequence of the different spatial wavefunctions, not the spin wavefunctions. The antisymmetric spatial wavefunction spreads out over a larger region of space, decreasing the unfavorable interactions between the two electrons. The three triplet states usually have similar energies in the absence of an external magnetic field, but split apart in the presence of a field.

The transition dipoles for transitions from the singlet ground state to excited triplet states are very different from the transition dipole for forming the excited singlet state. The transition dipoles for forming the triplet states are all zero, either because terms with opposite signs cancel or because each term includes an integral of the form  $\langle \alpha(1) | \beta(1) \rangle$ , which evaluates to zero. Excitations from the ground state to an excited triplet state therefore are formally forbidden. In practice, weak optical transitions between singlet and triplet states can be observed in some cases. Triplet states also can be created by *intersystem crossing* from excited singlet states. In most cases, intersystem crossing is brought about by coupling of the spin angular momentum with the local magnetic field due to orbital motion of the electrons. This is called *spin-orbit coupling*.

Most of the photochemical reactions of chlorophylls in solution occur from excited triplet states.

This is because excited triplet states typically have much longer lifetimes than the corresponding excited singlet states (tens or hundreds of microseconds as compared to nanoseconds), giving the excited molecule an extended opportunity to collide with a reaction partner such as  $O_2$ . The initial electron-transfer steps of photosynthesis, however, do not depend on random collisions, and these reactions all occur from excited singlet states. Excited triplet states form only as side reactions, sometimes by intersystem crossing but more commonly by electron-transfer processes in the reaction centers. When a chlorophyll triplet state does form, the excited molecule can transfer an electron to  $O_2$  to generate the superoxide radical ( $O_2^{\cdot-}$ ), which then can participate in a variety of destructive reactions with other cellular components. In addition,  $O_2$  is unusual in that its ground electronic state is a triplet state while its lowest excited state is a singlet state. Transfer of energy and spin from triplet chlorophyll can raise  $O_2$  to the excited singlet state, which again can initiate a variety of destructive reactions such as oxidation of unsaturated lipids. Carotenoids serve to protect photosynthetic antennas and reaction centers from these processes. Energy transfer to a carotenoid from triplet chlorophyll puts the carotenoid in an excited triplet state, but this lies too low in energy to drive formation of either superoxide or singlet  $O_2$ . The carotenoid decays quickly to the ground state with the release of heat.

The relatively long lifetimes of triplet states reflect, in part, the need for spin-orbit coupling to drive the conversion to the singlet ground state. However, the decay of the triplet state usually is much slower than the formation of this state by intersystem crossing from an excited singlet state, even if this also requires spin-orbit coupling. This is because the energy gap between the triplet state and the ground state usually is greater than the gap between the excited singlet state and the triplet state. The extra energy must be converted into highly excited vibrational modes of the molecule in the ground state. As discussed under Internal Conversion, the rate of this process falls off steeply as the energy gap increases.

## XVII. Spectral Bandshapes and Dynamics

### A. Vibronic Transitions

If a molecule in an excited state undergoes a conversion to some other state with a time constant  $\tau$ , the energy of the excited state will have an uncertainty of at least  $\hbar/\tau$ . This relationship can be derived by expressing the wavefunction of the transient state as a sum of wavefunctions for states with a distribution of energies (Atkins, 1993). The uncertainty in the energy manifests itself as a broadening of the absorption spectrum for creating the excited state: the shorter the time constant, the larger the absorption bandwidth. However, a measurement of the bandwidth does not necessarily allow one to determine the time constant, because the shapes and widths of electronic absorption and emission spectra also depend on the coupling of vibrational and electronic transitions and on the interactions of the chromophores with their surroundings. Let us first consider the contributions of vibrational transitions.

The complete wavefunction for a molecule includes nuclear wavefunctions in addition to electronic wavefunctions. Because electrons are much lighter than the nucleus, they move much more rapidly. We therefore can view the electrons as moving in an electric field of static nuclei, and the nuclei as moving in an average field of the electron cloud. This allows us to make the so-called *Born-Oppenheimer approximation*, in which the combined wavefunction is written as a product of separate wavefunctions for electrons and nuclei:

$$\Psi(\vec{r}, \vec{R}) \approx \psi(\vec{r})\chi(\vec{R}),$$

where  $\vec{r}$  and  $\vec{R}$  represent the electronic and nuclear coordinates, respectively. A combination of an electronic wavefunction and a particular nuclear wavefunction is termed a *vibronic level*. The Born-Oppenheimer approximation turns out to be acceptable for most molecules. This is especially important in spectroscopy, because it allows us to assign spectroscopic transitions as being primarily



electronic, vibrational or rotational in nature. It also helps to clarify how the shape of an electronic band depends on temperature and on the nuclear wavefunctions of the ground and excited electronic states.

For a diatomic molecule in a particular electronic state, the potential energy term in the nuclear Hamiltonian is approximately a quadratic function of the distance between the nuclei, with a minimum at the mean bond length. This Hamiltonian gives a set of nuclear (or vibrational) wavefunctions with equally spaced energies,  $E_j = (j + \frac{1}{2})h\nu$ , where  $\nu$  is the classical bond vibration frequency (see Infrared Spectroscopy). These are the *harmonic oscillator* wavefunctions.

Consider a transition from a given vibronic level of the electronic ground state,  $\psi_g(\vec{r})\chi_j(\vec{R})$ , to a particular level of the electronic excited state,  $\psi_e(\vec{r})\chi_k(\vec{R})$ . This transition involves a change from vibrational wavefunction  $\chi_j$  to  $\chi_k$  in addition to a change from electronic wavefunction  $\psi_g$  to  $\psi_e$ . However, the electronic and nuclear parts of the transition dipole usually can be separated, because the nuclei are essentially frozen in position during the excitation. This is known as the *Franck principle*. It also usually proves safe to make the *Condon approximation* that the electronic transition dipole is insensitive to small changes in the nuclear coordinates. With these assumptions, the overall transition dipole,  $\vec{\mu}_{e,k \leftarrow g,j}$ , is the product of a *nuclear overlap integral*  $\langle \chi_j | \chi_k \rangle$  and an electronic transition dipole that is averaged over the nuclear coordinates. The contribution that a particular vibronic transition makes to the overall dipole strength of an absorption band depends on  $|\vec{\mu}_{e,k \leftarrow g,j}|^2$ , and thus on the square of the nuclear overlap integral,  $|\langle \chi_j | \chi_k \rangle|^2$  in addition to the square of the electronic transition dipole. The square of the overlap integral is called a *Franck-Condon factor*. These factors can be calculated by standard formulas for the harmonic oscillator wavefunctions (Manneback, 1951).

The individual vibrational wavefunctions for a given electronic state are orthogonal, which means that  $\langle \chi_k | \chi_k \rangle = 1$  and  $\langle \chi_j | \chi_k \rangle = 0$  for all  $j \neq k$  (see Wavefunctions). Therefore, if the nuclear potential

energy surfaces are the same in the ground and excited electronic states, as shown in Fig. 12a, only transitions between corresponding vibrational levels have non-zero Franck-Condon factors, and these all have the same energy. But if the electronic excitation shifts the minimum of the potential energy surface along the vibrational coordinate, as is likely since it changes the electron distribution in the molecule,  $\langle \chi_j | \chi_k \rangle$  can be non-zero for  $j \neq k$ . The absorption spectrum then will include a family of vibronic transitions with different energies, as illustrated in Fig. 12b. The transition between the lowest vibrational levels of the two electronic states is called the *0–0 transition*. At low temperatures, almost all the molecules in the electronic ground state will be in the lowest vibrational state (the *zero-point* state), and transitions from this state to various vibrational levels of the excited state will contribute a shoulder on the higher-energy (blue) side of the absorption spectrum. At higher temperatures, some molecules will be in higher vibrational levels of the ground state and will contribute shoulders on both the blue and the red sides of the spectrum. Coupled vibrational transitions of solvent molecules will contribute additional, broad ‘phonon wings’ to each vibronic line.

As we discuss in Infrared Spectroscopy, all but the very simplest polyatomic molecules have multiple vibrational modes. To a first approximation, the overall vibrational wavefunction can be written as a product of the vibrational wavefunctions for the individual modes. The overall Franck-Condon factor for a transition then is simply a product of the Franck-Condon factors for all the separate modes. If we are interested in a sample with molecules in a distribution of nuclear states, the effective Franck-Condon factor usually represents a Boltzmann (thermal) average over this distribution.

### B. Homogeneous and Inhomogeneous Broadening

As mentioned above, absorption spectra are broadened by several additional effects. First, there is *lifetime broadening* brought about by the finite lifetime of the excited vibronic state and the time-

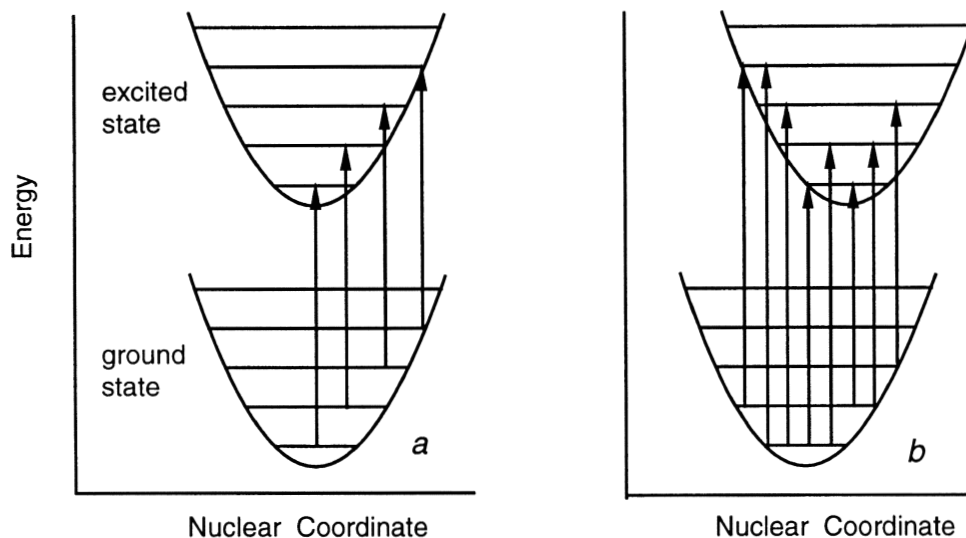


Fig. 12. Vibronic transitions. (a) If the nuclear potential energy surfaces are the same in the ground and excited electronic states, only vibronic transitions between corresponding vibrational levels have non-zero Franck-Condon factors, and the transitions starting in various levels all have the same energy. (b) If the nuclear potential energy surface is displaced in the excited state, vibronic transitions between different vibrational levels have non-zero Franck-Condon factors and the absorption spectrum includes a family of lines with different energies.

energy uncertainty relation ( $\Delta E \approx \hbar/\tau$ ). High-frequency fluctuations of the interactions of the molecule with its surroundings also can cause the energy gap between the excited and ground states to fluctuate rapidly, broadening the absorption line. These two effects contribute *homogeneous broadening*, which is similar for all the molecules in a sample. *Inhomogeneous broadening* occurs when slowly varying interactions with the surroundings give the individual molecules different transition energies. Absorption bands with significant contributions from charge-transfer transitions are particularly sensitive to local electric fields from the surroundings. In most cases, the broadened vibronic absorption lines smear together to give a broad spectrum that cannot be resolved cleanly into its individual components. However, individual absorption lines from molecules in different environments sometimes are well resolved at low temperature. Similar considerations apply to the shapes of fluorescence emission spectra.

### C. Spectral Hole Burning

The contributions of homogeneous and inhomogeneous broadening and phonon wings to individual

absorption lines can be resolved by the technique of *spectral hole burning*, in which a sample is illuminated continuously by a narrow-band laser at a very low temperature (typically  $\leq 4$  K) and the absorption spectrum is measured. Molecules that absorb at the laser frequency are excited selectively. The excited molecules then either undergo a reaction, giving rise to a product with a different absorption spectrum (*photochemical hole burning*) or return to the ground state with a slightly modified configuration or environment, again resulting in a change in absorption spectrum (*nonphotochemical hole burning*). Continued illumination of an inhomogeneous sample depletes the population of molecules that absorb at the laser frequency, 'burning' a trough or 'hole' in the absorption spectrum. The width of the hole at the 0–0 transition energy (the *zero-phonon hole*) provides a measure of the homogeneous broadening, and sometimes can be related to the dynamics of electronic transitions of the excited state. (The energy of the zero-point state can be broadened by electronic transitions, but not by vibrational relaxations.) The relative depths of holes for other vibronic transitions provide information on the Franck-Condon factors

and thus on the displacement of excited-state potential energy curve relative to the ground state. The strength of phonon side-bands provides information on interactions of the excited molecule with its surroundings. Small and his colleagues have applied these techniques to a variety of antenna complexes (Hayes et al., 2000; Jankowiak et al., 2000; Matsuzaki et al., 2000, 2001; Pieper et al., 2000; Ratsep et al., 2000; Wu et al., 2000; Reinot et al., 2001).

Closely related to hole burning is the technique of *fluorescence line-narrowing spectroscopy*, in which the fluorescence spectrum corresponding to the hole in the absorption spectrum is measured. For an application of this method to antenna complexes, see Wendling et al. (2000).

## XVIII. Spontaneous Fluorescence

### A. The Einstein A and B Coefficients

When an absorbing sample is exposed to continuous light, the steady-state rate at which atoms make transitions from the ground state to the excited state ( $rate_{e \leftarrow g}$ ) can be expressed in terms of the number of atoms in the ground state ( $N_g$ ), the dipole strength ( $D$ ) and the incident irradiance. Einstein's inquiry into the rate constants for these processes helped to clarify the distinction between stimulated emission, which is just the reverse of absorption, and the decay of excited states by *spontaneous* fluorescence. Einstein expressed the irradiance in terms of the energy density,  $\rho(\nu)$  (see Electromagnetic Radiation). For the rate of excitation, he obtained

$$rate_{e \leftarrow g} = B\rho N_g,$$

where  $B = 2\pi D/3n^2\hbar^2$ . Similarly, the rate of downward transitions by stimulated emission is

$$rate_{g \leftarrow e} = B\rho N_e,$$

where  $N_e$  is the number of excited molecules. The rate constant  $B$  is often called the *Einstein B coefficient*.

These expressions suggest that the ratio of atoms in the excited and ground states,  $N_e/N_g$ , would go to 1 at thermal equilibrium, when the rates of upward and downward transitions must balance ( $rate_{e \leftarrow g} = rate_{g \leftarrow e}$ ). But this is clearly incorrect: at equilibrium,  $N_e/N_g$  should be given by the Boltzmann expression  $N_e/N_g = \exp\left\{-\left(E_e - E_g\right)/k_B T\right\}$ . There must be another decay mechanism that is independent of the light intensity. If excited atoms can fluoresce spontaneously with rate constant  $A$  (the *Einstein A coefficient*), the total rate of downward transitions will be

$$rate_{g \leftarrow e} = B\rho N_e + AN_e.$$

An expression for  $A$  can be obtained by imagining that the absorbing and emitting species are in a windowless box, in equilibrium with the 'black-body' radiation from the walls of the box. The energy density of black-body radiation can be related to the temperature of the walls, using an expression derived by Planck. If we incorporate this expression for  $\rho(\nu)$  in the above equations for  $rate_{e \leftarrow g}$  and  $rate_{g \leftarrow e}$ , it follows that  $A$  is directly proportional to  $B$ , and hence to  $D$ . The relationship is:

$$A = 8\pi\hbar n^3 \nu^3 c^{-3} B = 32\pi^3 n D / 3\hbar\lambda^3$$

This result has several implications. First, since  $A$  is proportional to  $D$ , strong absorbers are inherently strong fluorescers. Second, other things being equal, the rate constant for fluorescence decreases with the cube of the wavelength. Molecules like chlorophyll and bacteriochlorophyll, which absorb and fluoresce in the red or near-IR region of the spectrum, thus should be less fluorescent than molecules with similar dipole strengths in the blue or UV. (The ratio of the molar absorption coefficient to the dipole strength also depends on the wavelength, but not so strongly. See Dipole Strength for more on this point.)

The reciprocal of Einstein's  $A$  coefficient is the *natural radiative lifetime* ( $\tau_r$ ) for fluorescence. If the excited state decayed solely by fluorescence, then the population of excited molecules created by a short excitation flash would decrease exponentially with a

time constant of  $1/A$ :

$$N_e(t) = N_e^0 \exp\{-t/\tau_r\} = N_e^0 \exp\{-t A\},$$

where  $N_e^0$  is the population at zero time. The observed decay usually is faster than this (i.e., the measured *fluorescence lifetime* is less than  $\tau_r$ ) because other decay mechanisms operate in parallel with fluorescence (see Fluorescence Yield and Lifetime). The lifetime and intensity of the observed fluorescence are, therefore, not predictable from the magnitude of  $A$  alone.

Although the foregoing arguments show that 'spontaneous' fluorescence must occur, they do not say anything about the underlying mechanism of this process. In the quantum theory fluorescence is not really spontaneous, but rather results from interactions with the 'zero-point' level of the radiation field. As described in Electromagnetic Radiation, the quantum states of light have energies  $E_j = (j+1/2)\hbar\nu$ , where the integer  $j$  is the number of photons in the field. The zero-point level refers to  $j = 0$  and  $E_0 = (1/2)\hbar\nu$ . Interactions of an electromagnetic field in this state with an excited molecule can cause the molecule to fluoresce, resulting in an increase in the number of photons in the field from 0 to 1.

### B. The Strickler-Berg Equation

So far, we have considered a system that absorbs and emits at a single frequency. The electronic absorption and emission bands of molecules are broadened by coupling to vibrational transitions and by heterogeneous interactions with the surroundings. Einstein's treatment was extended to such systems by Strickler and Berg (1962), who obtained the expression

$$\frac{1}{\tau_r} = A \approx \frac{8000 \ln 10 \pi c n^2}{\mathcal{N}_A \bar{\lambda}^3} \int \frac{\epsilon}{\nu} d\nu,$$

where

$$\bar{\lambda}^3 = \frac{\int F \bar{\nu}^{-3} d\bar{\nu}}{\int F d\bar{\nu}}.$$

In these expressions,  $F(\lambda)$  or  $F(\bar{\nu})$  is the fluorescence emission intensity at wavelength  $\lambda$  or wavenumber  $\bar{\nu}$ . The integral  $\int \frac{\epsilon(\nu)}{\nu} d\nu$  is taken over the molecule's absorption band, and is proportional to  $D$  (see Dipole Strength). The factor  $\bar{\lambda}^3$  is an average of the  $\lambda^3$  over the fluorescence emission band, and takes the place of the  $\lambda^3$  in the expression relating Einstein's  $A$  coefficient to  $D$ .

The Strickler-Berg expression assumes that thermal equilibration of the excited molecule with its surroundings occurs rapidly relative to the fluorescence lifetime. Although this assumption is not strictly valid in photosynthetic antennas or reaction centers, or even for chlorophylls in solution, the errors in the calculated values of  $\tau_r$  probably are relatively minor.

Ross (1975) showed that the left side of the Strickler-Berg equation also should include the ratio of the vibrational partition functions of the ground and excited states. In the case of bacteriochlorophyll, this factor appears to be close to 1 (Becker et al., 1991), and we have omitted it here for simplicity.

### C. Stokes Shifts

After a molecule is excited, the excess vibrational and rotational energy is lost to the environment very rapidly (usually within a few picoseconds). The excited state also may be stabilized by electronic and nuclear rearrangements of the solvent or protein environment. Consequently, the fluorescing state is lower in energy than the initially produced state and the fluorescence spectrum is shifted to longer wavelengths relative to the absorption spectrum. This shift to the red is termed the *Stokes shift*. It can be resolved temporally after excitation with a short flash, providing information on the dynamics and energetics of interactions of the excited molecule with its surroundings. The dynamics of the Stokes shift typically are multiphasic and can extend from subpicosecond to nanosecond or even microsecond time scales in viscous media.

## XIX. Time-Resolved Spectroscopy

### A. Time-Resolved Fluorescence

Although the rates of excited-state reactions can sometimes be inferred from spectral bandwidths or steady-state fluorescence anisotropy (see Linear Dichroism and Fluorescence Anisotropy), time-resolved measurements are the least ambiguous way of obtaining such information. Time-resolved measurements can be made of either fluorescence emission or changes in light absorption.

There are several ways of resolving the dynamics of excited-state emission, and the choice of technique depends mainly on the time resolution required. In the most straightforward technique, the sample is excited with a short pulse of light and emission perpendicular to the excitation direction is captured with a photodiode interfaced to an oscilloscope or digitizer. The wavelength at which the emission is detected can be selected with dichroic filters or a monochromator. If the emission is weak, a detector with a large gain such as a photomultiplier tube (PMT) or avalanche photodiode can be used. The response time of the detector and digitizer typically is a nanosecond or longer, which is comparable to the decay time of excitations in photosynthetic antenna complexes. This approach therefore has only limited applications in studies of antenna complexes.

A commonly used technique with a higher time resolution is *time-correlated single-photon counting*. Here, the sample is excited with a train of short pulses and the emission at a selected wavelength is detected with a fast PMT or a microchannel plate (MCP) detector. The MCP is an array of thin ( $\sim 10\ \mu\text{m}$  in diameter) capillaries ('channels'), each of which is subject to a large voltage gradient along its length. A photon incident on the detector ejects an electron that dislodges additional electrons as it travels down one of the channels. The short transit distance and the small cross section of the channel ensure that the response time and the spread in transit times are very short ( $\sim 150\ \text{ps}$  and  $\sim 25\ \text{ps}$ , respectively, for currently available detectors). In the photon-counting technique, the excitation and emission intensities are

attenuated until no more than a single emission photon is detected for each excitation pulse. The time at which the photon is detected relative to the excitation is measured, and a histogram is constructed of the number of photons detected as a function of this delay. The histogram is the transient profile of interest. Although a 10-ps wide input pulse is broadened to a 150-ps transient by the MCP and the detection electronics, a mathematical deconvolution procedure allows transients with rise or fall times as short as 30 ps to be measured reliably. Because this is a photon-counting technique, the signal/noise ratio is well characterized and goes as  $\sqrt{N}$ , where  $N$  is the number of photons counted. If  $N$  is sufficiently large, very small changes in the emission kinetics can be resolved.

In another technique, the sample is excited continuously with light whose intensity is modulated sinusoidally at a high frequency, typically on the order of 100 MHz, and the fluorescence signal is measured continuously. The fluorescence lifetime can be calculated from the phase shift of the fluorescence signal relative to the excitation, or from the relative amplitude of the modulation of the fluorescence.

Sub-picosecond time resolution of fluorescence can be achieved with a *streak camera*. Photons reaching the streak camera eject electrons from a photocathode. The electrons are accelerated and made to traverse a time-varying electric field between a pair of deflection plates. Electrons are deflected by varying angles, dependent on their time of arrival at the plates. Photoelectrons corresponding to the tail end of the fluorescence emission arrive later than those corresponding to the early part of the emission, for example. The deflected electrons reach a phosphor screen target, and the glow pattern on the screen is recorded. The temporal emission signal is thus converted to a spatial signal and the relationship between the two signals is determined by the shape of the time-varying field applied to the deflection plates. Time resolutions as high as 200 fs have recently been achieved with this technique. A disadvantage, in addition to the high cost of the instrumentation, is that streak cameras usually require a low-repetition

rate and high excitation irradiance. In photosynthetic antennas, high excitation intensities lead to singlet-singlet annihilation (see Resonance Energy Transfer), complicating the data analysis. For a recent study of an antenna system by this technique, see Gobets et al. (2001).

The method with the highest time resolution is a nonlinear optical method, in which the fluorescence signal is sampled by mixing with a 'gate' light pulse. The time resolution is determined mainly by the widths of the excitation and gate pulses, so that with femtosecond light pulses the time resolution is also in the femtosecond range. The emission from a thin sample is collected and focused along with the gate pulse onto a nonlinear crystal. The combined electric fields of the two pulses interact with the electrons of the crystal to generate a new radiation field at the sum of the frequencies of the two incident fields. This process is known as *fluorescence upconversion*. If the strength of the gate pulse is fixed, the intensity of the upconverted light is proportional to the emission light irradiance. Because polarization of the electrons of the crystal is essentially instantaneous, a necessary condition for upconversion is that the two fields be present simultaneously in the crystal. Typically, the arrival time of the gate pulse is swept across the temporal profile of the emission, and the irradiance of the upconverted light is plotted as a function of the time delay. The timing of the gate pulse is controlled with a motorized delay stage, which typically consists of a retro-reflecting mirror atop a linear slide. The gate beam ray entering the retroreflector is reflected back parallel to the incident ray but with a horizontal displacement, and is steered to the nonlinear crystal. By virtue of the fixed speed of light in air and the folded path of the beam along the delay stage, a movement of  $1.5\ \mu\text{m}$  of the stage changes the timing of the gate pulse by 10 fs. With high-quality slides and linear movements, a resolution of better than 1 fs is attainable. Wavelength selection is accomplished with a spectral filter after the nonlinear crystal and by tuning the angle of the crystal relative the incident beams. Fluorescence upconversion has been used extensively to study energy transfer in reaction centers and antenna complexes (Jimenez et al., 1996; King et al., 2000, 2001).

### B. Time-Resolved Absorbance Changes

In time-resolved absorption spectroscopy, the sample is excited with a short pulse of light and changes in its absorbance are measured as a function of time. As in fluorescence, the simplest method for studying time-resolved absorption also has the lowest time resolution. A weak 'probe' beam and an excitation flash are crossed in the sample, the probe beam is detected after the sample with either a PMT or a photodiode, and the signal is recorded with an oscilloscope or digitizer. A crucial difference between emission and absorption techniques is that the former gives a background-free signal. In absorption, we usually detect a small change superimposed on a large background signal that must be subtracted electronically. The probe beam can also be pulsed such that it lasts only for the duration of the time scan of interest. An intense burst of probe light is advantageous in sub-microsecond measurements because a continuous beam provides too few photons during short time intervals.

Picosecond or femtosecond time resolution can be achieved with a 'pump-probe' sampling technique similar to fluorescence upconversion. The pump and the probe beams are both comprised of short pulses that typically are derived from the same laser source. The time delay between the two pulses is varied by sending one of them through a delay stage. The change in the irradiance of the transmitted probe pulses is obtained as a function of the delay, giving a direct measure of the time-dependent transmittance change.

In contrast to emission spectroscopy, there are several different contributions to the signal in absorption spectroscopy: an increase in transmittance due to loss ('bleaching') of ground-state absorption, a transmittance decrease due to the development of excited-state absorption, and an apparent transmittance increase due to stimulated emission from the excited state. Stimulated emission occurs because the probe beam induces emission from the excited molecules and carries the emitted photons with it (see Spontaneous fluorescence). The relative contributions of these different components depend

on the sample and vary with detection wavelength. If the pump and probe pulses arrive at the sample simultaneously, the sample facilitates an interaction between the pump and the probe pulses such that additional, nonlinear signals are seen. These so-called ‘coherence artifacts’ last approximately for the duration of the temporal overlap. Usually, only the signals seen after the coherent signals have decayed are considered for analysis.

When the pump and the probe pulses are identical in wavelength and no spectral filtering is applied to the probe pulses, measurements of time-resolved changes in transmittance and stimulated emission are often called ‘one-color’ pump-probe spectroscopy. However, the wavelength spectrum of short light pulses can be very broad. A 15-fs pulse at 800 nm has a spectrum with significant intensity over a range of about 100 nm. Changes in transmittance at specific wavelengths therefore can be measured by sending the probe pulse through a monochromator or tunable spectral filter after the sample. A three-dimensional spectrum of transmittance plotted against time along one axis and wavelength along another can be very informative. This method has been called ‘pseudo two-color’ pump-probe spectroscopy, and has been applied with great success to the study of antenna complexes. By using a photodiode array to detect the dispersed probe light, signals at several hundred wavelengths can be recorded simultaneously, reducing the data collection time tremendously.

Focusing a short, intense light pulse into a liquid or glass can generate a short pulse called a *white-light continuum* that spans the 400–1000 nm range. Using such a continuum as a probe pulse makes possible true ‘two-color’ time-resolved spectroscopy.

Another variation of pump-probe spectroscopy is to examine how the delay between the pump pulse and an equally intense probe pulse affects some third property of an excited state, such as the yield of spontaneous emission (Nagarajan and Parson, 2000). Such techniques may have some advantage over conventional measurements of emission dynamics, but have not yet been widely applied.

Time-resolved emission and absorption anisotropy measurements have been used extensively in studies

of energy-transfer kinetics in antenna complexes. If the molecules in a sample are randomly oriented, a linearly polarized excitation beam selectively excites molecules whose transition dipoles are oriented along the polarization direction (see Linear Dichroism and Fluorescence Anisotropy). The emission and absorbance signals with polarizations parallel and orthogonal to the excitation polarization can be used to construct the time-dependent anisotropy signal. The anisotropy can be used to explore the dynamics of depolarization by energy transfer and the spatial distributions of the dipoles at intermediate stages of depolarization (Nagarajan et al., 1999).

## XX. Transition Dipoles

### A. Definition and Interpretation

The electric transition dipole is the fundamental molecular parameter that determines the strengths of most optical absorption bands. It also underlies linear dichroism, the dependence of absorbance on the polarization of the light relative to the molecular orientation. The dipole strength of a spectroscopic transition is the square of the magnitude of the transition dipole.

Classically, the *electric dipole* ( $\vec{\mu}$ ) of a set of charges located at discrete points is a vector  $(\mu_x, \mu_y, \mu_z)$  with  $x$ ,  $y$  and  $z$  components defined by

$$\mu_x = \sum_i q_i x_i,$$

where  $q_i$  and  $x_i$  are the charge and  $x$ -coordinate of charge  $i$ , and similarly for  $\mu_y$  and  $\mu_z$ . For continuous distributions of charge, we can replace the sum by an integral over all space:

$$\bar{\mu}_x = \iiint q(x, y, z) x \, dx \, dy \, dz$$

or

$$\vec{\mu} = \iiint q(\vec{r}) \vec{r} \, dx \, dy \, dz \equiv \int q(\vec{r}) \vec{r} \, d\vec{r},$$



where  $\vec{r}$  is a vector from the origin of the coordinate system to a given point ( $\vec{r} = (x, y, z)$ ).

Now consider a molecule that has two electronic states, a ground state with wavefunction  $\psi_g$  and an excited state with wavefunction  $\psi_e$ . The *transition dipole*,  $\vec{\mu}_{e \leftarrow g}$ , for excitation of an electron from  $\Psi_g$  to  $\Psi_e$  is the vector

$$\vec{\mu}_{e \leftarrow g} = e \int \Psi_e^* \vec{r} \Psi_g d\vec{r},$$

where  $e$  is the charge of an electron. In the bra-ket notation (see Mathematical Tools), this is written

$$\vec{\mu}_{e \leftarrow g} = \langle \Psi_e | e\vec{r} | \Psi_g \rangle = e \langle \Psi_e | \vec{r} | \Psi_g \rangle.$$

A transition dipole is an integral over all space of a product of three quantities: the position vector ( $\vec{r}$ ) and two different wavefunctions ( $\Psi_e^*$  and  $\Psi_g$ ). As discussed in Wavefunctions, both  $\Psi_e^*$  and  $\Psi_g$  depend on time as well as position.  $\Psi_g$  includes the factor  $\exp(-iE_g t / \hbar)$ , where  $E_g$  is the energy of the ground state, and  $\Psi_e^*$  includes the factor  $\exp(iE_e t / \hbar)$ , where  $E_e$  is the energy of the excited state. The transition dipole, therefore, is

$$\vec{\mu}_{e \leftarrow g} = e \langle \Psi_e | \vec{r} | \Psi_g \rangle = e \langle \psi_e | \vec{r} | \psi_g \rangle \exp\{i(E_e - E_g)t / \hbar\},$$

where  $\psi_e$  and  $\psi_g$  are the spatial parts of the wavefunctions. The factor  $\exp\{i(E_e - E_g)t / \hbar\}$  oscillates with time at a frequency proportional to the energy difference between the two states. Transition dipoles differ in this respect from the electric dipole of the system in either the ground or the excited state. These ‘permanent’ dipoles are given by  $\vec{\mu}_g = e \langle \Psi_g | \vec{r} | \Psi_g \rangle = e \langle \psi_g | \vec{r} | \psi_g \rangle$  and  $\vec{\mu}_e = e \langle \Psi_e | \vec{r} | \Psi_e \rangle = e \langle \psi_e | \vec{r} | \psi_e \rangle$ , which are independent of time. The transition dipole  $\vec{\mu}_{e \leftarrow g}$  can have a non-zero magnitude even if  $|\vec{\mu}_e|$  and  $|\vec{\mu}_g|$  are both zero, and vice versa.

The transition dipole also should be distinguished from the change in dipole that accompanies the excitation. This ‘difference dipole’ is  $\Delta\vec{\mu} = \vec{\mu}_e - \vec{\mu}_g = e \langle \Psi_e | \vec{r} | \Psi_e \rangle - e \langle \Psi_g | \vec{r} | \Psi_g \rangle$ , which again is independent of time. The transition dipole can be viewed as an actual oscillating electric dipole associated with a

‘superposition’ state that consists of a linear combination of the ground and excited states.

As mentioned above, the dipole strength of a transition is the square of  $|\vec{\mu}_{e \leftarrow g}|$ . The relationship between the transition dipole and the rate of absorption of light can be derived by starting with the wavefunctions that are solutions to the Schrödinger equation for the absorber in the absence of light, and treating the oscillating radiation field as a perturbation to the Hamiltonian (see Wavefunctions). If the external field oscillates at frequency  $|E_e - E_g|/\hbar$ , the field can interact with the oscillating transition dipole and induce transitions between the two states. The interaction energy is given by the dot product  $\vec{\mu}_{e \leftarrow g} \cdot \vec{E}$ , and the rate of transitions is proportional to  $|\vec{\mu}_{e \leftarrow g} \cdot \vec{E}|^2$ . In this semi-classical picture, the resonance condition for absorption ( $\hbar\nu = \Delta E$ ) is satisfied when the radiation field and the transition dipole oscillate at the same frequency. If the oscillations differ in frequency, the interaction energy will fluctuate between positive and negative values and will average to zero.

Because of the oscillatory time-dependent factor  $\exp\{i(E_e - E_g)t / \hbar\}$ , the absolute sign of the spatial part of a transition dipole is immaterial. Indeed, rotating a molecule by  $180^\circ$  will not affect any measurable spectroscopic properties as long as it does not alter the interactions of the molecule with its surroundings. Transition dipoles thus can be viewed as double-headed vectors. Note that the electric field of light ( $\vec{E}$ ) also oscillates rapidly back and forth along the polarization axis, and that the strength of the absorption depends only on the square of  $\vec{\mu}_{e \leftarrow g} \cdot \vec{E}$ , not the sign of  $\vec{\mu}_{e \leftarrow g} \cdot \vec{E}$  at any particular time. Perhaps for this reason, discussions of transition dipoles often refer only to the spatial factor  $e \langle \psi_g | \vec{r} | \psi_g \rangle$  and neglect the time-dependent factor.

Magnitudes of transition dipoles, like those of permanent dipoles, usually are given in units of debyes (1 debye =  $10^{-18}$  esu cm =  $3.336 \times 10^{-30}$  coulomb m). Because the charge of an electron is  $-4.803 \times 10^{-10}$  esu and  $1 \text{ \AA} = 10^{-8}$  cm, the dipole associated with a pair of positive and negative elementary charges separated by  $1 \text{ \AA}$  has a magnitude of 4.803 debyes.

### B. Theoretical Evaluations of Transition Dipoles

To illustrate the theoretical evaluation of a transition dipole, consider the simple quantum mechanical model of an electron in a one-dimensional box. Figure 13 shows the spatial wavefunction of the ground state ( $\psi_0$ ) and the first two excited states ( $\psi_1$  and  $\psi_2$ ) of this system. Since we have only one positional coordinate ( $x$ ), the transition dipole vector (if nonzero) must be oriented along this axis and we need only evaluate the integral  $e\langle\psi_1|x|\psi_0\rangle$  to obtain  $\vec{\mu}_{1\leftarrow 0}$ , or  $e\langle\psi_2|x|\psi_0\rangle$  for  $\vec{\mu}_{2\leftarrow 0}$ . Inspection of the figure shows that  $\vec{\mu}_{2\leftarrow 0}$  must be zero. This is because  $\psi_2$  and  $\psi_0$  have the same symmetry about  $x = 0$ : the product  $\psi_2(x)\psi_0(x)$  for any given value of  $x$  is the same as  $\psi_2(-x)\psi_0(-x)$ . The positional coordinate  $x$ , however, changes sign at zero, so that the product of  $x$  with  $\psi_2(x)\psi_0(x)$  for any  $x > 0$  is opposite in sign to the corresponding product for  $x < 0$ . The integral of this product over all  $x$  must, therefore, be zero. An excitation for which the transition dipole is zero or very small is said to be ‘forbidden.’

The situation is different for  $\vec{\mu}_{1\leftarrow 0}$  because  $\psi_1$  and  $\psi_0$  have different symmetries:  $\psi_1$  changes sign at  $x = 0$ . The product of  $x$  with  $\psi_1(x)\psi_0(x)$  thus has the same sign for corresponding positive and negative values of  $x$ , and its integral over all  $x$  is non-zero. An excitation with a non-zero transition dipole is said to be ‘allowed.’ Depending on the magnitude of the transition dipole, an excitation also can be described as ‘strongly’ or ‘weakly’ allowed. Strongly allowed transitions typically have transition dipoles between 10 and 100 debyes. Forbidden transitions can become weakly allowed as a result of structural distortions or as a result of interactions with the magnetic field of light.

Although the foregoing discussion might suggest otherwise, shifting the origin of the coordinate system does not affect the magnitude of a transition dipole. This follows from the fact that the wavefunctions are orthogonal, which means that  $\langle\psi_b|\psi_a\rangle = 0$  for any pair of nonidentical eigenfunctions  $\psi_b$  and  $\psi_a$  of the same Hamiltonian (see Wavefunctions). Shifting the origin of the coordinate system by an arbitrary

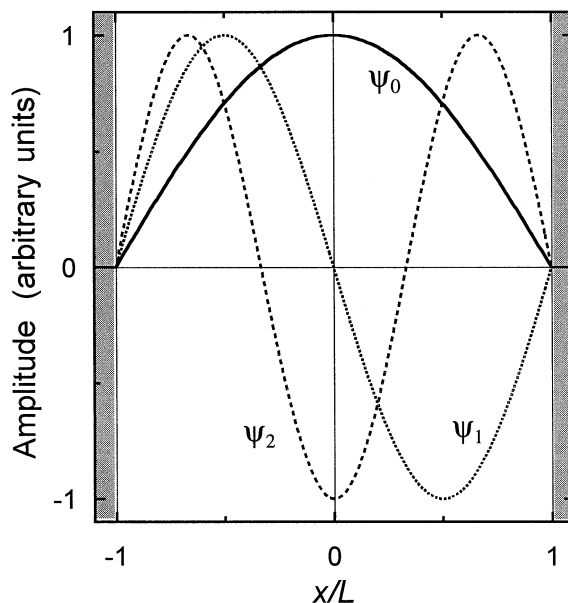


Fig. 13. Spatial wavefunctions for a particle in a one-dimensional box of length  $2L$  with infinitely high walls.  $\psi_0$  is the ground-state (lowest-energy) wavefunction;  $\psi_1$  and  $\psi_2$ , the lowest and next lowest excited states. Outside the box ( $x < -L$  or  $x > L$ , shaded areas), the wavefunctions are zero. Note that the number of times the wavefunction passes through zero inside the box increases progressively with the energy of the corresponding state. Wavefunctions  $\psi_0, \psi_2, \psi_4, \dots$  have ‘even’ or ‘gerade’ symmetry about  $x = 0$ , while wavefunctions  $\psi_1, \psi_3, \psi_5, \dots$  have ‘odd’ or ‘ungerade’ symmetry.

constant vector  $\vec{R}$  simply adds a term of the form  $e\vec{R}\langle\psi_a|\psi_b\rangle$  to the transition dipole, and the integral in this term is zero as long as the wavefunctions are orthogonal.

The transition dipole  $e\langle\psi_1|x|\psi_0\rangle$  for an electron in a box has dimensions of charge times length (esu cm), and its magnitude is proportional to the length of the box. In general, the magnitude of a transition dipole increases with the size of the molecular orbitals of the ground and excited states. Molecules such as chlorophylls and carotenoids, which have highly extended  $\pi$ -electron systems, thus are stronger absorbers than molecules with more localized electrons.

Transition dipoles can be calculated for a molecule with  $\pi$  electrons by writing the spatial wavefunctions as linear combinations of atomic  $p$  orbitals:

$$\psi_a = \sum_{i=1}^n C_i^a u_i,$$

where  $u_i$  represents an atomic  $p$  orbital on atom  $i$  and the sum runs over all the conjugated atoms. The coefficients ( $C_i^a$ ) can be found by standard quantum-mechanical treatments. The transition dipole then is given, to a reasonable approximation, by

$$\bar{\mu}_{e \leftarrow g} = \sqrt{2} e \sum_{i=1}^n C_i^e C_i^g \vec{r}_i,$$

where  $\vec{r}_i$  is the position of atom  $i$ . The factor of  $\sqrt{2}$  in this equation enters because the HOMO usually has two electrons with antiparallel spins, and there are two possible ways of assigning these electrons to  $\psi_g$  and  $\psi_e$  in the excited state. We assume here that the spins remain antiparallel, which means that excited state is a singlet state.

As an example, consider ethylene. The highest occupied molecular orbital (HOMO) of ethylene has a  $\pi$ -type wavefunction that can be approximated as

$$\psi_g = \frac{1}{\sqrt{2}} u_1 + \frac{1}{\sqrt{2}} u_2,$$

where  $u_1$  and  $u_2$  are atomic  $p_z$  orbitals of carbons 1 and 2, respectively. The lowest unoccupied molecular orbital (LUMO) can be represented similarly as

$$\psi_e = \frac{1}{\sqrt{2}} u_1 - \frac{1}{\sqrt{2}} u_2.$$

The HOMO is a bonding orbital, while the LUMO is antibonding. The transition dipole for this pair of orbitals is

$$\bar{\mu}_{e \leftarrow g} = \sqrt{2} e \left\{ \frac{1}{\sqrt{2}} \frac{1}{\sqrt{2}} \vec{r}_1 - \frac{1}{\sqrt{2}} \frac{1}{\sqrt{2}} \vec{r}_2 \right\} = \frac{\sqrt{2}}{2} e \vec{r}_{12},$$

where  $e \vec{r}_{12}$  is the vector from carbon 2 to carbon 1.

This result shows that the transition dipole for raising ethylene to its lowest excited singlet state is directed along the C=C bond, just as the transition dipole for an electron in a one-dimensional box is parallel to the box. Also, as we noted for an electron in a box, the transition dipole for ethylene is predicted to be proportional to the length of the  $\pi$ -system ( $|e \vec{r}_{12}|$ ). There is, however, a limit to this proportionality. If the molecule is stretched much beyond the mean length of a C=C bond, the description of the molecular orbitals as symmetric and antisymmetric combinations of atomic  $p$  orbitals begins to break down, and the electrons localize on one atom or the other. In the limit of widely separated atoms, the wavefunction coefficients become  $C_1^g = \pm 1$ ,  $C_2^g = 0$ ,  $C_1^e = 0$ , and  $C_2^e = \mp 1$ ; the transition dipole then goes to zero because the products  $C_1^g C_1^e$  and  $C_2^g C_2^e$  are both zero.

## XXI. Wavefunctions

### A. Wavefunctions, Operators and Expectation Values

One of the fundamental notions of quantum mechanics is that we can describe a particle such as an electron, or in principle any system, by a mathematical function of position and time  $\Psi(x, y, z, t)$  (or  $\Psi(\vec{r}, t)$ ). This function is called the particle's *wavefunction*. The wavefunction is interpreted as the *probability amplitude* that the particle is at a particular position at a given time. The probability of finding the particle in volume element  $d\vec{r}$  at time  $t$  ( $d\vec{r} = dx dy dz$ ) is  $\Psi^*(\vec{r}, t) \Psi(\vec{r}, t) d\vec{r}$ , where  $\Psi^*$  is the complex conjugate of  $\Psi$ . Hence, the total probability that the particle exists *somewhere* at time  $t$  is  $\int \Psi^* \Psi d\vec{r} = \int |\Psi|^2 d\vec{r}$ . In order for this interpretation to be physically meaningful,  $|\Psi|^2$  must be real, finite, and a single-valued function of position and time. These requirements put restrictions on the wavefunctions for physical systems.

In the bra-ket notation (see Mathematical Tools), the probability that the particle exists somewhere is written  $\langle \Psi | \Psi \rangle$ , which means the same thing

as  $\int \Psi^* \Psi d\vec{r}$ .

$\Psi$  is said to be an *eigenfunction* or *eigenvector* of the operator  $\tilde{a}$  if  $\tilde{a}\Psi = A\Psi$ , where  $A$  is just a number (possibly complex). This is an *eigenvalue* equation, and  $A$  is called the eigenvalue. Multiplying both sides of the eigenvalue equation on the left by  $\Psi^*$  and integrating over all space gives

$$\langle \Psi | \tilde{a} | \Psi \rangle = \langle \Psi | A | \Psi \rangle = A \langle \Psi | \Psi \rangle = A,$$

where we have assumed that the system with wavefunction  $\Psi$  exists, so  $\langle \Psi | \Psi \rangle = 1$ . The integral  $\langle \Psi | \tilde{a} | \Psi \rangle$  has a special meaning: it is the *expectation value* of the observable physical property that corresponds to operator  $\tilde{a}$ . This is the value we are most likely to obtain if we measure the property experimentally, assuming that the measurement is free of systematic errors. Thus if  $\Psi$  is an eigenfunction of operator  $\tilde{a}$ , the eigenvalue  $A$  is the expectation value of a measurement of the corresponding property. This quantum mechanical relationship is analogous to a classical physical equation that states how the property depends on position and time.

The operator that corresponds to the total energy ( $E$ ) of a system is called the *Hamiltonian operator* ( $\tilde{\mathcal{H}}$ ), or simply the Hamiltonian. The Hamiltonian includes terms for kinetic energy, electrostatic interactions of any charged particles in the system, magnetic interactions, and the interactions of the system with any external electromagnetic fields. If  $\tilde{\mathcal{H}}$  operates on the wavefunction of a system, multiplying the result of this operation by  $\Psi^*$  and then integrating over all space gives the expectation value of the total energy:

$$\langle \Psi | \tilde{\mathcal{H}} | \Psi \rangle = E.$$

### B. The Schrödinger Equation

The formal procedure for finding the wavefunction and energy of a system is to solve the *time-dependent Schrödinger equation*, which reads:

$$\tilde{\mathcal{H}}\Psi = i\hbar \frac{\partial \Psi}{\partial t}.$$

If a system is isolated from the surroundings so that its total energy is constant, then the Hamiltonian must be independent of time. In this situation, the wavefunction can be written as the product of two functions, one of which ( $\psi$ ) depends only on position and the other of which ( $\phi$ ) depends only on time. Replacing  $\Psi(\vec{r}, t)$  by  $\psi(\vec{r})\phi(t)$  in the time-dependent Schrödinger equation then leads to the *time-independent Schrödinger equation*:

$$\tilde{\mathcal{H}}\psi = E\psi,$$

where  $E$  (a constant) is the energy. In general, this expression has many solutions ( $\psi_i, \psi_j, \psi_k, \dots$ ), each with its own discrete value of  $E$  ( $E_i, E_j, E_k, \dots$ ). For a bound electron in an atom, the solutions are the familiar atomic orbitals ( $s, p, d, \dots$ ); for an electron in a molecule, they are the molecular orbitals. The energies of a free particle are not quantized (restricted to discrete values), but rather can take on any value.

Once the energy ( $E$ ) is known, the time-dependent Schrödinger equation also leads to a simple differential equation for the  $\phi(t)$ :

$$\frac{\partial}{\partial t} \phi(t) = -\frac{iE}{\hbar} \phi(t).$$

This equation has the solution

$$\phi_k(t) = \exp(-iE_k t / \hbar).$$

(We have omitted a phase shift that represents an arbitrary choice of  $t = 0$ .)  $\phi(t)$  is an oscillatory function that oscillates at frequency  $E_k / 2\pi\hbar$ , or  $E_k/h$ , and has both real and imaginary parts.

Combining the spatial and time-dependent factors, the complete wavefunction is

$$\Psi_k(\vec{r}, t) = \psi_k(\vec{r}) \exp(-iE_k t / \hbar).$$

The time-dependent factor drops out when we calculate the probability function  $|\Psi|^2$  because  $(e^{-ix})^* e^{-ix} = e^{ix} e^{-ix} = 1$ , but it is important for coherence effects and transitions of a system from one state to another.

The eigenfunctions of a constant Hamiltonian represent the possible *stationary states* of the system. A system in one of these states will remain there indefinitely with constant energy as long as the system is not perturbed by outside influences, *i.e.*, as long as the Hamiltonian does not change.

It often is useful to express the wavefunction of a complex system as a linear combination of terms from a set of simpler functions  $u_i(\vec{r})$ :

$$\Psi(\vec{r}, t) = \sum_i c_i(t) u_i(\vec{r}),$$

where the coefficients  $c_i$  are independent of position but can be functions of time. The  $u_i(\vec{r})$  then are said to constitute a *basis*. The wavefunctions of a molecule, for example, can be constructed from a combination of atomic orbitals centered on the individual atoms. The wavefunctions of a time-dependent system can be constructed similarly from the eigenfunctions of a constant Hamiltonian, particularly if the time dependence results from a relatively small perturbation of the system. For such a representation to be most useful, the basis functions must be *orthonormal*, which means that

$$\langle u_i | u_i \rangle = 1$$

$$\langle u_i | u_j \rangle = 0 \text{ for } i \neq j.$$

The eigenfunctions of  $\tilde{H}$  have these properties.

For a brief discussion of the contributions of electronic and nuclear wavefunctions to the overall wavefunction of a molecule, see Spectral Bandshapes. Spin wavefunctions are discussed under Singlet and Triplet States.

### Acknowledgement

Preparation of this chapter was supported in part by NSF grant MCB-9904618.

### References

- Alden RG, Johnson E, Nagarajan V and Parson WW (1997) Calculations of spectroscopic properties of the LH2 bacteriochlorophyll-protein antenna complex from *Rhodospseudomonas sphaeroides*. *J Phys Chem B* 101: 4667–4680
- Amesz J and Hoff AJ (1996) *Biophysical Techniques in Photosynthesis*. Kluwer Academic Publishers, Dordrecht
- Atkins PW (1993) *Molecular Quantum Mechanics*. Oxford University Press, New York
- Barzda V, Gulbinas V, Kananavicius R, Cervinskaskas V, van Amerongen H, van Grondelle R and Valkunas L (2001) Singlet-singlet annihilation kinetics in aggregates and trimers of LHCII. *Biophys J* 80: 2409–2421
- Becker M, Nagarajan V and Parson WW (1991) Properties of the excited singlet states of bacteriochlorophyll-*a* and bacteriopheophytin-*a* in polar solvents. *J Am Chem Soc* 113: 6840–6848
- Beekman LMP, Steffen M, van Stokkum IHM, Olsen JD, Hunter CN, Boxer SG and van Grondelle R (1997) Characterization of the light-harvesting antennas of photosynthetic purple bacteria by Stark spectroscopy. 1. LH1 antenna complex and the B820 subunit from *Rhodospirillum rubrum*. *J Phys Chem B* 101: 7284–7292
- Bixon M and Jortner J (1968) Intramolecular radiationless transitions. *J Chem Phys* 48: 715–726
- Braiman MS and Rothschild KJ (1988) Fourier transform infrared techniques for probing membrane protein structure. *Annu Rev Biophys Chem* 17: 541–570
- Breton J, Verméglio A, Garrigos M and Paillotin G (1981) Orientation of the chromophores in the antenna system of *Rhodospseudomonas sphaeroides*. In: Akoyunoglu G (ed) *Photosynthesis III. Structure and Molecular Organization of the Photosynthetic Apparatus*, pp 445–459. Balaban International Science Services, Philadelphia
- Breton J, Navedryk E, Allen JP and Williams JC (1997) Electrostatic influence of  $Q_A$  reduction on the IR vibrational mode of the 10a-ester C=O of  $H_A$  demonstrated by mutations at residues Glu L104 and Trp L100 in reaction centers from *Rhodobacter sphaeroides*. *Biochem* 36: 4515–4525
- Bublitz G and Boxer SG (1997) Stark spectroscopy: Applications in chemistry, biology and materials science. *Annu Rev Phys Chem* 48: 213–242
- Chynwat V and Frank HA (1995) Application of the energy gap law to S1 energies and dynamics of carotenoids. *Chem Phys* 194: 237–244
- Czarnecki K, Cua A, Kirmaier C, Holten D and Bocian DF (1999) Relationship between altered structure and photochemistry in mutant reaction centers in which bacteriochlorophyll replaces the photoactive bacteriopheophytin. *Biospectrosc* 5: 346–357
- Deng H and Callender R (1999) Raman spectroscopic studies of the structures, energetics, and bond distortions of substrates bound to enzymes. *Methods Enzymol* 308: 176–201
- Dexter DL (1953) A theory of sensitized luminescence in solids. *J Chem Phys* 21: 836–850
- Ebrey TG and Clayton RK (1969) Polarization of fluorescence from bacteriochlorophyll in castor oil, in chromatophores and as P870 in photosynthetic reaction centers. *Photochem Photobiol* 10: 109–117

- Förster T (1965) Delocalized excitation and excitation transfer. In: Sinanoglu O (ed) *Modern Quantum Chemistry, Part III*, pp 93–137. Academic Press, New York
- Frank HA, Bautista JA, Josue JS and Young AJ (2000) Mechanism of nonphotochemical quenching in green plants: Energies of the lowest excited singlet states of violaxanthin and zeaxanthin. *Biochem* 39: 2831–2837
- Gelbart WM, Freed KF and Rice SA (1970) Internal rotation and the breakdown of the adiabatic approximation: Many-phonon radiationless transitions. *J Chem Phys* 52: 2460–2473
- Gobets B, Kennis JTM, Ihalainen JA, Brazzoli M, Croce R, van Stokkum IHM, Bassi R, Dekker JP, van Amerongen H, Fleming GR and van Grondelle R (2001) Excitation energy transfer in dimeric light harvesting complex I: A combined streak-camera/fluorescence upconversion study. *J Phys Chem B* 105: 10132–10139
- Gouterman M (1961) Spectra of porphyrins. *J Mol Spectrosc* 6: 138–163
- Griffiths PR and deHaseth JA (1986) *Fourier Transform Infrared Spectrometry*. Wiley, New York
- Hanson LK (1991) Molecular orbital theory of monomer pigments. In: Scheer H (ed) *Chlorophylls*, pp 993–1014. CRC Press, Boca Raton
- Haugland RP, Yguerabide J and Stryer L (1969) Dependence of the kinetics of singlet-singlet energy transfer on spectral overlap. *Proc Natl Acad Sci USA* 63: 23–30
- Hayes JM, Matsuzaki S, Ratsep M and Small GJ (2000) Red chlorophyll *a* antenna states of Photosystem I of the cyanobacterium *Synechocystis* sp. PCC 6803. *J Phys Chem B* 104: 5625–5633
- Hu X and Spiro TG (1997) Tyrosine and tryptophan structure markers in hemoglobin ultraviolet resonance Raman spectra: mode assignments via subunit-specific isotope labeling of recombinant protein. *Biochem* 36: 15701–15712
- Itoh H and I'Haya Y (1964) The electronic structure of naphthalene. *Theor Chim Acta* 2: 247–257
- Ivancich A, Artz K, Williams JC, Allen JP and Mattioli TA (1998) Effects of hydrogen bonds on the redox potential and electronic structure of the bacterial primary electron donor. *Biochem* 37: 11812–11820
- Jankowiak R, Zazubovich V, Ratsep M, Matsuzaki S, Alfonso M, Picorel R, Seibert M and Small GJ (2000) The CP43 core antenna complex of Photosystem II possesses two quasi-degenerate and weakly coupled  $Q_y$  trap states. *J Phys Chem B* 104: 11805–11815
- Jimenez R, Dikshit SN, Bradforth SE and Fleming GR (1996) Electronic excitation transfer in the LH2 complex of *Rhodobacter sphaeroides*. *J Phys Chem* 100: 6825–6834
- Jordanides XJ, Scholes GD and Fleming GR (2001) The mechanism of energy transfer in the bacterial photosynthetic reaction center. *J Phys Chem B* 105: 1652–1669
- King BA, McAnaney TB, deWinter A and Boxer SG (2000) Excited state energy transfer pathways in photosynthetic reaction centers. 3. Ultrafast emission from the monomeric bacteriochlorophylls. *J Phys Chem B* 104: 8895–8902
- King BA, de Winter A, McAnaney T and Boxer SG (2001) Excited state energy transfer pathways in photosynthetic reaction centers. 4. Asymmetric energy transfer in the heterodimer mutant. *J Phys Chem B* 105: 1856–1862
- Knox RS and Gulen D (1993) Theory of polarized fluorescence from molecular pairs. Förster transfer at large electronic coupling. *Photochem Photobiol* 57: 40–43
- Krueger BP, Scholes GD and Fleming GR (1998) Calculation of couplings and energy-transfer pathways between the pigments of LH2 by the *ab initio* transition density cube method. *J Phys Chem B* 102: 5378–5386
- Kühn O and Sundström V (1997) Pump-probe spectroscopy of dissipative energy transfer dynamics in photosynthetic antenna complexes: A density matrix approach. *J Chem Phys* 107: 4154–4164
- Lakowicz JR (1999) *Principles of Fluorescence Spectroscopy*, 2nd Edition. Plenum Press, New York
- Lapouge K, Naveke G, Gall A, Ivancich A, Seguin J, Scheer H, Sturgis JN, Mattioli TA and Robert B (1999) Conformation of bacteriochlorophyll molecules in photosynthetic proteins from purple bacteria. *Biochem* 38: 11115–11121
- Levine IN (1999) *Quantum Chemistry*. Prentice Hall, Upper Saddle River, NJ
- Lippert E and Macomber JD (1995) *Dynamics During Spectroscopic Transitions*. Springer-Verlag, Berlin
- Manneback C (1951) Computation of the intensities of vibrational spectra of electronic bands in diatomic molecules. *Physica* 17: 1001–1010
- Mäntele W (1993) Infrared vibrational spectroscopy of the photosynthetic reaction center. In: Deisenhofer J and Norris JR (eds) *The Photosynthetic Reaction Center II*, pp 240–284. Academic Press, San Diego
- Mataga N and Kubota T (1970) *Molecular Interactions and Electronic Spectra*. Marcel Dekker, New York
- Matsuzaki S, Zazubovich V, Ratsep M, Hayes JM and Small GJ (2000) Energy transfer kinetics and low energy vibrational structure of the three lowest energy  $Q_y$  states of the Fenna-Matthews-Olson antenna complex. *J Phys Chem B* 104: 9564–9572
- Matsuzaki S, Zazubovich V, Fraser NJ, Cogdell RJ and Small GJ (2001) Energy transfer dynamics in LH2 complexes of *Rhodospseudomonas acidophila* containing only one B800 molecule. *J Phys Chem B* 105: 7049–7056
- Mattioli TA, Lin X, Allen JP and Williams JC (1995) Correlation between multiple hydrogen bonding and alteration of the oxidation potential of the bacteriochlorophyll dimer of reaction centers from *Rhodobacter sphaeroides*. *Biochem* 34: 6142–6152
- McHale JL (1999) *Molecular Spectroscopy*. Prentice Hall, Upper Saddle River, NJ
- Nagarajan V and Parson WW (2000) Femtosecond fluorescence depletion anisotropy: application to the B850 antenna complex of *Rhodobacter sphaeroides*. *J Phys Chem B* 104: 4010–4013
- Nagarajan V, Johnson ET, Williams JC and Parson WW (1999) Femtosecond pump-probe spectroscopy of the B850 antenna complex of *Rhodobacter sphaeroides* at room temperature. *J Phys Chem B* 103: 2297–2309
- Nakanishi K, Berova N and Woody RW, eds (1994) *Circular Dichroism: Principles and Applications*. VCH, New York
- Olsen JD, Sturgis JN, Westerhuis WH, Fowler GJ, Hunter CN and Robert B (1997) Site-directed modification of the ligands to the bacteriochlorophylls of the light-harvesting LH1 and LH2 complexes of *Rhodobacter sphaeroides*. *Biochem* 36: 12625–12632
- Parson WW and Warshel A (1987) Spectroscopic properties of photosynthetic reaction centers. 2. Application of the theory to *Rhodospseudomonas viridis*. *J Am Chem Soc* 109: 6152–6163

- Pieper J, Irrgang KD, Ratsep M, Voigt J, Renger G and Small GJ (2000) Assignment of the lowest  $Q_y$  state and spectral dynamics of the CP29 chlorophyll *a/b* antenna complex of green plants: A hole-burning study. *Photochem Photobiol* 71: 574–581
- Polivka T, Herek JL, Zigmantas D, Åkerlund H-E and Sundström V (1999) Direct observation of the (forbidden) S1 state in carotenoids. *Proc Natl Acad Sci USA* 96: 4914–4917
- Polivka T, Zigmantas D, Frank HA, Bautista JA, Herek JL, Koyama Y, Fujii R and Sundström V (2001) Near-infrared time-resolved study of the S-1 state dynamics of the carotenoid spheroidene. *J Phys Chem B* 105: 1072–1080
- Ramsay GD and Eftink MR (1994) Analysis of multidimensional spectroscopic data to monitor unfolding of proteins. *Meth Enzymol* 240: 615–645
- Ratsep M, Johnson TW, Chitnis PR and Small GJ (2000) The red-absorbing chlorophyll *a* antenna states of Photosystem I: A hole-burning study of *Synechocystis* sp. PCC 6803 and its mutants. *J Phys Chem B* 104: 836–847
- Reinot T, Zazubovich V, Hayes JM and Small GJ (2001) New insights on persistent nonphotochemical hole burning and its application to photosynthetic complexes. *J Phys Chem B* 105: 5083–5098
- Ross RT (1975) Radiative lifetime and thermodynamic potential of excited states. *Photochem Photobiol* 21: 401–406
- Sauer K (1995) *Biochemical Spectroscopy*, Academic Press, San Diego
- Schatz GC and Ratner MA (1993) *Quantum Mechanics in Chemistry*, Prentice Hall, Englewood Cliffs NJ
- Scherz A and Parson WW (1984) Exciton interactions in dimers of bacteriochlorophyll and related molecules. *Biochim Biophys Acta* 766: 666–678
- Scholes GD and Fleming GR (2000) On the mechanism of light harvesting in photosynthetic purple bacteria: B800 to B850 energy transfer. *J Phys Chem B* 104: 1854–1868
- Scholes GD, Gould IR, Cogdell RJ and Fleming GR (1999) Ab initio molecular orbital calculations of electronic couplings in the LH2 bacterial light-harvesting complex of *Rps. acidophila*. *J Phys Chem B* 103: 2543–2553
- Scholes GD, Jordanides XJ and Fleming GR (2001) Adapting the Förster theory of energy transfer for modeling dynamics in aggregated molecular assemblies. *J Phys Chem B* 105: 1640–1651
- Siebert F (1995) Infrared spectroscopy applied to biochemical and biological problems. *Methods Enzymol* 246: 501–526
- Siebrand W (1967a) Radiationless transitions in polyatomic molecules. I. Calculations of Franck-Condon factors. *J Chem Phys* 46: 440–447
- Siebrand W (1967b) Radiationless transitions in polyatomic molecules. II. Triplet-ground-state transitions in hydrocarbons. *J Chem Phys* 47: 2411–2422
- Sosnick TR, Fang X and Shelton VM (2000) Application of circular dichroism to study RNA folding transitions. *Meth Enzymol* 317: 393–409
- Stewart DH, Cua A, Chisholm DA, Diner BA, Bocian DF and Brudvig GW (1998) Identification of histidine 118 in the D1 polypeptide of Photosystem II as the axial ligand to chlorophyll Z. *Biochem* 37: 10040–10046
- Strickler SJ and Berg RA (1962) Relationship between absorption intensity and fluorescence lifetime of molecules. *J Chem Phys* 37: 814–822
- Struve WS (1989) *Fundamentals of Molecular Spectroscopy*. Wiley Interscience, New York
- Stryer L and Haugland RP (1967) Energy transfer: A spectroscopic ruler. *Proc Natl Acad Sci USA* 58: 719–726
- Sumi H (1999) Theory on rates of excitation-energy transfer between molecular aggregates through distributed transition dipoles with application to the antenna system in bacterial photosynthesis. *J Phys Chem B* 103: 252–260
- Trinkunas G, Herek JL, Polivka T, Sundstrom V and Pullerits T (2001) Exciton delocalization probed by excitation annihilation in the light-harvesting antenna LH2. *Phys Rev Lett* 86: 4167–4170
- Warshel A and Parson WW (1987) Spectroscopic properties of photosynthetic reaction centers. 1. Theory. *J Am Chem Soc* 109: 6143–6152
- Wendling M, Pullerits T, Przyjalowski MA, Vulto SIE, Aartsma TJ, van Grondelle R and van Amerongen H (2000) Electron-phonon coupling in the Fenna-Matthews-Olson Complex of *Prosthecochloris aestuarii* determined by temperature-dependent absorption and fluorescence line-narrowing measurements. *J Phys Chem B* 104: 5825–5831
- Westerhuis WHJ, Vos M, van Grondelle R, Ames J and Niederman RA (1998) Altered organization of light-harvesting complexes in phospholipid-enriched *Rhodobacter sphaeroides* chromatophores as determined by fluorescence yield and singlet-singlet annihilation measurements. *Biochim Biophys Acta* 1366: 317–329
- Wilson EB, Decius JC and Cross PC (1955) *Molecular Vibrations*. McGraw-Hill, New York
- Wu HM, Ratsep M, Young CS, Jankowiak R, Blankenship RE and Small GJ (2000) High-pressure and Stark hole-burning studies of chlorosome antennas from *Chlorobium tepidum*. *Biophys J* 79: 1561–1572
- Wynne K and Hochstrasser R (1993) Coherence effects in the anisotropy of optical experiments. *Chem Phys* 171: 179–188
- Zhou H and Boxer SG (1998a) Probing excited-state electron transfer by resonance Stark spectroscopy. 1. Experimental results for photosynthetic reaction centers. *J Phys Chem B* 102: 9139–9147
- Zhou H and Boxer SG (1998b) Probing excited-state electron transfer by resonance Stark spectroscopy. 2. Theory and application. *J Phys Chem B* 102: 9148–9160



# Chapter 4

## The Evolution of Light-harvesting Antennas

Beverley R. Green\*

*Botany Department, University of British Columbia, Vancouver, B.C. Canada V6T1Z4*

Summary .....	130
I. Introduction .....	130
II. Origins .....	131
A. Very Early Evolution .....	131
B. The rRNA 'Tree of Life' and the Five Groups of Photosynthetic Prokaryotes .....	132
III. How Proteins and Their Genes Evolve .....	136
A. How Sequences Change Over Time .....	136
1. Genetic Variation .....	136
2. Gene Duplication Has Played a Major Role in Evolution .....	136
3. Recruitment .....	137
4. Lateral Gene Transfer in Prokaryotes .....	137
5. Gene Transfer from Endosymbiont to Host Nucleus .....	137
6. Time-scale of Cellular Evolution: Adaptations and Catastrophic Extinctions .....	138
B. How Phylogenetic Relatedness is Assessed .....	138
1. Phylogenetic Trees .....	138
2. Rates of Evolution and Mutational Saturation .....	140
3. Some Common Problems with Trees .....	141
4. Gene Clusters—an Additional Source of Information .....	141
IV. Pigment Biosynthesis Genes .....	142
A. Did Chl or BChl Come First? .....	142
B. The Accessory Chls of Chloroplasts and Prochlorophytes .....	143
C. Isoprenoids and Carotenoids .....	144
D. Phycobilin Biosynthesis .....	145
V. Photosynthetic Reaction Centers and the Core Antenna Family .....	145
A. Three-Dimensional Structures of Reaction Centers and Core Antennas .....	145
B. The Core Complex Antenna Family .....	145
1. CP47, CP43 and IsiA .....	146
2. The Pcb's (Prochlorophyte Chl <i>a/b</i> Proteins) .....	147
VI. Phycobiliproteins .....	148
A. The family Tree—Duplication and Divergence .....	148
B. Losses .....	149
C. Cryptophyte Phycobiliproteins .....	150
VII. LHC Superfamily .....	150
A. A Family Unique to Cyanobacteria and Eukaryotes .....	150
B. The Three-helix Light-harvesting Antennas (LHCs) .....	151
1. Phylogenetic Relatedness of the Polypeptides .....	151
2. Reconstitution Experiments Suggest 'Molecular Opportunism' in Chl Binding .....	154
C. ELIPs, Seps and Hlips .....	155
D. Endosymbiosis and the Evolution of the LHC Superfamily .....	155
VIII. Single Membrane Helix Antennas of Purple and Green Filamentous Bacteria .....	155

---

\*Email: [brgreen@interchange.ubc.ca](mailto:brgreen@interchange.ubc.ca)

IX. Antenna Proteins Unique to Certain Groups .....	156
A. Chlorosomes and the FMO Protein of Green Bacteria .....	156
B. Peridinin-Chl a Protein of Dinoflagellates .....	156
X. The Big Picture: The Five Divisions of Photosynthetic Bacteria .....	157
References .....	160

## Summary

Light-harvesting antennas are central players in the conversion of solar energy to chemical energy. They have been evolving since the earliest anaerobic prokaryotes developed the first primitive photosystems. In the modern antennas, we see the results of many common processes of genetic change (duplication, divergence, acquisition and losses) as well as the primary and secondary endosymbiotic events that gave rise to the chloroplasts of photosynthetic eukaryotes. This chapter first reviews the assumptions and methods used in molecular evolution studies, then discusses the evolution of the enzymes involved in the synthesis of light-harvesting chromophores (chlorophylls, bacteriochlorophylls, phycobilins and carotenoids) and the evolution of the protein families that bind them, particular the core complex family, the LHC superfamily, and the phycobiliproteins. It is clear that the evolution of the proteins and the pigments were at least partly independent: ‘molecular opportunism’ resulted in the proteins’ binding whatever pigments were available, leading to the wide variety of chlorophyll-carotenoid pigment complexes that exist today. A model involving lateral gene transfer to account for the sharing of certain antennas by widely separated divisions of photosynthetic bacteria (including cyanobacteria) is proposed.

## I. Introduction

The evolution of light-harvesting systems cannot be separated from the evolution of early life. The development of even the most primitive ability to utilize the sun’s energy gave the earliest photoautotrophs enormously expanded opportunities to proliferate and diversify into new habitats. At the same time, early photoautotrophs would have had to cope with the damaging effects of solar radiation. In their modern descendants, we see a miniscule fraction of the great variety of adaptations to the two-edged sword of solar energy that must have existed during the last two or three billion years.

This chapter will examine the evolution of light-absorbing pigments, the enzymes involved in their

synthesis and the proteins that bind them to make light-harvesting antennas. In doing so, we must also consider the origins of the five groups of photosynthetic prokaryotes and the descendants of one of these groups, the chloroplasts. We will see that the evolution of the pigments and the proteins that bind them were not necessarily coupled. Furthermore, the pervasiveness of lateral gene transfer makes it unlikely that the five extant groups of photosynthetic prokaryotes had a common ancestor, even though their reaction centers and pigment biosynthesis enzymes probably did.

The advent of high through-put genomic and proteomic sequencing is having an enormous impact on the field of molecular evolution. New discoveries casting light on evolutionary processes may soon make some sections of this chapter obsolete. It will soon be possible to calculate phylogenetic trees based on large fractions of complete genomes, rather than a few specific proteins or rRNAs. The genomics capacity that has been applied to sequencing a few model organisms over the last few years is now being turned to other eukaryotes. This will provide the data needed to clarify the origin of chloroplasts and the effects of primary and secondary endosymbiosis on the genes encoding organelle proteins. It also will open up exciting possibilities for in vitro evolutionary

---

*Abbreviations:* BChl, Chl – bacteriochlorophyll, chlorophyll; CP43, CP47 – core antennas of PS II; ELIP – early light-induced protein; EST – expressed sequence tag, a cDNA sequence; Ga – billion years ago; Hlip – high light-induced protein of cyanobacteria; IsiA – Chl a protein induced by Fe limitation, product of *isiA* gene, also called CP43’; LHC – member of light-harvesting complex superfamily; Ohp – one-helix protein of *Arabidopsis*, similar to Hlip; Pcb – prochlorophyte Chl *a/b* protein; PsaA, PsaB – PS I reaction center-core antenna proteins; PS I, PS II – Photosystem I, Photosystem II; Sep – stress-induced two-helix proteins, members of LHC superfamily; RC – reaction center; Ycf17 – plastid open reading frame encoding an Hlip homolog

studies. With enough phylogenetic data, predictions can be made about sequences of ancestral proteins, which can then be synthesized and tested to discover their catalytic abilities (Golding and Dean, 1998; Chang and Donoghue, 2000). Molecular biology approaches make it possible to introduce genes for biosynthetic pathways into organisms that lack them, and observe the results. We may not be able to visit the past, but we can use advances in protein engineering to try out some of the possible scenarios.

## II. Origins

### A. Very Early Evolution

It is thought that the earth originated about 4.5 Ga (billion years before the present) (Chang, 1994) and that life may have originated as early as 4.0 Ga (Fig. 1). The earliest evidence suggestive of life comes from  $^{13}\text{C}/^{12}\text{C}$  ratios typical of fractionation by microbial metabolism, found in sedimentary rocks in Greenland dating from 3.8 Ga (Mojzsis et al., 1996). The earliest putative fossil microorganisms were found in strata dated to about 3.4 Ga (Schopf, 1993, 1994; Pflug, 2001; Schopf et al., 2002), although this claim has been challenged (Brasier et

al., 2002). Fossil prokaryotes are more common and well-documented in strata dated from about 2.8 Ga. Photographs of almost all the microfossils discovered up to 1991 can be found in 'The Proterozoic Biosphere', an enormous compendium edited by Schopf and Klein (1992), which also includes relevant sections on the early atmosphere. A variety of approaches to the study of early life and its environment can be found in the Nobel Symposium volume edited by Bengtson (1994).

Schopf (1993) has suggested that the majority of the early fossil cells were cyanobacteria, based on their size and filamentous nature. There is an unstated assumption here (and in many other papers on early fossil micro-organisms) that the sizes of cyanobacteria-like cells would be similar to those of their modern descendants, which live in much more complex and competitive environments. Pierson (1994) has argued persuasively that some of these fossil microorganisms could equally well have been members of the Chloroflexaceae (green gliding bacteria), and has pointed out the difficulty of distinguishing between phototrophs and chemolithotrophs on the basis of fossil evidence (Pierson, 2001). There are living chemolithotrophic bacteria with cell diameters up to 0.75 mm (Schulz and Jorgensen, 2001) and there may be many other large

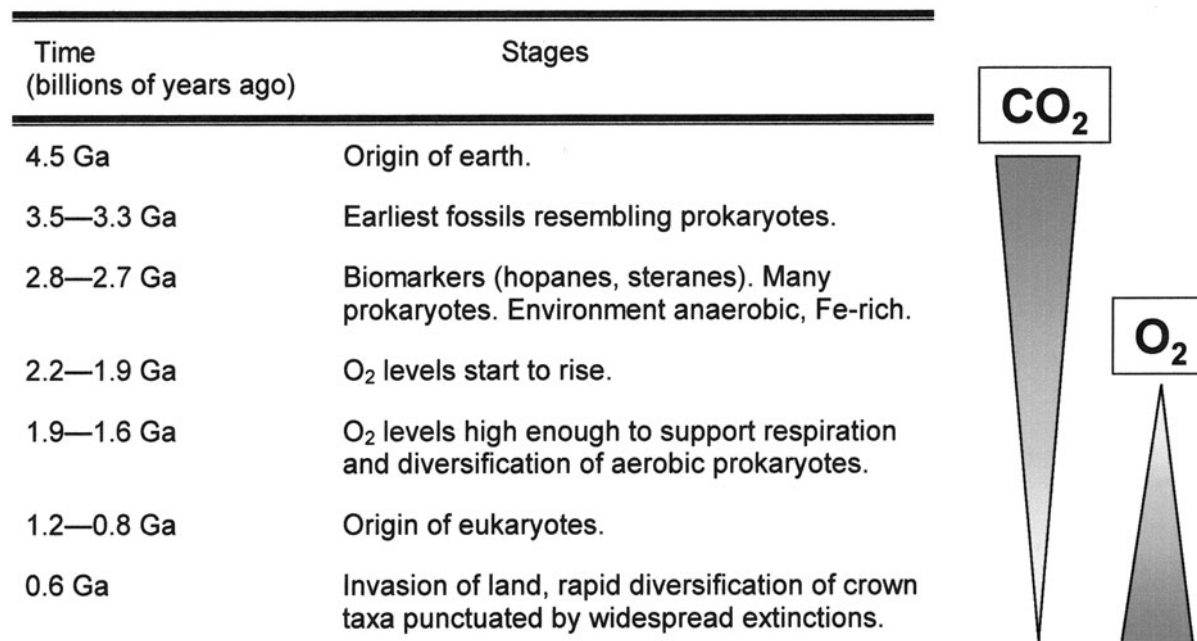


Fig. 1. Time-frame of the evolution of life. Rise of atmospheric oxygen was largely due to oxygenic photosynthesis. Ga, billions of years ago.

prokaryotes in little-explored habitats. Undoubtedly, simpler and smaller prokaryotes preceded the cyanobacteria-like organisms but were not as well preserved. The cyanobacterial electron transport chain with its two photosystems and ability to split water is clearly the result of extensive prior evolution. The very first living cells were probably chemolithotrophs, followed by simple photoautotrophic anaerobes (Nisbet and Sleep, 2001). To what extent these early photosynthesizers resembled modern obligate anaerobes such as the green sulfur bacteria is an open question.

It is now believed that the original atmosphere of the earth was anoxic and mildly reducing (Kasting et al., 1992; Kasting, 1993; Holland, 1994), and that most of the oxygen in the earth's present atmosphere is the result of oxygenic photosynthesis. A widely-cited model of atmospheric evolution (Kasting, 1993) suggests that  $O_2$  levels rose from  $10^{-4}$  to  $10^{-2}$  of present atmospheric levels sometime between 2.2 and 1.9 Ga (Holland, 1994). This is consistent with the increasing abundance of fossil cyanobacteria, and with the existence of 'red beds,' which are strata high in iron oxides. The rise in atmospheric  $O_2$  caused the oxidation of most of the available iron to Fe(III) and its subsequent precipitation. The resulting Fe limitation created serious nutritional deficiencies that have had evolutionary consequences to the present day (Section V; Chapter 17, Grossman et al.; Raven et al., 1999). By 1.9–1.6 Ga,  $O_2$  is thought to have reached 1–4% of present atmospheric levels (Kasting, 1993; Holland, 1994). This would have been enough to support extensive diversification of obligately aerobic heterotrophs. Much later (0.5–0.6 Ga), another big jump in  $O_2$  levels may have facilitated the Cambrian explosion of multicellular eukaryotes (Knoll, 1992).

Other evidence for the early existence of cyanobacteria-like organisms comes from molecular biomarkers, a different kind of fossil (Simoneit et al., 1998; Hayes, 2000; Moldowan and Jacobson, 2000). These molecules are the reduced carbon skeletons of biogenic macromolecules, in particular hopanes (from bacteriohopanepolyols) and steranes (from cholesterol and other steroids). In two recent studies, 2-methylhopanoids, characteristic of modern cyanobacteria, were found in two separate locations dated 2.5 and 2.7 Ga (Summons et al., 1999; Brocks et al., 1999). Given that cyanobacteria with their sophisticated electron transport chain could not have been the first cells to evolve, this would push back the

origin of cellular life to before 3 Ga.

There is no general agreement on when eukaryotes originated (Knoll, 1992; 1994). The earliest apparently eukaryotic fossil is a spiral-shaped organism named *Grypania* found in 2.1 Ga rocks (Han and Runnegar, 1993). The only evidence that it was a eukaryotic alga is its large size and apparent rigidity. However, the discovery of steranes as well as hopanes in 2.7 Ga shale (Brocks et al., 1999) suggests that organisms able to synthesize cholesterol could have been extant more than two billion years ago. This ability is now largely restricted to eukaryotes, but there is nothing to rule out the possibility that these biomarkers were left by one of the prokaryotic ancestors of eukaryotes. Large (up to 160  $\mu m$ ) spherical microfossils with processes suggestive of an underlying cytoskeleton have been found in 1.5 Ga shales (Javaux et al., 2001), and recognizable multicellular red algal fossils have been dated to about 1.2 Ga (Butterfield et al., 1990; Butterfield, 2000). There have been several claims that dinoflagellates and brown algae were in existence as early as 0.60–0.55 Ga (Butterfield and Rainbird, 1998; Xiao et al., 1998; Talyzina et al., 2000). If these are correct, the secondary endosymbioses that gave rise to these groups would have happened relatively soon after the primary endosymbiotic event that gave rise to the chloroplast. A summary of the major stages in the evolution of life and the atmosphere is given in Fig. 1.

### *B. The rRNA 'Tree of Life' and the Five Groups of Photosynthetic Prokaryotes*

As soon as protein sequencing methodology became available in the 1960s, it was applied to the study of evolutionary relationships, particularly in the pioneering work of Margaret Dayhoff and her collaborators (Dayhoff et al., 1978; Schwartz and Dayhoff, 1978). From the very beginning, it was clear that proteins with the same function from different organisms resembled each other, and that the degree of difference between sequences was roughly proportional to the evolutionary distance deduced from well-dated fossils. The genes now most commonly used in studying the relationships among groups of organisms are those encoding the two ribosomal RNAs. Because ribosomal structure must be extremely conservative for functional reasons, the rRNA sequences have changed very slowly, so it is possible to compare sequences across large evolutionary distances. Furthermore, rRNA

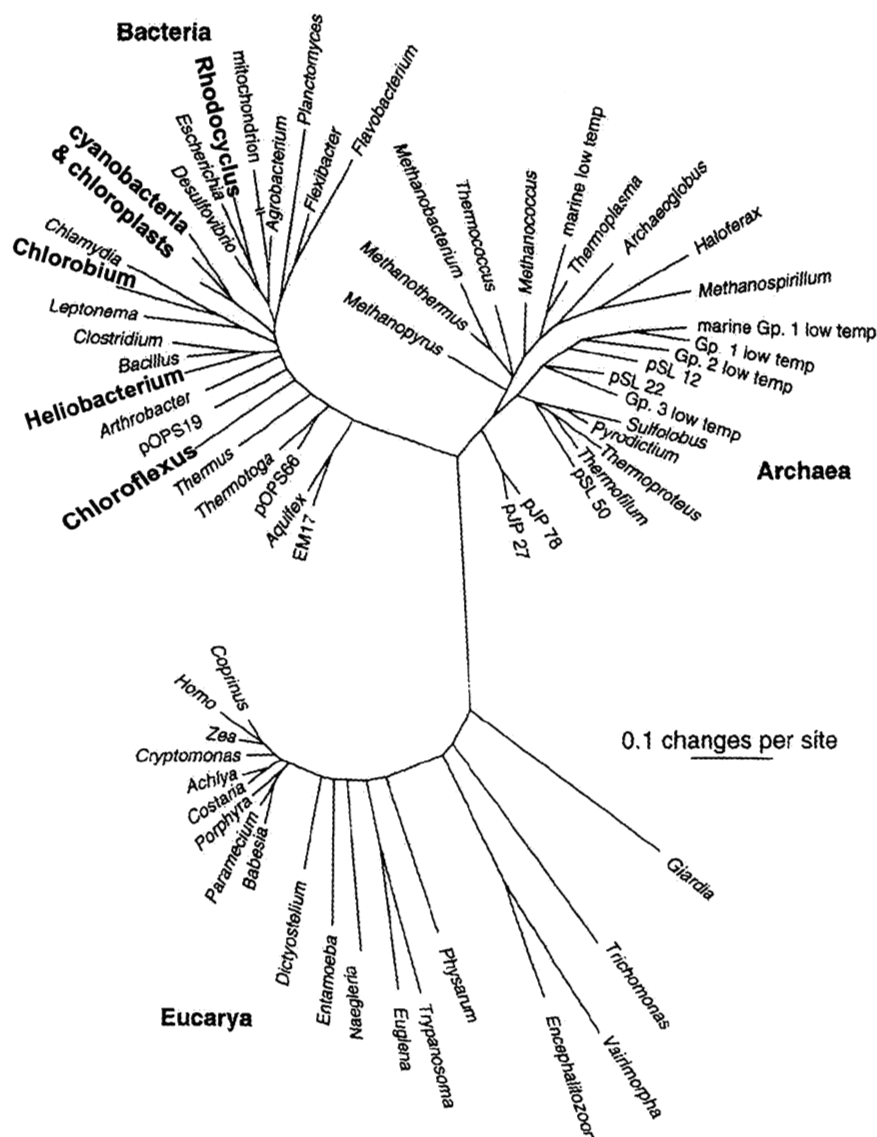


Fig. 2. Tree of Life based on 16S rRNA sequences showing the three domains of life. Representatives of the five groups of photosynthetic eubacteria are in bold. Adapted from Pace (1997).

genes are relatively large and therefore have a higher information content than most protein-coding genes. There is now an enormous database of rRNA sequences covering both prokaryotes and eukaryotes (<http://rrna.uia.ac.be>).

The sequencing of rRNA from many organisms yielded a 'Tree of Life' (Fig. 2), whose major feature was the division of all living organisms into three domains, Eubacteria, Archea (archebacteria) and Eucarya (eukaryotes) (Woese, 1987; Woese et al., 1990; Olsen et al., 1994). There is little argument about this fundamental division, which is supported

by many cellular attributes (Madigan et al., 1996; Pace, 1997), but there has been extensive debate over the location of the 'root' of the tree of life (Doolittle, 1995, 2000; Katz, 1998). Was the last common ancestor somewhere between the archebacteria and the eubacteria, with the eukaryotes being derived from one of these groups, or was it between the eukaryotic (nuclear) ancestor and the prokaryotic groups? The rRNA trees favor the former idea with eukaryotes being closer to archebacteria (Woese, 1987), but trees based on protein coding genes (Viale et al., 1994; Brown and Doolittle, 1997) and conserved

indels (insertions and deletions) (Gupta, 1998) give a variety of answers. It has become clear that the eukaryote genome is a mosaic of genes, some of which are closer to those of eubacteria and others closer to those of archaea (Golding and Gupta, 1995; Brown and Doolittle, 1997; Gupta, 1998; Katz, 1998; Rivera et al., 1998; Doolittle 1999). This has led to interesting hypotheses about how eukaryotes could have arisen from a fusion or symbiosis between a eubacterium and an archaebacterium (Doolittle, 1995; Gupta and Golding, 1996; Martin and Müller, 1998; Katz, 1998; Lopez-Garcia and Moreira, 1999; Martin, 1999).

In considering the evolution of photosynthesis and light-harvesting antennas, we first need to look at the photosynthetic prokaryotes. The only simplifying fact about these organisms is that they are all eubacteria! No photosynthetic archaebacteria have (yet) been discovered. The photosynthetic eubacteria fall into five distinct groups (Table 1), which are clearly separated from each other by both physiological and molecular sequence criteria (Blankenship, 1992, 1994; Stackebrandt et al., 1996; Madigan et al., 1996; Gupta et al., 1999; Olson, 2001). All the cyanobacteria are phototrophs, as are all the Chlorobiaceae (green sulfur bacteria), but the closest relatives of the heliobacteria are non-photosynthetic, low G+C, Gram-positive clostridia. The phototrophic members of the proteobacteria are scattered throughout that division, interspersed with non-photosynthetic relatives.

Unfortunately, the order in which the major eubacterial divisions diverged from each other cannot be resolved by molecular phylogeny (Woese, 1987; Stackebrandt et al., 1996; Hugenholtz et al., 1998).

This is due to two major factors. First of all, there have been so many changes over the three billion or more years since divergence from a common ancestor that even long sequences are mutationally saturated (Philippe and Forterre, 1999). Trees based on 16S and 23S rRNA sequences (Fig. 2), generally agree in showing that the deepest (earliest) phototrophic branch includes the green non-sulfur (gliding) bacteria such as *Chloroflexus* and *Heliothrix* (Woese, 1987; Stackebrandt et al., 1996), whose closest relatives are the *Deinococcus/Thermus* group. However, analysis of shared indels in heat-shock proteins suggested that the low G+C Gram-positive group that includes *Helio bacterium* was the earliest branching (Gupta, 1998; Gupta et al., 1999). The other major groups containing phototrophs appear to have radiated from each other within a short period of time (Woese, 1987; Ludwig and Schleifer, 1994; Hugenholtz et al., 1998). In some rRNA and protein trees, the cyanobacterial branch groups with the Gram-positive and proteobacterial branches (Woese, 1987; Viale et al., 1994), in some just with the Gram-positives (Hansmann and Martin, 2000), and in others with neither (Ludwig and Schleifer, 1994; Olsen et al., 1994). Trees based on proteins of the cytochrome *bc* complex have been interpreted as supporting clustering of cyanobacteria, Chlorobiaceae and Gram-positives, but the branches have low statistical support (Schütz et al., 2000).

The second major problem is lateral gene transfer. Analysis of whole genomes has provided solid evidence for a significant amount of lateral gene transfer between prokaryotic groups, even between archaebacteria and eubacteria (Rivera et al., 1998; Doolittle, 1999, 2000; Ochman et al., 2000; Koonin

Table 1. Photosynthetic prokaryotes and their light-harvesting antennas

Common Name	Taxonomic Group	Reaction Center	RC/core pigment	RC/core protein	Core Antenna	Peripheral Antennas
Heliobacteria	Low G+C Gram +	FeS-type	BChl <i>g</i>	PshA homodimer	Part of RC	none
Green sulfur bacteria	Chlorobiaceae	FeS-type	BChl <i>a</i>	PscA homodimer	Part of RC	Chlorosomes, FMO protein
Green nonsulfur (gliding) bacteria	Chloroflexaceae	Q-type	BChl <i>a</i>	L/M heterodimer	LH1	Chlorosomes
Purple bacteria	Proteobacteria	Q-type	BChl <i>a</i> or <i>b</i>	L/M heterodimer	LH1	LH2, LH3
Cyanobacteria	Cyanobacteriaceae	FeS-type (PS I)	Chl <i>a</i>	PsaA/PsaB heterodimer	Part of RC	Phycobilisomes?
		Q-type (PS II)	Chl <i>a</i>	D1/D2 (PsbA/D) heterodimer	CP47/CP43 (PsbB/PsbC)	Phycobilisomes

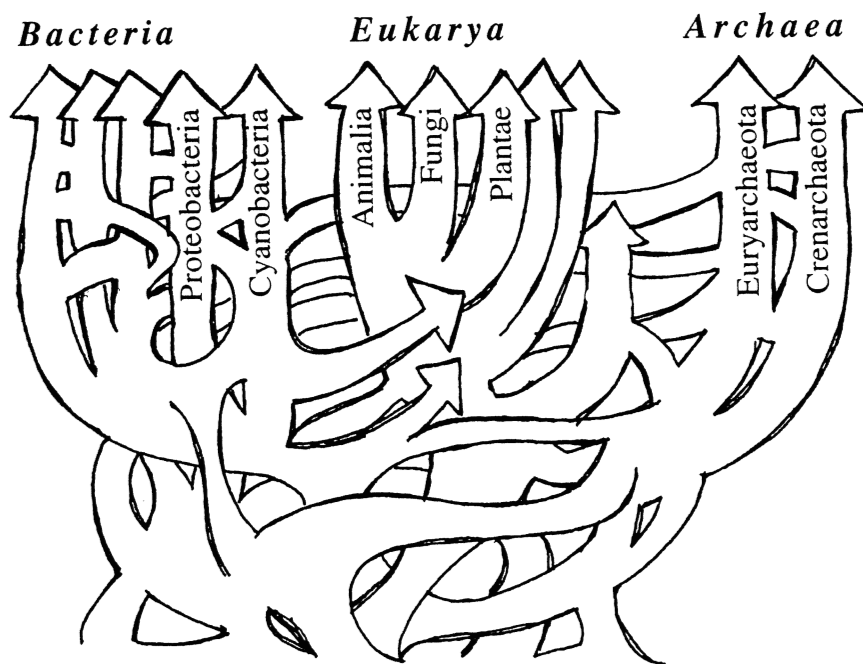


Fig. 3. Web of Life, taking into account lateral (horizontal) gene transfer. Adapted from Doolittle (1999).

et al., 2001; Raymond et al., 2002). What this means is that a modern prokaryote does not have a single line of descent from an ancestral prokaryote (Woese, 1998; Doolittle, 1999; Martin, 1999). The 'Tree of Life' (Fig. 2) is much closer to a 'Web of Life' (Fig. 3) (Doolittle, 1999). This has profound implications with respect to the origin of photosynthesis. Given the evidence for extensive lateral transfer between unrelated prokaryotes, we do not have to postulate a single common ancestor for all photosynthetic eubacteria. What we are analyzing at the level of primary sequence or three-dimensional structure is really the evolution of the protein or the protein family, not the evolution of its owners. We can quite legitimately restrict ourselves to studying the evolution of photosynthetic pigments, reaction centers and light-harvesting antennas without having to reconcile their evolution with the evolution of large groups of prokaryotes.

The way we look at photosynthetic reaction centers has changed dramatically over the last few years. Photosynthetic reaction centers (RC) have been traditionally classified as PS I-like, with FeS acceptors (FeS-type) or as PS II-like, with mobile quinones as acceptors (Q-type) (Nitschke and Rutherford, 1991; Blankenship, 1992). The heliobacteria and green sulfur bacteria have FeS-type RCs and are obligate

anaerobes (Table 1). However, the heliobacteria have BChl *g* (an isomer of Chl *a*) rather than BChl *a* in their RCs, and they do not have the chlorosomes and Fenna-Matthews-Olson protein that make up the peripheral antenna system of the Chlorobiaceae (Chapter 1, Green and Anderson; Chapter 6, Blankenship and Matsuura). In contrast, the green gliding bacteria (Chloroflexaceae) and the purple bacteria share Q-type RCs and LH1 antennas that have significant sequence similarity with each other, and both are generally facultative anaerobes, growing photosynthetically only in the absence of oxygen (with some exceptions, Chapter 5, Blankenship and Matsuura; Chapter 17, Young and Beatty). Among the prokaryotes, only the cyanobacteria have two photosystems and the ability to oxidize water.

How did five such very different groups of photosynthetic prokaryotes arise? Did any of them share a common ancestor to the exclusion of the others? Comparison of the recently determined 3D structures of Photosystem I (Schubert et al., 1998) and Photosystem II (Nield et al., 2000; Zouni et al., 2001) with the purple bacterial reaction center (Michel and Deisenhofer, 1988) show clearly that all the RCs are related structurally, as had been suggested earlier on spectroscopic grounds (Nitschke and Rutherford, 1991; Golbeck, 1993). In other words,



all photosynthetic reaction centers, whether they are FeS-type or Q-type, probably had a common ancestor. Although similar structures can arise by convergent evolution (reviewed in Russell, 1998) it is very unlikely that a structure as complex as a reaction center could have originated more than once. The possibility that the photosynthetic reaction centers of one or more of the five groups were acquired by lateral gene transfer is discussed further in Section X.

### III. How Proteins and Their Genes Evolve

In order to clarify some of the complications in dealing with molecular evolution over very long time-scales, we will first consider how protein sequences evolve and how their evolution is studied.

#### A. How Sequences Change Over Time

##### 1. Genetic Variation

Genetic material is not constant, but is continually undergoing small changes such as point mutations and small insertions and deletions (indels), and larger changes involving recombination and transposition. The smaller changes, quantified in terms of nucleotide or amino acid differences, are most useful for the derivation of phylogenetic trees. Most of the changes that occur do not become fixed in the population. Of those that are fixed, many cause no change at the protein level (due to the redundancy of the genetic code) or cause changes that are effectively neutral. A very small number may provide a selective advantage. Not all positions in a protein-coding gene will change at the same rate, since amino acids at the active site and in the hydrophobic core of the protein must be conserved, whereas residues on the surface of the molecule may be more free to vary. Different selective pressures also mean that different genes will have different rates of change. Even for the same gene, the rate of sequence change will not be constant over time.

The larger changes are not as easy to quantify, but are extremely important in providing genetic variability. Recombination provides a mechanism for shuffling of functional modules and the formation of novel combinations of domains, and it can result in the duplication or deletion of part or all of a gene. The result of domain shuffling is that there are many protein motifs that are widely distributed among

various protein families, e.g. ATP-binding motifs. Generation of different combinations of motifs/domains can provide the raw material for evolving new functions, and the formation of dimers or tetramers can introduce the possibility of allosteric control. The 1500 transcription factors of *Arabidopsis* show the wealth of combinatorial possibilities in regulating gene expression (Reichmann et al., 2000).

#### 2. Gene Duplication Has Played a Major Role in Evolution

Each new genome sequenced has reconfirmed Ohno's thesis that gene duplication played a major role in evolution (Ohno, 1970). The first careful analyses of the *E. coli* genome (Blattner et al., 1997; Riley and Labedan, 1997) showed that even in a prokaryote, many genes are members of gene families. This has been confirmed for every prokaryote and every eukaryote sequenced. In the case of *Arabidopsis*, 17% of the genes belong to gene families arranged in tandem arrays, showing their origin from small local duplications. Further, in several eukaryotic genomes it appears that whole sections have been duplicated (Wolfe and Shields, 1997; The Arabidopsis Genome Initiative, 2000), even in *Arabidopsis*, which was chosen as a model plant system because of its small genome size (Vision et al., 2000). The current model suggests that there was at least one complete duplication of the genome (tetraploidization) and many duplications of whole chromosome segments, each one followed by loss of some of the duplicated genes (Vision et al., 2000). Losses as well as gains contribute to diversification (Cavalier-Smith, 2002).

Gene duplication provides the raw material for adaptive evolution and the origin of novel functions. Once a gene has duplicated, it frees one of the copies from selective constraints so it can adapt to perform modified functions. This does not necessarily require the accumulation of a large number of small changes, but can happen with a single amino acid substitution (Golding and Dean, 1998), as in the case of the conversion of lactate dehydrogenase to malate dehydrogenase (Wilks et al., 1988). Most enzymes catalyze side-reactions, which means that one copy of an enzyme could undergo modifications that would make the minor activity the dominant one (O'Brien and Herschlag, 1999). Theoretical analysis suggests that both copies of a gene could diverge and lose activity as long as the total activity maintained the required level of functionality (Force et al., 1999;

Lynch and Force, 2000). Duplicate genes can be regulated independently, and divergence of 5' non-coding sequences involved in transcriptional regulation can facilitate the divergence of coding sequences (Force et al., 1999). Copies can also provide spare parts for domain shuffling and can originate new combinations of functions.

Most of the light-harvesting antenna proteins are members of large gene families, providing good examples of the possibilities created by gene duplication and divergence. With the exception of antennas unique to one or two taxonomic groups (Section VIII), the proteins of all the other antennas are members of just three extended families: the Core Complex family (Section V), the phycobiliprotein family (Section VI), and the LHC superfamily (Section VII) (Green and Durnford, 1996). The LHC superfamily was one of the first plant gene families to be recognized as such (Green et al., 1991). In fact, this family is not restricted to plants but has left a trail of relatives all the way from cyanobacterial genomes to the nuclear genomes of algae that obtained their chloroplasts by secondary endosymbiogenesis (Section VII; Chapter 1, Green and Anderson). In spite of the fact that there are only four kinds of light-harvesting chromophore (Chls, BChls, carotenoids and phycobilins), the proteins of the three families achieve flexibility in pigment binding by a range of variations on the three basic structural themes. In the course of evolution, this flexibility allowed them to continue to function while accumulating adaptive changes that optimized chromophore binding and allowed for fine-tuning of absorption maxima. This 'molecular opportunism' in binding whatever pigments were available also reinforces that idea that the proteins have evolved at least partly independently of the enzymes for pigment biosynthesis (Green, 2001).

### 3. Recruitment

Sometimes a protein can be recruited to an entirely new function. Lens crystallins, for example, have been recruited from different common enzymes in different vertebrates (Wistow, 1993). This may or may not involve gene duplication, and differences in function may even occur between two different locations in the same cell (Jeffery, 1999). These 'moonlighting proteins' can be advantageous for the cell by coordinating functions, and they illustrate the principle that 'organisms evolve by making use of

whatever is available' (Jeffery, 1999). However, they provide an unwanted complication for genomics researchers who are trying to identify open reading frames!

### 4. Lateral Gene Transfer in Prokaryotes

As pointed out in Section IIB, a major finding from the explosion of prokaryotic genome sequences is the prevalence of lateral gene transfer between distantly-related prokaryotes (Eisen, 2000; Ochman et al., 2000; Koonin et al., 2001). Genes involved in operational processes, e.g. metabolic pathways, are more likely to be transferred than are informational genes, i.e. those for transcription or translation (Jain et al., 1999). Genome-wide comparisons of the first 16 prokaryote genomes completely sequenced estimated the fraction of laterally-acquired sequences to be as high as 12% in *E. coli* K12 and 16% in *Synechocystis* 6803 (Ochman et al., 2000). Furthermore, there is strong evidence for gene transfer between archaea and eubacteria, especially in the thermophilic eubacteria *Aquiflex* and *Thermotoga*, which appear to have acquired their abilities to adapt to extreme temperatures by acquiring a significant number of genes from thermophilic archaebacteria (Deckert et al., 1998; Nelson et al., 1999). In the green sulfur bacterium *Chlorobium*, 12% of the genes more closely match archaeal than eubacterial homologs (Eisen et al., 2002). Although the estimated number of transferred genes depends on the methodology employed (Lawrence and Ochman, 2002; Ragan, 2002; Ragan and Charlebois, 2002), there is no doubt that there has been a significant amount of lateral transfer even between distantly related prokaryotes.

### 5. Gene Transfer from Endosymbiont to Host Nucleus

Understanding how endosymbionts became organelles is probably the most challenging question in evolutionary cell biology (Cavalier-Smith, 2000). Many genes were transferred from the eubacterial ancestors of mitochondria and chloroplasts to the nuclear compartments of their eukaryotic hosts during the primary endosymbioses. This process cannot be regarded as a number of simple translocations, since each transfer actually required several steps: (a) The integration of a *copy* of an organelle gene into the nuclear genome, (b) the acquisition or modifi-

cation of promoter sequences allowing the gene to be expressed in its new environment, (c) for those proteins that would be targeted back to the organelle, the acquisition of suitable presequences, and (d) the eventual elimination of the organelle's copy. Of course, many of the endosymbiont genes could be dispensed with since their functions would be provided by the host's nuclear genes. However, there are some cases where an endosymbiont gene replaced the host gene in the host's nucleus. It appears that some (cytosolic) glycolytic enzymes may have originated from the proteobacterial ancestor of the mitochondrion (Martin and Herrmann, 1998). Similarly, it appears that plant cytosolic phosphoglycerate kinase is of cyanobacterial origin (Martin and Schnarrenberger, 1997). Preliminary analysis of the *Arabidopsis* genome uncovered over 800 nuclear genes most closely matching cyanobacterial genes, and only 25% of those had a predicted chloroplast targeting presequence (Arabidopsis Genome Initiative, 2000). Martin et al. (2002) have estimated that as many as 4500 *Arabidopsis* nuclear genes (18% of the total) could be of cyanobacterial origin, and that the majority are not targeted to the chloroplast.

The relocation of a gene from an endosymbiont (mitochondrion or chloroplast) to the nucleus exposes it to different nucleotide substitution rates, codon preferences and selection pressures. The translocated gene may subsequently have a different rate of evolution compared to genes remaining in the organelle. For example, the mitochondrial ribosomal protein rps10 has evolved much faster in those plants where it is in the nucleus than in those where it is still in the mitochondrion (Adams et al., 2000). This is at least partly due to the fact that nucleotide substitution rates in plants are highest in the nucleus, intermediate in chloroplasts and low in mitochondria (Wolfe et al., 1987; Li, 1999).

During secondary endosymbiogenesis, where a non-photosynthetic eukaryote engulfed a photosynthetic red or green alga (Chapter 1, Green and Anderson; Delwiche and Palmer, 1997), it appears that the nuclear genes for plastid proteins were efficiently transferred to the secondary host's nucleus. In the cryptophyte *Guillardia theta*, the relict nucleus of the red algal ancestor (nucleomorph) carries only 30 genes for plastid-targeted proteins among the 464 predicted open-reading frames (Douglas et al., 2001). The degree to which endosymbiont genes replaced host genes is yet to be determined. We have found an

interesting case of replacement in a tertiary endosymbiosis, where a dinoflagellate lost its own plastid and acquired a haptophyte plastid, and the dinoflagellate *psbO* gene was replaced by the haptophyte *psbO* gene in the dinoflagellate nucleus (Ishida and Green, 2002).

## 6. Time-scale of Cellular Evolution: Adaptations and Catastrophic Extinctions

One more thing needs to be considered. It is very difficult for us to imagine the time scale of evolution, which probably extended over a period of at least three billion years. For every successful adaptation, there must have been millions of unsuccessful ones. Only a vanishingly small fraction of the organisms that ever lived has descendants in the present. Imagine a large, highly branched bush that looks dead except for a single leaf at the very end of each of a few small branches. Those leaves represent the extant divisions of bacteria, five of which have photosynthetic members. It is important to remember that some of the extinct organisms might have been able to survive quite well in some modern niche, but were wiped out during one of the massive extinctions that occurred repeatedly during earth's history, for reasons that had nothing to do with their potential selective advantage.

### B. How Phylogenetic Relatedness is Assessed

#### 1. Phylogenetic Trees

A phylogenetic tree is a representation of the evolutionary relationship among a group of organisms (or their genes). A good basic introduction to phylogenetic trees can be found in the books by Graur and Li (2000) and Hall (2001). more comprehensive treatments are given in Li (1999) and Hillis et al. (1995). A large number of programs are available free to academic users through J. Felsenstein's website (Felsenstein, 2002), and the NCBI website (<http://www3.ncbi.nlm.nih.gov/>). The PAUP package (Swofford, 1999) can be purchased for the price of a biochemistry textbook. Similar methods are used for nucleotide and amino acid sequence data, but construction of trees based on protein sequences avoids some of the problems that result when different groups of organisms have different base compositions and codon preferences, as well as the problem of mutational saturation at the third codon position. This is particularly important

over the long evolutionary distances involved in the evolution of photosynthesis. The journals *Molecular Biology and Evolution* and *Journal of Molecular Evolution* publish many papers concerning methods of phylogenetic inference and their pitfalls, as well as the most current results obtained with these methods.

The first step in phylogenetic tree construction involves the alignment of a group of related sequences. Sequence alignment is not a trivial matter (McClure et al., 1994; Higgins et al., 1996; Rost, 1999). Alignment algorithms generally move one sequence past the other, using a program that averages a similarity score over a sliding window and optimizes the length of segments aligned. For proteins, the similarity score is calculated from an amino acid substitution matrix (see below) such as one of the PAM matrices (Dayhoff et al., 1978), the JTT matrix (Jones et al., 1992), the WAG matrix (Whelan and Goldman, 2001) or the Blosom series (Henikoff and Henikoff, 1992, 1993). The final alignment is improved by editing after visual inspection, and those parts of the sequences that cannot be aligned are eliminated from the analysis. Prior knowledge of protein structure and functional modules can be very helpful in this situation. It is interesting to note that almost all rRNA sequence alignments are done by eye rather than by algorithm. This is not so old-fashioned as it sounds, because the human eye-brain combination has very sophisticated pattern-matching abilities and the enormous database of previously aligned sequences makes the job easier. In a group of aligned sequences, each position (column) is counted as one phylogenetic character, in the same way that a morphological characteristic (e.g. yellow versus green seeds) is counted as one character.

The biggest problem with most multiple sequence alignment programs is that they cannot handle large insertions and deletions effectively. In order not to run calculations on spurious alignments, I recommend doing a preliminary search to find matching blocks of sequence using a program like Macaw (Schuler et al., 1991) or Gapped Blast (Altschul et al., 1997), then deleting long segments not shared by all sequences. Insertions and deletions are potentially informative, but there is no theoretical basis for understanding their frequency or their size, as there is for amino acid or nucleotide substitutions. The common (and necessary) practice of eliminating indel regions in constructing phylogenetic trees unfortunately means that some potentially useful

information is lost. However, the presence or absence of an indel can be used as a discrete character in phylogeny under the assumption that the same indel probably would not occur more than once in the same position unless the two organisms had a common ancestor. Methods based on these 'signature sequences' attempt to exploit this information (Gupta, 1998; Gupta et al., 1999; Fast et al., 2001). Some caution is warranted with respect to very small indels (one or two amino acids) because of the possibility of independent parallel occurrences.

There are three basic methods of tree construction: parsimony, distance and maximum likelihood. It is common practice to calculate trees by all three methods for any given set of proteins, since each method has its own strengths and weaknesses (Hillis et al., 1998; Li, 1999; Graur and Li, 2000; Hall, 2001). All three methods give a branching order, i.e. indicate which taxon separated from the others first and which taxons remain clustered. Distance and maximum likelihood also give estimates of branch lengths, usually expressed in terms of the average number of changes per position along that branch. The validity of the tree is assessed statistically by methods such as bootstrap resampling (Felsenstein 1985, 1988; Hillis and Bull, 1993). Other methods of assessing the reliability of trees are discussed in the references cited above. A useful checklist of points to consider in evaluating any tree or submitting it for publication is given by Stewart (Box 2 in Stewart, 1993).

Maximum parsimony, the simplest method, is based on the idea that the tree that requires the smallest number of changes to explain the differences between sequences is the most likely to be correct. Only those positions that favor one possible tree over another (informative sites) are used in the calculations. Non-informative sites include invariant sites (sites not free to vary for structural or functional reasons) but are not restricted to them. Parsimony calculations on DNA sequences can take into account different ratios of transitions to transversions (calculated from the data), but cannot compensate for multiple hits or back-mutations, so they should not be used for distantly related sequences.

In distance methods, the final alignment is used to calculate a matrix of pairwise evolutionary distances for all the sequences, using an amino acid substitution matrix that represents the probability that one particular amino acid will be changed into another. Distance methods pick the tree with the minimum

overall length as the optimum tree. The commonly used Neighbor-Joining distance method (Saitou and Nei, 1987) groups the two closest sequences, calculates a revised distance between this pair and each of the other sequences, and continues grouping sequences and recalculating distances until the final tree is obtained. Distances are often corrected using the LogDet transformation, which has some statistical advantages (Lockhart et al., 1994).

There are a number of common amino acid substitution matrices in use. The PAM (point accepted mutation) matrices were originally calculated from observed amino acid substitutions in closely-related proteins, and they take into account the average number of nucleotide changes needed to convert one amino acid to another (Dayhoff et al., 1978). The JTT matrices (initials of the authors Jones, Taylor and Thornton, 1992) are updated mutation data matrices based on a much greater sample of protein sequences. The WAG matrix (Whelan and Goldman, 2001) was derived from the same large database using a more sophisticated mathematical approach based on maximum likelihood. There are also matrices optimized for the particular amino acid substitution patterns found in chloroplasts (Adachi et al., 2000), and mitochondria (Adachi and Hasegawa, 1996a). The Blosom matrices (Henikoff and Henikoff, 1992, 1993) were derived in a completely different way, from a database of sequence blocks conserved among distantly related sequences, and they are not related to any model of sequence evolution. They are optimized for database searching and alignment, and are not used for phylogenetic treeing.

Maximum likelihood (Adachi and Hasegawa, 1996b) uses the substitution matrix as a model of evolutionary change to calculate the likelihood of every possible tree for each position in the alignment. It then sums the likelihoods for each possible tree over the entire sequence and picks the tree with the highest likelihood. Needless to say, it is the most computationally intensive method, often requiring that only a subset of the sequences be analyzed. Faster algorithms that use computational shortcuts such as quartet puzzling (Strimmer and von Haeseler, 1996) are coming into use.

## *2. Rates of Evolution and Mutational Saturation*

In calculating evolutionary distances, it is necessary

to take into account two types of variation in evolutionary rates. 'Rates across sites' refers to the fact that the rate of change is not the same at each position in a sequence due to functional constraints on the molecule. This can be directly calculated for each site (Van de Peer et al., 1996); more commonly, the rates are assumed to follow a gamma distribution (Rzhetsky and Nei, 1994), and a correction employing this is incorporated into many tree-construction programs. The treatment of invariant sites is discussed by Lockhart et al. (1996).

There is also the problem that rates can vary over evolutionary time, i.e. a protein may have evolved faster in one taxonomic group than in a sister group. One approach in dealing with this is to combine as many different protein coding genes as possible, on the assumption that since the proteins have different functions, their rates of evolution are likely to vary in different ways from one taxon to another. The effects of different rates thus will tend to cancel out (Bauldauf et al., 2000; Moreira et al., 2000). This has been applied to mitochondrial protein genes (Cao et al., 1994) and to plastid-encoded proteins, where more than 40 sequences were either concatenated or calculated individually and the results were summed (Martin et al., 1998; Adachi et al., 2000; Martin et al., 2002). The sisterhood of red and green algae is solidly supported by trees based on nuclear elongation factor 2 (EF-2) and a fusion of 13 nuclear-encoded proteins (Moreira et al., 2000), but not by trees that consider RNA polymerase II (RPB1) alone (Stiller and Hall, 1997).

With very ancient separations, there is the problem of mutational saturation, in which the numbers of back mutations and multiple changes at a position are enough to obscure the evolutionary history. This problem has been extensively studied by H. Philippe and colleagues (Philippe and Adoutte, 1998; Philippe and Laurent, 1998; Philippe and Forterre, 1999). It is connected to a problem called 'long branch attraction' (Felsenstein, 1988; Philippe, 2000). A property of the tree-building methods is that the algorithms tend to group taxa on long branches with each other and place them at the base of the tree. A long basal branch can mean that that taxon branched off very early from the rest of the species, or it may simply mean that the molecule being studied had a higher rate of sequence change in that particular lineage. Conversely, sequences that are mutationally saturated will have shorter branches than they should have, i.e. the length of time since their divergence from their



neighbors is longer than it appears on the tree.

Problems involving rates cannot always be corrected. For example, in chloroplast 23S rDNA trees, *Euglena* sequences often cluster with dinoflagellate and apicomplexan sequences simply because all these groups have very divergent sequences (Zhang et al., 2000). The microsporidians, a group of unicellular protists lacking mitochondria, were originally placed near the base of the eukaryotic 18S rRNA tree, and it was hypothesized that they diverged before the ancestral eukaryote acquired a mitochondrion. However, when  $\alpha$  and  $\beta$ -tubulin genes were analyzed, the microsporidia grouped with the fungi (Keeling et al., 2000). It is possible that all the early-branching protist groups are misplaced in the eukaryotic tree because of rate variation problems (Philippe, 2000; Philippe et al., 2000; van de Peer et al., 2000). This is why it is difficult to establish an overall phylogenetic tree for all eukaryotes (Bauldauf et al., 2000; Van de Peer et al., 2000).

### 3. Some Common Problems with Trees

Use of an insufficient number of sequences or a biased selection of sequences, which is sometimes unavoidable due to lack of data, can give misleading results. So can the choice of a molecule with too few informative positions, e.g. a small, highly conserved protein. Several workers have recently suggested that codon usage bias and nucleotide composition can affect amino acid substitution patterns (Naylor and Brown, 1997; Barbrook et al., 1998; Foster and Hickey, 1999).

Then there is the problem of paralogous genes. If gene X was duplicated before the separation of the two species being compared, each species will have two sister genes (called paralogs) whose evolutionary histories may be different. If gene Y of one species is unwittingly compared with gene Z of the other, the tree relating them will be invalid, i.e. it is an 'apples-and-oranges' comparison. A determined effort needs to be made to find all the paralogs in both species before developing an evolutionary story.

A rooted tree is one in which the direction of evolution (order of branching) is implied, with the common ancestor at the base (root). For example, the hypothetical tree in Fig. 3 implies a common ancestor for all cellular life, whereas Fig. 2 makes no statement about a common ancestor. In the absence of information about this ancestor (the usual case), the sequences of interest (ingroup) are compared to one

or more sequences that are more distantly related to them than they are to each other (the outgroup). For example, myoglobin might be used as the outgroup in a tree of vertebrate hemoglobins. The root is then placed between the outgroup and the ingroup branches, on the assumption that this represents the common ancestor of the ingroup and the outgroup. It is often difficult to find suitable outgroup sequences that can be aligned with reasonable accuracy, without making unjustifiable (and untestable) assumptions. A poor choice of outgroup can distort relationships in a tree. Paralogs have been used to root the universal tree, with mixed success (Gogarten et al., 1989; Iwabe et al., 1989; Kollman and Doolittle, 2000). Considerable thought should go into the choice of outgroup, and unrooted trees should probably be seen more frequently, particularly when the evolution of a protein family rather than the evolution of a group of organisms is under consideration. The 'Tree of Life' in Fig. 2 is an unrooted tree because there is no conceivable outgroup when all of life is included.

Readers should not be discouraged by this recital of complications, but rather should be encouraged to look at phylogenetic tree construction as just another experimental approach, with the possible pitfalls and artifacts found in any laboratory method. Especially when evolutionary distances are very large, we must be willing to recognize the limits of our data. In the absence of a time machine, we may not be able to obtain all the answers we would like.

### 4. Gene Clusters—an Additional Source of Information

Genes encoding enzymes that belong to the same pathway or macromolecular complex are often found in clusters (Lawrence, 1999; Overbeek et al., 1999). These clusters can be conserved over long evolutionary distances, as is the case for subunits of ATP synthase and for ribosomal proteins in bacteria and organelles (Boore and Brown, 1998; Stoebe and Kowallik, 1999; Nikolaichik and Donachie, 2000). Since changes in gene order involve recombination mechanisms, there is less chance of convergent evolution (Boore and Brown, 1998). There is considerable debate about the biological benefits of gene clustering (reviewed in Lawrence, 1999); it has even been suggested that clustering benefits the genes, not the organisms, because it facilitates lateral transfer of a metabolic pathway and the spread of the genes in question, i.e. they are 'selfish operons' (Lawrence,

1999). Differences in gene order have been used to suggest lateral transfer of the photosynthesis gene cluster from an  $\alpha$ -proteobacterium to a  $\beta$ -proteobacterium (Igarashi et al., 2001). However, it is not clear whether the presence of a cluster carrying the pigment biosynthesis and reaction center genes in purple bacteria and *Heliobacterium* indicates genes that were received by lateral transfer, or whether these genes are just getting ready to travel. Photosynthesis genes are not clustered in *Chlorobium* (Eisen et al., 2002), *Synechocystis* (Kaneko et al., 1996) or *Chloroflexus* (R. E. Blankenship, personal communication).

#### IV. Pigment Biosynthesis Genes

Light-harvesting pigments are members of only three biochemical classes: porphyrins (Chl, BChl), bilins and carotenoids (Chapter 2, Scheer). Chlorophylls, bacteriochlorophylls and phycobilins share the early steps of their biosynthetic pathway with heme.

##### A. Did Chl or BChl Come First?

Does the presence or absence of individual pigments tell us anything about the evolution of photosynthetic prokaryotes? The answer to this question is unclear because of the very ancient nature of these biosynthetic pathways and the enormous evolutionary

distances among the five prokaryotic groups, as discussed in the previous section. In fact, this subject provides a good case study of the difficulties of developing a phylogenetic tree that is valid for very distant comparisons.

Figure 4 shows the final steps of chlorophyll and bacteriochlorophyll synthesis. Molecular structures can be found in Chapter 2 (Scheer) and in the reviews by Beale (1999), Bauer et al. (1993) and Suzuki et al. (1997). The common precursor of all Chls and BChls is divinylprotochlorophyllide *a* (also called [8-vinyl]-protochlorophyllide or Mg-2,4-divinylpheoporphyrin  $a_3$ -monomethyl ester), which is part of the light-harvesting antenna of the prochlorophyte *Prochloron* and at least two species of eukaryotic algae (Helfrich et al., 1999). This pigment may be more widespread than is commonly realized, because it could easily be misidentified as Chl *c*, which has very similar structure and spectroscopic properties (Chapter 2, Scheer). Figure 4 suggests that divinyl protochlorophyllide *a* may have been the ancestral light-harvesting pigment, and might even have been part of primitive reaction centers.

The last common intermediate of Chls and BChls is chlorophyllide *a*, which is formed by reduction of ring D by the light-independent protochlorophyllide reductase, except in higher plants. This is a three-subunit enzyme encoded by the *chlB*, *chlL* and *chlN* genes in cyanobacteria and algae, or by the related *bchB*, *bchL* and *bchN* genes of purple and green

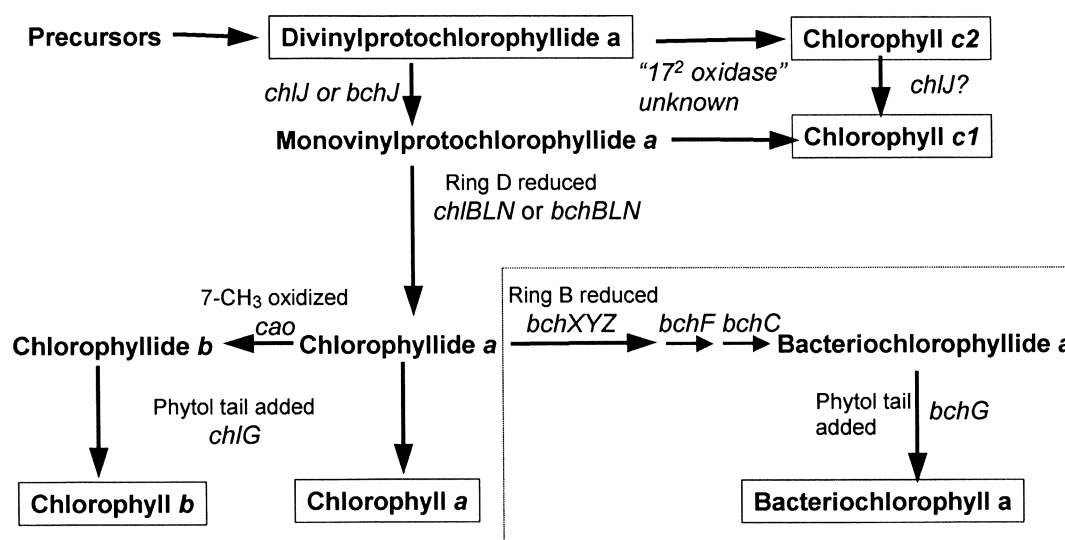


Fig. 4. Synthesis of Chls and BChl *a* from common intermediates. Note that chlorophyllide *a* is the common precursor to BChl *a*, Chl *a* and Chl *b*. Boxed pigments have been shown to have a light-harvesting role in at least one organism. The dotted box delineates reactions unique to BChl synthesis.



bacteria. BChl *a* synthesis also requires a second ring reduction, which is catalyzed by the products of three genes: *bchX*, *bchY*, *bchZ* which are related to the *bchL*, *bchN* and *bchB* genes by an apparent gene duplication (Burke et al., 1993a,b). Since the BchX, BchL and ChlL sequences are distantly related to the Type I nitrogenase Fe proteins (NifH) of non-photosynthetic bacteria, the latter were used for the root in a maximum likelihood analysis. This analysis showed that the *bchX* gene branched off first, before *bchL/chlL* diverged (Burke et al., 1993b). In order to rationalize this finding, the authors proposed that the ancestral enzyme was relatively non-specific and was able to catalyze both ring reductions, and that the ability to make BChl was lost in the line leading to the cyanobacteria and chloroplasts.

Lockhart et al. (1996) re-examined the question and showed that the previous analysis was distorted by the inclusion of invariant sites, i.e. those not free to vary between sequences of the same biological function. Furthermore, the nitrogenase genes would not be expected to have the same invariant sites as the pigment synthesis genes because nitrogenase has a different function and would therefore be subject to different selection pressures at different sites in the molecule. This calls into question the use of nitrogenase genes as an outgroup to root the tree. Lockhart et al. (1996) concluded that the data available did not favor any particular hypothesis.

In a more recent analysis, trees were made by all three standard methods (neighbor-joining, parsimony, and maximum likelihood) using gene sequences from *Heliobacillus*, *Chloroflexus* and *Chlorobium* as well as purple bacteria, cyanobacteria and plants (Xiong et al., 1998; 2000). The genes studied were *bchBLN/chlBLN* and *bchG/chlG* (Fig. 4) as well as the three genes that encode subunits of Mg chelatase, the first committed step in porphyrin biosynthesis (Chapter 2, Scheer). Both DNA and protein sequences were analyzed, and trees were also made from concatenated sequences of all seven genes. The results were somewhat surprising: in all the trees, *Chlorobium* and *Chloroflexus* genes were clustered, and so were the *Heliobacillus* and cyanobacterial genes. Furthermore, the majority of trees showed purple bacteria as the earliest branching group. The authors showed that unrooted trees gave the same topology as rooted trees, but they did not address the problem of invariant sites, although the rest of their analysis was careful and the branches had good statistical support. There is also the problem that the seven

genes analyzed by Xiong et al. (2000) encode subunits of only three enzymes, and therefore may not be representative of all the Chl and BChl synthesis genes. It was unfortunate that *bchXYZ* sequences were not included in the analysis.

On the basis of parsimony, it would seem simplest to assume that the first photosynthetic prokaryotes used earlier intermediates in the biosynthetic pathways, and that more steps were added later by gene duplication and divergence. If Chl *a* preceded BChl *a*, that would explain the presence of Chl *a* as well as BChl *a* in the reaction centers of green sulfur bacteria (Chapter 6, Blankenship and Matsuura; Kobayashi et al., 2000). Perhaps divinylprotochlorophyllide *a* was even earlier, since it is still being used in light-harvesting (Helfrich et al., 1999) and is the common intermediate in both Chl and BChl biosynthesis pathways.

Analyses over very long distances will always face the problem that rates of sequence evolution are unlikely to have remained constant. The apparent early divergence of the purple bacterial branch in the analysis of Xiong et al. (2000) may simply mean that the pigment biosynthesis genes are evolving faster in the proteobacterial line than in the other lines. Given the increasing number of examples of lateral gene transfer that contribute to confusing the phylogeny of whole metabolic pathways (e.g. isoprenoid biosynthesis, see below), questions involving large evolutionary distances should be attacked at the whole-genome level whenever possible (Green and Gantt, 2000).

### *B. The Accessory Chls of Chloroplasts and Prochlorophytes*

The three major groups of eukaryotic algae differ in the accessory Chls of their membrane-intrinsic LHCs (Chapter 1, Green and Anderson; Section VII). As shown in Figure 4, the synthesis of Chl *b* from Chl *a* requires only one additional step, catalyzed by the enzyme Chl *a* oxygenase (CaO) (Tanaka et al., 1998; Oster et al., 2000). Sequences of CaO from two prochlorophytes, two green algae and several higher plants are all related, suggesting that the *cao* gene had a common ancestor in prokaryotes and chloroplasts (Tomitani et al., 2000). These authors proposed that all cyanobacteria originally had the ability to make both Chl *b* and phycobilisomes and that the ability to make Chl *b* was retained while phycobilisomes were lost in the lines that led to

prochlorophytes and chloroplasts. This would have required multiple independent losses of CaO in the many cyanobacterial lines, especially since the closest relatives of each kind of prochlorophyte do not make Chl *b* (Wilmoth, 1995; Turner, 1997; Turner et al., 1999). Another possibility is that lateral gene transfer spread the *cao* gene among the three prochlorophytes and the ancestor of the chloroplast. The cyanobacterial ancestor of the chloroplast was not closely related to any of the prochlorophytes (Wilmoth, 1995; Turner, 1997; Turner et al., 1999). Both these models imply that the first photosynthetic eukaryote had the gene for CaO and made Chl *b*, which was subsequently lost in the lines leading to glaucophytes and red algae (Bryant, 1992).

Two groups recently succeeded in introducing the *cao* gene into *Synechocystis* PCC6803, and showed that Chl *b* was synthesized and incorporated into proteins (Satoh et al., 2001; Xu et al., 2001). When the gene was introduced into wild-type cells, Chl *b* made up 7–10% of total Chl and 8% of the Chl in the PsaA/PsaB reaction center complex of PS I (Satoh et al., 2001). When it was introduced into a PS I-less mutant with decreased ability to synthesize Chl, along with a gene for the major LHCII Chl *a/b* protein of pea, Chl *b* made up 60% of total Chl, even though the LHCII protein was rapidly turned over and did not accumulate to a significant extent. The Chl *b* was incorporated into PS II and was able to transfer energy to the reaction center (Xu et al., 2001). This shows that there is no absolute specificity for Chl *a*, and suggests that a variety of chlorins and bacteriochlorins could have been used successfully for both reaction centers and antennas during the last 3 billion years. The most striking example of a natural Chl substitution is the prokaryote *Acaryochloris marina* (reviewed in Boichenko et al., 2000), in which almost all the Chl *a* has been replaced by Chl *d*.

The specific Chls, and to a certain extent the BChls, found in any particular taxonomic group have historically been used as major taxonomic characters. However, there have always been a few anomalies, e.g. the eustigmatophytes, which are heterokonts according to all criteria except for their lack of Chl *c* (Green and Durnford, 1996; Chapter 11, Macpherson and Hiller). In addition to the transformation experiments with *Synechocystis*, a variety of reconstitution experiments also suggest that many antenna proteins can adapt to bind whatever Chls or BChls their owners are capable of synthesizing (Davis et al., 1996; Green, 2001). The Lhca1 apoprotein of

the red alga *Porphyridium*, which only binds Chl *a*, can be reconstituted with either Chl *b* or Chl *c*, chlorophylls that its ancestors may never have encountered (Grabowski et al., 2001).

The synthesis of Chls *c1* and *c2* from the protochlorophyllide precursors requires only the formation of a double bond in the propionate side-chain (Chapter 2, Scheer); this should require just one additional enzyme, the hypothetical '17<sup>2</sup> oxidase' (Fig. 4). Unfortunately, there is currently no information about either the enzymatic activity or the gene(s) involved. Since the Chls *c* are found only in algae whose chloroplasts were acquired by secondary symbiogenesis involving a red algal endosymbiont (heterokonts, cryptophytes, haptophytes and dinoflagellates, see Chapter 1, Green and Anderson), this implies that their red algal ancestor(s) should have been able to synthesize Chl *c*, even though no Chls *c* have so far been detected in red algae (Chapter 2, Scheer). This question should be re-examined with modern analytical methods.

The cryptophytes are the only algal group that has Chl *c* but retains phycobilins, and several bilins unique to this group have a double bond in the same propionate side chain as Chl *c* (Chapter 2, Scheer). This suggests that the same enzyme(s) may be used in the synthesis of both types of pigment.

### C. Isoprenoids and Carotenoids

Isoprenoids include many types of molecule important in photosynthesis: carotenoids, quinones, sterols and the phytol tails of the (B)Chls are all derived from a common precursor pool of isopentenyl diphosphate and its isomer dimethylallyl diphosphate. Two completely different pathways, the 1-deoxyxylulose 5-phosphate (DOXP) and mevalonate pathways, provide these 5-carbon diphosphate precursors (Chapter 2, Scheer). Most eukaryotes and all archaebacteria use only the mevalonate pathway, whereas the eubacteria use predominantly the DOXP pathway. However, some eubacteria also use part or all of the mevalonate pathway and a few appear to use it exclusively. Two analyses that included genomic, phylogenetic and biochemical data both suggested strongly that multiple lateral gene transfers and gene replacements must be invoked to explain the distribution of genes and pathways among the eubacteria (Boucher and Doolittle, 2000; Lange et al., 2000). Most photosynthetic eukaryotes have the mevalonate pathway in the cytoplasm and the DOXP pathway (like that of cyanobacteria) in the chloroplast.

However, the Chlorophyta (main line of green algae) appear to have retained the DOXP pathway but lost the mevalonate pathway (Schwender et al., 2001).

Carotenoid biosynthesis pathways are partly common to all photosynthetic organisms and partly specific to groups of bacteria or algae. The taxonomic distribution of particular carotenoids and the major biosynthetic pathways are given in Table 1 and Fig. 8 of Chapter 2 (Scheer). More information on carotenoids of anoxygenic bacteria is given by Takaichi (1999). Takaichi and Mimuro (1998) showed that neoxanthin is found only in the green (Chl *a/b*) line, and they suggested that neoxanthin was related to the presence of Chl *b*. However, this carotenoid is the precursor of abscisic acid, which may be the more relevant correlation. It has been suggested that neoxanthin synthase was derived from lycopene cyclase by gene duplication and divergence (Bouvier et al., 2000). The difference between a lycopene  $\epsilon$ -cyclase that adds one  $\epsilon$ -ring and another that adds two has been traced to a single amino acid switch (Cunningham and Gantt, 2001). Unfortunately, no molecular phylogenetic analysis on the genes common to all pathways appears to have been done, although most of the gene sequences are known.

#### *D. Phycobilin Biosynthesis*

All the phycobilin pigments, including phytochrome, are synthesized from heme via the common intermediate biliverdin IX $\alpha$  (Chapter 2, Scheer). The cyanobacterial bilin reductases that produce phycoerythrobilin, phycocyanobilin and phytychromobilin are members of a gene family, and provide a nice example of gene duplication followed by divergence (Frankenberg et al., 2001). They are distantly related to the red chlorophyll catabolite reductases of the Chl degradation pathway in higher plants (Wüthrich et al., 2000).

### **V. Photosynthetic Reaction Centers and the Core Antenna Family**

#### *A. Three-Dimensional Structures of Reaction Centers and Core Antennas*

More than ten years ago, it was suggested that both PS I-type and PS II-type reaction centers had enough similarities in design and function that they must have had a common ancestor (Nitschke and Rutherford, 1991; Golbeck, 1993). The high

resolution x-ray crystallographic structures of cyanobacterial PS I (Schubert et al., 1998; Fromme et al., 2001; Jordan et al., 2001; Chapter 8, Fromme et al.) and the purple bacterial RC (Michel and Deisenhofer, 1988), along with the lower resolution structure of PS II (Zouni et al. 2001; Chapter 7, Dekker and van Amerongen) show such strong similarities that there is no longer much doubt about their common origin. In contrast, there are substantial differences between the protein sequences, which can even be misleading in predicting the three-dimensional structure (Schubert et al., 1998). Although the two proteins that make up the reaction center of PS I have 11 membrane-spanning helices, as compared to the five helices of the purple RC, the arrangement of the inner (C-terminal) five helices of PsaA and PsaB is remarkably similar to those of the purple bacterial L and M subunits (Chapter 5, Robert et al.) and the D1/D2 subunits of PS II (Chapter 7, Dekker and van Amerongen; Zouni et al., 2001).

The outer (N-terminal) six helices of the PS I proteins PsaA and PsaB are structurally related to the six helices of CP43 and CP47, the core antennas of PS II (Schubert et al., 1998; Barber et al., 2000; Jordan et al., 2001; Zouni et al., 2001). It appears that in PS II, the antenna parts (CP47, CP43) are detached from the RC-protecting parts (D1, D2) but maintain the same relative positions in the macromolecular complex (Fig. 5). However, this conclusion is supported mainly by the three-dimensional similarity, as the amino acid sequence similarity between the PS I and PS II core antennas of cyanobacteria is not statistically convincing (reviewed in Schubert et al., 1998; Baymann et al., 2001). This means that any phylogenetic tree that attempts to include all photosynthetic reaction centers (Xiong et al., 1998) is questionable. Furthermore, in the cyanobacterial PS I structure, not all the antenna Chls are bound by the outer six helices; some are bound by the inner helices and some by other polypeptides of the PS I complex (Jordan et al., 2001; Chapter 8, Fromme et al.). What this means is that there has been a very long time for diversification and adaptation since the divergence of the two photosystems.

#### *B. The Core Complex Antenna Family*

The Core Complex antenna family as defined by Green and Durnford (1996) includes the six N-terminal helices of PsaA and PsaB along with CP47, CP43, IsiA and the prochlorophyte Pcb's (Chl *a/b* antennas). However, because the PS I core antennas

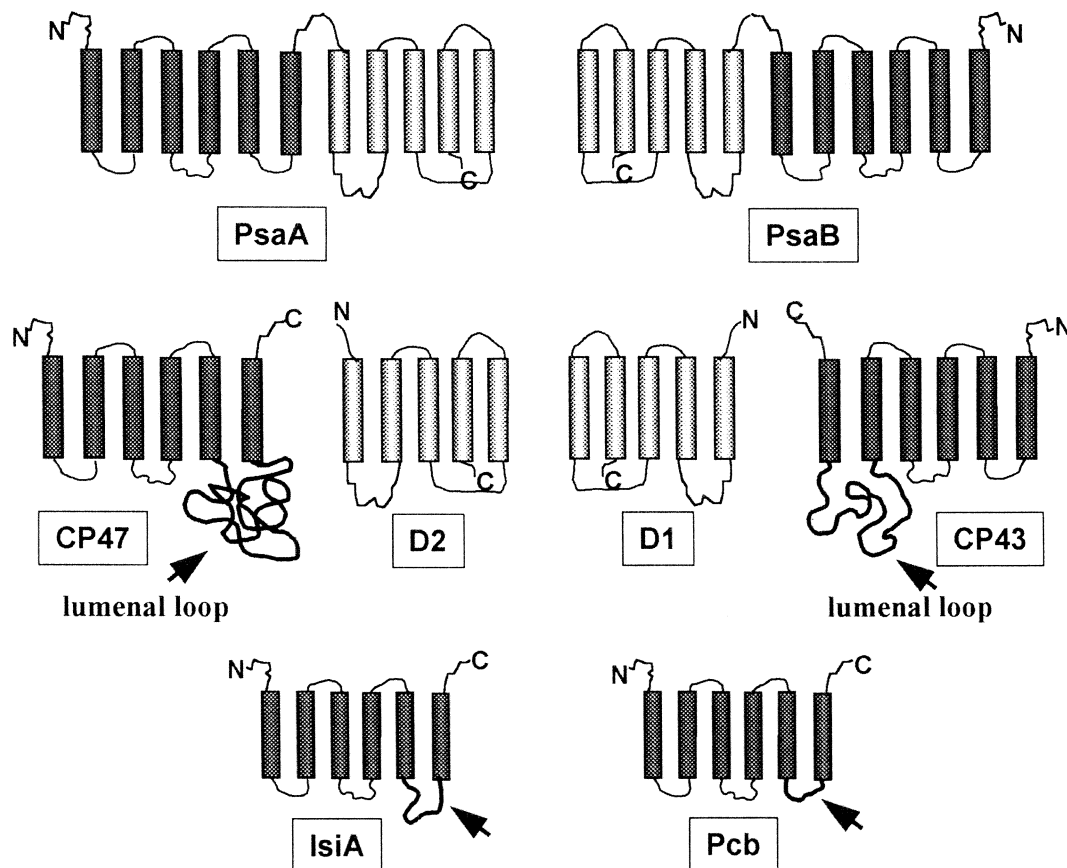


Fig. 5. Core Complex family of the cyanobacterial/chloroplast line (oxygenic photosynthesizers). The C-terminal five helices of PsaA and PsaB (PS I) are analogous to the D1 and D2 subunits of PS II; the outer six helices to CP47 and CP43. IsiA, iron deficiency-induced antenna protein; Pcb, prochlorophyte Chl *a/b* antenna proteins. Arrows: luminal loops between fifth and sixth transmembrane helices. These loops are much longer in CP43 and CP47 than in the other family members.

are so divergent (see above), the following discussion is mainly restricted to the other members of the family.

### 1. CP47, CP43 and IsiA

The cyanobacteria/plastid lineage is the only one that has multiple members of the Core Complex antenna family. In addition to CP47 (PsbB) and CP43 (PsbC), this family includes the IsiA proteins and the prochlorophyte Chl *a/b* proteins (Pcb), all of which are predicted to have six trans-membrane helices (Green and Durnford, 1996; Chapter 1, Green and Anderson). The major difference among them is in the length of the luminal loop between the fifth and sixth trans-membrane helices. These loops are much longer in CP47 and CP43 than in the Pcb,

IsiAs, or PsaA/B (Fig. 5). If the loop regions unique to CP47 and CP43 were detached, they would be equivalent to individual luminal proteins of 12 and 10 kDa respectively. The insertion(s) of these loop sequences could have been correlated with the acquisition of water-splitting ability, since there is considerable evidence that the loop regions are involved in binding and protecting the Mn-cluster Putnam-Evans and Bricker, 1997; Rosenberg et al., 1999).

The six-helix members of the Core Complex family have enough sequence similarity to be reliably aligned and used for phylogenetic tree construction (La Roche et al., 1996; van der Staay et al., 1998). These trees show that PsbB (CP47) is the most divergent member of the family, consistent with higher selective pressures due to its intimate connection with the

water-splitting apparatus. They are consistent with the idea that PsbB and PsbC (CP43) arose by duplication of an ancestral gene, and that the IsiA proteins are more closely related to PsbC than to PsbB.

The IsiA proteins of cyanobacteria are Chl *a*-binding proteins expressed only under conditions of Fe deprivation, during which the phycobilisomes and photosystems are down-regulated and total Chl/cell decreases (Reithman and Sherman, 1988; Ferreira and Straus, 1994). They bind only Chl *a*, since their owners make only Chl *a*. At least one *isiA* gene has been found in every cyanobacterium examined to date (Geiss et al., 2001; Ting et al., 2002). There has been an on-going debate about the function of these chlorophyll-proteins, with suggestions ranging from light-harvesting to energy dissipation to being a simple Chl reservoir (Burnap et al., 1993; Park et al., 1999; Geiss et al., 2001; Sandström et al., 2001; Chapter 1, Green and Anderson). Since most of the experimental studies had focused on PS II, it was a surprise when the IsiA Chl *a*-protein (also called CP43') was discovered to be associated with PS I, forming a ring of 18 subunits around the trimeric PS I complex, in both *Synechocystis* PCC 6803 (Bibby et al., 2001a) and *Synechococcus* PCC 7942 (Boekema et al., 2001). Both groups demonstrated energy transfer from CP43' to PS I, showing that CP43' acts as a PS I light-harvesting antenna under conditions of Fe deprivation. This would explain the observation that cyclic electron flow around PS I is enhanced under iron stress (Ivanov et al., 2000).

## 2. The Pcb's (Prochlorophyte Chl *a/b* Proteins)

'Prochlorophyte' refers to the three cyanobacteria (*Prochloron*, *Prochlorothrix*, *Prochlorococcus*) that differ from other cyanobacteria in having Chl *a/b* antennas and little or no phycobiliprotein antenna (Matthijs et al., 1995). These species are not closely related to each other or to the putative ancestor of the chloroplast (Wilmotte, 1994; Turner et al., 1999; Ting et al., 2002). Although *Prochlorococcus* was only discovered in 1988 (Chisholm et al., 1988) it is now recognized as an important member of the phytoplankton community in subtropical waters (reviewed in Partensky et al., 1999; Ting et al., 2002). It is most closely related to marine strains of *Synechococcus* (Hess et al., 2001) and together they account for a significant fraction of the ocean's productivity (reviewed in Ting et al., 2002). Genomes

of both high-light-adapted and low-light-adapted ecotypes have been sequenced (Hess et al., 2001). In contrast to the other two prochlorophytes, *Prochlorococcus* has divinyl-Chls *a* and *b*, i.e. the 8-vinyl side-chain has not been reduced, suggesting that the *chlJ* gene has been lost or is poorly expressed (Fig. 4).

The Pcb (prochlorophyte Chl *b*-binding) proteins are completely unrelated to the Chl *a/b* proteins of plants and chlorophyte algae (LaRoche et al., 1996). They bind both Chls *a* and *b*, or divinyl-Chl *a* and *b*, in various ratios depending on the organism (Matthijs et al., 1995; Partensky et al., 1999). *Prochlorothrix hollandica* has three *pcb* genes in a single operon; two closely related ones encoding polypeptides of about 34 kDa and a third (*pcbC*) that is more divergent and encodes a 38 kDa polypeptide (van der Staay et al., 1998). Different environmental isolates of *Prochlorococcus* have different numbers of *pcb* genes: the high-light adapted strain MED4 has only one (LaRoche et al., 1996), but the low-light strain SS120 has seven (Garczarek et al., 2000; 2001). In the low-light strain, but not the high-light strain, Pcb proteins form a ring around PS I (Bibby et al., 2001b), similar to the rings of CP43' subunits around PS I in *Synechocystis* (Bibby et al., 2001a) and *Synechococcus* (Boekema et al., 2001).

We earlier suggested that the *Prochlorothrix* and *Prochlorococcus* Pcb's could have originated through independent duplications and that the third *Prochlorothrix* gene (*pcbC*) was the result of a second independent duplication involving an ancestral gene more closely related to CP43 than IsiA (van der Staay et al., 1998). An interesting twist to this story has been added by the recent discovery of Fe-deficiency-induced genes that more closely resemble *Prochlorothrix pcbC* than *isiA*, in *Fischerella* and *Anabaena*, two cyanobacteria that do not make Chl *b* (Geiss et al., 2001). Figure 6 shows that *Prochlorothrix* PcbC and the PcbC-like proteins branch together and are distinctly separated from the IsiA proteins of the same species, with good bootstrap support. The other Pcb proteins appear to form species-specific clusters.

The Core Complex family is thus more widespread and diverse than was realized even a few years ago. It appears likely that iron limitation was a significant factor in driving the proliferation of this family. Cyanobacteria suffer the results of their own evolutionary success in inventing the ability to split water. Soluble Fe is in limited supply in the biosphere as a direct result of cyanobacterial activities, i.e. the pollution of the atmosphere by increasing levels of

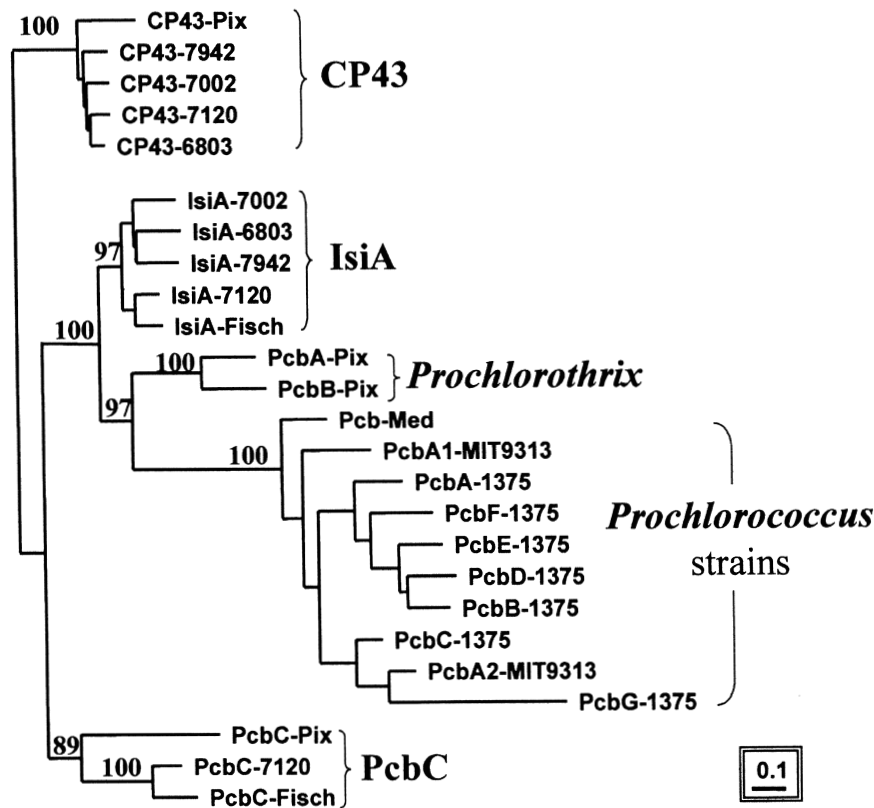


Fig. 6. Phylogenetic tree of core antenna family proteins: CP43, IsiA and Pcb, including the PcbCs of *Fischerella* (Fisch) and *Anabaena* PCC 7120 (7120) that do not bind Chl *b* and form a separate clade with *Prochlorothrix* PcbC (Pix). Tree was constructed by the Neighbor-Joining method (Saitou and Nei, 1987) using rate-corrected distances. Scale bar indicates 0.1 changes per amino acid position. Other CP43 and IsiA sequences from *Synechocystis* PCC 6803 (6803), *Anacystis nidulans* PCC 7942 (7942), *Synechococcus* PCC 7002 (7002) and *Anabaena* PCC 7120 (7120).

oxygen and the resultant precipitation of Fe during the Proterozoic era (Fig. 1). As a result, large areas of the world's oceans are very poor in Fe. These are the areas where *Prochlorococcus* and marine *Synechococcus* are found in abundance (Ting et al., 2002). The fact that members of this family can bind either Chl *a* alone or a mixture of Chl *a* and Chl *b* suggests they bind whatever pigments are made available to them, which in turn implies that the evolution of the proteins is separate from the evolution of the pigment biosynthesis pathways (Section IV; Green, 2001

## VI. Phycobiliproteins

### A. The family Tree—Duplication and Divergence

Phycobilisomes are found in cyanobacteria, glaucophytes and red algae (Chapter 7, Mimuro and Kikuchi;

Chapter 10, Gantt et al.; Sidler, 1995; MacColl, 1998). The phycobiliproteins bind a limited number of bilin pigments, which differ only in having a variable number of double bonds (5–8) and in having either one or two vinyl groups available for thioether linkage to the corresponding biliprotein (Chapter 2, Scheer). The major pigment proteins are phycoerythrin, phycoerythrocyanin, phycocyanin and allophycocyanin, each of which has  $\alpha$  and  $\beta$  protein subunits. This protein family gives a very good illustration of 'fine-tuning' by the polypeptide moiety; even though they contain a limited number of pigments, the pigment-proteins have a very broad range of light absorption between 490 and 600 nm, a range where the chlorophylls have very little absorption.

The extended family of  $\alpha$  and  $\beta$  polypeptides is a good example of multiple gene duplications and divergence resulting in functional diversity. Thanks to the large number of available sequences, their

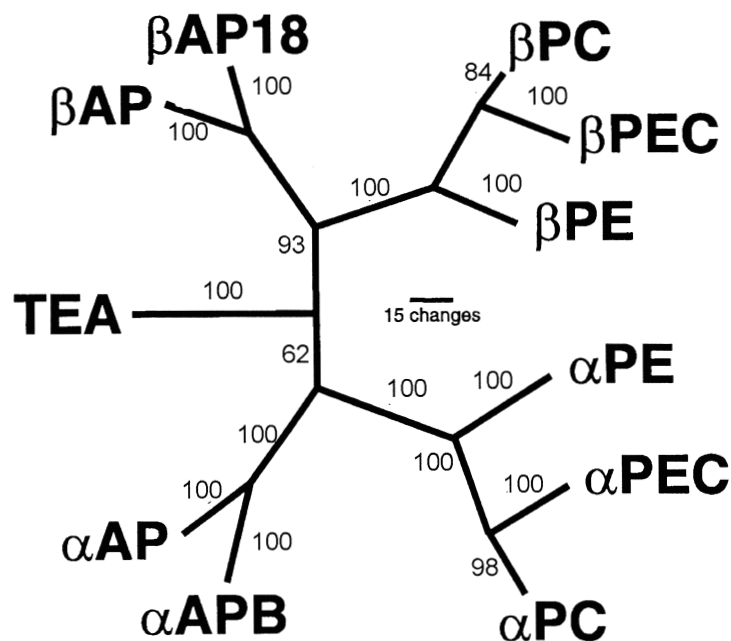


Fig. 7. Phylogenetic tree of the phycobiliproteins. AP, allophycocyanin; APB, allophycocyanin-B, PC, phycocyanin; PE, phycoerythrin; PEC, phycoerythrocyanin; TEA, linker. Numbers on a branch indicate the percent statistical support for the separation of that branch from the rest of the tree. Adapted from Apt et al. (1995).

relatively large size, and the availability of a number of crystallographic structures to aid in alignment, phylogenetic analysis has been particularly informative (Ducret et al., 1994; Apt et al., 1995). The  $\alpha$  and  $\beta$  subunits form two separate branches of the tree (Fig. 7), suggesting that tandem duplication of an ancestral gene early in the evolutionary history of the cyanobacteria gave an  $\alpha$ - $\beta$  operon and that subsequent rounds of duplication and divergence of the operon produced the family of phycobiliprotein genes. There are a number of subgroups in each class of phycobiliprotein, and their  $\alpha$  and  $\beta$  subunits appear to have co-evolved. This co-evolution is understandable when the large number of residues involved in  $\alpha$ - $\beta$  interaction is taken into account (Apt et al., 1995).

The large core-membrane linker polypeptide ( $L_{CM}$ ) that attaches the allophycocyanin cores to the photosynthetic membrane in the vicinity of Photosystem II is an evolutionary mosaic (Sidler, 1995). Its chromophore-binding N-terminal half is part of the  $\alpha/\beta$  family (TEA domain in Fig. 7), while the C-terminal half is related to the other linker polypeptides (Sidler, 1995). The TEA domain tends to cluster with the  $\alpha$ -allophycocyanins, but the position of the root in this tree is not very robust

(Ducret et al., 1994; Apt et al., 1995).

The phycobiliproteins have the globin fold (Schirmer et al., 1985) and bind their chromophores via Cys residues at comparable positions to those that bind globin hemes. However, sequence similarity is negligible, even when the three-dimensional structures are aligned (Bashford et al., 1987). Does this mean that the globins and the phycobiliproteins shared a common ancestor? The globin fold has been found in a number of other proteins such as colicins, which do not bind any heme or heme derivative (Holm and Sander, 1993). Profile analysis of all members of the globin superfamily, phycocyanin and colicin suggest that the latter two represent convergent evolution of a protein fold (Bashford et al., 1987; Holm and Sander, 1993; Moens et al., 1996).

### B. Losses

The picture above is the 'standard' phycobilisome. A number of cyanobacteria lack phycoerythrin, probably as a result of independent secondary losses; in some strains phycoerythrins are replaced with phycoerythrocyanin (Apt et al., 1995; MacColl, 1998). A strain of the red alga *Rhodella reticulata* possesses a functional phycoerythrin that has only  $\beta$



subunits, i.e. it has  $\beta_6$  trimers instead of  $(\alpha\beta)_3$  trimers (Thomas and Passaquet, 1999). *Acaryochloris marina*, an unusual cyanobacterium that has mainly Chl *d*, has rod-shaped structures made up of phycocyanin and allophycocyanin (Marquardt et al., 1997; Hu et al., 1999).

None of the Chl *a/b* containing prochlorophytes (cyanobacteria) has phycobilisomes. However, several strains of *Prochlorococcus* have genes for phycoerythrin subunits (Hess et al., 1996, 1999; Penno et al., 2000; Ting et al., 2001). Sequence analysis suggests that these genes are evolving rapidly (Ting et al., 2001). In the low-light-adapted strain SS120, these genes are expressed, although weakly, and both  $\alpha$  and  $\beta$  subunits accumulate (Hess et al., 1996; 1999). In the high-light-adapted strain MED4, no  $\alpha$  subunit gene could be detected in the complete genome sequence, and the  $\beta$  subunit gene is very divergent, lacking several highly conserved residues needed for chromophore binding (Hess et al., 2001; Ting et al., 2001).

### C. Cryptophyte Phycobiliproteins

Some unique phycobiliproteins are found in the cryptophytes (Chapter 11, Macpherson and Hiller; Glazer and Wedemayer, 1995; Wedemeyer et al., 1996), an algal group that acquired its chloroplast and nucleomorph (relict endosymbiont nucleus) from a red alga by secondary endosymbiogenesis (Chapter 1, Green and Anderson; Douglas and Penny, 1999; Zauner et al., 2000; Douglas et al., 2001). Cryptophytes do not form phycobilisomes, but rather  $\alpha_1\alpha_2\beta\beta$  dimers that are located in the thylakoid lumen (Ludwig and Gibbs, 1989). Any one species or strain contains only phycoerythrin or a so-called 'phycocyanin,' which is actually a phycoerythrin (Glazer and Wedemayer, 1995). They bind a number of novel bilins that further extend the range of wavelengths absorbed; their structures and absorbances are displayed in an excellent color graphic in the paper by Wedemeyer et al. (1996); see also Chapter 2 (Scheer). Two of the bilins unique to cryptophytes have a double bond in the same propionyl side chain as the double bond that distinguishes the Chls *c*. On the basis of parsimony, one would expect the same enzyme or close relatives to catalyze the two reactions. Perhaps the double bond in Chl *c* is the only trace of the phycobilin biosynthetic pathway that was possessed by all the

ancestral chromophytes before they lost the red algal nucleus and all the phycobiliprotein genes.

The chloroplast-encoded  $\beta$  subunits of cryptophytes cluster with red algal  $\beta$  subunits in phylogenetic trees (Ducret et al., 1994; Apt et al., 1995). However, the nuclear-encoded  $\alpha$  subunits show no sequence relatedness to  $\alpha$  subunits of other organisms, and in fact are not related to any other sequences in the databanks (Chapter 12, Macpherson and Hiller), not even the linkers of red algae (Apt et al., 2001). The crystal structure (Wilk et al., 1999) shows that these  $\alpha$  subunits have the same fold as a small linker polypeptide ( $L_{C-7.8}$ ) of a cyanobacterial allophycocyanin. This suggests that a linker polypeptide that was already binding a chromophore may have been recruited to a new role.

The phylogenetic trees of all  $\alpha$  and  $\beta$  subunits (Fig. 7) support Glazer's original idea (1976) that all the phycobiliproteins descend from one ancestral gene. Glazer and Wedemayer (1995) later suggested that cryptophyte biliproteins represented the ancestral state, and that the secondary endosymbiotic event involved the engulfing of a photosynthetic eukaryote with Chl *a*, Chl *c* and a phycoerythrin  $\beta$  subunit. However, the evidence that the cryptophyte and red algal chloroplasts are related is now so strong (Douglas and Penny, 1999; Zauner et al., 2000; Douglas et al., 2001) that it is much more likely that multiple losses (of phycocyanin, allophycocyanin and various linkers) were the consequence of secondary endosymbiogenesis.

## VII. LHC Superfamily

### A. A Family Unique to Cyanobacteria and Eukaryotes

The LHC family includes all the three-helix membrane-intrinsic Chl *a/b*, Chl *a/c* and Chl *a* protein complexes of photosynthetic eukaryotes, as well as the ELIPs (early light-induced proteins) of green algae and plants (Green et al., 1991; Green and Durnford, 1996; Chapter 1, Green and Anderson). The ELIPs are induced in response to high light, desiccation and other stresses, and they appear to have a photoprotective rather than a light-harvesting role (Adamska, 1997; Montané and Kloppestech, 2000).

The family also includes a number of one-helix

proteins whose sequences are related to the first and third helices of the three-helix antennas and ELIPs (Dolganov et al., 1995; Funk and Vermaas, 1997). The Hlips (high-light-induced proteins), also called Scps (small cab-like proteins), are found in all cyanobacteria so far examined. Genes for related one-helix proteins are also found in the chloroplast genomes of red algae, glaucophytes and cryptophytes (reviewed in Green and Kühlbrandt, 1995), the nucleomorph genome of a cryptophyte (Douglas et al., 2001), and the nuclear genome of *Arabidopsis* (Jansson, 1999; Jansson et al., 2000). Other members of the family, the two-helix Seps (stress-expressed proteins) (Heddad and Adamska, 2000) and the four-helix PsbS protein of PS II (Kim et al., 1992; Wedel et al., 1992), are nuclear encoded, like all the three-helix LHCs and ELIPs, and have been found only in higher plants. There is no evidence for members of the LHC superfamily outside of the cyanobacteria/plastid line.

The unifying signature of the LHC superfamily is a membrane-spanning helix with a motif of Chl-binding residues and a pattern of small and large amino acid side-chains that permit helices to pack together (Fig. 8). In the three dimensional structure of pea LHCII (Kühlbrandt et al., 1994), the first and third trans-membrane helices are doubly cross-linked by ionic bridges between the Glu on one helix and the Arg on the other. This pattern of residues is found in all the single-helix members of the family, suggesting that they may be able to form homodimers in vivo (Dolganov et al., 1995; Green and Kühlbrandt, 1995).

The first model for the origin of this family was inspired by the discovery of a four-helix member of the family, now called PsbS (Kim et al. 1992.; Wedel et al., 1992). The first pair of helices are highly related to the second pair of helices, suggesting that a two-helix ancestor underwent a tandem gene duplication-fusion event, giving a four helix intermediate that later lost one helix to give the ancestral three-helix protein (Green and Pichersky 1994; Green and Kühlbrandt 1995). The two-helix precursor would have originated from the fusion of a gene for a single-helix Hlip-like protein with another sequence encoding a potential membrane-spanning helix. This model appeared to be strengthened when genes for both one-helix (Ohps) and two-helix (Seps) members of the family were found in the *Arabidopsis* genome (Jansson, 1999; Heddad and Adamska, 2000;

Jansson et al., 2000). However, PsbS itself is almost certainly not an ancestral intermediate, since no *psbS* transcript has been found in the *Porphyra* or *Chlamydomonas* EST databases (Nikaido et al., 2000; B. R. Green, unpubl.). As of this writing, it appears that PsbS is a relatively modern invention, probably restricted to the higher plant line (Fig. 9).

A simpler hypothesis involves duplication of a chromosomal segment carrying an *hli*-like gene, with the inclusion of enough additional sequence between the two copies to promote the formation of the middle transmembrane helix. There would have been selective pressure for accumulation of hydrophobic residues in this middle segment, because it would have enabled the first and third helices to retain their original orientation in the membrane and to form the ionic bridges. There is no convincing sequence relatedness between the middle helices of LHCs and ELIPs, so they might have originated in separate events.

## B. The Three-helix Light-harvesting Antennas (LHCs)

### 1. Phylogenetic Relatedness of the Polypeptides

All the light-harvesting members of the LHC superfamily are predicted to have three trans-membrane helices and to fold similarly to LHCII of pea, whose structure has been determined by electron crystallography (Kühlbrandt et al., 1994). Phylogenetic trees based on all the available protein sequences (Durnford et al., 1999; Deane et al., 2000) showed several key points. First of all, the Chl *a/b* and Chl *a/c* proteins were clearly separated. Secondly, the divergence of the Chl *a/b* line into three groups, two of which are predominantly associated with only one photosystem, happened after its separation from the line leading to the Chl *a/c* proteins (Caron et al., 1996; Durnford et al., 1996; Green and Durnford, 1996). One of these branches includes Lhcb1,2,3 and 5 and the algal LHCIIIs, all of which are associated with PS II (Fig. 10). In the green alga *Chlamydomonas*, sequences can be clearly assigned to Lhcb4 (CP29) and Lhcb5 (CP26), which suggests that these complexes were distinct entities prior to the divergence of the streptophyte (plant) and chlorophyte (green algal) lineages (Teramoto et al., 2001). In contrast, the green algal LHCII sequences are on a

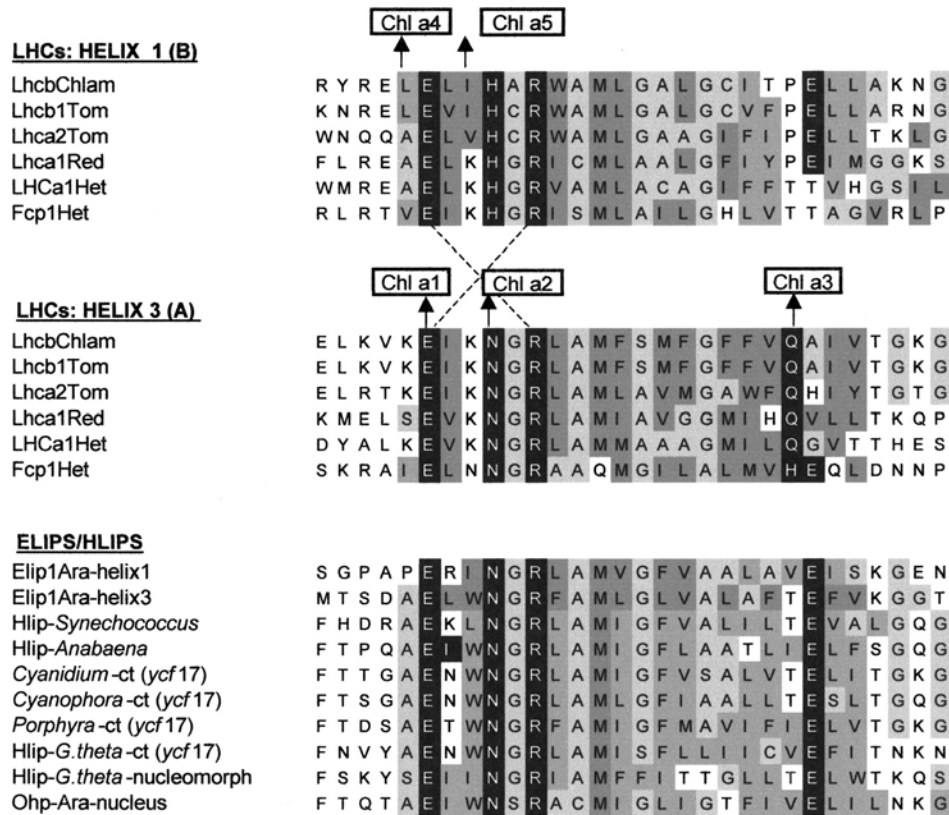


Fig. 8. Conserved sequence motifs in the trans-membrane helices of the LHC superfamily. The five boxed Chl *a*'s are those identified in the electron crystallographic structure of pea LHCII (Kühlbrandt et al., 1994); the residues binding them are in white letters on black background. Helices 1 and 3 are named B and A in Kühlbrandt et al.(1994). Dotted lines indicate a cross-linking ionic bridge between the Chl-binding Glu on one helix with the Arg on the other helix. The C-terminal conserved Glu in ELIPs, Hlips and helix 1 of LHCs may have a role in energy dissipation. Light grey background, small conserved residues; dark grey background, generic hydrophobic residues (FILMVWY). Lhca, PS I-associated; Lhcb, PS II-associated; Fcp, fucoxanthin Chl *a/c*; ct (ycf17), chloroplast-encoded Hlip; nucleomorph, nucleus indicate locations of genes for Hips and Ohp; Ohp, one-helix protein; Tom, tomato, Chlam, *Chlamydomonas reinhardtii*; Red, *Porphyridium cruentum*; Het, *Heterosigma akashiwo*; Ara, *Arabidopsis thaliana*; G. theta, *Guillardia theta*

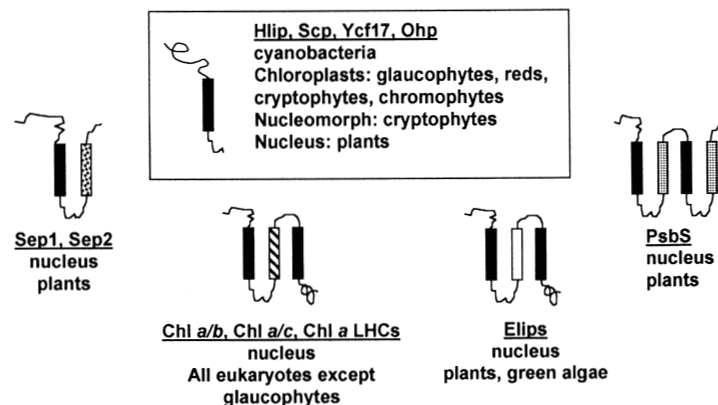


Fig. 9. Cartoon of LHC superfamily members with one, two, three and four transmembrane helices, and their locations. Black helix represents the conserved, probably ancestral helix characteristic of them all. The second helices of Seps, LHCs, ELIPs and the second and fourth helix of PsbS are shaded differently because there is no sequence similarity among them. Hlip or Scp, high-light-induced or 'small cab-like' proteins of cyanobacteria; Ycf17, protein encoded by chloroplast open reading frame ycf17; Ohp, one-helix protein of *Arabidopsis*; Sep, stress-induced proteins of *Arabidopsis*. Details in text.

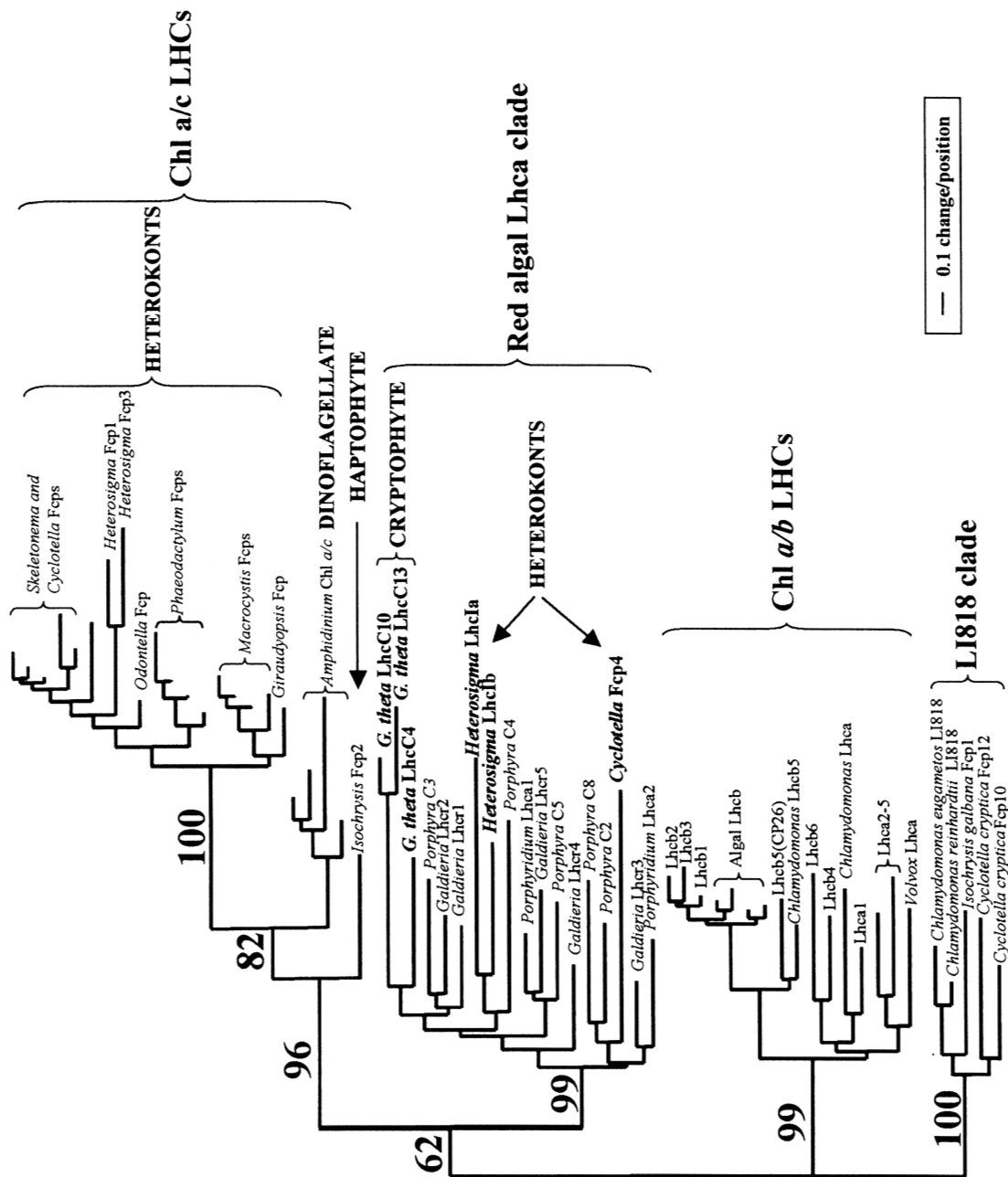


Fig. 10. Phylogenetic tree of the light-harvesting members of the LHC superfamily. Tree was generated by neighbor-joining; percent bootstrap statistical support (numbers on branches) are from maximum likelihood tree. Fcp, fucoxanthin-Chl *a/c* protein; Lhca, LHC associated with PS I; Lhcb, LHC associated with PS II. Sequences are from the diatoms *Skeletonema costatum*, *Cyclotella cryptica*, *Odontella sinensis* and *Phaeodactylum tricornutum*; the raphidophyte *Heterosigma akashiwo*, the dinoflagellate *Amphidinium carterae* CS-21, the haptophyte *Isochrysis galbana*, the cryptophyte *Guillardia theta*; and the red algae *Porphyra yezoensis*, *Galdieria sulphuraria* and *Porphyridium cruentum*. In the Chl *a/b* line, all sequences are from higher plants except as noted. Courtesy of Dr. Kenichiro Ishida.

separate branch from the higher plant Lhcb1, Lhcb2 and Lhcb3 sequences, suggesting that the three polypeptides of higher plant LHCII diversified after the streptophyte-chlorophyte split (Durnford et al., 1999; Teramoto et al., 2001).

Thirdly, the red algal Lhca's and the cryptophyte Chl *a/c* proteins were found at the base of the Chl *a/c* clade<sup>1</sup> (Durnford et al., 1999) or formed a sister group to the main Chl *a/c* branch (Deane et al., 2000). This was further support for the concept that the heterokont, haptophyte, cryptophyte and dinoflagellate lines (all those with Chl *a/c* LHCs) obtained their plastids from a red algal endosymbiont (Delwiche and Palmer, 1997; Douglas et al., 2001). However, recent analyses have added some complications. A sequence from the diatom *Cyclotella cryptica* and two sequences from the raphidophyte *Heterosigma akashiwo* are more closely related to the red algal Lhcas (associated only with PS I) than to the rest of the heterokont Chl *a/c* proteins (Eppard and Rhiel, 1998; Eppard et al., 2000; K. Ishida, unpublished). The tree shown in Fig. 10 includes these sequences and new red algal sequences from *Galdieria sulphuraria* (Marquardt et al., 2001) and the *Porphyra* EST database (Nikaido et al., 2000; K. Ishida, unpublished). Because of the amount of sequence divergence in this inclusive collection, only 132 amino acid positions (60–75% of the mature polypeptides) were used to construct the tree. The tree shows strong bootstrap support (99%) for a 'Red algal Lhca clade' which includes the cryptophyte and the anomalous heterokont sequences. The rest of the Chl *a/c* proteins form a separate, well-supported (96%) clade. However, support for a combined red algal Lhca-Chl *a/c* clade is weak (62%) in this particular tree.

The finding that all the cryptophyte Chl *a/c* protein sequences obtained so far cluster with the red algal LHCI suggests that these cryptophyte antenna proteins may be associated primarily with PS I, in agreement with some biochemical evidence (Bathke et al., 1999). The anomalous heterokont sequences that are solidly in the red algal clade suggest that the heterokont algae may also have an antenna specifically associated with PS I, something that has never been reported. The fact that red algae, and maybe cryptophytes, have LHC antennas associated only with PS I suggests the possibility that the ancestral LHC may have been PS I-associated, and that the

other Chl *a/c* and Chl *a/b* antennas evolved from this LHC separately in the red and green lineages, coincident with loss of phycobilisomes.

However, there is a newly recognized section of the LHC family that is common to both the Chl *a/c* and Chl *a/b* lineages, labeled 'LI818 clade' in Fig. 10 (Deane et al., 2000; Richard et al., 2000). Richard et al. (2000) were the first to point out that a very divergent haptophyte Chl *a/c* sequence (LaRoche et al., 1994) and two divergent *Cyclotella* sequences (Eppard et al., 2000) were most closely related to a mysterious *Chlamydomonas* protein named LI818 (Savard et al., 1996). They suggested that LI818 may have a photoprotective role during the early stages of chloroplast development and that members of the clade are probably quite ancient (Richard et al., 2000). It is possible that this clade is closest to the ancestral LHC.

## 2. Reconstitution Experiments Suggest 'Molecular Opportunism' in Chl Binding

As mentioned above, modern members of the LHC family have a considerable degree of flexibility in pigment binding, suggesting that their ancestors also were able to adapt to binding a variety of different Chls and carotenoids. Reconstitution experiments on Chl *a/b* proteins suggest that at least some of the eight Chl-binding sites common to all Chl *a/b* proteins can ligate either Chl *a* or *b* (Meyer et al. 1996; Giuffra et al., 1997; Bassi et al., 1999; Kleima et al., 1999). One of these proteins can even be reconstituted almost exclusively with Chl *b*, although with somewhat altered energy-transfer characteristics (Kleima et al., 1999). Furthermore, Grabowski et al. (2001) demonstrated that a red algal LHC apoprotein (LhcaR1) could be reconstituted with the pigments from either a higher plant or a chromophyte alga, and that the reconstituted pigment-protein could perform the critical function of transferring energy absorbed by the accessory Chl (Chl *b* or Chl *c*) to Chl *a*. Approximately eight Chls were bound per polypeptide chain, the same as the number bound when the protein was reconstituted with its own pigments, and close to the number found in the native complex. It therefore appears that the Chl-binding sites on the LHC protein may be conserved, but are not particularly specific for which Chl they bind, and in fact can bind Chls that their ancestors probably never encountered (Green, 2001).

<sup>1</sup> A clade is a monophyletic group that includes all the descendants of a common ancestor.

### C. ELIPs, Seps and Hlips

The interesting thing about these members of the LHC super family is that most of them are involved in photoprotection (Adamska, 1997). The three-helix ELIPs have been shown to bind carotenoids and a small amount of Chl (Adamska et al., 1999). They are not included in the tree of Fig. 10 because they have little sequence relatedness to the LHCs outside of the first and third transmembrane helix, so sequence alignments would be guesswork. They have not been seen in any alga in the red line, but it would be premature to conclude that they are restricted to the green line. The two-helix Sep1 and Sep2 are induced only by high light stress (Heddad and Adamska, 2000). The one-helix Hlips of the cyanobacterium *Synechocystis* PCC6803 are induced in response to high light stress, and to nutrient deprivation that leads to high light stress (Dolganov et al. 1995; He et al., 2001). The involvement of members of the LHC superfamily in carotenoid accumulation and high-light-stress response has led to the suggestion that the prokaryotic ancestors were originally high light-stress response proteins, with some three-helix members of the family later evolving the ability to cope with low light levels by binding more Chl (Green and Kühlbrandt, 1995; Gantt, 1998; Montané and Kloppstech, 2000).

### D. Endosymbiosis and the Evolution of the LHC Superfamily

No three-helix members of the LHC family have been found in cyanobacteria or in one group of photosynthetic eukaryotes, the glaucophytes (Steiner and Löffelhardt, 2002). The glaucophytes retain a vestige of the cyanobacterial proteo-glycan cell wall between the two envelope membranes of their chloroplast (also called a 'cyanelle'). Molecular data support the idea that this group of algae may have been the earliest to branch off from the common ancestor of all photosynthetic eukaryotes, prior to the divergence of the red and green lines (Bauldauf et al., 2000; Moreira et al., 2000). The glaucophyte plastid genome carries a gene for a single-helix Hlip, but we have no information about its function.

If this scenario is correct, it means that the three-helix members of the LHC family evolved in the common ancestor of the red and green algae, after they had diverged from the glaucophyte line. Since there are no plastid-encoded three-helix LHCs, the

existence of nucleus-encoded one-helix relatives suggests that a copy of the one-helix ancestral gene was first transferred to the nucleus in the red-green common ancestor and that the ancestral three-helix LHC evolved in the nucleus before the divergence of the red and green lines. It is most likely that these plastids still had phycobilisomes and made Chl *b* as well as Chl *a* (Bryant, 1992; Tomitani et al., 1999).

Many lines of evidence now support the idea that several algal groups obtained their plastids by secondary endosymbiosis (Chapter 1, Green and Anderson). The eukaryotic endosymbiont not only provided the plastid, but also transferred many nuclear genes to the new host's nucleus. The LHC trees support the idea that *Euglena* and *Chlorarachnion* acquired their chloroplasts from green algal endosymbionts (Deane et al., 2000), and that all Chl *a/c* plastids originated from a red algal endosymbiont. The evidence for the latter is particularly strong for the cryptophytes, which still have a relict nucleus (nucleomorph) from the red algal ancestor. In *Guillardia theta* there is an *hli* gene on the plastid genome and a different *hli* gene on the nucleomorph genome (Douglas et al., 2001). However, the three-helix LHC genes are found only in the nuclear genome (Deane et al., 2000; Chapter 11, Macpherson and Hiller).

### VIII. Single Membrane Helix Antennas of Purple and Green Filamentous Bacteria

Purple bacteria and green filamentous bacteria have membrane-intrinsic antennas that are multimers of a heterodimer consisting of one  $\alpha$  and one  $\beta$  polypeptide chain, 2–3 Bhl and one or two carotenoids (Chapter 5, Robert, Cogdell and van Grondelle; Zuber and Brunisholz, 1991; Zuber and Cogdell, 1995). The  $\alpha$  and  $\beta$  subunits are small polypeptides (5–7 kDa), each of which has one membrane-spanning helix containing a conserved His residue that binds a BChl. There are two types of antenna complex: the core LH1 (B875), believed to be a ring of 16 dimers around the reaction center, and the peripheral LH2 (B800-850) and LH3 (B800-820), organized in smaller rings separate from the reaction center. The LH polypeptide sequences do not contain enough information for phylogenetic tree construction because of their shortness and the preponderance of 'generic' hydropathic residues in the membrane-spanning domain. However, simple alignment shows

clearly that the  $\alpha$  subunits of all species are related to each other, and so are the  $\beta$  subunits (Zuber and Brunisholz, 1991; Zuber and Cogdell, 1995; see Fig. 2 in Chapter 5, Robert et al.). The  $\alpha$  and  $\beta$  subunits share only a conserved BChl-binding His, but given their functional similarities it is most likely they had a common ancestor.

The  $\alpha$  and  $\beta$  polypeptides of the green filamentous bacterium *Chloroflexus* are clearly related to the  $\alpha$  and  $\beta$  polypeptides of the purple bacteria (Zuber and Cogdell, 1995). The presence of related proteins in two such otherwise unrelated groups of bacteria suggests strongly that lateral gene transfer was involved, but does not tell us which group of bacteria originated this type of antenna. If  $\alpha$  and  $\beta$  subunits diverged subsequent to an ancestral gene duplication, the duplication must have predated the lateral transfer between the purple and green non-sulfur groups of bacteria.

The most interesting thing about protein comparisons in this family is that seemingly small differences in protein-chromophore interactions are responsible for a range of absorbing wavelengths from 800 nm to 890 nm in the Bchl *a* containing species (Chapter 5, Robert et al.). This is extended even further to 1015–1020 nm in the Bchl *b*-containing species *Blastochloris* (*Rhodospseudomonas*) *viridis* and *Ectothiorhodospira* *halochloris*. These interactions can be studied in vitro by reconstitution of mutant LH polypeptides with BChl *a* (Davis et al., 1997), or by the reconstitution of native polypeptides with a variety of natural and synthetic BChl derivatives (Davis et al., 1996; Fiedor et al., 2001). Furthermore, the high-resolution structures of two LH2s and one LH3 (McLuskey et al., 2001) provides the spatial information for designing detailed structure-function studies.

## IX. Antenna Proteins Unique to Certain Groups

In contrast to the Core Complex family, which is present in some form in the three groups of bacteria with PS I-type photosystems (cyanobacteria, green sulfur bacteria and heliobacteria), and the LHC superfamily, which is present in all cyanobacteria and photosynthetic eukaryotes, some antennas have a much more restricted distribution. In two of these cases, lateral gene transfer provides the best explanation for their pattern of occurrence.

### A. Chlorosomes and the FMO Protein of Green Bacteria

Chlorosomes are found in both the green sulfur bacteria (Chlorobiaceae) and the green gliding bacteria (Chloroflexaceae) (Chapter 6, Blankenship and Matsuura). The proteins of the *Chlorobium* chlorosome belong to several gene families and show evidence of domain swapping (Vassilieva et al., 2002). *Chloroflexus* chlorosomes have a simpler protein complement than those of *Chlorobium*, but at least two of their major proteins appear to be related to two of the *Chlorobium* proteins (Blankenship et al., 1995). This suggests a common but distant evolutionary origin for the two kinds of chlorosome. Several BChl biosynthesis genes of *Chlorobium* also appear more closely related to those of *Chloroflexus* (Xiong et al., 2000; Eisen et al., 2002; Xiong and Bauer, 2002). The two types of green bacteria are otherwise not at all related, and have different types of reaction centers and membrane-intrinsic antennas (Table 1), indicating the possibility of lateral gene transfer.

The FMO BChl *a* protein is found only in green sulfur bacteria. It owes its fame to the fact that the FMO trimer from *Prosthecochloris aestuarii* was the first chlorophyll-protein structure determined to high resolution (Matthews et al., 1979). However, it turned out to be quite atypical as it is the only such protein that consists of a  $\beta$ -barrel with the BChl wrapped inside. Its only relative in the databanks is the FMO protein from *Chlorobium*, which has an almost identical protein fold (Li et al., 1997). The origin of this protein is a mystery.

### B. Peridinin-Chl *a* Protein of Dinoflagellates

The peridinin-Chl *a* protein is found only in dinoflagellates (Chapter 11, Macpherson and Hiller). Its sequence has been determined for a number of species, and the sequences are all related. The larger members are clearly the result of duplication and fusion of two copies of a smaller gene (Norris and Miller, 1994; Hiller et al., 2001). There are no obvious relatives in the sequence databanks, and the three-dimensional structure has a unique fold (Hofmann et al., 1996). The most interesting thing about this antenna is that the carotenoids are the light-harvesting chromophore. There is a ratio of six or eight carotenoids to two Chl *a*'s, and the Chls appear to function largely to transfer energy from the carotenoids to membrane-intrinsic antennas or



reaction centers (Chapter 11, Macpherson and Hiller). It will be interesting to see if distant homologs eventually show up in sequence databases.

### **X. The Big Picture: The Five Divisions of Photosynthetic Bacteria**

The high-resolution structures of PS I, PS II and the purple bacterial reaction center have established that all photosystems had a common ancestor (Section V.A). If we accept the idea that bacterial genomes are mosaics that have been enriched by the incorporation of genes laterally acquired from other prokaryotes (Section III.4; Blankenship, 2001;), we can discuss the evolutionary history of antennas, reaction centers and pigment biosynthesis enzymes without being constrained by the (still unresolved) family tree of the five photosynthetic eubacterial divisions.

The first whole-genome comparison of representatives of the five divisions of photosynthetic bacteria has shown conclusively that there has been extensive lateral gene transfer among them (Raymond et al., 2002). Even when maximum likelihood methods were applied to 188 proteins found in all five taxa, it was not possible to find a consensus tree. Every possible phylogenetic tree was represented by more than a few examples!

Support for lateral gene transfer comes from ecological considerations as well as from genome comparisons. In nature, most prokaryotes are not found in pure culture, but rather in multi-species communities. Modern microbial mat communities can be made up of millimeter thick layers of Chloroflexaceae, cyanobacteria, purple bacteria and green sulfur bacteria in various combinations (Castenholz et al., 1992; Pierson, 1994; Castenholz and Pierson, 1995). Such mats are believed to have been very common in the Precambrian and to have given rise to sedimentary structures known as stromatolites, where many of the fossils of early prokaryotes have been found (Pierson, 1994; Schopf, 1994; Nisbet and Sleep, 2001). These would have provided suitable environments for lateral gene transfer among different types of prokaryote. Furthermore, the ancient microbial communities were not disturbed by the eukaryotic grazers and competitors that limit them today, so they could have harbored much more diverse populations of prokaryotes.

There have been a number of thoughtful attempts

to rationalize the evolution of reaction centers and antennas with the evolution of the five groups of photosynthetic bacteria (Pierson and Olson, 1989; Blankenship, 1992, 1994, 2001; Stackebrandt et al., 1996; Nitschke et al., 1998; Gupta et al., 1999; Baymann et al., 2001; Olson, 2001; Xiong and Bauer, 2002). There are several open questions. Was the last common ancestor of all photosystems a stripped-down homodimeric version of a Q-type RC with no core antenna, or did it already have a built-in core antenna and FeS electron acceptors? How could the two types of photosystem have evolved from this common ancestor and ended up in such divergent groups of bacteria? (Note that these questions do not consider the steps in the origin of the common ancestor itself). Then there is the problem of explaining how cyanobacteria acquired both kinds of reaction center and evolved the ability to extract electrons from water. And as can be seen in Table 1, there are different combinations of peripheral antennas and reaction centers to be explained.

The earliest true cells were probably lithotrophs with a primitive electron transport chain that enabled them to obtain energy by oxidizing reduced inorganic compounds (e.g. sulfides) using other inorganics (e.g. nitrate) as electron acceptors (Castresana and Moreira, 1999; Nisbet and Sleep, 2001). The earliest photoautotrophs evolved in an anaerobic environment rich in available iron and sulfides (Canfield and Raiswell, 1999), which would have been conducive to developing one-electron transfers using FeS centers. They would already have a cytochrome *b*-type complex (Nitschke et al., 1998; Schütz et al., 2000). It is generally assumed that the ancestral RC was homodimeric, like those of the present-day Chlorobiaceae and Heliobacteriaceae (Table 1). Because present-day green sulfur bacteria live in environments that most closely resemble that of the early earth, and because they have only 16 core antenna BChl *a* as compared to 30 BChl *g* for *Heliobacillus* and 96 Chl *a* for cyanobacterial PS I (Table 2, Chapter 1, Green and Anderson), I agree with Baymann et al. (2001) in favoring a chlorobial RC as closest to the ancestral RC (Fig. 11).

Both the Chlorobiaceae and the heliobacteria are obligate anaerobes with homodimeric FeS-type RCs, but all the members of the former group are photoautotrophs whereas the heliobacteria belong to the Gram-positive Firmicutes, most of which are not photosynthetic. This suggests that the heliobacteria may have acquired their RCs by lateral transfer, from

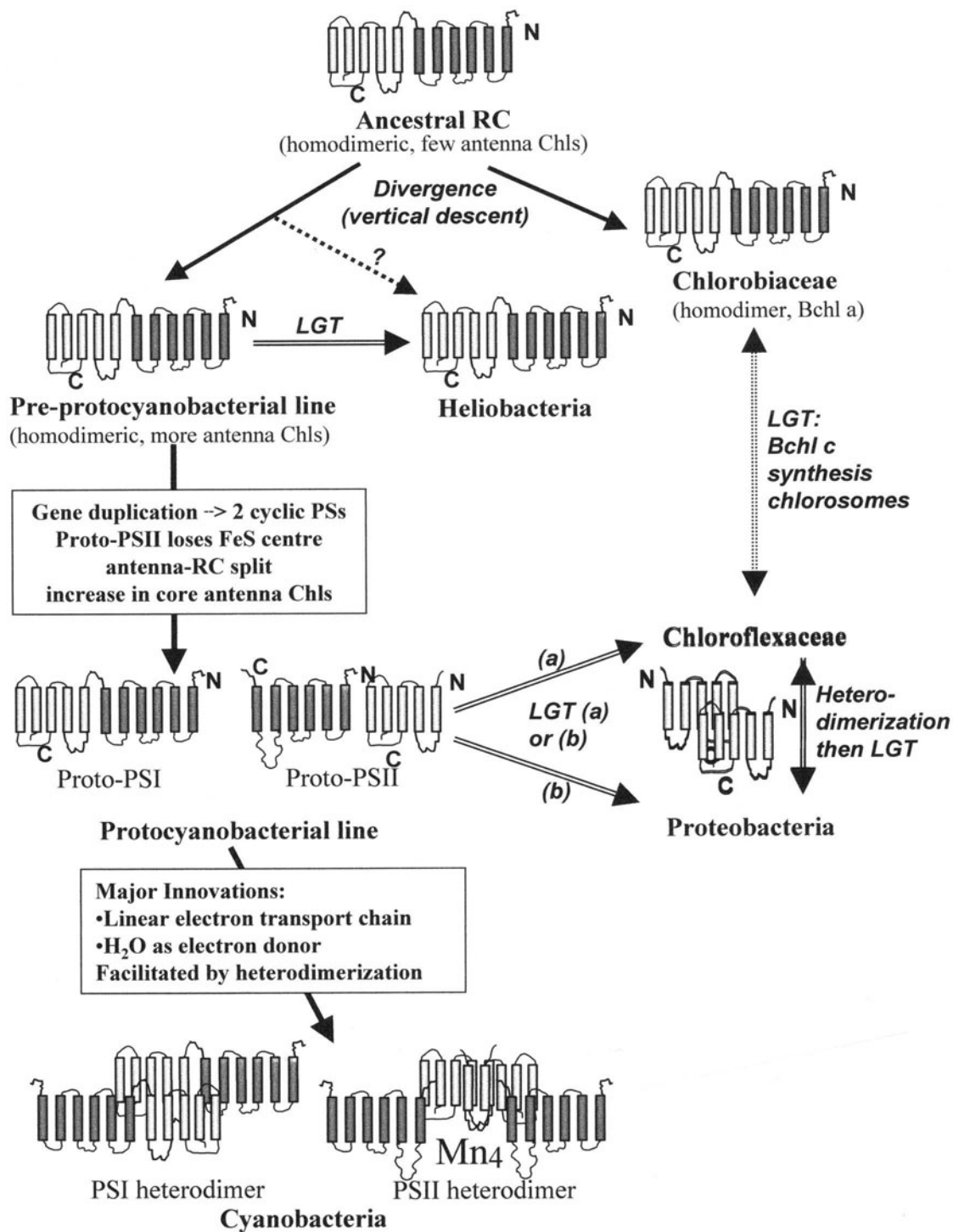


Fig. 11. Model for the origin of reaction centers and antennas in the five divisions of photosynthetic bacteria, taking into account the possibility of lateral gene transfer (LGT). Dark cylinders, membrane helices of core antennas; light cylinders, the five RC helices. See text for discussion.

either the green sulfur or cyanobacteria (Madigan and Ormerod, 1995). Most of the known strains of heliobacteria are found in association with cyanobacteria in rice paddies (Madigan and Ormerod, 1995). A number of heliobacterial and cyanobacterial proteins are close neighbors in phylogenetic trees, including a large cluster of ribosomal proteins, two elongation factors and an RNA polymerase subunit (Hansmann and Martin, 2000), subunits of the cytochrome bc complex (Schütz et al., 2000) and several BChl biosynthesis enzymes (Xiong et al., 2000; Xiong and Bauer, 2002). In addition, 24% of the 188 trees in the five-genome analysis support the clustering of *Synechocystis* 6803 and *Heliobacillus mobilis* (Raymond et al., 2002). However, given that some rRNA trees also support this relationship (Woese, 1987), the possibility of vertical descent cannot be completely ruled out (dotted arrow in Fig. 11).

According to the scheme presented in Fig. 11, PS II originated in the cyanobacterial line by duplication of the gene for the (still homodimeric) proto-PS I RC protein. Over time, the two photosystems diverged in sequence, proto-PS II lost its FeS center and developed the ability to exchange reduced quinones with the bilayer. At some point, the proto-PS II gene became split into a six-helix antenna part and a five-helix RC part. This fragmentation might have facilitated the loss of the FeS center, or the loss of the FeS center might have facilitated adaptation to separate RC and antenna. Either one might have helped to open up a pathway for the exchange of reduced quinones with the bilayer. Heterodimerization would have occurred later, because CP47 and CP43 are more similar in sequence to each other than to PsaA or PsaB. The origin of PS II from PS I is supported by some sequence similarities (Vermaas, 1994; Fromme et al. 1996; Schubert et al., 1998; Baymann et al. (2001), although the statistical support is not strong. The two most important innovations that followed were the joining of the two photosystems into a linear electron transport chain and the development of the ability to use water, one of the commonest molecules on earth, as an electron donor. As several authors have pointed out, this was probably arrived at through intermediate stages, using other electron donors such as Fe(II) and hydrogen peroxide (Blankenship and Hartman, 1998; Dismukes et al., 2001).

The splitting of the core antenna from RC in the proto-PS II would have made it possible for the RC

gene to have been transferred either to an ancestor of the Chloroflexaceae or to a proteobacterium (Fig. 11). Both the purple proteobacteria and the Chloroflexaceae are facultative photosynthesizers, i.e. they do not have an absolute requirement for light. Their RC proteins and their LH1 antenna proteins are related, and it is generally accepted that one group acquired these genes from the other by LGT (Blankenship, 1992). The LH1 antenna evolved in whichever line first acquired the photosystem. Heterodimerization of RC and LH1 would have allowed for further structural adaptations, and LH2 would have originated by gene duplication in the purple bacteria.

Another likely example of lateral transfer concerns the chlorosomes, which are found in both Chlorobiaceae and Chloroflexaceae. The chlorosome genes could have been acquired laterally by one group from the other. If BChl synthesis genes were transferred at the same time and replaced the original BChl genes (Eisen et al., 2002), it could explain why the two (otherwise very unrelated) kinds of 'green bacteria' appear as sister groups on trees of BChl synthesis enzymes (Xiong et al., 2000).

Figure 11 is very similar to the model proposed by Baymann et al. (2001) and is similar to an earlier model of Vermaas (1994) in proposing that Q-type RCs originated from FeS-type RCs by gene duplication. The model of Olson and Pierson (Pierson and Olson, 1989), updated by Olson (2001) posits that a very early ancestral prokaryote evolved both types of reaction center, and that subsequent diversification led to the loss of one type of RC or the other in every lineage except the cyanobacteria. Some earlier models proposed the reverse: that the cyanobacteria resulted from a fusion of two bacteria with different reaction center types (Blankenship, 1992, 1994; Xiong et al., 1998). The most recent version of that model attempts to include the Chl/BChl biosynthesis pathways in a rather complex scheme with an ancestral purple bacterial RC giving rise to heliobacterial and green sulfur bacterial lines with the acquisition of a six helix antenna, and subsequent fusion of the former with another descendant of the purple bacterial RC (Xiong and Bauer, 2002). All the models are reviewed by Olson (2001).

Regardless of how the five divisions of photosynthetic bacteria acquired their abilities, the ecologically determining event was the development of oxygen evolution in the cyanobacteria. The

resulting rise of O<sub>2</sub> levels in the mid-Proterozoic, with subsequent depletion of Fe(II), would have favored photosystems that were not based on FeS centers, i.e. it would have led to a competitive advantage for the cyanobacteria over the anaerobic green sulfur bacteria and heliobacteria. It is generally agreed that micro-organisms have played and still play a dominant role in determining the composition of the earth's atmosphere (Nisbet and Sleep, 2001; Kasting and Seifert, 2002). Without the cyanobacteria, there might never have been enough oxygen to support the evolution of multicellular life. And without the efficient harnessing of the sun's energy by the light-harvesting antennas, there would be little photosynthesis of any sort. Antennas can truly be considered among the most important molecules on earth!

## References

- Adachi J and Hasegawa M (1996a) Model of amino acid substitution in proteins encoded by mitochondrial DNA. *J Mol Evol* 42: 459–468
- Adachi J and Hasegawa M (1996b) MOLPHY: Programs for molecular phylogenetics. Version 2.2, pp 1–150. Computer Science Monographs 23, Institute of Statistical Mathematics, Tokyo
- Adachi J, Waddell PJ, Martin W and Hasegawa M (2000) Plastid genome phylogeny and a model of amino acid substitution for proteins encoded by chloroplast DNA. *J Mol Evol* 50: 348–358
- Adams KL, Daley DO, Qiu Y-L, Whelan J and Palmer JD (2000) Repeated, recent and diverse transfers of a mitochondrial gene to the nucleus in flowering plants. *Nature* 408: 354–357
- Adamska I (1997) ELIPs—light induced stress proteins. *Physiol Plant* 100: 794–805
- Adamska I, Roobol-Bóza M, Lindahl M and Andersson B (1999) Isolation of pigment-binding early light-inducible proteins from pea. *Eur J Biochem* 260: 453–460
- Altschul SF, Madden TL, Schäfer AA, Zhang J, Zhang Z, Miller W and Lipman DJ (1997) Gapped BLAST and PSI-BLAST: A new generation of protein database search programs. *Nucleic Acids Res* 25: 3389–3402
- Apt KE, Collier JL and Grossman AR (1995) Evolution of the phycobiliproteins. *J Mol Biol* 248: 79–96
- Apt KE, Metzner S and Grossman AR (2001) The subunits of phycoerythrin from a red alga: Position in phycobilisomes and sequence characterization. *J Phycol* 37: 64–70
- Arabidopsis Genome Initiative (2000) Analysis of the genome sequence of the flowering plant *Arabidopsis thaliana*. *Nature* 408: 796–815
- Barber J, Morris E and Büchel C (2000) Revealing the structure of the Photosystem II chlorophyll binding proteins, CP43 and CP47. *Biochim Biophys Acta* 1459: 239–247
- Barbrook AC, Lockhart PJ and Howe CJ (1998) Phylogenetic analysis of plastid origins based on *secA* sequences. *Curr Genet* 34: 336–341
- Bashford D, Chothia C and Lesk AM (1987) Determinants of a protein fold. Unique features of the globin amino acid sequences. *J Mol Biol* 196: 199–216
- Bassi R, Croce R, Cugini D and Sandoña D (1999) Mutational analysis of a higher plant antenna protein provides identification of chromophores bound into multiple sites. *Proc Natl Acad Sci USA* 96: 10056–10061
- Bathke L, Rhiel E, Krumbein WE and Marquardt J (1999) Biochemical and immunochemical investigations on the light-harvesting system of the cryptophyte *Rhodomonas* sp: Evidence for a Photosystem I specific antenna. *Plant Biology* 1: 516–523
- Bauer CE, Bollivar DW and Suzuki JY (1993) Genetic analyses of photopigment biosynthesis in eubacteria: A guiding light for algae and plants. *J Bacteriol* 175: 3919–3925
- Bauldauf SL, Roger AJ, Wenk-Siefert I and Doolittle, WF (2000) A kingdom level phylogeny of eukaryotes based on combined protein data. *Science* 290: 972–977
- Baymann F, Brugna M, Mühlhoff U and Nitschke W (2001) Daddy, where did (PS)I come from? *Biochim Biophys Acta* 1507: 291–310
- Beale SI (1999) Enzymes of chlorophyll biosynthesis. *Photosynth Res* 60: 43–73
- Bengtson S (ed) (1994) Early Life on Earth. 84<sup>th</sup> Nobel Symposium. Columbia University Press
- Bibby TS, Nield J and Barber J (2001a) A Photosystem II-like protein, induced under iron-stress, forms an antenna ring around the Photosystem I trimer in cyanobacteria. *Nature* 412: 743–745
- Bibby TS, Nield J, Partensky F and Barber J (2001b) Antenna ring around Photosystem I. *Nature* 413: 590
- Blankenship RE (1992) Origin and early evolution of photosynthesis. *Photosynth Res* 33: 91–111
- Blankenship RE (1994) Protein structure, electron transfer and evolution of prokaryotic photosynthetic reaction centers. *Antonie Van Leeuwenhoek* 65: 311–329
- Blankenship RE (2001) Molecular evidence for the evolution of photosynthesis. *Trends Plant Sci* 6: 4–6
- Blankenship RE and Hartman H (1998) The origin and evolution of oxygenic photosynthesis. *Trends Biochem Sci* 23: 94–97
- Blankenship RE, Olson JM and Miller M (1995) Antenna complexes from green photosynthetic bacteria. In: Blankenship RE, Madigan MT and Bauer CE (eds) *Anoxygenic Photosynthetic Bacteria* pp 399–435, Kluwer Academic Publishers, Dordrecht
- Blattner FR, Plunkett G, Bloch CA, Perna NT, Burland V, Riley M, Collado-Vides J, Glasner JD, Rode CK, Mayhew GF, Gregor J, Davis NW, Kirkpatrick HA, Goeden MA, Rose DJ, Mau B and Shao Y (1997) The complete genome sequence of *Escherichia coli* K-12. *Science* 277: 1453–1462
- Boekema EJ, Hifney A, Yakushevskaya AE, Piotrowski M, Keegstra W, Berry S, Michel K-P, Pistorius EK and Kruij J (2001) A giant chlorophyll-protein complex induced by iron deficiency in cyanobacteria. *Nature* 412: 745–748
- Boichenko VA, Klimov VV, Miyashita H and Miyachi S (2000) Functional characteristics of chlorophyll *d*-predominating photosynthetic apparatus in intact cells of *Acaryochloris marina*. *Photosynth Res* 65: 269–277
- Boore JL and Brown WM (1998) Big trees from little genomes: Mitochondrial gene order as a phylogenetic tool. *Curr Opin Genet Devel* 8: 668–674
- Boucher Y and Doolittle FW (2000) The role of lateral gene

- transfer in the evolution of isoprenoid biosynthesis pathways. *Molecular Microbiol* 37:703–716
- Bouvier F, D'Harlingue A, Backhaus RA, Kumagai MH and Camara B (2000) Identification of neoxanthin synthase as a carotenoid cyclase paralog. *Eur J Biochem* 267: 6346–6352
- Brasier MD, Green OR, Jephcoat AP, Kleppe AK, van Kranendonk MJ, Lindsay JF, Steele A and Grassineau NV (2002) Questioning the evidence for Earth's oldest fossils. *Nature* 416: 76–81
- Brocks JJ, Logan GA, Buick R and Summons RE (1999) Archean molecular fossils and the early rise of eukaryotes. *Science* 285: 1033–1036
- Brown JR and Doolittle WF (1997) Archaea and the prokaryote-to-eukaryote transition. *Microbiol Mol Biol Rev* 61: 456–502
- Bryant DA (1992) Puzzles of chloroplast ancestry. *Curr Biol* 2:240–242.
- Burke DH, Alberti M and Hearst JE (1993a) The *Rhodobacter capsulatus* chlorin reductase-encoding locus, *bchA*, consists of three genes, *bchX*, *bchY*, and *bchZ*. *J Bacteriol* 175: 2407–2413
- Burke DH, Hearst JE and Sidow A (1993b) Early evolution of photosynthesis—clues from nitrogenase and chlorophyll iron proteins. *Proc Natl Acad Sci USA*. 90:7134–7138
- Burnap RL, Troyan T and Sherman LA (1993) The highly abundant chlorophyll-protein complex of iron-deficient *Synechococcus* sp. PCC7942 (CP43') is encoded by the *isiA* gene. *Plant Physiol* 103: 893–902
- Butterfield NJ (2000) *Bangiomorpha pubescens* N. gen., n. sp.: Implications for the evolution of sex, multicellularity, and the Mesoproterozoic/Neoproterozoic radiation of eukaryotes. *Paleobiology* 26: 386–404
- Butterfield NJ and Rainbird RH (1998) Diverse organic-walled fossils, including possible dinoflagellates, from the Early Neoproterozoic of arctic Canada. *Geology* 26: 963–966
- Butterfield NJ, Knoll AH and Swett K (1990) A bangiophyte red alga from the Proterozoic of Arctic Canada. *Science* 250: 204–107
- Canfield DE and Raiswell R (1999) The evolution of the sulfur cycle. *Am J Sci* 299: 697–723
- Cao Y, Adachi J, Janke A, Pääbo S and Hasegawa M (1994) Phylogenetic relationships among eutherian orders estimated from inferred sequences of mitochondrial proteins: Instability of a tree based on a single gene. *J Mol Evol* 39: 519–527
- Caron L, Douady D, Quinet-Szely M, de Goër S and Bérkaloff C (1996) Gene structure of a chlorophyll *a/c*-binding protein from a brown alga: Presence of an intron and phylogenetic implications. *J Mol Evol* 43: 270–280
- Castenholz RW and Pierson BK (1995) Ecology of thermophilic anoxygenic phototrophs. In: Blankenship RE, Madigan MT and Bauer CE (eds) *Anoxygenic Photosynthetic Bacteria*, pp 87–103. Kluwer Academic Publishers, Dordrecht
- Castenholz RW, Bauld J and Pierson BK (1992) Photosynthetic Activity in Modern Microbial Mat-Building communities. In: Schopf JW and Klein C (eds) *The Proterozoic Biosphere, a Multidisciplinary Study*, pp 279–285. Cambridge University Press, Cambridge
- Castresana J and Moreira D (1999) Respiratory chains in the last common ancestor of living organisms. *J Mol Evol* 49: 453–460
- Cavalier-Smith T (2000) Membrane heredity and early chloroplast evolution. *Trends Plant Sci* 5: 174–182
- Cavalier-Smith T (2002) Chloroplast evolution: Secondary symbiogenesis and multiple losses. *Curr Biol* 12: R62–R64
- Chang S (1994) The planetary setting of prebiotic evolution. In Bengtson S (ed) *Early Life on Earth*. Nobel Symposium No. 84, pp 11–23. Columbia University Press, New York
- Chang SW and Donoghue MJ (2000) Recreating ancestral proteins. *Trends Ecol Evol* 15: 109–114
- Chisholm SW, Olson RJ, Zettler ER, Goerick R, Waterbury JB and Welschmeyer NA (1988) A novel free-living prochlorophyte abundant in the oceanic euphotic zone. *Nature* 334: 340–343
- Cunningham FX and Gantt E (2001) One ring or two? Determination of ring number in carotenoids by lycopene  $\epsilon$ -cyclases. *Proc Natl Acad Sci USA* 98: 2905–2910
- Davis CM, Parkes-Loach PS, Cook CK, Meadows KA, Bandilla M, Scheer H and Loach PA (1996) Comparison of the structural requirements for bacteriochlorophyll binding in the core light-harvesting complexes of *Rhodospirillum rubrum* and *Rhodobacter sphaeroides* using reconstitution methodology with bacteriochlorophyll analogs. *Biochemistry* 35: 3072–3084
- Davis CM, Bustamente PL, Todd JB, Parkes-Loach PS, McGlynn P, Olsen JD, McMaster L, Hunter CN and Loach PA (1997) Evaluation of structure-function relationships in the core light-harvesting complex of photosynthetic bacteria by reconstitution with mutant polypeptides. *Biochemistry* 36: 3671–3679
- Dayhoff MO, Schwartz RM and Orcutt BC (1978) A model of evolutionary change in proteins. In Dayhoff MO (ed) *Atlas of Protein Sequence and Structure*, Vol 5, Supplement 3, pp 345–352. National Biomedical Research Foundation, Washington, D.C.
- Deane JA, Fraunholz M, Su V, Maier U-G, Martin W, Durnford DG and McFadden GI (2000) Evidence for nucleomorph to host nucleus gene transfer: Light-harvesting complex proteins from cryptomonads and chlorarachniophytes. *Protist* 151: 239–252
- Deckert G, Warren PV, Gaasterland T, Young WG, Lenox AL, Graham DE, Overbeek R, Snead MA, Keller M, Aujay M, Huber R, Feldman RA, Short JM, Olsen GJ and Swanson RV (1998) The complete genome of the hyperthermophilic bacterium *Aquifex aeolicus*. *Nature* 392: 353–358
- Delwiche CF, Palmer JD (1997) The origin of plastids and their spread via secondary endosymbiosis. *Pl Syst Evol [Suppl.]* 11: 53–86
- Dismukes GC, Klimov VV, Baranov SV, Koslov YN, DasGupta J and Tyryshkin A (2001) The origin of atmospheric oxygen on Earth: The innovation of oxygenic photosynthesis. *Proc Natl Acad Sci USA* 98: 2170–2175
- Dolganov NAM, Bhaya D, Grossman AR (1994) Cyanobacterial protein with similarity to the chlorophyll *a/b* binding proteins of higher plants: evolution and regulation. *Proc Natl Acad Sci USA* 92:636–640
- Doolittle RF (1995) Of Archae and Eo: What's in a name? *Proc Natl Acad Sci USA* 92: 2421–2423
- Doolittle WF (1999) Phylogenetic classification and the universal tree. *Science* 284: 2124–2128.
- Doolittle WF (2000) The nature of the universal ancestor and the evolution of the proteome. *Curr Opin Struct Biol* 10: 355–358
- Douglas SE and Penny SL (1999) The plastid genome of the cryptophyte alga *Guillardia theta*: Complete sequence and

- conserved syntenic groups confirm its common ancestry with red algae. *J Mol Evol* 48: 236–244
- Douglas S, Zauner S, Fraunholz M, Beaton M, Penny S, Deng L-T, Wu X, Reith M, Cavalier-Smith R and Maier U-G (2001) The highly reduced genome of an enslaved algal nucleus. *Nature* 410: 1091–1096
- Ducret A, Sidler W, Frank G and Zuber H (1994) The complete amino acid sequence of R-phycoerythrin- $\alpha$  and  $\beta$  subunits from the red alga *Porphyridium cruentum*. Structural and phylogenetic relationships of the phycoerythrins within the phycoerythrin families. *Eur J Biochem* 221: 563–580
- Durnford DG, Aebersold R, Green BR (1996) The fucoxanthin-chlorophyll proteins from a chromophyte alga are part of a large multigene family: Structural and evolutionary relationships to other light harvesting antennae. *Mol Gen Genet* 253: 377–386
- Durnford DG, Deane JA, Tan S, McFadden GI, Gantt E and Green BR (1999) A phylogenetic assessment of the eukaryotic light-harvesting antenna proteins, with implications for plastid evolution. *J Mol Evol* 48: 59–68
- Eisen JA (2000) Horizontal gene transfer among microbial genomes: new insights from complete genome analysis. *Curr Opin Genet Devel* 10: 606–611
- Eisen JA and 35 others (2002) The complete genome sequence of *Chlorobium tepidum* TLS, a photosynthetic, anaerobic, green-sulfur bacterium. *Proc Natl Acad Sci* 99: 9509–9514
- Eppard M and Rhiel E (1998) The genes encoding light-harvesting subunits of *Cyclotella cryptica* (Bacillariophyceae) constitute a complex and heterogeneous family. *Mol Gen Genet* 260: 335–345
- Eppard M, Krumbein WE, von Haeseler A and Rhiel E (2000) Characterization of *fcp4* and *fcp12*, two additional genes encoding light harvesting proteins of *Cyclotella cryptica* (Bacillariophyceae) and phylogenetic analysis of this complex gene family. *Plant Biol* 2: 283–289
- Fast NM, Kissinger JC, Roos DS and Keeling PJ (2001) Nuclear-encoded, plastid-targeted genes suggest a single common origin for apicomplexan and dinoflagellate plastids. *Mol Biol Evol* 18: 418–426.
- Fiedler L, Leupold D, Teuchner K, Voigt B, Hunter CM, Scherz A and Scheer H (2001) Excitation trap approach to analyze size and pigment-pigment coupling: reconstitution of LH1 antenna of *Rhodospirillum rubrum* with Ni-substituted bacteriochlorophyll. *Biochemistry* 40: 3737–3747
- Felsenstein J (1985) Confidence limits on phylogenies: An approach using the bootstrap. *Evolution* 39: 783–791
- Felsenstein J (1988) Phylogenies from molecular sequences: Inference and reliability. *Annu Rev Genet* 22: 521–565
- Felsenstein J (2002) Phylip. (<http://evolution.genetics.washington.edu/phylip.html>)
- Ferreira F and Straus NA (1994) Iron deprivation in cyanobacteria. *J Appl Phycol* 6: 199–210
- Force A, Lynch M, Pickett FB, Amores A, Yan Y and Postlethwait J (1999) Preservation of duplicate genes by complementary, degenerative mutations. *Genetics* 151: 1531–1545
- Foster PG and Hickey DA (1999) Compositional bias may affect both DNA-based and protein-based phylogenetic reconstructions. *J Mol Evol* 48: 284–290
- Frankenberg N, Mukougawa K, Kohchi T and Lagarias JC (2001) Functional genomic analysis of the HY2 family of ferredoxin-dependent bilin reductases from oxygenic photosynthetic organisms. *Plant Cell* 13: 965–978
- Fromme P, Will HT, Schubert WD, Klukas O and Saenger W (1996) Structure of Photosystem I at 4.5-Å resolution—a short review including evolutionary aspects. *Biochim Biophys Acta* 1275: 76–83
- Fromme P, Jordan P and Krauss N (2001) Structure of Photosystem I. *Biochim Biophys Acta* 1507: 5–31
- Funk C and Vermaas W (1999) A cyanobacterial gene family coding for single-helix proteins resembling part of the light-harvesting proteins from higher plants. *Biochemistry* 38: 9397–9404
- Gantt E, Cunningham FX, Grabowski B and Tan S (1998) Relatedness of carotenoid-chlorophyll antenna complexes in algae and plants. In Garab G (ed.) *Photosynthesis: Mechanisms and Effects*, Vol I, pp 239–247. Kluwer Academic, Dordrecht
- Garczarek L, Hess WR, Holtzendorff J, van der Staay GWM and Partensky F (2000) Multiplication of antenna genes as a major adaptation to low light in a marine prokaryote. *Proc Natl Acad Sci USA* 97: 4098–4101
- Garczarek L, van der Staay GWM, Hess WR, Le Gall F and Partensky F (2001) Expression and phylogeny of the multiple antenna genes of the low-light adapted strain *Prochlorococcus marinus* SS120 (Oxyphotobacteria). *Plant Mol Biol* 46: 683–693
- Geiss U, Vinnemeier J, Schoor A and Hagemann M (2001) The iron-regulated *isiA* gene of *Fischerella muscicola* strain PCC 73103 is linked to a likewise regulated gene encoding a Pcb-like chlorophyll-binding protein. *FEMS Microbiol Lett* 197: 123–129
- Giuffra E, Zucchelli G, Sandonà D, Croce R, Cugini D, Garlaschi FM, Bassi R and Jennings RC (1997) Analysis of some optical properties of a native and reconstituted Photosystem II antenna complex, CP29-pigment binding sites can be occupied by chlorophyll *a* or chlorophyll *b* and determine spectral forms. *Biochemistry* 36: 12984–12993
- Glazer AN (1976) Phycoerythrins: Structure and function. *Photochem Photobiol Rev* 1: 71–115
- Glazer AN and Wedemayer GJ (1995) Cryptomonad biliproteins—an evolutionary perspective. *Photosynth Res* 46: 93–105
- Gogarten JP, Kibak H, Dittrich H, Taiz L, Bowman EJ, Manolson EJ, Poole RJ, Date T, Oshima T, Konishi J, Denda K and Yoshida M (1989) Evolution of vacuolar H<sup>+</sup>-ATPase: Implications for the origin of eukarya. *Proc Natl Acad Sci USA* 86: 6661–6665
- Golbeck JH (1993) Shared thematic elements in photochemical reaction centers. *Proc Natl Acad Sci USA* 90: 1642–1646
- Golding GB and Dean AM (1998) The structural basis of molecular adaptation. *Mol Biol Evol* 15: 355–369
- Golding GB and Gupta RS (1995) Protein-based phylogenies support a chimeric origin for the eukaryotic genome. *Mol Biol Evol* 12: 1–6
- Grabowski B, Cunningham FX Jr and Gantt E (2001) Chlorophyll and carotenoid binding in a simple red algal light-harvesting complex crosses phylogenetic lines. *Proc Natl Acad Sci USA* 98: 2911–2916
- Graur D and Li W-H (2000) Gene duplication, exon shuffling and concerted evolution. In: *Fundamentals of Molecular Evolution*, pp 249–322. Sinauer Associates, Inc., Sunderland
- Green BR (2001) Was ‘molecular opportunism’ a factor in the evolution of different photosynthetic light-harvesting pigment systems? *Proc Natl Acad Sci USA* 98: 2119–2121

- Green BR and Durnford DG (1996) The chlorophyll-carotenoid proteins of oxygenic photosynthesis. *Annu Rev Plant Physiol Plant Mol Biol* 47: 685–714
- Green BR and Gantt E (2000) Is photosynthesis really derived from purple bacteria? *J Phycol* 36: 983–985
- Green BR and Kühlbrandt W (1995) Sequence conservation of light-harvesting and stress-response proteins in relation to the three-dimensional molecular structure of LHCII. *Photosynth Res* 44: 139–148
- Green BR and Pichersky E (1994) Hypothesis for the evolution of three-helix Chl *a/b* and Chl *a/c* light-harvesting antenna proteins from two-helix and four-helix ancestors. *Photosynth Res* 39: 149–162
- Green BR, Pichersky E and Kloppstech K (1991) The chlorophyll *a/b*-binding light-harvesting antennas of green plants: The story of an extended gene family. *Trends Biochem Sci* 16: 181–186
- Gupta RS (1998) Protein phylogenies and signature sequences: A reappraisal of evolutionary relationships among archaeobacteria, eubacteria, and eukaryotes. *Microbiol Mol Biol Rev* 62: 1435–1491
- Gupta RS and Golding GB (1996) The origin of the eukaryotic cell. *Trends Biochem Sci* 21: 166–171
- Gupta RS, Mukhtar T and Singh B (1999) Evolutionary relationships among photosynthetic prokaryotes (*Helio-bacterium chlorum*, *Chloroflexus aurantiacus*, cyanobacteria, *Chlorobium tepidum* and proteobacteria): Implications regarding the origin of photosynthesis. *Mol Microbiol* 32: 893–906
- Hall BG (2001) *Phylogenetic Trees Made Easy: A How-To Manual for Molecular Biologists*. Sinauer Associates, Sunderland
- Han T-M and Runnegar B (1992) Megascopic eukaryotic algae from the 2.1-billion-year-old Negaunee iron-formation, Michigan. *Science* 257: 232–235
- Hansmann S and Martin W (2000) Phylogeny of 33 ribosomal and six other proteins encoded in an ancient gene cluster that is conserved across prokaryotic genomes: Influence of excluding poorly alignable sites from analysis. *Int J Syst Evol Microbiol* 50: 1655–1663
- Hayes JM (2000) Lipids as a common interest of microorganisms and geochemists. *Proc Natl Acad Sci USA* 97: 14033–14034
- He Q, Dolganov N, Björkman O and Grossman AR (2001) The high light-inducible polypeptides in *Synechocystis* PCC6803. Expression and function in high light. *J Biol Chem* 276: 306–314
- Helfrich M, Ross A, King GC, Turner AG and Larkum AWD (1999) Identification of [8-vinyl]-protochlorophyllide a in phototrophic prokaryotes and algae: Chemical and spectroscopic properties. *Biochim Biophys Acta* 1410: 262–272
- Hedddad M and Adamska I (2000) Light stress-regulated two-helix proteins in *Arabidopsis thaliana* related to the chlorophyll *a/b*-binding gene family. *Proc Nat Acad Sci USA* 97: 3741–3746
- Henikoff S and Henikoff JG (1992) Amino acid substitution matrices from protein blocks. *Proc Natl Acad Sci USA* 89: 10915–10919
- Henikoff S and Henikoff JG (1993) Performance evaluation of amino acid substitution matrices. *Proteins* 17: 49–61
- Hess WR, Partensky F, van der Staay GWM, Garcia-Fernandez JM, Börner T and Vaulot D (1996) Coexistence of phycoerythrin and a chlorophyll *a/b* antenna in a marine prokaryote. *Proc Natl Acad Sci USA* 93: 11126–11130
- Hess WR, Steglich C, Lichtlé C and Partensky F (1999) The phycoerythrins of *Prochlorococcus marinus* are associated to the thylakoid membrane and are encoded by a single large gene cluster. *Plant Mol Biol* 40: 507–521
- Hess WR, Roca G, Ting CS, Larimer F, Stilwagen S, Lamerdin J and Chisholm SW (2001) The photosynthetic apparatus of *Prochlorococcus*: Insights through comparative genomics. *Photosynth Res* 70: 53–71
- Higgins DG, Thompson JD and Gibson TJ (1996) Using CLUSTAL for multiple sequence alignments. *Methods in Enzymology* 266: 383–402
- Hiller RG, Crossley LG, Wrench PM, Santucci N and Hofmann E (2001) The 15-kDa forms of the apo-peridinin-chlorophyll *a* protein (PCP) in dinoflagellates show high identity with the apo-32 kDa PCP forms, and have similar N-terminal leaders and gene arrangements. *Mol Gen Genet* 266: 254–259
- Hillis DM and Bull JJ (1993) An empirical test of bootstrapping as a method for assessing confidence on phylogenetic analysis. *Syst Biol* 42: 182–192
- Hillis DM, Moritz C and Mable BK (eds) (1996) *Molecular Systematics*. Sinauer Associates, Sunderland
- Hofmann E, Wrench PM, Sharples FP, Hiller RG, Welte W and Diederichs K (1996) Structural basis of light harvesting by carotenoids: Peridinin-chlorophyll-protein from *Amphidinium carterae*. *Science* 272: 1788–1791
- Holland HD (1994) Early Proterozoic atmospheric change. In Bengtson S (ed) *Early Life on Earth*. Nobel Symposium No. 84, pp 237–244. Columbia Univ. Press, New York
- Holm L and Sander C (1993) Structural alignment of globins, phycocyanins and colicin-A. *FEBS Lett* 315: 301–306
- Hu Q, Marquardt J, Iwasaki I, Miyashita H, Kurano N, Mörschel E and Miyachi S (1999) Molecular structure, localization and function of biliproteins in the chlorophyll *a/d* containing oxygenic photosynthetic procaryote *Acaryochloris marina*. *Biochim Biophys Acta* 1412: 250–261
- Hugenholtz P, Goebel BM and Pace NR (1998) Impact of culture-independent studies on the emerging phylogenetic view of bacterial diversity. *J Bact* 180: 4765–4774
- Igarashi N, Harada J, Nagashima S, Matsuura K, Shimada K and Nagashima KVP (2001) Horizontal transfer of the photosynthesis gene cluster and operon rearrangement in purple bacteria. *J Mol Evol* 52: 333–341
- Ishida A and Green BR (2002) Second-hand and third-hand chloroplasts in dinoflagellates: Phylogeny of oxygen-evolving enhancer 1 (PsbO) protein reveals replacement of a nuclear-encoded plastid gene by that of a haptophyte tertiary endosymbiont. *Proc Natl Acad Sci USA* 99: 9294–9299
- Ivanov AG, Park Y-I, Miskiewicz E, Raven JA, Huner NPA and Öquist G (2000) Iron stress restricts photosynthetic intersystem electron transport in *Synechococcus* sp. PCC 7942. *FEBS Lett* 485: 173–177
- Iwabe N, Kuma K-I, Hasegawa M, Osawa S and Miyata T (1989) Evolutionary relationship of archaeobacteria, eubacteria, and eukarya inferred from phylogenetic trees of duplicated genes. *Proc Natl Acad Sci USA* 86: 9355–9359
- Jain R, Rivera MC and Lake JA (1999) Horizontal gene transfer among genomes: the complexity hypothesis. *Proc Natl Acad Sci USA* 96: 3801–3806
- Jansson S (1994) The light-harvesting chlorophyll *a/b*-binding



- proteins. *Biochim Biophys Acta* 1184:1–19
- Jansson S (1999) A guide to the Lhc genes and their relatives in *Arabidopsis*. *Trends Plant Sci* 4: 236–240
- Jansson S, Andersson J, Kim SJ and Jackowski G (2000) An *Arabidopsis thaliana* protein homologous to cyanobacterial high-light-inducible proteins. *Plant Mol Biol* 42: 345–351
- Javaux EJ, Knoll AH and Walter MR (2001) Morphological and ecological complexity in early eukaryotic ecosystems. *Nature* 412: 66–69
- Jeffery CJ (1999) Moonlighting proteins. *Trends Biochem Sci* 24:8–11
- Jones DT, Taylor WR and Thornton JM (1992) The rapid generation of mutation data matrices from protein sequences. *Computer Appl Biosci* 8: 275–282.
- Jordan P, Fromme P, Will HT, Klukas O, Saenger W and Krauss (2001) Three-dimensional structure of cyanobacterial Photosystem I at 2.5 Å resolution. *Nature* 411: 909–917
- Kaneko T, Sato S, Kotani H, Tanaka A, Asamizu E, Nakamura Y, Miyajima N, Hirose M, Sugiura M, Sasamoto S et al. (1996) Sequence analysis of the genome of the unicellular cyanobacterium *Synechocystis* sp. Strain PCC6803. II. Sequence determination of the entire genome and assignment of potential protein-coding regions. *DNA Res* 3: 109–136
- Kasting JF (1993) Earth's early atmosphere. *Science* 259: 920–926
- Kasting JF and Seibert JL (2002) Life and the evolution of Earth's atmosphere. *Science* 296: 1066–1067
- Kasting JF, Holland HD and Kump LR (1992) Atmospheric Evolution: the Rise of Oxygen. In Schopf JW and Klein C (eds) *The Proterozoic Biosphere, a multidisciplinary study*, pp 159–163. Cambridge University Press, Cambridge
- Katz LA (1998) Changing perspectives on the origin of eukaryotes. *Trends Ecol Evol* 13: 493–497
- Keeling PJ, Luker MA and Palmer JD (2000) Evidence from beta-tubulin phylogeny that microsporidia evolved from within the fungi. *Mol Biol Evol* 17: 23–31
- Kim S, Sandusky P, Bowlby NR, Aebersold R, Green BR, Vlahakis S, Yocum CF and Pichersky E (1992) Characterization of a spinach psbS cDNA encoding the 22 kDa protein of Photosystem II. *FEBS Lett* 314: 67–71
- Kleima FJ, Hobe S, Calkoen F, Urbanus ML, Peterman EJG, van Grondelle R, Paulsen H and van Amerongen H (1999) Decreasing the chlorophyll *a/b* ratio in reconstituted LHCII: Structural and functional consequences. *Biochemistry* 38: 6587–6596
- Knoll AH (1992) The early evolution of eukaryotes: A geological perspective. *Science* 256: 622–627
- Knoll AH (1994) Proterozoic and early Cambrian protists: Evidence for accelerating evolutionary tempo. *Proc Natl Acad Sci USA* 91:6743–6750
- Kobayashi M, Oh-oka H, Akutsu S, Akiyama M, Tominaga K, Kise H, Nishida F, Watanabe T, Amesz J, Koizumi M, Ishida N and Kano H (2000) The primary electron acceptor of green sulfur bacteria, bacteriochlorophyll 663, is chlorophyll *a* esterified with 2,6-phytydienol. *Photosynth Res* 63: 269–280
- Kollman JM and Doolittle RF (2000) Determining the relative rates of change for prokaryotic and eukaryotic proteins with anciently duplicated paralogs. *J Mol Evol* 51: 173–181
- Koonin EV, Makarova KS and Aravind L (2001) Horizontal gene transfer in prokaryotes: quantification and classification. *Annu Rev Microbiol* 55:709–42
- Kühlbrandt W, Wang DN, Fujiyoshi Y (1994) Atomic model of plant light-harvesting complex by electron crystallography. *Nature* 367:614–621
- Lange BM, Rujan R, Martin W and Croteau R (2000) Isoprenoid biosynthesis: The evolution of two ancient and distinct pathways across genomes. *Proc Natl Acad Sci USA* 97: 13172–13177
- LaRoche J, Henry D, Wyman K, Sukenik A, Falkowski P (1994) Cloning and nucleotide sequence of a cDNA encoding a major fucoxanthin-, chlorophyll *a/c*-containing protein from the chrysophyte *Isochrysis galbana*: Implications for evolution of the *cab* gene family. *Plant Mol Biol* 25:355–368
- LaRoche J, van der Staay GWM, Partensky F, Ducret A, Aebersold R, Li R, Golden SS, Hiller RG, Wrench PM Larkum AWD and Green BR (1996) Independent evolution of the prochlorophyte and green plant chlorophyll *a/b* light-harvesting proteins. *Proc Natl Acad Sci US* 93: 15244–14248
- Lawrence JG (1999) Selfish operons: The evolutionary impact of gene clustering in prokaryotes and eukaryotes. *Curr Opin Genet Devel* 9: 642–648
- Lawrence JG and Ochman H (2002) Reconciling the many faces of lateral gene transfer. *Trends Microbiol* 10: 1–4
- Li W-H (1997) *Molecular Evolution*. Sinauer Associates, Sunderland
- Li X-P, Björkman O, Shih C, Grossman AR, Rosenquist M, Jansson S and Niyogi KK (2000) A pigment-binding protein essential for regulation of photosynthetic light harvesting. *Nature* 403: 391–395
- Li YF, Zhou WL, Blankenship RE and Allen JP (1997) Crystal structure of the bacteriochlorophyll *a* protein from *Chlorobium tepidum*. *J Mol Biol* 271: 456–471
- Lockhart PJ, Steel MA, Hendy MD and Penny D (1994) Recovering evolutionary trees under a more realistic model of sequence evolution. *Mol Biol Evol* 11: 605–612
- Lockhart PJ, Larkum AWD, Steel MA, Wadell, PJ and Penny D (1996) Evolution of chlorophyll and bacteriochlorophyll: The problem of invariant sites in sequence analysis. *Proc Nat Acad Sci USA*. 93:1930–1934
- López-García P and Moreira D (1999) Metabolic symbiosis at the origin of eukaryotes. *Trends Biochem Sci* 24: 88–93
- Ludwig M and Gibbs SP (1989) Localization of phycoerythrin at the luminal surface of the thylakoid membrane in *Rhodomonas lens*. *J Cell Biol* 108: 875–884
- Ludwig W and Schleifer KH (1994) Bacterial phylogeny based on 16S and 23S rRNA sequence analysis. *FEMS Microbiol Rev* 15: 155–173
- Lynch M and Force A (2000) The probability of duplicate gene preservation by subfunctionalization. *Genetics* 154: 459–473
- MacColl R (1998) Cyanobacterial phycobilisomes. *J Struct Biol* 124: 311–334
- Madigan MT and Ormerod JG (1995) Taxonomy, physiology and ecology of heliobacteria. In: Blankenship RE, Madigan MT and Bauer CE (eds) *Anoxygenic Photosynthetic Bacteria*, pp 17–30. Kluwer Academic Publishers, Dordrecht
- Madigan MT, Martinko JM, Parker J (1996) *Brock Biology of Microorganisms* (8th ed), Chapter 17. Prentice Hall, Upper Saddle River
- Marquardt J, Senger H, Miyashita H, Miyachi S and Mörschel E (1997) Isolation and characterization of biliprotein aggregates from *Acaryochloris marina* a Prochloron-like prokaryote containing mainly chlorophyll *d*. *FEBS Lett* 410: 428–432
- Marquardt J, Lutz B, Wans S, Rhiel E and Krumbein WE (2001)

- The gene family coding for the light-harvesting polypeptides of Photosystem I of the red alga *Galdieria sulphuraria*. *Photosynth Res* 68: 121–130
- Martin W (1999) Mosaic bacterial chromosomes: a challenge en route to a tree of genomes. *BioEssays* 21: 99–104
- Martin W and Herrmann RG (1998) Gene transfer from organelles to the nucleus: how much, what happens, and why? *Plant Physiol* 118: 9–17
- Martin W and Müller M (1998) The hydrogen hypothesis of the first eukaryote. *Nature* 392: 37–41
- Martin W and Schnarrenberger C (1997) The evolution of the Calvin cycle from prokaryotic to eukaryotic chromosomes: A case study of functional redundancy in ancient pathways through endosymbiosis. *Curr Genet* 32: 1–18
- Martin W, Stoebe B, Goremykin V, Hansmann S, Hasegawa M and Kowallik KV (1998) Gene transfer to the nucleus and the evolution of chloroplasts. *Nature* 393: 162–165
- Martin W, Rujan T, Richly E, Hansen A, Cornelsen, Lins T, Leister D, Stoebe B, Hasegawa M and Penny D (2002) Evolutionary analysis of *Arabidopsis*, cyanobacterial, and chloroplast genomes reveals plastid phylogeny and thousands of cyanobacterial genes in the nucleus. *Proc Natl Acad Sci USA* 99: 12246–12251
- Matthews BW, Fenna RE, Bolognesi MC, Schmid MR and Olson JM (1979) Structure of a bacteriochlorophyll *a*-protein from the green photosynthetic bacterium *Prosthecochloris aestuarii*. *J Mol Biol* 131: 259–285
- Matthijs HCP, van der Staay GWM and Mur LR (1995) Prochlorophytes: The 'other' cyanobacteria? In: Bryant DA (ed) *The Molecular Biology of Cyanobacteria*, pp 49–64. Kluwer Academic Publishers, Dordrecht
- McClure MA, Vasi TK and Fitch WM (1994) Comparative analysis of multiple protein-sequence alignment methods. *Mol Biol Evol* 11: 571–592
- McLuskey K, Prince SM, Cogdell RJ and Isaacs NW (2001) The crystallographic structure of the B800-820 LH3 light-harvesting complex from the purple bacteria *Rhodospirillum rubrum* strain 7050. *Biochemistry* 40: 8783–8789
- Meyer M, Wilhelm C and Garab G (1996) Pigment-pigment interactions and secondary structure of reconstituted algal chlorophyll *a/b*-binding light-harvesting complexes of *Chlorella fusca* with different pigment compositions and pigment-protein stoichiometries. *Photosynth Res* 49: 71–81
- Michel H and Deisenhofer J (1988) Relevance of the photosynthetic reaction center from purple bacteria to the structure of Photosystem II. *Biochemistry* 27: 1–7
- Moens L, Vanfleteren J, Van de Peer Y, Peeters K, Kapp O, Czeluzniak J, Goodman M, Blaxter M and Vinogradov S (1996) Globins in nonvertebrate species: Dispersal by horizontal gene transfer and evolution of the structure-function relationships. *Mol Biol Evol* 13: 324–333
- Mojzsis SJ, Arrhenius G, McKeegan KD, Harrison TM, Nutman AP and Friend CRL (1996) Evidence for life on earth before 3,800 million years ago. *Nature* 384: 55–59
- Moldovan JM and Jacobson SR (2000) Chemical signals for early evolution of major taxa. *Biosignatures and taxon-specific biomarkers*. *Int Geol Rev* 42: 805–812
- Montané M-H and Kloppstech K (2000) The family of light-harvesting-related proteins (LHCs, ELIPs, HLIPs): Was the harvesting of light their primary function? *Gene* 258: 1–8
- Moreira D, Le Guyader H and Phillippe H (2000) the origin of red algae and the evolution of chloroplasts. *Nature* 405: 69–72
- Naylor GJP and Brown WM (1997) Structural biology and phylogenetic estimation. *Nature* 388: 527–528
- Neerken S and Amesz J (2001) The antenna reaction center complex of heliobacteria: Composition, energy conversion and electron transfer. *Biochim Biophys Acta* 1507: 278–290
- Nelson KE, Clayton RA, Gill SR, Gwinn ML, Dodson RJ, Haft DH, Hickey EK, Peterson JD, Nelson WC, Ketchum KA, McDonald L, Utterback TR, Malek JA, Linher KD, Garrett, MM, Stewart AM, Cotton MD, Pratt MS, Phillips CA, Richardson D, Heidelberg J, Sutton GG, Fleischmann, RD, Eisen JA, White O, Salzberg SL, Smith HO, Venter JC and Fraser CM (1999) Evidence for lateral gene transfer between Archaea and bacteria from genome sequence of *Thermotoga maritima*. *Nature* 399: 323–329
- Nield J, Orlova EV, Morris EP, Gowen B, van Heel M and Barber J (2000) 3D map of the plant Photosystem II supercomplex obtained by cryoelectron microscopy and single particle analysis. *Nature Struct Biol* 7: 44–47
- Nikaido I, Asamizu E, Nakajima M, Nakamura Y, Saga N and Tabata S (2000) Generation of 10,154 expressed sequence tags from a leafy gametophyte of a marine red alga, *Porphyra yezoensis*. *DNA Res* 7: 223–227
- Nikolaichik YA and Donachie WD (2000) Conservation of gene order amongst cell wall and cell division genes in Eubacteria, and ribosomal genes in Eubacteria and Eukaryotic organelles. *Genetica* 108: 1–7
- Nisbet EG and Sleep NH (2001) The habitat and nature of early life. *Nature* 409: 1083–1091
- Nitschke W and Rutherford AW (1991) Are all of the different types of photosynthetic reaction center variations on a common structural theme? *Trends Biochem Sci* 16: 241–243
- Nitschke W, Mühlenhoff U and Liebl U (1998) Evolution. In: Raghavendra AS (ed) *Photosynthesis, a Comprehensive Treatise*, pp 285–304. Cambridge University Press, Cambridge
- Norris BJ and Miller DJ (1994) Nucleotide sequence of a cDNA clone encoding the precursor of the peridinin-chlorophyll *a*-binding protein from the dinoflagellate *Symbiodinium* sp. *Plant Mol Biol* 24: 673–677
- O'Brien PJ and Herschlag D (1999) Catalytic promiscuity and the evolution of new enzyme activities. *Chem Biol* 6: 91–105
- Ochman H, Lawrence JG and Groisman EA (2000) Lateral gene transfer and the nature of bacterial innovation. *Nature* 405: 299–304
- Ohno S (1970) *Evolution by Gene Duplication*. Springer-Verlag, Berlin
- Olsen GJ, Woese CR and Overbeek R (1994) The winds of evolutionary change; breathing new life into microbiology. *J Bacteriol* 176: 1–6
- Olson JM (1970) Evolution of photosynthesis. *Science* 168: 438–446
- Olson JM (2001) 'Evolution of Photosynthesis' (1970), re-examined thirty years later. *Photosynth Res* 68: 95–112
- Oster U, Tanaka R, Tanaka A and Rüdiger W (2000) Cloning and functional expression of the gene encoding the key enzyme for chlorophyll *b* biosynthesis (CAO) from *Arabidopsis thaliana*. *Plant Journal* 21: 305–310
- Overbeek R, Fonstein M, D'Souza M, Pusch GD and Maltsev N (1999) The use of gene clusters to infer functional coupling. *Proc Natl Acad Sci USA* 96: 2896–2901
- Pace NR (1997) A molecular view of microbial diversity and the

- biosphere. *Science* 276: 732–740
- Park YI, Sandstrom S, Gustafsson P and Öquist (1999) Expression of the *isiA* gene is essential for the survival of the cyanobacterium *Synechococcus* sp. PCC 7942 by protecting Photosystem II from excess light under iron limitation. *Molec Microbiol* 32: 123–129
- Partensky F, Hess WR and Vaulot D (1999) *Prochlorococcus*, a marine photosynthetic prokaryote of global significance. *Microbiol Mol Biol Rev* 63: 106–127
- Penno S, Campbell L and Hess WR (2000) Presence of phycoerythrin in two strains of *Prochlorococcus* (cyanobacteria) isolated from the subtropical north Pacific ocean. *J Phycol* 36: 723–729
- Pflug HD (2001) Earliest organic evolution. Essay to the memory of Bartholomew Nagy. *Precambrian Res* 106: 79–91
- Philippe H (2000) Long branch attraction and protist phylogeny. *Protist* 151: 307–316
- Philippe H and Adoutte A (1998) The molecular phylogeny of Eukaryota: Solid facts and uncertainties. In Coombs GH, Vickerman K, Sleigh MA and Warren A (eds) *Evolutionary Relationships Among Protozoa*, pp 25–55. Chapman and Hall, London
- Philippe H and Forterre P (1999) The rooting of the universal tree of life is not reliable. *J Mol Evol* 49: 509–523
- Philippe H and Laurent J (1998) How good are deep phylogenetic trees? *Curr Opin Genet Devel* 8: 616–623
- Philippe H, Germot A and Moreira D (2000) The new phylogeny of eukaryotes. *Curr Opin Genet Devel* 10: 596–601
- Pierson BK (1994) The emergence, diversification and role of photosynthetic eubacteria. In Bengtson S (ed) *Early Life on Earth*. Nobel Symposium No. 84, pp 161–180. Columbia University Press, New York
- Pierson BK (2001) O phototroph, O chemotroph, where art thou? *Trends Microbiol* 9: 259–260
- Pierson BK and Olson JM (1989) Evolution of photosynthesis in anoxygenic photosynthetic prokaryotes. In: Cohen Y and Rosenberg (Eds) *Microbial Mats*, pp 402–427. American Society of Microbiologists, Washington, DC.
- Putnam-Evans C and Bricker TM (1997) Site-directed mutagenesis of the basic residues K-321 to (321)G in the CP47 protein of Photosystem II alters the chloride requirement for growth and oxygen-evolving activity in *Synechocystis* 6803. *Plant Molecular Biology*. 34:455–463
- Ragan M (2002) Reconciling the many faces of lateral gene transfer. *Trends Microbiol* 10: 4
- Ragan M and Charlebois RL (2002) Distributional profiles of homologous open reading frames among bacterial phyla: Implications for vertical and lateral transmission. *Int J Systematic Evol Microbiol* 52: 777–787
- Raven JA, Evans MCW and Korb RE (1999) The role of trace metals in photosynthetic electron transport in O<sub>2</sub>-evolving organisms. *Photosynth Res* 60: 111–150
- Raymond J, Zhaxybayeva O, Gogarten JP, Gerdes SY and Blankenship RE (2002) Whole-genome analysis of photosynthetic prokaryotes. *Science* 298: 1616–1620
- Reichmann JL, Heard J, Martin G, Reuber L, Jiang C-Z, Keddie J, Adam L, Pineda O, Ratcliffe OJ, Samaha RR, Creelman R, Pilgrim M, Broun P, Zhang JZ, Ghandehari D, Sherman BK and Yu G-L (2000) *Arabidopsis* transcription factors: Genome-wide comparative analysis among eukaryotes. *Science* 290: 2105–2110
- Richard C, Ouellet H and Guertin M (2000) Characterization of the LI818 polypeptide from the green unicellular alga *Chlamydomonas reinhardtii*. *Plant Mol Biol* 42: 303–316
- Riethman HC and Sherman LA (1988) Purification and characterization of an iron stress-induced chlorophyll-protein from the cyanobacterium *Anacystis nidulans* R2. *Biochim Biophys Acta* 935: 141–151
- Riley M and Labedan B (1997) Protein evolution viewed through *Escherichia coli* protein sequences: Introducing the notion of a structural segment of homology, the module. *J Mol Biol* 268: 857–868
- Rivera MC, Jain R, Moore JE and Lake JA (1998) Genomic evidence for two functionally distinct gene classes. *Proc Natl Acad Sci USA* 95: 6239–6244
- Rosenberg C, Christian J, Bricker TM and Putnam-Evans C (1999) Site-directed mutagenesis of glutamate residues in the large extrinsic loop of the Photosystem II protein CP 43 affects oxygen-evolving activity and PS II assembly. *Biochemistry* 38: 15994–16000
- Rost B (1999) Twilight zone of protein sequence alignments. *Prot Engineering* 12: 85–94
- Rujan T and Martin W (2001) how many genes in *Arabidopsis* come from cyanobacteria? An estimate from 386 protein phylogenies. *Trends Genet* 17: 113–120
- Russell RB (1998) Detection of protein three-dimensional side-chain patterns: New examples of convergent evolution. *J Mol Biol* 279: 1211–1227
- Rzhetsky A and Nei M (1994) Unbiased estimates of the number of nucleotide substitutions when substitution rate varies among different sites. *J Mol Evol* 38: 295–299
- Saitou N and Nei M (1987) The neighbor-joining method: A new method for reconstructing phylogenetic trees. *Mol Biol Evol* 4: 406–425
- Sandström S, Park Y-I, Öquist G and Gustafsson P (2001) CP43', the *isiA* gene product, functions as an excitation energy dissipator in the cyanobacterium *Synechococcus* sp. PCC 7942. *Photochem Photobiol* 74: 431–437
- Satoh S, Ikeuchi M, Mimuro M and Tanaka A (2001) Chlorophyll *b* expressed in cyanobacteria functions as a light-harvesting antenna in Photosystem I through flexibility of the proteins. *J Biol Chem* 276: 4293–4297
- Savard F, Richard C and Guertin M (1996) The *Chlamydomonas reinhardtii* LI818 gene represents a distant relative of the *cabI/II* genes that is regulated during the cell cycle and in response to illumination. *Plant Mol Biol* 32: 461–473
- Schirmer T, Bode W, Huber R, Sidler W and Zuber H (1985) X-ray crystallographic structure of the light-harvesting biliprotein C-phycoerythrin from the thermophilic cyanobacterium *Mastigocladus laminosus* and its resemblance to globin structures. *J Mol Biol* 184: 257–277
- Schopf JW (1993) Microfossils of the early archaean apex chert: New evidence of the antiquity of life. *Science* 260: 640–646
- Schopf JW (1994) The oldest known records of life: Early Archaean stromatolites, microfossils, and organic matter. In Bengtson S (ed) *Early Life on Earth*. Nobel Symposium No. 84, pp 193–206. Columbia University Press, New York
- Schopf JW and Klein C (1992) *The Proterozoic Biosphere, a multidisciplinary study*. Cambridge University Press, Cambridge
- Schopf JW, Kudryavtsev AB, Agresti DG, Wdowiak TJ and Czaja AD (2002) Laser-Raman imagery of Earth's earliest

- fossils. *Nature* 416: 73–76
- Schubert W-D, Klukas O, Saenger W, Witt HT, Fromme P and Krauss N (1998) A common ancestor for oxygenic and anoxygenic photosynthetic systems: A comparison based on the structural model of Photosystem I. *J. Mol. Biol.* 280: 297–314
- Schuler GD, Altschul SF and Lipman DJ (1991) A workbench for multiple alignment construction and analysis. *Proteins Struct Funct Genet* 9: 180–190
- Schultz HN and Jorgensen BB (2001) Big bacteria. *Annu Rev Microbiol* 55: 105–137
- Schütz M, Brugna M, Lebrun E, Baymann F, Huber R, Stetter K-O, Hauska G, Toci R, Lemesle-Meunier D, Tron P, Schmidt C and Nitschke W (2000) Early evolution of cytochrome *bc* complexes. *J Mol Biol* 300: 663–675
- Schwartz RM and Dayhoff MO (1978) Origins of prokaryotes, eukaryotes, mitochondria, and chloroplasts. *Science* 199: 395–403
- Schwender J, Gemunden C and Lichtenthaler HK (2001) Chlorophyta exclusively use the 1-deoxyxylulose 5-phosphate/2-C-methylerythritol 4-phosphate pathway for the biosynthesis of isoprenoids. *Planta* 212: 416–423
- Sidler WA (1995) Phycobilisome and phycobiliprotein structures. In: Bryant DA (ed) *The Molecular Biology of Cyanobacteria*, pp 140–216. Kluwer Academic, Dordrecht
- Simoneit BR, Summons RE and Jahnke LL (1998) Biomarkers as tracers for life on early earth and Mars. *Origins Life Evol Biosphere* 28: 475–483
- Stackebrandt, E., Rainey, F.A., Ward-Rainey, N (1996) Anoxygenic phototrophy across the phylogenetic spectrum: Current understanding and future perspectives. *Arch Microbiol.* 166: 211–223
- Steiner JM and Löffelhardt W (2002) Protein import into cyanelles. *Trends Pl Sci* 7: 72–77
- Stewart C-B (1993) The powers and pitfalls of parsimony. *Nature* 361: 603–607
- Stiller JW and Hall BD (1997) The origin of red algae: Implications for plastid evolution. *Proc Natl Acad Sci USA* 94: 4520–4525
- Stoebe B and Kowallik KV (1999) Gene-cluster analysis in chloroplast genomics. *Trends Genet* 15: 344–347
- Strimmer K and von Haeseler A (1996) Quartet puzzling: A quartet maximum-likelihood methods for reconstructing tree topologies. *Mol Biol Evol* 13: 964–969
- Summons RE, Jahnke LL, Hope JM and Logan GA (1999) 2-Methylhopanoids as biomarkers for cyanobacterial oxygenic photosynthesis. *Nature* 400: 554–557
- Suzuki JY, Bolivar DW and Bauer CE (1997) Genetic analysis of chlorophyll biosynthesis. *Annu Rev Genet* 31: 61–89
- Swofford DL (1999) Phylogenetic analysis using parsimony (and other methods) PAUP\* 4.0 (test version). Sinauer, Sunderland
- Takaichi S (1999) Carotenoids and carotenogenesis in anoxygenic photosynthetic bacteria. In: Frank HA, Young J, Britton G and Cogdell RJ (eds) *The Photochemistry of Carotenoids*, pp 39–69. Kluwer Academic Publishers, Dordrecht
- Takaichi S and Mimuro M (1998) Distribution and geometric isomerism of neoxanthin in oxygenic phototrophs- 9'-cis, a sole molecular form. *Plant Cell Physiol* 39: 968–977
- Talyzina NM, Moldovan JM, Johannisson A and Fago FJ (2000) Affinities of Early Cambrian acritarchs studied by using microscopy, fluorescence flow cytometry and biomarkers. *Rev Palaeobotany Palynology* 108: 37–53
- Tanaka A, Ito H, Tanaka R, Tanaka NK and Yoshida K (1998) Chlorophyll *a* oxygenase (CAO) is involved in chlorophyll *b* formation from chlorophyll *a*. *Proc Natl Acad Sci USA* 95: 12719–12723
- Teramoto H, Ono T and Minagawa J (2001) Identification of *Lhcb* gene family encoding the light-harvesting chlorophyll-*a/b* proteins of Photosystem II in *Chlamydomonas reinhardtii*. *Plant Cell Physiol* 42: 849–856
- Thomas J-C and Passaquet C (1999) Characterization of a phycoerythrin without  $\alpha$ -subunits from a unicellular red alga. *J Biol Chem* 274: 2472–2482
- Ting CS, Rocap G, King J and Chisholm SW (2001) Phycobiliprotein genes of the marine photosynthetic prokaryote *Prochlorococcus*: evidence for rapid evolution of genetic heterogeneity. *Microbiology* 147: 3171–3182
- Ting CS, Rocap G, King J and Chisholm SW (2001) Cyanobacterial photosynthesis in the oceans: The origins and significance of divergent light-harvesting strategies. *Trends Microbiol* 10: 134–142
- Tomitani A, Okada K, Miyashita H, Matthijs HCP, Ohno T and Tanaka A (1999) Chlorophyll *b* and phycobilins in the common ancestor of cyanobacteria and chloroplasts. *Nature* 400: 159–162
- Turner S (1997) Molecular systematics of oxygenic photosynthetic bacteria. *Pl Syst Evol (Suppl)* 11: 13–52
- Turner S, Pryer KM, Miao VPW and Palmer JD (1999) Investigating deep phylogenetic relationships among cyanobacteria and plastids by small subunit rRNA sequence analysis. *J Eukaryot Microbiol* 46: 327–338
- Van de Peer Y, Van der Auwera G and De Wachter R (1996) The evolution of stramenopiles and alveolates as derived by 'substitution rate calibration' of small ribosomal subunit RNA. *J Mol Evol* 42: 201–210
- Van de Peer Y, Baldauf SL, Doolittle WF and Meyer A (2000) An updated and comprehensive rRNA phylogeny of (Crown) eukaryotes based on rate-calibrated evolutionary distances. *J Mol Evol* 51: 565–576
- Van der Staay GWM, Yurkova N and Green BR (1998) The 38 kDa chlorophyll *a/b* protein of the prokaryote *Prochlorothrix hollandica* is encoded by a divergent *pcb* gene. *Plant Mol Biol* 36: 709–716
- Vassilieva EV, Stirewalt VL, Jakobs CU, Frigaard N-U, Baker MA, Sotak AM and Bryant DA (2002) Subcellular localization of chlorosome proteins in *Chlorobium tepidum* and characterization of three new chlorosome proteins: CsmF, CsmH and CsmX. *Biochemistry* 41: 4358–4370
- Vermaas WFJ (1994) Evolution of heliobacteria: Implications for photosynthetic reaction center complexes. *Photosynth Res* 41: 285–294
- Viale AM, Arakaki AK, Soncini FC and Ferreyra RG (1994) Evolutionary relationships among eubacterial groups as inferred from GroEL (chaperonin) sequence comparisons. *Int J Syst Bacteriol* 44: 527–533
- Vision TJ, Brown DG and Tanksley SD (2000) The origins of genomic duplications in *Arabidopsis*. *Science* 290: 2114–2117
- Wedel N, Klein R, Ljungberg U, Andersson B and Herrmann RG (1992) The single-copy gene *psbS* codes for a phylogenetically intriguing 22 kDa polypeptide of Photosystem II. *FEBS Lett* 314: 61–66
- Wedemeyer GJ, Kidd DG and Glazer AN (1996) Cryptomonad

- biliproteins: Bilin types and locations. *Photosynth Res* 48: 163–170
- Whelan S and Goldman N (2001) A general empirical model of protein evolution derived from multiple protein families using a maximum-likelihood approach. *Mol. Biol. Evol.* 18, 691–699
- Wilk K, Harrop SJ, Jankova L, Edler D, Keenan G, Sharples FP, Hiller RC and Curmi PMG (1999) Evolution of a light-harvesting protein by addition of new subunits and rearrangement of conserved elements: Crystal structure of a cryptophyte phycoerythrin at 1.63 Å. *Proc Natl Acad Sci USA* 96: 8901–8906
- Wilmotte A (1995) Molecular evolution and taxonomy of the cyanobacteria. In: Bryant DA (ed) *The Molecular Biology of Cyanobacteria*, pp 1–25. Kluwer Academic, Dordrecht
- Wistow G (1993) Lens crystallins: Gene recruitment and evolutionary dynamism. *Trends Biochem Sci* 18: 301–306
- Woese CR (1987) Bacterial Evolution. *Microbiol Rev* 51: 222–271
- Woese CR (1998) The universal ancestor. *Proc Natl Acad Sci USA* 95: 6854–6859
- Woese CR, Kandler O and Wheelis ML (1990) Towards a natural system of organisms: Proposal for the domains Archaea, Bacteria, and Eucarya. *Proc Natl Acad Sci USA* 87: 4576–4579
- Wolfe KH and Shields DC (1997) Molecular evidence for an ancient duplication of the entire yeast genome. *Nature* 387: 708–713
- Wolfe KH, Li W-H and Sharp PM (1987) Rates of nucleotide substitution vary greatly among plant mitochondrial, chloroplast, and nuclear DNAs. *Proc Natl Acad Sci USA* 84: 9054–9058
- Wüthrich K L, Bovet L, Hunziger PE, Donnison IS and Hörtensteiner S (2000) Molecular cloning, functional expression and characterisation of RCC reductase involved in chlorophyll catabolism. *Plant J* 21: 189–198
- Xiao SH, Knoll AH and Yuan XL (1998) Morphological reconstruction of *Miaohephyton bifurcatum*, a possible brown alga from the Neoproterozoic Doushantuo Formation, South China. *J Paleontology* 72: 1072–1086.
- Xiong J and Bauer CE (2002) Complex evolution of photosynthesis. *Annu Rev Plant Biol* 53: 503–521
- Xiong J, Inoue K and Bauer CE (1998) Tracking molecular evolution of photosynthesis by characterization of a major photosynthesis gene cluster from *Heliobacillus mobilis*. *Proc Nat Acad Sci US* 95: 14851–56
- Xiong J, Fischer WM, Inoue K, Nakahara M and Bauer CE (2000) Molecular evidence for the early evolution of photosynthesis. *Science* 289: 1724–1730
- Xu H, Vavilin D and Vermaas W (2001) Chlorophyll *b* can serve as the major pigment in functional Photosystem II complexes of cyanobacteria. *Proc Nat Acad Sci USA* 98: 14168–14173
- Zauner S, Fraunholz M, Wastl J, Penny S, Beaton B, Cavalier-Smith T, Maier U-G and Douglas S (2000) Chloroplast protein and centrosomal genes, a tRNA intron, and odd telomeres in an unusually compact eukaryotic genome, the cryptomonad nucleomorph. *Proc Natl Acad Sci USA* 97: 200–205
- Zhang Z, Green BR and Cavalier-Smith T (2000) Phylogeny of ultra-rapidly evolving dinoflagellate chloroplast genes: A possible common origin for sporozoan and dinoflagellate plastids. *J Mol Evol* 51: 26–40
- Zouni A, Witt H-T, Kern J, Fromme P, Krauss N, Saenger W and Orth P (2001) Crystal structure of Photosystem II from *Synechococcus elongatus* at 3.8 Å resolution. *Nature* 409: 739–743
- Zuber H and Cogdell RJ (1995) Structure and organization of purple bacterial antenna complexes. In: Blankenship, RE, Madigan MT and Bauer CE (eds): *Anoxygenic Photosynthetic Bacteria*, pp 315–348, Kluwer Academic, Dordrecht
- Zuber H and Brunisholz RA (1991) Structure and function of antenna polypeptides and chlorophyll-protein complexes: Principles and variability. In: Scheer H (ed.) *Chlorophylls*, pp 627–704, CRC Press, Boca Raton

# Chapter 5

## The Light-Harvesting System of Purple Bacteria

Bruno Robert\*

*Section de Biophysique des Protéines et des Membranes, DBCM/CEA and URA CNRS 2096,  
C.E. Saclay, 91191 Gif/Yvette, France*

Richard J. Cogdell

*Division of Biochemistry and Molecular Biology, Institute of Biomedical and Life Sciences,  
University of Glasgow, Glasgow G128QQ, U.K.*

Rienk van Grondelle

*Department of Physics and Astronomy, Vrije Universiteit, De Boelelaan 1081,  
1081 HV Amsterdam, The Netherlands*

Summary .....	170
I. Introduction .....	170
II. Components of the Light-Harvesting System of Purple Bacteria .....	171
A. Core Antennas .....	171
B. Peripheral Antennas .....	173
C. The 3-Dimensional Structure of LH2 from <i>Rps. acidophila</i> and <i>Rsp. molischianum</i> .....	174
III. Structure-Function Relationships in Bacterial Antennas .....	176
A. The Origin of the $Q_y$ Absorption Transition .....	176
B. Molecular Origin of the $Q_y$ Redshift: Experimental Evidence .....	178
C. What Makes the Difference between LH1 and LH2 Proteins? .....	180
IV. Energy Transfer in Light-Harvesting Proteins from Purple Bacteria .....	181
A. Energy Transfer between Carotenoid and Bacteriochlorophyll Molecules .....	181
B. Energy Transfer from the B800 BChl Molecules in LH2 .....	182
C. Excitation and Energy Transfer in the 850 nm Transition .....	184
D. LH2 to LH1 Transfers .....	185
E. Excitation in LH1 Rings: Equilibration and Transfer to Reaction Centers .....	186
V. Conclusion .....	188
Acknowledgments .....	188
References .....	188

---

\*Author for correspondence; email: brobert@cea.fr

## Summary

Antenna proteins from purple photosynthetic bacteria are by far the best-understood photosynthetic light-harvesting proteins, and among the best-characterized membrane proteins in any biological field. The photosynthetic membrane of purple bacteria is an exceptional case of a membrane for which structural information is available on the partner proteins involved in a biological process. The bacterial light-harvesting system constitutes an ideal source of experimental results for confronting theories to explain the functioning of these biological molecules in elementary physical and chemical terms, and for exploring light capture and transfer mechanisms at the level of the whole membrane. This chapter reviews the different aspects of our current knowledge on light-harvesting proteins from purple bacteria. A special emphasis is given to the biochemical properties of these complexes, their natural diversity, and the details of the known structures. The most recent results on the physical mechanisms that underlie their electronic properties, and on the cascade of the ultrafast excitation transfers that follow the absorption of the solar light are summarized. These are discussed in the light of the different models and calculations that have been performed from the crystal structure.

## I. Introduction

Light-Harvesting (LH) proteins from purple bacteria are probably the best-characterized photosynthetic antenna proteins with regard to structure and function and also from a spectroscopic point of view. Actually these proteins are among the best-characterized membrane proteins in any biological field, because they possess a combination of properties that make them particularly attractive for both biochemical and biophysical studies. Firstly, the light-harvesting system from most purple bacteria is comprised of only one or two different membrane protein-pigment complexes. Each of these complexes exhibits characteristic absorption properties, and they are naturally over-expressed in the photosynthetic membranes. In bacterial species that synthesize only one type of antenna complex, the absorption of the whole photosynthetic membrane therefore arises mainly from these pigment-protein complexes. Spectroscopic characterization of these proteins thus was started even before the first protocols to purify them were developed (Thorner, 1970; Clayton and Clayton, 1972). Secondly, the bacteriochlorophyll (BChl) molecules bound to these proteins exhibit absorption properties in the near infrared that are very different from those of isolated BChl, and which

depend critically on the type of antenna protein they are bound to. Denaturation of these proteins thus results in a dramatic change in their near infrared absorption spectra. This means that the quality of a preparation may be readily analyzed simply by recording its absorption spectrum. Because of this, biochemical characterization of these proteins was performed in early days of membrane protein biochemistry (for a review see Zuber and Cogdell, 1995), opening the way for a wide range of biophysical studies.

In the photosynthetic purple bacteria, the light-harvesting system generally contains a core antenna, also called LH1, which transfers excitation energy directly to the reaction centers. In BChl *a*-synthesizing bacteria, LH1 complexes typically absorb at 870–880 nm. Their absorption peak is shifted to about 1000 nm in BChl *b*-synthesizing species. Many bacterial species also contain peripheral antenna complexes, LH2, which transfer excitation energy to the reaction centers via LH1. LH2 complexes usually exhibit two major absorption transitions in the near infrared, at 800 and 850 nm in BChl *a*-containing bacteria. The near infrared absorption transitions of both LH1 and LH2 are thus considerably red-shifted relative to the absorption of isolated, monomeric BChl *a* (770 nm in most organic solvents). In LH complexes, BChl molecules responsible for a given  $Q_y$  absorption transition are usually referred to as B followed by the position of this transition, e.g. B800 or B850 (Fig. 1).

Both LH1 and LH2 are oligomers of an elementary unit, composed of a pair of small (5–7 kDa), very hydrophobic apoproteins, called  $\alpha$  and  $\beta$ , each of

---

*Abbreviations:* BChl – bacteriochlorophyll; CD – circular dichroism; Crt – carotenoid; FWHM – full width at half-maximum height; GPa – gigapascal; LH – light-harvesting; LH1 – core light-harvesting complex; LH2 – peripheral light-harvesting complex; NIR – near infrared; P – primary electron donor; *Rb.* – *Rhodobacter*; RC – reaction center; *Rps.* – *Rhodopseudomonas*; *Rsp.* – *Rhodospirillum*



which contains a single transmembrane helix as the major structural element (Zuber and Brunisholz, 1991). The successful crystallization of reaction centers from *Rhodopseudomonas (Rps.) viridis* (Deisenhofer et al., 1984) triggered attempts to crystallize both LH1 and LH2 from a wide range of bacterial species which, after more than ten years of struggle, resulted in the determination of the 3D-structure of LH2 from *Rps. acidophila* (McDermott et al., 1995) (Fig. 1) and later from *Rhodospirillum (Rsp.) molischianum* (Koepeke et al., 1996). Although a high-resolution structure of LH1 has not yet been obtained, a projection map at low resolution of this protein has been determined (Karrasch et al., 1995). Since LH1 and LH2 apoproteins are homologous, and these complexes are assembled on very similar principles, it was possible to build reasonable structural models of LH1 from this projection map with the help of the LH2 structure, (Papiz et al., 1996; Hu and Schulten, 1998). The membrane of purple photosynthetic bacteria is thus a unique example of a photosynthetic membrane for which the structures of the different partner proteins involved in the early steps of the photosynthetic process are known, and it provides an ideal source of experimental results for an attempt to explain the functioning of these biological molecules in elementary physical and chemical terms (Sundström et al., 1999).

## II. Components of the Light-Harvesting System of Purple Bacteria

### A. Core Antennas

Photosynthetic purple bacteria generally contain core antenna complexes, or LH1, in stoichiometric amounts with respect to the reaction centers (Sistrom, 1978). In some bacteria, such as *Rsp. rubrum* or *Rps. viridis* these proteins are the only antenna complex present. They are most often constituted from a single pair of  $\alpha\beta$  subunits. The polypeptides are encoded by the first two open reading frames from the *puf* operon (*pufA* and *pufB*), which also encodes the L and M subunits of the bacterial reaction center (Youvan et al., 1984; Naylor et al., 1999; see also chapter 16, Beatty and Young). In a few cases, evidence was obtained for the existence of more than one  $\alpha$  and/or  $\beta$  polypeptide type, for instance in *Chromatium vinosum* (Zuber and Brunisholz, 1991) and possibly in the BChl *b*-synthesizing bacterium

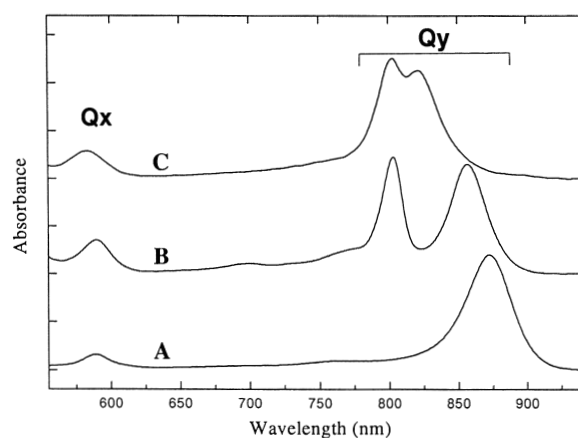


Fig. 1. Electronic absorption spectra ( $Q_x$  and  $Q_y$  transitions). A. LH1 from *Rsp. rubrum*, strain G<sup>+</sup>; B. LH2 (B800-850) from *Rps. acidophila*, strain 10050; C. LH3 (B800-820) from *Rps. acidophila*, strain 10050.

*Ectothiorhodospira halochloris*, although the antenna system of the latter is not yet fully characterized (see below). An additional polypeptide,  $\gamma$ , was found associated with LH1 from *Rps. viridis*, but its role is still unclear (Brunisholz et al., 1985). Each of the LH1 polypeptides binds a single BChl (*a* or *b*) molecule, through conserved His residues located in the transmembrane segment of the  $\alpha$  and  $\beta$  polypeptides. These LH1 proteins generally exhibit a single absorption transition in the near infrared, which usually is located between 875 and 890 nm (Fig 1). However, an 865-nm absorbing LH1 has been reported in *Roseococcus thiosulfatophilus*, a marine, aerobic species (Gall et al., 1999), and a 920-nm absorbing LH1 has been isolated from the thermophilic *Chromatium tepidum* species (Garcia et al., 1986; Fathir et al., 1998). BChl *b*-containing LH1 such as those found in *Rps. viridis* absorb at *ca* 1000 nm. Wild-type LH1 proteins contain one molecule of carotenoid per  $\alpha\beta$  pair (Cogdell et al., 1982; Arellano et al., 1998). Unlike LH2 complexes, LH1 is generally stable in the absence of colored carotenoids (although their absence often induces 5–10 nm blueshifts of the NIR absorption transition). When LH1 is dissociated into small subunits by octyl-glucoside treatment, the carotenoid molecule is lost (Jirsakova and Reiss-Husson, 1993; Loach and Parkes-Loach, 1995). This suggests that it lies, as in LH2, at the interface between  $\alpha\beta$  pairs. Upon removal of octyl-glucoside, LH1 subparticles obtained from carotenoid-containing proteins usually reassociate without their bound carotenoid and exhibit

$\alpha$	N-TERMINUS	HYDROPHOBIC REGION	C-TERMINUS
LH1-Rr		MWRIWQLFDPRQALVGLATFLFVLALLIHFIILLSTERFNWLEGASTKPVQTS	
LH1-Rs		MSKFYKIWMIFDPRRVFVAQGVFLFLAVMIHFILLSTPSYNWLEISAAKYNRVAAVE	
LH2-Rs		MTNGKIWLTVKPTVGVPFLSAAFIASVVIHAAVLTTTTLWPAYYQGSAAVAEE	
LH2-Ra		MNQGKIWTVVNPVSVGLPLLLGSVTVIAILVHAAVLSTTTWFPAYWQGGKKAA	
LH3-Ra		MNQGKIWTVVPPAFGLPLMLGAVAITALLVHAAVLTHTTWYAAFLQGGVKKAA	
$\beta$	N-TERMINUS	HYDROPHOBIC REGION	C-TERMINUS
LH1-Rr		EVKQESLSGITEGEAKFEHKIFTSSILVFFGVAAFAHLLVWIWRPWPVPGPNYS	
LH1-Rs		ADKSDLGYTGTLDEQAQELHSVYMSGLWPFFSAVAIVAHLAVTIWRPWF	
LH2-Rs		TDDLNVWPSGLTVAEEAEVHKQLILGTRVFGGMALIAHFLAAATPWL	
LH2-Ra		ADDVKGLTGLTAAESEFLHKHVIDGTRVFFVIAIFAHVLAFAFSPWLH	
LH3-Ra		AEVLTSEQAEEELHKHVIDGTRVFLVIAIAHFLAFTLTLPWLH	

Fig. 2. Primary amino acid structures of the  $\alpha$  (top) and  $\beta$  (bottom) antenna polypeptides of LH1, LH2 (B800-850) and LH3 (B800-820). Sequences were aligned relative to the conserved membrane His residues. In bold: amino acids involved in interactions with the bound BChl molecules (see text). Rr, *Rsp. rubrum*; Rs, *Rb. sphaeroides*; Ra, *Rps. acidophila* Ac7050.

absorption properties similar to those of the intact, untreated, LH1 complex (Loach and Parkes-Loach, 1995). In the case of *Rubrivivax gelatinosus* however, reassociation of LH1 requires the presence of hydroxyspheroidene, the carotenoid naturally synthesized by the bacterium (Jirsakova and Reiss-Husson, 1994).

Electron diffraction studies on 2-D-crystals of LH1 proteins from *Rsp. rubrum* gave rise to a low-resolution projection map of these complexes in the membrane plane (Karrasch et al., 1995). This projection map was published before the structure of LH2 was available, and it demonstrated that LH1 is composed of a circular association of  $\alpha\beta$  subunits. Sixteen  $\alpha\beta$  subunits are required to produce a complete closed circle (Karrasch et al., 1995). The central hole of these rings is large enough to contain the reaction center, and 2-D crystals of LH1-RC complexes clearly show that it does (Meckenstock et al., 1992a,b; Walz and Ghosh, 1997; Walz et al., 1998). Whether these closed, 16-membered rings truly exist *in vivo* is still matter of debate. It has become clear that in *Rb. sphaeroides* and *Rb. capsulatus* the small protein pufX also plays an important role in the structure and organization of the LH1-RC core. PufX is a short polypeptide (nearly the size of one antenna polypeptide) with a single membrane-spanning domain (Youvan et al., 1984). It is required for photosynthetic growth (Lilburn et al., 1992; Barz and Oesterhelt, 1994), and its proposed role is to form a pore in the LH1 ring, thus allowing quinones to move between the RC and the cytochrome *bc*<sub>1</sub> complex (Barz and Oesterhelt, 1994; McGlynn

et al., 1994; Barz et al., 1995; Cogdell et al., 1996). In an LH2-lacking, pufX-containing mutant from *Rb. capsulatus*, LH1 complexes were observed as open rings of approximately 12  $\alpha\beta$  subunits (3/4 of a turn) connected to form dimers via the holes left by the missing 4  $\alpha\beta$  subunits. These 'combined' LH1 surrounded two connected reaction centers (Jungas et al., 1999). However, the resolution of these projection maps was low enough to leave open the possibility of other interpretations. In a pufX<sup>-</sup> mutant of *Rb. sphaeroides*, a remarkable change of the linear dichroism spectrum of the membrane was observed. This change implies that all the RC proteins were aligned in the membrane plane, with the transition dipole of the primary electron donor almost perpendicular to the long axis of the photosynthetic membrane, which has a tubular shape (Frese et al., 2000). This preferential orientation of the RC was lost in the absence of pufX, concomitant with loss of the dimeric structure (Francia et al., 1999; Frese et al., 2000). How pufX induces this remarkable long-range ordering these proteins is still unknown.

Up to now, attempts to crystallize LH1 proteins have failed to produce crystals that diffract to the resolution required to produce useful 3-D structures. Thus little is known about the details of the LH1 structure. However, experiments combining site-selected mutagenesis and vibrational spectroscopy have shown that each BChl in these proteins interacts with a tryptophan residue through its acetyl carbonyl (Olsen et al., 1997; Sturgis et al., 1997), as in LH2 from *Rsp. molischianum* (Koepke et al., 1996, see below). Similar experiments have shown that, in

addition, these BChl molecules are involved in intermolecular interactions through their keto carbonyl groups. This group forms an H-bond with the protonated nitrogen atom of the imidazole sidechain whose non-protonated nitrogen serves as the ligand of the other BChl molecule in the same  $\alpha\beta$  subunit (Olsen et al., 1997). According to this 'interlocking' model, all of the BChl interactions with the surrounding  $\alpha$  and  $\beta$  apoproteins occur within the same  $\alpha\beta$  subunit, as in the LH2 complex from *Rsp. molischianum*. Another important conclusion from vibrational spectroscopy was that the structure of the BChl binding sites in these LH1 proteins is strongly conserved among most BChl *a*-containing bacterial species (Robert and Lutz, 1985).

### B. Peripheral Antennas

In addition to their core antenna, a number of bacterial species, including *Rb. sphaeroides*, *Rb. capsulatus*, and *Rps. acidophila*, also contain peripheral antenna, or LH2 complexes. The LH2 polypeptides are encoded by the *puc* operon (Youvan and Ismail, 1985), and their expression depends on the bacterial growth conditions (light intensity, temperature, and oxygen pressure) (Sistrom, 1978). Typical LH2 proteins, such as those which have been crystallized from *Rps. acidophila*, exhibit two electronic transitions in the near infrared, at 850 and 800 nm (Fig. 1B). These transitions arise from a ring of strongly-coupled BChls within the membrane phase and from 'monomer' BChls located closer to the membrane/cytosol interface, respectively (see below). The B850 molecules are bound to the  $\alpha$  and  $\beta$  polypeptides through a conserved His, homologous to those that bind the B875 molecules in LH1 complexes. These complexes consist of a ring of eight or nine  $\alpha\beta$  subunits, smaller than the LH1 ring (McDermott et al., 1995). In some bacteria, such as *Erythromicrobium ramosum* and *Chromatium purpuratum*, the main LH2 proteins absorb at shorter wavelengths, at 832 and 830 nm, respectively (Cogdell et al., 1990; Gall et al., 1999). LH2 proteins have not been yet found in BChl *b*-containing bacteria. However, *Ectothiorhodospira halochloris* exhibits, in the membrane, two transitions in the near infrared at 1020 and 800 nm, which could arise from LH2-type proteins (Steiner and Scheer, 1985). These proteins have not yet been fully characterized, and it remains possible that these bacteria possess a new light-harvesting system and no LH2.

In a number of bacterial strains (e.g. *Rb. sphaeroides* and *Rb. capsulatus*) LH2 proteins are built from a single type of  $\alpha$  and  $\beta$  apoproteins (Zuber and Brunisholz, 1991). However, other purple bacteria frequently possess more than one single copy of the *pucA* and *pucB* genes (up to six in *Rps. palustris* (Tadros, 1990; Tadros et al., 1993), and possibly even more in some *Rps. acidophila* strains (Brunisholz et al., 1987; Gardiner et al., 1992)). In some cases, only one  $\alpha\beta$  pair is expressed, the other genes remaining apparently silent (as in *Rsp. molischianum* (Germeroth et al., 1996; Sauer et al., 1996b)). In other cases (*Chromatium vinosum*, *Rps. palustris*, and *Rps. acidophila*), the peripheral light-harvesting system is composed of a mixture of different  $\alpha$  and  $\beta$  polypeptides. The exact role of these variant polypeptides is not yet fully understood. In some bacteria, such as *Rps. acidophila*, they are synthesized in low-light growth conditions, and they assemble independently to form LH2 rings with a red-most absorption transition at 820 nm instead of 850 nm (Brunisholz et al., 1987) (Fig. 1C). They contain natural variations at residues  $\alpha_{44}$  and  $\alpha_{45}$  (Brunisholz et al., 1987). These residues (Tyr and Trp, respectively) are involved in H-bond interactions with the 850-nm absorbing BChl molecules (Fowler et al., 1994). It was shown that the replacement of these amino acids by leucine and phenylalanine is directly responsible for the changes in the absorption spectrum (Fowler et al., 1992). However, in other bacteria, such as *Rps. palustris* and *Chromatium vinosum*, some  $\alpha\beta$  pairs share very high sequence similarity (Bissig et al., 1990; Tadros et al., 1993). In *Rps. palustris*, it was concluded recently that the unusual absorption properties of the LH2 complexes synthesized under low-light conditions could reflect rings containing mixtures of polypeptides (Gall and Robert, 1999). Structural studies, involving either X-ray crystallography or electron diffraction on 2-D crystals, have been performed on LH2 from *Rhodovulum sulfidophilus* (Savage et al., 1996) and on 820-nm absorbing LH2 from *Rps. acidophila* (McLuskey et al., 1999, 2001). In both these cases, the organization of the LH2, and in particular the structure and stoichiometry of the  $\alpha\beta$  ring, is very similar to that of the LH2 from *Rps. acidophila*.

In the LH2 structure of *Rps. acidophila*, one carotenoid molecule is visible (Cogdell et al., 1999). Carotenoids are an important component of the LH2 proteins, and seem necessary for their assembly. Mutant bacteria deficient in carotenoid synthesis are

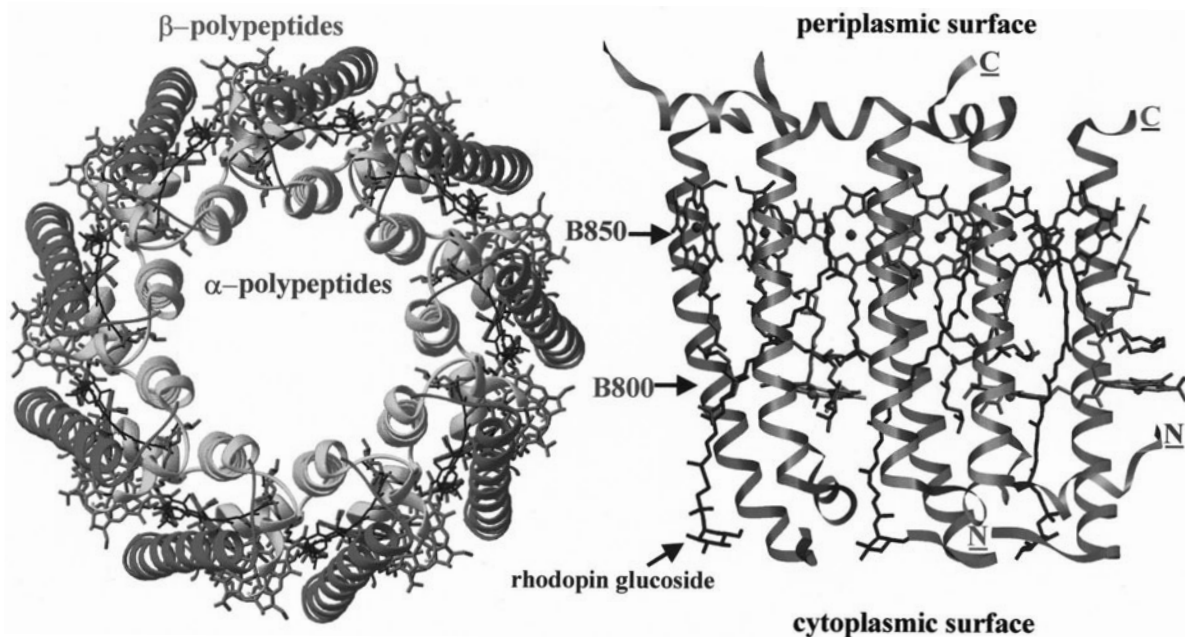


Fig. 3. Front view (in the plane of the membrane) and side view of the structure of LH2 proteins from *Rhodospseudomonas acidophila*, strain 10050, showing both nine-membered rings of  $\alpha$  and  $\beta$  polypeptides. In the color version (Color Plate 2) the  $\alpha$  and  $\beta$  polypeptides are shown in orange and green, respectively, the 850-nm absorbing BChl molecules in magenta, the 800-nm absorbing BChls in cyan and rhodopin glucoside in dark blue. See Color Plate 2.

generally unable to synthesize normal LH2 proteins, and a correlation was even found between the expression level of the *crtI* gene and that of LH2 proteins (Lang and Hunter, 1994). The structural role of the carotenoid molecule can be easily understood by considering that the carotenoid is located parallel to the  $\alpha$  and  $\beta$  polypeptides (Fig. 3) and mediates some of the hydrophobic interactions between these polypeptides (Cogdell et al., 1999). Recently, however, it was reported that the purple sulfur bacterium *Chromatium minutissimum* is able to fully assemble carotenoid-less LH2 protein in the presence of large amounts of carotenoid synthesis inhibitors (A. Moskalenko, unpublished). This finding may reflect the fact that LH2 proteins in sulfur, photosynthetic bacteria, possess a slightly different organization, which allows them to be assembled in the absence of colored carotenoids. There is still a discussion about the precise stoichiometry of carotenoid molecules in LH2. Although a large number of biochemical and spectroscopic data have indicated that there should be two functionally different carotenoid molecules per  $\alpha\beta$  subunit (Kramer et al., 1984), only one has been observed in the structures from *Rps. acidophila* (Cogdell et al., 1999) and *Rsp. molischianum* (Koepke et al., 1996).

Moreover, a recent pigment analysis showed convincingly that in detergent-purified LH2 from *Rb. sphaeroides* and *Rps. acidophila* the actual BChl: carotenoid stoichiometry is 3:1 (Arellano et al., 1998). However, additional experiments (and/or structures) are clearly required to demonstrate whether this stoichiometry holds for all LH2 antenna complexes, or whether it depends on growth and/or purification conditions.

### C. The 3-Dimensional Structure of LH2 from *Rps. acidophila* and *Rsp. molischianum*

Figure 3 shows the 2.5-Å crystal structure of LH2 from *Rps. acidophila* (Isaacs et al., 1995; Prince et al., 1997). It consists of a nonameric circular association of  $\alpha\beta$  heterodimers. This association produces, in the membrane plane, two concentric rings of helical  $\alpha$ - (inside ring) and  $\beta$ - (outside ring) polypeptides. Each polypeptide binds one BChl molecule non-covalently through the imidazole sidechain of a conserved His residue (Zuber and Brunisholz, 1991). These BChl molecules are sandwiched between the two polypeptide rings and form a ring of nine dimers of BChls. This ring of 18 BChl molecules gives rise to the red-most absorption



Fig. 4. Side views (across the plane of the membrane) of the  $\alpha\beta$  dimers from A. *Rhodospseudomonas acidophila* and B. *Rhodospirillum rubrum*. The carotenoid molecule and the hydrophobic tails of the BChl molecules are omitted from the *Rps. acidophila* structure for clarity. BChl molecules are shown in dark gray, amino acid sidechains involved in H-bonding the 850-nm absorbing BChl in light-gray. H-bonds are indicated as gray dotted lines. Note that the  $\alpha$  polypeptide in *Rps. acidophila* extends towards the adjacent  $\alpha\beta$  dimer, so that Tyr  $\alpha_{44}$  does not interact with the BChl  $a$  molecules bound to the represented dimer, but with one bound to the adjacent dimer. By contrast, in the LH1-related *Rsp. rubrum* structure, both the BChl molecules bound to a dimer interact with amino acids belonging to this dimer, namely Trp  $\alpha_{45}$  and  $\beta_{44}$ .

transition at 850 nm (van Grondelle et al., 1994). Each of these 18 BChls forms an H-bond via its acetyl carbonyl group with a neighboring amino acid residue (Tyr  $\alpha_{44}$  or Trp  $\alpha_{45}$ ), confirming a prediction from earlier spectroscopic studies (Fowler et al., 1994; Sturgis et al., 1995b). Note that the BChl bound to the  $\beta$  subunit interacts with Tyr  $\alpha_{44}$  of the neighboring  $\alpha$  subunit (Fig. 4). These proteins thus have an H-bond network that is complete only when the ring is fully assembled. Each  $\alpha\beta$  subunit binds one additional BChl molecule near the interface between the membrane and the cytosol, through the oxygen atom of the formylated N-terminal of the  $\alpha$  polypeptide. This binding site is very polar and is mainly composed of aminoacids from the  $\beta$  polypeptide. The BChl molecules bound to these sites form a ring of nine 'monomer' BChls spaced by about 21 Å with their macrocycles nearly in the membrane plane. They give rise to the 800-nm absorption band of these proteins. Again, the acetyl carbonyl group of each of these BChls forms an H-bond with the neighboring Arg  $\beta_{21}$ .

The crystal structure of the *Rps. acidophila* LH2 contains one carotenoid per  $\alpha\beta$  unit, a rhodopin

glucoside with its main axis oriented nearly perpendicular to the membrane plane (Fig. 3). One of its ends reaches the cytosolic face of the membrane, while the other forms van der Waals contacts with the  $\alpha$ -bound BChl of the adjacent  $\alpha\beta$  subunit. In between, the carotenoid also forms van der Waals contacts with the 800-nm absorbing BChl molecule. Most of the contacts between the  $\alpha$  and  $\beta$  polypeptides are mediated either through this carotenoid molecule (between adjacent subunits) or through the phytyl tails of the 850-nm absorbing molecules, which lie parallel to these polypeptides, and run from the BChl macrocycle to the periplasmic side.

If the LH2 from *Rps. acidophila* can be considered as a 'typical' peripheral antenna protein of purple bacteria, the LH2 from *Rsp. rubrum* is, by contrast, a very unusual complex. Sequence comparisons show that its  $\alpha$  and  $\beta$  polypeptides are more related to those of the LH1 complexes (Germeroth et al., 1993). Using resonance Raman spectroscopy, it could further be concluded that the binding sites of the red-most absorbing BChls in these complexes were very similar to those of LH1 (Germeroth et al., 1993). Its crystal structure was

therefore of particular interest, as it could give information about the structure of the LH1, for which no highly diffracting crystals have yet been reported. The overall structure of the LH2 protein from *Rsp. molischianum* is similar to that of LH2 of *Rps. acidophila*, except that it is an octameric ring of  $\alpha$  and  $\beta$  apoproteins, which therefore binds only 24 BChls (instead of 27 in the case of *Rps. acidophila*) (Koepke et al., 1996). Apart from that difference in the number of apoproteins forming the ring, the major difference is in the binding site of the 800-nm absorbing BChl (B800). In *Rsp. molischianum* LH2, the plane of these B800 molecules is rotated by 90 degrees compared with the LH2 from *Rps. acidophila*, and is tilted away from the membrane plane (Fig. 3B). The detailed protein-BChl interactions also are different in this complex. It is important to note that the B850 BChl molecules are H-bonded by tryptophan residues, one belonging to the  $\alpha$  and the other to the  $\beta$  polypeptide, as in LH1 proteins (Olsen et al., 1994; Sturgis et al., 1997). Each  $\alpha\beta$  subunit thus forms, in terms of H-bonds to BChl, an independent unit (Fig. 4B).

### III. Structure-Function Relationships in Bacterial Antennas

#### A. The Origin of the $Q_y$ Absorption Transition

The  $Q_y$  electronic transitions of LH2 and LH1 proteins are dramatically red-shifted relative to those of monomeric BChl in organic solvents. Understanding the mechanisms of this red-shift is particularly important, as in purple bacteria, in contrast with oxygen-evolving organisms, the funneling of the excitons towards the RC is strongly driven by the gradient in the energy of the electronic transitions of the different light-harvesting complexes. As discussed above, antennas from purple bacteria generally contain a large number of BChl cofactors, and those present in the intra-membrane part of these proteins are in close contact with each other, forming large arrays of 16, 18 or 32 interacting molecules. How precisely the arrangement of the pigments in the complexes determines the observed  $Q_y$  electronic transition is what we wish to understand.

Depending on the strength of the pigment-pigment interactions, the  $Q_y$  transition could simply be the sum of the electronic transitions of all the pigments (if there are no, or only weak interactions), or in the

other extreme (i.e. with strong interactions), it could arise from one giant electronic transition that is a collective property of the whole set of BChl molecules (Chapter 2, Scheer). In reality, the situation is even more complex, since the electronic properties of a set of identical, interacting, molecules depend not only on the strength of the intermolecular interactions, but also on variations in the properties of the individual molecules. In an assembly of chemically identical molecules, differences in the local physico-chemical properties can arise either from slight differences in their conformations and/or the conformation of the immediate surroundings, or from dynamic fluctuations of the system. Because of these two effects, usually referred to as static and dynamic disorder, chemically identical molecules must be considered as different, and despite their interactions, each molecule will tend to retain its individual physico-chemical properties. In the extreme case of strongly interacting molecules in the absence of disorder, the set of interacting molecules will behave as one supermolecule, and the excited state can be described by exciton theory, where the excitation is coherently delocalized over the whole set of interacting molecules. If the interactions are weaker, and the disorder larger, the excited state will become localized on one or a subset of molecules, and will hop incoherently from one of these subsets to another. These limiting cases thus involve physically different origins of the electronic transition(s) of the complex, and they can result in different spectroscopic properties.

The evolution of the system with time also depends on the extent of delocalization of the excitation. If the excited states are delocalized over the whole set of interacting molecules, with the new energy levels given by the diagonalization of the interaction Hamiltonian, the time evolution of the excited state occurs via relaxations between these energy levels, generally through energy exchange with vibrations of the system. This is called phonon-induced relaxation between exciton levels. If the excitation is (even partially) localized, the time evolution will be described by a similar initial relaxation, followed by incoherent hopping of the excitation. When the excitation is fully localized, the energy transfer is described by Förster theory (or adapted versions of it, see below). Also, during the hopping process the system permanently exchanges phonon/vibration energy with its surroundings, and, in that sense, the two relaxation processes are similar. The true situation



may be somewhere in between these two limiting cases, and the important factor deciding which of these processes actually occurs is the ratio of the coupling between electronic transitions ( $V$ ) and the disorder ( $\Delta$ ). Determining which of these cases applies to the  $Q_y$  transitions of the LH1 and LH2 proteins is thus essential in order to understand their properties fully, and is closely related to the question of the extent to which the spectrum reflects BChl/BChl electronic or pigment/protein interactions (Chapter 3, Parson).

Most calculations have concerned LH2 rings, the three-dimensional structure of which is known. As well documented by a number of authors (McDermott et al., 1995; Sauer et al., 1996a), using an exciton model for LH2 can lead to the prediction of the correct position for the  $Q_y$  of these proteins. However, such a prediction alone does not validate the pure exciton model (Monshouwer and van Grondelle, 1996; Sturgis and Robert, 1996). Firstly, it is now known that both the 820- and 850-nm absorbing LH2 of *Rps. acidophila* exhibit very similar structures (McLuskey et al., 2001). If an exciton calculation is performed for both these proteins, variations of site energies have to be taken into account so that the calculation does not lead to exactly same prediction for their  $Q_y$  transitions. Secondly, the pure exciton model predicts that the lowest excitonic level has close to zero dipole strength, and as a consequence, would not be fluorescent at very low temperature. This is certainly not the case, as shown for LH2s from both *Rb. sphaeroides* and *Rps. capsulatus*. In fact, both LH2 complexes fluoresce with a rate two–three times faster than monomeric BChl in solvent (Monshouwer et al., 1997).

To overcome these problems, it is necessary to introduce disorder in the LH2 system, i.e. to introduce into the calculation the fact that all the BChl may not, at a given instant, have exactly the same optical properties. In order to fully explain the behavior of the LH2 fluorescence as a function of temperature, it had to be assumed that the disorder was about two times larger than the pigment-pigment coupling strength (van Grondelle et al., 1997). Such a high value implies that, in LH2 rings, the disorder is high enough to destroy the delocalization of the exciton over the whole set of molecules, or, more simply, that the properties of the pigments in each ring are sufficiently different so that they cannot be considered as an assembly of identical molecules. Analysis of the results of a variety of spectroscopic methods led

to the conclusion that an excitation in the 850-nm ring of the LH2 is coherent over a few (2–4) BChl molecules (Pullerits et al., 1995; Monshouwer et al., 1997; Kennis et al., 1997a; Kuhn and Sundström, 1997).

Thus, the 850 ring of the LH2 likely behaves as a system in which the different pigments are strongly coupled, but where the disorder is large enough to prevent the complete collective behavior of these coupled pigments. Most recent calculations attempting to predict the CD signal of LH2 also reflect this dual character of these rings. LH2 proteins generally exhibit strong, conservative CD signals in the 850-nm region (positive rotational strength on the blue side, negative on the red side (Cogdell and Scheer, 1985)), which have been attributed to strong BChl-BChl excitonic interactions. Surprisingly, the zero crossing of this signal does not coincide with the absorption maximum but is at about 6–7 nm longer wavelength (Sauer et al., 1996a; Koolhaas et al., 1997, 2000). Furthermore, in a mutant of *Rb. sphaeroides* lacking the B800 BChl molecule, a broad, weak, negative CD-band around 780 nm (Koolhaas et al., 1998) was observed, which was ascribed to the upper exciton band of the B850 ring. Although a large disorder is introduced in these calculations (which should, as discussed above, result in localization of the excitation), to predict the CD signal correctly, with its red-shifted zero-crossing, requires the full ring (Koolhaas et al., 1997). The reason for this is that the contribution to the CD signal of LH2 resulting from the nearest neighbor interactions is very small, as they have almost parallel transition dipoles. The maximum contribution originates from interactions between dipoles separated by about a quarter of the ring. In short, the CD ‘remembers’ the excitonic properties of the ring, in spite of the disorder which effectively localizes the excitation on a few BChl molecules (Somsen et al., 1996b). From these calculations, the magnitude of the nearest neighbor dipole-dipole coupling matrix elements were calculated to be 300 and 230  $\text{cm}^{-1}$  for intra- and inter-dimer nearest neighbors, respectively (Koolhaas et al., 1998).

In contrast, LH1 proteins, in which similar or stronger BChl-BChl interactions would be expected, exhibit a more complex, weaker, non-conservative signal in the 875 nm region, which may vary from complex to complex. Moreover, biochemical reconstitutions of LH1 proteins after dissociation have shown that, depending on the reconstitution



procedure, proteins exhibiting similar absorption maxima can exhibit totally different CD signals in their  $Q_y$  region (Parkes-Loach et al., 1988; Lapouge et al., 2000). One probable reason is that the transition dipoles in LH1 are oriented even more in the plane of the ring than in LH2. As a consequence, all contributions to the CD cancel and the signal becomes sensitive to small variations in the orientation and position of the transition dipoles. Thus, for LH1, there is no straightforward relationship between the CD signal and the absorption maximum, and extracting the coupling factors from the CD spectra is extremely complicated and so far not solved.

### *B. Molecular Origin of the $Q_y$ Redshift: Experimental Evidence*

As mentioned above, 850-nm and 820-nm absorbing LH2 from *Rps. acidophila* exhibit very similar molecular structures. Although they certainly play an important role, BChl-BChl interactions alone may thus not entirely explain the electronic properties of LH proteins from purple bacteria. To explain these spectral differences, it is necessary to address other factors that contribute to tuning the absorption of these proteins. In the last decade, spectroscopic studies, often in combination with genetic techniques, have led to considerable progress in our understanding of these factors, which underlie the electronic properties of bacterial antennas. Different types of protein-BChl interactions may influence the absorption properties of LH complexes. Besides direct interactions (such as H-bond formation) the surrounding protein provides to the BChl molecules an environment with given dielectric properties, and it may, by steric hindrance, influence the conformation of their conjugated macrocycles, or of the conjugated chemical groups located peripheral to this macrocycle.

Crystallographic studies show that the BChl bound to the  $\beta$  polypeptide of the 850-nm absorbing pair in LH2 from *Rps. acidophila* is significantly distorted (Prince et al., 1997). This distortion may modify the absorption of this molecule (and thus of the BChl dimer, which would then be constituted of two spectroscopically unequivalent molecules). Resonance Raman studies have confirmed the existence of a distorted BChl in these proteins; moreover evidence was given that this distorted conformation exists in both LH1 and LH2 proteins (Lapouge et al., 1999). Furthermore, calculation of the CD spectrum of LH2

required the two bacteriochlorophylls bound to the  $\alpha$  and  $\beta$  polypeptides to be spectrally different, with the  $\beta$  BChl about 300  $\text{cm}^{-1}$  redder than the  $\alpha$  BChl (Koolhaas et al., 1998). A similar difference was predicted to exist by quantum chemical calculations (Alden et al., 1997). Recently, the structure of the 820-nm absorbing LH2 from strain 7050 of *Rps. acidophila* was deduced from X-ray crystallographic studies (McLuskey et al., 2001). On the basis of this structure, it was proposed that the absence of H-bonds from residues Tyr  $\alpha_{44}$  and Trp  $\alpha_{45}$ , which have been replaced by Phe and Leu, induces an out-of-plane rotation of the acetyl carbonyl groups of the red-most absorbing BChls. The exact quantitative relationship between this rotation and the  $Q_y$  blue shift observed upon the removal of the H-bond still remains to be established. It is unclear whether the rotation alone is large enough to deconjugate the acetyl group from the BChl macrocycle and account for the observed 850 to 820 nm spectral shift (Gudowska-Nowak et al., 1990). As detailed in Lapouge et al. (1999), deducing the conformation of the BChl molecules precisely from X-ray crystallographic studies is a demanding task and requires highly diffracting crystals. However, deconjugation of a carbonyl from the BChl macrocycle should be accompanied by a clear signature in the resonance Raman spectra (Ridge et al., 2000). The combination of such spectroscopic measurements with higher-resolution structural data for the 820-nm absorbing LH2 from *Rps. acidophila* and other bacterial strains should help in evaluating the factors that have a role in tuning the absorption of these complexes.

More than a decade ago, it was postulated that the residues located at positions  $\alpha_{44}$  and  $\alpha_{45}$  play a role in tuning the spectroscopic properties of LH2 from *Rps. acidophila* (Brunisholz et al., 1987). At these positions, a Leu-Phe doublet was found in 820-nm absorbing LH2, in contrast with the usually found Tyr-Trp doublet (or Tyr-Tyr in *Rb. sphaeroides*) in 850-nm absorbing complexes (bolded in Fig. 2). Selective mutations of each of these Tyr to Phe resulted in a blue-shift of the B850 transition by about 15 nm, and doubly-mutated proteins exhibited electronic properties close to those of the low-light, B800-820 LH2 complexes from *Rps. acidophila* (Fowler et al., 1992). In the same complexes, it was shown by Raman spectroscopy that in wild-type LH2 these tyrosines form H-bonds with the acetyl carbonyl groups of the 850-nm absorbing BChl molecules (Fowler et al., 1994). Replacing one or

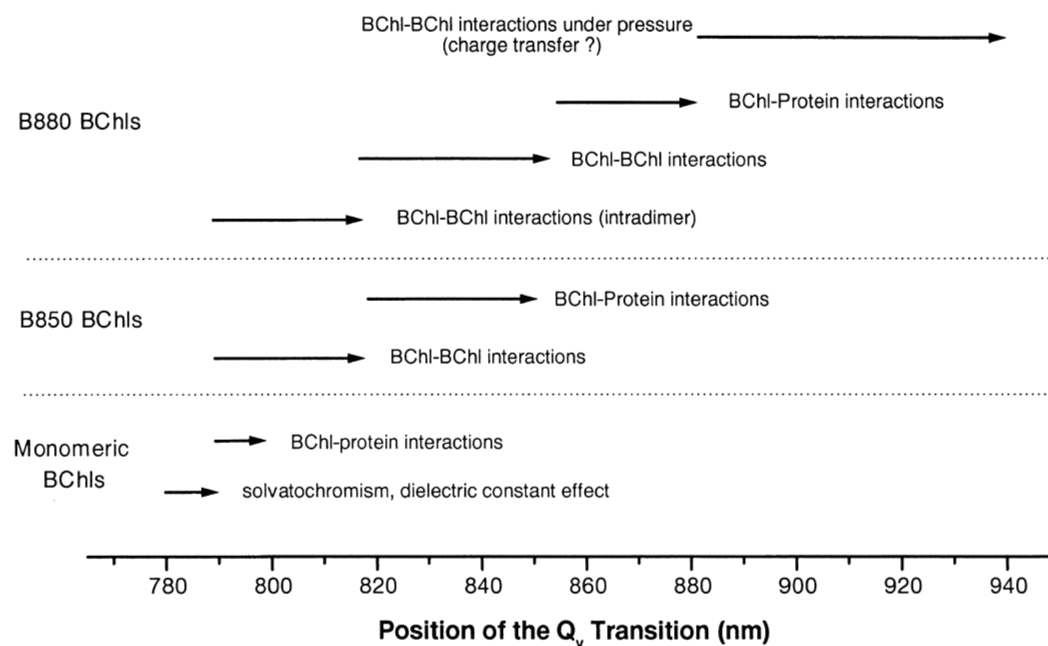


Fig. 5. Overview of the known mechanisms involved in tuning the position of the  $Q_y$  electronic transition of BChl molecules in antenna complexes from purple bacteria. Additional mechanisms, such as conformation changes of the molecules, also could play a role, particularly in the shift of the  $Q_y$  transitions of B850 and B880 from 790 to 820 nm (third and fifth arrows from the bottom). However, no conformational change is observed during the transition of *Rsp. rubrum* LH1 from B820 to B873 (B. Robert, unpublished).

both of these residues by leucine or phenylalanine removes these interactions without measurable reorganization of the BChl binding sites. This, together with the fact that the conservative part of the CD spectrum of the mutant proteins is, though blue-shifted, otherwise identical to that of the wild-type, suggested that these H-bonds have a direct effect on the LH2 absorption, which does not involve the excitonic interactions (Sturgis and Robert, 1996) (Fig. 5).

Spectroscopic studies on naturally 820-nm absorbing LH2 confirmed that the tuning in vivo of the LH2 absorption from 850 to 820 nm is indeed accompanied by the loss of these H-bonds (Sturgis et al., 1995a,b; Sturgis and Robert, 1997; Gall et al., 1999). A similar mechanism was found in LH1 proteins. By a combination of spectroscopy and genetic techniques, it was shown that the conserved Trps  $\alpha_{43}$  and  $\beta_{47}$  form H-bonds with the acetyl carbonyl of the 875-nm absorbing BChls in LH1. When these Trps are replaced by phenylalanines in *Rb. sphaeroides* LH1, the loss of each of these interactions shifts the  $Q_y$  transition of these complexes about 10 nm to the blue (Olsen et al., 1994; Sturgis et al., 1997). In *Roseococcus thiosulfatophilus* LH1

proteins, which absorb at 865 nm, the acetyl carbonyl of the BChl molecules are free from interactions (Gall et al., 1999). This alone may explain the unusual absorption of this complex. A number of changes in the absorption of both LH1 and LH2 proteins, due to mutations of the  $\alpha$  and  $\beta$  polypeptides, were thus ascribed to the tuning of the absorption of individual BChl monomers in these proteins by H-bond formation (Sturgis and Robert, 1997). It is not however yet clear whether these H-bonds have a direct effect on the absorption of the LH proteins or whether the latter is due to the properties of the sidechains in the immediate environment of the BChl molecules.

In LH2 proteins from *Rb. sphaeroides* Arg  $\beta_{21}$  forms an H-bond with the acetyl carbonyl of the B800 (McDermott et al., 1995). When this interaction is broken by mutation, the  $Q_y$  transition of this molecule blue shifts by about 10 nm, towards 790 nm (Fowler et al., 1997; Gall et al., 1997). Depending on the precise nature of the amino acid at position  $\beta_{21}$ , the  $Q_y$  absorption of the B800 BChl in LH2 varies between 780 and 792. It was proposed that this additional 12 nm variation was due to changes in the local dielectric constant around the BChl (Gall et al., 1997). Combination of the H-bond together with the

effect of a low dielectric constant almost fully accounts for the entire red-shift (from 770 to 800 nm) experienced by the  $Q_y$  transition of BChl *a* upon binding in the B800 site. However, it is clear that these shifts are not sufficient to fully explain the position of the 875 and 850 nm transitions in LH1 and LH2 proteins (Fig. 1), and that BChl/BChl interactions need to be taken into account.

Direct experimental evidence that protein-BChl interactions are not the major cause for the absorption difference between LH1 and LH2 came from massive, non-directed, mutagenesis experiments performed on *Rb. capsulatus* LH2. These experiments showed that a set of three mutations in the  $\beta$  subunit was sufficient to transform LH2 into 'pseudo LH1' proteins, i.e. proteins possessing the same absorption as LH1 (Delagrave et al., 1995). It was shown further that the sequence changes did not alter either the protein-BChl interactions or the conformations of the BChls in any of these mutants (Hu et al., 1998). Another direct piece of evidence that BChl/BChl interactions play an important role in tuning the absorption of both LH1 and LH2 came from measurements conducted at high hydrostatic pressure. High pressure shifts the  $Q_y$  transition of LH1 from *Rsp. rubrum* gradually to the red (with a slope of nearly 1000 cm<sup>-1</sup>/GPa), although the conformations and the specific protein/BChl interactions are not affected (Sturgis et al., 1998) (Fig. 5).

BChl/BChl interactions may affect the absorption of the interacting pigments by a number of mechanisms. Excitonic interactions, i.e. interactions between the excited electronic states, may occur between closely located pigments. This type of interaction has often been considered to be the major mechanism underlying the red-shift of LH1 and LH2 (see below, and for a general discussion van Grondelle et al. (1994)). However, additional mechanisms exist. BChls in close contact form a large part of each other's environment, i.e. their interactions may also be solvatochromic. Finally, the situation may be even more complex if the interactions between these molecules, maybe in combination with the asymmetric electrostatic environment provided by the protein, perturb the properties of the excited states. For example, it was shown by Stark spectroscopy that the  $Q_y$  transitions of both LH1 and LH2 exhibit a strong charge-transfer character, with LH1 significantly larger than LH2 (Gottfried et al., 1991; Beekman et al., 1997a,b). This charge-transfer character, which is not present in the  $Q_y$  transitions of

monomeric pigments, could arise in the  $\alpha\beta$  (BChl)<sub>2</sub> dimer, and possibly is one of the reasons why LH1 and LH2  $Q_y$  transitions experience such a large red-shift in vivo (Somsen et al., 1998). Up to now, the role of these different mechanisms in the red-shift of the  $Q_y$  of the bacterial LH has not been fully quantified. Factors influencing the  $Q_y$  transitions are summarized graphically in Fig. 5.

### C. What Makes the Difference between LH1 and LH2 Proteins?

As discussed in Section III, non-directed mutagenesis experiments performed on *Rb. capsulatus* LH2, have shown convincingly that most of the difference in absorption between LH1 and LH2 resides in BChl-BChl interactions. However, many experimental results point to fundamental differences between these proteins in the nature of the lowest electronic excited states: their CD spectra are totally different, the inhomogeneous broadening of the  $Q_y$  transition of LH1 is larger than that of LH2, and the magnitude of the Stark effect is larger in LH1. However, it seems possible that this whole set of different spectral properties arises from only a limited number of variations in the structure of the  $\alpha$  and  $\beta$  polypeptides. For instance, the  $\alpha$  and  $\beta$  polypeptides of LH2 in *Rsp. molischianum* are both homologous to those normally found in LH1 (Germeroth et al., 1993). However, its  $Q_y$  transition lies at 850 nm, and it shares a number of spectral properties with normal LH2 proteins. On the other hand, the CD signal associated with this transition is nearly identical to that of LH1 proteins (Visschers et al., 1995). The situation is similar in the case of pseudo-LH1 (pLH1) mutants obtained by non-directed mutagenesis and phenotypic screening of the  $\beta$  polypeptide of *Rb. capsulatus* LH2 (Hu et al., 1998). Some combinations of mutations resulted in absorption properties in the infrared nearly identical to those of LH1 proteins. In addition to shifting the position of the  $Q_y$  transition, these mutations increased the inhomogeneous broadening of the absorption band.

Analysis of the sequences of these pLH1 mutants has shown that a series of mutations on the N-terminal side of the transmembrane helix of the  $\beta$  polypeptide is able to give the LH2 complex most of the spectral properties typical for LH1. These mutations are located towards the cytoplasmic side of the membrane, i.e. on the opposite side of the membrane relative to the BChl binding site. Also

striking is that, among the huge number of screened mutants, none could be found which would both exhibit LH1-like absorption and still bind the 800-nm absorbing BChl (Hu et al., 1998). These results strongly suggest that the difference between LH1 and LH2 originates, at least partly, from the overall geometry of the LH polypeptides, i.e. from the factors that govern the angles between the  $\alpha\beta$  subunits, which would in turn influence the angles between the BChl pairs in the complex. Among these factors, the presence of the 800-nm absorbing BChl and the volumes of the amino acids at the ends of the membrane helices of both  $\alpha$  and  $\beta$  polypeptides are expected to play a dominant role in tuning the supramolecular organization of these polypeptides. They could thus determine, indirectly, the electronic properties of the LH proteins. It may be speculated that in the 'LH1' configuration the intra- $\alpha\beta$  BChl dimer is more tightly coupled, thus giving rise to the larger Stark effect and stronger excitonic interactions, both leading to the further red-shift. Future work involving site-selected mutations inspired from the sequences of these pseudo-LH1 should clarify the roles of the different amino acids involved in these mechanisms.

#### IV. Energy Transfer in Light-Harvesting Proteins from Purple Bacteria

##### A. Energy Transfer between Carotenoid and Bacteriochlorophyll Molecules

Carotenoid (Crt) molecules in photosynthetic pigment-protein complexes have three major functions: (i) they capture photons in the blue and green spectral range, i.e. in a spectral region where BChl molecules absorb poorly but where the solar spectrum is maximum, and transfer that energy to BChl; (ii) they protect the organism against oxidative stress, as they can quench BChl triplet states and singlet oxygen; and (iii) as evidenced by the LH2 crystal structures, they have a structural role by participating in the overall organization and stability of the LH complexes from photosynthetic purple bacteria (Frank and Cogdell, 1995). In the known structures of the LH2 proteins, the only resolved carotenoid molecule is in van der Waals contact with both the 800-nm and the 850-nm absorbing BChl molecules (Fig. 3), and thus is ideally located for both singlet-singlet and triplet-triplet transfer

mechanisms (McDermott et al., 1995; Freer et al., 1996).

The intense absorption of carotenoids in the blue-green spectral range arises from the second singlet excited state ( $S_2$ ), the lowest one ( $S_1$ ) being optically forbidden. However, in isolated carotenoids the carotenoid  $S_2$  state decays in about 100–200 fs, (Shreve et al., 1991b; Ricci et al., 1996) via internal conversion to  $S_1$ , which lives for several picoseconds, depending on the number of conjugated C=C double bonds. As the emission spectra of  $S_2$  and  $S_1$  overlap with the  $Q_x$  and  $Q_y$  absorption bands of BChl molecules, respectively, energy transfer from the carotenoid to the BChls can occur via either the  $S_2 \rightarrow Q_x$  or the  $S_1 \rightarrow Q_y$  channels (Trautman et al., 1990; Shreve et al., 1991a). The overall efficiency of Crt-to-BChl energy transfer is highly variable, ranging from nearly 100% in LH2 of *Rb. sphaeroides* to 55% in *Rps. acidophila* (and several similar complexes) and as low as ~30% in LH1 of *Rsp. rubrum* (Cogdell et al., 1981; Angerhofer et al., 1986; Noguchi et al., 1990; Cogdell et al., 1992). This, however, does not seem to be due to structural differences between these LH (actually explaining these differences in yield would require tremendous variations in the structure of these complexes) but rather to type of carotenoid. With respect to the effect of length of conjugation, carotenoids with fewer conjugated double bonds generally have longer  $S_1$  lifetimes and thereby allow more time for transfer from this state (Frank et al., 1993). As well, it may also depend on the propensity of the singlet excited state of some carotenoids to de-excite via a fission process (leading from a singlet excited state to a pair of triplet states) (Rademaker et al., 1979).

In LH2 from *Rb. sphaeroides* and *Rps. acidophila*, carotenoid molecules transfer excitation energy to both 800- and 850-nm absorbing BChls. On the LH2 of *Rb. sphaeroides* about 25% of the energy reaches the 850-nm absorbing BChls via the 800-nm absorbing BChls, while about 75% is transferred directly to them (Kramer et al., 1984; Chadwick et al., 1987). These transfers are extremely fast, as it could be shown that the 850-nm  $Q_y$  state is populated within 200 fs after carotenoid excitation (Trautman et al., 1990; Shreve et al., 1991a). Because this rate is similar to that of the carotenoid  $S_2 \rightarrow S_1$  decay, it is highly probable that these two processes compete with each other. The transfer of excitation from the carotenoid to the BChl may thus occur via the two processes:  $S_2 \rightarrow B850$  and  $S_2 \rightarrow S_1 \rightarrow B850/B800 Q_y$ .

Although precise measurements of the kinetics of these processes have been achieved by a number of groups (Andersson et al., 1996; Ricci et al., 1996; Krueger et al., 1998; Walla et al., 2000), due to the extreme difficulty of these experiments more work seems needed to reach a consensus on the exact path and speed of these transfers. From the rates observed and the proportion of excitation transferred to the different pigments, it is possible to draw general models of the transfer events. However, there is still no general agreement on the number of carotenoids bound per LH2, or on the parameters that determine this number. In particular, it is unclear whether the number of carotenoids is the same for all LH2, or whether it depends on growth conditions.

Energy transfer from carotenoid to both the 800- and 830-nm absorbing BChls in LH2 from *Chr. purpuratum* has been modeled on the basis of the presence of two carotenoids per  $\alpha\beta$  pair (Andersson et al., 1996). In this model, one carotenoid transfers excitations exclusively to the B800 (through its  $S_1$  state), and the other to the B830 (through both  $S_1$  and  $S_2$ ). Recently, it was shown that the carotenoid absorption spectrum displayed a significant band-shift on BChl excitation, and the shift was about three times larger for B800 than for B850 excitation. The observed spectral differences strongly suggest the presence of two carotenoids per  $\alpha\beta$  subunit, one reacting to the field induced by the 800-nm excited state, and the other more closely connected with the 850-nm state (Herek et al., 1998). However, a direct demonstration of the presence of these two carotenoid molecules would help in clarifying the experimental results in this area.

In spirilloxanthin-containing LH1 (*Rsp. rubrum*, *Rps. marina*) the transfer of excitation energy from the spirilloxanthin to BChl *a* is low (about 30%) (Duysens, 1952). Excitation of this carotenoid to its allowed  $S_2$  state not only leads to energy transfer and relaxation to the forbidden  $S_1$  state, but also results in formation of triplets with a relatively high quantum yield. Since the triplet yield was found to depend on the presence of a relatively weak magnetic field (about 40% reduction in a field of .1 T), it was suggested that this direct triplet formation occurs by the process of singlet fission (Rademaker et al., 1979). This process does not occur with spirilloxanthin in organic solvents, and is unusual since most carotenoids cannot be excited directly to a triplet state. Measurements of the fluorescence quantum yield in a variety of LH complexes showed

that the fast triplet formation in fact competed with the energy transfer to BChl, and that this phenomenon was not restricted to spirilloxanthin (Kingma et al., 1985a,b). It was shown recently by femtosecond spectroscopy that, in LH1 of *Rsp. rubrum*, the  $S_2$  excited state decayed within 100 fs, generating the  $S_1$  state, the BChl  $Q_x$  state, and a new state that in a few picoseconds led to the well-characterized triplet (Gradinaru et al., 2001). This new state could be a double triplet state localized on the originally excited carotenoid. However, precisely how this state decays into the normal triplet state is so far unknown. These and other results on light-harvesting carotenoids show that much remains to be discovered in these systems.

### *B. Energy Transfer from the B800 BChl Molecules in LH2*

When LH2 is excited in the 800-nm absorbing ring of BChl molecules of the LH2 proteins, the excitation should be largely localized on a single molecule. The distance between these molecules (about 21 Å center-to-center) is much too large for strong excitonic effects to take place. However, the excitation can be transferred from a given B800 molecule either to another B800 molecule, or to BChl(s) in the strongly coupled B850 ring (Kramer et al., 1984; Monshouwer and van Grondelle, 1996; Wu et al., 1997; Salverda et al., 2000). Direct evidence of B800-to-B800 transfer is provided by the fact that, at low temperature, the fluorescence from the B800 is largely depolarized. This depolarization was used to estimate the kinetics of transfer within the B800 ring, taking into account that the 800-to-850 transfer occurs with a time constant of about 1.5 ps (Kramer et al., 1984). A value of about 500 fs was obtained, from which it was calculated that the distance between B800 BChls is about 21 Å, a value that is remarkably close to that deduced from the crystallographic structure of the protein.

Several groups have studied energy transfer within the B800 ring by measuring time-resolved anisotropy decay. These measurements have been performed at both low and room temperature, and with LH2 complexes isolated from *Rb. sphaeroides*, *Rps. palustris* (Hess et al., 1993), *Rps. acidophila* (Ma et al., 1998) and *Rsp. molischianum* (M. Wendling unpublished). From the results obtained, a consistent view of this process has emerged. According to this picture, B800-to-B800 energy transfer is fast at low

temperature (300–500 fs) and slows down to about 1 ps at room temperature (Hess et al., 1993). At low temperature, the fast relaxation following excitation of the 800 nm Q<sub>y</sub> transition may give direct evidence for energy transfer in the B800 band. In *Rb. sphaeroides* LH2, an isotropic decay has been shown to occur on the blue side of this band within 400 to 500 fs, a lifetime that corresponds well to the rise kinetics observed on the red side (Monshouwer et al., 1995b; Monshouwer and van Grondelle, 1996). Similar results were reported for LH2 from *Rps. acidophila* (Wu et al., 1996a; Ma et al., 1998). In LH2 from *Rsp. molischianum* at 77K, the isotropic and anisotropic decays both occur in about 0.8 to 0.9 ps (M. Wendling, unpublished results), i.e. twice slower than observed in *Rps. acidophila* and *Rb. sphaeroides*, although the anisotropy decay does not necessarily have the same decay time as the blue to red relaxation. As mentioned above, the positioning of the B800 BChl is quite different in the structures of *Rps. acidophila* and *Rsp. molischianum* LH2. It was recently calculated that the dipole-dipole coupling between B800 BChls is smaller in *Rsp. molischianum*, and this difference is large enough to account for the observed difference in energy transfer rate (M. Wendling, unpublished). Experiments at room temperature are more demanding because the faster 800-to-850 energy transfer reduces the time during which depolarization may be observed. Although a lifetime as short as 300 fs was reported for *Rps. acidophila* LH2 (Ma et al., 1997), recent 3-pulse photon echo peak shift experiments on LH2 of *Rsp. molischianum* and *Rps. acidophila* yielded for both LH2s a 1 ps decay phase in the peak shift, which was ascribed to B800-to-B800 energy transfer (Joo et al., 1996; Salverda et al., 2000). This result implies a time constant of 2 ps for hopping within the B800 ring. The remarkable temperature dependence (slower at higher temperature) originates from the spectral overlap term in the Förster equation, which decreases at higher temperatures because of band broadening (Hess et al., 1995a; Pullerits et al., 1997). The same broadening increases the rate of B800-to-B850 energy transfer.

From B800, excitation is rapidly transferred to the B850, thus jumping from the outer ring of well separated BChls to the intramembrane ring where neighboring BChls have strong excitonic interactions. This transfer step puts the excitation into a plane that it will not leave afterwards, as both the B875 of the LH1 proteins and the primary electron donor (P) of

the reaction centers are located in this same plane (Hunter, 1995). Energy transfer from B800 to B850 has been studied extensively, probably because its characterization can be performed on isolated LH2 proteins, and also because it involves well-separated electronic transitions. By the late 1980s, it was established that the time constant for this transfer was less than a picosecond (Sundström et al., 1986; Freiberg et al., 1988). Subsequent experiments using femtosecond pulsed lasers demonstrated that the time constant for energy transfer from B800 to B850 is about 700 fs at room temperature (Shreve et al., 1991a) and slows to about 1 ps at 77 K and about 2 ps at 4 K (Monshouwer et al., 1995a; Pullerits et al., 1997).

The availability of site-selected mutants of LH2 complexes with altered absorption properties has made it possible to study the mechanism of 800-to-850 transfer in detail (Hess et al., 1994; Fowler et al., 1997). As discussed above, the B850 transitions in LH2 mutants from *Rb. sphaeroides* bearing a single or double mutation of Tyr $\alpha_{44}$  and  $\alpha_{45}$  are blue-shifted to 839 and 826 nm, respectively (Fowler et al., 1992). Similarly, mutations of Arg  $\beta_{21}$  shift the B800 transition to 780 nm (Gall et al., 1997). This system is thus ideal for studying how the transfer rate evolves with the spectral overlap, and for a quantitative assessment of the physical mechanisms underlying this particular step of excitation transfer.

A proper analysis of the rate of energy transfer from B800 to B850 is more complicated than one might have expected. Evaluating the spectral overlap between the B800 and B850 BChls requires one to take into account, not only the main 800- and 850-nm absorption bands (which overlap only very weakly), but also the large manifold of excitonic and vibrational sublevels of the B850 ring. Although the results obtained at different temperatures with the mutant strains could be accounted for qualitatively in a simple Förster model (Hess et al., 1994; Fowler et al., 1997), quantitative calculations indicated that energy transfer from B800 to B850 would be much slower than observed if it occurred only by the Förster mechanism (Pullerits et al., 1997; Herek et al., 2000). A second channel for energy transfer was suggested to involve higher-energy excitonic transitions of the B850 ring (Wu et al., 1996b; Kuhn and Sundström, 1997). These transitions occur in the region of 780 nm, where they overlap the emission spectrum of B800. Because the rate of energy transfer in the Förster picture is proportional to the dipole



strength of the acceptor, and the higher-energy exciton transitions of B850 have only small dipole strengths, one might expect that energy transfer to these transitions would be very slow. However, the coupling matrix elements for energy transfer cannot be calculated correctly on the basis of the dipole strengths observed in the absorption spectrum. Instead, it is necessary to evaluate the interactions of a B800 BChl with each of the individual B850 BChls, which will be located at various distances and with various orientations (Sumi, 1999). The asymmetric position of the B800 molecule relative to the B850 ring breaks the symmetry of the interactions, with the result that B850 transitions that are 'forbidden' in absorption can be coupled significantly to the B800  $Q_y$  transition. In addition, disorder in the B850 ring must be considered. The spectral overlap must be calculated for each realization of the disorder (i.e. for each individual ring) and then averaged. Such a calculation requires lineshape parameters and electronic couplings that cannot be obtained directly from the ensemble emission and absorption spectra and so must be measured or calculated independently. Scholes and Fleming recently performed calculations in which they took lineshape parameters from photon echo experiments (Joo et al., 1996; Scholes et al., 1999) and electronic couplings from quantum mechanical calculations (Scholes and Fleming, 2000). These calculations led to faster energy transfer kinetics, though still twice slower than those observed experimentally.

CD experiments performed on LH2 mutants from *Rb. sphaeroides* devoid of the 800-nm absorbing BChl have identified a weak transition at about 780 nm, which most likely arises from the B850 exciton manifold (Koolhaas et al., 1998). The position, intensity and shape of this transition could be reproduced well by assuming a dipole-dipole coupling between the BChls of the B850 ring of about 300  $\text{cm}^{-1}$  and a disorder of 400  $\text{cm}^{-1}$  (FWHM) (Koolhaas et al., 1998; Koolhaas et al., 2000). As discussed above, this band provides an additional spectral overlap between the B800 transition and the B850 excitonic manifold at room temperature. The overlap would become significantly smaller at low temperature as the 800-nm transition becomes extremely narrow. It was thus suggested that the slowing of the transfer kinetics between room temperature and 4 K results from the progressive disappearance of this spectral overlap, i.e. from the progressive closure of one of the excitation transfer paths (Sundström et al.,

1999). From the observed temperature dependence of the kinetics, about 50% of the excitation transfer at room temperature was estimated to involve the upper edge of the 850-nm exciton band. However, additional channels for excitation transfer cannot be fully excluded. It was proposed that carotenoid could mediate the 800-to-850 coupling (Pullerits et al., 1997). Studies of LH2 complexes devoid of carotenoids, which recently have been reported to assemble in purple sulfur bacteria such as *Chr. minutissimum* (Krikunova et al., 2002), would help to test this hypothesis.

### C. Excitation and Energy Transfer in the 850 nm Transition

As discussed above, it is clear that the B850 BChls in LH2 are strongly coupled. A value of about 250–400  $\text{cm}^{-1}$  for the BChl-to-BChl coupling in this structure has been reported by many groups (Monshouwer and van Grondelle, 1996; Sauer et al., 1996a; Alden et al., 1997; Pullerits et al., 1997; Koolhaas et al., 1998; Krueger et al., 1998; Novoderezhkin et al., 1999). Nevertheless, the molecular origin of the 850 nm transition is quite complex to determine precisely. However, the time evolution of the excited state in the B850 ring depends on the origin of the absorption band and, as a consequence, the study of the evolution of the excited state after excitation with a short pulse may yield additional information. Over the past few years, a large number of advanced spectroscopic techniques have been applied to address this problem, including time-resolved absorption (Visser et al., 1995; Chachisvilis et al., 1997; Kennis et al., 1997b; Nagarajan et al., 1999), fluorescence upconversion (Jimenez and Fleming, 1996), three-pulse photon echo peak shift (Jimenez et al., 1997), and other non-linear techniques (Leupold et al., 1993). Although general agreement has not yet been reached on every aspect of this problem, this field has progressed tremendously in the past decade.

Excitation of the 850-nm transition results in a bleaching and stimulated emission that shift very rapidly towards the red of the transition. Most groups have reached the same conclusion, though using different techniques, namely that at least two different events occur during this process. There is first a very fast phase (50 fs) that arises from relaxation due to the coupling of the electronic transition to rapid fluctuations in the protein environment following the initial excitation (Monshouwer et al., 1998; Jimenez



and Fleming, 1996) and a slower phase, which is thought to correspond to an excitation redistribution over nonequivalent energetic sites (Visser et al., 1995; Jimenez and Fleming, 1996). This redistribution proceeds by steps as fast as 100 fs, and is complete in less than a picosecond. Different isotropic and anisotropic decay times measured in LH2 suggest that the 100 fs steps occurring during the excitation redistribution do not correspond to hopping of the excitation from monomer to monomer (Pullerits and Sundström, 1996; Chachisvilis et al., 1997). Instead, the excitation probably is distributed over more than one BChl molecule, and the hopping occurs between groups of BChls. Estimates of the precise localization of the excitation is still a matter of controversy, but most studies were found to be consistent with a delocalization length of the exciton varying between two and six BChl molecules at 1 ps after excitation (Pullerits and Sundström, 1996).

It must be pointed out that the picture of excitation redistribution through a series of Förster-type energy-transfer events, where the excitation hops between subsets of BChls in the ring, does not seem able to explain some of the experimental data observed for LH2. Among those, the most striking are the low-frequency oscillatory phenomena, which have been observed after excitation with ultra-short pulses (Chachisvilis et al., 1994; Monshouwer et al., 1998). Such low-frequency oscillations usually are explained by coherent nuclear motions in the ground or excited state. However, they are observable in both LH1 and LH2 for several picoseconds after excitation, i.e. long after the excitation is supposed to have equilibrated through a large number of energy-transfer steps. In a recent simulation of the dynamics the following schematic view emerged. If one assumes that the excitons are coupled only weakly to their environment, coherent nuclear motions induced by the femtosecond excitation and the relaxation in the excitonic manifold occur independently during the first 100 fs. Hopping sets in on a slower time scale, destroying the coherent nuclear motion of the excited state (Novoderezhkin et al., 1999). From the amplitude of the peakshifts observed in three-pulse photon echo peak shift experiments, it may indeed be concluded that the coupling of the electronic transition to the environment in photosynthetic pigment-proteins is relatively weak, for instance when compared to dye molecules in solution (Jimenez et al., 1997; Yu et al., 1997). However, in reality, the

interplay between electronic and nuclear degrees of freedom and their interaction with the environment should be explicitly accounted for.

Energy transfer between 850-nm absorbing rings of different LH2 proteins is particularly difficult to study. First, it requires performing experiments on whole membranes, i.e. facing the yet unsolved problem of heterogeneity of such biological samples. Second, as the different rings are expected to be spectroscopically quite similar, and since the polarization is entirely lost after absorption by the first 850 nm ring, there are currently very few data that can be safely used to characterize this step. At low temperature, the induced bleaching and emission continue to shift to the red with time between 3 and 10 ps after excitation (Chachisvilis et al., 1997; Freiberg et al., 1998). This long-time dynamics was assigned to excitation transfer among LH2 rings (Freiberg et al., 1998), thus suggesting that the inhomogeneity of the electronic properties of individual LH2 rings is large enough to reveal the 850-to-850 excitation transfer between rings. These values are consistent with calculations on systems containing more than a single ring, which predicted a time constant of about 7 ps for LH2-to-LH2 transfer (Hu et al., 1997). These kinetics for the 850-to-850 transfer, assuming that the 3–10 ps process reflects energy transfer, match quite well with the numbers obtained for LH2-to-LH1 transfer (see below). The distances between LH2 rings and between LH2 and LH1 rings could be quite similar. The donor-acceptor spectral overlaps for  $B_{850} \rightarrow B_{850}$  and  $B_{850} \rightarrow LH1$  energy transfer also are similar, at least at room temperature when the spectra are broad. Therefore, studies of LH2-to-LH1 energy transfer should in principle also yield information on the kinetics of LH2-to-LH2 transfers.

#### *D. LH2 to LH1 Transfers*

LH2-to-LH1 ring energy transfer is easily observable because of the differences of the absorption and fluorescence spectra of the two complexes. Energy transfer at both room and low temperatures has been measured in membranes from different purple bacterial strains by a number of groups (Sundström et al., 1986; van Grondelle et al., 1987; Freiberg et al., 1989; Zhang et al., 1992; Mueller et al., 1993; van Grondelle et al., 1994; Hess et al., 1995b; Nagarajan and Parson, 1997). Most of the results

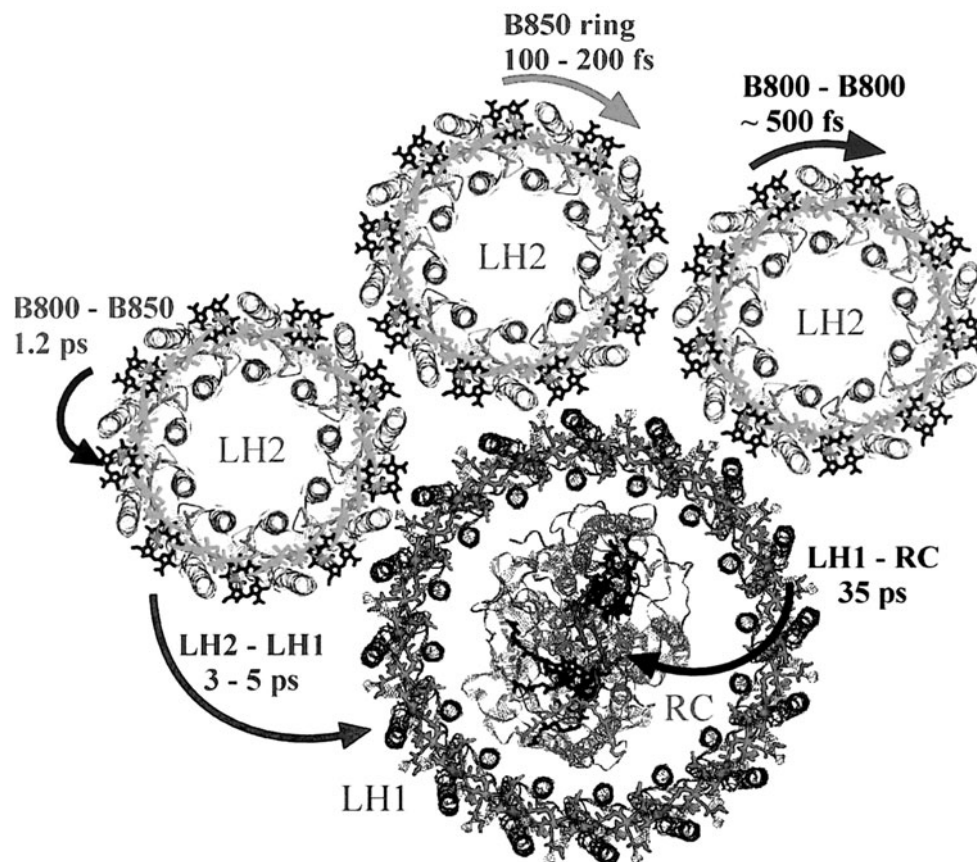


Fig. 6. Overview of the energy-transfer steps in the photosynthetic membrane of purple bacteria at room temperature. See Color Plate 3.

obtained are in fair agreement, and it may be safely concluded that a large part of LH2-to-LH1 energy transfer occurs with a time constant of 3 to 5 picoseconds (Hess et al., 1995b). Part of the LH2-to-LH1 energy transfer occurs on a time scale of several tens of picoseconds, and this may be assigned to LH2-to-LH2 transfer before one of the LH2 delivers the excitation to an LH1 (Nagarajan and Parson, 1997). As neither the number of LH2 per LH1, nor the organization of LH2 around (or, at least in the vicinity of) LH1 is very well defined, it is difficult to evaluate how long excitations should hop between different LH2 rings before being transferred to LH1. Calculations based on a photosynthetic unit modeled on the *Rsp. molischianum* LH2 structure, in which LH2 directly surrounds LH1, have predicted that LH2-to-LH1 transfers should occur with 3–5 picosecond kinetics (Hu et al., 1997) (Fig. 6).

#### E. Excitation in LH1 Rings: Equilibration and Transfer to Reaction Centers

The ultimate goal of the photosynthetic light-harvesting process is the transfer of excitation energy to reaction centers, which is achieved by LH1 antennas (Fig. 6). Fully understanding this process would ideally require the determination of two parameters. First, what is the organization of LH1 around the reaction centers, and in particular, how many  $\alpha\beta$  subunits surround how many reaction centers (see above)? And second, what precisely is the nature of the excitation in LH1?

The first events following energy absorption in LH1 have been reported to be quite similar to those occurring in LH2, consisting of a very fast energy redistribution that is completed within *ca.* half a picosecond (Bradforth et al., 1995; Visser et al., 1995; Kumble et al., 1996; Chachisvilis et al., 1997; Monshouwer et al., 1998). If exciton hopping lies at

the basis of the spectral dynamics, each hop occurs in about 100 femtoseconds. Due to the inhomogeneous broadening of LH1, this hopping results in ultra-fast downhill energy transfer, and thus in an apparent shift of the observed bleaching and emission when excitation occurs on the blue wing of the LH1 absorption. Comparison of isotropic and anisotropic decays in LH1 from *Rb. sphaeroides* (Chachisvilis et al., 1997) and *Rps. viridis* (Monshouwer et al., 1998) led to the conclusion that, as in LH2, the excitation in LH1 cannot be localized on a single BChl molecule (Chachisvilis et al., 1997). However, the precise degree of localization of excitation in LH1 is still unknown. Comparing the initial peak-shift value measured by three-pulse photon echo peak shift spectroscopy for LH1 in its native and dissociated forms suggests that dissociation of LH1 does not affect the excitation delocalization (Yu et al., 1997). As dissociated forms of LH1 exhibit the spectral properties of a BChl dimer, it was concluded that the excitation is localized on a very small number of BChl molecules, probably a dimer. Simulations aimed at reproducing the experimental pump-probe spectrum measured after excitation by an ultra-short pulse suggested that the excitation is shared by about four BChl molecules (Pullerits and Sundström, 1996). Though there are still some uncertainties on the precise number of BChls that share the excitation, it is worth noting that most results converge towards small numbers as compared to 32, the total number of BChls in the LH1 ring. As in LH2, low-frequency oscillatory phenomena have been observed in LH1, and these survive for quite a long time compared to the hopping time in the ring (Chachisvilis et al., 1994, 1995; Bradforth et al., 1995; Jimenez et al., 1997; Monshouwer et al., 1998).

The last step of the energy-transfer process takes the excitation from the LH1 to the reaction center. The rate of this reaction has been measured by a number of groups (for a review see Freiberg, 1995), as it contains an important piece of information on the overall excitation trapping process. This overall trapping process may be trap-limited (i.e. limited by the charge-separation rate in the reaction centers), diffusion-limited (i.e. limited by the migration of the excitation in the antenna proteins), or transfer-to-the-trap limited (i.e. limited by the rate of excitation transfer from LH1 to the RC). When reaction centers are fully able to perform charge separation, trapping kinetics ranging from about 35 to about 80 picoseconds have been measured by time-resolved

absorption and fluorescence techniques (Sundström et al., 1986; van Grondelle et al., 1987; Visscher et al., 1989; Beekman et al., 1994; Freiberg et al., 1996). It is not yet completely clear why there are such discrepancies between measurements, but their origin probably lies in the poor characterization of whole membranes of a given organism. For instance, an increasing ratio of LH2 to LH1 will decrease the probability of finding the excitation on LH1, thereby slowing the trapping kinetics. Secondly, the oxidation state of the special pair is known to affect the excited-state lifetime, with the excitation living three to four times longer in oxidized reaction centers ( $P^+$ ) than in reduced ( $P$ ). Finally, the way the membranes have been prepared and stored, and the age and growth conditions of the bacterial culture are likely to play a role in determining the overall architecture of the samples. It seems possible that these parameters could account for the factor of almost three between the various reported measurements. However, all the values appear to be extremely slow compared to the kinetics of both the primary charge separation and the ring-to-ring transfer in the photosynthetic membrane. This implies that energy transfer from the LH1 to the special pair is the rate-limiting step of the overall energy-trapping process, which means that the latter is transfer-to-trap-limited (Beekman et al., 1994; Somsen et al., 1994; Timpmann et al., 1995; Somsen et al., 1996a). On the other hand, it was reported that the trapping time depends on the redox state of reaction center components other than  $P$ , because significantly slower kinetics were found for 'closed' reaction centers, i.e. proteins in which the first quinone had been reduced (Timpmann et al., 1993). This conclusion, which suggests a trap-limited excitation process was recently re-addressed (Trissl et al., 1999). It appears that the dependence of the observed kinetics upon the redox state of this quinone is only 7% in *Rsp. rubrum*, in good agreement with the transfer-to-trap-limited model. A slightly stronger dependence was found for *Rps. viridis*, but the transfer-to-trap limitation seems to reflect quite well the situation in most bacteria that contain only LH1.

Considering the organization of LH1 around the reaction centers as observed by electronic microscopy and the models that were derived from these experiments, it appears that the distance between the LH1 BChl and  $P$  in reaction centers is always very large. Though this might just be due to the size of reaction centers, it was speculated that the large distance could play a role in avoiding oxidation of

the BChl from LH1 by the oxidized primary donor (P) (Sundström et al., 1999). Indeed, it is possible to oxidize these BChls chemically by ferricyanide, which suggests that their redox potential is close to, or even lower than that of P (Picorel et al., 1984). Oxidation of even one molecule of BChl per LH1 ring is sufficient to quench its singlet excited state dramatically and render it useless as an antenna complex (Law and Cogdell, 1997). It was noted that if the LH1-to-P distance must be kept large, then a circular organization of LH1 around the reaction centers is the only way to keep the trapping efficiency high (Fleming and van Grondelle, 1997). The fact that only a small number of LH1 excited states are degenerate with P also contributes to an increased localization of the excitation on P, and therefore a higher trapping rate. We speculate that both these contributions are essential for the proper functioning of the whole excitation-transfer process. Formation of rings, or of portions of rings around the reaction centers would thus be a very important feature of the ultimate photosynthetic efficiency in purple photosynthetic bacteria.

## V. Conclusion

The study of light-harvesting proteins of purple photosynthetic bacteria has led to the description of a quite complex biological system and of its different components at an unprecedented level of both physics and biology. Not only has this achievement involved a tremendous number of experimental techniques that previously had been applied in biology only sparingly (if at all), but also it has reached a point where one can reasonably hope to understand, from a physical point of view, the details of a process involving multiple components of a biological membrane. Although in the last decade most of the points of controversy concerning the kinetics and the mechanisms of excitation transfer in the intracytoplasmic membrane of photosynthetic purple bacteria have been resolved, it is likely that this particular field of photosynthesis will continue to grow in the future. Indeed it offers exciting opportunities to develop in new directions, including the mechanism of insertion and supramolecular organization of membrane proteins *in vivo* and the most advanced aspects of theory for energy transfer in well-defined molecular assemblies.

## Acknowledgments

RJC thanks the BBSRC for financial support and his numerous coworkers and colleagues who have contributed to many of the studies referred to here.

## References

- Alden RG, Johnson E, Nagarajan V, Parson WW, Law CJ and Cogdell RJC (1997) Calculations of spectroscopic properties of the LH2 bacteriochlorophyll-protein antenna complex from *Rhodospseudomonas acidophila*. *J Phys Chem B* 101: 4667–4680
- Andersson PO, Cogdell RJ and Gillbro T (1996) Femtosecond dynamics of carotenoid-to-bacteriochlorophyll a energy transfer in the light-harvesting antenna complexes from the purple bacterium *Chromatium purpuratum*. *Chem Phys* 210: 195–217
- Angerhofer A, Cogdell RJ and Hipkins MF (1986) A spectral characterization of the light-harvesting pigment-protein complexes from *Rhodospseudomonas acidophila*. *Biochim Biophys Acta* 848: 333–341
- Arellano JB, Raju BB, Naqvi KR and Gillbro T (1998) Estimation of pigment stoichiometries in photosynthetic systems of purple bacteria: Special reference to the (absence of) second carotenoid in LH2. *Photochem Photobiol* 68: 84–87
- Barz WP and Oesterhelt D (1994) Photosynthetic deficiency of a *pufX* deletion mutant of *Rhodobacter sphaeroides* is suppressed by point mutations in the light-harvesting complex genes *pufB* or *pufA*. *Biochemistry* 33: 9741–9752
- Barz WP, Venturoli G, Francia F, Melandri BA, Vermeglio A and Oesterhelt D (1995) The PufX protein of *Rhodobacter sphaeroides* is required for efficient ubiquinone ubiquinol exchange between the reaction center and the cytochrome *bc<sub>1</sub>* complex. In: Mathis P (ed) *Photosynthesis: From Light to Biosphere*, pp 427–432. Kluwer Academic Publishers, Dordrecht
- Beekman LMP, van Mourik F, Jones MR, Visser HM, Hunter CN and van Grondelle R (1994) Trapping kinetics in mutants of the photosynthetic purple bacterium *Rhodobacter sphaeroides*: Influence of the charge separation rate and consequences for the rate-limiting step in the light-harvesting process. *Biochemistry* 33: 3143–3147
- Beekman LMP, Frese RN, Fowler GJS, Ortiz de Zarate I, Cogdell RJ, van Stokkum I, Hunter CN and van Grondelle R (1997a) Characterization of the light-harvesting antennas of photosynthetic purple bacteria by Stark spectroscopy. 2. LH2 complexes: Influence of the protein environment. *J Phys Chem B* 101: 7293–7301
- Beekman LMP, Steffen M, van Stokkum I, Olsen JD, Hunter CN, Boxer SG and van Grondelle R (1997b) Characterization of the light-harvesting antennas of photosynthetic purple bacteria by Stark spectroscopy. 1. LH1 antenna complex and the B820 subunit from *Rhodospirillum rubrum*. *J Phys Chem B* 101: 7284–7292
- Bissig I, Wagner-Huber V, Brunisholz RA and Zuber H (1990) Multiple antenna complexes in various purple photosynthetic bacteria. *FEMS Symp* 53: 199–210

- Bradforth SE, Jimenez R, Dikshit SN and Fleming GR (1995) Electronic excitation transfer in bacterial light harvesting complexes. In: Mathis P (ed) *Photosynthesis: From Light to Biosphere*, pp 23–28. Kluwer Academic Publishers, Dordrecht
- Brunisholz RA, Cuendet PA, Theiler R and Zuber H (1981) The complete amino acid sequence of the single light harvesting protein from chromatophores of *Rhodospirillum rubrum* G-9<sup>+</sup>. *FEBS Lett* 129: 150–154
- Brunisholz RA, Jay F, Suter F and Zuber H (1985) The light-harvesting polypeptides of *Rhodopseudomonas viridis*. The complete amino-acid sequences of B1015- $\alpha$ , B1015- $\beta$  and B1015- $\gamma$ . *Biol Chem Hoppe-Seyler* 366: 87–98
- Brunisholz RA, Bissig I, Niederer E, Suter F and Zuber H (1987) Structural studies on the light-harvesting polypeptides of *Rp. acidophila*. In: Biggins J (ed) *Progress in Photosynthesis Research*, Vol 1, pp 13–16. Nijhoff, Dordrecht
- Chachisvilis M, Pullerits T, Jones MR, Hunter CN and Sundström V (1994) Vibrational dynamics in the light-harvesting complexes of the photosynthetic bacterium *Rhodobacter sphaeroides*. *Chem Phys Lett* 224: 345–354
- Chachisvilis M, Fidler H, Pullerits T and Sundström V (1995) Coherent nuclear motions in light-harvesting pigments and dye molecules, probed by ultrafast spectroscopy. *J Raman Spectrosc* 26: 513–522
- Chachisvilis M, Kuehn O, Pullerits T and Sundström V (1997) Excitons in photosynthetic purple bacteria: Wavelike motion or incoherent hopping? *J Phys Chem B* 101: 7275–7283
- Chadwick BW, Zhang C, Cogdell RJ and Frank HA (1987) The effects of lithium dodecyl sulfate and sodium borohydride on the absorption spectrum of the B800-850 light-harvesting complex from *Rhodopseudomonas acidophila* 7750. *Biochim Biophys Acta* 893: 444–451
- Clayton RK and Clayton BJ (1972) Relations between pigments and proteins in the photosynthetic membranes of *Rhodopseudomonas spheroides*. *Biochim Biophys Acta* 283: 492–504
- Cogdell RJ and Scheer H (1985) Circular dichroism of light-harvesting complexes from purple photosynthetic bacteria. *Photochem Photobiol* 42: 669–678
- Cogdell RJ, Hipkins MF, MacDonald W and Truscott TG (1981) Energy transfer between the carotenoid and the bacteriochlorophyll within the B-800-850 light harvesting pigment-protein complex of *Rhodopseudomonas sphaeroides*. *Biochim Biophys Acta* 634: 191–202
- Cogdell RJ, Lindsay JG, Valentine J and Durant I (1982) A further characterization of the B890 light-harvesting pigment-protein complex from *Rhodospirillum rubrum* strain S1. *FEBS Lett* 150: 151–154
- Cogdell RJ, Hawthornthwaite AM, Evans MB, Ferguson LA, Kerfeld C, Thornber JP, Van Mourik F and Van Grondelle R (1990) Isolation and characterization of an unusual antenna complex from the marine purple sulfur photosynthetic bacterium *Chromatium purpuratum* BN5500. *Biochim Biophys Acta* 1019: 239–244
- Cogdell RJ, Andersson PO and Gillbro T (1992) Carotenoid singlet states and their involvement in photosynthetic light-harvesting pigments. *J Photochem Photobiol B* 15: 105–112
- Cogdell RJ, Fyfe PK, Barrett SJ, Prince SM, Freer AA, Isaacs NW, McGlynn P and Hunter CN (1996) The purple bacterial photosynthetic unit. *Photosynth Res* 48: 55–63
- Cogdell RJ, Fyfe PK, Howard TD, Fraser N, Isaacs NW, Freer AA, McKluskey K and Prince SM (1999) The structure and function of the LH2 complex from *Rhodopseudomonas acidophila* strain 10050, with special reference to the bound carotenoid. In: Frank HA, Young AJ, Britton G and Cogdell RJ (eds) *The Photochemistry of Carotenoids*, pp 71–80. Kluwer Academic Publishers, Dordrecht
- Deisenhofer J, Epp O, Miki K, Huber R and Michel H (1984) X-ray structure analysis of a membrane protein complex. Electron density map at 3 Å resolution and a model of the chromophores of the photosynthetic reaction center from *Rhodopseudomonas viridis*. *J Mol Biol* 180: 385–398
- Delagrave S, Goldman ER and Youvan DC (1995) Context dependence of phenotype prediction and diversity in combinatorial mutagenesis. *Protein Eng* 8: 237–242
- Duysens LNM (1952) Transfer of Excitation Energy in Photosynthesis. Ph.D. Thesis, University of Utrecht, Utrecht
- Fathir I, Ashikaga M, Tanaka K, Katano T, Nirasawa T, Kobayashi M, Wang Z-Y and Nozawa T (1998) Biochemical and spectral characterization of the core light harvesting complex 1 (LH1) from the thermophilic purple sulfur bacterium *Chromatium tepidum*. *Photosynth Res* 58: 193–202
- Fleming GR and van Grondelle R (1997) Femtosecond spectroscopy of photosynthetic light-harvesting systems. *Curr Opin Struct Biol* 7: 738–748
- Fowler GJS, Visschers RW, Grief GG, Van Grondelle R and Hunter CN (1992) Genetically modified photosynthetic antenna complexes with blueshifted absorbance bands. *Nature* 355: 848–850
- Fowler GJS, Sockalingum GD, Robert B and Hunter CN (1994) Blue shifts in bacteriochlorophyll absorbance correlate with changed hydrogen bonding patterns in light-harvesting 2 mutants of *Rhodobacter sphaeroides* with alterations at  $\alpha$ -Tyr-44 and  $\alpha$ -Tyr-45. *Biochem J* 299: 695–700
- Fowler GJS, Hess S, Pullerits T, Sundström V and Hunter CN (1997) Role of  $\beta$  Arg-10 in the B800 bacteriochlorophyll and carotenoid pigment environment within the light-harvesting LH2 complex of *Rhodobacter sphaeroides*. *Biochemistry* 36: 11282–11291
- Francia F, Wang J, Venturoli G, Melandri BA, Barz WP and Oesterhelt D (1999) The Reaction center-LH1 antenna complex of *Rhodobacter sphaeroides* contains one pufX molecule which is involved in dimerization of this complex. *Biochemistry* 38: 6834–6845
- Frank HA and Cogdell, RJ (1995) Carotenoids in photosynthesis. *Photochem Photobiol* 63: 257–264
- Frank HA, Farhoosh R, Gebhard R, Lugtenburg J, Gosztola D and Wasielewski MR (1993) The dynamics of the S1 excited states of carotenoids. *Chem Phys Lett* 207: 88–92
- Freer A, Prince S, Sauer K, Papiz M, Hawthornthwaite-Lawless A, McDermott G, Cogdell R and Isaacs NW (1996) Pigment-pigment interactions and energy transfer in the antenna complex of the photosynthetic bacterium *Rhodopseudomonas acidophila*. *Structure (London)* 4: 449–462
- Freiberg A (1995) Coupling of antennas to reaction centers. In: Blankenship RE, Madigan MT and Bauer CE (eds) *Anoxygenic Photosynthetic Bacteria*, pp 385–398. Kluwer Academic Publishers, Dordrecht
- Freiberg A, Godik VI, Pullerits T and Timpmann KE (1988) Directed picosecond excitation transport in purple photosynthetic bacteria. *Chem Phys* 128: 227–235
- Freiberg A, Allen JP, Williams J and Woodbury NW (1996)

- Energy trapping and detrapping by wild type and mutant reaction centers of purple non-sulfur bacteria. *Photosynth Res* 48: 309–319
- Freiberg A, Jackson JA, Lin S and Woodbury NW (1998) Subpicosecond Pump-Supercontinuum Probe Spectroscopy of LH2 Photosynthetic Antenna Proteins at Low Temperature. *J Phys Chem A* 102: 4372–4380
- Frese RN, Olsen JD, Branvall R, Westerhuis WHJ, Hunter CN and Van Grondelle R (2000) The long-range supraorganization of the bacterial photosynthetic unit: A key role for PufX. *Proc Natl Acad Sci USA* 97: 5197–5202
- Gall A and Robert B (1999) Characterization of the different peripheral light-harvesting complexes from high- and low-light grown cells from *Rhodospseudomonas palustris*. *Biochemistry* 38: 5185–5190
- Gall A, Fowler GJS, Hunter CN and Robert B (1997) Influence of the protein binding site on the absorption properties of the monomeric bacteriochlorophyll in *Rhodobacter sphaeroides* LH2 complex. *Biochemistry* 36: 16282–16287
- Gall A, Yurkov V, Vermeglio A and Robert B (1999) Certain species of the Proteobacteria possess unusual bacteriochlorophyll *a* environments in their light-harvesting proteins. *Biospectroscopy* 5: 338–345
- Garcia D, Parot P, Vermeglio A and Madigan MT (1986) The light-harvesting complexes of a thermophilic purple sulfur photosynthetic bacterium *Chromatium tepidum*. *Biochim Biophys Acta* 850: 390–5
- Gardiner AT, MacKenzie RC, Barrett SJ, Kaiser K and Cogdell RJ (1992) The genes for the peripheral antenna complex apoproteins from *Rhodospseudomonas acidophila* 7050 form a multigene family. In: Murata N, (ed) *Research in Photosynthesis*, Vol 1, pp 77–80. Kluwer Academic Publishers, Dordrecht
- Germeroth L, Lottspeich F, Robert B and Michel H (1993) Unexpected similarities of the B800-850 light-harvesting complex from *Rhodospirillum rubrum* to the B870 light-harvesting complexes from other purple photosynthetic bacteria. *Biochemistry* 32: 5615–21
- Germeroth L, Reilaender H and Michel H (1996) Molecular cloning, DNA sequence and transcriptional analysis of the *Rhodospirillum rubrum* B800/850 light-harvesting genes. *Biochim Biophys Acta* 1275: 145–150
- Gottfried DS, Stocker JW and Boxer SG (1991) Stark effect spectroscopy of bacteriochlorophyll in light-harvesting complexes from photosynthetic bacteria. *Biochim Biophys Acta* 1059: 63–75
- Gradinaru CC, Kennis JTM, Papagiannakis E, van Stokkum IHM, Cogdell RJ, Fleming GR, Niederman RA and van Grondelle R (2001) An unusual pathway of excitation energy deactivation in carotenoids: Singlet-to-triplet conversion on an ultrafast timescale in a photosynthetic antenna. *Proc Nat Acad Sci USA* 98: 2364–2369
- Gudowska-Nowak E, Newton MD and Fajer J (1990) Conformation and environmental effects on bacteriochlorophyll optical spectra: Correlations of calculated spectra with structural studies. *J Phys Chem* 94: 5795–5801
- Herek JL, Polivka T, Pullerits T, Fowler GJS, Hunter CN and Sundström V (1998) Ultrafast carotenoid band shifts probe structure and dynamics in photosynthetic antenna complexes. *Biochemistry* 37: 7057–7061
- Herek JL, Fraser NJ, Pullerits T, Martinsson P, Polivka T, Scheer H, Cogdell RJ and Sundström V (2000) B800 forward B850 energy transfer mechanism in bacterial LH2 complexes investigated by B800 pigment exchange. *Biophys J* 78: 2590–2596
- Hess S, Feldchtein F, Babin A, Nurgaleev I, Pullerits T, Sergeev A and Sundström V (1993) Femtosecond energy transfer within the LH2 peripheral antenna of the photosynthetic purple bacteria *Rhodobacter sphaeroides* and *Rhodospseudomonas palustris* LL. *Chem Phys Lett* 216: 247–257
- Hess S, Visscher KJ, Pullerits T, Sundström V, Fowler GJS and Hunter CN (1994) Enhanced rates of subpicosecond energy transfer in blue-shifted light-harvesting LH2 mutants of *Rhodobacter sphaeroides*. *Biochemistry* 33: 8300–8305
- Hess S, Aakesson E, Cogdell RJ, Pullerits T and Sundström V (1995a) Energy transfer in spectrally inhomogeneous light-harvesting pigment-protein complexes of purple bacteria. *Biophys J* 69: 2211–2225
- Hess S, Chachisvilis M, Timpmann K, Jones MR, Fowler GJS, Hunter CN and Sundström V (1995b) Temporally and spectrally resolved subpicosecond energy transfer within the peripheral antenna complex (LH2) and from LH2 to the core antenna complex in photosynthetic purple bacteria. *Proc Natl Acad Sci USA* 92: 12333–12337
- Hu Q, Sturgis JN, Robert B, Delagrave S, Youvan DC and Niederman RA (1998) Hydrogen bonding and circular dichroism of bacteriochlorophylls in the *Rhodobacter capsulatus* light harvesting 2 complex altered by combinatorial mutagenesis. *Biochemistry* 37: 10006–10015
- Hu X and Schulten K (1998) Model for the light-harvesting complex I (B875) of *Rhodobacter sphaeroides*. *Biophys J* 75: 683–694
- Hu X, Ritz T, Damjanovic A and Schulten K (1997) Pigment organization and transfer of electronic excitation in the photosynthetic unit of purple bacteria. *J Phys Chem B* 101: 3854–3871
- Hunter CN (1995) Rings of light. *Curr Biol* 5: 826–828
- Isaacs NW, Cogdell RJ, Freer AA and Prince SM (1995) Light-harvesting mechanisms in purple photosynthetic bacteria. *Curr Opin Struct Biol* 5: 794–797
- Jimenez R and Fleming GR (1996) Ultrafast spectroscopy of photosynthetic systems. In: Ames J and Hoff AJ (eds) *Biophysical Techniques in Photosynthesis*, pp 63–73. Kluwer Academic Publishers, Dordrecht
- Jimenez R, van Mourik F, Yu JY and Fleming GR (1997) Three-pulse photon echo measurements on LH1 and LH2 complexes of *Rhodobacter sphaeroides*: A nonlinear spectroscopic probe of energy transfer. *J Phys Chem B* 101: 7350–7359
- Jirsakova V and Reiss-Husson F (1993) Isolation and characterization of the core light-harvesting complex B875 and its subunit form, B820, from *Rhodocyclus gelatinosus*. *Biochim Biophys Acta* 1183: 301–308
- Jirsakova V and Reiss-Husson F (1994) A specific carotenoid is required for reconstitution of the *Rubrivivax gelatinosus* B875 light harvesting complex from its subunit form B820. *FEBS Lett* 353: 151–154
- Joo T, Jia Y, Yu J-Y, Jonas DM and Fleming GR (1996) Dynamics in isolated bacterial light harvesting antenna (LH2) of *Rhodobacter sphaeroides* at room temperature. *J Phys Chem* 100: 2399–2409
- Jungas C, Ranck J-L, Rigaud J-L, Joliet P and Vermeglio A (1999) Supramolecular organization of the photosynthetic



- apparatus of *Rhodobacter sphaeroides*. EMBO J 18: 534–542
- Karrasch S, Bullough PA and Ghosh R (1995) The 8.5 Å projection map of the light-harvesting complex I from *Rhodospirillum rubrum* reveals a ring composed of 16 subunits. EMBO J 14: 631–668
- Kennis JTM, Streltsov AM, Permentier H, Aartsma TJ and Ames J (1997a) Exciton coherence and energy transfer in the LH2 antenna complex of *Rhodospseudomonas acidophila* at low temperature. J Phys Chem B 101: 8369–8374
- Kennis JTM, Streltsov AM, Vulto SIE, Aartsma TJ, Nozawa T and Ames J (1997b) Femtosecond dynamics in isolated LH2 complexes of various species of purple bacteria. J Phys Chem B 101: 7827–7834
- Kingma H, van Grondelle R and Duysens LNM (1985a) Magnetic field effects in photosynthetic bacteria. I. Magnetic field-induced bacteriochlorophyll emission changes in the reaction center and the antenna of *Rhodospirillum rubrum*, *Rhodospseudomonas sphaeroides* and *Prosthecochloris aestuarii*. Biochim Biophys Acta 808: 363–382
- Kingma H, van Grondelle R and Duysens LNM (1985b) Magnetic field effects in photosynthetic bacteria. II. Formation of triplet states in the reaction center and the antenna of *Rhodospirillum rubrum* and *Rhodospseudomonas sphaeroides*. Magnetic field effects. Biochim Biophys Acta 808: 383–399
- Koepeke J, Hu X, Muenke C, Schulten K and Michel H (1996) The crystal structure of the light-harvesting complex II (B800-850) from *Rhodospirillum rubrum*. Structure (London) 4: 581–597
- Koolhaas MHC, van der Zwan G, Frese RN and van Grondelle R (1997) Red shift of the zero crossing in the CD spectra of the LH2 antenna complex of *Rhodospseudomonas acidophila*: A structure-based study. J Phys Chem B 101: 7262–7270
- Koolhaas MHC, Frese RN, Fowler GJS, Bibby TA, Georgakopoulou S, van der Zwan G, Hunter CN and van Grondelle R (1998) Identification of the upper exciton component of the B850 bacteriochlorophylls of the LH2 antenna complex, using a B800-free mutant of *Rhodobacter sphaeroides*. Biochemistry 37: 4693–4698
- Koolhaas MHC, van der Zwan G and van Grondelle R (2000) Local and nonlocal contributions to the linear spectroscopy of light-harvesting antenna systems. J Phys Chem B 104: 4489–4502
- Kramer HJM, van Grondelle R, Hunter CN, Westerhuis WHJ and Ames J (1984) Pigment organization of the B800-850 antenna complex of *Rhodospseudomonas sphaeroides*. Biochim Biophys Acta 765: 156–165
- Krikunova M, Kummrow A, Voight B, Rini M, Lokstein H, Moskalenko A, Scheer H, Razjivin A and Leupold D (2002) Fluorescence of native and carotenoid-depleted LH2 from *Chromatium minutissimum*, originating from simultaneous two-photon absorption in the spectral range of the presumed (optically 'dark') S-1 state of carotenoids. FEBS Lett 528: 227–229
- Krueger BP, Scholes GD and Fleming GR (1998) Calculation of couplings and energy-transfer pathways between the pigments of LH2 by the ab initio transition density cube method. J Phys Chem B 102: 5378–5386
- Kuhn O and Sundström V (1997) Pump-probe spectroscopy of dissipative energy transfer dynamics in photosynthetic antenna complexes: A density matrix approach. J Chem Phys 107: 4154–4164
- Kumble R, Palese S, Visschers RW, Dutton PL and Hochstrasser RM (1996) Ultrafast dynamics within the B820 subunit from the core (LH-1) antenna complex of *Rs. rubrum*. Chem Phys Lett 261: 396–404
- Lang HP and Hunter CN (1994) The relationship between carotenoid biosynthesis and the assembly of the light-harvesting LH2 complex in *Rhodobacter sphaeroides*. Biochem J 298: 197–205
- Lapouge K, Nèveke A, Gall A, Seguin J, Scheer H, Sturgis J and Robert B (1999) Conformation of bacteriochlorophyll molecules in photosynthetic proteins from purple bacteria. Biochemistry 38: 11115–11121
- Lapouge K, Nèveke A, Robert B, Scheer H and Sturgis JN (2000) Exchanging cofactors in the core antennas from purple bacteria: Structure and properties of Zn-bacteriopheophytin-containing LH1. Biochemistry 39: 1091–1099
- Law CJ and Cogdell RJ (1997) The effect of chemical oxidation on the fluorescence of the LH1 complex from the purple bacterium *Rhodobium rubrum*. FEBS Lett 432: 27–30
- Leupold D, Voigt B, Pfeiffer M, Bandilla M and Scheer H (1993) Nonlinear polarization spectroscopy (frequency domain) studies of excited state processes: The B800-850 antenna of *Rhodobacter sphaeroides*. Photochem Photobiol 57: 24–28
- Lilburn TG, Haith CE, Prince RC and Beatty JT (1992) Pleiotropic effects of pufX gene deletion on the structure and function of the photosynthetic apparatus of *Rhodobacter capsulatus*. Biochim Biophys Acta 1100: 160–170
- Loach PA and Parkes-Loach PS (1995) Structure-function relationships in core light-harvesting complexes (LH1) as determined by characterization of the structural subunit and by reconstitution experiments. Blankenship RE, Madigan MT and Bauer CE (eds) Anoxygenic Photosynthetic Bacteria, pp 437–471. Kluwer Academic Publishers, Dordrecht
- Ma Y-Z, Cogdell RJ and Gillbro T (1997) Energy transfer and exciton annihilation in the B800-850 antenna complex of the photosynthetic purple bacterium *Rhodospseudomonas acidophila* (Strain 10050). A femtosecond transient absorption study. J Phys Chem B 101: 1087–1095
- Ma Y-Z, Cogdell RJ and Gillbro T (1998) Femtosecond energy-transfer dynamics between bacteriochlorophylls in the B800-820 antenna complex of the photosynthetic purple bacterium *Rhodospseudomonas acidophila* (Strain 7750). J Phys Chem B 102: 881–887
- McDermott G, Prince SM, Freer AA, Hawthornthwaite-Lawless AM, Papiz MZ, Cogdell RJ and Isaacs NW (1995) Crystal structure of an integral membrane light-harvesting complex from photosynthetic bacteria. Nature 374: 517–521
- McGlynn P, Hunter CN and Jones MR (1994) The *Rhodobacter sphaeroides* PufX protein is not required for photosynthetic competence in the absence of a light harvesting system. FEBS Lett 349: 349–353
- McLuskey K, Prince SM, Cogdell RJ and Isaacs NW (1999) Crystallization and preliminary X-ray crystallographic analysis of the B800-820 light-harvesting complex from *Rhodospseudomonas acidophila* strain 7050. Acta Crystallogr, Sect D: Biol Crystallogr D55: 885–887
- McLuskey K., Prince SM, Cogdell RJ, Isaacs NX (2001) The crystallographic structure of the B800-820 LH3 light-harvesting complex from the purple bacterium *Rhodospseudomonas acidophila* strain 7050. Biochemistry 40: 8783–8789
- Meckenstock RU, Brunisholz RA and Zuber H (1992a) The



- light-harvesting core-complex and the B820-subunit from *Rhodopseudomonas marina*. Part I. Purification and characterization. FEBS Lett 311: 128–134
- Meckenstock RU, Krusche K, Brunisholz RA and Zuber H (1992b) The light-harvesting core-complex and the B820-subunit from *Rhodopseudomonas marina*. Part II. Electron microscopic characterization. FEBS Lett 311: 135–138
- Monshouwer R and van Grondelle R (1996) Excitations and excitons in bacterial light-harvesting complexes. Biochim Biophys Acta 1275: 70–75
- Monshouwer R, De Zarate IO, van Mourik F, Picorel R, Cogdell RJ and van Grondelle R (1995a) Energy transfer in the LH 2 complex of *Rb. sphaeroides* and *Rps. acidophila* studied by sub picosecond absorption spectroscopy. In: Mathis P (ed) Photosynthesis: From Light to Biosphere, pp 91–94. Kluwer Academic Publishers, Dordrecht
- Monshouwer R, Ortiz de Zarate I, van Mourik F and van Grondelle R (1995b) Low-intensity pump-probe spectroscopy on the B800 to B850 transfer in the light harvesting complex II of *Rhodobacter sphaeroides*. Chem Phys Lett 246: 341–6
- Monshouwer R, Abrahamsson M, van Mourik F and van Grondelle R (1997) Superradiance and exciton delocalization in bacterial photosynthetic light-harvesting systems. J Phys Chem B 101: 7241–7248
- Monshouwer R, Baltuska A, van Mourik F and van Grondelle R (1998) Time-resolved absorption difference spectroscopy of the LH-1 antenna of *Rhodopseudomonas viridis*. J Phys Chem A 102: 4360–4371
- Nagarajan V and Parson WW (1997) Excitation energy transfer between the B850 and B875 antenna complexes of *Rhodobacter sphaeroides*. Biochemistry 36: 2300–2306
- Nagarajan V, Johnson ET, Williams JC and Parson WW (1999) Femtosecond pump-probe spectroscopy of the B850 antenna complex of *Rhodobacter sphaeroides* at room temperature. J Phys Chem B 103: 2297–2309
- Naylor GW, Addlesee HA, Gibson LCD and Hunter CN (1999) The photosynthetic gene cluster of *Rhodobacter sphaeroides*. Photosynth Res 62: 121–139
- Noguchi T, Hayashi H and Tasumi M (1990) Factors controlling the efficiency of energy transfer from carotenoids to bacteriochlorophyll in purple photosynthetic bacteria. Biochim Biophys Acta 1017: 280–290
- Novoderezhkin V, Monshouwer R and van Grondelle R (1999) Exciton (de)localization in the LH2 antenna of *Rhodobacter sphaeroides* as revealed by relative difference absorption measurements of the LH2 antenna and the B820 subunit. J Phys Chem B 103: 10540–10548
- Olsen JD, Sockalingum GD, Robert B and Hunter CN (1994) Modification of a hydrogen bond to a bacteriochlorophyll *a* molecule in the light-harvesting 1 antenna of *Rhodobacter sphaeroides*. Proc Natl Acad Sci USA 91: 7124–7128
- Olsen JD, Sturgis JN, Westerhuis WHJ, Fowler GJS, Hunter CN and Robert B (1997) Site-directed modification of the ligands to the bacteriochlorophylls of the light-harvesting LH1 and LH2 complexes of *Rhodobacter sphaeroides*. Biochemistry 36: 12625–12632
- Papiz MZ, Prince SM, Hawthornthwaite-Lawless AM, McDermott G, Freer AA, Isaacs NW and Cogdell RJ (1996) A model for the photosynthetic apparatus of purple bacteria. Trends Plant Sci 1: 198–206
- Parkes-Loach PS, Sprinkle JR and Loach PA (1988) Reconstitution of the B873 light-harvesting complex of *Rhodospirillum rubrum* from the separately isolated  $\alpha$ - and  $\beta$ -polypeptides and bacteriochlorophyll *a*. Biochemistry 27: 2718–2727
- Picorel R, Lefebvre S and Gingras G (1984) Oxidation-reduction of B800-850 and B880 holochromes isolated from three species of photosynthetic bacteria as studied by electron-paramagnetic resonance and optical spectroscopy. Eur J Biochem 142: 305–311
- Prince SM, Papiz MZ, Freer AA, McDermott G, Hawthornthwaite-Lawless AM, Cogdell RJ and Isaacs NW (1997) Apoprotein structure in the LH2 complex from *Rhodopseudomonas acidophila* strain 10050: Modular assembly and protein pigment interactions. J Mol Biol 268: 412–423
- Pullerits T and Sundström V (1996) Photosynthetic light-harvesting pigment-protein complexes: Toward understanding how and why. Acc Chem Res 29: 381–389
- Pullerits T, Chachisvilis M and Sundström V (1995) Exciton dynamics and delocalization length in B850 molecules of LH2 of *Rhodobacter sphaeroides*. In: Mathis P (ed) Photosynthesis: From Light to Biosphere, pp 107–110. Kluwer Academic Publishers, Dordrecht
- Pullerits T, Hess S, Herek JL and Sundström V (1997) Temperature dependence of excitation transfer in LH2 of *Rhodobacter sphaeroides*. J Phys Chem B 101: 10560–10567
- Rademaker H, Hoff AJ and Duysens LNM (1979) Magnetic field-induced increase of the yield of (bacterio)chlorophyll emission of some photosynthetic bacteria and of *Chlorella vulgaris*. Biochim Biophys Acta 546: 248–255
- Ricci M, Bradforth SE, Jimenez R and Fleming GR (1996) Internal conversion and energy transfer dynamics of spheroidene in solution and in the LH-1 and LH-2 light-harvesting complexes. Chem Phys Lett 259: 381–390
- Ridge JP, Fyfe PK, McAuley KE, van Brederode ME, Robert B, van Grondelle R, Isaacs NW, Cogdell RJ and Jones MR (2000) An examination of how structural changes can affect the rate of electron transfer in a mutated bacterial photoreaction center. Biochem J 352: 567–578
- Robert B and Lutz M (1985) Structures of antenna complexes of several Rhodospirillales from their resonance Raman spectra. Biochim Biophys Acta 807: 10–23
- Salverda JM, van Mourik F, van der Zwan G and van Grondelle R (2000) Energy transfer in the B800 rings of the peripheral bacterial light-harvesting complexes of *Rhodopseudomonas acidophila* and *Rhodospirillum rubrum* studied with photon echo techniques. J Phys Chem B 104: 11395–11408
- Sauer K, Cogdell RJ, Prince SM, Freer A, Isaacs NW and Scheer H (1996a) Structure-based calculations of the optical spectra of the LH2 bacteriochlorophyll-protein complex from *Rhodopseudomonas acidophila*. Photochem Photobiol 64: 564–576
- Sauer PRR, Lottspeich F, Unger E, Mentle R and Michel H (1996b) Deletion of a B800-850 light-harvesting complex in *Rhodospirillum rubrum* DSM119 leads to 'revertants' expressing a B800-820 complex: Insights into pigment binding. Biochemistry 35: 6500–6507
- Savage H, Cyrklaff M, Montoya G, Kühlbrandt W and Sinning I (1996) Two-dimensional structure of light harvesting complex II (LHII) from the purple bacterium *Rhodovulum sulfidophilum* and comparison with LHII from *Rhodopseudomonas acidophila*. Structure (London) 4: 243–252
- Scholes GD and Fleming GR (2000) On the mechanism of light

- harvesting in photosynthetic purple bacteria: B800 to B850 Energy Transfer. *J Phys Chem B* 104: 1854–1868
- Scholes GD, Gould IR, Cogdell RJ and Fleming GR (1999) Ab initio molecular orbital calculations of electronic couplings in the LH2 bacterial light-harvesting complex of *Rps. acidophila*. *J Phys Chem B* 103: 2543–2553
- Shreve AP, Trautman JK, Frank HA, Owens TG and Albrecht AC (1991a) Femtosecond energy-transfer processes in the B800–850 light-harvesting complex of *Rhodobacter sphaeroides* 2.4.1. *Biochim Biophys Acta* 1058: 280–288
- Shreve AP, Trautman JK, Owens TG, Frank HA and Albrecht AC (1991b) In vivo energy transfer studies in photosynthetic systems by subpicosecond timing. *Proc SPIE-Int Soc Opt Eng* 1403: 394–399
- Sistrom WR (1978) Control of antenna pigment components in photosynthetic bacteria. In: Clayton RK (ed) *The Photosynthetic Bacteria*, pp 841–848. Plenum, New York
- Somsen OJG, van Mourik F, van Grondelle R and Valkunas L (1994) Energy migration and trapping in a spectrally and spatially inhomogeneous light-harvesting antenna. *Biophys J* 66: 1580–1596
- Somsen OJG, Valkunas L and van Grondelle R (1996a) A perturbed two-level model for exciton trapping in small photosynthetic systems. *Biophys J* 70: 669–683
- Somsen OJG, van Grondelle R and van Amerongen H (1996b) Spectral broadening of interacting pigments: Polarized absorption by photosynthetic proteins. *Biophys J* 71: 1934–1951
- Somsen OJG, Chernyak V, Frese RN, van Grondelle R and Mukamel S (1998) Excitonic interactions and Stark spectroscopy of light harvesting systems. *J Phys Chem B* 102: 8893–8908
- Steiner R and Scheer H (1985) Characterization of a B800/1020 antenna from the photosynthetic bacteria *Ectothiorhodospira halochloris* and *Ectothiorhodospira abdelmalekii*. *Biochim Biophys Acta* 807: 278–284
- Sturgis JN and Robert B (1996) The role of chromophore coupling in tuning the spectral properties of peripheral light-harvesting protein of purple bacteria. *Photosynth Res* 50: 5–10
- Sturgis JN and Robert B (1997) Pigment binding-site and electronic properties in light-harvesting proteins of purple bacteria. *J Phys Chem B* 101: 7227–7231
- Sturgis JN, Hageman G, Tadros MH and Robert B (1995a) Biochemical and spectroscopic characterization of the B800–850 light-harvesting complex from *Rhodobacter sulfidophilus* and its B800–830 spectral form. *Biochemistry* 34: 10519–10524
- Sturgis JN, Jirsakova V, Reiss-Husson F, Cogdell RJ and Robert B (1995b) Structure and properties of the bacteriochlorophyll binding site in peripheral light-harvesting complexes of purple bacteria. *Biochemistry* 34: 517–523
- Sturgis JN, Olsen JD, Robert B and Hunter CN (1997) Functions of conserved tryptophan residues of the core light-harvesting complex of *Rhodobacter sphaeroides*. *Biochemistry* 36: 2772–2778
- Sturgis JN, Gall A, Ellervee A, Freiberg A and Robert B (1998) The effect of pressure on the bacteriochlorophyll a binding sites of the core antenna complex from *Rhodospirillum rubrum*. *Biochemistry* 37: 14875–14880
- Sumi H (1999) Theory on rates of excitation-energy transfer between molecular aggregates through distributed transition dipoles with application to the antenna system in bacterial photosynthesis. *J Phys Chem B* 103: 252–260
- Sundström V, Van Grondelle R, Bergström H, Aakesson E and Gillbro T (1986) Excitation-energy transport in the bacteriochlorophyll antenna systems of *Rhodospirillum rubrum* and *Rhodobacter sphaeroides*, studied by low-intensity picosecond absorption spectroscopy. *Biochim Biophys Acta* 851: 431–46
- Sundström V, Pullerits T and van Grondelle R (1999) Photosynthetic light harvesting: Reconciling dynamics and structure of purple bacterial LH2 reveals function of photosynthetic unit. *J Phys Chem B* 103: 2327–2346
- Tadros MH (1990) Gene structure, organization and expression of the light-harvesting B800–850  $\alpha$  and  $\beta$  polypeptides in photosynthetic bacteria. *FEMS Symp* 53: 19–31
- Tadros MH, Katsiou E, Hoon MA, Yurkova N and Ramji DP (1993) Cloning of a new antenna gene cluster and expression analysis of the antenna gene family of *Rhodopseudomonas palustris*. *Eur J Biochem* 217: 867–75
- Thornber JP (1970) Photochemical reactions of purple bacteria as revealed by studies of three spectrally different carotene bacteriochlorophyll-protein complexes isolated from *Chromatium*, strain D. *Biochemistry* 9: 2688–2698
- Timpmann K, Freiberg A and Sundström V (1995) Energy trapping and detrapping in the photosynthetic bacterium *Rhodopseudomonas viridis*: Transfer-to-trap-limited dynamics. *Chem Phys* 194: 275–283
- Timpmann K, Zhang FG, Freiberg A and Sundström V (1993) Detrapping of excitation energy from the reaction center in the photosynthetic purple bacterium *Rhodospirillum rubrum*. *Biochim Biophys Acta* 1183: 185–193
- Trautman JK, Shreve AP, Violette CA, Frank HA, Owens TG and Albrecht AC (1990) Femtosecond dynamics of energy transfer in B800–850 light-harvesting complexes of *Rhodobacter sphaeroides*. *Proc Natl Acad Sci U S A* 87: 215–219
- Trissl HW, Law CJ and Cogdell RJ (1999) Uphill energy transfer in LH2-containing purple bacteria at room temperature. *Biochim Biophys Acta* 1412: 149–172
- van Grondelle R, Bergström H, Sundström V and Gillbro T (1987) Energy transfer within the bacteriochlorophyll antenna of purple bacteria at 77 K, studied by picosecond absorption recovery. *Biochim Biophys Acta* 894: 313–326
- van Grondelle R, Dekker JP, Gillbro T and Sundström V (1994) Energy transfer and trapping in photosynthesis. *Biochim Biophys Acta* 1187: 1–65
- van Grondelle R, Monshouwer R and Valkunas L (1997) Photosynthetic light-harvesting. *Pure Appl Chem* 69: 1211–1218
- Vischer KJ, Bergström H, Sundström V, Hunter CN and van Grondelle R (1989) Temperature dependence of energy transfer from the long wavelength antenna BChl-869 to the reaction center in *Rhodospirillum rubrum*, *Rhodobacter sphaeroides* (w.t. and M21 mutant) from 77 to 177 K, studied by picosecond absorption spectroscopy. *Photosynth Res* 22: 211–217
- Vischers RW, Germeroth L, Michel H, Monshouwer R and van Grondelle R (1995) Spectroscopic properties of the light-harvesting complexes from *Rhodospirillum molischianum*. *Biochim Biophys Acta* 1230: 147–154
- Visser HM, Somsen OJG, von Mourik F, Lin S, van Stokkum IHM and van Grondelle R (1995) Direct observation of sub-picosecond equilibration of excitation energy in the light-

- harvesting antenna of *Rhodospirillum rubrum*. *Biophys J* 69: 1083–1099
- Walla PJ, Linden PA, Hsu C-P, Scholes GD and Fleming GR (2000) Femtosecond dynamics of the forbidden carotenoid S1 state in light-harvesting complexes of purple bacteria observed after two-photon excitation. *Proc Natl Acad Sci USA* 97: 10808–10813
- Walz T and Ghosh R (1997) Two-dimensional crystallization of the light-harvesting I-reaction center photounit from *Rhodospirillum rubrum*. *J Mol Biol* 265: 107–111
- Walz T, Jamieson SJ, Bowers CM, Bullough PA and Hunter CN (1998) Projection structures of three photosynthetic complexes from *Rhodobacter sphaeroides*: LH2 at 6 Å, LH1 and RC-LH1 at 25 Å. *J Mol Biol* 282: 833–845
- Wu H-M, Ratsep M, Jankowiak R, Cogdell RJ and Small GJ (1997) Comparison of the LH2 antenna complexes of *Rhodopseudomonas acidophila* (Strain 10050) and *Rhodobacter sphaeroides* by high-pressure absorption, high-pressure hole burning and temperature-dependent absorption spectroscopies. *J Phys Chem B* 101: 7641–7653
- Wu H-M, Reddy NRS, Cogdell RJ, Muenke C, Michel H and Small GJ (1996a) A comparison of the LH2 antenna complex of three purple bacteria by hole burning and absorption spectroscopies. *Mol Cryst Liq Cryst Sci Technol, Sect A* 291: 163–173
- Wu H-M, Savikhin S, Reddy NRS, Jankowiak R, Cogdell RJ, Struve WS and Small GJ (1996b) Femtosecond and hole-burning studies of B800's excitation energy relaxation dynamics in the LH2 antenna complex of *Rhodopseudomonas acidophila* (Strain 10050). *J Phys Chem* 100: 12022–12033
- Youvan DC and Ismail S (1985) Light-harvesting II (B800-B850 complex) structural genes from *Rhodopseudomonas capsulata*. *Proc Natl Acad Sci U S A* 82: 58–62
- Youvan DC, Bylina EJ, Alberti M, Begusch H and Hearst JE (1984) Nucleotide and deduced polypeptide sequences of the photosynthetic reaction-center, B870 antenna and flanking polypeptides from *R. capsulata*. *Cell* 37: 949–957
- Yu J-Y, Nagasawa Y, van Grondelle R and Fleming GR (1997) Three pulse echo peak shift measurements on the B820 subunit of LH1 of *Rhodospirillum rubrum*. *Chem Phys Lett* 280: 404–410
- Zuber H and Brunisholz RA (1991) Structure and function of antenna polypeptides and chlorophyll-protein complexes: principles and variability. In: Scheer H (ed) *Chlorophylls*, pp 627–703. CRC Press, Boca Raton
- Zuber H and Cogdell RJ (1995) Structure and organization of purple bacterial antenna complexes. In: Blankenship RE, Madigan MT and Bauer CE (eds) *Anoxygenic Photosynthetic Bacteria*, pp 315–348. Kluwer Academic Publishers, Dordrecht

# Chapter 6

## Antenna Complexes from Green Photosynthetic Bacteria

Robert E. Blankenship\*

*Department of Chemistry and Biochemistry, Center for the Study of Early Events in Photosynthesis, Arizona State University, Tempe, AZ 85287-1604 U.S.A.*

Katsumi Matsuura

*Department of Biology, Tokyo Metropolitan University, Minamiohsawa 1-1, Tokyo 192-0397, Japan*

Summary .....	195
I. Introduction .....	196
A. Classes of Green Photosynthetic Bacteria .....	196
B. Cellular Organization .....	196
C. Pigment Content .....	199
II. Chlorosome Structure, Pigment Stoichiometry and Protein Content .....	201
A. Overall Chlorosome Structure, Composition and Preparation .....	201
B. Pigment Organization in Chlorosomes .....	201
C. Proteins in Chlorosomes .....	202
D. The Chlorosome Baseplate .....	203
III. Redox-Dependent Regulation of Energy Transfer in Chlorosomes .....	204
A. Redox Regulation in Green Bacteria .....	204
B. Quinones: A Newly Found Component in Chlorosomes .....	205
IV. Fenna-Matthews-Olson Protein .....	207
V. Kinetics and Pathways of Energy Transfer in Chlorosomes and Membranes of Green Bacteria .....	209
VI. Conclusions and Future Work .....	210
Acknowledgment .....	211
References .....	211

### Summary

Green photosynthetic bacteria contain unique peripheral antenna complexes known as chlorosomes. Chlorosome complexes are optimized for light collection at low levels. The chlorosome is composed of large amounts of pigment and relatively little protein. The pigments consist principally of bacteriochlorophylls *c*, *d* or *e* plus carotenoids, along with small amounts of bacteriochlorophyll *a*. The bacteriochlorophylls *c*, *d* or *e* are organized into pigment oligomers with relatively little or no involvement of protein in determining the pigment arrangement. The bacteriochlorophyll *a* is associated with a protein as a pigment-protein complex. Additional membrane-associated antenna complexes are energy transfer intermediates between the chlorosome and the reaction center. These include the Fenna-Matthews-Olson protein in the green sulfur bacteria, and integral membrane antenna complexes similar to the purple bacterial LHI complex in the green nonsulfur bacteria. The green sulfur bacteria antenna system is regulated by redox potential, so that excitations are efficiently quenched at high redox potentials and never reach the reaction center. This regulation is mediated by quinone molecules that are localized in the chlorosome complex and is thought to protect the cell from light-induced superoxide formation under conditions of transient oxygen exposure.

---

\*Author for correspondence, email: blankenship@asu.edu

## I. Introduction

### A. Classes of Green Photosynthetic Bacteria

The green photosynthetic bacteria are anoxygenic phototrophs that contain unique antenna complexes known as chlorosomes. The chlorosome is an antenna system that is well adapted to conditions of extremely low light flux. It presents an extraordinarily high absorption cross section to incoming light, while at the same time utilizing a minimum of cellular resources in its construction. It is thus an ideal system for organisms that live in conditions where they receive little light and must grow using only photosynthesis as an energy source.

There are two families of green bacteria. One family is the Chlorobiaceae, also called the green sulfur bacteria (Trüper and Pfennig, 1992). These organisms are strict anaerobes and contain an Fe-S type of reaction center similar to Photosystem I (Feiler and Hauska, 1995; Sakurai et al., 1996; Olson, 1998). In addition, they contain the BChl *a*-containing trimeric Fenna-Matthews-Olson (FMO) antenna protein complex, which is discussed in more detail below. The green sulfur bacteria exemplify the physiological characteristics given above, in that they are obligate photoautotrophs and are often found at the very lowest levels of the photic zone, either in lake or microbial mat environments (van Gemerden and Mas, 1995). The most widely studied green sulfur bacteria are a deep emerald green color, which gives the entire group its name. However, some species, especially those that contain BChl *e*, are brown in color.

The other family of green bacteria is the Chloroflexaceae, often called the green gliding, green filamentous or green nonsulfur bacteria (Pierson and Castenholz, 1992, 1995). They are facultatively aerobic and contain a pheophytin-quinone type of reaction center similar to that found in Photosystem II and the purple bacteria (Feick et al., 1995). The only member of this family that has been well studied is the thermophilic organism *Chloroflexus aurantiacus*. These organisms are less obviously dependent on carrying out photosynthesis in low light environments, and are often found in hot spring microbial

mats, where they are either surface exposed or underlie a layer of cyanobacteria. The contrast between some of the properties of the chlorosomes in the two families of green bacteria is interesting and provides clues to their different environmental and physiological characteristics. Table I summarizes some of the characteristics of the antenna systems and reaction centers from the two families of green bacteria.

Another group of anoxygenic photosynthetic organisms that is closely related to the green nonsulfur bacteria is represented by *Heliothrix oregonensis* (Pierson et al., 1985) and a recently isolated species, *Roseiflexus castenholzii* (Hanada et al., 2002). Available information indicates that most of the phylogenetic, metabolic and physiological characteristics of these organisms are similar to those of the green nonsulfur bacteria, except for the absence of the characteristic chlorosome antenna complex. In addition to *Heliothrix oregonensis* and *Roseiflexus castenholzii*, several species of uncultured organisms appear to belong in this group (Boomer et al., 2000).

The two families of green bacteria appear to be only very distantly related, based on 16S r-RNA analysis (Gibson et al., 1985; Woese, 1987). Metabolically and physiologically the two groups are very different, and for some time it has been considered likely that the information needed to build the chlorosome was laterally transferred between the two groups of organisms (Blankenship, 1992). However, recent sequencing of genes involved in bacteriochlorophyll *a* biosynthesis has indicated that at least this portion of the genetic information needed to carry out photosynthesis is closely related in the two groups of organisms (Xiong et al., 2000). Whether this represents a close relationship of the rest of the photosynthetic apparatus or other metabolic pathways remains to be determined. The comparison of the complete genome sequences of representatives of the two groups, just recently completed but not yet fully analyzed or published, should firmly establish just how they are related.

### B. Cellular Organization

The characteristic feature of green photosynthetic bacteria is the peripheral light-harvesting structure known as the chlorosome (Fig. 1). This complex, described in detail in Section II, is attached to the cytoplasmic side of the inner cell membrane, which, in contrast to the intracytoplasmic membrane of

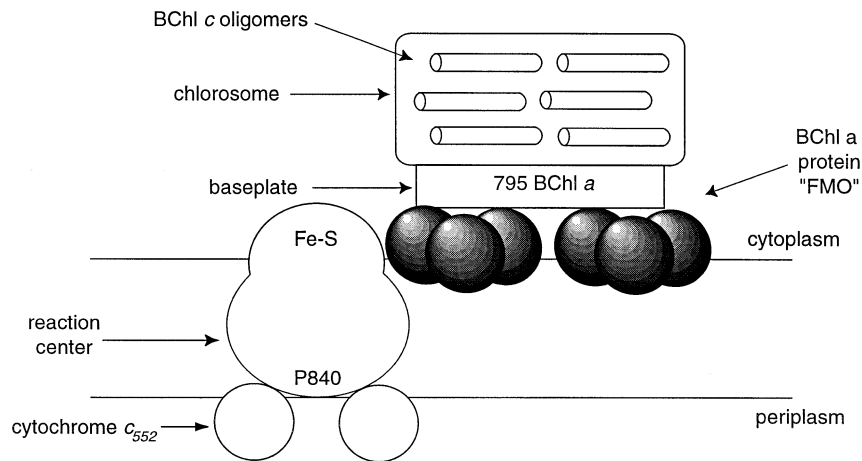
**Abbreviations:** BChl – bacteriochlorophyll; Chl – chlorophyll;  $E_m$  – redox midpoint potential; FMO – Fenna-Matthews-Olson;  $F_{ox}$  – fluorescence intensity under oxidized conditions;  $F_{red}$  – fluorescence intensity under reduced conditions; LH – light harvesting; MK – menaquinone

Table 1. Characteristics of Antennas and Reaction Centers of Green Photosynthetic Bacteria

Family	Representative Organism	Chlorosome Pigments	Chlorosome Absorption Maximum (nm)	FMO Antenna Protein	Integral Membrane Antenna	Reaction Center Type	Reaction Center Pigment Content	Reaction Center Photobleaching Maximum (nm)
Chloroflexaceae (Green non sulfur)	<i>Chloroflexus aurantiacus</i>	BChl <i>c</i>	740	No	B808-866	Pheo-Q	3 BChl <i>a</i> 3 BPh <i>a</i>	865
Chloroflexaceae (Green non sulfur)	<i>Roseiflexus castenholzii</i>	None	NA	No	B801-878	Pheo-Q	3 BChl <i>a</i> 3 BPh <i>a</i>	865
Chlorobiaceae (Green sulfur)	<i>Chlorobium tepidum</i>	BChl <i>c</i>	750	Yes	None (RC)	Fe-S	16 BChl <i>a</i> 4 Chl <i>a</i> <sub>670</sub>	840
Chlorobiaceae (Green sulfur)	<i>Chlorobium vibrioforme</i>	BChl <i>d</i>	725	Yes	None (RC)	Fe-S	16 BChl <i>a</i> 4 Chl <i>a</i> <sub>670</sub> Note 1	840
Chlorobiaceae (Green sulfur)	<i>Chlorobium phaeobacteroides</i>	BChl <i>e</i>	712	Yes	None (RC)	Fe-S	16 BChl <i>a</i> 4 Chl <i>a</i> <sub>670</sub> Note 1	840

Note 1. Reaction center pigment composition is assumed by analogy to related organisms but has not been experimentally determined.

### Chlorosome-Green Sulfur Bacteria



### Chlorosome-Green Nonsulfur Bacteria

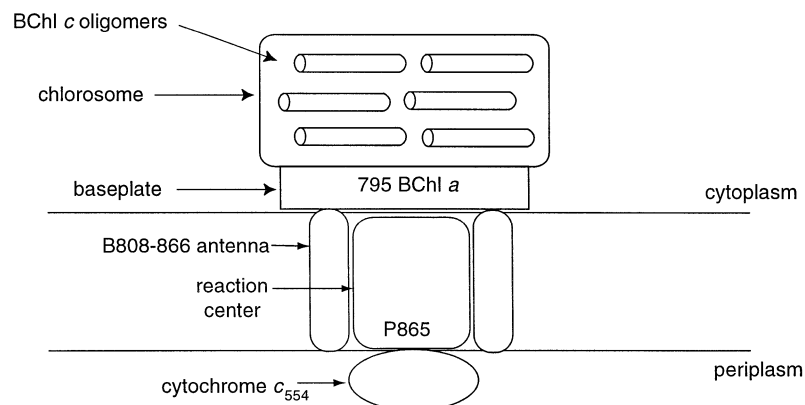


Fig. 1. Schematic structural models of chlorosomes from green sulfur bacteria (top) and green nonsulfur bacteria (bottom).

purple bacteria, is not invaginated. The chlorosome structure contains all the BChl *c*, *d* or *e* in the cell and a small amount of BChl *a* that is an integral part of the chlorosome, in a complex known as the baseplate (discussed below).

The BChl *a* in green bacteria is mostly contained in membrane-bound antenna pigment-proteins and in the reaction centers. The best studied of the BChl *a*-containing antenna pigment-proteins is the Fenna-Matthews-Olson or (FMO) protein (Matthews and Fenna, 1980). It is a peripheral membrane protein

found only in the green sulfur bacteria, and is discussed in more detail below. The green sulfur bacteria do not have any known integral membrane antenna complexes, except the reaction center complex itself, which contains some antenna pigments. The green sulfur bacterial reaction center is generally similar to Photosystem I, in that it contains a series of Fe-S clusters as early electron acceptors bound to a homodimeric core reaction center protein complex of two 82 kDa proteins (Büttner et al., 1992). However, the green sulfur bacterial complex



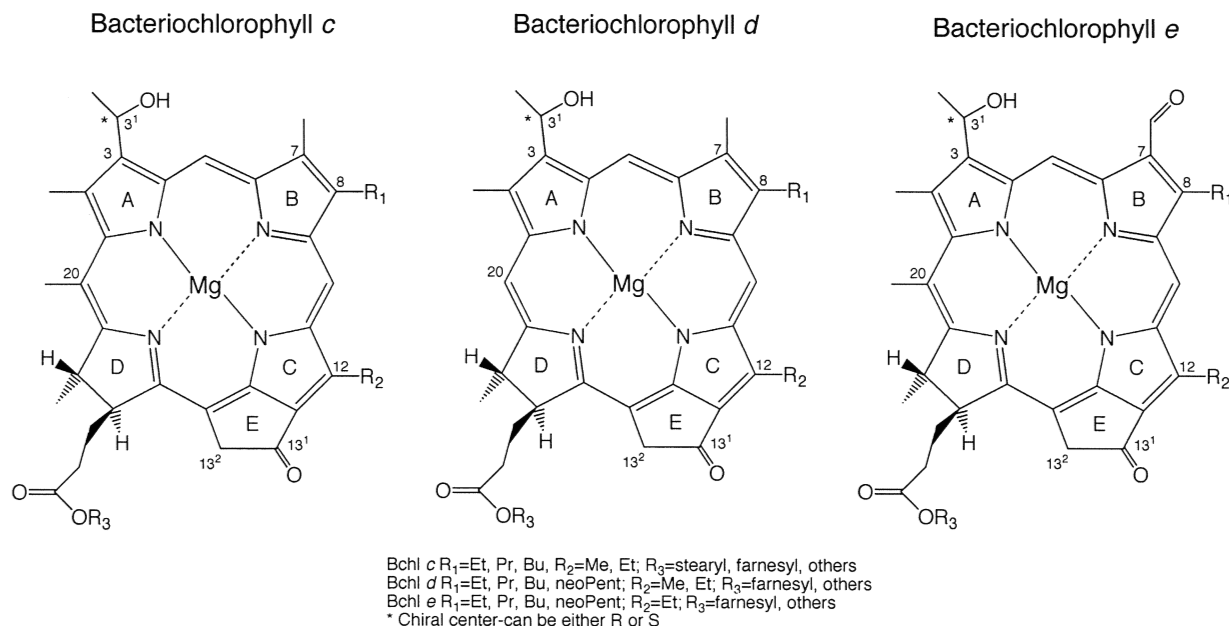


Fig. 2. Structures of bacteriochlorophylls *c*, *d* and *e*. IUPAC nomenclature is used for the numbering of the carbon atoms and the designations of the rings.

contains many fewer pigments than Photosystem I. Recent analytical measurements indicate that the reaction center complex contains 16 molecules of BChl *a* (Griesbeck et al., 1998; Permentier et al., 2000) and four molecules of a pigment with the same macrocycle as Chl *a* but with a different esterifying tail (van de Meent et al., 1992; Permentier et al., 2000). The Chl *a* serves as the primary electron acceptor. The primary electron donor BChl *a*, probably a special pair, absorbs at 840 nm.

The green nonsulfur bacteria contain an integral membrane antenna complex known as the B808-865 complex. This complex has been sequenced in *Chloroflexus* and appears by sequence to be most closely related to the LH1 complex found in purple photosynthetic bacteria (Wechsler et al., 1985b, 1987, 1991; Zuber and Brunisholz, 1991; Watanabe et al., 1995). However, a significant difference is that the B808-865 complex contains two spectral types of BChl *a*, absorbing at 808 and 865 nm instead of the one type of BChl *a* that typically absorbs at 870 to 880 nm in LH1 complexes. This makes the *Chloroflexus* complex spectrally more similar to the LH2 class of purple bacterial antenna complexes. Whether the B808-865 antenna complex is organized in a large ring that surrounds the reaction center, as the LH1 complexes appear to be in purple bacteria, or is organized in smaller rings that are more

peripheral to the reaction center, as the LH2 complexes are (Cogdell et al., 1999), is not known, although the former arrangement seems the more likely.

The *Chloroflexus* reaction center is generally similar to that found in the purple bacteria except that it does not contain an H subunit (Feick et al., 1995). The H subunit is found on the cytoplasmic side of the membrane in the purple bacteria in the position occupied by the chlorosome in the green nonsulfur bacteria. The primary electron donor absorbs at 865 nm.

Schematic structural models of the chlorosomes and associated antenna and reaction center complexes in the two families of green bacteria are shown in Fig. 1.

### C. Pigment Content

Most green bacteria contain both BChl *a* and either BChl *c*, BChl *d* or BChl *e* (Scheer, 1991; Oelze and Golecki, 1995; Blankenship et al., 1995; Olson, 1998). The structures of the latter pigments are shown in Fig. 2, and are collectively known as chlorobium chlorophylls. A preferred nomenclature for these pigments has been proposed (Smith, 1994). Chemically, the chlorobium chlorophylls are more closely related to the true chlorophylls than to

bacteriochlorophyll *a* in that the double bond in ring B is not reduced. This feature makes them chemically classified as chlorins instead of bacteriochlorins. One unique feature of the chlorobium chlorophylls is the lack of the bulky carboxymethyl substituent at the 13<sup>2</sup> position on ring E that is found in all other chlorophyll-type pigments. A second unique chemical feature is the hydroxyethyl substituent at the 3 position on ring A. In addition, the 3<sup>1</sup> carbon is asymmetric and both R and S diastereomers are often found in significant quantities (Smith et al., 1982; Brune et al., 1987; Bobe et al., 1990; Chiefari et al., 1995; Ishii et al., 2000). The final unusual feature of these pigments is the remarkable pigment heterogeneity found in chlorosomes. BChls *c*, *d* and *e*, unlike all other chlorophylls, are not single compounds, but rather are groups of chemically related compounds (Smith, 1994). The pigment heterogeneity occurs primarily at the C-8 and C-12 positions, where varying alkyl substituents are found. In addition, the tails are somewhat variable, especially in the green nonsulfur bacteria, which can incorporate a wide range of alcohols into the tail (Larsen et al., 1995).

The characteristic structural feature of BChl *c* that distinguishes it from BChl *d* and *e* is the presence of a methyl substituent at the C-20 position. BChl *d* has a hydrogen substituent at C-20. BChl *e* has methyl at C-20 and a formyl group at C-7. BChl *f*, with hydrogen at C-20 and formyl at C-7 is the logical final member of the series of pigments. It has never been found in any natural organism, but its properties have been investigated in model compounds (Tamiaki et al., 2000).

In almost all cases cells contain only a single type of chlorobium chlorophyll, BChl *c*, *d* or *e*, which functions exclusively as an antenna pigment and is contained only in the chlorosomes (Oelze and Golecki, 1995; Blankenship et al., 1995). Typical absorption maxima in vivo for these pigments are 740–750 nm for BChl *c* (740 nm is typical of green nonsulfur bacteria and 750 nm is typical for green sulfur bacteria), 725 for BChl *d* and 712 for BChl *e*. An exception is found in some strains of *Chlorobium limicola* in which both BChl *c* and *d* occur in significant quantities (Steensgaard et al., 1999, 2000b). BChl *c*, *d* or *e* constitutes about half the mass of the chlorosomes, as shown in Table 2.

Almost nothing is known about the biosynthetic pathways for the chlorobium chlorophylls (see Porra, 1997, for review). This represents an area that is in need of further research. The mechanism(s) by which the organism regulates the biosynthesis of the two

types of chlorophylls (e.g. BChl *a* and *c*) found in the cell and fine tunes the pigment composition to the light availability are also not known. One aspect of bacteriochlorophyll *c* biosynthesis that has seen some progress is the attachment of the esterifying tail. In *Chloroflexus*, two related enzymes are found, one that attaches the phytol tail to form BChl *a* and the other that attaches the tail to form BChl *c* (Lopez et al., 1996; Schoch et al., 1999). These are coded for by the *bchG* and *bchG2* genes, respectively.

Evidence is now overwhelming that the pigments in chlorosomes are organized into pigment oligomers, in which the pigments are in direct van der Waals contact and proteins are of secondary importance in determining the pigment geometry (Blankenship et al., 1995). The structures of the BChl *c* type pigments clearly lend themselves to self-aggregation. The OH group on ring A has been implicated in the formation of a variety of aggregated species in vitro. The lack of the bulky carboxymethyl substituent on ring E permits them to pack together more closely than other chlorophylls or bacteriochlorophylls (Oba and Tamiaki, 1999). There is a large literature on aggregation properties of BChl *c* and related pigments, which is reviewed in Blankenship et al. (1995).

Carotenoids are also present in all chlorosomes as light-harvesting pigments and quenchers of the triplet state of bacteriochlorophylls. In *Chlorobium* species, the molar ratio of carotenoids to BChl *c* is around 1/10 (Table 2) (Frigaard et al., 1997). In BChl *e* containing species such as *Chlorobium phaeobacteroides*, a broad absorption band around 520 nm is observed and has been suggested to be due to carotenoids. However, the effects of inhibiting carotenoid biosynthesis (Arellano et al., 2000b) or extracting carotenoids by organic solvents (Cox et al., 1998), and comparisons with the spectra of aggregates of extracted BChl *e* (Smith et al., 1983, Saga et al., 2001) indicate that this band reflects an aggregated form of BChl *e*. In *Chloroflexus* chlorosomes, the molar ratio of carotenoids to BChl *c* is more than 1/5. Although a part of the carotenoids are carotenoid glucoside and carotenoid glucoside with fatty acids, which are suggested to be present in chlorosome envelope (Tsuji et al., 1995, Takaichi et al., 1995), the molar ratio of hydrophobic carotenoids ( $\beta$ -carotene and  $\gamma$ -carotene) to BChl *c* is still about 1/5 after extensive washing of chlorosomes with SDS to remove the envelope and baseplate components (Tsuji et al., 1995).

Table 2. Estimated Chemical Composition of Typical Chlorosomes (% Dry weight)

	BChl <i>c</i>	BChl <i>a</i>	carotenoids	quinones	other lipids	protein
Chloroflexaceae (Green non sulfur)	43	2	8	5	13	30
Chlorobiaceae (Green sulfur)	54	0.2	4	3.8	11	27

The composition was estimated from the data in Frigaard et al. (1997), Holo et al. (1985) and Schmidt (1980). Note that preparations used for each study were different in strains, growth conditions, and preparation methods. Other components, which are not known as definite components so far, were assumed to be zero.

## II. Chlorosome Structure, Pigment Stoichiometry and Protein Content

### A. Overall Chlorosome Structure, Composition and Preparation

The structures of chlorosomes from the two families of green bacteria are generally similar (Fig. 1), with a flattened ellipsoidal shape of dimensions 100 to 200 nm long, 30 to 70 nm wide and 10 to 12 nm thick (Oelze and Golecki, 1995; Staehelin et al., 1978, 1980). The smaller dimensions apply to the green nonsulfur bacteria, while the chlorosomes from the green sulfur bacteria are larger in all dimensions. Internal rod-like features 5–10 nm in diameter are observed. Several models have appeared that propose detailed molecular structures of the oligomers packing together to form the rods visualized by electron microscopy (Matsuura et al., 1993; Holzwarth and Schaffner, 1994; Nozawa et al., 1994; Novoderezhkin and Fetisova, 1997; van Rossum et al., 2001).

Each chlorosome has been estimated to contain roughly 10,000 molecules of BChl *c* (Olson, 1980a, 1998), although a direct measurement of this number was apparently not made. Recent measurements using single molecule fluorescence techniques and dynamic light scattering in chlorosomes of *Chlorobium tepidum* have found approximately 250,000 BChl *c* per chlorosome (Montaño et al., 2001b). In addition to the BChl *c* (*d* or *e*), chlorosomes contain a much smaller amount of BChl *a*, with the precise values depending on the species and growth conditions (Oelze and Golecki, 1995), together with proteins, glycolipids, BChl *a*, carotenoids and quinones. The relative contents of these additional components are indicated in Table 2.

The inside of the chlorosomes is thought to be very hydrophobic and the currently accepted view is that the chlorosome is surrounded by a lipid monolayer that consists mainly of monogalactosyl diglyceride (MGDG) with the hydrocarbon tails

pointed toward the interior of the chlorosome and the polar head groups pointed to the chlorosome surface. In addition, chlorosomes contain a number of proteins that are all thought to be localized in the envelope (see below).

Chlorosomes can be detached from the cytoplasmic membranes by using chaotropic agents such as 2 M NaSCN, (Gerola and Olson, 1986) or some detergents (Feick and Fuller, 1984). Isolated chlorosomes are generally stable, and maintain their overall structure as well as their light-harvesting function.

### B. Pigment Organization in Chlorosomes

The far-red absorption spectrum of BChl *c* in the chlorosomes is red-shifted some 70–80 nm with respect to that of monomeric BChl *c* in organic solvents, reflecting the specific organization of the pigments. The pigment organization of BChl *c* is unique among all photosynthetic systems, since the pigments are not bound to proteins but aggregated by themselves to create the higher, functional structure. The spectral red shift is caused by the chromophore-chromophore interactions among BChl *c* molecules rather than pigment-protein interactions.

A. A. Krasnovsky first proposed the concept of aggregated pigments as models for pigment organization in chlorosomes of green bacteria. (Krasnovsky and Pakshina, 1959; Bystrova et al., 1979; Krasnovsky and Bystrova, 1980). This pioneering work clearly established many of the basic features of chlorosomes, which have been confirmed and extended (and sometimes rediscovered!) by later workers.

The following pieces of evidence support the concept of the protein-free organization of BChl *c*. First, BChl *c* in non-polar solvents can form aggregates whose spectra resemble those of chlorosomes. For reviews of these properties see Blankenship et al., (1995), Tamiaki (1996) and Olson (1998). BChl *c* has the ability to form oligomers

through the ligation of an oxygen atom in one molecule to the central magnesium atom in another molecule. Protein-free pigment-lipid aggregates resembling chlorosomes in various aspects also can be formed in the aqueous phase with BChl *c* and galactolipids (Hirota et al., 1992ab; Miller et al., 1993). Second, proteins can be extracted from chlorosomes with SDS without affecting the spectral properties of the BChl *c* (Griebenow et al., 1989, 1991; Holzwarth et al., 1990a). By contrast, the aggregated spectral form of BChl *c* can be converted reversibly to the monomeric form by hexanol in intact chlorosomes (Brune et al., 1987; Matsuura and Olson, 1990; Zhu et al., 1995). Finally, proteins have been shown to be located only in the chlorosome envelope and not in the hydrophobic interior (Wullink et al., 1991; Chung and Bryant, 1996), and no proteins have been unambiguously shown to be BChl *c*-binding proteins.

The organization of BChl *c* (*d* or *e*) oligomers to form higher-order structures also appears to be based on protein-free self aggregation of the pigments. In native chlorosomes, the excitation transition dipoles of BChl *c* (*d* or *e*) are highly ordered with respect to the long axis of the ellipsoidal chlorosomes, based on linear dichroism and fluorescence polarization measurements (Betti et al., 1982; Fetisova et al., 1986, 1988; Griebenow et al., 1991; Mimuro et al., 1994). A similar higher organization of pigments was observed in protein-free pigment-lipid aggregates in the aqueous phase (Hirota et al., 1992ab). When the aggregates were embedded in a polyacrylamide gel and the gel was elongated in one direction to orient the particles, a large linear-dichroism signal resembling that of native chlorosomes was observed. This observation strongly suggests that a higher-order structure of BChl *c* (*d* or *e*) in chlorosomes, which probably corresponds to the rod structure observed in the electron microscope, is also formed without the involvement of proteins.

Understanding the detailed structural arrangement of the bacteriochlorophyll *c* pigments in the chlorosome has been a subject of intense investigation. Unfortunately, crystals of chlorosomes or aggregated BChl *c* have not yet been obtained so an X-ray structure has not been possible. An X-ray structure of dimers of a model compound of BChl *d* has been described (Barkigia et al., 1997), but this dimer does not have any interactions between the 3<sup>1</sup>-hydroxyethyl substituent and the central metal (Zn in this compound). These interactions are well

established by spectroscopic analyses, so this dimer does not appear to be a building block of the larger aggregates that are found in chlorosomes. Perhaps the most direct experimental method that has been applied to determine the structure of the pigments in aggregates is solid state NMR (Nozawa et al., 1994; Balaban et al., 1995; Mizoguchi et al., 1998, 2000; Wang et al., 1999; van Rossum et al., 2001).

### C. Proteins in Chlorosomes

Although proteins now are not considered to be involved in the basic organization of BChl *c* in chlorosomes, it is also true that proteins are important components in chlorosomes. The sizes, sequences, and locations of chlorosomal proteins have been extensively studied, but the functions of these proteins are not known except in the case of the CsmA protein, which has recently been shown to be the BChl *a*-binding baseplate protein in *Chloroflexus* chlorosomes (see below).

Isolated chlorosomes from *Cf. aurantiacus* contain three major proteins, CsmA, CsmN and CsmM, with apparent molecular masses of 3.7, 11 and 18 kDa, as well as a minor component of 5.8 kDa (Feick and Fuller, 1984; Bryant, 1994). The amino acid sequence of CsmA has been chemically determined (Wechsler et al., 1985a) and the true mass is 5.7 kDa, which is in agreement with the deduced mass from the sequence of the *csmA* gene encoding this protein (Theroux et al., 1990). The genes for CsmN and CsmM also have been isolated and sequenced (Niedermeier et al., 1994) and the two polypeptides are 145 and 97 amino acids long and have true molecular masses of 15.5 and 10.8 kDa, respectively. These chlorosomal proteins are located in the lipid envelope, as demonstrated by gold labeling electron microscopy (Wullink et al., 1991).

In chlorosomes of green sulfur bacteria, Chung et al., (1994) found ten different polypeptides and Chung and Bryant (1996) identified five proteins as CsmA, CsmB, CsmC, CsmD, and CsmE as both genes and polypeptides. All of these five polypeptides are components of the chlorosome envelope by protease susceptibility mapping and agglutination experiments with isolated chlorosomes. No proteins have been shown to be located in the hydrophobic interior of chlorosomes. An additional five polypeptides were identified as CsmF, CsmH, CsmI, CsmJ, and CsmX and were also suggested to be envelope proteins (Vassilieva et al., 2000). Recent results by Vassilieva

et al. (2001) indicate that CsmI and CsmJ, and possibly also CsmX, contain FeS centers. The functions of these FeS centers are not yet known, but may possibly relate to the redox regulation of energy transfer in green sulfur bacteria described in Section III. Among all the known chlorosome proteins, CsmA is the only polypeptide that has significant similarity between green sulfur bacteria and *Chloroflexus*.

The CsmA protein was originally suggested to be involved in BChl *c* organization in chlorosomes of *Cf. aurantiacus* (Feick and Fuller, 1984; Wechsler et al., 1985a; Niedermeier et al., 1992; Lehmann et al., 1994a,b) and the green sulfur bacteria (Wagner-Huber et al., 1988, 1991). This was primarily based on the facts that CsmA is the most abundant protein in the chlorosomes and that the characteristic absorption band of BChl *c* around 740 nm is significantly decreased following proteolytic digestion of this protein. In a proposed model seven BChl *c* molecules coordinate to glutamine and asparagine residues (Wechsler et al., 1985a). However, proteins from several green sulfur bacteria that are similar to the CsmA protein were sequenced and none of the seven putative BChl *c* binding residues was found to be conserved (Wagner-Huber, 1988; Chung et al., 1994). The suggestion that the CsmA protein is a BChl *c*-binding protein has been replaced by the currently accepted view that BChl *c* in chlorosomes is organized by self-aggregation without proteins.

Chung et al. (1998) inactivated the *csmA* gene in the green sulfur bacterium *Chlorobium vibrioforme* and found that CsmA is required for the viability of the cells. CsmC, on the other hand, was found to be dispensable. The absence of CsmC caused a small red shift in the near-infrared absorption maximum of BChl *d* in whole cells and chlorosomes, but chlorosomes were assembled and could be isolated. The doubling time of the CsmC-deficient mutant was approximately twice that of the wild-type strain. Fluorescence emission measurements suggested that energy transfer from the bulk BChl *d* to another pigment, perhaps BChl *a*, emitting at 800–804 nm, was less efficient in the mutant cells lacking CsmC than in wild-type cells.

The functions of none of the chlorosomal proteins are known, with the exception of the CsmA protein, described below. Clearly, more research is needed to elucidate their functions. It is likely that some of these proteins are involved in chlorosome assembly.

#### D. The Chlorosome Baseplate

All chlorosomes contain a small amount of BChl *a* that absorbs at approximately 795 nm (Schmidt, 1980; Betti et al., 1982; Feick and Fuller, 1984; Gerola and Olson, 1986). In the green nonsulfur bacteria, the amount of this 'baseplate' BChl is about 1:20 compared to BChl *c* (Table 2). The green sulfur bacteria contain much less of this component. Sometimes it is difficult to observe in absorption spectra, but it is always apparent in fluorescence spectra of isolated chlorosomes (Causgrove et al., 1990). The excitation energy of the baseplate BChl is intermediate between the energies of the chlorosome and membrane chromophores, and the baseplate is almost certainly physically located at the interface between these two pigment pools, although this has not been shown directly. The nature of the baseplate is discussed below.

The minor Mr 5.8 kDa protein in *Chloroflexus* chlorosomes, whose sequence is still not known, was originally proposed as the binding site of the 795 nm baseplate BChl *a* that forms the link between the chlorosome and the membrane-associated pigment-proteins (Feick and Fuller, 1984). However, recent results (discussed below) (Sakuragi et al., 1999; Montañó et al., 2001a) clearly indicate that the 5.7 kDa CsmA protein forms the pigment-protein in the baseplate.

A specific BChl *a*-protein (795 nm) has been postulated in the envelope of chlorosomes as the baseplate to mediate energy transfer from BChl *c* to the FMO protein in green sulfur bacteria (Gerola and Olson 1986) and to the LH protein in *Chloroflexus*. The Q<sub>y</sub> absorption band of BChl *a* in the baseplate has a maximum at 795 nm, which is red shifted 25 nm compared to that of the monomeric form of this pigment in methanol, probably due to the pigment-protein interaction.

The baseplate complex in *Cf. aurantiacus* is clearly a pigment-protein complex, based on its spectroscopic properties and its sensitivity to protease digestion, SDS treatment, alkaline treatment (van Walree et al., 1999) and heating (Y. Zhu, D. Smith and R. E. Blankenship, unpublished). However, the most convincing evidence comes from the recent biochemical studies by Sakuragi et al. (1999) and Montañó et al., (2000), which conclusively establish the CsmA protein as part of the baseplate. Based on a series of experiments with proteolytic digestion, alkaline treatment and a treatment using hexanol,

sodium cholate and Triton X-100, it was strongly suggested that BChl *a* is associated with the CsmA protein in *Cf. aurantiacus* (Sakuragi et al., 1999). Following that study, the baseplate protein was isolated as the complex of the CsmA protein, BChl *a* and carotenoid (Montaño et al., 2001a).

A surprising finding in these studies is that there is a large amount of  $\beta$ -carotene in the purified baseplate preparation, with an estimated stoichiometry of 2-3  $\beta$ -carotene per BChl *a*. In addition, a previously unreported long-wavelength pigment form absorbing at 865 nm was found in the purified baseplate. Biochemical and spectroscopic evidence suggests that this band is not due to contamination from the B808-865 integral membrane antenna complex. Purification of the baseplate complex from green sulfur bacteria has not yet been reported.

The localization of the chlorosomal proteins has been investigated in chlorosomes from *Cf. aurantiacus* by immunogold labeling electron microscopy by Wullink et al. (1991). Their results suggested that CsmA is located in the chlorosome envelope, mainly on the side distal to the cytoplasmic membrane. Considering the function of BChl *a* as the mediator of excitation energy from BChl *c* in chlorosomes to the reaction centers in the cytoplasmic membranes, BChl *a* in chlorosomes and its associated protein are expected to be located at the region in contact with the cytoplasmic membrane. The immunolocalization findings are therefore surprising. A possible explanation for the apparent contradiction is that the location of CsmA might not be restricted to the attachment site of the chlorosome to the cytoplasmic membrane, or the arrangement of the chlorosome attachment site may have been distorted during cell breakage when the chlorosome preparations were made. More structural studies of the location of various chlorosome proteins are needed.

As described above, CsmA from green sulfur bacteria has a significant sequence homology to that from *Chloroflexus*. Two regions with sequences of G-H-W and I-N-R/Q-N-A-Y are highly conserved (Wagner-Huber et al., 1988; Wagner-Huber et al., 1991). The estimated molar ratio of BChl *a* to CsmA in *Cb. tepidum* was comparable to the ratio estimated in *Cf. aurantiacus* (Sakuragi et al., 1999). Therefore, it is reasonable to postulate that the CsmA protein is also involved in the BChl *a* organization in chlorosomes of green sulfur bacteria.

The conserved histidine residue in the CsmA protein is a very suitable candidate as a BChl *a*

ligand, as seen in the FMO protein (Tronrud et al., 1986; Li et al., 1997) as well as in other photosynthetic proteins including reaction centers and light-harvesting systems in purple bacteria.

### III. Redox-Dependent Regulation of Energy Transfer in Chlorosomes

#### A. Redox Regulation in Green Bacteria

A variety of lines of evidence suggest that a redox-dependent regulation of energy transfer occurs in green sulfur bacteria. Early work showed that the fluorescence emission intensity of green sulfur bacterial antennas is highly dependent on redox potential, which is not typical behavior of isolated photosynthetic antenna complexes (Karapetyan et al., 1980; van Dorssen et al., 1986a). Later work suggested a specific redox-activated regulation of energy transfer in the green sulfur bacteria (Blankenship et al., 1990, 1993; Wang et al., 1990). This effect appears to involve a direct chemical titration of redox groups in the chlorosome antennas, and is observed in whole cells, isolated membranes and purified chlorosomes. There is no indication of phosphorylation in this system, as the effect is easily observed in purified systems with no phosphorylation substrates present. In the oxidized form, the redox groups efficiently quench excited states in the antenna system, reducing the overall energy transfer efficiency from nearly 100% to 10% or less. Redox titrations of fluorescence in isolated chlorosomes gave a pH-dependent midpoint potential of -146 meV versus the normal hydrogen electrode (Blankenship et al., 1993). Additional work revealed a similar redox modulation in the isolated Fenna-Matthews-Olson (FMO) protein that underlies the chlorosome (Zhou et al., 1994). The effect therefore operates on at least two levels, within the chlorosome itself and in the FMO protein. Whether these two effects have similar molecular mechanisms is not yet clear. Recent work has provided a likely molecular mechanism involving quinones for the redox control effect in chlorosomes. This is discussed in more detail in the next section.

Do these redox effects on the antenna system reflect a real cellular control mechanism? Such an effect could serve to protect the cell from transient exposure to oxidizing conditions, in particular to oxygen. The green sulfur bacteria contain a reaction center that has very low-potential iron sulfur centers



as early acceptors and reduces ferredoxin directly in a manner similar to Photosystem I (Feiler and Hauska, 1995). The reduced ferredoxin diffuses freely in the cytoplasm and is utilized in the cell's carbon reduction cycle, which is a reverse TCA cycle (Buchanan and Arnon, 1990; Sirevåg, 1995). The reduced ferredoxins will readily react with oxygen to form superoxide, which leads to a variety of damaging photooxidative products. By preventing charge separation under oxygenic conditions by quenching excitations in the antenna system, green bacterial cells avoid producing these toxic substances. Thus, they appear to have a system that permits them to survive transient exposures to oxygen without incurring irreversible cellular damage. While this proposed mechanism of cellular protection is appealing in many ways, it has not been directly demonstrated and remains an area in need of further study.

Green sulfur bacteria are found in a variety of environments, often just below the chemocline in stratified lakes (Trüper and Pfennig, 1992; Ormerod, 1992). The chemocline is the transition between the oxygenated water near the surface and the anaerobic water deeper in the lake. Sulfide levels are very low above the chemocline and higher below it. The chemocline represents the transition from oxidizing to reducing conditions. Under these conditions cells will be exposed occasionally to moderate oxygen levels and a mechanism that provided even partial protection from oxidative damage would be of enormous adaptive advantage.

The redox effects are missing in whole cells and are much diminished in isolated chlorosomes of the green nonsulfur bacterium *Chloroflexus aurantiacus* (Wang et al., 1990; Frigaard and Matsuura, 1999). *Chloroflexus* has an entirely different physiology and ecology with respect to oxygen. *Chloroflexus* usually lives in close proximity to cyanobacteria, and therefore is often under aerobic, even hyperoxic conditions (Pierson and Castenholz, 1992; Ormerod, 1992). If the same redox control mechanism that is found in the green sulfur bacteria were present in *Chloroflexus*, it would severely limit their ability to carry out photosynthesis under aerobic conditions. However, *Chloroflexus* is not vulnerable to oxidative damage in the same way that the green sulfur bacteria are, because its reaction center does not directly reduce ferredoxin. Its carbon reduction cycle, while not fully understood, clearly does not involve free ferredoxin as does the reverse TCA cycle (Sirevåg, 1995). Therefore, a redox modulation effect similar

to that found in the green sulfur bacteria would provide no selective advantage for *Chloroflexus*, and actually would prevent them from carrying out photosynthesis under most natural conditions.

### B. Quinones: A Newly Found Component in Chlorosomes

Isoprenoid quinones were recently found to occur in chlorosomes (Frigaard et al., 1997). Chlorosomes of *Chlorobium tepidum* contain significant amounts of chlorobiumquinone (1'-oxomenaquinone-7) and menaquinone-7 (MK-7). The molecular structures of these quinones are shown in Fig. 3. MK-10 is present in chlorosomes of the green filamentous bacterium *Chloroflexus aurantiacus* (Frigaard et al., 1997). The molar ratio of total quinone to BChl *c* in the chlorosomes is approximately 1:10 (Table 2). Most of the chlorobiumquinone and part of the MK-7 in the green sulfur bacteria *Chlorobium tepidum* and *Chlorobium phaeobacteroides* are located in the chlorosomes (Frigaard et al., 1997).

Chlorobiumquinone and MK-7 are the major isoprenoid quinones in many species of green sulfur bacteria and probably are present in all representatives of this group (Imhoff and Bias-Imhoff, 1995). Chlorobiumquinone was detected in green sulfur bacteria more than 30 years ago and was proposed to be involved in photosynthetic electron transfer; but little was known about its function or intracellular location (Frydman and Rappaport, 1963; Powls et al., 1968; Redfearn and Powls, 1968; Powls and Redfearn, 1969). Chlorobiumquinone has not been

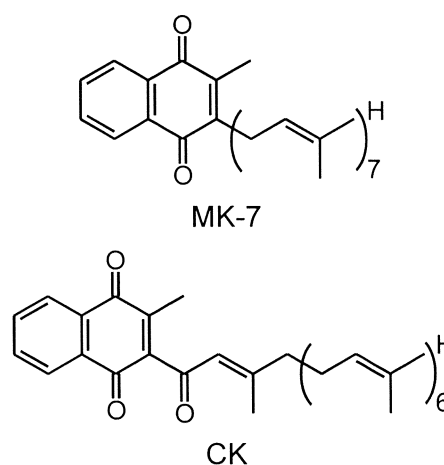


Fig. 3. Molecular structures of menaquinone-7 (MK-7) and chlorobiumquinone (CK) found in green sulfur bacteria.



found in any group of organisms other than green sulfur bacteria.

Isoprenoid quinones are very hydrophobic and presumably are located in the interior of the chlorosomes rather than in the chlorosome envelope. This was confirmed by SDS treatment of chlorosomes, which extracts envelope components without affecting the BChl *c* organization in the hydrophobic interior (Frigaard et al., 1998). SDS does not extract any quinones from chlorosomes of either *Cb. tepidum* or *Cf. aurantiacus*.

To identify the redox species that quenches fluorescence, a pigment-lipid aggregate consisting of BChl *c* and galactolipid in aqueous solution was used (Frigaard et al., 1997). The redox effect on BChl *c* emission in the BChl *c*-galactolipid aggregates was small, but was enhanced if chlorobiumquinone was added before the aggregates were made. Oxidized chlorobiumquinone was suggested to act as the quencher of BChl *c* fluorescence.

Although chlorobiumquinone is an effective quencher, other quenchers may also be important. Menaquinones are also present in chlorosomes of green sulfur bacteria and show a quenching effect in the BChl *c*-galactolipid aggregates. Menaquinone is the sole quinone component in *Chloroflexus* chlorosomes as described above, and small redox effects on the fluorescence intensity can be observed in *Chloroflexus* chlorosomes. Even in the absence of quinones, BChl *c*-galactolipid aggregates show redox-dependent fluorescence changes. Van Noort et al. (1997) have described redox effects on excited-state lifetimes in BChl *c* oligomers in hexane. From EPR measurements on reduced and oxidized samples, BChl *c* radicals in the oxidized BChl *c* oligomers were suggested to act as quenchers.

The presence of the different quenching mechanisms was also observed when freeze-dried chlorosomes from *Cb. tepidum* were extracted with hexane to remove carotenoids, BChl *a* and quinones. The BChl *c* aggregates remained intact in the hexane-extracted chlorosomes as judged from the absorption spectrum, but the BChl *c* fluorescence under oxidizing conditions increased 3-fold and the ratio of the BChl *c* fluorescence under reducing conditions to the fluorescence under oxidizing conditions ( $F_{\text{red}}/F_{\text{ox}}$ ) decreased from 40 to about 3. The extracted components are thus not necessary for BChl *c* aggregation but are likely to be involved in formation of a redox-dependent excitation quencher. The  $F_{\text{red}}/F_{\text{ox}}$  ratio in BChl *c*-galactolipid aggregates in an

aqueous buffer also is about 3 (Frigaard et al., 1997; van Noort et al., 1997). Thus, a  $F_{\text{red}}/F_{\text{ox}}$  ratio of about 3 is probably a property of pure BChl *c* aggregates. This value is also close to the BChl *c*  $F_{\text{red}}/F_{\text{ox}}$  ratio found in *Chloroflexus* chlorosomes and hexanol-treated *Chlorobium* chlorosomes.

As described above, the midpoint potential ( $E_m$ ) of the major fluorescence quenching in chlorosomes from *Chlorobium vibrioforme* is approximately -150 mV at pH 7 (one-electron reaction) and decreases by 60 mV per pH unit, indicating that one proton is taken up along with the electron (Blankenship et al., 1990, 1993). This  $E_m$  is significantly lower than the  $E_m$  of chlorobiumquinone in ethanol, 39 mV at pH 7 (Redfearn and Powls, 1968). However, the  $E_m$  values of the quinones in ethanol refer to a two-electron reaction whereas the  $E_m$  of chlorosomal fluorescence quenching refers to a one-electron reaction. The chlorobiumquinones in the chlorosomes may be located in a specific environment where they interact with aggregated BChl *c*. It is possible that the  $E_m$  of chlorosomal fluorescence quenching reflects the  $E_m$  of a semiquinone/oxidized quinone couple or of a chlorobiumquinone-BChl *c* radical complex. A function of the 1'-oxo group in the chlorobiumquinone molecule may be to stabilize such a semiquinone or a complex species.

The physiological significance of the fluorescence quencher on energy transfer from chlorosomes to the reaction center was directly shown from flash-induced electron transfer reactions (Frigaard and Matsuura 1999). The primary electron donor to the reaction center in green sulfur bacteria is a bound cytochrome *c*. Light energy absorbed by the BChl *c* antenna is transferred to the reaction center via baseplate BChl *a* and FMO proteins. Measurements of flash-induced cytochrome *c* oxidation in whole cells of *Cb. tepidum* showed that energy transfer from the BChl *c* was highly inhibited under aerobic conditions. When BChl *c* was selectively excited, the half-saturation light intensity for cytochrome *c* photooxidation increased about 30-fold under aerobic conditions compared to anaerobic conditions (Fig. 4a). Such a redox effect was not observed when BChl *a* (mainly in FMO proteins) was excited (Fig. 4b). Thus, the fluorescence quenching mechanism in chlorosomes of green sulfur bacteria regulates energy transfer from the major light-harvesting pigment to the reaction center.

Although *Chloroflexus* chlorosomes also show a small fluorescence quenching under oxidizing

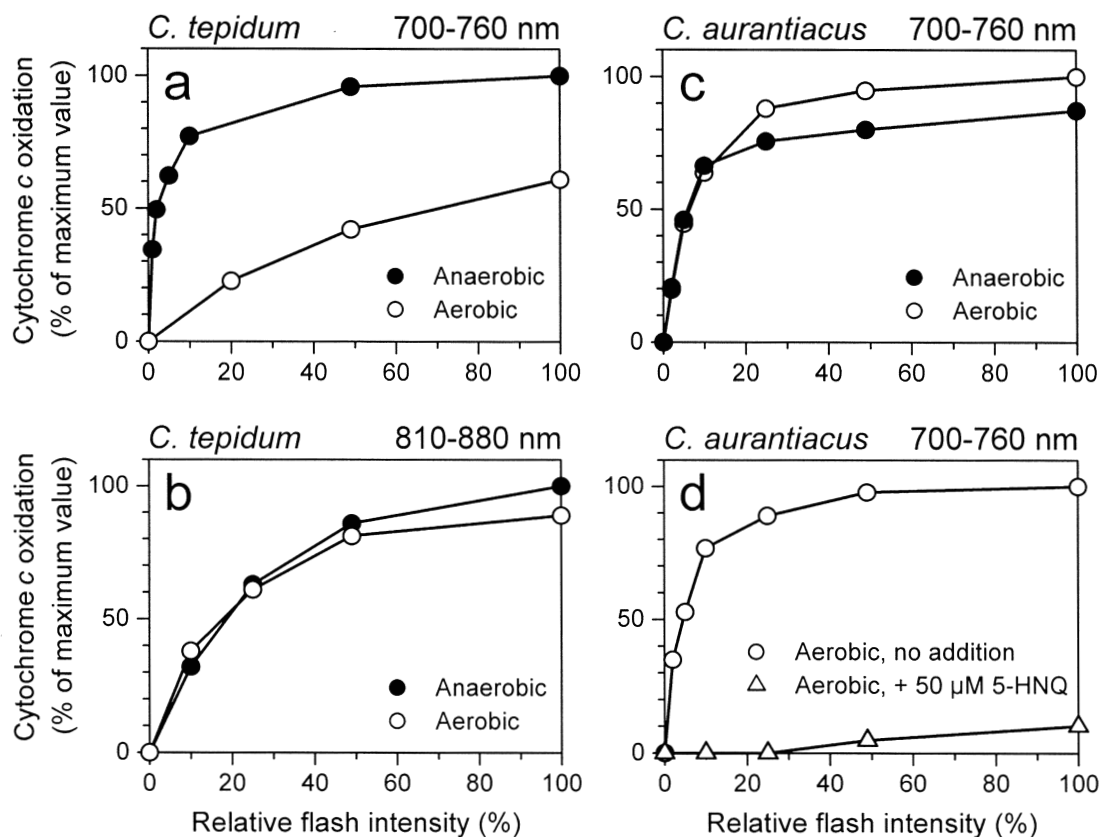


Fig. 4. Effects of environmental redox states on energy transfer from chlorosomes to the reaction center measured by flash-induced oxidation of cytochrome *c* as a function of flash intensity. (a) *Chlorobium tepidum* cells excited at 700–760 nm (wavelengths absorbed by chlorosomes) under aerobic or anaerobic conditions. (b) *Chlorobium tepidum* cells excited at 810–880 nm (wavelengths absorbed by FMO proteins and the reaction centers). (c) *Chloroflexus aurantiacus* cells excited with light absorbed by chlorosomes. (d) *Chloroflexus aurantiacus* cells excited under aerobic conditions with light absorbed by chlorosomes in the presence and absence of externally added 5-hydroxy-1,4-naphthoquinone.

conditions as described above, cytochrome *c* photooxidation was not affected by the transition from anaerobic to aerobic conditions even when BChl *c* was excited (Fig. 4c). This means that the redox-dependent change in the fluorescence intensity in *Chloroflexus* chlorosomes is independent of the energy flow from chlorosomes to the reaction center. However, the addition of low concentrations of certain quinones (e.g. 5-hydroxy-1,4-naphthoquinone) to *Chloroflexus* cells under aerobic conditions induces a quenching of the BChl *c* fluorescence and inhibits photosynthetic electron transfer when BChl *c* is specifically excited (Fig. 4d) (Frigaard et al., 1999). Addition of quinones thus causes the chlorosomal energy transfer in *Chloroflexus aurantiacus* to exhibit a sensitivity to  $O_2$  similar to that observed in green sulfur bacteria. To have a large quenching effect the

quinone must be sufficiently hydrophobic and have a carbonyl or hydroxyl group in the alpha position to one of the quinone oxygen atoms (Frigaard et al., 1999; Tokita et al., 2000). Since chlorobiumquinone (1'-oxomonaquinone-7) has such a structure, it is highly probable that chlorobiumquinone is the physiological quencher that mediates the regulation of energy transfer from BChl *c* to the reaction center in green sulfur bacteria.

#### IV. Fenna-Matthews-Olson Protein

A water-soluble protein that contains BChl *a* was isolated and extensively characterized by John Olson and co-workers (Olson, 1966, 1978, 1980a,b, 1998). The X-ray structure of this protein was determined

by Roger Fenna and Brian Matthews (Fenna and Matthews, 1975; Matthews et al., 1979; Matthews and Fenna, 1980; Tronrud et al., 1986; Tronrud and Matthews, 1993). The protein has come to be known as the Fenna-Matthews-Olson or FMO protein, although it is also often called the BChl *a* protein. The FMO protein was the first chlorophyll-containing protein to have its structure determined. Much of what we know about how chlorophyll-type pigments interact with proteins has been learned from studies of this protein.

The structure of the FMO protein has been determined from two species of green sulfur bacteria, *Prosthecochloris aestuarii* 2K and *Chlorobium tepidum* (Tronrud et al., 1986, 1993; Li et al., 1997). Figure 5 shows the structure of the FMO protein from *Chlorobium tepidum*. The FMO protein consists of primarily  $\beta$ -sheet secondary structure, with 17  $\beta$ -sheets wrapped into a 'taco shell' structure. Seven molecules of BChl *a* are inside the shell. Each BChl *a* molecule has a unique binding site within the protein so that they are all inequivalent. Five of them are coordinated to histidine residues, one to a backbone carbonyl and one to a structured water molecule. The protein has a trimeric quaternary structure, with a threefold axis of symmetry in the center of the complex. The subunits are held together primarily by salt linkages and other polar interactions (Li et al., 1997).

The FMO protein has been studied intensely by spectroscopic (Philipson and Sauer, 1972; Johnson and Small, 1991; Savikhin and Struve, 1994; Savikhin et al., 1994b, 1997, 1998; van Mourik et al., 1994; Reddy et al., 1995; Freiberg et al., 1997; Louwe et al., 1997a, 1998; Vulto et al., 1997, 1998a; Franken et al., 1998; Rätsep et al., 1998, 1999; Matsuzaki et al., 2000; Wendling et al., 2000) and theoretical methods (Pearlstein, 1992; Gülen, 1996; Louwe et al., 1997b; Vulto et al., 1998b, 1999; Renger and May, 1998; Iseri and Gülen, 1999; Owen and Hoff, 2001). In pioneering early theoretical work, Pearlstein and coworkers (Pearlstein and Hemenger, 1978; Whitten et al., 1980; Pearlstein, 1992; Lu and Pearlstein, 1993) estimated the strength of the exciton coupling among the pigments both within a protein monomer and between monomers in the trimeric complex and proposed that the lowest energy pigment is pigment #7 in the Fenna and Matthews numbering system. Attempts to simulate the absorption and CD spectra of the FMO complex were only partially successful.

The view of the electronic properties of this well-

studied complex has changed dramatically in the past several years. The lowest energy BChl is now almost conclusively identified as #3. In addition, the strength of excitonic coupling among the seven pigments is now considered to be weaker than was previously thought, so that some of the near IR absorption transitions are largely localized on a single molecule instead of primarily delocalized over several molecules (Louwe et al., 1997a,b; Vulto et al., 1998b; Iseri and Gülen, 1999).

FMO complexes have been isolated from a number of green sulfur bacteria and all appear to be highly similar, although subtle spectral differences are found, especially in the low temperature absorption and CD spectra (Francke and Ames, 1997). The precise structural differences that lead to these spectral differences are not yet understood. The amino acid sequences of the FMO proteins from *Prosthecochloris aestuarii* 2K and *Chlorobium tepidum* are 78% identical (Daurat-Larroque et al., 1986; Dracheva et al., 1992).

The FMO protein is thought to be located between the chlorosome and the cytoplasmic membrane. Electron microscopic studies have revealed a paracrystalline array with periodicity of 6 nm (Staehelin et al., 1980). However, the characteristic trimeric structure of the FMO was not resolvable in these studies and whether this crystalline array is actually the FMO protein has not been directly demonstrated with immunolabeling. The quantitative information now available suggests that it may not be the FMO protein (Remigy et al., 1999; Permentier et al., 2000).

Linear dichroism spectroscopy was used to demonstrate that the threefold symmetry axis of the trimeric FMO complex is oriented perpendicular to the surface of the membrane, so that the disk-like complex lies flat on the membrane (Melkozernov et al., 1998). This arrangement is consistent with electron microscopy studies of the isolated reaction center complex from *Chlorobium tepidum*, which has associated FMO protein (Remigy et al., 1999). These studies as well as biochemical analysis (Permentier et al., 2000) suggest that two FMO molecules are tightly associated with each reaction center complex. It is thus surprising that the FMO protein is readily isolated from green sulfur bacteria under relatively mild conditions. This raises the possibility that there are two distinct pools of FMO protein, one tightly associated with the reaction center and one that is not. The *Cb. tepidum* genome contains

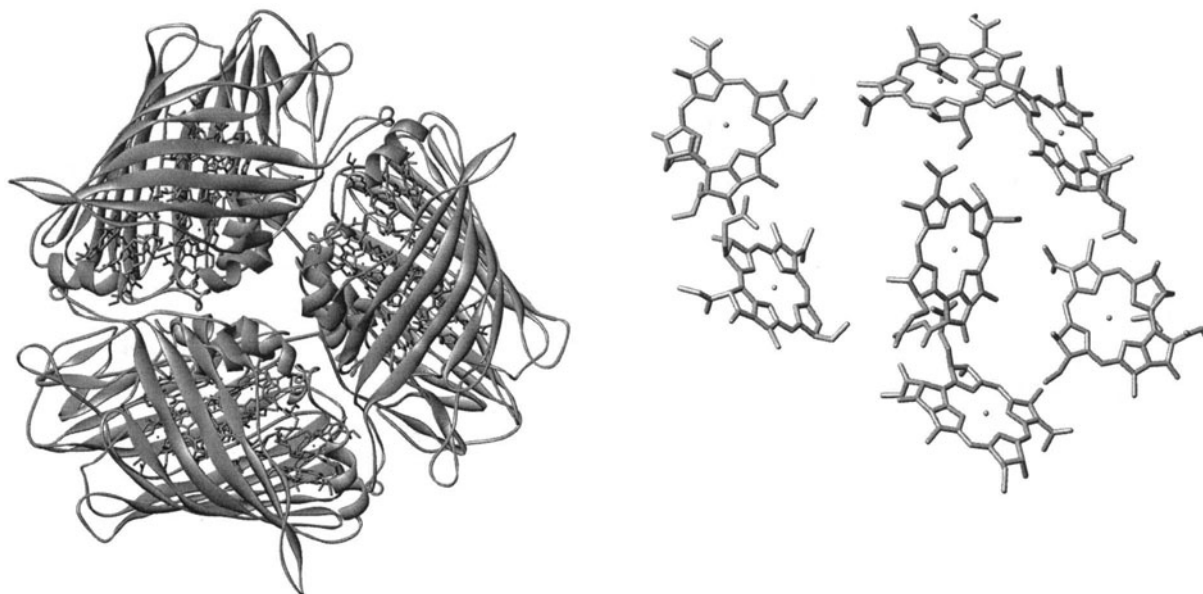


Fig. 5. Structure of the Fenna-Matthews-Olson protein from *Chlorobium tepidum* as determined by Li et al. (1997). (Left) Ribbon diagram of the structure of the trimer of the FMO protein, including protein and bacteriochlorophyll *a* pigments. (Right) View of the pigment arrangement in one subunit. The phytyl tails of the bacteriochlorophyll *a* molecules have been omitted for clarity. Figure produced from Protein Data Bank file 1KSA using Web Lab Viewer from Molecular Simulations, Inc.

only a single FMO gene (D. Bryant, personal communication), so there are not distinct but similar gene products. However, post-translational modification of the FMO protein could cause some molecules to associate preferentially with the reaction center. More quantitative data on the amounts of FMO protein in cells and various biochemical preparations as well as more detailed biochemical and structural analysis of the two pools of FMO proteins would be useful.

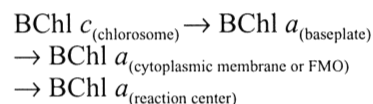
Li et al. (1997) proposed that the FMO protein is partially buried in the membrane and suggested, on the basis of somewhat different hydrophobicities of the two surfaces of the protein, that one side is buried in the membrane and the other is in contact with the chlorosome. However, both the membrane-associated and chlorosome-associated surfaces are likely to be hydrophobic and the hydrophobicity differences of the surfaces of the two sides of the trimeric protein complex do not differ greatly, so this assignment remains tentative.

The FMO protein appears to be an essential cell component, as attempts to delete it genetically have to date proven lethal (Zhou, 1995; Hu, 2001). A major difficulty in constructing mutants of green

sulfur bacteria is the fact that these organisms are obligate photoautotrophs (Trüper and Pfennig, 1992) and if photosynthesis is significantly disrupted the organisms do not survive. Efforts to establish heterotrophic growth conditions for the green sulfur bacteria have so far proven unsuccessful.

## V. Kinetics and Pathways of Energy Transfer in Chlorosomes and Membranes of Green Bacteria

The overall energy transfer pathway of green bacteria follows the sequence:



Each successive pigment species has progressively red-shifted absorption and fluorescence spectra. The descending energy levels thus provide a 'funneling' of excitations into the reaction center. Several research groups studied the kinetics of energy transfer by steady-state and time-resolved fluorescence and

absorption techniques, and a generally consistent picture has emerged. This is reviewed in van Grondelle et al., 1994; Blankenship et al., 1995; Olson, 1998 and is not considered here in detail. The data support a sequential energy transfer pathway from the BChl *c* (*d* or *e*) pigments in the body of the chlorosome to the baseplate to the membrane-bound antenna complexes and finally to the reaction centers. However, most of these measurements did not have high enough time resolution to reveal ultrafast components that have been observed in chlorosomes from both *Chloroflexus* and *Cb. tepidum* (Savikhin et al., 1994a; Savikhin et al., 1995, 1996). These components complicate the picture of the energy transfer system significantly and need to be further investigated.

Because the chlorosome antenna is so large, it seems likely that 'tuning' of the pigment absorption into an energetic gradient within the chlorosome is important for ensuring that the overall efficiency of energy collection is high. There are now some indications from a variety of sources that this is indeed the case (Holzwarth et al., 1990b; Griebenow et al., 1991; Lin et al., 1991; Matsuura et al., 1993; Steensgaard et al., 1999, 2000).

There have not been any reports of the kinetics of energy transfer from carotenoid to BChl in chlorosomes. Early steady-state measurements indicated that the efficiency of energy transfer was 55%, although the interpretation was made that the carotenoid transferred energy primarily to BChl *c* (van Dorssen et al., 1986b). More recent measurements have given generally similar values of 50–80% (Melø et al., 2000). However, it now appears that there are two pools of carotenoid in chlorosomes, part in the main body that is expected to transfer to BChl *c* and part in the baseplate that is expected to transfer directly to BChl *a* (see above). This issue needs to be reinvestigated with new preparations. Ultrafast measurements with higher time resolution are needed to resolve the carotenoid-to-BChl energy transfer, which is usually in the femtosecond time regime. Recent measurements on triplet quenching in chlorosomes suggest that carotenoids can quench BChl *a* triplets, which supports the view that a significant fraction of the carotenoid is closely associated with the BChl *a* in the baseplate (Melø et al., 2000; Carbonera et al., 2001). Similar conclusions were reached by Arellano et al. (2000a) using the BChl *e* containing organism *Chlorobium phaeobacterioides*.

The kinetics and efficiency of energy transfer from the FMO protein to the reaction center in green sulfur bacteria are poorly understood. The close structural arrangement of FMO and reaction center, which most investigators agree must be present, suggests that there should be a rapid and efficient energy transfer between the two complexes. However, the FMO protein is unable to transfer energy to the reaction center in isolated FMO-RC complexes (Ohoka et al., 1998; Neerken et al., 1998). One possible explanation of this result is that the complexes are somehow damaged during preparation and the relative geometrical arrangement disrupted so that energy transfer is inhibited, although the complexes are still tightly bound to each other. While this possibility cannot be ruled out, it seems unlikely, especially since the efficiency of energy transfer from FMO to reaction center also is low in subcellular membrane preparations (Francke et al., 1996). Another possible explanation might be that the redox regulation that is seen in the chlorosome also occurs in the FMO protein (see above). It may be that the redox conditions of these measurements were not optimal for high efficiency of energy transfer. This issue remains to be resolved.

## VI. Conclusions and Future Work

Our understanding of the structure and function of chlorosomes advanced dramatically in the last 10 years of the 20th century. It seems clear now that the major light-harvesting pigment, BChl *c* (*d* or *e*) is organized into the functional structure by self-aggregation of pigment molecules without binding to proteins. The aggregate structure is unique among all photosynthetic antenna systems, and makes a very dense package of chlorophyll molecules possible. Redox-dependent regulation of energy transfer in chlorosomes of green sulfur bacteria is another unique characteristic. Chlorobiumquinone, which is found only in green sulfur bacteria among all organisms, is located almost solely in chlorosomes and is largely responsible for the redox-dependent energy-transfer regulation. Most chlorosomal proteins were sequenced and one of them, CsmA found in both green bacterial groups, was shown to bind BChl *a* to form the baseplate that functionally connects chlorosomes to the membrane. With the quinones and proteins, all the major components in chlorosomes are now identified. The FMO protein,

which transfers excited energy from the baseplate to the membrane in green sulfur bacteria, is tightly bound to the reaction center complex.

In spite of the clarification of these important points, many problems remain to be solved. Information on the structure of the baseplate pigment-protein complex is especially needed, since this complex is essential for efficient energy transfer from the chlorosome antenna to the membrane. The detailed structural arrangement of BChl *c* molecules in chlorosomes also needs to be clarified. The observation that the chlorophyll forms in chlorosomes appear to be heterogeneous suggests that there may be a family of aggregated pigment structures that differ in detail. The roles of the minor BChl *c* forms in energy transfer need elucidating, and the kinetics of energy transfer among the various components must be measured and analyzed theoretically. The dense aggregates of large numbers of chlorophyll molecules could lend themselves to a physical mechanism of energy transfer that is unique among the photosynthetic antenna.

Little is known about biosynthesis and assembly of chlorosomes; for example, we do not know whether chlorosomes can divide into daughter chlorosomes or are newly assembled without parent chlorosomes. Evolutionary relationships between chlorosomes of the two groups of green bacteria should be clarified soon based on the sequences of the whole genomes of representatives from both groups. The origin of the unique antenna, the chlorosome, also may be clarified in relation to the early evolution of photosynthesis. Industrial applications of antenna systems without proteins is another important field to be studied, and could lead to improved, or even radically new devices for solar energy capture.

## Acknowledgment

We thank Dr. N.-U. Frigaard for the preparation of Figs. 3 and 4 and information on chlorosomal quinones and proteins.

## References

- Arellano JB, Melø TB, Borrego CM, Garcia-Gil J and Naqvi KR (2000a) Nanosecond laser photolysis studies of chlorosomes and artificial aggregates containing bacteriochlorophyll *e*: Evidence for the proximity of carotenoids and bacteriochlorophyll *a* in chlorosomes from *Chlorobium phaeobacteroides* strain CL1401. *Photochem Photobiol* 72: 669–675
- Arellano JB, Psencik J, Borrego CM, Ma YZ, Guyoneaud R, Garcia-Gil J and Gillbro T (2000b) Effect of carotenoid biosynthesis inhibition on the chlorosome organization in *Chlorobium phaeobacteroides* strain CL1401. *Photochem Photobiol* 71: 715–723
- Balaban TS, Holzwarth AR, Schaffner K, Boender GJ, Degroot HJM (1995) CP-MAS C-13-nmr dipolar correlation spectroscopy of C-13-enriched chlorosomes and isolated bacteriochlorophyll-*c* aggregates of *Chlorobium tepidum*—the self-organization of pigments is the main structural feature of chlorosomes. *Biochemistry* 34:15259–15266
- Barkigia KM, Melamed D, Sweet RM, Smith KM and Fajer J (1997) Self-assembled zinc pheoporphyrin dimers. Models for the supramolecular antenna complexes of green photosynthetic bacteria? *Spectrochimica Acta A* 53: 463–469
- Betti JA, Blankenship RE, Natarajan LV, Dickinson LC and Fuller RC (1982) Antenna organization and evidence for the function of a new antenna pigment species in the green photosynthetic bacterium *Chloroflexus aurantiacus*. *Biochim Biophys Acta* 680: 194–201
- Blankenship RE (1992) Origin and early evolution of photosynthesis. *Photosynth Res* 33: 91–111
- Blankenship RE, Wang J, Causgrove TP and Brune DC (1990) Efficiency and kinetics of energy transfer in chlorosome antennas from green photosynthetic bacteria. In: Baltscheffsky M (ed) *Current Research in Photosynthesis*, Vol II, pp 17–24. Kluwer Academic Publishers, Dordrecht
- Blankenship RE, Cheng PL, Causgrove TP, Brune DC, Wang SHH, Choh JU and Wang J (1993) Redox regulation of energy transfer efficiency in antennas of green photosynthetic bacteria. *Photochem Photobiol* 57: 103–107
- Blankenship RE, Olson JM and Miller M (1995) Antenna complexes from green photosynthetic bacteria. In: Blankenship RE, Madigan MT and Bauer CE (eds) *Anoxygenic Photosynthetic Bacteria*, pp 399–435. Kluwer Academic Publishers, Dordrecht
- Bobe FW, Pfennig N, Swanson KL and Smith KM (1990) Red shift of absorption maxima in chlorobiineae through enzymic methylation of their antenna bacteriochlorophylls. *Biochemistry* 29: 4340–4348
- Boomer SM, Pierson BK, Austinhirst R and Castenholz RW (2000) Characterization of novel bacteriochlorophyll-*a*-containing red filaments from alkaline hot springs in Yellowstone National Park. *Arch Microbiol* 174: 152–161 SEP
- Brune DC, Nozawa T and Blankenship RE (1987) Antenna organization in green photosynthetic bacteria. I. Oligomeric bacteriochlorophyll *c* as a model for the 740 nm-absorbing bacteriochlorophyll *c* in *Chloroflexus aurantiacus* chlorosomes. *Biochemistry* 26: 8644–8652
- Bryant DA (1994) Gene nomenclature recommendations for green photosynthetic bacteria and heliobacteria. *Photosynth Res* 41: 27–28
- Buchanan BB and Arnon DI (1990) A reverse Krebs cycle in photosynthesis—Consensus at last. *Photosynth Res* 24: 47–53
- Büttner M, Xie D-L, Nelson H, Pinther W, Hauska G and Nelson N. (1992) Photosynthetic reaction center genes in green sulfur bacteria and in Photosystem I are related. *Proc Natl Acad Sci USA* 89: 8135–8139
- Bystrova MI, Mal'gosheva IN and Krasnovskii AA (1979) Study

Arellano JB, Melø TB, Borrego CM, Garcia-Gil J and Naqvi KR (2000a) Nanosecond laser photolysis studies of chlorosomes and artificial aggregates containing bacteriochlorophyll *e*: Evidence for the proximity of carotenoids and bacteriochlorophyll *a* in chlorosomes from *Chlorobium phaeo-*

- of molecular mechanism of self-assembly of aggregated forms of BChl *c*. *Mol Biol (English Trans)* 13: 582–594
- Carbonera D, Bordignon E, Giacometti G, Agostini G, Vianelli A and Vannini C (2001) Fluorescence and absorption detected magnetic resonance of chlorosomes from green bacteria *Chlorobium tepidum* and *Chloroflexus aurantiacus*. A comparative study. *J Phys Chem. B* 105: 246–255
- Causgrove TP, Brune DC, Wang J, Wittmershaus BP and Blankenship RE (1990) Energy transfer kinetics in whole cells and isolated chlorosomes of green photosynthetic bacteria. *Photosynth Res* 26: 39–48
- Chiefari J, Griebenow K, Balaban TS, Holzwarth AR and Schaffner K (1995) Models for the pigment organization in the chlorosomes of photosynthetic bacteria—Diastereoselective control of in-vitro Bacteriochlorophyll-C(S) aggregation. *J Phys Chem* 99: 16194–16194
- Chung S and Bryant DA (1996) Characterization of *csmA* genes, encoding a 7.5-kDa protein of the chlorosome envelope, from the green sulfur bacteria *Chlorobium vibrioforme* 8327D and *Chlorobium tepidum*. *Arch Microbiol* 166:234–244
- Chung S, Frank G, Zuber H and Bryant DA (1994) Genes encoding two chlorosome components from the green sulfur bacteria *Chlorobium vibrioforme* strain 83271D and *Chlorobium tepidum*. *Photosynth Res* 41: 261–275
- Chung SH, Shen GZ, Ormerod J and Bryant DA (1998) Insertional inactivation studies of the *csmA* and *csmC* genes of the green sulfur bacterium *Chlorobium vibrioforme* 8327: The Chlorosome protein *csmA* is required for viability but *csmC* is dispensable. *FEMS Lett* 164: 353–361
- Cogdell RJ, Isaacs NW, Howard TD, McLuskey K, Fraser NJ and Prince SM (1999) How photosynthetic bacteria harvest solar energy. *J Bacteriol* 181: 3869–3879
- Cox RP, Miller M, Aschenbrucker J, Ma Y-Z and Gillbro T (1998) The role of bacteriochlorophyll *e* and carotenoids in light harvesting in brown-colored green sulfur bacteria. In: Garab G (ed) *Photosynthesis: Mechanism and Effects*, Vol I, pp 149–152, Kluwer Academic Publishers, Dordrecht
- Daurat-Larroque ST, Brew K and Fenna RE (1986) The complete amino acid sequence of a bacteriochlorophyll *a*-protein from *Prosthecochloris aestuarii*. *J Biol Chem* 261: 3607–3615
- Dracheva S, Williams JC and Blankenship RE (1992) Cloning and sequencing of the FMO-protein gene from *Chlorobium tepidum*. In: Murata N (ed) *Research in Photosynthesis*, pp 53–56. Kluwer Academic Publishers, Dordrecht
- Feick RG and Fuller RC (1984) Topography of the photosynthetic apparatus of *Chloroflexus aurantiacus*. *Biochemistry* 23: 3693–3700
- Feick R, Shiozawa JA and Ertlmaier A (1995) Biochemical and spectroscopic properties of the reaction center of the green filamentous bacterium *Chloroflexus aurantiacus*. In: Blankenship RE, Madigan MT and Bauer CE (eds) *Anoxygenic Photosynthetic Bacteria*, pp 699–708. Kluwer Academic Publishers, Dordrecht
- Feiler U and Hauska G (1995) The reaction center from green sulfur bacteria. In: Blankenship RE, Madigan MT and Bauer CE (eds) *Anoxygenic Photosynthetic Bacteria*, pp 665–685. Kluwer Academic Publishers, Dordrecht
- Fenna RE, Matthews BW (1975) Chlorophyll arrangement in a bacteriochlorophyll protein from *Chlorobium limicola*. *Nature* 258: 573–577
- Fetisova ZG, Kharchenko and Abdourakhmanov IA (1986) Strong orientational ordering of the near-infrared transition moment vectors of light-harvesting antenna bacterioviridin in chromatophores of the green photosynthetic bacterium *Chlorobium limicola*. *FEBS Lett* 199: 234–236
- Fetisova ZG, Freiberg AM and Timpmann KE (1988) Long-range molecular order as an efficient strategy for light harvesting in photosynthesis. *Nature* 334: 633–634
- Franke C and Ames J (1997) Isolation and pigment composition of the antenna system of four species of green sulfur bacteria. *Photosynth Res* 52: 137–146
- Franke C, Otte SCM, Miller M, Ames J and Olson JM (1996) Energy transfer from carotenoid and FMO protein in subcellular preparations from green sulfur bacteria. Spectroscopic characterization of an FMO-reaction center core complex at low temperature. *Photosynth Res* 50: 71–77
- Franken EM, Neerken S, Louwe RJW, Ames J and Aartsma TJ (1998) A permanent hole burning study of the FMO antenna complex of the green sulfur bacterium *Prosthecochloris aestuarii*. *Biochemistry* 37: 5046–5051
- Freiberg A, Lin S, Timpmann K and Blankenship RE (1997) Exciton dynamics in FMO bacteriochlorophyll protein at low temperatures. *J Phys Chem B* 101: 7211–7220
- Frigaard NU and Matsuura K (1999) Oxygen uncouples light absorption by the chlorosome antenna and photosynthetic electron transfer in the green sulfur bacterium *Chlorobium tepidum*. *Biochim Biophys Acta* 1412: 108–117
- Frigaard NU, Takaichi S, Hirota M, Shimada K and Matsuura K (1997) Quinones in chlorosomes of green sulfur bacteria and their role in the redox-dependent fluorescence studied in chlorosome-like bacteriochlorophyll *c* aggregates *Arch Microbiol* 167: 343–349
- Frigaard NU, Matsuura K, Hirota M, Miller M and Cox RP (1998) Studies of the location and function of isoprenoid quinones in chlorosomes from green sulfur bacteria. *Photosynth Res* 58: 81–90
- Frigaard N, Tokita S and Matsuura K (1999) Exogenous quinones inhibit photosynthetic electron transfer in *Chloroflexus aurantiacus* by specific quenching of the excited bacteriochlorophyll *c* antenna. *Biochim Biophys Acta* 1413: 108–116
- Frydman B and Rappaport H (1963) Non-chlorophyllous pigments of *Chlorobium thiosulfatophilum*—chlorobiumquinone. *J Am Chem Soc* 85: 823–825
- Gerola PD and Olson JM (1986) A new bacteriochlorophyll alpha-protein complex associated with chlorosomes of green sulfur bacteria. *Biochim Biophys Acta* 848: 69–76
- Gibson J, Ludwig W, Stackebrandt E and Woese CR (1985) The phylogeny of the green photosynthetic bacteria: Absence of a close relationship between *Chlorobium* and *Chloroflexus*. *Syst Appl Microbiol* 6: 152–156
- Griebenow K and Holzwarth AR (1989) Pigment organization and energy transfer in green bacteria. 1. Isolation of native chlorosomes free of bound bacteriochlorophyll *a* from *Chloroflexus aurantiacus* by gel-electrophoretic filtration. *Biochim Biophys Acta* 973: 235–240
- Griebenow K, Holzwarth AR, Van Mourik F and van Grondelle R (1991) Pigment organization and energy transfer in green bacteria. 2. Circular and linear dichroism spectra of protein-containing and protein-free chlorosomes isolated from *Chloroflexus aurantiacus* Strain Ok-70-fl. *Biochim Biophys Acta* 1058: 194–202
- Griesbeck C, Hager-Braun C, Rogl H and Hauska G (1998)



- Quantitation of P840 reaction center preparations from *Chlorobium tepidum*: Chlorophylls and FMO protein. *Biochim Biophys Acta* 1365: 285–293
- Gülen D (1996) Interpretation of the excited-state structure of the Fenna-Matthews-Olson pigment protein complex of *Prosthecochloris aestuarii* based on the simultaneous simulation of the 4 K absorption, linear dichroism, and singlet-triplet absorption difference spectra: A possible excitonic explanation? *J Phys Chem* 100: 17683–17689
- Hanada S, Takaichi S, Matsuura K and Nakamura K (2002) *Roseiflexus castenholzii* gen. nov., sp. nov., a thermophilic, filamentous, photosynthetic bacterium which lacks chlorosomes. *Int J Syst Evol Microbiol* 52: 187–193
- Hirota M, Moriyama T, Shimada K, Miller M, Olson JM and Matsuura K (1992a) High degree of organization of bacteriochlorophyll *c* in chlorosome-like aggregates spontaneously assembled in aqueous solution. *Biochim Biophys Acta* 1099: 271–274
- Hirota M, Tsuji K, Shimada K and Matsuura K (1992b) Composition and organization of chlorosome-like bacteriochlorophyll *c*-lipid aggregates in aqueous solution. In: Murata N (ed) *Research in Photosynthesis, Vol I*, pp 81–84, Kluwer Academic Publishers, Dordrecht
- Holo H, Broch-Due, M. and Ormerod JG (1985) Glycolipids and the structure of chlorosomes in green bacteria. *Arch Microbiol* 143: 94–99
- Holzwarth AR and Schaffner K (1994) On the structure of bacteriochlorophyll molecular aggregates in the chlorosomes of green bacteria. A molecular modelling study. *Photosynth Res* 41: 225–233
- Holzwarth AR, Griebenow K and Schaffner K. (1990a) A photosynthetic antenna system which contains a protein-free chromophore aggregate. *Z Naturforsch* 45c: 203–206
- Holzwarth AR, Müller MG and Griebenow K (1990b) Picosecond energy transfer kinetics between pigment pools in different preparations of chlorosomes from the green bacterium *Chloroflexus aurantiacus*. *J Photochem Photobiol B* 5: 457–465
- Hu D (2001) Investigation of the Fenna-Matthews-Olson protein from photosynthetic green sulfur bacteria. Ph.D. Dissertation, Arizona State University, Tempe
- Imhoff JM and Bias-Imhoff U (1995) Lipids, quinones and fatty acids of anoxygenic phototrophic bacteria. In: Blankenship RE, Madigan MT and Bauer CE (eds) *Anoxygenic Photosynthetic Bacteria*, pp 179–205. Kluwer Academic Publishers, Dordrecht
- Iseri EI and Gülen D (1999) Electronic excited states and excitation transfer kinetics in the Fenna-Matthews-Olson protein of the photosynthetic bacterium *Prosthecochloris aestuarii* at low temperatures. *European Biophys J with Biophys Lett* 28: 243–253
- Ishii T, Kimura M, Yamamoto T, Kirihaata M and Uehara K (2000) The effects of epimerization at the 3<sup>1</sup>-position of bacteriochlorophylls *c* on their aggregation in chlorosomes of green sulfur bacteria. Control of the ratio of 3(1) epimers by light intensity. *Photochem Photobiol* 71: 567–573
- Johnson SG and Small GJ (1991) Excited state structure and energy transfer dynamics of the bacteriochlorophyll *a* protein from *Prosthecochloris aestuarii*. *J Phys Chem* 95: 471–479
- Karapetyan NV, Swarthoff T, Rijgersberg CP and Ames J (1980) Fluorescence emission spectra of cells and subcellular preparations of a green photosynthetic bacterium. Effects of dithionite on the intensity of the emission bands. *Biochim Biophys Acta* 593: 254–260
- Krasnovsky AA and Bystrova MI (1980) Self-assembly of chlorophyll aggregated structures. *BioSystems* 12: 181–194
- Krasnovsky AA and Pakshina EV (1959) The photochemical and spectral properties of bacterioviridin of green sulfur bacteria. *Doklady Acad Nauk SSSR (English Trans)* 127: 215–218
- Larsen KL, Miller M, Cox RP (1995) Incorporation of exogenous long-chain alcohols into bacteriochlorophyll-*c* homologs by *Chloroflexus aurantiacus*. *Arch Microbiol* 163: 119–123
- Lehmann RP, Brunisholz RA and Zuber H (1994a) Structural differences in chlorosomes from *Chloroflexus aurantiacus* grown under different conditions support the BChl *c*-binding function of the 5.7 kDa polypeptide. *FEBS Lett* 342: 319–324
- Lehmann RP, Brunisholz RA and Zuber H (1994b) Giant circular dichroism of chlorosomes from *Chloroflexus aurantiacus* treated with 1-hexanol and proteolytic enzymes. *Photosynth Res* 41: 165–173
- Li YF, Zhou W, Blankenship RE and Allen J (1997) Crystal structure of the bacteriochlorophyll *a* protein from *Chlorobium tepidum*. *J Molec Bio* 271: 456–471
- Lin S, Van Amerongen H and Struve WS (1991) Ultrafast pump-probe spectroscopy of bacteriochlorophyll *c* antennae in bacteriochlorophyll *a*-containing chlorosomes from the green photosynthetic bacterium *Chloroflexus aurantiacus*. *Biochim Biophys Acta* 1060: 13–24
- Lopez J, Ryan S and Blankenship RE (1996) Sequence of the *bchG* Gene from *Chloroflexus aurantiacus*: The relationship between chlorophyll synthase and other polyprenyltransferases. *J Bacteriol* 178: 3369–3373
- Louwe RJW, Vrieze J, Aartsma TJ and Hoff AJ (1997a) Toward an integral interpretation of the optical steady-state spectra of the FMO-complex of *Prosthecochloris aestuarii*. 1. An investigation with linear-dichroic absorbance-detected magnetic resonance. *J Phys Chem B* 101: 11273–11279
- Louwe RJW, Vrieze J, Hoff AJ and Aartsma TJ (1997b) Toward an integral interpretation of the optical steady-state spectra of the FMO-complex of *Prosthecochloris aestuarii*. 2. Exciton simulations. *J Phys Chem B* 101: 11280–11287
- Louwe RJW, Aartsma TJ, Gast P, Hulsebosch RJ, Nan HM, Vrieze J and Hoff AJ (1998) The triplet state of the FMO complex of the green sulfur bacterium *Prosthecochloris aestuarii* studied with single-crystal EPR. *Biochim Biophys Acta—Bioenergetics* 1365: 373–384
- Lu XY and Pearlstein RM (1993) Simulations of Prosthecochloris bacteriochlorophyll *a*-protein optical-spectra improved by parametric computer-search. *Photochem Photobiol* 57: 86–91
- Matsuura K and Olson JM (1990) Reversible conversion of aggregated bacteriochlorophyll-*c* to the monomeric form by 1-Hexanol in chlorosomes from *Chlorobium* and *Chloroflexus*. *Biochim Biophys Acta* 1019: 233–238
- Matsuura K, Hirota M, Shimada K and Mimuro M (1993) Spectral forms and orientation of bacteriochlorophyll-*c* and bacteriochlorophyll-*a* in chlorosomes of the green photosynthetic bacterium *Chloroflexus aurantiacus*. *Photochem Photobiol* 57: 92–97
- Matsuzaki S, Zazubovich V, Rätsep M, Hayes JM and Small GJ (2000) Energy transfer kinetics and low energy vibrational structure of the three lowest energy Q<sub>y</sub> states of the Fenna-

- Matthews-Olson antenna complex. *J Phys Chem B* 104: 9564–9572
- Matthews BW and Fenna RE (1980) Structure of a green bacteriochlorophyll protein. *Acc Chem Res* 13: 309–317
- Matthews BW, Fenna RE, Bolognesi MC, Schmid MF, Olson JM (1979) Structure of a bacteriochlorophyll *a*-protein from the green photosynthetic bacterium *Prosthecochloris-aestuarii*. *J Mol Biol* 131: 259–285
- Melkozernov AN, Olson JM, Li Y-F, Allen JP and Blankenship RE (1998) Orientation and excitonic interactions of the Fenna-Matthews-Olson protein in membranes of the green sulfur bacterium *Chlorobium tepidum*. *Photosynth Res* 56: 315–328
- Melø TB, Frigaard NU, Matsuura K and Razi Naqvi K (2000) Electronic energy transfer involving carotenoid pigments in chlorosomes of two green bacteria: *Chlorobium tepidum* and *Chloroflexus aurantiacus*. *Spectrochim Acta A* 56A: 2001–2010
- Miller M, Gillbro T and Olson JM (1993) Aqueous aggregates of bacteriochlorophyll *c* as a model for pigment organization in chlorosomes. *Photochem Photobiol* 57: 98–102
- Mimuro M, Hirota M, Nishimura Y, Moriyama T, Yamazaki I, Shimada K and Matsuura K. (1994) Molecular organization of bacteriochlorophyll in chlorosomes of the green photosynthetic bacterium *Chloroflexus aurantiacus*: Studies of fluorescence depolarization accompanied by energy transfer processes. *Photosynthesis Res* 41: 181–191
- Mizoguchi T, Sakamoto S, Koyama Y, Ogura K and Inagaki F (1998) The structure of the aggregate form of bacteriochlorophyll *c* showing the  $Q_y$  absorption above 740 nm as determined by the ring current effects on  $^1\text{H}$  and  $^{13}\text{C}$  nuclei and by  $^1\text{H}$ - $^1\text{H}$  intermolecular NOE correlations. *Photochem Photobiol* 67: 239–248
- Mizoguchi T, Hara K, Nagae H and Koyama Y (2000) Structural transformation among the aggregate forms of bacteriochlorophyll *c* as determined by electron absorption and NMR spectroscopies: Dependence on the stereoisomeric configuration and on the bulkiness of the 8-C side chain. *Photochem Photobiol* 71: 596–609
- Montaño G, Wu H-M, Lin S, Brune DC and Blankenship RE (2001a) Isolation and characterization of the B795 baseplate light-harvesting complex from the chlorosomes of *Chloroflexus aurantiacus*. *Biophys J* 80: 30a
- Montaño G, Bowen B, Woodbury NW, Labelle J, Pizziconi V and Blankenship RE, (2001b) Determination of the number of bacteriochlorophyll molecules per chlorosome light-harvesting complex in *Chloroflexus aurantiacus* and *Chlorobium tepidum*. In: PS2001: Proceedings of the 12th International Congress on Photosynthesis. S15-020. CSIRO Publishing, Melbourne (CD-ROM)
- Neerken S, Permentier HJ, Francke C, Aartsma TJ and Ames J (1998) Excited states and trapping in reaction center complexes of the green sulfur bacterium *Prosthecochloris aestuarii*. *Biochemistry* 37: 10792–10797
- Niedermeier G, Scheer H and Feick RG (1992) The functional role of protein in the organization of bacteriochlorophyll-*c* in chlorosomes of *Chloroflexus aurantiacus*. *Eur J Biochem* 204: 685–692
- Niedermeier G, Shiozawa JA, Lottspeich F and Feick RG (1994) Primary structure of two chlorosome proteins from *Chloroflexus aurantiacus*. *FEBS Lett* 342: 61–65
- Novoderezhkin VI and Fetisova ZG (1997) Oligomerization of light-harvesting pigments as a structural factor optimizing the photosynthetic antenna function. 3. Model of oligomeric pigment organization in antennae of green bacteria. *Mol Biol* 31: 435–440
- Nozawa T, Ohtomo K, Suzuki M, Nakagawa H, Shikama Y, Konami H, and Wang ZY (1994) Structures of chlorosomes and aggregated BChl *c* in *Chlorobium tepidum* from solid state high resolution CP/MAS C-13 NMR. *Photosynth Res* 41: 211–223
- Oba T and Tamiaki H (1999) Why do chlorosomal chlorophylls lack the C13(2)-methoxycarbonyl moiety? An in vitro model study. *Photosynth Res* 61: 23–31
- Oelze J and Golecki JR (1995) Membranes and chlorosomes of green bacteria: Structure, composition and development. In: Blankenship RE, Madigan MT and Bauer CE (eds) *Anoxygenic Photosynthetic Bacteria*, pp 259–278. Kluwer Academic Publishers, Dordrecht
- Oh-oka H, Kamei S, Matsubara H, Lin S, van Noort PI and Blankenship RE (1998) Transient Absorption Spectroscopy of Energy Transfer and Trapping Processes in the Reaction Center of *Chlorobium tepidum*. *J Phys Chem* 102: 8190–8195
- Olson JM (1966) Chlorophyll-protein complexes derived from green photosynthetic bacteria. In: Vernon LP and Seely GR (eds) *The Chlorophylls* pp 413–425 Academic Press, New York
- Olson JM (1978) Bacteriochlorophyll *a*-proteins from green bacteria. In: Clayton RK and Sistrom RS (eds) *The Photosynthetic Bacteria*, pp 161–178. Plenum Press, New York
- Olson JM (1980a) Chlorophyll organization in green photosynthetic bacteria. *Biochim Biophys Acta* 594: 33–51
- Olson JM (1980b) Bacteriochlorophyll *a*-proteins of two green photosynthetic bacteria. *Meth Enzymol* 69: 336–344
- Olson JM (1998) Chlorophyll organization and function in green photosynthetic bacteria. *Photochem Photobiol* 67: 61–75
- Ormerod JG (1992) Physiology of the photosynthetic prokaryotes. In: Mann NH and Carr NG (eds) *Photosynthetic Prokaryotes*, pp 93–120. Plenum, New York
- Owen GM and Hoff AJ (2001) Absorbance detected magnetic resonance spectra of the FMO complex of *Prosthecochloris aestuarii* reconsidered: Exciton simulations. *J Phys Chem B* 105: 1458–1463
- Pearlstein RM (1992) Theory of the optical spectra of the bacteriochlorophyll-*a* antenna protein trimer from *Prosthecochloris aestuarii*. *Photosynth Res* 31: 213–226
- Pearlstein RM and Hemenger RP (1978) Bacteriochlorophyll electronic-transition moment directions in bacteriochlorophyll *a*-protein. *Proc Natl Acad Sci USA* 75: 4920–4924
- Permentier HP, Schmidt KA, Kobayashi M, Akiyama M, Hager-Braun C, Neerken, S, Miller M and Ames J. (2000) Composition and optical properties of reaction core complexes from the green sulfur bacteria *Prosthecochloris aestuarii* and *Chlorobium tepidum*. *Photosynth Res* 64: 27–39
- Philipson KD and Sauer K (1972) Exciton interaction in a bacteriochlorophyll-protein from *Chloropseudomonas ethylica*. Absorption and circular dichroism at 77 K. *Biochem* 11: 1880–1885
- Pierson BK and Castenholz RW (1992) The family Chloroflexaceae. In: Balows A, Trüper HG, Dworkin M, Schliefer KH, and Harder W (eds) *The Prokaryotes*, pp 3754–3774. Springer-Verlag, Berlin

- Pierson BK and Castenholz RW (1995) Taxonomy and physiology of filamentous anoxygenic phototrophs. In: Blankenship RE, Madigan MT and Bauer CE (eds) *Anoxygenic Photosynthetic Bacteria*, pp 31–47. Kluwer Academic Publishers, Dordrecht
- Pierson BK, Giovannoni SJ, Stahl DA and Castenholz RW (1985) *Heliothrix oregonensis*, gen.-nov., sp.-nov., a phototrophic filamentous gliding bacterium containing bacteriochlorophyll *a*. *Arch Microbiol* 142: 164–167
- Porra, RJ (1997) Recent progress in pophyrin and chlorophyll biosynthesis. *Photochem Photobiol* 65: 492–516
- Powls R and Redfearn ER (1969) Quinones of the chlorobacteriaceae—properties and possible function. *Biochim Biophys Acta* 172: 429–437
- Powls R, Redfearn E and Trippett S (1968) The structure of chlorobiumquinone. *Biochem Biophys Res Commun* 33: 408–411
- Rätsep M, Blankenship RE and Small GJ (1999) Energy transfer and spectral dynamics of the three lowest energy Q(y)-states of the Fenna-Matthews-Olson antenna complex. *J Phys Chem B* 103: 5736–5741
- Rätsep M, Wu H-M, Hayes JM, Blankenship RE, Cogdell RJ and Small GJ (1998) Stark hole-burning studies of three photosynthetic complexes. *J Phys Chem B* 102: 4035–4044
- Reddy NRS, Jankowiak R and Small GJ (1995) High-pressure hole-burning studies of the bacteriochlorophyll *a* antenna complex from *Chlorobium tepidum*. *J Phys Chem* 99: 16168–16178
- Redfearn ER and Powls R (1968) The quinones of green photosynthetic bacteria. *Biochem J* 106: 50P
- Remigy HW, Stahlberg H, Fotiadis D, Muller SA, Wolpensinger B, Engel A, Hauska G and Tsiotis G (1999) The reaction center complex from the green sulfur bacterium *Chlorobium tepidum*: A structural analysis by scanning transmission electron microscopy. *J Mol Bio* 290: 851–858
- Renger Th and May V (1998) Ultrafast exciton motion in photosynthetic antenna systems: The FMO complex. *J Phys Chem A* 102: 4381–4391
- Saga Y, Matsuura K and Tamiaki H (2001) Spectroscopic studies on self-aggregation of bacteriochlorophyll-*e* in non-polar organic solvents: Effects of stereoisomeric configuration at the 31-position and alkyl substituents at the 81-position. *Photochem. Photobiol* 74: 72–80
- Sakuragi Y, Frigaard NU, Shimada K and Matsuura K (1999) Association of the bacteriochlorophyll *a* with the CsmA protein in chlorosomes of the photosynthetic green filamentous bacterium *Chloroflexus aurantiacus*. *Biochim et Biophys Acta—Bioenergetics* 1413: 172–180
- Sakurai H, Kusumoto N and Inoue K (1996) Function of the reaction center of green sulfur bacteria. *Photochem Photobiol*, 64: 5–13
- Savikhin S and Struve WS (1994) Ultrafast energy transfer in FMO trimers from the green bacterium *Chlorobium tepidum*. *Biochem* 33: 11200–11208
- Savikhin S, Zhou WL, Blankenship RE and Struve WS (1994a) Femtosecond energy transfer and spectral equilibration in bacteriochlorophyll *a*—Protein antenna trimers from the green bacterium *Chlorobium tepidum*. *Biophys J* 66: 110–113
- Savikhin S, Zhu Y, Lin S, Blankenship RE and Struve WS (1994b) Femtosecond spectroscopy of chlorosome antennas from the green photosynthetic bacterium *Chloroflexus aurantiacus*. *J Phys Chem* 98: 10322–10334
- Savikhin S, van Noort PI, Zhu Y, Lin S, Blankenship RE and Struve WS (1995) Ultrafast energy transfer in light harvesting chlorosomes from the green sulfur bacterium *Chlorobium tepidum*. *Chem Phys* 194: 245–258
- Savikhin S, Zhu Y, Blankenship RE and Struve WS (1996) Intraband energy transfers in the BChl *c* antenna of chlorosomes from the green photosynthetic bacterium *Chloroflexus aurantiacus*. *J Phys Chem* 100: 17978–17980
- Savikhin S, Buck DR and Struve WS (1997) Pump-probe anisotropies of Fenna-Matthews-Olson protein trimers from *Chlorobium tepidum*: A diagnostic for exciton localization? *Biophys J* 73: 2090–2096
- Savikhin S, Buck DR and Struve WS (1998) Toward level-to-level energy transfers in photosynthesis: The Fenna-Matthews-Olson Protein. *J Phys Chem B* 102: 5556–5565
- Scheer H (1991) Structure and occurrence of chlorophylls. In: Scheer H (ed) *Chlorophylls*, pp 3–30. CRC Press, Boca Raton
- Schmidt K (1980) A comparative study on the composition of chlorosomes [*chlorobium vesicles*] and cytoplasmic membranes from *Chloroflexus aurantiacus* strain Ok-70-fl and *Chlorobium limicola f thiosulfatophilum* strain 6230. *Arch Microbiol* 124: 21–31
- Schoch S, Oster U, Mayer K, Feick R and Rüdiger W. (1999) Substrate specificity of overexpressed bacteriochlorophyll synthase from *Chloroflexus aurantiacus*. In: Argyroudi-Akoyunoglou JH and Senger H, Eds, *The Chloroplast: From Molecular Biology to Biotechnology*, pp 213–216. Kluwer Academic Publishers, Dordrecht
- Sirevåg R (1995) Carbon metabolism in green bacteria. In: Blankenship RE, Madigan MT and Bauer CE (eds) *Anoxygenic Photosynthetic Bacteria*, pp. 871–883. Kluwer Academic Publishers, Dordrecht
- Smith KM (1994) Nomenclature of the bacteriochlorophylls *c*, *d*, and *e*. *Photosynth Res* 41: 23–26
- Smith KM, Goff DA, Fajer J and Barkigia KM (1982) Chirality and structures of bacteriochlorophylls *d*. *J Am Chem Soc* 104: 3747–9
- Smith KM, Kehres LA and Fajer J (1983) Aggregation of bacteriochlorophylls *c*, *d*, and *e*. Models for the antenna chlorophylls of green and brown photosynthetic bacteria. *J Am Chem Soc* 105: 1387–1389
- Staehelin LA, Golecki JR, Fuller RC and Drews G (1978) Visualization of the supramolecular architecture of chlorosomes (*Chlorobium* type vesicles) in freeze-fractured cells of *Chloroflexus aurantiacus*. *Arch Microbiol* 119: 269–277
- Staehelin LA, Golecki JR and Drews G (1980) Supramolecular organization of chlorosomes (chlorobium vesicles) and of their membrane attachment sites in *Chlorobium limicola*. *Biochim Biophys Acta* 589: 30–45
- Steensgaard DB, van Walree CA, Baneras L, Borrego CM, Garcia-Gil J, Holzwarth AR (1999) Evidence for spatially separate bacteriochlorophyll *c* and bacteriochlorophyll *d* pools within the chlorosomal aggregate of the green sulfur bacterium *Chlorobium limicola*. *Photosynthesis Research* 59: 231–241
- Steensgaard DB, van Walree CA, Permentier H, Baneras L, Borrego CM, Garcia-Gil J, Aartsma TJ, Amesz J and Holzwarth AR (2000) Fast energy transfer between BChl *d* and BChl *c* in chlorosomes of the green sulfur bacterium *Chlorobium limicola*. *Biochim Biophys Acta* 1457: 71–80
- Takaichi S, Tsuji K, Matsuura K and Shimada K (1995) A monocyclic carotenoid glucoside ester is a major carotenoid in

- the green filamentous bacterium *Chloroflexus aurantiacus*. *Plant Cell Physiol* 36: 773–778
- Tamiaki H (1996) Supramolecular structure in extramembraneous antennae of green photosynthetic bacteria. *Coordination Chem Rev* 148: 183–197
- Tamiaki H, Kubo M and Oba T (2000) Synthesis and self-assembly of zinc methyl bacteriopheophorbide-f and its homolog. *Tetrahedron* 56: 6245–6257
- Theroux SJ, Redlinger TE, Fuller RC and Robinson SJ (1990) Gene encoding the 5.7 kilodalton chlorosome protein of *Chloroflexus aurantiacus*: Regulated message levels and a predicted carboxy terminal protein extension. *J Bacteriol* 172: 4497–4504
- Tokita S, Frigaard NU, Hirota M, Shimada K and Matsuura K (2000) Quenching of bacteriochlorophyll fluorescence in chlorosomes from *Chloroflexus aurantiacus* by exogenous quinones. *Photochem Photobiol* 72: 345–350
- Tronrud DE and Matthews BW (1993) Refinement of the structure of a water-soluble antenna complex from green photosynthetic bacteria with incorporation of the chemically determined amino acid sequence. In: Norris J and Deisenhofer H (eds) *The Photosynthetic Reaction Center*, Vol 1 pp 13–21. Academic Press, San Diego
- Tronrud DE, Schmid MF and Matthews BW (1986) Structure and X-ray amino acid sequence of a bacteriochlorophyll *a* protein from *Prosthecochloris aestuarii* refined at 1.9 Å resolution. *J Mol Biol* 188: 443–454
- Trüper HG and Pfennig N (1992) The family Chlorobiaceae. In: Balows A, Trüper HG, Dworkin M, Schliefer KH and Harder W (eds) *The Prokaryotes*, 2nd Ed., pp 3583–3592. Springer-Verlag, Berlin
- Tsuji K, Takaichi S, Matsuura K and Shimada K (1995) Specificity of carotenoids in chlorosomes of the green filamentous bacterium, *Chloroflexus aurantiacus*. In: Mathis P (ed) *Photosynthesis: From Light to Biosphere*, Vol 4, pp 99–103. Kluwer Academic Publishers, Dordrecht
- Van de Meent, EJ, Kobayashi M, Erkelens C, Van Veelen PA, Otte SCE, Inoue K, Watanabe T and Ames J (1992) The nature of the primary electron acceptor in green sulfur bacteria. *Biochim Biophys Acta* 1102: 371–378
- van Dorssen RJ, Gerola PD, Olson JM and Ames J (1986a) Optical and structural properties of chlorosomes of the photosynthetic green sulfur bacterium *Chlorobium limicola*. *Biochim Biophys Acta* 848: 77–82
- van Dorssen RJ, Vasmel H and Ames J (1986b) Pigment organization and energy-transfer in the green photosynthetic bacterium *Chloroflexus-aurantiacus*.2. The chlorosome. *Photosynth Res* 9: 33–45
- van Gemerden H and Mas J (1995) Ecology of phototrophic sulfur bacteria. In: Blankenship RE, Madigan MT and Bauer CE (eds) *Anoxygenic Photosynthetic Bacteria*, pp 49–85. Kluwer Academic Publishers, Dordrecht
- van Grondelle R, Dekker JP, Gillbro T and Sundström W (1994) Energy transfer and trapping in photosynthesis. *Biochim Biophys Acta* 1187: 1–65
- van Mourik F, Verwijst RR, Mulder JM and van Grondelle R (1994) Singlet-triplet spectroscopy of the light-harvesting BChl *a* complex of *Prosthecochloris aestuarii*. The nature of the low energy 825 nm transition. *J Phys Chem* 98: 10307–10312
- van Noort PI, Zhu Y, LoBrutto R and Blankenship RE (1997) Redox effects on the excited-state lifetime in chlorosomes and bacteriochlorophyll *c* oligomers. *Biophys J* 72: 316–325
- van Rossum BJ, Steensgaard DB, Mulder FM, Boender GJ, Schaffner K, Holzwarth AR, de Groot HJM (2001) A refined model of the chlorosomal antennae of the green bacterium *Chlorobium tepidum* from proton chemical shift constraints obtained with high-field 2-D and 3-D MAS NMR dipolar correlation spectroscopy *Biochemistry* 40: 1587–1595
- van Walree CA, Sakuragi Y, Steensgaard DB, Bosinger CS, Frigaard NU, Cox RP, Holzwarth AR and Miller M (1999) Effect of alkaline treatment on bacteriochlorophyll *a*, quinones and energy transfer in chlorosomes from *Chlorobium tepidum* and *Chlorobium phaeobacteroides*. *Photochem Photobiol* 69: 322–328
- Vassilieva EV, Frigaard N-F and Bryant DA (2000) Chlorosomes: The light-harvesting complexes of green bacteria. *The Spectrum* 13: 7–13
- Vassilieva EV, Antonkine ML, Zybilov BL, Yang F, Jakobs CU, Golbeck JH and Bryant DA (2001) Electron transfer may occur in the chlorosome envelope: The CsmI and CsmJ proteins of chlorosomes are 2Fe-2S ferredoxins. *Biochemistry* 40: 464–473
- Vulto SIE, Streltsov AM and Aartsma TJ (1997) Excited state energy relaxation in the FMO complexes of the green bacterium *Prosthecochloris aestuarii* at low temperatures. *J Phys Chem B* 101: 4845–4850
- Vulto SIE, Neerken S, Louwe RJW, de Baat MA, Ames J and Aartsma TJ (1998a) Excited-state structure and dynamics in FMO antenna complexes from photosynthetic green sulfur bacteria. *J Phys Chem B* 102: 10630–10635
- Vulto SIE, de Baat MA, Louwe RJW, Permentier HP, Neef T, Miller M, van Amerongen H and Aartsma TJ (1998b) Exciton simulations of optical spectra of the FMO complex from the green sulfur bacterium *Chlorobium tepidum* at 6 K. *J Phys Chem B* 102: 9577–9582
- Vulto SIE, de Baat MA, Neerken S, Nowak FR, van Amerongen H, Ames J and Aartsma TJ (1999) Excited state dynamics in FMO antenna complexes from photosynthetic green sulfur bacteria: A kinetic model. *J Phys Chem B* 103: 8153–8161
- Wagner-Huber R, Brunisholz R, Frank G and Zuber H (1988) The BChl *c/e*-binding polypeptides from chlorosomes of green photosynthetic bacteria. *FEBS Lett* 239: 8–12
- Wagner-Huber R, Fischer UR, Brunisholz R, Rumbeli G, Frank G and Zuber H (1991) The primary structure of the presumable BChl *d*-binding polypeptide of *Chlorobium Vibrioforme* f. *thiosulfatophilum*. *Biochim Biophys Acta* 1060: 97–105
- Wang J, Brune DC and Blankenship RE (1990) Effects of oxidants and reductants on the efficiency of excitation transfer in green photosynthetic bacteria. *Biochim Biophys Acta* 1015: 457–463
- Wang ZY, Umetsu M, Kobayashi M, Nozawa T (1999) C-13- and N-15-NMR studies on the intact bacteriochlorophyll *c* dimers in solutions. *J Am Chem Soc* 121: 9363–9369
- Watanabe Y, Feick RG and Shiozawa JA (1995) Cloning and sequencing of the genes encoding the light-harvesting B806-866 polypeptides and initial studies on the transcriptional organization of Puf2b, Puf2a and Puf2c in *Chloroflexus-aurantiacus*. *Arch Microbiol* 163: 124–130
- Wechsler T, Suter F, Fuller RC and Zuber H. (1985a) The complete amino acid sequence of the bacteriochlorophyll *c*

- binding polypeptide from chlorosomes of the green photosynthetic bacterium *Chloroflexus aurantiacus*. FEBS Lett 181: 173–178
- Wechsler T, Brunisholz R, Suter F, Fuller RC and Zuber H. (1985b) The complete amino acid sequence of a bacteriochlorophyll *a* binding polypeptide isolated from the cytoplasmic membrane of the green photosynthetic bacterium *Chloroflexus aurantiacus*. FEBS Lett 191:34–38
- Wechsler TD, Brunisholz RA, Frank G, Suter F and Zuber H. (1987) The complete amino acid sequence of the antenna polypeptide B806-866- $\beta$  from the cytoplasmic membrane of the green bacterium *Chloroflexus aurantiacus*. FEBS Lett 210:189–94
- Wechsler TD, Brunisholz RA, Frank G, Zuber H (1991) Isolation and protein chemical characterization of the B806-866 antenna complex of the green thermophilic bacterium *Chloroflexus aurantiacus*. J Photochem Photobiology B. 8: 189–197
- Wendling M, Pullerits T, Przyjalowski MA, Vulto SIE, Aartsma TJ van Grondelle R and van Amerongen HV (2000) Electron-vibrational coupling in the Fenna-Matthews-Olson complex of *Prosthecochloris aestuarii* determined by temperature-dependent absorption and fluorescence line-narrowing measurements. J Phys Chem B 104: 5825–5831
- Whitten WB, Olson JM and Pearlstein RM (1980) 7-fold exciton splitting of the 810-nm band in bacteriochlorophyll *a*-proteins from green photosynthetic bacteria. Biochim Biophys Acta 591: 203–207 1980
- Woese CR (1987) Bacterial evolution. Microbiol Rev 51: 221–271
- Wullink W, Knudsen J, Olson JM, Redlinger TE and Van Bruggen EFJ (1991) Localization of polypeptides in isolated chlorosomes from green phototrophic bacteria by immunogold labeling electron microscopy. Biochim Biophys Acta 1060: 97–105
- Xiong J, Fischer WM, Inoue K, Nakahara M, Bauer CE (2000) Molecular evidence for the early evolution of photosynthesis. Science 289: 1724–1730
- Zhou W (1995) Studies of the bacteriochlorophyll *a* protein from the photosynthetic green sulfur bacterium *Chlorobium tepidum*. Ph. D. Dissertation, Arizona State University, Tempe
- Zhou W, LoBrutto R, Lin S and Blankenship RE (1994) Redox effects on the bacteriochlorophyll *a*-containing Fenna-Matthews-Olson protein from *Chlorobium tepidum*. Photosynth Res 41: 89–96
- Zhu YW, Ramakrishna BL, van Noort, PI and Blankenship RE (1995) Microscopic and spectroscopic studies of untreated and hexanol-treated chlorosomes from *Chloroflexus aurantiacus*. Biochim Biophys Acta 1232: 197–207
- Zuber H and Brunisholz RA (1991) Structure and function of antenna polypeptides and chlorophyll-protein complexes: Principles and variability. In: Scheer H (ed) Chlorophylls, pp 627–703. CRC Press, Boca Raton

# Chapter 7

## Light-Harvesting in Photosystem II

Herbert van Amerongen\*

*Laboratory of Biophysics, Department of Agrotechnology and Food Sciences,  
Dreijenlaan 3, 6703 HA Wageningen, The Netherlands*

Jan P. Dekker\*

*Faculty of Sciences, Division of Physics and Astronomy, Vrije Universiteit,  
De Boelelaan 1081, 1081 HV Amsterdam, The Netherlands*

Summary .....	220
I. Introduction .....	220
II. The Photosystem II Genes and Proteins .....	221
III. Individual Photosystem II Antenna Complexes .....	222
A. Major Peripheral Antenna Complexes (LHCII) .....	222
1. Structure .....	222
2. Xanthophylls: Identity, Location and Function .....	224
3. Location and Identity of the Chlorophylls .....	226
4. Chlorophyll-Xanthophyll Contacts .....	228
5. Xanthophyll → Chlorophyll Singlet Energy Transfer .....	228
6. Chlorophyll <i>b</i> → Chlorophyll <i>b</i> and Chlorophyll <i>a</i> Singlet Energy Transfer .....	229
7. Chlorophyll <i>a</i> → Chlorophyll <i>a</i> Singlet Energy Transfer .....	229
8. Singlet Excitation Energy Transfer throughout and between LHCII Trimers .....	230
B. Minor Peripheral Antenna Complexes (CP29, CP26, CP24) .....	231
1. General Features .....	231
2. CP29 .....	231
3. CP26 and CP24 .....	232
C. Other Proteins Associated with the Peripheral Antenna .....	233
D. CP47 and CP43 .....	234
IV. Reaction Center Containing Photosystem II Complexes .....	235
A. The Isolated Photosystem II Reaction Center .....	235
1. Biochemistry and Structure .....	235
2. Spectroscopy .....	236
3. Energy Transfer and Trapping .....	236
B. Photosystem II Core Complexes .....	237
C. Photosystem II Supercomplexes .....	240
D. Photosystem II Membranes .....	242
V. Overall Trapping of Excitation Energy .....	242
References .....	245

---

\*Authors for correspondence, email: Herbert.vanAmerongen@wur.nl or dekker @nat.vu.nl

## Summary

Photosystem II (PS II) of green plants represents one of the most complex systems in plant biology. It consists of at least 29 different types of proteins, binds a huge number of pigments (chlorophylls and carotenoids), produces the oxygen that we breathe and plays essential roles in many regulation mechanisms of the photosynthesis. In this chapter, we discuss the mechanisms of light-harvesting and trapping of excitation energy in green plant PS II. We describe structural models of the pigment-binding proteins of PS II and their supramolecular organization, and consider the energy transfer processes between pigments in individual complexes, with an emphasis on the major trimeric light-harvesting complex II (LHCII) of PS II, which is by far the best studied protein of the PS II antenna. Energy transfer between different complexes also is addressed, as well as studies on complete PS II complexes. In contrast to many previous studies, we conclude that the relatively long excited-state lifetime in PS II should be explained by a combination of three different factors: 1) the relatively slow energy transfer in the outer antenna, 2) the small number of chlorophylls that connect the antenna to the reaction center, and 3) the relatively slow charge separation in the reaction center. The process of excitation trapping can therefore not be classified as being purely diffusion-, transfer-to-the-trap-, or trap-limited.

## I. Introduction

Photosystem II (PS II) is a large supramolecular pigment-protein complex embedded in the thylakoid membranes of green plants, algae and cyanobacteria. Its major task is to collect light energy and to use this for the reduction of plastoquinone, the oxidation of water and the formation of a transmembrane pH gradient. It consists of at least 29 different types of protein subunits, many of which are intrinsically bound to the thylakoid membranes. Some subunits are involved in the capturing of solar energy and the regulation of the energy flow, others are directly or indirectly involved in the oxidation of water to molecular oxygen.

The most elementary functions of PS II (primary charge separation and secondary electron transport) are carried out by two proteins known as D1 and D2, which together constitute the reaction center (RC). These subunits bind the so-called primary reactants, which include the primary electron donor of PS II, known as P680. The electronic excitation of P680 initiates the transfer of an electron from P680 to a

pheophytin (Ph), resulting in the oxidation of the chlorophyll (P680<sup>+</sup>) and the reduction of the pheophytin (Ph<sup>-</sup>), and thus in a charge separation. The electron on the Ph molecule is taken up by a complex of two quinones and a non-heme iron, which after proton uptake produces reduced plastoquinone. Reduction of P680<sup>+</sup> proceeds via a redox-active tyrosine of the D1 protein and a cluster of four manganese ions, which after the accumulation of four oxidizing equivalents oxidizes water to molecular oxygen.

Photosystem II has a number of unique properties. Perhaps the most important is the extremely high redox potential of P680<sup>+</sup> (~ +1.2 V), which is much higher than the redox potentials of all other known photosystems and is sufficient to oxidize water to molecular oxygen. The evolution of the capability to use water as source of electrons has allowed photosynthetic organisms to proliferate to an enormous extent, and has finally resulted in our present oxygenic atmosphere.

The high redox potential of P680<sup>+</sup> implies that more energy will be stored in the charge-separated products in PS II than in any other photosystem (Diner and Babcock, 1996). This has placed large constraints upon the energetics of the primary processes of PS II. In order to support the high free energy of charge separation in PS II, it is necessary that the energetic input be as large as possible. This is achieved by keeping the absorption wavelength of the primary electron donor as short as possible. At the same time, however, the absorption wavelength of the primary electron donor can not be shorter than that of most antenna chlorophylls, because the uphill

---

*Abbreviations:* ADMR – absorbance-detected magnetic resonance;  $\beta$ -Car –  $\beta$ -carotene;  $\beta$ -DM – dodecyl- $\beta$ ,D-maltoside; C – monomeric PS II core complex; CD – circular dichroism; Chl – chlorophyll; DCCD – N,N'-dicyclohexylcarbodiimide; ELIP – early light-induced protein; IC – internal conversion; L – loosely bound trimeric LHCII; LD – linear dichroism; LHCII – light-harvesting complex II; Lut – lutein; M – moderately bound trimeric LHCII; Neo – Neoxanthin; 3PEPS – three-pulse photon echo peak shift; Ph – pheophytin; PS II – Photosystem II; RC – reaction center; S – strongly bound trimeric LHCII; S-S – singlet-singlet; S-T – singlet-triplet; T-S – triplet-minus-singlet; Vio – violaxanthin; Zea – zeaxanthin



energy transfer would considerably slow down the overall process of charge separation. Indeed, of all known primary electron donors P680 absorbs at the shortest wavelength and creates the shallowest trap of excitation energy within its antenna (Jennings et al., 1993a,b). The shallow trap of excitation energy means that at physiological temperatures (at which the thermal energy has about the same value as the energy gradient from the PS II chlorophyll *a* antenna molecules to P680)<sup>1</sup> the excitation energy has a roughly equal probability to be localized anywhere on the complete antenna (~150 chlorophyll *a* antenna molecules), and that the overall time for the trapping of the excitation energy by P680 will be relatively long.

In the following sections we first introduce the genes and proteins of PS II, then we describe in detail the spectroscopy and function of the various individual chlorophyll-protein complexes of the PS II antenna (Green and Durnford, 1996), then we discuss how the various antenna proteins connect to the D1 and D2 proteins and how this affects the transfer and trapping of the excitation energy, and finally we describe the spectroscopy and function of the complete PS II antenna system.

## II. The Photosystem II Genes and Proteins

Table 1 lists the 29 genes and gene products that are known to be associated with PS II in green plants. Some of these genes are encoded by the chloroplast genome, others by the nuclear genome. The list is not complete, since it lacks the so-called early light-induced proteins (ELIPs), proteins that are transiently synthesized by the nuclear genome under greening conditions (Jansson, 1994). Also the list does not include PS II proteins like the extrinsic PsbU and PsbV polypeptides, which occur only in cyanobacteria and do not have counterparts in higher plants. The list, however, includes the recently discovered membrane protein called LhbA (Ruf et al., 2000) or PsbZ (Swiatek et al., 2001), which is encoded by the conserved chloroplast open reading frame *ycf9*. This protein is associated with the peripheral antenna protein CP26 (Ruf et al., 2000) and controls the interaction between the PS II core complex and the peripheral antenna (Swiatek et al., 2001). It is expected that more such small proteins associated

with the peripheral antenna remain to be discovered (Ruf et al., 2000). Table 1 also lists the molecular mass and the number of transmembrane  $\alpha$ -helices of each gene product, and the smallest possible complex of proteins, associated with the PS II reaction center (PS II RC), in which each gene product is located (see Sections III and IV for definitions of the various complexes). Table 2 lists the chromophores associated with the various complexes.

It is now generally accepted that PS II is organized as a dimer in the granal parts of the thylakoid membrane (Santini et al., 1994; Hankamer et al., 1997a). Stromal PS II may perhaps be monomeric (Bassi et al., 1995), but probably contains all the PS II antenna proteins, with the possible exception of the Lhcb2 protein (Jansson et al., 1997). The total antenna size of stromal PS II is about 130 Chl (*a+b*) per RC (Jansson et al., 1997), which suggests the presence of all monomeric LHCII complexes (Lhcb4-6) and one or two trimeric LHCII complexes (Table 2). The total antenna size of granal PS II is about 210–250 Chl (*a+b*), suggesting the presence of two or three additional trimeric LHCII complexes.

Many details of the structural organization of the various pigment-protein complexes have been obtained by electron crystallography of two-dimensional crystals of trimeric LHCII (Kühlbrandt et al., 1994), the CP47-RC complex (Rhee et al., 1997, 1998) and the dimeric oxygen-evolving PS II core complex (Hankamer et al., 1999) and by X-ray diffraction of three-dimensional crystals of the PS II core complex from *Synechococcus elongatus* (Zouni et al., 2001). The LHCII structure reveals the positions and orientations of 3 transmembrane  $\alpha$ -helices, 12 chlorophyll and 2 carotenoid molecules per monomeric subunit, and is discussed in more detail in Section III.A (see below). It is commonly believed that the related monomeric proteins CP29, CP26 and CP24 have very similar organizations (Green and Kühlbrandt, 1995). The PS II core structure reveals the positions and orientations of a large number of transmembrane  $\alpha$ -helices, as well as those of the electron transport co-factors and of 32 chlorophyll and two pheophytin molecules (Zouni et al., 2001). This complex contains the PsbA-F, PsbH-O and PsbX proteins, as well as the extrinsic PsbU and PsbV proteins only found in cyanobacteria, and is discussed in more detail in Sections III.D, IV.A and IV.B.

<sup>1</sup> At 293 K the thermal energy  $k_B T$  is about  $4 \times 10^{-21}$  J, or 25 meV, or 200 cm<sup>-1</sup>, or 10 nm around 675 nm.

Table 1. List of PS II genes and gene products from green plants, listed in the order of decreasing mass

No.	Gene (origin)	Protein	Protein Mass (kDa)	No. TM $\alpha$ -Helices <sup>a</sup>	Location (smallest possible unit) <sup>b</sup>
1	<i>psbB</i> (c) <sup>c</sup>	CP47	56.3 <sup>d</sup>	6	CP47-RC
2	<i>psbC</i> (c)	CP43	50.1	6	core
3	<i>psbD</i> (c)	D2	39.4	5	RC
4	<i>psbA</i> (c)	D1	38.0	5	RC
5	<i>Lhcb4</i> (n)	CP29	28.4	3	C <sub>2</sub> S
6	<i>Lhcb5</i> (n)	CP26	26.6	3	C <sub>2</sub> S
7	<i>PsbO</i> (n)	33 kDa, OEC33	26.5	-	Core
8	<i>Lhcb2</i> (n)	LHCIIb <sup>e</sup>	24.8	3	C <sub>2</sub> S
9	<i>Lhcb1</i> (n)	LHCIIb	24.6	3	C <sub>2</sub> S
10	<i>Lhcb3</i> (n)	LHCIIb <sup>e</sup>	24.6	3	C <sub>2</sub> SM
11	<i>Lhcb6</i> (n)	CP24	22.7	3	C <sub>2</sub> SM
12	<i>PsbS</i> (n)	PSII-S	21.7	4	??
13	<i>PsbP</i> (n)	23 kDa, OEC23	20.2	-	Core
14	<i>PsbQ</i> (n)	17 kDa, OEC17	16.5	-	Core
15	<i>PsbR</i> (n)	10 kDa	10.2	-	Core
16	<i>psbE</i> (c)	$\alpha$ -Cyt.b559	9.3	1	RC
17	<i>psbH</i> (c)	PSII-H	7.7	1	Core
18	<i>psbZ</i> (c)	LhbA or PSII-Z	6.6	2	associates with CP26
19	<i>PsbW</i> (n)	PSII-W	5.9	1	RC
20	<i>psbN</i> (c)	PSII-N	4.7	1	Core
21	<i>psbF</i> (c)	$\beta$ -Cyt.b559	4.4	1	RC
22	<i>psbL</i> (c)	PSII-L	4.4	1	CP47-RC
23	<i>psbK</i> (c)	PSII-K	4.3	1	CP47-RC
24	<i>PsbX</i> (n)	PSII-X	4.2	1	Core
25	<i>psbI</i> (c)	PSII-I	4.2	1	RC
26	<i>psbJ</i> (c)	PSII-J	4.1	1	??
27	<i>psbT<sub>c</sub></i> (c)	PSII-T <sub>c</sub>	3.8	1	CP47-RC
28	<i>psbM</i> (c)	PSII-M	3.8	1	Core
29	<i>PsbT<sub>n</sub></i> (n)	PSII-T <sub>n</sub>	3.3	-	Core

<sup>a</sup> the no.  $\alpha$ -helices refers to the number of transmembrane  $\alpha$ -helices. <sup>b</sup> the smallest possible PS II RC-containing unit to which the protein is connected. RC refers to the isolated PS II RC complex (Section IV.A), CP47-RC to the isolated PS II RC complex with connected CP47 protein, core to the fully functional PS II core complex (Section IV.B), while C<sub>2</sub>S and C<sub>2</sub>SM refer to PSII-LHCII supercomplexes consisting of a dimeric PS II core complex (C<sub>2</sub>) and a strongly bound trimeric LHCII complex (S) or a moderately bound LHCII complex (M) (Section IV.C). <sup>c</sup> c and n refer to chloroplast and nuclear origin, respectively. <sup>d</sup> the masses of all *Psb* gene products are those of spinach (Hankamer et al., 1997a). The *Lhcb* gene products are those of tomato except *Lhcb4*, which is from barley (Jansson, 1994). The *PsbZ* (LhbA) protein is from tobacco (Ruf et al., 2000). <sup>e</sup> occurs usually in a single copy together with two *Lhcb1* proteins in trimeric LHCIIb (Jansson, 1994)

### III. Individual Photosystem II Antenna Complexes

#### A. Major Peripheral Antenna Complexes (LHCII)

##### 1. Structure

Most of the pigments in PS II are bound to the major

peripheral antenna complexes, called LHCII. These trimeric pigment-protein complexes are not unique in composition and consist of various combinations of three very similar proteins, encoded by genes *Lhcb1*, *Lhcb2* and *Lhcb3*, which usually occur in a ratio of about 8:3:1 (Jansson, 1994). The *Lhcb1* and *Lhcb2* polypeptides have only 14 differences in their amino acid sequences, while the *Lhcb3* polypeptide deviates more in sequence from the other two and

Table 2. Pigment composition of PS II complexes

Complex	Phe <i>a</i>	Chl <i>a</i>	Chl <i>b</i>	$\beta$ -Car	Lut	Vio <sup>a</sup>	Neo	No/RC <sup>b</sup>
PS II RC <sup>c</sup>	2	6	0	2	0	0	0	1
CP47 <sup>d</sup>	0	16	0	2–3	0	0	0	1
CP43 <sup>d</sup>	0	13	0	2–3	0	0	0	1
CP29 <sup>e</sup>	0	6	2	0	0.7–1.0	0.6–1.3	0.5–0.6	1
CP26 <sup>f</sup>	0	6	3	0	~1	~0.5	~0.5	1
CP24 <sup>g</sup>	0	5	5	0	?	?	?	1
LHCII <sup>h</sup>	0	7–8	5–6	0	2	0.3–1	1	~12
total / RC <sup>i</sup>	2	138–150	70–82	6–8	~27	6–16	~14	
core (C) <sup>d</sup>	2	35	0	6–8	0	0	0	
CS <sup>j</sup>	2	68–71	20–23	6–8	~8	2–5	~4	
CSM <sup>k</sup>	2	94–100	40–46	6–8	~15	4–10	~8	
CSML <sup>l</sup>	2	115–124	55–64	6–8	~21	5–13	~11	

<sup>a</sup> Violaxanthin is partially converted into zeaxanthin and/or antheraxanthin under conditions of light stress. <sup>b</sup> No/RC refers to the number of (monomeric) protein copies per RC in PS II membranes. The number of LHCII proteins must be regarded as a rough average, because this number can vary depending on plant species and growth conditions. <sup>c</sup> Eijkelhoff et al., 1996. <sup>d</sup> Vasil'ev et al., 2001. <sup>e</sup> Bassi et al., 1999; Pascal et al., 1999; Ruban et al., 1999. <sup>f</sup> Frank et al., 2000. <sup>g</sup> Pagano et al., 1998. <sup>h</sup> Kühlbrandt et al., 1994; Peterman et al., 1997c; Ruban et al., 1999. <sup>i</sup> Sum of PS II RC, CP47, CP43, CP29, CP26, CP24 and LHCII, each multiplied with the number denoted in No/RC. <sup>j</sup> CS refers to one half of the most common PSII-LHCII supercomplex (C<sub>2</sub>S<sub>2</sub>) and consists of PS II core, CP29, CP26 and (trimeric) LHCII complexes in a 1:1:1:1 ratio. <sup>k</sup> CSM consists of PS II core, CP29, CP26, CP24 and (trimeric) LHCII complexes in a 1:1:1:1:2 ratio. <sup>l</sup> CSML consists of PS II core, CP29, CP26, CP24 and (trimeric) LHCII complexes in a 1:1:1:1:3 ratio.

also is somewhat smaller (it lacks a number of amino acids at the N-terminus).

A major step forward in the understanding of light harvesting in PS II was the elucidation of the structure of LHCII by Kühlbrandt and coworkers (Kühlbrandt et al., 1994), who combined results from electron diffraction and electron microscopy on two-dimensional crystals of LHCII at cryogenic temperatures. Crystals were grown from native LHCII, containing the gene products encoded by *Lhcb1*, *Lhcb2* and *Lhcb3*, but the stoichiometry of these proteins in the crystals is not known. The resolution of the structure was 3.4 Å parallel to the plane of the trimer (which is also the plane of the 2-D crystals and the plane of the membrane), but 4.4–4.9 Å perpendicular to this plane. This resolution provided a somewhat crude model of the structure (Kühlbrandt et al., 1994). The model shows large parts of the protein backbone as well as the locations and approximate orientations of twelve chlorophylls and two carotenoids in each monomer (Fig. 1). Particularly well-resolved are the three transmembrane  $\alpha$ -helices (A, B and C—also numbered as 3, 1 and 2, respectively) and a short amphiphilic helix (D) at the interface of the protein and the water surroundings.

Helices A and B are exceptionally long for transmembrane helices, make an angle of about 30° with the normal to the membrane plane, and are held together at least in part by a pair of inter-helix ion pairs. A stereo representation of the LHCII pigments is given in Color Plate 4. Helix C is shorter and is oriented normal to the membrane. The structure of a considerable part of the protein, in particular most of the connecting parts between the helices as well as the C- and N-termini, was not resolved. Noteworthy is the N-terminal part, which is known to contain a lipid binding site and which is involved in trimerization (Nussberger et al., 1993; Hobe et al., 1995). It also contains (except for the *Lhcb3* gene product) a phosphorylation site. Phosphorylation of the latter site is believed to cause 'lateral' movement of LHCII between the granal and lamellar parts of the thylakoid membranes (Bassi et al., 1997).

In view of the light-harvesting function, the pigments are of particular interest. The model shows twelve chlorophylls (Chls) and two carotenoids (xanthophylls) per LHCII monomer. The two resolved xanthophylls were found to have an important structural role and were tentatively identified as lutein (Lut), because the other xanthophylls violaxanthin

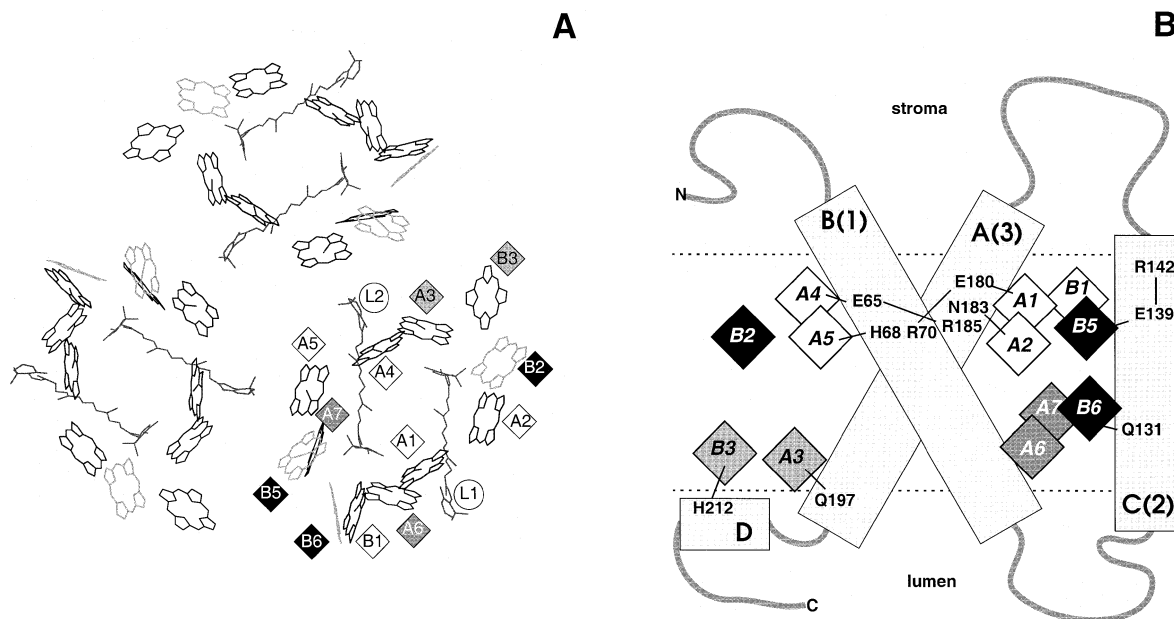


Fig. 1. Structure of the trimeric LHCII complex (Kühlbrandt et al., 1994). A) Top view of the chromophores resolved in the 3.4 Å crystal structure. L1 and L2 indicate the positions of the xanthophylls; A1–B6 indicate the sites of the Chls, numbered according to Kühlbrandt et al. (1994). The grey-scale of numbers and background in the squares corresponds to that in B. B) Schematic representation of the  $\alpha$ -helices, the location of the chlorophylls and known pigment binding sites in LHCII. Helices are indicated by characters A–D, numbers in parentheses refer to the numbering based on the amino acid sequence (from N- to C-terminus). Also indicated are amino acids known to bind Chl or to be involved in intramembrane charge pairs in LHCII. The chlorophylls in white and black have been shown to be Chl *a* and Chl *b*, respectively; those in grey have been proposed to have a mixed character (see text and Table 4). See stereogram of pigments in Color Plate 4.

(Vio) and neoxanthin (Neo) were present in substoichiometric amounts in the crystallization mixture. The identity of the Chls (Chl *a* or Chl *b*) in the structure could not be resolved from the structural data. The seven Chls closest to the two resolved xanthophylls were tentatively attributed to Chl *a*. As discussed in the following sections, reconstitution experiments after overexpression of the genes in *E. coli* have indicated that this attribution was only partially correct. It should be noted that the pea LHCII that was used as starting material for crystallization contained eight Chls *a* and six Chls *b* per monomer. These numbers vary slightly across species and for maize, values of seven Chls *a* and five Chls *b* per monomer were reported (Remelli et al., 1999).

LHCII, as the main protein constituent of the thylakoid membranes, should be considered not only as a light-harvesting pigment protein complex, but also as a main structural element of the thylakoid membrane. It has been well established that it plays an important role in the formation and stabilization

of the grana and in the lateral separation of the two photosystems (Garab and Mustárdy, 1999). LHCII also provides structural flexibility to the granal thylakoids (Barzda et al., 1996), which is largely independent of the activity of the photochemical apparatus, and most likely driven by a thermo-optic effect, i.e., the local thermal fluctuations due to the dissipation of the excess excitation energy (Cseh et al., 2000). This type of light-dependent structural flexibility of LHCII, probably in concert with its pH-dependent flexibility (Ruban et al., 1998), may play an essential role in regulatory processes, such as the dissipation of excess excitation energy (Jennings et al., 1991; Horton et al., 1996; Barzda et al., 1999), and the regulation of phosphorylation by light (Zer et al., 1999).

## 2. Xanthophylls: Identity, Location and Function

LHCII from dark-adapted plants usually contains Lut, Neo and Vio in a ratio of about 2:1:0.07–1, depending on the aggregation state, source and

biochemical isolation procedure (Peterman et al., 1997c; Ruban et al., 1999). This points to a total of four binding sites per monomeric subunit of a trimer, which have now indeed been recognized. The first two sites bind the xanthophylls seen in the crystal structure (Kühlbrandt et al., 1994) which make an internal central crossbrace in the complex (Fig. 1). Both sites can be occupied by either Lut or Vio, but with a very strong preference for Lut (Croce et al., 1999b; Hobe et al., 2000), whereas the binding affinity for Neo is extremely small (Hobe et al., 2000). The third site was not recognized in the crystal structure, but on the basis of reconstitution studies it was concluded to be near helix C (2) and to be specific for Neo (Croce et al., 1999b). Hobe et al. (2000) found that the affinity for Lut is 25 times lower. From linear-dichroism (LD) experiments it was concluded that the angle between Neo and the normal to the trimer plane is  $57^\circ \pm 1.5^\circ$ , close to the value for the central transmembrane xanthophylls in the crystal structure. The fourth site is probably exclusively occupied by Vio. It was recently shown by Ruban et al. (1999) that approximately one Vio is bound per monomeric subunit of LHCII, but the binding is weak and the xanthophyll is very easily lost upon isolation. Gruszecki et al. (1999) proposed a model in which a fraction of the Vio molecules that are in a cis-conformation are located on one site of the membrane, while the major fraction is in an all-trans-conformation and is transmembrane. It was proposed that the loosely-bound Vio is involved in the xanthophyll cycle, in which Vio is de-epoxidated to form zeaxanthin (Zea) under high-light conditions (Ruban et al., 1999). Changes have been observed in the conformation of (at least) one of the xanthophylls in LHCII upon aggregation with the use of resonance Raman spectroscopy (Ruban et al., 1995). The corresponding xanthophyll could not be unambiguously assigned, although it was presumed to be Lut. In a more recent study, Ruban et al. (2000) showed that a fraction of the Neo molecules undergoes a structural change upon oligomerization of LHCII.

The interpretation of spectroscopic measurements on LHCII is helped considerably by differences in absorption properties of the xanthophylls in the four binding sites. It is consistently found that Neo has its red-most absorption peak at  $487 \pm 1$  nm (Peterman et al., 1997c; Croce et al., 1999a,b; Gradinaru et al., 2000; Ruban et al., 2000) whereas both Lut and Vio peak more to the red (Peterman et al., 1997c; Croce et al., 1999a,b; Gruszecki et al., 1999; Ruban et al.,

2000; Gradinaru et al., 2000). Monomeric LHCII contains no Vio and it shows besides the Neo absorption an additional peak at 494–495 nm, which is ascribed to the two Lut molecules (Peterman et al., 1997c; Croce et al., 1999b; Ruban et al., 2000). Croce et al. (2000) even found small differences for both Lut molecules in monomeric reconstituted LHCII complexes. For trimeric LHCII, which also contains (substoichiometric amounts of) Vio, an additional small absorption band was observed around 510 nm, and was assigned to Vio (Peterman et al., 1997c; Gradinaru et al., 2000). However, Ruban et al. assigned the 510 nm band to a Lut molecule (Ruban et al., 2000) and it was claimed that one of the luteins has a different conformation in the trimer than in the monomer. The difference in the absorption spectrum of Lut in monomers and trimers would then be due to a conformational difference. Below, we stick to our own assignment (Vio corresponds to 510 nm) for the discussion of singlet transfer from xanthophyll to Chl and triplet transfer from Chl to xanthophyll, but the different assignment of Ruban et al. should be kept in mind.

The central xanthophylls (luteins) absorbing maximally at 494 nm are probably structurally important (Kühlbrandt et al., 1994) and give rise to efficient singlet energy transfer to Chl and in addition accept a large fraction of the Chl *a* triplets (Peterman et al., 1997c). This means that there must be close contacts between these xanthophylls and at least some Chl *a* residues.

The triplet quenching is physiologically important for the following reasons. The excitation energy transfer from Chl *b* to Chl *a* is rather fast (the main part of the energy transfer proceeds within 1 ps—see below) and therefore most of the excitations are present on Chl *a* during the excited-state lifetime in PS II (on the order of several tens to hundreds of ps). There is a finite probability for a singlet excitation to transform into a triplet excitation via a spin flip (a process called intersystem crossing) which consequently leads to Chl *a* triplets. These triplets are potentially harmful for the system since they can react with molecular oxygen to form singlet oxygen ( $^1\text{O}_2^*$ ), a highly reactive and destructive species. However, the xanthophylls quench the Chl *a* triplets rather effectively, because of efficient triplet transfer from Chl *a* to xanthophyll. The rate of transfer was estimated to be  $>(0.5 \text{ ns})^{-1}$  by Schödel et al. (1998). The energy of the xanthophyll triplets is too low to allow the formation of singlet oxygen and thus the

Table 3. List of mutations in three studies to identify the pigments that bind at specific binding sites in LHCII

site	Remelli et al. (1999)	Yang et al. (1999)	Rogl and Kühlbrandt (1999)
A1	RE70/180IV		E180A
A2	N183V		N183A
A3	Q197V	Q197E, Q197S	Q197L
A4	ER65/185VL	EH65/68QL	E65A
A5	H68I	H68F, H68L EH65/68QL	H68A
A6	P82V		LG77/78VF
B3	H212V	H212F, H212L	H212A
B5	E139L FR139/142LL		E139A
B6	Q131V, Q131E	Q131E, Q131S	Q131A

xanthophylls fulfill a protective role (Siefermann-Harms, 1987; Nechushtai et al., 1988; Siefermann-Harms and Angerhofer, 1998).

In contrast to the central xanthophylls, the Neo at the third binding position was found to perform badly in singlet excitation energy transfer and triplet quenching (Peterman et al., 1997c). One might wonder about the function of the Neo in LHCII. Croce et al. (1999b) found that reconstituted complexes with Neo suffer less from photooxidation in the presence of oxygen than complexes without Neo and it was therefore proposed that Neo is actively involved in the scavenging of  $^1\text{O}_2^*$ .

The Vio at the fourth binding position, absorbing maximally at 510 nm, was found to be efficient in singlet energy transfer to Chl and in accepting triplets from Chl *a* (Peterman et al., 1997c). In complexes with substoichiometric amounts of Vio, a relatively large fraction of the Chl *a* triplets were transferred to Vio, indicating that Vio at this binding position plays an important photophysical role (it should be noted that the 510 nm absorption band was assigned to Lut by Ruban et al., 2000).

Finally, we would like to mention the work of Pogson et al. (1998) who studied *Arabidopsis* mutants with altered xanthophyll compositions. It turns out that plants are still viable in the complete absence of lutein, violaxanthin and neoxanthin, but the xanthophylls appear to be necessary for optimal rates of seedling development and photoprotection.

### 3. Location and Identity of the Chlorophylls

In order to understand the light harvesting and photoprotection in LHCII in detail, one needs to know the identities of the Chls. The longest-wavelength absorption band of Chl *b* lies around 650 nm whereas it is located near 670 nm for Chl *a*. Because of this large energy difference, singlet excitations have a strong tendency to be located on Chl *a*. Therefore, the identities of the pigments is of crucial importance for the routes of energy transfer. On the other hand, dangerous triplets are also predominantly generated on Chl *a* and effective triplet quenching requires close contacts with xanthophyll molecules.

The identity of the Chls was recently addressed by studying reconstituted LHCII complexes in which individual Chl binding sites had been mutated to non-bonding sites (Remelli et al., 1999; Rogl and Kühlbrandt, 1999; Yang et al., 1999). In order to facilitate the discussion, we denote the binding sites of the chlorophylls by a capital and a number, corresponding to the numbering of the chlorophylls as originally given by Kühlbrandt and coworkers (Kühlbrandt et al., 1994; Fig. 1a,b; Color Plate 4). Thus site A1 binds Chl *a*1, etc. The original assignment was based on the assumption that the triplets that are predominantly formed on Chl *a* have to be quenched by the two xanthophylls that are observable in the crystal structure. For triplet quenching to be efficient, Van der Waals contact is required and this formed the rationale for the

Table 4. Ligands and types of chlorophyll of the proposed chlorophyll binding sites in trimeric LHCII and CP29 (for references, see text)

site	LHCII ligand	LHCII type of Chl	CP29 ligand	CP29 type of Chl
A1	Glu	a	Glu	a
A2	Asn	a	His	a
A3	Gln	mixed	Gln	mixed
A4	Glu	a	Glu	a
A5	His	a <sup>a</sup>	His	a
A6	Gly <sup>b</sup>	mixed or b	-	-
A7	?	mixed or b	-	-
B1	?	a	-	-
B2	?	b	-	-
B3	His	mixed	His	mixed
B5	Glu	b	Glu	mixed
B6	Gln	b	Glu	mixed

<sup>a</sup> required for stability. <sup>b</sup> peptide carbonyl

identification of the seven central Chls as Chl *a*. The presence of additional xanthophylls, however, invalidates this line of reasoning.

Table 3 lists the various mutations that have been introduced in the different studies in order to reveal the identities of the individual pigments. Rogl and Kühlbrandt concluded that the Chls at sites A1 and A2 are indeed Chl *a*, whereas those at sites B5 and B6 are Chl *b* (Table 4). The same conclusion was reached by Remelli et al. (1999). Also the results of Yang et al. (1999) strongly suggest that the Chl at B6 is a Chl *b*. The binding site A5 for Chl *a* was mutated in all three studies and although reconstituted complexes could be obtained, the stability was reported to be much lower in two of these studies: either 1.5–3 Chls were lacking (Yang et al. 1999), or no trimers could be formed (Rogl and Kühlbrandt, 1999). Remelli et al. found the loss of only one Chl *a* when A5 was mutated, whereas the number of Chl *b* molecules and xanthophylls per LHCII monomer did not change.

Some controversial results were obtained when mutating A3 and B3. Yang et al. (1999) found a loss of approximately 1 Chl *a* and 1 Chl *b* upon changing B3 and it was suggested that binding a Chl at position A3 might require the presence of a Chl at position B3. Conversely, mutating A3 led to the loss of ~0.5 Chl *a* and ~0.5 Chl *b*, suggesting that this site has no preference for binding either Chl *a* or Chl *b*. Also Remelli et al. concluded that the Chl at A3 was a Chl

*a* in 50% of the cases and a Chl *b* in the other 50%. They found that mutation of B3 led to the loss of only one Chl per monomer, again a Chl *a* in 50% and a Chl *b* in the other 50% of the cases. Rogl and Kühlbrandt concluded that both the Chls at A3 and B3 are Chl *a*, but they did not determine the Chl to protein ratio and could not be confident about the exact number of Chls present. The discrepancy might partly be related to disregarding the possibility of mixed binding sites.

Rogl and Kühlbrandt found that mutation of A4 and A6 led to the formation of unstable trimers (for the latter mutant also no Neo was bound) and no conclusions were drawn about the identity of the corresponding pigments. Remelli et al. concluded that the Chl at A4 is a Chl *a* and that at B2 is a Chl *b*, whereas on average 1.5 Chl *b* and 0.5 Chl *a* are located at sites A6 and A7. Finally, they observed that mutation of site A1 led to the loss of ~1.5 Chl *a*, from which it was concluded that the Chls at A1 and B1, which are very close together, are both Chl *a*.

In conclusion, the results of the three groups seem to agree in most cases and are consistent with the original 'Kühlbrandt assignment' with a few exceptions: B1 probably binds a Chl *a*, sites A3 and B3 have each mixed character (0.5 Chl *a* and 0.5 Chl *b*), and A6 and A7 together bind ~1.5 Chl *b* and ~0.5 Chl *a*. These conclusions agree with the results of some spectroscopic studies (see below). Even for trimeric and aggregated LHCII, where part of the



xanthophyll in the 4th position is supposed to be present, it was concluded that 1–2 Chls *a* per trimer are not in contact with a xanthophyll (Barzda et al., 2000). These Chls might correspond to the Chls at site B1 or B3.

#### 4. Chlorophyll-Xanthophyll Contacts

It was found by Rogl and Kühlbrandt (1999) and by Croce et al. (1999a) that in reconstituted complexes, where the B5 and B6 binding sites were mutated in such a way that no Chl could bind at these positions, 50% less Neo was bound, indicating that Neo is located near these two Chl *b* pigments in the vicinity of helix C (helix 2). When LHCII is reconstituted without Neo, strong changes are observed in the Chl *b* regions of the absorption, circular dichroism (CD) and LD spectra (Croce et al., 1999a,b). Much weaker changes occur in the Chl *a* region, which is understandable if most Chls *a* are relatively far away from Neo. Most Chl *a* molecules are probably located next to the central xanthophylls, although one is possibly located next to Vio in the 4<sup>th</sup> position. Evidence for this was given by Peterman et al. (1997c), who detected an ~80% efficiency of Chl *a* to xanthophyll triplet transfer in monomeric LHCII (largely depleted of the xanthophyll at fourth binding site) and a significantly higher efficiency in trimeric LHCII (with partly occupied fourth binding site).

Additional spectroscopic observations confirm this view. Sub-picosecond pump-probe experiments show that singlet excitation of Chl *a* (at 670 and 680 nm) leads to spectral changes at 494 nm (Lut) and 510 nm (Vio), whereas excitation of Chl *b* leads to a pronounced absorption change at 486 nm (Neo) (Gradinaru et al., 1998c). Similarly, absorbance detected magnetic resonance (ADMR) and flash-induced triplet-minus-singlet (T-S) spectroscopy showed that triplets on Lut (494 nm) and Vio (510 nm) cause characteristic absorption changes in the Chl *a* Q<sub>y</sub> region, whereas similar features are absent in the Chl *b* Q<sub>y</sub> region (Carbonera and Giacometti, 1992; van der Vos et al., 1994; Peterman et al., 1995, 1997c; Naqvi et al., 1997; Barzda et al., 1998). These experiments strongly indicate that most Chl *a* molecules are in contact with the central xanthophylls (mainly Lut), that one Chl *a* is possibly next to Vio at the 4<sup>th</sup> binding site, and that Neo is in contact with some Chl *b* molecules at sites B5 and B6. Xanthophyll-chlorophyll contacts can influence the

Chl lifetimes (Naqvi et al., 1997; van Amerongen and van Grondelle, 2001) and might be important for regulatory processes.

#### 5. Xanthophyll → Chlorophyll Singlet Energy Transfer

Several experimental subpicosecond transient absorption studies have been performed with the aim of observing the energy transfer kinetics from xanthophyll to Chl in LHCII (Peterman et al., 1997b; Connelly et al., 1997a,b; Gradinaru et al., 2000; Walla et al., 2000; Croce et al., 2001). In these studies, the xanthophyll → Chl energy transfer was observed to take place mainly within several hundreds of femtoseconds (fs). Together with the fact that extensive spectral overlap exists and a broad spectral window has to be probed, to disentangle many processes, this makes the experiments and their interpretation quite complicated. Several years ago, contradictory conclusions were reached about the identities of the Chls that accept the excitations. Connelly et al. (1997) excited LHCII from *Arabidopsis thaliana* at 475 and 490 nm at room temperature. Upon excitation at the latter wavelength, a component with a time constant of 142 fs was observed, and was attributed to direct energy transfer from xanthophyll to Chl *b*. Transfer from xanthophyll to Chl *a* appeared to be absent. These authors presented a model in which two Chl *b* molecules are close to the central xanthophylls. This particular model conflicts with other results (Section III.A.3). It should be noted that at the excitation wavelengths, besides Lut and Chl *b*, Neo also is expected to be excited, and Neo is in close contact with two Chl *b* molecules (see above).

Excitation at 500 nm (mainly Chl *b* and Lut) showed rapid energy transfer (~220 fs) from a xanthophyll to a Chl *a* spectral form peaking around 675 nm, whereas excitation at 514 nm (mainly Chl *b* and Vio at the fourth binding position) led to transfer to Chl *a* at 670 nm (Peterman et al., 1997b). No direct transfer from xanthophyll to Chl *b* was observed. Although the time resolution was not as high as in the study by Connelly et al. (1997a), Peterman et al. argued that only a small fraction of xanthophyll → Chl *b* transfer could have been missed in the experiment. The contacts of both Lut and Vio with Chl *a* molecules with different absorption characteristics are in agreement with T-S results (van der Vos et al.,

1991; Peterman et al., 1997c). Walla et al. (2000) concluded from one- and two-photon femtosecond experiments that transfer takes mainly place from xanthophyll to Chl *a*. Recently, Gradinaru et al. (2000) concluded from an elaborate subpicosecond transient absorption study on trimeric LHCII from spinach that Lut and Vio (i. e. the Xan with an absorption peak at 510 nm) transfer almost exclusively towards Chl *a*, whereas Neo transfers to Chl *b*. In a femtosecond transient absorption study on reconstituted LHCII monomers, Croce et al. (2001) confirmed that the single Neo molecule transfers almost exclusively to Chl *b*. The two Lut molecules were found to transfer both to Chl *b* and Chl *a*. It was estimated that 40–50% of the excitations on the xanthophylls (both Lut and Neo) are transferred to Chl *b*. Given the fact that Neo transfers almost exclusively to Chl *b*, it must be concluded that in these experiments excitations from Lut are predominantly transferred to Chl *a* and that a fraction (between 10 and 25%) is transferred to Chl *b*. Therefore, the results of both groups are in fair agreement with each other (and with the pigment assignments given above).

#### 6. Chlorophyll *b* → Chlorophyll *b* and Chlorophyll *a* Singlet Energy Transfer

The approximate rate of excitation energy transfer from Chl *b* to Chl *a* in LHCII was estimated by studying membranes from *Chlamydomonas reinhardtii* with the use of fluorescence upconversion (Eads et al., 1989). The observed time constant was  $0.5 \pm 0.2$  ps. An additional slower component of  $4 \pm 2$  ps was observed (for isolated LHCII) in a transient absorption study by Kwa et al. (1992b). The presence of at least two components was confirmed in subsequent studies by Du et al. (1994), Pålsson et al. (1994) and Bittner et al. (1994, 1995). In more recent transient absorption studies, in which the entire  $Q_y$  region was probed, a more complete picture was obtained for the Chl *b* → Chl *a* transfer. Visser et al. (1996) performed experiments at 77 K and observed transfer components of <300 fs (~40%), 600 fs (~40%) and ~6 ps (~20%) after exciting Chl *b* at 650 nm, suggesting that one of the five Chl *b* molecules per monomeric subunit transfers energy much more slowly than the others, with a time constant well above 1 ps. Similar results were obtained by Connelly et al. (1997b) at room temperature, with transfer

times (180 fs, 480 fs and 6ps) and relative contributions that were similar to those observed by Visser et al. (1996), although some variation was found for different preparations. The above-mentioned experiments were performed on trimeric LHCII. It was concluded by Kleima et al. (1997) that all observed transfer processes occur within a monomeric subunit: the distances between pigments on different monomers are simply too large to explain the subpicosecond transfer steps, whereas the slowest process is observed for both monomers and trimers (Kleima et al., 1997). Agarwal et al. (2000) applied three-pulse photon echo peak shift (3PEPS) measurements and found evidence for some Chl *b* → Chl *b* energy transfer, but the relative amount, when compared to the amount of Chl *b* → Chl *a* transfer, was not determined.

We can summarize these results by concluding that most of the singlet excitations created either on xanthophyll or Chl *b* are transferred within one ps to Chl *a* molecules within the same monomeric subunit. Further transfer of singlet excitations then takes place almost exclusively between Chl *a* molecules.

#### 7. Chlorophyll *a* → Chlorophyll *a* Singlet Energy Transfer

In an early singlet-singlet annihilation study on LHCII aggregates from spinach by Gillbro et al. (1988) it was concluded that the average nearest-neighbor time for transfer between Chl *a* molecules is less than 5 ps. Later studies were directed at obtaining information about specific transfer steps out of the multitude of processes that are expected to take place. In a (polarized) transient absorption study at room temperature by Kwa et al. (1992b), transfer times ranging from <2 ps to 15–35 ps were observed. The latter time was tentatively assigned to transfer between monomers. A relatively slow process of 13 ps also was observed by Mullineaux et al. (1993) in a photon-counting study, although it was clear that faster processes also should be present. This was confirmed by Pålsson et al. (1994), who observed times of ~2 ps and 10–20 ps. Savikhin et al. (1994) found transient absorption depolarization times ranging from 5 ps at room temperature to many tens of picoseconds at cryogenic temperatures, whereas Bittner et al. (1995) found a ~14 ps spectral equilibration above 670 nm at 12 K. All these studies had in common that energy transfer was observed on

a time scale significantly longer than 1 ps, which was more or less the upper limit for transfer from xanthophyll and Chl *b* towards Chl *a*.

An extensive study of the Chl *a* → Chl *a* transfer kinetics in trimeric LHCII was performed by Visser et al. (1996, 1997) at 77 K. At this temperature the absorption spectrum shows an increased fine structure with respect to room temperature, which allows more detailed observations. It was shown that excitation at 663 nm gave rise to a ~2 ps transfer time, whereas excitation around 670 nm led to transfer steps of ~400 fs and ~15 ps. Similar experiments were performed by Gradinaru et al. (1998b) on monomeric LHCII at 77K. In general, the results were comparable to those observed on trimers but additional details were resolved. Excitation at 663 nm showed a transfer time of  $5 \pm 1$  ps towards longer wavelength pigments and it was argued that this transfer originated from only one Chl *a* pigment. After excitation at 669 nm, two downhill transfer times of 300 fs and 12 ps were observed, while excitation towards longer wavelengths revealed at least one other picosecond component. Thus, it is clear that even within a monomer some 'slow' processes are present. Recent 3PEPS measurements at room temperature gave Chl *a* equilibration times ranging from 300 fs to 6 ps (Agarwal et al., 2000).

It was recently discussed that the large variation in observed transfer times (hundreds of fs to over 10 ps) can be explained by energy transfer within the monomeric subunits (van Amerongen and van Grondelle, 2001). The spread in transfer times is, to a large extent, explained by large variations in the pigment-pigment distances and their relative orientations and to a lesser extent by a variation in site energies.

### 8. Singlet Excitation Energy Transfer throughout and between LHCII Trimers

Most of the ultrafast measurements mentioned above focus on individual excitation energy transfer steps, which can be monitored if the Chl *a* molecules that are involved have slightly different absorption characteristics. In other words, *spectral* equilibration is monitored. For the overall light-harvesting process, however, it is also important to study transfer between spectrally identical pigments (for instance on different monomeric subunits or trimers), which gives rise to *spatial* equilibration. This subject can be addressed by singlet-singlet (S-S) annihilation experiments. In

S-S annihilation studies usually intense (sub)pico-second laser pulses are used to excite a sample. Due to these intense pulses, several singlet excitations can be created simultaneously in a photosynthetic complex. While migrating through the complex, these excitations can end up on the same molecule, which leads to the loss of one singlet excitation (annihilation) due to internal conversion (IC). The process of IC is extremely fast and occurs on a time scale of ~100 fs. Studying the annihilation kinetics can provide information about the speed of excitation transfer throughout the domain (van Amerongen et al., 2000). Because xanthophyll or Chl *b* to Chl *a* excitation transfer is extremely fast and essentially unidirectional (see above), only transfer between Chl *a* molecules is important for the annihilation process.

Bittner et al. (1994) performed S-S annihilation experiments on trimeric LHCII and fitted the annihilation process with an exponential decay with a time constant of 28 ps. Barzda et al. (2001) obtained an annihilation rate for trimers of  $(24 \text{ ps})^{-1}$  at room temperature. The annihilation experiments were also performed on lamellar aggregates of LHCII. After normalizing the annihilation rate to the annihilation rate per trimer, a value of  $(16 \text{ ps})^{-1}$  was obtained (Barzda et al., 2000). Loosely speaking, this means that in an aggregate of *X* trimers it takes on average  $X \times 16$  ps before two Chl *a* excitations meet. If one excitation is replaced by a stationary trap, for instance a triplet, this average time would double to  $X \times 32$  ps. This time is the spatial equilibration time (first passage time or migration  $\tau_{\text{mig}}$ ) per excitation. The time of 32 ps in one trimeric LHCII complex is actually remarkably slow. For instance, in the PS I core complex the entire trapping process (resulting in primary charge separation) takes only ~23 ps (van Grondelle et al., 1994), although the number of Chl *a* molecules is ~4 times higher than in trimeric LHCII. Moreover, the rate-limiting step for trapping in PS I is probably transfer to the trap, meaning that spatial equilibration in the antenna occurs on a much faster time scale than in LHCII. The difference in the average Chl *a* to Chl *a* transfer times in LHCII and PS I is probably caused by the different Chl *a* densities in the two complexes. It was recently illustrated that the observed annihilation rate is in reasonable agreement with the pigment assignment given above and the previous results from polarized and ultrafast experiments (Van Amerongen and Van Grondelle, 2001).

## *B. Minor Peripheral Antenna Complexes (CP29, CP26, CP24)*

### *1. General Features*

Besides the major trimeric peripheral antenna complexes LHCII, the outer antenna of PS II also contains the 'minor' complexes CP29, CP26, CP24. These proteins show large homology with LHCII, especially regarding the Chl binding sites, and bind approximately 8–10 Chls (*a* and *b*), besides several xanthophylls (Table 2). They also share many spectroscopic properties with LHCII (Zucchelli et al., 1994) and their overall fold is thought to be similar to that of LHCII (Green and Kühlbrandt, 1995; Sandona et al., 1998). In general, one copy of each protein is found per PS II RC and together the minor complexes bind 15% of the Chls in PS II. Therefore, their role in light harvesting seems to be less pronounced than that of LHCII, although their role in regulatory mechanisms can be important in view of the location close to the PS II core (Section IV.C). A possible role of these complexes in regulatory mechanisms is strengthened by the finding that a larger fraction of Vio is converted to Zea in CP26 and CP29 than in trimeric LHCII (Wentworth et al., 2000). In addition, CP26 and CP29, but not LHCII or CP24, bind DCCD, an inhibitor of non-photochemical quenching (Ruban et al., 1992; Pesaresi et al., 1997). The DCCD binding site of CP29 is probably also involved in the binding of Ca<sup>2+</sup> ions, suggesting a photophysical role (Jegerschöld et al., 2000).

### *2. CP29*

For a long time knowledge about the minor complexes lagged behind that of LHCII because of problems in isolating sufficient amounts of pure and intact protein. However, a large amount of information has recently become available due to the expression of the CP29 apoprotein in *E. coli*, and the successful reconstitution of a complex (rCP29) that is almost indistinguishable from native CP29 (nCP29) from maize (Giuffra et al., 1996; Sandona et al., 1998).

Six of the Chl binding sites that were identified in LHCII are identical in CP29. Moreover, the site B6 for Chl *b* is a Gln in LHCII and a Glu in CP29, whereas site A2 is an Asn in LHCII and a His in CP29, also potential chlorophyll-binding ligands (Bassi et al., 1999). These eight sites presumably bind the eight Chls in CP29. In a detailed study, all

the binding amino acids were selectively mutated to non-binding residues to study the Chl identities and their spectroscopic properties (Bassi et al., 1999). nCP29 from maize binds six Chls *a* and two Chls *b*. Mutating site A2, A4 or A5 led to the loss of one Chl *a* molecule, whereas mutating site A3, B3, B5 or B6 did not lead to the loss of only one type of pigment. Therefore, the latter were referred to as mixed sites. No stable complex could be obtained when site A1 was mutated, but from indirect evidence it was concluded that A1 binds Chl *a* (Bassi et al., 1999). Despite the fact that some sites may show mixed occupancy, there is a remarkable 'plateau region' where variation of the Chl *a* to Chl *b* ratio in the reconstitution mixture does not lead to variation in the ratio within the complex. This suggests that a Chl *a* at one mixed binding site preferentially sits next to a Chl *b* on the neighboring binding site (and vice versa). A significant decrease of the Chl *a* to Chl *b* ratio in the reconstitution mixture did result in a decrease of the Chl *a* to Chl *b* ratio in the complex, but the opposite was not possible, i.e., a large increase of the Chl *a* to Chl *b* ratio could not be achieved (Giuffra et al., 1997). Similar results were obtained for LHCII (Kleima et al., 1999) and CP24 (Pagano et al., 1998), but one Chl *a* molecule appeared to be necessary for stable trimeric LHCII and stable CP24. Recently, it was reported that LHCII can also be reconstituted without any Chl *a* (Schmid et al., 2001).

It is interesting to compare the Chl identities in CP29 to those in LHCII (Table 4). Sites A1, A2, A4 and A5 presumably bind Chl *a* in both proteins, whereas A3 and B3 consistently are mixed sites. However, sites B5 and B6 are thought to bind exclusively Chl *b* in LHCII. When the Glu of site B6 in CP29 is changed into a Gln, the amino acid found here in LHCII, a relative increase in the amount of Chl *b* is observed, and when the Gln of (reconstituted) LHCII is changed into a Glu, an increased amount of bound Chl *a* is found (Bassi et al., 1999). These results indicate that the difference in binding preference for Chl *a* or Chl *b* is at least partly determined by the nature of the amino acid at site B6 (Gln or Glu).

nCP29 from maize binds 0.9 Lut, 0.5 Neo and 0.6 Vio per complex and rCP29 can be prepared with similar xanthophyll contents (Bassi et al., 1999). It was found that the mutation E166V leads to the loss of 1 xanthophyll in rCP29 in a site called L2 (Bassi et al., 1999). The resulting complex after reconstitution contains 0.84 Lut, 0.04 Neo and 0.12 Vio, indicating

that one site (L1) is predominantly occupied by Lut while the other site has a mixed character, not crucial for refolding. The occupancy of the xanthophyll binding sites appears to be slightly different in CP29 from spinach, where 0.7 Lut, 0.6 Neo and 0.7 Vio were observed per complex (Pascal et al., 1999), or 1.0 Lut, 0.6 Neo and 1.3 Vio (Ruban et al., 1999), one more xanthophyll than observed by the other groups.

In analogy with LHCII (see above), CP29 has a 496 nm absorption band at cryogenic temperatures that is probably due to Lut and Vio, whereas a smaller peak at 483 nm can be ascribed to Neo (Pascal et al., 1999). The absorption spectrum of CP29 in the  $Q_y$  region is dominated by the absorption of Chl *a*, but at cryogenic temperatures Chl *b* bands are clearly revealed at 638 and 650 nm (Zucchelli et al., 1994; Pascal et al. 1999). The Chl *b* bands also contribute in a pronounced way to the CD and LD spectra. Bassi et al. (1999) tried to correlate the individual absorption bands with specific Chls by comparing the absorption spectra of reconstituted complexes with and without mutated binding sites. Sites A2, A4 and A5 were associated with Chl *a* absorption bands at 680, 676 and 675 nm, respectively. Mutation of mixed sites led to clear changes in both the Chl *a* and Chl *b* spectral regions: B3 (639 and 679 nm), A3 (638 and 668 nm), B5 (650 and 678 nm) and B6 (652 and 678 nm). Subsequently, it was concluded that Chl A1 most likely absorbs around 669 nm. These assignments should be considered with some caution. The removal of specific pigments may induce changes of the absorption of the remaining pigments due to changed excitonic interactions (pigment-pigment interactions) or conformational changes (pigment-protein interactions) (Van Amerongen and Van Grondelle, 2001). This might be the reason for the apparent discrepancy with a sub-ps pump-probe study, in which CP29 was excited at 77 K, at either 640 or 650 nm (Gradinaru et al. 1998a). Excitation at 640 nm was followed by transfer (time constant ~350 fs) to a relatively 'red' Chl *a* whereas excitation at 650 nm was followed by transfer to a relatively 'blue' Chl *a* (time constant ~2.2 ps), i.e., just opposite to what one might expect from the work of Bassi et al. (1999). Also from hole-burning measurements it was concluded that transfer from the 'red' Chl *b* is slower than transfer from the 'blue' Chl *b* (Pieper et al., 2000).

Most of the Chls *a* contribute to the absorption band around 676 nm. Although the absorption peak of Chl A2 is possibly at lower energy than those of

the other Chls, the energetic separation is relatively small. This is in agreement with recent fluorescence line-narrowing experiments, where it is observed that the fluorescence at 4 K arises from at least 3 different Chl *a* molecules (Pascal et al., 2000). This is readily explained by the fact that the spacing of the energy levels of different pigments is less than the inhomogeneous spread in energy of the individual pigments, a situation that is similar to that of LHCII (Peterman, 1997a; Pieper et al., 1999a,b).

Nonpolarized sub-ps pump-probe spectroscopy has also been applied in the Chl *a*  $Q_y$  region (Gradinaru et al., 1998a). Due to the overlap of the absorption bands only two transfer processes could be observed, a very fast one of ~300 fs and a much slower process of 10–13 ps. In view of the rather isolated position of the Chl pair at sites A3–B3, it seems most likely that the latter process reflects transfer from the Chl *a* of this pair to the pool of other Chl molecules.

### 3. CP26 and CP24

Various results have been reported for the pigment composition of CP26. Chl *a*/Chl *b* ratios of 3.3 (van Amerongen et al., 1994b), 2.5 (Ruban et al., 1999) and 2.2 (Dainese and Bassi, 1991) were found. Comparison of the low-temperature absorption spectrum of CP29 and CP26 (Zucchelli et al., 1994) shows relatively more absorption in the Chl *b* region, indicating that the Chl *a*/Chl *b* ratio is smaller for CP26 than for CP29, where it is close to 3.0. Several papers have described spectroscopic properties of CP26 (Jennings et al., 1993a,b; van Amerongen et al., 1994; Zucchelli et al., 1994;), and the LD and CD spectra in the  $Q_y$  region resemble to a large extent those of CP29 (Pascal et al., 1999), indicating a similar chlorophyll organization. In the Soret region clear differences are observed, probably because of differences in the xanthophyll composition and/or location. Ruban et al (1999) proposed that CP26 strongly binds (at least) one Lut in the center, and that a Neo binds at a similar site as the Neo in LHCII, whereas a Vio molecule is bound loosely at a peripheral position. Ros et al. (1998) reconstituted CP26 after overexpression of the apoprotein in *E. coli*. They were not able to obtain a Chl *a*/Chl *b* ratio higher than 1.4, whereas it appeared to be possible to obtain a reconstituted complex without any Chl *a*. More recently, reconstituted CP26 was obtained with 6 Chl *a*, 3 Chl *b*, 1 Lut, 0.55 Neo and 0.45 Vio per complex (Frank et al., 2000).

Isolation and purification of CP24 is a difficult task. Pagano et al. (1998) were able to reconstitute CP24 after overexpression of the apoprotein in *E. coli*. The spectroscopic properties and pigment composition were compared to those of the isolated wild-type complex. They found a Chl *a* to Chl *b* ratio of 1.2 for the isolated complex, whereas values varying from 0.9 to 1.6 had been observed before. Reconstituted complexes with a Chl *a* to Chl *b* ratio of 0.12 to 1.4 could be obtained when the pigment composition of the reconstitution mixture was varied. The absorption and CD spectra of the complexes with a ratio of 1.0 resembled those of the isolated CP24. Taking into account the sensitivity of the ratio in the complex to the ratio in the reconstitution mixture, which again had a 'plateau region', it was argued that CP24 most likely contains 5 Chls *a*, 5 Chls *b* and 2 xanthophylls (Lut and Vio).

### *C. Other Proteins Associated with the Peripheral Antenna*

There are at least two other types of PS II proteins that belong to the group of nuclear-encoded Chl *a/b* binding proteins and are related to trimeric LHCII (Section III.A) and the minor peripheral antenna complexes (Section III.B). The first type is formed by the group of early light-inducible proteins (ELIPs). These proteins are transiently induced during greening or during the exposure to light stress, and show significant sequence homology with LHCII (Grimm et al., 1989), in particular in the regions of the transmembrane helices A and B (Fig. 1). A first report on the isolation and purification of a 17 kDa ELIP from pea has appeared recently and a preliminary spectroscopic characterization was presented (Adamska et al., 1999). The protein was found to bind lutein and Chl *a* in a ratio of about 2:1. The emission and excitation spectra reported in this paper, however, suggest that the pigments are bound differently than in LHCII, despite the presence of at least four conserved putative chlorophyll-binding amino acid residues. The chlorophylls emitted at 674 nm, which is close to the emission wavelength of free Chl *a* and about 6 nm blue-shifted compared to that of all trimeric and monomeric LHCII proteins. In addition, the xanthophylls did not transfer any excitation energy to Chl *a*, which is in clear contrast to LHCII and very unlikely for a functional light-harvesting protein (see above).

The second type of protein is the PSII-S protein,

which is encoded by the nuclear *PsbS* gene. This protein has recently gained increased attention, because its presence in thylakoid membranes seems to be directly related to the physiologically highly important process of non-photochemical quenching (Li et al., 2000), by which excess excitation energy is harmlessly converted into heat. The protein is characterized by four membrane-spanning helices (Wedel et al., 1992; Kim et al., 1992), i.e., one more than most other proteins of this family, and is probably very hydrophobic. The protein is found in grana membranes, but its location relative to other proteins is unclear. A number of reports have suggested that it should be located between the PS II core and the peripheral antenna (Kim et al., 1994), but the evidence is indirect and needs confirmation by other methods. Biochemical studies have indicated that the C<sub>2</sub>S<sub>2</sub> PSII-LHCII complexes (Section IV.C) are depleted of the PSII-S protein (Hankamer et al., 1997b; Harrer et al., 1998; Eshaghi et al., 1999; Nield et al., 2000c). EM studies on PSII-LHCII super- and megacomplexes and semi-crystalline grana membrane fragments from wild-type *Arabidopsis thaliana* and from the *npq4* mutant lacking the PSII-S protein have suggested that the PSII-S protein is not located in the direct vicinity of the PSII-LHCII supercomplexes and most likely is located in the LHCII-enriched regions of the grana membranes (Yakushevska et al., 2001a).

It presently is not clear whether or not the PSII-S protein binds pigments. It is now generally agreed that the protein is stable in the absence of chlorophylls and carotenoids (Funk et al., 1995b). The PSII-S protein differs in this respect from the light-harvesting proteins of the Cab-gene family, which require pigments in order to fold to their native conformations (Paulsen, 1995). Research by Funk and co-workers has indicated that the PSII-S protein is a chlorophyll-binding protein (Funk et al., 1994, 1995a), but spectroscopic research in our laboratory suggests that the chlorophylls and carotenoids are not bound to the protein in these preparations in a similar way as in the light-harvesting proteins of the Cab-gene family, and instead show all the characteristics of loosely or unspecifically connected pigments (E. J. G. Peterman and C. Funk, unpublished). It has been suggested that the PSII-S protein transiently binds pigments in order to reduce the presence of free Chl in the membranes (Paulsen, 1995), which can be dangerous because of its ability to generate singlet oxygen (see above). However, for such a protein one expects an



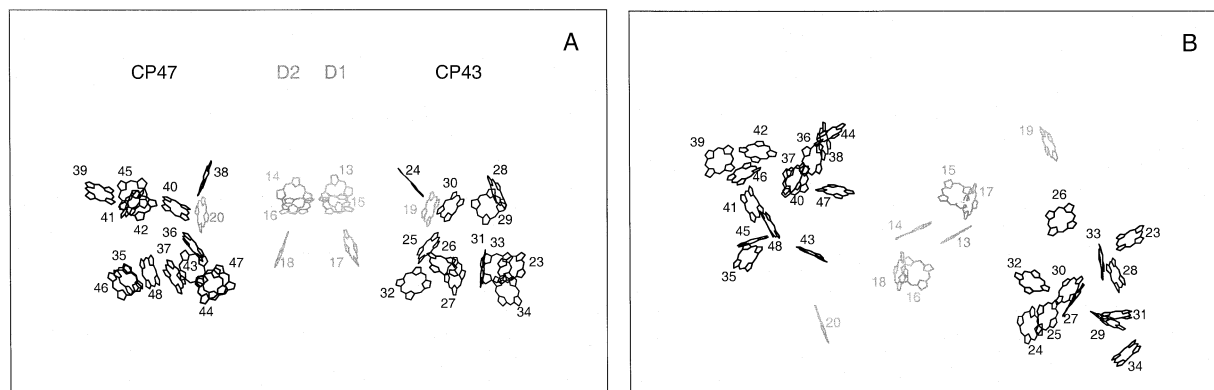


Fig. 2. A) side view and B) top view of the pigments of a PS II monomer, obtained from the dimeric PS II core complex from *Synechococcus elongatus* (Zouni et al., 2001). The chromophores bound to CP47 and CP43 are depicted in black, while those bound to D1/D2 are depicted in grey. The numbers correspond to the numbers deposited in the Protein DataBank (accession number 1FE1). All depicted chromophores have been identified as Chl *a*, except for numbers 17 and 18, which are Ph *a* molecules. The numbers of the chromophores in grey correspond to: 13 = P<sub>D1</sub>, 14 = P<sub>D2</sub>, 15 = Chl<sub>D1</sub>, 16 = Chl<sub>D2</sub>, 17 = Pheo<sub>D1</sub>, 18 = Pheo<sub>D2</sub>, 19 = Chl<sub>D1</sub>, 20 = Chl<sub>D2</sub> (nomenclature from Zouni et al., 2001).

efficient quenching of Chl *a* triplets, and even this was not observed in the isolated complex (E. J. G. Peterman and C. Funk, unpublished). Overexpression of the gene in *E. coli* and 'reconstitution' experiments should shed more light on this issue.

#### D. CP47 and CP43

It has long been thought that CP47 and CP43 each form six transmembrane  $\alpha$ -helices in the thylakoid membrane and that conserved histidine residues in these helices provide the ligands for most of the chlorophylls (Bricker, 1990), suggesting an organization of the chlorophylls in two layers near the two surfaces of the membrane. The recent structural data (Zouni et al., 2001) clearly support this view (Fig. 2), and in addition suggest an evolutionary relationship between the core antenna proteins of PS II and PS I (Schubert et al., 1998). Both proteins bind approximately 14 chlorophyll *a* molecules (Barbato et al., 1991; Rhee et al., 1998). The center-to-center distances between the nearest chlorophylls range between 8.5 and 13.5 Å (Zouni et al., 2001). The only other chromophore is  $\beta$ -carotene, of which at least two molecules are present in both core antenna proteins.

Both CP47 and CP43 have been isolated and purified in non-ionic detergents with the preservation of most of their spectroscopic features. The CP43 core antenna protein binds less strongly to the PS II RC complex than CP47, and can be separated from

the RC by a mild detergent treatment. It binds only weakly to anion-exchange columns, and a relatively high pH is required to separate the complex from free chlorophylls and other contaminations (Dekker et al., 1995). The CP47 protein can be separated from the PS II RC complex by a treatment with dodecylmaltoside and LiClO<sub>4</sub> (Ghanotakis et al., 1989). This treatment appears to preserve the spectral properties of CP47 relatively well (Kwa et al., 1992a).

The 4 K absorption spectra of both proteins reveal major spectral forms peaking near 682, 678, 669 and 661 nm. The room-temperature absorption spectrum of CP43 peaks at shorter wavelengths than that of CP47 (670 nm vs. 675 nm), probably because the 669 nm spectral form has a greater oscillator strength in CP43 than in CP47. Each protein has a unique and very characteristic spectroscopic feature at low temperatures. For CP43 this is the extremely sharp absorption peak at 682.5 nm (Breton and Katoh, 1987; Dekker et al., 1995), which probably has a bandwidth (fwhm) of not more than 2.7 nm at 4 K (Groot et al., 1999) and which is, to our knowledge, the narrowest chlorophyll absorption peak observed in any Chl-containing complex. The narrow band and a much broader band peaking at about 680 nm form two different red-most transitions in CP43 (Groot et al., 1999; Jankowiak et al., 2000). A clear peak near 682.5 nm was also observed in the 4 K absorption spectrum of a well-resolved PS II core preparation (Van Leeuwen, 1993). The CP47 complex gives rise to a minor spectral form peaking near 690



nm (Chang et al., 1994; Groot et al., 1995), which also has been observed in PS II core complexes. The  $Q_y$  transition of this spectral form is perpendicular to the plane of the membrane (van Dorssen et al., 1987b), unlike that of most other 'red' spectral forms, which usually are oriented parallel to the plane of the membrane. The 690 nm spectral form is largely responsible for the well-known F695 fluorescence band of PS II at 77 K, and has a relatively broad bandwidth (fwhm  $\sim 10$  nm), which is primarily determined by inhomogeneous broadening (Den Hartog et al., 1998). Both the 690-nm band of CP47 and the sharp 682.5-nm feature of CP43 probably arise from a state with an oscillator strength corresponding to that of only one chlorophyll (van Dorssen et al., 1987a; Groot et al., 1999), however it is not likely that both features reflect chlorophylls in corresponding positions in the two proteins, because the orientations are clearly different. A number of spectroscopic observations have suggested that excitonic coupling plays an important role in CP47 and CP43 (Groot et al., 1995; Groot et al., 1999).

In contrast to all other major PS II proteins, the core antenna proteins CP47 and CP43 have not been investigated in detail by ultrafast spectroscopy. A single-photon timing study of CP47 was reported by De Paula et al. (1994), but the time resolution of the experiments was not sufficient to reveal much detail of the energy transfer dynamics. Recent experiments indicated that most of the energy transfer dynamics at 77 K occurs within 2–3 ps in both complexes (de Weerd et al., 2002).

#### IV. Reaction Center Containing Photosystem II Complexes

##### A. The Isolated Photosystem II Reaction Center

###### 1. Biochemistry and Structure

The biochemical isolation and purification of the Photosystem II reaction center (PS II RC) was first reported in 1987 by Nanba and Satoh (1987). Their widely followed method makes use of the fact that the RC complex is the most stable of all pigment-protein complexes of PS II membranes in the presence of the moderately deleterious detergent Triton X-100 and binds most strongly to anion-exchange columns. Thus, a relatively simple isolation procedure is employed: PS II membranes are solubilized by Triton

X-100, after which the pigment-protein complexes are bound to an anion-exchange column, washed with Triton X-100 and exchanged for a mild detergent like dodecyl- $\beta$ ,D-maltoside ( $\beta$ -DM) to obtain preparations with optimal stability (Satoh, 1996). It is also possible to isolate the PS II RC without the use of Triton X-100 by applying a combination of dodecylmaltoside and  $\text{LiClO}_4$  (Ghanotakis et al., 1989; Eijkelhoff et al., 1996) and to obtain a PS II RC preparation with a lower chlorophyll content (see below) by using  $\text{Cu}^{2+}$ -affinity chromatography (Vacha et al., 1995).

It is now commonly accepted that isolated PS II RCs consist of equimolar amounts of the D1 and D2 subunits, the  $\alpha$ - and  $\beta$ -subunits of cytochrome *b*-559 and the *PsbI* gene product (Satoh, 1996). PS II RC complexes from green plants isolated without Triton X-100 also contain about equimolar amounts of the poorly stainable *PsbW* gene product, whereas complexes isolated with Triton X-100 contain only sub-equimolar amounts of this protein (Eijkelhoff, 1997; Shi and Schröder, 1997). D1 and D2 show amino acid sequence homology with the L and M subunits of purple bacterial reaction centers (Michel and Deisenhofer, 1988), in line with the idea that both RCs are of the same type, and bind the organic co-factors that are involved in the primary charge separation reactions (chlorophyll *a*, pheophytin *a*, plastoquinone). The function of the other subunits, however, is largely unknown.

Highly purified PS II RCs bind 6 Chl *a*, 2 Ph *a* and 2  $\beta$ -Car molecules (Eijkelhoff et al., 1996; Zheleva et al., 1996), i.e., they bind two chlorophylls and one carotenoid more than the related bacterial RCs. The only reliable method reported thus far to obtain a lower Chl content is based on  $\text{Cu}^{2+}$ -affinity chromatography, which gives PS II RCs binding 5 Chl *a*, 2 Ph *a* and 1  $\beta$ -Car molecules (Vacha et al., 1995). In this preparation, one of the peripheral Chl molecules (Chl- $Z_{D1}$  or Chl- $Z_{D2}$ , see below) is missing. The  $\beta$ -Car molecules have been reported to be either in the 15-*cis* (Bialek-Bylka et al., 1995) or all-*trans* conformation (Yruela et al., 1998). Part of the  $\beta$ -Car can be released from the complex by washing with Triton X-100 (De las Rivas et al., 1993; Eijkelhoff et al., 1996), suggesting a location near the periphery of the complex. Isolated PS II RC complexes do not contain plastoquinone (Nanba and Satoh, 1987).

The 3.8 Å structure of the PS II core complex (Zouni et al., 2001; Fig. 2) indicates that in the center of the complex 4 Chl *a* and 2 Ph *a* molecules are

located in similar positions and orientations as the corresponding molecules in the purple bacterial reaction center (except that the Chl molecules constituting the 'special pair' are observed at a larger Mg-Mg distance of 10 Å), and that two additional Chl *a* molecules (called Chl-Z<sub>D1</sub> and Chl-Z<sub>D2</sub>) are bound near the periphery of the complex, ligated to the conserved histidines at positions 118 and 117 of D1 and D2, respectively. These chlorophylls are located at 23.7 and 23.9 Å from the nearest pheophytin molecules and at 24.5 and 24.6 Å from the 'accessory' chlorophylls (Zouni et al., 2001; Table 4). Chl-Z<sub>D2</sub> is probably important for an efficient flow of excitation energy from the core antenna to the photochemical reaction center (Lince and Vermaas, 1998), while Chl-Z<sub>D1</sub> can be photooxidized with low yield in PS II core complexes at low temperature (Stewart et al., 1998). One cytochrome *b*-559 molecule was also identified in the 3.8 Å structure (Zouni et al., 2001). It is located near D2 at the periphery of the PS II core complex, and the nearest chlorophyll is Chl-Z<sub>D2</sub> at a center-to-center distance of 27 Å.

## 2. Spectroscopy

Despite the rather similar organizations of the central four chlorophyll and two pheophytin molecules in the RCs of PS II and purple bacteria, the absorption spectra are strikingly different. In the purple bacterial reaction center, the absorption bands of the low-exciton band of the special pair (880 nm), the accessory chlorophylls (800 nm) and the pheophytins (770 nm) are clearly separated. In addition, the higher-energy exciton band of the special pair is known to contribute to the low-energy side of the 800 nm band. In PS II, however, the Q<sub>y</sub> transitions of all chlorophylls and pheophytins occur at about 675 nm, and only at cryogenic temperatures can some fine structure in the absorption spectrum be observed with bands peaking near 670 and 679 nm and a shoulder at 683 nm.

There is some evidence that the peripheral chlorophylls absorb maximally on the 'blue' side of the Q<sub>y</sub> absorption (670–675 nm), and that all 'red' absorption (679–683 nm) is caused by the central four chlorophylls and two pheophytins of the complex (Dekker and van Grondelle, 2000; Germano et al., 2001), though at least in cyanobacteria one of the 'special pair' chlorophylls may absorb at slightly shorter wavelength (Diner et al., 2001). An important issue is the strength of the excitonic interactions in

the PS II RC. Based on the discovery of a differently-oriented high-energy exciton component of P680 at 667 nm (Kwa et al., 1994) a model has been proposed in which the coupling between the six central chlorins is relatively weak (about 100 cm<sup>-1</sup>)<sup>2</sup> and of similar magnitude as the intrinsic disorder (Durrant et al., 1995). In this so-called 'multimer' model there is no 'special pair' and for each realization of the disorder the excitation may be localized on basically any combination of neighboring chlorins. It is not difficult to imagine that at sufficiently low temperatures such a system shows a very complex behavior. In some RCs the excitations become localized on pigments involved in fast charge separation (P680), while in other RCs the excitations become localized on pigments not active in fast electron transfer (the so-called 'trap' state) (Groot et al., 1994, 1996).

## 3. Energy Transfer and Trapping

The kinetics of energy transfer and trapping have been studied by several groups using both ultrafast absorbance-difference and fluorescence techniques. After some intense debates in the literature, it seems now generally accepted that primary charge separation reactions at room temperature are strongly multiphasic with main components of about <1, 8, 20 and/or 50 ps (Müller et al., 1996; Donovan et al., 1997; Greenfield et al., 1997; Klug et al., 1998). Thus, the formation of the primary radical pair takes more time in isolated PS II RCs than in bacterial reaction centers, where the average formation time of the primary radical pair is shorter than 10 ps.

The primary photosynthetic reactions in the PS II RC have recently been reviewed (Dekker and van Grondelle, 2000) and interpreted in terms of A) energy transfer, B) charge separation, C) charge stabilization and D) relaxation (protein conformational change) (Fig. 3). In this view, the energy transfer processes (A) proceed predominantly in two time domains. The transfer of excitation energy within the six central chlorins of the RC probably is ultrafast, with time constants of ~100 and ~500 fs (Durrant et al., 1992; Merry et al., 1996), whereas the energy transfer from the peripheral chlorophylls to the central core occurs much more slowly, in about 20–30 ps (Roelofs et al., 1993; Rech et al., 1994; Schelvis et al., 1994). At least part of the primary charge

<sup>2</sup> An occurrence of low- and high-energy exciton bands at 679 (or 683) and 667 nm, respectively, corresponds to a maximal coupling strength of 130 (or 175) cm<sup>-1</sup> (in the case of a dimer).

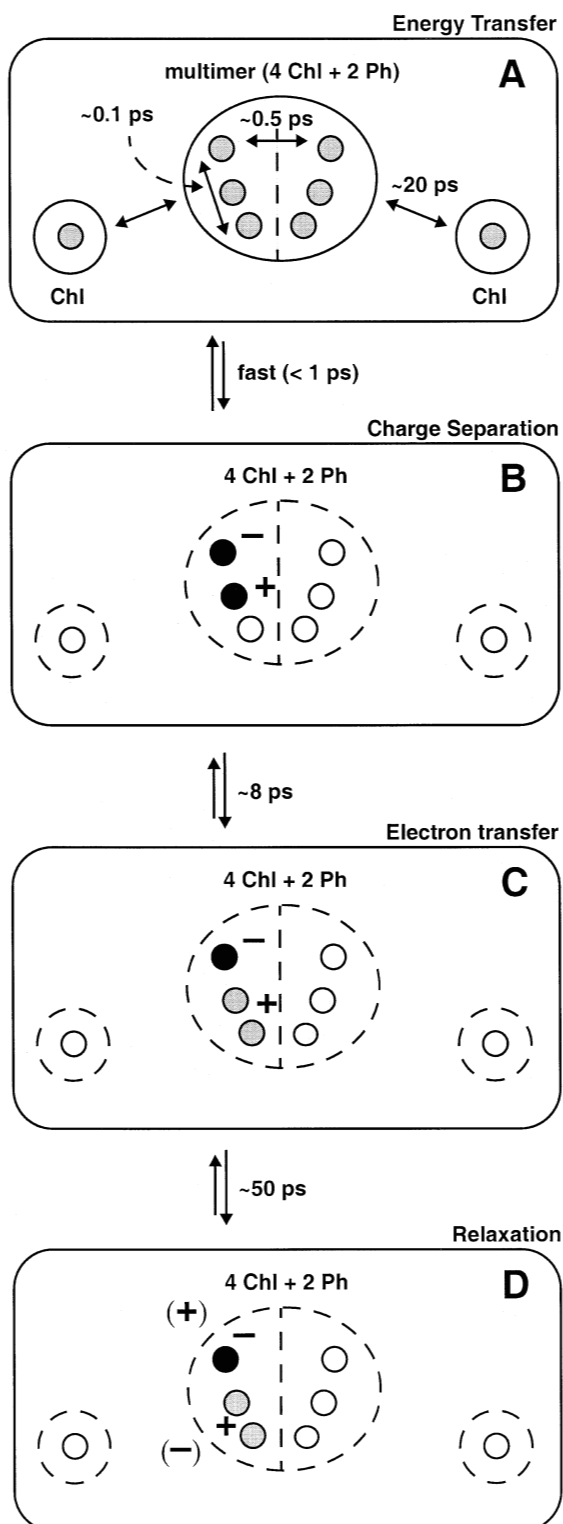


Fig. 3. Schematic representation of the energy transfer, primary charge separation, stabilization and relaxation reactions in the PS II RC (adapted from Dekker and van Grondelle, 2000). For details see text.

separation (B) is thought to occur within less than 1 ps but with a low yield, because the equilibrium between singlet-excited P680 and the primary radical pair is probably towards the singlet-excited states (Blomberg et al., 1998). The ultrafast part of this reaction probably starts from the singlet-excited 'accessory' Chl on the active branch (Dekker and van Grondelle, 2000), which has been shown to transfer an electron rapidly to the neighboring BPh in purple bacterial reaction centers (Van Brederode and van Grondelle, 1999). Charge separation starting from the 'special pair' Chl on the active branch probably occurs in reaction (C), in which a charge stabilization reaction also may occur by electron transfer from a 'special pair' Chl to the 'accessory' Chl that was oxidized in reaction (B). If the charge-separated state with the cation on the 'special pair' is lower in free energy than the state with the cation on the 'accessory' chlorophyll, as is usually the case in bacterial reaction centers (van Brederode and van Grondelle, 1999), then this electron transfer will shift the equilibrium between the excited state and the radical pair towards the radical pair and result in a stabilization of the charge-separation reaction. It has been suggested that this process occurs in about eight ps (Dekker and van Grondelle, 2000). Slow relaxation reactions (D) of the radical pair may proceed by conformational changes of the protein, induced by the creation of the two charges (Konermann et al., 1997), and are most likely responsible for the  $\sim 50$  ps kinetics.

At very low temperatures the charge stabilization reaction (C) may not occur to a significant extent, and the uphill parts of the energy transfer (A) and/or initial charge separation reactions (B) may slow down considerably. Both processes proceed between almost isoenergetic states, which in view of the disorder means that they can proceed slightly downhill in some complexes (and thus are fast and weakly dependent on temperature) and slightly uphill in other complexes (and thus become retarded significantly at very low temperatures).

### B. Photosystem II Core Complexes

The smallest PS II unit fully capable of maintaining high rates of oxygen evolution and plastoquinone reduction is the PS II core complex. In this complex all constituents of the PS II RC complex are present, as well as the core antenna proteins CP47 and CP43, the extrinsic PsbO protein indirectly involved in water oxidation, and a number of low-mass proteins

(Bricker and Ghanotakis, 1996). Also all inorganic cofactors required for oxygen evolution are present. Of all low-mass PS II proteins, a possible function is only known for the PSII-L subunit. This protein seems to be required for efficient electron transport from Tyr-Z to P680<sup>+</sup> (Hoshida et al., 1997).

There is overwhelming evidence that the PS II core complex is organized as a dimer in the stacked, appressed regions of the thylakoid membrane. Although monomeric complexes are generally slightly less stable and active, it is clear that the dimerization is not required for photochemical activity (Dekker et al., 1988). Highly purified PS II core complexes bind about 35 Chl *a*, 2 Ph *a* and 6–10  $\beta$ -Car molecules per monomeric unit (Barbato et al., 1991; van Leeuwen et al., 1991). The 3.8 Å crystal structure revealed the locations of 35 Chl *a* and 2 Ph *a* molecules, but the  $\beta$ -Car molecules remained undetected at this resolution (Vasil'ev et al., 2001). It is possible that a few chlorophylls escaped detection thus far, in particular in the peripheral (CP43) parts of the complex.

The 77 K fluorescence spectrum of the PS II core complex shows characteristic peaks at 695 and 685 nm, which are generally referred to as F-695 and F-685, respectively. To discuss the origin of both types of emission, we show plots of the quantum yield and peak wavelength of F-695 and F-685 as functions of temperature (Fig. 4). F-685 is the dominant fluorescing species between room temperature and about 80 K, over which temperature range it gradually red-shifts from about 683 nm at room temperature to 686 nm at 70 K. The extent of the red shift in the PS II core complex is smaller than observed for purified CP47, but larger than for CP43 (Fig. 4), from which we conclude that F-685 represents fluorescence from singlet excited states equilibrated over basically all core antenna pigments (i.e., CP47, CP43 and possibly also PS II RC pigments). The yield of this component is probably determined by the equilibrium between the radical pair and the singlet excited states, while the red-shift of F-685 may be caused by the higher probability of the excitation to locate on the red-shifted chlorophylls of the CP47 complex at lower temperatures (Section III.D).

F-695, on the other hand, is the dominant fluorescing species at temperatures below 80 K. Upon cooling to 4 K, its yield increases dramatically, while its peak maximum blue-shifts from 694 nm at 77 K to 690 nm at 4 K (Fig. 4). The blue shift and increased intensity upon cooling to 4 K were explained

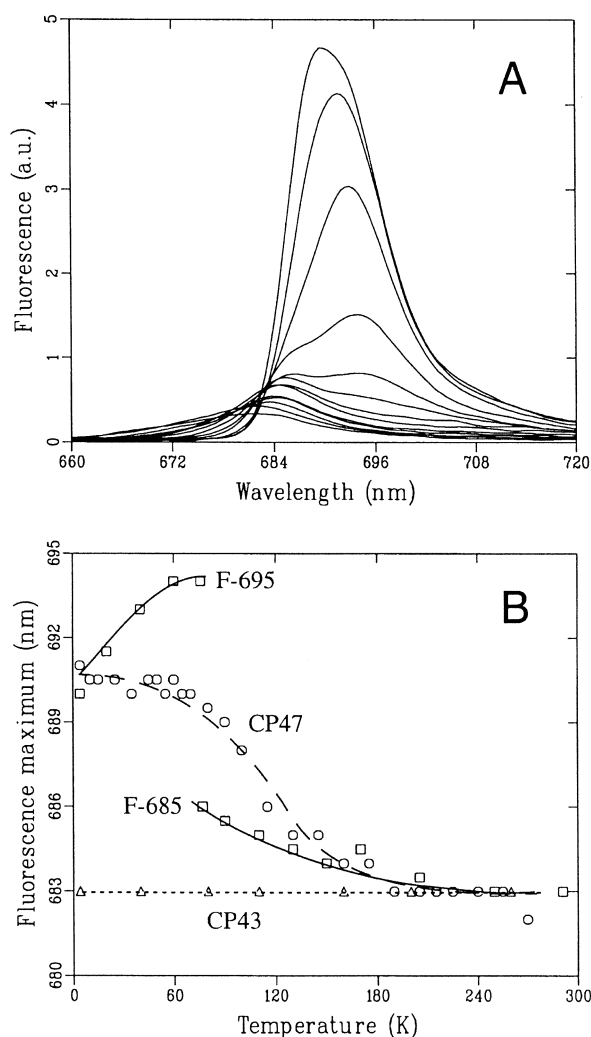


Fig. 4. A) Emission spectra of PS II core complexes upon excitation at 590 nm at (from top to bottom)  $T = 4, 20, 40, 60, 77, 90, 110, 130, 150, 170, 205, 250$  and  $291$  K. B) Wavelength maxima of the emission spectra of PS II core (squares), CP47 (circles) and CP43 (triangles) complexes as a function of temperature (adapted from Dekker et al., 1995).

by the inhomogeneous distribution of the 690 nm pigment of CP47 (Dekker et al., 1995). In complexes in which the 690 nm chlorophyll absorbs at a relatively long wavelength the thermal energy may not be sufficient to allow uphill energy transfer to P680 at intermediate temperatures, thus giving rise to long-lived fluorescence, which should be red-shifted because only the low-energy part of the inhomogeneous distribution is involved. In complexes in which the 690 nm chlorophyll absorbs at a relatively short wavelength, however, much less thermal energy

is required for the energy transfer to P680, and the excitation most likely will result in charge separation and a low fluorescence quantum yield. The emission therefore will shift to the blue with decreasing temperature as energy transfer to P680 slows down or is even blocked in a larger fraction of the complexes. The fluorescence quantum yield in PS II core complexes at 4 K was estimated to be about 75% compared to that of isolated CP47 (Dekker et al., 1995), indicating that at 4 K most of the excitations on the F-695 chlorophyll are not transferred to P680. We conclude that F-695 represents a trap of excitation energy, whereas F-685 represents the combined singlet excited states in equilibrium with the radical pair.

Recent studies on the low-temperature emission properties of monomeric CP47-RC complexes have indicated that at 1.2 K the downhill energy transfer from RC to CP47 chlorophylls also is limited (Den Hartog et al., 1998), which suggests that in this complex the distance between the lowest energy pigments of CP47 and RC is larger than the Förster radius ( $\sim 5$  nm). At room temperature, however, the energy transfer between CP47 and RC should be very efficient. The most straightforward explanation of these results is that the CP47 chlorophyll(s) closest to the RC core absorb at a relatively short wavelength. The nearest distances between the chlorophylls of CP47 or CP43 and RC are relatively large (about 2.1 nm, Zouni et al., 2001; Fig. 2 and Table 4).

In dimeric complexes energy transfer between the two monomers occurs efficiently at room temperature (Jahns and Trissl, 1997). Most likely, this energy transfer takes place between CP47 chlorophylls. The Mg-Mg distance between the nearest chlorophylls on each side of the dimer is 2.73 nm, as calculated from the crystal structure (Zouni et al., 2001; Table 4).

Since a previous review (van Grondelle et al., 1994) almost no new data have been presented on the kinetics of energy transfer and trapping in the PS II core complex. At that time, most authors interpreted data obtained with open reaction centers (containing oxidized  $Q_A$ ) in terms of a fast equilibration of the excitation energy (within 10 ps), followed by a decay phase of about 40–80 ps attributed to a trap-limited charge separation and a phase of about 200–500 ps attributed to charge stabilization due to electron transfer from Ph- to  $Q_A$  (see, e.g., Schatz et al., 1988). These numbers cannot be regarded as very accurate, because the extent to which annihilation effects contributed to the kinetics reported by the various

groups is not clear and/or because the specific aggregation state of the investigated complexes (monomer, dimer or larger aggregate) was not determined.

Nevertheless, the recent progress in the understanding of the structure of PS II suggests that at least some of the previous interpretations need revision. In particular, the proposed fast ( $<10$  ps) equilibration of excitation energy seems unlikely in view of the large distance between the chlorophylls of the PS II RC and the core antenna proteins (see above). In addition, the two extra chlorophylls of the PS II RC are very likely not the only ‘connecting’ chlorophylls in the PS II core complex, because the pheophytins and the peripheral chlorophylls of the RC are located at about equal distances to the closest core antenna chlorophylls (Zouni et al., 2001; Table 4). Moreover, the transfer from the peripheral chlorophylls to P680 takes about 20 ps. Thus, the situation seems similar to that in the purple bacterial photosystem, where there is a long distance between the RC and the LH1 core antenna and energy transfer from LH1 to the RC determines the total charge separation time of about 50 ps (Beekman et al., 1994). The 40–80 ps kinetics in the PS II core complex may therefore be attributed, at least in part, to a transfer-to-the-trap-limited charge separation reaction (Vasil’ev et al., 2001; de Weerd et al., 2002). In contrast to the purple bacterial photosystem, the core antenna system does not surround the RC in PS II and excitations can only move from CP47 (or CP43) directly to the RC and not to CP43 (or CP47). Even in dimeric PS II core complexes the only possible contact between core antenna chlorophylls is that between two adjacent CP47 proteins (Fig. 2; Section IV.C). The 40–80 ps kinetics could, therefore, include separate contributions from CP47 and CP43 which do not necessarily have exactly the same average kinetics. The attribution of the 200–500 ps kinetics also may be less straightforward than initially assumed (Schatz et al., 1988) because these kinetics occur not only on the same time scale as the charge stabilization reaction, but probably also on the time scale of fluorescence from excited states in the reaction center (Merry et al., 1998).

In closed PS II (with  $Q_A$  reduced) the two main decay phases were shown to slow approximately three-fold to about 200–250 and 1300 ps, which was explained by an increase of the free energy of the primary radical pair by the negative charge on  $Q_A$ , causing a shift of the equilibrium between the excited

state and the radical pair towards the excited state (Schatz et al., 1988). While the picture of trap-limited charge separation may still hold, additional mechanisms (a rate-limiting decay of the excited state in the reaction center as discussed above and recombination luminescence) could play a role in the overall kinetics.

### C. Photosystem II Supercomplexes

The largest isolated and purified PS II particles are the PSII-LHCII supercomplexes, of which there are now more than a dozen characterized by electron microscopy and single particle image averaging (Boekema et al., 1995, 1998, 1999a,b, 2000a; Nield et al., 2000a,b). They all consist of a dimeric PS II core complex, surrounded by a variable number of trimeric and monomeric LHCII proteins. The most common and best characterized supercomplex is the so-called  $C_2S_2$  supercomplex, a two-fold symmetrical complex. Biochemical data have indicated that each half consists of a PS II core complex (referred to as 'C'), a 'strongly' bound trimeric LHCII complex (referred to as 'S'), a CP29 protein and a CP26 protein (Hankamer et al., 1997b; Harrer et al., 1998). The S trimer most likely consists of two Lhcb1 and one Lhcb2 proteins (Hankamer et al., 1997b). Other supercomplexes also contain a CP24 protein and a 'moderately' bound trimeric LHCII complex (referred to as 'M'), whereas a rather small number of supercomplexes also contain a 'loosely' bound trimeric LHCII (referred to as 'L') (Harrer et al., 1998; Boekema et al., 1999a,b). Figure 5 shows the approximate location of the S, M and L trimer with respect to the dimeric PS II core complex. The M trimer most likely consists of two Lhcb1 and one Lhcb3 protein, because Lhcb3 is not present in the  $C_2S_2$  supercomplexes (Hankamer et al., 1997b) but present in larger associations (Boekema et al., 1999a). Additional evidence comes from a complex isolated by Bassi and Dainese (1992). This complex consists of the Lhcb1, Lhcb3, Lhcb4 and Lhcb6 polypeptides in a 2:1:1:1 ratio. Based on the location of the Lhcb4 (CP29) and Lhcb6 (CP24) proteins in the supercomplex (Fig. 5) it seems reasonable to assume that the M trimer is involved in this complex and thus contains the minor Lhcb3 protein. Electron microscopy also has revealed the way the dimeric supercomplexes can be attached to each other. Three different associations or megacomplexes have been recognized, the so-called type I, type II and type III

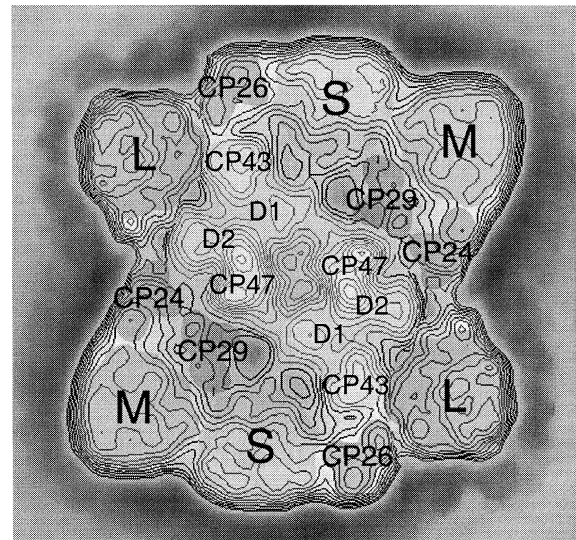
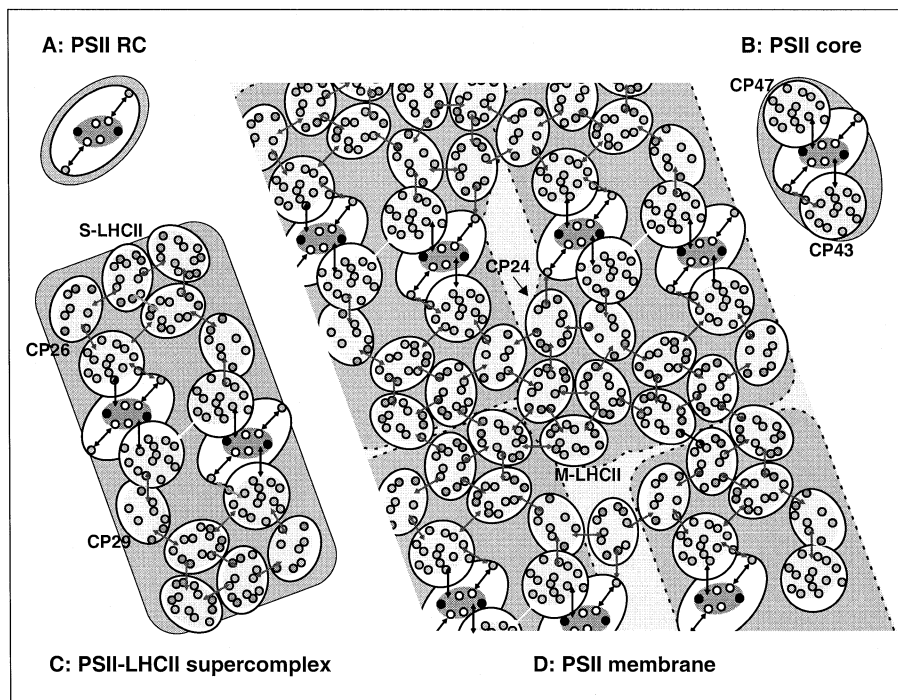


Fig. 5. Constructed image of a 'complete' PSII-LHCII supercomplex, the hypothetical  $C_2S_2M_2L_2$  supercomplex (adapted from Boekema et al., 1999b). S, M and L refer to strongly, moderately and loosely bound LHCII, respectively.

associations (Boekema et al., 1999a,b). In all megacomplexes the minor proteins CP26 and CP24 seem to be very important for the interactions between the supercomplexes.

It is becoming increasingly clear that the  $C_2S_2$ ,  $C_2S_2M$  or  $C_2S_2M_2$  supercomplexes form the basic unit of PS II in at least a large part of the grana membranes, in particular because the characteristic shapes of these complexes are clearly observed in a partially disrupted grana membrane fragment (van Roon et al., 2000). The structure of the  $C_2S_2$  supercomplex seems also conserved between green plants and green algae, because very similar structures were observed in spinach and in *Chlamydomonas reinhardtii* (Nield et al., 2000b). It is not clear, however, how the various PSII-LHCII supercomplexes make up the complete grana membrane, or how they connect to the LHCII that is not present in these complexes. There are, on the average, about eight trimeric LHCII complexes per PS II dimer in the grana membranes (Jansson, 1994). However, the most common  $C_2S_2$  and  $C_2S_2M$  supercomplexes accommodate only two and three trimeric LHCII complexes per PS II dimer, respectively, while supercomplexes with more than four trimeric LHCII complexes per PS II dimer are extremely rare in spinach (Boekema et al., 1999a,b). For instance, the hypothetical complex depicted in Fig. 5, with six





**Fig. 6.** Schematic representation of the most important energy transfer and trapping processes in (A) the PS II RC complex, (B) a monomeric PS II core complex, (C) the  $C_2S_2$  PSII-LHCII supercomplex and (D) a part of a membrane with a regular array of  $C_2S_2M$  PSII-LHCII supercomplexes. In (D) the supercomplexes are contoured by dashed lines and depicted with a stronger grey-scale than the surrounding membrane. The pigments are indicated as circles in white (the four central chlorophylls of the PS II RC), black (Ph *a*), light grey (antenna Chl *a*) and dark grey (Chl *b*), and are placed at *approximate* positions according to the various crystal structures. The figure indicates that the trapping process ( $\tau_{\text{trap}}$ , represented by the dark area in the center of the PS II RC complex) is relatively important in the PS II RC complex, that the delivery of the excitation energy ( $\tau_{\text{del}}$ , represented by the black arrows) plays an important role in the PS II core complex, and that the migration processes ( $\tau_{\text{mig}}$ , represented by the grey arrows) are significant in the PSII-LHCII supercomplexes and the PS II membranes. The light grey areas represent areas in which ultrafast energy transfer among groups of chlorophylls is expected in core and peripheral antenna proteins, whereas the white arrows represent a few less likely (relatively slow) energy transfer routes. See Color Plate 5.

LHCII trimers, was not observed at all in a dataset of more than 17,000 particles (Boekema et al., 1999a). A partial answer was given by an analysis by electron microscopy of paired grana membrane fragments, in which a rather common semi-regular array of  $C_2S_2M$  supercomplexes was observed in spinach (Boekema et al., 2000b) and of  $C_2S_2M_2$  supercomplexes in *Arabidopsis thaliana* (Yakushevska et al., 2001b). The analysis suggested that many PSII-LHCII supercomplexes in one membrane face only LHCII in the other, which implies that energy transfer from one membrane to the next is very important in grana membranes. A possible existence of LHCII-only domains in the thylakoid membranes was corroborated by the structural characterization of a supramolecular complex consisting of seven trimeric LHCII complexes (Dekker et al., 1999). Spectros-

copic characteristics of an aggregated LHCII complex of very similar size were recently reported by Ruban et al. (1999).

It is also becoming increasingly clear that the supramolecular organization of PS II is heterogeneous on various levels. The heterogeneity is not restricted to the segregation into grana stacks, margins and stroma lamellae (Jansson et al., 1997), but also occurs in the direct environment of the  $C_2S_2$  supercomplexes (the presence or absence of M- and/or L-types of LHCII trimers and the presence or absence of monomeric LHCII proteins) and in the complete macromolecular organization of the PSII-LHCII supercomplexes (Boekema et al., 1999a,b, 2000b).

Initial spectroscopic experiments indicate that PSII-LHCII supercomplexes and PS II membranes are very similar with regard to the general spectroscopic



properties of PS II (Eshaghi et al., 2000) and the decay of the oxidized primary electron donor P680<sup>+</sup> (Schilstra et al., 1999). Experiments using ultrafast spectroscopy to monitor the excitation dynamics and trapping have not yet been reported.

#### D. Photosystem II Membranes

Only a few reports with new results on this topic have been presented since 1994 and we again refer to the review of van Grondelle et al. (1994) for details. Compared to PS II core complexes the excitation energy transfer in PS II membranes or in chloroplast fragments has been found to be even more heterogeneous, with additional phases in the 300–600 ps and 2–3 ns time range for open and closed reaction centers, respectively. The general conclusion was that the exciton/radical pair equilibrium model describes the excitation energy transfer and trapping in PS II reasonably well, but that at least some type of heterogeneity has to be proposed to explain the data. Among the possible types of heterogeneity, 1) a heterogeneous charge-separation process, 2) the so-called  $\alpha/\beta$  heterogeneity and 3) heterogeneous organization of the peripheral antenna with tightly bound and loosely associated trimeric LHCII were considered (van Grondelle et al., 1994). The recent results on the native associations of PS II and LHCII (Boekema et al., 1999a,b) indicate that the latter type of heterogeneity will play a very important role.

An important aspect of the PS II membranes is the fact that the distance between the two adjacent membranes is small (about 2 nm), so that resonance energy transfer from one layer to the next is very well possible. This is particularly important in PS II membranes with partially ordered macrodomains, where it was shown that many PS II units in one layer face only LHCII in the other (Boekema et al., 2000b). Experimental evidence for the occurrence of fast excitation energy transfer from one layer to the next has been provided by fast photovoltage experiments (Trissl et al., 1987; Leibl et al., 1989). It was concluded that a so-called 'excitonic short-circuit' between layers occurs on a faster time scale than the average trapping time.

We conclude that more work is needed to obtain a better idea of the excitation decay mechanisms in intact PS II, including fast spectroscopic measurements on well-defined PSII-LHCII supercomplexes. Detailed measurements of excitation decay in monomeric and dimeric PS II core particles also are

required in order to clarify whether dimerization is one of the tools by which PS II can regulate its overall efficiency.

#### V. Overall Trapping of Excitation Energy

In this section, we will give a rough description of the overall trapping of excitation energy in PS II. As indicated above, the description is far from complete because many essential details of the structure and dynamics of PS II are still lacking. Nevertheless, some essential ingredients can be discussed that will have to be taken into account for proper modeling.

We start by presenting some theoretical background, which is mostly based on a recent overview (van Grondelle and Somsen, 1999). In the incoherent limit, the excited-state dynamics of a photosynthetic system follows a Master equation:

$$\frac{dp_i}{dt} = -k_i p_i + \sum_j (p_j k_{ji} - p_i k_{ij}) - \delta_{iRC} p_{RC} k_{RC} \quad (1)$$

Here  $p_i$  is the time-dependent probability (population) to find the excitation at site  $i$  in the network of pigment molecules, while  $p_{RC}$  is the population of the primary donor. Furthermore,  $k_i$  is the rate of loss from a site due to fluorescence, internal conversion and intersystem crossing,  $k_{RC}$  is the rate of charge separation,  $k_{ij}$  is the Förster rate of energy transfer from site  $i$  to site  $j$  and  $\delta$  is the Kronecker delta. The latter is equal to 1 if pigment  $i$  is the primary donor and is 0 otherwise. Note that a unidirectional charge separation is considered here, i.e., no charge recombination is taken into account at the moment.

The solution of Eq. (1) is a sum of  $N$  exponential decays, where  $N$  is the number of pigments of the system under consideration, including the primary donor. These components merge into a continuous distribution of decay times in an ensemble of non-identical systems (non-identical as a result of, for instance, inhomogeneous broadening). Some of the faster decay times may be observed as equilibration phenomena. In trapping experiments with largely nonselective excitation and detection, the fast decay components usually have very small amplitudes and only a mono-exponential decay from thermal equilibrium is observed. The resulting expression for this time  $\tau$  (the total excited-state lifetime or total trapping time) is a sum of three contributions:

$$\tau = \tau_{trap} + \tau_{mig} + \tau_{del} \quad (2)$$

in which  $\tau_{trap}$  represents the trapping time in the reaction center,  $\tau_{del}$  represents the delivery of the excitation energy to the reaction center and  $\tau_{mig}$  represents the migration of the excitation energy in the light-harvesting antenna. When either  $\tau_{trap}$ ,  $\tau_{del}$  or  $\tau_{mig}$  dominates the overall expression (i.e., represents the slowest process), the decay kinetics are said to be 'trap-limited,' 'transfer-to-the-trap-limited' or 'diffusion-limited,' respectively.

In Fig. 6 we visualize the most essential processes in a PS II RC complex (A), a PS II core complex (B), a  $C_2S_2$  PSII-LHCII supercomplex (C) and a single PS II membrane (D). The trapping process (represented by the central red (or dark grey) areas in Fig. 6) occurs in the multimer of four chlorophylls and two pheophytins in the PS II RC. The delivery of excitations to the RC multimer (represented by the dark blue (or black) arrows in Fig. 6) is provided mainly by the core antenna proteins CP47 and CP43 (Fig. 6B), but may also contain some contributions from the peripheral chlorophylls in the PS II RC (Fig. 6A) and from LHCII in the adjacent membrane (not shown). The migration of excitations between the various antenna complexes (represented by the green (or grey) arrows in Fig. 6) occurs to a significant extent in PSII-LHCII supercomplexes (Fig. 6C) and is very important in PS II membranes (Fig. 6D).

In the case of trap-limited kinetics, charge separation is much slower than energy transfer. In this case,  $\tau \sim \tau_{trap}$  and depends only on the rate constant of primary charge separation ( $k_{RC}$ ) and the equilibrium excited-state population of the primary donor ( $\rho_{eq}$ ):

$$\tau_{trap}^{-1} = k_{RC} \rho_{eq} \text{ with } \rho_{eq} = 1 / \sum_i \exp \frac{E_{RC} - E_i}{k_B T} \quad (3)$$

in which  $E_{RC}$  and  $E_i$  represent the excited state energies of the pigments of the RC and of site  $i$ , respectively,  $T$  is the absolute temperature and  $k_B$  is the Boltzmann constant. Within the context of this model, the overall lifetime increases when the antenna size increases, because the probability to find the excitation on the primary donor decreases accordingly. Measurements of PS II complexes of different antenna size have indeed indicated that the overall lifetime is longer for the larger complexes (see above), based on which several authors have suggested that the PS II kinetics are trap-limited (Schatz et al., 1988). In this model, extrapolation to a P680/Chl ratio of 1 gives the intrinsic rate of charge separation, which according to Schatz et al. (1988) would be about  $(2.7 \text{ ps})^{-1}$ . The

time-resolved data on the PS II RC complex (see above), however, indicate that in addition to the intrinsic rate of charge separation in the RC (which even may be an order of magnitude faster than  $(2.7 \text{ ps})^{-1}$ ), the rate of charge stabilization by electron transfer and relaxation also is important (discussed in Section IV.A.3).

The delivery term,  $\tau_{del}$ , becomes important when transfer between the antenna and the primary donor is significantly slower than energy transfer between the antenna pigments. Beekman et al. (1994) performed a detailed analysis of the trapping kinetics of the photosynthetic unit of the purple bacterium *Rhodospirillum rubrum*, which probably consists of an RC (partly) surrounded by a single ring of  $\alpha\beta$ -pigment-protein pairs that form the LH1 core antenna. It was concluded that the total lifetime of 50–60 ps is 'transfer-to-the-trap-limited,' i.e.,  $\tau_{del}$  in this case is the dominant term on the right-hand side of Eq. (2).

In the typical case of approximately equal excited-state energies of the delivery and other antenna Chls,  $\tau_{del}$  is given by (van Amerongen et al., 2000):

$$\tau_{del} \approx \frac{x}{z} \left( \frac{1}{k_D} - \frac{1}{k_h} \right) \approx \frac{x}{z} \frac{1}{k_D} \quad (4)$$

Here  $k_D$  is the rate of excitation energy transfer from a delivery site or linker Chl to the RC,  $k_h$  is the rate of energy transfer between neighboring pigments (in the case of a regular lattice of antenna pigments),  $z$  is the number of linker Chls and  $x$  is the number of Chls in the antenna (including the linker Chls). We start by considering a hypothetical core complex in which all excitations in CP47 and CP43 are delivered to the primary donor via the two peripheral Chls in the RC. These two Chls, which function as linker Chls in this hypothetical case, transfer their excitations to the primary donor with a time constant of approximately 20 ps (Section IV.A.3). In this case,  $\tau_{del}$  would be 280 ps, assuming 14 Chls in both CP47 and CP43 and 2 linker Chls. This is much larger than the measured trapping kinetics for the PS II core complex (40–80 ps, Section IV.B) and excludes the possibility that the peripheral Chls of the RC function as the sole linker sites for excitation delivery from the antenna to the primary donor. Therefore, it can be argued that CP47 and CP43 also contain pigments which transfer excitations to the RC with a similar or faster rate. The presently available structural data indeed appear to confirm this view (Zouni et al., 2001; Fig. 2). Table 5 shows that Chl43 of CP47 and

Table 5. Center-to-center distances between chlorophylls and/or pheophytins on the same (core 1) or different (mon 1 and mon 2, core 1 and core 2) monomeric subunits, calculated from the crystal structures of LHCII from pea (Kühlbrandt et al., 1994) and the PS II core complex from *Synechococcus elongatus* (Zouni et al., 2001).

Residue 1	Residue 2	Center-to-center distance (Å)
A4 LHCII (mon 1)	A5 LHCII (mon 2)	16.4
A4 LHCII (mon 1)	B5 LHCII (mon 2)	17.2
A5 LHCII (mon 1)	A5 LHCII (mon 2)	18.3
Chl43 CP47 (core 1)	ChlZ D2 (core 1)	20.9
Chl26 CP43 (core 1)	ChlZ D1 (core 1)	21.1
Chl43 CP47 (core 1)	Ph D2 (core 1)	21.3
Chl26 CP43 (core 1)	Ph D1 (core 1)	21.6
Chl32 CP43 (core 1)	Ph D1 (core 1)	24.5
Chl47 CP47 (core 1)	Ph D2 (core 1)	25.5
ChlZ D2 (core 1)	Ph D2 (core 1)	23.7
ChlZ D1 (core 1)	Ph D1 (core 1)	23.9
ChlZ D1 (core 1)	Chl D1 (core 1)	24.5
ChlZ D2 (core 1)	Chl D2 (core 1)	24.6
Chl44 CP47 (core 1)	Chl44 CP47 (core 2)	27.3
ChlZ D1 (core 1)	Chl42 CP47 (core 2)	30.7
ChlZ D1 (core 1)	Chl39 CP47 (core 2)	30.9

Chl26 of CP43 are at very similar center-to-center distances to the peripheral Chl and Ph molecules of D2 and D1, respectively.

The migration time  $\tau_{mig}$  is often called the ‘average first passage time’ and reflects the average time for an excitation to reach the primary donor for the first time (Pearlstein, 1982; Valkunas, 1986; Somsen et al., 1994), at least in the case when  $\tau_{del}$  can be ignored. Otherwise, the average first passage time is equal to the sum of  $\tau_{mig}$  and  $\tau_{del}$ .  $\tau_{mig}$  will dominate Eq. (2) when the rate of charge separation is much faster than the (average) rate of energy transfer (and  $k_D$  is not slower than  $k_h$ ), in which case the entire charge-separation process becomes migration- or diffusion-limited.

For a regular light-harvesting antenna structure with dimension  $d$  and size  $N$ ,  $\tau_{mig}$  can be expressed as:

$$\tau_{mig} = 0.5Nf_d(N)k_h^{-1} \quad (5)$$

The structure function  $f_d(N)$  is of the order of unity ( $0.5 < f_d(N) < 1.0$ ) for an antenna-RC complex containing many tens to several hundreds of pigments, and as a rough approximation  $f_d(N)$  can be considered independent of the number of pigments within this

range. It was shown above (Section III.A.8) that a number  $X$  of LHCII trimers leads to a contribution of  $X \times 32$  ps to the total trapping time. The average number of LHCII trimers per RC is approximately 4 and thus LHCII contributes  $\sim 130$  ps to the total trapping time (Barzda et al., 2001). The Chl  $a$  organization in monomeric CP29, CP26 and CP24 is probably very similar to that in monomeric LHCII (see above) and one might expect an additional  $\sim 30$  ps contribution to the total value of  $\tau_{mig}$ . The total number of Chl  $a$  molecules in CP47 and CP43 ( $\sim 28$ ) is close to that of trimeric LHCII, but the Chl  $a$  density is probably higher and therefore the contribution to  $\tau_{mig}$  is minor. We stress that the organization of LHCII in the PS II membranes is very heterogeneous and that there are large variations in the local LHCII environments of the PS II units, which suggests that there may be a very large variation in  $\tau_{mig}$  (and in  $\tau_{trap}$ ).

Recently, it was shown that the number of excited states after 150 and 250 ps in PS II preparations with varying antenna size could be modeled satisfactorily by assuming that the rate of energy transfer is much faster than the rate of charge separation (Barter et al., 2001). It was pointed out by the authors that the

model is not necessarily correct on a microscopic level, but that it offers a way to describe the free energy of the system as a function of time in a meaningful way. It was concluded that energy transfer is not the rate-limiting step in the trapping process. We have presented evidence, however, that energy transfer is a relatively slow process and can not be ignored (Barzda et al., 2001).

We conclude by saying that there are no clear-cut data available from which it follows that either  $\tau_{trap}$ ,  $\tau_{mig}$ , or  $\tau_{del}$  dominates the total trapping time in PS II in vivo, or that any of these terms can be totally neglected. On the contrary, it seems more likely that all three terms contribute significantly to the total trapping time. In order to increase our understanding on the trapping process in PS II, more refined structural data are needed as well as kinetic data on well-defined preparations. Also an understanding of the energetics of the charge-separation process itself is crucial, since these energetics determine the extent to which the various charge separation, stabilization and recombination reactions occur, which will significantly contribute to the observed decay rates.

## References

- Adamska I, Roobol-Boza M, Lindahl M and Andersson B (1999) Isolation of pigment-binding early light-inducible proteins from pea. *Eur J Biochem* 260: 453–460
- Agarwal R, Krueger BP, Scholes GD, Yang M, Yom J, Mets L and Fleming GR (2000) Ultrafast energy transfer in LHC-II revealed by three-pulse photon echo peak shift measurements. *J Phys Chem B* 104: 2908–2918
- Barbato R, Race HL, Friso G and Barber J (1991) Chlorophyll levels in the pigment-binding proteins of Photosystem II. *FEBS Lett* 286: 86–90
- Barter LMC, Bianchetti M, Jeans C, Schilstra MJ, Hankamer B, Diner BA, Barber J, Durrant JR and Klug DR (2001) Relationship between excitation energy transfer, trapping, and antenna size in Photosystem II. *Biochemistry* 40: 4026–4034
- Barzda V, Peterman EJG, Calkoen F, van Grondelle R and van Amerongen H (1998) The Influence of aggregation on the triplet formation in light-harvesting chlorophyll *a/b* pigment-protein complex II of green plants. *Biochemistry* 37: 546–551
- Barzda V, Jennings RC, Zucchelli G and Garab G (1999) Kinetic analysis of light-induced fluorescence quenching in light-harvesting chlorophyll *a/b* pigment-protein complex of Photosystem II. *Photochem Photobiol* 70: 751–759
- Barzda V, Vengris M, Valkunas L, van Grondelle R and van Amerongen H (2000) Generation of fluorescence quenchers from the triplet states of chlorophylls in the major light-harvesting complex II from green plants. *Biochemistry* 39: 10468–10477
- Barzda V, Gulbinas V, Kananavicius R, van Amerongen H, van Grondelle R and Valkunas L (2001) Singlet-singlet annihilation kinetics in aggregates and trimers of LHCII. *Biophys J* 80: 2409–2421
- Bassi R and Dainese P (1992) A supramolecular light-harvesting complex from chloroplast Photosystem-II membranes. *Eur J Biochem* 204: 317–326
- Bassi R, Marquardt J and Lavergne J (1995) Biochemical and functional properties of Photosystem II in agranal membranes from maize mesophyll and bundle-sheath chloroplasts. *Eur J Biochem* 233: 709–719
- Bassi R, Sandona D and Croce R (1997) Novel aspects of chlorophyll *a/b*-binding proteins. *Physiol Plant* 100: 769–779
- Bassi R, Croce R, Cugini D and Sandona D (1999) Mutational analysis of a higher plant antenna protein provides identification of chromophores bound into multiple sites. *Proc Natl Acad Sci USA* 96: 10056–10061
- Beekman LMP, van Mourik F, Jones MR, Visser HM, Hunter CN and van Grondelle R (1994) Trapping kinetics in mutants of the photosynthetic purple bacterium *Rhodobacter sphaeroides*: Influence of the charge separation rate and consequences for the rate-limiting step in the light-harvesting process. *Biochemistry* 33: 3143–3147
- Bialek-Bylka GE, Tomo T, Satoh K and Koyama Y (1995) 15-cis- $\beta$ -carotene found in the reaction center of spinach Photosystem II. *FEBS Lett* 363: 137–140
- Bittner T, Irrgang KD, Renger G and Wasielewski MR (1994) Ultrafast excitation energy transfer and exciton-exciton annihilation processes in isolated light harvesting complexes of Photosystem II (LHCII) from spinach. *J Phys Chem* 98: 11821–11826
- Bittner T, Wiederrecht GP, Irrgang KD, Renger G and Wasielewski M (1995) Femtosecond transient absorption spectroscopy on the light-harvesting Chl *a/b* protein complex of Photosystem II at room temperature and 12 K. *Chem Phys* 194: 311–322
- Blomberg MRA, Siegbahn PER and Babcock GT (1998) Modeling electron transfer in biochemistry: A quantum chemical study of charge separation in *Rhodobacter sphaeroides* and Photosystem II. *J Am Chem Soc* 120: 8812–8824
- Boekema EJ, Hankamer B, Bald D, Kruij J, Nield J, Boonstra AF, Barber J and Rögner M (1995) Supramolecular structure of the Photosystem II complex from green plants and cyanobacteria. *Proc Natl Acad Sci USA* 92: 175–179
- Boekema EJ, van Roon H and Dekker JP (1998) Specific association of Photosystem II and light-harvesting complex II in partially solubilized Photosystem II membranes. *FEBS Lett* 424: 95–99
- Boekema EJ, van Roon H, Calkoen F, Bassi R and Dekker JP (1999a) Multiple types of association of Photosystem II and its light-harvesting antenna in partially solubilized Photosystem II membranes. *Biochemistry* 38: 2233–2239
- Boekema EJ, van Roon H, van Breemen JFL and Dekker JP (1999b) Supramolecular organization of Photosystem II and its light-harvesting antenna in partially solubilized Photosystem II membranes. *Eur J Biochem* 266: 444–452
- Boekema EJ, van Breemen JFL, van Roon H and Dekker JP (2000a) Conformational changes in Photosystem II supercomplexes upon removal of extrinsic subunits. *Biochemistry* 39: 12907–12915
- Boekema EJ, van Breemen JFL, van Roon H and Dekker JP (2000b) Arrangement of Photosystem II supercomplexes in

- crystalline macrodomains within the thylakoid membranes of green plants. *J Mol Biol* 301: 1123–1133
- Breton J and Katoh S (1987) Orientation of the pigments in Photosystem II: Low temperature linear-dichroism study of a core particle and of its chlorophyll-protein subunits isolated from *Synechococcus* sp. *Biochim Biophys Acta* 892: 99–107
- Bricker TM (1990) The structure and function of CPa-1 and CPa-2 in Photosystem II. *Photosynth Res* 24: 1–13
- Bricker TM and Ghanotakis DF (1996) Introduction to oxygen evolution and the oxygen-evolving complex. In Ort DR and Yocum CF (eds) *Oxygenic Photosynthesis: The Light Reactions*, pp 113–136. Kluwer Academic Publishers, Dordrecht
- Carbonera D and Giacometti CG (1992) Optically detected magnetic resonance of pigments in light harvesting complex (LHCII) of spinach. *Rend Fis Acc Lincei* 3: 361–368
- Chang H-C, Jankowiak R, Yocum CF, Picorel R, Alfonso M, Seibert M and Small GJ (1994) Exciton level structure and dynamics in the CP47 antenna complex of Photosystem II. *J Phys Chem* 98: 7717–7724
- Connelly JP, Müller MG, Bassi R, Croce R and Holzwarth AR (1997a) Femtosecond transient absorption study of carotenoid to chlorophyll energy transfer in the light-harvesting complex II of Photosystem II. *Biochemistry* 36: 281–287
- Connelly JP, Müller MG, Hucke M, Gatzert G, Mullineaux CW, Ruban AV, Horton P and Holzwarth AR (1997b) Ultrafast spectroscopy of trimeric light-harvesting complex II from higher plants. *J Phys Chem B* 101: 1902–1909
- Croce R, Remelli R, Varotto C, Breton J and Bassi R (1999a) The neoxanthin binding site of the major light harvesting complex (LHCII) from higher plants. *FEBS Lett* 456: 1–6
- Croce R, Weiss S and Bassi R (1999b) Carotenoid-binding sites of the major light-harvesting complex II of higher plants. *J Biol Chem* 274: 29613–29623
- Croce R, Müller MG, Bassi R and Holzwarth AR (2001) Carotenoid-to-chlorophyll energy transfer in recombinant major light-harvesting complex (LHCII) of higher plants. I. Femtosecond transient absorption measurements. *Biophys J* 80: 901–915
- Cseh Z, Rajagopal S, Tsonev T, Busheva M, Papp E and Garab G (2000) Thermooptic effect in chloroplast thylakoid membranes. Thermal and light stability of pigment arrays with different levels of structural complexity. *Biochemistry* 39: 15250–15257
- Dainese P and Bassi R (1991) Subunit stoichiometry of the chloroplast Photosystem-II antenna system and aggregation state of the component chlorophyll *a/b* binding proteins. *J Biol Chem* 266: 8136–8142
- De Las Rivas J, Telfer A and Barber J (1993) Two coupled  $\beta$ -carotene molecules protect P680 from photodamage in isolated Photosystem II reaction centres. *Biochim Biophys Acta* 1142: 155–164
- De Paula JC, Liefshitz A, Hinsley S, Lin W, Chopra V, Long K, Williams SA, Betts S and Yocum CF (1994) Structure-function-relationships in the 47-kDa antenna protein and its complex with the Photosystem II reaction-center core. Insights from picosecond fluorescence decay kinetics and resonance Raman spectroscopy. *Biochemistry* 33: 1455–1466
- De Weerd FL, van Stokkum IHM, van Amerongen H, Dekker JP and van Grondelle R (2002) Pathways for energy transfer in the core light-harvesting complexes CP43 and CP47 of Photosystem II. *Biophys J* 82: 1586–1597
- Dekker JP and van Grondelle R (2000) Primary charge separation in Photosystem II. *Photosynth Res* 63: 195–208
- Dekker JP, Boekema EJ, Witt HT and Rögner M (1988) Refined purification and further characterization of oxygen-evolving and Tris-treated Photosystem II particles from the thermophilic cyanobacterium *Synechococcus* sp. *Biochim Biophys Acta* 936: 307–318
- Dekker JP, Hasselødt A, Pettersson Å, van Roon H, Groot M-L and van Grondelle R (1995) On the nature of the F695 and F685 emission of Photosystem II. In Mathis P (ed) *Photosynthesis: From Light to Biosphere*, Vol I, pp 53–56. Kluwer Academic Publishers, Dordrecht
- Dekker JP, van Roon H and Boekema EJ (1999) Heptameric association of light-harvesting complex II trimers in partially solubilized Photosystem II membranes. *FEBS Lett* 449: 211–214
- Den Hartog FTH, Dekker JP, van Grondelle R and Völker S (1998) Spectral distributions of 'trap' pigments in the CP47 and CP47RC complexes of Photosystem II at low temperature. A fluorescence line-narrowing and hole-burning study. *J Phys Chem B* 102: 11007–11016
- Diner BA and Babcock GT (1996) Structure, dynamics, and energy conversion efficiency in Photosystem II. In Ort DR and Yocum CF (eds) *Oxygenic Photosynthesis: The Light Reactions*, pp 213–247. Kluwer Academic Publishers, Dordrecht
- Diner BA, Schlodder E, Nixon PJ, Coleman WJ, Rappaport F, Lavergne J, Vermaas WJ and Chisholm DA (2001) Site-directed mutations of D1-198 and D2-197 of Photosystem II in *Synechocystis* PCC6803: Sites of primary charge separation and cation and triplet stabilization. *Biochemistry* 40: 9265–9281
- Donovan B, Walker LA II, Kaplan D, Bouvier M, Yocum CF and Sension RJ (1997) Structure and function in the isolated reaction center complex of Photosystem II. 1. Ultrafast fluorescence measurements of PS II. *J Phys Chem B* 101: 5232–5238
- Du M, Xie X, Mets L and Fleming GR (1994) Direct observation of ultrafast energy-transfer processes in light-harvesting complex II. *J Phys Chem* 98: 4736–4741
- Durrant JR, Hastings G, Joseph DM, Barber J, Porter G and Klug DR (1992) Subpicosecond equilibration of excitation energy in isolated Photosystem II reaction centers. *Proc Natl Acad Sci USA* 89: 11632–11636
- Durrant JR, Klug DR, Kwa SLS, van Grondelle R, Porter G and Dekker JP (1995) A multimer model for P680, the primary electron donor of Photosystem II. *Proc Natl Acad Sci USA* 92: 4798–4802
- Eads DD, Castner Jr. EW, Alberty R, Mets L and Fleming GR (1989) Direct observation of energy transfer in a photosynthetic membrane: chlorophyll *b* to chlorophyll *a* transfer in LHC. *J Phys Chem* 93: 8271–8275
- Eijkelhoff C (1997) The Photosystem II reaction center: Biochemical and biophysical aspects of photosynthesis in green plants. Doctoral Thesis, Vrije Universiteit Amsterdam
- Eijkelhoff C, van Roon H, Groot M-L, van Grondelle R and Dekker JP (1996) Purification and spectroscopic characterization of Photosystem II reaction center complexes isolated with or without Triton X-100. *Biochemistry* 35: 12864–12872
- Eshaghi S, Andersson B and Barber J (1999) Isolation of a highly

- active PSII-LHCII supercomplex from thylakoid membranes by a direct method. *FEBS Lett* 446: 23–26
- Eshaghi S, Turcsányi E, Vass I, Nugent J, Andersson B and Barber J (2000) Functional characterization of the PSII-LHC II supercomplex isolated by a direct method from spinach thylakoid membranes. *Photosynth Res* 64: 179–187
- Frank HA, Kumar Das S, Bautista JA, Bruce D, Vasil'ev S, Crimi M, Croce R and Bassi R (2001) Photochemical behavior of xanthophylls in the recombinant Photosystem II antenna complex, CP26. *Biochemistry* 40: 1220–1225
- Funk C, Schröder WP, Green BR, Renger G and Andersson B (1994) The intrinsic 22 kDa protein is a chlorophyll-binding subunit of Photosystem II. *FEBS Lett* 342: 261–266
- Funk C, Schröder WP, Napiwotzki A, Tjus SE, Renger G and Andersson B (1995a) The PSII-S protein of higher plants—a new type of pigment-binding protein. *Biochemistry* 34: 11133–11141
- Funk C, Adamska I, Green BR, Andersson B and Renger G (1995b) The nuclear-encoded chlorophyll-binding photosystem-II-S protein is stable in the absence of pigments. *J Biol Chem* 270: 30141–30147
- Garab G and Mustárdy L (1999) Role of LHCII-containing macrodomains in the structure, function and dynamics of grana. *Austr J Plant Physiol* 26: 649–658
- Germano M, Shkuropatov AY, Permentier H, de Wijn R, Hoff AJ, Shuvalov VA and van Gorkom HJ (2001) Pigment organization and their interactions in reaction centers of Photosystem II: Optical spectroscopy at 6 K of reaction centers with modified pheophytin composition. *Biochemistry* 40: 11472–11482
- Ghanotakis DF, de Paula JC, Demetriou DM, Bowlby NR, Petersen J, Babcock GT and Yocum CF (1989) Isolation and characterization of the 47 kDa protein and the D1-D2-cytochrome *b*-559 complex. *Biochim Biophys Acta* 974: 44–53
- Gillbro T, Sandström Å, Spangfort M, Sundström V and van Grondelle R (1988) Excitation energy annihilation in aggregates of chlorophyll *a/b* complexes. *Biochim Biophys Acta* 934: 369–374
- Giuffra E, Cugini D, Croce R and Bassi R (1996) Reconstitution and pigment-binding properties of recombinant CP29. *Eur J Biochem* 238: 112–120
- Giuffra E, Zucchelli G, Sandona D, Croce R, Cugini D, Garlaschi FM, Bassi R and Jennings RC (1997) Analysis of some optical properties of a native and reconstituted Photosystem II antenna complex, CP29: Pigment binding sites can be occupied by chlorophyll *a* or chlorophyll *b* and determine spectral forms. *Biochemistry* 36: 12984–12993
- Gradinaru CC, Pascal AA, van Mourik F, Robert B, van Grondelle R and van Amerongen H (1998a) Ultrafast evolution of the excited states in the minor chlorophyll *a/b* complex CP29 from green plants studied by energy-selective pump-probe spectroscopy. *Biochemistry* 37: 1143–1149
- Gradinaru CC, Özdemir S, Gülen D, van Stokkum IHM, van Grondelle R and van Amerongen H (1998b) The flow of excitation in LHCII monomers. Implications for the structural model of the major plant antenna. *Biophys J* 75: 3064–3077
- Gradinaru CC, van Stokkum IHM, van Grondelle R and van Amerongen H (1998c) Ultrafast absorption changes of the LHCII carotenoids upon selective excitation of the chlorophylls. In *Photosynthesis: Mechanisms and Effects* In: Garab G (ed), pp 277–281. Kluwer Academic Publishers, Dordrecht
- Gradinaru CC, van Stokkum IHM, van Grondelle R and van Amerongen H (2000) Identifying the pathways of energy transfer between carotenoids and chlorophylls in LHCII and CP29. A multicolor, femtosecond pump-probe study. *J Phys Chem B* 104: 9330–9342
- Green BR and Durnford DG (1996) The chlorophyll-carotenoid proteins of oxygenic photosynthesis. *Ann Rev Plant Physiol Plant Mol Biol* 47: 685–714
- Green BR and Kühlbrandt W (1995) Sequence conservation of light-harvesting and stress-response proteins in relation to the 3-dimensional molecular structure of LHCII. *Photosynth Res* 44: 139–148
- Greenfield SR, Seibert M, Govindjee and Wasielewski MR (1997) Direct measurement of the effective rate constant for primary charge separation in isolated Photosystem II reaction centers. *J Phys Chem B* 101: 2251–2255
- Grimm B, Kruse E and Kloppstech K (1989) Transiently expressed early light-inducible thylakoid proteins share transmembrane domains with light-harvesting chlorophyll-binding proteins. *Plant Mol Biol* 13: 583–593
- Groot M-L, Peterman EJG, van Kan PJM, van Stokkum IHM, Dekker JP and van Grondelle R (1994) Temperature dependent triplet and fluorescence quantum yields of the Photosystem II reaction center described in a thermodynamic model. *Biophys J* 67: 318–330
- Groot M-L, Peterman EJG, van Stokkum IHM, Dekker JP and van Grondelle R (1995) Triplet and fluorescing states of the CP47 antenna complex of Photosystem II studied as a function of temperature. *Biophys J* 68: 281–290
- Groot M-L, Dekker JP, van Grondelle R, den Hartog FTH and Völker S (1996) Energy transfer and trapping in isolated Photosystem II reaction centers of green plants at low temperature. A study by spectral hole-burning. *J Phys Chem* 100: 11488–11495
- Groot M-L, Frese RN, de Weerd FL, Bromek K, Pettersson Å, Peterman EJG, van Stokkum IHM, van Grondelle R and Dekker JP (1999) Spectroscopic properties of the CP43 core antenna protein of Photosystem II. *Biophys J* 77: 3328–3340
- Gruszecki WI, Grudziński W, Banaszek-Glos A, Matula M, Kernen P, Krupa Z and Sielewiesiuk (1999) Xanthophyll pigments in light-harvesting complex II in monomolecular layers: Localisation, energy transfer and orientation. *Biochim Biophys Acta* 1412: 173–183
- Hankamer B, Barber J and Boekema EJ (1997a) Structure and membrane organization of Photosystem II from green plants. *Ann Rev Plant Phys Plant Mol Biol* 48: 641–672
- Hankamer B, Nield J, Zheleva D, Boekema E, Jansson S and Barber J (1997b) Isolation and characterization of monomeric and dimeric Photosystem II complexes from spinach and their relevance to the organisation of Photosystem II in vivo. *Eur J Biochem* 243: 422–429
- Hankamer B, Morris EP and Barber J (1999) Revealing the structure of the oxygen-evolving core dimer of Photosystem II by cryoelectron crystallography. *Nature Struct Biol* 6: 560–564
- Harrer R, Bassi R, Testi MG and Schäfer C (1998) Nearest-neighbour analysis of a Photosystem II complex from *Marchantia polymorpha* L. (liverwort), which contains reaction centre and antenna proteins. *Eur J Biochem* 255: 196–205
- Hobe S, Foster R, Klinger J and Paulsen H (1995) N-proximal



- sequence motif in light-harvesting chlorophyll *a/b*-binding protein is essential for the trimerization of light-harvesting chlorophyll *a/b* complex. *Biochemistry* 34: 10224–10228
- Hobe S, Niemeier H, Bender A and Paulsen H (2000) Carotenoid binding sites in LHCIIb. Relative affinities towards major xanthophyll of higher plants. *Eur J Biochem* 267: 616–624
- Horton P, Ruban AV and Walters RG (1996) Regulation of light-harvesting in green plants. *Annual Review of Plant Physiology and Plant Molecular Biology* 47: 655–684
- Hoshida H, Sugiyama R, Nakano Y, Shiina T and Toyoshima Y (1997) Electron paramagnetic resonance and mutational analysis of Photosystem II-L subunit in the oxidation step of Tyr-Z by P680<sup>+</sup> to form the Tyr-Z<sup>+</sup>P680Pheo<sup>-</sup> state in Photosystem II. *Biochemistry* 36: 12053–12061
- Jahns P and Trissl H-W (1997) Indications for a dimeric organization of the antenna-depleted reaction center core of Photosystem II in thylakoids of intermittent light grown pea plants. *Biochim Biophys Acta* 1318: 1–5
- Jankowiak R, Zazubovich V, Rätsep M, Matsuzaki S, Alfonso M, Picorel R, Seibert M and Small GJ (2000) The CP43 core antenna complex of Photosystem II possesses two quasi-degenerate and weakly coupled Q<sub>y</sub>-trap states. *J Phys Chem B* 104: 11805–11815
- Jansson S (1994) The light-harvesting chlorophyll *a/b* proteins. *Biochim Biophys Acta* 1184: 1–19
- Jansson S, Stefánsson H, Nyström U, Gustafsson P and Albertsson P-Å (1997) Antenna protein composition of PS I and PS II in thylakoid sub-domains. *Biochim Biophys Acta* 1320: 297–309
- Jegerschöld C, Rutherford AW, Mattioli TA, Crimi M and Bassi R (2000) Calcium binding to the Photosystem II subunit CP29. *J Biol Chem* 275: 12781–12788
- Jennings RC, Garlaschi FM and Zucchelli G (1991) Light-induced fluorescence quenching in the light-harvesting chlorophyll *a/b* protein complex. *Photosynth Res* 27: 57–64
- Jennings RC, Garlaschi FM, Bassi R, Zucchelli G, Vianelli A and Dainese P (1993a) A study of photosystem-II fluorescence emission in terms of the antenna chlorophyll-protein complexes. *Biochim Biophys Acta* 1183: 194–200
- Jennings RC, Bassi R, Garlaschi FM, Dainese P and Zucchelli G (1993b) Distribution of the chlorophyll spectral forms in the chlorophyll-protein complexes of Photosystem II antenna. *Biochemistry* 32: 3203–3210
- Kim S, Sandusky P, Bowlby NR, Aebershold R, Green BR, Vlahakis S, Yocum CF and Pichersky E (1992) Characterization of a spinach psbS cDNA-encoding 22 kDa protein of Photosystem II. *FEBS Lett* 314: 67–71
- Kim S, Pichersky E and Yocum CF (1994) Topological studies of spinach 22 kDa protein of Photosystem II. *Biochim Biophys Acta* 1188: 339–348
- Kleima FJ, Gradinaru CC, Calkoen F, van Stokkum IHM, van Grondelle R and van Amerongen H (1997) Energy transfer in LHCII monomers at 77K studied by sub-picosecond transient absorption spectroscopy. *Biochemistry* 36: 15262–15268
- Kleima FJ, Hobe S, Calkoen F, Urbanus ML, Peterman EJG, van Grondelle R, Paulsen H and van Amerongen H (1999) Decreasing the chlorophyll *a/b* ratio in reconstituted LHCII: Structural and functional consequences. *Biochemistry* 38: 6587–6596
- Klug DR, Durrant JR and Barber J (1998) The entanglement of excitation energy transfer and electron transfer in the reaction centre of Photosystem II. *Philos Trans Roy Soc* 356: 449–464
- Konermann L, Gatzen G and Holzwarth AR (1997) Primary processes and structure of the Photosystem II reaction center. 5. Modeling of the fluorescence kinetics of the D1-D2-cyt-*b*559 complex at 77 K. *J Phys Chem B* 101: 2933–2944
- Kühlbrandt W, Wang DN and Fujiyoshi Y (1994) Atomic model of plant light-harvesting complex by electron crystallography. *Nature* 367: 614–621
- Kwa SLS, van Kan PJM, Groot ML, van Grondelle R, Yocum CF and Dekker JP (1992a) Spectroscopic comparison of D1-D2-cytochrome *b*-559 and CP47 complexes of Photosystem II. In: Murata N (ed) *Research in Photosynthesis*, Vol. I, pp 263–266. Kluwer Academic Publishers, Dordrecht
- Kwa SLS, van Amerongen H, Lin S, Dekker JP, van Grondelle R and Struve WS (1992b) Ultrafast energy transfer in LHC-II trimers from the Chl *a/b* light-harvesting antenna of Photosystem II. *Biochim Biophys Acta* 1102: 202–212
- Kwa SLS, Eijkelhoff C, van Grondelle R and Dekker JP (1994) Site-selection spectroscopy of the reaction center complex of Photosystem II. I. Triplet-minus-singlet absorption difference: A search for a second exciton band of P-680. *J Phys Chem* 98: 7702–7711
- Leibl W, Breton J, Deprez J and Trissl H-W (1989) Photoelectric study on the kinetics of trapping and charge stabilization in oriented PS-II membranes. *Photosynth Res* 22: 257–275
- Li X-P, Björkman O, Shih C, Grossman AR, Rosenquist M, Jansson S and Niyogi KK (2000) A pigment-binding protein essential for regulation of photosynthetic light harvesting. *Nature* 403: 391–395
- Lince MT and Vermaas W (1998) Association of His117 in the D2 protein of Photosystem II with a chlorophyll that affects excitation-energy transfer efficiency to the reaction center. *Eur J Biochem* 256: 595–602
- Merry SAP, Kumazaki S, Tachibana Y, Joseph DM, Porter G, Yoshihara K, Barber J, Durrant JR and Klug DR (1996) Sub-picosecond equilibration of excitation energy in isolated Photosystem II reaction center revisited: Time-dependent anisotropy. *J Phys Chem* 100: 10469–10478
- Merry SAP, Nixon PJ, Barter LMC, Schilstra M, Porter G, Barber J, Durrant JR and Klug DR (1998) Modulation of quantum yield of primary radical pair formation in Photosystem II by site-directed mutagenesis affecting radical cations and anions. *Biochemistry* 37: 17439–17447
- Michel H and Deisenhofer J (1988) Relevance of the photosynthetic reaction center from purple bacteria to the structure of Photosystem II. *Biochemistry* 27: 1–7
- Müller MG, Huckle M, Reus M and Holzwarth AR (1996) Primary processes and structure of the Photosystem II reaction center. 4. Low-intensity femtosecond transient absorption spectra of D1-D2-cyt-*b*559 reaction centers. *J Phys Chem* 100: 9527–9536
- Mullineaux CW, Pascal AA, Horton P and Holzwarth AR (1993) Excitation-energy quenching in aggregates of the LHC-II chlorophyll-protein complex. A time-resolved fluorescence study. *Biochim Biophys Acta* 1141: 23–28
- Naqvi KR, Melo TB, Raju BB, Javorfi T, Simidjiev I and Garab G (1997) Quenching of chlorophyll *a* singlets and triplets by carotenoids in light-harvesting complex of Photosystem II: Comparison of aggregates with trimers. *Spectrochim Acta A* 53: 2659–2667
- Naqvi KR, Javorfi T, Melo TB and Garab G (1999) More on the



- catalysis of internal conversion in chlorophyll-*a* by an adjacent carotenoid in light-harvesting complex (Ch1*a/b* LHCII) of higher plants: Time-resolved triplet-minus-singlet spectra of detergent-perturbed complexes. *Spectrochim Acta A* 55: 193–204
- Nanba O and Satoh K (1987) Isolation of a Photosystem II reaction center consisting of D-1 and D-2 polypeptides and cytochrome *b*-559. *Proc Natl Acad Sci USA* 84: 109–112
- Nechustai R, Thornber JP, Patterson LK, Fessenden RW and Levanon H (1988) Photosensitization of triplet carotenoid in photosynthetic light-harvesting complex of Photosystem II. *J Phys Chem* 92: 1165–1168
- Nield J, Orlova EV, Morris EP, Gowen B, van Heel M and Barber J (2000a) 3D map of the plant Photosystem II supercomplex obtained by cryoelectron microscopy and single particle analysis. *Nature Struct Biol* 7: 44–47
- Nield J, Kruse O, Ruprecht J, da Fonseca P, Buchel C and Barber J (2000b) Three-dimensional structure of *Chlamydomonas reinhardtii* and *Synechococcus elongatus* Photosystem II complexes allows for comparison of their oxygen-evolving complex organization. *J Biol Chem* 275: 27940–27946
- Nield J, Funk C and Barber J (2000c) Supermolecular structure of Photosystem II and location of the PsbS protein. *Phil Trans R Soc Lond B* 355: 1337–1344
- Nussberger S, Dörr K, Wang DN and Kühlbrandt W (1993) Lipid-protein interactions in crystals of plant light-harvesting complex. *J Mol Biol* 234: 347–356
- Pagano A, Cinque G and Bassi R (1998) In vitro reconstitution of the recombinant Photosystem II light-harvesting complex CP24 and its spectroscopic characterization. *J Biol Chem* 273: 17154–17165
- Pålsson LO, Spangfort MD, Gulbinas V and Gillbro T (1994) Ultrafast chlorophyll *b*-chlorophyll *a* excitation energy transfer in the isolated light harvesting complex, LHCII, of green plants. Implications for the organisation of chlorophylls. *FEBS Lett* 339: 134–138
- Pascal AA, Gradinaru CC, Wacker U, Peterman EJG, Calkoen F, Irrgang K-D, Horton P, Renger G, van Grondelle R, Robert B and van Amerongen H (1999) Spectroscopic characterization of the spinach Lhcb4 protein (CP29), a minor light-harvesting complex of Photosystem II. *Eur J Biochem* 262: 817–823.
- Pascal AA, Peterman EJG, Gradinaru CC, van Amerongen H, van Grondelle R and Robert B (2000) Structure and interactions of the chlorophyll *a* molecules in the higher plant Lhcb4 antenna protein. *J Phys Chem B* 104: 9317–9321
- Paulsen H (1995) Chlorophyll *a/b*-binding proteins. *Photochem Photobiol* 62: 367–382
- Pearlstein RM (1982) Exciton migration and trapping in photosynthesis. *Photochem Photobiol* 35: 835–84.
- Pesaresi P, Sander D, Giuffra E and Bassi R (1997) A single point mutation (E166Q) prevents dicyclohexylcarbodiimide binding to the Photosystem II subunit CP29. *FEBS Lett* 402: 151–156
- Peterman EJG, Dukker FM, van Grondelle R and van Amerongen H (1995) Chlorophyll *a* and carotenoid triplet states in light-harvesting complex II of higher plants. *Biophys J* 69: 2670–2678
- Peterman EJG, Pullerits T, van Grondelle R and van Amerongen H (1997a) Electron-phonon coupling and vibronic fine structure of light-harvesting complex II of green plants; Temperature dependent absorption and high-resolution fluorescence spectroscopy. *J Phys Chem B* 101: 4448–4457
- Peterman EJG, Monshouwer R, van Stokkum IHM, van Grondelle R and van Amerongen H (1997b) Ultrafast singlet excitation transfer from carotenoids to chlorophylls via different pathways in light-harvesting complex II of green plants. *Chem Phys Lett* 264: 279–284
- Peterman EJG, Gradinaru CC, Calkoen F, Borst JC, van Grondelle R and van Amerongen H (1997c) The xanthophylls in light-harvesting complex II of higher plants: Light harvesting and triplet quenching. *Biochemistry* 36: 12208–12215
- Pieper J, Rätsep M, Jankowiak R, Irrgang K-D, Voigt J, Renger G and Small GJ (1999a)  $Q_y$ -level structure and dynamics of solubilized light-harvesting complex II of green plants: Pressure and hole burning studies. *J Phys Chem B* 103: 2412–2421
- Pieper J, Irrgang K-D, Rätsep M, Jankowiak R, Schrötter Th, Voigt J, Small GJ and Renger G (1999b) Effects of aggregation on trimeric light-harvesting complex II of green plants: A hole-burning study. *J Phys Chem B* 103: 2412–2421
- Pieper J, Irrgang K-D, Rätsep M, Voigt J, Renger G and Small GJ (2000) Assignment of the lowest  $Q_y$ -state and spectral dynamics of the CP29 chlorophyll *a/b* antenna complex of green plants: A hole-burning study. *Photochem Photobiol* 71: 574–581
- Pogson BJ, Niyogi KK, Björkman O and DellaPenna D (1998) Altered xanthophyll compositions adversely affect chlorophyll accumulation and nonphotochemical quenching in *Arabidopsis* mutants. *Proc Natl Acad Sci USA* 95: 13324–13329
- Rech T, Durrant JR, Joseph MD, Barber J, Porter G and Klug DR (1994) Does slow energy transfer limit the observed time constant for radical pair formation in photosystem II reaction centers? *Biochemistry* 33: 14768–14774
- Remelli R, Varotto C, Sander D, Croce R and Bassi R (1999) Chlorophyll binding to monomeric light-harvesting complex—A mutation analysis of chromophore-binding residues. *J Biol Chem* 274: 33510–33521
- Rhee K-H, Morris EP, Zheleva D, Hankamer B, Kühlbrandt W and Barber J (1997) Two-dimensional structure of plant Photosystem II at 8 Å resolution. *Nature* 389: 522–526
- Rhee K-H, Morris EP, Barber J and Kühlbrandt W (1998) Three-dimensional structure of the plant Photosystem II reaction centre at 8 Å resolution. *Nature* 396: 283–286
- Roelofs TA, Kwa SLS, van Grondelle R, Dekker JP and Holzwarth AR (1993) Primary processes and structure of the Photosystem II reaction center. II. Low temperature picosecond fluorescence kinetics of a D1-D2-Cytochrome *b*-559 reaction center complex isolated by short Triton-exposure. *Biochim Biophys Acta* 1143: 147–157
- Rogl H and Kühlbrandt W (1999) Mutant trimers of Light-harvesting complex II exhibit altered pigment content and spectroscopic features. *Biochemistry* 38: 16214–16222
- Ros F, Bassi R and Paulsen H (1998) Pigment-binding properties of the recombinant Photosystem II subunit CP26 reconstituted in vitro. *Eur J Biochem* 253: 653–658
- Ruban AV, Walters RG and Horton P (1992) The molecular mechanism of the control of excitation-energy dissipation in chloroplast membranes—inhibition of  $\Delta$ -pH-dependent quenching of chlorophyll fluorescence by dicyclohexylcarbodiimide. *FEBS Lett* 309: 175–179
- Ruban AV, Horton P and Robert B (1995) Resonance Raman spectroscopy of the Photosystem II light-harvesting complex of green plants: a comparison of trimeric and aggregated states. *Biochemistry* 34: 2333–2337

- Ruban AV, Pesaresi P, Walker U, Irrgang KD, Bassi R and Horton (1998) The relationship between the binding of dicyclohexylcarbodiimide and quenching of chlorophyll fluorescence in the light-harvesting proteins of Photosystem-II. *Biochemistry* 37: 11586–11591
- Ruban AV, Lee PJ, Wentworth M, Young AJ and Horton P (1999) Determination of the stoichiometry and strength of binding of xanthophylls to the Photosystem II light harvesting complexes. *J Biol Chem* 274: 10458–10465
- Ruban AV, Pascal AA and Robert B (2000) Xanthophylls of the major photosynthetic light-harvesting complex of plants: Identification, conformation and dynamics. *FEBS Lett* 477: 181–185
- Ruf S, Biehler K and Bock R (2000) A small chloroplast-encoded protein as a novel architectural component of the light-harvesting antenna. *J Cell Biol* 149: 369–377
- Sandona D, Croce R, Pagano A, Crimi M and Bassi R (1998) Higher plants light harvesting proteins. Structure and function as revealed by mutation analysis of either protein or chromophore moieties. *Biochim Biophys Acta* 1365: 207–214
- Santini C, Tidu V, Tognon G, Ghirelli Magaldi A and Bassi R (1994) Three-dimensional organization of the higher plant Photosystem II reaction centre and evidence for its dimeric organization in vivo. *Eur J Biochem* 221: 307–315
- Satoh K (1996) Introduction to the Photosystem II reaction center—isolation and biochemical and biophysical characterization. In: Ort DR and Yocum CF (eds) *Oxygenic Photosynthesis: The Light Reactions*, pp 193–211, Kluwer Academic Publishers, Dordrecht
- Savikhin S, van Amerongen H, Kwa SLS, van Grondelle R and Struve WS (1994) Low-temperature energy transfer in LHC-II trimers from the Chl *a/b* light-harvesting antenna of Photosystem II. *Biophys J* 66: 1597–1603
- Schatz GH, Brock H and Holzwarth AR (1988) Kinetic and energetic model for the primary processes in Photosystem II. *Biophys J* 54: 397–405
- Schelvus JPM, van Noort PI, Aartsma TJ and van Gorkom HJ (1994) Energy transfer, charge separation and pigment arrangement in the reaction center of Photosystem II. *Biochim Biophys Acta* 1184: 242–250
- Schilstra MJ, Nield J, Dörner W, Hankamer B, Carradus M, Barter LMC, Barber J, and Klug DR (1999) Similarity between electron donor side reactions in the solubilized Photosystem II-LHC II supercomplex and Photosystem-II-containing membranes. *Photosynth Res* 60: 191–198
- Schmid VHR, Thome P, Ruhle W, Paulsen H, Kühlbrandt W and Rogl H (2001) Chlorophyll *b* is involved in long-wavelength spectral properties of light-harvesting complexes LHC I and LHC II. *FEBS Lett* 499: 27–31
- Schödel R, Irrgang K-D, Voigt J and Renger G (1998) Rate of carotenoid triplet formation in solubilized light-harvesting complex II (LHCII) from spinach. *Biophys J* 75: 3143–3153
- Schubert W-D, Klukas O, Saenger W, Witt HT, Fromme P and Krauss N (1998) A common ancestor for oxygenic and anoxygenic photosynthetic systems: A comparison based on the structural model of Photosystem I. *J Mol Biol* 280: 297–314
- Shi L-X and Schröder WP (1997) Compositional and topological studies of the PsbW protein in spinach thylakoid membranes. *Photosynth Res* 53: 45–53
- Siefermann-Harms D (1987) The light-harvesting and protective functions of carotenoids in photosynthetic membranes. *Physiol Plant* 69: 561–568
- Siefermann-Harms D and Angerhofer A (1998) Evidence for an O<sub>2</sub>-barrier in the light-harvesting chlorophyll-*a/b*-protein complex LHC II. *Photosynth Res* 55: 83–94
- Somsen OJG, van Mourik F, van Grondelle R and Valkunas L (1994) Energy migration and trapping in a spectrally and spatially inhomogeneous light-harvesting antenna. *Biophys J* 66: 1580–1596
- Stewart DH, Cua A, Chisholm DA, Diner BA, Bocian DF and Brudvig GW (1998) Identification of histidine 118 in the D1 polypeptide of Photosystem II as the axial ligand to chlorophyll Z. *Biochemistry* 37: 10040–10046
- Swiatek M, Kuras R, Sokolenko A, Higgs D, Olive J, Cinque G, Muller B, Eichacker LA, Stern DB, Bassi R, Herrmann RG and Wollman FA (2001) The chloroplast gene *ycf9* encodes a Photosystem II (PS II) core subunit, PsbZ, that participates in PS II supramolecular architecture. *Plant Cell* 13: 1347–1367
- Trissl H-W, Breton J, Deprez J and Leibl W (1987) Primary electrogenic reactions of Photosystem II as probed by the light-gradient method. *Biochim Biophys Acta* 893: 305–319
- Vacha F, Joseph DM, Durrant JR, Telfer A, Klug DR, Porter G and Barber J (1995) Photochemistry and spectroscopy of a five-chlorophyll reaction center of Photosystem II isolated by using a Cu affinity column. *Proc Natl Acad Sci USA* 92: 2929–2933
- Valkunas L (1986) Influence of structural heterogeneity on energy migration in photosynthesis. *Laser Chem* 6: 253–267
- van Amerongen H and van Grondelle R (2001) Understanding the energy transfer function of LHCII, the major light-harvesting complex of green plants. *J Phys Chem B* 105: 604–617
- Van Amerongen H, van Bolhuis BM, Betts S, Mei R, van Grondelle R, Yocum CF and Dekker JP (1994) Spectroscopic characterization of CP26, a chlorophyll *a/b* binding protein of the higher plant Photosystem II reaction center. *Biochim Biophys Acta* 1188: 227–234
- Van Amerongen H, Valkunas L and van Grondelle R (2000) *Photosynthetic excitons*. World Scientific, Singapore.
- Van Brederode ME and van Grondelle R (1999) New and unexpected routes for ultrafast electron transfer in photosynthetic reaction centers. *FEBS Lett* 455: 1–7
- Van der Vos R, Carbonera D and Hoff AJ (1991) Microwave and optical spectroscopy of carotenoid triplets in light-harvesting complex LHCII of spinach by absorbance-detected magnetic resonance. *Appl Magn Res* 2: 179–202
- Van der Vos R, Franken EM and Hoff AJ (1994) ADMR study of the effect of oligomerisation on the carotenoid triplets and on triplet-triplet transfer in light harvesting complex II (LHCII) of spinach. *Biochim Biophys Acta* 1188: 243–250
- Van Dorssen RJ, Plijter JJ, Dekker JP, den Ouden A, Ames J and van Gorkom HJ (1987a) Spectroscopic properties of chloroplast grana membranes and of the core of Photosystem II. *Biochim Biophys Acta* 890: 134–143
- Van Dorssen RJ, Breton J, Plijter JJ, Satoh K, van Gorkom HJ and Ames J (1987b) Spectroscopic properties of the reaction center and of the 47 kDa chlorophyll protein of Photosystem II. *Biochim Biophys Acta* 893: 267–274
- Van Grondelle R and Somsen OJG (1999) Excitation energy transfer in photosynthesis. In Andrews DL and Demidov AA (eds) *Resonance energy transfer*, pp 366–398. John Wiley and Sons, Chichester

- Van Grondelle R, Dekker JP, Gillbro T and Sundström V (1994) Energy transfer and trapping in photosynthesis. *Biochim Biophys Acta* 1187: 1–65
- Van Leeuwen PJ (1993) The redox cycle of the oxygen-evolving complex of Photosystem II. Doctoral Thesis, University of Leiden
- Van Leeuwen PJ, Nieveen MC, van de Meent EJ, Dekker JP and van Gorkom HJ (1991) Rapid and simple isolation of pure Photosystem II core and reaction center particles from spinach. *Photosynth Res* 28: 149–153
- Van Roon H, van Breemen JFL, de Weerd FL, Dekker JP and Boekema EJ (2000) Solubilization of green plant thylakoid membranes with *n*-dodecyl- $\alpha$ -D-maltoside. Implications for the structural organization of the Photosystem II, Photosystem I, ATP synthase and cytochrome *b<sub>6</sub>f* complexes. *Photosynth Res* 64: 155–166
- Vasil'ev S, Orth P, Zouni A, Owens TG and Bruce D (2001) Excited-state dynamics in Photosystem II: Insights from the X-ray crystal structure. *Proc Natl Acad Sci USA* 98: 8602–8607
- Visser HM, Kleima FJ, van Stokkum IHM, van Grondelle R and van Amerongen H (1996) Probing the many energy-transfer processes in the photosynthetic light-harvesting complex II at 77 K using energy-selective sub-picosecond transient absorption spectroscopy. *Chem Phys* 210: 297–312
- Visser HM, Kleima FJ, van Stokkum IHM, van Grondelle R and van Amerongen H (1997) Probing the many energy-transfer processes in the photosynthetic light-harvesting complex II at 77 K using energy-selective sub-picosecond transient absorption spectroscopy. *Chem Phys* 215: 299
- Walla PJ, Yom J, Krueger BP and Fleming GR (2000) Two-photon excitation spectrum of light-harvesting complex II and fluorescence upconversion after one- and two-photon excitation of the carotenoids. *J Phys Chem B* 104: 4799–4806
- Wedel N, Klein R, Ljungberg U, Andersson B and Herrmann RG (1992) The single-copy gene *psbS* codes for a phylogenetically intriguing 22 kDa polypeptide of Photosystem II. *FEBS Lett* 314: 61–66
- Wentworth M, Ruban AV and Horton P (2000) Chlorophyll fluorescence quenching in isolated light harvesting complexes induced by zeaxanthin. *FEBS Lett* 471: 71–74
- Yakushevska AE, Ruban AV, Jensen PE, van Roon H, Niyogi KK, Horton P, Dekker JP and Boekema EJ (2001a) Supramolecular organization of Photosystem II and its associated light-harvesting antenna in the wild-type and *npq4* mutant of *Arabidopsis thaliana*. In: PS2001 Proceedings: 12th International Congress on Photosynthesis, S5–006. CSIRO Publishing, Melbourne (CD-ROM)
- Yakushevska AE, Jensen PE, Keegstra W, van Roon H, Scheller HV, Boekema EJ and Dekker JP (2001b) Supermolecular organization of Photosystem II and its associated light-harvesting antenna in *Arabidopsis thaliana*. *Eur J Biochem* 268: 6020–6028
- Yang C, Kosemund K, Cornet C and Paulsen H (1999) Exchange of pigment-binding amino acids in light-harvesting chlorophyll *a/b* protein. *Biochemistry* 38: 16205–16213
- Yruela I, Tomas R, Sanjuan ML, Torrado E, Aured M and Picorel R (1998) The configuration of  $\beta$ -carotene in the Photosystem II reaction center. *Photochem Photobiol* 68: 729–737
- Zer H, Vink M, Keren N, Dilly-Hartwig HG, Paulsen H, Herrmann RG, Andersson B and Ohad I (1999) Regulation of thylakoid protein phosphorylation at the substrate level: Reversible light-induced conformational changes expose the phosphorylation site of the light-harvesting complex II. *Proc Natl Acad Sci USA* 96: 8277–8282
- Zheleva D, Hankamer B, and Barber J (1996) Heterogeneity and pigment composition of isolated Photosystem II reaction centers. *Biochemistry* 35: 15074–15079
- Zheleva D, Sharma J, Panico M, Morris HR and Barber J (1998) Isolation and characterization of monomeric and dimeric Photosystem II complexes. *J Biol Chem* 273: 16122–16127
- Zouni A, Witt HT, Kern J, Fromme P, Krauss N, Saenger W and Orth P (2001) Crystal structure of Photosystem II from *Synechococcus elongatus* at 3.8 angstrom resolution. *Nature* 409: 739–743
- Zucchelli G, Dainese P, Jennings RC, Breton J, Garlaschi FM and Bassi R (1994) Gaussian decomposition of absorption and linear dichroism spectra of outer antenna complexes of Photosystem II. *Biochemistry* 33: 8982–8990

# Chapter 8

## Structure and Function of the Antenna System in Photosystem I

Petra Fromme<sup>\*1,3</sup>, Eberhard Schlodder<sup>\*1</sup> and Stefan Jansson<sup>\*2</sup>

<sup>1</sup> Max-Volmer-Laboratorium für Biophysikalische Chemie, Fakultät II, Technische Universität Berlin, Straße des 17 Juni 135, 10623 Berlin, Germany; <sup>2</sup> Department of Plant Physiology, University of Umeå, Sweden; <sup>3</sup> Department of Chemistry and Biochemistry, Arizona State University, Tempe, AZ 85287-1604, U.S.A.

Summary .....	254
I. Introduction .....	254
II. The Architecture of Cyanobacterial Photosystem I .....	255
A. The Protein Subunits .....	255
1. Oligomeric Structure of PS I and Interaction with External Antenna Complexes .....	255
2. The Two Large Subunits (PsaA and PsaB) .....	255
3. The Stromal Subunits (PsaC, PsaD and PsaE) .....	256
4. The Small, Integral-Membrane Subunits .....	257
B. The Electron Transport Chain .....	259
III. Structural Organization of the Core Antenna System .....	261
A. Arrangement of the Chlorophylls .....	261
B. The 'Red' Chlorophylls .....	262
C. The Linker Chl Dimers .....	264
D. The Chl Trimer and Tetramer .....	265
E. Carotenoids .....	265
IV. Plant Photosystem I .....	266
A. Polypeptides Unique to Plants .....	266
B. The External Antenna System of PS I in Plants .....	266
C. Heterogeneity of the External PS I Antenna .....	268
D. Pigment Composition of LHC I .....	268
E. Long-Wavelength Chls .....	269
F. The Architecture of the Plant PS I Antenna .....	270
V. Excitation Energy Transfer and Trapping in PS I .....	270
A. Structure and Spectra .....	271
B. Kinetics of Energy Transfer .....	271
C. Simulations .....	273
D. Function of Carotenoids .....	274
E. Energy Transfer in PS I from Higher Plants .....	274
Acknowledgment .....	275
References .....	275

---

\*Authors for correspondence, email: petra.fromme@asu.edu; eber0535@mailbox.tu-berlin.de; stefan.jansson@plantphys.umu.se

## Summary

Photosystem I (PS I) is a large, membrane protein complex, consisting of 12–15 proteins and more than 100 bound cofactors, that catalyzes light-driven electron transfer across the photosynthetic membrane in cyanobacteria, green algae and plants. Photosystem I is unique compared to other photosynthetic systems because the majority of the antenna pigments and the cofactors of the electron transport system are bound to the same protein subunits. Photosystem I can therefore be regarded as a joint reaction center-core antenna system. In this chapter, PS I is described with respect to both structure and function. The kinetics of energy transfer and trapping are discussed in the light of the structural information. We also discuss models for the interaction of PS I with the external antenna complexes in cyanobacteria and plants.

## I. Introduction

Plants, green algae and cyanobacteria use the energy of sunlight to drive the synthesis of carbohydrates from CO<sub>2</sub> and water. Two large protein complexes, the Photosystems I and II, catalyze the first steps of this energy conversion, the light-induced charge separation across the photosynthetic membrane. In plants, these complexes are found in the chloroplast thylakoid membrane.

Photosystem I (PS I) captures sunlight by a large antenna system consisting of chlorophylls (Chls) and carotenoids and transfers the energy to the reaction center of the complex, which mediates the light-driven electron transfer from the soluble electron carrier proteins plastocyanin or cytochrome *c*<sub>6</sub> at the lumenal side to ferredoxin or flavodoxin at the stromal side of the thylakoid membrane. (For reviews on PS I see Golbeck, 1996, Brettel, 1997 and Manna and Chitnis, 1999)

The PS I core complex of cyanobacteria consists of 12 protein subunits, which coordinate 127 cofactors. The reaction center and most of the core antenna pigments are harbored by the same protein subunits (PsaA and PsaB). This is in contrast to type II reaction centers, which either have no core antenna, as in the case of purple bacterial reaction centers, or have antenna pigments bound to subunits distinct from the subunits that coordinate the reaction center cofactors, as is the case in Photosystem II (PS II). The close structural connection between the antenna system and the reaction center in PS I results

in a very sophisticated and efficient light-capturing system. When one photon is absorbed by PS I at room temperature, the probability that a charge separation occurs is greater than 98%. After light absorption, the electron is transferred along a chain of electron carriers consisting of six Chls, two phylloquinones and three [4Fe-4S] clusters.

In cyanobacterial membranes, the PS I complex is present both as a monomer and as a trimer with a molecular weight of more than 10<sup>6</sup>. Under low light conditions, the cyanobacterial PS I can interact with phycobilisomes, which are extrinsic membrane light-harvesting complexes, in order to increase the absorption cross-section of the light-capturing system (Mullineaux, 1994). It was reported recently that under iron deficiency a ring of 18 subunits of the membrane-bound IsiA protein surrounds the trimeric PS I complex and transfers energy to the core antenna system of PS I (Bibby et al., 2001; Boekema et al., 2001).

In plants and green algae, light harvesting complex I (LHC I), an integral membrane protein, is closely associated with Photosystem I to increase the antenna size (Knoetzel et al., 1992; Jansson et al., 1996; Haldrup et al., 2000, Jensen et al., 2000,). As far as is known, the PS I holocomplex, which consists of the core complex and the LHC I, exists in the membrane only as a monomer.

Information concerning the structure of PS I is available from a variety of biochemical and biophysical investigations, as well as from a recent X-ray structure of cyanobacterial PS I at 2.5 Å resolution (Jordan et al., 2001). The organization of the antenna system of PS I is discussed in this chapter with respect to the structure and function of the complex as a whole.

---

*Abbreviations:* A – accessory Chl; A<sub>1</sub> – spectroscopically identified secondary electron acceptor in PS I, a phylloquinone; A<sub>0</sub> – spectroscopically identified primary electron acceptor in PS I, a Chl *a* monomer; Chl(s) – chlorophyll(s); ETC – electron transfer chain; F<sub>X</sub>, F<sub>A</sub>, and F<sub>B</sub> – [4Fe-4S] iron-sulfur clusters; P700 – primary electron donor in PS I; pbRC – purple bacterial reaction center; PS I – Photosystem I; RC – reaction center

## II. The Architecture of Cyanobacterial Photosystem I

### A. The Protein Subunits

Photosystem I is highly conserved among plants, green algae and cyanobacteria. In all these organisms, the complex contains two large subunits (PsaA and PsaB) and at least eight smaller subunits (PsaC, PsaD, PsaE, PsaF, PsaI, PsaJ, PsaK and PsaL). The arrangement of these subunits in the cyanobacterial complex is shown in Fig. 1 and Color Plate 6. The large PsaA and PsaB subunits coordinate most of the components of the electron transfer chain (ETC). These cofactors include the primary donor (P700), the monomeric accessory Chls (A), the primary electron acceptor ( $A_0$ ), an additional Chl *a* monomer, the two phylloquinones ( $A_1$ ), and  $F_X$ , a [4Fe-4S] iron-sulfur cluster. In addition, 79 antenna Chl *a* molecules and most of the carotenoids of the core antenna system are bound to the PsaA and PsaB subunits. Subunit PsaC carries the two terminal FeS clusters ( $F_A$  and  $F_B$ ). Subunits PsaC, PsaD and PsaE are located on the stromal side of the membrane. The N-terminal domain of subunit PsaF is exposed to the luminal side of the membrane. In plants, this subunit is involved in docking of plastocyanin. Subunits PsaI, PsaJ, PsaK and PsaL are small, integral membrane proteins that are located around the periphery of PsaA and PsaB.

In addition to the ten, highly conserved subunits listed above, PS I from cyanobacteria contains two more small, integral membrane proteins that have not so far been found in plants (PsaM, and the recently discovered PsaX). These subunits are located peripherally to PsaA and PsaB, as shown in Fig. 1.

Photosystem I of green algae and higher plants also contains the PsaG, PsaH, PsaN and PsaO subunits in addition to the ten conserved subunits. The complex from these organisms also contains the LHC-I antenna pigment-protein complex, which includes four different polypeptides (Lhca1-4). The structures and functions of PsaG, PsaH, PsaN, PsaO and LHC I will be discussed below in Section IV.

#### 1. Oligomeric Structure of PS I and Interaction with External Antenna Complexes

Early evidence for a trimeric organization of PS I in cyanobacteria came from electron microscopy (Boekema et al., 1987). It is now well established

that PS I trimers exist in the cyanobacterial membrane in vivo (Hladik and Sofrova, 1991). The ratio between monomers and trimers is probably regulated by the salt concentration (Kruip et al., 1994) and light intensity. However, the physiological function of the trimerization is still under discussion. It has been proposed that the main purpose of the trimer is to increase the antenna size for optimal light-capturing under low light intensity (Karapetyan et al., 1999). Experimental evidence that the trimerization is essential for growth of cyanobacteria at limiting light intensities came from experiments on light adaptation of the thermophilic cyanobacterium *Synechococcus elongatus*. In this organism, the ratio of monomeric to trimeric PS I changes in vivo as a function of the light intensity (Fromme, 1998). At low light intensity, mutants lacking the PsaL subunits, which are essential for trimer formation, grow at one-tenth the rate of wild-type cells (Fromme, 1998).

Under iron deficiency, a ring of IsiA subunits surrounds the trimeric PS I, and could provide a further increase of the antenna size (Bibby et al., 2001; Boekema et al., 2001b). IsiA is related to CP43, and more distantly to CP47, the subunits of PS II coordinating the core antenna Chl *a* molecules (Chapter 4, Green). There has been considerable debate about whether IsiA functions as an antenna or just as a photoprotective device, but most investigations have focused on its relationship to PS II.

#### 2. The Two Large Subunits (PsaA and PsaB)

The major protein subunits of PS I, PsaA and PsaB, show large homology to each other and are suggested to have evolved via gene duplication. Eleven transmembrane helices were predicted from hydrophobicity plots (Fish et al., 1985) in agreement with the data derived from the recent X-ray structure analysis (Jordan et al., 2001). There is a conserved sequence containing two cysteines in the loop between transmembrane helices h and i (formerly called helices VII and IX). This site coordinates the [4Fe4S] cluster  $F_X$ . The C-terminal five transmembrane helices (g, h, i, j and k) surround the electron transfer chain (Fig. 1A). Their organization shows similarities to the arrangement of the L and M subunits in purple bacterial RCs and D1/D2 in PS II (Deisenhofer et al., 1995; Zouni et al., 2001), supporting the idea that all photo-reaction centers derive from a common ancestor (Nitschke and Rutherford, 1991; Blankenship, 1992; Schubert et al., 1998).

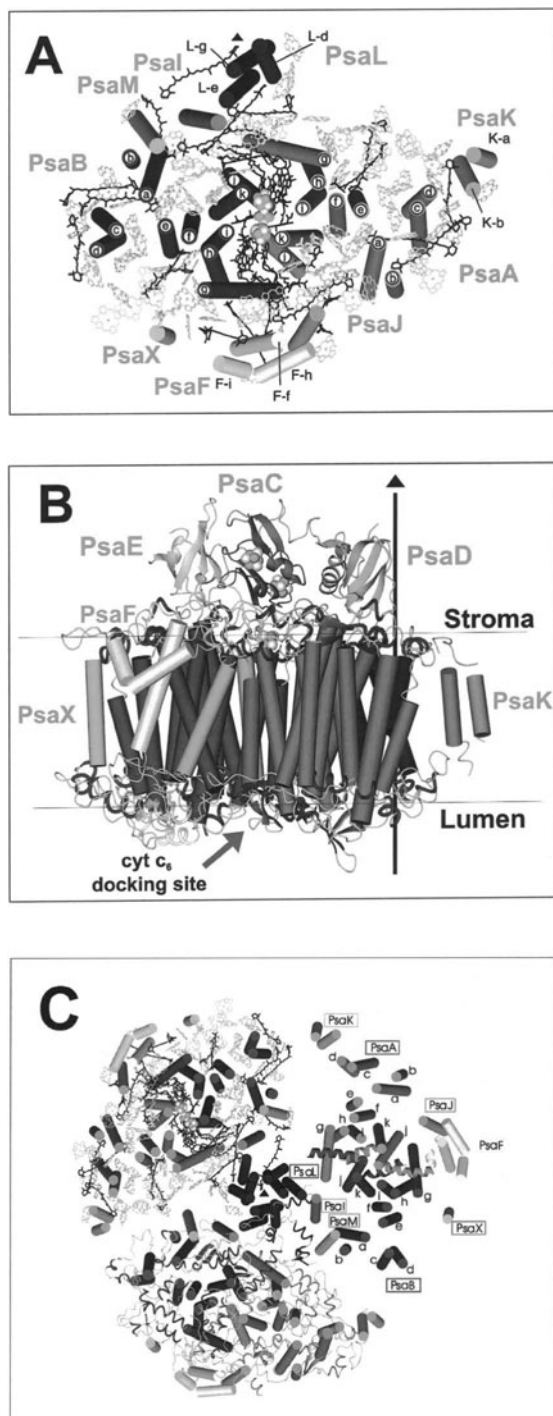


Fig. 1. (A) and (B): Arrangement of protein subunits and cofactors in one monomeric unit of Photosystem I. Transmembrane helices are shown as cylinders. Chlorophylls are represented by their head-groups, with the ring substituents omitted for clarity. The carotenoids and lipids also are shown. The Fe/S atoms of the [4Fe-4S] clusters are represented by small spheres. (A) View from the stromal side onto the membrane plane, showing only the transmembrane part of Photosystem I; (B) view along the membrane plane, with the organic cofactors omitted for clarity. The arrow indicates the threefold symmetry axis of the trimeric structure (C) Organization of the PS I trimer. View from the stromal side onto the membrane plane, with the stromal subunits omitted for clarity. Different structural elements are shown in

In spite of this common origin, the function of the C-terminal domain has been modified in PS I. Whereas the D1 and D2 proteins in PS II bind only two Chls of the antenna system (Zouni et al., 2001), the C-terminal region of PsaA and PsaB coordinates 27 antenna Chls in addition to the reaction center Chls. The whole central antenna domain of the core antenna system is a unique feature of PS I.

The arrangement of the six N-terminal transmembrane helices can be regarded as a trimer of three pairs of helices: a/b, c/d and e/f. In Color Plate 6, the  $\alpha$  helices are shown as cylinders, with the blue and red helices belonging to subunits PsaA and PsaB, respectively. These two subunits are related to each other by a local twofold symmetry axis extending from P700 to F<sub>X</sub>.

Closely attached to subunits PsaA and PsaB, four lipids have been identified, three molecules of phosphatidylglycerol (PG) and one monogalactosyl-diacylglyceride (MDGD) (Jordan et al., 2001). Lipids were detected previously by biochemical techniques in PS I core complexes consisting exclusively of PsaA and PsaB (Makewicz et al., 1996). The 2.5-Å structure shows that four lipids are indeed an essential part of PS I. Instead of being located close to the detergent-exposed side of PS I, they are located in the core of PsaA and PsaB at positions related by the pseudo C<sub>2</sub> symmetry (Fig. 1A) and Color Plate 6A.

### 3. The Stromal Subunits (PsaC, PsaD and PsaE)

Three subunits (PsaC, PsaD and PsaE) are located on the stromal side of PS I, providing the docking site for ferredoxin (Fig. 1B). Subunit PsaC (8.9 kDa) carries the two terminal iron-sulfur clusters (F<sub>A</sub> and F<sub>B</sub>). The clusters can be distinguished spectroscopically by their low-temperature EPR spectra (for review see Golbeck, 1999). The important role of subunit PsaC in coordination of the two terminal FeS clusters was previously suggested based on a conserved sequence motif CXXCXXCXXXCP, which occurs twice in the *psaC* gene (Mühlenhoff et al., 1993). A homology of PsaC to bacterial ferredoxins containing two [4Fe4S] clusters was



suggested from strong sequence similarity. The structure of PsaC exhibits a pseudo twofold symmetry similar to that of bacterial ferredoxins (Adman et al., 1973). However, PsaC differs from these ferredoxins in ways that could be significant for its function in the PS I complex. The N-terminus is extended by two amino acids, and the C-terminus by 14. This region of the PsaC subunit forms the contact site to subunits PsaA and PsaB. In addition, the loop connecting the two  $\alpha$ -helices has an insertion of ten amino acids. This loop is exposed to the putative ferredoxin/ flavodoxin docking site, suggesting a role in the interaction with these mobile electron-carrier proteins.

The arrangement of FeS clusters  $F_A$  and  $F_B$  in PS I was a matter of debate for many years (for reviews see Golbeck, 1993, 1996). However, spectroscopic results give strong evidence that  $F_B$  is the terminal cluster (Diaz-Quintana et al., 1998; Fischer et al., 1999; Golbeck, 1999). The recent, high resolution X-ray structure shows unambiguously that the FeS cluster  $F_B$  is indeed the distal cluster that performs the final electron transfer step to ferredoxin/ flavodoxin, whereas  $F_A$  is located in the vicinity of  $F_X$ . The center-to-center distance from  $F_X$  to  $F_A$  is only 14.9 Å, while that to  $F_B$  is 22 Å. The two clusters  $F_A$  and  $F_B$  are separated by a center-to-center distance of 12 Å, which is remarkably similar to the distance that Adman et al. (1973) found between the clusters in the bacterial ferredoxin. A sequential electron transport from  $F_X$  to  $F_A$  to  $F_B$  is therefore most likely. The similar structures strongly indicate a common evolutionary origin of bacterial ferredoxin and PsaC.

The structure of subunit PsaE (8 kDa) was first determined in solution by  $^1\text{H}$  and  $^{15}\text{N}$  NMR (Falzone et al., 1994). The structures of PsaE in solution and in the Photosystem I complex are nearly identical with respect to its compact core of five antiparallel stranded  $\beta$ -sheets. However, the CD loop that connects  $\beta$ -strands  $\beta_C$  and  $\beta_D$  is flexible in solution, but twisted in PsaE bound to PS I, where it interacts with subunits PsaA and PsaB. The position of PsaE in the complex, in close vicinity to the putative ferredoxin docking site, confirms previous biochemical data showing that PsaE is involved in the anchorage of ferredoxin (Rousseau et al., 1993; Sonoike et al., 1993; Strotmann and Weber, 1993). The N-terminus of PsaE is

surface-exposed, which is an interesting finding because in barley PsaE can be crosslinked with ferredoxin-NADP reductase (FNR) via its N-terminal extension (Andersen et al., 1992a).

The largest of the three stromal subunits, PsaD, forms the part of the stromal hump that is close to the trimerization domain, in agreement with previous suggestions based on electron microscopy of PS I complexes from mutants lacking this subunit (Kruip et al., 1997). This arrangement also is in agreement with crosslinking experiments, which showed that PsaD can be crosslinked to subunit PsaL in cyanobacteria as well as in plants (Xu et al., 1994a; Jansson et al., 1996). The main structural motifs of PsaD are one four-stranded and one two-stranded antiparallel  $\beta$ -sheet. The N and C termini are both exposed to the stromal surface, in agreement with studies of protease accessibility and biotin labeling (Xu et al., 1994b). In addition, investigations on mutant PS I lacking the 24 residues from the carboxyl terminus of PS I have shown that this surface-exposed domain of PsaD is not essential for the assembly of PsaD into the PS I complex (for review see Manna and Chitnis, 1999). The most striking structural feature of PsaD is the C-terminal 'clamp' formed by the sequence region D94 to D122, which wraps around PsaC. This feature explains previous results that showed that PsaD is needed for correct orientation of PsaC (Li et al., 1991; Golbeck, 1992). Furthermore, the structure suggests that PsaD is directly involved in electron transfer to ferredoxin, in agreement with a large amount of previous biochemical data (Zanetti and Merati, 1987; Zilber and Malkin, 1992; Lelong et al., 1994; Sétif et al., 1995; Lelong et al., 1996).

#### 4. The Small, Integral-Membrane Subunits

The PS I complex of cyanobacteria consists of 12 different protein subunits, of which PsaA and PsaB and seven small subunits, PsaF, PsaI, PsaJ, PsaK, PsaL, PsaM and PsaX, are embedded in the membrane. The seven small subunits surround the large subunits PsaA and PsaB (Fig. 1).

PsaL (16.6 kDa), PsaI (4.3 kDa) and PsaM (3.4 kDa) are located 'inside' the trimer at the monomer-monomer interfaces. (See Fig. 1 and Color Plate 6.) PsaL forms most of the contact sites within the

---

(Fig. 1. continued) each of the three monomers. In the top right monomer, the transmembrane helices are shown as cylinders and the subunits are labeled. The top left monomer shows the complete set of cofactors along with the transmembrane helices. In the lower monomer, the  $\alpha$ -helices of the stromal and luminal loop regions are shown as ribbons. (1JB0.pdb file, Jordan et al., 2001). See Color Plate 6.

trimerization domain. This subunit contains three transmembrane helices and several surface helices and short  $\beta$ -sheets, of which transmembrane helix L-g and  $\alpha$ -helices L-c and L-h, located at the stromal and luminal sides respectively, form most of the contact sites. It had been suggested earlier that subunits PsaL are located in the trimerization domain, because PsaL deletion mutants of cyanobacteria contain only PS I monomers (Chitnis and Chitnis, 1993; Chitnis et al., 1993). In addition to its structural function, PsaL coordinates three Chls that functionally link the antenna systems within the trimer.

PsaI and PsaM each contains only one transmembrane helix. PsaI is located close to PsaL, in agreement with previous studies (Xu et al., 1995; Jansson et al., 1996). The main functions of these small subunits probably are stabilization of the antenna system and the quaternary structure of PS I as a whole. As mentioned above, subunit PsaM has been identified so far only in cyanobacteria, although an open reading frame for it is found in the liverwort chloroplast genome (Ohya et al., 1986).

PsaF, PsaJ and PsaX are located on the side of the monomeric complex that is distal to the trimerization domain (Fig. 1 and Color Plate 5). In the 1980s, PsaF (15 kDa) was expected to be an extrinsic subunit located on the luminal side of PS I. This suggestion was based mainly on the fact that subunit PsaF contains two pre-sequences, one for import into the chloroplast and a second for import into the thylakoid lumen. Recently, it was shown that PsaF is imported via the SEC pathway, which also is used for import of the luminal electron carrier plastocyanin (Karnauchoff et al., 1994). Hippler et al. (1999) were able to cross-link plant subunit PsaF to plastocyanin, indicating a possible role of PsaF in docking of this soluble electron donor. However, evidence for at least a partial intrinsic location of PsaF in the membrane came from the finding that PsaF could not be removed with chaotropic agents such as urea or NaBr (Chitnis et al., 1995), but could be extracted by detergents such as Triton X-100 (Bengis and Nelson, 1977). Interaction of PsaF with the stromal subunit PsaE was indicated by crosslinking experiments (Armbrust et al., 1996).

The 2.5 Å structure shows that the N-terminus of PsaF is located in the lumen (Fig. 1). This part of the protein contains several 3/10 and  $\alpha$  helices. The N-terminal region of plant PsaF shows an insertion at the C-terminal end of helix F-c that could allow this part of PsaF to come close to the putative plastocyanin

binding site in plants. This arrangement is in good agreement with previous biochemical experiments. Deletion of PsaF in the green algae *Chlamydomonas reinhardtii* leads to a dramatically reduced electron transfer from plastocyanin to P700<sup>+</sup> (Farah et al., 1995; Drepper et al., 1996; Hippler et al., 1997). By contrast, PsaF is not involved in docking of either plastocyanin or cytochrome  $c_6$  in cyanobacteria (Xu et al., 1994d), and deletion of PsaF in cyanobacteria has no effect on the reduction kinetics of these electron carriers (Xu et al., 1994c). In the cyanobacterial structure, the sequence region F87 to F112 forms one transmembrane helix followed by a short loop. An unusual structural feature of PsaF is the finding of two short helices that penetrate but do not cross the membrane (F-h and F-i). These helices form a V-like arrangement that penetrates about 1/3 of the way across the membrane (Fig. 1B). The C-terminus is located on the stromal side of the membrane in close vicinity to PsaE, in agreement with crosslinking studies (Armbrust et al., 1996). Although several Chls and carotenoids are located in close vicinity to PsaF, the subunit does not provide a fifth ligand to a Mg of a Chl. Subunit PsaF is located close to the small subunit PsaJ, in agreement with deletion mutant and crosslinking experiments on the cyanobacterium *Synechocystis* (Xu et al., 1994d) and on plant (barley) PS I (Jansson et al., 1996). PsaJ contains one transmembrane helix and coordinates three Chl molecules.

One function of PsaF and PsaJ probably is stabilization of the core antenna system. This structural region also could be the interaction site for the external antenna complexes. The unusual V-shaped helix arrangement of PsaF could be a recognition site for docking of phycobilisomes. Evidence for this speculation came from the finding that a mutant of *S. elongatus*, lacking PsaF, showed no phenotype at normal light intensity but was unable to grow at low light intensities (Fromme and Jordan, unpublished). The mutant cells died after 10 days, expressing so much allophycocyanine that the culture had a turquoise color.

A possible function of PsaJ was revealed by the recent finding that cells under iron deficiency form a giant ring of 18 subunits of the IsiA protein surrounding the PS I trimer (Bibby et al., 2001; Boekema et al., 2001b). Under iron deficiency the phycobilisomes are completely degraded, suggesting that the IsiA ring functions as an external antenna system for PS I. Modeling of the 2.5 Å structure in a

low-resolution electron density map indicated a direct interaction of some of the Chls of PsaJ with this antenna ring (Boekema et al., 2001b).

A new, twelfth subunit, PsaX, has been identified in the cyanobacterial structure. This protein was seen previously in PSI preparations from other thermophilic cyanobacteria, but the gene sequence has not been identified so far. PsaX is located at the detergent-exposed surface in close vicinity to PsaB. It contains one transmembrane helix and coordinates one Chl.

Interaction with external antenna systems is also a possible role for PsaK, the small subunit located at the 'edge' of the complex close to PsaA. This subunit contains two transmembrane helices and binds two antenna Chls, which under iron deficiency might also interact with Chls of the IsiA ring. In this respect, it is interesting that PsaK has been isolated with the LHC 1 complex in higher plants and has been shown to cross-link to Lhca3 (Jansson et al., 1996; Jensen et al., 2000).

### B. The Electron Transport Chain

The electron transport chain in PS I consists of six Chls, two phyloquinones and three 4Fe4S clusters. As Fig. 2 shows, the organic cofactors are arranged in two branches, A and B. The A-branch consists of Chls eC-A1, eC-B2, eC-A3 and the phyloquinone  $Q_K$ -A; the B-branch consists of eC-B1, eC-A2, eC-B3 and  $Q_K$ -B. The cofactors in the A and B branches are coordinated by subunits PsaA and PsaB, respectively, with the exception of the second pair of Chls. The 'accessory' Chl belonging to the A-branch (eC-B2) is coordinated by PsaB, while that belonging to the B-branch (eC-A2) is coordinated by PsaA.

The first Chl pair (eC-A1 and eC-B1) is located close to the luminal side of the reaction center and is assigned to P700. In contrast to the purple bacterial RC, where the special pair is a homodimer of two BChl molecules, P700 is a heterodimer: eC-B1 is a Chl *a* molecule, whereas eC-A1 is the C-13 epimer of Chl *a* (Chl *a'*). In addition, the H-bonding is very asymmetric. The Chl *a'* in the A-branch forms three hydrogen bonds to the protein, while eC-B1 has no hydrogen bonds. This asymmetry could explain why the spin in  $P700^{+}$  is located mainly on the eC-B1 molecule (Käb et al., 2001). When P700 is excited to its lowest excited singlet state ( $P700^*$ ), it transfers an electron in about 1 ps to an electron acceptor ( $A_0$ ) that has been identified spectroscopically as a molecule of Chl *a*.  $P700^*$  is a very strong reductant,

with a midpoint redox potential of about  $-1.3$  V.  $\Delta G^\circ$  for the initial charge-separation step ( $P700 A_0 \rightarrow P700^{+} A_0^{-}$ ) is estimated to be about 250 meV. (See Brettel, 1997 for a review on the kinetics and energetics of electron transfer in PS I.)

The Chls of the third pair (eC-A3 and eC-B3 in Fig. 2) are located close to the middle of the membrane, at positions similar to the positions of the bacterio-phytyls in the reaction center of purple bacteria. One (or both) of these Chls most probably represent the spectroscopically identified electron acceptor  $A_0$ . The two Chls form hydrogen bonds to the hydroxyl groups of tyrosines A696 and B676. The axial ligands of Chls eC-A3 and eC-B3 are provided by methionine residues MetA688 and MetB668, which are located to give Mg-S distances of 2.6 Å. This is remarkable, because the interactions between the hard acid  $Mg^{2+}$  and methionine sulfur as a soft base are expected to be weak. Mutational studies suggest that these methionines are critical for the function of the electron-transfer chain (Fairclough et al., 2001; Ramesh et al., 2001). The functional implications of the lack of a strong fifth ligand to the  $Mg^{2+}$  atom of these Chls remain to be clarified.

The Chls of the second pair (eC-B2 and eC-A2 in Fig. 2) are located approximately midway between the first and third pairs, at center-to-center distances of 11.7 and 11.9 Å from eC-A1 and eC-B1, respectively. The edge-to-edge distances to the Chls of P700 are only 3.1 and 3.3 Å. The structure thus

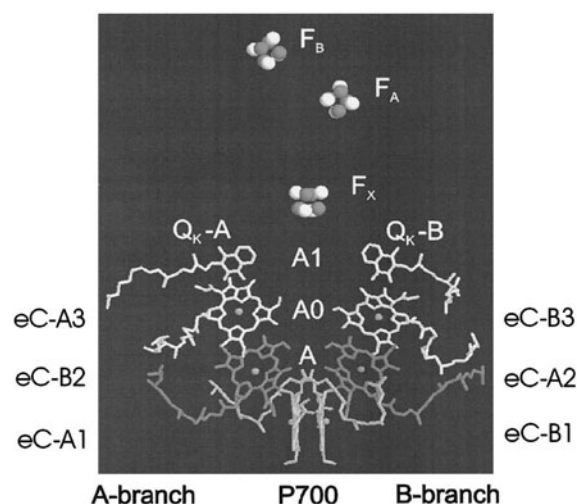


Fig. 2. The cofactors of the electron transport chain. The labeling of the individual Chls corresponds to the protein subunit that provides the ligand to the central Mg atom.

suggests that eC-A2 and/or eC-B2 represent a transient electron acceptor (A) that mediates electron transfer from P700 to  $A_0$ . Their central  $Mg^{2+}$  ions are axially coordinated by water molecules that are hydrogen-bonded to asparagine residues AsnA604 (eC-A2) and AsnB591 (eC-B2). The coordination of  $Mg^{2+}$  by water differs from the coordination of the 'accessory Chls' in bacterial reaction centers, where a histidine provides the fifth ligand for each  $Mg^{2+}$ . Neither eC-B2 nor eC-A2 forms any hydrogen-bonds to the protein. Their chlorin rings are roughly parallel to those of the next Chls of the electron transport chain, eC-A3 and eC-B3.

The edge-to-edge distance between the Chls of the second and third pairs is only 3.3 Å in both cofactor branches, and therefore is in the same range as the distance between P700 and the second pair of Chls. Due to the close proximity of the second and third pair of Chls the spectroscopic features of the electron acceptor  $A_0$  could be influenced by interactions between the eC-B2/eC-A3 and eC-A2/eC-B3 Chl pairs. This idea is supported by the finding that the difference spectrum  $A_0/A_0^-$  indicates the presence of a nearby Chl (Hastings et al., 1995a,b).

The next electron-transfer step is the transfer of the electron from  $A_0$  to phyloquinone, which occurs with a time constant of 20 to 50 ps (Hecks et al., 1994; Brettel and Vos, 1999). The free energy gap for this step is estimated to be about equal to the reorganization energy  $\lambda$  (i.e.  $\Delta G^0 = -\lambda$ ), which is the optimal condition for rapid electron transfer (Marcus and Sutin, 1985; Iwaki et al., 1996). The structure of PS I at 2.5 Å resolution shows two phyloquinones at a center-to-center distance of 8.6 Å from  $A_0$ . This is in agreement with photovoltage measurements, which indicate that the component of the distance between  $A_0$  and  $A_1$  normal to the membrane is about 20% of the corresponding distance between P700 and  $A_1$  (Kumazaki et al., 1994). The distance between P700<sup>++</sup> and  $A_1^-$  was determined by pulsed EPR measurements to be  $25.4 \pm 0.3$  Å (Bittl et al., 1997; Dzuba et al., 1997), which would fit to the 26 Å center-to-center distances of the cofactor pairs  $Q_K-B/eC-A1$  and  $Q_K-A/eC-B1$ .

The binding sites in PS I for phyloquinones  $Q_K-A$  and  $Q_K-B$  are very similar. The quinone planes are  $\pi$ -stacked 3.0 to 3.5 Å from the indole rings of the conserved tryptophans TrpA697 and TrpB677, which are located on stromal-surface  $\alpha$ -helices between

transmembrane helices j and k. Both phyloquinones have a hydrogen bond from the carbonyl-oxygen ortho to the phytyl chain to the amide NH group of a Leu residue (LeuA722 for  $Q_K-A$  and LeuB706 for  $Q_K-B$ ). In contrast to all other tight quinone-binding sites identified in proteins so far (Ermler et al., 1994; Deisenhofer et al., 1995; Iwata et al., 1995; Xia et al., 1997; Abramson et al., 2000), the second carbonyl-group is not hydrogen bonded. Perhaps the asymmetric hydrogen bonding contributes to the low midpoint reduction potential ( $\sim -800$  mV) of the phyloquinone in PS I as compared to the structurally similar menaquinone in reaction centers of *Rhodospseudomonas viridis* ( $\sim -150$  mV).

From the phyloquinone, the electron is transferred to a series of three bound iron-sulfur clusters:  $A1 \rightarrow F_X \rightarrow F_A \rightarrow F_B$ . The iron sulfur clusters put PS I in the group of ferredoxin-reducing or type I reaction centers. Electron transfer from  $A_1^-$  to the first FeS cluster  $F_X$  shows biphasic kinetics with time constants of about 20 and 250 ns, which has been taken as evidence for two active branches (Guergova-Kuras et al., 2001; for a review see Brettel and Leibl, 2001). This reoxidation of  $A_1^-$  is probably the rate-limiting step of the electron transfer from P700\* to the terminal iron-sulfur cluster  $F_B$ . The sulfur ligands to the [4Fe4S] cluster of  $F_X$  are provided by cysteines A578 and A587 from PsaA and B565 and B574 from PsaB. This binding motif is located between transmembrane helices h and i (Jordan et al., 2001). It seems significant that  $F_X$  forms no hydrogen bonds with the protein. The lack of hydrogen bonding to the metal cluster could contribute to the strongly negative reduction potential (around  $-600$  mV) of this FeS cluster. Other factors such as a low polarity of the protein environment and low solvent accessibility also could be important in this regard.

$F_X$  plays a prominent structural role in addition to its essential role in electron transfer. The twofold symmetry axis that relates the two large subunits PsaA and PsaB to each other runs exactly through the center of  $F_X$ . Recently it was shown that special enzymes are involved in the assembly of  $F_X$ , and that this assembly is a prerequisite for the binding of PsaC, PsaD and PsaE to the integral membrane part of PS I (Shen et al., 2002, 2002a, see also Schwabe and Kruip, 2000 for a review on PS I assembly).

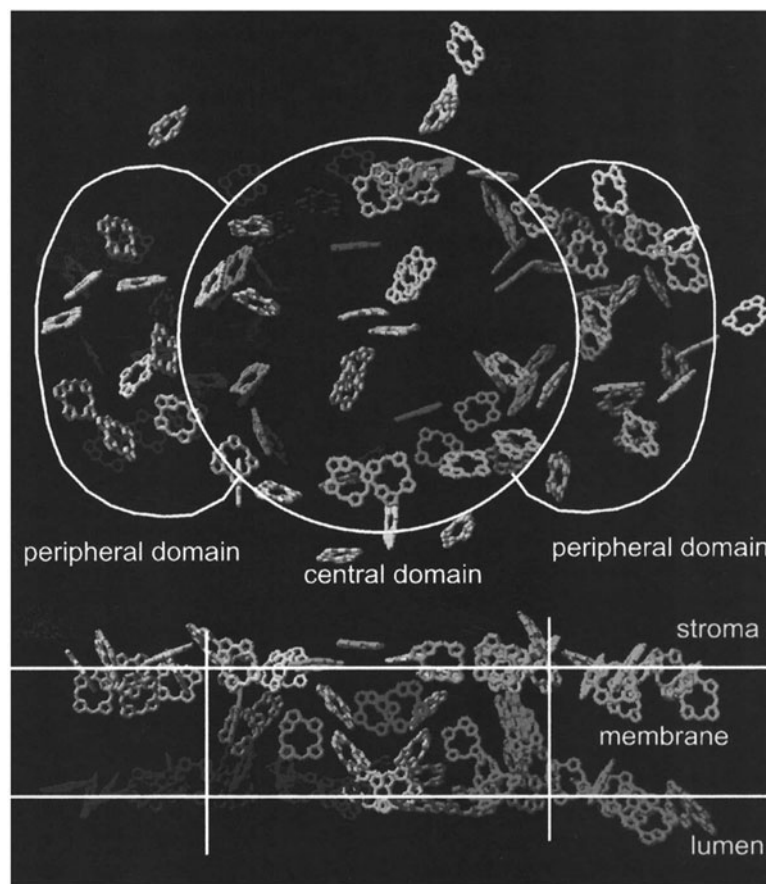


Fig. 3. The arrangement of the Chls in one monomer of Photosystem I. Only the ring planes of the Chls are shown for clarity. Top: view from the stromal side onto the membrane plane. Bottom: view along the membrane plane. See Color Plate 7.

### III. Structural Organization of the Core Antenna System

#### A. Arrangement of the Chlorophylls

The most interesting and complex feature of PS I is the integral antenna system consisting of 90 Chl *a* molecules and 22 carotenoids. The antenna pigments surround the central reaction center structure formed by the C-terminal five transmembrane helices (g-k) of subunits PsaA and PsaB (Figs. 1A and 3 and Color Plates 6 and 7).

The X-ray structure at 2.5 Å resolution (Jordan et al., 2001) shows a unique arrangement of antenna pigments in PS I that is very different from the highly symmetric bacteriochlorophyll arrangements in the light harvesting complexes of purple bacteria (Karrasch et al., 1995; McDermott et al., 1995). The

Chls are arranged outside the inner ring of helices, most of them coordinated by the large subunits PsaA/B; however, the small subunits PsaJ, PsaK, PsaL, PsaM and PsaX and a phosphatidylglycerol (PG) also axially ligate (either directly or indirectly via water molecules) 11 of the Chls. These Chls are located peripherally to the antenna Chls bound to PsaA/B. Figure 3 and Color Plate 7 show the pigment arrangement in the core antenna. The antenna system can be divided into a central part where the Chls are distributed over the whole depth of the membrane, and two peripheral parts where the Chls are ordered in two layers at the stromal and luminal sides of the membrane. However, the layer arrangement also extends to the central domain, so that within the two layers a ring-shaped pigment arrangement surrounding the reaction center is visible (Byrdin et al., 2002)

In total, 79 Chls of the antenna system are

coordinated by PsaA and PsaB. These pigments are colored green and blue in Color Plate 7. The 11 Chls bound to the small subunits are shown in yellow and the Chls of the electron transfer chain in orange. A total of 34 Chls (18 of PsaA and 16 of PsaB) are located in the stromal layer (light green/blue) and 35 Chls (17 of PsaA and 18 of PsaB) are in the luminal layer (dark green/blue). In the central domain, 10 Chls (5 of PsaA and 5 of PsaB) are located closer to the middle of the membrane, indicated by medium green/blue color.

Of the 79 antenna Chls coordinated by PsaA and PsaB, 64 are located in homologous positions in PsaA and PsaB and are related by the pseudo- $C_2$  symmetry. The remaining 15 sites that coordinate Chls are not conserved between PsaA and PsaB. Most of these 'additional' Chls are located in the luminal and stromal layers, where they seem to fill some of the gaps in the structure. Almost all the Chls are separated by  $Mg^{2+}$ - $Mg^{2+}$  distances between 7 and 16 Å, a range in which fast excitation energy transfer is possible by the Förster mechanism (Förster, 1965). Although 61 Chls in PsaA and PsaB are coordinated to imidazole side chains of His, some are coordinated to oxygen atoms of Gln, Asp or Glu side chains, to the hydroxyl groups of Tyr, to peptide carbonyl oxygen atoms or to water molecules (Jordan et al., 2001). It is interesting that only 3 of the 15 'additional' Chls that do not follow the twofold symmetry are coordinated by histidines, whereas 59 of the 64 symmetry-related Chls are coordinated by histidines. These differences in  $Mg^{2+}$ -coordination, in protein environment and in Chl-Chl distances and orientations give rise to a heterogeneously broadened absorption band in the  $Q_y$ -region (see below). Most remarkable are the so-called red Chls that absorb at wavelengths above 700 nm.

The Chls of the electron transport chain (shown in orange in Color Plate 7) and the antenna system are well separated from each other, so that none of the antenna Chls comes closer than 20 Å to P700. However, there are two Chl molecules (antenna Chls A40 and B39) that seem to connect the antenna system structurally to the electron transfer chain. These are located in the middle of the membrane about 13 Å from the two Chl molecules assigned to  $A_0$  (Fig. 4A). They are close to the Chl dimers formed by Chls B37 and B38 on the PsaB side and Chls A38 and A39 on the PsaA side, which could function as intermediate local 'traps' for excitation energy. Recent calculations of excitonic couplings

between the Chls and simulations of optical spectra suggest that a significant amount of the excitation energy proceeds to P700 via Chls A40 and B39 and the A38/39 and B37/38 dimers (Byrdin et al., 2002). These six pigments are therefore termed 'linker' Chls.

### B. The 'Red' Chlorophylls

Photosystem I contains some Chls that absorb between 700 and 740 nm, i.e. at longer wavelengths than P700. These are the so called 'long-wavelength' or 'red' Chls. The number of these pigments varies among different organisms (Shubin et al., 1992; Pålsson et al., 1998; Melkozernov et al., 2000b). PS I of *S. elongatus* contains about ten red Chls per PS I monomer, as shown by spectroscopic investigations (Pålsson et al., 1998).

Several different functional roles for the long-wavelength Chls have been proposed (Trissl, 1993; Karapetyan et al., 1999). First, many cyanobacteria live under light-limited conditions in their natural habitat. Under these conditions, it would be useful for the cells to use far red light, which is not captured by the bulk antenna Chls of the green algae. However, one must take into consideration that far red light is absorbed by water. The intensity of light in the range between 700 and 740 nm is diminished to about 10% in 1 m depth (Chapter 15, Falkowski and Chen). The disadvantage of the additional long-wavelength antenna Chls would be that they slow down trapping. Indeed, it has been demonstrated experimentally that the trapping time of different cyanobacteria is directly correlated to the number of Chls that absorb at wavelengths >700 nm (Gobets et al., 2001). We will return to this point in Section V.

Other authors have proposed that the red Chls might be located close to the reaction center to facilitate trapping by focusing the excitation energy towards P700 (van Grondelle et al., 1994). In this case, the long-wavelength Chls may decrease the rate of flow of excitation energy from the central domain back to the peripheral domains.

Another possible function for the long-wavelength Chls located at the periphery of the core complex could be to provide 'entrance points' of the excitation energy from external antenna complexes to the core antenna of PS I.

The red shift could be caused by specific pigment-pigment or pigment-protein interactions. The most prominent cofactor-cofactor interaction is the

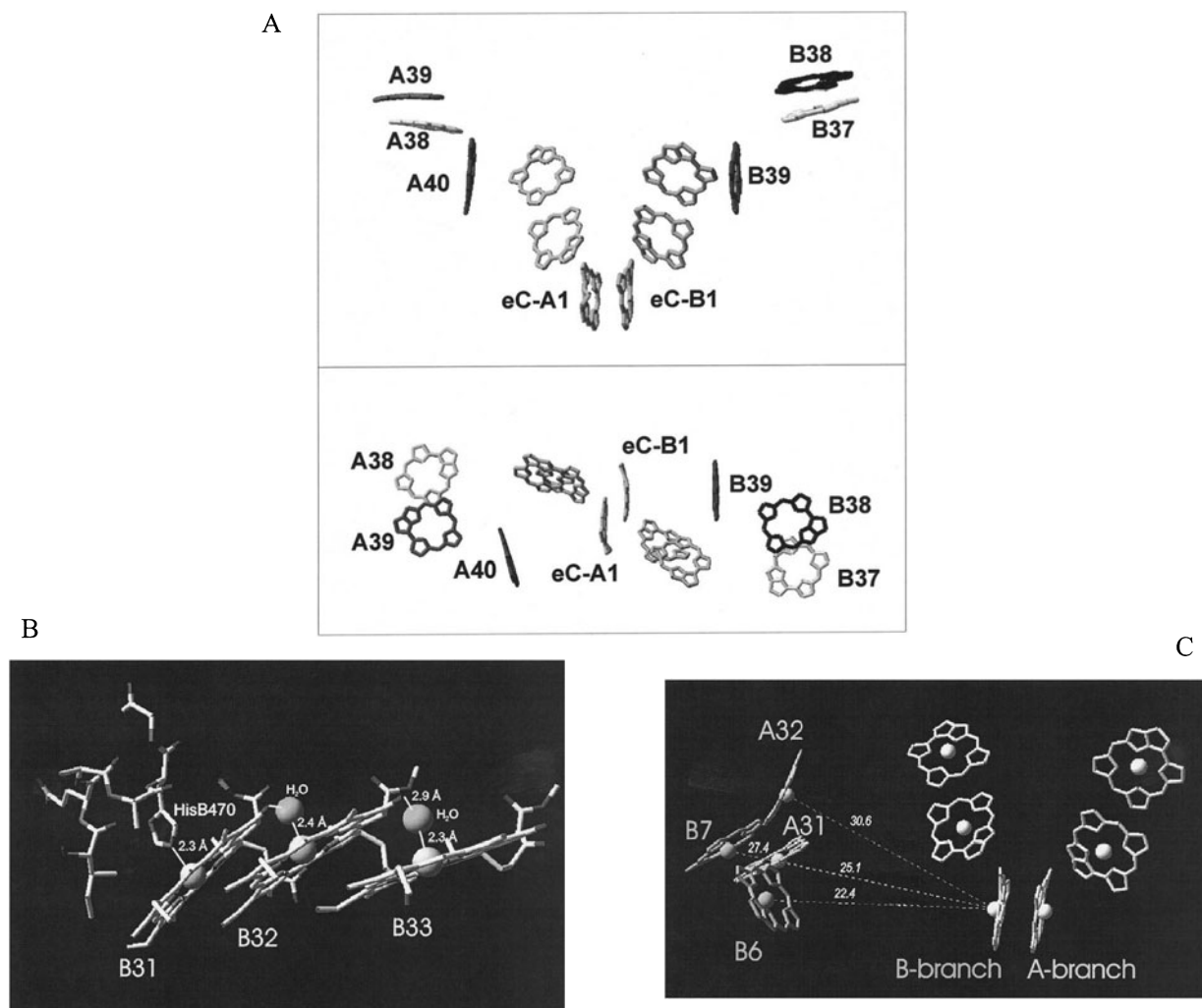


*Fig. 4.* Detailed views of strongly-coupled antenna Chls that may have a specific function in light harvesting. (A) Chls of the antenna system, which are located at close distance to the electron transfer chain. The A-branch is located on the left, the B-branch on right. Chls A40 and B39 are located close to the third pair of Chls of the electron transfer chain and are called linker Chls. The Chl pairs A38/39 and B37/38 are referred to as linker dimers in this chapter. (B) A trimer of Chls coordinated by PsaB. Only B31 is coordinated directly by a His residue of PsaB; B32 and B33 are coordinated by bridging water molecules. (C) Location of a Chl tetramer in relation to the electron-transfer chain. Chls B6 and B7 may be long-wavelength Chls that are not present in monomeric PS I.

excitonic coupling between the Chls, but interactions with adjacent carotenoids or aromatic amino acid residues also could contribute to the red shift. Protein-cofactor interactions that could influence the energetic and spectroscopic properties of the Chls include (a) differences in the dielectric constant of the local environment (Altmann et al., 1992; Sundström and van Grondelle, 1995), (b) electrostatic interactions with charged amino acid side chains (Eccles and Honig, 1983), and (c) differences in  $Mg^{2+}$ -ligation, H-bonding and deviations from planarity of the

chlorine ring induced by the protein binding site (Gudowska-Nowak et al., 1990). Because of the complexity of these interactions, the transition energies can not be derived directly from the structure. However, the excitonic coupling between the Chls can be calculated based on the 2.5 Å structure. The strongest excitonically coupled Chls are listed in Table 1 (Byrdin et al., 2002). It is very likely that the long-wavelength Chls can be found among these coupled Chls. Figure 4 shows some possible candidates for the red Chls in the 2.5 Å structure.



*Table 1.* Characteristics of the most strongly coupled dimers in PS I: center-to-center distance, excitonic interaction energy (J) calculated in the point-dipole and extended-dipole approximations, and cosine of the angle ( $\beta$ ) between the transition dipoles (see also Byrdin et al., 2002)

Chl <i>a</i> dimers	Distance between ring -centers [Å]	Excitonic coupling [cm <sup>-1</sup> ] (point dipole approx.)	Excitonic coupling [cm <sup>-1</sup> ] (extended dipole )	Cos ( $\beta$ )
eC-A1-eC-B1	5.76	414.8	138.3	-0.53
B31-B32	8.29	-247.7	-252.0	0.99
B32-B33	8.03	-241.8	-203.6	0.97
A12-A14	8.35	-230.9	-218.1	0.99
A32-B7	8.89	210.9	244.4	-0.83
B37-B38	7.51	-205.7	-172.1	-0.63
eC-A2-eC-B3	7.75	189.4	141.6	-0.33
A10-A18	9.11	-180.6	-190.4	0.86
B9-B17	8.74	-179.4	-160.9	0.89
A38-A39	7.97	-167.8	-145.7	-0.71
A33-A34	9.85	-162.4	-193.8	0.87
eC-B2-eC-A3	8.29	157.4	130.5	-0.34
A31-A32	9.92	145.8	158.5	-0.90
A36-A37	10.21	-141.0	-158.9	0.99
A26-A27	9.14	-138.4	-135.1	-0.20
B24-B25	9.04	-134.9	-129.5	-0.18
A20-A21	10.10	-131.6	-135.4	0.97
B18-B19	10.28	-124.0	-129.2	0.91
B14-B15	9.25	-122.5	-120.6	-0.17
A16-A17	9.24	-120.9	-120.6	-0.15
B27-B28	10.35	-120.9	-123.2	0.99
B35-B36	10.53	-120.1	-127.8	0.98
A16-A25	10.84	-113.3	-123.7	0.97
A29-A30	10.12	-110.8	-99.9	0.96
A7-A6	10.62	-108.8	-112.8	0.81
B29-B30	11.62	103.0	120.7	-1.00
B14-B23	11.38	-96.8	-103.8	0.99
eC-A1-eC-B2	11.90	-92.1	-104.8	0.50
eC-B1-eC-A2	12.14	-87.0	-98.8	0.55

### C. The Linker Chl Dimers

Two prominent Chl *a* dimers are formed by Chls A38/A39 coordinated to PsaA and B37/B38 coordinated to PsaB (Fig. 4a). Both are located near

the stromal side of the membrane. Their chlorin head groups are oriented parallel to the membrane and are stacked at 3.5 Å separation with small lateral shifts so that the center-to-center distances are only 8.2 Å and 7.6 Å, respectively. Their  $\pi$  electron systems

partially overlap. These Chls are coordinated by amino acids in the loops that connect transmembrane helices k and j and coordinate the phyloquinones. Significantly, helix j also provides the residues that coordinate both P700 and  $A_0$ . Furthermore, the single linker Chls A40 and B39 are coordinated by the only histidine in the transmembrane helix k. These two Chls and the A38/39 and B37/38 dimers are the only Chls coordinated by the sequence region that coordinates the cofactors of the electron-transport chain. The linker dimers are related by pseudo- $C_2$  symmetry, one dimer located close to PsaF, the other close to PsaL. Each of the two Chl *a* pairs is located within a relatively short center-to-center distance (16 Å) to one of the 'connecting' Chls, A38/A39 to A40 and B37/B38 to B39. It has been proposed that excitation energy can transfer at reasonable rates from these Chl *a* dimers to the electron-transfer chain via the two connecting Chls, suggesting that the dimers play a special role in excitation energy transfer (Jordan et al., 2001).

#### D. The Chl Trimer and Tetramer

Chlorophyll molecules B31, B32 and B33 form a trimer, which is located at the luminal side of the membrane close to PsaX (Fig. 4b). One of the Chls (B31) is coordinated to HisB470 of subunit PsaB, but the Mg atoms of the other two Chls are coordinated by water molecules. The three Chls are stacked like a staircase. The chlorin planes are almost parallel, with interplanar separations of 3.5 to 3.7 Å but laterally shifted, resulting in center-to-center distances of 8.3 Å. This geometry implies that the transition dipole moments of the chlorin rings are roughly parallel, indicating that the lowest energy exciton band carries most of the oscillator strength. The topography of this trimer shows homologies to the structures of aggregates of small organic Chl derivatives (Kratky and Dunitz, 1977). It is remarkable that the crystals of these aggregates show an absorption maximum at 740 nm. This extreme red shift was explained by strong excitonic interactions supported by  $\pi$ - $\pi$  interactions within the stacks. There is only one Chl *a* trimer in the PS I complex, possibly because a counterpart related by the pseudo- $C_2$  symmetry would interfere with the monomer-monomer contact in the trimer. Two different functions of this trimer can be proposed: The trimer could be used for capturing long-wavelength light as discussed above, or could be involved in excitation energy

transfer from the antenna ring of 18 IsiA proteins that functions as an external antenna system for PS I under iron deficiency. Modeling of the PS I trimer into the electron density map shows that Chl B33 of the trimer might be strongly attached to the antenna system of IsiA.

Four excitonically coupled Chls (A31, A32, B6 and B7) are located on the luminal side of the membrane at the interface between PS I monomers (Fig. 4c). Chlorophylls A31 and A32 have symmetry-related counterparts in B29 and B30, and are all coordinated by histidines. Chls B6 and B7 are coordinated by Asp and Glu, respectively, and have no  $C_2$ -symmetry analogue on the PsaA side of the antenna system. Taking into account the strong excitonic coupling, a large red shift is expected for the low-energy exciton band of the tetramer (Byrdin et al., 2002). The tetramer is located close to the interface between subunits PsaA, PsaB and PsaL at the trimerization domain. It also is relatively close to P700 (the center-to-center distance between B6 and eC-A1 is about 22 Å) (Fig. 4c). Therefore, the tetramer could serve as a functional 'trap' of the excitation energy close to the RC, or as the entrance point for excitation energy from the other monomers within the trimerization domain, via the three Chls coordinated by PsaL. This location of red Chls could explain the loss of two Chls absorbing at 719 nm when the PS I trimer of *S. elongatus* is split into monomers (Pålsson et al., 1998).

#### E. Carotenoids

The structure of PS I at 2.5 Å resolution shows the positions of 22 carotenoids, in good agreement with previous spectroscopic and biochemical investigations. The carotenoids are all modeled with  $\beta$ -carotene, in agreement with earlier biochemical studies showing that  $\beta$ -carotene is the most abundant carotene in PSI (Coulal et al., 1989; Makewicz et al., 1996). However, the 2.5 Å resolution is not high enough to exclude the possibility that some of the carotenoids are xanthophylls. Of the 22 carotenoids, 17 are in the all-trans conformation, whereas five have one or two cis bonds (two are modeled as 9-cis, and one each as 9,9'-cis, 9,13'-cis and 13-cis). All the carotenoids are located in the integral-membrane part of PS I, with only a few of the head groups being closer to the stromal or luminal side. Ten carotenoid molecules are bound to PsaA and PsaB by hydrophobic interactions, and some of the carotenoids

are bound to PsaF and PsaJ, thereby structurally linking these subunits to the PsaA/PsaB core. The 22 carotenoids are in van der Waals contact ( $< 3.6 \text{ \AA}$ ) to 60 Chl *a* head groups (Fig. 5).

Carotenoids fulfill several important functions in photosynthesis, including light harvesting, photoprotection by quenching Chl *a* triplet states, protection against singlet oxygen, dissipation of excess energy as heat, and structural stabilization (for reviews see Cogdell, 1985; Frank and Cogdell, 1995; Bialek-Bylka et al., 1998; Frank, 1999). It is now well established that the most important of these functions is photoprotection. The carotenoids quench excited Chl *a* triplet states, which otherwise could generate toxic singlet oxygen (Cogdell, 1985; Frank, 1999; Section V). This function is of importance in vivo since most cells are frequently overexposed to light, and cells lacking carotenoids are very sensitive to light (Roemer et al., 1995). The PS I structure shows that most of the proposed red Chls (e.g., the linker dimers A38/39 and B37/38 and the tetramer A31/A32/B6/B7) are in close vicinity to carotenoids. This is essential for photoprotection because the red Chls are most probably the location where triplet states in the antenna system are formed by intersystem crossing. About 80% of the fluorescence is emitted from these Chls at room temperature (Pålsson et al., 1998).

The 2.5 Å structure shows that carotenoids also play a structural role in PS I. The interaction between the peripheral subunits and the PsaA/B core is mediated to a large extent by van der Waals interactions between hydrophobic helices and the carotenoids. The carotenoids thus appear to provide a 'hydrophobic glue.' Car 22, which is located in the trimerization domain may have an important function in trimerization of PS I due to hydrophobic contacts with the three subunits.

#### IV. Plant Photosystem I

##### A. Polypeptides Unique to Plants

Although a high-resolution structure has not been obtained for higher plant PS I, it is very likely that the proteins that are common to plants and cyanobacteria are structurally and functionally similar, so that the cyanobacterial structure can serve as a framework to discuss the structure and function of plant PS I. However, higher plants contain eight subunits that

are not present in cyanobacteria: PsaG, PsaH, PsaN, PsaO and the LHC I proteins Lhca1-4. These proteins have a peripheral localization in PS I (Section IV.F), as one might expect if they were added to the complex relatively late in evolution.

The PsaG and PsaK protein sequences of plants are both similar to cyanobacterial PsaK (Kjærulff et al., 1993). Apparently, a gene duplication event and subsequent divergent evolution gave rise to the PsaK and PsaG proteins of plants. There are actually two *PsaK* genes in the cyanobacterial genome, but since neither of these is significantly more similar to higher plant *PsaG* than the other, it is not clear which is related more directly to the ancestor of *PsaG*. This means that it is unclear whether PsaK or PsaG occupies the position of cyanobacterial PsaK in the plant PS I complex. However, PsaK appears to be in contact with Lhca3 in plants (Jansson et al., 1996; Jensen et al., 2000), suggesting that PsaK is located in the same position as its cyanobacterial homologue (see discussion on antenna structure below).

PsaH is a 9 kD protein present on the stromal side of the complex in close contact with PsaL, PsaI (Jansson et al., 1996) and PsaD (Andersen et al., 1992b), in the region where the three monomers of the trimeric form of cyanobacterial PS I interact. It has been shown that PsaH is involved in the interaction of LHC II with PS I and perhaps provides a docking site for this antenna complex (Lunde et al., 2000). As discussed below, plants lacking PsaH are not capable of performing state transitions.

The PsaN subunit is located in the lumen (Nielsen et al., 1994) and seems to interact with PsaF in the binding of plastocyanin, a process that in plants (in contrast to cyanobacteria) is dependent on PsaF. PsaF is an essential protein in plants, but antisense plants with very low levels of PsaF have been constructed (Haldrup et al., 2000). The deficient plants have a significantly reduced capacity for plastocyanin oxidation, are severely impaired in growth and are light-stressed even at moderate light intensities. Absence of PsaN is less detrimental, but also reduces the capacity for plastocyanin oxidation (Haldrup et al., 1999).

##### B. The External Antenna System of PS I in Plants

The Lhca proteins of the plant PS I peripheral antenna system are homologous to LHC proteins found in PS II (Green et al., 1991; Green and Pichersky, 1994).

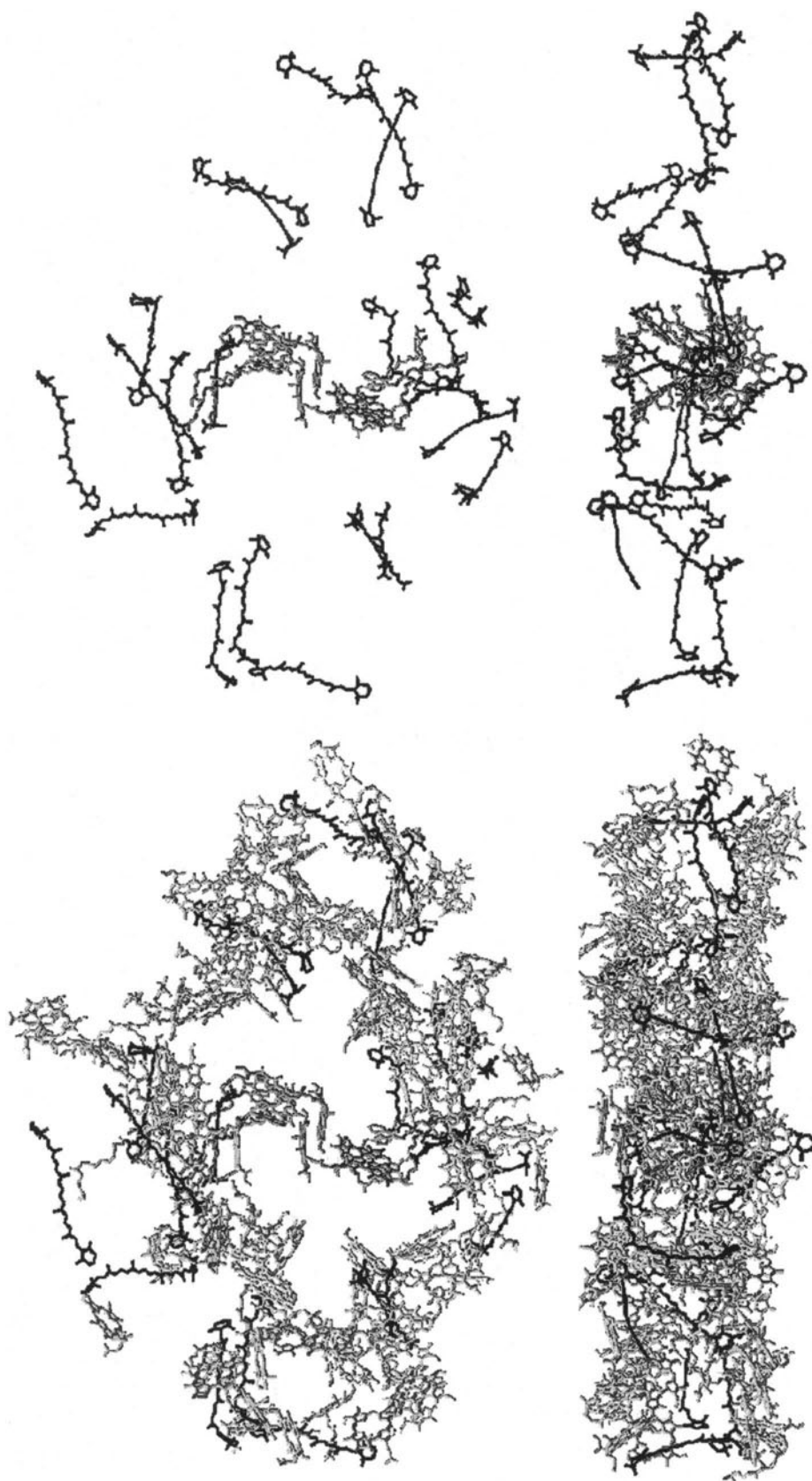


Fig. 5. The location of the carotenoids and Chls in Photosystem I: In the left part of the figure the Chls with their ring substituents and their large phytol chains are shown in gray and the carotenoids in black. This part of the figure shows the dense packing of the Chls and carotenoids. It is clear that the cofactors, which contribute 30% of the total mass of the Photosystem I, occupy a large part of the volume. On the right side of the figure, the Chls are omitted for clarity and the arrangement of the carotenoids is depicted. For the top part of the figure the view direction is from the stromal side onto the membrane plane; for the bottom part, the view is parallel to the membrane plane.

The four LHC proteins that are specific for PS I, Lhca1, Lhca2, Lhca3 and Lhca4, are named to reflect the order in which their genes were cloned and sequenced (Jansson, 1994). The Lhca polypeptides have molecular masses between 20 and 25 kDa. Lhca3 is the largest, but the relative order of the others depends on the plant species, and the apparent order can vary with the gel system. On the sequence level, the Lhca polypeptides are more similar to each other than to the Lhcb polypeptides, but the Lhca1 protein is somewhat different in this respect. Especially in the loops connecting the transmembrane helices, Lhca1 resembles Lhcb4 (CP29) more than the other LHC proteins, suggesting that Lhca1 and Lhcb4 play analogous roles in PS I and PS II, respectively. Two additional genes encoding proteins with high similarity to the Lhca proteins have been identified recently in the genome of *Arabidopsis thaliana* and named *Lhca5* and *Lhca6* (Jansson, 1999). The corresponding gene products have not yet been detected, however, and the mRNA levels seem much lower than those of Lhca1-4, so these proteins probably are not 'normal' protein components of LHC I.

The major LHC II complex is trimeric, and the proteins of the minor Lhcb proteins (CP29, CP26 and CP24) are monomeric proteins. In contrast, the Lhca proteins seem to be organized as dimers (Jansson et al., 1996). Lhca1 and Lhca4 form a stable heterodimer, while the Lhca2 and Lhca3 proteins appear to form weak homodimers. However, dimers of Lhca2 and Lhca3 have never been purified and properly characterized, so the homodimeric structure of these proteins has only been inferred from circumstantial evidence. It has also been suggested that other dimers could be formed.

In addition to the Lhca polypeptides, a fraction of LHC II is associated with PS I. The amount varies; LHC II accumulates in low light and the fraction of LHC II that is associated with PS I depends on the spectral composition of the light, as manifested by the so-called 'state transition' phenomenon (Chapter 13, Krause and Jahns; Chapter 15, Falkowski). This binding apparently can not occur in antisense plants lacking Psal, so it is very likely that LHC II binds to the PS I complex at the position of Psal (Lunde et al., 2000). PS I complexes without LHC I proteins but retaining LHC II can sometimes be prepared (Sarvari et al., 1995), showing that LHC I is not necessary for binding of LHC II to PS I.

### C. Heterogeneity of the External PS I Antenna

The antenna protein composition of PS I is variable. The amount of Lhca polypeptides generally decreases at higher light intensities, although the pattern for the individual polypeptides is not clear (Bailey et al., 2001). PS I complexes in different thylakoid regions differ in the amount of Lhca polypeptides (Jansson et al., 1997) and even the spectral composition of the growth light influences the Lhca polypeptide composition (S. Benson, personal communication). Finally, as mentioned above, the amount of LHC II bound to the PS I complex varies with both light quantity and quality. Although it is difficult to measure the amount of LHC II bound to PS I directly, it has been estimated that several (at least three) LHC II trimers sometimes associate with PS I (Jansson et al., 1997). Taken together, these data indicate that the peripheral antenna of PS I is flexible. Several regulatory mechanisms evidently determine the polypeptide composition of the peripheral antenna of PS I in a manner that is not yet understood.

### D. Pigment Composition of LHC I

Surprisingly little is known about the pigment composition of LHC I. It is clear, however, that the protein binds the carotenoids lutein,  $\beta$ -carotene and violaxanthin in addition to Chls *a* and *b* (Jansson, 1994). Violaxanthin can be photoconverted to antheraxanthin and zeaxanthin in the xanthophyll cycle. These conversions have an important role in the peripheral antenna of Photosystem II, but occur also in Photosystem I (Thayer and Björkman, 1992).  $\beta$ -carotene is not found in LHC II, which instead binds neoxanthin.

Attempts to measure the pigment stoichiometry of LHC I have not been very conclusive. The PS I/LHC I complex (often called PS I-200) has been suggested to have Chl *a/b* ratios of 6.1 (Knötzel et al., 1992), 7.2 (Pålsson et al., 1995), and 7.7 (Lee and Thornber, 1997). If the pigment composition of the PS I core (96 Chl *a*) is subtracted from that of PS I-200, 110 Chls should be bound to the LHC I proteins; however, some workers have estimated the Chl content of LHC I to be lower than this. Lee and Thornber (1995), for example, suggested 80 Chls. Keeping in mind that the antenna polypeptide composition is variable (see above), the lack of consensus on the pigments is not surprising. The biochemical procedures for preparing LHC I complexes are harsher

than those employed for the LHC II proteins, and are most certainly prone to result in pigment losses. In any case, the Chl *a/b* ratio of LHC I seems to be similar to that of the monomeric (minor) LHC proteins of PS II (that is 2.5–3.0) and is very different from that of trimeric LHC II, which binds almost as many Chl *b* as Chl *a*. The carotenoid content of LHC I is perhaps even less certain, but Lee and Thornber's (1995) estimate of 6–7 violaxanthins, 10 luteins, and 12  $\beta$ -carotenes is typical.

Recent advances in reconstitution systems could potentially give new opportunities to estimate the pigment content of the Lhca proteins (Schmid et al., 1997). However, since it is possible to reconstitute LHC proteins with abnormal pigment compositions, such as complexes containing only Chl *a* or only Chl *b* (Schmidt et al., 2001), no clear-cut answers have been obtained from reconstituted systems so far.

### E. Long-Wavelength Chls

Like the cyanobacterial complex, PS I from higher plants contains long-wavelength or 'red' Chls. Some of these are present in the core complex, presumably in the same locations as those found in cyanobacteria. However, at low temperature, the major fluorescence emission from PS I is around 730 nm and originates from chlorophylls associated with LHC I. The Lhca1/Lhca4 heterodimer has a low-temperature fluorescence peak around 730 nm and has therefore been named LHCI-730 (Lam et al., 1984). The 'red' Chls seem to be associated primarily with Lhca4 (Schmid et al., 1997, Tjus et al., 1995), but the observation that the spectrum of the heterodimer is different from that of the monomers (Melkozernov et al., 1998) suggests that the red Chls may be located at the interface of the two proteins. These red pigments are reported to absorb light of about 705 nm (Mukerji and Sauer, 1993; Ihalainen et al., 2000), and consequently to have an unusually large difference in wavelength between the absorbance and emission maxima (Stokes shift). It has been suggested that Chl *b* molecules are necessary for the formation of the red pigments (Schmid et al., 2001).

Preparations of Lhca2 and Lhca3 fluoresce at 680 nm, and these proteins consequently were named LHCI-680 (Lam et al., 1984; Knoetzel et al., 1992). There is, however, emerging evidence that this fluorescence peak may be artificial. Figure 6 shows the low-temperature fluorescence spectra of leaves

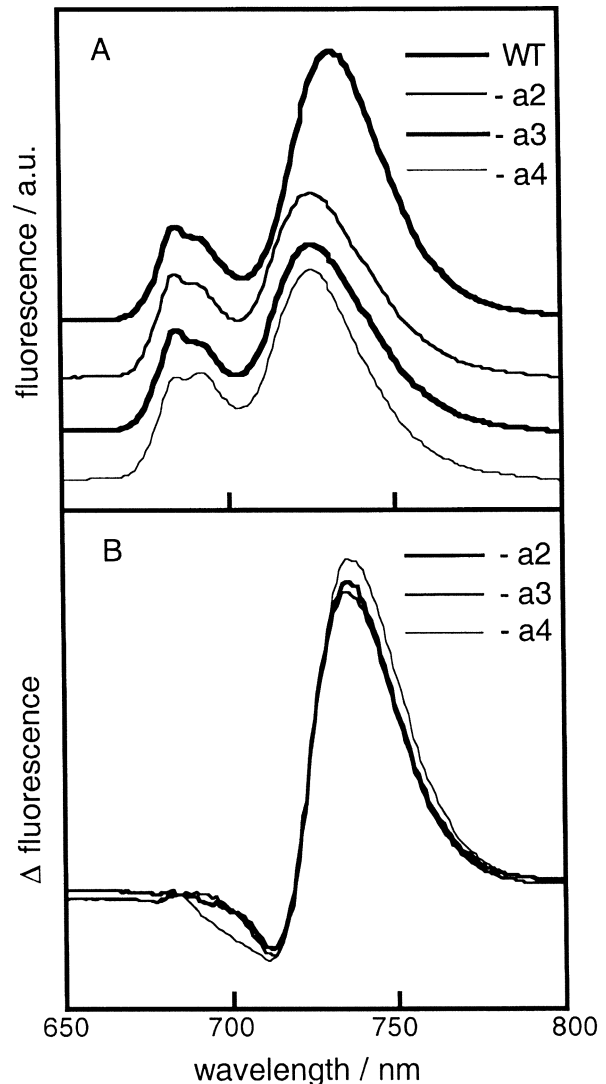


Fig. 6. 77 K fluorescence emission spectra of wild-type (wt) Arabidopsis plants and of plants lacking specific Lhca polypeptides. Leaves from plants transformed with antisense constructs for Lhca2, Lhca3 or Lhca4 were excited at 400 nm. (A) Fluorescence emission spectra, normalized to the Photosystem II emission peak. The spectra are displaced vertically for clarity. (B) Difference spectra (wt *minus* antisense plant). The emission spectra of the three different antisense plants are virtually identical.

from wild-type *Arabidopsis* plants and from antisense plants that lack one of the Lhca proteins. The fluorescence spectrum of plants that are completely devoid of Lhca2, but retain Lhca1 and Lhca4, is essentially the same as that of plants without Lhca4, which therefore do not contain LHCI-730, and the same is true for antisense plants that lack Lhca3 (Zhang et al., 1997; Ganeteg et al., 2001). This

indicates that all the PS I antenna proteins may contribute to the long-wavelength fluorescence *in vivo*, although other explanations cannot be definitely excluded. A possible cause of the lack of long-wavelength fluorescence in preparations of Lhca2 and Lhca3 is that the emitting pigments are located on the interface between the monomers, or between the monomers and the reaction center complex. In preparations of these proteins, which have monomerized as a result of the necessary detergent treatment, these pigments could either have dissociated or be in a different chemical environment, resulting in a lack of red-shifted pigments. If this is correct, the names LHCI-680 and LHCI-730 are inappropriate. We suggest that the complexes instead should be named after the polypeptide content, e.g. Lhca2, Lhca3 and the Lhca1/Lhca4 heterodimer. The role of the red Chls in LHC I is, like that of the red Chls in the PS I core, unclear. However, antenna function in far-red enriched light environments seems to be a reasonable possibility (Rivadossi et al., 1999).

#### F. The Architecture of the Plant PS I Antenna

Although we lack a high-resolution structure of plant PS I, it is possible to develop a working model for the peripheral antenna system of PS I if all the data on subunit interactions are put together (Fig. 7). Chemical cross-linking indicates that PsaH is in contact with PsaD, PsaL and PsaI, PsaK with Lhca3, and Lhca2 with Lhca3, and that Lhca4 is in contact with either Lhca2 or Lhca3 (Jansson et al., 1996). The finding that PsaH is necessary for interaction of mobile LHC II with PS I suggests that these proteins are in contact. In addition, Lhca3 is much less stable in the absence of Lhca2, indicating that Lhca3 probably is located peripherally in the complex (Ganeteg et al., 2001). This conclusion is consistent with the assumption that plant PsaK occupies the same position as its cyanobacterial counterpart, and that Lhca3 is located next to it.

This information, taken with the fact that LHC I is found on one side of the complex (Boekema et al., 2001a), suggests the model shown in Fig. 7. Here it is assumed that one homodimer each of Lhca2 and Lhca3, and two Lhca1/4 heterodimers, associate with each PS I. The number of LHC II trimers is not fixed, but here two Lhcb1/2 trimers have been modeled close to the PsaH protein. In the absence of a three-dimensional structure, this model should be regarded

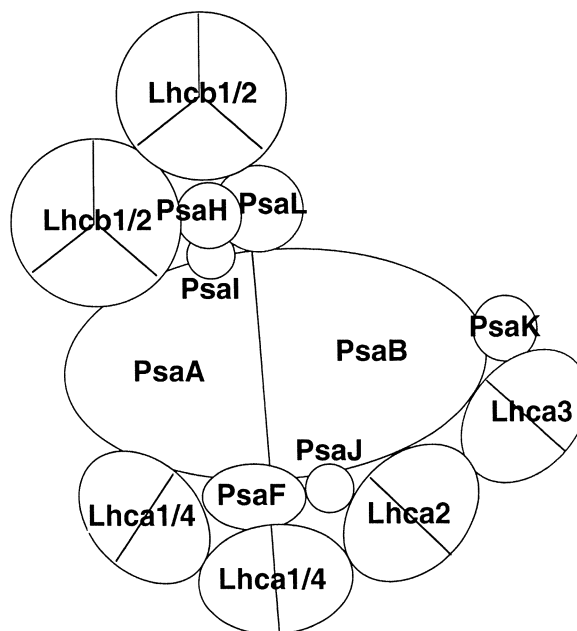


Fig. 7. Structural model of the plant Photosystem I. See text for details.

as tentative, bearing in mind that the antenna protein composition varies in ways we do not understand.

#### V. Excitation Energy Transfer and Trapping in PS I

This section focuses on energy transfer in PS I from *S. elongatus*, for which the three-dimensional structure at 2.5 Å resolution has been described in Sections II and III. For recent reviews on excitation energy transfer in PS I including plant PS I, see Melkozernov (2001) and Gobets and van Grondelle (2001). In the PS I from *S. elongatus*, the six reaction center Chls are surrounded by a core antenna system consisting of 90 Chls and 22 carotenoids (Figs. 3 and 5). It is their function to harvest solar energy and to transfer this energy to the reaction center (RC), where the excitation energy is converted into a charge-separated state. The criteria for efficiency of an antenna system are (i) a maximal cross section for light absorption over a wide spectral range, (ii) the ability to trap the excitation energy with minimal losses, and (iii) high stability due to effective protection against photodestruction.



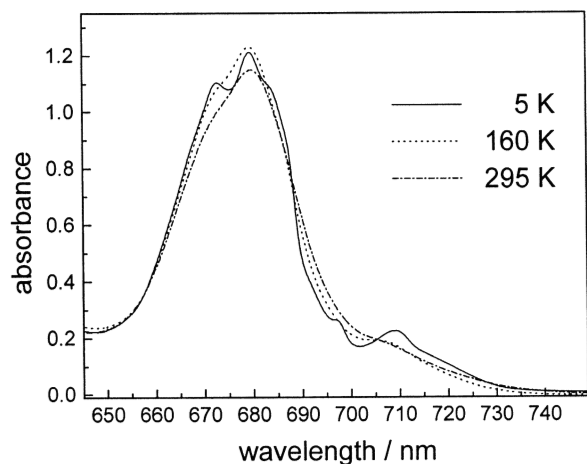


Fig. 8. Steady-state absorption spectrum of the trimeric PS I core complex from *S. elongatus* in the  $Q_y$ -region at various temperatures. Note that the absorption extends beyond 740 nm. (Byrdin et al., 2002).

### A. Structure and Spectra

The mean center-to-center distance between neighboring Chls in the cyanobacterial PS I is 9.9 Å, which is only slightly above the diameter of the chlorin ring. This dense packing indicates that excitonic interactions have to be taken into account for a description of the spectral and functional properties of PS I. Table 1 summarizes the most strongly coupled Chl dimers. Using the point-dipole approximation, the excitonic coupling energy of the two Chls constituting P700 (eC-A1 and eC-B1) is significantly larger than all the other couplings (Table 1, column 3). However, calculations using the extended dipole approximation (Pearlstein, 1992) or the point-monopole method (Chang, 1977), which probably are more reliable, indicate that the couplings between other pairs of Chls in the reaction center of PS I are of comparable strength (column 4).

Figure 8 illustrates that the absorption spectrum in the  $Q_y$  region of trimeric PS I complexes from *S. elongatus* is highly heterogeneous. The  $Q_y$  absorption maximum is centered at about 680 nm, but at low temperature (5 K) clearly exhibits multiple bands (Pålsson et al., 1998; Byrdin et al., 2000). Absorption bands at about 708 nm and 720 nm with oscillator strengths corresponding to approximately five and four Chls, respectively, are attributed to the long-wavelength ('red') Chls, which play a crucial role in the kinetics of energy transfer and trapping because they absorb at wavelengths longer than that of the

primary electron donor, P700. The spectral heterogeneity can be explained by strong pigment-pigment interactions of tightly coupled dimers and trimers and site-energy differences arising from pigment-protein-interactions (Section III). It should be noted that there is a considerable redistribution of absorption as a function of temperature. Upon lowering temperature, the absorption in the red region above 705 nm increases at the expense of the absorption in region between 688 and 705 nm. Such a redistribution of absorption also has been found for PS I in *Synechocystis* sp. and *Spirulina platensis*. (Cometta et al., 2000; Rätsep et al., 2000).

### B. Kinetics of Energy Transfer

The excited-state dynamics of PS I complexes have been studied intensively by time-resolved absorption and fluorescence spectroscopy. The short center-to-center distances between the Chls in the antenna system suggest very fast energy transfer. Indeed, the average rate constant for energy transfer (hopping) between two Chls has been reported to be between  $(200 \text{ fs})^{-1}$  and  $(100 \text{ fs})^{-1}$  (Du et al., 1993; Kennis et al., 2001). The trapping of the excitation energy by charge separation can be followed by measuring the fluorescence decay. Figure 9 shows the decay-associated spectra of excitation energy-transfer processes in monomeric PS I core complexes from *Synechocystis* sp. PCC 6803 (A) and trimeric PS I core complexes from *S. elongatus* (B) and *Spirulina platensis* (C), as measured using a synchroscan streak camera with excitation at 400 nm (Gobets et al., 2001). In PS I from *S. elongatus*, the lifetime of the dominant decay component is about 35 ps, with good agreement between various groups (Holzwarth et al., 1993; Dorra et al., 1998; Byrdin et al., 2000; Gobets et al., 2001; Kennis et al., 2001). The spectrum associated with the trapping is virtually independent of the excitation wavelength (Hastings et al., 1995a). It resembles closely the steady-state emission spectrum, which exhibits a maximum at 721 nm and a shoulder at 685 nm at room temperature (Fig. 9B, closed triangles). This indicates that the largest part of the fluorescence is emitted from the long-wavelength Chls. Time-resolved fluorescence measurements in species that have different contents of 'red' Chls show clearly that these Chls slow down the trapping (Gobets et al., 2001). In Fig. 9A-C, the increase of the trapping lifetime from 23 to 50 ps is correlated with the amount and the transition energies

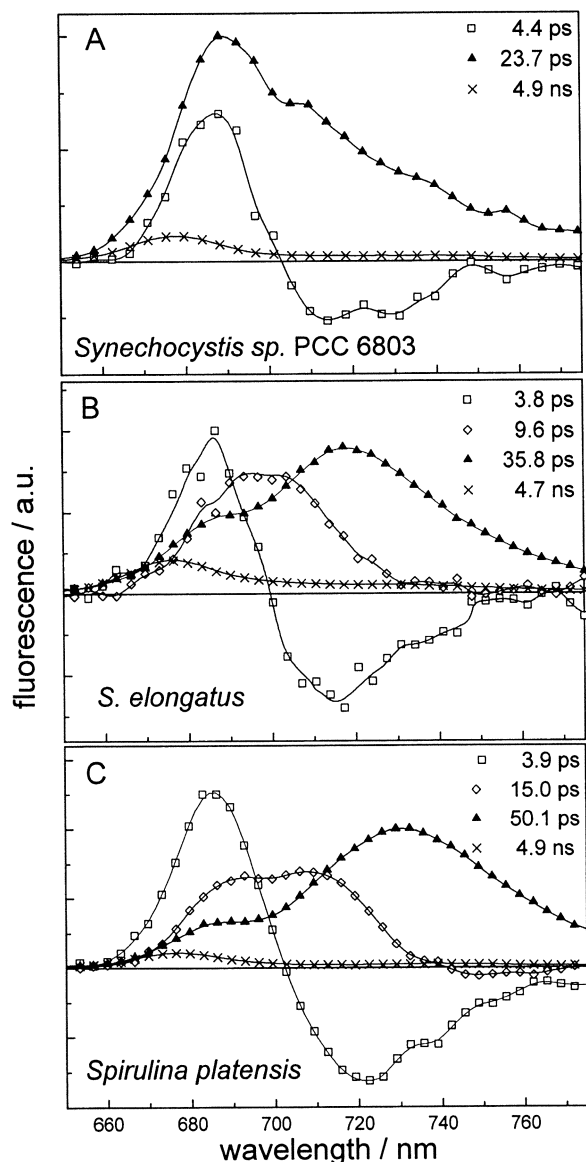


Fig. 9. Decay-associated spectra of fluorescence from cyanobacterial PS I core complexes upon excitation at 400 nm at room temperature: (A) Monomeric PS I from *Synechocystis* sp. PCC 6803; (B) trimeric PS I from *S. elongatus*; (C) trimeric PS I from *Spirulina platensis*. The small 4.9 ns component can be attributed to a small fraction of uncoupled Chls present in the preparations (Gobets et al., 2001).

of the long-wavelength Chls in the different species.

Remarkably, the oxidation state of P700 has only a small effect on the fluorescence lifetime at room temperature (Byrdin et al., 2000). A detailed single-photon counting study revealed that the fluorescence lifetime is about 3 ps longer for PS I with P700 in the

oxidized state than with P700 reduced, where fast quenching occurs by charge separation. A fluorescence induction effect corresponding to this difference in lifetimes showed an increase of ~12% in the fluorescence yield upon P700 oxidation at 295 K. These results indicate that the oxidized donor (P700<sup>+</sup>) is almost as good a quencher as the reduced donor. P700<sup>+</sup> exhibits a broad, flat absorption that extends into the far red beyond 800 nm and provides spectral overlap with the emission bands of all the core-antenna pigments, so that P700<sup>+</sup> can effectively act as an excitation energy acceptor. The subsequent fast radiationless decay of (P700<sup>+</sup>)<sup>\*</sup> probably constitutes the quenching mechanism (for a detailed discussion of the quenching mechanism see Trissl, 1997; and Byrdin et al., 2000).

As a consequence of the spectral heterogeneity of the antenna, excitation energy redistribution processes directed towards thermal equilibration take place. Kinetic components with transfer lifetimes in the 2–15 ps range have been resolved (Holzwarth et al., 1993; Hastings et al., 1995a; Dorra et al., 1998; Byrdin et al., 2000; Gobets et al., 2001; Kennis et al., 2001). In the decay-associated spectra shown in Fig. 9, energy redistribution between antenna Chls absorbing at different wavelengths gives rise to spectra with positive and negative amplitudes. These spectra are ‘conservative,’ in that the overall fluorescence remains approximately constant. In PS I from *S. elongatus*, the spectrum of the 3.8 ps component (Fig. 9B, squares) is positive below 700 nm and negative at wavelengths longer than 700 nm, indicating energy transfer from the bulk antenna to the red pigments. In addition, a 9.6 ps component (Fig. 9B, diamonds) peaks around 700 nm and barely drops below zero. This component has been assigned to a slower energy-transfer process, during which trapping occurs to a great extent (Gobets et al., 2001). However, single-photon counting experiments have yielded only one energy-transfer component, with a time constant of 12–14 ps (Dorra et al., 1998; Byrdin et al., 2000). The reason for this discrepancy remains to be clarified.

The fast and efficient trapping explains the low fluorescence yield of PS I core complexes, which is only about 1% at room temperature. Figure 10A shows the temperature dependence of the relative fluorescence yield for PS I with P700 in the reduced (triangles) or oxidized (squares) state. Upon lowering the temperature, the fluorescence yield increases by a factor of ~20 for PS I with reduced P700, as

compared to a factor of  $\sim 10$  for PS I with oxidized P700. The inset shows steady-state fluorescence spectra at different temperatures. The maximum emission shifts to the red from 721 nm at 295 K to 733 nm at 5 K. The increase in the fluorescence yield with decreasing temperature can be explained on the assumption that a significant part of the excitation is trapped on the energetically lowest-lying antenna pigments, because uphill energy transfer becomes impossible at low temperature. As a consequence, the yield of charge separation decreases by about a factor of 2 upon lowering the temperature from 295 K to 5 K (Fig. 10B and Pålsson et al., 1998). At 5 K, the fluorescence is mainly associated with long-lived fluorescence components with time constants between 0.4 and 4 ns (Byrdin et al., 2000).

### C. Simulations

Structure-based calculations have been performed to simulate simultaneously the optical spectra of PS I from *S. elongatus* (absorption, linear and circular dichroism and emission) and the energy-transfer kinetics by application of excitonic coupling theory in order to reveal relationships between structure and function (Byrdin et al., 2002). The assignment of transition energies to all the structurally defined Chls is the most critical point in these calculations. The assignment strategy was guided by symmetry relations, by considerations regarding the axial ligands and H-bonding to the Chls, by functional arguments concerning the location of the red pigments (Section III), and by fine tuning of the transition energies of the bulk pigments to improve the simulations of the spectra. The long-wavelength absorption was assigned to the tightly coupled cluster of four Chls near the trimerization domain (A31-A32-B7-B6) and the A38/39 and B37/38 dimers, which also are strongly coupled and are close to the linker Chls A40 and B39 (Figs. 4a and 4c). If the spectral heterogeneity caused by excitonic coupling and heterogeneous site energies is neglected (i.e., if all Chls are assumed to have the same  $Q_y$  transition energy), the walk of excitations through the antenna will be random. The time constant for trapping in such a system is predicted to be about 60 ps, which is significantly longer than the time observed experimentally ( $\sim 35$  ps). As a result of excitonic coupling and/or interactions of Chls eC-A1 and eC-B1 with the protein, the low-energy exciton band of P700 in *S. elongatus* is located at 703 nm. This puts the absorption of P700

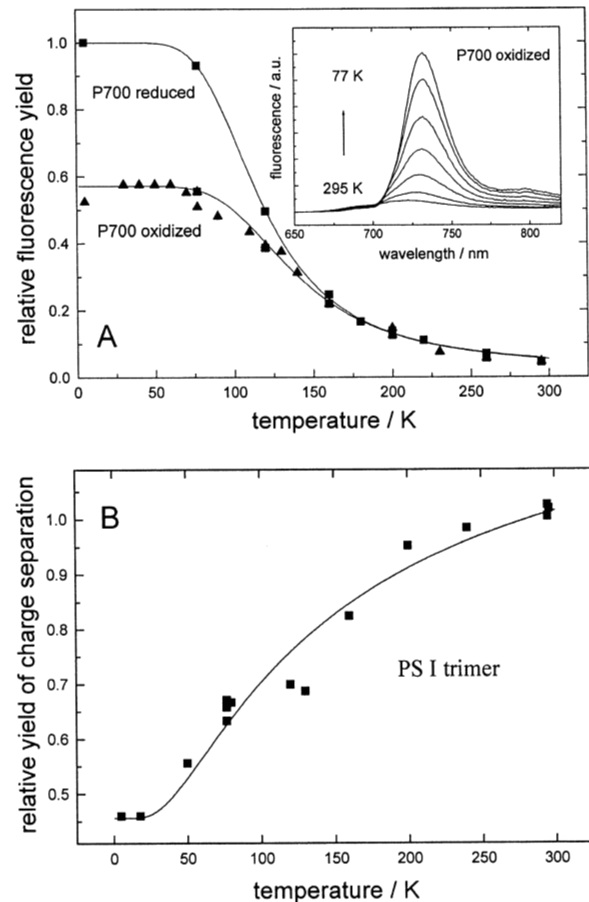


Fig. 10. (A) Temperature dependence of the fluorescence yield of trimeric PS I complexes from *S. elongatus* with P700 in the reduced or oxidized state. The inset shows steady-state emission spectra at different temperatures. Note the increase of yield (the area below the curve) and the shift of the emission maximum to longer wavelengths upon lowering the temperature. (B) Temperature dependence of the yield of charge separation in trimeric PS I complexes from *S. elongatus* (Pålsson et al., 1998; Byrdin et al., 2000)

at longer wavelengths than all the other Chls except for the red Chls. The resulting energy gradient towards the trap imposes a directionality and is calculated to speed up trapping to about 25 ps if the wavelengths of the red Chls are set to 680 nm. A trapping time of 25 ps is similar to that observed in PS I complexes with the least amount of red Chls. If the long-wavelength absorption of PS I from *S. elongatus* attributed to the tetramer (A31-A32-B7-B6) and to the two linker dimers (A38/39 and B37/38) also is taken into account, the calculated trapping time agrees well with the experimental value ( $\sim 35$  ps) (Byrdin et al., 2002).

The parameters used in this modeling assume both fast transfer between Chls (Förster radius = 78 Å), and fast trapping (intrinsic rate constant for primary charge-separation =  $0.87 \text{ ps}^{-1}$ ). The effects of varying these parameters indicate that the excited-state dynamics are not limited purely by either the rate constant for electron transfer ('trap-limited') or the rate of energy transfer to the trap ('transfer-limited'). Instead, PS I appears to be well balanced between these two extremes.

Similar calculations can be used to analyze situations in which the arrangement of the Chls is modified, for example by removal of the linker and/or the linker dimer Chls, removal of outlying Chls in the small subunits in order to simulate deletion mutants, or removal of antenna Chls located in the middle of the membrane (Byrdin et al., 2002). Interestingly, removing the linker Chls has almost no effect on the calculated trapping time, indicating that these Chls are not required for efficient trapping. The variation between the longest and shortest trapping times was found to be only about threefold, corresponding to a difference in quantum efficiency of only 3% between ~98% and ~95%. This result indicates that the system is optimized for robustness rather than for extremely fast trapping.

#### D. Function of Carotenoids

Carotenoids in PS I absorb in the range from 450–550 nm, where absorption by Chl *a* is weak. The close contact to the Chls facilitates fast excitation energy transfer from the carotenoids to the Chls (Kennis et al, 2001). Singlet energy transfer to Chl *a* from the lowest excited states of the  $\beta$ -carotenes occurs with a time constant of 1.2 ps, and transfer from the second excited state with a time constant of 170 fs (Kennis et al., 2001). The overall transfer efficiency was estimated to be about 90%. On the basis of the absorption spectrum of the PS I core complexes, the contribution of the carotenoids to light harvesting in PS I can be estimated to be about 20 %, neglecting light harvesting and energy transfer to PS I by phycobilisomes.

The high stability of the PS I complex depends mainly on the effective protection against photo-destruction by the carotenoids. The major role of the carotenoids (Car) is, besides light harvesting, to quench Chl triplet states to prevent the formation of singlet oxygen. Chl *a* triplet states are formed in the antenna by intersystem crossing from the lowest

excited singlet state. The triplet excitation transfer from Chl to Car proceeds through the electron-exchange mechanism, which requires close proximity between Chl and Car as found in the 2.5 Å structure (Section III and Fig. 5). The kinetics of triplet-triplet energy transfer from Chl *a* to Car has been determined by transient absorption spectroscopy (Schlodder et al., 2001). The transfer occurs with time constants of ~14 ns (~60%) and ~120 ns (~40%). The kinetics were found to be essentially independent of temperature. Interestingly, the structure revealed that no  $\beta$ -carotene molecule is located in the vicinity of P700. This excludes quenching of the triplet state of the primary electron donor ( $^3\text{P700}$ ) by carotenoids.  $^3\text{P700}$  is formed by charge recombination of the radical pair  $\text{P700}^+\text{A}_0^-$  after singlet-triplet mixing when the electron transfer to  $\text{A}_1$  is blocked. At temperatures below 50 K, the decay kinetics of  $^3\text{P700}$  is similar to that of Chl *a* triplet states in organic solvents and is independent of temperature. Above 50 K the decay rate increases with increasing temperature, indicating a decay pathway with an activation energy of about 40 meV. At room temperature, the decay time constant is 4 to 6  $\mu\text{s}$  (Schlodder et al., 2001). The process of the activated decay is not well understood, but probably represents a protective mechanism to prevent formation of singlet oxygen in the reaction center.

#### E. Energy Transfer in PS I from Higher Plants

The PS I holocomplex from higher plants and green algae consists of the core complex and the peripheral antenna complex LHC I, which binds about another 100 Chl *a* and/or *b* molecules (Section IV). This higher structural complexity of the PS I holocomplex results in even more complex energy-transfer dynamics compared to those in the PS I core complexes. To get information on the energy transfer in PS I from higher plants, studies have been performed with isolated (native and reconstituted) subunits of the LHC I (for a recent review see Melkozernov, 2001) and with the intact PS I holocomplex (for reviews see van Grondelle et al., 1994; Gobets and van Grondelle, 2001). Studies of the excitation energy transfer in the isolated Lhca1 and Lhca4 monomer and the Lhca1/Lhca4 heterodimer (also called LHCI-730) revealed that excitation energy transfer from Chl *b* to Chl *a* occurs within 500–600 fs. Redistribution of excitation energy between different spectral forms of Chl *a*, i.e. energy

transfer from the major Chl *a* pool with an absorption maximum around 679 nm to Chl *a* molecules absorbing at longer wavelengths, takes place within a few picoseconds. These Chls absorbing at longer wavelength show an emission maximum at about 730 nm (Melkozernov et al., 2000a, 2002). For a detailed discussion of the location of red Chls in PS I from higher plants see Section IV E. Several kinetic components have been resolved in studies of the excitation energy transfer and trapping kinetics in the PS I holocomplexes from spinach (Turconi et al., 1994), maize (Croce et al., 2000) and *Arabidopsis thaliana* (Ihalainen et al., 2002). The fastest components with lifetimes between 2 and 17 ps were attributed to excitation energy equilibration between bulk and long-wavelength Chl forms. Slower components with lifetimes of about 50 and 120 ps, which display emission spectra with all-positive amplitudes, have been ascribed to the overall trapping in the PS I complexes from higher plants. The observation of at least two trapping components have been taken as an indication that trapping in PS I from higher plants does not occur from a thermally equilibrated state and that the excitation energy transfer is diffusion-limited. It has been proposed that the faster (50 ps) component originates from trapping of excitation energy within the core complex whereas the slower component may reflect uphill energy transfer from the red-spectral forms of the LCH I to the core complex.

## Acknowledgment

This work was supported by the Deutsche Forschungsgemeinschaft (Sfb 498, TP A1).

## References

- Abramson J, Riistama S, Larsson G, Jasaitis A, Svensson-Ek M, Laakkonen L, Puustinen A, Iwata S and Wikstrom M. (2000) The structure of the ubiquinol oxidase from *Escherichia coli* and its ubiquinone binding site. *Nat Struct Biol* 7: 910–917
- Adman ET, Sieker LC and Jensen LH (1973) The Structure of a bacterial ferredoxin. *J Biol Chem* 248: 3987–3996
- Altmann RB, Renge I, Kador L and Haarer D (1992) Dipole moment differences of nonpolar dyes in polymeric matrices: Stark Effect and photochemical hole burning. *J Chem Phys* 97: 5316–5322
- Andersen B, Scheller HV and Moller BL (1992a) The PSI-E subunit of Photosystem I binds ferredoxin:NADP<sup>+</sup> oxidoreductase. *FEBS Lett* 311: 169–73
- Andersen B, Koch B and Scheller HV (1992b) Structural and functional analysis of the reducing side of Photosystem I. *Physiol Plant* 84: 154–161
- Armbrust TS, Chitnis PR and Guikema JA (1996) Organization of Photosystem I polypeptides examined by chemical crosslinking. *Plant Physiol* 111: 1307–1312
- Bailey S, Walters R, Jansson S and Horton P (2001) Acclimation of *Arabidopsis thaliana* to the light environment: The existence of separate low light and high light responses. *Planta* 213: 794–801
- Bengis C and Nelson N (1977) Subunit structure of chloroplast Photosystem I reaction center. *J Biol Chem* 252: 4564–4569
- Bialek-Bylka GE, Fujii R, Chen CH, Oh-oka H, Kamiesu A, Satoh K, Koike H, Koyama Y (1998) 15-*cis* carotenoids found in the reaction center of the green sulfur bacterium *Chlorobium tepidum* and in Photosystem I reaction center of the cyanobacterium *Synechococcus vulcanus*. *Photosynth Res* 58: 135–142
- Bibby TS, Nield J and Barber J (2001) Iron deficiency induces the formation of an antenna ring around trimeric Photosystem I in cyanobacteria. *Nature* 412: 743–745
- Bittl R, Zech SG, Fromme P, Witt HT and Lubitz W (1997) Pulsed EPR structure analysis of Photosystem I single crystals: Localization of the phyloquinone acceptor. *Biochemistry* 36: 12001–12004
- Blankenship RE (1992) Origin and early evolution of photosynthesis. *Photosynth Res* 33: 91–111
- Boekema EJ, Jensen PE, Schlodder E, van Breemen JFL, van Roon H, Scheller HV and Dekker JP (2001a) Green plant Photosystem I binds light harvesting complex I on one side of the complex. *Biochemistry* 40: 1029–1036
- Boekema EJ, Hifney A, Yakushevskaya AE, Piotrowski M, Keegstra W, Berry S, Michel KP, Pistorius EK and Kruij J (2001b) A giant chlorophyll-protein complex induced by iron deficiency in cyanobacteria. *Nature* 412: 745–748
- Boekema EJ, Dekker JP, van Heel MG, Rögner M, Saenger W, Witt I and Witt HT (1987) Evidence for a trimeric organization of the Photosystem I complex from the thermophilic cyanobacterium *Synechococcus* sp. *FEBS Lett* 217: 283–286
- Brettel K (1997) Electron transfer and arrangement of the redox cofactors in Photosystem I. *Biochim Biophys Acta* 1318: 322–373
- Brettel K and Leibl W (2001) Electron transfer in Photosystem I. *Biochim Biophys Acta* 1507: 100–114
- Brettel K and Vos MH (1999) Spectroscopic resolution of the picosecond reduction kinetics of the secondary electron acceptor A<sub>1</sub> in Photosystem I. *FEBS Lett* 447: 315–317
- Byrdin M, Rimke I, Schlodder E, Stehlik D and Roelofs TA (2000) Decay kinetics and quantum yields of fluorescence in Photosystem I from *Synechococcus elongatus* with P700 in the reduced and oxidized state: Are the kinetics of excited state decay trap-limited or transfer-limited? *Biophys J* 79: 992–1007
- Byrdin M, Jordan P, Krauß N, Fromme P, Stehlik D and Schlodder E (2002) Light harvesting in Photosystem I—Modeling based on the 2.5 Å structure of Photosystem I from *Synechococcus elongatus*. *Biophys J* 83: 433–457
- Chang JC (1977) Monopole effects on electronic excitation interactions between large molecules. I. Application to energy transfer in chlorophylls. *J Chem Phys* 67: 3901–3909
- Chitnis PR, Xu Q, Chitnis VP and Nechustai R (1995) Function

- and organization of Photosystem I polypeptides. *Photosynth Res* 44: 23–40
- Chitnis VP and Chitnis PR (1993) PsaL subunit is required for the formation of Photosystem I trimers in the cyanobacterium *Synechocystis* sp. PCC 6803. *FEBS Lett* 336: 330–334
- Chitnis VP, Xu Q, Yu L, Golbeck JH, Nakamoto H, Xie DL and Chitnis PR (1993) Target inactivation of the gene PsaL encoding a subunit of Photosystem I of the cyanobacterium *Synechocystis* PCC 6803. *J Biol Chem* 268: 11678–11684
- Cogdell RJ (1985) Carotenoids in photosynthesis. *Pure Appl Chem* 57: 723–728
- Cometta A, Zucchelli G, Karapetyan NV, Engelmann E, Garlaschi FM and Jennings RC (2000) Thermal behavior of long wavelength absorption transitions in *Spirulina platensis* Photosystem I trimers. *Biophys J* 79: 3235–3243
- Coufal J, Hladik J and Sofrova D (1989) The carotenoid content of Photosystem I-pigment-protein-complexes of the cyanobacterium *Synechococcus elongatus*. *Photosynthetica* 23: 603–616
- Croce R, Dorra D, Holzwarth AR and Jennings RC (2000) Fluorescence decay and spectral evolution in intact Photosystem I of higher plants. *Biochemistry* 39: 6341–6348
- Deisenhofer J, Epp O, Sinning I and Michel H (1995) Crystallographic refinement at 2.3 Å resolution and refined model of the photosynthetic reaction centre from *Rhodospseudomonas viridis*. *J Mol Biol* 246: 429–57
- Diaz-Quintana A, Leibl W, Bottin H and Sétif P (1998) Electron transfer in Photosystem I reaction centers follows a linear pathway in which iron-sulfur cluster FB is the immediate electron donor to soluble ferredoxin. *Biochemistry* 37: 3429–39
- Dorra D, Fromme P, Karapetyan NV and Holzwarth AR (1998) Fluorescence kinetics of Photosystem I: Multiple fluorescence components. In: Garab G (ed) *Photosynthesis: Mechanism and Effects*, Vol I, pp 587–590. Kluwer Academic Publishers, Dordrecht
- Drepper F, Hippler M, Nitschke W and Haehnel W (1996) Binding dynamics and electron transfer between plastocyanin and Photosystem I. *Biochemistry* 35: 1282–95
- Du M, Xie X, Jia Y, Mets L and Fleming GR (1993) Direct observation of ultrafast energy transfer in PS I core antenna. *Chem Phys Lett* 201: 535–542
- Dzuba SA, Gast P and Hoff AJ (1997) Electron spin echo of spin polarized radical pairs in the intact quinone reconstituted plant Photosystem I reaction center. *Chem Phys Lett* 236: 595–602
- Eccles J and Honig B (1983) Charges amino acids as spectroscopic determinants for chlorophyll in vivo. *Proc Natl Acad Sci USA* 80: 4959–4962
- Ermler U, Fritzsche G, Buchanan SK and Michel H (1994) Structure of the photosynthetic reaction centre from *Rhodobacter sphaeroides* at 2.65 Å resolution: Cofactors and protein-cofactor interactions. *Structure* 2: 925–36
- Fairclough WV, Evans MCW, Purton S, Rigby SEJ and Heathcote P (2001) Site-directed mutagenesis of PsaA: M684 in *Chlamydomonas reinhardtii*. In: PS2001: Proceedings 12th International Congress on Photosynthesis, S6-022. CSIRO Publishing, Melbourne [CD-ROM]
- Falzone CJ, Kao YH, Zhao J, MacLaughlin KL, Bryant DA and Lecomte JT (1994) <sup>1</sup>H and <sup>15</sup>N NMR assignments of PsaE, a Photosystem I subunit from the cyanobacterium *Synechococcus* sp. strain PCC 7002. *Biochemistry* 33: 6043–51
- Farah J, Rappaport F, Choquet Y, Joliot P and Rochaix JD (1995) Isolation of a psaF-deficient mutant of *Chlamydomonas reinhardtii*: Efficient interaction of plastocyanin with the Photosystem I reaction center is mediated by the PsaF subunit. *EMBO J* 14: 4976–84
- Fischer N, Sétif P and Rochaix JD (1999) Site-directed mutagenesis of the PsaC subunit of Photosystem I. F<sub>B</sub> is the cluster interacting with soluble ferredoxin. *J Biol Chem* 274: 23333–40
- Fish L, Kück U and Bogorad L (1985) Two partially homologous adjacent light-inducible maize chloroplast genes encoding polypeptides of the P700 chlorophyll a protein complex of Photosystem I. *J Biol Chem* 260: 1413–1421
- Förster T (1965) Delocalized excitation and excitation transfer. In: Sinnanoglu O (ed) *Modern Quantum Chemistry*, Vol IIIB, pp 93–137. Academic Press, New York
- Frank HA (1999) Incorporation of carotenoids into reaction center and light-harvesting pigment-protein complexes. In: Frank HA, Young AJ, Britton G and Cogdell RJ (eds) *The Photochemistry of Carotenoids*, pp 235–244. Kluwer Academic Publishers, Dordrecht
- Frank H and Cogdell RJ (1995) Carotenoids in photosynthesis. *Photochem Photobiol* 63: 257–264
- Fromme P (1998) Structure and function of Photosystem I. Habilitationsschrift. Technical University Berlin, Berlin Germany
- Ganeteg U, Strand Å, Gustafsson P and Jansson S (2001) The properties of the chlorophyll *a/b*-binding proteins Lhca2 and Lhca3 studied in vivo using antisense inhibition. *Plant Physiol* 127: 150–158
- Gobets B, van Stokkum IHM, Rögner M, Kruip J, Schlodder E, Karapetyan NV, Dekker JP and van Grondelle R (2001) Time resolved fluorescence emission measurements of Photosystem I particles of various cyanobacteria: A unified compartmental model. *Biophys J* 81: 407–424
- Gobets B, and van Grondelle R (2001) Energy transfer and trapping in Photosystem I. *Biochim Biophys Acta* 1507: 80–99
- Golbeck JH (1992) Structure and function of Photosystem I. *Annu Rev Plant Physiol* 43: 293–324
- Golbeck JH (1993) The structure of Photosystem I. *Curr Opin Struc Biol* 3: 508–514
- Golbeck JH (1996) Photosystem I. *Plant Physiol* 111: 661–669
- Golbeck JH (1999) A comparative analysis of the spin state distribution of in vitro and in vivo mutants of PsaC. *Photosynth Res* 61: 107–144
- Green BR, Pichersky E and Kloppstech K (1991) Chlorophyll *a/b* binding proteins: An extended family. *Trends Biochem Sci* 16: 181–188 (1991)
- Green BR and Pichersky E (1994) Hypothesis for the evolution of three-helix Chl *a/b* and Chl *a/c* light-harvesting antenna proteins from two-helix and four-helix ancestors. *Photosynth Res* 39: 149–162
- Gudowska-Nowak E, Newton MD and Fajer J (1990) Conformational and environmental effects on bacteriochlorophyll optical spectra: Correlations of calculated spectra with structural results. *J Phys Chem* 94: 5795–5801
- Guergova-Kuras M, Boudreaux B, Joliot A, Joliot P and Redding K (2001) Evidence for two active branches for electron transfer in Photosystem I. *Proc Natl Acad Sci USA* 98: 4437–4442
- Haldrup A, Naver H and Scheller HV (1999) The interaction

- between plastocyanin and Photosystem I is inefficient in transgenic *Arabidopsis* plants lacking the PSI-N subunit of Photosystem I. *Plant J* 17: 689–698
- Haldrup A, Simpson DJ and Scheller HV (2000) Down-regulation of the PSI-F subunit of Photosystem I in *Arabidopsis thaliana*. The PSI-F subunit is essential for photoautotrophic growth and antenna function. *J Biol Chem* 275: 31211–31218
- Hastings G, Reed LJ, Lin S and Blankenship B (1995a) Excited State Dynamics in Photosystem I: Effects of detergent and excitation wavelength. *Biophys J* 69: 2044–2055
- Hastings G, Hoshina S, Webber AN and Blankenship RE (1995b) Universality of energy and electron transfer processes in Photosystem I. *Biochemistry* 34: 15512–22
- Hecks B, Wulf K, Breton J, Leibl W and Trissl HW (1994) Primary charge separation in Photosystem I: A two step electrogenic charge separation connected with  $P700^+A_0^-$  and  $P700^+A_1^-$  formation. *Biochemistry* 33: 8619–8624
- Hippler M, Drepper F, Farah J and Rochaix JD (1997) Fast electron transfer from cytochrome  $c_6$  and plastocyanin to Photosystem I of *Chlamydomonas reinhardtii* requires Psf. *Biochemistry* 36: 6343–9
- Hippler M, Drepper F, Rochaix JD and Mühlenhoff U (1999) Insertion of the N-terminal part of Psf from *Chlamydomonas reinhardtii* into Photosystem I from *Synechococcus elongatus* enables efficient binding of algal plastocyanin and cytochrome  $c_6$ . *J Biol Chem* 274: 4180–4188
- Hladik J and Sofrova D (1991) Does the trimeric form of Photosystem I reaction center of cyanobacteria in vivo exist? *Photosynth Res* 29: 171–175
- Holzwarth AR, Schatz G, Brock H and Bittersmann E (1993) Energy transfer and charge separation kinetics in Photosystem I. Part I: Picosecond transient absorption and fluorescence study of cyanobacterial Photosystem I particles. *Biophys J* 64: 1813–1826
- Ihalainen JA, Gobets B, Sznee K, Brazzoli M, Croce R, Bassi R, van Grondelle R, Korppi-Tommola JEI and Dekker JP (2000) Evidence for two spectroscopically different dimers of light-harvesting complex I from green plants. *Biochemistry* 39: 8625–8631
- Ihalainen JA, Jensen PE, Haldrup A, van Stokkum IHM, van Grondelle R, Scheller, HV, and Dekker JP (2002) Pigment Organization and energy transfer dynamics in isolated Photosystem I complexes from *Arabidopsis thaliana* depleted of the PSI-G, PSI-K, PSI-L or PSI-N subunit. *Biophys J* 83: 2190–2201
- Iwaki M, Kumazaki S, Yoshihara K, Erabi T and Itoh S (1996)  $\Delta G^\circ$  dependence of the electron transfer rate in the photosynthetic reaction center of plant Photosystem I: Natural optimization of reaction between chlorophyll  $a$  ( $A_0$ ) and quinone. *J Phys Chem* 100: 10802–10809
- Iwata S, Ostermeier C, Ludwig B and Michel H (1995) Structure at 2.8 Å resolution of cytochrome  $c$  oxidase from *Paracoccus denitrificans*. *Nature* 376: 660–669
- Jansson S (1994) The light-harvesting chlorophyll  $a/b$ -binding proteins. *Biochim Biophys Acta* 1184: 1–19
- Jansson S (1999) A guide to the Lhc genes and their relatives in *Arabidopsis*. *Trends Plant Sci* 4: 236–240
- Jansson S, Andersen B and Scheller HV (1996) Nearest-neighbor analysis of higher-plant Photosystem I holocomplex. *Plant Physiol* 112: 409–420
- Jansson S, Stefánsson H, Nyström U, Gustafsson P and Albertsson PÅ (1997) Antenna protein composition of PS I and PS II in thylakoid sub-domains. *Biochim Biophys Acta* 1320: 297–309
- Jensen PE, Gilpin M, Knoetzel J and Scheller HV (2000) The PSI-K subunit of Photosystem I is involved in the interaction between light harvesting complex 1-680 and the Photosystem I reaction center core. *J Biol Chem* 275: 24701–24708
- Jordan P, Fromme P, Klukas O, Witt HT, Saenger W and Krauß N (2001) Three-dimensional structure of cyanobacterial Photosystem I at 2.5 Å resolution. *Nature* 411: 909–917
- Jung YS, Vassiliev IR, Qiao F, Yang F, Bryant DA and Golbeck JH (1996) Modified ligands to  $F_A$  and  $F_B$  in Photosystem I. Proposed chemical rescue of a [4Fe-4S] cluster with an external thiolate in alanine, glycine, and serine mutants of Psf. *J Biol Chem* 271: 31135–31144
- Karapetyan NV, Holzwarth AR and Rögner M (1999) The Photosystem I trimer of cyanobacteria: Molecular organization, excitation dynamics and physiological significance. *FEBS Lett* 460: 395–400
- Karnauchov I, Cai DG, Schmidt I, Herrmann, RG and Klossgen, RB (1994) The thylakoid translocation of subunit-3 of Photosystem I, the Psf gene-product, depends on a bipartite transit peptide and proceeds along an azide-sensitive pathway. *J Biol Chem* 269: 32871–32878
- Karrasch S, Bullough PA and Ghosh R (1995) The 8.5 Å projection map of the light harvesting complex I from *Rhodospirillum rubrum* reveals a ring composed of 16 subunits. *EMBO J* 14: 631–638
- Käb H, Fromme P, Witt HT and Lubitz W (2001) Orientation and Electronic Structure of the Primary Electron Donor Radical Cation in Photosystem I: A Single Crystal EPR and ENDOR Study. *J Phys Chem B* 105: 1225–1239
- Kennis JTM, Gobets B, van Stokkum IHM, Dekker JP, van Grondelle R and Flemming GR (2001) Light harvesting by chlorophylls and carotenoids in the Photosystem I core complex of *Synechococcus elongatus*: A fluorescence upconversion study. *J Phys Chem* 105: 4485–4494
- Knoetzel J, Svendsen I and Simpson DJ (1992) Identification of the Photosystem I antenna polypeptides in barley. Isolation of three pigment-binding antenna complexes. *Eur J Biochem* 206: 209–215
- Kratky C and Dunitz JD (1977) Ordered aggregation states of chlorophyll and some of its derivatives. *J Mol Biol* 113: 431–442
- Kruip J, Bald D, Boekema EJ and Rögner M (1994) Evidence for the existence of trimeric and monomeric Photosystem I complexes in thylakoid membranes from cyanobacteria. *Photosynth Res* 40: 279–286
- Kruip J, Chitnis PR, Lagoutte B, Rögner M and Boekema EJ (1997) Structural organization of the major subunits in cyanobacterial Photosystem I—Localization of subunits PsfC, -D, -E, -F, and -J. *J Biol Chem* 272: 17061–17069
- Kumazaki S, Kandori H, Petek H, Yoshihara K and Ikegami I (1994) Primary photochemical processes in P700 enriched Photosystem I particles: Trap limited excitation decay and primary charge separation. *J Phys Chem* 98: 10335–10342
- Lam E, Ortiz W and Malkin R (1984) Chlorophyll  $a/b$  proteins of Photosystem I. *FEBS Lett* 168: 10–14
- Lee AI and Thornber JP (1995) Analysis of the pigment stoichiometry of pigment-protein complexes from barley. *Plant Physiol* 107: 565–574



- Lelong C, Boekema EJ, Kruip J, Bottin H, Rögner M and Sétif P (1996) Characterization of a redox active cross-linked complex between cyanobacterial Photosystem I and soluble ferredoxin. *EMBO J* 15: 2160–8
- Lelong C, Sétif P, Lagoutte B and Bottin H (1994) Identification of the amino acids involved in the functional interaction between Photosystem I and ferredoxin from *Synechocystis* sp. PCC 6803 by chemical cross-linking. *J Biol Chem* 269: 10034–10039
- Li N, Zhao JD, Warren PV, Warden JT, Bryant DA and Golbeck JH (1991) PsaD is required for the stable binding of PsaC to the Photosystem I core protein of *Synechococcus* sp. PCC 6301. *Biochemistry* 30: 7863–7872
- Lunde C, Jensen PE, Haldrup A, Knoetzel J and Scheller HV (2000) The PSI-H subunit of Photosystem I is essential for state transitions in plant photosynthesis. *Nature* 408: 613–615
- Makewicz A, Radunz A and Schmidt GH (1996) Comparative immunological detection of lipids and carotenoids on peptides of Photosystem I from higher plants and cyanobacteria. *Z Naturforsch* 51c: 319–328
- Manna P and Chitnis PR (1999) Function and molecular genetics of Photosystem I. In: Singhal GS, Renger G, Sopory SK, Irrgang KD and Govindjee (eds) *Concepts in Photobiology: Photosynthesis and Photomorphogenesis*, pp 221–263. Narosa Publishing House, New Delhi
- Marcus RA and Sutin N (1985) Electron transfer in chemistry and biology. *Biochim Biophys Acta* 811, 265–322
- McDermott G, Prince SM, Freer AA, Hawthornthwaite-Lawless AM, Papiz MZ, Cogdell RJ and Isaacs NW (1995) Crystal structure of an integral membrane light-harvesting complex from photosynthetic bacteria. *Nature* 374: 517–521
- Melkozernov AN (2001) Excitation energy in Photosystem I from the oxygenic organisms. *Photosyn. Res* 70: 129–153
- Melkozernov AN, Schmid VHR, Schmidt GW and Blankenship RE (1998) Energy distribution in heterodimeric light-harvesting complex LHCl-730 of Photosystem I. *J Phys Chem B* 102: 8183–8189.
- Melkozernov AN, Lin S, Schmid VHR, Paulsen H, Schmidt GW and Blankenship RE (2000a) Ultrafast excitation dynamics of low energy pigments in reconstituted peripheral light-harvesting complexes of Photosystem I. *FEBS Lett* 471: 89–92
- Melkozernov AN, Lin S and Blankenship RE (2000b) Excitation dynamics and heterogeneity of energy equilibration in the core antenna of Photosystem I from the cyanobacterium *Synechocystis* sp. PCC 6803. *Biochemistry* 39: 1489–98
- Melkozernov, AN, Schmid, VHR, Lin, S, Paulsen H, and Blankenship RE (2002) Excitation energy transfer in the Lhca1 subunit of LHC I-730 peripheral antenna of Photosystem I. *J Phys Chem* 106: 4313–4317
- Mühlenhoff U, Hachnel W, Witt HT and Herrmann RG (1993) Genes encoding eleven subunits of Photosystem I from the thermophilic cyanobacterium *Synechococcus* sp. *Gene* 127: 71–78
- Mukerji I and Sauer K (1993) Energy transfer dynamics of an isolated light harvesting complex of Photosystem I from spinach: Time-resolved fluorescence measurements at 295 K and 77 K. *Biochim Biophys Acta* 1142: 311–321
- Mullineaux CW (1994) Excitation energy transfer from phycobilisomes to Photosystem I in a cyanobacterial mutant lacking Photosystem II. *Biochim Biophys Acta* 1184: 71–77
- Nielsen VS, Mant A, Knoetzel J, Möller BL and Robinson C (1994) Import of barley Photosystem I subunit N into the thylakoid lumen is mediated by a bipartite presequence lacking an intermediate processing site. *J Biol Chem* 269: 3762–3766
- Nitschke W and Rutherford AW (1991) Photosynthetic reaction centres: Variations on a common structural theme? *Trends Biochem Sci* 16: 241–5
- Ohyama K, Fukazawa H, Kohchi T, Shirai H, Tohru S, Sano S, Umesono K, Shiki Y, Takeuchi M, Chang Z, Aota SI, Inokuchi H and Ozeki H (1986) Chloroplast gene organization deduced from complete sequence of liverwort *Marchantia polymorpha* Chloroplast DNA. *Nature* 322: 572–574
- Pålsson LO, Tjus SE, Andersson B and Gillbro T (1995) Ultrafast energy transfer dynamics resolved in isolated spinach light-harvesting complex I and the LHC I-730 subpopulation. *Biochim Biophys Acta* 1230: 1–9
- Pålsson LO, Flemming C, Gobets B, van Grondelle R, Dekker JP and Schlodder E (1998) Energy transfer and charge separation in Photosystem I: P700 oxidation upon selective excitation of the long-wavelength antenna chlorophylls of *Synechococcus elongatus*. *Biophys J* 74: 2611–2622
- Pierlstein RM (1992) Theoretical interpretation of antenna spectra. In: Scheer H (ed) *Chlorophylls*, pp 1047–1078. CRC Press, Boca Raton
- Ramesh VM, Gibasiewicz K, Lin S and Webber AN (2001) Specific mutations of the PsaB methionine axial ligand to chlorophyll A<sub>0</sub> of PS I in *Chlamydomonas reinhardtii*. In *PS2001: Proceedings 12th International Congress on Photosynthesis*, S6-025. CSIRO Publishing, Melbourne [CD-ROM]
- Rätsep M, Johnson TW, Chitnis PR and Small GJ (2000) The red-absorbing chlorophyll *a* antenna states of Photosystem I: A hole-burning study of *Synechocystis* sp. PCC 6803 and its mutants. *J Phys Chem* 104: 836–847
- Rivados A, Zucchelli G, Garlaschi FM and Jennings RC (1999) The importance of PS I chlorophyll red forms in light-harvesting by leaves. *Photosynth Res* 60: 209–215
- Roemer S, Senger H and Bishop NI (1995) Characterization of the carotenoid less strain of *Scenedesmus obliquus* mutant C-6E, a living Photosystem I model. *Bot Acta* 108: 80–86
- Rousseau F, Sétif P and Lagoutte B (1993) Evidence for the involvement of PSI-E subunit in the reduction of ferredoxin by Photosystem I. *EMBO J* 12: 1755–1765
- Sárvári E, Malatinszky G and Nyitrai P (1995) Organisation of Photosystem I antenna. In: Mathis P (ed), *Photosynthesis: From Light to Biosphere*, Vol I, pp 195–198. Kluwer Academic Publishers, Dordrecht
- Schlodder E, Falkenberg K, Gergeleit M and Brettel K (1998) Temperature dependence of forward and reverse electron transfer from A<sub>1</sub><sup>+</sup>, the reduced secondary electron acceptor in Photosystem I. *Biochemistry* 37: 9466–9476
- Schlodder E, Paul A und Çetin M (2001) Triplet States in Photosystem I Complexes from *Synechococcus elongatus*. In *PS2001: Proceedings 12th International Congress on Photosynthesis*, S6-015. CSIRO Publishing, Melbourne [CD-ROM]
- Schmid VH, Cammarata KV, Bruns BU and Schmidt GW (1997) In vitro reconstitution of the Photosystem I light-harvesting complex LHCl-730: Heterodimerization is required for antenna pigment organization. *Proc Natl Acad Sci USA* 94: 7667–7672
- Schmid VHR, Thomé P, Rühle W, Paulsen H, Kühlbrandt W and

- Rogl H (2001) Chlorophyll *b* is involved in long-wavelength spectral properties of light-harvesting complexes LHC I and LHC II. *FEBS Lett* 499: 27–31
- Schwabe TME and Kruij J (2000) Biogenesis and assembly of Photosystem I. *Indian J Biochem Biophys* 37: 351–359
- Schubert WD, Klukas O, Saenger W, Witt HT, Fromme P and Krauss N (1998) A common ancestor for oxygenic and anoxygenic photosynthetic systems: A comparison based on the structural model of Photosystem I. *J Mol Biol* 280: 297–314
- Sétif P, Hanley J, Barth P, Bottin H and Lagoutte B (1995) Ferredoxin reduction by PS I with wild type, deleted and site-directed mutants from the cyanobacterium *Synechocystis* sp. PCC6803. In: Mathis P (ed) *Photosynthesis: From Light to Biosphere*, Vol I, pp 23–28. Kluwer Academic Publishers, Dordrecht
- Shen G, Zhao J, Reimer SK, Antonkine ML, Cai Q, Weiland SM, Golbeck JH and Bryant DA (2002) Assembly in Photosystem I. I. Inactivation of the *rubA* gene encoding a membrane-associated rubredoxin in the cyanobacterium *Synechococcus* sp. PCC 7002 causes a loss of Photosystem I activity. *J Biol Chem* 277: 20343–20354
- Shen G, Antonkine ML, van Der Est A, Vassiliev IR, Brettel K, Bittl R, Zech S, Zhao J, Stehlik D, Bryant DA and Golbeck JH (2002a) Assembly of Photosystem I. II. Rubredoxin is required for the in vivo assembly of FX in *Synechococcus* sp. PCC 7002 as shown by optical and EPR spectroscopy. *J Biol Chem* 277: 20355–20366
- Shubin VV, Bezsmertnaya IN and Karapetyan NV (1992) Isolation from *Spirulina* membranes of two Photosystem I-type complexes, one of which contains chlorophyll responsible for the 77 K fluorescence band at 760 nm. *FEBS Lett* 309: 340–342
- Sonoike K, Hatanaka H and Katoh S (1993) Small subunits of Photosystem I reaction center complexes from *Synechococcus elongatus*. II. The *psaE* gene product has a role to promote interaction between the terminal electron acceptor and ferredoxin. *Biochim Biophys Acta* 1141: 52–57
- Strotmann H and Weber N (1993) On the function of PsaE in chloroplast Photosystem I. *Biochim Biophys Acta* 1143: 204–210
- Sundström V and van Grondelle R (1995) Kinetics and excitation transfer and trapping in purple bacteria. In: Blankenship RE, Madigan MT and Bauer CE (eds) *Anoxygenic Photosynthetic Bacteria*, pp 349–372. Kluwer Academic Publishers, Dordrecht
- Thayer SS and Björkman O (1992) Carotenoid distribution and deepoxidation in thylakoid pigment-protein complexes from cotton leaves and bundle-sheath cells of maize. *Photosynth Res* 33: 213–225
- Trissl HW (1993) Long wavelength absorbing antenna pigments and heterogeneous absorption bands concentrate excitons and increase absorption cross section. *Photosynth Res* 35: 247–263
- Trissl HW (1997) Determination of the quenching efficiency of the oxidized primary donor of Photosystem I, P700<sup>+</sup>: Implications for the trapping mechanism. *Photosynth Res* 54: 237–240
- Turconi S, Weber, G, Schweitzer, H, Strotmann H and Holzwarth, AR (1994) Energy transfer and charge separation in Photosystem I. 2. Picosecond fluorescence study of various PS I particles and light-harvesting complex isolated from higher plants. *Biochim Biophys Acta* 1187: 324–334
- van Grondelle, R, Dekker JP, Gillbro T and Sundström V (1994) Energy transfer and trapping in photosynthesis. *Biochim Biophys Acta* 1187: 1–65
- Xia D, Yu CA, Kim H, Xia JZ, Kachurin AM, Zhang L, Yu L and Deisenhofer J (1997) Crystal structure of the cytochrome *bc<sub>1</sub>* complex from bovine heart mitochondria. *Science* 277: 60–66
- Xu Q, Armbrust TS, Guikema JA and Chitnis PR (1994a) Organization of Photosystem I polypeptides: A structural interactions between PsaD and PsaL subunits. *Plant Physiol* 106: 1057–1063
- Xu Q, Guikema JA and Chitnis PR (1994b) Identification of surface-exposed domains on the reducing side of Photosystem I. *Plant Phys* 106: 617–624
- Xu Q, Jung YS, Chitnis VP, Guikema JA, Golbeck JH and Chitnis PR (1994c) Mutational analysis of Photosystem I polypeptides in *Synechocystis* sp. PCC 6803. Subunit requirements for reduction of NADP<sup>+</sup> mediated by ferredoxin and flavodoxin. *J Biol Chem* 269: 21512–8
- Xu Q, Yu L, Chitnis VP and Chitnis PR (1994d) Function and organization of Photosystem I in a cyanobacterial mutant strain that lacks PsaF and PsaJ subunits. *J Biol Chem* 269: 3205–11
- Xu Q, Hoppe D, Chitnis VP, Odom WR, Guikema JA and Chitnis PR (1995) Mutational analysis of Photosystem I polypeptides in the cyanobacterium *Synechocystis* sp. PCC 6803. Targeted inactivation of *psaL* reveals the function of *psaL* in the structural organization of *psaL*. *J Biol Chem* 270: 16243–50
- Zanetti G and Merati G (1987) Interaction between Photosystem I and ferredoxin. Identification by chemical cross-linking of the polypeptide which binds ferredoxin. *Eur J Biochem*. 169: 143–6
- Zhang H, Goodman HM and Jansson S (1997) Antisense inhibition of the Photosystem I antenna protein Lhca4 in *Arabidopsis thaliana*. *Plant Physiol* 115: 1525–1531
- Zilber AL and Malkin R (1992) Organization and topology of Photosystem I subunits. *Plant Physiol* 99: 901–911
- Zouni A, Witt HT, Kern J, Fromme P, Krauß N, Saenger W and Orth P (2001) Crystal structure of Photosystem II from *Synechococcus elongatus* at 3.8 Å resolution. *Nature* 409: 739–743

# Chapter 9

## Antenna Systems and Energy Transfer in Cyanophyta and Rhodophyta

Mamoru Mimuro\*

*Department of Technology and Ecology, Hall of Global Environmental Research,  
Kyoto University, Yoshida-Honmachi, Sakyo-ku, Kyoto 606-8501, Japan*

Hiroto Kikuchi

*Department of Physics, Nippon Medical School, 2-297-2 Kosugi-cho,  
Nakahara-ku, Kawasaki, 211-0063, Japan*

Summary .....	282
I. Introduction .....	282
II. Molecular Architecture of Antenna Systems in Cyanobacteria and Red Algae .....	282
A. Membrane-bound Antenna Complexes .....	282
B. Antenna Complexes Outside of Membranes—Phycobiliproteins .....	283
1. Molecular Organization of Phycobiliproteins .....	283
2. Spectroscopic Properties of Phycobiliproteins .....	287
3. Binding of Chromophores to Phycobiliproteins .....	287
4. Evolution of the Phycobiliprotein Family and Linkage to the Globin Family .....	288
5. Phycobilisome Architecture .....	290
III. Energy Flow in Antenna Systems of Cyanobacteria .....	291
IV. Three-Dimensional Structures of Phycobiliproteins .....	292
A. Basic Structures .....	292
B. Allophycocyanin .....	293
C. Phycocyanin .....	295
D. Phycoerythrocyanin .....	296
E. Phycoerythrin .....	296
F. Cryptophycean Phycoerythrin .....	297
G. Modification of the Three-Dimensional Structures by Linker Polypeptides .....	297
V. Electronic States of Chromophores in Phycobiliproteins .....	298
A. Relationship between Chromophore Configurations and Electronic States .....	298
1. Chromophore Species .....	298
2. Configuration of the Bound Chromophore .....	298
3. Electrostatic Fields from the Surrounding Protein .....	298
4. The Protonation State of the Chromophore .....	299
5. Interactions Between Chromophores .....	299
B. Dynamic Fluctuations of Phycobiliprotein Structures .....	299
VI. Energy Transfer .....	301
A. Theory of Energy Transfer .....	301
B. Experimental Analyses in C-PC .....	301
VII. Concluding Remarks .....	302
Acknowledgments .....	302
References .....	302

---

\* Author for correspondence, email: mamo\_mi@bio.h.kyoto-u.ac.jp

## Summary

The molecular architecture and energy transfer processes in the phycobilin-chlorophyll antenna systems of *Cyanophyta*, *Glaucophyta*, *Rhodophyta* and *Cryptophyta* are discussed with an emphasis on the molecular structures of the individual phycobiliprotein building blocks. The assembly of phycobilisomes from phycobiliproteins is explained, from the binding of chromophores to the individual apoproteins to the binding of phycobilisomes to thylakoid membranes. Structure-function relationships in phycobiliproteins are discussed in the light of the crystal structures and a normal-mode analysis. The normal-mode analysis helps to clarify aspects of the protein structure that are critical for determining the optical properties of phycobiliproteins. A gradient of energy levels in phycobilisomes is realized by binding of specific linker polypeptides to common building blocks. Energy-transfer processes are clearly shown by the time-resolved fluorescence spectra of intact cells and isolated phycobilisomes. The rate of energy transfer between weakly interacting chromophores can be described by the Förster mechanism, and the predictions agree well with the experimental results. Evolution of phycobiliproteins seems to have increased both the number of chromophores per unit monomer and the range of energy levels in the complex, so as to capture an increasing fraction of the available solar energy. Further analyses on the basis of crystal structures should lead to an improved understanding of how interactions of the chromophores with the protein maximize the efficiency of light capture.

## I. Introduction

Phycobiliproteins are pigment-protein complexes that form major components of the photosynthetic antenna systems of *Cyanophyta* (cyanobacteria), *Glaucophyta*, *Rhodophyta* (red algae) and *Cryptophyta*. In the *Cyanophyta*, *Glaucophyta* and *Rhodophyta*, they occur mainly as large, supermolecular complexes called phycobilisomes, which line the surface of the photosynthetic membrane. Phycobiliproteins and phycobilisomes have been studied extensively by both biochemical and crystallographic techniques. The genes encoding the apoproteins and related colorless proteins have been sequenced and the regulation of their biosynthesis has been elucidated in considerable detail. In this chapter, we will describe recent progress on the structure and function of phycobiliproteins and phycobilisomes from biochemical and biophysical points of view. Regulation of the expression of phycobiliprotein genes will be discussed elsewhere in this book. For other review articles on phycobiliproteins and phycobilisomes, the reader is referred to Gantt (1980), Scheer (1981), Glazer (1985), Sidler (1994), MacColl (1998) and Mimuro et al. (1999).

**Abbreviations:** APC – allophycocyanin; Chl – chlorophyll; PC – phycocyanin; PCB – phycocyanobilin; PE – phycoerythrin; PEB – phycoerythrobilin; PEC – phycoerythrocyanin; PUB – phycourobilin; PVB – phycoviolobilin; RC – reaction center; x-PC and x-PE – forms of phycocyanin and phycoerythrin with different chromophore compositions

## II. Molecular Architecture of Antenna Systems in Cyanobacteria and Red Algae

### A. Membrane-bound Antenna Complexes

The antenna systems of *Cyanophyta*, *Glaucophyta*, *Rhodophyta* and *Cryptophyta* contain two kinds of antenna components: one is associated with integral membrane proteins, and the other is located on the periphery of the photosynthetic membrane. With the exception of the carotenoid-protein complexes of dinoflagellates and the chlorosomes of green bacteria, photosynthetic antennas outside membranes occur only in the above four taxa, and they differ both structurally and functionally from the antenna systems found in other plants or bacteria.

In thylakoid membranes of oxygenic photosynthetic organisms, there are two reaction center (RC) complexes, PS I and PS II (Fig. 1). PS II removes electrons from water molecules and passes them to PS I, which reduces NADP for assimilation of CO<sub>2</sub>. The individual RC complexes contain many different polypeptides, including several kinds of chlorophyll-proteins. The PS I RC is comprised of two major polypeptides (the *psaA* and *psaB* gene products), which bind approximately 100 molecules of Chl *a* and 10 molecules of  $\beta$ -carotene (Jordan et al., 2001). These Chls can be classified functionally into either electron-transfer components or antenna pigments, and most of Chls are part of the antenna. On the other hand, the electron-transfer Chls of the PS II RC are associated with two relatively small

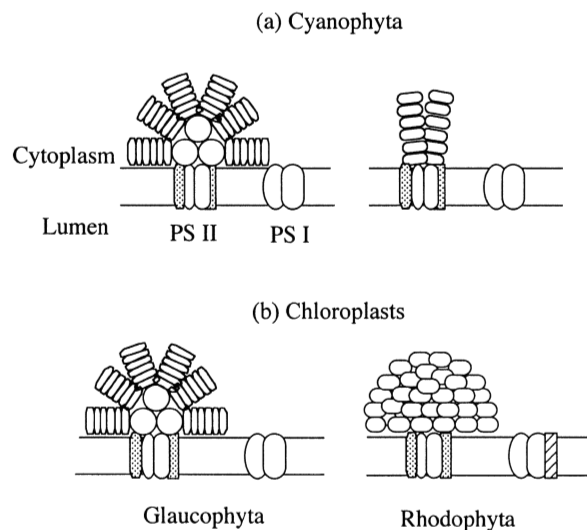


Fig. 1. Arrangement of phycobilin-Chl *a* antenna systems in (a) Cyanophyta and (b) chloroplasts of Glaucophyta and Rhodophyta. Two photosynthetic units (PS I and II) are located in the membrane. The proteins represented by stippled symbols are CP47 and CP43, the core antennas of PS II, and those without stippling are reaction center proteins or phycobiliproteins. Phycobilisomes are located outside the membrane on the cytoplasmic (cyanobacterial) or stromal (chloroplast) surface. Phycobilisomes with hemidiscoidal shapes (*upper and lower left*) are common in Cyanophyta and Glaucophyta, and rod-like phycobilisomes (*upper right*) are found in the simple cyanobacterium *Gloeobacter violaceus*. Hemidiscoidal and hemispherical (*lower right*) morphologies are found in Rhodophyta, which also have a Chl *a*-binding LHC I (hatched) associated with the PS I core complex

polypeptides (the *psbA* and *psbD* gene products, D<sub>1</sub> and D<sub>2</sub>), which together bind only 6 Chls and 2 pheophytins (Zouni et al., 2001). Additional polypeptides (the *psbB* and *psbC* gene products, CP47 and CP43) associate with the D<sub>1</sub> and D<sub>2</sub> proteins to form complexes that bind a total of approximately 30 Chl *a* molecules and 10  $\beta$ -carotenes. Recently, crystal structures of the PS I (Krauß et al., 1996; Klukas et al., 1999a,b; Jordan et al., 2001) and PS II (Rhee et al., 1998; Zouni et al., 2001) core complexes from a cyanobacterium were resolved at resolutions of 2.5 and 3.8 Å, respectively.

In addition to the fundamental antenna systems of PS I and PS II described above, some prokaryotic cells that contain Chl *b* (*Prochloron*, *Prochlorothrix*) have an unusual Chl-protein called prochlorophyte chlorophyll binding protein (Pcb), which is thought to be related to CP43 (Green and Dunford, 1996; La Roche et al., 1996). *Acaryochloris marina* contains Chl *d* as a major Chl that is found in CP43/CP47 as

well as PsaA/PsaB (Miyashita et al., 1996). On the other hand, an additional antenna protein called LHC I is associated with the PS I core complex in red algae (Rhodophyta) (Wolfe et al., 1994). This protein is assigned to the LHC superfamily, which occurs in the antenna system in all oxygenic photosynthetic organisms except for prokaryotes and Glaucophyta. However, under conditions of light stress, cyanobacteria synthesize small proteins called the 'high-light induced proteins' (Hlips), which share sequence similarity with the first and third transmembrane helices of the LHC superfamily (Dolganov et al., 1995; Chapter 4, Green).

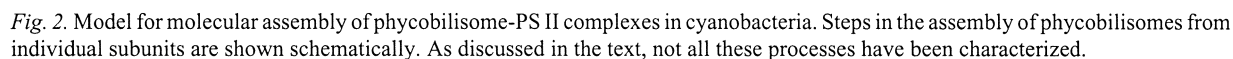
### B. Antenna Complexes Outside of Membranes—Phycobiliproteins

Cyanophyta, Glaucophyta, Rhodophyta and Cryptophyta contain another type of antenna pigments, the phycobiliproteins. Phycobiliproteins are water-soluble proteins that attach externally to the photosynthetic membrane. In Cyanophyta, Glaucophyta and Rhodophyta, phycobiliproteins form large assembled structures called phycobilisomes that are located on the stromal side of membranes (Section II.B.5). In Cryptophyta, individual phycobiliproteins are located on the luminal side of membranes and do not form phycobilisomes (Chapter 11, Hiller and Macpherson).

#### 1. Molecular Organization of Phycobiliproteins

Figure 2 shows a schematic model of construction of the phycobilin-Chl *a* antenna system in cyanobacteria. Essentially the same scheme applies to Glaucophyta and Rhodophyta. The basic unit of all phycobiliproteins is a heterodimer of  $\alpha$  and  $\beta$  subunits, each of which can carry either one, two or three chromophores depending on molecular species (Fig. 3). This unit is conventionally referred to as a monomer. Three of the  $\alpha\beta$  monomers associate to form an  $(\alpha\beta)_3$  trimer, which is the basic building block of phycobilisomes. The trimers assemble into hexamers  $((\alpha\beta)_6)$  and larger structures with the help of additional 'linker' polypeptides, some of which also have bound pigments.

The chromophores bound to phycobiliproteins are called phycobilins. These include four kinds of open-chain tetrapyrroles, whose molecular structures are shown in Fig. 4. The various chromophores differ in the number of conjugated double bonds and their



There are at least four types of phycobiliproteins: phycoerythrin (PE), phycoerythrocyanin (PEC), phycocyanin (PC) and allophycocyanin (APC), which differ in amino acid sequence, the number of chromophores per subunit, and the identities of the chromophores. The compositions of the individual phycobiliproteins are summarized in Table 1. The allophycocyanins include two additional molecular species (APC-B and the ‘anchor polypeptide’), whose energy levels are lower than those of APC. APC-B is sometimes abbreviated to APB. PC and PE also have subclasses with variations in the chromophore species.

Individual phycobiliprotein subunits are hereafter identified by  $\alpha$  or  $\beta$  with a superscript indicating the type of phycobiliprotein, for example  $\alpha^{\text{PC}}$  or  $\beta^{\text{PC}}$  in the case of PC. As mentioned above, the functional unit for the formation of phycobilisomes is an  $(\alpha\beta)_3$  trimer containing three identical  $\alpha\beta$  monomers. Two such trimers form a hexamer, and in the case of PE one copy of an additional subunit ( $\gamma$ ) is also present per hexamer. Under physiological conditions, the minimum unit is the trimer and the monomer is not present. To obtain monomers, a high concentration of chaotropic anion is required (Murakami et al., 1981). In APC, each  $\alpha$ - or  $\beta$ -subunit carries one PCB, whereas in PC, the  $\alpha$ -subunit carries one PCB and the  $\beta$ -subunit has two. In PEC, the  $\alpha$ -subunit has one PVB, and the  $\beta$ -subunit carries two PCBs. PE and PC have several patterns that are identified by a prefix B, b, C or R. C-PE has five PEBs (two in the  $\alpha$ -subunit and three in the  $\beta$ -subunit). B-PE and b-PE are optically very similar, with the same chromophore composition in the  $\gamma$  subunit. They both have absorption maxima at 560 and 545 nm with a shoulder around 500 nm; however, the relative absorption of

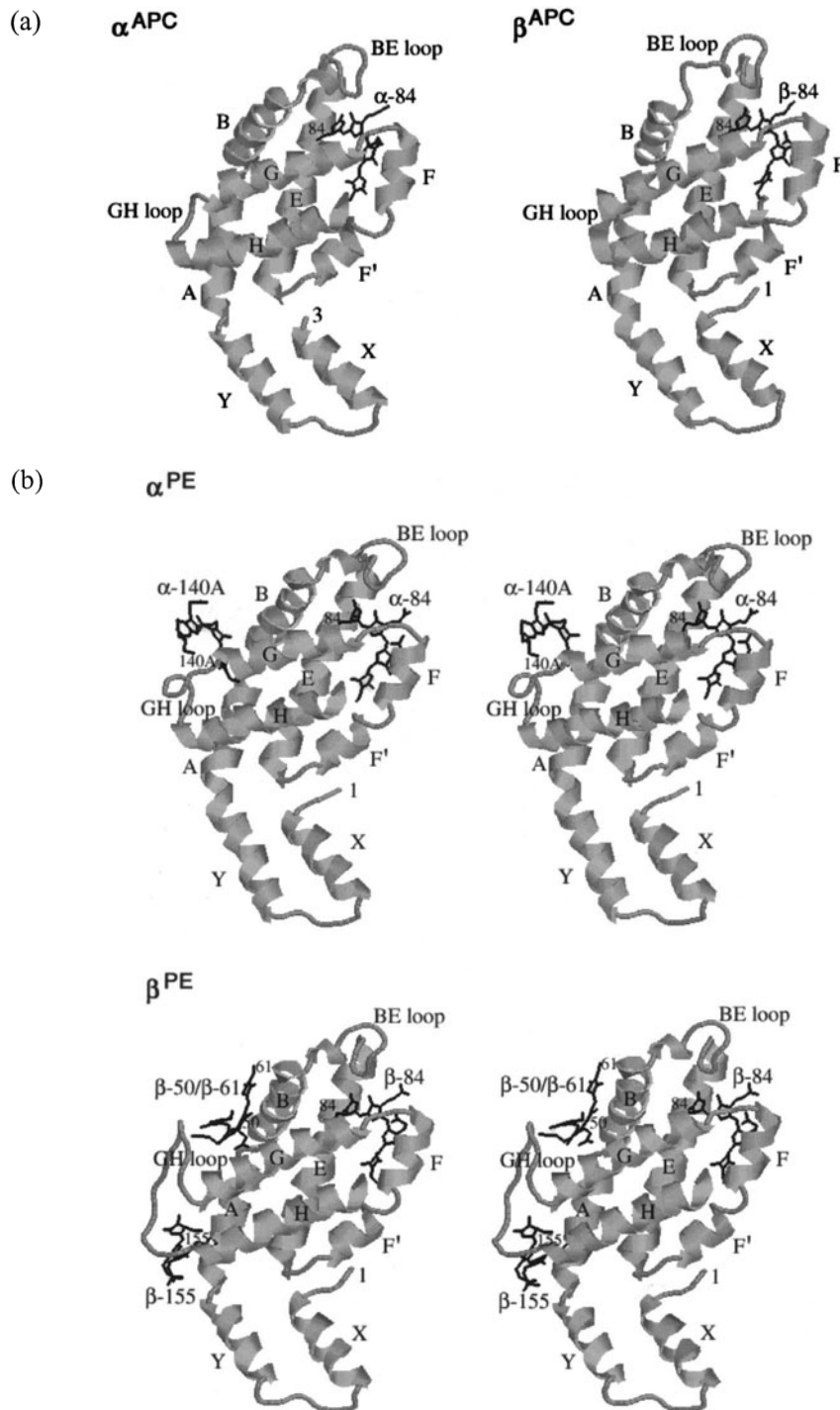


*Fig. 3.* (a) Crystal structures of  $\alpha$ - (left) and  $\beta$ - (right) subunits of APC (top) (Brejc et al., 1996; 1ALL.PDB).  $\alpha$ -helical structural elements are labeled X, Y, A, B, E, F', F, G and H. The amino termini are labeled 1 (or 3 in  $\alpha^{APC}$ , where residues 1 and 2 are disordered). The label 84 on the E helices shows the position of cysteine 84, to which the  $\alpha$ -84 or  $\beta$ -84 chromophore is bound. The  $\alpha$ - and  $\beta$ -subunits fold very similarly but their bilins have slightly different orientations, particularly in ring D. (b) Stereo view of crystal structures of the  $\alpha$ - (middle) and  $\beta$ - (bottom) subunits of R-PE (Chang et al., 1996; 1LIA.PDB). One additional chromophore ( $\alpha$ -140) is attached to the  $\alpha$ -subunit, and two additional chromophores ( $\beta$ -155 and  $\beta$ -50/ $\beta$ -61) to the  $\beta$ -subunit. The attachment sites for these chromophores are labeled 140A, 50, 61 and 155 (see the corresponding cysteines of *b*-PE in Table 2).



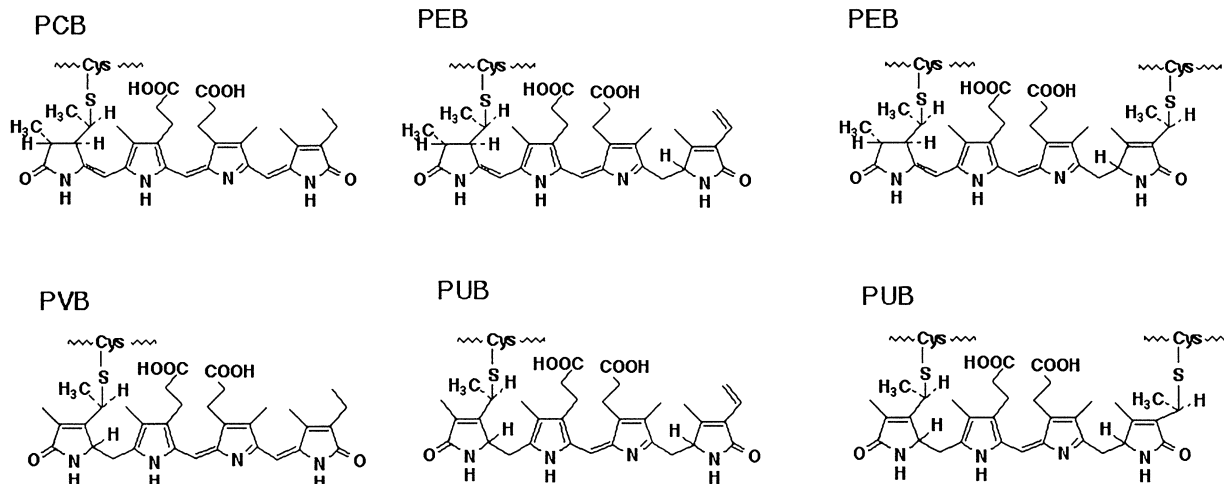


Fig. 4. Molecular structures of the four phycobilins. PCB, phycocyanobilin; PEB, phycoerythrobilin; PVB, phycoviolobilin; and PUB, phycourobilin. The thioether links to Cys residues of the apoproteins also are shown. Pyrrole ring A is on the left in each structure, and D on the right

Table 1. Molecular species of phycobiliproteins and linker polypeptides

Phycobiliprotein	Subunit composition	Chromophores in		Linkers
		$\alpha$ -subunit	$\beta$ -subunit	
Allophycocyanin (APC)				$L_C^{7,8}$ ( $L_C^{8,9}$ ), $L_{CM}$
APC	$(\alpha\beta)_3$	1PCB	1PCB	
APC-B	$(\alpha\beta)_2\alpha^{APB}\beta$	1PCB	1PCB	
Phycocyanin (PC)				$L_R^{8,9}$ , $L_R^{34}$ , $L_{RC}^{29,5}$
C-PC	$(\alpha\beta)_3$	1PCB	2PCB	
R-PC	$(\alpha\beta)_3$	1PCB	1PCB, 1PEB	
Phycoerythrocyanin (PEC)	$(\alpha\beta)_3$	1PVB	2PCB	$L_R^{35}$
Phycoerythrin (PE)				$L_R^{35}$
C-PE	$(\alpha\beta)_3$	2PEB	3PEB	
b-PE	$(\alpha\beta)_6\gamma$	2PEB	3PEB	
		(2PEB & 2PUB in $\gamma$ )		
B-PE	$(\alpha\beta)_6\gamma$	2PEB	3PEB	
		(2PEB & 2PUB in $\gamma$ )		
R-PE	$(\alpha\beta)_6\gamma$	2PEB	2PEB, 1PUB	
		(2PEB & 2PUB in $\gamma$ )		

In the case of PE, numbers in parentheses represent the chromophore composition of the  $\gamma$  subunit. Molecular weights of linker polypeptides of *M. lamosus* are given as superscripts for APC, C-PC and PEC, and those of *F. diplosiphon* for C-PE. The molecular weights are variable, depending on the species.

this shoulder is somewhat higher in B-PE than in b-PE. R-PE has two PEB in the  $\alpha$ -subunit, two PEB and one PUB in the  $\beta$ -subunit, and 2 PEB and 2 PUB on the  $\gamma$ -subunit.

All naturally occurring cyanobacteria and red algae produce APC and PC, even though many cyanobacteria do not synthesize either PEC or PE, (Bryant, 1982). An exception is a species of *Prochlorococcus*

that reportedly contains only PE (Partensky et al., 1999). Almost all species of red algae synthesize PE, but several species resemble cyanobacteria in having only PC and APC. Cryptomonad phycobiliproteins have different peptide sequences and three-dimensional structures, and will be discussed separately in Section IV.F.

## 2. Spectroscopic Properties of Phycobiliproteins

Each of the four kinds of phycobiliprotein has characteristic optical properties (Fig. 5). APC absorbs maximally between 650 and 655 nm; PC, between 595 and 640 nm; PEC, between 570 and 575 nm; and PE, between 500 and 565 nm. The differences in the absorption spectra are caused by several factors, including variations in the chemical species and the three-dimensional conformation of the bound chromophore and differences in the electric field from the protein surrounding the chromophore (Section V.A). In general, the absorption maximum shifts to the red with an increase in the number of conjugated double bonds.

Phycobiliproteins are highly fluorescent. The fluorescence yield of PC was estimated to be higher than 30% on the basis of the fluorescence lifetime of isolated C-PC (Yamazaki et al., 1984). This yield is not particularly high compared to the fluorescence yields of many chromophores in solution. For example, Chl *a* in organic solvents has a fluorescence yield of approximately 30%. However, the fluorescence yield of Chl *a* in antenna systems is decreased to less than 10% of the yield in organic solvents, whereas the fluorescence yield of phycobilins remains high even in the antenna. Energy transfer between the chromophores occurs very efficiently in phycobiliproteins, with the result that most of the fluorescence is emitted by the chromophore whose energy level is the lowest in the complex. PE, for example, emits at 575 nm; PC, at 640 to 645 nm; and APC at 660 to 663 nm. In the case of ACP-B and the anchor polypeptide, emission maxima were observed between 680 and 685 nm or longer. The fluorescence properties are very important when we monitor energy transfer in phycobiliproteins (Section III).

## 3. Binding of Chromophores to Phycobiliproteins

The phycobilin chromophores of phycobiliproteins are bound to the polypeptide chain at conserved positions, either by one cysteinyl thioether linkage through the vinyl substituent on pyrrole ring A of the phycobilin, or by two such linkages through the vinyl substituents on rings A and D (Fig. 4). In almost all cases, one phycobilin is attached at ring A to cysteine 84 of the  $\alpha$ -subunit, and a second phycobilin is bound similarly to cysteine 84 of the  $\beta$ -subunit; these

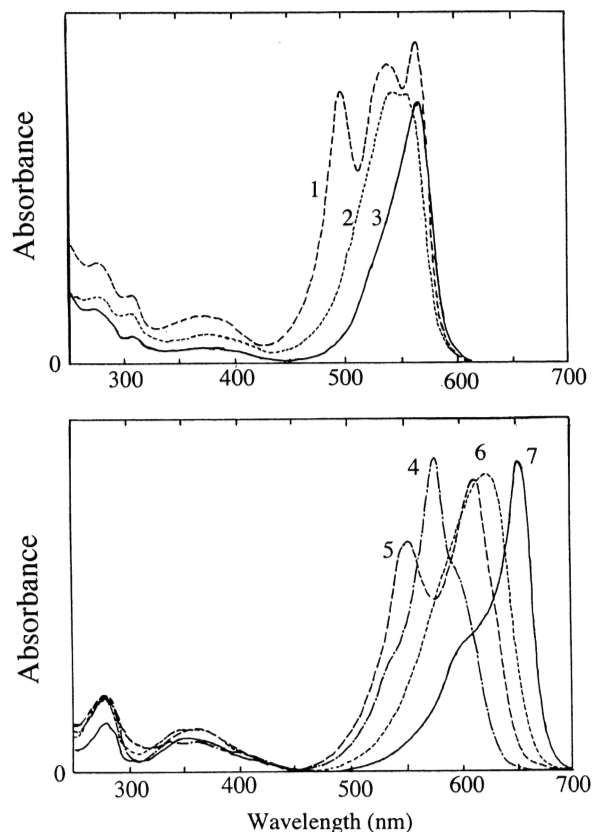


Fig. 5. Absorption spectra of various phycobiliproteins. (1) RPE, (2) B-PE, (3) C-PE, (4) PEC, (5) R-PC, (6) C-PC and (7) APC. The spectra were measured in phosphate buffer (10 mM, pH 6.0) at room temperature. Under these conditions, the protein aggregates to form the trimer or hexamer, and the monomer is not present.

chromophores are called  $\alpha$ -84 or  $\beta$ -84 for convenience. (The amino acid sequences of phycobiliproteins usually are numbered on the basis of the numbering in PC because the crystal structure of PC was the first to be solved. This convention necessitates occasional insertions or deletions in the numbering for other phycobiliproteins.) PC, PEC and PE bind a second chromophore to cysteine 155 in the  $\beta$ -subunit, and the chromophore attached here is called  $\beta$ -155 (Figs. 3 and 6). In PE, the  $\alpha$ -subunit also binds a second phycobilin at cysteine 140B, and cysteines 50 and 61 of the  $\beta$ -subunit bind a third phycobilin through rings A and D. These chromophores are denoted  $\alpha$ -140 and  $\beta$ -50/ $\beta$ -61.

The phycobilin contents of several cyanobacterial phycobiliproteins are shown in Table 1. PEC and PC differ in the chromophore attached to cysteine  $\alpha$ -84,

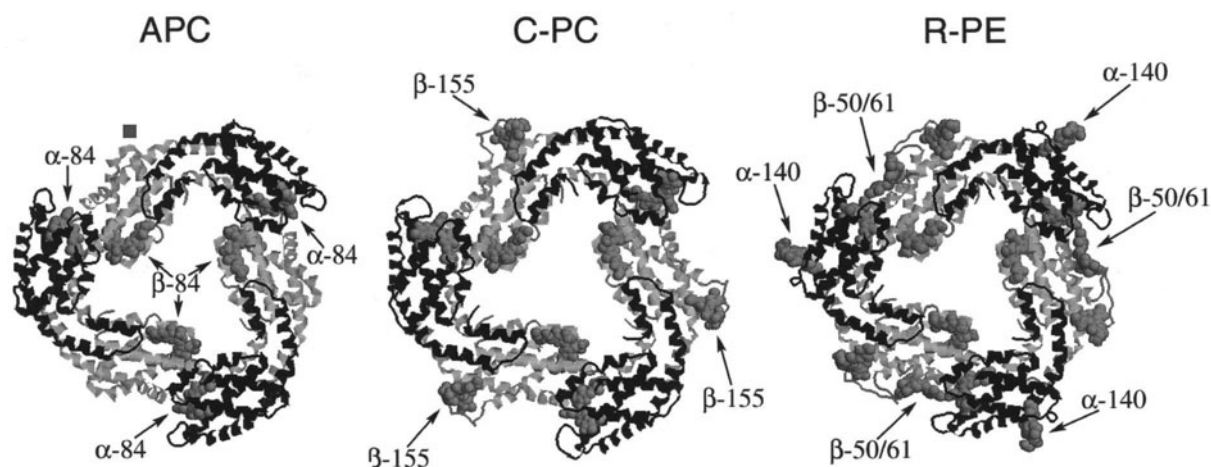


Fig. 6. Crystal structures of three phycobiliproteins (APC, C-PC, and R-PE). These  $(\alpha\beta)_3$  trimers are drawn on the basis of the structures of APC (Brejc et al., 1995; 1ALL.PDB), C-PC (Düring et al., 1991; 1CPC.PDB), and R-PE (Chang et al., 1996; 1LIA.PDB). Each basic block, the  $(\alpha\beta)_3$  trimer, is shown from a viewpoint along the symmetry axis, and chromophores are shown in space-filling representation. APC has one  $\alpha$ -84 chromophore in each  $\alpha$ -subunit (dark gray) and one  $\beta$ -84 chromophore in each  $\beta$ -subunit (light gray). In C-PC,  $\beta$ -155 chromophores are added compared to APC. In R-PE,  $\alpha$ -140 chromophores and  $\beta$ -50/ $\beta$ -61 chromophores are added compared to C-PC. See Color Plate 8.

which is PCB in PC and PVB in PEC. APC containing PUB (phycocyanin WH8501) also has been isolated (Swanson et al., 1991). To express this diversity, it has been proposed that phycobiliproteins be renamed with a two- or three-letter prefix identifying the phycobilin composition (MacColl, 1998). According to this proposal, PEC is CV-phycocyanin and phycocyanin WH8501 is CU-phycocyanin, where C, U, and V represent PCB, PUB, and PVB, respectively.

The folding and oligomerization of phycobiliproteins packs the  $\alpha$ -84 and  $\beta$ -84 chromophores centrally around the symmetry axis of the trimer, and puts the  $\alpha$ -140,  $\beta$ -155 and  $\beta$ -50/ $\beta$ -61 chromophores, if they are present, on the outside (Fig. 6). Variations in the chromophores bound to cysteines  $\alpha$ -140,  $\beta$ -155 and  $\beta$ -50/ $\beta$ -61 require only relatively small adjustments in the tertiary and quaternary structure of the protein. The three-dimensional structures of all the phycobiliproteins thus are very similar. The wide separation of the binding sites avoids short-range interactions between chromophores, which could lead to quenching of fluorescence.

#### 4. Evolution of the Phycobiliprotein Family and Linkage to the Globin Family

All phycobiliproteins except for the  $\alpha$ -subunit of *Cryptophyta* have been assigned to the globin family

of proteins because they fold to form a globin-like domain, even though the level of amino acid identity is not statistically significant. (Ducret et al, 1994; Sidler, 1994; Apt et al, 1995). The similarity in the three-dimensional structures and the conserved chromophore binding site in myoglobin and phycobiliproteins support the view that these proteins emerged from a common ancestor. Hardison (1998) has pointed out the continuous presence of the globin family from bacteria to eukaryotes, and non-photosynthetic prokaryotes have been reported to contain globin-family proteins that could be related to the phycobiliproteins (Wakabayashi et al., 1986). Phycocyanins are assumed to have branched off from an ancestral hemoprotein gene very early, so that the present-day proteins do not have enough sequence similarity to the rest of the globin family to make an entirely convincing tree of all the globins.

A phylogenetic tree of phycobiliproteins can be drawn (Fig. 7 in Chapter 4, Green) since their sequence identity is in the range of 20 to 30% (Table 2). The proteins presumably have evolved by duplication of the gene encoding an individual subunit, followed by mutations of amino acid residues at multiple sites. One point of interest is the branching of the linker protein  $L_{CM}$  away from the  $\alpha$ - and  $\beta$ -subunits of APC (Redlinger and Gantt, 1982).  $L_{CM}$ , which is sometimes called the 'anchor' protein,

Table 2. Primary sequence of several typical phycobiliproteins

Alpha-subunit		1	50	90
APC	--SIVTKSIVNRAAEARYLS	↓	↓	↓
C-PC	MKTPLTEAVALLASOGREFLS	↓	↓	↓
PEC	MKTPLTEAVALLASOGREFLS	↓	↓	↓
C-PE	MKSIVTTVIAAAAPAGRFP	↓	↓	↓
b-PE	MKSIVTTVIAAAAPAGRFP	↓	↓	↓
Beta-subunit		1	50	90
APC	MQDAITSVINSSVQGGKYLDRSAIQK	↓	↓	↓
C-PC	MQDAITSVINSSVQGGKYLDRSAIQK	↓	↓	↓
PEC	MQDAITSVINSSVQGGKYLDRSAIQK	↓	↓	↓
C-PE	MQDAITSVINSSVQGGKYLDRSAIQK	↓	↓	↓
b-PE	MQDAITSVINSSVQGGKYLDRSAIQK	↓	↓	↓
Alpha-subunit		91	140	141
APC	YLRITGIVAGDVTPIEEIGV	↓	↓	↓
C-PC	YLRITGIVAGDVTPIEEIGV	↓	↓	↓
PEC	YLRITGIVAGDVTPIEEIGV	↓	↓	↓
C-PE	YLRITGIVAGDVTPIEEIGV	↓	↓	↓
b-PE	YLRITGIVAGDVTPIEEIGV	↓	↓	↓
Beta-subunit		91	140	141
APC	YLRITGIVAGDVTPIEEIGV	↓	↓	↓
C-PC	YLRITGIVAGDVTPIEEIGV	↓	↓	↓
PEC	YLRITGIVAGDVTPIEEIGV	↓	↓	↓
C-PE	YLRITGIVAGDVTPIEEIGV	↓	↓	↓
b-PE	YLRITGIVAGDVTPIEEIGV	↓	↓	↓

The APC sequence is from *S. platensis* (Sidler et al., 1981), C-PC from *Agmenellum quadruplicatum* (Pilot and Fox, 1984; Schirmer et al., 1986), PEC from *M. laminosus* (Füglstadler et al., 1983), C-PE from *Calothrix* PCC 7601 (Sidler et al., 1986), and b-PE from *P. cruentum* (Sidler et al., 1989). Residues responsible for binding chromophores (cysteine, C) or stabilizing the chromophores (aspartic acid, D) are printed in white on black backgrounds. Other residues that are conserved in both the  $\alpha$  and  $\beta$  subunits are shown in dark gray, and residues that are conserved only in one subunit are in light gray. The PGGNXY motif is boxed. The sequence numbering is based on the  $\beta$ -subunit of C-PC, and requires some deletions and/or insertions in the other sequences. Bars and letters above the sequences indicate the  $\alpha$ -helical regions of C-PC.

contains a chromophore binding site and associates with APC subunits in phycobilisomes (see below). The separation of  $L_{CM}$  from the  $\alpha$ - and  $\beta$ -subunits thus may be critical for the evolution of phycobilisomes. However, there are two contradictory analyses of the branching point of the anchor polypeptide (Ducret et al., 1994; Apt et al., 1995). Another interesting, and possibly related feature is the grouping of the  $\alpha$ - and  $\beta$ -subunits of APC. Although Sidler (1994) has suggested that these two subunits belong to the same branch of the phylogenetic tree, other analyses favor placing them on different branches (Ducret et al., 1994; Apt et al., 1995). The phylogenetic tree of phycobiliproteins thus remains to be clearly resolved.

Comparisons of the chromophore attachment sites in various phycobiliproteins suggest that the attachment site at cysteine  $\alpha$ -84 or  $\beta$ -84 has been conserved in APC, PC, PEC, C-PE, B-PE and b-PE, and may be primordial. During evolution, each additional binding site apparently was acquired by insertion of a small peptide containing a cysteine residue as an attachment site. In line with this scheme, the total number of chromophores per  $\alpha\beta$  unit increases with time in the phylogenetic tree: APC has two chromophores, PC and PEC have three, and PE has five. As noted above, these additional chromophores are found in loops on the protein surface and are at the periphery of the  $(\alpha\beta)_3$  structure (Fig. 6). Along with each new chromophore-binding cysteine, an aspartic acid residue also was added, probably to tailor the electronic states of the chromophore (see below). The combination of a cysteine residue as a binding site and a nearby aspartic acid residue thus appears to be a critical index for the evolutionary development of phycobiliproteins. The choice of the chromophore also changed with evolution. The phycobiliproteins at the periphery have chromophores that absorb light at shorter wavelengths (higher energy) than those at the center. This selection of molecular species ensures a high probability of light absorption over a very broad spectrum and creates a gradient of energy levels that favors efficient energy transfer to the core (see below).

### 5. Phycobilisome Architecture

Phycobiliproteins function in assembled forms, phycobilisomes, in cyanobacteria, *Glaucophyta* and red algae, while a much smaller form is the functional unit in *Cryptophyta* (Section IV.F). Phycobilisomes

were first discovered on the surface of thylakoid membranes in the red alga *Porphyridium cruentum* (Gantt and Conti, 1966), and subsequently were found in many species of cyanobacteria and *Glaucophyta* (Giddings et al., 1983). The overall morphology of phycobilisomes has been investigated extensively by electron microscopy (Gantt and Conti, 1966; Gantt et al., 1968). There are two typical types of morphology, hemidisoidal and hemiellipsoidal (Fig. 1). The hemidisoidal shape is found throughout phycobilin-containing organisms, whereas the hemiellipsoidal shape is seen mainly in cells rich in PE. A third, rod-like morphology was described in the cyanobacterium *Gloeobacter violaceus*, but is exceptional (Guglielmi et al., 1981).

The basic structure of hemidisoidal phycobilisomes consists of a set of rods radiating from a central core (Fig. 2). Each of the rods is constructed from a pile of phycobiliprotein  $(\alpha\beta)_3$  units. These units contain PC as an essential constituent, and often contain PE and/or PEC as well, depending on the organism. The core, which attaches to the thylakoid membrane, is made up of a small and variable number of APC units. In an AN112 mutant of *Synechococcus* PCC 6301 the core contains only two dodecamer APC units, while in *Mastigocladus laminosus* it contains three dodecamer and two hexamer units (Glazer et al., 1985). However, the basic morphology always consists of a pile of cylinders aligned laterally.

The structure of hemiellipsoidal phycobilisomes is less clear. However, antibodies raised against PE bind to the outer surface and antibodies to APC bind to the flat end part of hemiellipsoidal phycobilisomes (Gantt et al., 1976), suggesting that the overall morphology is identical to that of hemidisoidal phycobilisomes. Since APC has the lowest energy levels of all the phycobiliproteins, a gradient of energy level to thylakoid membranes exists in both types of phycobilisomes.

In addition to phycobiliproteins, phycobilisomes contain colorless linker polypeptides that connect the phycobiliproteins (Fig. 2). Linker polypeptides are abbreviated L with a subscript to indicate their location in the phycobilisome and, in some cases, a superscript for the molecular mass in kD (Glazer, 1985). There are four types of linkers: linkers within the rod structure ( $L_R$ ), linkers that connect the rod to the core ( $L_{RC}$ ), linkers within the core ( $L_C$ ), and linkers that connect the core to the thylakoid membrane ( $L_{CM}$ ).  $L_{CM}$  appears to be a unique species,

but each of the other three groups includes several different proteins.  $L_R^8$  and  $L_R^9$  are small polypeptides that sit on the distal ends of rods;  $L_R^{34}$ ,  $L_R^{35}$ , and  $L_{RC}^{29.5}$  are involved in elongating the rod and positioning the hexamers within the rod (de Lorimier et al., 1990).  $L_C$  is usually a small polypeptide with a molecular mass of 9 kDa;  $L_{CM}$  (the anchor polypeptide) is a much larger protein with a molecular mass in the range of 60 to 120 kDa (Redlinger and Gantt, 1982).

Because the molecular structure of the C-PE trimer is very similar to those of PC and APC, replacing PC by C-PE during chromatic adaptation (Grossman et al., 1993) probably does not change the overall morphology of phycobilisomes. However, the association of the  $\gamma$ -subunit with B-PE or R-PE may lead to a somewhat different morphology (Ficner and Huber, 1993).

### III. Energy Flow in Antenna Systems of Cyanobacteria

Phycobilisomes are efficient antenna systems and the light energy they absorb is transferred rapidly to the RC in the thylakoid membranes through antenna complexes in the membranes. The steps of the energy-transfer process can be resolved by fluorescence spectroscopy, as shown in Fig. 7A for whole cells of the cyanobacterium *Anabaena variabilis* (M-3) at  $-196^\circ\text{C}$  (Mimuro, 1990). Upon excitation of C-PC at 580 nm, the emission peaking at 645 nm shortly after the excitation comes from PC, which absorbed most of the 580-nm excitation flash in these experiments. Fluorescence at 660 nm from APC grows on a time scale of several hundred ps after the excitation, and is followed by emission from the Chl *a* of both PS II (685 and 695 nm) and PS I (730 nm).

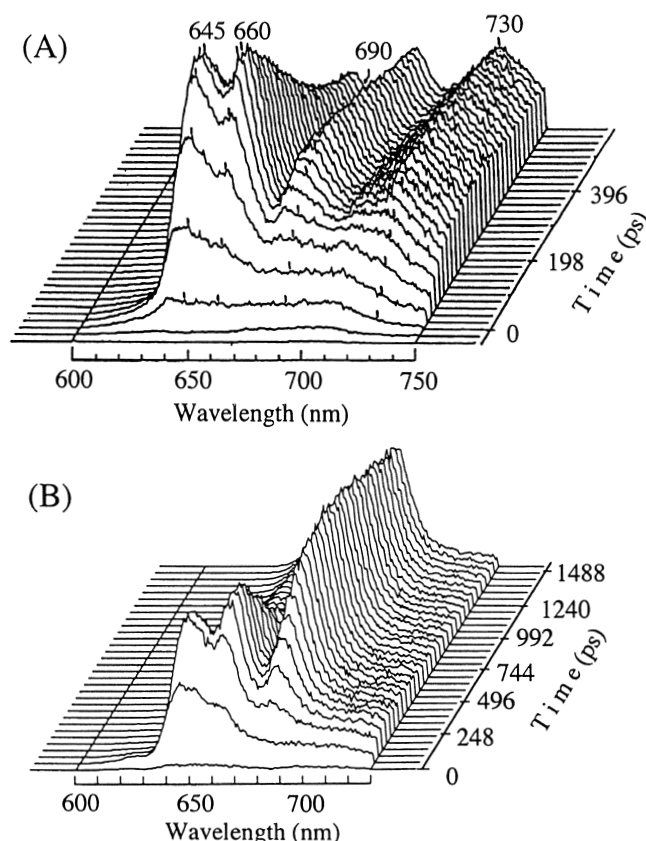


Fig. 7. Excitation energy flow in the cyanobacterium *Anabaena variabilis* (M-3). Time-resolved fluorescence spectra at  $-196^\circ\text{C}$  in intact cells (A) (Mimuro, 1990) and isolated phycobilisomes (B) (Mimuro et al., 1989) are shown. An excitation wavelength of 580 nm was used to excite C-PC preferentially.

Yamazaki et al. (1984) have made similar measurements in the red alga *Porphyridium cruentum* and *Anacystis nidulans* (*Synechococcus* sp. PCC 6301)).

The excitation spectrum for PS I emission at low temperature shows that phycobilisomes serve as an antenna for PSI as well as PS II (Ley and Butler, 1977; Mimuro and Fujita, 1977), but the pathways of energy transfer from phycobilisomes to PS I are not entirely clear. There are two possible pathways: a direct route from phycobilisomes to the PS I core complex, as proposed by Mullineaux et al. (1994, 1997), and an indirect route via PS II. Ley and Butler (1977) showed that about 50% of the energy absorbed by phycobilisomes is transferred to PS I when the PS II traps are open, and that this portion increases to more than 90% when the PS II traps are closed. Because the probability of charge recombination in PS II RCs is usually very low when the traps are open (less than 1% in intact cells (Haug et al., 1972; Arnold, 1991)), it is unlikely that the transfer of energy to PS I represents only the excess energy released by charge-recombination. It appears, rather, to reflect either a direct connection of phycobilisomes to PS I or a constitutive process in which energy flows transiently through the PS II antenna. If phycobilisomes are connected directly to PS I, we might expect the rise time of phycobilin-sensitized emission from PS I at low temperature to be much shorter than that of emission from PS II; however, to our knowledge, such fluorescence kinetics have not been described. In the measurements shown in Fig. 7A, for example, fluorescence from PS I and PS II rose with essentially the same kinetics.

Evidence for heterogeneous energy levels in phycobiliproteins was found in time-resolved fluorescence spectra of intact cells (Mimuro, 1990) and isolated phycobilisomes (Mimuro et al., 1989) (Fig. 7). The emission peak of PC shifted from 638 nm to 645 nm with time, suggesting a successive shift of the main population of excited components. A smaller shift from 660 to 663 nm occurred in APC. In PS II, the emission maximum appeared initially at 684 nm and then shifted to 695 nm. Since the 685- and 695-nm components are known to be distinct (Murata and Satoh, 1986), the shift of the emission spectrum probably reflects movements of the excitation through a succession of components rather than a relaxation of a homogeneous population. In the case of PS I Chl *a*, the peak appeared first at approximately 715 nm and then shifted to 730 nm with time. This shift of the Chl *a* emission also

suggests a migration of the excitation among several spectral components of PS I.

The transfer of energy from PC to APC is particularly clear in the time-resolved emission spectrum when PC is excited in isolated phycobilisomes (Fig. 7B). Shifts of the emission maxima again were discernible; the emission peaked initially at 638, 660, and 680 nm for PC, APC and the final emitter, respectively, and shifted to 645, 666, and 686 nm, respectively, with time. These results suggest that each component of the phycobilisome is significantly heterogeneous.

The sequence of energy transfer in the phycobilisome antenna follows the gradient of energy levels in the pigments. At the connecting site of phycobilisomes to membranes, there are two specialized phycobiliproteins,  $\alpha^{APB}$  and the anchor polypeptide ( $L_{CM}$ ), either of which could, in principle, serve as the energy donor to the Chl *a* antenna in the membranes. The pigment in these proteins has a fluorescence maximum around 685 nm, very close to the level of the Chl *a* antenna. The functions of  $\alpha^{APB}$  and  $L_{CM}$  were examined by fluorescence polarization spectroscopy (Mimuro et al., 1986b). The excitation polarization spectrum at  $-196^\circ\text{C}$  showed that  $L_{CM}$  was connected to the antenna in the membranes. This was confirmed by studies of a mutant lacking the  $L_{CM}$  gene (Zhao et al., 1992). The  $\alpha^{APB}$  does not transfer energy to Chl *a* in the membranes, and therefore, is postulated to be the terminal pigment in the phycobilisome.

The overall efficiency of energy transfer from phycobilisomes to the RC has been estimated to be about 80 to 90% by comparison of the excitation spectrum of fluorescence with absorption spectrum. Compared with the antenna systems of other organisms, this value is not particularly high. Energy flow in red algae has not been discussed extensively. However, the time-resolved fluorescence spectra show that the flow in these organisms is essentially identical to that in cyanobacteria (Yamazaki et al., 1984).

#### IV. Three-Dimensional Structures of Phycobiliproteins

##### A. Basic Structures

Three-dimensional structures of the four known kinds of phycobiliproteins are similar, despite the relatively low level of amino acid identity in the primary



sequences (Table 2). As mentioned above, phycobiliproteins are assigned to the globin family and their overall folding is similar to that of myoglobin. Their  $\alpha$ -helical structural elements were, therefore, named following the scheme used for myoglobin (Schirmer et al., 1985).

The  $(\alpha\beta)_3$  trimer which has a three-fold axis serves as the basic block of a phycobilisome (Fig. 6). The  $\alpha$ - and  $\beta$ -subunits are almost alike in three-dimensional structure, although they differ in molecular mass and amino acid sequence. Both subunits are composed of nine  $\alpha$ -helices connected by irregular turns (Fig. 3). The tertiary structures of  $\alpha^{PC}$  and  $\beta^{PC}$  resemble those of  $\alpha^{APC}$  and  $\beta^{APC}$  except in the loop between the G and H helices of  $\beta^{PC}$ . Ten additional amino acid residues are inserted here in  $\beta^{PC}$ , and one of these residues binds an additional chromophore (Fig. 6).

Each  $\alpha$ - or  $\beta$ -subunit consists of two domains. Since one of these domains has a fold similar to that of myoglobin, this domain is sometimes called the globin-like domain and its  $\alpha$ -helices are named A, B, E, F, G, and H after the corresponding helices of myoglobin. The other domain consists of two additional helices that stick out from the globin-like domain and are unique to phycobiliproteins. These helices are named X and Y, and we call this domain the X-Y helices domain. Because all the phycobilins are attached in the globin-like domain, this domain may be said to have the function of light harvesting, while the X-Y helices domain might be said to form the basic block structure of the phycobilisome. Helix F is divided into two helices (F and F'), giving a total

of nine helices in the order X, Y, A, B, E, F', F, G, and H from the N-terminal end of the protein (Schirmer et al., 1986). The three-dimensional structures of many phycobiliproteins are available in the Brookhaven Protein Data Bank database (<http://www.rcsb.org/pdb>). The file names and resolutions as of October, 2002 are shown in Table 3.

### B. Allophycocyanin (APC)

The  $\alpha^{APC}$  and  $\beta^{APC}$  subunits of *Spirulina platensis* consist of 160 and 161 amino acid residues, respectively (Sidler et al., 1981; Brejc et al., 1995). Each subunit has only one chromophore, phycocyanobilin (PCB) (Chapman et al., 1967), which is bound covalently to the polypeptide at cysteine 84 ( $\alpha$ -84 or  $\beta$ -84) (Fig. 3).

The crystal structure analysis and refinement of the APC  $(\alpha\beta)_3$  trimer was first reported from *S. platensis* at 2.3 Å resolution (Brejc et al., 1995; Brookhaven Protein Data Bank file 1ALL.PDB). Although the sequence identity between the subunits is only 38% for the consensus sequences,  $\alpha^{APC}$  and  $\beta^{APC}$  have the same folding pattern and almost identical structures (Fig. 3). However, there are two significant differences between the  $\alpha^{APC}$  and  $\beta^{APC}$  subunits. One is in the N-terminal region of the protein, which is shorter by two residues in  $\alpha^{APC}$  than in  $\beta^{APC}$  (Fig. 3 and Table 2). The other is in the BE loop, where the 63rd amino acid is deleted in  $\beta^{APC}$ . Due to this deletion, the BE loop is more kinked in  $\beta^{APC}$  than in  $\alpha^{APC}$ , and the first part of the BE loop of

Table 3. Crystal structure of phycobiliproteins found in Brookhaven Protein Data Bank at the end of October, 2002

Phycobiliprotein	PDB file name	Resolution	Deposition Date	Reference
APC	1ALL	2.30 Å	01-Mar-1995	Brejc et al., 1995
	1B33	2.30 Å	15-Dec-1998	Reuter et al., 1999
C-PC	1CPC	1.66 Å	11-Oct-1990	Düring et al., 1991
	1GH0	2.20 Å	29-Oct-2000	Wang et al., 2001
	1HA7	2.20 Å	28-Mar-2001	Padyana et al., 2001
	1I7Y	2.50 Å	11-Mar-2001	Adir et al., 2001
	1KTP	1.60 Å	17-Jan-2002	Adir et al., unpublished
	1PHN	1.65 Å	21-Jun-1995	Stec et al., 1999
R-PC	1F99	2.40 Å	09-Jul-2000	Jiang et al., 2001
R-PE	1B8D	1.90 Å	29-Jan-1999	Ritter et al., 1999
	1EYX	2.25 Å	09-May-2000	Contreras-Martel et al., 2001
	1LIA	2.80 Å	29-Jan-1996	Chang et al., 1996
PE 545	1QGW	1.63 Å	10-May-1999	Wilk et al., 1999

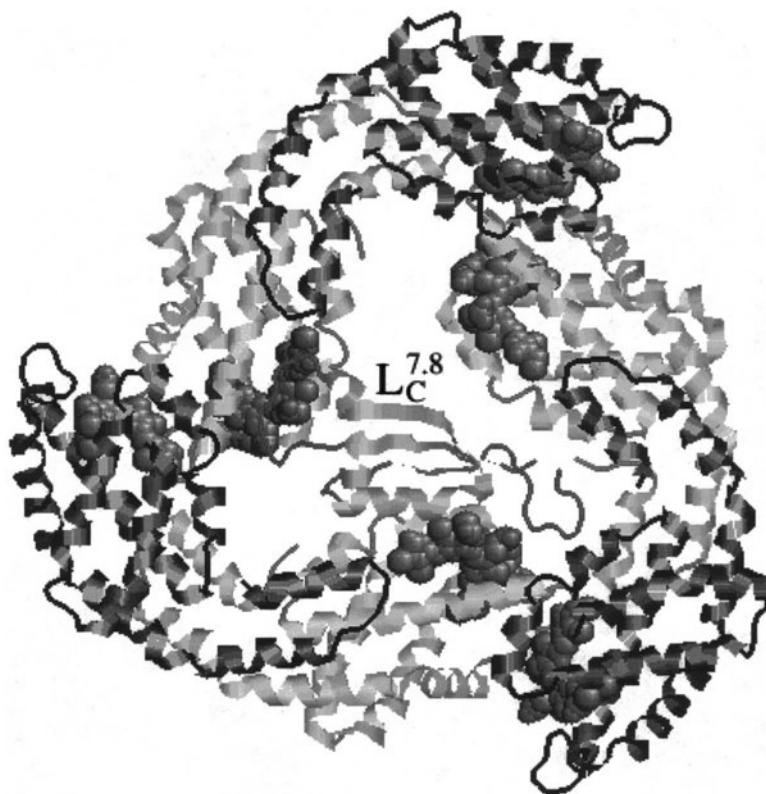


Fig. 8. The APC ( $\alpha\beta$ )<sub>3</sub> with the linker polypeptide  $L_C^{7.8}$  in the cavity of the trimer. The figure was drawn on the basis of PDB structure file 1B33.PDB (Reuter et al., 1999). The  $\alpha$  and  $\beta$  subunits of APC are shown with a ribbon representation in dark or light gray, respectively, and all the chromophores ( $\alpha$ -84 and  $\beta$ -84) are shown by a space-filling representation. The  $L_C^{7.8}$  linker polypeptide interacts directly with the two of the three  $\beta$ -84 chromophores (Reuter et al., 1999). See Color Plate 9.

the  $\beta^{APC}$  monomer interacts with the chromophore  $\alpha$ -84 of the neighboring monomer (Fig. 6). In contrast, the corresponding part of the BE loop in  $\alpha^{APC}$  (from  $\alpha$ -61 to  $\alpha$ -66) is completely exposed to the solvent and does not make any contacts with the chromophore. The second part of the BE loop in both  $\alpha^{APC}$  and  $\beta^{APC}$  is important for the protein-chromophore interactions within the same subunit (Fig. 3). This region consists of the conserved motif PGGNxY from amino acid residues 69 to 76 (residues 73 and 74 are deleted). Its conformation is almost identical in the two subunits, although  $\beta^{APC}$  has a methylated asparagine at position 72 with the methyl group pointing towards chromophore  $\beta$ -84.

The crystal structure of *M. laminosus* APC with a linker polypeptide has been described at 2.2 Å resolution (Reuter et al., 1999; 1B33.PDB) (Fig. 8). (The numbering of the amino acid residues differs in this report because of the neglect of a deletion.) The ( $\alpha\beta$ )<sub>3</sub> complex from this organism contains one copy of the  $L_C^{7.8}$  linker polypeptide, which has a molecular

mass of 7.8 kDa (formerly thought to be 8.9 or 10 kDa). The linker polypeptide is located in the central channel of the APC trimer. It has an elongated shape and consists of a three-stranded  $\beta$ -sheet (Leu3-Leu9, Tyr26-Pro32, and Lys49-Leu55), two  $\alpha$ -helices (Leu22-Thr25, which has only one turn, and Tyr33-Met46), and connecting random-coil segments. Approximately half the surface area of the linker is buried in the complex. The binding of  $L_C^{7.8}$  breaks the  $C_3$  symmetry of the trimer, and the trimer is flattened along the  $C_3$  symmetry axis (Reuter et al., 1999). Interestingly, the  $L_C^{7.8}$  linker polypeptide is not bound to all three  $\alpha\beta$  monomers in the trimer; it binds predominantly to two of the  $\beta$ -subunits and it interacts directly with the chromophores of these subunits (Reuter et al., 1999).

Binding of a linker polypeptide induces changes in the absorption properties of APC. In the monomer, the absorption maximum is located at 615 nm, and either of the two chromophores has almost the same absorption maximum (Füglister et al., 1987). When

the monomer APC forms the trimer without a linker polypeptide, the maximum is at 650 nm with two shoulders at approximately 620 and 600 nm. When a linker polypeptide was bound to the trimer, the absorption maximum shifted to the red by 1 or 2 nm, and the shoulder at 620 nm disappeared, while the 600-nm shoulder remained. The extinction coefficient of the 650-nm band increased, accompanied by a decrease in the 620-nm extinction. These two bands therefore were assigned to the  $\beta$ -chromophores that interact directly with the linker polypeptide (Reuter et al., 1999).

These results indicate that differences in the protein structures result in differences in the electric fields around the chromophores (Schneider et al., 1995). The absorption and emission properties of the chromophores are important for energy transfer (Section VI). The sequence homology of the first part of the BE loop in APC, PC, and b-PE is not high between two subunits, whereas the second part is more conserved (Table 2). Hopefully, crystal structures of the APC- $L_{CM}$  complex and of complexes containing both  $L_C^{7,8}$  and  $L_{CM}$  will lead to better understanding of energy transfer in the phycobilisome core and from the core to the PS II antenna in thylakoid membranes.

The  $\alpha^{APC}$  and  $\beta^{APC}$  subunits of the  $\alpha\beta$  monomer interact predominantly through their hydrophobic X and Y helices. In this arrangement, the  $\alpha$ -84 and  $\beta$ -84 chromophores are separated at the ends of individual subunits by a center-to-center distance of 45 Å. However, when a trimer is formed by three identical monomers, the  $\alpha$ -84 chromophore in each monomer is located relatively near the  $\beta$ -84 chromophore of an adjacent monomer, with a center-to-center distance of about 21 Å. This location of chromophores in the trimer is conserved in all known phycobiliproteins and appears to be a basic strategy for efficient energy transfer between trimers.

The crystal structure of APC isolated from a red alga *Porphyra yezoensis* has been described at 2.2 Å resolution (Liu et al., 1999); however, the coordinates are not available through the Protein Data Bank at the time of writing.

### C. Phycocyanin (PC)

The two subunits of *M. lamosus* consist of 162 ( $\alpha^{PC}$ ) and 172 ( $\beta^{PC}$ ) amino acid residues (Frank et al., 1978). The blue-colored, deep-red-fluorescent PC is the predominant form of PC and contains three PCB chromophores per  $\alpha\beta$  monomer. PCBs are covalently

attached to the polypeptides through cysteines  $\alpha$ -84,  $\beta$ -84, and  $\beta$ -155. The maximum wavelength of light absorption ranges from 595 to 640 nm.

The crystal structure of the PC trimer was first solved in *M. lamosus* (Schirmer et al., 1985, 1986, 1987). The structure of PC from the cyanobacterium *Fremyella diplosiphon* (C-PC) then was reported at 1.66 Å resolution (Düring et al., 1991; 1CPC.PDB), followed by that of PC from *C. caldarium* at 1.65 Å resolution (Stec et al., 1999; 1PHN.PDB). Recently, several additional crystal structures of PC were reported (Adir et al., 2001 (1I74), 2002 (1KTP); Padyana et al., 2001 (1HA7); Wang et al., 2001 (1GH0); Table 3).

The folding pattern of  $\alpha^{PC}$  and  $\beta^{PC}$  is the same as in APC. However, the sequence identity between  $\alpha^{PC}$  and  $\beta^{PC}$  is 26%, which is lower than that in APC. This difference between APC and PC results mainly from an insertion of ten residues ( $\beta$ -150 to  $\beta$ -159) in PC at the end of the GH loop ( $\beta$ -145 to  $\beta$ -155) and the start of helix H ( $\beta$ -156 to  $\beta$ -172). A PCB chromophore is attached through  $\beta$ -Cys155 in this insertion. The absorption maximum of this chromophore (596 nm) is the shortest of the three chromophores in the  $\alpha\beta$  monomer of PC (Mimuro et al., 1986a). The ten-residue insertion thus is significant for functional aspects of the phycobilisome.

The PGGNxY motif in the BE loop is conserved in  $\beta^{PC}$ , but is not well conserved in  $\alpha^{PC}$  (Table 2). This could reflect the fact that the PGGNxY motif of  $\alpha^{PC}$  is exposed to the solvent and does not interact with peptides of other phycobiliproteins, while the PGGNxY motif of the  $\beta^{PC}$  interacts with the  $\alpha$ -84 of the neighboring monomer (Fig. 6).

The arrangement of chromophores  $\alpha$ -84 and  $\beta$ -84 in the PC trimer is essentially identical to that in APC; the third chromophore,  $\beta$ -155, is distant from both  $\alpha$ -84 and  $\beta$ -84, with a center-to-center distance of 45 Å. When the hexamer is formed by face-to-face attachment of two trimers, the chromophores in the two trimers are arranged in close proximity to each other. This arrangement again facilitates fast and efficient energy transfer between the rod components. The linker protein also plays an important role in energy transfer in the rod by forming an energy gradient to the core (Glauser et al., 1993), but its location in the structure is still unknown.

As for R-PC, the amino acid sequences of the R-PC subunits in the red alga *P. cruentum* are known (Ducret et al., 1994). R-PC from this alga resembles C-PC in forming ( $\alpha^{RPC}\beta^{RPC}$ )<sub>3</sub> trimers, but differs in the replacement of PCB by PEB at the  $\beta$ -155 position

(Glazer, 1985; Ducret et al., 1994). The crystal structure of R-PC from the red alga *Polysiphonia urceolata* at 2.4 Å was reported (Jiang et al., 2001; 1F99). In this R-PC, the  $\beta$ -155 chromophore is also PEB, not PCB.

#### D. *Phycoerythrocyanin (PEC)*

Many cyanobacteria do not synthesize either PEC or PE (Bryant, 1982). However, *M. laminosus* does synthesize PEC, and the amino acid sequences of all three phycobiliproteins, APC, PC, and PEC, from *M. laminosus* have been determined (Frank et al., 1978; Sidler et al., 1981; Füglistaller et al., 1983).  $\alpha^{\text{PEC}}$  has 162 amino acid residues and carries the purple-colored phycoviolobin (PVB);  $\beta^{\text{PEC}}$  has 171 residues with PCBs at  $\beta$ -Cys84 and  $\beta$ -Cys155. Their amino acid sequences are similar to those of the PC subunits. PEC crystals from *M. laminosus* have been characterized by Rübéli et al. (1985), and the three-dimensional structure has been described at 2.7 Å resolution (Düring et al., 1990). The protein and chromophore structures of the PEC subunits are very similar to those of PC except for the substitution of PVB for PCB in the  $\alpha$ -subunit, and the spatial arrangement of the chromophores in the PEC trimer is essentially identical to that in PC (Düring et al., 1990). The conjugated  $\pi$ -electronic system in PVB is shorter than that in PCB, extending over only three of the four pyrrole rings (Fig. 4). PVB absorbs light around 575 nm and has the highest energy level in phycobilisomes consisting of PEC, PC and APC. PEC usually is located on the periphery of the phycobilisome, allowing for energy transfer to the pigments with lower energies.

Optical spectroscopy and NMR measurements have shown that the PVB in the  $\alpha$ -subunit of PEC can undergo an isomerization of the C15-C16 double bond between ring C and D (Zhao et al., 1995a, 1995b; Förstendorf et al., 1997). Some authors have speculated that PEC can act as a photoreceptor similar to phytochrome (Brune et al., 1988). However, the exact physiological role of the photoreaction is not known.

#### E. *Phycoerythrin (PE)*

B-PE consists of three different subunits and its basic unit is an  $(\alpha\beta)_6\gamma$  aggregate. The  $(\alpha\beta)_6$  structure is formed by face-to-face aggregation of the trimer  $(\alpha\beta)_3$ , which is the basic unit in APC or PC. The

structure of the trimer  $(\alpha\beta)_3$  is similar to that of APC and PC. However, the chromophores differ from those of APC and PC.  $\alpha^{\text{BPE}}$  contains two PEBs per monomer;  $\beta^{\text{BPE}}$  has three PEBs; and  $\gamma^{\text{BPE}}$  has two PEBs and two PUBs. The conjugated  $\pi$ -electron systems of these chromophores are shorter than that in PCB, the predominant chromophore of APC and PC. PEB resembles PVB in having three of the four pyrrole rings conjugated, but these are rings A, B and C in PEB, and rings B, C and D in PVB (Fig. 4). In PUB, the conjugated region is shorter still, including only rings B and C.

The three-dimensional structure of B-PE from the red alga *Porphyridium sordidum* is known at 2.2 Å resolution (Ficner et al., 1992), and that of b-PE from *P. cruentum* at 2.3 Å resolution (Ficner et al., 1993). b-PE and B-PE have very similar subunit structures and compositions  $((\alpha\beta)_6\gamma)$ , and both have absorption maxima at 560 and 545 nm with a shoulder around 500 nm. However, the relative absorption of this shoulder is somewhat higher in B-PE than in b-PE. Again, the three-dimensional structures of the  $\alpha$ - and  $\beta$ -subunits resemble those of APC, PC and PEC (Schirmer et al., 1987; Düring et al., 1991; Brejc et al., 1995).

The  $\alpha^{\text{bPE}}$  and  $\beta^{\text{bPE}}$  subunits are both slightly larger than the corresponding PC subunits, containing 164 and 177 amino acid residues, respectively (Sidler et al., 1989). The five PEBs are attached to cysteines  $\alpha$ -84,  $\alpha$ -140,  $\beta$ -84,  $\beta$ -155 and  $\beta$ -50/ $\beta$ -61. (Cysteines  $\beta$ -50 and  $\beta$ -61 provide two cysteinyl-thioether linkages to the same PEB through the vinyl substituents on pyrrole rings A and D (Fig. 4).) The maximum wavelength of light absorption is 540–560 nm.

The main differences between the b-PE and PC structures arise from deletion of residues  $\alpha$ -67 and  $\alpha$ -68 in the  $\alpha$ -subunit, insertion of four residues (CVPR) beginning with cysteine 140 in the  $\alpha$ -subunit, and the insertion of five residues beginning with threonine 148 in the  $\beta$ -subunit (Table 2). These alterations make the sequence identity between the  $\alpha$ - and  $\beta$ -subunits in b-PE lower than that in PC. The deletion of residues  $\alpha$ -67 and  $\alpha$ -68 changes the BE loop in the  $\alpha$ -subunit and affects the interaction with the chromophore  $\alpha$ -84. This may be related to variations in the absorption spectrum of the chromophore  $\alpha$ -84. The insertion of four amino acids at  $\alpha$ -140 extends the GH loop, and allows PEB to be attached to the additional cysteine residue at this position. The insertion of five amino acid residues at

$\beta$ -148 extends the GH loop in the  $\beta$ -subunit. The enlarged GH loop interacts with the additional chromophore of the  $\beta$ -subunit, the  $\beta$ -50/ $\beta$ -61 chromophore. This feature is found in B-PE or R-PE in addition to b-PE, and can be seen in the R-PE structure shown in Fig. 6. The two additional chromophores ( $\alpha$ -140 and  $\beta$ -50/ $\beta$ -61) in PE compared with PC could be one of the strategies for gathering excitation energy into the phycobilisome core, in addition to absorbing light at shorter wavelengths.

The crystal structure of R-PE from *P. urceolata* was determined at 2.8 Å resolution (Chang et al., 1996; 1LIA.PDB). This structure was recently refined to a resolution 1.9 Å (Jiang et al., 1999), but the model is not yet found in the PDB. The crystal structure of R-PE from *G. monilis* has been described at 1.90 Å resolution (Ritter et al., 1999; 1B8D.PDB). The three-dimensional structure of R-PE (Fig. 3b) is similar to that of B-PE from *P. sordidum* except for two main differences in the chromophore composition. The  $\gamma$ -subunit has three PUBs and one PEB in R-PE, but two PUBs and two PEBs in B-PE. The  $\beta$ -subunit has PUB bound to  $\beta$ -50/ $\beta$ -61 in R-PE, but PEB in B-PE. The crystal structure of R-PE from *Gracilaria chilensis* at 2.4 Å resolution has also been described (Contreras-Martel et al., 2001; 1EYX).

Although the amino acid sequence and optical properties of C-PE are well known (Table 2), its three-dimensional structure has not yet been described.

### F. Cryptophycean Phycoerythrin (PE)

The phycobiliproteins of *Cryptophyta* differ from those of cyanobacteria and red algae in several respects (Glazer and Wedemayer 1995; Wedemayer et al., 1996; Chapter 11, Hiller and Macpherson). First, phycobilisomes are not found in *Cryptophyta*; instead, a phycobiliprotein dimer serves as the functional unit. In addition, each of the known species of cryptophytes contains only one type of phycobiliprotein, which is invariably either PC or PE; APC has not been detected (Sidler, 1994). This restriction, however, still allows substantial variation of the absorption spectrum: typical examples are PE545, PE565, and PC645, where the numbers indicate the absorption maxima. A third difference is that the phycobiliproteins attach to the lumenal side of the thylakoid membranes, not to the cytoplasmic side as in cyanobacteria and red algae. Accompanying this

localization, the PS II fluorescence maximum at  $-196^\circ\text{C}$  changes from 685 nm to 688 nm (Mimuro et al., 1998).

Like other phycobiliproteins, cryptophycean phycobiliproteins consist of  $\alpha$ - and  $\beta$ -subunits. But while the  $\beta$ -subunit is similar to other  $\beta$ -subunits, the  $\alpha$ -subunit has a shorter primary sequence. This variation results in a significant difference in the three-dimensional structures. Wilk et al. (1999) have described the crystal structure of PE545 from *Rhodomonas* CS24 at 1.63 Å resolution. The functional unit is an ( $\alpha_1\beta$ )( $\alpha_2\beta$ ) heterodimer. A striking feature of the  $\alpha$ -subunits is the presence of  $\beta$ -sheet structure that has not been found in other phycobiliproteins. In the  $\beta$ -subunit, the N-terminal part is different; the X-Y helices are replaced by a single Y-helix, which does not protrude from the globin-fold domain. Thus the hydrophobic domain that forms the interface between monomers in other phycobiliproteins is missing in the cryptophycean PE, preventing the formation of higher-order structures such as an ( $\alpha\beta$ )<sub>3</sub> trimer.

The arrangement of chromophores in PE545 is unlike that in any of the other known structures. One chromophore is bound to each  $\alpha$ -subunit and three to the  $\beta$ -subunit. One chromophore on the  $\beta$ -subunit links to the protein through two thioether bonds ( $\beta$ -50/ $\beta$ -61). This chromophore in the  $\alpha_1\beta$  monomer is located close to the corresponding chromophore in the  $\alpha_2\beta$  monomer, leading to exciton absorption bands with relatively strong circular dichroism (MacColl et al., 1998; Wilk et al., 1999). The chromophore of the  $\alpha$ -subunit monomer appears to serve as the final energy acceptor in the ( $\alpha\alpha$ ,  $\alpha\beta$ ) complex.

### G. Modification of the Three-Dimensional Structures by Linker Polypeptides

Binding of linker polypeptides to phycobiliproteins affects the energy levels of the chromophores, probably through modifications of protein structure. The sensitivity of the optical properties of individual chromophores to binding of linker polypeptides was seen clearly in the PC of *Synechocystis* sp. PCC 6701. PC hexamers located at the outer end, middle, and core end of a rod bind three different colorless linker polypeptides, with molecular masses of 31.5, 33.5 and 27 kDa, respectively (Glazer, 1985). The complexes of the outer, middle, and core-end hexamer with their linker polypeptides have fluorescence

maxima at 643, 648 and 652 nm, respectively. This gradient of decreasing energy levels towards the inside of the rod structure parallels the absorption maxima (Glazer, 1985; Glauser et al., 1993), and causes a successive shift of the emission maximum in time-resolved fluorescence spectra (Mimuro et al., 1989). These results indicate that, in addition to connecting the phycobiliprotein building blocks, linker polypeptides create a gradient in the energy levels that insures efficient energy transfer to RCs in the membranes.

Similar phenomena are observed in APC trimers (Glazer, 1985; Füglistaller et al., 1987). The APC core contains four different kinds of trimers:  $(\alpha_3^{\text{APC}} \beta_3^{\text{APC}}) \cdot \text{L}_C$ ,  $(\alpha_3^{\text{APC}} \beta_3^{\text{APC}}) \cdot (\alpha_3^{\text{APC}} \beta_2^{\text{APC}} \beta_{16.2}^{\text{APC}}) \cdot \text{L}_{\text{CM}}$  and  $(\alpha^{\text{APB}} \alpha_2^{\text{APC}} \beta_3^{\text{APC}}) \cdot \text{L}_C$ . Binding of  $\text{L}_C$  ( $\text{L}^{8.9}$ ) induces a small red shift of the absorption maximum from 650 to 652 nm and a shift of the emission maximum from 660 to 663 nm (Füglistaller et al., 1987). Changes in the three-dimensional structure by binding of a linker polypeptide were reported (Reuter et al., 1999). The  $\text{L}_C^{7.8}$  linker polypeptide is not bound to all three  $\alpha\beta$  monomers in the trimer; it binds predominantly to two of the  $\beta$ -subunits and it interacts directly with the chromophores of these subunits (Reuter et al., 1999). The binding of  $\text{L}_C^{7.8}$  breaks the  $\text{C}_3$  symmetry of the trimer, and the trimer is flattened along the  $\text{C}_3$  symmetry axis (Reuter et al., 1999). These observations indicate that three-dimensional structure of APC is modified through binding of a linker polypeptide. Changes in absorption properties may arise partly from changes in configuration of chromophores due to binding of the linker polypeptides, in addition to the direct interaction of a linker polypeptide with two  $\beta$  chromophores.

Although some uncertainties remain in the structures of phycobilisomes, the structural information obtained by X-ray crystallography has revealed how phycobilisomes are organized to facilitate a high efficiency of energy transfer.

## V. Electronic States of Chromophores in Phycobiliproteins

### A. Relationship between Chromophore Configurations and Electronic States

The absorption and emission properties of phycobiliproteins are determined by the electronic states of the chromophores. Five main factors affect the

energies of these states: (1) the chemical species of chromophore, (2) the configuration of the bound chromophore, (3) electrostatic fields from the protein, (4) pigment-protein interactions that alter the protonation state of the chromophore, and (5) interactions between chromophores. We will discuss each of these factors in turn.

### 1. Chromophore Species

Each of the four kinds of chromophores found in phycobilisomes (PUB, PEB, PVB and PCB) has two keto groups, seven C-C double bonds and one C-N double bond (Glazer, 1985). The energy levels depend primarily on the number of conjugated double bonds, and to a lesser extent on the side chains of the tetrapyrroles. As the number of conjugated double bonds increases, the absorption maximum shifts to the red. The actual numbers of conjugated double bonds are five in PUB, six in PEB, eight in PVB, and nine in PCB.

### 2. Configuration of the Bound Chromophore

In phycobiliproteins, even the same kind of chromophore can have different configurations. For example, although the  $\alpha$ -84 chromophores are PCBs in both PC and APC, their bound configurations differ. Figure 9 shows these configurations. Molecular orbital calculations indicate that the chromophore with a more planar configuration, such as the APC chromophore in Fig. 9, should absorb at a longer wavelength. However, this effect is not necessarily seen because the interactions between the chromophore and its surroundings also can differ in the two proteins as described below.

### 3. Electrostatic Fields from the Surrounding Protein

The chromophores in all the phycobiliproteins are buried in the protein and thus can be affected by electrostatic fields from the surrounding amino acid residues. The shift of the absorption maximum in APC 30 nm to the red relative to the maximum in PC probably results partly from such interactions between the chromophore and the surrounding protein. Differences in interactions with the protein could also account for the fact that  $\alpha^{\text{APB}}$  and the anchor polypeptide absorb and emit still lower energies even though they contain the same chromophore (PCB) as

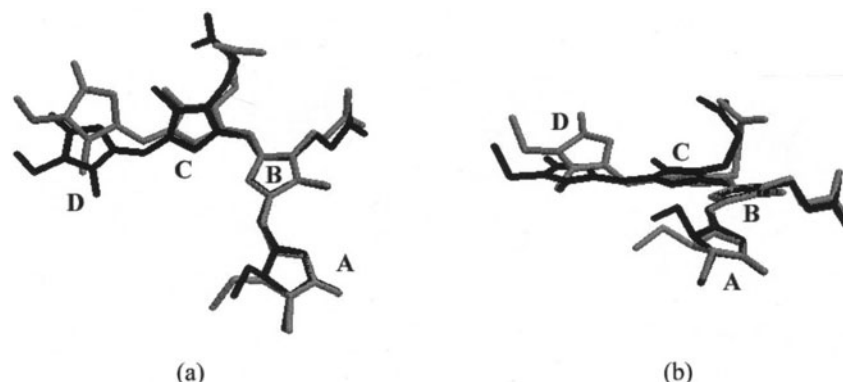


Fig. 9. (a) The  $\alpha$ -84 chromophore configurations in APC (black) and C-PC (gray) when the pyrrole rings B of the two are superposed. The coordinates are from 1ALL.PDB (Brejc et al., 1995) and 1CPC.PDB (Düring et al., 1991). A, B, C, or D represents the name of the pyrrole ring. (b) The structures viewed from another direction to emphasize the twist angle between the C and D rings in C-PC.

C-PC and APC. ( $\alpha^{\text{APB}}$  and the anchor polypeptide have absorption maxima around 658 and 671 nm and a fluorescence maximum around 680 nm.) However, the three dimensional structures of  $\alpha^{\text{APB}}$  and the anchor polypeptide are not yet known.

#### 4. The Protonation State of the Chromophore

The structures shown in Fig. 4 are the neutral chromophores, in which the nitrogen of one of the four pyrrole rings (ring C), is not protonated. The chromophores in many phycobiliproteins probably are protonated on this nitrogen. Irrespective of whether they have one or two covalent links to the protein, the PCB, PVB, PEB and PUB chromophores in phycobilisomes are situated close to a conserved aspartate residue. In the crystal structures of C-PC (Düring et al., 1991, 1CPC.PDB), one of the carboxylate oxygens of the Asp side chain is 2.82 Å from the nitrogen of pyrrole B of chromophore  $\alpha$ -84, and 2.66 Å from the nitrogen of pyrrole C (Fig. 10b). Assuming that the carboxylate group is ionized, both the nitrogens most likely will be protonated and the chromophore will have an overall charge of +1. This protonation is expected to modify the electronic state of the chromophore considerably. Kikuchi et al. (1997) showed that the experimentally observed spectroscopic properties of PC can be reproduced well if the nitrogens of pyrroles B and C are both protonated, but that if the nitrogen of pyrrole C is unprotonated, the calculated oscillator strength for excitation to the lowest excited singlet state becomes very small and the absorption maximum moves to a shorter wavelength. The aspartic acid residue

therefore has a strong influence on the electronic states through the protonation of the chromophore, and this presumably is why it is conserved in almost all phycobiliproteins. In the  $\alpha$ -subunits of PC, the  $\alpha$ -84 chromophore interacts with Asp 87; in the  $\beta$ -subunit, the  $\beta$ -84 chromophore interacts with Asp 87 and the  $\beta$ -155 chromophore interacts similarly with Asp 39.

#### 5. Interactions Between Chromophores

With the exception of the cryptophycean PE545, where two chromophores bound to the  $\beta$  subunit of the ( $\alpha_1\beta$ ,  $\alpha_2\beta$ ) heterodimer are located in van der Waals contact (Wilk et al., 1999), the distances between chromophores in phycobiliproteins are too large for pigment-pigment interactions to be very significant. The special features of the circular dichroism (CD) spectrum of PE545 can be explained by this interaction. In this case, the spectroscopic properties can no longer be assigned to individual chromophores, but instead represent cooperative properties of the complex. Of course, the absorption properties of the complex still depend on the four factors discussed above.

#### B. Dynamic Fluctuations of Phycobiliprotein Structures

A normal-mode analysis was carried out to investigate the dynamic structures of phycobiliproteins and explore the effects of vibrations on the spectroscopic properties (Kikuchi et al., 2000). The dynamic structures of the phycobiliprotein subunits were



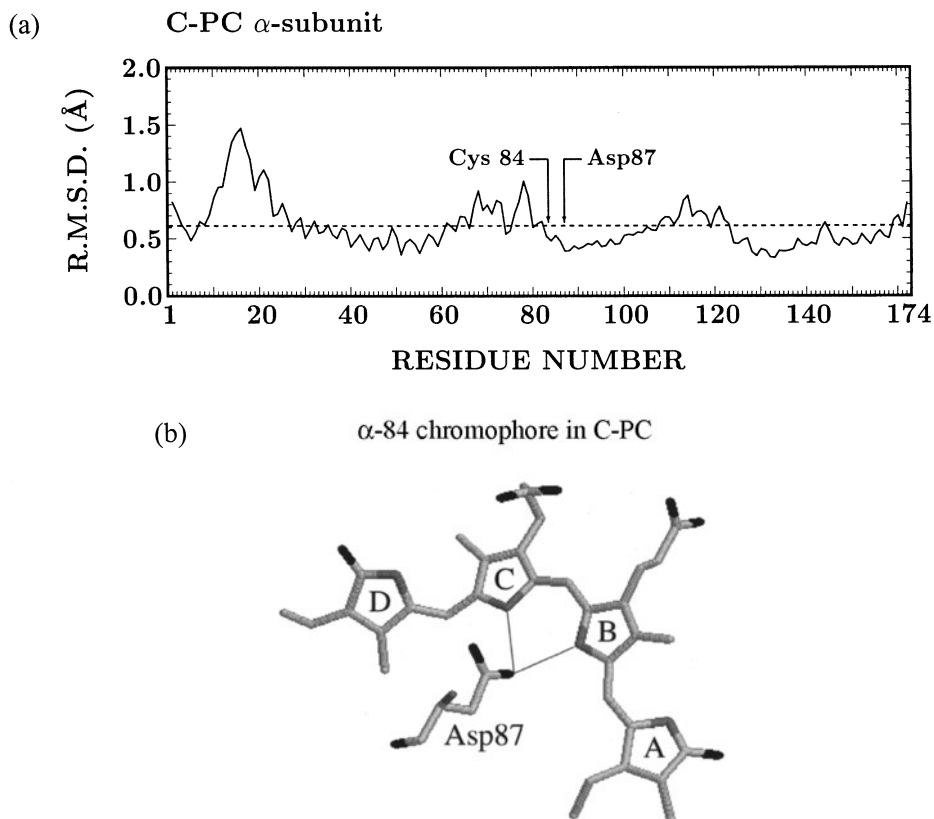


Fig. 10. Fluctuation of the positions of  $C\alpha$  atoms of individual amino acid residues in C-PC (a) and structure of the protein near the PCB chromophore in the C-PC  $\alpha$ -subunit (b). (a) The root-mean square fluctuations were obtained by normal-mode analysis of the C-PC  $\alpha$ -subunit (Kikuchi et al., 2000). As crystal structure data of C-PC, 1CPC.PDB (Düring et al., 1991) is used. (b) The PCB chromophore is bound to cysteine 84, and is oriented to place the nitrogen atoms of pyrrole rings B and C approximately equidistant from one of the carboxylate oxygens of aspartic acid 87. This structure is found in many phycobiliproteins.

expressed in terms of correlated movements of segments consisting of consecutive amino acids. The  $\alpha$ - and  $\beta$ -subunits of PC were classified into eight segments whose movements were either positively correlated, negatively correlated, or uncorrelated.

Normal-mode analysis allows one to estimate the fluctuations of  $C\alpha$  atoms of individual amino acids. In the PC  $\alpha$ -subunit, Asp 87 was found to have the smallest fluctuations, in line with the proposal that the positioning of its carboxyl group is critical in order to induce protonation of the  $\alpha$ -84 chromophore (Fig. 10). The  $\alpha$ -84 chromophore is located in a pocket where movements of the pigment are restricted by interactions with the protein and vice versa. In the  $\beta$ -subunit of PC, aspartic acids 87 and 39 both had small fluctuations.

Kikuchi et al. (2000) also examined the module structures of PC. The concept of module structures was introduced by Go (Go, 1981, 1983). Kikuchi et

al. found that the X-Y helices domain was very similar to a module in pyruvate phosphate dikinase, a multiphosphotransfer enzyme that synthesizes phosphoenolpyruvate (Herzberg et al., 1996). The three-dimensional structure of the X-Y helices domain is highly unusual; a similar domain structure has not yet been found in any other proteins except for pyruvate phosphate dikinase. The PC subunit presumably acquired the X-Y helices domain by adding a DNA base sequence encoding the X-Y helices to the 5' end of the gene for the globin-like domain. Such an event might have enabled phycobilisomes to assemble, because the X-Y helices domain seems to be critical for formation of the  $\alpha\beta$  unit. In line with this picture, PE545 from the cryptophyte *Rhodomonas* CS24, which lacks the X-Y helices domain, does not form higher aggregates.

## VI. Energy Transfer

### A. Theory of Energy Transfer

The time-resolved fluorescence spectra shown in Fig. 7A indicate that the overall flow of energy from phycobilisomes to Chl *a* in the thylakoid membranes is a very fast process. However, the rapid shift of the emission to longer wavelengths does not necessarily reflect the elementary steps of energy transfer. Studies from both experimental and theoretical perspectives are necessary in order to elucidate the rates of these individual steps.

Energy transfer in phycobiliproteins competes with other relaxation processes of excited states, including internal conversion, intersystem crossing, fluorescence and photochemical reactions. Since phycobiliproteins have a large extinction coefficient ( $\epsilon \sim 10^5 \text{ M}^{-1}\text{cm}^{-1}$ ), the natural radiative lifetime is relatively short ( $\tau \sim 10^{-8} \text{ s}$ ). Therefore, high transfer efficiency demands a very short transfer time. As discussed in Chapter 3 (Parson and Nagarajan), there are two main mechanisms of energy transfer, the electron exchange interaction (Dexter, 1953) and the Coulomb interaction mechanism (Förster, 1948). The exchange mechanism requires an overlap of wavefunctions between the donor (D) and acceptor (A), and thus usually occurs only between molecules that are in van der Waals contact. The Coulomb mechanism does not require orbital overlap.

As shown by the crystal structures, the center-to-center distances between the chromophores in most phycobiliproteins are at least 20 Å, even after trimer units are incorporated into a phycobilisome. It is, therefore, reasonable to assume that the chromophores interact only weakly. (An exception is cryptophycean PE545, where two  $\beta$  chromophores are almost in van der Waals contact (Wilk et. al., 1999.) In the case of weak interactions, the Förster mechanism gives the rate constant for energy transfer ( $k_{ET}$ ) as:

$$k_{ET} = \frac{9000(\ln 10)\kappa^2 c^4}{128\pi^5 n^4 \tau_D} (R_{DA})^{-6} \int F_D(\nu) \epsilon_A(\nu) \nu^{-4} d\nu.$$

Here  $\kappa$  is the orientation factor ( $\kappa = \cos \theta - 3 \cos \beta_1 \cos \beta_2$ );  $\theta$  is the angle between the transition dipoles ( $\vec{\mu}_D$  and  $\vec{\mu}_A$ ) of the donor (D) and acceptor (A);  $\beta_1$  is the angle between  $\vec{\mu}_D$  and the vector connecting D and A ( $\vec{R}_{DA}$ );  $\beta_2$  is the angle between  $\vec{\mu}_A$  and  $\vec{R}_{DA}$ ;  $c$  is the speed of light;  $n$  is the refractive index of the medium;  $R_{DA}$  is the distance between D

and A;  $F_D(\nu)$  is the fluorescence of D at frequency  $\nu$ ;  $\epsilon_D(\nu)$  is the molar absorption coefficient of A; and  $\tau_D$  is the emission lifetime of D in the absence of A. According to this equation, the rate constant is determined mainly by the spectral overlap integral and the intermolecular distance. The rate constant decreases with the sixth power of  $R_{DA}$ . In the case of PC, both  $R_{DA}$  and the orientation factor  $\kappa$  are known from the X-ray structure, and energy levels of individual chromophores are known by spectral analyses (see below). The transfer rate thus can be calculated numerically and compared with experimental data. This is an exceptional case in pigment-protein complexes, because in many other cases either the structure or the energy levels of the individual chromophores, or both, are unknown.

### B. Experimental Analyses in C-PC

The crystal structure of C-PC is known in several species (Section IV.C). There are three types of chromophores,  $\alpha$ -84,  $\beta$ -84 and  $\beta$ -155. An analysis of the energy levels of the chromophores in the trimer puts chromophore  $\beta$ -155 at the highest level, with an absorption maximum between 598 and 601 nm, chromophore  $\alpha$ -84 at an intermediate level (618–622 nm), and chromophore  $\beta$ -84 lowest (632–634 nm) (Mimuro et al., 1986a). The  $\alpha$ -84 chromophore in one monomer is located at the interface between two monomers, closest to the  $\beta$ -84 chromophore in an adjacent monomer ( $R_{DA} \approx 21 \text{ Å}$ ). The  $\beta$ -155 chromophore is located at the outside of the trimer, at distances of about 45 Å from  $\alpha$ -84 and  $\beta$ -84. Based on the energy levels, distances and relative orientations, the direction of energy flow is easily predicted to be from the  $\beta$ -155 to  $\beta$ -84 and from  $\alpha$ -84 to  $\beta$ -84. A most interesting process is from the  $\alpha$ -84 chromophore to  $\beta$ -84, because of their relatively close location. Using the Förster equation, Sauer and Scheer (1988) estimated the interaction energy between these chromophores to be  $56 \text{ cm}^{-1}$  and estimated  $k_{ET}$  for this step to be  $1.53 \times 10^{12} \text{ sec}^{-1}$ , giving an expected transfer time of 0.6 ps. They also calculated the rates of other transfer steps; however, these are more difficult to resolve experimentally because multiple decay processes overlap.

Direct information on energy-transfer processes in phycobiliproteins has been obtained by spectroscopic measurements in the time region between 100 fs and 10 ps. Measurements of transient absorption changes and time-resolved fluorescence spectra or

decay have provided complementary results, although absorbance measurements provide somewhat higher time resolution. Time-resolved spectroscopic measurements on C-PC trimers were carried out by several groups. Gillbro et al. (1993) measured pulse-induced changes of absorption and stimulated emission in C-PC trimers from *M. lamosus*, and found that the anisotropy of the signals decayed with a time constant of 500 fs. Hucke et al. (1993) also found a decay time of 500 fs in PEC trimers, and Sharkov et al. (1994) measured a similar time of 440 fs in APC trimers. Since the center-to-center distances between the  $\alpha$ -84 and  $\beta$ -84 chromophores are almost the same in PC, PEC and APC, the anisotropy decay time can be regarded as the time constant for energy transfer between these chromophores. The observed time constant is close to the 0.6 ps predicted by the equation 1, suggesting that the Förster mechanism applies to phycobiliproteins (Gillbro et al., 1993). Measurements on C-PC with linker polypeptides also have been achieved (Pizarro and Sauer, 2001), and are important for understanding energy transfer in vivo.

When two chromophores are close enough to each other to form exciton absorption and emission bands, the electronic states are mixed and should be viewed as belonging to the complex as a whole (Chapter 3, Parson and Nagarajan). As discussed above, this is likely to be the situation for the pair of  $\beta$ -50/ $\beta$ -61 chromophores in the cryptophycean PE545 dimer, which are essentially in van der Waals contact (Wilk et al., 1999) and probably give rise to the exciton CD bands of the dimer (MacColl et al., 1998). The fastest decay time constant of 2.4 ps measured in the PE545 dimer by two-photon fluorescence (MacColl et al., 1998) thus probably cannot be assigned to stochastic energy transfer between these chromophores. The fluorescence decay kinetics do appear to depend on pigment-pigment interactions, however, because monomerization affects them strongly in addition to changing the absorption and CD spectra. This suggests that the 2.4-ps step reflects a relaxation between two exciton states of the dimer.

## VII. Concluding Remarks

Phycobiliproteins have efficiencies of energy transfer in the range of 80 to 90%. Though high by some measures, this is lower than the efficiency of other photosynthetic antenna systems, suggesting that the

molecular organization of phycobiliproteins falls short of ideal. The main factors that affect the transfer efficiency include the chemical and physical properties of the chromophores, the configurations of the chromophores in their binding sites on the proteins, direct and indirect effects of the protein (local electric fields, perturbations of the ionization states of the chromophores, and suppression of chemical reactivities), the orientations of the transition dipoles, and the distances between chromophores. Although it might seem that little would be left for study on this point, this is far from true. Crystallographic studies are providing an abundance of structural information on new and modified phycobiliproteins, and normal-mode analysis has opened a new approach to examining how fluctuations of the protein structure affect the spectroscopic properties and function of the antenna. These studies should shed new light on the interactions of the chromophores with each other and with the proteins.

## Acknowledgments

We are grateful to Profs. I. Yamazaki and T. Katoh for their collaboration on the analysis of energy transfer processes in cyanobacteria, and to Dr. A. Murakami for his comments and help for preparation of the manuscript. We acknowledge Drs. W.W. Parson, R.B. Green and E. Gantt for their critical reading of the manuscript.

## References

- Adir N, Dobrovetsky E and Lerner N (2001) Structure of C-phycocyanin from the thermophilic cyanobacterium *Synechococcus vulcanus* at 2.5 Å: Structural implications for thermal stability in phycobilisome assembly. *J Mol Biol* 313: 71–81
- Adir N, Vainer R and Lerner N (2002) Refined structure of c-phycocyanin from the cyanobacterium *Synechococcus vulcanus* at 1.6 Å: Insights into the role of solvent molecules in thermal stability and cofactor structure. *Biochim Biophys Acta* 1556: 168–174.
- Apt KE, Collier JL and Grossman AR (1995) Evolution of the phycobiliproteins. *J Mol Biol* 248: 79–96
- Arnold WA (1991) Experiments. *Photosynth Res* 27: 73–82
- Beale SI (1994) Biosynthesis of cyanobacterial tetrapyrrole pigments: Hemes, chlorophylls and phycobilins. In: Bryant DA (ed) *The Molecular Biology of Cyanobacteria*, pp. 139–216. Kluwer Academic Publishers, Dordrecht
- Beale SI (1999) Enzymes of chlorophyll biosynthesis. *Photosynth Res* 60: 43–73
- Brejč K, Ficner R, Huber R and Steinbacher S (1995) Isolation,

- crystallization, crystal structure analysis and refinement of allophycocyanin from the cyanobacterium *Spirulina platensis* at 2.3 Å resolution. *J Mol Biol* 249: 424–440
- Brune W, Wilczok T and Waclawek R (1988) Indications for photoreversible reactions in the range of phycochrome *b* absorption obtained by automated microscopic image-analysis of germinating *Anabaena akinetes*. *Cytobios* 216: 39–48
- Bryant DA (1982) Phycoerythrocyanin and phycoerythrin: Properties and occurrence in cyanobacteria. *J Gen Microbiol* 128: 835–844
- Chang WR, Jiang T, Wan ZL, Zhang JP, Yang ZX and Liang DC (1996) Crystal structure of R-phycoerythrin from *Polysiphonia urceolata* at 2.8 Å resolution. *J Mol Biol* 262: 721–731
- Chapman DJ, Cole WJ and Siegelman HW (1967) Chromophores of allophycocyanin and R-phycoerythrin. *Biochem J* 105: 903–905
- Contreras-Martel C, Martinez-Oyanedel J, Bunster M, Legrand P, Piras C, Vermede X and Fontecilla-Camps JC (2001) Crystallization and 2.2 Å resolution structure of R-phycoerythrin from *Gracilaria chilensis*: A case of perfect hemihedral twinning. *Acta Crystallogr D* 57: 52–60
- de Lorimier R, Guglielmi G, Bryant DA and Stevens SE Jr (1990) Structure and mutation of a gene encoding a 33000-molecular weight phycocyanin-associated linker polypeptide. *Arch Microbiol* 153: 541–549
- Dexter DL (1953) A theory of sensitized luminescence in solids. *J Chem Phys* 21: 836–850
- Dolganov NAM, Bhaya D and Grossman AR (1995) Cyanobacterial protein with similarity to the chlorophyll *a/b* binding proteins of higher plants: Evolution and regulation. *Proc Natl Acad Sci USA* 92: 636–640
- Ducet A, Sidler W, Frank G and Zuber H (1994) Complete amino acid sequence of R-phycoerythrin I  $\alpha$ - and  $\beta$ -subunits from the red alga *Porphyridium cruentum*. *Eur J Biochem* 221: 563–580
- Düring M, Huber R, Bode W, Rumbeli R and Zuber H (1990) Refined three-dimensional structure of phycoerythrocyanin from the cyanobacterium *Mastigocladus laminosus* at 2.7 Å. *J Mol Biol* 211: 633–644
- Düring M, Schmidt GB and Huber R (1991) Isolation, crystallization, crystal structure analysis and refinement of constitutive C-phycoerythrin from the chromatically adapting cyanobacterium *Fremyella diplosiphon* at 1.66 Å resolution. *J Mol Biol* 217: 577–592
- Ficner R and Huber R (1993) Refined crystal structure of phycoerythrin from *Porphyridium cruentum* at 0.23-nm resolution and localization of the  $\gamma$  subunit. *Eur J Biochem* 218: 103–106
- Ficner R, Lobeck K, Schmidt G and Huber R (1992) Isolation, crystallization, crystal structure analysis and refinement of B-phycoerythrin from the red alga *Porphyridium sordidum* at 2.2 Å resolution. *J Mol Biol* 228: 935–950
- Förstendorf H, Parbel A, Scheer H and Siebert F (1997) Z,E isomerization of the  $\alpha$ -84 phycoviolobin chromophore of phycoerythrocyanin from *Mastigocladus laminosus* investigated by Fourier-transform infrared difference spectroscopy. *FEBS Lett* 402: 173–176
- Förster Th (1948). Zwischenmolekulare Energiewanderung und Fluoreszenz. *Ann Physik Leipzig* 2: 55–75
- Frank G, Sidler W, Widmer H and Zuber H (1978) The complete amino-acid sequence of both subunits of C-phycoerythrin from the cyanobacterium *Mastigocladus laminosus*. *Hoppe-Seyler's Z Physiol Chem* 359: 1491–1507
- Füglister P, Suter F and Zuber H (1983) The complete amino-acid sequence of both subunits of phycoerythrocyanin from the thermophilic cyanobacterium *Mastigocladus laminosus*. *Hoppe Seyler's Z Physiol Chem* 364: 691–712
- Füglister P, Rumbeli R, Suter F and Zuber H (1984) Minor polypeptides from the phycobilisome of the cyanobacterium *Mastigocladus laminosus*. Isolation, characterization and amino-acid sequences of a colorless 8.9 kDa polypeptide and of a 16.2 kDa phycobiliprotein. *Hoppe-Seyler's Z Physiol Chemie* 365: 1085–1096
- Füglister P, Mimuro M and Zuber H (1987) Allophycocyanin complexes of the phycobilisome from *Mastigocladus laminosus* influence of the linker polypeptide L8<sup>9</sup> on the spectral properties of the phycobiliprotein subunits. *Biol Chem Hoppe-Seyler* 368: 353–367
- Gantt E (1980) Structure and function of phycobilisomes: Light-harvesting pigment complexes in red and blue-green algae. *Int Rev Cytol* 66: 45–80
- Gantt E and Conti SF (1966) Granules associated with the chloroplast lamellae of *Porphyridium cruentum*. *J Cell Biol* 29: 423–434
- Gantt E, Edwards MR and Conti SF (1968) Ultrastructure of *Porphyridium aeruginosum*, a blue-green colored Rhodophyta. *J Phycol* 4: 65–71
- Gantt E, Lipschultz CA and Zilinskas BA (1976) Further evidence for a phycobilisome model from selective dissociation, fluorescence emission, immunoprecipitation and electron microscope. *Biochim Biophys Acta* 430: 375–388
- Giddings TH Jr, Wasmann C and Staehelin LA (1983) Structure of the thylakoids and envelope membranes of the cyanella of *Cyanophora paradoxa*. *Plant Physiol* 71: 409–419
- Gillbro T, Sharkov AV, Kryukov IV, Khoroshilov EV, Kryukov PG, Fischer R and Scheer H (1993) Förster energy transfer between neighboring chromophores in C-phycoerythrin trimers. *Biochim Biophys Acta* 1140: 321–326
- Glauser M, Sidler W and Zuber H (1993) Isolation, characterization and reconstitution of phycobiliprotein rod-core linker polypeptide complexes from the phycobilisomes of *Mastigocladus laminosus*. *Photochem Photobiol* 57: 344–351
- Glazer AN (1985) Light harvesting by phycobilisomes. *Annu Rev Biophys Chem* 14: 47–77
- Glazer AN and Wedemayer GJ (1995) Cryptomonad biliproteins—an evolutionary perspective. *Photosynth Res* 46: 93–105
- Go M (1981) Correlation of DNA exonic regions with protein structural units in hemoglobin. *Nature* 291: 90–92
- Go M (1983) Modular structural units, exons, and function in chicken lysozyme. *Proc Natl Acad Sci USA* 80: 1964–1968
- Green BR and Dunford DG (1996) The chlorophyll-carotenoid proteins of oxygenic photosynthesis. *Annu Rev Plant Physiol Mol Biol* 47: 685–714
- Grossman AR, Schaefer MR, Chaing GG and Collier JL (1993) The phycobilisome, a light-harvesting complex responsive to environmental conditions. *Microbiol Rev* 57: 725–749
- Guglielmi G, Cohen-Bazire G and Bryant DA (1981) The structure of *Gloeobacter violaceus* and its phycobilisomes. *Arch Microbiol*, 129: 181–189
- Hardison R (1999) Hemoglobin from bacteria to man: evolution of different patterns of gene expression. *J Exp Biol* 201: 1099–1117

- Haug A, Jaquet DD, Beall HC (1972) Light emission from the *Scenedesmus obliquus* wild type, mutant 8, and mutant II strains, measured under steady-state conditions between 4 nanoseconds and 20 seconds. *Biochim Biophys Acta* 283: 92–99
- Herzberg O, Chen CCH, Kapadia G, McGuire M, Carroll LJ, Noh SJ and Dunaway-Mariano D (1996) Swiveling-domain mechanism for enzymatic phosphotransfer between remote reaction sites. *Proc Natl Acad Sci USA* 93: 2652–2657
- Hucke M, Schweitzer G, Holzwarth AR, Sidler W and Zuber H (1993) Studies on chromophore coupling in isolated phycobiliproteins IV Femtosecond transient absorption study of ultrafast excited state dynamics in trimeric phycoerythrocyanin complexes. *Photochem Photobiol*, 57: 76–80
- Jiang T, Zhang JP and Liang D (1999) Structure and function of chromophores in R-phycoerythrin at 1.9 Å resolution. *Proteins Struct Func Genet* 34: 224–231
- Jiang T, Zhang JP, Chang WR and Liang DC (2001) Crystal structure of R-phycoerythrin and possible energy transfer pathways in the phycobilisome. *Biophys J* 81: 1171–1179
- Jordan P, Fromme P, Witt HT, Klukas O, Saenger W and Krauß N (2001) Three-dimensional structure of cyanobacterial photosystem I at 2.5 Å resolution. *Nature* 411: 909–917
- Kikuchi H, Sugimoto T and Mimuro M (1997) An electronic state of the chromophore, phycocyanobilin, and its interaction with the protein moiety in C-phycoerythrin: Protonation of the chromophore. *Chem Phys Lett* 274: 460–465
- Kikuchi H, Wako H, Yura K, Go M and Mimuro M (2000) Significance of a two-domain structure in subunits of phycobiliproteins revealed by the normal mode analysis. *Biophys J* 79: 1587–1600
- Klukas O, Schubert WD, Jordan P, Krauß N, Fromme P, Tobias H and Saenger W (1999a) Photosystem I, an improved model of the stromal subunits PsuA, PsuB and PsuE. *J Biol Chem* 274: 7351–7360
- Klukas O, Schubert WD, Jordan P, Krauß N, Fromme P, Tobias H and Saenger W (1999b) Localization of two phylloquinones, Q<sub>k</sub> and Q<sub>k</sub>', in an improved electron density map of Photosystem I at 4 Å resolution. *J Biol Chem* 274: 7361–7367
- Krauß N, Schubert WD, Klukas O, Fromme P, Witt HT and Saenger W (1996) Photosystem I at 4 Å resolution represents the first structural model of a joint photosynthetic reaction centre and core antenna system. *Nature, Struct Biol* 3: 965–973
- La Roche J, van der Staay GWM, Partensky F, Ducret A, Aebersold R, Li R, Golden SS, Hiller RG, Wrench PM, Larkum AWD and Green BR (1996) Independent evolution of the Prochlorophyte and green plant chlorophyll *a/b* light harvesting proteins. *Proc Natl Acad Sci USA* 93: 15244–15248
- Ley AC and Butler WL (1977) The distribution of excitation energy between photosystem I and II in *Porphyridium cruentum*. In: Miyachi S, Katoh S, Fujita Y and Shibata K (eds), *Photosynthetic Organelles*, pp. 33–46. Japanese Society of Plant Physiologists, Tokyo
- Liu JY, Jiang T, Zhang JP and Liang DC (1999) Crystal structure of allophycocyanin from red algae *Porphyra yezoensis* at 2.2-Å resolution. *J Biol Chem* 274: 16945–16952
- MacColl R (1998) Cyanobacterial phycobilisomes. *J Struct Biol* 24: 311–34
- MacColl R, Malak H, Gryczynski I, Eisele LE, Mizcewski GJ, Franklin E, Sheikh H, Montelese D, Hopkins S and MacColl LC (1998) Phycoerythrin 545: Monomers, energy migration, bilin topography, and monomer/dimer equilibrium. *Biochem* 37: 417–423
- Mimuro M (1990) Studies on excitation energy flow in the photosynthetic pigment system; Structure and energy transfer mechanism. *Bot Mag Tokyo* 103: 233–253
- Mimuro M and Fujita Y (1977) Estimation of chlorophyll *a* distribution in the photosynthetic pigments systems I and II of the blue-green alga *Anabaena variabilis*. *Biochim Biophys Acta* 459: 376–389
- Mimuro M, Fuglistaller P, Rumbeli R and Zuber H (1986a). Functional assignment of chromophores and energy transfer in C-phycoerythrin isolated from the thermophilic cyanobacterium *Mastigocladus laminosus*. *Biochim Biophys Acta* 848: 155–166
- Mimuro M, Lipschultz CA and Gantt E (1986b) Energy flow in the phycobilisome core of *Nostoc* sp (MAC): Two independent terminal pigments. *Biochim Biophys Acta* 852: 126–132
- Mimuro M, Yamazaki I, Tamai N and Katoh T (1989) Excitation energy transfer in phycobilisomes at –196 °C isolated from the cyanobacterium *Anabaena variabilis* (M-3): evidence for plural transfer pathways to the terminal emitter. *Biochim Biophys Acta* 973: 153–162
- Mimuro M, Tamai N, Murakami A, Watanabe M, Erata M, Watanabe M, Tokutomi M and Yamazaki I (1998) Multiple pathways of the excitation energy flow in the photosynthetic pigment system of a cryptophyte, *Cryptomonas* sp. (CR-1). *Phycological Res* 46, 155–164
- Mimuro M, Kikuchi H and Murakami A (1999) Structure and function of phycobilisomes. In Singhal GS, Renger G, Sopory SK, Irrgang KD and Govindjee (eds) *Concepts in Photobiology: Photosynthesis and Photomorphogenesis*, pp. 104–135, Kluwer Academic Publishing, Dordrecht
- Miyashita H, Ikemoto H, Kurano N, Adachi K, Chihara M and Miyachi M (1996) Chlorophyll *d* as major pigment. *Nature* 383: 402
- Mullineaux CW (1994) Excitation energy transfer from phycobilisomes to Photosystem I in a cyanobacterial mutant lacking photosystem II. *Biochim Biophys Acta* 1184: 71–77
- Mullineaux CW, Tobin MJ and Jones GR (1997) Mobility of photosynthetic complexes in thylakoid membranes. *Nature* 390: 421–424
- Murakami A, Mimuro M, Ohki K and Fujita Y (1981) Absorption spectrum of allophycocyanin isolated from *Anabaena cylindrica*: Variation of the absorption spectra induced by changes in the physico-chemical environment. *J Biochem* 89: 79–86
- Murata N and Satoh K (1986) Absorption and fluorescence emissions by intact cells, chloroplasts and chlorophyll-proteins complexes. In: Ames J, Govindjee and Fork D C (eds), *Light Emission by Plants and Bacteria*, pp. 137–159. Academic Press, New York
- Padyana AK, Bhat VB, Madyastha KM, Rajashankar DR and Ramakumar S (2001) Crystal structure of a light-harvesting protein C-phycoerythrin from *Spirulina platensis*. *Biochem Biophys Res Comm* 282: 892–898
- Partensky F, Hess WR and Vault D (1999) Prochlorococcus, a marine photosynthetic prokaryote of global significance.

- Microbiol Mol Biol Rev 63: 106–127
- Pilot TJ and Fox JL (1984) Cloning and sequencing of the genes encoding the alpha and beta subunits of C-phycoerythrin from the cyanobacterium *Agmenellum quadruplicatum*. Proc Natl Acad Sci USA 81: 6983–6987
- Pizarro SA and Sauer K (2001) Spectroscopic study of the light-harvesting protein C-phycoerythrin associated with colorless linker polypeptides. Photochem Photobiol 73: 556–563
- Redlinger T and Gantt E (1982) A  $M_r$  95,000 polypeptide in *Porphyridium cruentum* phycobilisomes and thylakoids: Possible function in linkage of phycobilisomes to thylakoids and in energy transfer. Proc Natl Acad Sci USA 79: 5542–5546
- Reuter W, Wiegand G, Huber R and Than ME (1999) Structural analysis at 2.2 Å of orthorhombic crystals presents the asymmetry of the allophycocyanin-linker complex, AP-L $\zeta$ <sup>8</sup>, from phycobilisomes of *Mastigocladus laminosus*. Proc Natl Acad Sci USA 96: 1363–1368
- Rhee KH, Morris EP, Barber J and Kühlbrandt W (1998) Three-dimensional structure of the plant Photosystem II reaction center at 8 Å resolution. Nature 396: 283–286
- Ritter S, Hiller RG, Wrench PM, Welte W and Diederichs K (1999) Crystal structure of a phycoerythrin-containing phycocyanin at 1.90-Å resolution. J Struct Biol 126: 86–97
- Rümbeli R, Schirmer T, Bode W, Sidler W and Zuber H (1985) Crystallization of phycoerythrocyanin from the cyanobacterium *Mastigocladus laminosus* and preliminary characterization of two crystal forms. J Mol Biol 186: 197–200
- Sauer K and Scheer H (1988) Excitation transfer in C-phycoerythrin Förster transfer rate and exciton calculation based on new crystal structure from *Agmenellum quadruplicatum* and *Mastigocladus laminosus*. Biochim Biophys Acta 936: 157–170
- Scheer H (1981) Biliprotein. Angew Chem 93: 230–250
- Schirmer T, Bode W, Huber R, Sidler W and Zuber H (1985) X-ray crystallographic structure of the light-harvesting biliprotein C-phycoerythrin from the thermophilic cyanobacterium *Mastigocladus laminosus* and its resemblance to globin structures. J Mol Biol 184: 257–277
- Schirmer T, Huber R, Schneider M, Bode W, Miller M and Hackert ML (1986) Crystal structure analysis and refinement at 2.5 Å of hexameric C-phycoerythrin from the cyanobacterium *Agmenellum quadruplicatum*. The molecular model and its implications for light-harvesting. J Mol Biol 188: 651–676
- Schirmer T, Bode W and Huber R (1987) Refined three dimensional structures of two cyanobacterial C phycoerythrins at 2.1 and 2.5 Å resolution. A common principle of phycobilin-protein interaction. J Mol Biol 196: 677–695
- Schneider S, Prenzel CJ, Brehm G, Gottschalk L, Zhao KH and Scheer H (1995) Resonance-enhanced cars spectroscopy of biliproteins. Influence of aggregation and linker proteins on chromophore structure in allophycocyanin (*Mastigocladus laminosus*). Photochem Photobiol 62: 847–854
- Sharkov AV, Kryukov IV, Khoroshilov EV, Kryukov PG, Fisher R, Scheer H and Gillbro T (1992) Femtosecond energy transfer between chromophores in allophycocyanin trimers. Chem Phys Lett 191: 633–638
- Sidler W (1994) Phycobilisomes and phycobiliprotein structures. In: Bryant DA (ed) The Molecular Biology of Cyanobacteria, pp 139–216. Kluwer Academic Publishers, Dordrecht
- Sidler W, Gysi J, Isker E and Zuber H (1981) The complete amino acid sequence of both subunits of allophycocyanin: A light harvesting protein-pigment complex from the cyanobacterium *Mastigocladus laminosus*. Hoppe-Seyler's Z Physiol Chem 362: 611–628
- Sidler W, Kumpf B, Rüdiger W and Zuber H (1986) The complete amino-acid sequence of C-phycoerythrin from the cyanobacterium *Fremyella diplosiphon*. Bio Chem Hoppe-Seyler 367: 627–642
- Sidler W, Kumpf B, Suter F, Klotz AV, Glazer AN and Zuber H (1989) The complete amino-acid sequence of the  $\alpha$  and  $\beta$  subunits of B-phycoerythrin from the rhodophycean alga *Porphyridium cruentum*. Bio Chem Hoppe-Seyler 370: 115–124
- Stec B, Troxler RF and Teeter MM (1999) Crystal structure of C-Phycocyanin from *Cyanidium caldarium* provides a new perspective on phycobilisome assembly. Biophys J 76: 2912–2921
- Swanson RV, Ong LJ, Wilbanks SM and Glazer AN (1991) Phycoerythrins of marine unicellular cyanobacteria. II. Characterization of phycobiliproteins with unusually high phycoerythrin content. J Biol Chem 266: 9528–9534
- Wakabayashi S, Matsubara H and Webster DA (1986) Primary sequence of a dimeric bacterial haemoglobin from *Vitreoscilla*. Nature 322: 481–483
- Wang XQ, Li LN, Chang WR, Zhang JP, Gui LL, Guo BJ and Liang DC (2001) Structure of C-phycoerythrin from *Spirulina platensis* at 2.2 Å resolution: A novel monoclinic crystal form for phycobiliproteins in phycobilisomes. Acta Crystallogr D 57: 784–792
- Wedemayer GJ, Kidd DG and Glazer AN (1996) Cryptomonad biliproteins: Bilin types and locations. Photosynth Res 48: 163–170
- Wilk E, Harrop SJ, Jankova L, Edler D, Keenan G, Sharples F, Hiller RG and Curmi MG (1999) Evolution of a light-harvesting protein by addition of new subunits and rearrangement of conserved elements: Crystal structure of a cryptophyte phycoerythrin at 1.63-Å resolution. Proc Natl Acad Sci USA 96: 8901–8906
- Wolfe GR, Cunningham FX Jr, Dunford D, Green BR and Gantt E (1994) Evidence for a common origin of chloroplasts with light-harvesting complexes of different pigmentation. Nature 367: 566–568
- Yamazaki I, Mimuro M, Mura T, Yamazaki T, Yoshihara K and Fujita Y (1984) Excitation energy transfer in the light harvesting antenna system of the red alga *Porphyridium cruentum* and the blue-green alga *Anacystis nidulans*: Analysis of time-resolved fluorescence spectra. Photochem Photobiol 39: 233–240
- Zhao J, Zhou J and Bryant DA (1992) Energy transfer processes in phycobilisomes as deduced from analyses of mutants of *Synechococcus* PCC 7002. In: Murata N (ed), Research in Photosynthesis, Vol I, pp 25–32. Kluwer Academic Publishers, Dordrecht
- Zhao KH, Haessner R, Cmiel E and Scheer H (1995a) Type-I reversible photochemistry of phycoerythrocyanin involves Z/E-isomerization of  $\alpha$ -84 phycoviolobin chromophore. Biochim Biophys Acta 1228: 235–243
- Zhao KH and Scheer H (1995b) Type-I and type-II reversible photochemistry of phycoerythrocyanin a-subunit from *Mastigocladus laminosus* both involve Z, E isomerization of

phycoviolobin chromophore and are controlled by sulfhydryls in apoprotein. *Biochim Biophys Acta* 1228: 244–253  
Zouni A, Witt HT, Kern J, Fromme P, Krauß N, Saenger W and

Orth P (2001) Crystal structure of photosystem II from *Synechococcus elongatus* at 3.8 Å resolution. *Nature* 409: 739–743



# Chapter10

## Antenna Systems of Red Algae: Phycobilisomes with Photosystem II and Chlorophyll Complexes with Photosystem I

Elisabeth Gantt\*, Beatrice Grabowski and Francis X. Cunningham, Jr.  
*Department of Cell Biology and Molecular Genetics, Microbiology Building,  
University of Maryland, College Park MD 20742, U.S.A.*

Summary .....	307
I. Introduction .....	308
II. Structure and Composition of the Antenna Systems .....	308
A. Photosystems I and II are Discrete and Each has an Antenna Complex .....	308
B. Phycobilisomes and Phycobiliproteins .....	309
1. Phycobilisome Structure .....	309
2. Phycobiliprotein Characteristics .....	310
3. Linker Polypeptides .....	312
C. Chlorophylls and Carotenoids .....	312
1. Chlorophylls .....	312
2. Carotenoids .....	313
D. Light Harvesting Complex of PS I (LHC I) .....	313
1. LHC I in Red Algae but not in Glaucocystophytes .....	313
2. Characteristics Common to Red Algal LHC Polypeptides .....	314
III. Phylogenetic Implications of LHC Structure and Function .....	315
IV. Light Acclimation Responses .....	315
A. Intensity Effects .....	316
B. Wavelength Effects .....	316
V. Energy Distribution .....	318
VI. Future Problems to be Addressed .....	319
Acknowledgments .....	319
References .....	319

### Summary

Red algae have two types of light-harvesting antennas: the phycobilisome which is directly connected to the reaction centers of Photosystem II, and a LHC I complex connected to the reaction centers of PS I. The structure of red algal phycobilisomes is much like those of cyanobacteria, with a central allophycocyanin core surrounded by phycocyanin and with phycoerythrin on the periphery. In many reds the phycobilisome size is larger due mainly to a greater phycoerythrin content. The presence of LHC I may be regarded as a considerable advance in extending the light absorbing capacity in photosynthetic eukaryotes; an exception exists in the glaucocystophytes where LHC complexes have not yet been found. Chlorophyll *a* is the only type of chlorophyll present, while the presence of chlorophyll *d* is still in doubt. Zeaxanthin, and sometimes lutein, is the predominant carotenoid. Though zeaxanthin does not appear to function as an antenna pigment, in vitro reconstitution studies show its necessity for LHC stability and chlorophyll insertion. Phylogenetic relatedness of rhodophyte LHCs with those of higher plants, chromophytes, and dinophytes is evident in the high conservation of critical residues in three intrinsic membrane regions and in the successful reconstitution of red algal LHC polypeptides with pigments of other groups. Convincing evidence for excitation energy transfer

\*Author for correspondence, email: eg37@umail.umd.edu

between PS I and PS II is lacking. Photoacclimation to high light intensity is manifested by a per cell reduction of thylakoid area and chlorophyll, a decrease in the phycoerythrin content per phycobilisome, and a decline in LHC I polypeptides. In cells acclimated to light absorbed primarily by chlorophyll (red) the RC 1 content decreases and the RC 2 increases, in contrast to the opposite response with phycobilisome-absorbing green light. Complementary chromatic adaptation to red or green light, i.e. changes in phycobilisome pigments as in certain cyanobacteria, does not occur in reds.

## I. Introduction

Red algae are morphologically and developmentally diverse eukaryotic algae ranging in complexity from single cells to multicellular macrophytic forms. The presence of phycoerythrin in most of the species, and the absence of flagellated stages are two identifying features of this group of organisms. Morphologically, the chloroplasts of red algae appear highly similar to cells of cyanobacteria. The red algae are either red or blue-green in color depending on whether the orange-red phycoerythrin (PE) or the blue phycocyanin (PC) are the predominant pigments. Phycobiliproteins are water soluble pigments in which phycobilin chromophores are covalently linked to apoproteins. The phycobiliproteins are assembled in highly organized supramolecular complexes, phycobilisomes (PBS), wherein the chromophores are oriented for maximal absorption and transfer of energy from higher to lower energy states (Glazer, 1989; Chapter 9, Mimuro and Kikuchi). Phycobilisomes cover the stromal surface of thylakoids, which do not exhibit grana-like stacked regions. These characteristics, together with the simple photosynthetic pigment composition in red algae and cyanobacteria, were convincing factors in developing the argument that cyanobacteria are the progenitors of red algal chloroplasts.

Also considered in this chapter are the glaucocystophytes (*Cyanophora*, *Glaucocystis*) whose chloroplasts may be close to the cyanobacterial endosymbiont ancestor. Glaucocystophytes are often classified

with the red algae (Cavalier-Smith, 1993) largely because their cyanelles have the appearance and pigmentation of cyanobacteria (Löffelhardt et al., 1997), but unlike chloroplasts they appear to have retained the ancestral cyanobacterial cell wall layers.

This short chapter is not intended to be historically comprehensive but will concentrate on red algal antenna features exclusively. In comparison, many reviews tend to combine phycobiliproteins and PBS and include cyanobacterial features (Glazer, 1985; Gantt, 1986; Grossman et al., 1995), and tend to emphasize aspects of wavelength regulated phycobiliprotein synthesis. Reviews specifically on photoacclimation of rhodophytes, and the photosynthetic membrane structure are generally sparse (Gantt, 1980, 1990; Talarico and Maranza, 2000). Here we hope to highlight important questions on the organization of thylakoid membrane structure in red algae and the co-ordinated biosynthesis and interaction of the major antenna components in these organisms. We also emphasize recent results on LHC I polypeptide characteristics that demonstrate a close functional relatedness among eukaryotic LHCs that was not imagined until a few years ago.

## II. Structure and Composition of the Antenna Systems

### A. Photosystems I and II are Discrete and Each has an Antenna Complex

Photosystems with their respective antennas can be isolated as discrete functioning units, as has been demonstrated in *Porphyridium cruentum* (Gantt, 1990, 1996). This simple unicellular red alga is currently the model system for the reds and it has been analyzed in greatest detail. Antenna complexes of relatively few other red algal species have been studied. These include *Rhodella violacea*, *Galdieria sulphuraria* (syn. *Cyanidium caldarium*), and to a lesser extent, *Porphyra umbilicalis* and *Aglaothamnion neglectum*.

**Abbreviations:** APC – allophycocyanin; Car – carotenoid(s); Chl – chlorophyll(s); L<sub>CM</sub> – linker polypeptide for phycobilisome core-thylakoid association; LHC – light-harvesting complex; *LhcaR1*, *LhcaR2* – genes encoding LHC I polypeptides of red algae; LHC I – light-harvesting complex of PS I; PBS – phycobilisome(s); P<sub>700</sub> – absorbance change used to assay PS I activity; PC – phycocyanin (*Cyanophyceae*: C-PC, *Rhodophyceae*: R-PC); PE – phycoerythrin (*Bangiophyceae*: large (B-PE) or small (b-PE) mol. wt., *Rhodophyceae*: large (R-PE) or small (r-PE) mol. wt.); PS I – Photosystem I; PS II – Photosystem II; Q<sub>A</sub> – primary acceptor of PS II; RC 1 – reaction center of PS I; RC 2 – reaction center of PS II; Zea – zeaxanthin

The localization of the photosystems and their light harvesting complexes within the photosynthetic membrane is summarized in Fig. 1 as represented for *P. cruentum* cells grown under optimal conditions (Cunningham et al., 1989). A Photosystem I (PS I) holocomplex isolated from *P. cruentum* has about 150 Chl *a* molecules per  $P_{700}$ , of which about 100 molecules are in the reaction center core complex (RC1) when it is separated from the light-harvesting complex (LHC I) polypeptides (Wolfe et al., 1994b). Phycobilisomes, with about 2,300 chromophores/PBS for *P. cruentum* are among the largest photosynthetic antenna complexes and are the major light gathering system of PS II (Gantt, 1996).

PS II preparations from *Cyanidium caldarium*, which were highly active ( $2375 \mu\text{mol O}_2/\text{mg Chl h}^{-1}$ ), lacked LHC II polypeptides yet contained the PS II core components and the polypeptides of the  $\text{O}_2$ -evolving complex similar to cyanobacteria (Enami et al., 1995). These results indicate that the red algal PS II system is more closely related to those of cyanobacteria than those of higher plants. Independent confirmation exists from preparations of PS II isolated from *P. cruentum* thylakoids demonstrating the core antenna polypeptides CP43, CP47 plus D1 and D2. At present there is no evidence in this alga,

or any other red alga, for the presence of LHC II polypeptides as attested to by their absence on SDS-PAGE gels and the lack of immunoreactivity with antibodies to higher plant LHC IIs (Tan et al., 1995; Wolfe et al., 1994b). There is also no evidence for the presence of peripheral core antennas equivalent to CP24, CP26, and CP29 of higher plants (Bassi et al., 1999; Sandoña et al., 1998). It is thus reasonable to conclude that about 45 Chl *a*/ $Q_A$  molecules, as found by us for *P. cruentum*, are typical of red algal RC 2. Analysis of *Galdieria sulphuraria* suggests that this is also the case for this species (Marquardt and Riehl, 1997; Marquardt, 1998; Marquardt et al., 2001).

## B. Phycobilisomes and Phycobiliproteins

### 1. Phycobilisome Structure

Cyanobacterial phycobilisome structure, as comprehensively reviewed by Sidler (1994; Chapter 9, Mimuro and Kikuchi), has been more extensively characterized than that of red algae. However, the overall structure appears virtually the same except for species-specific variations in size and shape. In both groups they serve as energy guides (Glazer, 1989). Rhodophyte PBS tend to be larger than those

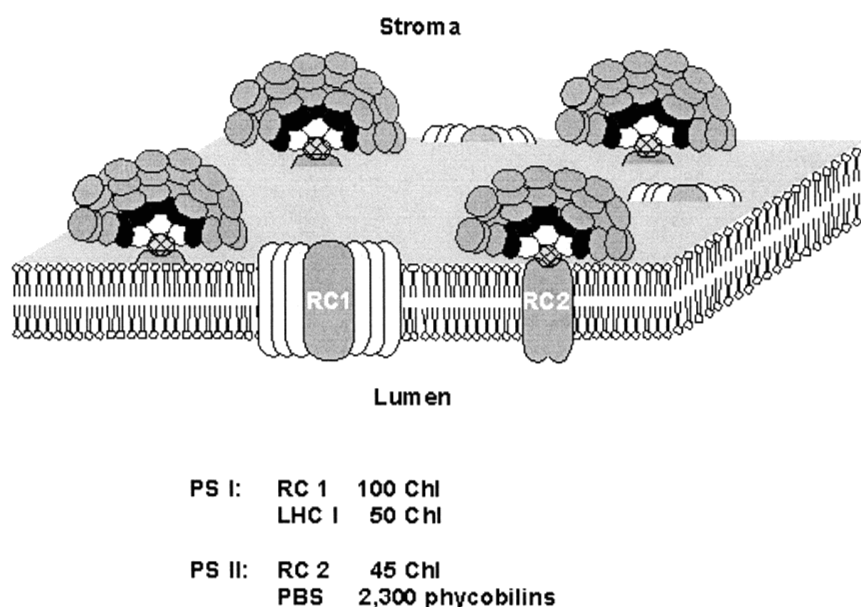


Fig. 1. Photosynthetic apparatus representative of a red alga (*Porphyridium cruentum*). Phycobilisomes (represented as viewed in cross section with part of the outer shell removed) showing the phycocerythrin layer (gray) on the periphery, followed by a phycocyanin layer (black), and allophycocyanin (light gray) in the core, and the  $L_{CM}$ -thylakoid linker (hatched) which connects the phycobilisome to the RC 2 (dimer) centers to which excitation energy is transferred. The RC 1 has a multi-peptide LHC I complex (green). PS I contains most of the Chl *a*, while PS II has the larger antenna with several thousand chromophores.

in most cyanobacteria and glaucocystophytes. Phycobilisomes of *G. pacifica* are among the largest in size (63 nm long, 38 nm wide, 38 nm high) and exceed those of *P. cruentum* (50 nm long, 33 nm wide, 30 nm high). The morphology of PE-rich PBS, as in *G. pacifica* and *P. cruentum*, tends to be hemispherical, with PE rods on the periphery attached to the central core composed of PC and APC (Gantt, 1980). However, although rich in PE, the PBS of *R. violacea* are hemidiscoidal (Bernard et al., 1996; Ritz et al., 1998), as is also the case in the PC-rich *C. paradoxa* and in *G. sulphuraria* (Marquardt, 1998). Sometimes both hemidiscoidal and hemispherical PBS are found in the same alga, as exemplified in field-collected *Porphyra umbilicalis* (Algarra et al., 1990). It is possible that a shape change may be one manifestation of less peripheral PE in the rods. However, in *P. cruentum* cells grown under high light, the PBS size decreased with an attendant 25% reduction of B-PE (Cunningham et al., 1989) as compared to those in cells grown in low light, but there was no notable change in PBS shape.

## 2. Phycobiliprotein Characteristics

Phycobiliproteins are water soluble antenna pigments that are readily released upon cell breakage to produce vibrant blue- or orange to red-colored solutions. Chemically, the chromophores are linear tetrapyrroles that are covalently bound to the apoprotein by thioether linkages to one or two rings (rings A/D) (MacColl and Guard-Friar, 1987; Chapter 2, Scheer). Amino acid sequences of the apoproteins show that the chromophores are always attached to cysteine residues and that the sequences surrounding the chromophores tend to be very highly conserved (Apt et al., 1995). Most of the phycobiliproteins are composed of  $\alpha$  and  $\beta$  protein subunits. They tend to be more stable as aggregates of  $3\alpha + 3\beta$  (trimer), or as  $6\alpha + 6\beta$  (hexamer). The most stable are the large aggregates of phycoerythrins (designated as B-PE or R-PE) which have a combination of  $\alpha$ ,  $\beta$ , and  $\gamma$  subunits and total molecular masses of about 260,000 kDa. Spectrally, the red algal phycobiliproteins are similar to those in cyanobacteria (Chapter 9, Mimuro and Kikuchi), and an extensive analysis of their amino acid sequences has confirmed that they form two distinct evolutionary lines that originate from a common ancestor (Apt et al., 1995).

The absorption and fluorescence characteristics of the major types of phycobiliproteins common in

rhodophytes are summarized in Table 1, and typical spectra are seen in Fig. 2. The principal chromophore types are phycocyanobilin and phycoerythrobilin. The former is mainly present in PC, APC, and  $L_{CM}$  (PBS-thylakoid linker), while the latter is common to all PEs. Phycourobilin is a third type of chromophore that is found in many rhodophyte PE (Chapter 2, Scheer).

The phycobiliproteins most abundant in PBS are B-PE, b-PE (bangiophycean, e.g. *Porphyridium cruentum*), and R-PE (rhodophycean, e.g. *Griffithsia monilis*). In addition to the more common  $\alpha$ - and  $\beta$ -subunits, the B- and R-PEs have  $\gamma$ -subunits. Interestingly, the  $\gamma$ -subunits appear to also serve as stabilizing linkers, because in the less stable b-PE and r-PE (45–120 kDa) the  $\gamma$ -subunits are absent. Phycoerythrobilin chromophores, covalently linked, are generally present on all  $\alpha$  and most  $\beta$  subunits of b-PE, B-PE and R-PE. Phycourobilin chromophores are present in R-PE, B-PE and r-PE and are the predominantly found on  $\gamma$ - and  $\beta$ -subunits (Ritter et al., 1999; Ficner and Huber, 1993). Some interesting novel high molecular weight PE are being found as more red algal pigments are being examined. A fresh-water *Audouinella* species was found to have phycocyanobilin in addition to the phycoerythrobilin and phycourobilin (Glazer et al. 1997). Yet another phycobilin containing PE, in *Rhodella reticulata*, totally lacked  $\alpha$ -subunits (Thomas and Passaquet, 1999).

Rhodophyte PEs absorb maximally in the 500–565 nm range (Fig. 2), with the 500 nm absorbance attributable to phycourobilin. The peripheral location of PE as an outer shell of the PBS and the fluorescence emission of these phycobiliproteins at 575–580 nm are energetically consistent with the functional transfer to PC.

Deep blue-colored PC absorb maximally around 620–630 nm (Fig. 2) and fluoresce at about 640–650 nm (Table 1). R-PC is purplish in color and is a spectral variant that contains phycoerythrobilin chromophores as well as phycocyanobilin chromophores, but nevertheless has the typical fluorescence emission of PCs. The aqua-colored APC, absorbing at the longest wavelength (650 nm), are located at the centers of PBS (Fig. 1). When present as trimers, as in the PBS core, the fluorescence emission occurs at 660 nm vs. the 650 nm emission for the monomer stage (Zhang et al., 1998). APC-B and  $L_{CM}$  are the longest wavelength components in PBS. The  $L_{CM}$ , the linker between the PBS core and the thylakoid

Table 1. Pigments, pigment binding polypeptides, and phycobilisome linker polypeptides in rhodophytes

		Absorption Maxima (nm)	Fluorescence (nm)
Thylakoid pigments:			
Chlorophylls:	Chl <i>a</i>	438, 670 (432, 618, 665) <sup>a</sup>	678
Carotenoids:	$\beta$ -carotene	(454, 480) <sup>b</sup>	—
	zeaxanthin	485 (422, 450, 481) <sup>a</sup>	—
	lutein	485 (425, 448, 476) <sup>b</sup>	—
LHC I polypeptides:		19.5a, 19.5b kDa	
		21.0	
		22.0	
		22.5	
		23.0	
		23.5	
Phycobilisome pigments:			
phycoerythrin:	b-PE	545, 563	575
	B-PE	498, 545, 563	575
	R-PE	498, 542, 565	578
phycocyanin:	C-PC	620	655
	R-PC	553, 615	640
allophycocyanin:	APC	650	660
	APC-B	618, 673	680
*L <sub>CM</sub>		650	680
Phycobilisome linkers:			
colored	*L <sub>CM</sub> PBS core-thylakoid, 93 kDa, phycocyanobilin chromophore		
	L $\gamma^1$ PE-PE, 33 kDa, urobilin chromophore		
	L $\gamma^2$ PE-PE, 32 kDa, "		
	L $\gamma^3$ PE-PE, 30 kDa, "		
uncolored	L <sub>RC</sub> core-rod PC, 27 kDa		
	L <sub>C</sub> APC-B, 13 kDa		

Spectral maxima are for pigment-proteins in aqueous buffer at room temperature. Parenthesis and *italics* are extracted pigments in <sup>a</sup>methanol or <sup>b</sup>acetone. Source material mainly from *Porphyridium cruentum* or *Rhodella violacea*. \*L<sub>CM</sub> is identified both as the terminal PBS pigment and as a PBS-thylakoid linker.

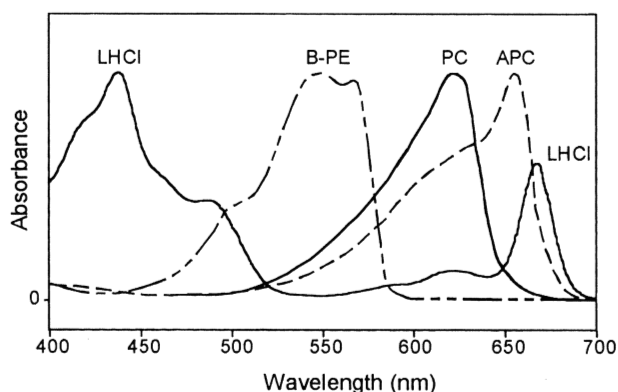


Fig. 2. Absorption spectra of antenna pigment-proteins in an aqueous medium. Allophycocyanin (---), phycocyanin (—) and phycoerythrin (----) are from phycobilisomes, and Chl *a* is in the LHC I complex (heavy line). The shoulder at about 490 nm is due to the carotenoid zeaxanthin which is not an antenna pigment.

membrane, has an emission maximum at about 680 nm in solution at room temperature, and a maximum of about 685 nm at  $-196^{\circ}\text{C}$ . With a molecular weight of about 92–95 kDa (*P. cruentum*), the  $L_{\text{CM}}$  is the largest single type of polypeptide in the PBS, with only one to a few molecules per PBS. The function of APC-B in the PBS is not fully understood because in cyanobacterial mutants it was found not to be required for PBS assembly and energy transfer (Bryant, 1991). The positional phycobiliprotein order, from the periphery to the core of the *P. cruentum* PBS as depicted in Fig. 1, represents the arrangement of pigments absorbing from higher to lower energy states. The structural integrity of PBS, free of RC 2, can be ascertained by the distinctive fluorescence emission at about 685 nm ( $-196^{\circ}\text{C}$ ), when excited through any of the component phycobiliproteins. However, when functionally coupled to RC 2 the fluorescence peak is at 695 nm ( $-196^{\circ}\text{C}$ ) showing that energy is transferred to Chl *a*. Thus, the major energy transfer path begins with the excitation of PE, energy transfer to PC, then APC, and last to the  $L_{\text{CM}}$  and then to RC 2 (Scheme 1).

Whether energy transfer occurs from APC-B to  $L_{\text{CM}}$ , or directly to RC 2, is not known.

### 3. Linker Polypeptides

Linker polypeptides are required for the appropriate arrangement of phycobiliproteins and for functional PBS structure. The majority of the linkers are uncolored, but some contain chromophores. Those of known function from *R. violacea* and *P. cruentum* are listed in Table 1. Three red-colored linkers (L) are  $\gamma$ -subunits of PEs, and one is the blue-colored  $L_{\text{CM}}$  core-membrane linker. One small uncolored linker is associated with APC-B, and another is required for attaching PC rods to the PBS core. However, the function of most linker polypeptides remains to be elucidated. In well resolved SDS-PAGE gels of *R. violacea* a rather prominent colorless polypeptide is noted at about 45 kDa and at least two other uncolored ones are found at 23 kDa and 16.5 kDa

(Bernard et al., 1996). Moreover, seven potential linker polypeptides (at 52, 45, 40, 36, 34, 28, 27 kDa) are prominent in *P. cruentum* PBS (Gantt, 1990).

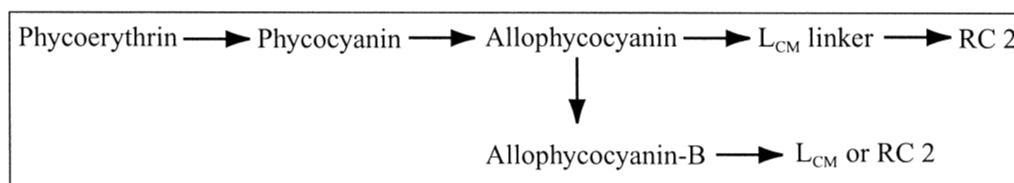
It is of interest to note that the  $\alpha$  and  $\beta$  apoproteins are generally chloroplast encoded, unlike most of the linkers which are nuclear encoded. This is evident from chloroplast genome sequences, and from translation inhibitor studies as in *R. violacea* (Bernard et al., 1996). Some of the colored  $\gamma$ -subunits appear to have other functions in addition to stabilizing PE aggregates and absorbing light. For example, an R-PE  $\gamma$ -subunit of *A. neglectum* has an N-terminal extension with a sequence uncharacteristic of phycobiliproteins but suggestive of a transit peptide that directed polypeptide import into pea chloroplasts (Apt et al., 1993).

### C. Chlorophylls and Carotenoids

For the phycobiliproteins, which are soluble in an aqueous medium, the spectral characteristics are relatively easy to assess. This is not the case for the two other major pigment classes: the Chls and carotenoids. In their 'native' state (i.e. attached to proteins) they differ in their absorption peaks from those extracted by organic solvents, with the latter usually shifting toward shorter wavelengths (Jeffrey et al., 1997). This blue-shift is illustrated by the different absorption maxima of the native complexes and extracted pigments from *P. cruentum*, which has a very simple pigment composition (Fig. 2, Table 1). In native pigment-protein complexes, Chl *a* has an absorption maximum at about 438 nm in the blue Soret wavelength region and another in the red region at about 670 nm, and a fluorescence emission at about 678 nm (excited at 438 nm). For Chl extracts in organic solvents the spectral maxima shift toward shorter wavelengths, i.e. 432 and 665 nm for Chl *a*.

#### 1. Chlorophylls

Chlorophyll *a* is usually the only type of Chl present in red algae. Occurrence of Chl *d* (Chapter 2, Scheer)



Scheme 1

was reported many years ago in red macrophytes by Manning and Strain (1943). Natural occurrence of this pigment was not given full credence until Chl *d* was unequivocally established in the oxygenic photosynthetic prokaryote *Acaryochloris*, where it accounts for most of the Chl content (Miyashita et al., 1996, 1997). However, verification of Chl *d* in field-collected rhodophytes is difficult since epiphytic micro-algae may contaminate the samples. Conclusive evidence of Chl *d* in isolated red algal PS I or PS II complexes would more convincingly demonstrate the existence this Chl in rhodophytes.

## 2. Carotenoids

Since the carotenoid composition of relatively few red algae has been critically examined, very little is known about the variety and function of carotenoids in this group thus far. In *P. cruentum*,  $\beta$ -carotene but not  $\alpha$ -carotene, has been routinely found in thylakoids in our laboratory, but this carotenoid is not an antenna pigment. We have also found small concentrations of cryptoxanthin, and antheraxanthin, but since they are present in only submolar amounts (Stransky and Hager, 1970; Cunningham et al., 1989) they are not important in this species, even if they serve as accessory pigments in other organisms. Zeaxanthin is the major carotenoid in *P. cruentum*, and also in *G. sulphuraria* (Marquardt, 1998). However, it cannot be regarded as an antenna pigment because when excited it does not show energy transfer to Chl. Nevertheless, it serves a critical function as it is required for stable insertion of Chl in LHC I (Grabowski et al., 2000). Lutein occurs in some of the 'higher' reds such as in *Batrachospermum* where it was identified by Stransky and Hager (1970). Presumably lutein is present in the LHC I complexes of these organisms, and like zeaxanthin, contributes to structural stability but in addition also serves as an accessory pigment as in green algae and higher plants. Carotenoid depletion, arising from treatment with the carotenoid pathway inhibitor norflurazon, severely affected the photosystems in *G. sulphuraria* with major pigment reductions in the PS II core complex and the LHC I complex, as well as the energetic uncoupling of PBS (Marquardt, 1998).

### D. Light Harvesting Complex of PS I (LHC I)

The gain of peripheral light-harvesting proteins for enhancement of light absorption and energy transfer

to the photosynthetic reaction centers was a major advancement in the evolution of chloroplasts. The acquisition of LHCs probably arose early in chloroplast evolution (Chapter 4, Green), and most eukaryotic photosynthetic organisms contain membrane-intrinsic light harvesting complexes (LHCs) associated with both Photosystems I and II. Cyanobacteria, the presumed ancestors of chloroplasts (Delwiche et al., 1995; Moreira et al., 2000), made use of PBS as light harvesting antennas for PS II, but did not acquire membrane-intrinsic peripheral LHCs. The eukaryotic glaucocystophytes, (like *Cyanophora*) may be extant examples of organisms wherein a cyanobacterial symbiont is in transition to becoming a chloroplast.

### 1. LHC I in Red Algae but not in Glaucocystophytes

Rhodophyte LHCs, first discovered in *P. cruentum* and associated only with RC I, have a simple pigment complement of Chl *a*, zeaxanthin, and  $\beta$ -carotene (Wolfe et al. 1994a). The LHC I of *P. cruentum* consists of at least seven polypeptides, ranging in size from 19.5 to 23 kDa (Wolfe et al., 1994a, Tan et al., 1997b). At this time it is not known if every LHC polypeptide binds Chl and carotenoids and in what proportion. However, from the predicted amino acid sequences of LhcaR1 and LhcaR2 (Tan et al., 1997a, 1997b) eight putative Chl-binding sites are evident as discussed below.

Rhodophyte LHCs in the same molecular weight range as those of *P. cruentum* have been isolated from *G. sulphuraria*, and have also been found to be associated only with PSI (Marquardt and Rhiel, 1997). LHCI polypeptides of the expected molecular weight have been identified immunologically in seven other red algae: *Achrochaetium*, *Bangia*, *Callithamnion* (*Aglaothamnion*), *Cyanidium*, *Polysiphonia*, and *Spermothamnion*, indicating a wide distribution of LHC I in the rhodophytes (Wolfe et al., 1994a; Tan et al., 1997a). In the *Cyanidium* species used in our laboratory we also found a strong immunoreactive band with anti-LHC I at about 33 kDa, a band not present in the *Galdieria* species (formerly known as *Cyanidium*) used by Marquardt and Rhiel (1997).

Glaucocystophytes have chloroplasts that have a structurally similar thylakoid arrangement to that of rhodophytes, with PBS on the stromal side of the membranes. Although they are related to rhodophytes they appear to lack LHC polypeptides, and thus their



chloroplasts are more akin to cyanobacteria. In analyzing the PS I components in thylakoids and isolated complexes from the glaucocystophyte *Cyanophora paradoxa*, Koike et al. (2001) were unable to detect LHC I polypeptides that were recognized by antibodies to LHC I polypeptides of *Porphyridium* or *Chlamydomonas*. Also, from their determination of the PS I/PS II stoichiometry and Chl analysis they found that the total Chl content is accounted for by the RC 1 and RC 2, with little remaining that could be in LHC I. Koike et al (2001) reasonably suggest that LHC-related genes in eukaryotes were acquired later and are thus not present in the glaucocystophytes

## 2. Characteristics Common to Red Algal LHC Polypeptides

Like the Chl *a/b*-binding LHCs of green plants, the red algal LHCI polypeptides are encoded in the nucleus (Tan et al., 1997a; Marquardt et al., 2000, 2001). The polypeptides encoded by two of the red algal LHC genes, *LhcaR1* and *LhcaR2* ('*Lhca*' indicates PSI affinity and '*R1*' and '*R2*' the first and second rhodophyte gene), of the *P. cruentum* multiprotein complex (Tan et al., 1997a,b) correspond

in sequence and structure to the basic LHC model of Kühlbrandt et al. (1994), with three predicted transmembrane helices (Fig. 3). The rhodophyte LHCs do not appear to have the small fourth helix near the lumen characteristic of the higher plant LHC II (Tan et al., 1997a, b).

The *P. cruentum* Chl *a*-binding LHCs were found to be immunologically related to higher-plant Chl-*a/b* proteins as well as to fucoxanthin-Chl-*a/c* antenna complexes (Wolfe et al., 1994a), and these relationships are also reflected in the sequence and conserved regions (Tan et al., 1997a,b). The *P. cruentum* LHC I polypeptides, *LhcaR1* and *LhcaR2*, are particularly well conserved, relative to plant LHCs, in the two central transmembrane helices, in the N-terminal flanking sequences between the helices on the stromal side that contain two putative carotenoid-binding sites, and in the eight putative Chl *a*-binding sites. Helices 1 and 3 of the *P. cruentum* LHCs each have three Chl *a*-binding sites and helix 2 has two Chl-binding sites also conserved in higher plant LHCs. The stabilizing residues thought to form ionic bonds between helices 1 and 3 (E56, R155 and R61, E150) are also identical to the consensus residues of green plant LHCs (Tan et al. 1997a,b). An interesting feature of the second helix is that the

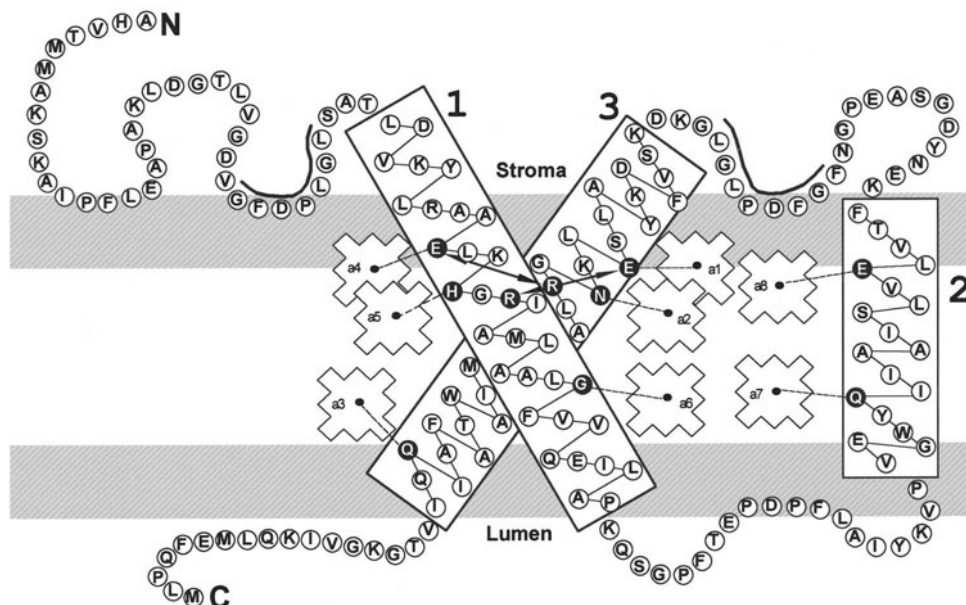


Fig. 3. Model for *LhcaR1* of *Porphyridium cruentum* with three transmembrane helices. Those residues in white text on a dark background are believed to function as Chl-binding ligands or in stabilization of helices 1 and 3. Black lines above residues on the stromal side mark amino acids that may be involved in pigment stabilization, and gray areas represent the membrane lipid bilayer. The model is a modification of that proposed by Tan et al., 1997b and Grabowski et al. (2001).

putative Chl-binding sites are separated by 8 a.a. residues, a feature shared by the chromophytes, but not by chlorophyte LHCs which have a spacing of 7 a.a. residues as can be seen in sequence comparisons (Green and Kühlbrandt 1995, Passaquet and Lichtlé 1996, Tan et al. 1997a, Durnford et al 1999). This spacing could be merely a coincidence, or it may prove to be a significant structural feature.

A comparison of the amino acid sequences deduced from seven red algal LHC I cDNAs that have been sequenced, *LhcaR1* and *LhcaR2* from *P. cruentum* and five from *G. sulphuraria* (Marquardt et al., 2000, 2001), shows that they are highly similar in molecular weight and have up to 81% similarity in the three predicted transmembrane helix regions. *G. sulphuraria*, therefore, also has a multi-peptide LHC I family, similar to *P. cruentum* where 7 polypeptides have been identified so far (Tan et al., 1997b). All the *G. sulphuraria* genes appear to have introns (Marquardt et al., 2001).

### III. Phylogenetic Implications of LHC Structure and Function

In higher plants, possession of Chl *a* and *b* in association with LHCs and the carotenoid pigments of the xanthophyll cycle is regarded as an advantage for success on land. The increased absorbance in the range 450–550 nm provided by Chl *c* and fucoxanthin in chromophytes, and by peridinin in dinophytes can be advantageous in the varied light quality in marine environments. Although LHC proteins are highly conserved across many taxa (Green and Durnford, 1996; Chapter 4, Green), they bind very different pigments in different taxonomic groups, e.g. Chls *a* and *b* and lutein in chlorophytes, Chls *a* and *c* and fucoxanthin in chromophytes; Chls *a* and *c* and peridinin in dinophytes; and Chl *a* and zeaxanthin in most rhodophytes. How did this diversity in pigment binding evolve? Were the pigment binding sites inherent in the ancestral protein, binding whatever pigments were available, or alternatively, did binding sites for specific pigments arise within the various taxa. Recent evidence suggests that the former, termed ‘molecular opportunism’ by Green (2001) may describe the evolution of pigment binding in the LHCs (Grabowski et al. 2001).

In vitro reconstitution experiments showing that certain Chl-binding sites in higher plant LHCs are able to bind either Chl *a* or Chl *b* interchangeably and

that functional LHCs can be assembled with a variety of higher plant carotenoid types and ratios (Bassi et al., 1999; Rogl and Kühlbrandt, 1999) indicate that a certain plasticity may be inherent in LHCs. The conceivable transitional nature of the *Porphyridium* chloroplast between cyanobacteria and photosynthetic eukaryotes and the simpler structure of its LHCs make this rhodophyte an ideal candidate for investigating this apparent flexibility of pigment binding.

The *LhcaR1* of *Porphyridium cruentum* normally has eight Chl *a* and four zeaxanthin molecules, although as few as one zeaxanthin/polypeptide was found sufficient for insertion of the full Chl complement (Grabowski et al., 2000). The pigments typical of a chlorophyte (*Spinacea oleracea*; Chls *a* and *b* plus lutein), a chromophyte (*Thallasiosira fluviatilis*; Chls *a*, *c*, plus fucoxanthin and diadinoxanthin), and a dinophyte (*Prorocentrum micans*; Chls *a*, *c*, plus peridinin) were found to functionally bind to this protein as evidenced by their participation in energy transfer to Chl *a*, the terminal acceptor pigment (Grabowski et al., 2001). These results not only demonstrate the functional relatedness of rhodophyte and higher plant LHCs but also suggest that eight Chl-binding sites per polypeptide are an ancestral trait, and that the flexibility to bind various Chl and carotenoid pigments was retained throughout the evolution of LHCs.

A summary of pigment-binding results in Table 2 shows that the rhodophyte LHC polypeptide retains a flexibility to functionally bind pigments foreign to its evolutionary history and that almost certainly evolved along separate phylogenetic lines i.e., rhodophytes, chlorophytes, chromophytes and dinophytes. We suggest that the diversity in the pigment composition of LHCs of different taxa is not primarily reflective of protein diversity but rather is representative of diverse pigment synthesis enzymes that developed in taxa for optimization of light energy utilization under differing light environments.

### IV. Light Acclimation Responses

It should be noted that results of acclimation studies discussed in this chapter relate mainly to experiments performed under controlled laboratory conditions mostly of unicellular red algae. Light adaptive responses, largely relating to natural i.e. field conditions, are summarized for fresh-water rhodo-

Table 2. Pigments from distantly-related photosynthetic organisms form functional in vitro complexes with a rhodophyte (LhcaR1) polypeptide

	Mol pigment/mol polypeptide									
	Chl <i>a</i>	Chl <i>b</i>	Chl <i>c</i>	Zea	Fuco	Diadin	$\beta$ -car	Lut	Neo	Vio
Pigment Source:										
Rhodophyte <sup>1</sup>	8.2	–	–	4.04	–	–	0.33	–	–	–
Chlorophyte <sup>2</sup>	6.2	1.8	–	–	–	–	0.10	2.4	0.73	1.20
Chromophyte <sup>3</sup>	7.0	–	1.0	–	8.0	1.9	–	–	–	–

<sup>1</sup>*Porphyridium cruentum*, <sup>2</sup>spinach, <sup>3</sup>*Thallasiosira fluviatilis*. Zea, zeaxanthin; fuco, fucoxanthin; diadin, diadinoxanthin;  $\beta$ -car,  $\beta$ -carotene; lut, lutein; neo, neoxanthin; vio, violaxanthin; as in Grabowski et al (2001).

phytes in Sheath and Hambrook (1990), and marine species were recently reviewed by Talarico and Maranza (2000). Light intensity and light quality are important factors in pigment composition and in photosynthetic competence, and generally higher pigment content is found in algae grown at lower light intensity (Cunningham et al., 1989; Gantt 1990; Ritz et al., 2000; Zucchi and Necchi, 2001). However, light acclimation responses are not identical in all red algal species as pointed out in a comparative study of eight red algal fresh-water species (Necchi and Zucchi 2001, Zucchi and Necchi, 2001). The influence of nutrient availability, temperature, salinity, pH may be equally important. For example, in the field, the growth of macro-algae tends to increase in the winter and decrease in the summer (Lüning, 1993). Thus meaningful comparisons on light acclimation in short term field studies can be difficult to interpret. From controlled laboratory studies on *P. cruentum* it is known that the cell growth state is very important since pigmentation can significantly differ between cells in log phase and early stationary phase at a constant light intensity. In stationary phase cells we found a reduction of PBS/thylakoid area (Levy and Gantt, 1988), which did not occur in cells analyzed from the mid to late log phase of growth (Cunningham et al. 1989).

#### A. Intensity Effects

The absorbance capacity per cell decreases with increasing light intensity in cells grown in white light. Irradiance effects may result in significant changes in thylakoid area per cell, PBS composition and size, and changes in PS I/PS II stoichiometry. Generally, an increase of light intensity (white light) causes a reduction of the major photosynthetic components per cell (Cunningham et al., 1989; Ritz et al., 2000). The acclimation responses are relatively straightforward, for *P. cruentum* at least. The content

of Chl/thylakoid area and the number of PBS/thylakoid area remain relatively constant even though the overall pigment content per cell decreases in high light-grown cells (Table 3). From cells grown in white light ( $10 \mu\text{mol m}^{-2} \text{s}^{-1}$ ) we can recover 20% Chl in the PS II polypeptide region and 80% in the PS I region (with a total Chl recovery of 92%) (Aizawa et al., 1997). This is in good agreement with estimates on thylakoids (Cunningham et al., 1989, 1990) for low light-grown cells. It is noteworthy that the PSI/PSII stoichiometry (shown by  $Q_A/P_{700}$  determinations) is little changed by the intensity of white light (Table 3).

In high light (white) the decrease in Chl content is almost entirely from the reduction of the PS I antenna size. Isolated PS I holocomplexes from high light-grown cells of *P. cruentum* had 25% less Chl than those of low light-grown cells (Tan et al., 1995). A concomitant progressive decline in LHC I polypeptide band intensity (on SDS-PAGE) accompanied the decrease in Chl content. Acclimation to high light intensity in PBS is shown by a 25% reduction of PE, which in *P. cruentum* is entirely of the B-PE type (Cunningham et al., 1989). In extensive kinetic studies of photoacclimated cells of *R. violacea*, Ritz et al. (2000) found that the terminal PE content of PBS declined in high light, as also did the thylakoid area per cell. Both of these rhodophytes display the same fundamental acclimation characteristics.

#### B. Wavelength Effects

The photosystem stoichiometry adjusts differentially when cells are grown in light primarily absorbed by the PBS antenna of PS II (green light) vs. light absorbed primarily by Chl (red) most of which is normally associated with PS I (Table 3). Red algae, in contrast to some cyanobacteria (Chapter 17, Grossman et al.), do not undergo complementary chromatic adaptation with major changes in the PE/

Table 3. Photoacclimation responses of the photosynthetic apparatus of *Porphyridium cruentum* grown in different light intensities and qualities

	Irradiance intensity ( $\mu\text{mol m}^{-2} \text{s}^{-1}$ )	Chl/cell (pg)	Thylak./cell ( $\mu\text{m}^2$ )	$Q_A/P_{700}$ (mol/mol)	$Q_A/\text{PBS}$ (mol/mol)	$P_{700}/\text{PBS}$	$Q_A+P_{700}$ PBS
White light:	6	1.7	630	0.54	2.9	5.4	8.2
	35	1.8	580	0.45	2.8	6.2	8.9
	180	0.6	300	0.43	3.0	6.8	9.8
	280	0.6	250	0.53	3.9	7.6	11.6
Green light:	15	1.6	nd	0.26	1.6	6.3	7.9
Red light:	15	1.5	nd	1.21	4.3	3.6	7.9

Table 4. Light quality photoacclimation responses in light primarily absorbed by phycobilisomes (green) or primarily by chlorophyll (red)

	Density per $\mu\text{m}^2$ thylakoid membrane area		
	PBS	RC 1	RC 2
Green light: ( $15 \mu\text{mol m}^{-2} \text{s}^{-1}$ )	$400/\mu\text{m}^2$	$2520/\mu\text{m}^2$	$630/\mu\text{m}^2$
Red light: ( $15 \mu\text{mol m}^{-2} \text{s}^{-1}$ )	$450/\mu\text{m}^2$	$1580/\mu\text{m}^2$	$1890/\mu\text{m}^2$

PC ratio when grown under different light quality. *P. cruentum* cells grown in green light, primarily absorbed by PE, acclimate by increasing the number of PS I and decreasing the number of PS II, without any significant change in the PBS composition or size (Table 4) (Cunningham et al., 1990). Under red light, PS II reaction center number increases relative to the numbers of PS I and PBS. Based on the measured PBS density of  $400/\mu\text{m}^2$  membrane area in green light-grown cells and  $450/\mu\text{m}^2$  in red light-grown cells, and on the PS I and PS II reaction center content, the photosystem densities per unit membrane were estimated as shown in Table 4 (Mustardy et al., 1992). In Fig. 4 is shown how many photosystems of each type would occur relative to the area occupied by a PBS in *P. cruentum*. In this species, conservative calculations made in our laboratory predict that more than half of the thylakoid area is occupied by PS I, PS II, Cyt/ $b_6$  and  $\text{CF}_1$  components.

The spatial distribution of PS I and PS II reaction centers in membranes from red- and green-light grown cells were probed with gold-coupled antibody to the reaction centers (Mustardy et al., 1992). We ascertained that both photosystems are distributed throughout the photosynthetic membranes, without any gross sequestrations of either photosystem. In attempting to assess the distance between the reaction centers we came to the conclusion that PS I and PS II reaction centers tend to occur as small clusters as suggested in Fig. 4. For PS I 25% of the total PS I

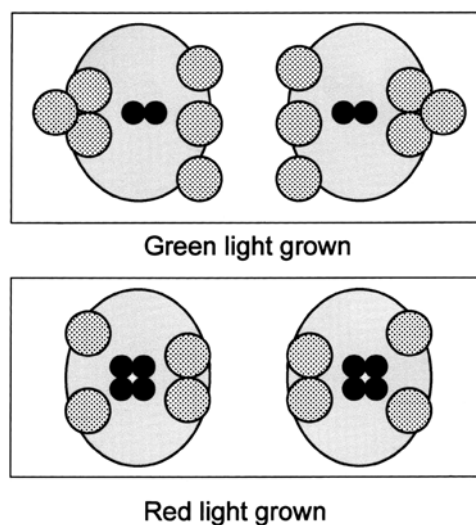


Fig. 4. Stoichiometric representation of photosystem distribution in cells of *Porphyridium cruentum* grown in green or red light. Photosystem I (stippled) and Photosystem II (black) complexes are shown stoichiometrically relative to the phycobilisome (large gray circles) and as viewed through the thylakoid looking from the lumenal toward the stromal surface. Direct physical association of PS II centers and PBS has been shown. Various distributions and groupings of PS I centers are possible, but physical association between PS I centers and phycobilisomes is not implied.

centers in the thylakoid membrane were immuno-tagged. The greatest percentage (42%) of PS II centers were tagged in thylakoids with the lower total PS II density, whereas in those with the higher PS II

density the percentage decreased (29%) (Mustardy et al., 1992). Furthermore, the sum of gold-label particles was higher when PSI and PS II centers were labeled separately, then when labeled simultaneously. Clustered centers would tend to bind proportionately less immunol-label if the reaction centers and the gold-antibody-particle used are in the same size range, as was the case in these experiments. The clustering of PS II centers, consistent with the immunolabeling, has independent support from dimers observed in the fracture plane of thylakoid membranes. Freeze-fracture studies on red algal thylakoids have repeatedly indicated groups of dimers near PBS (Gantt, 1980; Mörschel and Mühlethaler, 1983). Moreover, four to five PS II/PBS were proposed as a functional unit in red light-grown cells (Ley, 1984; Cunningham et al., 1990) in *P. cruentum*. Therefore, PS II tetramers in such cell are proposed (Fig. 4).

For red algae there is no direct evidence that PS I exists as trimers (as allowed for in Fig. 4), but such an extrapolation could be made since PS I trimers are clearly evident in cyanobacteria (Jordan et al., 2001; Chapter 8, Fromme et al.). Having experimentally addressed this question, we have not been able to obtain conclusive results. Furthermore, in fractionated thylakoids of *Cyanophora* Koike et al. (2001) were not able to demonstrate the existence of PS I trimers for this glaucocystophyte. It is possible that trimers, if they occur in reds or glaucocystophytes, are not sufficiently stable under the isolation conditions used, including those applied for cyanobacteria where trimers have been repeatedly shown.

## V. Energy Distribution

Photoinhibition and attendant photodamage is a problem when the energy of light absorbed by the antenna systems cannot be utilized or otherwise dissipated. One might expect red algae, which have low light compensation points (Gantt, 1990), to be more sensitive to photoinhibition. To the contrary, rhodophytes have been shown to be rather resistant to photodamage from high light and to have rapid recovery times after exposure (Lee and Vonshak, 1988; Hanelt et al., 1992). Classic manifestations of photoinhibition such as that in higher plants involving light-dependent phosphorylation of PS II have not been clearly demonstrated in reds. In an examination of the involvement of state transitions in *P. cruentum*,

Biggins et al. (1984) were unable to show a light-dependent phosphorylation in whole cells. Such results were clearly inconsistent with those from higher plants, but are fully consistent with the findings of Pursiheimo et al. (1998) who examined thylakoid protein phosphorylation of evolutionarily divergent species. In PBS-containing organisms (the cyanobacterium *Synechocystis* PCC6803 and the red alga *Ceramium tenuicorne*) light-dependent phosphorylation was absent in PS II core proteins, unlike in green plants. Interestingly, their findings led them to suggest that absence of PS II core protein phosphorylation in PBS-containing organisms demonstrates that it is unnecessary for the proper function of PS II.

Excitation energy from the PBS is directly transferred to RC 2 where it is converted to photochemical energy resulting in O<sub>2</sub>-evolution and electron transfer to RC 1. Transfer from PBS to RC 2 is well established in whole cells, and functional activity of isolated PBS/RC 2 complexes has been demonstrated (cf. Gantt, 1990). A direct association of PBS and PS I has not as yet been demonstrated. However, one could speculate that PS I and PS II centers might be brought sufficiently close, within the less than 10 nm distance required for excitation energy transfer. It can also be speculated that PBS may somehow become attached to PS I by a conformational change occurring in thylakoid membrane components, or by a migration of PBS from PS II to PS I reaction centers.

In green plants an excitation transfer connection between PS II and PS I (state change) can be brought about by phosphorylation of LHC II polypeptides and their migration to PS I (Chapter 13, Krause and Johns). With the apparent lack of LHC II polypeptides in red algae, this mechanism of preventing damage from over-excitation of RC 2 is not likely. State changes in green plants, as measured by a decrease in PS II fluorescence, occur relatively slowly, with durations of minutes. In red algae the apparent state changes are orders of magnitude faster, and the increase of PS I fluorescence appears to be independent of the quenching in PS II fluorescence (Bruce et al. 1986, Delphin et al. 1996).

What alternatives exist in red algae to dissipate energy and prevent photoinhibition, if the energy is not redistributed by the reaction centers? Dissipation through fluorescence or thermal conversion are recognized alternatives, but direct evidence is still lacking. In cyanobacteria, from whole cell fluores-

cence studies, Mullineaux et al. (1997) favor the hypothesis that over-excitation from excess PBS energy to RC 2 is prevented by the physical detachment of the PBS and their movement and attachment to RC 1.

A compelling set of experiments was performed that critically addressed the state 1 and 2 transitions in the unicellular red alga *Rhodella violacea* and elucidated critical factors that resolve apparent inconsistencies (Delphin et al., 1995, 1996, 1998). These experiments showed that inhibition of protein phosphorylation did not influence the state 1 and 2 transitions (Delphin et al. 1995), thus supporting previous findings (Biggins et al. (1984). They further demonstrated that the PS II quenched fluorescence state results from the  $\Delta pH$  across the membrane and not from the reduction of the plastoquinone pool (Delphin et al. 1996). Even very low intensities of green light (state 2 light), absorbed only by PBS antenna of PS II, were sufficient for inducing the  $\Delta pH$ . The PS II fluorescence quenching was relaxed upon uncoupling the  $\Delta pH$  gradient, and by activation of ATPase, hence it was proposed that the quenching relaxation is related to the utilization of the  $\Delta pH$  by ATP synthase (Delphin et al. 1998). The collective results make it clear that substantial differences exist in the excitation energy distribution in red algae and green plants.

## VI. Future Problems to be Addressed

Red algae, despite a paucity of defined mutants and the lack of genetic transformation systems, provide rare opportunities for exploring basic questions of excitation energy transfer among pigment complexes and of membrane topography. Many years have elapsed since the discovery of PBS in red algae. Yet many interesting problems remain unresolved, the primary one being how PBSs are functionally connected to RC 2. Such a functional connection very likely includes phycocyanobilin chromophore(s) on the  $L_{CM}$  and the companion Chl chromophores in parallel orientation within a distance of less than 10 nm. Is excitation energy transferred first to the core antenna, or directly to the reaction center Chls? Reconstitution experiments with RC 2 components are feasible and are especially attractive because of the relatively simple polypeptide composition. Ascertaining the physical and functional binding of PBS to RC 1 can be readily approached by relatively

straightforward in vitro reconstitution of purified intact components. Also, red algal thylakoid membranes provide excellent material for determining the potential function domains within intact membranes by examining the topographic distribution of RC1, RC 2, ATP synthase, and the Cyt  $b_6f$  complex. One simple approach would be to combine atomic force microscopy, which has high resolution potential, with primary antibody labeling for identification of thylakoid complexes.

The photoprotection mechanism(s) in red algae are certainly interesting and remain to be elucidated. Clearly the state 1 and 2 changes are different from those of green plants. Also to be clarified is the means by which non-photochemical quenching takes place, which, given the carotenoid composition of LHC 1 of *P. cruentum*, must rely on zeaxanthin without other attendant quenching cycle carotenoids. Pigment and LHC I protein reconstitution experiments begun in our laboratory suggest that 'molecular opportunism' may be a significant factor in the evolution of light-harvesting complexes and pigment binding. Expanding such studies to more red algal LHCs and a variety of pigments and concentrations can enhance our understanding of the expansion of differentially pigmented algal groups which retained the fundamental protein structure.

## Acknowledgments

We would like to thank DOE for past support for research on the photosynthetic apparatus of red algae, and NSF (MCB 9631257) for more recent partial support.

## References

- Aizawa K, Tan S and Gantt E (1997) Rapid separation and analysis of chlorophyll-proteins from the red alga *Porphyridium cruentum*. Proceedings of the First Annual Meeting Japanese Soc Marine Biotechnol 1: 69A
- Algarra P, Thomas J-C and Mousseau A (1990) Phycobilisome heterogeneity in the red alga *Porphyra umbilicalis*. Plant Physiol 92: 570-576
- Apt KE, Hoffman NE and Grossman AR (1993) The gamma subunit of R-phycoerythrin and its possible mode of transport into the plastid of red algae. J Biol Chem 268:16208-16215
- Apt KE, Collier JL and Grossman AR (1995) Evolution of the phycobiliproteins. J Mol Biol 248: 79-96
- Bassi R, Croce R, Cugini D and Sandoñá D (1999) Mutational analysis of a higher plant antenna protein provides identification



- of chromophores bound into multiple sites. *Proc Natl Acad Sci USA* 96:10056–10061
- Bernard C, Etienne A-L and Thomas J-C (1996) Synthesis and binding of phycoerythrin and its associated linkers to the phycobilisome in *Rhodella violacea* (Rhodophyta): Compared effects of high light and translation inhibitors. *J Phycol* 32: 265–271
- Biggins J, Campbell CL and Bruce D (1984) Mechanism of the light state transition in photosynthesis II. Analysis of phosphorylated polypeptides in the red alga *Porphyridium cruentum*. *Biochim Biophys Acta* 767: 138–144.
- Bruce D, Hanzlick CA, Hancock LE, Biggins J and Knox RS (1986) Energy distribution in the photochemical apparatus of *Porphyridium cruentum*: Picosecond fluorescence spectroscopy of cells in state 1 and state 2 at 77 K. *Photosynth Res* 10: 283–290
- Bryant DA (1991) Cyanobacterial phycobilisomes: Progress toward complete structural and functional analysis via molecular genetics. In: Bogorad L and Vasil IL (eds) *Cell Cultures and Somatic Cell Genetics of Plants*, Vol 7B: The Photosynthetic Apparatus: Molecular Biology and Operation, pp 257–300. Academic Press, San Diego
- Cavalier-Smith T (1993) Kingdom protozoa and its 18 phyla. *Microbiol Rev* 57:953–994
- Cunningham FX, Jr, Dennenberg RJ, Mustardy L, Jursinic PA and Gantt E (1989) Stoichiometry of Photosystem I, Photosystem II, and phycobilisomes in the red alga *Porphyridium cruentum* as a function of growth irradiance. *Plant Physiol* 91:1179–1187
- Cunningham FX, Jr, Dennenberg RJ, Jursinic PA and Gantt E (1990) Growth under red light enhances Photosystem II relative to Photosystem I and phycobilisomes in the red alga *Porphyridium cruentum*. *Plant Physiol* 93: 888–895
- Delphin E, Duval J-C, Etienne A-L and Kirilovsky D (1996) State transitions or  $\Delta$ -pH dependent quenching of Photosystem II fluorescence in red algae. *Biochemistry* 35:9435–9445
- Delphin E, Duval J-C, Etienne A-L and Kirilovsky D (1998)  $\Delta$ pH-dependent Photosystem II fluorescence quenching induced by saturating, multiturnover pulses in red algae. *Plant Physiol* 118: 103–113
- Delphin E, Duval J-C and Kirilovsky D (1995) Comparison of state 1-state 2 transitions in the green alga *Chlamydomonas reinhardtii* and in the red alga *Rhodella violacea*: Effect of kinase and phosphatase inhibitors. *Biochim Biophys Acta* 1232: 91–95
- Delwiche C, Kuhsel M and Palmer JD (1995) Phylogenetic analysis of *tufA* sequences indicates a cyanobacterial origin of all plastids. *Mol Phylogeny and Evol* 4:110–128
- Durnford DG, Deane JA, Tan S, McFadden GI, Gantt E and Green BR (1999) A phylogenetic assessment of the eukaryotic light-harvesting antenna proteins, with implications for plastid evolution. *J Molec Evolution* 48: 59–68.
- Enami I, Murayama H, Ohta H, Kamo M, Nakazato K, Sehn J-R (1995) Isolation and characterization of a Photosystem II complex from the red alga *Cyanidium caldarium*: Association of cytochrome c-550 and a 12 kDa protein with the complex. *Biochim Biophys Acta*. 1232: 208–216.
- Ficner R, Huber R (1993) Refined crystal structure of phycoerythrin from *Porphyridium cruentum* at 0.23 nm resolution and localization of the  $\alpha$ -subunit. *Eur J Biochem* 218: 103–106
- Gantt E (1980) Structure and function of phycobilisomes: Light harvesting pigment complexes in red and blue-green algae. *Intl Rev Cytol* 66: 45–80
- Gantt E (1986) Phycobilisomes. In: Staehelin LA and Arntzen CJ (eds) *Encyclopedia of Plant Physiology. Photosynthetic Membranes and Light-Harvesting Systems: Photosystem III*, 19: 260–268. Springer-Verlag, Berlin
- Gantt E (1990) Pigmentation and photoacclimation. In Cole KM and Sheath RG (eds) *Biology of the Red Algae*, pp 203–219. Cambridge University Press, Cambridge
- Gantt E (1996) Pigment protein complexes and the concept of the photosynthetic unit: Chlorophyll complexes and phycobilisomes. *Photosynth Res* 48: 47–53.
- Glazer AN (1985) Light harvesting by phycobilisomes. *Annu Rev Biophys Chem* 14: 47–77
- Glazer AN (1989) Light guides. Directional energy transfer in a photosynthetic antenna. *J Biol Chem* 264: 1–4
- Glazer AN, Chan CF and JA West (1997) An unusual phycocyanobilin-containing phycoerythrin of several bluish-colored, acrochaetoid, freshwater red algal species. *J Phycol* 33: 617–624
- Grabowski B, Tan S, Cunningham FX, Jr and Gantt, E (2000) Characterization of the *Porphyridium cruentum* Chl *a*-binding LHC by in vitro reconstitution: LHCaR1 binds 8 Chl *a* molecules and proportionately more carotenoids than CAB proteins. *Photosynth Res* 63: 85–96
- Grabowski B, Cunningham FX, Jr and Gantt, E (2001) Chlorophyll and carotenoid binding in a simple red algal LHC crosses phylogenetic lines. *Proc Natl Acad Sci USA*. 98: 2911–2916
- Green BR (2001) Was 'molecular opportunism' a factor in the evolution of different photosynthetic light-harvesting systems? *Proc Natl Acad Sci USA*. 98: 2119–2121
- Green BR and Durnford (1996) The chlorophyll-carotenoid proteins of oxygenic photosynthesis. *Ann Rev Plant Physiol Plant Molec Biol* 47: 685–714
- Green BR and Kühlbrandt W (1995) Sequence conservation of light-harvesting and stress-response proteins in relation to the 3-dimensional molecular-structure of LHCII. *Photosynth Res* 44: 139–148
- Grossman AR, Bhaya D, Apt KE and Kehoe DM (1995) Light-harvesting complexes in oxygenic photosynthesis: Diversity, control, and evolution. *Annu Rev Genet* 29: 231–88
- Hanelt D, Huppertz K and Nultsch W (1992) Photoinhibition of photosynthesis and its recovery in red algae. *Bot Acta* 105: 278–284
- Jeffrey SW, Mantoura RFC and Wright SW (eds) (1997) *Phytoplankton Pigments in Oceanography: Guidelines to Modern Methods*, UNESCO, Paris
- Jordan P, Fromme P, Witt HT, Klukas O, Saenger W and Krauss N (2001) Three-dimensional structure of cyanobacterial Photosystem I at 2.5 Å resolution. *Nature* 411: 909–917
- Kühlbrandt W, Wang DN and Fujiyoshi Y (1994) Atomic model of plant light-harvesting complex by electron crystallography. *Nature* 367: 614–621
- Koike H, Shibata M, Yasutomi K, Kashino Y and K Satoh (2001) Identification of Photosystem I components from a glaucocystophyte, *Cyanophora paradoxa*: the PsdD protein has an N-terminal stretch homologous to higher plants. *Photosynth Res* 65: 207–217
- Lee YK and Vonshak A (1988) The kinetics of photoinhibition and its recovery in the red alga *Porphyridium cruentum*. *Arch*



- Microbiol 150: 529–533
- Levy I and Gantt E (1988) Light acclimation of *Porphyridium purpureum* (Rhodophyta): Growth, photosynthesis, and phycobilisomes. J Phycol 24: 452–458
- Ley AC (1984) Effective absorption cross-sections in *Porphyridium cruentum*. Implications for energy transfer between phycobilisomes and Photosystem II reaction centers. Plant Physiol 74: 451–454
- Löffelhardt W, Bohnert HJ and Bryant DA (1997) The cyanelles of *Cyanophora paradoxa*. Critical Rev Plant Sci 16: 393–413
- Lüning K (1993) Environmental and internal control of seasonal growth in seaweeds. Hydrobiologia 260/262: 1–14
- MacColl R and Guard-Friar D (1987) Phycobiliproteins. CRC Press, Boca Raton
- Manning WM and Strain HH (1943) Chlorophyll *d*, a green pigment of red algae. J Biol Chem 151: 1–19
- Marquardt J (1998) Effects of carotenoid depletion on the photosynthetic apparatus of *Galdieria sulphuraria* (Rhodophyta) strain that retains its photosynthetic apparatus in the dark. J Plant Physiol 152: 372–380
- Marquardt J and Rhiel E (1997) The membrane-intrinsic light-harvesting complex of the red alga *Galdieria sulphuraria* (formerly *Cyanidium caldarium*): Biochemical and immunochromatographic characterization. Biochim et Biophys Acta 1320: 153–164
- Marquardt J, Wans S, Rhiel E, Randolph A and Krumbein WE (2000) Intron-exon structure and gene copy number of a gene encoding for a membrane intrinsic light-harvesting polypeptide of the red alga *Galdieria sulphuraria*. Gene 255: 257–265
- Marquardt J, Lutz B, Wans S, Rhiel E and Krumbein WE (2001) The gene family coding for the light-harvesting polypeptides of Photosystem I of the red alga *Galdieria sulphuraria*. Photosynth Res 68: 121–130
- Miyashita H, Ikemoto H, Kurano N, Adachi K, Chihara M and Miyachi S (1996) Chl *d* as a major pigment. Nature 383: 402
- Miyashita H, Adachi K, Kurano N, Ikemoto H, Chihara M and Miyachi S (1997) Pigment composition of a novel oxygenic photosynthetic prokaryote containing chlorophyll *d* as the major chlorophyll. Plant Cell Physiol 38: 274–281
- Moreira D, Le Guyader H and Philippe H (2000) The origin of red algae and the evolution of chloroplasts. Nature 405: 69–72
- Mörschel E and Mühlethaler K (1983) On the linkage of exoplasmic freeze-fracture particles to phycobilisomes. Planta 158: 451–457
- Mullineaux CW, Tobin MJ and Jones GR (1998) Mobility of photosynthetic complexes in thylakoid membranes. Nature 390: 421–424
- Mustardy L, Cunningham FX Jr and Gantt E (1992) Photosynthetic membrane topography: Quantitative in situ localization of Photosystem I and II. Proc Natl Acad Sci USA 89: 10021–10025
- Necchi O Jr and Zucchi MR (2001) Photosynthetic performance of freshwater Rhodophyta in response to temperature, irradiance, pH and diurnal rhythm. Phycolog Res 49: 305–318
- Passaquet C and Lichtlé C (1995) Molecular study of a light-harvesting apoprotein of *Giraudyopsis stellifer* (Chryso-phyceae). Plant Molec. Biol. 29: 135–148
- Pursiheimo S, Rintamäki E, Baena-Gonzales E and Aro E-M (1998) Thylakoid protein phosphorylation in evolutionarily divergent species with oxygenic photosynthesis. FEBS Lett 423: 178–182
- Ritter S, Hiller RG, Wrench PM, Welte W, Diederichs K (1999) Crystal structure of a phycourobilin-containing phycoerythrin at 1.90-Å resolution. J Struct Biol 126: 86–97
- Ritz M, Lichtlé C, Spilar A, Joder A, Thomas J-C and Etienne A-L (1998) Characterization of phycocyanin-deficient phycobilisomes from a pigment mutant of *Porphyridium* sp. (Rhodophyta). J Phycol 34: 835–843
- Ritz M, Thomas J-C, Spilar A and Etienne A-L (2000) Kinetics of photoacclimation in response to a shift to high light of the red alga *Rhodella violacea* adapted to low irradiance. Plant Physiol 123: 1415–1425
- Rogl H and Kühlbrandt W (1999) Mutant trimers of light-harvesting complex II exhibit altered pigment content and spectroscopic features. Biochemistry 38: 16214–16222
- Sandonà D, Croce R, Pagano A, Crimi M and Bassi R (1998) Higher plant light harvesting proteins. Structure and function as revealed by mutation analysis of either protein or chromophore moieties. Biochim. Biophys. Acta 1365: 207–214
- Sheath RG and Hambrook JA (1990) Freshwater ecology. In: Cole KM and Sheath RG (eds) Biology of the Red Algae, pp 423–453. Cambridge University Press, Cambridge
- Sidler W A (1994) Phycobilisome and phycobiliprotein structures. In: Bryant DA (ed) The Molecular Biology of the Cyanobacteria, pp 139–246. Kluwer Academic Publishers, Dordrecht
- Stransky H and Hager A (1970) Das Carotenoidmuster und die Verbreitung des lichtinduzierten Xanthophyllzyklus in verschiedenen Algenklassen IV. Cyanophyceae und Rhodophyceae. Arch Microbiol 72: 84–96
- Talarico L and Maranza G (2000) Light adaptive responses in red macroalgae: An overview. J Photochem Photobiol B: Biology 56: 1–11
- Tan S, Wolfe GR, Cunningham FX Jr and Gantt E (1995) Decrease of polypeptides in the PS I antenna complex with increasing growth irradiance in the red alga *Porphyridium cruentum*. Photosynth Res 45: 1–10
- Tan S, Cunningham FX, Jr and Gantt E (1997a) *LHCR1* of the red alga *Porphyridium cruentum* encodes a polypeptide of the LHCI complex with seven potential chlorophyll *a*-binding residues that are conserved in most LHCS. Plant Molec Biol 33: 157–167
- Tan S, Ducret A, Aebersold R and Gantt E (1997b) Red algal LHCI genes have similarities with both Chl *a/b*- and *a/c*-binding proteins: A 21 kDa polypeptide encoded by *Lhcr2* is one of the six LHCI polypeptides. Photosynth Res 53: 129–140
- Thomas J-C and Passaquet C (1999) Characterization of a phycoerythrin without  $\alpha$ -subunits from a unicellular red alga. J Biol Chem 274: 2472–2482
- Wolfe GR, Cunningham FX Jr, Durnford D, Green BR and Gantt E (1994a) Evidence for a common origin of chloroplasts with light-harvesting complexes of different pigmentation. Nature 367: 566–568
- Wolfe GR, Cunningham FX Jr, Grabowski B and Gantt E (1994b) Isolation and characterization of Photosystem I and II from the red alga *Porphyridium cruentum*. Biochim Biophys Acta 1188: 357–366
- Zhang J-M, Zheng X-G, Zhang J-P, Zhao F-I, Xie J, Wang H-Z, Zhao J-Q, Jiang L-Y (1998) Studies of the energy transfer among allophycocyanin from phycobilisomes of *Polysiphonia urceolata* by time-resolved fluorescence isotropic and

anisotropic spectroscopy. *Photochem Photobiol* 68: 777–784  
Zucchi MR and Necchi O Jr (2001) Effects of temperature,  
irradiance and photoperiod on growth and pigment content in

some freshwater red algae in culture. *Phycolog Res* 49: 103-  
114

# Chapter 11

## Light-Harvesting Systems in Chlorophyll *c*-Containing Algae

Alisdair N. Macpherson

*Department of Biophysical Chemistry, Umeå University, SE-901 87 Umeå, Sweden*

Roger G. Hiller\*

*Biology Department, Macquarie University, North Ryde, NSW Australia 2109*

Summary .....	324
I. Introduction .....	324
A. Pigments .....	324
B. Proteins .....	326
II. Groups Having One Main Light Harvesting System .....	328
A. Lhcf (FCP), the Intrinsic LHC of Haptophyte and Heterokont Algae .....	328
1. Isolation .....	328
2. Spectroscopy .....	329
3. Genes and Sequences .....	330
B. LHC from <i>Pleurochloris</i> .....	332
C. Lhcv (VCP) from <i>Nannochloropsis</i> and <i>Monodus</i> .....	333
III. Groups Having Two Distinct Light Harvesting Systems .....	333
A. Cryptophytes .....	333
1. Phycobiliprotein Components .....	333
a. PE545 .....	334
2. Lhcc, the Intrinsic LHC of Cryptophytes .....	337
3. Interaction of the Phycobiliproteins with Lhcc and/or the Photosystems .....	338
B. Dinoflagellates .....	339
1. Peridinin-Chlorophyll <i>a</i> -Protein (PCP) .....	340
a. Spectroscopy .....	342
b. Reconstitution .....	345
2. Lhcd (iPCP), the Intrinsic LHC of Dinoflagellates .....	345
3. Interactions Between the Systems .....	346
IV. Concluding Remarks .....	347
Acknowledgments .....	348
References .....	348

---

\*Author for correspondence, email: rhiller@rna.bio.mq.edu.au

## Summary

Our knowledge of the diverse peripheral light-harvesting complexes (LHCs) found in species of algae which contain chlorophyll (Chl) *c* as an accessory pigment is reviewed. Sequencing of genes encoding intrinsic LHCs with three putative transmembrane helices is proceeding rapidly in all groups, but basic biochemistry, particularly of the LHC components attached to PS I-enriched complexes, is currently neglected. All LHCs appear to have two different environments for Chl *c*, and the longer wavelength forms ( $> 640$  nm) have their  $Q_y$  transition in the plane of the membrane, or the long axis of the particle. A limited amount of time-resolved spectroscopic data has been interpreted as excluding Chl *c* as an intermediate in energy transfer between either phycobilins or carotenoids and Chl *a*, but this may be premature. All the light-harvesting proteins seem to be encoded by multigene families, and for diatoms and brown algae, many genes have been sequenced. This will allow the role of individual gene products in determining the adaptive responses to environmental variation to be appraised.

For those groups which possess an additional water-soluble antenna (cryptophytes and dinoflagellates), high-resolution ( $< 2.0$  Å) structures of the antennas are available. These are directing theoretical and transient spectroscopic studies of some of the most fundamental aspects of light harvesting, and the unique peridinin-chlorophyll *a*-protein (PCP) has already received appreciable attention. The cryptophyte PE545 has recently been crystallized as an  $(\alpha_1\beta)(\alpha_2\beta)$  heterodimer, in distinct contrast to the  $(\alpha\beta)_6$  structure of cyanobacterial phycobilins. However, the comparable interchromophore distances suggest that the fundamentals of light harvesting will be similar in both groups. The lack of a structure for any of the intrinsic light-harvesting proteins with three helices, which are common to all the groups, is a serious drawback to understanding the detailed mechanisms of light-harvesting and the role of carotenoids in particular.

## I. Introduction

Chlorophyll (Chl) *c* is found in widely diverse classes of algae, all of which have resulted from secondary or tertiary endosymbioses (McFadden, 2001). As Chl *c*-like pigments have also been found in the prochlorophyte section of the cyanobacteria, it is likely that the ancestral primary symbiont retained Chl *c* and this was transferred independently to several different algal lines whose descendants are extant (Larkum and Howe, 1997). The progression of simple branches may well have been complicated by lateral gene transfer, although there is no compelling evidence for this in the sequences of the light-harvesting proteins.

### A. Pigments

The photosynthetic antennas of marine algae are adapted to maximize the collection of the relatively

low levels of blue-green light penetrating the water column and a characteristic feature of these species is a relatively high carotenoid content associated with possession of Chl *c*. In brown algae, and diatoms and dinoflagellates (planktonic microalgae), fucoxanthin or peridinin (Fig. 1) is the primary carotenoid. Together with Chl *c*, these carotenoids are responsible for extending the light harvesting capabilities of the organism beyond the Soret band of Chl *a* to  $\sim 570$  nm (Larkum and Barrett, 1983; Hiller et al., 1991; Hiller, 1999). In cryptophytes, a single type of phycobiliprotein is also utilized to capture a significant fraction of the longer wavelength light that would otherwise be lost for photosynthetic purposes. Most marine algae also adapt to changing light intensity, or spectral quality, by varying the amount of light-harvesting proteins, with concomitant changes in the pigment content (Chapter 15, Falkowski and Chen).

The energy levels of carotenoids in general, and peridinin in particular, are shown in a generalized form in Fig. 2, along with chlorophyll *a*  $Q_x$  and  $Q_y$  states. The intense absorption in the blue-green region of the visible spectrum is attributed to the allowed transition from the ground  $S_0$  ( $1^1A_g^-$ ) state to the second excited singlet  $S_2$  ( $1^1B_u^+$ ) state. The  $S_2$  state of carotenoids decays within 300 fs to the lower-lying excited singlet  $S_1$  ( $2^1A_g^-$ ) state, which in turn decays

---

*Abbreviations:* Chl – chlorophyll; DBV – 15,16-dihydrobiliverdin; FCP – fucoxanthin-chlorophyll *a/c*-protein; HL – high light; LHC – light-harvesting complex; LL – low light; MBV – mesobiliverdin; PC – phycocyanin; PCB – phycocyanobilin; PCP – peridinin-chlorophyll *a*-protein; PE – phycoerythrin; PEB – phycoerythrobilin; PS I – Photosystem I; PS II – Photosystem II; VCP – violaxanthin-chlorophyll *a*-protein

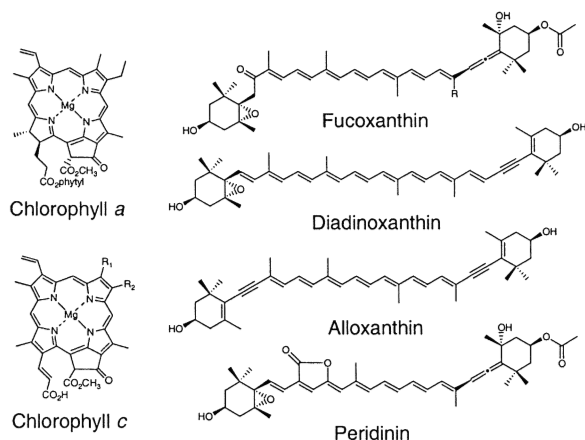


Fig. 1. Structures of some of the main pigments making up the Chl *c*-containing LHCs: Chl *a* (phytyl = 3,7,11,15-tetramethyl-2-hexadecenyl); Chl *c* (Chl *c*<sub>1</sub>: R<sub>1</sub> = CH<sub>3</sub>, R<sub>2</sub> = CH<sub>2</sub>CH<sub>3</sub>; Chl *c*<sub>2</sub>: R<sub>1</sub> = CH<sub>3</sub>, R<sub>2</sub> = CH=CH<sub>2</sub>; Chl *c*<sub>3</sub>: R<sub>1</sub> = COOCH<sub>3</sub>, R<sub>2</sub> = CH=CH<sub>2</sub>); fucoxanthin (R = H; 19'-hexanoyloxyfucoxanthin: R = CH<sub>2</sub>OCOC<sub>5</sub>H<sub>11</sub>); diadinoxanthin; alloxanthin; peridinin.

to the ground state.

Although one-photon transitions between the *S*<sub>0</sub> and *S*<sub>1</sub> states are forbidden by symmetry (Christensen, 1999; Frank, 2001), both peridinin and fucoxanthin possess an unusual structure with low symmetry and a conjugated carbonyl group (Fig. 1), and weak emission from the *S*<sub>1</sub> state is observed (Shreve et al., 1991; Mimuro et al., 1992). Furthermore, the *S*<sub>1</sub> lifetime of these xanthophylls shows an exceptional dependence upon the solvent polarity, varying from 7–173 ps (Bautista et al., 1999b; Frank et al., 2000; Zigmantas et al., 2001). It has been proposed that a short-lived (~1–3.5 ps) intramolecular charge transfer state lies below the *S*<sub>1</sub> state in polar solvents and relaxation to this third excited state competes with *S*<sub>1</sub> → *S*<sub>0</sub> internal conversion, thereby reducing the *S*<sub>1</sub> lifetime.

The inherently short lifetimes of the carotenoid excited states need not preclude efficient singlet excitation energy transfer to lower-lying chlorophyll states if the pigments are sufficiently close (in van der Waals contact) and the electronic interactions are large. Indeed, ultrafast kinetic measurements of higher plant LHCII trimers suggest that carotenoid-to-chlorophyll energy transfer can occur from the *S*<sub>2</sub> state with a remarkably high yield and rate of up to 80% and (33 fs)<sup>-1</sup>, respectively (Macpherson et al., 2002; Chapter 7, van Amerongen and Dekker).

Calculations of the electronic couplings driving energy transfer from the excited singlet states of

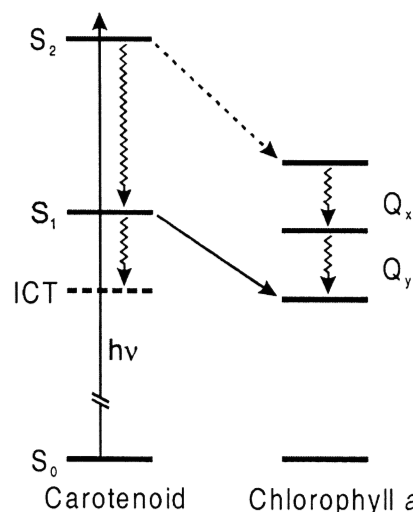


Fig. 2. Energy level scheme showing two possible pathways of carotenoid to chlorophyll energy transfer. Energy transfer from the *S*<sub>2</sub> state of the carotenoid to the *Q*<sub>x</sub> state of Chl *a* may be a significant pathway for some carotenoids (e.g. violaxanthin), but for others (e.g. peridinin), transfer from *S*<sub>1</sub> to *Q*<sub>y</sub> dominates. Three *Q* levels are indicated for Chl *a*; the *Q*<sub>y</sub> 0-0, *Q*<sub>y</sub> 0-1/ *Q*<sub>x</sub> 0-0, and *Q*<sub>x</sub> 0-1. The two *Q* levels of Chl *c* lie at energies similar to the 0-0 and 0-1 levels of the Chl *a* *Q*<sub>x</sub> state. An intramolecular charge transfer (ICT) state lying below the carotenoid *S*<sub>1</sub> state is also indicated.

carotenoids are complicated by the close proximity of the pigments in the LHCs and the breakdown of the point dipole approximation (Chapter 3, Parson and Nagarajan). However, quantitative evaluations of the full Coulombic interactions, including higher order electrostatic terms (Nagae et al., 1993), have been made by Damjanović et al. (2000) for the peridinin-chlorophyll *a*-protein (PCP). The calculated Coulombic couplings were considerably larger than those determined for an electron exchange mechanism, even for transfer from the optically 'forbidden' *S*<sub>1</sub> state to the Chl *a* *Q*<sub>y</sub> state. The lower symmetry of peridinin (and fucoxanthin), and distortions and red-shifts induced by the protein environment, will result in increased mixing of the *S*<sub>2</sub> and *S*<sub>1</sub> states and an enhancement of the *S*<sub>1</sub> transition dipole and *S*<sub>1</sub>–*Q*<sub>y</sub> coupling.

As an accessory light-harvesting pigment, Chl *c*, which has a fully unsaturated tetrapyrrole ring system and an acrylic acid side chain (Fig. 1), is somewhat anomalous. Compared to Chl *a*, the *Q*<sub>y</sub> (0,0) transition (at ~636 nm *in vivo*) is relatively weak, but the Soret band, with a maximum absorbance at ~450–460 nm, is more intense. However, in most organisms, carotenoids also absorb strongly in this region. Even

in the cryptophytes, where carotenoid absorption is not a strong feature, some species have very little Chl *c*. In the chrysophytes (Heterokonta, Table 1), *Ochromonas* (Grevby and Sundqvist, 1992) has a typical fucoxanthin-containing light-harvesting complex (LHC) but no Chl *c*, whereas *Giraudyopsis* retains Chl *c* in its LHC (Lichtlé et al., 1995). On the other hand, photosynthetic dinoflagellates typically possess a membrane-intrinsic LHC with peridinin, diadinoxanthin and a significant amount of Chl *c* (60% of the Chl *a* content). They also have a second water-soluble, extrinsic light-harvesting protein containing only peridinin and Chl *a*.

Although for many years it was generally accepted that there were only two types of Chl *c* (Chl *c*<sub>1</sub> and Chl *c*<sub>2</sub>, see Fig. 1), many different forms are now recognized (reviewed by Jeffrey and Anderson, 2000). The proliferation of Chl *c* types (Chl *c*/Chl *a* ratio > 0.5) is a particular feature of the haptophyte algae and is accompanied by some unusual carotenoid derivatives, e.g. 19'-butanoyloxy- and 19'-hexanoyloxy-fucoxanthin (Garrido and Zapata, 1998). The variants of Chl *c* also include nonpolar forms which

elute from a reversed-phase high-performance liquid chromatography (HPLC) column in the vicinity of Chl *a* and these have usually been described as 'phytylated' Chl *c*. One of these forms found in *Emiliana* has now been identified as a Chl *c*<sub>2</sub> moiety esterified to a monogalactosyldiacylglyceride (MGDG), rather than phytol (Garrido et al., 2000; Chapter 2, Scheer). Notwithstanding the fact that little is known about the role of the many forms of Chl *c*, it may be expected that all these forms are attached to the ubiquitous intrinsic LHCs which have three membrane-spanning helices and display a rich variation in pigmentation.

### B. Proteins

Although no high-resolution structure is available for any light-harvesting protein containing Chl *c*, derived amino acid sequences are available from many algal groups. These sequences, while showing a likely common origin with the much studied Chl *a*/*b*-binding LHCs of plants (Green and Durnford, 1996; Chapter 4, Green), provide no real information

Table 1. Representative organisms of algal groups together with their pigments

Algal Group	Representative Organisms	Chl <i>c</i> Type	Main Light-Harvesting Carotenoids	LHC Gene	LHC Initials
<u>Haptophyta</u>	<i>Emiliana</i> , <i>Isochrysis</i> , <i>Pavlova</i>	<i>c</i> <sub>1</sub> - <i>c</i> <sub>3</sub> and galactosyl derivatives	Fucoxanthin and 19'-acyloxy derivatives	<i>Lhcf</i>	
<u>Heterokonta</u>					
Bacillariophyceae (diatoms)	<i>Cyclotella</i> , <i>Cylindrotheca</i> , <i>Odontella</i> , <i>Phaeodactylum</i> , <i>Skeletonema</i> , <i>Thalassiosira</i>	<i>c</i> <sub>1</sub> and <i>c</i> <sub>2</sub>	Fucoxanthin	<i>Lhcf</i>	FCP
Phaeophyceae (brown algae)	<i>Dictyota</i> , <i>Fucus</i> , <i>Laminaria</i> , <i>Macrocystis</i>	<i>c</i> <sub>1</sub> and <i>c</i> <sub>2</sub>	Fucoxanthin	<i>Lhcf</i>	FCP, Cac
Raphidophyceae	<i>Heterosigma</i>	<i>c</i> <sub>1</sub> and <i>c</i> <sub>2</sub>	Fucoxanthin	<i>Lhcf</i>	FCP
Chrysophyceae	<i>Giraudyopsis</i> <i>Ochromonas</i>	+ -	Fucoxanthin		
Xanthophyceae	<i>Pleurochloris</i>	+	Diadinoxanthin, Vaucherixanthin, Heteroxanthin		
Eustigmatophyceae	<i>Monodus</i> , <i>Nannochloropsis</i>	-	Violaxanthin, Vaucherixanthin	<i>Lhcv</i>	VCP
<u>Cryptophyta</u>	<i>Cryptomonas</i> , <i>Guillardia</i> , <i>Rhodomonas</i>	<i>c</i> <sub>2</sub>	Alloxanthin	<i>Lhcc</i>	Cac
<u>Dinophyta</u> (dinoflagellates)	<i>Alexandrium</i> , <i>Amphidinium</i> , <i>Gonyaulax</i> , <i>Heterocapsa</i> , <i>Symbiodinium</i>	<i>c</i> <sub>2</sub>	Peridinin	<i>Lhcd</i>	acPCP, iPCP

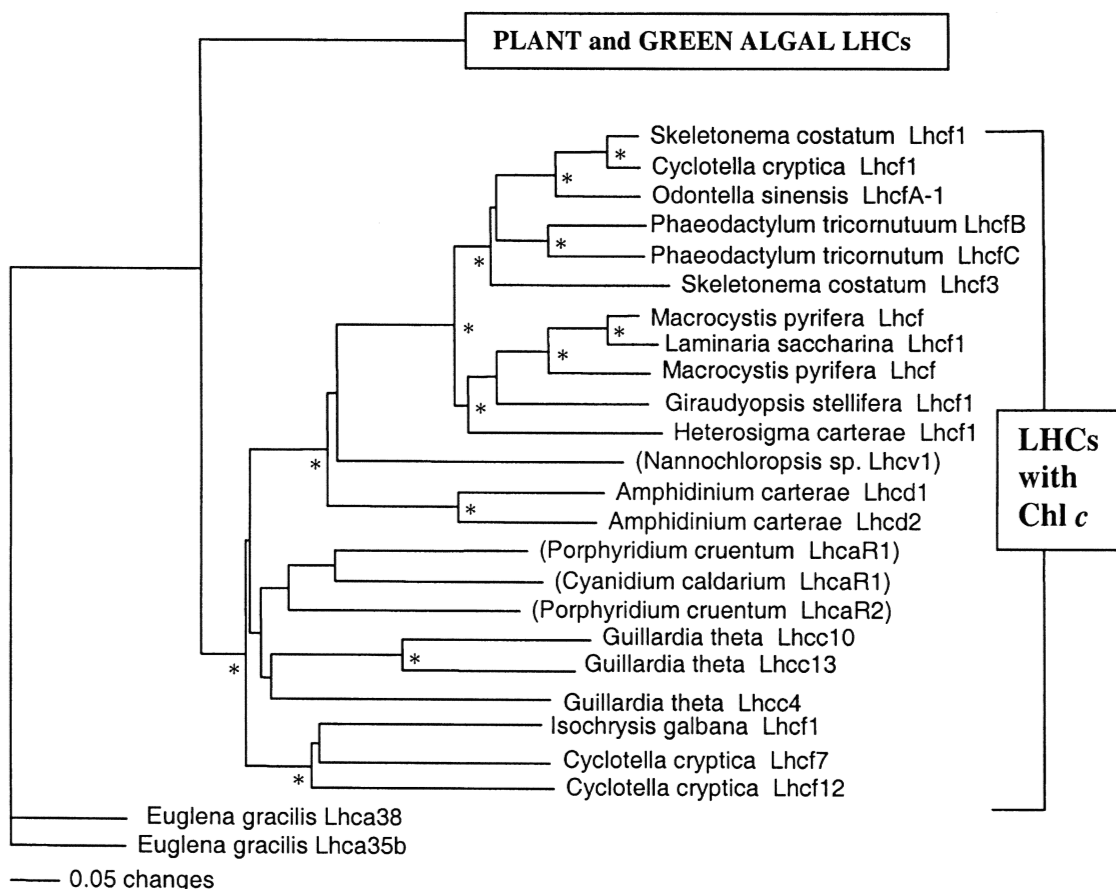


Fig. 3. Phylogenetic tree showing the relationships of LHCs containing Chl *c* (adapted from Deane et al., 2000). Bootstrap values higher than 75% (on average) are marked by an asterisk. Related LHCs not containing Chl *c* are bracketed.

on possible Chl *c* or carotenoid binding sites. The sequences do emphasize a conservation of four or five Chl *a* binding sites on transmembrane helices 1 and 3.

In the past, a number of different trivial names have been used to describe these related light-harvesting proteins, but of these, only FCP for those containing fucoxanthin, has achieved almost universal usage. Given the plethora of terms, it has been proposed that the genes and their proteins be designated in a way that emphasizes their inter-relationship (Jansson et al., 1999). Each group is designated by a four-letter code in which the fourth letter defines the type. Lhcf corresponds to FCP and Lhcd to iPCP, the intrinsic light-harvesting proteins of the peridinin-containing dinoflagellates. This simple rationalization may well require the addition of a fifth letter as a sequence becomes aligned with a function, as for Lhca and Lhcb, the LHCs associated

with Photosystem I (PS I) and Photosystem II (PS II) of higher plants, respectively. The relationships between these Chl *c*-containing proteins are shown in Fig. 3.

A glance at Fig. 3 shows a wide divergence of Lhcf and it may be that some of these are preferentially associated with PS I. It may also reflect the disproportionate number of Lhcf gene sequences available compared to those from other groups. In this chapter the four-letter code will be given at the beginning of the appropriate section, but the established trivial name, or simply LHC, will be used in the text.

The isolation of Chl *c*-containing LHCs which show excellent energy transfer from carotenoid and Chl *c* to Chl *a* is now readily achievable for many species of algae. Washed thylakoids are solubilized with digitonin or glycosidic detergents (such as *n*-dodecyl  $\beta$ -D-maltoside), at a w/w ratio of 20–100



detergent/Chl *a*. After centrifugation through a continuous sucrose gradient, three main bands are usually formed, with a PS I-enriched component at the bottom and the dominant LHC towards the top. A presumed PS II band is located near to the LHC.

The ease of isolation of the LHC, which often contains the greater part of the Chl in the thylakoids, is somewhat of a trap. Despite the obvious heterogeneity of the proteins, further purification is rarely undertaken and it may be that the second most abundant carotenoid present is localized on a separate polypeptide (De Martino et al., 2000). It is clear from published LHC polypeptide profiles that either there is a greater range of LHC peptide masses than predicted from the cDNA sequences, or there is considerable contamination and/or breakdown.

The thylakoids of chromophyte algae do not form stacks connected by single lamellae, but are arranged rather uniformly, either in groups of three appressed membranes, or in the case of cryptophytes, as two loosely associated membranes (Chapter 1, Green and Anderson). In immuno-electron microscopy (EM) studies, the LHC and PS I appear to be uniformly distributed along both the internal and external membranes (Pysznik and Gibbs, 1992; Lichtlé et al., 1992a,b). A consequence of this is that a separate PS I-containing membrane fragment cannot be isolated by mechanical means and it is generally suggested that there is no separate PS I LHC, as there is in higher plants and green algae. Our view is that this presumption may be premature, given the large families of genes already demonstrated, and that all detergent-derived PS I preparations contain a component of LHC which is rarely investigated (Berkaloff et al., 1990; Büchel and Wilhelm, 1993; Bathke et al., 1999; De Martino et al., 2000).

Two groups of algae (cryptophytes and dinoflagellates) possess a second accessory water-soluble light-harvesting protein for which high-resolution structures, as well as amino acid sequences, are available. The combination of high-resolution structural information with modern ultrafast spectroscopy offers many opportunities for understanding light harvesting in its most fundamental aspects. These two systems should also be valuable for elucidating the more physiologically relevant problems of light harvesting, such as the interaction between the many different protein molecules which make up the system and its adaptive response to the environment.

No attempt will be made in this chapter to catalogue

the light-harvesting proteins of every algal group. It will also be restricted to those groups which have Chl *c* in only the strictest sense. Algae such as *Mantoniella*, which have a Chl *c*-like component, but are otherwise in the Chl *a/b* category, are not included. On the other hand, the Eustigmatophyceae (Table 1) are included, as the LHC sequence of *Nannochloropsis* is clearly related to the Lhcf (Sukienik et al., 2000). Information will be confined to those systems for which there is a substantial body of biochemical, genetic and/or physiological data. Light-harvesting by the inner antennas surrounding the photosystems, e.g. by CP43 and CP47 in PS II, and PsaA and PsaB in PS I, will also not be discussed, as the amino acid sequences that have been derived indicate a high degree of identity across all algal and plant groups (Green and Durnford, 1996; Chapter 4, Green); they are dealt with in the context of the individual photosystems (Chapter 7, van Amerongen and Dekker; Chapter 8, Fromme, et al.)

## II. Groups Having One Main Light Harvesting System

Although not every algal group has been examined in detail, all the groups utilize a peripheral LHC with three membrane-spanning  $\alpha$ -helices and, with the exception of the cryptophytes and dinoflagellates, probably belong in this category. As shown in Table 1 and Fig. 3, most is known about the groups which use fucoxanthin as the principal light-harvesting carotenoid. Furthermore, the available data suggests, despite some considerable amino acid sequence differences between the taxa, that heterokont and haptophyte fucoxanthin-chlorophyll *a/c*-protein (FCP) LHCs are sufficiently similar to be treated as a single group (Fawley et al., 1987). Of the other algae in this category, only the LHCs of the xanthophyte *Pleurochloris meiringensis* and the eustigmatophytes *Nannochloropsis* and *Monodus* have been sufficiently investigated to warrant discussion.

### A. Lhcf (FCP), the Intrinsic LHC of Haptophyte and Heterokont Algae

#### 1. Isolation

Intrinsic LHCs in which fucoxanthin is the dominant carotenoid have been isolated from several different

algal groups. Discounting some of the earlier reports (reviewed in Hiller et al. 1991) where Triton X-100 was commonly used as a solubilizing detergent, the ratio of fucoxanthin to Chl *a* is typically 0.6–1.3 (Berkaloff et al., 1990; Passaquet et al., 1991), although ratios as high as ~2 have been reported (Friedman and Alberte, 1984). An average of five Chl *a* per 17–22 kDa polypeptide and a Chl *c*/Chl *a* ratio of 0.1–0.4, suggests a total of six or seven Chls per FCP. However, as few FCP isolation procedures involve any further purification beyond sucrose-density gradient separation of the solubilized thylakoids, these figures may be on the low side.

De Martino et al. (2000) separated the dominant FCP band from *Laminaria*, as well as FCP complexes obtained by subjecting the PS I- and PS II-enriched bands to a second detergent treatment, into a brown and a green fraction with an additional non-denaturing isoelectric focusing step. The brown fraction from each of the three complexes had a Chl *a*:Chl *c*:fucoxanthin ratio of 6:2:7 (or 8) per 20 kDa polypeptide and violaxanthin was only found in the green fractions. Katoh et al. (1989) obtained an FCP preparation from *Dictyota* which showed efficient energy transfer from Chl *c* and fucoxanthin to Chl *a*, when monitored at the fluorescence emission maximum of 677 nm. A functional particle was estimated to contain seven monomers, each monomer consisting of 13 Chl *a*, 3 Chl *c*, ten fucoxanthins and one violaxanthin associated with an apoprotein of 54 kDa. However, this is somewhat enigmatic as the molecular mass of the FCP polypeptide determined by gel electrophoresis is ~20 kDa (Passaquet et al., 1991). Assuming that these pigments are found on two polypeptides of 20 kDa, the *Dictyota* FCP would have a pigment composition similar to the FCPs isolated using glycosidic detergents from a number of organisms in several different laboratories.

## 2. Spectroscopy

Information on the organization of the pigments from these different preparations can be summarized as follows. Fucoxanthin is located in two different molecular environments; one of these extends the absorbance as far as ~570 nm (Fig. 4). Linear dichroism (LD) spectra of thylakoids show that the transition of this carotenoid is located at < 35° to the plane of the membrane (Hsu and Lee, 1987; Mimuro et al., 1990a; Hiller and Breton, 1992). This form of fucoxanthin is readily lost on mistreatment of the

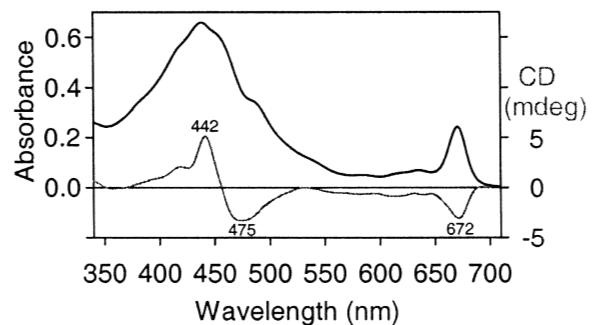


Fig. 4. Absorption (upper) and CD (lower) spectra of the FCP of *Pavlova lutherii*. Second derivative analysis of the absorption spectrum indicates peaks at 440, 455, 492, 541, 585, 634 and 671 nm.

FCP by increasing the temperature, or by adding sodium dodecyl sulfate (SDS) or Triton X-100. It is also lost when the FCP is incorporated into a squeezed polyacrylamide gel to make LD measurements (Hiller and Breton, 1992). In *Pavlova* (Fig. 4) and *Dictyota*, fucoxanthin shows almost no circular dichroism (CD) in the 540 nm region at room temperature. The signals observed at 440 (+), 673 (–) and 475 (–) nm were assigned to the Soret and  $Q_y$  bands of Chl *a* and to a second form of fucoxanthin, respectively (Mimuro et al., 1990a).

The detection of dichroism bands to the red of the Chl *a*  $Q_y$  absorption band at 671 nm suggests the presence of a long-wavelength form of Chl *a*. Two spectroscopically distinct Chl *c* forms absorbing at 632 and 638 nm were also detected in the same complex at 77 K. The brown FCP fraction from *Laminaria*, which has a Chl  $c_1$ /Chl  $c_2$  ratio of 0.64, shows similar behavior with a weak shoulder at 641 nm, in addition to the 633 nm maximum (Pascal et al., 1998). Although it might be tempting to equate the two Chl *c* forms with Chl  $c_1$  and  $c_2$ , it should be noted that cryptophyte and dinoflagellate LHCs which contain only Chl  $c_2$ , also show some evidence of two forms (Sections III.A.2 and III.B.2).

Resonance Raman spectroscopy was used to investigate the environment of the Chl *c* binding sites in the brown fraction of the major FCP of *Laminaria* at 77 K, by examining the position of the 9-keto-carbonyl band upon excitation of Chl *c* at 457.9 nm. The observation of two bands at 1679 and 1693  $\text{cm}^{-1}$ , downshifted from unbound Chl *c* in tetrahydrofuran (1707  $\text{cm}^{-1}$ ), confirms that there are two discrete populations of Chl *c*; one having a medium-strength hydrogen bond and the other in either a polar, or only

weakly interacting, environment (Pascal et al., 1998). Fucoxanthin was also studied in the same complex and the resonance Raman spectra clearly establish that this xanthophyll is bound in an *all-trans* conformation. However, the increase in intensity of two very weak out-of-plane modes when 514.5 nm excitation was used suggests that there is a subpopulation of fucoxanthins, perhaps one or two of the eight, with a highly twisted *all-trans* configuration.

We are aware of only one time-resolved study of an FCP complex. Trautman et al. (1990) measured the formation of the Chl *a* bleaching at 670 nm following excitation of the fucoxanthin in *Phaeodactylum* thylakoids between 500 and 540 nm and reported rise times of 0.5 and 2 ps with relative amplitudes of 1.7:1. Although the excited singlet state lifetimes of fucoxanthin were not determined in vivo, one possible interpretation of these kinetics is that there are two different binding sites from which the S<sub>1</sub> state of fucoxanthin can transfer energy to Chl *a* with an efficiency of at least 90%. Such a high energy transfer efficiency is consistent with that determined from the steady state fluorescence excitation spectrum of the thylakoids or isolated LHC, but only at wavelengths  $\geq 520$  nm (Shreve et al., 1991). To reconcile the apparent independence of the Chl *a* rise kinetics from excitation wavelength, and the lower steady-state efficiency of  $\sim 60\%$  between 450 and 500 nm, it was suggested that a fraction of the carotenoids is uncoupled from Chl *a*. The possible involvement of Chl *c* as an energy transfer intermediate between fucoxanthin and Chl *a* has not yet been investigated by time-resolved spectroscopy.

### 3. Genes and Sequences

Genes encoding complete FCPs have been reported from *Cyclotella* (Eppard and Rhiel, 1998; Eppard et al., 2000), *Odontella* (Kroth-Pancic, 1995), *Phaeodactylum* (Bhaya and Grossman, 1993), *Skeletonema* (Smith et al., 1997), *Laminaria* (Caron et al., 1996; De Martino et al., 2000), *Macrocystis* (Apt et al., 1995), *Isochrysis* (LaRoche, 1994), *Heterosigma* (Durnford et al., 1996) and *Giraudyopsis* (Passaquet and Lichtlé, 1995), with partial sequences available from *Thalassiosira* (Leblanc et al., 1999) and *Pavlova* (Hiller et al., 1993). With the possible exception of *Isochrysis*, it is likely that all FCPs are encoded by multigene families and up to twelve different light-

harvesting polypeptides have been detected (Durnford and Green, 1994).

In several cases, sufficient genes have been sequenced to permit separation into two classes. *Cyclotella* is particularly interesting as four of the eight genes sequenced are 'aberrant' forms (only 32–38% identity at the amino acid level), and three of these have most affinity with the Lhcf of *Isochrysis*, which is itself on a side branch of the main Chl *c*-containing lineage (Fig. 3). The fourth clone (Fcp4) is incomplete, but has a fairly strong affinity with the rhodophyte LHCs associated with PS I, especially towards the N-terminus (Eppard et al., 2000).

Despite the lack of recognizable lateral heterogeneity in the thylakoid membrane (Pysznik and Gibbs, 1992; Lichtlé et al., 1992a), it is possible that some of these derived LHC forms are preferentially associated with PS I. However, the LHCs associated with the PS I and PS II of *Laminaria* have a pigment content very similar to the main LHC fraction, and De Martino et al. (2000) concluded that there is no special PS I LHC. They also noted that the six *Lhcf* genes they isolated translate to give proteins with no variation in at least seven of the putative pigment-binding amino acids. Interestingly, one of the genes (*Lhcf3*) showed significant differences from the other five in both identity and pI. The differences were especially marked between helices 2 and 3 and at the C-terminus, which might be consistent with a different attachment point compared to the more abundant *Lhcf* forms.

The predicted size of FCP proteins is 17 to 23 kDa, in agreement with that found for the major polypeptide band on SDS polyacrylamide gels. As it is clear that all FCPs are members of the three-helix family typified by the LHCII of higher plants, the smaller size of FCPs compared to the latter is of interest and a model based on the Fcp2 sequence of *Cyclotella* is shown in Fig. 5. Much of the difference occurs in the lumenally-located loop, between transmembrane helices 1 and 2, and in the N-terminal region before the first membrane-spanning helix. As the resolution of these regions is not well defined in the Kühlbrandt et al. (1994) structure of higher plant LHC, we have no idea what these differences mean. It might be speculated that the difference in the N-terminal region is related to the different arrangement of the thylakoids, which are composed of three parallel appressed membranes, rather than a stack of many, as in higher plants.

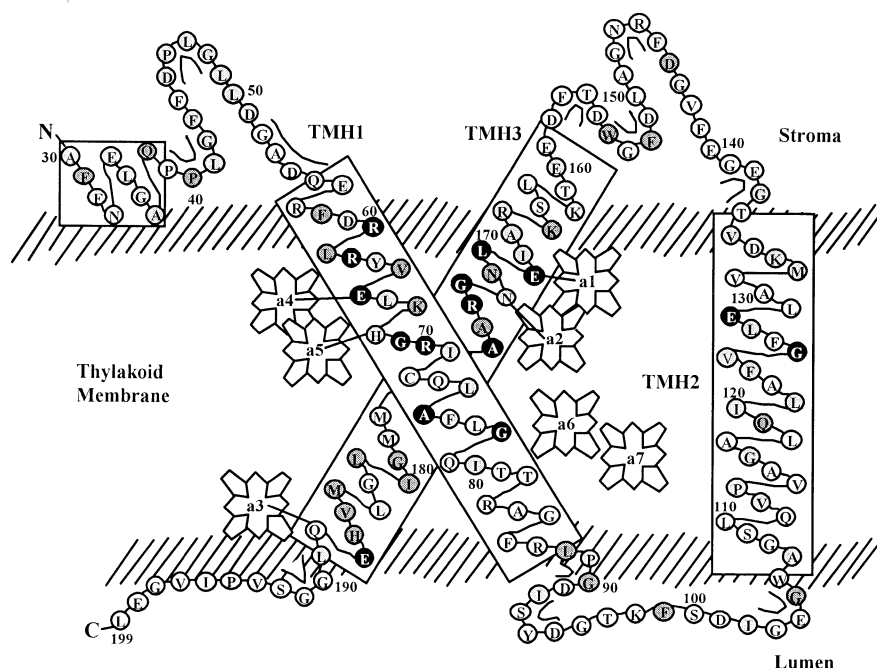


Fig. 5. Fcp2 sequence of *Cyclotella* (Eppard and Rhiel, 1998) modeled on the three transmembrane helix structure of LHCII (Kühlbrandt et al., 1994). White letters on black are conserved in all FCPs and some Chl *a/b* proteins. The gray residues are those conservatively-substituted in most LHCs. TMH, Trans-Membrane Helix. Thin lines beside groups of residues indicate predicted beta-turns.

The sequence identity between the FCPs and chlorophyll *a/b*-binding proteins is highest for the first and third helices and at least four conserved Chl *a* binding sites can be identified. As the fifth ligand for the central Mg atom of chlorophylls is now known to be very varied (Kühlbrandt et al., 1994), there are plenty of potential candidates for the remaining Chl *a* and Chl *c*. By analogy with LHCII of higher plants, the second transmembrane helix has been considered a possible Chl *c*-binding domain and, in particular, there are conserved glutamic acid and glutamine residues (Caron et al., 1996). As already noted, there is a similar number of fucoxanthin and Chl *a* molecules per polypeptide, but the residues involved in positioning the carotenoids close to the Chls cannot be predicted. In the peridinin–chlorophyll *a*-protein (PCP), the conjugated part of the carotenoid is surrounded by hydrophobic amino acids, but all eight peridinins are associated with different sequences.

The availability of complete FCP gene sequences opens the possibility for studies of the effects of environment on gene expression. In both *Giraudyopsis* (Passaquet and Lichtlé, 1995) and

*Thalassiosira* (Leblanc et al., 1999), the mRNA levels of dark-adapted cultures increased dramatically after the transition to light. In *Giraudyopsis*, expression of the FCP message became undetectable 11 hours after a subsequent return to darkness.

The similarity of the many members of the gene families makes elucidation of the roles of the different genes difficult. In *Macrocystis* (Apt et al., 1995), the *Lhcf* transcripts are ~1.2 or 1.6 kb, the difference lying in the length of the 3' untranslated region. Both the 1.2 and 1.6 kb transcript levels increased when cultures were transferred from high to low intensity white light, and low blue light was more effective than low white light. The levels of transcripts of the six genes sequenced were also examined under the same illumination conditions. The '*fcpD*' levels remained almost constant under all light conditions, but were greatly reduced by the middle of the dark cycle. In contrast, levels of '*fcpF*' dramatically increased under low blue or white light, but barely changed in the middle of the dark cycle following growth in mid-blue light. These studies show that by utilizing Northern blotting with gene-specific probes to individual *Lhcf*s, or semi-quantitative reverse

transcriptase-dependent polymerase chain reaction (RT-PCR) protocols employing gene-specific primers, a much greater understanding of the adaptation of the light harvesting system to changes in environmental conditions is attainable. Unfortunately the gene sequences of all, or most, of the members of the family have to be completed first!

### B. LHC from *Pleurochloris*

The LHC from *Pleurochloris* is the most extensively studied of any Xanthophyceae algae. The thylakoids have a Chl *c*/Chl *a* ratio of 0.05 and the LHC separated by sucrose density centrifugation has a Chl *c*/Chl *a* ratio of 0.22 (Wilhelm et al., 1988). The xanthophylls diadinoxanthin, vaucheriaxanthin ester and heteroxanthin are also strongly enriched in the LHC, with a total xanthophyll to Chl *a* ratio of 0.54. In this earlier work, a digitonin to Chl *a* ratio of 40:1 was used to solubilize the thylakoids and significant amounts of the above xanthophylls remained attached to the PS I fraction. At 77 K this PS I fraction had a fluorescence emission maximum at 715 nm, together with a shoulder at 695 nm, whereas the LHC had a peak at 685 nm. In subsequent work (Büchel and Wilhelm, 1993), the ratio of digitonin to Chl *a* was increased to 90:1 and the initial PS I preparation was treated to a second solubilization step with a Triton X-100:*n*-dodecyl  $\beta$ -D-maltoside:Chl *a* ratio of 20:90:1. From this, a fraction designated LHCI, with a Chl *c*/Chl *a* ratio of only 0.03, was obtained. This LHC had a fluorescence emission maximum at 702 nm, together with a shoulder at 686 nm, and a different polypeptide composition—approximately equal amounts of 17 and 21 kDa polypeptides, compared to a single polypeptide of 22 kDa for LHCII.

Some further support for the existence of a separate LHC associated with PS I was obtained from a freeze-fracture EM study. The PS I particles were observed as discrete patches on the PF<sub>2</sub> protoplasmic face and their dimensions were consistent with a core of PS I plus an LHC antenna (Büchel et al., 1992). Unfortunately there is no further data available for this PS I-associated antenna and the spectroscopic data discussed below relates exclusively to the LHCII.

When the LHCII is damaged or aged, excitation at 490 nm results in emission at 635 nm from Chl *c* and it was suggested that this was evidence that Chl *c* mediates energy transfer from the xanthophylls to

Chl *a* (Wilhelm et al., 1988). However no excitation spectrum was presented and some direct excitation of Chl *c* cannot be ruled out. We also consider it unlikely that Chl *c* uncoupled from Chl *a* would remain coupled to the xanthophylls.

Circular dichroism spectra suggest that while Chl *c* has little or no dichroism, the organization of Chl *a* is rather different from that in higher plant LHCs (Büchel and Garab, 1997). In the Chl *a* Q<sub>y</sub> region, the isolated *Pleurochloris* LHC shows a single intense negative CD band at 679 nm, 8 nm to the red of the absorption maximum. The absence of a split CD signal indicative of excitonic interactions, is in distinct contrast to higher plant LHCII (Chapter 7, van Amerongen and Dekker). From fits of the absorption and CD spectra with Gaussians centered at 670, 679 and 690 nm, it was concluded that the negative band centered at 679 nm represented only ~10% of the Chl *a*, but accounted for almost 80% of the CD signal. Although the amount of Chl *a* per 22 kDa polypeptide is unknown, the above result suggests only a single unique Chl *a* is involved. In contrast to the FCPs, the CD signal in the carotenoid region is rather weak.

The linear dichroism spectra of intact thylakoids show an intense positive band at 680 nm, together with a much smaller negative band at 659 nm and a complex pattern of bands of both signs at shorter wavelengths, assigned to carotenoids and the Chl Soret peaks (Büchel and Garab, 1998). The LHC also has a positive LD band at 680 nm, and this is accompanied by an almost equal strength negative band at 665 nm. However, the spectrum is dominated by a structured negative signal in the range 350 to 520 nm. As for the FCP complexes, there is little doubt that incorporation of the LHC of *Pleurochloris* (but not the thylakoids) into a polyacrylamide gel results in an unknown degree of decomposition (Hiller and Breton, 1992). Comparable LD studies, in which the orientation is achieved in a different medium, e.g. gelatine, are required to settle this point. Nevertheless in *Pleurochloris*, as in other LHCs containing Chl *c*, there is a small population of long wavelength Chl *a* which show a positive LD, indicating that the Q<sub>y</sub> transition lies in the plane of the thylakoids, or at less than 35° to the long axis of the LHC. This suggests that one or more of the conserved Chl *a* molecules is the source of the positive LD.

### *C. Lhcv (VCP) from Nannochloropsis and Monodus*

As with many other algal groups, the pigments involved in light harvesting have been established by recording the action spectra for photosynthesis, or the fluorescence excitation spectra for Chl *a* emission. In the Eustigmatophyceae, violaxanthin and perhaps vaucherixanthin ester (or its free form) act as accessory light-harvesting pigments (Owens et al., 1987). Strictly speaking these heterokonts should not be included in this review, since they do not possess a Chl *c*-containing LHC. However, the amino acid sequence derived for the main LHC, a violaxanthin-chlorophyll *a*-protein (VCP), aligns it close to the FCPs (Sukenic et al., 2000), as shown in Fig. 3. Stringent Southern blotting suggests only a single *Lhcv* gene is present, although it was noted that less stringent conditions produced several additional bands. This gene encodes a mature protein of 18.4 kDa, which is significantly smaller than the 26 kDa molecular mass that was determined by gel electrophoresis by Sukenic et al. (1992). The lower value is, however, consistent with the observation of a major polypeptide of 20 kDa in the thylakoids of similar species (Chrystal and Larkum, 1987). Antibodies to the 26 kDa apoprotein precipitated a major *in vitro* translation product of 28 kDa and a minor one of < 20 kDa. Thus, it is not impossible that a family of LHC genes encodes the light-harvesting proteins of *Nannochloropsis*, as in all the other algae.

In the absence of chlorophylls other than Chl *a*, the VCP isolated from *Nannochloropsis* shows a prominent xanthophyll absorption band at ~480 nm. Sukenic et al. (1992) reported the composition of the VCP to be 9 Chl *a*, 4 violaxanthins, and 2 vaucherixanthins per 26 kDa polypeptide, but if the mass is really 18.1 kDa, the ratio might be 6:3:1.5. Unfortunately, the light harvesting function of the xanthophylls is lost in the presence of even mild detergents (Brown, 1987; Sukenic et al., 1992). Trautman et al. (1990) estimated the energy transfer efficiency in the thylakoids to be 60–70%, and their transient absorption measurements indicate that this energy transfer probably proceeds directly from the S<sub>2</sub> state of the carotenoids to Chl *a* (Fig. 2).

A similar LHC was isolated from a *Monodus* sp. following solubilization with digitonin. A single polypeptide of ~23 kDa was observed and this VCP retained some energy transfer from the carotenoids to Chl *a* (Arsalane et al., 1992). Relative to Chl *a*,

violaxanthin and vaucherixanthin ester were present in a 28:13:100 ratio in this LHC, almost the same as for whole cells. Thus, it appears that the eustigmatophytes and xanthophytes have a carotenoid-to-Chl *a* ratio only half that of the FCPs and the intrinsic LHC of dinoflagellates (Section III.B.2).

## III. Groups Having Two Distinct Light Harvesting Systems

Two groups of algae, the cryptophytes and dinoflagellates, possess a peripheral water-soluble light-harvesting complex in addition to the universal membrane-intrinsic LHC. These additional light-harvesting proteins are not related to the three-helix LHCs.

### A. Cryptophytes

Cryptophytes are unique, utilizing both phycobiliproteins and intrinsic Chl *c*-containing light harvesting proteins in their light-harvesting apparatus. The LHC is most closely related to the LHCs of red algae (Fig. 3). The phycobiliproteins differ from those of the red algae and cyanobacteria in their location in the chloroplast, subunit structure and the occurrence of only one type of phycoerythrin (PE) or phycocyanin (PC) in a species. A number of immun-EM studies have firmly established that the phycobiliproteins are located in the thylakoid lumen (Spear-Bernstein and Miller, 1989; Ludwig and Gibbs, 1989; Rhiel et al., 1989; Lichtlé et al., 1992b; Vesik et al., 1992), confirming earlier work by Gantt et al. (1971). Some of these have also suggested that within the lumen the phycobilin occurs as stacks or rows (Ludwig and Gibbs, 1989; Lichtlé et al., 1992b; Vesik et al., 1992), although there is no real consensus. Since the PE is known to be a heterodimer of 60 kDa, whose dimensions are 75 Å × 60 Å × 40 Å (Wilk et al., 1999), there could be as many as seven PE molecules in some form of aggregate to account for the width (typically up to 300 Å) of the thylakoid lumen in cells grown at low light.

#### 1. Phycobiliprotein Components

The bilin pigments of these proteins are linear tetrapyrroles (for structures, see Chapter 2, Scheer). Although only PE or PC is found in any one species, this is an oversimplification as the spectral coverage,



especially of PC forms, is far wider than that of the PCs from cyanobacteria. Allophycocyanin has never been found in cryptophytes. Different phycobilins are designated by the predominant species of chromophore (PE are red-colored and contain at least one phycoerythrobilin, and PC are blue) together with the wavelength of maximum absorbance (see Table 2). The general structure of the proteins will be described here as a heterodimer of the form  $(\alpha_1\beta)(\alpha_2\beta)$ . Both MacColl et al. (1998) and Wilk et al. (1999) followed the convention derived from phycobilins in the phycobilisome, that the tightly linked  $\alpha\beta$  combination is a monomer and  $(\alpha_1\beta)(\alpha_2\beta)$  is therefore a heterodimer. However, in using this nomenclature, the large structural differences between the cryptophyte and cyanobacterial or rhodophyte phycobiliproteins should not be overlooked (Chapter 9, Mimuro and Kikuchi; Chapter 10, Gantt et al.).

The heterodimer is made up of two identical ~18.5 kDa  $\beta$  subunits and two shorter non-identical  $\alpha$  subunits ( $\alpha_1$ : 8.1–8.8 kDa;  $\alpha_2$ : 7–7.5 kDa). The amino acid sequence of each  $\beta$  subunit of PE or PC has a high degree of identity with the  $\beta$  subunit of the rhodophytes, including the N-methyl asparagine at residue  $\beta$ -72, and three bilin chromophores are covalently attached. The  $\alpha$  subunits only carry a single chromophore and their amino acid sequences have no counterparts in the databases. Many different types of bilin are utilized on both subunits (Table 2; reviewed in Glazer and Wedemayer, 1995). The gene for the  $\beta$  subunit is located on the chloroplast genome (Reith and Douglas, 1990), while the  $\alpha_1$  and  $\alpha_2$  genes are nuclear encoded (Jenkins et al., 1990) and arranged in pairs in an opposed orientation (M. Broughton and R. G. Hiller, unpublished).

A striking feature of cryptophyte phycobilins is the occurrence of many (at least eight for PE545) electrophoretically-distinct proteins from each species. Originally Hiller and Martin (1987) proposed a model in which all combinations of four different isoelectric forms of the  $\alpha$  subunits ( $\alpha_1$ ,  $\alpha_1'$ ,  $\alpha_2$ , and  $\alpha_2'$ ) might be combined with the  $\beta$  subunits to give ten possible variants. From a series of detailed studies on PE545, PC612 and PC645, MacColl et al. (1998, 1999a,b) suggest that the heterodimer is unstable in dilute solution at low pH and dissociates into  $\alpha\beta$  monomers. To our knowledge, the different isoforms of the monomers ( $\alpha_1\beta$ ,  $\alpha_2\beta$ , etc) have not yet been separated and characterized, and no evidence of monomer heterogeneity has been presented. Nevertheless, to account for more than three heterodimer isoforms, a number of different  $\alpha$  subunit forms are required and these are undoubtedly present, as shown by Southern blotting, genomic sequencing and N-terminal protein sequencing (R. G. Hiller, M. Broughton, G. Harrison and P. M. Wrench, unpublished). We note that the purified PE used to grow the crystals that resulted in a high-resolution structure also shows evidence of electrophoretic variability. However, it is possible that some of the variation results from the interaction of the chromophores with the reagents used to generate the isoelectric focusing gradients.

#### a. PE545

Some of the main features of the X-ray generated high-resolution (1.63 Å) structure of PE545 are shown in the figures below. A surface view (Fig. 6 and Color Plate 10) reveals that two  $\beta$  subunits are on opposite

Table 2. Bilin types and locations on cryptomonad biliproteins (Glazer and Wedemayer, 1995)

Biliprotein	$\alpha$ -Cys-18 (19)	$\beta$ -DiCys-50,61	$\beta$ -Cys-82	$\beta$ -Cys-158
PE545	Cys-DBV (562)	DiCys-PEB (550)	Cys-PEB (550)	Cys-PEB (550)
PE555	Cys-PEB (550)	DiCys-DBV (562)	Cys-PEB (550)	Cys-PEB (550)
PE566 <sup>1</sup>	Cys-Bilin 584 (584)	DiCys-Bilin 584 (584)	Cys-PEB (550)	Cys-Bilin 584 (584)
PE566 <sup>2</sup>	Cys-Bilin 618 (618)	DiCys-Bilin 584 (584)	Cys-PEB (550)	Cys-Bilin 584 (584)
PC569	Cys-PCB (643)	DiCys-Bilin 584 (584)	Cys-PCB (643)	Cys-Bilin 584 (584)
PC612	Cys-PCB (643)	DiCys-DBV (562)	Cys-PCB (643)	Cys-PCB (643)
PC645	Cys-MBV (684)	DiCys-DBV (562)	Cys-PCB (643)	Cys-PCB (643)

DBV, 15,16-dihydrobiliverdin; PEB, phycoerythrobilin; PCB, phycocyanobilin; MBV, mesobiliverdin. The numbers in parentheses indicate the long wavelength absorption maxima of solutions of bilin peptides in 10 mM trifluoroacetic acid. See Chapter 2 (Scheer) for structures of all these bilins. PE566<sup>1,2</sup> refers to strains Bermani and CBD, respectively. The bilins of PC630 have not been characterized.



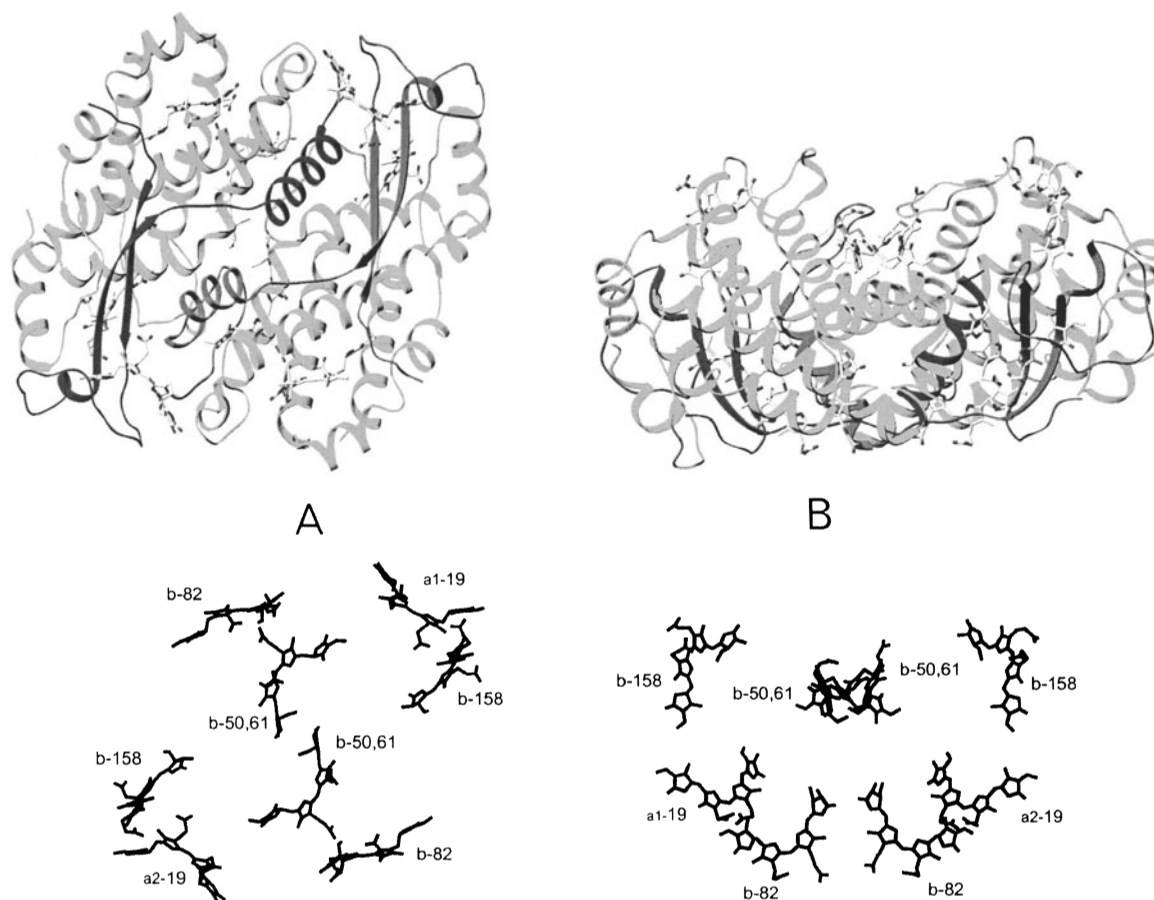


Fig. 6. PE545 from *Rhodomonas*, as ribbon diagram of polypeptide chain (top) and with chromophores dissected out (bottom). A, viewed from below; B, viewed from the side. a, chromophore attached to  $\alpha$ -subunits (dark ribbon); b,  $\beta$ -subunit. See Color Plates 10 and 11.

sides and that they sandwich the  $\alpha$  subunits. The chromophore arrangements are shown in the bottom part of Fig. 6. The positions of the three  $\beta$  subunit chromophores on the polypeptide chain are identical to those in rhodophyte PE, but the different secondary structure of the protein results in the two doubly-linked  $\beta$ -50,61 phycoerythrobilin (PEB) chromophores approaching end-to-end with the pyrrole A rings essentially parallel and in van der Waals contact (Wilk et al., 1999). The other chromophores, including the 15,16-dihydrobiliverdin (DBV) on the  $\alpha$  subunits, are spaced at 21–22 Å from their nearest neighbor, comparable to the 19 and 26 Å distances observed in rhodophyte PE (Chapter 9, Mimuro and Kikuchi).

Given the similarity of the amino acid sequences of rhodophyte and cryptophyte  $\beta$  subunits, it is interesting to note the structural variations required to accommodate the completely different organization of the holoprotein. A superposition of the two  $\beta$

subunits onto the rhodophyte  $\beta$  subunit indicates that the cryptophyte subunits mainly differ in the folding of the X and Y helices in and under the N-terminus, together with a small twist of the GH loop (Wilk et al., 1999). The  $\alpha$  subunits have a  $\beta$  sheet at the N-terminus and a short  $\alpha$ -helix towards the C-terminus (Fig. 6), which packs with helices B and E of a  $\beta$  subunit. Although the  $\alpha$  subunit amino acid sequences are not related to any other protein in the database, a remarkably similar folding of a short linker polypeptide to allophycocyanin in the phycobilisome has been reported (Reuter et al., 1999; Chapter 9, Mimuro and Kikuchi; see also Color Plate 9 of Chapter 9). It is uncertain if this indicates a real relationship between the  $\alpha$  subunits of PE545 and the  $L_C^{7,8}$  linker protein from *Mastigocladus*.

A striking feature of the three dimensional structure is the large number of ordered water molecules which fill a very polar cleft ( $\sim 20 \text{ Å} \times 5\text{--}10 \text{ Å} \times 15 \text{ Å}$ )

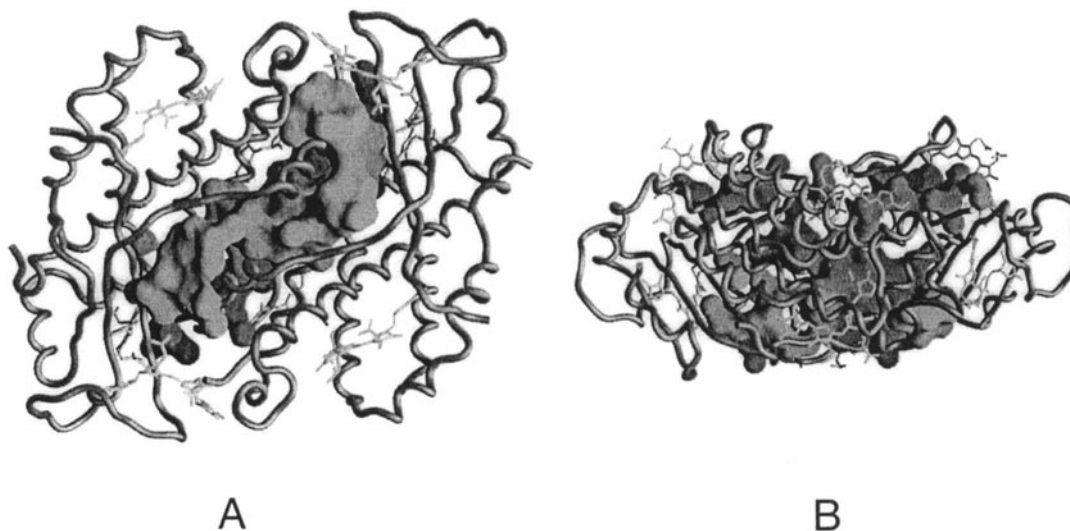


Fig. 7. Structure of PE545 with the ordered water molecules shown in the central cleft. (A) View down the pseudo two-fold axis with the slot (solid) formed of ordered water molecules. (B) Orthogonal view with the  $\beta$ -50,61 chromophores on top, near the center. The slot enters from the bottom and is not symmetric about the pseudo two-fold axis running up the page.

in the center of the protein (Fig. 7). It is tempting to suggest that this might be a docking site for a linker protein attaching the PE to the thylakoid membrane. However as the PE has been isolated from low light grown cells, most of the phycobiliproteins could not be adjacent to the membrane, but rather, associated with other PE molecules. In searching for a linker protein, phycobiliproteins extracted from cells grown under high light may be a better starting point.

It is interesting to compare the PE545 structure with that envisaged from analysis of the extensive spectroscopic data accumulated by MacColl's group over many years (MacColl et al., 1998, 1999a,b), combined with the biochemistry of separated  $\alpha\beta$  units. The concentration-dependent dissociation of the heterodimers into  $\alpha\beta$  monomers at pH 4.5 was monitored by dynamic light scattering and by size exclusion chromatography. At pH 4.5, the absorbance of PE545 from *Rhodomonas lens* was reduced by ~20% compared to that at pH 6.0, and this was accompanied by a somewhat larger decrease of the visible CD bands and a blue shift of the fluorescence maximum from 584–585 to 581 nm. The observation of only small changes in the ultraviolet CD indicated that the secondary structure was largely unaltered.

The difference spectrum between the heterodimer (pH 6.0) and monomer (pH 4.5) CD had maxima at 538 (+) and 564 (–) nm, and a shape very similar to the heterodimer CD spectrum. A similar difference

spectrum was obtained after permanganate treatment. To account for the negative CD band, which is absent in native rhodophyte phycoerythrin ( $\alpha_6\beta_6\gamma$ ), exciton coupling between a pair of closely-spaced chromophores was proposed to exist across the dimer interface, as was indeed observed in the X-ray-derived structure. It is worth noting that the pH 6.0-minus-pH 4.5 difference CD spectrum is distinctly asymmetrical, and that the crystal structure suggests that interactions between the  $\beta$ -50,61 phycoerythrobilin (PEB) chromophores are not the only ones broken by separation of the monomers. Each  $\alpha$ -19 DBV (15,16-dihydrobiliverdin) appears to be coupled with  $\beta$ -82 and  $\beta$ -50,61 bilins from the opposite  $\beta$  subunit (Fig. 6), and this coupling will also be disrupted upon dissociation.

Since the CD spectrum of the  $\alpha\beta$  monomers was significantly stronger than that attributed to the intermonomer interactions, MacColl et al. (1998, 1999b) speculated that there must be another pair of bilins ( $\alpha$ -19 DBV and a  $\beta$  PEB) in close proximity within the monomer. However, the PEB chromophores attached to the  $\beta$  polypeptide also show a negative CD band in ~1 M urea, pH 4.0 (MacColl et al., 1994). Although the structure shows no strongly interacting pair of chromophores within a monomer, it is possible that the situation in PE545 is similar to that in PCP (Section III.B.1.a), and weak interactions between all the chromophores have to be evaluated

to reproduce the CD spectra (Carbonera et al., 1999). Unfortunately, no structure-based calculations of the CD have been reported.

There is little published kinetic data available to compare with the Förster resonance energy transfer times calculated from the structure of PE545 (Wilk et al., 1999). Using 2-photon excitation, fluorescence decay times of 2.4, 483 and 2505 ps were reported for the PE545 heterodimer. At pH 4.0, where the monomer predominates, the lifetimes were 39, 423 and 2500 ps (MacColl et al., 1998). The 2500 ps component was assigned to emission from the lowest-energy bilin and the 2.4 ps component to the energy migration time among the chromophores. In the heterodimer, a fast rate of  $(0.4 \text{ ps})^{-1}$  was calculated for a single transfer between the pair of  $\beta$ -50,61 phycoerythrobilins formed across the monomer-monomer interface (Wilk et al., 1999). The next fastest pairwise transfer times were between the  $\beta$ -82 and  $\beta$ -50,61 PEB chromophores of one monomer and the  $\alpha$ -19 DBV chromophore of the other monomer (12–28 ps). The transfer times to the DBV chromophore within the  $\alpha\beta$  monomers were estimated to be considerably slower ( $\geq 150$  ps for  $\beta$  subunit C, and  $\geq 450$  ps for  $\beta$  subunit D), although high rates of  $(15\text{--}100 \text{ ps})^{-1}$  were still predicted for transfer between isoenergetic PEB chromophores on a single  $\beta$  subunit.

The steady state fluorescence polarization reported by MacColl et al. (1999b) is essentially zero for excitation wavelengths up to 540 nm, but thereafter increases rapidly in the region of negative CD to a final value of  $\sim 0.2$  at 600 nm. This change in polarization was assigned to a combination of three processes: intra- and inter-monomer internal conversion between the exciton levels of two sets of coupled chromophores and energy transfer from DBV to PEB within a monomer. Ultrafast time-resolved anisotropy measurements may prove to be a profitable avenue of future research.

As shown in Table 2, the positions of all the chromophores have been established, as they can be isolated still covalently attached to their tryptic peptides. The subtle variation between PE545 and PE555, where the novel DBV chromophore is attached to the  $\alpha$  subunits of PE545, but doubly linked at  $\beta$ -50,61 in PE555, is particularly noteworthy. In all other cases, it is the  $\alpha$  subunit that binds the bilin that is lowest (or one of the lowest) in energy in 10 mM trifluoroacetic acid. Like PE555, the DBV is also attached at  $\beta$ -50,61 in PC612 and PC645, but

the other  $\beta$  subunit chromophores are phyco-cyanobilins (PCB) lying at lower energy. The CD spectra of these biliproteins are similar to PE545 in that they show a strong negative band at long wavelengths and both the positive and negative CD bands decrease upon disruption of the heterodimer. MacColl et al. (1999a) propose that the  $\beta$ -50,61 DBV chromophores of PC612 are not coupled across the monomer-monomer interface because a negative CD band on the blue side was not observed. The three changes in the fluorescence polarization spectrum at  $\sim 550$ , 590 and 640 nm were assigned to energy transfer from DBV, transfer from PCB to a coupled pair of PCBs within the monomer and to internal conversion between this pair of PCBs, respectively (MacColl et al., 1999b).

## 2. *Lhcc*, the Intrinsic LHC of Cryptophytes

The intrinsic LHC isolated by SDS-polyacrylamide gel electrophoresis, or by solubilizing the thylakoids in digitonin, contains most of the Chl *c* and has two principal polypeptides of 20 and 24 kDa (Ingram and Hiller, 1983; Rhiel et al., 1986). Assuming twelve Chls per polypeptide, a detailed analysis of the pigment composition of *Cryptomonas rufescens* complexes suggests each LHC unit contains ten Chl *a*, two Chl *c*, four alloxanthins (5% in a *cis* form) and one crocoxanthin (Lichtlé et al., 1987). Significantly higher Chl *c* contents (Chl *c*<sub>2</sub>/Chl *a* ratio of 0.59–0.71) have been reported for the LHC of *Cryptomonas maculata* by Rhiel et al. (1986), and for *Rhodomonas* sp. (formerly *Chroomonas* sp.) by Ingram and Hiller (1983).

A PS I-specific LHC in cryptophytes is strongly suggested by the work of Bathke et al. (1999). Western blotting of five fractions isolated from *Rhodomonas* sp. thylakoids solubilized with 5% *n*-dodecyl  $\beta$ -D-maltoside revealed LHC polypeptides of 17, 21 and 22 kDa that were specific to PS I. The lowermost band from the sucrose gradient was identified as a PS I-LHCI fraction and it contained a 17 kDa polypeptide which cross-reacted with a higher plant PS I LHC antibody. Distinguishing features of this PS I-containing band were red-shifted absorption (681 nm) and emission maxima (712 nm), and a low Chl *c* content (a Chl *c*<sub>2</sub>/Chl *a* ratio of 0.10 was estimated for the LHC component).

The linear dichroism spectra of a digitonin-solubilized LHC preparation of *Rhodomonas salina* was studied at room temperature and at 10 K (Hiller

et al., 1992). Stability of the LHC in the polyacrylamide gel used to orient the samples by squeezing was excellent, in contrast to the situation with FCPs. This was not unexpected, as the dimeric or trimeric complex isolated by the cold SDS green gel technique is also extremely stable (Ingram and Hiller, 1983). The large amount of Chl *c* in the LHC of *Rhodomonas salina* is particularly noticeable in the 10 K absorption spectrum, with clear peaks at ~463, 588, and 640 nm. At 10 K, both Chl *a* and Chl *c* show red-shifted positive LD peaks in the  $Q_y$  region at 676 and 645 nm, respectively. This indicates that these transitions lie in the plane of the membrane and that a subset of pigments is involved. A weak additional peak observed at 659 nm may be the LD counterpart of a shoulder seen in the absorption spectrum at ~662 nm, the low intensity reflecting an alignment at close to the magic angle. The observation of complex negative features between 570 and 630 nm, a region where the Chl *a*  $Q_x$  transition will also make a contribution, is further evidence of heterogeneity and suggests that there is more than one form of Chl *c*.

Although it is more than 15 years since the cryptophyte LHC was isolated, amino acid sequences for *Guillardia theta* (formerly *Cryptomonas phi*) have only recently become available (Deane et al., 2000) and emphasize the link between cryptophytes and red algae (Fig. 3). The 20 and 24 kDa polypeptides, which are present in approximately equal amounts, are very similar for the first 181 and 173 residues, respectively (inserting gaps in the longer peptide to maximize the alignment), and the difference in size comes from the extended C-terminus. As the C-terminus is in the lumen in the Kühlbrandt et al. (1994) model for the LHC, it may be that this is involved in positioning of the PE (see below). The molecular masses of the derived mature proteins are 20,667 (Lhcc10), and 21,778 kDa (Lhcc13), the latter being not quite in agreement with the gel data. Since cryptophyte LHCs form a family with many members, it may be that this discrepancy will disappear as more genes are sequenced.

### 3. Interaction of the Phycobiliproteins with Lhcc and/or the Photosystems

Despite early work (Haxo and Fork, 1959) which demonstrated that the cryptophyte phycoerythrins acted as light-harvesting pigments, only a few studies

have investigated the pathways of energy transfer from phycobilins in algal cells. Lichtlé et al. (1980) recorded the low temperature absorption and fluorescence spectra of *Cryptomonas rufescens* cells and observed clear PE566 bands in the excitation spectra when the emission was monitored at 685 nm, but not at 730 nm. They concluded that the phycoerythrin transferred its energy preferentially to PS II and that the photosystems were connected by an intrinsic chlorophyll protein, which could transfer energy to either system. However, the presence of uncoupled PE566 (indicated by the strong fluorescence at 630 nm) complicates the interpretation of the excitation spectra, since a significant fraction of the emission at 685 nm will be from PE566. In contrast, relatively weak PE566 emission was observed upon 560 nm excitation in the studies of Bruce et al. (1986), and PE566 makes a clear contribution to the 77 K excitation spectra monitored at both 688 and 725 nm.

Lichtlé et al. (1987) obtained four bands after centrifugation of digitonin-solubilized *Cryptomonas* cells broken in a French press. In addition to the PS I-enriched, LHC-enriched, and PE566 bands, a band lying below, but continuous with, the PE566 band was identified as containing PE566 complexes coupled to PS II. In the absence of any comparable preparations from other laboratories, this claim is worth evaluating. From the polypeptide profile and the PS II activity, measured as 2,6-dichlorophenolindophenol (DCIP) reduction, it is clear that this fraction is enriched in PS II. It also contains some LHC, as the Chl *a*:Chl *c* ratio was slightly lower than in the whole cells. The 77 K fluorescence spectrum is dominated by emission from uncoupled PE566, with a maximum at 625 nm. Nevertheless, the observation of some Chl *a* emission at 686 nm when 550 nm excitation was used, suggests that some PE566 is coupled. The different fractions were also examined by negative staining electron microscopy and small particles believed to be PE were seen close to, or attached to, the thylakoid vesicles of the PS II-enriched fraction. However, PE particles were observed in all the fractions and were found surrounding vesicles, in chains and in rods, as well as occurring as isolated units and so these results do not support, or negate, the existence of a PE-PS II particle.

The PS II-enriched band also contained polypeptides of 77–97 kDa and it was suggested that these might be related to the phycobilisome linker

ApcE of red algae (Lichtlé et al., 1987). However, this gene is not present in the plastid genome of the cryptophyte *Guillardia* (Douglas and Penny, 1999). It may also be relevant that PsbB (CP47) and PsbC (CP43) in *Guillardia* are well conserved and show no features that might indicate a docking site for a phycobilin. It seems to us more plausible to have association of PE with the LHC (Lichtlé et al., 1992b; Bathke et al., 1999) with a low binding constant, rather than a specific interaction of a putative PE linker with the core.

From the data on *Cryptomonas rufescens* it can be calculated that there are about two PE566 molecules for each LHC, assuming 12 Chl per polypeptide of average molecular mass 22 kDa. It is reasonable to assume that there is only one ~60 kDa PE directly associated with a LHC and that the second one associates with this PE from the other luminal face. This would result in a minimal lumen cross-section of 160 Å and, as already noted, the lumen cross-section may be 300 Å, or more, so there could be more than two PE per LHC, or the PE could be excluded from one of the luminal faces.

Hiller et al. (1992) used LD to search for oriented forms of PE545 in whole cells of *Rhodomonas* at 10 K, but the 520 to 580 nm region was featureless under conditions where there was a strong positive dichroism from Chl *a*. Subtracting the contribution of the intrinsic LHC from the whole cell LD spectrum revealed a small positive component at 570 nm, which was attributed to the cryptoviolin chromophore of the  $\alpha$  subunits. However, if a special linking component exists, it could be best looked for by both spectroscopy and biochemistry using cells grown at high light when the PE content is low. It is also reasonable to query whether a linker containing a chromophore is necessary at all. The rate constant for excitation energy transfer described by Förster theory (Chapter 3, Parson and Nagarajan), depends upon the distance between the centers of the chromophores ( $R^{-6}$ ), an orientation factor ( $\kappa^2$ ), the radiative rate of the donor ( $k_f^D$ ), and the degree of overlap of the donor fluorescence with the absorbance of the acceptor.

PE545 represents the most extreme case with respect to the overlap integral between the PE545 emission at 585 nm and the  $Q_y$  absorbance of Chl *a* at ~670 nm. In this case, transfer to the Chl  $Q_x$  state of Chl *a* makes a significant contribution, but the overlap integral calculated for both Chl *a* transitions is only as large as that for Chl *c* as the acceptor (MacColl

and Berns, 1978). However, reducing the distance between the chromophores, or increasing the orientation factor, can easily compensate for a less favorable overlap integral.

The existence of an intermediate between phycobilins and Chl *a* can, in principle, be confirmed by fast kinetic experiments. However, if the lifetime of the intermediate is significantly shorter than its formation time, the excited state population will be too low to detect and the decay of the excited states of the phycobilins will be the rate-limiting step. Thus, the failure to detect Chl *c* emission upon excitation of PE566 (or the carotenoids) of intact cells of *Cryptomonas* sp. CR-1 at 77 K (Mimuro et al., 1998) does not necessarily rule out its involvement as an energy transfer intermediate. Moreover, the observation of fluorescence decay times for PE545 (110 ps) and PE566 (100 ps) which are faster than for PC645 (250 ps) in whole cells at 77 K, despite a 4.3- or 2.5-fold decrease in overlap with Chl *a*, provides some support for Chl *c* functioning as an intermediate in the PE-containing species (Bruce et al., 1986). Regardless of the pathway, the time-resolved emission spectra of these studies indicate a preferential transfer of energy from the phycobilins to PS II, followed by slow spillover to PS I.

### *B. Dinoflagellates*

Photosynthetic dinoflagellates are a somewhat heterogeneous group of organisms, which have acquired chloroplasts from a variety of sources. In some cases these chloroplasts are utilized and then discarded, in others they have become true permanent chloroplasts, and in yet others the status is uncertain. The only light-harvesting systems that will be considered here are those containing the highly-oxygenated carotenoid peridinin, the characteristic and major carotenoid of dinophytes.

There are usually, but not always, two light-harvesting components: the unique water-soluble PCP, and an LHC (Lhcd) which, as already noted, is a member of the three-helix family of light-harvesting proteins. There are reports of species which completely lack PCP (Prézelin and Haxo, 1976), but small amounts of PCP may become insoluble, particularly if the cells are frozen before PCP extraction. On the other hand, Prézelin (1976) determined that the PCP of *Heterocapsa pygmaea* (formerly *Glenodinium* sp.) cultivated in low light conditions can make a substantial contribution to

light-harvesting, binding up to 50% of the peridinin and 18% of the whole cell Chl *a*. In other species, the amount of peridinin released in the form of water-soluble PCP is reported to reach 70–95% of the total cellular peridinin content (Meeson et al., 1982; Prézelin, 1987).

As PCP contains the same carotenoid as the LHC, its function seems, superficially, to be redundant. It requires ~40 amino acids to bind a peridinin in PCP, whereas the LHC needs only half that number. It may be that there is some limit to which the LHC can be laterally added to the photosystems, and adding PCP in a third dimension overcomes this restriction and permits a larger cross-section around each photosystem.

### 1. Peridinin-Chlorophyll *a*-Protein (PCP)

Since its purification and characterization in 1976 (Haxo et al., 1976; Prézelin and Haxo, 1976), the peridinin-chlorophyll *a*-protein has been the subject of numerous studies at the physiological, molecular and structural levels. In contrast to the LHC (Section III.B.2), PCP genes encode a single holoprotein and are without introns. The mature apoprotein is either found in the form of a monomer of 32 kDa, which binds eight peridinins and two Chl *a*, or a dimer of 15 kDa polypeptides, in which each monomer binds four peridinins and a Chl *a*. Spectroscopically the two types are very similar (Prézelin and Haxo, 1976; Song et al., 1976; Carbonera et al., 1999), as are up to thirteen isoforms with different isoelectric points (Iglesias-Prieto et al., 1991). We note that PCP forms from *Alexandrium* containing ten or twelve peridinins per two Chl *a* have also been reported (Ogata and Kodama, 1993). However, the absorption spectra presented by Ogata et al. (1994) and Akimoto et al. (1996) display a 475 to 669 nm absorbance ratio of ~3.9, almost identical to that of the main PCP from *Amphidinium* (Sharples et al., 1996).

Each organism contains many PCP genes (> 5000 in *Gonyaulax*), which are tandemly arranged (Le et al., 1997), and the heterogenous nature of the protein is clearly indicated by differences in the amino acid sequences (Sharples et al., 1996; Hiller et al., 2001a). Nevertheless, these sequences, and also those derived from quite different species with 32 kDa protein forms, show a high degree of identity (Fig. 8). The amino acid sequence of the 32 kDa polypeptide indicates that it arose by a gene duplication and fusion (Norris and Miller, 1994), since the two halves

are ~55% identical and joined by a spacer region (underlined in Fig. 8). In addition, the 15 kDa PCP polypeptide of *Heterocapsa* and of a *Symbiodinium* sp. from the sea anemone *Anthopleura elegantissima* also shows a high degree of sequence homology with both domains of *Amphidinium* (Hiller et al., 2001a; Weis et al., 2002).

A second divergent form of PCP eluting from a cation-exchange column at much higher salt concentrations (designated high salt PCP), was isolated by Sharples et al. (1996). The 34 kDa polypeptide of this variant has just a 31% primary sequence identity with the abundant PCP forms (Hiller et al., 1999), and binds only six peridinins per two Chl *a*. Its role has yet to be determined, but it makes up less than 3% of the total PCP in *Amphidinium*.

The determination of the structure of the main form of PCP from *Amphidinium carterae* at 2.0 Å resolution by X-ray crystallography (Hofmann et al., 1996) has given a particular impetus to spectroscopic experiments, and renewed interest in peridinin in its own right (Bautista et al., 1999b; Zigmantas et al., 2001). Structurally, PCP forms a boat-shaped monomer with a hydrophobic interior enclosing two pigment clusters, each containing four peridinins in van der Waals contact (3.3–3.8 Å) with a Chl *a* (Fig. 9 and Color Plate 12). The centers of the two Chl *a* macrocycles are separated by 17.4 Å and the fifth ligand for the Mg atom is provided by a water molecule linked to a Histidine residue (positions 125 and 289 in Fig. 8). In each pigment cluster the peridinins are arranged as two pairs, crossing at  $56 \pm 6^\circ$  at a distance of less than 4 Å to each other.

In the crystal, the PCP monomers form a non-crystallographic trimer in the form of a flattened disc (Fig. 10). Essentially the same pigment arrangement is predicted for *Heterocapsa*, since the amino acid sequences of the protein regions in contact with the pigments in the *Amphidinium* structure are conserved (Hiller et al., 2001a). There is no direct evidence as to the location of PCP, e.g. from immunogold labeling, but the gene sequence predicts a precursor with a typical lumen-directing sequence (Norris and Miller, 1994). It has been suggested that the trimer may be the PCP form found in vivo and that the flattened disc could make contact with the LHC, allowing efficient Förster energy transfer to occur (Hofmann et al., 1996). Indeed the LHC differs from other chromophyte LHCs, particularly at the C-terminus, but other differences from the LHCII of higher plants, such as



1				50		100
Musc	MAM.KVRAAG	LILLLSFCLS	CWV.....	FVPGPRHVGP	.VAAGALG..	MMAAAPAYA
Hete	MAK..ARKAC	.VLA AVLALT	.GLRQSA...	FVPGPRGLAP	MAAAGGMLA.	MAGAAPAHA↓
Symb	MVRG.ARKAI	AVG.VAVAVA	CGLQKHNL..	FVPGPR..H.	AAPVAAAAS	MMAPAAAFAD
Amph	MVRG.GKAV	VLATVAFCAT	SVVQKTCG..	FVPSPLRQRA	AAAGAAASVA	TWFAPAFAFAD
Gony	MGRSRTVRAL	ATGVVVLAAT	RCLHKPANHS	FVPGPLRRNA	APAAAAASAA	TMLAPAFAFAD
Alex					D EIGDAAAKLIG	DASYAFAKEV
					↑	DCNNGIFLQA
						PGKFQPLEAL
101					150	200
Musc						
Hete						
Symb	KAIDKMIEMG	AAADPKLLKD	AAEAHHKAIG	SISGPNGVTS	RADWDVNAA	IGRVVASVPK
Amph	KAIDKMIEMG	AAADPQLLKA	AAEAHHKAIT	TVSGANGVTS	RADWDVNAA	LGRVISAVPE
Gony	KAIDKMIEMG	VQADPKLLKA	AAEAHHKAIG	SISGPNGVTS	RADWDVNAA	LGRVISAVPE
Alex	K-I-KH-V					ATVMDVNSV
						SGITDPVPA
						YMKSLVNGAD
						AEKAYEGFLA
201					250	300
Musc						
Hete						
Symb	FKDVVEKNQV	ATASAPAVV.	PSGDKIGEAA	KALSDASYPF	IKDIDWLSDI	YLGKLPKGT
Amph	FKDVVEKNQV	TSAAGPATV.	PSGDTIGVAA	QKLSDASYPF	LKQIDWLSDI	YLGKLPKGT
Gony	FKDVVEKNQV	STAAAPPTVS	ASGDAIGEAA	KKLSEQSYPF	LKDINWLSDI	YLGKLPKGT
						SKKAIATDKM
						IMMGAKADGN
						LLKAAAQAHH
						QAIGSIDANG
301					350	376
Musc	VATLDDYTAI	NSAIGHMIAS	VPASKTMDVY	NAFAKFSLGS	DVGPMMSKV	NAADAKAAVE
Hete	VTTLDYEA	NAAIGHMVAS	AGESKTMDVY	NVFAFNZLKG	DVGPMMSKV	NAADAKAAVE
Symb	VTSADYEA	NAAIGHMVAS	VPKTTMDVY	NSMAGV.VDS	SVPNLFSKV	NPLDAVAAK
Amph	VTSADYEA	NAAIGHMVAS	VPKSTMDVY	KAMASV.TDT	GIPLNMF	SVK
Gony	VTSADYEA	NAAIGHMVAS	VPKSTMDVY	KAMASV.TDT	GIPLNMF	SVK
						AFYTFKDVVL
						AAQR*
						AFYTFKDVVQ
						AASQVA*

Fig. 8. Alignment of amino acid sequences of 32 and 15 kDa PCP forms. Musc, *Symbiodinium muscatinei* (Weis et al., 2002); Hete, *Heterocapsa* (Hiller et al., 2001); Symb, *Symbiodinium* (Norris and Miller, 1994); Amph, *Amphidinium*, (Sharples et al., 1996); Gony, *Gonyaulax* (Le et al., 1997); Alex, *Alexandrium* (Ogata et al., 1994). A space is indicated by a dot, an arrow marks the start of the mature protein and the spacer region is underlined. The sequences of the mature 32 kDa proteins are ~85% identical and *Heterocapsa* shares a 68% identity with the C-terminal domain of *Amphidinium*. Regions of significant sequence difference in the 15 kDa form are shown in *italic* face, and stop codons are indicated by an asterisk. The alignment was produced by the program Pileup with manual alignment of the *Heterocapsa* and *S. muscatinei* leader sequences (Hiller et al., 2001).



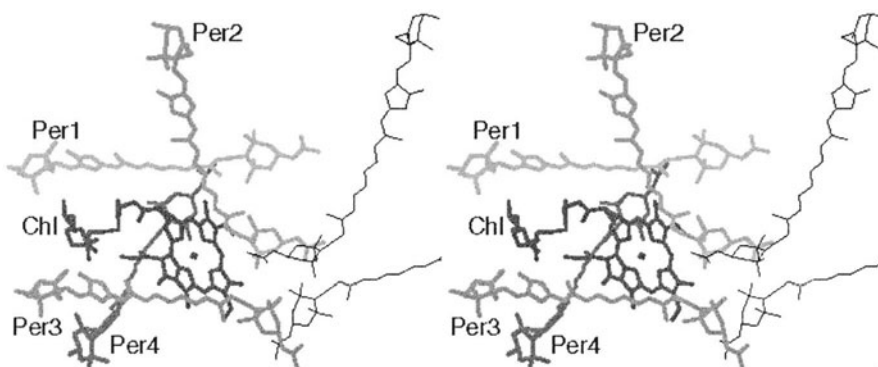


Fig. 9. Stereo view of the four peridinin and one Chl *a* in a pigment cluster in PCP. The thin lines show a peridinin pair from the adjacent cluster within the monomer. Reprinted from Hoffman et al. (1996). With permission from the American Association for the Advancement of Science.

the number of residues in the loops, are shared with the FCPs.

Direct energy transfer to the inner antenna of PS II has also been suggested (Mimuro et al., 1990b). However, even though the chloroplast DNA of dinoflagellates is very atypical (Zhang et al., 1999), PsbB (CP47) and PsbC (CP43) are not, and they contain no obvious modification which would suggest an interaction with a PCP trimer. The possibility of a location close to PS I should also not be discounted, as dinoflagellate PsbA and PsbB genes predict a product which is very different from that in higher plants and green algae, especially in regions outside the thylakoid membrane (Barbrook and Howe, 2000; Hiller, 2001). In the absence of lateral heterogeneity, energy could still be channeled from PCP to PS II, even if bound to a PS I component.

#### a. Spectroscopy

The absorption spectra of purified PCP from *Amphidinium* (Fig. 11) and *Heterocapsa* display a Chl *a*  $Q_y$  maximum at 670 nm and 673 nm, respectively, identical to the 35 and 15 kDa forms of *Symbiodinium* sp. at room temperature (Iglesias-Prieto et al., 1991). The high salt form of *Amphidinium* has an intermediate absorption maximum at 671 nm. These differences in the Chl *a* maxima of the three PCP types extend to the Soret region of the absorption spectra and also to the emission spectra. In each case, the fluorescence maximum is ~3 nm to the red of the  $Q_y$  absorption maximum.

At low temperature, three distinct bands become apparent in the 600–630 nm region. (Prézelin and Haxo, 1976; Ogata et al., 1994; Kleima et al., 2000b).

Simulations of the absorption spectrum of *Amphidinium*, combined with an examination of the CD and LD spectra, enabled Kleima et al. (2000b) to assign the band at 625 nm to the  $Q_x$  transition, and bands at 604 and 615 nm to vibronic components of the  $Q_y$  transition. They also utilized the LD spectrum in a simulation of the Chl *a*  $Q_y$  absorption band to determine that the two Chl *a* molecules are not identical, but have  $Q_y$  maxima separated by ~1 nm at 77 K. Somewhat larger differences of 2.8–3.7 nm were reported for *Symbiodinium* sp. at room temperature (Iglesias-Prieto et al., 1991), although these values were obtained by spectral decomposition of the Chl *a*  $Q_y$  absorption band utilizing Gaussians of very different bandwidth and area.

The observation of a negative CD band ~3 nm to the red of the  $Q_y$  absorption maximum (Fig. 11) has also been attributed to Chl *a* heterogeneity (Ogata et al., 1994). However, the difference in CD and absorption band shape led Kleima et al. (2000b) to suggest that a conservative component, in addition to a larger non-conservative spectral component (with the same shape as the absorption), is responsible for this red shift. Moreover, simulations of the conservative component verified that the coupling of the Chls within a PCP monomer is very weak ( $<10$  cm<sup>-1</sup>).

The absorption and CD spectra of PCP are dominated by contributions from the peridinin (Fig. 11). A derivative analysis indicates that the absorption maxima of peridinin are red-shifted in *Heterocapsa* (480 and 526 nm) and the high salt form of *Amphidinium* (485 and 527 nm), compared to *Amphidinium* (474 and 513 nm). Originally, the strong positive and negative CD bands were

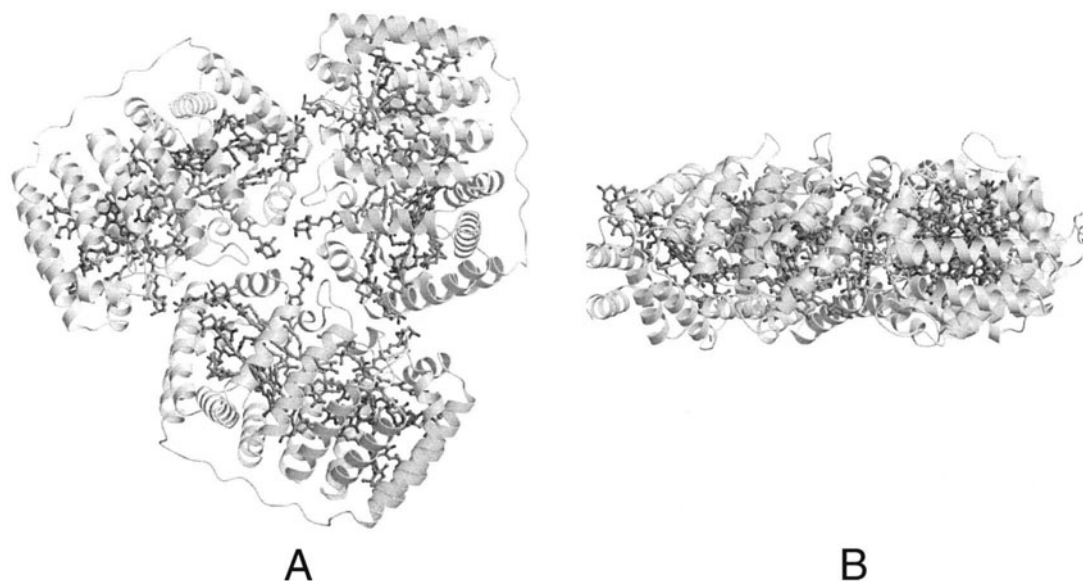


Fig. 10. (A) Top and (B) side views of trimeric PCP (Hiller 1999). See Color Plate 12.

interpreted as being conservative and resulting from two non-interacting sets of excitonically-coupled peridinin dimers, with all the peridinins arranged at right angles to each other around the Chl *a* (Song et al., 1976). Without taking into account the X-ray-derived structure, Pilch and Pawlikowski (1998) modeled the CD spectra on the basis of a rectangular tetramer of relatively strongly coupled peridinin molecules and calculated pairwise interactions of up to 2200 cm<sup>-1</sup>.

The crystal structure confirms that there are two pairs of peridinins within each cluster and, within each pair, the peridinins are in van der Waals contact. However, they cross at an angle of ~56° and structure-based calculations suggest that five smaller (~100–300 cm<sup>-1</sup>) pairwise interactions between the four peridinins within a cluster contribute to the CD. Furthermore, to successfully reproduce the general features of the *Amphidinium* and *Heterocapsa* CD spectra in the region of the carotenoid and Soret band absorption, all possible interactions between the eight peridinins and two chlorophylls in a double cluster have to be taken into account (Carbonera et al., 1999). In particular, the simulations reveal that the intercluster interaction energies between the two chlorophylls and between most of the peridinins in one cluster and the pigments of the opposite cluster are significant and necessary to obtain satisfactory agreement in the Soret band region. Further

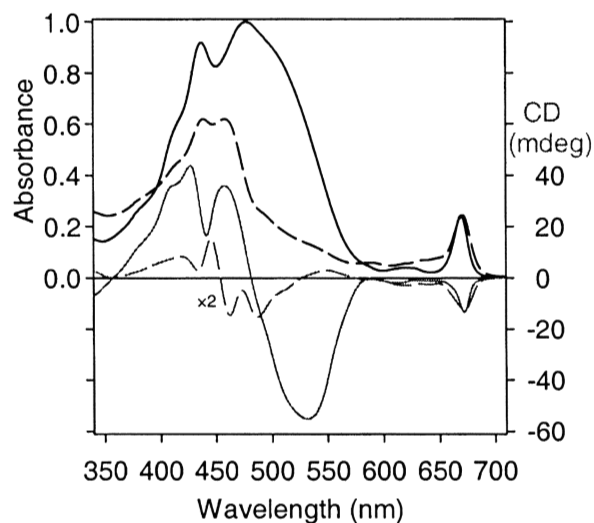


Fig. 11. Absorption (black) and CD (gray) spectra of the PCP (solid line) and LHC (dashed line) of *Amphidinium carterae*. The spectra were normalized relative to the Chl *a* Q<sub>y</sub> band intensity for a PCP absorption maximum of 1.

improvements to the fit were realized by allowing the 0–0 energies (543, 485, 518 and 535 nm) and dipole strengths of the four peridinins in a cluster to vary. We note that the CD spectrum of the high salt form of PCP shows a markedly reduced positive CD band in the 420–430 nm region, but is otherwise rather similar in appearance (Sharples et al., 1996).

Fluorescence excitation spectra indicate that the peridinin transfer energy to Chl *a* with a high efficiency (>85%), which may be wavelength dependent (Akimoto et al., 1996). Time-resolved spectroscopic measurements with sufficient time resolution were first reported by Bautista et al. (1999a). A single exponential rise time of 3.2 ps was obtained in the Chl *a* bleaching region at 670 nm, after selectively exciting the peridinin in *Amphidinium* PCP at 530 nm. A peridinin-to-Chl *a* energy transfer efficiency of 76% from the  $S_1$  state, with a  $(4.2 \text{ ps})^{-1}$  rate, can be determined from this rise time and the  $S_1$  lifetime reported for peridinin in methanol (13.4 ps). However, the  $S_1$  lifetime of peridinin is remarkably solvent dependent (Bautista et al., 1999b; Zigmantas et al., 2001), and the calculated energy transfer efficiency will rise to 91% if the intrinsic  $S_1$  lifetime in the protein environment in the absence of energy transfer is similar to that in benzyl alcohol (35 ps).

From a global and target analysis of the transient absorption spectra recorded between ~450 to 700 nm, Kreuger et al. (2001) suggest that ~25–50% of the energy transferred to Chl *a* proceeds directly from the  $S_2$  state of peridinin. Additional energy transfer from the  $S_1$  state (2.0 ps lifetime), as well as a minor amount (~3%) from the intramolecular charge transfer state of peridinin, and a 10–18% subpopulation of 'disconnected' peridinin were other pathways suggested by their analysis. However, fluorescence upconversion measurements rule out the possibility of significant energy transfer from the  $S_2$  state. The  $S_2$  lifetime of peridinin dissolved in ethanol or benzyl alcohol is exceptionally short ( $43 \pm 3$  fs) and, within experimental error, it is the same in PCP (A.N. Macpherson, unpublished). In PCP, Zigmantas et al. (2002) monitored the decay of the stimulated emission from the intramolecular charge transfer (ICT) state at 930 nm and observed matching rise kinetics in the Chl *a* bleaching region at 670 nm with 2.5 ps (major) and 0.7 ps (minor) components. They propose that energy transfer from the intramolecular charge transfer state is an important pathway and that this state is populated directly from the  $S_2$  state. If energy transfer does not occur from this ICT state, its function may be regulatory; harmlessly converting excess energy to heat (Bautista et al., 1999).

The high-resolution structure has been used to model the energy transfer between the calculated electronic states of all the chromophores within one

pigment cluster of a PCP monomer (Damjanović et al., 2000). The semi-empirical calculations suggest that the peridinin are excitonically coupled and that energy transfer from the allowed  $S_2$  state is much too slow to compete with internal conversion to the peridinin  $S_1$  state. The calculations therefore predict that energy is transferred solely from the  $S_1$  state of peridinin to Chl *a*, although the transfer rates determined for a Coulombic coupling mechanism were considerably larger than those derived from the experimental lifetimes. In this case, transfer to both the  $Q_x$  and  $Q_y$  states of Chl *a* is feasible on spectral overlap grounds. However, the calculated  $S_1$ – $Q_x$  couplings were small and it was concluded that the  $S_1$ – $Q_y$  pathway will be dominant.

Damjanović et al. (2000) also suggested that peridinin 612 (Per2, Fig. 9), which is poorly oriented with respect to the Chl *a*  $Q_y$  transition, very rapidly transfers its energy to other peridinin (mainly Per1) at the  $S_2$  level and plays little, if any, direct role in transfer to Chl *a*. The time-resolved anisotropy measurements made by Kreuger et al. (2001) do not exclude the possibility of a limited amount of energy transfer between the  $S_2$  states of the peridinin. However, another explanation of the depolarization (to an anisotropy of 0.29) upon  $S_1$  formation is a change in the orientation of the  $S_1$  transition dipole.

The high-resolution structure has also been used to model the rate of energy transfer between the Chls of the trimer, assuming a Förster mechanism (Kleima et al., 2000a). From time-resolved fluorescence anisotropy measurements, two very different depolarization times were resolved. The shorter anisotropy decay component (6.8 ps) was assigned to the equilibration time between the Chls within a monomer and the 350 ps lifetime to inter-monomer equilibration. The experimental results were used to model the energy transfer times between isoenergetic Chls and, for Chls in adjacent monomers, time constants ranging from 0.66–12.1 ns (Table 3) were predicted. Not only are the distances quite large, but the  $Q_y$  transitions are rather poorly oriented with respect to those in the neighboring monomer (Fig. 12).

These calculations have important implications for the operation of PCP as a light harvesting protein in vivo. It had been speculated that the energy would be equilibrated among the Chls of the trimer (Hoffman et al., 1996) in a manner analogous to the bacterial LHC (Chapter 5, Robert, Cogdell and van Grondelle). However, the relatively slow inter-monomer rates

Table 3. The calculated time constants ( $\tau$ ) for Förster energy transfer between the chlorophylls of two PCP monomers. (Kleima et al., 2000a)

Chl Pair	R (Å)	$\kappa^2$	$\tau$
1,2	17.35	0.292	14.6 ps
1,3	54.88	1.822	2.34 ns
1,4	40.53	1.055	0.66 ns
2,3	55.37	0.373	12.1 ns
2,4	43.65	0.380	2.84 ns

The numbering and distances (R) are indicated in Fig. 12. The orientation factor ( $\kappa^2$ ) was determined for a  $Q_y$  transition dipole moment rotated  $4.5^\circ$  from the y-axis.

indicate this is unlikely, as the onward flow of energy from PCP towards the reaction centers is probably significantly faster (Section III.B.3). For this process to be efficient, each PCP monomer must be located adjacent to an acceptor protein, such as an LHC, which is plausible if the in vivo state of both is trimeric. Some preliminary calculations indicate that this requires the Chl *a* in adjacent proteins to be separated by no more than 40–50 Å (Kleima et al., 2000a) assuming a favorable orientation of transition dipoles.

### b. Reconstitution

A functional PCP can be reconstituted from heterologously-expressed apoprotein mixed with pigments extracted from native PCP. The conditions are a simple mixing at 4 °C of pigments dissolved in ethanol with apoprotein in Tris or Tricine buffers to give a final ethanol concentration of 15%. After purification on an anion exchange column, the excitation spectrum for Chl *a* emission is almost identical to that of native PCP, as are the absorbance and circular dichroism spectra. Expression constructs of the N-terminal domain alone of monomeric PCP could also be reconstituted and they presumably form dimers, since the spectroscopic properties are similar to those of dimeric PCP from *Heterocapsa*. Preliminary studies show that Chl *a* can be replaced by Chl *b* or Chl *d*, but not by Bchl. Peridinin cannot be replaced by fucoxanthin or siphonaxanthin, possibly because their head groups will project well into the contact region between the N- and C-terminal domains (Hiller et al., 2001b). The manipulation of PCP via this reconstitution system in conjunction with the many spectroscopic techniques noted above should considerably increase our understanding of

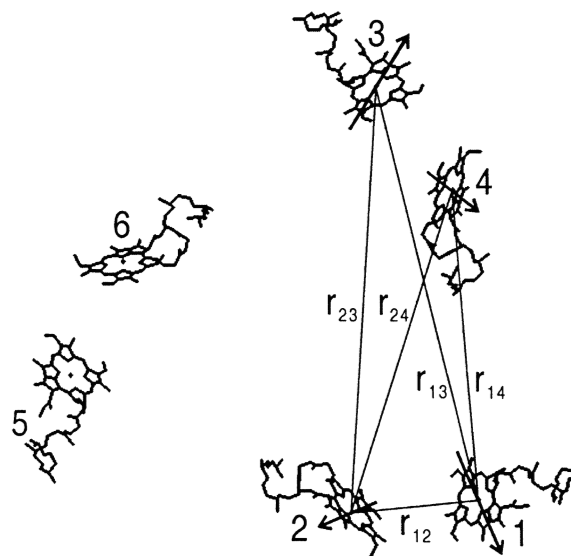


Fig. 12. Chl *a* organization in a PCP trimer. Chl *a* 1 and 2 belong to one monomer, as do 3 and 4, and the arrows indicate the transition dipole moments. The center-to-center distances between the Chls are listed in Table 3 (Kleima et al., 2000a).

carotenoid–Chl energy transfer.

### 2. Lhcd (iPCP), the Intrinsic LHC of Dinoflagellates

The intrinsic LHC, isolated from thylakoids solubilized in digitonin or glycosidic detergents as a brown band upon sucrose gradient centrifugation, has been investigated by a number of groups (Hiller et al., 1993; Iglesias-Prieto et al., 1993; Jovine et al., 1995). This LHC has a principal polypeptide of ~19 kDa and, for the digitonin solubilized *Amphidinium* complex, a pigment composition of 7 Chl *a*, 4 Chl *c*<sub>2</sub>, 12 peridinin and two diadinoxanthins. The peridinin content of the *Amphidinium* and *Heterocapsa* LHC solubilized with glycosidic detergents is somewhat lower (Table 4). Nevertheless, it is remarkable that the carotenoid content in the LHC exceeds that of Chl *a* on a molar basis for all the algae. The relatively high levels of Chl *c*<sub>2</sub> are also notable. In clear blue oceanic waters, the amount of light harvested by Chl *c*<sub>2</sub> is calculated to be up to 30% of the total absorbed light, at least in species of dinoflagellates where PCP is absent (Johnsen et al., 1994).

Both peridinin and Chl *c*<sub>2</sub> appear to transfer energy efficiently to Chl *a* in these preparations and fluorescence is observed at ~676 nm. This energy

Table 4. Composition of dinoflagellate LHCs

Organism	Fraction of Chl <i>a</i> in the thylakoids	Chl <i>c</i> / Chl <i>a</i>	peridinin/ Chl <i>a</i>	diadinoxanthin/
<i>Amphidinium</i>	~72%	0.60	1.4	0.3
<i>Symbiodinium</i>	45%	1.0	2.0	present
<i>Heterocapsa LL</i>	–	0.62	1.1	0.3
<i>Heterocapsa HL</i>	–	0.60	0.9	0.6

transfer is easily disrupted by heating or treating the LHC with SDS, as fluorescence is observed from Chl *c* at ~643 nm and the excitation spectrum of the Chl *a* emission indicates that the peridinin is disconnected (Hiller et al., 1993; Iglesias-Prieto et al., 1993). Similarly, LHC preparations obtained by solubilizing the thylakoids with SDS or Deriphat 160-C, the detergents originally used to isolate complexes prior to 1993 (Prézelin, 1987; Knoetzel and Rensing, 1990), show the same behavior (Jovine et al., 1995).

The 77 K absorption and fluorescence excitation spectra of *Amphidinium* show peaks at 634 and 649 nm, which were attributed to two forms of Chl *c*<sub>2</sub>. Peaks at similar positions were also observed in the 10 K LD spectrum of thylakoids (Hiller et al., 1993), and at 635 and 647 nm in the 77 K fluorescence excitation spectrum of *Alexandrium tamarense* (formerly *Protogonyaulax tamarensis*) cells (Mimuro et al., 1990b). In common with the *Dictyota*, *Pavlova* and *Pleurochloris* LHC, the CD spectrum of the *Amphidinium* LHC has a red-shifted (–) Chl *a* Q<sub>y</sub> band (Fig. 11). This band has the same intensity and peak position (673 nm) as the PCP of *Amphidinium*, but a larger bandwidth. A feature which appears to be unique to the *Amphidinium* LHC, is a broad band with positive dichroism at 550 nm. This may be associated with the red-shifted peridinin forms absorbing at 542 nm.

The amino acid sequence(s) are known for the *Amphidinium* protein and indicate that, while there is a fairly high identity with the Lhcf<sub>s</sub> at the N-terminus, the C-terminus is very different (Hiller et al., 1995). In the tree shown in Fig. 3, the dinoflagellate LHC is quite close to the FCPs (Lhcf), but depending on the analysis, and perhaps on the sequence used for the comparison, it has also been positioned at the base of the chromophyte lineage close to the anomalous Lhcf of *Isochrysis* (Caron et al., 1996). A three-helix model based on the LHCI structure of Kühlbrandt et al. (1994) has been presented, and five conserved Chl

*a* binding sites were identified (Hiller, 1999).

### 3. Interactions Between the Systems

Given the dual nature of the light-harvesting machinery of dinoflagellates it is of considerable interest to understand how PCP interacts with the intrinsic LHC. Since both complexes contain so much peridinin it is not possible to selectively excite only one of the complexes in whole cells. There appears to be just one time-resolved study of the emission from chlorophylls in whole cells following predominantly excitation of peridinin. Mimuro et al. (1990b) excited *Alexandrium tamarense* cells at 77 K with 6 ps pulses at 540 nm and observed fluorescence peaks appearing in the order F649–F670–F683–F698/709/724–F689. The prompt appearance of the 649 nm component was attributed to direct excitation of Chl *c*, which decayed with a major lifetime of ~40 ps. The 670 nm component had a rise time of ~18 ps and a decay component of ~55 ps, matching the rise of F683 (assigned to CP43). The subsequent formation of the F698/709/724 and F689 components was attributed to spillover from PS II to PS I and to excitation of CP47, respectively.

It should be noted that the fluorescence emission maximum of the isolated LHC of *Alexandrium* is not known, and neither is the distribution of peridinin between the PCP and LHC complexes. It is tempting to ascribe the 670 nm emission to PCP (672 nm for *Alexandrium cohorticula* at 77 K, Ogata et al., 1994), and that at 683 nm to the LHC (681–683 nm at 77 K, Hiller et al., 1993; Iglesias-Prieto et al., 1993). However, if the ~55 ps formation time of F683 reflects energy transfer from the PCP to LHC, the absorption of the 540 nm pulses by peridinin in PCP would have to greatly exceed that in the LHC, otherwise a much faster intra-LHC peridinin-to-Chl *a* rise component should be present. Studies of *Amphidinium* and *Heterocapsa* grown at low light indicate that approximately equal amounts of

peridinin are found in both complexes (R. G. Hiller and F. P. Sharples, unpublished), and in *Symbiodinium* grown at 10× higher light levels, PCP contains at most 15% of the peridinin (Iglesias-Prieto et al., 1993). There is a pressing need for some fast kinetic studies on whole cells, thylakoids and isolated LHC to accurately resolve the energy transfer kinetics from both peridinin and Chl *c*.

Since the amount of PCP is so variable, both by species and environmental conditions, it is worth reviewing what is known at the molecular level. Following an early indication (Roman et al., 1988) that levels of PCP may be light regulated at the transcriptional level, ten Lohuis and Miller (1998) investigated the levels of transcripts of LHC and PCP in relation to light intensity and degree of cytosine methylation. Under the highest light growth conditions (HL: 100  $\mu\text{mol m}^{-2} \text{s}^{-1}$ ), the transcript levels were relatively low, but after transfer to 'moderate' light (ML: 20  $\mu\text{mol m}^{-2} \text{s}^{-1}$ ), the PCP and LHC transcripts increased 34- and 6-fold, respectively. When the light was decreased further (LL: < 2  $\mu\text{mol m}^{-2} \text{s}^{-1}$ ), the levels of PCP transcript increased to 87× the HL, but that of the LHC declined. The LHC is synthesized as a polypeptide and the message was found to be 6.1 kb, with two very minor species at 2.7 and 1.5 kb (Hiller et al., 1995). The ~6.0 and ~3.0 kb messages were found for cells grown in LL and ML, but only the ~3.0 kb species was present in cells grown under HL (ten Lohuis et al., 1998). It is not known whether these differences result from the expression of separate LHC genes at LL intensity, or whether there is some form of differential mRNA splicing. A partial LHC genomic sequence suggests that the latter is a definite possibility, as there are introns at conserved positions towards the C-terminus of each LHC unit, including the first one adjacent to the putative transit peptide. It was postulated that all LHC messages would include the first LHC unit and as many as nine subsequent LHC units would be attached to this one (Hiller et al., 1999). It may be relevant that the heterogeneous Edman-determined amino acid sequence has the highest degree of identity with the first unit, rather than that at the polyA tail, although in the absence of full-length sequences of the gene from either cDNA or genomic DNA, this result must be interpreted cautiously.

Some data are available (Iglesias-Prieto and Trench, 1997) for the distribution of Chl *a* between PCP, LHC and Photosystems I and II in three different *Symbiodinium* sp. cultured in saturating light (HL:

250  $\mu\text{mol m}^{-2} \text{s}^{-1}$ ), versus low light (LL: 40  $\mu\text{mol m}^{-2} \text{s}^{-1}$ ). For cells grown in LL, the LHC contained 60–70% of the fractionated Chl *a* and PCP only 5–7%. The total Chl *a* per cell was significantly lower in all three species grown under HL, with ~2 and ~3-fold reductions in the LHC and PCP, respectively. The changes in total Chl *a* associated with PS I correlated with the P700 content and it was also suggested that the size of the antenna surrounding the PS I core increased in low light.

*Symbiodinium microadriaticum*, as cultured by the Santa Barbara group, contains both monomeric and dimeric PCP (Iglesias-Prieto et al., 1991). Separation of the different isoforms indicates that the acidic forms are comprised solely of dimeric PCP. The relative amounts of monomeric and dimeric PCP depend upon the growth conditions, and a four-fold increase in the dimeric form (~64% of the PCP) was calculated for LL cells (Iglesias-Prieto and Trench, 1997). Stochaj and Grossman (1997) studied the proteins of the *Symbiodinium* sp. from the anemone *Aiptasia pallida* grown in culture under LL and compared them to those produced *in hospite*. The cultured cells (from an identical algal strain) produced exclusively the monomeric 35 kDa form of PCP, whereas the dimeric 14 kDa form predominated in cells extracted from the host anemone. In addition, both the intensity and chromaticity of the light effect changes in the relative abundance of the different isoelectric forms of *Heterocapsa*, with acidic isoforms becoming more prevalent in low blue light (Jovine et al., 1992). The mechanisms and implications of these differences in PCP expression remain to be determined.

#### IV. Concluding Remarks

A wish list of all the data we would like to have on a light-harvesting protein would include many items relating structure and kinetics, as well as a knowledge of the roles played by the many different gene products. We would hope to integrate this reductionist viewpoint with the rest of photosynthesis. For PCP and cryptophyte phycobilins this is now a distinct possibility, but for the LHCs containing Chl *c*, progress is very slow and a high-resolution structure may be a long way off (the LHCII of higher plants is still below the resolution required to be of maximum use).

Although we are not aware of any pigment-



reconstitution studies of heterologously-expressed Chl *a/c*-binding proteins, such as those reported for the LHCII of higher plants (Chapter 7, van Amerongen and Dekker), the reconstitution of a red algal LHC with Chl *c*, together with Chl *a* and either fucoxanthin or peridinin, has been reported (Grabowski et al., 2001; Chapter 10, Gantt, Grabowski and Cunningham). A pigment stoichiometry of 7 Chl *a*: 1 Chl *c*: 8 fucoxanthin: 2 diadinoxanthin per mole of expressed polypeptide was determined and the absorption spectrum closely resembles that of a native FCP. However, the fluorescence excitation spectra suggest that not all the carotenoids transfer their energy to Chl *a*. Nevertheless, these results further underline the potential of this type of approach to understanding energy transfer in the Chl *c*-containing LHCs. The application of two dimensional electrophoresis combined with mass spectrometry has also not been reported for any LHC.

It is ten years since the first sequences for the Chl *c*-containing LHCs were determined and there are now more than fifty available from a wide range of algae. We need no new sequences unless they fill in gaps in the LHC families of organisms already extensively studied. What we do need is a concerted attack on all fronts, spectroscopic, structural and environmental, on the LHCs of perhaps one or two organisms from the chromophyte and dinophyte groups. These could become the spinach of the algal light-harvesting world!

## Acknowledgments

The authors are supported by the Swedish Natural Science Research Council (NFR) and the Australian Research Council. They thank Erhard Rhiel for Fig. 5, Paul Curmi for Fig. 6 and Eckhard Hoffman for Fig. 10 and the interchromophore distances in Table 3.

## References

- Akimoto S, Takaichi S, Ogata T, Nishimura Y, Yamazaki I and Mimuro M (1996) Excitation energy transfer in carotenoid-chlorophyll protein complexes probed by femtosecond fluorescence decays. *Chem Phys Lett* 260: 147–152
- Apt KE, Clendennen SK, Powers DA and Grossman AR (1995) The gene family encoding the fucoxanthin chlorophyll proteins from the brown alga *Macrocystis pyrifera*. *Mol Gen Genet* 246: 455–464
- Arsalane W, Rousseau B and Thomas JC (1992) Isolation and characterization of native pigment-protein complexes from two Eustigmatophyceae. *J Phycol* 28: 32–36
- Barbrook AC and Howe CJ (2000) Minicircular plastid DNA in the dinoflagellate *Amphidinium operculatum*. *Mol Gen Genet* 263: 152–158
- Bathke L, Rhiel E, Krumbein WE and Marquardt J (1999) Biochemical and immunochemical investigations on the light-harvesting system of the cryptophyte *Rhodomonas* sp.: Evidence for a Photosystem I specific antenna. *Plant Biol* 1: 516–523
- Bautista JA, Hiller RG, Sharples FP, Gosztola D, Wasielewski M and Frank HA (1999a) Singlet and triplet energy transfer in the peridinin-chlorophyll *a*-protein from *Amphidinium carterae*. *J Phys Chem A* 103: 2267–2273
- Bautista JA, Connors RE, Raju BB, Hiller RG, Sharples FP, Gosztola D, Wasielewski MR and Frank HA (1999b) Excited state properties of peridinin: Observation of a solvent dependence of the lowest excited singlet state lifetime and spectral behavior unique among carotenoids. *J Phys Chem B* 103: 8751–8758
- Berkaloff C, Caron L and Rousseau B (1990) Subunit organization of PS I particles from brown algae and diatoms: Polypeptide and pigment analysis. *Photosynth Res* 23: 181–193
- Bhaya D and Grossman AR (1993) Characterization of gene clusters encoding the fucoxanthin chlorophyll proteins of the diatom *Phaeodactylum tricornutum*. *Nucleic Acids Res* 21: 4458–4466
- Brown JS (1987) Functional organization of chlorophyll *a* and carotenoids in the alga, *Nannochloropsis salina*. *Plant Physiol* 83: 434–437
- Bruce D, Biggins J, Steiner T and Thewalt M (1986) Excitation energy transfer in the cryptophytes. Fluorescence excitation spectra and picosecond time-resolved emission spectra of intact algae at 77 K. *Photochem Photobiol* 44: 519–525
- Büchel C and Garab G (1997) Organization of the pigment molecules in the chlorophyll *a/c* light-harvesting complex of *Pleurochloris meiringensis* (xanthophyceae). Characterization with circular dichroism and absorbance spectroscopy. *J Photochem Photobiol B: Biol* 37: 118–124
- Büchel C and Garab G (1998) Organization of the pigment molecules in the thylakoids and the chlorophyll *a/c* light-harvesting complex of a xanthophyte alga, *Pleurochloris meiringensis*. A linear dichroism study. *J Photochem Photobiol B: Biol* 44: 199–204
- Büchel C and Wilhelm C (1993) Isolation and characterization of a Photosystem I-associated antenna (LHCI) and a Photosystem I-core complex from the chlorophyll *c*-containing alga *Pleurochloris meirengis* (Xanthophyceae). *J Photochem Photobiol B: Biol* 20: 87–93
- Büchel C, Wilhelm C, Hauswirth N, and Wild A (1992) Evidence for a lateral heterogeneity by patch-work like areas enriched with Photosystem I complexes in the three thylakoid lamellae of *Pleurochloris meiringensis* (Xanthophyceae). *Crypt Bot* 2: 375–386
- Carbonera D, Giacometti G and Segre U (1996) Carotenoid interactions in peridinin chlorophyll *a* proteins from dinoflagellates. Evidence for optical excitons and triplet migration. *J Chem Soc, Faraday Trans* 92: 989–993
- Carbonera D, Giacometti G, Segre U, Hofmann E and Hiller RG (1999) Structure-based calculations of the optical spectra of



- the light-harvesting peridinin–chlorophyll–protein complexes from *Amphidinium carterae* and *Heterocapsa pygmaea*. *J Phys Chem B* 103: 6349–6356
- Caron L, Douady D, Quinet-Szely M, de Goër S and Berkaloﬀ C (1996) Gene structure of a chlorophyll *a/c*-binding protein from a brown alga: Presence of an intron and phylogenetic implications. *J Mol Evol* 43: 270–280
- Christensen RL (1999) The electronic states of carotenoids. In: Frank HA, Young AJ, Britton G and Cogdell RJ (eds) *Photochemistry of Carotenoids*, pp 137–159. Kluwer Academic Publishers, Kluwer
- Chrystal J and Larkum AWD (1987) Pigment-protein complexes and light harvesting in eustigmatophyte algae. In: Biggins J (ed) *Progress in Photosynthesis Research*, Vol II, pp 189–192. Martinus Nijhoff Publishers, Dordrecht
- Damjanović A, Ritz T and Schulten K (2000) Excitation transfer in the peridinin-chlorophyll-protein of *Amphidinium carterae*. *Biophys J* 79: 1695–1705
- De Martino A, Douady D, Quinet-Szely M, Rousseau B, Crepineau F, Apt K and Caron L (2000) The light-harvesting antenna of brown alga: Highly homologous proteins encoded by a multigene family. *Eur J Biochem* 267: 5540–5549
- Deane JA, Fraunholz M, Su V, Maier U-G, Martin W, Durnford DG and McFadden GI (2000) Evidence for nucleomorph to host nucleus gene transfer: Light-harvesting complex proteins from cryptomonads and chlorarachniophytes. *Protist* 151: 239–252
- Douglas SE and Penny SL (1999) The plastid genome of the cryptophyte alga, *Guillardia theta*: Complete sequence and conserved syntenic groups confirm its common ancestry with red algae. *J Mol Evol* 48: 236–244
- Durnford DG and Green BR (1994) Characterization of the light harvesting proteins of the chromophytic alga, *Olisthodiscus luteus* (*Heterosigma carterae*). *Biochim Biophys Acta* 1184: 118–123
- Durnford DG, Aebersold R and Green BR (1996) The fucoxanthin-chlorophyll proteins from a chromophyte alga are part of a large multigene family: Structural and evolutionary relationships to other light-harvesting antennae. *Mol Gen Genet* 253: 377–386
- Eppard M and Rhie E (1998) The genes encoding light-harvesting subunits of *Cyclotella cryptica* (Bacillariophyceae) constitute a complex and heterogeneous family. *Mol Gen Genet* 260: 335–345
- Eppard M, Krumbein WE, von Haeseler A and Rhie E (2000) Characterization of fcp4 and fcp12, two additional genes encoding light harvesting proteins of *Cyclotella cryptica* (Bacillariophyceae) and phylogenetic analysis of this complex gene family. *Plant Biol* 2: 283–289
- Fawley MW, Morton SJ, Stewart KD and Mattox KR (1987) Evidence for a common evolutionary origin of light-harvesting fucoxanthin chlorophyll *a/c*-protein complexes of *Pavlova gyra* (Prymnesiophyceae) and *Phaeodactylum tricornutum* (Bacillariophyceae). *J Phycol* 23: 377–381
- Frank HA (2001) Spectroscopic studies of the low-lying singlet excited electronic states and photochemical properties of carotenoids. *Arch Biochem Biophys* 385: 53–60
- Frank HA, Bautista JA, Josue J, Pendon Z, Hiller RG, Sharples FP, Gosztola D and Wasielewski MR (2000) Effect of the solvent environment on the spectroscopic properties and dynamics of the lowest excited states of carotenoids. *J Phys Chem B* 104: 4569–4577
- Friedman AL and Alberte RS (1984) A diatom light-harvesting pigment-protein complex. Purification and characterization. *Plant Physiol* 76: 483–489
- Gantt E, Edwards MR and Provasoli L (1971) Chloroplast structure of the Cryptophyceae. Evidence for phycobiliproteins within intrathylakoidal spaces. *J Cell Biol* 48: 280–290
- Garrido JL and Zapata M (1998) Detection of new pigments from *Emiliania huxleyi* (Prymnesiophyceae) by high-performance liquid chromatography, liquid chromatography–mass spectrometry, visible spectroscopy, and fast atom bombardment mass spectrometry. *J Phycol* 34: 70–78
- Garrido JL, Otero J, Maestro MA and Zapata M (2000) The main nonpolar chlorophyll *c* from *Emiliania huxleyi* (Prymnesiophyceae) is a chlorophyll *c*<sub>2</sub>-monogalactosyldiacylglyceride ester: A mass spectrometry study. *J Phycol* 36: 497–505
- Glazer AN and Wedemayer, GJ (1995) Cryptomonad biliproteins—an evolutionary perspective. *Photosynth Res* 46: 93–105
- Grabowski B, Cunningham FX Jr. and Gantt E (2001) Chlorophyll and carotenoid binding in a simple red algal light-harvesting complex crosses phylogenetic lines. *Proc Natl Acad Sci USA* 98: 2911–2916
- Green BR and Durnford DG (1996) The chlorophyll-carotenoid proteins of oxygenic photosynthesis. *Annu Rev Plant Physiol Plant Mol Biol* 47: 685–714
- Grevby C and Sundqvist C (1992) Characterization of light-harvesting complex in *Ochromonas danica* (Chrysophyceae). *J Plant Physiol* 140: 414–420
- Haxo FT and Fork DC (1959) Photosynthetically active accessory pigments of cryptomonads. *Nature* 184: 1051–1052
- Haxo FT, Kycia, JH, Somers GF, Bennett A and Siegelman HW (1976) Peridinin-chlorophyll *a* proteins of the dinoflagellate *Amphidinium carterae* (Plymouth 450). *Plant Physiol* 57: 297–303
- Hiller RG (1999) Carotenoids as components of the light-harvesting proteins of eukaryotic algae. In: Frank HA, Young AJ, Britton G and Cogdell RJ (eds) *Photochemistry of Carotenoids*, pp 81–98. Kluwer Academic Publishers, Dordrecht
- Hiller RG (2001) ‘Empty’ minicircles and petB/atpA and psbD/psbE (cyt<sub>b</sub><sub>559</sub>  $\alpha$ ) genes in tandem in *Amphidinium carterae* plastid DNA. *FEBS Lett* 505: 449–452
- Hiller RG and Breton J (1992) A linear dichroism study of photosynthetic pigment organisation in two fucoxanthin-containing algae. *Biochim Biophys Acta* 1102: 365–370
- Hiller RG and Martin CD (1987) Multiple forms of a type I phycoerythrin from a *Chroomonas* sp. (Cryptophyceae) varying in subunit composition. *Biochim Biophys Acta* 923: 98–102
- Hiller RG, Anderson JM and Larkum AWD (1991) The chlorophyll-protein complexes of algae. In: Scheer H (ed) *The Chlorophylls*, pp 529–547. CRC Publications, Boca Raton
- Hiller RG, Scaramuzzi CD and Breton J (1992) The organisation of photosynthetic pigments in a cryptophyte alga: A linear dichroism study. *Biochim Biophys Acta* 1102: 360–364
- Hiller RG, Wrench PM, Gooley, AP, Shoebridge G and Breton J (1993) The major intrinsic light-harvesting protein of *Amphidinium*: Characterization and relation to other light-harvesting proteins. *Photochem Photobiol* 57: 125–131
- Hiller RG, Wrench PM and Sharples FP (1995) The light-harvesting chlorophyll *a-c*-binding protein of dinoflagellates:

- A putative polyprotein. FEBS Lett 363: 175–178
- Hiller RG, Broughton MJ, Wrench PM, Sharples FP, Miller DJ and Catmull J (1999) Dinoflagellate light-harvesting proteins: Genes, structure and reconstitution. In Argyroudi-Akoyonoglou JH and Senger H (eds) *The Chloroplast: From Molecular Biology to Biotechnology*, pp 3–10. Kluwer Academic Publishers, Dordrecht
- Hiller RG, Crossley LG, Wrench PM, Santucci N and Hofmann E (2001a) The 15-kDa forms of the apo-peridinin-chlorophyll *a* protein (PCP) in dinoflagellates show high identity with the apo-32 kDa PCP forms, and have similar N-terminal leaders and gene arrangements. *Mol Gen Genet* 266: 254–259
- Hiller RG, Sharples FP, Catmull J, Puskeiler R and Miller DJ (2001b) Reconstitution of the peridinin-chlorophyll *a*-protein (PCP) from heterologously expressed apoprotein and isolated pigments. In: PS 2001: Proceedings of the 12th International Congress on Photosynthesis, S31-021. CSIRO Publishing, Melbourne (CD-ROM)
- Hofmann E, Wrench PM, Sharples FP, Hiller RG, Welte W and Diederichs K (1996) Structural basis of light harvesting by carotenoids: Peridinin-chlorophyll-protein from *Amphidinium carterae*. *Science* 272: 1788–1791
- Hsu B-D and Lee J-Y (1987) Orientation of pigments and pigment-protein complexes in the diatom *Cylindrotheca fusiformis*. A linear-dichroism study. *Biochim Biophys Acta* 893: 572–577
- Iglesias-Prieto R and Trench RK (1997) Acclimation and adaptation to irradiance in symbiotic dinoflagellates. II. Response of chlorophyll-protein complexes to different photon-flux densities. *Mar Biol* 130:23–33
- Iglesias-Prieto R, Govind NS and Trench RK (1991) Apoprotein composition and spectroscopic characterization of the water-soluble peridinin-chlorophyll *a*-proteins from three symbiotic dinoflagellates. *Proc R Soc Lond B* 246: 275–283
- Iglesias-Prieto R, Govind NS and Trench RK (1993) Isolation and characterization of three membrane-bound chlorophyll-protein complexes from four dinoflagellate species. *Phil Trans R Soc Lond B* 340: 381–392
- Ingram K and Hiller RG (1983) Isolation and characterization of a major chlorophyll *a/c*<sub>2</sub> light-harvesting protein from a *Chroomonas* species (Cryptophyceae). *Biochim Biophys Acta* 772: 310–319
- Jansson S, Green BR, Grossman AR and Hiller RG (1999) A proposal for extending the nomenclature of light-harvesting proteins of the three transmembrane helix type. *Plant Mol Biol Rep* 17: 221–224
- Jeffrey SW and Anderson JM (2000) *Emiliania huxleyi* (Haptophyta) holds promising insights for photosynthesis. *J Phycol* 36: 449–452
- Jenkins J, Hiller RG, Speirs J and Godovac-Zimmermann J (1990) A genomic clone encoding a cryptophyte phycoerythrin  $\alpha$ -subunit. Evidence for three  $\alpha$ -subunits and an N-terminal membrane transit sequence. *FEBS Lett* 273: 191–194
- Johnsen G, Nelson NB, Jovine RVM and Prézélin BB (1994) Chromoprotein- and pigment-dependent modeling of spectral light absorption in two dinoflagellates, *Prorocentrum minimum* and *Heterocapsa pygmaea*. *Mar Ecol Prog Ser* 114: 245–258
- Jovine RVM, Triplett EL, Nelson NB and Prézélin BB (1992) Quantification of chromophore pigments, apoprotein abundance and isoelectric variants of peridinin-chlorophyll *a*-protein complexes (PCPs) in the dinoflagellate *Heterocapsa pygmaea* grown under variable light conditions. *Plant Cell Physiol* 33: 733–741
- Jovine RVM, Johnsen G and Prézélin BB (1995) Isolation of membrane bound light-harvesting-complexes from the dinoflagellates *Heterocapsa pygmaea* and *Prorocentrum minimum*. *Photosynth Res* 44: 127–138
- Katoh T, Mimuro M and Takaichi S (1989) Light-harvesting particles isolated from a brown alga, *Dictyota dichotoma*. A supramolecular assembly of fucoxanthin-chlorophyll-protein complexes. *Biochim Biophys Acta* 976: 233–240
- Kleima FJ, Hofmann E, Gobets B, van Stokkum IHM, van Grondelle R, Diederichs K and van Amerongen H (2000a) Förster excitation energy transfer in peridinin-chlorophyll-*a*-protein. *Biophys J* 78: 344–353
- Kleima FJ, Wendling M, Hofmann E, Peterman EJG, van Grondelle R, and van Amerongen H (2000b) Peridinin chlorophyll *a* protein: Relating structure and steady-state spectroscopy. *Biochemistry* 39: 5184–5195
- Knoetzel J and Rensing L (1990) Characterization of the photosynthetic apparatus from the marine dinoflagellate *Gonyaulax polyedra*. I. Pigment and polypeptide composition of the pigment-protein complexes. *J Plant Physiol* 136: 271–279
- Krueger BP, Lampoura SS, van Stokkum IHM, Papagiannakis E, Salverda JM, Gradinaru CC, Rutkauskas D, Hiller RG and van Grondelle R (2001) *Biophys J* 80: 2843–2855
- Kroth-Pancic PG (1995) Nucleotide sequence of two cDNAs encoding fucoxanthin chlorophyll *a/c* proteins in the diatom *Odontella sinensis*. *Plant Mol Biol* 27: 825–828
- Kühlbrandt W, Wang DN and Fujiyoshi Y (1994) Atomic model of plant light-harvesting complex by electron crystallography. *Nature* 367: 614–621
- Larkum AWD and Barrett J (1983) Light-harvesting processes in algae. *Adv Bot Res* 10: 1–219
- Larkum T and Howe CJ (1997) Molecular aspects of light-harvesting processes in algae. *Adv Bot Res* 27: 257–330
- LaRoche J, Henry D, Wyman K, Sukenik A and Falkowski P (1994) Cloning and nucleotide sequence of a cDNA encoding a major fucoxanthin-, chlorophyll *a/c*-containing protein from the chrysophyte *Isochrysis galbana*: Implications for evolution of the *cab* gene family. *Plant Mol Biol* 25: 355–368
- Le QH, Markovic P, Hastings JW, Jovine RVM and Morse D. (1997) Structure and organization of the peridinin-chlorophyll *a*-binding protein gene in *Gonyaulax polyedra*. *Mol Gen Genet* 255: 595–604
- Leblanc C, Falcatore A, Watanabe M and Bowler C (1999) Semi-quantitative RT-PCR analysis of photoregulated gene expression in marine diatoms. *Plant Mol Biol* 40: 1031–1044
- Lichtlé C, Jupin H, and Duval JC (1980) Energy transfers from Photosystem II to Photosystem I in *Cryptomonas rufescens* (Cryptophyceae). *Biochim Biophys Acta* 591: 104–112
- Lichtlé C, Duval JC and Lemoine Y (1987) Comparative biochemical, functional and ultrastructural studies of photosystem particles from a Cryptophyceae: *Cryptomonas rufescens*; isolation of an active phycoerythrin particle. *Biochim Biophys Acta* 894: 76–90
- Lichtlé C, Spilar A and Duval JC (1992a) Immunogold localization of light-harvesting and Photosystem I complexes in the thylakoids of *Fucus serratus* (Phaeophyceae). *Protoplasma* 166: 99–106
- Lichtlé C, McKay RML and Gibbs SP (1992b) Immunogold

- localization of Photosystem I and Photosystem II light-harvesting complexes in cryptomonad thylakoids. *Biol Cell* 74: 187–194
- Lichtlé C, Arsalane W, Duval JC and Passaquet C (1995) Characterization of the light-harvesting complex of *Giraudyopsis stellifer* (Chrysophyceae) and effects of light stress. *J Phycol* 31: 380–387
- Ludwig M and Gibbs SP (1989) Localization of phycoerythrin at the lumenal surface of the thylakoid membrane in *Rhodomonas lens*. *J Cell Biol* 108: 875–884
- MacColl R and Berns DS (1978) Energy transfer studies on cryptomonad biliproteins. *Photochem Photobiol* 27:343–349
- MacColl R, Lam I, Choi CY and Kim J (1994) Exciton splitting in phycoerythrin 545. *J Biol Chem* 269: 25465–25469
- MacColl R, Malak H, Gryczynski I, Eisele LE, Mizejewski GJ, Franklin E, Sheikh H, Montellese D, Hopkins S and MacColl LC (1998) Phycoerythrin 545: Monomers, energy migration, bilin topography and monomer/dimer equilibrium. *Biochemistry* 37: 417–423
- MacColl R, Eisele LE, Dhar M, Ecuyer J-P, Hopkins S, Marrone J, Barnard R, Malak H and Lewitus AJ (1999a) Bilin organization in cryptomonad biliproteins. *Biochemistry* 38: 4097–4105
- MacColl R, Eisele LE and Marrone J (1999b) Fluorescence polarization studies on four biliproteins and a bilin model for phycoerythrin 545. *Biochim Biophys Acta* 1412: 230–239
- Macpherson AN, Paulsen H and Gillbro T (2002) Ultrafast carotenoid-to-chlorophyll singlet energy transfer in the light-harvesting complex II of higher plants. In: PS 2001: Proceedings of the 12th International Congress on Photosynthesis, S31-025/S2-001. CSIRO Publishing, Melbourne (CD-ROM)
- McFadden GI (2001) Primary and secondary endosymbiosis and the origin of plastids. *J Phycol* 37: 951–959
- Meeson BW, Chang SS and Sweeney BM (1982) Characterization of peridinin-chlorophyll *a*-proteins from the marine dinoflagellate *Ceratium furca*. *Bot Mar* 25: 347–350
- Mimuro M, Katoh T and Kawai H (1990a) Spatial arrangements of pigments and their interaction in the fucoxanthin-chlorophyll *a/c* protein assembly (FCPA) isolated from the brown alga *Dictyota dichotoma*. Analysis by means of polarized spectroscopy. *Biochim Biophys Acta* 1015: 450–456
- Mimuro M, Tamai N, Ishimaru T and Yamazaki I (1990b) Characteristic fluorescence components in photosynthetic pigment system of a marine dinoflagellate, *Protogonyaulax tamarensis*, and excitation energy flow among them. Studies by means of steady-state and time-resolved fluorescence spectroscopy. *Biochim Biophys Acta* 1016: 280–287
- Mimuro M, Nagashima U, Takaichi S, Nishimura Y, Yamazaki I and Katoh T (1992) Molecular structure and optical properties of carotenoids for the in vivo energy transfer function in the algal photosynthetic pigment system. *Biochim Biophys Acta* 1098: 271–274
- Mimuro M, Tamai N, Murakami A, Watanabe M, Erata M, Watanabe MM, Tokutomi M and Yamazaki I (1998) Multiple pathways of excitation energy flow in the photosynthetic pigment system of a cryptophyte, *Cryptomonas* sp. (CR-1). *Phycol Res* 46: 155–164
- Nagae H, Kakitani T, Katoh T and Mimuro M (1993) Calculation of the excitation transfer matrix elements between the  $S_2$  or  $S_1$  state of carotenoid and the  $S_2$  or  $S_1$  state of bacteriochlorophyll. *J Chem Phys* 98: 8012–8023
- Norris BJ and Miller DJ (1994) Nucleotide sequence of a cDNA clone encoding the precursor of the peridinin-chlorophyll *a*-binding protein from the dinoflagellate *Symbiodinium* sp. *Plant Mol Biol* 24: 673–677
- Ogata T and Kodama M (1993) In: Smayda TJ and Shimizu Y (eds) *Toxic Phytoplankton Blooms in the Sea*, pp 901–905. Elsevier, New York
- Ogata T, Kodama M, Nomura S, Kobayashi M, Nozawa T, Katoh T and Mimuro M (1994) A novel peridinin-chlorophyll *a* protein (PCP) from the marine dinoflagellate *Alexandrium cohorticula*: A high pigment content and plural spectral forms of peridinin and chlorophyll *a*. *FEBS Lett* 356: 367–371
- Owens TG, Gallagher JC and Alberte RS (1987) Photosynthetic light-harvesting function of violaxanthin in *Nannochloropsis* spp. (Eustigmatophyceae). *J Phycol* 23: 79–85
- Pascal AA, Caron L, Rousseau B, Lapouge K, Duval J-C and Robert B (1998) Resonance Raman spectroscopy of a light-harvesting protein from the brown alga *Laminaria saccharina*. *Biochemistry* 37: 2450–2457
- Passaquet C and Lichtlé C (1995) Molecular study of a light-harvesting apoprotein of *Giraudyopsis stellifer* (Chrysophyceae). *Plant Mol Biol* 29: 135–148
- Passaquet C, Thomas JC, Caron L, Hauswirth N, Puel F and Berkalo C (1991) Light-harvesting complexes of brown algae: Biochemical characterization and immunological relationships. *FEBS Lett* 280: 21–26
- Pilch M and Pawlikowski M (1998) Circular dichroism (CD) study of peridinin-chlorophyll *a* protein (PCP) complexes from marine dinoflagellate algae. The tetramer approach. *J Chem Soc, Faraday Trans* 94: 227–232
- Prézelin BB (1976) The role of peridinin-chlorophyll *a*-proteins in the photosynthetic light adaptation of the marine dinoflagellate, *Glenodinium* sp. *Planta* 130: 225–233
- Prézelin BB (1987) Photosynthetic physiology of dinoflagellates. In: Taylor FJR (ed) *The Biology of Dinoflagellates*, pp 174–223. Blackwell, Oxford
- Prézelin BB and Haxo FT (1976) Purification and characterization of peridinin-chlorophyll *a*-proteins from the marine dinoflagellates *Glenodinium* sp. and *Gonyaulax polyedra*. *Planta* 128: 133–141
- Pysznik AM and Gibbs SP (1992) Immunocytochemical localization of Photosystem I and the fucoxanthin-chlorophyll *a/c* light-harvesting complex in the diatom *Phaeodactylum tricorutum*. *Protoplasma* 166: 208–217
- Reith M and Douglas S (1990) Localization of  $\beta$ -phycoerythrin to the thylakoid lumen of *Cryptomonas*  $\Phi$  does not involve a signal peptide. *Plant Mol Biol* 15: 585–592
- Reuter W, Wiegand G, Huber R and Than ME (1999) Structural analysis at 2.2 Å of orthorhombic crystals presents the asymmetry of the allophycocyanin-linker complex, AP-LC<sup>7,8</sup>, from phycobilisomes of *Mastigocladus laminosus*. *Proc Natl Acad Sci USA* 96: 1363–1368
- Rhiel E, Krupinska K and Wehrmeyer W (1986) Effects of nitrogen starvation on the function and organization of the photosynthetic membranes in *Cryptomonas maculata* (Cryptophyceae). *Planta* 169: 361–369
- Rhiel E, Kunz J and Wehrmeyer W (1989) Immunocytochemical localization of phycoerythrin-545 and of a chlorophyll *a/c* light harvesting complex in *Cryptomonas maculata* (Cryptophyceae). *Bot Acta* 102: 46–53
- Roman SJ, Govind NS, Triplett EL and Prézelin BB (1988) Light regulation of peridinin-chlorophyll *a*-protein (PCP) complexes

- in the dinoflagellate, *Glenodinium* sp. *Plant Physiol* 88: 594–599
- Sharples FP, Wrench PM, Ou K and Hiller RG (1996) Two distinct forms of the peridinin-chlorophyll *a*-protein from *Amphidinium carterae*. *Biochim Biophys Acta* 1276: 117–123.
- Shreve AP, Trautman JK, Owens TG and Albrecht AC (1991) A femtosecond study of electronic state dynamics of fucoxanthin and implications for photosynthetic carotenoid-to-chlorophyll energy transfer mechanisms. *Chem Phys* 154: 171–178
- Smith GJ, Gao Y and Alberte RS (1997) The fucoxanthin-chlorophyll *a/c* proteins comprise a large family of coexpressed genes in the marine diatom *Skeletonema costatum* (Greve). Characterization of eight unique cDNAs. *Plant Physiol* 114: 1136
- Song PS, Koka P, Prézélin BB and Haxo FT (1976) Molecular topology of the photosynthetic light-harvesting pigment complex, peridinin-chlorophyll *a*-protein, from marine dinoflagellates. *Biochemistry* 15: 4422–4427
- Spear-Bernstein L and Miller KR (1989). Unique location of the phycobiliprotein light-harvesting pigment in the cryptophyceae. *J Phycol* 25: 412–419
- Stochaj WR and Grossman AR (1997) Differences in the protein profiles of cultured and endosymbiotic *Symbiodinium* sp. (Pyrrophyta) from the anemone *Aiptasia pallida* (Anthozoa). *J Phycol* 33: 44–53
- Sukenik A, Livne A, Neori A, Yacobi YZ and Katcoff D (1992) Purification and characterization of a light-harvesting chlorophyll-protein complex from the marine eustigmatophyte *Nannochloropsis* sp. *Plant Cell Physiol* 33: 1041–1048
- Sukenik A, Livne A, Apt KE and Grossman AR (2000) Characterization of a gene encoding the light-harvesting violaxanthin-chlorophyll protein of *Nannochloropsis* sp. (Eustigmatophyceae). *J Phycol* 36: 563–570
- ten Lohuis MR and Miller DJ (1998) Light-regulated transcription of genes encoding peridinin chlorophyll *a* proteins and the major intrinsic light-harvesting complex proteins in the dinoflagellate *Amphidinium carterae* Hulburt (Dinophyceae). Changes in cytosine methylation accompany photoadaptation. *Plant Physiol* 117: 189–196
- Trautman JK, Shreve AP, Owens TG and Albrecht AC (1990) Femtosecond dynamics of carotenoid-to-chlorophyll energy transfer in thylakoid membrane preparations from *Phaeodactylum tricornutum* and *Nannochloropsis* sp. *Chem Phys Lett* 166: 369–374
- Vesk M, Dwarte D, Fowler S and Hiller RG (1992) Freeze fracture immunocytochemistry of light-harvesting pigment complexes in a cryptophyte. *Protoplasma* 170: 166–176.
- Weis VM, Verde EA and Reynolds WS (2002) Characterization of a short form peridinin-chlorophyll-protein (PCP) cDNA and protein from the symbiotic dinoflagellate *Symbiodinium muscatinei* (Dinophyceae) from the sea anemone *Anthopleura elegantissima* (Cnidaria). *J Phycol* 38: 157–163
- Wilhelm C, Büchel C and Rousseau B (1988) The molecular organization of chlorophyll-protein complexes in the Xanthophyceae alga *Pleurochloris meiringensis*. *Biochim Biophys Acta* 934: 220–226
- Wilk KE, Harrop SJ, Jankova L, Edler D, Keenan G, Sharples F, Hiller RG and Curmi PMG (1999) Evolution of a light-harvesting protein by addition of new subunits and rearrangement of conserved elements: Crystal structure of a cryptophyte phycoerythrin at 1.63-Å resolution. *Proc Natl Acad Sci USA* 96: 8901–8906
- Zhang Z, Green, BR and Cavalier-Smith T (1999) Single gene circles in dinoflagellate chloroplast genomes. *Nature* 400: 155–159
- Zigmantas D, Polívka T, Hiller RG, Yartsev A and Sundström V (2001) Spectroscopic and dynamic properties of the peridinin lowest singlet excited states. *J Phys Chem A* 105: 10296–10306
- Zigmantas D, Polívka T, Hiller RG and Sundström V (2002) Energy transfer pathways in the peridinin chlorophyll-*a* protein complex as revealed by the near-infrared time-resolved spectroscopy. In: PS2001 Proceedings: 12th International Congress on Photosynthesis, S2-031. CSIRO Publishing, Melbourne (CD-ROM)

# Chapter 12

## Biogenesis of Green Plant Thylakoid Membranes

Kenneth Cline\*

*Horticultural Sciences and Plant Molecular and Cellular Biology,  
University of Florida, Gainesville, FL 32611, U.S.A.*

Summary .....	353
I. Introduction .....	354
II. Methodologies for Higher Plant Chloroplasts .....	354
III. Overview of Localization Processes .....	356
A. Targeting Elements .....	356
B. Overall Pathway From Cytosol To Thylakoids .....	356
C. Evolutionary Origins of Translocation Machineries .....	356
D. Four Thylakoid Translocation/Integration Systems .....	358
E. Genetic and Biochemical Identification of Pathways and Components Are Consistent .....	358
IV. Different Mechanisms Address Different Translocation Problems .....	359
A. Sec Pathway .....	359
B. $\Delta$ pH-Dependent/Tat Pathway .....	361
C. cpSRP Pathway .....	361
D. The Spontaneous Pathway .....	363
V. The In Vivo Site of Thylakoid Protein Transport and Insertion .....	364
VI. Chlorophyll Synthesis And The Insertion Of Antenna Proteins .....	364
A. Regulation of LHC Gene Expression by the Chlorophyll Synthetic Pathway .....	364
B. Chlorophyll Requirement for Antenna Stability and Integration .....	365
C. Topology of Chlorophyll Synthesis .....	365
D. Does Chlorophyll Drive the Insertion of Antenna Proteins? .....	367
VII. Future Prospects .....	367
References .....	368

### Summary

Biogenesis of chloroplast thylakoid membranes involves the synthesis of proteins, lipids, and pigments and their assembly into an elaborate membrane system containing four different supramolecular photosynthetic complexes. In addition, because these biogenetic processes begin during early stages of plastid development, where plastids contain little internal membrane, thylakoid membrane formation also entails substantial membrane flow from the envelope. Most thylakoid proteins are encoded in the nucleus and synthesized in the cytosol—the remainder are encoded and synthesized in the plastid. Nuclear-encoded thylakoid proteins are imported into the plastid by a translocation apparatus that evolved after endosymbiosis, and the imported proteins are routed into thylakoids by translocation systems that evolved in prokaryotes prior to endosymbiosis. Four different translocation pathways have been described for thylakoids. The Sec pathway transports proteins in an unfolded conformation to the lumen; the  $\Delta$ pH-dependent/Tat pathway transports folded proteins to the lumen; the spontaneous pathway integrates one class of membrane proteins; the cpSRP pathway appears

---

\*Email: kcline@ufl.edu

dedicated to targeting and assembly of multispanning LHC proteins. Assembly of LHC proteins represents an interesting situation. A novel component of the cpSRP system has been employed to specifically adapt the SRP system to posttranslational integration. In addition, LHC proteins require chlorophyll for their integration and stability. Thus the site(s) of chlorophyll synthesis likely determine the exact site of LHC integration. Although the thylakoid membrane is the site of translocation/integration in immature and mature chloroplasts, evidence increasingly points to the inner envelope membrane as the site of insertion during very early plastid developmental stages, and envelope invagination combined with vesicular traffic as the vehicle for relocating lipids and proteins to the plastid interior. In such a scenario, the translocons and chlorophyll biosynthetic enzymes should be located in the envelope in developing proplastids. Recent cloning of the genes for these proteins should soon allow a test of this hypothetical mechanism.

## I. Introduction

Biogenesis of photosynthetic membranes in plant and algal chloroplasts is possibly the most complex membrane assembly process in the eukaryotic cell. The components of the four different supramolecular complexes participating in the light reactions are synthesized in two different compartments in the cell. Current estimates place the number of thylakoid proteins participating in photosynthesis at 75 to 100. In higher plants, 33 of these are encoded and synthesized in the plastid (Herrmann, 1999; Race et al., 1999; Peltier et al., 2000). The remainder are encoded in the nucleus and synthesized in the cytosol. In addition to the proteins directly involved in photosynthesis, a variety of other thylakoid proteins play a role in biogenesis and homeostasis of the membranes and these are also encoded in the nucleus (Settles and Martienssen, 1998; Dalbey and Robinson, 1999; Keegstra and Cline, 1999). Nuclear-encoded proteins encounter and pass several membrane and soluble compartments en-route to their thylakoid destination. This is different from the majority of other membrane-targeted proteins, which cross or integrate into only one membrane during their entire lifetime. Thus, nuclear-encoded thylakoid proteins encounter several molecular machines for transmembrane translocation and also chaperone or pilot molecules to ferry them across aqueous compartments. Upon arriving at their destination, the polypeptides must be met by their plastid-encoded partners to assemble functional complexes (Wollman

et al., 1999; Choquet and Vallon, 2000).

Not only is exquisite choreography required to combine nuclear-encoded and plastid encoded subunits in exact stoichiometry, but many proteins are also ligated to prosthetic groups. Chlorophyll, carotenoids, metal ions and other co-factors must enter the assembly process at some point. In some cases, co-factor acquisition can be uncoupled from localization processes (Howe and Merchant, 1994). However, in others such as with chlorophyll binding proteins, integration into the membrane is strictly coupled to pigment assembly (see below).

One additional complexity in higher plant chloroplasts is that assembly occurs over a wide range of developmental stages, ranging from early differentiation of the proplastid, where internal membranes are virtually absent and both proteins and bilayer accumulate simultaneously, to fully developed chloroplasts, where the assembly processes are required primarily for maintenance. The result is that biogenesis mechanisms must operate under varied organelle architectures and at strikingly different rates (Mullet, 1988; Dahlin and Cline 1991; Fig. 1). Indeed, an important challenge is to describe the mechanisms that assemble internal membranes in situations where little or no internal membrane pre-exists.

## II. Methodologies for Higher Plant Chloroplasts

Several experimental techniques have been employed to study the biogenesis of thylakoid proteins, each with its own strengths and weaknesses. Much of the information presented in this chapter derives from reconstituted *in vitro* assays with intact plant chloroplasts, isolated thylakoids, stromal extract, and purified components. Detailed methods for the

---

*Abbreviations:* Chl – chlorophyll; cpSRP – chloroplast signal recognition particle; ER – endoplasmic reticulum; GGPP – geranylgeranyl pyrophosphate; LHC – light harvesting chlorophyll-binding protein; LTD – lumen-targeting domain; POR – protochlorophyllide oxidoreductase; SRP – signal recognition particle; STD – stromal targeting domain; Tat – twin arginine translocation

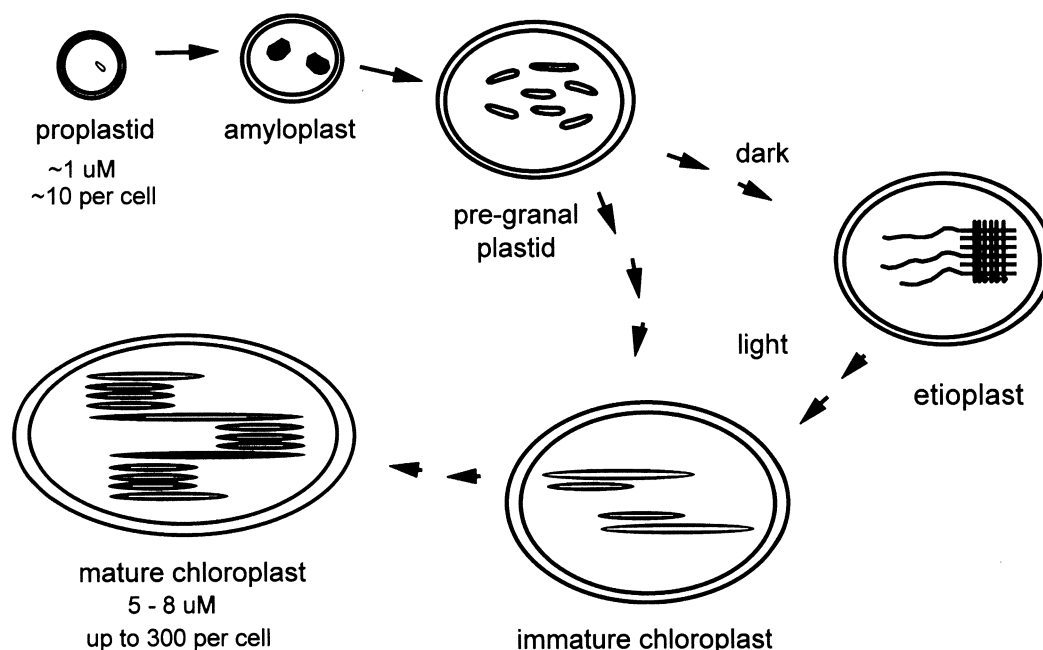


*Fig. 1.* The pathway for development of chloroplasts from proplastids. All plastids have a double membrane envelope that encloses an aqueous stroma. When seeds are germinated in the dark, plastids develop into etioplasts, which contain internal membranes consisting of prolamellar bodies and prothylakoids. Upon illumination, etioplasts develop rapidly into chloroplasts with a highly elaborated thylakoid membrane. When seedlings develop normally in the light, proplastids proceed directly to chloroplasts without the intermediate etioplast stage. During periods of rapid membrane synthesis, invaginations of the inner envelope membrane as well as stromally localized vesicles can be seen (not shown).

basic assays can be found at <http://www.hos.ufl.edu/clineweb/>. In vitro assays permit experimental conditions to be controlled more precisely and generally are more conducive to determining mechanisms involved in the process. One frequent criticism of in vitro assays is that they employ radiotracer amounts of precursor proteins and that low levels of import and transport are obtained (Cline et al., 1985; Hooper and Eggink, 1999). However, since the early 1990s, chemical quantities of precursors have been produced by over-expression in bacteria, allowing import and localization to be measured under optimal substrate concentrations. Such assays showed that isolated chloroplasts are capable of in vivo rates of import and assembly. Pfisterer et al. (1982) estimated that each chloroplast in a rapidly developing monocot leaf imports ~15,000 total proteins per minute and assembles ~3000 LHC proteins per minute. In vitro import rates of ~40,000 proteins per minute per chloroplast and LHC *in organello* assembly rates of 10,000 proteins per min have been achieved (Cline et al., 1993). The limited number of analyses conducted with bacterially

expressed precursors has yielded essentially the same results as those obtained with radiotracer levels of precursors (Cline et al., 1993; Yuan et al., 1993). On the other hand, a valid criticism of in vitro studies is that they are conducted with partly developed chloroplasts rather than developing proplastids, and may not represent the precise situation that occurs in the very early stages of thylakoid formation.

Genetic studies have played an important role in component discovery, in querying the pathways and the components involved in vivo, and in dissecting regulatory mechanisms (Smith and Kohorn, 1994; Voelker and Barkan, 1995; Settles et al. 1997; Sundberg et al., 1997; Voelker et al., 1997; Jarvis et al., 1998; Amin et al., 1999; Klimyuk et al., 1999; Walker et al., 1999; Bauer et al., 2000; Motohashi et al., 2001). Interrogation of intact organisms, either those containing transgenes encoding modified precursors (Lawrence and Kindle, 1997; Kindle, 1998; Rensink et al. 1998), or under specialized conditions to enhance early developmental events (Hooper and Eggink, 1999) has also been employed. The focus of this chapter will be restricted to protein



transport and assembly in higher plant chloroplasts and will emphasize those processes as they apply to the antenna proteins.

### III. Overview of Localization Processes

#### A. Targeting Elements

Nuclear-encoded thylakoid proteins are synthesized in the cytosol as precursor proteins and localized by post-translational import into the plastid (Fig. 2; Cline and Henry, 1996; Schnell 1998; Keegstra and Cline, 1999). Precursors possess amino-terminal plastid targeting peptides called transit peptides that direct proteins to and into the plastid. Plastid targeting peptides (also called stroma targeting domains or STDs) share compositional features, but lack sequence consensus. Several web-based programs are relatively good at identifying functional plastid-targeting transit peptides (ChloroP <http://www.cbs.dtu.dk/services/ChloroP/>, Target P <http://www.cbs.dtu.dk/services/TargetP/>). Precursors to thylakoid proteins contain additional targeting information that determines their ultimate location in the thylakoid membrane system. Proteins destined for the thylakoid lumen and some integral thylakoid proteins have bipartite transit peptides in which the carboxyl proximal domain is a thylakoid targeting signal sequence (referred to as a lumen targeting domain or LTD). These sequences are removed concomitant with or shortly after thylakoid localization. Cleaved LTDs resemble bacterial signal peptides with a charged amino terminus, hydrophobic core region, and hydrophilic cleavage region (Cline and Henry, 1996) and are accurately predicted with the program SignalP <http://www.cbs.dtu.dk/services/SignalP/>.

The majority of integral membrane proteins possess targeting sequences present in the mature proteins sequence. These targeting sequences appear to comprise the hydrophobic transmembrane domains of the proteins. However, definitively ascribing targeting function to such sequences is very difficult because of their essential nature in anchoring the protein in the bilayer. Recently, a novel class of targeting element for antenna proteins was described that enables imported proteins to interact post-translationally with a unique form of the signal recognition particle (SRP) (see below). Plastid-encoded thylakoid proteins consist primarily of

integral membrane proteins or extrinsic proteins associated with the stromal face of the thylakoids (Race et al., 1999). By and large, these proteins are made without cleavable targeting sequences and for most; the targeting elements have not been identified. Exceptions are cytochrome *f* and probably PsbK, which contain amino-terminal signal peptides.

#### B. Overall Pathway From Cytosol To Thylakoids

In vitro analysis played a major role in defining the pathways taken by thylakoid precursor proteins to their functional locations. Thylakoid proteins are assembled in isolated chloroplasts by a two-step mechanism in which the precursors are first imported into the stroma and are then transported across or integrated into the thylakoid membrane. A large body of evidence supports this model, including the kinetics of stromal intermediate appearance during import into chloroplasts (Reed et al., 1990; Cline et al., 1992a), accumulation of stromal intermediates in import assays when thylakoid transport is specifically inhibited (Cline et al., 1989, 1992b, 1993), progression of intermediates into thylakoids upon inhibitor removal (Cline et al., 1993; Creighton et al., 1995), and reconstitution of intermediate precursor transport into isolated thylakoids (Cline and Henry, 1996). A study of the assembly pathway of plastocyanin in intact *Chlamydomonas* cells provides in vivo support for such a two-step pathway (Howe and Merchant, 1993), as does analysis of plants with mutations in thylakoid translocation machinery (Voelker and Barkan, 1995).

#### C. Evolutionary Origins of Translocation Machinery

Studies during the past decade support a model for thylakoid protein assembly that has been termed 'conservative sorting' (Hartl et al., 1986). The genes for thylakoid proteins were originally present in the genome of the prokaryotic endosymbiont, an organism similar to a cyanobacterium, and the proteins were assembled into and across the membranes by prokaryotic systems called protein 'export' mechanisms (Schatz and Dobberstein, 1996). Most of those genes were relocated to the host nuclear genome during the course of evolution and were successfully deleted from the organelle genome upon acquisition of a plastid targeting mechanism. Such a mechanism imports the nuclear encoded proteins

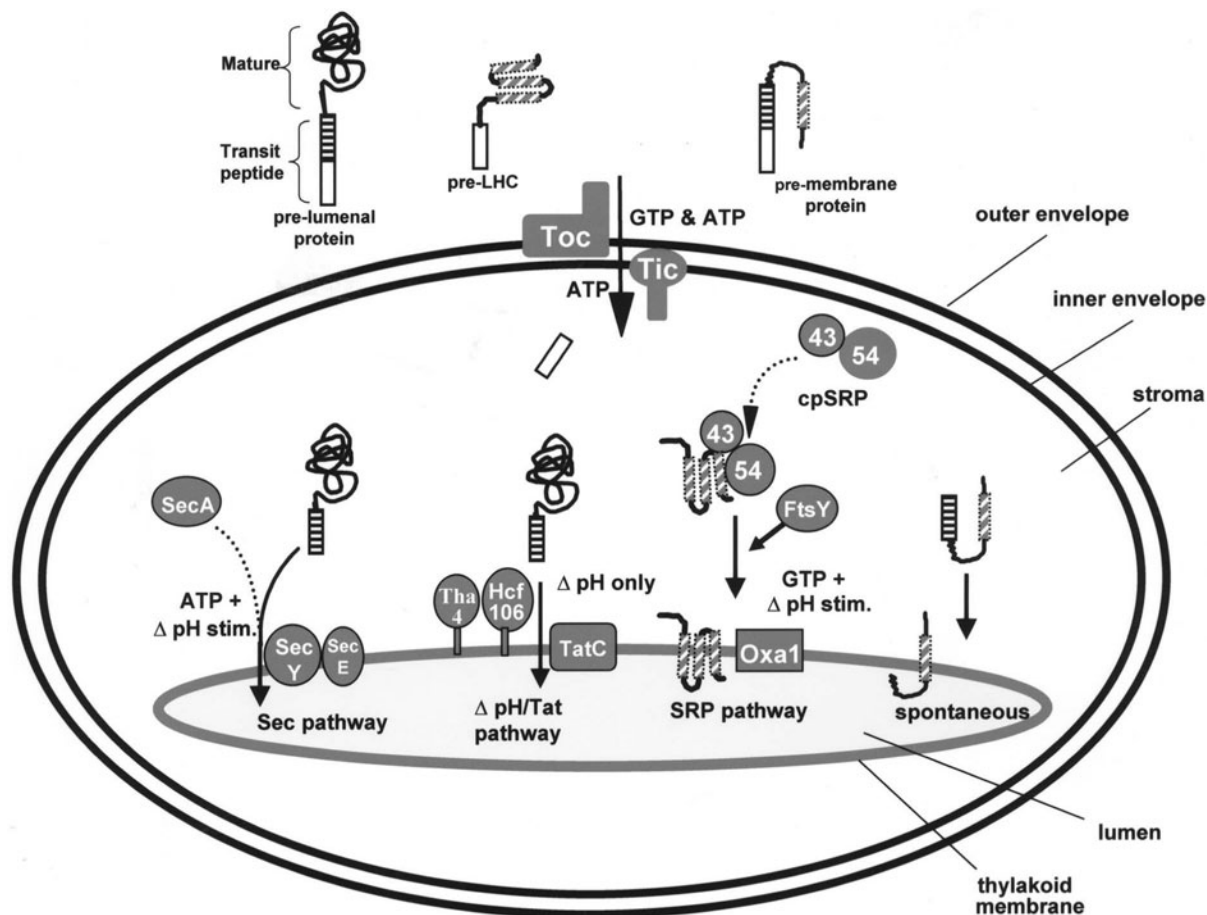


**Fig. 2.** Working model for localization of thylakoid proteins. Precursor proteins are imported across the envelope into the stroma by the general import machinery that consists of the Translocon in the Outer Chloroplast envelope (Toc) and the Translocon in the Inner Chloroplast envelope (Tic). The chloroplast-targeting domain of the transit peptide (open rectangles) is removed by the stromal processing protease. Lumen-targeting domains (striped rectangles) and transmembrane domains (slashed rectangles) direct thylakoid translocation of intermediate precursors in by one of four different mechanisms. The chloroplast Sec pathway employs chloroplast orthologs of the bacterial SecA ATPase and SecY/ SecE translocon. The chloroplast SRP pathway, which integrates the LHC protein family into the membrane, shares some characteristics with the ER and bacterial SRP pathway. Orthologous components are the chloroplast SRP54 protein and the chloroplast FtsY protein. The only known membrane component of this system is an ortholog of the mitochondrial Oxa1p, which facilitates insertion of mitochondrial inner membrane proteins but is not coupled to SRP. The cpSRP43 protein is a novel component that confers post-translational capabilities on cpSRP54. The  $\Delta$ pH-dependent pathway is orthologous to the bacterial Tat pathway and employs three membrane proteins whose function is not currently known. Membrane proteins with short lumen domains integrate into the membrane by an apparently spontaneous mechanism that is driven by hydrophobic interactions between transmembrane domains and the bilayer. Details on the operation of these systems are presented in the text. A listing of their known substrates is given in Table 1.

into the plastid matrix or stroma (Race et al., 1999). Imported proteins then enter pathways conserved from the prokaryotic endosymbiont. The general protein import apparatus in the plastid envelope, which delivers proteins to the stroma, contains several novel protein components and thus fits the model of a translocation machine that evolved post-endosymbiosis (Chen and Schnell, 1999; May and Soll, 1999). The identified thylakoid targeting and

translocation systems are all homologous to prokaryotic protein export systems (Settles and Martienssen, 1998; Dalbey and Robinson, 1999; Keegstra and Cline 1999). Recent studies indicate that at least some plastid-encoded proteins also employ conserved mechanisms for their thylakoid integration (Voelker and Barkan, 1995; Nilsson et al., 1999; Zhang et al., 2001). As will be seen below, in vitro as well as in vivo investigations support this

model. Figure 2 shows a working model for the localization of nuclear-encoded thylakoid proteins.

#### *D. Four Thylakoid Translocation/Integration Systems*

Four precursor-specific thylakoid targeting pathways have been identified (Fig. 2). One pathway appears to employ an unassisted mechanism for insertion of proteins into the membrane and is currently referred to as the 'spontaneous' pathway. The other three pathways have distinctive energy requirements and translocation machinery; two are named based on homology to bacterial export systems (Sec and SRP) and one based on the unique energy requirement of a trans-thylakoid pH gradient ( $\Delta$ pH-dependent pathway). With the exception of cpSRP43, components of the thylakoid translocation machinery are homologous to bacterial proteins involved in protein export (Settles and Marteinssen, 1998; Dalbey and Robinson, 1999, Keegstra and Cline, 1999). Surprisingly, components of two of the pathways, Oxa1p and Hcf106, were first described for organelle transport. As will be discussed below, each pathway appears to address a specific translocation requirement of its substrates. Even the limited list of substrates shown in Table 1 demonstrates that assembly of each supramolecular complex requires participation of more than one pathway.

#### *E. Genetic and Biochemical Identification of Pathways and Components Are Consistent*

Genetic and biochemical approaches have played complementary roles in identifying components and assigning them to pathways. For example, cpSecA, cpSecY, and cpSecE were identified by biochemical homology-based approaches and were tested in vitro for function (Nakai et al., 1994; Yuan et al., 1994; Mori et al., 1999, Shuenemann et al., 1999). Similarly, *thai* (cpSecA) mutant maize plants accumulated lower levels of the same group of substrate proteins as those shown to require Sec components in vitro (Voelker and Barkan, 1995) as well as the plastid-encoded cytochrome *f*, which was later confirmed as a cpSecA-dependent substrate by biochemical experiments (Nohara et al., 1996; Mould et al., 1997).

Hcf106 was identified by mutant analysis (Voelker and Barkan, 1995, Settles et al., 1997). Tha4 was simultaneously identified by genetic (Walker et al., 1999) and biochemical (Mori et al., 1999) approaches.

Accumulation of substrates of the  $\Delta$ pH-dependent pathway was specifically reduced in *hcf106* and *tha4* mutant plants. Isolation of Hcf106 led to the identification of homologous bacterial systems (called Tat for twin arginine translocation) that employ Hcf106 homologues (Mori and Cline, 2001). Orthologs of Hcf106, Tha4, and a third component called TatC are encoded on the same operon in *E. coli*, and are frequently linked in other bacteria. Genetic experiments showed that the *E. coli* TatC gene is essential for Tat pathway transport (see Mori and Cline, 2001 for review). A chloroplast TatC ortholog (cpTatC) was identified by homology-based cloning and shown to be a thylakoid protein with antibodies raised to a cpTatC peptide (Mori et al., 2001). Antibodies to Hcf106, Tha4, or cpTatC specifically reduced transport of  $\Delta$ pH-dependent pathway substrates (Mori et al., 1999, 2001). Recently, *Arabidopsis* mutants of the cpTatC gene were shown to be defective in thylakoid biogenesis (Motohashi et al., 2001).

cpSRP54 was identified by biochemical experiments as a component of a stromal complex with the Lhcb1 stromal intermediate and also as being essential for Lhcb1 integration into isolated thylakoids (Li et al., 1995). A cpSRP54 null mutant called *ffc* showed significant delay in greening of the first leaves, reduced accumulation of at least six members of the LHC family, and reduced accumulation of the plastid-encoded D1 protein (Amin et al., 1999). cpSRP43 was simultaneously identified by biochemical (Shuenemann et al. 1998) and genetic approaches (Klimyuk et al., 1999). In vitro, cpSRP43 is essential for integration of Lhcb1. The cpSRP43 mutant, called *chaos*, is viable but mildly chlorotic and exhibits reduced accumulation of the same LHC family members as the cpSRP54 mutant, but is not deficient in D1 or other photosystem core components (Amin et al., 1999; Klimyuk et al., 1999). The chloroplast Oxa1p homologue (cpOxa1p) was first identified genetically as a chlorotic mutant (*albino3*) deficient in thylakoids (Sundberg et al., 1997) and then implicated in Lhcb1 integration by antibody inhibition studies (Moore et al., 2000). cpFtsY was cloned by homology to the bacterial FtsY protein and placed on the pathway by biochemical experiments (Kogata et al., 1999; Tu et al., 1999).

One significant difference between in vitro and genetic experiments concerns the severity of the defects when a component is disabled or absent. For example, in vitro transport of Sec-dependent

substrates OE33 and plastocyanin in the absence of cpSecA or in the presence of antibodies to cpSecY is severely reduced (Nakai et al., 1994; Yuan et al., 1994; Mori et al., 1999). In contrast, the accumulation of plastocyanin and OE33, while reduced in *tha1* plants, was still significant, generally about 20–30% of wild type (Voelker et al., 1995). Whereas antibodies severely reduce the transport of  $\Delta$ pH-dependent pathway substrates (Mori et al., 1999, 2001), those same substrates accumulated in low but significant amounts in *hcf106* and *tha4* mutant plants (Voelker and Barkan, 1994; Walker et al., 1999). Voelker and Barkan (1995) employed pulse labeling and immunoprecipitation to obtain a more realistic assessment of transport impairment in these mutants. In *tha1* mutants little if any pulse-labeled Sec-dependent precursor proteins were processed to mature size; rather they accumulated as intermediates. A similar result was obtained with pulse-labeled substrates OE23 and OE17 in the *hcf106* mutant plants. Chloroplasts isolated from *hcf106* plants are completely defective in  $\Delta$ pH-dependent pathway transport (Settles et al., 1997; Summer et al., 2000). Thus, one explanation for the apparent discrepancy is that in vivo a reduced rate of turnover compensates for a low rate of transport, thereby allowing significant accumulation. Among the possible reasons for reduced turnover is that a thylakoid protease fails to localize properly in the mutant.

The individual cpSRP mutants show the mildest apparent impairment of a pathway—affected LHC protein accumulation appeared to be ~30–50% of wild type (Amin et al., 1999). However, the *ffc/chaos* double mutant was recently shown to be more severely deficient in LHC proteins (with the exception of Lhcb4), thereby verifying that cpSRP is the major in vivo pathway for LHCs (Hutin et al., 2002). One possible reason for the apparent leakiness of the single mutants is that other components can substitute for missing components in vivo, e.g. an hsp70 protein or some other chaperone.

Although mutations in certain components have mild to moderate effects on the accumulation of pathway substrates, mutations in some membrane-localized components are so severe that little can be determined regarding specific pathway utilization. Null cpSecY mutants produce very little internal membrane and have reduced amounts of virtually all of the thylakoid proteins (Roy and Barkan, 1998). Similarly, *albino3* mutant plants (Sundberg et al., 1997) and cpTatC mutant plants (Motohashi et al.,

2001) were chlorotic and produced little internal membrane. Such severe phenotypes are likely pleiotropic in nature, reflecting the fact that loss of certain subunits of photosynthetic complexes destabilize the entire complex. Given the severity of such mutations, interpretations based on the accumulation of thylakoid proteins are suspect and biochemical data must be used solely for information on pathway utilization. In the case of *albino 3*, disruption of an algal orthologous gene was much more informative. Disruption of the *Chlamydomonas* Alb3(cpOxa1p) resulted in selective reduction of Lhc proteins to only 5 to 10% of wild type (Bellafigliore et al., 2002). Whether the difference reflects a greater role for cpOxa1p in plants than in algae remains to be determined. Nevertheless, the results with *Chlamydomonas* provide confirmation that this component plays an important role in Lhc protein integration/assembly.

#### IV. Different Mechanisms Address Different Translocation Problems

The multiplicity of different translocation systems appears to reflect distinctive translocation problems presented by each subset of precursor proteins. The two major types of translocation process are transport of large hydrophilic domains into the lumen and insertion of membrane domains into the bilayer. There are two systems that primarily transport luminal proteins, Sec and the  $\Delta$ pH-dependent/Tat. There are two systems that integrate membrane proteins, the spontaneous and the SRP systems. The SRP pathway appears to function posttranslationally for the LHC family of proteins that span the membrane three times and require pigment for insertion. These systems have recently been reviewed (Eichacker and Henry, 2001; Mori and Cline, 2001; Schleiff and Kloesgen, 2001) and the reader should consult these reviews for a more in-depth discussion.

##### A. Sec Pathway

The limited number of studies on the Sec pathway indicate that it operates similarly to the well-characterized bacterial Sec pathway (Keegstra and Cline, 1999). In the bacterial system, proteins bind to SecA at the membrane and are threaded across the bilayer by the reciprocating action of the translocation motor SecA, which inserts and de-inserts as a func-

Table 1. Translocation pathway utilization by thylakoid proteins

Complex	protein	pathway	method	location
PS II	OE33 (PsbO)	Sec	B <sup>1</sup> , G <sup>2</sup>	lumen
	OE23 (PsbP)	$\Delta$ pH	B, G	lumen
	OE17 (PsbQ)	$\Delta$ pH	B, G	lumen
	PsbT	$\Delta$ pH	B	lumen
	PsbW	Spontaneous	B	membrane
	PsbX	Spontaneous	B	membrane
	PsbY	Spontaneous	B	membrane
	PsbS	Spontaneous	B,G	membrane
	D1 (PsbA)	cpSRP54/cpSecY	B, G	membrane
Cyt <i>b/f</i>	cyt <i>f</i>	Sec	B,G	membrane/lumen
	Rieske	$\Delta$ pH/Sec?	B	membrane
PS I	PsaN	$\Delta$ pH	B	lumen
	PsaK	Spontaneous	B	membrane
	PsaF	Sec	B	membrane
Antenna	Lhcb1	cpSRP	B,G	membrane
	Lhcb2	cpSRP	B <sup>3</sup> ,G	membrane
	Lhcb3	cpSR	G	membrane
	Lhcb5	cpSRP	B,G	membrane
	Lhcb6	cpSRP	G	membrane
	Lhca1	cpSRP	B,G	membrane
	Lhca2	cpSRP	B <sup>3</sup> ,G	membrane
	Lhca3	cpSRP	G, B <sup>3</sup>	membrane
	Lhca4	cpSRP	G	membrane
ATP synthase	CF0 II	Spontaneous		membrane
Other	Hcf136	$\Delta$ pH	B	lumen
	P16	$\Delta$ pH	B	lumen
	Pftf	$\Delta$ pH	B	membrane
	ELIP	Spontaneous	B	membrane

<sup>1</sup> B, biochemical evidence, <sup>2</sup> G, genetic evidence. Biochemical data on PsbW, X, Y, S, and Lhcb5 can be found in Woolhead et al. (2001), on PsaK in Mant et al. (2001), on Hcf136 in Hynds et al. (2000), and on P16 in Mant et al. (1999). Genetic data on the LHC proteins can be found in Amin et al. (1999) and Hutin et al. (2002). <sup>3</sup> B\* is biochemical data from transit complex formation with in vitro translation products (K. Cline, unpublished). Other biochemical and genetic evidence is discussed in the text or in Keegstra and Cline (1999). Roles of PS II proteins and LHCs are discussed in more detail in Chapter 7 (Dekker and Amerongen), and PS I proteins and LHCs in Chapter 8 (Fromme et al.).

tion of its ATP binding and hydrolysis cycle (Economou, 1999). The proteins cross the membrane through a translocation channel made up in part by the SecYEG protein complex. Importantly, the proteins cross the membrane in an unfolded conformation in both the bacterial and thylakoid Sec systems. Bacterial and thylakoid Sec systems transport soluble luminal proteins as well as integrate membrane proteins (Table 1). In bacteria, SecA appears to function primarily in translocation of larger hydrophilic regions that flank signal peptides

or hydrophobic signal-anchors on the carboxyl proximal side (Dalbey and Kuhn, 2000). In this way, Sec systems can both transport soluble proteins and integrate membrane proteins. The limited number of known substrates verifies this dual capability for the thylakoid Sec system. Recent proteomic analyses suggest that the lumen contains many tens and possibly even hundreds of proteins of which ~50% are predicted to be targeted by the Sec system (Peltier et al., 2000, 2002; Schubert et al., 2002). Thus it is likely that the primary role of the Sec system will be

to transport luminal proteins. Because the Sec system transports proteins in an unfolded conformation, it is important that Sec substrates be readily unfolded. In this regard, the OE33 protein, a Sec substrate, is reported to be a naturally unfolded protein (Lydakis-Simantiris et al., 1999). In addition, Sec pathway substrates that function with co-factors must assemble with their prosthetic groups in the lumen rather than the stroma. Examples of such Sec substrates are plastocyanin and cytochrome *f* (Merchant and Dreyfuss, 1998).

### *B. ΔpH-Dependent/Tat Pathway*

Much less is known regarding the operation of the ΔpH-dependent and homologous bacterial Tat systems, but it is clear that these systems complement Sec in capabilities. Their distinctive features are a consensus RR (Arg-Arg) motif in their signal peptides, the sole use of the pH gradient for translocation energy (in thylakoids) and their ability to transport folded proteins (see Mori and Cline, 2001 for review). The ΔpH-dependent system has been directly shown to transport folded polypeptides with diameters of ~2–3 nm (Clark and Theg, 1997; Hynds et al., 1998). Documented substrates of the thylakoid system range in size from 3,600 D to 36,000 D, and the presence of a twin arginine in its signal peptide suggests that polyphenoloxidase (~60 kD) is also translocated by the ΔpH-dependent system. The conformation of authentic substrates during transport has not been established, although indirect evidence suggests that iOE23 and iOE17 are tightly folded when presented to the transport machinery (Creighton, 1995; Musser and Theg, 2000). If these substrates are all folded prior to transport, a putative channel would have to expand to ~5 nm. Most of the substrates of the bacterial Tat system are cofactor-binding proteins that are assembled with their prosthetic groups in the cytoplasm. These proteins have a range of sizes but are estimated to present the translocation system with diameters up to 7 nm, which is larger than the thickness of the bilayer (Berks et al., 2000). At present, the Rieske protein is the only co-factor binding protein shown to use the ΔpH-dependent system (Molik et al., 2001). However, an ascorbate peroxidase as well as polyphenyloxidase are predicted to be ΔpH-dependent system substrates based on the presence of twin arginines in their LTDs.

The manner by which these systems translocate

folded proteins and at the same time maintain the membrane in an ion-tight state (Teter and Theg, 1998) is an intriguing puzzle. Recent work in our lab indicates that in thylakoids, assembly of the translocon is a regulated process that occurs in several steps (Cline and Mori, 2001). Precursors bind to an ~700 kD receptor complex of cpTatC and Hcf106 in a twin arginine-dependent reaction. Upon imposition of the pH gradient, Tha4 is recruited and appears to join with the precursor-receptor complex (Mori and Cline, 2002). Following translocation, the components dissociate. The structure of the active translocon is not known with any certainty. However, imaging of an overexpressed TatA/B complex (Sargent et al., 2001) and unpublished data (K. Cline) suggests a channel. One attractive possibility is that multiples of Tha4 and/or Hcf106 assemble around a core cpTatC to form a dynamic flexible channel that expands or contracts to fit the transported substrate. Quantitative immunoblotting shows that cpTatC is present in thylakoids at about 18,000 copies per chloroplast, similar to the estimated number of ΔpH-dependent pathway translocation sites (Asai et al., 1999), whereas Hcf106 and Tha4 are present at five- to ten-fold the number of translocation sites (Mori et al., 2001). The stoichiometry is consistent with a dynamic channel model. In addition, this model would allow for integration of membrane proteins because transmembrane domains could partition into the bilayer between monomeric channel components. The ΔpH-dependent pathway integrates the membrane protein Pftf, a bitopic homologue of the FtsH protease (Summer et al., 2000).

The tentative conclusion here is that the ΔpH-dependent pathway serves to translocate proteins that either must remain folded during translocation or that when folded in the stroma, are sufficiently stable that unfolding by the Sec pathway is inefficient. Consistent with this view is the observation that substrates of the ΔpH-dependent pathway are inefficiently transported *in vitro* by the Sec pathway, even when equipped with an efficient Sec signal peptide (Clausmeyer et al., 1993; Henry et al., 1997).

### *C. cpSRP Pathway*

Current data indicates that the posttranslational cpSRP system is dedicated to the integration of the multispanning membrane proteins that comprise the LHC antenna family. *In vitro* studies have described in some detail the operation of certain parts of the

cpSRP system for the integration of Lhcb1. The precursor protein is imported into the stroma and processed to mature size by the stromal processing protease. Concurrently, Lhcb1 binds to two components of the cpSRP, thereby forming a transit complex (Li et al., 1995; Shuenemann et al., 1998). Transit complex formation occurs with intact chloroplasts and can also be reconstituted simply by combining stromal extract or purified cpSRP with LHCP translation products (Payan and Cline, 1991; Groves et al., 2001). This posttranslational action of cpSRP is a novel capability not possessed by other SRPs, which are strictly co-translational (Cline and Henry, 1996). Similar to other SRP54s, the cpSRP54 protein binds to hydrophobic peptides, in this case the third transmembrane domain of Lhcb1 (High et al., 1997). cpSRP43 binds a conserved 18 amino acid peptide of Lhcb1 (L18) that is located between its second and third transmembrane domains (Delille et al., 1999; Tu et al., 2000). If the L18 sequence is absent, cpSRP54 binds only weakly and transiently to hydrophobic segments, unless they are presented as nascent chains. Thus, the posttranslational action of cpSRP can be ascribed to the participation of cpSRP43 and the L18 peptide. This is a novel adaptation to the eukaryotic situation, wherein a nuclear-encoded thylakoid protein of necessity must interact with translocation machinery post-translationally.

The events subsequent to formation of the transit complex are less clear. GTP hydrolysis and a chloroplast homologue of FtsY (cpFtsY) are required for integration (Kogata et al., 1999; Tu et al., 1999). FtsY is a bacterial GTPase that interacts with the bacterial SRP and regulates its GTPase activity. FtsY is homologous to the  $SR\alpha$  subunit of the receptor for ER SRP (Dalbey and Kuhn, 2000). In the ER system, binding of nascent precursor chains to SRP, interaction of the SRP-nascent chain complex with  $SR\alpha$ , and delivery of the ribosome-nascent chain complex to the Sec61 translocon is considered to be the targeting phase of protein transport across the ER. Similarly, FtsY is thought to participate in targeting bacterial precursors to the translocon, currently thought to consist of SecYEG, and for certain proteins also SecA and YidC, an Oxa1p homologue (Dalbey and Kuhn, 2000). Both the bacterial and the chloroplast FtsY proteins have been reported to partition between soluble and membrane-bound states (Kogata et al., 1999; Tu et al., 1999). In *E. coli*, membrane

association is required for FtsY function, an indication that its site of action is on the membrane (Zelazny et al., 1997). By analogy with the ER and bacterial systems, cpSRP and FtsY may serve to target LHC proteins to a specific location on the membrane, possibly a specific translocon.

A chloroplast Oxa1p homologue (Alb3 or cpOxa1p) is the only known component of the cpSRP translocon (Moore et al., 2000). Oxa1p is a mitochondrial inner membrane protein that participates in the insertion of integral inner membrane proteins from the matrix side (Hell et al., 1997). Oxa1p is capable of facilitating both N-tail insertion and C-tail insertion. As such, it is ideal for the integration of multispinning membrane proteins. Experiments in bacteria indicate that YidC (an Oxa1 homologue) functions in concert with the SecY/E translocon (Dalbey and Kuhn, 2000). Antibody inhibition experiments with thylakoids suggest that cpSecY does not play a role in the integration of LHC proteins (Mori et al., 1999). This mode of operation of Oxa1p occurs in yeast mitochondria, which lack a Sec homologous system. Nevertheless, this must be further examined. For example, a second SecY protein is predicted from the *Arabidopsis* genomic sequence (accession #AC007071), is represented by an expressed sequence tag (EST), and is predicted to be chloroplast localized. The second SecY is quite diverged from the protein called cpSecY and would not be recognized by the antibodies produced to cpSecY. One thing is clear from several lines of evidence: cpSecA does not participate in LHC integration (Keegstra and Cline, 1999).

Exactly how many of the LHC family members employ cpSRP and FtsY is not known with certainty. Assignments are more reliable when both biochemical data and genetic data are available. As mentioned, conclusive biochemical data is only available for Lhcb1 and partial biochemical data is available for another five family members. Genetic data is now available for most family members (Hutin et al., 2002) (Table 1). In the case of Lhcb4 (CP29), it appears to disagree with the biochemical data, which shows a cpOxa1p requirement for Lhcb4 (Woolhead et al., 2001). The tentative conclusion is that most closely related LHC members require the cpSRP system for integration into the membrane, whereas the more distant family members, ELIP and PsbS, do not. Rather, these latter two proteins appear to be



```

a3      1 ---GNPAYPGGPFFFNPLGFGKD--
a5      1 ---LEPGYPGGPLLNPLGLAKD--
a4      1 ---GEVGYPGG-IFNPLNFAPT--
b6      1 ---GDQGYPGG-RFFPLGLAGK--
b3      1 ---GNDLYPGGQYFDPLGLADD--
L18     1 ---VDPLYPGG-SFDPLGLADD--
b2      1 ---LDPLYPGG-AFDPLNLAED--
b1      1 ---EDLLYPGG-SFDPLGLATD--
b5      1 ---EDKLHPGG-PFDPLGLAKD--
b4      1 LDPEKRIYPGG-YFDPLGLAAD--
a1      1 -DPEKKKYPGG-AFDPLGYSKD--
a2      1 -----VGYPGGLWFDPLGWGSGSP
consensus 1      e lypGG fdPLgla d

```

Fig. 3. Alignment of the L18 region of the LHC family of apoproteins from *Arabidopsis thaliana*. Best matches were determined by clustal alignment between L18 and the region between the predicted second and third transmembrane domains of the respective LHC proteins. The pictured alignment was done by ClustalW and Boxshade. The accession numbers for Lhca1-5 are S25435, AAD28767, AAA18206, AAA32760, and AF134121, respectively. The accession numbers for Lhcb 1-6 are CAA27540, AAD28771, AAD28773, AAD28775, AF134129, and AF134130, respectively.

integrated by the spontaneous mechanism (Kruse and Kloppstech, 1992; Kim et al., 1999; Woolhead et al., 2001). This conclusion is consistent with the presence or absence of L18-homologous sequences. Nuclear-encoded proteins lacking an L18 sequence are not likely to be substrates for cpSRP. All of the Lhca and Lhcb members in *Arabidopsis* contain sequences homologous to the pea Lhcb1 L18 with identities ranging from 50–83% (Fig. 3). PsbS and ELIPs lack L18 sequences, consistent with biochemical and genetic studies.

At present, little is known regarding the use of cpSRP components for insertion of plastid-encoded proteins. A study in which a homologous chloroplast translation system was used to produce nascent chains of the D1 polypeptide detected an interaction with cpSRP54 (Nilsson et al., 1999). As the D1 protein is cotranslationally inserted into the thylakoids, D1 should not require cpSRP43. Of interest is that a second population of cpSRP54 is associated with plastid ribosomes and with thylakoidal-associated ribosome nascent chain complexes, and this cpSRP54 is not associated with cpSRP43 (Schuenemann et al., 1998). A recent analysis of D1 integration found cpSecY in close contact with D1 translation intermediates (Zhang et al., 2001). The potential implication of these findings, that cpSRP54 lacking cpSRP43, docks with the Sec translocon, is intriguing but requires further study. Nevertheless, it suggests that as with the situation in bacteria, translocation systems have the capacity to operate in different combinatorial modes, i.e. cpSRP54 can operate with cpOxa1p under certain circumstances and with cpSecY under others. Also, as cpSecA has not been

detected in association with D1 nascent chains, it suggests that cpSecY can function as a channel without employing cpSecA as a motor.

#### D. The Spontaneous Pathway

The spontaneous pathway is usually employed by membrane proteins that possess pairs of hydrophobic helices (where one can be a signal peptide) with short luminal domains (see Schleiff and Kloege, 2001 for review). Single transmembrane domain proteins with short transferred hydrophilic domains can frequently also insert into the bilayer without assistance of translocation machinery. Insertion into the membrane appears to be driven by hydrophobic interactions that are sufficient to compensate for the energy debt required to move a hydrophilic segment across the bilayer. Several of the thylakoid proteins that insert into thylakoids without any apparent assistance fit that model. However, the need for translocation machinery (cpSRP and cpOxa1p) for LHC insertion and the apparent spontaneous insertion of PsbS and ELIP is not readily understandable. One early idea regarding the SRP requirement was that cpSRP binding was essential to maintain solubility of hydrophobic membrane proteins in the stroma (Payan and Cline, 1991). However, ELIP and PsbS are as hydrophobic or more hydrophobic than the LHCs, based on GRAVY analysis (Kyte and Doolittle, 1982). Thus cpSRP utilization must relate to some other property of the substrates. One potential role of cpSRP is to target LHC apoproteins to the sites of chlorophyll ligation, considering that chlorophyll *b* is essential for LHC insertion (see below).

## V. The In Vivo Site of Thylakoid Protein Transport and Insertion

In vitro data for transport and insertion of nuclear-encoded thylakoid proteins definitively show that the thylakoid membrane is the site of translocation in isolated chloroplasts. Evidence for this conclusion comes from efficient reconstituted assays with purified thylakoids but not envelope membranes (Cline, 1986), the use of ATP synthase inhibitors tentoxin and venturicidin to alter energy sources for transport (Cline, 1992, Yuan and Cline, 1994), subfractionation data showing that cpSecY, cpTatC, and cpOxa1p are exclusively located in the thylakoid membrane (K.Cline, unpublished), and the demonstration that translocated proteins assemble with pre-existing photosynthetic complexes (Cline 1988; Kuttkat et al., 1995; Hashimoto et al., 1997). On the other hand, the site of translocation in vivo has not been thoroughly examined.

Several observations suggest that in the early stages of plastid development, the envelope may be the site of thylakoid protein integration and transport. One comes from studies of *Chlamydomonas* cells that are induced to produce thylakoid proteins rapidly by preinduction of mRNAs at 38 °C, followed by light induction of thylakoid formation (Hoover et al., 1991; Hoover and Eggink, 1999). Under these conditions, the colorless plastids are primed for rapid production of photosynthetic membranes. The earliest photosynthetic membranes produced after the shift to light appeared to emanate from the chloroplast envelope. Correlation of spectrophotometric properties and morphologic characteristics argue that LHC and functional photosystems are produced in the envelope prior to the appearance of any internal membranes. Although this experimental setup is arguably non-physiological, it does show that thylakoid protein assembly can occur in the envelope. In this scenario, thylakoid proteins would be inserted into the envelope and proceed to the plastid interior via inner envelope invaginations and/or membrane vesicles.

The notion that the envelope is the initial site of thylakoid protein transport and integration has been proposed several times and deserves serious consideration for a variety of reasons. The first is the fact that proplastids are virtually devoid of internal membranes and that membranes are not known to form de novo. Second, the envelope is the site of synthesis of most of the polar lipids of the thylakoids,

yet soluble lipid carrier proteins have not been detected (Joyard et al., 1998). Membrane vesicles have been consistently seen in the stroma of developing plastids as have infoldings (or invaginations) of the inner envelope membrane (Carde et al., 1982). Such vesicles can be induced in chloroplasts in vivo by low temperature (Morre et al., 1991), a condition known to arrest membrane trafficking through the endomembrane system. More recent studies have suggested that a vesicle transport system employs traditional components of endomembrane vesicle trafficking (Kim et al., 2001) as well as a novel protein call VIPP1 that is required for thylakoid accumulation and has a dual localization in envelope and thylakoids (Kroll et al., 2001). Thus it appears that a system capable of transferring membrane from envelope to thylakoids is in place.

At present, the composition of the vesicles is unknown. Although they might consist entirely of lipid bilayer, it is more likely that they carry newly inserted thylakoid proteins. A model that would allow for conservation of translocation mechanism and would be consistent with the in vivo results with *Chlamydomonas*, and the in vitro results with partially developed chloroplasts would be for translocon components, e.g. cpTatC, cpSecY, cpOxa1p, to be initially inserted in the envelope regardless of developmental stage. During early chloroplast development, the insertion site of new thylakoid proteins would be solely in the inner envelope. As translocons are relocated via vesicles to thylakoids, the major site of insertion would shift to the thylakoids. Clearly an important test of this hypothesis will be to determine the site of integration of translocon proteins and to determine their membrane location during plastid development. As antibodies are now available for all known translocon components, this should be feasible.

## VI. Chlorophyll Synthesis And The Insertion Of Antenna Proteins

### A. Regulation of LHC Gene Expression by the Chlorophyll Synthetic Pathway

Chlorophyll (Chl) synthesis and availability play several significant roles in the biogenesis of antenna proteins. The Chl biosynthetic pathway regulates the expression of LHC genes. Although a number of factors, most prominently light, are necessary for

LHC gene expression, chloroplast development has a controlling influence on expression (Surpin and Chory, 1997). Specifically, if biogenesis of thylakoids is arrested or disrupted LHC genes are repressed, as if the plants were dark grown. A number of different approaches have implicated chlorophyll precursors as signaling factors for LHC expression. For example, treatment with inhibitors that induce accumulation of Mg-protoporphyrin IX or Mg-protoporphyrin IX dimethyl ester inhibit LHC expression in the light, implicating the Mg ligation step in nuclear signaling (Johanningmeier and Howell, 1984). Recent cloning of the *gun5* mutant reinforces that interpretation. Gun (genomes uncoupled) mutants express LHC genes in photobleached plants. Gun5 encodes the H subunit of Mg chelatase (Mochizuki et al., 2001). However, signaling appears to be more complex than accumulation of the Mg ligated intermediates because mutants of the I subunit of Mg chelatase, which also accumulate intermediates, behave as wild-type. While future studies will unravel the intricacies of plastid signaling factors, it is now clear that flow through the chlorophyll biosynthetic pathway serves as a regulatory point for controlling expression of LHC genes.

### ***B. Chlorophyll Requirement for Antenna Stability and Integration***

Such tight regulation of LHC synthesis reflects the fact that Chl availability is required for accumulation of Chl binding proteins in chloroplast membranes (see Paulsen, 1997 for review). For example, in a null *Arabidopsis* mutant of the chlorophyll(ide) *a* oxygenase gene that completely lacks Chl *b*, all of the Lhcb proteins fail to accumulate (Espineda et al., 1999). This and earlier studies (Apel and Klopstech, 1980; Bennett, 1981) led to the conclusion that in the absence of Chl, LHC proteins are unstable to proteases and degraded. Several labs have reported the characterization of thylakoid proteases capable of degrading Lhcb proteins (Hooper and Hughes, 1992; Lindahl et al., 1995; Tziveleka and Argyroudi-Akoyunoglou 1998). Even in vitro, imported LHC that is prevented from inserting into the bilayer is subject to significant degradation (K. Cline, unpublished). Mutant LHCs are degraded even more rapidly (Cline et al., 1989; Kohorn and Tobin, 1989; Reid et al., 1990).

Recent studies indicate that Chl is required for insertion of antenna proteins. Prior work had

established that etioplast membranes are incapable of integrating LHC proteins and that some greening is necessary before they became competent (Chitnis et al., 1987). Kuttkat et al. (1997) directly asked whether chlorophyll is required for Lhcb1 insertion with etioplast inner membranes. They showed that when etioplast membranes were allowed to synthesize the Chl analogs Zn pheophytin *a* and *b*, they became competent for integration of Lhcb. In their experiments, they found that Zn pheophytin *b* was sufficient for insertion, whereas Zn pheophytin *a* was not. Adamska et al. (2001) recently showed that Chl *a*, but not chlorophyll *b*, is required for insertion of ELIP proteins. This suggests that protein insertion must occur at the exact site of the last step of Chl synthesis, which would be addition of the acyl tail by chlorophyll synthetase. Alternatively, it is possible that after synthesis, chlorophyll is bound by a putative chlorophyll carrier protein or chaperone until ligated to antenna proteins. Several candidates for such a carrier have been suggested (Paulsen 1997).

### ***C. Topology of Chlorophyll Synthesis***

Whether or not Chl can move following synthesis, it is likely that the protein integration site will be on the same membrane as the enzymes involved in the latter steps of Chl synthesis. Thus the location of Chl biosynthetic enzymes likely determines the site of insertion during development. Chlorophyll synthesis can be broken down into steps carried out in the plastid stroma and steps carried out in association with a plastid membrane (Fig. 4). The steps of chlorophyll (and heme) synthesis from ALA up to protoporphyrinogen IX occur in the plastid stroma (von Wettstein et al., 1995; Rudiger, 1997; Beale, 1999). The present discussion will focus on the enzymes of the later steps of chlorophyll synthesis, which are membrane associated. There are several excellent reviews on the biosynthesis of chlorophylls (Rudiger, 1997; Beale, 1999) that should be consulted for detailed descriptions of the process; an overview is given in Chapter 2 (Scheer).

Although the location of the enzymes of the membrane-associated steps should be diagnostic for the location of pigment ligation, their localization has not been a trivial matter. For example, two separate enzymes catalyze oxidation of protoporphyrinogen IX, one in the mitochondrion and one in the plastid. The plastid protoporphyrinogen oxidase has been localized to both the envelope and the thylakoids

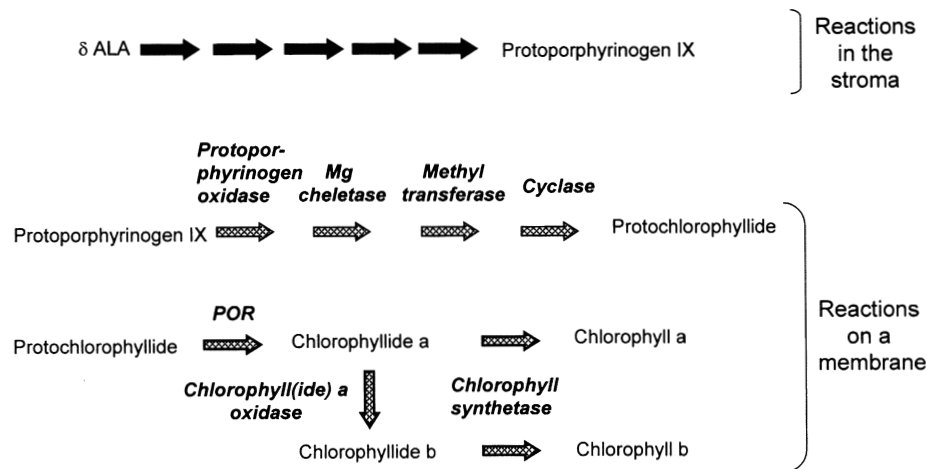


Fig. 4. Topography of chlorophyll synthesis in higher plant chloroplasts. Steps from  $\Delta$ ALA to protoporphyrinogen IX are catalyzed by enzymes located in the plastid stroma and are designated by black arrows. Steps from protoporphyrinogen IX to chlorophylls *a* and *b* are carried out in association with a membrane, either the envelope or internal membranes of etioplasts and chloroplasts as discussed in the text. Enzymes catalyzing these steps are in italics and stippled arrows designate the steps.

(Che et al., 2000; Watanabe et al., 2001). Mg chelatase is reported to partition between envelope and stroma of chloroplasts depending on the Mg concentration (Nakayama et al., 1998). Protochlorophyllide oxidoreductase (POR) has been the focus of many of the studies on the location of chlorophyll biosynthetic enzymes (for reviews see Ledbedev and Timko, 1998; Sundqvist and Dahlin, 1997). It has been shown to be located on the envelope, on developing thylakoids, and on the inner membranes of etioplasts. Localization studies can be complicated in plants where two isoforms of POR are expressed. In plants such as barley and *Arabidopsis*, the A form (PORA) is expressed in darkness and accumulates in large quantities in the inner etioplast membranes, where it plays the predominant role in shaping the prolamellar body. Upon transfer to light, expression and plastid import of PORA is severely downregulated and the existing protein is degraded. PORB is constitutively expressed and after transfer to light becomes the major form of POR. In a recent study (Barthelemy et al., 2000) analyzed the location of POR proteins (A and B) and protochlorophyllide during progressive stages of greening barley. They found that POR and protochlorophyllide were predominantly localized in the inner (thylakoids) during early stages of greening, but shifted to the envelope in mature chloroplasts. When expressed on a stoichiometric basis, the total thylakoid POR and protochlorophyllide were in great excess over those located in the envelope during developmental stages and roughly equivalent

in mature chloroplasts. As POR lacks putative transmembrane anchors, its association with the membrane depends on peripheral association with the membranes. This might explain its dual location within the plastid during development. However, it doesn't explain the surprising finding that in mature spinach chloroplasts, POR was located on the outer leaflet of the outer envelope membrane (Joyard et al., 1990).

The location of protoporphyrinogen oxidase, Mg chelatase, and POR at various stages of development will lead to a greater understanding of the collaboration between envelope and internal membranes in pigment synthesis. However, the locations of the last two enzymes in the chlorophyll synthesis pathway ultimately mark the site of protein insertion. Chlorophyll synthetase activity has been found only in interior membranes of etioplasts and chloroplasts (Rudiger, 1997). This is consistent with in vitro analysis showing thylakoids to be the site of LHC insertion (see above). In etioplasts, the enzymatic activity prefers GGPP as a substrate. A putative chlorophyll synthetase was identified several years ago (Gaubier et al., 1995). The bacterially expressed *Arabidopsis* enzyme prefers GGPP rather than phytidyl-PP, similar to the etioplast enzyme activity rather than the thylakoid enzyme activity (Rudiger, 1997). Whether or not two enzymes are responsible for chlorophyll synthetase activity is unknown; however, the putative Chl synthetase is present as a single copy in the *Arabidopsis* genome.

The localization of chlorophyll(ide) *a* oxidase is also of importance because chlorophyll *b* is required for insertion and stability of LHC proteins. The chlorophyll(ide) *a* oxidase gene was recently cloned (Espineda et al., 1998; Tanaka et al., 1998). Originally thought to use chlorophyll *a* as a substrate, recent in vitro studies indicate that chlorophyllide *a* is the preferred substrate (Oster et al., 2000). The location of this enzyme has not yet been reported. An important question is: 'where are chlorophyll synthetase and chlorophyll(ide) *a* oxidase located during early stages of the development of proplastids to chloroplasts?' Because of the difficulty of isolating proplastids as well as partly developed chloroplasts, it will be necessary to employ immunocytochemical techniques to determine the location of these enzymes as a function of developmental stage. The availability of cloned genes for these proteins should make this approach possible.

#### *D. Does Chlorophyll Drive the Insertion of Antenna Proteins?*

It is not presently known whether chlorophyll and/or xanthophyll ligation provides some sort of driving force for insertion of antenna proteins into the bilayer. However, the fact that in vitro insertion requires chlorophyll *b* for Lhcb1 and chlorophyll *a* for ELIP strongly implicates pigments in such a role, or at least in stabilizing the inserted state (see Paulsen, 1997 for review). It has been shown in reconstitution experiments that pigments induce conformational changes in denatured LHC proteins that lead to formation of pigment-protein complexes. Thus, one possibility is that pigment availability at the site of insertion coordinately binds to transmembrane domains as they insert into the bilayer. In the case of cpSRP-dependent family members, the targeting stage of the process may deliver the LHC protein to the membrane at the exact location of chlorophyll availability. Whether such a process occurs awaits more detailed dissection of the events that occur during the integration step.

Hooper and co-workers suggest quite a different model for chlorophyll participation in the insertion step (Hooper and Eggink, 1999, 2001). They suggest that import of LHCs into the plastid is tightly coupled with chlorophyll availability in the envelope, such that chlorophyll binding to transmembrane domains promotes diversion of the protein from the general import Toc translocon and folding into the envelope

bilayer. When chlorophyll is absent or insufficient, import stalls just subsequent to transit peptide removal by the stromal processing protease, and the stalled proteins are retrieved by cytosolic processes. The primary experimental observation leading to this model is that in *Chlamydomonas* cells, Lhcb of mature size is found in cytoplasmic vacuoles, and that such vacuolar sequestration is enhanced under conditions where LHC precursors are synthesized in vast excess over chlorophyll. Although this proposed integration mechanism is intriguing, it is difficult to reconcile with other observations of LHC assembly, as it would occur without prior entry into the stroma. As mentioned above, when Lhcb1 insertion in vitro is inhibited by ionophores (Cline et al., 1988) or by depletion of stromal ATP (Cline, unpublished), the protein is efficiently imported into the chloroplast, but accumulates in the stroma complexed with the cpSRP (Payan and Cline, 1991). Furthermore, the recent results of Nussaume and coworkers (Hutin et al., 2002) showing that the cpSRP is essential for LHC accumulation argue strongly that imported LHC proteins are assembled via a stromal intermediate that interacts with cpSRP. The finding of mature sized LHC in *Chlamydomonas* vacuoles is puzzling. However, because other proteins, including the large subunit of Rubisco and the  $\alpha$  subunit of the coupling factor, both of which are synthesized on plastid ribosomes, are also found in the *Chlamydomonas* cytoplasmic vacuoles (Park et al., 1999), it is more likely that a general degradation pathway is responsible for scavenging stromal proteins and that imported but unassembled stromal LHC is transferred to vacuoles by that process.

### **VII. Future Prospects**

Although much progress has been made in understanding the pathways and mechanisms of thylakoid protein assembly, several areas are particularly ready for further investigation. Mechanistic aspects of two pathways are still unclear in any system. It is still totally unclear how the  $\Delta$ pH/Tat-dependent systems transport large folded domains without causing the membrane to become nonspecifically permeable. Nor is it obvious how the pH gradient facilitates the transport. With regards to the SRP system, what interactions specify targeting and docking to the membrane and to what does the transit complex dock? In particular, does SRP target to some particular

site on the membrane other than simply the cpOxal translocon? How does the cpOxal<sub>p</sub> translocon facilitate LHC insertion? Here, an important question will be the coordination between protein integration and chlorophyll synthesis. Thus, the specific location of the components of these two merging pathways must be determined.

A second major area of future investigation will be to learn the mechanisms of assembly of plastid-synthesized proteins. Preliminary studies suggest that there may be important differences between assembly mechanisms of imported vs. plastid-synthesized proteins.

Finally, an extremely important area for further investigation will be to unravel events and mechanisms during other stages of plastid development. What are the mechanisms of vesicle formation, movement, and fusion, and what is the vesicle cargo. It will also be important to determine the site of thylakoid protein translocation in developing proplastids, and the site(s) of pigment synthesis. Answering these questions now appears to be feasible due to developments in genetics and biochemistry over the past several years, and the increased availability of genomics and proteomic technology.

## References

- Adamska I, Kruse E and Kloppstech K (2001) Stable insertion of the early light-induced proteins into etioplast membranes requires chlorophyll *a*. *J Biol Chem* 276: 8582–8587
- Amin P, Sy DA, Pilgrim ML, Parry DH, Nussaume L and Hoffman NE (1999) *Arabidopsis* mutants lacking the 43- and 54-kilodalton subunits of the chloroplast signal recognition particle have distinct phenotypes. *Plant Physiol* 121: 61–70
- Apel K and Kloppstech K (1980) The effect of light on the biosynthesis of the light-harvesting chlorophyll *a-b* protein—evidence for the requirement of chlorophyll *a* for the stabilization of the apoprotein. *Planta* 150: 426–430
- Asai T, Shinoda Y, Nohara T, Yoshihisa T and Endo T (1999) Sec-dependent pathway and Delta pH-dependent pathway do not share a common translocation pore in thylakoidal protein transport. *J Biol Chem* 274: 20075–20078
- Barthélemy X, Bouvier G, Radunz A, Docquier S, Schmid G and Franck F (2000) Localization of NADPH-protochlorophyllide reductase in plastids of barley at different greening stages. *Photosynth Res* 64: 63–76
- Bauer J, Chen K, Hiltbunner A, Wehrli E, Eugster M, Schnell D and Kessler F (2000) The major protein import receptor of plastids is essential for chloroplast biogenesis. *Nature* 403: 203–207
- Beale SI (1999) Enzymes of chlorophyll biosynthesis *Photosynth Res* 60: 43–73
- Bellafiore S, Ferris P, Naver H, Gohre V and Rochaix J-D (2002) Loss of Albino3 Leads to the Specific Depletion of the Light-Harvesting System. *Plant Cell* 14: 2303–2314
- Bennett J (1981) Biosynthesis of the light-harvesting chlorophyll *a-b* protein-polypeptide turnover in darkness. *Eur J Biochem* 118: 61–70
- Berks BC, Sargent F and Palmer T (2000) The Tat protein export pathway. *Mol. Microbiol.* 35: 260–274
- Carde JP, Joyard J and Douce R (1982) Electron-microscopic studies of envelope membranes from spinach plastids. *Biol Cell* 44: 315
- Che FS, Watanabe N, Iwano M, Inokuchi H, Takayama S, Yoshida S and Isogai A (2000) Molecular characterization and subcellular localization of protoporphyrinogen oxidase in spinach chloroplasts. *Plant Physiol.* 124: 59–70
- Chen X and Schnell DJ (1999) Protein import into chloroplasts. *Trends Cell Biol.* 9: 222–227
- Chitnis PR, Nechushtai R and Thornber JP (1987) Insertion of the precursor of the light-harvesting chlorophyll *a/b*-protein into the thylakoids requires the presence of a developmentally regulated stromal factor. *Plant Mol Biol* 10: 3–11
- Choquet Y and Vallon O (2000) Synthesis, assembly and degradation of thylakoid membrane proteins. *Biochimie.* 82: 615–34
- Clark SA and Theg SM (1997) A folded protein can be transported across the chloroplast envelope and thylakoid membranes. *Mol. Biol. Cell* 8: 923–934
- Clausmeyer S, Klosgen RB and Herrmann RG (1993) Protein import into chloroplasts. The hydrophilic luminal proteins exhibit unexpected import and sorting specificities in spite of structurally conserved transit peptides. *J Biol Chem* 268: 13869–76
- Cline K (1986) Import of proteins into chloroplasts—membrane integration of a thylakoid precursor protein reconstituted in chloroplast lysates. *J Biol Chem* 261: 4804–4810
- Cline K (1988) Light-harvesting chlorophyll-*a/b* protein—membrane insertion, proteolytic processing, assembly into LHC-II, and localization to appressed membranes occurs in chloroplast lysates. *Plant Physiol* 86: 1120–1126
- Cline K and Henry R (1996) Import and routing of nucleus-encoded chloroplast proteins. *Annu. Rev. Cell Dev. Biol.* 12: 1–26
- Cline K and Mori H (2001) Thylakoid ΔpH-dependent precursor proteins bind to a cpTatC-Hcf106 complex before Tha4-dependent transport. *J Cell Biol* 154: 719–729
- Cline K, Werner-Washburne M, Lubben TH and Keegstra K (1985) Precursors to two nuclear-encoded chloroplast proteins bind to the outer envelope membrane before being imported into chloroplasts. *J Biol Chem* 260: 3691–3696
- Cline K, Fulsom DR and Viitanen PV (1989) An imported thylakoid protein accumulates in the stroma when insertion into thylakoids is inhibited. *J Biol Chem* 264: 14225–14232
- Cline K, Henry R and Yuan JG (1992a) Translocation of nucleus-encoded proteins into and across the thylakoid membranes. *Photosynth Res* 34: 93–93
- Cline K, Ettinger WF and Theg SM (1992b) Protein-specific energy-requirements for protein-transport across or into thylakoid membranes—two luminal proteins are transported in the absence of ATP. *J Biol Chem* 267: 2688–2696
- Cline K, Henry R, Li CJ and Yuan J (1993) Multiple pathways for protein transport into or across the thylakoid membrane. *EMBO J* 12: 4105–4114



- Creighton AM, Hulford A, Mant A, Robinson D and Robinson C (1995) A monomeric, tightly folded stromal intermediate on the delta pH-dependent thylakoidal protein transport pathway. *J Biol Chem* 270: 1663–1669
- Dahlin C and Cline K (1991) Developmental regulation of the plastid protein import apparatus. *Plant Cell* 3: 1131–1140
- Dalbey RE and Kuhn A (2000) Evolutionarily related insertion pathways of bacterial, mitochondrial and thylakoid membrane proteins. *Annu Rev Cell Dev Biol* 16: 51–87
- Dalbey RE and Robinson C (1999) Protein translocation into and across the bacterial plasma membrane and the plant thylakoid membrane. *Trends Biochem Sci* 24: 17–22
- DeLille J, Peterson EC, Johnson T, Moore M, Kight A and Henry R (2000) A novel precursor recognition element facilitates posttranslational binding to the signal recognition particle in chloroplasts. *Proc Natl Acad Sci U S A* 97: 1926–1931
- Economou A (1999) Following the leader: bacterial protein export through the Sec pathway. *Trends Microbiol* 7: 315–320
- Eichacker LA and Henry R (2001) Function of a chloroplast SRP on thylakoid protein transport. *Biochim Biophys Acta* 1541: 120–134
- Espineda CE, Linford AS, Devine D and Brusslan JA (1999) The AtCAO gene, encoding chlorophyll *a* oxygenase, is required for chlorophyll *b* synthesis in *Arabidopsis thaliana*. *Proc Natl Acad Sci USA* 96: 10507–10511
- Gaubier P, Wu HJ, Laudie M, Delseny M and Grellet F (1995) A chlorophyll synthetase gene from *Arabidopsis thaliana*. *Mol Gen Genet* 249: 58–64
- Groves MR, Mant A, Kuhn A, Koch J, Dubel S, Robinson C and Sinning I (2001) Functional characterization of recombinant chloroplast signal recognition particle. *J Biol Chem* 276: 27778–27786
- Hartl FU, Schmidt B, Wachter E, Weiss H and Neupert W (1986) Transport into mitochondria and intramitochondrial sorting of the Fe/S protein of ubiquinol-cytochrome *c* reductase. *Cell* 47: 939–951
- Hashimoto A, Ettinger WF, Yamamoto Y and Theg SM (1970) Assembly of newly imported oxygen-evolving complex subunits in isolated chloroplasts: Sites of assembly and mechanism of binding. *Plant Cell* 9: 441–452
- Hell K, Herrmann J, Pratje E, Neupert W and Stuart RA (1997) Oxa1p mediates the export of the N- and C-termini of pCoxII from the mitochondrial matrix to the intermembrane space. *FEBS Lett* 418: 367–370
- Henry R, Carrigan M, McCaffrey M, Ma X and Cline K (1997) Targeting determinants and proposed evolutionary basis for the Sec and the Delta pH protein transport systems in chloroplast thylakoid membranes. *J Cell Biol* 136: 823–832
- Herrmann RG (1999) Biogenesis and evolution of photosynthetic (thylakoid) membranes. *Biosci Rep* 5: 355–365
- High S, Henry R, Mould RM, Valent Q, Meacock S, Cline K, Gray JC and Lührink J (1997) Chloroplast SRP54 interacts with a specific subset of thylakoid precursor proteins. *J Biol Chem* 272: 11622–11628
- Hoover JK and Eggink LL (1999) Assembly of light-harvesting complex II and biogenesis of thylakoid membranes in chloroplasts. *Photosynth Res* 61: 197–215
- Hoover JK and Eggink LL (2001) A potential role of chlorophylls *b* and *c* in assembly of light-harvesting complexes. *FEBS Lett* 489: 1–3
- Hoover J and Hughes MJ (1992) Purification and characterization of a membrane-bound protease from *Chlamydomonas reinhardtii*. *Plant Physiol* 99: 932–937
- Hoover JK, Boyd CO and Paavola LG (1991) Origin of thylakoid membranes in *Chlamydomonas reinhardtii* y-1 at 38 °C. *Plant Physiol* 96: 1321–1328
- Howe G and Merchant S (1993) Maturation of thylakoid lumen proteins proceeds post-translationally through an intermediate in vivo. *Proc Natl Acad Sci U S A* 90: 1862–1866
- Howe G and Merchant S (1994) Role of heme in the biosynthesis of cytochrome *c*<sub>6</sub>. *J Biol Chem* 269: 5824–5832
- Hutin C, Havaux M, Carde JP, Kloppstech K, Meierhoff K, Hoffman N and Nussaume L (2002) Double mutation cpSRP43—/cpSRP54— is necessary to abolish the cpSRP pathway required for thylakoid targeting of the light-harvesting chlorophyll proteins. *Plant J* 29: 531–543
- Hynds PJ, Robinson D and Robinson C (1998) The sec-independent twin-arginine translocation system can transport both tightly folded and misfolded proteins across the thylakoid membrane. *J Biol Chem* 273: 34868–34874
- Hynds PJ, Plucken H, Westhoff P and Robinson C (2000) Different lumen-targeting pathways for nuclear-encoded versus cyanobacterial/plastid-encoded Hcf136 proteins. *FEBS Lett* 467: 97–100
- Jarvis P, Chen LJ, Li H, Peto CA, Fankhauser C and Chory J (1998) An *Arabidopsis* mutant defective in the plastid general protein import apparatus. *Science* 282: 100–103
- Johanningmeier U and Howell SH (1984) Regulation of light-harvesting chlorophyll-binding protein mRNA accumulation in *Chlamydomonas reinhardtii*. Possible involvement of chlorophyll synthesis precursors. *J Biol Chem* 259: 13541–13549
- Joyard J, Block M, Pineau B, Albrieux C and Douce R (1990) Envelope membranes from mature spinach chloroplasts contain a NADPH:protochlorophyllide reductase on the cytosolic side of the outer membrane. *J Biol Chem* 265: 21820–21827
- Joyard J, Teyssier E, Mieg C, Berny-Seigneurin D, Marechal E, Block MA, Dorne AJ, Rolland N, Ajlani G and Douce R (1998) The biochemical machinery of plastid envelope membranes. *Plant Physiol* 118: 715–723
- Keegstra K and Cline K (1999) Protein import and routing systems of chloroplasts. *Plant Cell* 11: 557–570
- Kim SJ, Jansson S, Hoffman NE, Robinson C and Mant A (1999) Distinct ‘assisted’ and ‘spontaneous’ mechanisms for the insertion of polytopic chlorophyll-binding proteins into the thylakoid membrane. *J Biol Chem* 274: 4715–4721
- Kim YW, Park DS, Park SC, Kim SH, Cheong GW and Hwang I (2001) *Arabidopsis* dynamin-like 2 that binds specifically to phosphatidylinositol 4-phosphate assembles into a high-molecular weight complex in vivo and in vitro. *Plant Physiol* 127: 1243–1255
- Kindle KL (1998) Amino-terminal and hydrophobic regions of the *Chlamydomonas reinhardtii* plastocyanin transit peptide are required for efficient protein accumulation in vivo. *Plant Mol Biol* 38: 365–377
- Klimyuk VI, Persello-Cartieaux F, Havaux M, Contard-David P, Schuenemann D, Meierhoff K, Gouet P, Jones JD, Hoffman NE and Nussaume L (1999) A chromodomain protein encoded by the *Arabidopsis* CAO gene is a plant-specific component of the chloroplast signal recognition particle pathway that is involved in LHCP targeting. *Plant Cell* 11: 87–99
- Kogata N, Nishio K, Hirohashi T, Kikuchi S and Nakai M (1999)



- Involvement of a chloroplast homologue of the signal recognition particle receptor protein, FtsY, in protein targeting to thylakoids. *FEBS Lett* 447: 329–333
- Kohorn BD and Tobin EM (1989) A hydrophobic, carboxy-proximal region of a light-harvesting chlorophyll *a/b* protein is necessary for stable integration into thylakoid membranes. *Plant Cell* 1: 159–166
- Kroll D, Meierhoff K, Bechtold N, Kinoshita M, Westphal S, Vothknecht UC, Soll J and Westhoff P (2001) VIPP1, a nuclear gene of *Arabidopsis thaliana* essential for thylakoid membrane formation. *Proc Natl Acad Sci U S A* 98: 4238–4242
- Kruse E and Kloppstech K (1992) Integration of early light-inducible proteins into isolated thylakoid membranes. *Eur J Biochem* 208: 195–202
- Kuttkat A, Grimm R and Paulsen H (1995) Light-harvesting chlorophyll *a/b*-binding protein inserted into isolated thylakoid binds pigments and is assembled into trimeric light-harvesting complex. *Plant Physiol* 4: 1267–1276
- Kuttkat A, Edhofer I, Eichacker LA and Paulsen H (1997) Light-harvesting chlorophyll *a/b*-binding protein stably inserts into etioplast membranes supplemented with Zn-pheophytin *a/b*. *J Biol Chem* 272: 20451–20455
- Kyte J and Doolittle RF (1982) A simple method for displaying the hydropathic character of a protein. *J Mol. Biol.* 157: 105–132
- Lawrence SD and Kindle KL (1997) Alterations in the *Chlamydomonas* plastocyanin transit peptide have distinct effects on in vitro import and in vivo protein accumulation. *J Biol Chem* 272: 20357–20363
- Lebedev N and Timko MP (1998) Protochlorophyllide photoreduction. *Photosynth Res* 58: 5–23
- Li X, Henry R, Yuan J, Cline K and Hoffman NE (1995) A chloroplast homologue of the signal recognition particle subunit SRP54 is involved in the posttranslational integration of a protein into thylakoid membranes. *Proc Natl Acad Sci USA* 92: 3789–3793
- Lindahl M, Yang DH and Andersson B (1995) Regulatory proteolysis of the major light-harvesting chlorophyll *a/b* protein of Photosystem II by a light-induced membrane-associated enzymic system. *Eur J Biochem* 231: 503–509
- Lydakis-Simantiris N, Hutchison RS, Betts SD, Barry BA and Yocum CF (1999) Manganese stabilizing protein of Photosystem II is a thermostable, natively unfolded polypeptide. *Biochemistry* 38: 404–414
- Mant A, Kieselbach T, Schroder WP and Robinson C (1999) Characterisation of an *Arabidopsis thaliana* cDNA encoding a novel thylakoid lumen protein imported by the delta pH-dependent pathway. *Planta* 207: 624–627
- Mant A, Woolhead CA, Moore M, Henry R and Robinson C (2001) Insertion of Psak into the thylakoid membrane in a 'horse-shoe' conformation occurs in the absence of signal recognition particle, nucleoside triphosphates or functional Albino3. *J Biol Chem* 276: 36125–36130
- May T and Soll J (1999) Chloroplast precursor protein translocon. *FEBS Lett* 452: 52–56
- Merchant S and Dreyfuss BW (1998) Posttranslational assembly of photosynthetic metalloproteins. *Annu Rev Plant Phys* 49: 25–51
- Mochizuki N, Brusslan JA, Larkin R, Nagatani A and Chory J (2001) *Arabidopsis* genomes uncoupled 5 (GUN5) mutant reveals the involvement of Mg-chelatase H subunit in plastid-to-nucleus signal transduction. *Proc Natl Acad Sci U S A* 98: 2053–2058
- Molik S, Karnauchov I, Weidlich C, Herrmann RG and Klösgen RB (2001) The Rieske Fe/S protein of the cytochrome *b<sub>6</sub>/f* complex in chloroplasts: Missing link in the evolution of protein transport pathways in chloroplasts? *J Biol Chem* 276: 42761–42766
- Moore M, Harrison MS, Peterson EC and Henry R (2000) Chloroplast Oxa1p homolog albino3 is required for post-translational integration of the light harvesting chlorophyll-binding protein into thylakoid membranes. *J Biol Chem* 275: 1529–1532
- Mori H and Cline K (2001) Post-translational protein translocation into thylakoids by the Sec and ΔpH-dependent pathways. *Biochim Biophys Acta* 1541: 80–90
- Mori H and Cline K (2002) A twin arginine signal peptide and the pH gradient trigger reversible assembly of the thylakoid ΔpH/Tat translocase. *J Cell Biol* 157: 205–210
- Mori H, Summer EJ, Ma X and Cline K (1999) Component specificity for the thylakoidal Sec and Delta pH-dependent protein transport pathways. *J Cell Biol* 146: 45–55
- Mori H, Summer EJ and Cline K (2001) Chloroplast TatC plays a direct role in thylakoid ΔpH-dependent protein transport. *FEBS Lett* 501: 65–68
- Morre DJ, Sellden G, Sundqvist C and Sandelius AS (1991) Stromal low-temperature compartment derived from the inner membrane of the chloroplast envelope. *Plant Physiol* 97: 1558–1564
- Motohashi R, Nagata N, Ito T, Takahashi S, Hobo T, Yoshida S and Shinozaki K (2001) An essential role of a TatC homologue of a Delta pH-dependent protein transporter in thylakoid membrane formation during chloroplast development in *Arabidopsis thaliana*. *Proc Natl Acad Sci USA* 98: 10499–10504
- Mould RM, Knight JS, Bogsch E and Gray JC (1997) Azide-sensitive thylakoid membrane insertion of chimeric cytochrome *f* polypeptides imported by isolated pea chloroplasts. *Plant J* 11: 1051–1058
- Mullet JE (1988) Chloroplast development and gene-expression. *Annu Rev Plant Phys* 39: 475–502
- Musser SM and Theg SM (2000) Characterization of the early steps of OE17 precursor transport by the thylakoid Delta pH/Tat machinery. *Eur J Biochem* 267: 2588–2598
- Nakai M, Goto A, Nohara T, Sugita D and Endo T (1994) Identification of the SecA protein homolog in pea chloroplasts and its possible involvement in thylakoidal protein transport. *J Biol Chem* 269: 31338–31341
- Nakayama M, Masuda T, Bando T, Yamagata H, Ohta H and Takamiya K-I (1998) Cloning and expression of the soybean chlH gene encoding a subunit of Mg-chelatase and localization of the Mg<sup>2+</sup> concentration-dependent ChlH protein within the chloroplast. *Plant Cell Physiol* 39: 275–284
- Nilsson R, Brunner J, Hoffman NE and van Wijk KJ (1999) Interactions of ribosome nascent chain complexes of the chloroplast-encoded D1 thylakoid membrane protein with cpSRP54. *EMBO J* 18: 733–742
- Nohara T, Asai T, Nakai M, Sugiura M and Endo T (1996) Cytochrome *f* encoded by the chloroplast genome is imported into thylakoids via the SecA-dependent pathway. *Biochem Biophys Res Commun* 224: 474–478

- Oster U, Tanaka R, Tanaka A and Rudiger W (2000) Cloning and functional expression of the gene encoding the key enzyme for chlorophyll *b* biosynthesis (CAO) from *Arabidopsis thaliana*. *Plant J* 21: 305–10
- Park H, Eggink LL, Roberson RW and Hooper JK (1999) Transfer of proteins from the chloroplast to vacuoles in *Chlamydomonas reinhardtii* (Chlorophyta): A pathway for degradation. *J Phycol* 35: 528–538
- Paulsen H (1997) Pigment ligation to proteins of the photosynthetic apparatus in higher plants. *Physiol Plantarum* 100: 760–768
- Payan LA and Cline K (1991) A stromal protein factor maintains the solubility and insertion competence of an imported thylakoid membrane protein. *J Cell Biol* 112: 603–613
- Peltier JB, Friso G, Kalume DE, Roepstorff P, Nilsson F, Adamska I and van Wijk KJ (2000) Proteomics of the chloroplast: systematic identification and targeting analysis of luminal and peripheral thylakoid proteins. *Plant Cell* 3: 319–341
- Peltier JB, Emanuelsson O, Kalume DE, Ytterberg J, Friso G, Rudella A, Liberles DA, Soderberg L, Roepstorff P, von Heijne G and van Wijk KJ (2002) Central functions of the luminal and peripheral thylakoid proteome of *Arabidopsis* determined by experimentation and genome-wide prediction. *Plant Cell* 14: 211–236
- Pfisterer J, Lachmann P and Kloppstech K (1982) Transport of proteins into chloroplasts. Binding of nuclear-coded chloroplast proteins to the chloroplast envelope. *Eur J Biochem* 126: 143–148
- Race HL, Herrmann RG and Martin W (1999) Why have organelles retained genomes? *Trends Genet* 9: 364–370
- Reed JE, Cline K, Stephens LC, Bacot KO and Viitanen PV (1990) Early events in the import/assembly pathway of an integral thylakoid protein. *Eur J Biochem* 194: 33–42
- Rensink WA, Pilon M and Weisbeek P (1998) Domains of a transit sequence required for in vivo import in *Arabidopsis* chloroplasts. *Plant Physiol* 118: 691–699
- Rüdiger W (1997) Chlorophyll metabolism: from outer space down to the molecular level. *Phytochem* 46: 1151–1167
- Sargent F, Gohlke U, De Leeuw E, Stanley NR, Palmer T, Saibil HR and Berks BC (2001) Purified components of the *Escherichia coli* Tat protein transport system form a double-layered ring structure. *Eur J Biochem* 268: 3361–3367
- Schatz G and Dobberstein B (1996) Common principles of protein translocation across membranes. *Science* 271: 1519–1525
- Schlieff E and Klösgen R-B (2001) Without a little help of my friends—Direct insertion of proteins into chloroplast membranes. *Biochim Biophys Acta* 1541: 22–33
- Schnell DJ (1998) Protein targeting to the thylakoid membrane. *Annu Rev Plant Physiol Plant Mol Biol* 49: 97–126
- Schubert M, Petersson UA, Haas BJ, Funk C, Schröder WP and Kieselbach T (2002) Proteome map of the chloroplast lumen of *Arabidopsis thaliana*. *J Biol Chem* 277: 8354–8365
- Schuenemann D, Gupta S, Persello-Cartiaux F, Klimyuk VI, Jones JDG, Nussaume L and Hoffman NE. (1998) A novel signal recognition particle targets light-harvesting proteins to the thylakoid membranes. *Proc Natl Acad Sci U S A* 95: 10312–10316
- Schuenemann D, Amin P, Hartmann E and Hoffman NE (1999) Chloroplast SecY is complexed to SecE and involved in the translocation of the 33-kDa but not the 23-kDa subunit of the oxygen-evolving complex. *J Biol Chem* 274: 12177–12182
- Settles AM and Martienssen R (1998) Old and new pathways of protein export in chloroplasts and bacteria. *Trends in Cell Biol* 8: 494–501
- Settles AM, Yonetani A, Baron A, Bush DR, Cline K and Martienssen R (1997) Sec-independent protein translocation by the maize Hcf106 protein. *Science* 278: 1467–1470
- Smith TA and Kohorn BD (1994) Mutations in a signal sequence for the thylakoid membrane identify multiple protein transport pathways and nuclear suppressors. *J Cell Biol* 126: 365–74
- Summer EJ, Mori H, Settles H and Cline K (2000) The thylakoid delta pH-dependent pathway machinery facilitates RR-independent N-tail protein integration. *J Biol Chem* 275: 23483–23490
- Sundberg E, Slagter JG, Fridborg I, Cleary SP, Robinson C and Coupland G (1997) ALBINO3, an *Arabidopsis* nuclear gene essential for chloroplast differentiation, encodes a chloroplast protein that shows homology to proteins present in bacterial membranes and yeast mitochondria. *Plant Cell* 9: 717–730
- Sundqvist C and Dahlin C (1997) With chlorophyll pigments from prolamellar bodies to light-harvesting complexes. *Physiol Plantarum* 100: 748–759
- Surpin M and Chory J (1997) The co-ordination of nuclear and organellar genome expression in eukaryotic cells. *Essays Biochem* 32: 113–125
- Tanaka A, Ito H, Tanaka R, Tanaka NK, Yoshida K and Okada K (1998) Chlorophyll *a* oxygenase (CAO) is involved in chlorophyll *b* formation from chlorophyll *a*. *Proc Natl Acad Sci USA* 95: 12719–12723
- Teter SA and Theg SM (1998) Energy-transducing thylakoid membranes remain highly impermeable to ions during protein translocation. *Proc Natl Acad Sci USA* 95: 1590–1594
- Tziveleka LA, Argyroudi-Akoyunoglou JH (1998) Implications of a developmental-stage-dependent thylakoid-bound protease in the stabilization of the light-harvesting pigment-protein complex serving Photosystem II during thylakoid biogenesis in red kidney bean. *Plant Physiol* 117: 961–970
- Tu CJ, Schuenemann D and Hoffman NE (1999) Chloroplast FtsY, chloroplast signal recognition particle and GTP are required to reconstitute the soluble phase of light-harvesting chlorophyll protein transport into thylakoid membranes. *J Biol Chem* 274: 27219–27224
- Tu CJ, Peterson EC, Henry R and Hoffman NE (2000) The L18 domain of light-harvesting chlorophyll proteins binds to chloroplast signal recognition particle 43. *J Biol Chem* 275: 13187–1318790
- Voelker R and Barkan A (1995) Two nuclear mutations disrupt distinct pathways for targeting proteins to the chloroplast thylakoid. *EMBO J* 14: 3905–3914
- Voelker R, Mendel-Hartvig J and Barkan A (1997) Transposon-disruption of a maize nuclear gene, *tha1*, encoding a chloroplast SecA homologue: In vivo role of cp-SecA in thylakoid protein targeting. *Genetics* 145: 467–478
- von Wettstein D, Gough S and Kannangara CG (1995) Chlorophyll Biosynthesis. *Plant Cell* 7: 1039–1057
- Walker MB, Roy LM, Coleman E, Voelker R and Barkan A (1999) The maize *tha4* gene functions in sec-independent protein transport in chloroplasts and is related to hcf106. *J Cell Biol* 147: 267–276
- Watanabe N, Che FS, Iwano M, Takayama S, Yoshida S and Isogai A (2001) Dual targeting of spinach protoporphyrinogen oxidase II to mitochondria and chloroplasts by alternative use

- of two in-frame initiation codons. *J Biol Chem* 276: 20474–20481
- Wollman FA, Minai L and Nechushtai R (1999) The biogenesis and assembly of photosynthetic proteins in thylakoid membranes. *Biochim Biophys Acta* 1411: 21–85
- Woolhead CA, Thompson SJ, Moore M, Tissier C, Mant A, Rodger A, Henry R and Robinson C (2001) Distinct Albino3-dependent and -independent pathways for thylakoid membrane protein insertion. *J Biol Chem* 276: 40841–40846
- Yuan J and Cline K (1994) Plastocyanin and the 33-kDa subunit of the oxygen-evolving complex are transported into thylakoids with similar requirements as predicted from pathway specificity. *J Biol Chem* 269: 18463–18467
- Yuan JG, Henry R and Cline K (1993) Stromal factor plays an essential role in protein integration into thylakoids that cannot be replaced by unfolding or by heat-shock protein hsp70. *Proc Natl Acad Sci USA* 90: 8552–8556
- Yuan J, Henry R, McCaffery M and Cline K (1994) SecA homologue in protein transport within chloroplasts: Evidence for endosymbiont-derived sorting. *Science* 266: 796–798
- Zelazny A, Seluanov A, Cooper A and Bibi E (1997) The NG domain of the prokaryotic signal recognition particle receptor, FtsY, is fully functional when fused to an unrelated integral membrane polypeptide. *Proc Natl Acad Sci USA* 94: 6025–6029
- Zhang L, Paakkari V, Suorsa M and Aro EM (2001) A SecY homologue is involved in chloroplast-encoded D1 protein biogenesis. *J Biol Chem* 276: 37809–37814

# Chapter 13

## Pulse Amplitude Modulated Chlorophyll Fluorometry and its Application in Plant Science

G. Heinrich Krause and Peter Jahns

*Institute of Plant Biochemistry, Heinrich Heine University Düsseldorf,  
Universitätsstrasse 1, D-40225 Düsseldorf, Germany*

Summary .....	373
I. Introduction .....	374
II. The Measuring Principle of the Pulse Amplitude Modulation Fluorometer .....	374
III. Initial and Variable Fluorescence .....	375
A. Initial Fluorescence .....	375
B. Variable Fluorescence .....	376
IV. Ratio of Maximum Variable to Maximum Total Fluorescence, $F_v/F_m$ .....	378
V. Fluorescence Quenching .....	379
A. Photochemical Quenching .....	380
B. Non-photochemical Quenching .....	381
1. Basics—The Two Definitions of Non-photochemical Quenching .....	381
2. Resolution of qN Components .....	382
3. Energy-dependent Quenching, qE .....	383
a. Role of the Xanthophyll Cycle .....	384
b. Mechanism .....	384
c. Quenching of Initial Fluorescence .....	385
4. State-Transition Quenching, qT .....	386
5. Photoinhibitory Quenching, qI .....	386
VI. Photosynthetic Yield and Rate of Linear Electron Transport Determined by Fluorescence Analysis .....	388
A. Quantum Efficiency of Photosystems II and I .....	388
B. Electron Transport through PS II .....	390
VII. Application of Chlorophyll Fluorescence in the Study of Mutants .....	391
VIII. Conclusion and Perspectives .....	392
Acknowledgment .....	393
References .....	393

### Summary

The development of the pulse amplitude modulation technique to measure chlorophyll *a* fluorescence has provided an important, widely used tool to investigate various photosynthetic processes in a non-invasive manner. The present chapter is focused on a number of chlorophyll fluorescence parameters that are frequently applied in plant science and can be easily determined in vascular plants. Modes of measurement and details of interpretation of these parameters, as well as examples of applications are described to provide the reader with a comprehensive treatise on the scope of the method of modulation fluorometry. This includes the discussion of still uncertain or speculative explanations, imperfection of current models and problems concerning possible errors in the exact determination of certain parameters. Particular emphasis is put on the effects of stress conditions that directly or indirectly affect the energy conversion in Photosystem II and thus influence fluorescence emission from plant leaves, i.e. are reflected by photochemical and non-photochemical fluorescence quenching phenomena. The chapter also considers the growing use of the fluorescence method including video imaging of fluorescence to identify and study plant mutants.

## I. Introduction

A small fraction of the light energy absorbed by the photosynthetic antennae is re-emitted as chlorophyll (Chl) *a* fluorescence. At physiological temperatures, the predominant source of fluorescence is the antenna of Photosystem II (PS II). As the primary photochemical reaction and radiationless deactivation of excited pigments in PS II compete for photon energy with fluorescence emission, the latter is influenced in a complex manner directly or indirectly by photosynthetic processes. Thus, the extent and kinetics of Chl fluorescence emission bears valuable information. Precise measurement of fluorescence signals under well-defined conditions can be used to assess a variety of reactions related to photosynthesis. The development of refined techniques to record and analyze Chl fluorescence signals led to many investigations, done both *in vitro* with isolated chloroplasts, thylakoids and PS II particles, and *in vivo* with intact leaves of vascular plants, as well as with photosynthetic microorganisms. These studies provided far-reaching interpretation of Chl fluorescence phenomena and made fluorescence a powerful non-invasive tool in plant science. Before about 1985, this tool was utilized by a relatively small group of specialists only. The introduction of 'pulse-amplitude-modulation' fluorometers (Schreiber, 1986), which are commercially available and easy to operate, led to a wide use of the Chl fluorescence technique among plant scientists. Particularly in stress physiology, modulation fluorometers are frequently applied both in the laboratory and in the field to detect adverse effects of environmental biotic and abiotic stress factors, as well as acclimation processes in plants. In parallel, highly sensitive fluorometers were developed, based on the 'pump and probe' and 'fast-repetition-rate' techniques, which allow the measurement of Chl fluorescence in aquatic ecosystems, e.g. of phytoplankton in the oceans, where the Chl concentration is extremely low (Kolber and Falkowski, 1993; Falkowski and Kolber, 1995;

Kolber et al., 1998; Behrenfeld et al., 1998). Non-modulated fluorometry was optimized for analyses of fast fluorescence transients (Strasser et al., 1995).

Basic Chl fluorescence phenomena have been addressed in an earlier article (Krause and Weis, 1991), which also considered previous reviews. Several further reviews have appeared since, covering various aspects of Chl fluorescence methods (Karukstis, 1991; Dau 1994; Govindjee, 1995; Joshi and Mohanty, 1995; Mohammed et al., 1995; Schreiber et al., 1998; Lazár, 1999). The present chapter is focused on Chl *a* fluorescence of terrestrial vascular plants, as can be routinely monitored by pulse-amplitude-modulated fluorometry in the time range of microseconds to minutes at physiological temperatures. The significance of fluorescence parameters will be pointed out and examples for their use in plant science discussed, but a complete review of the immense number of applications cannot be given here.

## II. The Measuring Principle of the Pulse Amplitude Modulation Fluorometer

The technical details of the method have been well described for the PAM fluorometer (Schreiber, 1986; Schreiber et al., 1986). The principle of measurement in comparison to 'non-modulated' instruments is briefly summarized below.

In fluorometers using non-modulated continuous light (see Schreiber, 1983, for technical review), an 'actinic', photosynthetically active light beam (usually blue or short-wavelength red) of medium to high intensity induces both photosynthesis and Chl fluorescence. By suitable optical filters, this actinic light is shielded from the detector to which the red fluorescence, e.g. in the range of maximum emission at about 685 nm (or in the far-red region), is admitted. This technique has several severe disadvantages that are eliminated by the modulation system. With 'non-modulated' fluorometers (i) it is often difficult to determine the initial fluorescence yield,  $F_0$ ; (ii) the signal size depends on the intensity of the actinic beam; (iii) stray light from the environment disturbs fluorescence recording; (iv) quenching processes cannot be resolved *in vivo*. Nevertheless, such instruments may be well suited to record fast fluorescence induction in dark-adapted leaves (see Section III.B below).

*Abbreviations:* Ax – antheraxanthin; Chl – chlorophyll; LHCII – light harvesting complex of Photosystem II; PAR – photosynthetically active radiation (400–700 nm);  $\Phi_p$  – quantum yield of photosynthesis ( $O_2$  evolution or  $CO_2$  assimilation);  $\Phi_{PSII}$ ,  $\Phi_{PSI}$  – quantum efficiency of Photosystem II, Photosystem I; PQ – plastoquinone; PS I – Photosystem I; PS II – Photosystem II;  $Q_A$  – primary quinone-type electron acceptor of Photosystem II; Vx – violaxanthin; Zx – zeaxanthin

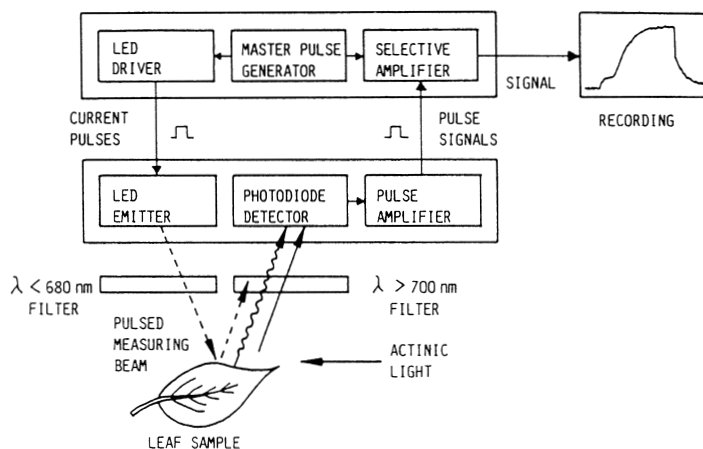


Fig. 1. Scheme of the measuring principle of pulse modulation chlorophyll fluorometry. Pulsed weak 'measuring' light from a light emitting diode (LED) is passed through an optical short-pass filter to the leaf sample. The fluorescence detector is shielded by a long-pass filter that prevents disturbance by stray light from the LED. A selective amplifier assures that only modulated fluorescence induced by the measuring light contributes to the signal. From Schreiber (1986) with kind permission from Kluwer Academic Publishers.

In the pulse-amplitude-modulated fluorometer (e.g. the PAM system), a very weak pulsed beam ( $\lambda < 680$  nm, pulse time  $1 \mu\text{s}$  and pulse frequency 1.6 kHz or 100 kHz in the PAM 101) from a light-emitting diode is used as a 'measuring' beam to induce fluorescence, which is detected at wavelengths  $\lambda > 710$  nm (Fig. 1). The amplifier selects only the modulated fluorescence. The amplitude and frequency of pulses of the measuring beam are set low enough to keep PS II in the 'dark-adapted' state in which initial fluorescence,  $F_0$ , is recorded. Then non-modulated actinic, photosynthetically active light of a higher intensity is applied as continuous illumination leading to steady-state photosynthesis. Superimposed high-intensity saturating light pulses of about 1 s are used to 'close' all PS II reaction centers and thus to obtain maximum fluorescence emission. The actinic light alters the fluorescence yield according to the light-induced changes in the state of PS II (Fig. 2). Actinic light of any wavelength and of very high intensities does not directly interfere with the fluorescence signal. A modulation fluorometer with a mechanical chopped measuring beam was already used in early basic studies by Duysens and Sweers (1963). In the modern electronic systems, response time, sensitivity and selectivity for the pulsed fluorescence have been immensely improved and allow time resolution of measurements below 1 ms.

### III. Initial and Variable Fluorescence

#### A. Initial Fluorescence

When all reaction centers of PS II are 'open', i.e. the primary quinone electron acceptor  $Q_A$  is in the oxidized state, a minimum 'initial' fluorescence yield,  $F_0$  or 'O', also called 'minimal', 'dark-level', or 'constant' fluorescence (Figs. 2–4), is obtained (Duysens and Sweers, 1963; Butler, 1978). With the modulation fluorometer,  $F_0$  can be conveniently recorded in dark-adapted leaves (Figs. 2, 4), provided the light energy input from the measuring beam is low enough to avoid any  $Q_A^-$  accumulation; a signal slowly increasing with time would indicate a too high intensity of the measuring beam. Weak far-red light exciting predominantly Photosystem I (PS I) may facilitate complete oxidation of intersystem electron carriers and of  $Q_A$ .

After strong actinic illumination and return to darkness (or more exactly, to illumination with weak measuring light only), a transient apparent increase in  $F_0$  (not shown in Fig. 4), lasting several minutes, can be observed under certain conditions (Mano et al., 1995). This was interpreted as indicating donation of electrons from stromal reductants to the plastoquinone pool and  $Q_A$ . Based on studies of wild-type and transgenic tobacco (*Nicotiana tabacum*) plants, the transient post-illumination fluorescence rise has been attributed to the action of

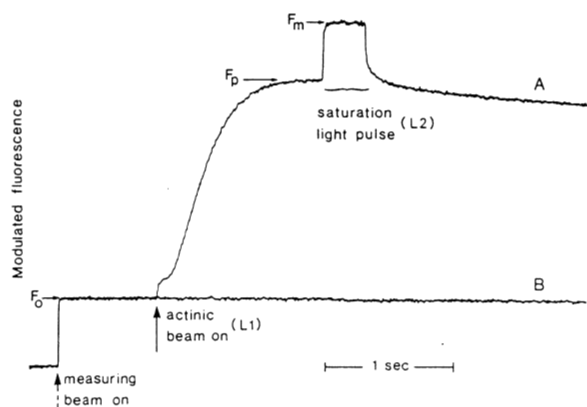


Fig. 2. Signal of modulated Chl *a* fluorescence from a leaf of *Phaseolus vulgaris* (trace A) and an ethanolic Chl extract (trace B) demonstrating the response to continuous white actinic light of moderate intensity (L1, 20 W m<sup>-2</sup>) and to a superimposed saturating light pulse (L2, 2000 W m<sup>-2</sup>). Note the absence of any change in the signal from the Chl extract upon illumination with non-modulated light. From Schreiber et al. (1986) with kind permission from Kluwer Academic Publishers.

plastidic NAD(P)H: plastoquinone oxidoreductase (Section VII).

In C<sub>3</sub> plants, F<sub>0</sub> measured at room temperature predominantly represents PS II fluorescence. However, PS I fluorescence contributes to the signal, particularly in the wavelength region  $\lambda > 710$  nm, where modulated fluorescence usually is detected. This is evident from spectral analyses of fluorescence lifetimes (Gilmore et al., 2000; for reviews of earlier literature see Holzwarth, 1991; Krause and Weis, 1991). The PSI-associated component of F<sub>0</sub> was shown to vary in Chl *b*-deficient *chlorina* mutants of barley (*Hordeum vulgare*) compared to the wild-type (Gilmore et al., 2000).

According to an estimation by Pfündel (1998), the contribution of PS I to F<sub>0</sub> is about 30% in C<sub>3</sub> species and about 50% in C<sub>4</sub> species of the NADP-malic enzyme type, because of the higher total PS I/PS II ratio in the latter. These results confirm earlier measurements with a two channel modulation fluorometer (Genty et al., 1990a) allowing fluorescence recording at 690 and 730 nm. At the long wavelength, a proportion of F<sub>0</sub> of about 30% in C<sub>3</sub> plants and 50% in the C<sub>4</sub> species maize was found not to participate in non-photochemical quenching and was tentatively attributed to PS I. In a special emitter-detector unit developed for the PAM system, fluorescence is excited with modulated blue light (maximum emission at 450 nm) and can be recorded in the region of 660–710 nm, which minimizes the

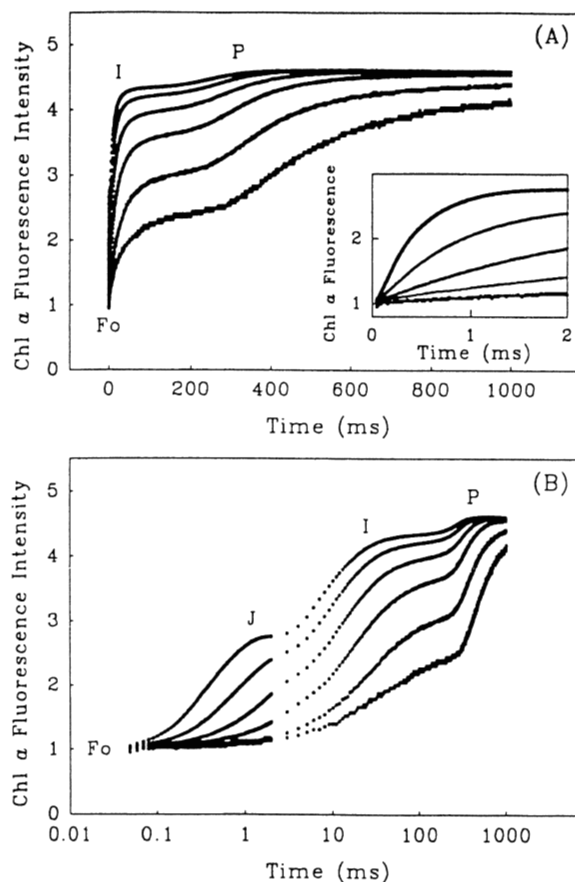


Fig. 3. Chl *a* fluorescence induction of a dark-adapted leaf of *Camellia japonica* irradiated with different intensities (from 18 W m<sup>-2</sup>, lower traces, to 576 W m<sup>-2</sup>, upper traces) of actinic light. Signals of non-modulated fluorescence, normalized at the F<sub>0</sub> level, are plotted (A) in linear and (B) in logarithmic time scale. The inset depicts the fluorescence rise in the first 2 ms of illumination (with 36 to 576 W m<sup>-2</sup>). From Strasser et al. (1995) with kind permission from the American Society for Photobiology.

PS I contribution to F<sub>0</sub> (Schreiber, 1994). The F<sub>0</sub> level can be altered by several factors, as discussed in section V.

### B. Variable Fluorescence

Actinic light causes a transient polyphasic increase of fluorescence emission within about 1 s to a peak, F<sub>p</sub> or 'P' (Figs. 2, 3 and 4A), which is followed by a decline (quenching) during several minutes to a low terminal level close to F<sub>0</sub> (Kautsky effect; Fig. 4). The fluorescence increment above F<sub>0</sub> originates from antennae of PS II and is defined as 'variable fluorescence' or F<sub>v</sub>. In the PAM system, the pulse frequency of the measuring beam is automatically



increased during actinic illumination to obtain a higher signal to noise ratio. The fluorescence rise can also be precisely recorded with instruments operating with non-modulated light, e.g. the 'Plant Efficiency Analyzer' (PEA), which is designed for analysis of fast transients during the first two seconds of fluorescence induction (Strasser et al., 1995). As first established by Duysens and Sweers (1963), the rise of variable fluorescence reflects photochemical reduction of  $Q_A$  or 'closing' of PS II reaction centers. The kinetics of the fluorescence rise is very complex and has been the subject of numerous studies (see Krause and Weis, 1991). In high actinic light, usually at least three phases of the rise can be distinguished, particularly when the transient is displayed in logarithmic time scale (Fig. 3). The times and amplitudes of these phases strongly depend on experimental conditions. The steps of the polyphasic rise, marked by inflections in the induction curve between the various phases (Fig. 3), were originally termed 'O-I<sub>1</sub>-I<sub>2</sub>-P' (Neubauer and Schreiber, 1987; Schreiber and Neubauer, 1987) and are equivalent to the steps 'O-J-I-P' studied by Strasser et al. (1995) and Srivastava et al. (1997).

The O-J phase represents reduction of  $Q_A$  to  $Q_A^-$ . The following phases reflect 'thermal' processes that only indirectly result from the photochemical reaction. Sometimes a dip, 'D', in the fluorescence transient is observed after J. When recorded in low or moderate light (see Fig. 3), the O-J phase (identical with 'O-I' of earlier literature and also called 'plateau' level,  $F_{PI}$ ) seems to reflect  $Q_A$  reduction in PS II <sub>$\beta$</sub>  units with 'Q<sub>B</sub>-nonreducing' reaction centers. PS II <sub>$\beta$</sub>  units have a small antenna size and are supposedly located in the stroma lamellae and grana margins of the thylakoids. A population of PS II <sub>$\beta$</sub>  apparently contains Q<sub>B</sub>-nonreducing (or sometimes termed 'inactive') centers incapable of fast electron transfer from  $Q_A$  to  $Q_B$  (for details see Govindjee, 1990; Krause and Weis, 1991). However, as discussed by Lazár (1999), the O-J rise in low light is complex and Q<sub>B</sub>-reducing centers may contribute substantially to this phase.

In a study of photoinhibition in leaves and isolated chloroplasts of spinach (van Wijk et al., 1993), the O-J phase (measured in low light) was insensitive to high-light pretreatment, whereas the J-P rise and electron transport capacity were strongly affected. Apparently, the Q<sub>B</sub>-nonreducing units, which have been suggested to represent a reserve pool for re-assembly of active PS II <sub>$\alpha$</sub>  in the 'PS II repair cycle' (Guenther and Melis, 1989; Guenther et al., 1990)

are much more resistant to high-light stress than PS II <sub>$\alpha$</sub> . This was recently confirmed for leaves of tropical plants exposed to the full spectrum of natural sunlight (Krause et al., 1999a).

If the actinic light is saturating, i.e. high enough to fully reduce the PS II acceptor side including the PQ pool, maximum  $F_V$  is reached and P becomes identical with the maximum total fluorescence emission,  $F_M$ . In saturating light, all  $Q_A$  is supposed to become reduced during the fast O-J phase. The fact that the J level is lower than P indicates a transient quenching of non-photochemical nature, which is not fully understood. At least in part, the quenching at J seems to be controlled by a transient limitation of electron donation to the PS II reaction center, possibly involving quenching by the radical  $P_{680}^+$ . The J-I phase has been interpreted as the relaxation of this quenching. Both the O-J and J-I phase have been shown to be influenced by the PS II donor side including the water oxidizing system (Schreiber and Neubauer, 1987). It was hypothesized (Schreiber and Krieger, 1996) that the thermal phases, in particular the J-I phase, are based on a recombination type fluorescence (resulting from recombination of the primary radical pair in PS II), which is quenched at the J level. The usually smaller I-P phase is thought to reflect reduction of the plastoquinone (PQ) pool, which is known to be a fluorescence quencher in the oxidized state (Vernotte et al., 1979). Due to the slow thermal phases, the rise from O to P requires at least 100 to 200 ms even in strong actinic light (for a recent review see Schreiber et al., 1998).

The O-J-I-P transient can be used routinely to detect stress effects in plant leaves. In heat-treated pea leaves, an additional fast step termed 'K' was detected in the range of 200–300  $\mu$ s (Srivastava et al., 1997). The O-K phase became dominant in the fluorescence rise after severe heat stress and has been interpreted to result from inhibition of the water-oxidation system and, in addition, from changes in the antenna architecture of PS II.

Besides recording of the fast fluorescence rise, the modulation fluorometer allows the analysis of  $Q_A^-$  re-oxidation in the dark (or more correctly, under the modulated measuring beam) after  $Q_A$  has been fully reduced by strong single-turnover flashes. The 'dark-decay' of variable fluorescence occurs in three phases. These represent electron transfer from  $Q_A^-$  to  $Q_B$  (i) in PS II centers that contain bound  $Q_B$  (lifetime,  $\tau \approx 500 \mu$ s), and (ii) in centers with an empty  $Q_B$  site requiring PQ binding prior to electron transfer ( $\tau \approx$

10 ms). The very slow third phase ( $\tau \approx 2$  s) seems to reflect the decay of the J level representing  $Q_B$ -nonreducing PS II units (see Cao and Govindjee, 1990).

Stress conditions affecting the PS II acceptor side may alter the kinetics of  $Q_A^-$  re-oxidation (Richter et al., 1990). Upon exposure of spinach leaves grown at room temperature to high light at 4 °C, the subsequently determined lifetime of the second, but not the first phase of the dark-decay of fluorescence was significantly prolonged, indicating an inhibition at the  $Q_B$  binding site of the D1 protein (Briantais et al., 1992). However, this was obviously a minor or transient effect; the major change was a strong decrease in the yield of  $F_V$  (Section V). When the plants had been cold-acclimated prior to the strong irradiation at low temperature, the effect was much less pronounced.

#### IV. Ratio of Maximum Variable to Maximum Total Fluorescence, $F_V/F_M$

As derived from the fluorescence model of Butler and coworkers (Butler, 1978), the ratio of maximum variable to maximum total fluorescence  $F_V/F_M = (F_M - F_0)/F_M$ , represents the potential quantum efficiency of the photochemical reaction in PS II. This relationship is valid also for more complex models considering connectivity between PS II units, as it is based on the fluorescence yield in the two extreme states where all reaction centers are either open or closed (Section VI.1). In earlier studies,  $F_V/F_M$  was usually determined by 77K fluorescence recorded in the 685–695 nm region. It was found that this ratio is remarkably uniform in mature, unstressed leaves among different species and ecotypes (Björkman and Demmig, 1987). The modulation fluorometer has made it very convenient to measure  $F_V/F_M$  in a non-invasive manner at room temperature. After recording  $F_0$  in a dark-adapted leaf, a saturating non-modulated light pulse (duration usually about 0.8 to 1 s) reduces  $Q_A$ ,  $Q_B$  and the PQ pool, and the fluorescence rises to  $F_M$  (Fig. 4A). The mean value of  $F_V/F_M$ ,  $0.832 \pm 0.004$ , found for  $C_3$  species at 77K (Björkman and Demmig, 1987), is in the range of  $F_V/F_M$  observed with the PAM system at 20 °C, but slightly lower than expected from the mean optimal quantum yield of photosynthetic  $O_2$  evolution at room temperature. For  $C_3$  plants, this was determined under non-photorespiratory conditions as  $0.106 \pm 0.001$  mol  $O_2$

mol<sup>-1</sup> photons (Björkman and Demmig, 1987), corresponding to a PS II quantum efficiency of 0.848, if one assumes equal distribution of photons between PS I and PS II and a minimum of 8 e<sup>-</sup> needed to evolve 1  $O_2$ . There are certainly intrinsic differences between the two methods of  $F_V/F_M$  determination, as indicated by comparative studies (Krause and Somersalo, 1989; Adams et al., 1990a). Donor side limitations will have less effect at 77K than at 20 °C, as at low temperature  $Q_A^-$  is not readily re-oxidized.  $Q_B$  and the PQ pool remain in the oxidized state and may act as static quenchers. In contrast, at room temperature, the quenching by the PQ pool (Vernotte et al., 1979), which accounts for about 15% of  $F_V$ , supposedly is eliminated during the I-P phase of the fluorescence rise (Schreiber and Neubauer, 1987). This may result in a slight overestimation of potential PS II efficiency. Therefore, Schreiber et al. (1995) suggested to measure the I level instead of  $F_M$  to determine PS II efficiency, which would also allow the application of much shorter pulses. However, this approach has found little use in practice.

On the other hand, at ambient temperatures a significant underestimation of  $F_V/F_M$  results from the contribution of PS I to  $F_0$  at  $\lambda > 710$  nm (Section III.A). This effect is more pronounced in  $C_4$  plants of the NADP-malic enzyme type than in  $C_3$  plants. Pfündel (1998) calculated from his study of  $C_3$ ,  $C_3$ - $C_4$  intermediate and  $C_4$  plants a corrected  $F_V/F_M$  of 0.88 for pure PS II fluorescence. Such high  $F_V/F_M$  values are, indeed, obtained with a PAM emitter-detector system that minimizes PS I contribution by recording fluorescence in the red region around 685 nm (Schreiber, 1994). A disadvantage of such a setup is its lower measuring sensitivity.

Despite these uncertainties, determination of  $F_V/F_M$  has become a widely used method to obtain an approximate measure of potential PS II efficiency in intact plant leaves. Light absorbed in excess of utilization in photosynthesis, particularly in combination with other stress factors, causes a sustained lowering of  $F_V/F_M$  when measured after an appropriate period (usually between 10 min and 1 h) of dark adaptation. The decline in  $F_V/F_M$  predominantly results from a decrease in  $F_V$  and, in certain cases, from an increase in  $F_0$ . Usually, these changes are reversible upon return to optimal conditions. As a result of stress exerted by excessive light, the decrease in  $F_V/F_M$  is closely related to 'photo-inhibition' of photosynthesis. In numerous studies, a linear correlation between decline in  $F_V/F_M$  and

inhibition of optimal quantum yield of photosynthesis,  $\Phi_p$  (i.e. yield of  $O_2$  evolution or  $CO_2$  assimilation in strictly limiting light) has been observed (Demmig and Björkman, 1987; see also Krause and Weis, 1991) making  $F_v/F_M$  a practical indicator of photoinhibition. In principle, the decrease in  $F_v/F_M$  results from an increase in thermal deactivation of excited Chl at the expense of photochemical activity and fluorescence emission. Thus, reductions in  $F_v/F_M$  express persistent 'non-photochemical' fluorescence quenching processes (Section V).

Theoretically, a linear relationship between  $F_v/F_M$  and  $\Phi_p$  is expected, if one assumes a gradual increase in the overall rate constant of thermal deactivation,  $k_D$ , accompanied by a gradual decrease in the rate constant of the photochemical reaction,  $k_p$ . However, studies of fluorescence induction (Krause et al., 1990) and thermoluminescence (Briantais et al., 1992) make it more likely that the decline in  $F_v/F_M$  is caused by a growing population of fully inactive PS II units exhibiting no variable fluorescence, while the remaining PS II units remain largely unchanged in their activity. It has been suggested that in the inactive population, the reaction centers have been transformed to quenchers (e.g. by damage to the D1 protein), which convert the excitation energy to heat. Moreover, a population with strong quenching centers in the antennae of PS II created by the action of the xanthophyll zeaxanthin may be responsible for the lowered fluorescence yield (Gilmore et al., 1995; Horton et al., 1996). In view of the exciton-radical pair equilibrium models of primary photochemistry (Section VI.1 and Chapter 7, van Amerongen and Dekker), it appears difficult, if not impossible, to discriminate between fluorescence quenching in the reaction center and antenna.

In a simple model considering two such populations (Giersch and Krause, 1991), a curvilinear relationship between  $F_v/F_M$  and  $\Phi_p$  or PS II efficiency was obtained. However, if cooperativity between PS II units, i.e. excitation energy transfer from active to quenching units was taken into account, a quasi-linear relationship appeared that fitted with data from photoinhibited isolated chloroplasts. Intact leaves, however, are more complex, as optical properties (Bornman et al., 1991), gradients of photoinhibition from upper to lower leaf sides (Krause and Somersalo, 1989) and possible differences in chloroplast structure come into play. Thus different relationships between  $F_v/F_M$  and  $\Phi_p$  can be found

(Björkman, 1987). When stress factors primarily affect sites other than PS II (e.g. in photosynthetic carbon metabolism), no linear correlation of  $F_v/F_M$  with  $\Phi_p$  can be observed. This has been demonstrated for water-stressed plants (Adams et al., 1990a), chilling-sensitive plants exposed to excess light at low temperatures (Tyystjärvi et al., 1989; Adams et al., 1990a) or plants irradiated with supplemental UV-B light (Nogués and Baker, 1995; Allen et al., 1997). Moreover, it should be considered that in chilling-sensitive species, PS I may be equally or more sensitive to high-light stress at chilling temperature than PS II (Sonoike, 1996; Terashima et al., 1998; Barth and Krause, 1999). Generally, there is no correlation between the capacity of photosynthesis (i.e. rate in saturating light) and  $F_v/F_M$ , because in saturating light,  $CO_2$  assimilation, but not the photochemical reaction is limiting.

Overall,  $F_v/F_M$  appears as a valuable, however, only approximate measure of potential PS II efficiency and may serve in many cases as a sensitive indicator of changes in photosynthetic performance under limiting light. However, for each plant system studied, the relationship between  $F_v/F_M$  and  $\Phi_p$  has to be established by direct measurements of photosynthesis.

## V. Fluorescence Quenching

Following the peak or maximum, fluorescence emission in continuous actinic light declines within minutes in several phases to a low steady-state ('terminal') level (Fig. 4A). The quenching is a complex phenomenon. Although the principles of the different quenching mechanisms were recognized in earlier studies (Briantais et al., 1985; Krause and Weis, 1991), the pulse modulation method made it very convenient to separate quenching components *in vivo*. One major component is the 'photochemical' quenching,  $qP$ , which is related to the redox state of  $Q_A$ . When saturating pulses are added repetitively during the fluorescence decline in continuous light, a rise of fluorescence to a maximum  $F_M'$  indicates closure of the fraction of reaction centers that had been open with  $Q_A$  in the oxidized state (Fig. 4A, C). This indicates that the fluorescence quenching in continuous light is caused in part by competition of the primary photochemical reaction with fluorescence emission. On the other hand, Fig. 4A demonstrates that the original  $F_M$  level of the dark-adapted state is not reached during continuous actinic illumination,

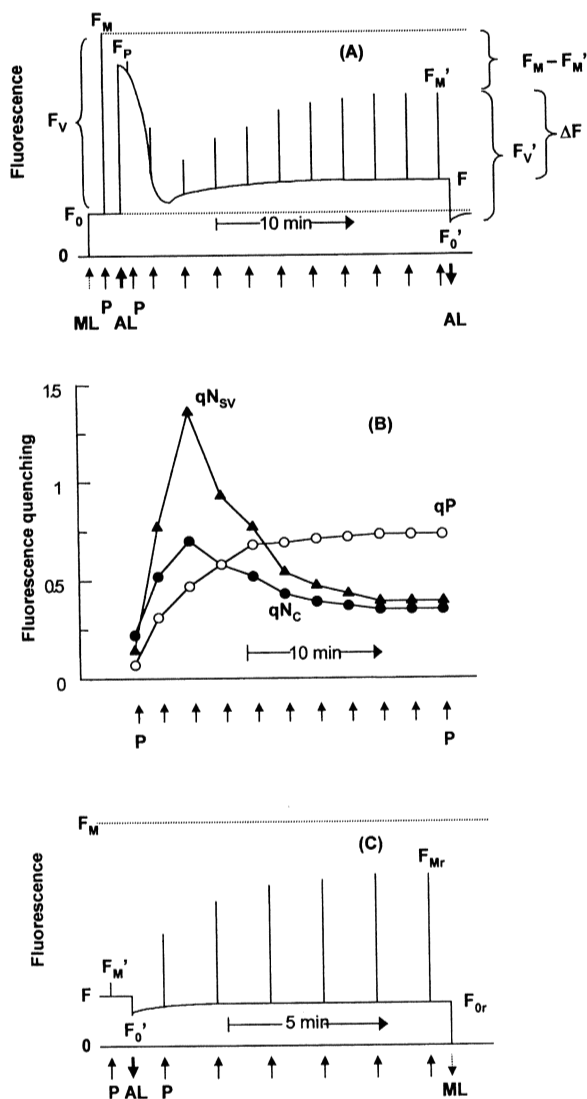


Fig. 4. Schematic presentation of Chl *a* fluorescence signals and derived quenching parameters from a plant leaf, as can be recorded with a modulation fluorometer. Depicted parameters:  $F_0$ ,  $F_M$ ,  $F_V$ , initial, maximum and variable Chl fluorescence yield in the dark-adapted state;  $F_0'$ ,  $F_M'$ ,  $F_V'$ , initial, maximum and variable Chl fluorescence yield in the light;  $F$ , total Chl fluorescence yield after 10 min dark relaxation of preilluminated leaves;  $qN_{SV}$ , non-photochemical fluorescence quenching, Stern-Volmer type;  $qN_C$ , nonphotochemical quenching coefficient;  $qP$ , photochemical quenching coefficient.

A. Determination of  $F_0$  and  $F_0'$  in weak modulated measuring light (ML), of  $F_M$  and  $F_M'$  by means of saturating light pulses (P) and of photochemical quenching ( $qP$ ), non-photochemical quenching ( $qN$ ) and photosynthetic yield of PS II ( $\Phi_{PSII}$ ) under moderate continuous light (around  $300 \mu\text{mol m}^{-2} \text{s}^{-1}$ ) and repetitive saturating pulses (P). Calculation of parameters:  $F_V = F_M - F_0$ ;  $F_V' = F_M' - F_0'$ ;  $\Delta F = F_M' - F$ ;  $\Phi_{PSII} = (F_M' - F)/F_M'$ .

B. Calculated values of photochemical quenching,  $qP$ , and non-

revealing 'non-photochemical' quenching processes,  $qN$ .

### A. Photochemical Quenching

As variable fluorescence may vary between zero (in the  $F_0$  state; all  $Q_A$  oxidized) and  $F_V$  (maximum variable fluorescence; all  $Q_A$  reduced), photochemical quenching,  $qP$ , is defined as the fraction of  $F_V$  (or  $F_V'$ , see below) quenched by oxidized  $Q_A$ , i.e. by utilization of excitons in photochemistry. According to this definition, at any time in continuous light,  $qP$  can be calculated from the fluorescence yield,  $F$ , and the maximal ( $F_M'$ ) and minimal ( $F_0'$ ) fluorescence (cf. Fig. 4A, B):

$$qP = (F_M' - F)/(F_M' - F_0') = (F_M' - F)/F_V'. \quad (1)$$

It should be noted that non-photochemical quenching occurring simultaneously with photochemical quenching results in a lowered maximum variable fluorescence,  $F_V'$ . Determination of  $F_V'$  and  $qP$  require measurement of  $F_0'$ , the minimal fluorescence level in the light, which may differ considerably from dark-adapted  $F_0$  due to non-photochemical quenching (Section V.B). An approximate value for  $F_0'$  can be obtained by switching off the actinic light and irradiating with weak far-red light to enhance reoxidation of  $Q_A^-$ . The transient fluorescence minimum attained within a few seconds then represents  $F_0'$  (Fig. 4A, C). However, the software of commercial modulation fluorometers usually calculates  $qP$  based on  $F_0$  rather than  $F_0'$ . This may result in significant errors, particularly in strong light when  $qP$  is small and  $qN$  high.

The parameter  $qP$  is an approximate measure of the fraction of reaction centers possessing oxidized  $Q_A$ . However, the relationship between  $qP$  and the

photochemical quenching,  $qN$ . For  $qN$ , two frequently used calculation methods, namely  $qN_{SV}$  and  $qN_C$  are compared. Parameters were calculated from the fluorescence signal shown in A at each saturating pulse (P) after turning on the actinic light (AL) as indicated by the corresponding arrows. Quenching parameters were calculated using:  $qP = (F_M' - F)/F_V'$ ;  $qN_{SV} = F_M/F_M' - 1$ ;  $qN_C = 1 - F_V'/F_V$ .

C. Relaxation of non-photochemical quenching in the dark after exposure to strong continuous actinic light (around  $2000 \mu\text{mol m}^{-2} \text{s}^{-1}$  for 20 min), determined by means of saturating light pulses (P). Calculation of parameters after 10 min dark relaxation (in this case,  $qT$  can be neglected):  $F_{Vr} = F_{Mr} - F_{Or}$ ;  $qE_{SV} \approx F_M/F_M' - F_M/F_{Mr}$ ;  $qI_{SV} \approx F_M/F_{Mr} - 1$ ;  $qE_C \approx 1 - F_V'/F_{Vr}$ ;  $qI_C \approx 1 - F_V'/F_V$ . (For further explanations see text.)

redox state of  $Q_A$  is not strictly linear. Depending on the degree of antenna connectivity allowing excitation energy transfer from PS II units with closed to units with open centers, a curvilinear relationship results (Trissl and Lavergne, 1994), and the fraction of PS II centers with oxidized  $Q_A$  is supposedly smaller than  $qP$ , except for extreme values, i.e.  $qP = 1$  and  $qP = 0$ .

As the Calvin cycle is the predominant process that finally accepts the electrons transported through PS II, the redox state of  $Q_A$  and thus  $qP$  are strongly influenced by photosynthetic carbon metabolism. During fluorescence induction in a dark-adapted leaf under moderate light,  $qP$  is low in the first minutes and gradually increases when the Calvin cycle becomes active and the stomates open (Fig. 4B). It may take 20 to 30 min or even longer to reach the steady-state of photosynthesis and  $qP$ , particularly when leaves had been dark-adapted for a long time, e.g. overnight. Optimal utilization of photochemical energy in carbon metabolism (including photorespiration) is characterized by high  $qP$  values. When light absorption exceeds the requirement by carbon assimilation,  $qP$  declines and approaches zero in extremely strong light. Likewise, under a given moderate irradiance, the light energy may become excessive, when environmental conditions restrict  $CO_2$  assimilation. This will lead to decreases in  $qP$ . Thus,  $qP$  may serve as a valuable indicator of 'light stress' combined with other stress factors.

### B. Non-photochemical Quenching

#### 1. Basics—The Two Definitions of Non-photochemical Quenching

Quenching of fluorescence that is not related to reoxidation of  $Q_A$ , as manifested by a lower value of  $F_M'$  in comparison to  $F_M$  (Fig. 4A,C), has been termed 'non-photochemical' quenching,  $qN$  (or NPQ). One type of such quenching, a persistent decrease in  $F_V/F_M$  related to photoinhibition of PS II, has already been mentioned in Section IV. It can be seen from Fig. 4B that  $qN$  develops roughly antiparallel to  $qP$  during fluorescence induction of a dark-adapted leaf. Under moderate actinic light,  $qN$  rises to a maximum during the first minutes, while  $qP$  is low. As  $qP$  increases,  $qN$  declines towards the steady state of photosynthesis (Fig. 4B).

In the literature, different definitions of non-photochemical quenching parameters can be found. In many studies, the Stern-Volmer equation

(Govindjee, 1995; Lakowicz, 1999) has been used to calculate  $qN$ , designated in the following as ' $qN_{SV}$ .' This term is identical with the frequently used abbreviation 'NPQ.' The Stern-Volmer approach considers the quenching of maximum fluorescence so that no  $F_0$  determination is required:

$$qN_{SV} = (F_M - F_M')/F_M' = F_M/F_M' - 1. \quad (2)$$

The parameter  $qN_{SV}$  is equivalent to the relative increase in the overall rate constant of non-photochemical energy conversion in PS II. The fluorescence yield is

$$F = k_F / \sum k_i, \quad (3)$$

where  $k_F$  is the rate constant of fluorescence emission and  $\sum k_i$  the sum of rate constants of all competing energy-converting reactions in PS II. In the state of  $F_M$ , the rate constant of the photochemical reaction,  $k_P$ , is zero; it follows that  $\sum k_i = k_N$ , the sum of rate constants of all non-photochemical reactions. Using Eqs. (3) and (4), this gives

$$F_M = k_F / k_N \text{ and} \quad (4)$$

$$qN_{SV} = (k_N' - k_N)/k_N = \Delta k_N / k_N, \quad (5)$$

where  $k_N'$  is the sum of non-photochemical rate constants in the quenched state and  $k_N$  refers to the initial dark-adapted state. Thus,  $qN_{SV}$  provides a measure of the increase in non-photochemical energy conversion under high-light stress. In highly excessive light,  $qN_{SV}$  values of 3 to 4 or even higher can be observed. However, one should be aware that this is a relative measure, as it refers to the initial dark-adapted state of the leaf. If the leaf is affected by previous stress (e.g. in case of 'chronic photo-inhibition' indicated by a lowered  $F_V/F_M$  ratio),  $qN_{SV}$  values may be misleading. When  $qN_{SV}$  is used to evaluate stress responses, calculations should be based on non-stressed leaves whenever possible.

With the modulation fluorometer,  $F_0$ ,  $F_0'$ ,  $F_V$  and  $F_V'$  can be routinely determined (Fig. 4A, C). In analogy to the photochemical quenching coefficient,  $qP$ , Schreiber et al. (1986) defined  $qN$  as the fraction of  $F_V$  quenched by non-photochemical processes. To distinguish such quenching coefficient (values between 0 and 1) from the Stern-Volmer type parameter, we designate this fraction of  $F_V$  here as  $qN_C$ :

$$qN_C = 1 - (F'_M - F'_0)/(F_M - F_0) = 1 - F'_V/F_V \quad (6)$$

When quenching of  $F_0$  is neglected, i.e.  $F'_0 = F_0$  (as may be the case with commercial software), the approximate value is

$$qN_C = (F_M - F'_M)/F_V \quad (7)$$

The two quenching coefficients,  $qP$  and  $qN_C$ , as defined by Schreiber and coworkers, are related to total quenching of variable fluorescence,  $q_C$ , according to

$$1 - q_C = (1 - qP)(1 - qN_C) \quad (8)$$

The physical meaning of  $qN_C$  is, however, considerably more complex than for  $qN_{SV}$ . In a model study, Havaux et al. (1991) pointed out that the coefficient  $qN_C$  depends on both non-photochemical and photochemical events in PS II. This results from the fact that  $F_V$ , which is related to the photochemical reaction, is considered in calculating  $qN_C$ , but not in the parameter  $qN_{SV}$ . Thus, in stress physiology, the Stern-Volmer approach ( $qN_{SV}$ ) appears as the preferable method to assess changes in non-photochemical energy dissipation.

## 2. Resolution of $qN$ Components

Based on different relaxation kinetics in the dark, three components of non-photochemical quenching can be resolved. These are (i) energy-dependent quenching,  $qE$ , which is related to pH-regulated processes in the antennae of PS II, (ii) state-transition quenching,  $qT$ , which depends on the redox-regulated phosphorylation state of LHCII and (iii) photo-inhibitory quenching,  $qI$ , which is related to photoinactivation of PS II and in part is based on damage to the reaction center. As for total non-photochemical quenching, the single components can be expressed either as quenching coefficients defined as the fraction of variable fluorescence quenched ( $qE_C$ ,  $qT_C$ ,  $qI_C$ , with values between 0 and 1) or based on the Stern-Volmer equation ( $qE_{SV}$ ,  $qT_{SV}$ ,  $qI_{SV}$ ). For reasons discussed above, the Stern-Volmer type quenching appears to be the more suitable method to express the impact of non-photochemical processes on energy conversion in PS II. In analogy to equation 6, the single Stern-Volmer type quenching parameters denote the contribution of the different processes to the increase in the overall non-

photochemical rate constant,  $k_N$ . The Stern-Volmer type quenching components are simply additive:

$$qN_{SV} = qE_{SV} + qT_{SV} + qI_{SV} \quad (9)$$

whereas the quenching coefficients referring to  $F'_V$  are related to each other according to the more complex equation

$$(1 - qN_C) = (1 - qE_C)(1 - qT_C)(1 - qI_C) \quad (10)$$

Moreover, the Stern-Volmer parameters are easier to determine, since  $F'_0$  measurement is not required.

Nevertheless, the quenching coefficients of Eq. (10) have been proven useful in many studies to characterize the state of leaves under stress conditions. With increasing PAR,  $qE_C$  exhibits a typical light-saturation curve. When light saturation of  $qE_C$  is reached, formation of high  $qI_C$  can be expected. Quantum yield of photosynthesis under saturating  $CO_2$  (mol  $O_2$  evolved or  $CO_2$  fixed per mol photons absorbed) decreases in an antiparallel fashion with increasing  $qE_C$ . A negative correlation between  $qE_C$  and quantum yield has been observed in isolated intact chloroplasts (Krause and Laasch, 1987) and leaf discs of spinach (Quick et al., 1989). In other studies (Peterson et al., 1988; Peterson, 1989), a linear relationship between quantum yield and the ratio  $qP/qN_C$  (up to values of 1.6) was reported. According to a model by Weis and Berry (1987), quantum efficiency of PS II and rates of electron transport related to  $CO_2$  assimilation can be calculated using  $qP$  and  $qN_C$  (Section VI). Thus, quenching coefficients may serve to estimate photosynthetic performance.

The three components of  $qN$  have been identified by applying repetitive saturating light pulses during the dark relaxation of quenching (Demmig and Winter, 1988; Horton and Hague, 1988; Quick and Stitt, 1989; Walters and Horton, 1991; Jahns and Krause, 1994) (see idealized trace in Fig. 4C). When the maximum variable fluorescence observed after actinic illumination during the dark relaxation period in barley (*Hordeum vulgare*) leaves was extrapolated back to the time of darkening, three phases of  $F_V$  increase with half-times of about 1 min, 5 min and several hours were resolved (Quick and Stitt, 1989). A better fitting deconvolution was obtained by back extrapolation of the semilogarithmic plot of  $\log qN_C$  versus dark time assuming exponentially decaying components (Walters and Horton, 1991). That

approach resulted in  $t_{1/2}$  of 1 min, 5–10 min and >30 min. The respective quenching components have been termed  $qN_f$  ('fast'),  $qN_m$  ('medium') and  $qN_s$  ('slow'). The three components were attributed to  $qE$ ,  $qT$  and  $qI$  (Horton and Hague, 1988; Quick and Stitt 1989). This interpretation was supported by the effects of various inhibitors and uncouplers. For instance, fluoride, which inhibits dephosphorylation of phospho-LHCII and thus traps the thylakoid system in state 2 (in which phospho-LHCII is detached from PS II so that excitation of PS I is favored in relation to PS II, see also Section V.B.4), abolished relaxation of  $qN_m$ . Similar  $t_{1/2}$  values were obtained for pea (*Pisum sativum*) leaves by analyzing the plot of  $\log F_v$  versus relaxation time (Jahns and Krause, 1994). Calculated  $qN_m$  was light-saturated below 400  $\mu\text{mol photons m}^{-2} \text{s}^{-1}$  and did not exceed values above 0.1. In intermittent light grown pea leaves that are devoid of most Chl *a/b* antenna complexes,  $qN_m$  was absent (Jahns and Krause, 1994). In isolated intact chloroplasts (Krause et al., 1982),  $qE$  was found to relax faster ( $t_{1/2} \approx 15$  s) than in leaves.

There are several complications regarding the extrapolation method. Relatively high apparent  $qT_c$  values (0.4 to 0.6) were obtained in barley leaves upon exposure to excess light (Quick and Stitt, 1989; Walters and Horton, 1991), although state transition is known to be suppressed by strong illumination (Section V.B.4). Fluorescence analyses at 77 K (Walters and Horton, 1991; see also Walters and Horton, 1993) indicated that in low light,  $qN_m$  is a reliable measure of  $qT$ , whereas in high light at least part of  $qN_m$  is due to other quenching processes. The authors suggested that  $qE$  strongly contributes to the  $qN_m$  component in high light. But given the fact that  $qI$  is heterogeneous and has a relatively fast relaxing component (Section V.B.5), it cannot be excluded that in high light also  $qI$  contributes to  $qN_m$ . A further problem is that often the medium phase of relaxation cannot be well resolved. Particularly at chilling temperatures, relaxation of quenching is slowed down and deconvolution of  $qN$  components can be problematic (e.g. Koroleva et al., 1994). Care should also be taken that the saturating pulses do not interfere with the relaxation of quenching. Apparently, such effects can be excluded if the time interval between pulses of 3000  $\mu\text{mol m}^{-2} \text{s}^{-1}$  is at least 100 s (Quick and Stitt, 1989; Walters and Horton, 1991).

As  $qT$  is largely suppressed under high-light stress,  $qN$  formed during excessive illumination of leaves can be resolved into approximate values for  $qE$  and

$qI$ . In spinach leaves (Leitsch et al., 1994) and sun leaves of tropical trees (Thiele et al., 1997) following high-light exposure,  $F_v/F_M$  and  $F_0$  increased in the dark and reached plateau values after about 10 min. This phase can be attributed predominantly to relaxation of  $qE$ . Further relaxation of quenching was stimulated by low light indicating 'recovery' from photoinhibition of PS II, i.e. relaxation of  $qI$ . Thus, for practical purposes,  $qE$  and  $qI$  can roughly be calculated from fluorescence recordings as depicted in Fig. 4C, using initial,  $F_{0r}$ , and maximum fluorescence,  $F_{Mr}$  measured after 10 min relaxation in darkness:

$$qE_{sv} \approx (F_{Mr}/F'_M - 1) F_M/F_{Mr} = F_M/F'_M - F_M/F_{Mr} \quad (11)$$

$$qI_{sv} \approx (F_M - F_{Mr})/F_{Mr} = F_M/F_{Mr} - 1, \quad (12)$$

$$\text{where } qN_{sv} \approx qE_{sv} + qI_{sv}. \quad (13)$$

Corresponding quenching coefficients according to Schreiber et al. (1986) are

$$qE_c \approx 1 - (F'_M - F_0)/(F_{Mr} - F_{0r}) = 1 - F'_v/F_{vr}; \quad (14)$$

$$qI_c \approx 1 - (F_{Mr} - F_{0r})/(F_M - F_0) = 1 - F_{vr}/F_v, \quad (15)$$

$$\text{where } 1 - qN_c \approx (1 - qE_c)(1 - qI_c). \quad (16)$$

It should be noted that  $qE$  and  $qI$  values calculated according to this approximation may contain small contributions of  $qT$  depending on experimental conditions.

In the following, the characteristics and possible mechanisms of the three quenching components are discussed.

### 3. Energy-dependent Quenching, $qE$

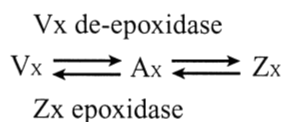
The quenching  $qE$  is caused by the energization of the thylakoid membrane. During short-term (several min) exposure of leaves to strong light  $qE$  is the major component of  $qN$ , as well as of total quenching. There is wide agreement that  $qE$  represents a 'down regulation' of PS II, i.e. an enhanced thermal dissipation of excitation energy in the antennae in response to excessive light absorption. The photoprotection of PS II by the  $qE$  mechanism was first demonstrated in vitro with isolated chloroplasts



(Krause and Behrend, 1986). The degree of energy-dependent quenching is known to depend on two factors, (i) the size of the  $\Delta\text{pH}$  across the thylakoid membrane and (ii) the amount of zeaxanthin (Zx) and possibly of antheraxanthin (Ax) present in the thylakoids. It was shown by Briantais et al. (1979) that  $qE_{\text{SV}}$  is linearly related to the  $\text{H}^+$  concentration in the thylakoid lumen (see also Krause and Weis, 1991). It should be noted that the relationship between  $qE_{\text{C}}$  (defined as quenching coefficient) and  $[\text{H}^+]$  is non-linear.

#### a. Role of the Xanthophyll Cycle

Zeaxanthin (Zx) and antheraxanthin (Ax) are formed in the xanthophyll cycle from the di-epoxide violaxanthin (Vx), when the Vx de-epoxidase in the thylakoid lumen is activated by low pH in high light. In low light or darkness, Vx is restored by Zx epoxidase localized on the stromal side of the thylakoids:



No plausible function of the long-known xanthophyll cycle (Yamamoto et al., 1962) was found until Demmig et al. (1987) suggested a role of Zx in thermal energy dissipation expressed as non-photochemical quenching. Since then, in numerous studies, close linear correlations between Zx contents of leaves and  $qN_{\text{SV}}$  (presumably measured under conditions where  $qE_{\text{SV}}$  was its major component) was documented (Demmig-Adams and Adams, 1992; 1996a, 1999). Again, such a linear relationship applies for Stern-Volmer type quenching only. Also the mono-epoxide Ax, the intermediate of Zx formation, has been suggested to facilitate formation of qE (see Gilmore, 1997). In several investigations, a closer correlation between  $qN_{\text{SV}}$  and  $\text{Zx} + \text{Ax}$  than between  $qN_{\text{SV}}$  and Zx alone was found (e.g. Demmig-Adams and Adams, 1996b). In vitro studies indicated that only Ax formed in the de-epoxidation reaction is effective in enhancing the quenching, but not that formed by epoxidation of Zx (Gilmore et al., 1994). For details on the xanthophyll cycle and its physiological significance, the reader is referred to Chapters 14 and 15 of this volume, and to several chapters in *The Photochemistry of Carotenoids*, a recent volume in this series (Frank et al., 1999).

Enhanced thermal dissipation of excitation energy related to  $\Delta\text{pH}$ -dependent quenching has been demonstrated in isolated thylakoids by means of photoacoustic spectroscopy (e.g. Mullineaux et al., 1994; Yahyaoui et al., 1998). However, this technique was apparently not suitable to detect the increase in heat release that is supposedly related to formation of Zx and Ax (Yahyaoui et al., 1998).

#### b. Mechanism

There is an extensive literature on the possible mechanism of qE and the roles of the  $\Delta\text{pH}$  and xanthophyll cycle, which is not intended to be reviewed here (for a detailed review see Horton et al., 1996, 1999). In short, the acidification of the thylakoid lumen seems to cause conformational changes of chlorophyll *a,b*-binding antenna proteins of the light harvesting complex of PS II (LHCII) by protonation of acidic amino acid residues accessible at the luminal side of the membrane. The conformational changes are viewed as the basis of qE formation. They seem to be influenced by  $\text{Mg}^{2+}$  concentration and alkalization of the stroma (Noctor et al., 1993; Ruban and Horton, 1995a) and might be related to a cation exchange (protons for magnesium ions) at the inner membrane surface and  $\text{Mg}^{2+}$  transfer from lumen to stroma (Krause, 1978; Briantais et al., 1979; Mohanty et al., 1995). The hypothesis of allosteric changes of the LHCII is supported by certain characteristics of qE. Formation and relaxation of qE are usually slower than changes in the proton gradient (Bilger et al., 1988; Horton et al., 1996) and are correlated with apparent absorbance (light scattering) changes at about 535 nm (Krause, 1974; Bilger et al., 1988; Noctor et al., 1993; Bilger and Björkman, 1994; Horton et al., 1996). In isolated chloroplasts, formation and relaxation of qE were shown to be temperature-dependent, with activation energies around 65 kJ mol<sup>-1</sup> typical for enzymatic reactions, (Krause, 1992).

The presence of Zx (and Ax) is supposed to facilitate strongly the formation of qE at a given  $\Delta\text{pH}$ . No quenching is caused by these xanthophylls in the absence of lumen acidification. Particularly, the minor (inner) LHCII complexes, CP29, CP26 and CP24 (encoded by the *Lhcb4*, *Lhcb5* and *Lhcb6* genes, respectively) which are enriched in xanthophyll cycle pigments (Bassi et al., 1993; Färber et al., 1997) seem to be involved in the enhancement of qE by action of Zx. This is supported by experiments

with intermittent light grown pea plants (Jahns and Schweig, 1995) and by fluorescence lifetime studies with *chlorina* mutants of barley deficient in the major (outer) LHCII encoded by the *Lhcb1*, *Lhcb2* and *Lhcb3* genes (Briantais et al., 1996; Gilmore et al., 1996). According to Noctor et al. (1991), the presence of Zx is not obligatory for qE formation, and maximum qE can be induced at high  $Mg^{2+}$  concentration by a very high  $\Delta pH$  alone. However, in other studies with isolated thylakoids only about half-maximal  $qE_C$  values were obtained at maximum  $\Delta pH$ , when the xanthophyll cycle was inhibited (Thiele and Krause, 1994; Jahns and Schweig, 1995). In vivo, by blocking the de-epoxidase with dithiothreitol, a substantial Zx-independent qE component can be demonstrated (Adams et al., 1990b; Demmig-Adams et al., 1990), but this is never close to maximal qE seen in the absence of the inhibitor. From their experiments with intermittent light grown plants, Jahns and Schweig (1995) concluded that Zx-dependent qE mainly results from Zx interaction with the minor LHCII complexes, in particular with *Lhcb5* (CP26), whereas the outer LHCII are responsible for Zx-independent quenching.

The central role of Zx for qE was underlined by the analysis of xanthophyll cycle mutants of *Chlamydomonas reinhardtii* and *Arabidopsis thaliana* (Niyogi et al., 1997, 1998). Algae and plants deficient in Vx de-epoxidase (so-called *npq1* mutants), that were unable to generate Zx, showed little or no qE formation. On the other hand, when a permanently high Zx content was present in mutants deficient in Zx epoxidase (so-called *npq2* mutants), qE was generated more rapidly in comparison with wild type plants/algae.

At present, it is not clear whether Zx-independent qE does play a significant role in vivo when the xanthophyll cycle is active. There are indications that at the start of strong illumination in vivo, when Zx levels are still low, but a high  $\Delta pH$  is built up, considerable Zx-independent quenching may occur (Horton and Ruban, 1992, and our unpublished observations). That the Zx-independent component results from the presence of Ax, as suggested by Gilmore and Yamamoto (1993) appears unlikely, as such quenching was observed in the absence of substantial amounts of both Ax and Zx (Thiele and Krause, 1994). In the steady state of photosynthesis, when Zx has been formed and a more moderate  $\Delta pH$  is present due to its utilization in ATP synthesis, Zx-dependent qE seems to dominate, as indicated by the

close correlation between Zx content and  $qE_{sy}$ .

Several models have been suggested regarding the synergistic action between  $\Delta pH$  and Zx (or Zx+Ax) resulting in the allosteric changes of LHCII that are supposed to be responsible for qE (Horton and Ruban, 1992; Horton et al., 1996, 1999; Gilmore, 1997; Gilmore et al., 1998). Most evidence suggests that the same mechanism is underlying both the Zx-dependent and -independent qE. Presumably, the conformational changes caused by protonation of LHCII complexes lead to the formation of a fluorescence quencher. Binding of Zx (and Ax) seems to enhance the quenching, whereas Vx acts as an 'anti-quencher.' From the appearance of a short-lifetime component of fluorescence in the quenched state, Gilmore et al. (1995) concluded that a quenching complex of protonated LHCII and xanthophyll is formed. The quenching is supposed to be achieved either by interaction between Chl molecules ('concentration quenching') with Zx and Ax supporting a conformation with strong pigment aggregation (model of Horton and coworkers) or by direct singlet-singlet energy transfer from Chl to xanthophyll molecules (Frank et al., 1994; Owens, 1994). The latter appears possible due to the low-lying singlet excited state of Zx resulting from its larger conjugated  $\pi$  electron system. As discussed by Horton et al. (1996, 1999), both ways of quenching possibly take place within the quenching complex. The putative qE mechanism has found strong support from studies with isolated LHCII complexes (Horton et al., 1996; Ruban et al., 1996).

Recent analysis of another NPQ-mutant (called *npq4*) of *Arabidopsis* indicated that an intrinsic subunit of PS II, PsbS (Kim et al., 1994; Funk et al., 1995), is essential for qE (Li et al., 2000). The *npq4* mutant is devoid of PsbS, but exhibits normal  $\Delta pH$  and xanthophyll cycle activity. Interestingly, that mutant not only lacked qE but also the pH-induced conformational changes indicated by the apparent absorbance change at 535 nm. This may indicate that binding of one or more protons to PsbS may be required for qE (Li et al., 2000). It is unclear, however, whether the quenching process occurs in PsbS itself or if protonation of PsbS induces quenching, e.g. in *Lhcb4*, *Lhcb5* or *Lhcb6*.

### c. Quenching of Initial Fluorescence

In agreement with the qE site being in the Chl *a,b*-binding antennae, where the xanthophyll cycle

pigments are located, qE was found to be associated with a quenching of  $F_0$ , at first wrongly attributed to state 1–state 2 transition (Bilger and Schreiber, 1986). The  $F_0$  quenching has been confirmed in numerous studies (see Horton and Ruban, 1992, 1993; Spunda et al., 1997; Thiele et al., 1997). At maximal qE, about 20–30% and in extreme cases up to 50% of  $F_0$  are quenched. The variability of  $F_0$  has consequences for the exact determination of quenching coefficients (Sections V.A. and V.B.2). Matters become more complex as the  $F_0$  quenching has been found to depend on the wavelength of fluorescence emission.  $F_0$  is quenched considerably less at 730 nm than at 690 nm, as observed with a modulated two channel Hansatech fluorometer (Genty et al., 1990a). Obviously, the PS I component of  $F_0$  at  $\lambda > 710$  nm, which is about 30% in  $C_3$  plants and 50% in NADP-malic enzyme-type  $C_4$  species (Section III.A), does not participate in the quenching.

#### 4. State-Transition Quenching, qT

It has long been known that imbalances in the distribution of excitation energy between the two photosystems cause so-called state transitions that optimize the energy allocation (Bennett et al., 1980; Allen et al., 1981). The sensor of such imbalances appears to be the intersystem electron carrier plastoquinone (PQ). Dark-adapted leaves usually are in 'state 1', in which the PAR excites PS II more than PS I. Strong reduction of the PQ pool under this condition induces a decrease in the absorption cross section of PS II in favor of PS I; the system shifts towards 'state 2'. If in state 2 the actinic light is preferentially absorbed by PS I, the PQ pool becomes more oxidized and the state transition is reversed. The decrease in PS II absorption cross section during state 1–state 2 transition is reflected by a quenching of Chl fluorescence, termed qT. The transition is known to be achieved by phosphorylation of the peripheral LHCII that is controlled by the redox state of PQ and/or the cytochrome  $b_6f$  complex (Allen, 1992; Anderson, 1992). The phosphorylated LHCII is supposed to be detached from PS II, to move from the grana to the stroma lamellae of the thylakoids and to transfer absorbed light energy to PS I. The reversal of qT is mediated by a phosphatase and occurs in the dark with a half-time of about 4–8 min. Accordingly, qT relaxation can be abolished by NaF, a phosphatase inhibitor. The state transition may be viewed as one expression of a larger system of redox

control of photosynthesis including the control of transcription of plastidic genes encoding for PS I and PS II reaction center proteins (Pfannschmidt et al., 1999).

Theoretically, the above mechanism of state transition should result in quenching of  $F_0$  proportional to the decrease in  $F_M$ . This has, in fact, been confirmed by a study with isolated spinach chloroplasts incubated with ATP in low light. Analysis of 77K fluorescence showed  $F_0$  quenching together with a decrease in PS II and increase in PS I fluorescence (Krause and Behrend, 1983). The decrease in the fluorescence ratio PS II/PS I at 77K can serve to estimate qT under conditions when qE and qI are absent (Walters and Horton, 1991; 1993).

However, the concept that the light energy absorbed by the phosphorylated LHCII complexes is transferred to PS I is still debated. A linear relationship between the quenching of the PS II/PS I fluorescence ratio (at 77K) and qT with a slope of 1.0 was found, but this slope should be larger than 1.0, if energy transfer to PS I does occur (Walters and Horton, 1991). No significant  $F_0$  quenching at room temperature associated with qT has been observed (Walters and Horton, 1993). Based on these results, the authors suggested that qT is caused by a non-photochemical dissipative process in the phosphorylated LHCII complexes. At present, no final decision between these differing views is possible.

The state transition appears to be a physiologically important regulation to optimize photosynthesis in low, limiting light, where quenching coefficients,  $qT_c$ , between 0.1 to 0.2 can be observed (Horton and Hague, 1988; Walters and Horton, 1991; Jahns and Krause, 1994). Thus, qT is a relatively small quenching component, but can account for a significant portion of qN in low light. Adjustment of the PS II absorption cross section is of particular significance in environments with fluctuating conditions of light flux and light quality (see Chapter 15, this volume). Under excessive light, qT appears to be largely suppressed, possibly through control by the high-energy state resulting from a high  $\Delta pH$  (Ferryhough et al., 1984; Oxborough et al., 1987; Walters and Horton, 1991).

#### 5. Photoinhibitory Quenching, qI

Non-photochemical quenching related to photo-inhibition of PS II, qI, describes the slowly relaxing ( $t_{1/2} > 10$  min) components of qN that remain after qE

and  $qT$  have relaxed following a light-dark transition. As discussed in Section IV,  $qI$  is often expressed as a persistent decrease in  $F_v/F_m$ , the potential efficiency of PS II. This parameter is preferred in many studies because of the close empirical relationship between  $F_v/F_m$  and optimal quantum yield of photosynthesis. When with increasing actinic light, photosynthesis and  $qE_c$  reach saturation,  $qI$  becomes a major component of total  $qN$  (Walters and Horton, 1993), the degree of it depending on PAR and time of irradiation, as well as on genotype and acclimation state of the plant. Relaxation of  $qI$  ('recovery') from photoinhibition usually proceeds faster in low light (optimally at about  $30 \mu\text{mol m}^{-2} \text{s}^{-1}$ ) than in the dark (Skogen et al., 1986; Leitsch et al., 1994). In most cases,  $qI$  results almost exclusively from quenching of  $F_v$ , whereas  $F_0$  remains constant or exhibits an increase (e.g. Schnettger et al., 1994; Hong and Xu, 1999). Like  $qE$ ,  $qI$  indicates enhanced thermal dissipation of excitation energy in PS II, as shown by fluorescence characteristics at 77K (Demmig and Björkman, 1987; Somersalo and Krause, 1989).  $F_v$  of both PS II and PS I at 77K are quenched, but the decrease in PS I fluorescence is less pronounced which results in a lowered PS II/PS I fluorescence ratio.

Different mechanisms contribute to  $qI$  formation as is obvious from distinct phases of recovery kinetics seen in low light (Leitsch et al., 1994). Photoinhibition of PS II and the associated fluorescence quenching has in many studies been assigned to an inactivation of the PS II reaction center, where particularly the D1 protein is affected and exhibits fast turnover viewed as a repair process (see Aro et al., 1993). In excessive light, inactive PS II centers accumulate in which the D1 protein is 'marked' for degradation. No net degradation of D1 occurs; rather, proteolysis of D1 seems to proceed at the same rate as newly synthesized D1 becomes available for replacement (Aro et al., 1992; Schnettger et al. 1992, 1994). Obviously, the inactive centers act as fluorescence quenchers keeping the PS II unit in the  $F_0$  state (Krause et al., 1990; Briantais et al., 1992; Hong and Xu, 1999). However, as discussed below, inactivation and turnover of D1 appears to occur as the last line of defense against adverse effects of excessive light.

In experiments with spinach leaves, a fast phase of  $qI$  relaxation (up to about one hour) was shown to be unrelated to turnover of the D1 protein, as this phase was not abolished in the presence of streptomycin, an inhibitor of plastidic protein synthesis. A second

slower phase of recovery (several hours) was inhibited by streptomycin, indicating that only the more slowly relaxing component of  $qI$  is based on D1 protein inactivation (Leitsch et al., 1994; Thiele et al., 1996). The fast phase of  $qI$  relaxation was found to be closely associated with reconversion of Zx or Zx+Ax to Vx in the xanthophyll cycle (Thiele et al., 1996; 1998). In the presence of dithiothreitol, which fully inhibited formation of Zx during strong illumination, the fast recovery phase was absent and only slow  $qI$  relaxation supposedly related to D1 turnover was seen (Thiele et al., 1996). In a study with pea plants, both phases of  $qI$  relaxation were found to be kinetically related to Zx epoxidation (Jahns and Mische, 1996). Interestingly, a persistent high level of Zx in the thylakoid membrane as present in the *npq2* mutant of *Chlamydomonas* (Niyogi et al., 1997) not only reduced strongly the inactivation of PS II but also the degradation of D1 upon high-light stress (Jahns et al., 2000), indicating a protective role of Zx against photoinactivation of the PS II reaction center.

The mechanism of the Zx-dependent  $qI$  has not been clarified. One has to assume that during long periods of high-light stress, Zx (or Ax) is increasingly bound to other sites of the LHCII than for  $qE$  formation. In contrast to  $qE$ , a putative quenching complex should still be effective after the  $\Delta pH$  has relaxed and should not change  $F_0$ . Slow dissociation of Zx and Ax could make these xanthophylls available for epoxidation and result in  $qI$  reversion. An interaction of Zx with the reaction center core has also been discussed (Jahns and Mische, 1996; Färber et al., 1997; Verhoeven et al., 1999). The reported conversion of  $\beta$ -carotene to Zx during turnover of the D1 protein in *Chlamydomonas reinhardtii* (Depka et al., 1998; Jahns et al., 2000) might represent Zx formation in the reaction center core. However, no strict experimental evidence is available so far to support this view.

In leaves that are constitutively adapted and well acclimated to high-light stress and have a large pool and high turnover of xanthophyll cycle pigments, Zx-related  $qI$  seems to dominate, and D1 inactivation and degradation to play a minor role. This was demonstrated for spinach cold-acclimated under excess light and for young sun leaves of tropical forest trees (Krause et al., 1995; 1999b; Thiele et al., 1996, 1997). Also in leaves of high mountain plants, D1 protein turnover under light stress was found to be strongly reduced (Streb et al., 1997). After severe stress, in particular when exerted by low temperatures

combined with excessive light, high Zx+Ax levels may be maintained for extended periods, e.g. over night. In such cases, very slow relaxation of qI was also correlated with epoxidation (Adams et al., 1995; Jahns and Miele, 1996; Verhoeven et al., 1996; Demmig-Adams et al., 1998). It is unknown whether or to what extent D1 turnover is involved here.

It has been suggested that (part of) qI results from a persistent  $\Delta pH$  sustained in the dark (or low light) by ATP hydrolysis (see Gilmore, 1997). This implies that the impact of preceding stress hinders the normal inactivation of the plastidic ATP synthase in the dark. ATP could be supplied by respiration, which is consistent with increased dark respiration rates seen upon photoinhibitory irradiation of leaves (Somersalo and Krause, 1990). Except for the mode of  $\Delta pH$  formation, the mechanism of such qI would be identical with that of qE, although it does not account for the absence of  $F_0$  quenching in qI. In experiments with spinach, a significant part of qI could be reversed by infiltration with the uncoupler nigericin (Ruban and Horton, 1995b). But since no  $\Delta pH$  could be detected upon chloroplast isolation, the nigericin-sensitive qI was ascribed to a conformational change that is reversed by action of nigericin. A recent study (Koroleva et al., 1998) demonstrated an ATP-dependent quenching that was relaxed by uncoupling with nigericin in spinach thylakoids isolated immediately after strong illumination of leaves at 4°C. In spinach in the field during winter at leaf temperatures between -5 and +6 °C, high Zx+Ax levels were retained over night and associated with a substantial nigericin-sensitive qI. Leaves of *Cucurbita maxima* (pumpkin), a chilling-sensitive species, exposed to high light at 4 °C exhibited a nigericin-sensitive qI component persisting for several hours at room temperature in low light (30  $\mu\text{mol m}^{-2} \text{s}^{-1}$ ), while slow de-epoxidation still took place for about one hour. As maintenance of an active de-epoxidase requires an acidic thylakoid lumen, these data suggest that, in fact, a low  $\Delta pH$  built up by ATP hydrolysis and sustained Zx+Ax levels are responsible for part of qI. A strongly reduced epoxidase activity (Färber and Jahns, 1998) possibly supports the retaining of high levels of Zx and Ax. It should be noted that depending on conditions only a fraction of qI can be attributed to this mechanism.

In summary, qI may consist of at least three components, based on (i) a persistent  $\Delta pH$  and Zx+Ax level causing qE-type quenching, (ii) bound de-epoxidized xanthophylls that maintain a dissipative

state in the absence of a  $\Delta pH$  and (iii) inactivation of the PS II reaction center as manifested by subsequent D1 protein degradation and replacement. The roles of Zx and D1 protein turnover in non-photochemical quenching processes are schematically illustrated in Fig. 5.

## VI. Photosynthetic Yield and Rate of Linear Electron Transport Determined by Fluorescence Analysis

### A. Quantum Efficiency of Photosystems II and I

Genty et al. (1989) were first to report that in the steady state of photosynthesis or, more generally, at any time during continuous actinic illumination, the product of qP and  $F_v'/F_m'$  (the potential efficiency of PS II in the light) is proportional to the apparent quantum yield of  $\text{CO}_2$  assimilation. This applied for  $C_3$  and  $C_4$  plants under a variety of experimental conditions. As discussed above (V.B.1), the reduction in  $F_v/F_m$  caused by actinic light is an expression of non-photochemical quenching. In the model proposed by the authors, the product  $qP \cdot F_v'/F_m'$  represents the quantum efficiency of PS II-driven electron transport,  $\Phi_{\text{PS II}}$ . With Eq. (1) for qP one obtains

$$\begin{aligned}\Phi_{\text{PS II}} &= qP \cdot F_v'/F_m' = (F_m' - F)/F_m' \\ &= \Delta F/F_m',\end{aligned}\quad (17)$$

where F is the total fluorescence yield in the light and  $\Delta F$  the fluorescence increment obtained with a saturating pulse (Fig. 4A). Thus, valuable information on PS II electron transport can be obtained just from the response of fluorescence to a saturating light pulse given during continuous illumination. Due to its simplicity, this approach has found wide application.

Equation (17) is based on the model of Butler (1978), assuming a limitation of the primary photochemical reaction by the exciton transfer from the antennae to the reaction center. In contrast, the now widely accepted 'exciton-radical pair equilibrium model' (Schatz et al., 1988; Holzwarth, 1991; Holzwarth and Roelofs, 1992) is based on fast equilibration of excitation energy between antennae and reaction center and on reversibility of the primary charge separation. Model calculations that also considered connectivity between PS II units (Trissl and Lavergne, 1994; Lavergne and Trissl, 1995) have

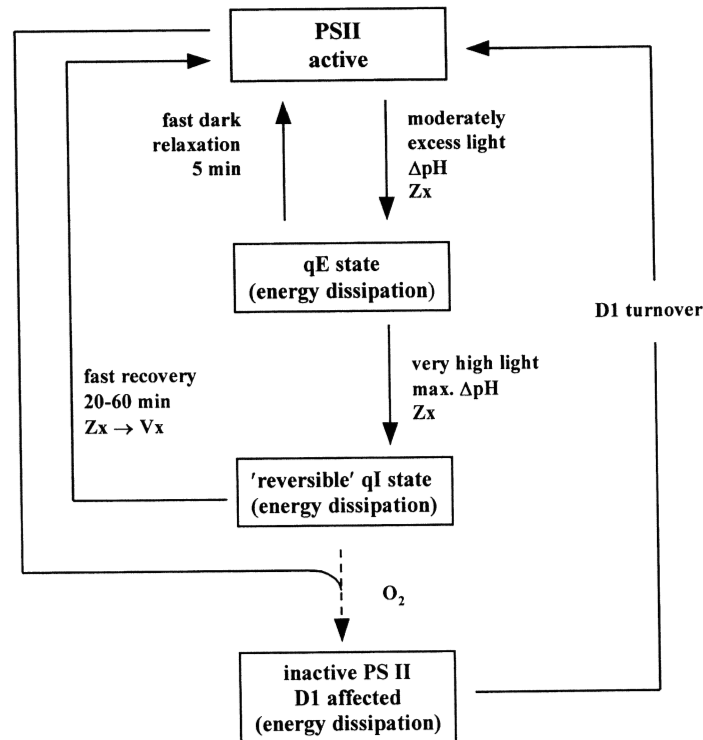


Fig. 5. Scheme of hypothetical energy-dissipating states of PS II related to non-photochemical fluorescence quenching. Moderate light stress is thought to predominantly induce the fast relaxing qE state by action of the trans-thylakoid  $\Delta pH$  and zeaxanthin (plus antheraxanthin). Stronger and longer lasting light stress leads to a reversible qI state in which supposedly more persistent binding of zeaxanthin is involved. When these protective mechanisms are overcharged, enhanced formation of active oxygen species from ground-state  $O_2$  may inactivate the D1 protein in the reaction center. For reasons of simplicity, a possible contribution of a sustained  $\Delta pH$  to the qI state and of xanthophyll involvement in relation to D1 turnover (see text) are not considered in the scheme. Adapted from Thiele et al. (1996) with permission from Elsevier Science.

confirmed that equation (17) is approximately valid for this complex model. It was calculated that  $\Delta F/F_M'$  only slightly (by about 14%) underestimated the quantum efficiency of PS II. In a notable episode, an article by Holzwarth (1993), entitled 'Is it time to throw away your apparatus for chlorophyll fluorescence induction?' was prompted by an earlier model study of Trissl et al. (1993) that contained a subsequently corrected computation error (Lavergne and Trissl, 1995).

Studies on numerous plant species in most cases did not show a strictly linear correlation between  $\Phi_{PSII}$  and apparent quantum yield of  $CO_2$  assimilation or  $CO_2$ -dependent  $O_2$  evolution,  $\Phi_p$ . In particular, deviations from linearity were reported for  $C_3$  plants when  $\Delta F/F_M'$  and  $\Phi_p$  were determined as function of PAR under photorespiratory conditions (Genty et al., 1990b; Harbinson et al., 1990). This is plausible, as photorespiration reduces net  $CO_2$  fixation at a given electron flux. A strong increase in the ratio  $\Phi_{PSII}/\Phi_p$

with temperature found for a  $C_3$  plant in normal air was interpreted as a result of enhanced photorespiration (Oberhuber and Edwards, 1993). Under non-photorespiratory conditions, as well as in  $C_4$  plants,  $\Phi_{PSII}/\Phi_p$  was low and did not change significantly with temperature. In leaves of  $C_4$  plants such as maize (*Zea mays*), where photorespiration is minimal, the model provided reasonable estimates of  $CO_2$  assimilation at varying  $CO_2$  concentrations, temperatures and light fluxes (Edwards and Baker, 1993). When photorespiration was suppressed in  $C_3$  plants by saturating  $CO_2$ , the plots of  $\Phi_{PSII}$  versus  $\Phi_p$  were approximately linear under high and moderate light. The plots deviated from linearity in the region of high quantum yield ( $\Phi_p$  values above 0.04) as measured under low, limiting light (Seaton and Walker, 1990; Öquist and Chow, 1992). A similar relationship between  $\Phi_{PSII}$  and measured electron transport rates was obtained with isolated thylakoids (Hormann et al., 1994). The curvilinear relation

between  $\Phi_{\text{PSII}}$  and  $\Phi_{\text{p}}$  (in the absence of photorespiration) was uniform among many species including  $C_3$ ,  $C_4$  and CAM plants, except for barley leaves (Öquist and Chow, 1992). The curvature of the correlation can be minimized, if 'true' quantum yields of  $\text{CO}_2$  assimilation,  $\Phi_{\text{CO}_2^*}$ , are determined, considering the fraction of absorbed light and the rate of  $\text{CO}_2$  release by mitochondrial respiration (Oberhuber et al., 1993). The latter, however, is difficult to assess in a leaf under illumination. Remaining small deviations from linearity, seen below 5% of full sunlight, were tentatively attributed to variations in mitochondrial respiration or other processes, such as electron transfer to  $\text{O}_2$  and nitrogen assimilation (Oberhuber et al., 1993). Thus, the relationship between  $\Phi_{\text{PSII}}$  and  $\Phi_{\text{p}}$  has to be established for the plant system investigated and conditions applied in order to obtain exact information on  $\Phi_{\text{p}}$  from fluorescence data. But for many species, similar relationships can be expected under standardized conditions.

Photoinhibited leaves exhibited reduced maximum values of both  $\Phi_{\text{p}}$  and  $\Phi_{\text{PSII}}$ , but the relationships between the two parameters were very similar to those of non-inhibited control leaves (Öquist and Chow, 1992). When fluorescence was monitored in sun leaves of tropical trees in situ during the course of the day, photoinhibition became apparent by reductions in  $\Phi_{\text{PSII}}$ , when after high-light exposure the PAR declined towards sunset or due to shading by clouds (Krause et al., 1995). The relationship between  $\Phi_{\text{PSII}}$  and  $\Phi_{\text{p}}$  did not change under drought stress (Cornic and Briantais, 1991). An approximately linear correlation between  $\Phi_{\text{PSII}}$  and  $\Phi_{\text{p}}$ , measured at high  $\text{CO}_2$  and an intermediate PAR, was observed in sugar beet (*Beta vulgaris*) leaves subjected to increasing iron deficiency (Morales et al., 1998). These examples show that the model can be well applied to study stress effects in plant leaves.

The 'Genty model' has also been tested by simultaneous measurements of  $\Phi_{\text{PSII}}$  and absorbance changes around 810 to 830 nm representing the quantum efficiency of PS I,  $\Phi_{\text{PSI}}$  (Harbinson et al., 1989; 1990; Genty et al., 1990b; Klughammer and Schreiber, 1994). Under conditions where cyclic electron transport around PS I was supposedly negligible, linear correlations between  $\Phi_{\text{PSII}}$  and  $\Phi_{\text{PSI}}$  were found. PS I activity can now be conveniently measured with a supplementary device of the PAM system (Klughammer and Schreiber, 1998). Using a modulated dual wavelength (810 versus 860 nm)

measuring light, P700 oxidation in actinic light is recorded as absorbance change,  $\Delta A_{810}$ . The maximal absorbance change,  $\Delta A_{810_{\text{max}}}$ , obtained under saturating far-red light (or by a short saturating pulse of white light), denotes full oxidation of P700 and provides a measure of PS I electron transport capacity. The proportion of P700 that remains reduced in the steady state of illumination then is

$$\text{P700}_{\text{red}} = 1 - \Delta A_{810} / \Delta A_{810_{\text{max}}}, \quad (18)$$

which may be taken as an estimate of  $\Phi_{\text{PSI}}$  (Genty et al., 1990b).

In a more complex model (Weis and Berry, 1987), two PS II populations, one with 'normal' activity and the other with energy-dissipating reaction centers were postulated. This model predicts a linear negative correlation between  $\Phi_{\text{S}}/qP$  and  $qN_{\text{C}}$ , where  $\Phi_{\text{S}}$  is the quantum yield of PS II electron transport in the steady state and  $\Phi_{\text{S}}/qP$  denotes the quantum yield of open reaction centers. Such linear correlation has been documented for several species (Weis and Berry, 1987; Sharkey et al., 1988; Öquist and Chow, 1992). An exception was barley, which showed a curvilinear relationship. As it is now well established that the qE component of qN is based on energy dissipation in the Chl *a/b* antennae rather than in the reaction centers, the model of Weis and Berry would need some modification. However, from their comparative study, Öquist and Chow (1992) concluded that on an empirical basis, both models provide useful means to predict photosynthetic function from fluorescence measurements. But the authors point out that the relationships between photosynthesis and fluorescence in the two models are not universal. The model of Weis and Berry (1987) requires  $F_0$  determination to calculate qP and  $qN_{\text{C}}$  values, which makes the model of Genty et al. (1989) easier to apply.

### B. Electron Transport through PS II

From the fluorescence parameter  $\Phi_{\text{PSII}}$  (equation 17), rates of PS II-driven electron transport,  $J_{\text{F}}$ , can be calculated. As  $\Phi_{\text{PSII}}$  represents the number of electrons transferred per photon absorbed by PS II, the rate of electron transport ( $\text{mol e}^- \text{m}^{-2} \text{s}^{-1}$ ) is

$$J_{\text{F}} = \Phi_{\text{PSII}} \cdot I \cdot a \cdot f, \quad (19)$$

where  $I$  is the incident PAR ( $\text{mol photons m}^{-2} \text{s}^{-1}$ ),  $a$  is the fraction of light absorbed by the leaf, and  $f$  the



fraction of absorbed light energy distributed to PS II (Krall and Edwards, 1992). The absorbance can be measured with an integrating sphere (Demmig and Björkman, 1987; Krause et al., 1995) and usually is around 0.84 in non-succulent mature leaves. Young developing leaves may, however, have a significantly lower absorbance depending on the pigment content per leaf area unit. For the steady state of photosynthesis, an approximately even distribution of excitation energy between PS II and I can be assumed, i.e.  $f = 0.5$ . In many cases, for 'normal' mature leaves,  $J_F$  can be estimated without determination of  $\alpha$  using the simple equation

$$J_F = 0.42 \Phi_{PSII} \cdot I. \quad (20)$$

If the net  $\text{CO}_2$  assimilation rate,  $A_{\text{CO}_2}$ , is measured simultaneously with fluorescence, the number of electrons transported through PS II per mol  $\text{CO}_2$  fixed,  $e^-/\text{CO}_2 = J_F/A_{\text{CO}_2}$ , is obtained (Krall and Edwards, 1992). The theoretical minimum of  $e^-/\text{CO}_2$  is 4. Data from measurements under different PAR show values of  $e^-/\text{CO}_2$  between about 5 and 6 in  $\text{C}_4$  plants and 9–13 in  $\text{C}_3$  plants (under air levels of  $\text{CO}_2$ ). The much higher values exhibited by  $\text{C}_3$  species were attributed to  $\text{CO}_2$  loss by photorespiration. In a study of tropical trees under full natural sunlight (Krause et al., 1995),  $e^-/\text{CO}_2$  increased during the 'midday depression' of photosynthesis to values between 15 and 23. Such decreased efficiency of net  $\text{CO}_2$  fixation may be explained by increased rates of photorespiration due to partial closure of stomates and very high leaf temperatures. Also enhanced rates of electron transfer to  $\text{O}_2$  (Mehler reaction) may contribute to increased  $e^-/\text{CO}_2$  ratios. Thus, simultaneous determination of  $J_F$  and  $A_{\text{CO}_2}$  allows to estimate the partitioning of PS II electron transport between reactions that do or do not result in carbon gain (Cornic and Briantais, 1991).

With commercially available instrumentation (MINI-PAM),  $J_F$  can be determined in a rapid succession of saturating pulses applied, e.g. every 10 s, under stepwise increasing actinic irradiance (White and Critchley, 1999). From the data, a light-saturation curve of  $J_F$  is obtained termed 'rapid light curve' that provides useful information on the state of the photosynthetic apparatus, for instance on the maximum electron transport rate at the chosen time of measurement.

## VII. Application of Chlorophyll Fluorescence in the Study of Mutants

Chl fluorescence has become one of the most powerful tools not only to study and characterize but particularly to identify mutants with defects that affect photosynthetic electron transport. The most simple method for this purpose is the detection of the so-called high Chl fluorescence (*hcf*) phenotype of randomly generated mutants. This method has already been introduced more than 30 years ago by Garnier (1967) and Bennoun and Levine (1967) for the detection of mutants in green algae. The basic concept of this method is that any inhibitory effect on electron flow through the photosynthetic electron transport chain will result in an increased portion of excitation energy that is re-emitted as Chl fluorescence. Since the early 1980s, when this method was applied by Miles (1980; 1982) to higher plants, a large number of *hcf* mutants have been identified in *Chlamydomonas reinhardtii*, *Zea mays*, *Hordeum vulgare* and *Arabidopsis thaliana* (e.g. Bennoun and Delepelaire, 1982; Simpson et al., 1985; Somerville 1986; Taylor et al., 1987; Dinkins et al., 1994, 1999; Meurer et al., 1996).

Mutants that can be isolated on the basis of the *hcf* phenotype usually cover all kinds of defects in the functions of PS II, cytochrome *b<sub>6</sub>f*, PS I, photophosphorylation,  $\text{CO}_2$  fixation and other processes related to the photosynthetic electron transport. The most important advantage of the *hcf* phenotype is that it can easily be determined just by eye under illumination of plants/algae with UV light. Thus, this procedure does not require any expensive instrumentation. However, the information about the specificity of an identified mutant is low. The determination of a few parameters by pulse modulation fluorometry can subsequently be used for a classification of the different mutants. Plants with defects in complexes of the photosynthetic electron transport chain can be simply identified by determining PS II fluorescence parameters such as  $F_v/F_m$ ,  $qN$  and  $qP$  in combination with measurements of the redox kinetics of P700 (Section VI.1), all during a 5 to 10 min illumination period with non-saturating actinic light (Meurer et al., 1996). PS II mutants are expected to show no or a strongly decreased yield of maximum variable fluorescence,  $F_v$  (Simpson and von Wettstein, 1980; Meurer et al., 1996) while PS I mutants can be identified by the absence of P700 absorbance changes (Harbinson

and Woodward, 1987; Meurer et al., 1996). Mutants with defects in the electron transport chain between plastoquinone and plastocyanin show a similarly high  $F_v$  as PS I mutants, but are distinguishable from those by the presence of PS I-related absorbance changes in the far-red region (Meurer et al., 1996). Moreover, a variety of other mutants with deficiencies in assimilation of  $\text{CO}_2$ ,  $\text{NO}_3^-$  and  $\text{SO}_4^{2-}$  can be identified by the *hcf* phenotype. Thus, screening for the *hcf* phenotype helps to identify mutants with a wide range of primary lesions, ranging from defects in the expression of proteins and the assembly of protein complexes to more complex phenomena like disturbed regulation of enzyme activities and signal transduction.

In a different approach, the post-illumination fluorescence rise (transient apparent  $F_0$  increase; Section III.A) has been used to identify and study transgenic tobacco plants containing mutated plastidic genes encoding subunits of the NAD(P)H:plastoquinone oxidoreductase (Kofer et al., 1998; Burrows et al., 1998). By combining molecular-genetic methods with analyses of Chl fluorescence and P700 absorbance changes, the functionality of this enzyme in chloroplasts has been proven.

Refined methods of fluorescence measurement have emerged during the last years based on the progress in video imaging of Chl fluorescence by the application of Charge-Coupled Device (CCD) cameras in combination with computer videoboards (see Kramer and Crofts, 1996). The development of these techniques made it rather simple and thus practical to map the photosynthetic performance of the surface of a leaf, different leaves of a plant or leaves from different plants on a single image (Daley et al., 1989; Mott et al., 1993; Genty and Meyer, 1994; Rolfe and Scholes, 1995; Siebke and Weis, 1995; Lichtenthaler, 1996; Lichtenthaler et al., 1996; Meyer and Genty, 1998). However, video imaging of fluorescence is not only useful for monitoring the heterogeneity of photosynthetic activities and stress responses in different regions of a leaf or a plant, but it is also an important method for screening photosynthetic mutants.

The progress in computer technology made it also very simple and affordable to do kinetic fluorescence imaging (although the time resolution is rather low), increasing the yield of information during the screening for mutants dramatically. Kinetic fluorescence imaging may allow a specific screening for more limited genetic defects. This helps to

significantly reduce the number of mutants that have to be investigated in more detail by other (biochemical, biophysical or genetic) methods.

Using such imaging procedures, Niyogi and co-workers were able to identify several mutants with defects in non-photochemical quenching of Chl fluorescence (Niyogi et al., 1997, 1998; Niyogi, 1999; Li et al., 2000). Physiological and genetic analysis of the mutants brought large progress in the understanding of the different mechanisms that may be involved in photoprotection by thermal energy dissipation (Section V.B.3). Fluorescence imaging together with modulated fluorescence recording and fluorescence spectroscopy at 77K served to identify state transition mutants of *Chlamydomonas reinhardtii* (Kruse et al., 1999).

One severe limitation of most video imaging systems is the rather low time resolution, which e.g. does not allow for an exact measurement of  $F_0$  and  $F_M$ . Any more detailed analysis of kinetics requires therefore the use of a separate instrumentation such as modulation fluorometers which can be used for time resolved analyses of fluorescence transients. A method to calculate  $F_0'$  from fluorescence images and thus to obtain the values for qP and  $F_v'/F_M'$  has been published by Oxborough and Baker (1997). Very recently a new imaging instrument has been developed which combines the advantage of modulated measuring light with video imaging of chlorophyll fluorescence (L. Nedbal, personal communication). This technique may open the door for more refined screening procedures and allow to identify new, so far unapproachable mutants.

## VIII. Conclusion and Perspectives

The Chl fluorescence parameters discussed in this chapter are easy to measure in leaves of vascular plants both in the laboratory and in the field by means of standard commercial instruments. This simplicity has allowed the wide application of modulated fluorescence. The review of the literature, however, shows that the interpretation of parameters supplied by modulation fluorometers is complex, the underlying mechanisms are not fully clarified and theoretical models have limitations. Moreover, problems of accurate measurements, e.g. of  $F_0$  and  $F_M$  under varying conditions may arise. Nevertheless, fluorescence parameters provide important information on photosynthetic performance in plants, even if

on a half-empirical basis. Care should always be taken not to over-interpret fluorescence data, and to cross-check their validity by other methods in the plant system studied.

As standard equipment for fluorometry has been improved in the last decade almost to perfection, a trend towards more specialized applications can be seen. Progress is apparent in fluorescence analyses of systems with very low Chl content such as phytoplankton, both by means of non-modulated (Kolber et al., 1998) and modulated fluorescence (Schreiber, 1998). Such measurements require a 1000 to 10 000 times higher sensitivity than for fluorescence detection in plant leaves with high Chl density (see Chapter 15). Highly sensitive modulation fluorometers can now be applied to measure Chl fluorescence in a single cell, protoplast or even chloroplast (Schreiber, 1998; Goh et al., 1999). Other specialties include measurement inside a leaf with a fiber-optic microprobe (Schreiber et al., 1996), underwater fluorometry (Schreiber et al., 1997) and determination of the transmittance of ultraviolet light through the leaf epidermis (Bilger et al., 1997). Refined and specialized equipment will certainly open further fields for the Chl fluorescence method.

## Acknowledgment

The authors thank the Deutsche Forschungsgemeinschaft (SFB 189) for support of research related to the subject of this chapter.

## References

- Adams WW III, Demmig-Adams B, Winter K and Schreiber U (1990a) The ratio of variable to maximum chlorophyll fluorescence from Photosystem II, measured in leaves at ambient temperature and at 77K, as an indicator of the photon yield of photosynthesis. *Planta* 180: 166–174
- Adams WW III, Demmig-Adams B and Winter K (1990b) Relative contributions of zeaxanthin-related and zeaxanthin-unrelated types of 'high-energy-state' quenching of chlorophyll fluorescence in spinach leaves exposed to various environmental conditions. *Plant Physiol* 92: 302–309
- Adams WW III, Demmig-Adams B, Verhoeven AS and Barker DH (1995) 'Photoinhibition' during winter stress: Involvement of sustained xanthophyll cycle-dependent energy dissipation. *Aust J Plant Physiol* 22: 261–276
- Allen DJ, McKee IF, Farage PK and Baker NR (1997) Analysis of limitations to CO<sub>2</sub> assimilation on exposure of leaves of two *Brassica napus* cultivars to UV-B. *Plant Cell Environ* 20: 633–640
- Allen JF (1992) Protein phosphorylation in regulation of photosynthesis. *Biochim Biophys Acta* 1098: 275–335
- Allen JF, Bennett J, Steinback KE and Arntzen CJ (1981) Chloroplast protein phosphorylation couples plastoquinone redox state to distribution of excitation energy between photosystems. *Nature* 291: 25–29
- Anderson JM (1992) Cytochrome *b<sub>6</sub>f* complex: Dynamic molecular organization, function and acclimation. *Photosynth Res* 34: 341–357
- Aro E-M, Kettunen R and Tyystjärvi E (1992) ATP and light regulate D1 protein modification and degradation. *FEBS Lett* 297: 29–33
- Aro E-M, Virgin I and Andersson B (1993) Photoinhibition of Photosystem II. Inactivation, protein damage and turnover. *Biochim Biophys Acta* 1143: 113–134
- Barth C and Krause GH (1999) Inhibition of Photosystem I and II in chilling-sensitive and chilling-tolerant plants under light and low-temperature stress. *Z Naturforsch* 54c: 645–657
- Bassi R, Pineau B, Dainese P and Marquardt J (1993) Carotenoid-binding proteins of Photosystem II. *Eur J Biochem* 212: 297–303
- Behrenfeld MJ, Prasil O, Kolber, ZS, Babin M and Falkowski PG (1998) Compensatory changes in Photosystem II electron turnover rates protect photosynthesis from photoinhibition. *Photosynth Res* 58: 259–268
- Bennett J, Steinback KE and Arntzen CJ (1980) Chloroplast phosphoproteins: Regulation of excitation energy transfer by phosphorylation of thylakoid membrane polypeptides. *Proc. Natl. Acad. Sci. USA* 77: 5253–5257
- Bennoun P and Delepelaire P (1982) Isolation of photosynthesis mutants in *Chlamydomonas*. In: Hallick R, Edelman M and Chua N (eds) *Methods in Chloroplast Molecular Biology*, pp 25–38. Elsevier, New York
- Bennoun P and Levine RP (1967) Detecting mutants that have impaired photosynthesis by their increased level of fluorescence. *Plant Physiol* 42: 1284–1287
- Bilger W and Björkman O (1994) Relationships among violaxanthin deepoxidation, thylakoid membrane conformation, and non-photochemical chlorophyll fluorescence quenching in leaves of cotton, *Gossypium hirsutum* L. *Planta* 193: 238–246
- Bilger W and Schreiber U (1986) Energy-dependent quenching of dark-level chlorophyll fluorescence in intact leaves. *Photosynth Res* 10: 303–308
- Bilger W, Heber U and Schreiber U (1988) Kinetic relationship between energy-dependent fluorescence quenching, light scattering, chlorophyll luminescence and proton pumping in intact leaves. *Z. Naturforsch* 43c: 877–887
- Bilger W, Veit M, Schreiber L and Schreiber U (1997) Measurement of leaf epidermal transmittance of UV radiation by chlorophyll fluorescence. *Physiol Plant* 101: 754–763
- Björkman O (1987) Low-temperature chlorophyll fluorescence in leaves and its relationship to photon yield of photosynthesis in photoinhibition. In: Kyle DJ, Arntzen CJ and Osmond CB (eds) *Photoinhibition*, pp 123–144. Elsevier, Amsterdam
- Björkman O and Demmig B (1987) Photon yield of O<sub>2</sub> evolution and chlorophyll fluorescence characteristics at 77K among vascular plants of diverse origins. *Planta* 179: 489–504
- Bornman JF, Vogelmann TC and Martin G (1991) Measurement of chlorophyll fluorescence within leaves using a fibreoptic microprobe. *Plant Cell Environ* 14: 719–725

- Briantais J-M, Vernotte C, Picaud M and Krause GH (1979) A quantitative study of the slow decline of chlorophyll *a* fluorescence in isolated chloroplasts. *Biochim Biophys Acta* 548: 128–138
- Briantais J-M, Vernotte C, Krause GH and Weis E (1985) Chlorophyll *a* fluorescence of higher plants: Chloroplasts and leaves. In: Govindjee, Ames J and Fork DC (eds) *Light Emission by Plants and Bacteria*, pp 539–583 Academic Press, Orlando
- Briantais J-M, Ducruet J-M, Hodges M and Krause GH (1992) The effects of low temperature acclimation and photoinhibitory treatments on Photosystem 2 studied by thermoluminescence and fluorescence decay kinetics. *Photosynth Res* 31: 1–10
- Briantais J-M, Dacosta J, Goulas Y, Ducruet J-M and Moya I (1996) Heat stress induces in leaves an increase of the minimum level of chlorophyll fluorescence,  $F_0$ : A time-resolved analysis. *Photosynth Res* 48: 189–196
- Burrows PA, Sazanov LA, Svab Z, Maliga P and Nixon PJ (1998) Identification of a functional respiratory complex in chloroplasts through analysis of tobacco mutants containing disrupted plastid *ndh* genes. *EMBO J* 17: 868–876
- Butler WJ (1978) Energy distribution in the photosynthetic apparatus of photosynthesis. *Annu Rev Plant Physiol* 29: 345–378
- Cao J and Govindjee (1990) Chlorophyll *a* fluorescence transient as an indicator of active and inactive Photosystem II in thylakoid membranes. *Biochim Biophys Acta* 1015: 180–188
- Cornic G and Briantais J-M (1991) Partitioning of photosynthetic electron flow between  $CO_2$  and  $O_2$  reduction in a  $C_3$  leaf (*Phaseolus vulgaris* L.) at different  $CO_2$  concentrations and during drought stress. *Planta* 183: 178–184
- Daley PF, Raschke K, Ball JT and Berry JA (1989) Topography of photosynthetic activity of leaves obtained from video images of chlorophyll fluorescence. *Plant Physiol* 9: 1233–1238
- Dau H (1994) Molecular mechanisms and quantitative models of variable Photosystem II fluorescence. *Photochem Photobiol* 60: 1–23
- Demmig B and Björkman O (1987) Comparison of the effect of excessive light on chlorophyll fluorescence (77K) and photon yield of  $O_2$  evolution in leaves of higher plants. *Planta* 171: 171–184
- Demmig B and Winter K (1988) Characterisation of three components of non-photochemical fluorescence quenching and their response to photoinhibition. *Aust J Plant Physiol* 15: 163–177
- Demmig B, Winter K, Krüger A and Czygan F-C (1987) Photoinhibition and zeaxanthin formation in intact leaves. A possible role of the xanthophyll cycle in the dissipation of excess light energy. *Plant Physiol* 84: 218–224
- Demmig-Adams B and Adams WW III (1992) Photoprotection and other responses of plants to high light stress. *Annu Rev Plant Physiol Plant Mol Biol* 43: 599–626
- Demmig-Adams W and Adams WW III (1996a) The role of xanthophyll cycle carotenoids in the protection of photosynthesis. *Trends Plant Sci* 1: 21–26.
- Demmig-Adams W and Adams WW III (1996b) Xanthophyll cycle and light stress in nature: Uniform response to excess direct sunlight among higher plant species. *Planta* 198: 460–470
- Demmig-Adams B, Adams WW III, Heber U, Neimanis S, Winter K, Krüger A, Czygan F-C, Bilger W and Björkman O (1990) Inhibition of zeaxanthin formation and of rapid changes in radiationless energy dissipation by dithiothreitol in spinach leaves and chloroplasts. *Plant Physiol* 92: 293–301
- Demmig-Adams B, Moeller DL, Logan BA and Adams WW III (1998) Positive correlation between levels of retained zeaxanthin + antheraxanthin and degree of photoinhibition in shade leaves of *Schefflera arboricola* (Hayata) Merrill. *Planta* 205: 367–374.
- Demmig-Adams B, Adams WW III, Effert V and Logan BA (1999) Ecophysiology of the xanthophyll cycle. In: Frank HA, Young AJ, Britton G and Cogdell RJ (eds) (1999) *The Photochemistry of Carotenoids*, pp 245–269, Kluwer Academic Publishers, Dordrecht
- Depka B, Jahns P and Trebst A (1998)  $\beta$ -Carotene to zeaxanthin conversion in the rapid turnover of the D1 protein of Photosystem II. *FEBS Lett* 424: 267–270
- Dinkins RD, Bandaranayake H, Green BR and Griffiths AJF (1994) A nuclear photosynthetic electron transport mutant of *Arabidopsis thaliana* with altered expression of the chloroplast *petA* gene. *Curr. Genet* 25: 282–288
- Dinkins RD, Bandaranayake H, Baeza L, Griffiths AJF and Green BR (1997) *hcf5*, a nuclear photosynthetic electron transport mutant of *Arabidopsis thaliana* with a pleiotropic effect on chloroplast gene expression. *Plant Physiol* 113: 1023–1031
- Duysens LNM and Sweers HE (1963) Mechanism of the two photochemical reactions in algae as studied by means of fluorescence. In: Jap Soc Plant Physiol (ed) *Studies on Microalgae and Photosynthetic Bacteria*, pp 353–372. University of Tokyo Press, Tokyo
- Edwards GE and Baker NR (1993) Can  $CO_2$  assimilation in maize leaves be predicted accurately from chlorophyll fluorescence analysis? *Photosynth Res* 37: 89–102
- Falkowski PG and Kolber Z (1995) Variations of chlorophyll fluorescence yields in phytoplankton in the world oceans. *Aust J Plant Physiol* 22: 341–355
- Färber A and Jahns P (1998) The xanthophyll cycle of higher plants: Influence of antenna size and membrane organization. *Biochim Biophys Acta* 1363: 47–58
- Färber A, Young AJ, Ruban AV, Horton P and Jahns P (1997) Dynamics of xanthophyll-cycle activity in different antenna subcomplexes in the photosynthetic membranes of higher plants: The relationship between zeaxanthin conversion and nonphotochemical fluorescence quenching. *Plant Physiol* 115: 1609–1618
- Fernyhough P, Foyer C and Horton P (1984) Increase in the level of thylakoid protein phosphorylation in maize mesophyll chloroplasts by decrease in the transthylakoid pH gradient. *FEBS Lett* 176: 133–138
- Frank HA, Cua A, Chynwat V, Young AJ, Gozola D and Wasielewski MR (1994) Photophysics of the carotenoids associated with the xanthophyll cycle in photosynthesis. *Photosynth Res* 41: 389–395
- Frank HA, Young AJ, Britton G and Cogdell RJ (eds) (1999) *The Photochemistry of Carotenoids*. Kluwer Academic Publishers, Dordrecht
- Funk C, Schröder WP, Napiwotzki A, Tjies SE, Renger G and Andersson B (1995) The PS II-S protein of higher plants: A new type of pigment-binding protein. *Biochemistry* 34: 11133–11141
- Garnier J (1967) Une méthode de détection, par photographie, de

- souches d'Algues vertes émettant in vitro une fluorescence anormale. CR Acad Sci Paris Ser D 265: 874–877
- Genty B and Meyer S (1994) Quantitative mapping of leaf photosynthesis using chlorophyll fluorescence imaging. Aust J Plant Physiol 22: 277–284
- Genty B, Briantais J-M and Baker NR (1989) The relationship between quantum yield of photosynthetic electron transport and quenching of chlorophyll fluorescence. Biochim Biophys Acta 990: 87–92
- Genty B, Wonders J and Baker NR (1990a) Non-photochemical quenching of  $F_0$  in leaves is emission wavelength dependent: Consequences for quenching analysis and its interpretation. Photosynth Res 26: 133–139
- Genty B, Harbinson J and Baker NR (1990b) Relative quantum efficiencies of the two photosystems of leaves in photorespiratory and non-photorespiratory conditions. Plant Physiol Biochem 28: 1–10
- Giersch C and Krause GH (1991) A simple model relating photoinhibitory fluorescence quenching in chloroplasts to a population of altered Photosystem II reaction centers. Photosynth Res. 30: 115–121
- Gilmore AM (1997) Mechanistic aspects of xanthophyll cycle-dependent photoprotection in higher plant chloroplasts and leaves. Physiol Plant 99: 197–209
- Gilmore AM and Yamamoto HY (1993) Linear models relating xanthophylls and lumen acidity to non-photochemical fluorescence quenching. Evidence that antheraxanthin explains zeaxanthin-independent quenching. Photosynth Res. 35: 67–78
- Gilmore AM, Mohanty N and Yamamoto HY (1994) Epoxidation of zeaxanthin and antheraxanthin reverses non-photochemical quenching of Photosystem II chlorophyll *a* fluorescence in the presence of trans-thylakoid  $\Delta$ pH. FEBS Lett 350: 271–274
- Gilmore AM, Hazlett TL and Govindjee (1995) Xanthophyll cycle-dependent quenching of Photosystem II chlorophyll *a* fluorescence: Formation of a quenching complex with a short fluorescence lifetime. Proc Natl Acad Sci USA 92: 2273–2277
- Gilmore AM, Hazlett TL, Debrunner PG and Govindjee (1996) Photosystem II chlorophyll *a* fluorescence lifetimes and intensity are independent of the antenna size differences between barley wild-type and *chlorina* mutants: Photochemical quenching and xanthophyll cycle-dependent nonphotochemical quenching of fluorescence. Photosynth Res 48: 171–187
- Gilmore AM, Shinkarev VP, Hazlett TL and Govindjee (1998) Quantitative analysis of the effects of intrathylakoid pH and xanthophyll cycle pigments on chlorophyll *a* fluorescence lifetime distributions and intensity in thylakoids. Biochem 37: 13582–13593
- Gilmore AM, Itoh S and Govindjee (2000) Global spectral-kinetic analysis of room temperature chlorophyll *a* fluorescence from light-harvesting antenna mutants of barley. Phil Trans R Soc Lond B 355: 1371–1384
- Goh C-H, Schreiber U and Hedrich R (1999) New approach of monitoring changes in chlorophyll *a* fluorescence of single guard cells and protoplasts in response to physiological stimuli. Plant Cell Environ 22: 1057–1070
- Govindjee (1990) Photosystem II heterogeneity: The acceptor side. Photosynth Res 25: 151–160
- Govindjee (1995) Sixty-three years since Kautsky: Chlorophyll *a* fluorescence. Aust J Plant Physiol 22: 131–160
- Guenther JE and Melis A (1989) The physiological significance of Photosystem II heterogeneity in chloroplasts. Photosynth Res 23: 105–109
- Guenther JE, Nemson JA and Melis A (1990) Development of Photosystem II in dark grown *Chlamydomonas reinhardtii*. A light-dependent conversion of PS II $_{\beta}$ ,  $Q_B$ -nonreducing centers to the PS II $_{\alpha}$ ,  $Q_B$ -reducing form. Photosynth Res 24: 35–46
- Harbinson J and Woodward FI (1987) The use of light-induced absorbance changes at 820 nm to monitor the oxidation state in leaves. Plant Cell Environ 10: 131–140
- Harbinson J, Genty B and Baker NR (1989) Relationship between the quantum efficiencies of Photosystems I and II in pea leaves. Plant Physiol 90: 1029–1034
- Harbinson J, Genty B and Baker NR (1990) The relationship between  $CO_2$  assimilation and electron transport in leaves. Photosynth Res 25: 213–224
- Havaux M, Strasser RJ and Greppin H (1991) A theoretical and experimental analysis of the  $q_P$  and  $q_N$  coefficients of chlorophyll fluorescence quenching and their relation to photochemical and nonphotochemical events. Photosynth Res 27: 41–55
- Holzwarth AR (1991) Excited state kinetics in chlorophyll systems and its relationship to the functional organization of the photosystems. In: Scheer H (ed) Chlorophylls, pp 1125–1151, CRC Press, Boca Raton
- Holzwarth AR (1993) Is it time to throw away your apparatus for chlorophyll fluorescence induction? Biophys J 64: 1280–1281
- Holzwarth AR and Roelofs TA (1992) Recent advances in the understanding of chlorophyll excited state dynamics in thylakoid membranes and isolated reaction center complexes. J Photochem Photobiol B 15: 45–62
- Hong S-S and Xu D-Q (1999) Light-induced increase in initial chlorophyll fluorescence  $F_0$  level and the reversible inactivation of PS II reaction centers in soybean leaves. Photosynth Res 61: 269–280
- Hormann H, Neubauer C and Schreiber U (1994) On the relationship between chlorophyll fluorescence quenching and the quantum yield of electron transport in isolated thylakoids. Photosynth Res 40: 93–106
- Horton P and Hague A (1988) Studies on the induction of chlorophyll fluorescence in isolated barley protoplasts. IV. Resolution of non-photochemical quenching. Biochim Biophys Acta 932: 107–115
- Horton P and Ruban AV (1992) Regulation of Photosystem II. Photosynth Res. 34: 375–385
- Horton P and Ruban AV (1993)  $\Delta$ pH-dependent quenching of the  $F_0$  level of chlorophyll fluorescence in spinach leaves. Biochim Biophys Acta 1142: 203–206
- Horton P, Ruban AV and Walters RG (1996) Regulation of light harvesting in green plants. Annu Rev Plant Physiol Plant Mol Biol 47: 655–684
- Horton P, Ruban AV and Young AJ (1999) Regulation of the structure and function of the light-harvesting complexes of Photosystem II by the xanthophyll cycle. In: Frank HA, Young AJ, Britton G and Cogdell RJ (eds) (1999) The Photochemistry of Carotenoids, pp 271–291, Kluwer Academic Publishers, Dordrecht
- Jahns P and Krause GH (1994) Xanthophyll cycle and energy-dependent fluorescence quenching in leaves from pea plants grown under intermittent light. Planta 192: 176–182
- Jahns P and Miesch B (1996) Kinetic correlation of recovery from photoinhibition and zeaxanthin epoxidation. Planta 198: 202–210

- Jahns P and Schweig S (1995) Energy-dependent fluorescence quenching in thylakoids from intermittent light grown pea plants: Evidence for an interaction of zeaxanthin and the chlorophyll *a/b* binding protein CP26. *Plant Physiol Biochem* 33: 683–687
- Jahns P, Depka B and Trebst A (2000) Xanthophyll cycle mutants from *Chlamydomonas reinhardtii* indicate a role of zeaxanthin in the D1 protein turnover. *Plant Physiol Biochem* 38: 371–376
- Joshi MK and Mohanty P (1995) Probing photosynthetic performance by chlorophyll fluorescence: Analysis and interpretation of fluorescence parameters. *J Sci Indust Res* 54: 155–174
- Karukstis KK (1991) Chlorophyll fluorescence as a physiological probe of the photosynthetic apparatus. In: Scheer H (ed) *Chlorophylls*, pp 769–795. CRC Press, Boca Raton
- Kim S, Pichersky E and Yocum CF (1994) Topological studies of spinach 22 kDa protein of Photosystem II. *Biochim Biophys Acta* 1188: 339–348.
- Klughammer C and Schreiber U (1994) An improved method, using saturating light pulses, for the determination of Photosystem I quantum yield via P700<sup>+</sup>-absorbance changes at 830 nm. *Planta* 192: 261–268
- Klughammer, C and Schreiber U (1998) Measuring P700 absorbance changes in the near infrared spectral region with a dual wavelength pulse modulation system. In: Garab G (ed) *Photosynthesis: Mechanisms and Effects*, Vol V, pp 4357–4360. Kluwer, Dordrecht
- Kofer W, Koop H-U, Wanner G and Steinmüller K (1998) Mutagenesis of the genes encoding subunits A, C, H, I, J and K of the plastid NAD(P)H-plastoquinone-oxidoreductase in tobacco by polyethylene glycol-mediated plastome transformation. *Mol Gen Genet* 258: 166–173
- Kolber Z and Falkowski PG (1993) Use of active fluorescence to estimate phytoplankton photosynthesis in situ. *Limnol Oceanogr* 38: 1646–1665
- Kolber ZS, Prášil O and Falkowski PG (1998) Measurements of variable chlorophyll fluorescence using fast repetition rate techniques: defining methodology and experimental protocols. *Biochim Biophys Acta* 1367: 88–106
- Koroleva OY, Brüggemann W and Krause GH (1994) Photoinhibition, xanthophyll cycle and in vivo chlorophyll fluorescence quenching of chilling-tolerant *Oxyria digyna* and chilling-sensitive *Zea mays*. *Physiol Plant* 92: 577–584
- Koroleva OY, Carouge N, Pelle B, Scholl S and Krause GH (1998) Sustained trans-thylakoid proton gradient induced by light stress at low temperatures? Possible effects on the xanthophyll cycle. In: Garab G (ed) *Photosynthesis: Mechanisms and Effects*, Vol III, pp 2325–2328. Kluwer, Dordrecht
- Krall JP and Edwards GE (1992) Relationship between Photosystem II activity and CO<sub>2</sub> fixation in leaves. *Physiol Plant* 86: 180–187
- Kramer DM and Crofts AR (1996) Control and measurement of photosynthetic electron transport in vivo. In: Baker NR (ed) *Photosynthesis and the Environment*, pp 25–66. Kluwer, Dordrecht
- Krause GH (1974) Changes in chlorophyll fluorescence in relation to light-dependent cation transfer across thylakoid membranes. *Biochim Biophys Acta* 333: 301–313
- Krause GH (1978) Effects of uncouplers on Mg<sup>2+</sup>-dependent fluorescence quenching in isolated chloroplasts. *Planta* 138: 73–78
- Krause GH (1992) Effects of temperature on energy-dependent fluorescence quenching in chloroplasts. *Photosynthetica* 27: 249–252
- Krause GH and Behrend U (1983) Characterization of chlorophyll fluorescence quenching in chloroplasts by fluorescence spectroscopy at 77K. II. ATP-dependent quenching. *Biochim Biophys Acta* 723: 176–181
- Krause GH and Behrend U (1986) ΔpH-dependent chlorophyll fluorescence quenching indicating a mechanism of protection against photoinhibition of chloroplasts. *FEBS Lett* 200: 298–302
- Krause GH and Laasch H (1987) Energy-dependent chlorophyll fluorescence quenching in chloroplasts correlated with quantum yield of photosynthesis. *Z Naturforsch* 42c: 581–584
- Krause GH and Somersalo S (1989) Fluorescence as a tool in photosynthesis research: Application in studies of photoinhibition, cold acclimation and freezing stress. *Phil Trans R Soc Lond B* 313: 281–293
- Krause GH and Weis E (1991) Chlorophyll fluorescence and photosynthesis: The basics. *Annu Rev Plant Physiol Plant Mol Biol* 42: 313–349
- Krause GH, Vernotte C and Briantais J-M (1982) Photoinduced quenching of chlorophyll fluorescence in intact chloroplasts and algae. Resolution into two components. *Biochim Biophys Acta* 679: 116–124
- Krause GH, Somersalo S, Zumbusch E, Weyers B and Laasch H (1990) On the mechanism of photoinhibition in chloroplasts. Relationship between changes in fluorescence and activity of Photosystem II. *J Plant Physiol* 136: 472–479
- Krause GH, Virgo A and Winter K (1995) High susceptibility to photoinhibition of young leaves of tropical forest trees. *Planta* 197: 583–591
- Krause GH, Schmude C, Garden G, Koroleva OY and Winter K (1999a) Effects of solar ultraviolet radiation on the potential efficiency of Photosystem II in leaves of tropical plants. *Plant Physiol* 121: 1349–1358
- Krause GH, Carouge N and Garden H (1999b) Long-term effects of temperature shifts on xanthophyll cycle and photoinhibition in spinach (*Spinacia oleracea*). *Aust J Plant Physiol* 26: 125–134
- Kruse O, Nixon PJ, Schmid GH and Mullineaux CM (1999) Isolation of state transition mutants of *Chlamydomonas reinhardtii* by fluorescence video imaging. *Photosynth Res* 61: 43–51
- Lakowicz JR (1999) *Principles of Fluorescence Spectroscopy*. 2nd edition. Kluwer Academic Publishers/Plenum Publishers, New York
- Lavergne J and Trissl H-W (1995) Theory of fluorescence induction in Photosystem II: Derivation of analytical expressions in a model including exciton-radical pair equilibrium and restricted energy transfer between photosynthetic units. *Biophys J* 68: 2474–2492
- Lazár D (1999) Chlorophyll *a* fluorescence induction. *Biochim Biophys Acta* 1412: 1–28
- Leitsch J, Schnettger B, Critchley C and Krause GH (1994) Two mechanisms of recovery from photoinhibition in vivo: Reactivation of Photosystem II related and unrelated to D1-protein turnover. *Planta* 194: 15–21
- Li XP, Björkman O, Shih C, Grossman AR, Rosenqvist M, Jansson S and Niyogi KK (2000) A pigment-binding protein essential for regulation of photosynthetic light harvesting.



- Nature 403: 391–395
- Lichtenthaler HK (1996) Vegetation stress: An Introduction to the stress concept in plants. *J Plant Physiol* 148: 4–14
- Lichtenthaler HK, Lang M, Sowinska M, Heisel F and Miehe JA (1996) Detection of vegetation stress via a new high-resolution fluorescence imaging system. *J. Plant Physiol* 148: 599–612
- Mano J, Miyake C, Schreiber U and Asada K (1995) Photoactivation of the electron flow from NADPH to plastoquinone in spinach chloroplasts. *Plant Cell Physiol* 36: 1589–1598
- Meurer J, Meierhoff K and Westhoff P (1996) Isolation of high-chlorophyll-fluorescence mutants of *Arabidopsis thaliana* and their characterisation by spectroscopy, immunoblotting and Northern hybridisation. *Planta* 198: 385–396
- Meyer S and Genty B (1998) Mapping intercellular CO<sub>2</sub> mole fraction (C-I) in *Rosa rubiginosa* leaves fed with abscisic acid by using chlorophyll fluorescence imaging—significance of C-I estimated from leaf gas-exchange. *Plant Physiol* 116: 947–957
- Miles CD (1980) Mutants of higher plants: Maize. *Methods Enzymol* 69: 3–23
- Miles CD (1982) The use of mutations to probe photosynthesis in higher plants. In: Hallick R, Edelman M and Chua N (eds) *Methods in Chloroplasts Molecular Biology*, pp 75–109. Elsevier, New York
- Mohammed GH, Binder WD and Gillies SL (1995). Chlorophyll fluorescence: A review of its practical forestry applications and instrumentation. *Scand J Forest Res* 10: 383–410
- Mohanty N, Gilmore AM and Yamamoto HY (1995) Mechanism of non-photochemical chlorophyll fluorescence quenching. II. Resolution of rapidly reversible absorbance changes at 530 nm and fluorescence quenching by the effects of antimycin, dibucaine and cation exchanger, A23187. *Aust J Plant Physiol* 22: 239–247
- Morales F, Abadía A and Abadía J (1998) Photosynthesis, quenching of chlorophyll fluorescence and thermal energy dissipation in iron-deficient sugar beet leaves. *Aust J Plant Physiol* 25: 403–412
- Mott KA, Cardon ZG and Berry JA (1993) Asymmetric patchy stomatal closure for the 2 surfaces of *Xanthium strumarium* L. leaves at low humidity. *Plant Cell Environ* 16: 25–34
- Mullineaux CW, Ruban AV and Horton P (1994) Prompt heat release associated with  $\Delta$ pH-dependent quenching in spinach thylakoid membranes. *Biochim Biophys Acta* 1185: 119–123
- Neubauer C and Schreiber U (1987) The polyphasic rise of chlorophyll fluorescence upon onset of strong continuous illumination: I. Saturation characteristics and partial control by the Photosystem II acceptor side. *Z Naturforsch* 42c: 1246–1254
- Niyogi KK (1999) Photoprotection revisited: Genetic and molecular approaches. *Annu Rev Plant Physiol Plant Mol Biol* 50: 333–359
- Niyogi KK, Björkman O and Grossman AR (1997) *Chlamydomonas* xanthophyll cycle mutants identified by video imaging of chlorophyll fluorescence quenching. *Plant Cell* 9: 1369–1380
- Niyogi KK, Grossman AR and Björkman O (1998) *Arabidopsis* mutants define a central role for the xanthophyll cycle in the regulation of photosynthetic energy conversion. *Plant Cell* 10: 1121–1134
- Noctor G, Rees D, Young A and Horton P (1991) The relationship between zeaxanthin, energy-dependent quenching of chlorophyll fluorescence and the trans-thylakoid pH gradient in isolated chloroplasts. *Biochim Biophys Acta* 1057: 320–330
- Noctor G, Ruban AV and Horton P (1993) Modulation of  $\Delta$ pH-dependent nonphotochemical quenching of chlorophyll fluorescence in spinach chloroplasts. *Biochim Biophys Acta* 1183: 339–344
- Nogués S and Baker NR (1995) Evaluation of the role of damage to Photosystem II in the inhibition of CO<sub>2</sub> assimilation in pea leaves on exposure to UV-B radiation. *Plant Cell Environ* 18: 781–787
- Oberhuber W and Edwards GE (1993) Temperature dependence of the linkage of quantum yield of Photosystem II to CO<sub>2</sub> fixation in C<sub>4</sub> and C<sub>3</sub> plants. *Plant Physiol* 101: 507–512
- Oberhuber W, Dai Z-Y and Edwards GE (1993) Light dependence of quantum yields of Photosystem II and CO<sub>2</sub> fixation in C<sub>4</sub> and C<sub>3</sub> plants. *Photosynth Res* 35: 265–274
- Öquist G and Chow WS (1992) On the relationship between quantum yield of Photosystem II electron transport, as determined by chlorophyll fluorescence and the quantum yield of CO<sub>2</sub>-dependent O<sub>2</sub> evolution. *Photosynth Res* 33: 51–62
- Owens TG (1994) Excitation energy transfer between chlorophylls and carotenoids. A proposed molecular mechanism for non-photochemical quenching. In: Baker NR and Bowyer JR (eds) *Photoinhibition of Photosynthesis. From Molecular Mechanisms to the Field*, pp 95–109. Bios Scientific Publishers, Oxford
- Oxborough K and Baker NR (1997) Resolving chlorophyll *a* fluorescence images of photosynthetic efficiency into photochemical and non-photochemical components—calculation of  $q_P$  and  $F_V'/F_M'$  without measuring  $F_0'$ . *Photosynth Res* 54: 135–142
- Oxborough K, Lee P and Horton P (1987) Regulation of thylakoid protein phosphorylation by high-energy-state quenching. *FEBS Lett* 221: 211–214
- Peterson RB (1989) Partitioning of noncyclic photosynthetic electron transport to O<sub>2</sub>-dependent dissipative processes as probed by fluorescence and CO<sub>2</sub> exchange. *Plant Physiol* 90: 1322–1328
- Peterson RB, Sivak MN and Walker DA (1988) Relationship between steady-state fluorescence yield and photosynthetic efficiency in spinach leaf tissue. *Plant Physiol* 88: 158–163
- Pfannschmidt T, Nilsson A and Allen JF (1999) Photosynthetic control of chloroplast expression. *Nature* 397: 625–628
- Pfündel (1998) Estimating the contribution of Photosystem I to total leaf chlorophyll fluorescence. *Photosynth Res* 56: 185–195
- Quick WP and Stitt M (1989) An examination of factors contributing to non-photochemical quenching of chlorophyll fluorescence in barley leaves. *Biochim Biophys Acta* 977: 287–296
- Quick WP, Scheibe R and Stitt M (1989) Use of tentoxin and nigericin to investigate the possible contribution of  $\Delta$ pH to energy dissipation and the control of electron transport in spinach leaves. *Biochim Biophys Acta* 974: 282–288
- Richter M, Rühle W and Wild A (1990) Studies on the mechanism of Photosystem II photoinhibition. A two-step degradation of D1 protein. *Photosynth Res* 24: 229–235
- Rolfe SA and Scholes JD (1995) Quantitative imaging of chlorophyll fluorescence. *New Phytol* 131: 69–79
- Ruban AV and Horton P (1995a) Regulation of non-photochemical quenching of chlorophyll fluorescence in plants.



- Aust J. *Plant Physiol* 22: 221–230
- Ruban AV and Horton P (1995b) An investigation of the sustained component of nonphotochemical quenching of chlorophyll fluorescence in isolated chloroplasts and leaves of spinach. *Plant Physiol* 108: 721–726
- Ruban AV, Young AJ and Horton P (1996) Dynamic properties of the minor chlorophyll *a/b* binding proteins of Photosystem II, an in vitro model for photoprotective energy dissipation in the photosynthetic membrane of green plants. *Biochem* 35: 674–678
- Schatz GH, Brock H and Holzwarth AR (1988) A kinetic and energetic model for the primary processes in Photosystem II. *Biophys J* 54: 397–405
- Schnettger B, Leitsch J and Krause GH (1992) Photoinhibition of Photosystem 2 in vivo occurring without net protein degradation. *Photosynthetica* 27: 261–265
- Schnettger B, Critchley C, Santore UJ, Graf M and Krause GH (1994) Relationship between photoinhibition of photosynthesis, D1 protein turnover and chloroplast structure: Effects of protein synthesis inhibitors. *Plant Cell Environ* 17: 55–64
- Schreiber U (1983) Chlorophyll fluorescence yield changes as a tool in plant physiology. I. The measuring system. *Photosynth Res* 4: 361–373
- Schreiber U (1986) Detection of rapid induction kinetics with a new type of high-frequency modulated chlorophyll fluorometer. *Photosynth Res* 9: 261–272
- Schreiber U (1994) New emitter-detector-cuvette assembly for measuring modulated chlorophyll fluorescence of highly diluted suspensions in conjunction with the PAM fluorometer. *Z. Naturforsch* 49c: 646–656
- Schreiber U (1998) Chlorophyll fluorescence: New instrumentation for special applications. In: Garab G (ed) *Photosynthesis: Mechanisms and Effects*, Vol V, pp 4253–4258
- Schreiber U and Krieger A (1996) Two fundamentally different types of variable chlorophyll fluorescence in vivo. *FEBS Lett* 397: 131–135
- Schreiber U and Neubauer C (1987) The polyphasic rise of chlorophyll fluorescence upon onset of strong continuous illumination: II. Partial control by the Photosystem II donor side and possible ways or interpretation. *Z. Naturforsch* 42c: 1255–1264
- Schreiber U, Schliwa U and Bilger W (1986) Continuous recording of photochemical and non-photochemical chlorophyll fluorescence quenching with a new type of modulation fluorometer. *Photosynth Res* 10: 51–62
- Schreiber U, Hormann H, Neubauer C and Klughammer C (1995) Assessment of Photosystem II photochemical quantum yield by chlorophyll fluorescence quenching analysis. *Aust J Plant Physiol* 22: 209–220
- Schreiber U, Kühl M, Klimant I and Reising H (1996) Measurement of chlorophyll fluorescence within leaves using a modified PAM fluorometer with a fiber-optic microprobe. *Photosynth Res* 47: 103–109
- Schreiber U, Gademan, R, Ralph PJ and Larkum AWD (1997) Assessment of photosynthetic performance of *Prochloron* in *Lissoclinum patella* in hospite by chlorophyll fluorescence measurements. *Plant Cell Physiol* 38: 945–951
- Schreiber U, Bilger W, Hormann H and Neubauer C (1998) Chlorophyll fluorescence as a diagnostic tool: Basics and some aspects of practical relevance. In: Raghavendra AS (ed) *Photosynthesis. A Comprehensive Treatise*, pp 320–336. Cambridge University Press, Cambridge, U.K.
- Seaton GGR and Walker DA (1990) Chlorophyll fluorescence as a measure of photosynthetic carbon assimilation. *Proc R Soc Lond B* 242: 29–35
- Sharkey TD, Berry JA and Sage RF (1988) Regulation of photosynthetic electron-transport in *Phaseolus vulgaris* L., as determined by room-temperature chlorophyll *a* fluorescence. *Planta* 176: 415–424
- Siebek K and Weis E (1995) Imaging of chlorophyll-*a* fluorescence in leaves—topography of photosynthetic oscillations in leaves of *Glechoma hederacea*. *Photosynth Res* 45: 225–237
- Simpson DJ and von Wettstein D (1980) Macromolecular physiology of plastids. XIV. *Viridis* mutants in barley: Genetic, fluoroscopic and ultrastructural characterisation. *Carlsberg Res Commun* 45: 283–314
- Simpson DJ, Machold O, Hoyer-Hansen G and von Wettstein D (1985) Chlorina mutants of barley (*Hordeum vulgare* L.). *Carlsberg Res Commun* 50: 223–238
- Skogen D, Chaturvedi R, Weidemann F and Nilsen S (1986) Photoinhibition of photosynthesis: effect of light quality and quantity on recovery from photoinhibition in *Lemna gibba*. *J Plant Physiol* 126: 195–205
- Somersalo S and Krause GH (1989) Photoinhibition at chilling temperature. Fluorescence characteristics of unhardened and cold-acclimated spinach leaves. *Planta* 177: 409–416
- Somersalo S and Krause GH (1990) Reversible photoinhibition of unhardened and cold-acclimated spinach leaves at chilling temperatures. *Planta* 180: 181–187
- Somerville CR (1986) Analysis of photosynthesis with mutants of higher plants and algae. *Annu Rev Plant Physiol* 37: 467–507
- Sonoike K (1996) Photoinhibition of Photosystem I: Its physiological significance in the chilling sensitivity of plants. *Plant Cell Physiol* 37: 239–347
- Spunda V, Kalina J, Marek MV and Naus J (1997) Regulation of photochemical efficiency of Photosystem 2 in Norway spruce at the beginning of winter and in the following spring. *Photosynthetica* 33: 91–102
- Srivastava A, Guissé B, Greppin, H and Strasser RJ (1997) Regulation of antenna structure and electron transport in Photosystem II of *Pisum sativum* under elevated temperature probed by the fast polyphasic chlorophyll *a* fluorescence transient: OKJIP. *Biochim Biophys Acta* 1320: 95–106
- Strasser RJ, Srivastava A and Govindjee (1995) Polyphasic chlorophyll *a* fluorescence transient in plants and cyanobacteria. *Photochem Photobiol* 61: 32–42
- Streb P, Feierabend J and Bligny R (1997) Resistance to photoinhibition of Photosystem II and catalase and antioxidative protection in high mountain plants. *Plant Cell Environ* 20: 1030–1040
- Taylor WC, Barkan A and Martienssen RA (1987) Use of nuclear mutants in the analysis of chloroplast development. *Dev Genet* 8: 305–320
- Terashima I, Noguchi K, Itoh-Nemoto T, Park Y-M, Kubo A and Tanaka K (1998) The cause of PS I photoinhibition at low temperatures in leaves of *Cucumis sativus*, a chilling-sensitive plant. *Physiol Plant* 103: 295–303
- Thiele A and Krause GH (1994) Xanthophyll cycle and thermal energy dissipation in Photosystem II: Relationship between

- zeaxanthin formation, energy-dependent fluorescence quenching and photoinhibition. *J Plant Physiol* 144: 324–332
- Thiele A, Schirwitz K, Winter K and Krause GH (1996) Increased xanthophyll cycle activity and reduced D1 protein inactivation related to photoinhibition in two plant systems acclimated to excess light. *Plant Science* 115: 237–250
- Thiele A, Winter K and Krause GH (1997) Low inactivation of D1 protein of Photosystem II in young canopy leaves of *Anacardium excelsum* under high-light stress. *J Plant Physiol* 151: 286–292
- Thiele A, Krause GH and Winter K (1998) In situ study of photoinhibition of photosynthesis and xanthophyll cycle activity in plants growing in natural gaps of the tropical forest. *Aust J Plant Physiol* 25: 189–195
- Trissl H-W and Lavergne J (1994) Fluorescence induction from Photosystem II: Analytical equations for yields of photochemistry and fluorescence derived from analysis of a model including exciton-radical pair equilibrium and restricted energy transfer between photosynthetic units. *Aust J Plant Physiol* 22: 183–193
- Trissl H-W, Gao Y and Wulf K (1993) Theoretical fluorescence induction curves derived from coupled differential equations describing the primary photochemistry of Photosystem II by an exciton/radical pair equilibrium. *Biophys J* 64: 984–998
- Tyystjärvi E, Ovaska J, Karunen P and Aro E-M (1989) The nature of light-induced inhibition of Photosystem II in pumpkin (*Cucurbita pepo* L) leaves depends on temperature. *Plant Physiol* 91: 1069–1074
- van Wijk KJ, Schnettger B, Graf M and Krause GH (1993) Photoinhibition and recovery in relation to heterogeneity of Photosystem II. *Biochim Biophys Acta* 1142: 59–68
- Verhoeven AS, Adams WW III and Demmig-Adams B (1996) Close relationship between the state of the xanthophyll cycle pigments and Photosystem II efficiency during recovery from winter stress. *Physiol Plant* 96: 567–576
- Verhoeven AS, Adams WW III, Demmig-Adams B, Croce R and Bassi R (1999) Xanthophyll cycle pigment localization and dynamics during exposure to low temperatures and light stress in *Vinca major*. *Plant Physiol* 120: 727–737
- Vernotte C, Etienne AL and Briantais J-M (1979) Quenching of the system II chlorophyll fluorescence by the plastoquinone pool. *Biochim Biophys Acta* 545: 519–527
- Walters RG and Horton P (1991) Resolution of components of non-photochemical chlorophyll fluorescence quenching in barley leaves. *Photosynth Res* 27: 121–133
- Walters RG and Horton P (1993) Theoretical assessment of alternative mechanisms for non-photochemical quenching of PS II fluorescence in barley leaves. *Photosynth Res* 36: 119–139
- Weis E and Berry JA (1987) Quantum efficiency of Photosystem II in relation to 'energy'-dependent quenching of chlorophyll fluorescence. *Biochim Biophys Acta* 894: 198–208
- White AJ and Critchley C (1999) Rapid light curves: A new fluorescence method to assess the state of the photosynthetic apparatus. *Photosynth Res* 59: 63–72
- Yahyaoui W, Harnois J and Carpentier R (1998) Demonstration of thermal dissipation of absorbed quanta during energy-dependent quenching of chlorophyll fluorescence in photosynthetic membranes. *FEBS Lett* 440: 59–63
- Yamamoto HY, Nakayama TOM and Chichester CO (1962) Studies on the light and dark interconversions of leaf xanthophylls. *Arch Biochem Biophys* 97: 168–173

# Chapter 14

## Photostasis in Plants, Green Algae and Cyanobacteria: The Role of Light Harvesting Antenna Complexes

Norman P.A. Huner\*

*Department of Biology, University of Western Ontario, London, Canada N6A 5B7*

Gunnar Öquist

*Umeå Plant Science Center, Umeå University, S-907 81 Umeå, Sweden*

Anastasios Melis

*Department of Plant Biology, 411 Koshland Hall,  
University of California, Berkeley, CA 94720, U.S.A.*

Summary .....	402
I. Introduction .....	402
A. Adaptation, Acclimation and Stress .....	403
B. Photostasis .....	403
II. Stress and Photostasis .....	404
A. State Transitions and Photosystem Stoichiometry .....	404
B. Photoprotection .....	405
1. High Light .....	405
2. Drought .....	406
3. High Temperature .....	407
C. Photodamage .....	407
III. Acclimation And Photostasis .....	409
A. Growth Irradiance .....	409
B. Growth Temperature .....	410
1. Green Algae and Cyanobacteria .....	410
2. Evergreen Plants .....	410
3. Herbaceous Winter Annuals .....	412
C. Nutrient Limitations .....	413
IV. Chloroplast Biogenesis and Photostasis .....	415
V. Sensing Mechanisms Involved in Photostasis .....	416
Acknowledgments .....	416
References .....	417

---

\* Author for correspondence, email: [nhuner@julian.uwo.ca](mailto:nhuner@julian.uwo.ca)

## Summary

The structural, as well as the functional, light-harvesting antenna size of the photosystems in plants, green algae and cyanobacteria may vary as a function of either short term stress or long term acclimation to high or low irradiance, suboptimal or supraoptimal temperatures as well as limitations in nutrient and water availability. Modulation of antenna size in response to such environmental perturbations is part of a complex response called photoacclimation. A common effect of changes in these environmental factors is the creation of an imbalance between the energy absorbed through photochemistry and the energy utilized through the electrochemical reactions of electron transport which are coupled to the metabolic reduction of C, N and S. Either short term stress or long term acclimation to these environmental conditions, independently or in combination, may lead to irreversible photodamage or the induction of photoprotective mechanisms. Since there is a consensus in the literature that the structure and function of Photosystem II are generally more sensitive to changes in these environmental conditions than Photosystem I, we focus our discussion on the role of the light-harvesting antenna of Photosystem II in photoprotection through the maintenance of a balance between energy input through photochemistry and subsequent energy utilization through metabolism. The predisposition of photosynthetic organisms to maintain such a balance in energy budget is defined as photostasis. Any change in either photon flux, temperature, nutrient status or water availability may cause an imbalance in energy budget which occurs whenever  $\sigma_{\text{PSII}} \cdot I > n \cdot \tau^{-1}$  where  $\sigma_{\text{PSII}}$  is the functional absorption cross section of PS II,  $I$  is the incident photon flux,  $n$  is the number of photosynthetic units and  $\tau^{-1}$  is the rate at which metabolism consumes photosynthetically generated electrons. Photosynthetic acclimation, induced by short and long term exposures to low or high light, low temperature, nutrient and water limitation, is discussed with respect to the modulation of  $\sigma_{\text{PSII}}$ ,  $I$ , and metabolic sink capacity ( $\tau^{-1}$ ) to restore photostasis and minimize photodamage to PS II in plants, green algae and cyanobacteria. It appears that the plastoquinone pool and/or the Cyt  $b_6/f$  complex may act as the primary sensor for the maintenance of photostasis. We suggest that sensing/signaling associated with environmentally induced energy imbalances in terrestrial plants, green algae and cyanobacteria appears to exert a broad influence on diverse molecular, physiological and developmental process which is consistent with the concept of a 'grand design of photosynthesis' initially proposed by Daniel Arnon in 1982.

## I. Introduction

Energy in the form of light enters the biosphere through the process of photosynthesis and ultimately sustains virtually all living organisms. The primary photochemical reactions of PS II and PS I are dependent upon the absorption of light by the light-harvesting antenna pigments and the subsequent excitation migration to reaction centers,  $P_{680}$  and  $P_{700}$  to induce a stable charge separation. Distinct integral membrane chlorophyll-protein complexes are

associated with the reaction center proteins of PS II (PsbA and PsbD) and PS I (PsaA and PsaB) to facilitate the absorption of light and subsequently transfer the excitation energy to the respective reaction centers (Jansson, 1994; Green and Durnford, 1996). The Lhcb family of polypeptides that function as light-harvesting antenna for PS II, and the Lhca family of polypeptides that function as light-harvesting antenna for PS I typically noncovalently bind the pigments Chl  $a$ , Chl  $b$  as well as carotenoids. Violaxanthin, a light-harvesting xanthophyll, can be photo-converted to the energy quenching molecules antheraxanthin and zeaxanthin which are involved in the non-photochemical dissipation of light energy whenever the absorption of light energy exceeds the capacity for  $\text{CO}_2$  assimilation (Demmig-Adams and Adams, 1996; Horton et al., 1996; Yamamoto and Bassi, 1996; Niyogi et al., 1998; Demmig-Adams et al., 1999; Gilmore and Govindjee, 1999; Yamamoto et al., 1999). Recently, Li et al. (2000) isolated a mutant of *Arabidopsis thaliana*, designated *nqp4-1*,

*Abbreviations:* EPS – epoxidation state of xanthophyll cycle pigments;  $I$  – absorbed photon flux; Lhca, Lhcb(1-6) – polypeptides of LHCI, LHCII; LHCI, LHCII – light-harvesting antennas of PS I, PS II; PQ – plastoquinone; PsaA/PsaB – polypeptides of PS I reaction center;  $Q_A$  – primary quinone acceptor of PS II; qE – energy-dependent quenching of fluorescence; qN – non-photochemical quenching of fluorescence; qP – photochemical quenching of fluorescence;  $\Phi_{\text{app}}\text{CO}_2$  – apparent quantum yield of  $\text{CO}_2$  assimilation;  $\Phi_{\text{app}}\text{O}_2$  – apparent quantum yield of  $\text{O}_2$  evolution;  $\sigma_{\text{PSII}}$  – functional absorption cross-section of PS II;  $\tau^{-1}$  – rate of electron consumption

that is defective in non-photochemical quenching of excess light. Although all other LHC polypeptides associated with PS II (Lhcb1-Lhcb6) were present at normal levels, *nqp4-1* lacks the PsbS gene product (Li et al., 2000), an intrinsic chlorophyll-binding protein associated with PS II (Funk et al., 1995). Although the precise location of PsbS within the PS II supermolecular complex has yet to be determined unequivocally (Nield et al., 2000), it is clear that PsbS functions in a photoprotective rather than a light-harvesting role.

Since changes in environmental conditions such as light, temperature, water and nutrient availability may modulate the photochemical reactions of photosynthesis to a different extent than the biochemical reactions involved in carbon reduction cycle, photorespiration, nitrogen and sulfur assimilation, photosynthetic organisms must constantly balance the energy absorbed through photochemistry versus the energy utilized through metabolism. The predisposition of photosynthetic organisms to maintain a balance in energy budget is defined as photostasis.

#### A. Adaptation, Acclimation and Stress

Plants, algae and cyanobacteria can experience and must adjust to wide daily and seasonal fluctuations in environmental conditions such as light and temperature. Responses to these changes can be divided into two principal components. Adaptation is a *genotypic* response to environmental changes which results in alterations to the genome that are stable and remain in the population over generations. In contrast, acclimation is a response induced by an environmental change which causes a *phenotypic* alteration with no change in genetic complement. Acclimation is usually initiated by a *stress* response which can be defined as transient, physiological, biochemical and molecular perturbations to short, abrupt changes in the environment. Although this stress response may initially exhibit a dampening phenomenon, exposure to the stress for extended periods of time may subsequently establish a new stable, acclimated state which usually involves some developmental change in response to the new environmental condition (Falk et al., 1996). Thus, terrestrial plants, green algae and cyanobacteria that are able to acclimate to an initial stress condition are considered *stress tolerant* whereas those organisms that are unable to acclimate and eventually succumb

to the initial stress are considered to be *susceptible or sensitive*.

#### B. Photostasis

Research over the past decade on photosynthetic acclimation to light in terrestrial plants, green algae and cyanobacteria has shown that the pigment and polypeptide compositions of LHCII, LHCI and cyanobacterial phycobilisomes are not fixed but are, in fact, very dynamic (Anderson, 1986; Falkowski and LaRoche, 1991; Melis, 1991; Fujita et al., 1994; Grossman et al., 1994). The antenna size of the photosystems is variable and inversely related to growth irradiance which reflects a photoacclimation mechanism which attempts to maintain a balance between energy input through photochemistry and subsequent energy utilization through metabolism (Melis et al., 1985; Anderson et al., 1995; Huner et al., 1998; Melis, 1998). The ability to adjust the light-harvesting capacity in response to growth irradiance to maintain this energy balance is indicative of photostasis with respect to the absorption of light by chloroplasts (Melis, 1998). Since the photosynthetic apparatus of plants and green algae resides in the chloroplast whereas the genes that code for the light-harvesting polypeptides are nuclear encoded, clearly photostasis must involve the exchange of information between the chloroplast and the nucleus, perhaps via the elusive 'plastid factor' (Taylor, 1989; Gray, 1996; Kropat et al., 1997, 2000). The oxidation of PS II by PS I via the intersystem electron chain is considered to be the rate limiting process in photosynthetic electron transport (Haehnel, 1984). According to Durnford and Falkowski (1997):

$$\text{Energy Absorption} = \sigma_{\text{PSII}} \cdot \mathbf{I}$$

where  $\sigma_{\text{PSII}}$  is the functional absorption cross-sectional area of PS II and  $\mathbf{I}$  is the incident photon flux. This product is, by and large, insensitive to temperature in the biologically significant range. Under light saturating conditions, the rate of utilization of the absorbed light through temperature-sensitive photosynthetic electron transport and the ultimate use of these photosynthetic electrons to reduce carbon, oxygen, nitrogen and sulfur can be estimated as:

$$\text{Energy Utilization} = n \cdot \tau^{-1}$$

where  $n$  is the number of photosynthetic units and

$\tau^{-1}$  is the rate at which photosynthetic electrons are consumed metabolically through C assimilation, N and S assimilation, as well as through the photorespiratory pathway. Thus, photostasis would be attained whenever energy absorption equals energy utilization. Falkowski and Chen (Chapter 15) have derived an equation which denotes this balance or photostatic state.

$$\sigma_{\text{PSII}} \cdot I = n \cdot \tau^{-1}$$

Consequently, photoacclimation, which may be defined as the specific mechanism by which an organism attempts to regain the photostatic state after exposure to some environmental change, should be induced whenever

$$n \cdot \tau^{-1} > \sigma_{\text{PSII}} \cdot I > n \cdot \tau^{-1}.$$

Accordingly, exposure to excess excitation energy or 'excitation pressure' (Huner et al., 1998) could be induced by changes in several different environmental parameters such as: (1) increasing growth irradiance at constant temperature which would increase  $I$ , (2) decreasing growth temperature at a constant irradiance which would decrease  $\tau^{-1}$ , (3) drought which would lead to stomal closure and  $\text{CO}_2$  limitations in C3 plants which would decrease  $\tau^{-1}$  and (4) by nutrient limitations such as iron, nitrogen or sulfur deprivation which would also potentially decrease  $\tau^{-1}$ . In all cases, photostasis could be attained by either reducing  $\sigma_{\text{PSII}}$  by reducing light-harvesting antenna size and/or reducing the effective absorption cross-sectional area of PS II through an increased capacity for non-photochemical quenching in the antenna. These mechanisms to adjust  $\sigma_{\text{PSII}}$  would reduce photosynthetic efficiency measured as either the apparent quantum yield of  $\text{CO}_2$  assimilation ( $\Phi_{\text{app}} \text{CO}_2$ ) or the apparent quantum yield of  $\text{O}_2$  evolution ( $\Phi_{\text{app}} \text{O}_2$ ). In addition,  $I$  could be reduced either by changing leaf angle relative to the incident radiation, leaf optical properties (Vogelmann et al., 1996), chloroplast orientation within mesophyll cells (Brugnoli and Björkman, 1992) or position in the water column in the case of green algae and cyanobacteria (Falkowski, 1983). However, during exposure to either low temperature or high light, photostasis also could be attained by increasing sink capacity ( $\tau^{-1}$ ). This may be accomplished by elevating the levels of Calvin cycle enzymes which would increase the capacity for  $\text{CO}_2$  assimilation ( $P_{\text{max}}$ ) or

photorespiration relative to electron transport.

Alternatively, the attainment of photostasis upon exposure to low, limiting irradiance may be attained either by increasing  $\sigma_{\text{PSII}}$  through an increase in light-harvesting antenna size and/or through an increase in the effective absorption cross-sectional area of PS II as a result of a reduction in the capacity for non-photochemical quenching. These mechanisms to adjust  $\sigma_{\text{PSII}}$  would increase both  $\Phi_{\text{app}} \text{CO}_2$  and  $\Phi_{\text{app}} \text{O}_2$ . Clearly, in nature, photoautotrophs may exploit any one or a combination of these mechanisms to attain photostasis in an environment which exhibits daily as well as seasonal changes in irradiance, temperature, water availability and nutrient status.

## II. Stress and Photostasis

### A. State Transitions and Photosystem Stoichiometry

Maximum photosynthetic efficiency of oxygenic photosynthesis requires the co-ordinated interaction of PS II and PS I in linear electron transport. Although the spectral distribution of the solar radiation reaching the earth is characterized by approximately constant emission in the photosynthetically active region of 450 to 700 nm, this emission profile is attenuated significantly due to filtering through either aquatic environments (Falkowski, 1983), crop and forest canopies (Björkman and Ludlow, 1972), or through a single leaf (Vogelmann et al., 1996). Such attenuation inevitably results in a short-term imbalance in the absorption of light between PS II and PS I which causes a decreased efficiency of linear electron transport. In terrestrial plants and green algae, light absorbed preferentially by PS II relative to PS I (state 2) leads to an over-reduction of the PQ pool whereas preferential excitation of PS I relative to PS II (state 1) results in oxidation of the PQ pool. The reduction of the PQ pool induces a thylakoid protein kinase to phosphorylate reversibly a portion of the peripheral Lhcb antenna polypeptides which subsequently migrate from PS II in the stacked thylakoid regions to PS I in the unstacked regions (Allen et al., 1981). Recently, Lunde et al. (2000) reported that a specific PS I subunit, PS I-H, is an absolute requirement for state transitions in *Arabidopsis thaliana*. In the absence of PS I-H, LHCII can not transfer energy to PS I. Oxidation of the PQ pool stimulates the dephosphorylation of

these Lhcb polypeptides through a protein phosphatase which results in the subsequent migration of this population of Lhcb from unstacked thylakoids back to PS II present in granal stacks. Thus, the regulation of state 1–state 2 transitions by the redox state of the thylakoid PQ pool reflects a mechanism to counteract the uneven absorption of light by PS I and PS II by adjustment of  $\sigma_{\text{PSII}}$  to maintain photostasis and to ensure maximum photosynthetic efficiency on a short term basis. The mechanism by which state transitions occur in cyanobacteria remains controversial (Bruce et al., 1989).

However, in addition to light induced state transitions, nitrogen assimilation in the green alga, *Selenastrum minutum*, can also induce state transitions (Turpin and Bruce, 1990). Nitrogen-limited cultures of this green alga respond to the increased demand for ATP during  $\text{NH}_4^+$  assimilation (ATP / NADPH = 5) relative to either  $\text{NO}_3^-$  (ATP / NADPH = 1.2) or  $\text{CO}_2$  assimilation (ATP / NADPH = 1.5) by undergoing a state transition. This results in the redirection of excitation energy away from PS II and towards PS I to ensure an increased production of ATP by cyclic electron transport (Turpin and Bruce, 1990).

In photosynthesis, it is assumed that PS I and PS II are connected in series with PS II reducing the intersystem electron components (PQ, Cyt  $b_6f$ , PC) and PS I oxidizing these electron carriers. Alterations in the relative contents of PS I and PS II reaction centers represent another mechanism to ensure equal rates of electron flow through both PS I and PS II to maximize the photosynthetic efficiency (Allen and Pfannschmidt, 2000). Modulation of PS I/PS II stoichiometry reflects adjustments of  $n$ . It has been proposed by Fujita et al. (1994) that modulation of photosystem stoichiometry is a response to changes in the redox state of the intersystem electron transport chain. Pfannschmidt et al. (1999) have shown that the transcription of the chloroplast encoded *psbA* and *psaAB* are controlled by the redox state of the PQ pool. Thus, over-reduction of the PQ pool by the preferential excitation of PS II not only favors the phosphorylation of LHCII but also the activation of *psaAB* transcription and the repression of *psbA*. Conversely, oxidation of the PQ pool by preferential excitation of PS I not only favors de-phosphorylation of LHCII but also the activation of transcription of *psbA* and the repression of *psaAB* (Pfannschmidt et al., 1999; Allen and Pfannschmidt, 2000). Thus, PQ, the redox sensor that controls state transitions, also

appears to be the sensor that regulates chloroplast photosystem stoichiometry. It appears that redox regulation of state transitions may be a mechanism to balance excitation energy on a very short time scale under light limiting conditions whereas redox regulation of photosystem stoichiometry through control of chloroplast gene transcription may represent a longer-term mechanism to correct for imbalances in the excitation of PS I and PS II (Allen and Pfannschmidt, 2000).

## B. Photoprotection

### 1. High Light

Photoinhibition of photosynthesis is defined as the light dependent decrease in photosynthetic rate which may occur whenever the photon flux is in excess of that required for photosynthesis (Long et al., 1994), that is, whenever

$$\sigma_{\text{PSII}} \cdot I > n \cdot \tau^{-1}.$$

Photoinhibition is usually measured as a decrease in either  $\Phi_{\text{app}} \text{O}_2$ ,  $\Phi_{\text{app}} \text{CO}_2$  or the maximum photochemical efficiency of PS II ( $F_v/F_m$ ) estimated through room temperature Chl *a* fluorescence (Krause and Weis, 1991). The use of the term 'photoinhibition' has lead to some confusion in the literature. First, photoinhibition is used with reference to the decrease in photosynthetic efficiency due to the irreversible inhibition of the function of PS II reaction centers as a consequence of irreversible photo-oxidative damage to the D1 reaction center polypeptide (Aro et al., 1993; Ohad et al., 1994; Melis, 1999). We will refer to this process as photodamage. To counteract this irreversible PS II photodamage, photoautotrophs have evolved a complex PS II repair mechanism which involves the removal of damaged D1 polypeptide followed by its replacement through de novo synthesis of the D1 polypeptide and its subsequent assembly into functional PS II reaction centers. Thus, in this context, photoinhibition of PS II is the result of an imbalance between the rate of repair of PS II versus the rate of damage (Melis, 1999). However, the term photoinhibition is also used with reference to the reversible decrease in photosynthetic efficiency as a consequence of an increase in thermal energy dissipation (qN, non-photochemical quenching) which leads to a decrease in the effective  $\sigma_{\text{PSII}}$  and a down regulation of PS II activity (Öquist et al.,



1992). This process, or any other process, which protects PS II from over-excitation will be referred to as 'photoprotection' (Öquist et al., 1992a).

Under normal physiological conditions, energy-dependent quenching (qE) is considered to be the major component of total qN and is dependent upon the extent of pH across the thylakoid membrane (Horton et al., 1996). It has been suggested that qE is the result of a localized H<sup>+</sup> domain within Lhcb and that, as a consequence, the site of energy-dependent quenching is the major PS II light-harvesting polypeptides, Lhcb1 and Lhcb2 (Horton et al., 1996). However, the roles of LHCII versus the minor antenna complexes of PS II in the mechanism of qE have been controversial (Falk et al., 1994; Jahns and Krause, 1994; Chapter 13, Krause and Jahns). However, recently Li et al. (2000) isolated a mutant of *Arabidopsis thaliana*, designated *nqp4-1*, that is deficient in non-photochemical quenching. Although all other LHC polypeptides associated with PS II (Lhcb1-Lhcb6) were present at levels comparable to the wild type, *nqp4-1* lacks the *PsbS* gene (Li et al., 2000) which codes for an intrinsic chlorophyll-binding protein associated with PS II (Funk et al., 1995). Although the precise location of PsbS within the PS II supermolecular complex has yet to be determined unequivocally (Nield et al., 2000), it is clear that PsbS functions in photoprotection of PS II rather than in light-harvesting.

Carotenoids are generally considered to function either to harvest light or to protect the photosynthetic apparatus through the de-excitation of singlet oxygen (<sup>1</sup>O<sub>2</sub>) and / or the triplet excited state of chlorophyll (Yamamoto and Bassi, 1996; Yamamoto et al., 1999). However, it is now established that the xanthophyll, zeaxanthin, is involved in the nonphotochemical dissipation of excess light (Demmig-Adams and Adams, 1996; Demmig-Adams et al., 1999). The xanthophyll cycle consists of the light-dependent de-epoxidation of the diepoxide violaxanthin, via the monoepoxide antheraxanthin, to the epoxide-free zeaxanthin (Yamamoto and Bassi, 1996). Furthermore, these xanthophyll carotenoids are associated with both the major LHCII components (Lhcb1 and Lhcb2) as well as the minor LHCII antenna (Thayer and Björkman, 1992). There is now a consensus that a close relationship exists between qN, thylakoid pH, the xanthophyll cycle and the antenna complexes (Demmig-Adams and Adams, 1996; Gilmore, 1997; Gilmore et al., 1998; Gilmore and Govindjee, 1999; Gilmore and Ball, 2000). However, non-photo-

chemical quenching is not always correlated with zeaxanthin accumulation due to xanthophyll cycle activity (Hurry et al., 1997).

The reversible interconversion of the light-harvesting xanthophyll, violaxanthin, to the energy quencher, zeaxanthin, can occur over periods of minutes to hours upon exposure to excessive radiation. Recently Logan et al. (1998a) examined the xanthophyll cycle-dependent energy dissipation during the rapid transfer of shade-adapted *Cucurbita pepo* L. and *Vinca major* L. to full sun light under field conditions. Damage to PS II reaction centers was considered to be minimal since no strong depressions in the pre-dawn values of Fv/Fm were observed, which is consistent with the report regarding daily exposure of wheat to high light (Hurry et al., 1992). However, a rapid increase in the xanthophyll cycle conversion state measured as zeaxanthin plus antheraxanthin as a fraction of total xanthophylls was observed with a concomitant decrease in PS II photochemical efficiency upon exposure to full sunlight. Thus, acclimation to high light appears to result in a persistent engagement of de-epoxidized xanthophylls for energy dissipation through PS II antenna (Logan et al., 1998a) which, as a result, leads to a decrease in  $\sigma_{\text{PSII}}$ .

## 2. Drought

Somerville and Ogren (1982) showed that a series of mutants of *Arabidopsis thaliana* deficient in the photorespiratory pathway could grow only under non-photorespiratory conditions. This pathway is initiated by the fixation of O<sub>2</sub> by Rubisco producing phosphoglycerate plus phosphoglycolate which is metabolized in the photorespiratory pathway to form the Calvin cycle intermediate glycerate-3-phosphate, CO<sub>2</sub> and NH<sub>3</sub>. Although it appears that photorespiration should be a wasteful process, it could serve as important energy sink ( $\tau^{-1}$ ) through its consumption of ATP and NADPH thus preventing the overreduction of the photosynthetic electron transport chain and photoinhibition. Transgenic tobacco exhibiting reduced levels of the photorespiratory enzymes, glycolate oxidase (Yamaguchi and Nishimura, 2000) or glutamate synthase (Kozaki and Takeba, 1996) indeed are more sensitive to photoinhibition than the respective wild types. However, the protective role of photorespiration may be especially important under stress conditions such as drought (Wingler et al., 1999; 2000). Although

there is a consensus that water stress inhibits photosynthesis, the underlying mechanism of this inhibition remains controversial (Keck and Boyer, 1974; Tezara et al., 1999, Cornic 2000). Drought stress stimulated photorespiration in barley mutants with reduced activities of chloroplastic glutamine synthetase, glycine decarboxylase or serine:glyoxylate aminotransferase. However, this was coupled with a several-fold increase in the de-epoxidation state of xanthophyll-cycle carotenoids in the drought-stressed barley mutants with a concomitant decrease in quantum yield for photosynthesis compared with the wild type barley (Wingler et al., 1999). Thus, it appears that drought-stressed barley may maintain photostasis through a combination of enhanced sink capacity ( $\tau^{-1}$ ) due to the stimulation of photorespiration coupled with a decrease in  $\sigma_{\text{PSII}}$ .

### 3. High Temperature

It has been known for sometime that the inhibition of whole leaf photosynthesis by high temperatures is primarily the result of the high temperature-induced destabilization of chloroplast thylakoid membranes (for review see Berry and Björkman, 1980). PS II appears to be more sensitive than PS I to heat inactivation which is a consequence of the heat instability of the oxygen evolving complex of PS II and also the heat sensitivity of the association between LHCII and the PS II reaction complex (Cheniae and Martin 1970; Armond et al., 1978; Armond and Staehelin, 1979). A short-term response to heat stress exhibited by most plants is the redistribution of excitation energy in favor of PS I (Weis, 1985) which would protect PS II through a decrease in  $\sigma_{\text{PSII}} \cdot I$ . In addition, the accumulation of chloroplast heat shock proteins appears to stabilize PS II against high temperatures (Heckathorn et al., 1998).

Plant species adapted to high temperatures appear to exhibit a photosynthetic apparatus with an enhanced stability to heat stress which may also be due to changes in thylakoid membrane lipid composition (Berry and Björkman, 1980). However, the role and the mechanism by which lipid-protein interactions stabilize thylakoids to high temperatures has yet to be resolved. Isoprenes have been implicated in the stabilization of the lipid phase of thylakoid membranes (Sharkey and Singsaas, 1995). In addition to their roles in light-harvesting, non-photochemical quenching of excess energy as well as quenching of triplet chlorophyll and singlet oxygen, it has been

suggested that carotenoids may also act as thylakoid membrane stabilizers during high light and heat stress (Havaux, 1998). Barley plants grown under sustained high irradiance at elevated temperature exhibited a reduced  $\sigma_{\text{PSII}}$  and a marked increase in the amount of free carotenoids compared to barley grown at moderate light and temperature conditions (Havaux et al., 1998).

### C. Photodamage

The D1/D2 heterodimer reaction center proteins of PS II function in primary photochemistry as well as the oxidation of water. These specialized functions of PS II occur in a microenvironment characterized by an abundance of oxygen coupled with the potential for exposure to excess excitation energy and transient formation of strong oxidants. Whenever the absorbed light energy exceeds the capacity of the organism either to use the trapped energy through photosynthesis (photochemical quenching, qP) or to dissipate it as heat through nonphotochemical quenching (qN), damage to PS II may occur (Osmond, 1994). The D1 protein of PS II is the primary site of photodamage which may be the result of either donor-side (Anderson et al., 1998) or acceptor-side limitations in PS II (Melis, 1999). Furthermore, exposure to excess light in oxygenic organisms may result in the formation of damaging reactive oxygen species either through the reduction of  $\text{O}_2$  to yield the superoxide anion radical ( $\text{O}_2^{\cdot-}$ ) or through energy transfer from excited triplet chlorophyll to ground state  $\text{O}_2$  to form singlet oxygen ( $^1\text{O}_2$ ) (Asada, 1996). If unchecked, irreversible photoinhibition due to photooxidative damage to PS II may lead to significant decreases in plant productivity (Baker, 1991). Recent evidence indicates that the chloroplast-targeted heat shock protein 70 (HSP70) may be involved both in the protection of PS II during photoinhibition as well as in the repair of damaged PS II in *Chlamydomonas reinhardtii* (Drzymalla et al., 1996; Schroda et al., 1999) and tomato (Heckathorn et al., 1998). Furthermore, several recent reports have indicated a selective, in vivo photoinhibition of PS I in chilling sensitive (Sonoike, 1998; Terashima et al., 1998) as well as cold tolerant plants (Havaux and Davaud, 1994; Ivanov et al., 1998).

The rate constant for photodamage to PS II has been shown to be a linear function of irradiance in plants and green algae (Baroli and Melis, 1996; Tyystjarvi and Aro, 1996). These data are consistent

with recent reports indicating a reciprocity between irradiance and the time of illumination for PS II inactivation, which has been interpreted to indicate that PS II acts a 'photon counter' (Park et al., 1995; Anderson et al., 1998). If this model is correct, then photodamage to PS II depends solely on the total number of photons absorbed and not the rate of photon absorption. Thus, the light-harvesting antenna size of PS II must modulate the rate of photodamage, and as a consequence, PS II reaction centers with large light-harvesting antennas should exhibit faster rates of photodamage than PS II reaction centers with small light-harvesting antennas. However, the effect of PS II light-harvesting size on the rate of PS II photodamage is still controversial (Ghirardi et al., 1987; Cleland and Melis, 1987; Leverenz et al., 1992; Tyytjärvi et al., 1994). Furthermore, more recent evidence supports the notion that PS II antenna size modulates PS II photodamage in higher plants (Park et al., 1997), green algae (Baroli and Melis, 1998) and cyanobacteria (Nakajima et al., 1998).

The dependence of PS II photodamage on PS II light-harvesting antenna size is consistent with the concept of PS II as a 'photon counter' with the probability for the loss of one PS II after the absorption of between  $10^5$  to  $10^7$  photons (Anderson et al., 1998). However, if PS II photodamage is dependent solely on the number of photons absorbed by PS II, then photodamage to PS II should be insensitive to the capacity to utilize the absorbed light energy via the photosynthetic electron transport and  $\text{CO}_2$  assimilation and should occur independent of temperature. Recent evidence indicates that increased capacity for photosynthetic electron transport and  $\text{CO}_2$  assimilation do protect against photoinhibitory damage (Öquist and Huner, 1992; Öquist et al., 1992b; Park et al., 1996a,b; Baroli and Melis, 1998). Furthermore, sensitivity to photodamage is exacerbated by exposure of plants to low temperatures (Huner et al., 1993; Krause, 1994). Thus, any environmental condition that either limits the rate of photosynthesis or the capacity of any metabolic sink to consume photosynthetically generated electrons ( $\text{CO}_2$  limitation, N-limitation, suboptimal temperatures) or enhances the rate of light absorption relative to the rate of electron transport (high light, increased light-harvesting antenna size) will result in an energy imbalance, that is,  $\sigma_{\text{PSII}} \cdot I > n \cdot \tau^{-1}$ . These conditions would increase the 'excitation pressure' on PS II and consequently result in an over-reduction of the PQ

pool which would shift the relative redox state of  $Q_A$  from oxidized to reduced thereby increasing the probability of photodamage to PS II. However, it has been reported that for a number of species the onset of photoinhibition can be detected when less than 40% of  $Q_A$  is in the reduced state which indicates that photodamage to PS II may occur when the majority of PS II reaction centers are still open (Öquist and Huner, 1993). Since photodamage was not distinguished from photoprotection in this latter study, the interpretation of these data with respect to the role of the redox state of  $Q_A$  and PS II photodamage remains equivocal. It would appear that the mitigation of PS II photodamage is a complex phenomenon. Although there is a finite probability for the photo-inactivation of PS II, this probability will vary with the state of acclimation of the photosynthetic apparatus (Anderson et al., 1998).

In contrast to chloroplasts, the cyanobacterium, *Synechococcus* sp. PCC 7942, possesses three homologous genes for the D1 protein of PS II reaction centers (Campbell et al., 1995), designated *psbAI*, *psbAII* and *psbAIII*. The *psbAI* gene encodes form 1, designated D1:1; *psbAII* and *psbAIII* encode form 2, designated D1:2. Mutants expressing D1:2 exhibit greater tolerance to photoinhibition than wild-type cells that express D1:1. Recently, it has been shown that exposure of wild-type *Synechococcus* sp PCC 7942 to low temperature induces a transient exchange of the D1:1 form for the D1:2 form of the PS II reaction center polypeptide, resulting in an increased tolerance to photoinhibition (Campbell et al., 1995). There is a consensus that a rapid cycle of damage and repair of the D1 polypeptide during photoinhibition is an intrinsic feature of PS II (Osmond, 1994; Melis, 1999). A decrease in membrane lipid unsaturation inhibits subsequent recovery from photoinhibition through an impairment of the D1 repair process in cyanobacteria (Nishida and Murata, 1996). This appears to occur because of an inability to process the newly synthesized D1 protein, which results in the accumulation of inactive PS II reaction centers. Moreover, exposure to cold enhances thylakoid fatty acid unsaturation and increases the tolerance of cyanobacteria to low temperature photoinhibition as well as chilling injury (Nishida and Murata, 1996). It has been proposed that modulation of membrane fluidity may act as a primary mechanism to sense changes in temperature in cyanobacteria (Murata and Los, 1997).

### III. Acclimation And Photostasis

#### A. Growth Irradiance

Growth irradiance modulates the size and composition of the light-harvesting antennas of PS I and PS II (Anderson, 1986; Sukenik et al., 1987; Tanaka and Melis, 1997; Melis, 1998). Species of the green alga *Dunaliella* exhibit a remarkable range in their capacity to adjust PS II antenna size (Sukenik et al., 1987; Tanaka and Melis, 1997; Melis, 1998). Generally, there is an inverse relationship between growth irradiance and antenna size. Thus, low growth light promotes large PS I and PS II antenna size whereas growth at high light generates a small photosynthetic unit size. This adjustment in PS II antenna size is the result of changes in the size of peripheral antenna of PS II and PS I, that is changes in LHCII and LHCI, rather than changes in the core antenna of PS II and PS I (Fig. 1). Similar changes in light-harvesting antenna size due to alterations in the levels of peridinin-Chl *a* protein complexes and the intrinsic *a/c*-containing light-harvesting proteins have also been observed during photoacclimation of the dinoflagellate, *Amphidinium carterae* (ten Lohuis and Miller, 1998). Figure 1A depicts a generalized view of the peripheral Chl *a/b* light-harvesting antenna as well as the core complex, consisting of CP47, CP43 and the reaction center proteins (D1/D2), of *Dunaliella salina* grown under low light. The peripheral PS II light-harvesting antenna is thought to consist of trimeric forms of Lhcb1 and Lhcb2 (Fig. 1, trimer) plus monomeric forms consisting of one of each of Lhcb3, Lhcb4, Lhcb5 and Lhcb6 (Fig. 1, m). In PS II, changes in light-harvesting antenna size are a consequence of the assembly of a variable number of Lhcb1/Lhcb2 trimers (Melis, 1998). Figure 1B illustrates the antenna organization after growth under moderate irradiance. Under these conditions, the content of peripheral Lhcb1/Lhcb2 trimers has decreased relative to that for growth under low light with no major changes in the polypeptide composition of the PS II core complex. Under high growth irradiance, PS II is thought to contain minimum levels of trimeric Lhcb1/Lhcb2. Initial growth under high light followed by a shift to low irradiance results in the recovery of maximum PS II antenna size within 12 to 24 h. However, low light grown cells subsequently shifted to high light exhibit only a very slow decline in LHCII abundance (Melis, 1998). Thus, it appears that it is easier to

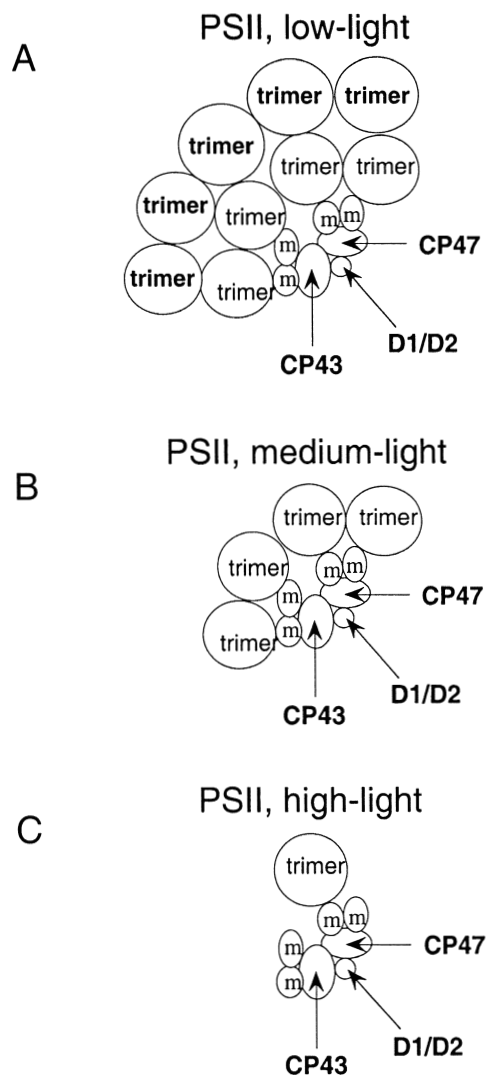


Fig. 1. Schematic models illustrating the effects of growth irradiance on the LHCII subunit composition and size in the green alga *Dunaliella salina*. Trimers of *D. salina* LHCII are composed of two subunits of Lhcb1 and 1 subunit of Lhcb2. Monomers (m) of LHCII are one subunit each of Lhcb3, Lhcb4, Lhcb5 and Lhcb6. Adapted from Melis (1998).

biosynthesize and assemble LHCII than it is to degrade this Chl-protein complex. In response to growth irradiance, these data are consistent with the notion that one mechanism to maintain photostasis is through modulation of  $\sigma_{\text{PSII}}$ . In addition to this mechanism, plants, green algae and cyanobacteria also modulate PS II/PS I stoichiometry (Fujita, 1994; Melis, 1998).

Although terrestrial plants exhibit the capacity to photoacclimate (Anderson, 1986; Anderson et al.,

1995), the extent of the photoacclimatory response is dampened relative to that of green algae (Falkowski and LaRoche, 1991). This apparently lower degree of plasticity with respect to the photoacclimation response in plants versus certain green algal species such as *Chlorella vulgaris* and *Dunaliella salina* and *Dunaliella tertiolecta* may, in part, reflect the physical impact of canopy structure, leaf angle and the inherent light gradients within a single leaf on light absorption. All of these factors would help to maintain photostasis through affecting the rate of light absorption ( $\sigma_{\text{PSII}} \cdot I$ ) by modulating  $I$ .

## B. Growth Temperature

### 1. Green Algae and Cyanobacteria

Low-temperature acclimation of the unicellular green algae, *Chlorella vulgaris* and *Dunaliella salina*, results in a depression of the capacity for  $\text{CO}_2$  assimilation and photosynthetic efficiency calculated on a per cell basis concomitant with an increase in the total xanthophyll pool size as well as a lower epoxidation state of the xanthophyll cycle pigments due to the conversion of violaxanthin to zeaxanthin (Maxwell et al., 1995a). In addition, cold acclimation of these green algae is associated with: a six-fold lower chlorophyll content per cell, a lower abundance of *Lhcb* mRNA as well as *Lhcb* polypeptides (Maxwell et al., 1995b) and an increased level of the carotenoid-binding protein, *Cbr*, than non-acclimated control cells (Krol et al., 1997). However, these algae appear unable to up-regulate carbon metabolism and thus are unable to adjust the number of electron-consuming sinks during growth and development at low temperature (Savitch et al., 1996). As a consequence, algal cultures grown at low temperature exhibited a distinctive yellow color (Huner et al., 1998). The repression in the accumulation of *Lhcb* mRNA and *Lhcb* polypeptides is not due to sucrose suppression (Jang and Sheen, 1994), since the capacity for sucrose accumulation is depressed upon cold acclimation of *Chlorella vulgaris* (Savitch et al., 1996).

Cultures grown at low temperature exhibit a three to four-fold increased tolerance to photoinhibition (Maxwell et al., 1995a). Thus, *Chlorella vulgaris* and *Dunaliella salina* alter their pigmentation significantly in response to low growth temperature or high growth irradiance. This reflects a reduction in light-harvesting capacity coupled with an increased

capacity to dissipate excess light nonphotochemically as heat through zeaxanthin and possibly lutein, which results in a decrease in  $\sigma_{\text{PSII}}$ .

Photosynthetic adjustment of *Chlorella* and *Dunaliella* to growth at low temperature and moderate irradiance is comparable to cells grown at high light with respect to pigmentation, gas exchange, sensitivity to photoinhibition as well as the accumulation of *Lhcb* and *Cbr* polypeptides (Maxwell et al., 1995a; Krol et al., 1997). This cannot be explained as either a simple growth temperature effect or as a simple irradiance response. Cultures grown at 5 °C and 150  $\mu\text{mol m}^{-2} \text{s}^{-1}$  (low temperature, medium light) or at 27 °C and 2200  $\mu\text{mol m}^{-2} \text{s}^{-1}$  (high temperature, high light) are both adjusted to growth at high PS II 'excitation pressure.' Conversely, cultures grown at either 27 °C and 150  $\mu\text{mol m}^{-2} \text{s}^{-1}$  (high temperature, medium light) or 5 °C and 20  $\mu\text{mol m}^{-2} \text{s}^{-1}$  (low temperature, low light) are both adjusted to low 'excitation pressures' (Huner et al., 1998). Similar conclusions regarding the role of PS II 'excitation pressure' have been reported for thermal and photoacclimation of *Laminaria saccharina* (Machalek et al., 1996), the expression of early light-inducible proteins (ELIPs) in barley (Montane et al., 1999) as well as systemic signaling of oxidative stress in *Arabidopsis thaliana* (Karpinski et al., 1999). However, Machalek et al. (1996) have shown that although thermal acclimation is similar to photoacclimation in many respects, it is not identical to photoacclimation.

Changes in pigmentation in the filamentous, nonheterocystous cyanobacterium, *Plectonema boryanum*, grown under ambient  $\text{CO}_2$  and either low temperature or high irradiance reflect adjustments in  $\sigma_{\text{PSII}}$  analogous to that observed in *Chlorella* and *Dunaliella* (Miskiewicz et al., 2000). In contrast to *Plectonema boryanum*, changes in pigmentation in *Synechococcus* sp. PCC 7002 cultures induced by low temperature are not due to either limitations in photosynthesis or low temperature photoinhibition of PS II but are a consequence of low temperature-induced nitrogen limitation (Sakamoto and Bryant, 1998). Thus, the energy imbalance as reflected by chlorosis of *Synechococcus* sp. PCC 7002 at low temperature, appears to be due to a limitation in sink capacity ( $\tau^{-1}$ ).

### 2. Evergreen Plants

In overwintering Scots pine (*Pinus sylvestris*), the

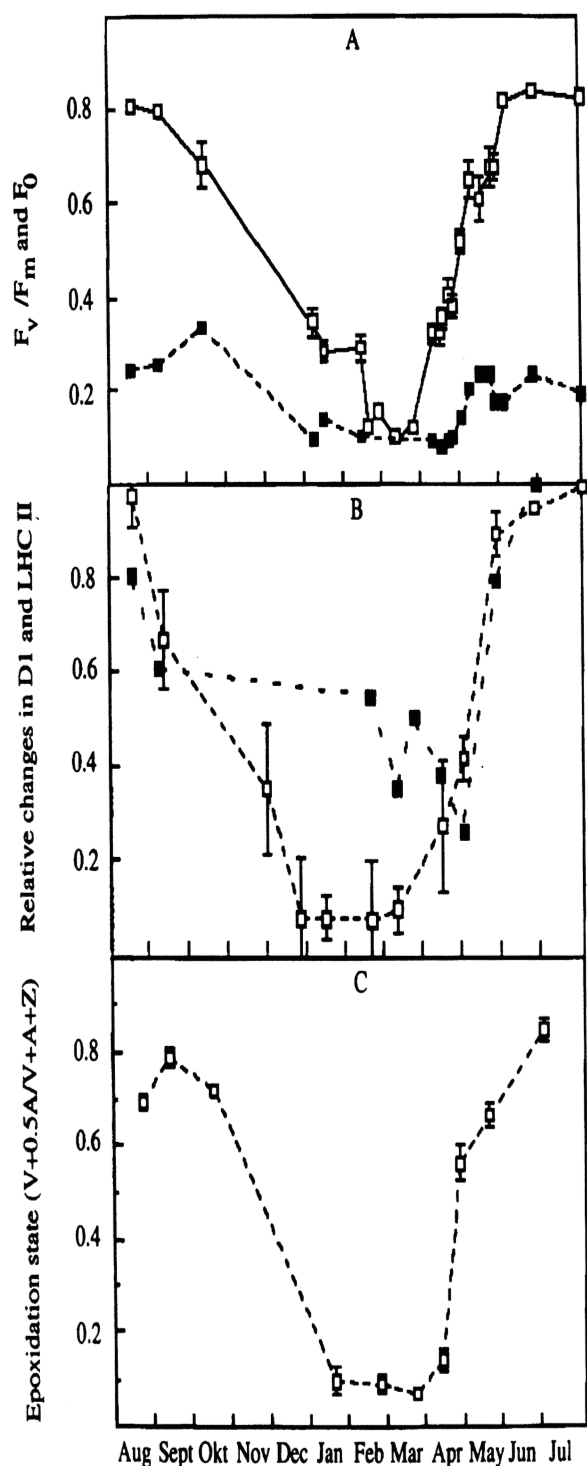


Fig. 2. (A) Seasonal variations in the photochemical efficiency of PS II ( $F_v/F_m$ ) (open symbols) and intrinsic fluorescence yield when all PS II centers are open ( $F_0$ ; closed symbols) in needles of Scots pine. (B) Seasonal variations in the D1 protein (open symbols) and the LHCII protein complex (closed symbols) in

light-harvesting antenna responds to high light and low temperatures by both an increase in the total xanthophyll pool size as well as an increased de-epoxidation of the xanthophyll cycle pigments (Ottander et al., 1995). Adams and coworkers have documented this characteristic response in several winter evergreen species such as *Pinus ponderosa* and *Malva neglecta* (Verhoeven et al., 1999), *Mahonia repens* (Logan et al., 1998b), *Vinca major* (Logan, et al., 1998a) and *Euonymus kiautschovicus* (Verhoeven et al., 1998) exposed to mild winter conditions. The xanthophyll cycle exhibits persistent engagement over night resulting in the de-epoxidation of xanthophyll cycle pool when the nocturnal temperatures are below freezing. In contrast, the xanthophyll cycle is disengaged when the nocturnal temperatures are above freezing resulting in the epoxidation of zeaxanthin and antheraxanthin to violaxanthin. It is suggested that the de-epoxidation of the xanthophyll pool efficiently protects PS II from photodynamic damage by decreasing  $\sigma_{PSII}$  due to an increased capacity for non-radiative dissipation of excess absorbed energy when low temperature limits the rate of photosynthesis (Demmig-Adams and Adams, 1996; Gilmore, 1997; Gilmore and Ball, 2000).

The mechanism of persistent engagement of zeaxanthin and antheraxanthin and the associated high capacity for non-radiative heat dissipation of absorbed light in the light-harvesting antenna is not well understood. Ottander et al. (1995) suggest that the persistent non-radiative heat dissipation of overwintering Scots pine is not only due to xanthophyll cycle activity but is also due to a reorganization of the entire light-harvesting antenna complex to maximize thermal dissipation. In Scots pine exposed to the severe, natural winter conditions of Northern Sweden, there was a close match throughout the winter between the epoxidation state of the xanthophyll cycle pigments and the change in variable fluorescence determined as the ratio of  $F_v/F_m$  (Fig. 2, A and C; Ottander et al. 1995). These winter stress responses may be regarded as adjustments for the safe dissipation of absorbed light under conditions when photosynthesis is largely inhibited due to impaired Photosystem II function as reflected by the breakdown of the D1 protein (Fig. 2B). The winter-induced aggregation of the

(Fig. 2. Continued) needles of Scots pine. (C) Seasonal variations in the epoxidation state of the xanthophyll cycle pigments in needles of Scots pine. V, violaxanthin; A, antheraxanthin; Z, zeaxanthin. (From Ottander et al., 1995).



light-harvesting chlorophyll antenna of Photosystem II which is reversed in the spring, appears to be a very efficient mechanism to dissipate absorbed excitation energy non-radiatively. Thus photostasis is maintained during the winter months by a reduction of the functional absorption cross section of PS II ( $\sigma_{\text{PSII}}$ ) under conditions where the capacity for  $\text{CO}_2$  assimilation is limited ( $n \cdot \tau^{-1}$ ). This reorganization of the light-harvesting apparatus of Scots pine during the winter may represent not only a mechanism to maintain photostasis but also a mechanism to maintain large stocks of chlorophyll in a quenched, protected state when photosynthesis is inhibited and to allow for rapid recovery of photosynthesis during the spring. This may be of great significance to the success of conifers in cold climates and help explain why conifers have become so successful in temperate and subarctic climates with cold winters (Öquist and Martin, 1986).

Overwintering of the herbaceous evergreen, periwinkle (*Vinca minor* L.), results in approximately 50% lower apparent  $\Phi_{\text{app}} \text{O}_2$  and  $P_{\text{max}}$  than comparable plants in the summer (Fig. 3A). Seasonal fluctuations in the zeaxanthin and violaxanthin contents as a consequence of the changing canopy cover in the spring and snow cover in the winter are characteristic of periwinkle leaves (Fig. 3B). Leaves from natural stands of periwinkle with the highest zeaxanthin contents typically were the least sensitive to laboratory photoinhibition conditions. However, the accumulation of zeaxanthin is not always correlated to increased non-photochemical quenching of chlorophyll fluorescence and protection against photoinhibition (Hurry and Huner, 1992; Hurry et al., 1996b; Hurry et al., 1997). This is consistent with the presence of both a zeaxanthin-independent and a zeaxanthin-dependent mechanism for the down regulation of PS II (Horton et al., 1996). During the late fall and early spring, the xanthophyll cycle is induced in leaves of *Vinca minor* L. resulting in an reduction of  $\sigma_{\text{PSII}}$  due to an enhancement of non-radiative dissipation of excess light with minimal changes in either Chl a/b ratios, LHCII abundance or LHCII composition and organization.

### 3. Herbaceous Winter Annuals

Cold tolerant cereals such as winter rye and winter wheat must grow and develop at low temperatures for maximum cold tolerance and successful winter survival in temperate climates. Thus, in contrast to

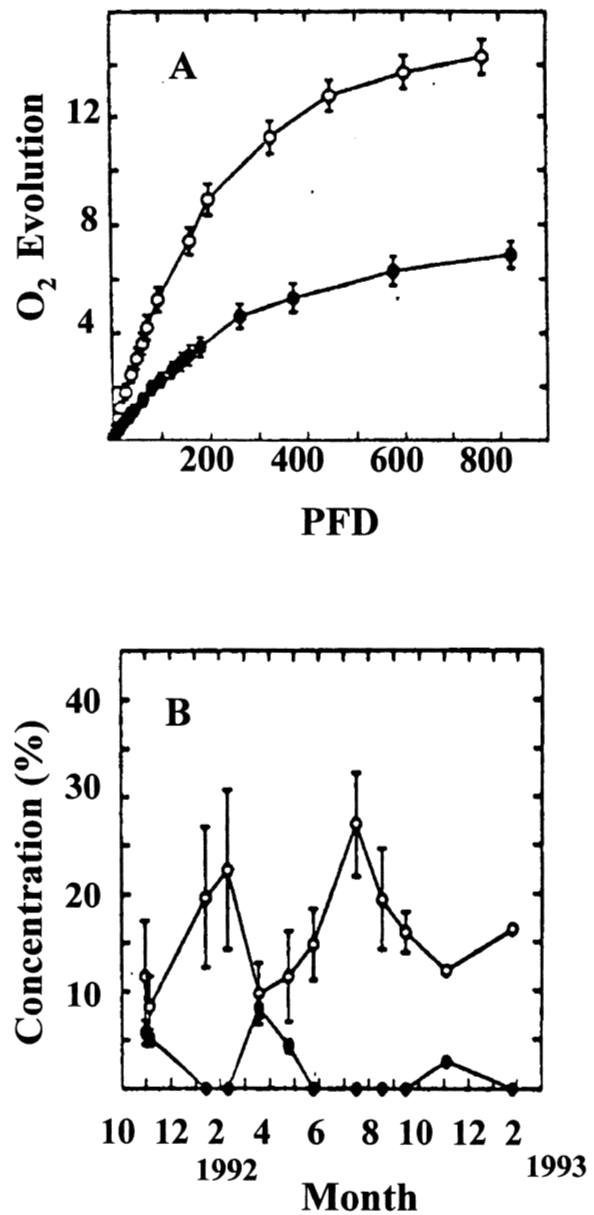


Fig. 3. (A) Effects of summer (open circles) and winter conditions (closed circles) on the light response curve for  $\text{CO}_2$  saturated,  $\text{O}_2$  evolution of *Vinca minor* L. leaves from a natural stand. (B) Seasonal variations in zeaxanthin (closed circles) and violaxanthin (open circles) content in *Vinca minor* L. leaves. Numbers indicate months of the year starting October (10) 1991. From Rezanoff (1993).

most evergreen plants, these plant species maintain the capacity for active photosynthesis during prolonged exposure to low, non-freezing temperatures during the cold acclimation period in the autumn with minimal changes in pigment content and



composition as well as no significant changes in the contents of Lhcb1, Lhcb2, D1, Cyt  $b_6f$ , PC, PsA/PsaB and the  $\gamma$ -subunit of the chloroplast ATP synthase complex (Gray et al., 1998). Somersalo and Krause (1990) were the first to report that cold acclimation of spinach results in an increased tolerance to photoinhibition, a result that was subsequently confirmed for winter rye and wheat (Öquist et al., 1993). This increased tolerance to photoinhibition was primarily due to an increased capacity to keep  $Q_A$  oxidized as a consequence of an elevated photosynthetic capacity with no change in photosynthetic efficiency (Öquist and Huner, 1992; 1993). The potential to keep  $Q_A$  oxidized and the potential to increase the photosynthetic capacity as a consequence of cold acclimation are correlated with both tolerance to photoinhibition and the capacity of winter rye and wheat cultivars to develop maximum freezing tolerance (Öquist et al., 1993; Gray et al., 1997).

The increased capacity of rye, wheat, rape and *Arabidopsis thaliana* to keep  $Q_A$  oxidized appears to be a consequence of a cold acclimation-induced stimulation of mRNA and protein levels associated with the major regulatory enzymes of photosynthetic carbon metabolism: Rubisco, stromal and cytosolic fructose biphosphatase, and sucrose phosphate synthase (Hurry et al., 1996a). This is translated into increased growth rates under potentially photoinhibitory conditions (Hurry et al., 1992). Thus, the elevated sucrose levels normally associated with cold acclimation do not result in the repression of photosynthetic gene expression in *Arabidopsis*, rye or wheat (Hurry et al., 1996a) contrary to current models related to sucrose regulation of plant gene expression (Jang and Sheen, 1994). It appears that increased cold tolerance and tolerance to photoinhibition may be the result of a 'reprogramming' of carbon metabolism and partitioning in these species (Hurry et al., 1996a). Thus, in contrast to *Chlorella vulgaris* and *Dunaliella salina*, winter wheat and winter rye appear to maintain photostasis primarily through an adjustment in sink capacity ( $n \cdot \tau^{-1}$ ) in response to growth at low temperatures with minimal changes in the structure and function of the photochemical apparatus (Gray et al., 1998). In addition to  $CO_2$  assimilation,  $O_2$  reduction through the Mehler reaction appears to play an important role as an electron sink while photorespiration plays a minimal role in the maintenance of photostasis in cold acclimated winter wheat. In contrast, both

photorespiration and the Mehler reaction appear to play a significant role in maintenance of energy balance in high light-grown winter wheat (Savitch et al., 2000). However, this response appears to be species specific since tolerance to low temperature photoinhibition in spinach appears to be a consequence of adjustments in carotenoid composition and xanthophyll cycle activity and hence a decrease in  $\sigma_{PSII}$  (Krause et al., 1999; Verhoeven et al., 1999).

Gray et al. (1997) have shown that the photosynthetic response and tolerance to photoinhibition of cold acclimated wheat and rye is not due to either temperature or light per se but rather to PS II 'excitation pressure' similar to the results for *Chlorella* and *Dunaliella*. Although growth of winter rye at low temperatures has minimal effects on the content and the pigment-protein composition of LHCII, development at low temperature does result in a significant reorganization of the supramolecular structure of LHCII as indicated by chloroplast ultrastructure, freeze-fracture of thylakoids and separation of Chl-protein complexes of isolated rye thylakoids by non-denaturing SDS-PAGE (Huner et al., 1993). Growth temperature modulates LHCII organization such that the oligomeric or trimeric form of LHCII predominates at 20 °C whereas the monomeric form predominates at 5 °C. Furthermore, these changes in structural stability were associated with a specific decrease in the *trans*- $\Delta^3$ -hexadecenoic acid (*trans*-16:1) content (Krol et al., 1988), a unique thylakoid membrane fatty acid specifically esterified to C-2 of thylakoid phosphatidylglycerol (PG) only (Harwood, 1980). In vitro reconstitution experiments indicated that PG containing *trans*-16:1 is specifically bound to LHCII and required to stabilize the trimeric form in rye thylakoids (Krupa et al., 1992). This is consistent with the recent identification of a specific binding site for PG on Lhcb which is required for LHCII trimerization (Nußberger et al. 1993; Hobe et al., 1995). Presumably the reversible transition from monomeric to trimeric state would effect  $\sigma_{PSII}$  (Horton et al., 1996). However, the functional significance of these changes in the stability of LHCII organization in cereals during acclimation to low temperature have yet to be elucidated.

### C. Nutrient Limitations

Growth of higher plants such as sugar beet, peach and pear under Fe deficiency induces significant leaf chlorosis which is associated with a decrease in

photosynthetic capacity as a consequence of a co-ordinated decrease in the content of LHCII, electron transport components and Rubisco (Terry, 1983; Taylor and Terry, 1986; Winder and Nishio, 1995). Although total Chl per leaf area decreases during growth under Fe deficiency, the reaction centers that are present under these conditions are fully active. Thus, the observed decrease in absorbance of sugar beet leaves grown under Fe deficiency is due to a decrease in the number of PS II units per leaf area (Spiller and Terry, 1980; Abadía et al., 2000). In addition to the decrease in the apparent size of LHCII, growth under Fe deficient conditions increases the extent of non-photochemical quenching associated with PS II. This is primarily due to the stimulation of the xanthophyll cycle (Abadía et al., 2000). Thus, we suggest that these observations are consistent with the thesis that plants grown under Fe deficient conditions attempt to maintain photostasis by: (1) decreasing  $I$  by lowering total pigment content per leaf area through a decrease in the number of PS II units per leaf area; (2) decreasing  $\sigma_{\text{PSII}}$  by lowering the LHCII content and increasing the zeaxanthin and antherxanthin contents relative to violaxanthin. Furthermore, the observation that Rubisco content is reduced during growth under Fe deficient conditions ensures that the rate of light absorption ( $\sigma_{\text{PSII}} \cdot I$ ) matches the capacity for  $\text{CO}_2$  assimilation ( $\tau^{-1}$ ).

We note with interest that chlorotic leaves of plants grown under Fe deficient conditions will turn green when exposed to an irradiance lower than the growth irradiance even though the plants are still under Fe deficient conditions (Abadía et al., 2000). Thus, the induction of this chlorotic state can not be due to Fe deficiency per se but must be due to an interaction of Fe deficiency and growth irradiance. This modulation of pigmentation in response to Fe deficiency in higher plants is strikingly similar to that described above for *Chlorella vulgaris* in response to growth temperature. Thus, we suggest that the changes in pigmentation, LHCII content and photosynthetic capacity in sugar beet in response to Fe deficiency may reflect acclimation to increased 'excitation pressure' induced by Fe limitation.

In *Chlamydomonas reinhardtii*, both phosphate and sulfate limitations independently result in a decrease in both photosynthetic capacity ( $P_{\text{max}}$ ) as well as  $\Phi_{\text{app}} \text{O}_2$  (Wykoff et al., 1998). Concomitantly, nutrient limited *Chlamydomonas* exhibited reduced efficiency of energy transfer from LHCII to PS II

reaction centers due to the combined effects of increased capacity for xanthophyll cycle-dependent, non-photochemical quenching of excess energy plus the induction of a state 2 transition during exposure to nutrient-limited conditions. These alterations result in a reduction in photosynthetic electron flow when this green alga is limited in either P or S. Thus, the photoacclimation response induced by nutrient limitations in order to maintain photostasis in this green alga, at least in part, appears to involve an adjustment of  $\sigma_{\text{PSII}}$ .

Cyanobacterial cultures deficient in macronutrients such as C, N, S and P typically exhibit chlorosis which reflects, in part, phycobilisome degradation (Grossman et al., 1994; Chapter 17, Grossman et al.). This degradation process is an ordered process in *Synechococcus* and *Synechocystis* sp. In addition, exposure of *Synechococcus* sp. to C-limitations induces the accumulation of a 42 kDa carotenoid binding protein concomitant with the reduction in phycobilisome content. The abundance of this carotenoid-binding protein is light dependent (Reddy et al., 1989). It has been proposed that phycobilisome degradation during nutrient limitation may provide a source of amino acids for the acclimation process. This 'trimming mechanism' is rapidly reversed upon readdition of the limiting nutrient (Grossman et al., 1994). However, since the size and number of phycobilisomes is reduced, photostasis potentially would be maintained as a consequence of the decrease in  $\sigma_{\text{PSII}}$  thus preventing the over-excitation of the photosynthetic apparatus.

Cyanobacteria exhibit an impressive capacity to alter the composition of electron carriers of the thylakoid membrane in response to limitations in micronutrients such as Fe and Cu (Straus, 1994). However, it is also well documented that iron-deficiency reduces both the phycobillin and chlorophyll containing antennas in cyanobacteria (Grossman et al., 1994). One of the most interesting changes observed in *Synechococcus*, *Synechocystis* and *Anabaena* is an induction of an iron stress-induced chlorophyll protein complex associated with Photosystem II (Guikema and Sherman, 1983; Leonhardt and Straus, 1994). This chlorophyll protein complex, denoted CP43', is encoded by the *isiA* gene which has close sequence similarity to *psbC*, the gene which encodes CP43 (Straus, 1994). It was proposed that CP43' may functionally replace CP43 as part of the core antenna of PS II or simply function

as a chlorophyll reservoir to facilitate recovery from iron deficiency (Burnap et al., 1993). However, picosecond Chl *a* fluorescence life-time measurements indicate inefficient energy transfer from CP43' to PS II reaction centers (Falk et al., 1995). Recently, Park et al. (1999) showed that CP43' protects Photosystem II from excess light in iron-starved cells of *Synechococcus* sp. PCC 7942. They suggested that CP43' functions as a non-radiative dissipator of absorbed light, thus protecting Photosystem II from light stress under iron deficiency. In contrast, recent structural evidence indicates that CP43' appears to be primarily associated with PS I rather than PS II (Bibby et al., 2001; Boekema et al., 2001; Huner et al., 2001). It is suggested that the ring structure formed around PS I by CP43' functions as an antenna for PS I (Bibby et al., 2001; Boekema et al., 2001). Thus, any possible role of CP43' in photoprotection during iron stress requires further investigation.

#### IV. Chloroplast Biogenesis and Photostasis

Angiosperms produce etiolated seedlings when exposed to prolonged darkness (Leech, 1984). Chloroplast biogenesis and assembly of the photosynthetic apparatus have been examined in monocots and dicots by exposure of etiolated seedlings to continuous or intermittent illumination (Akoyunoglou, 1984).

Early light-inducible proteins (ELIPs) are thylakoid polypeptides induced under high light stress and are related to the Lhcb/Lhca family of Chl *a/b* light-harvesting polypeptides (Green and Durnford, 1996). It has been suggested that ELIPs bind zeaxanthin and act as Chl scavengers after the light-dependent breakdown of thylakoid Chl-protein complexes (Krol et al., 1995; Adamska, 1997). Kloppstech and co-workers were the first to report that ELIPs are transiently expressed during greening of etiolated barley seedlings and mature leaves exposed to high-light stress (Meyer and Kloppstech, 1984). Similar light-inducible, carotenoid binding proteins (Cbr) have been detected in species of the green alga, *Dunaliella* (Levy et al., 1993; Krol et al., 1997; Banet et al., 2000). Recently, Heddad and Adamska (2000) identified two new light-stress enhanced proteins in *Arabidopsis thaliana*, Sep1 and Sep2, which exhibit ELIP consensus sequences and appear to be related to the Chl *a/b*-binding gene family.

Although the precise role of Sep1 and Sep2 is unknown, it is suggested that they are involved in photoprotection rather than light-harvesting (Heddad and Adamska, 2000).

The sensitivity of photoautotrophs to potential energy imbalances during the biosynthesis and assembly of the photochemical apparatus, which process in itself is light dependent, was examined by Krol et al. (1999). Greening of etiolated wild-type and the chlorina *f2* mutant of barley under continuous illumination at 20 °C resulted in transient fluctuations in the epoxidation state of the xanthophyll cycle pigments (EPS) which reflect the photoconversion of the light-harvesting xanthophyll, violoxanthin, to the energy quenching pigments, antheraxanthin and zeaxanthin (Demmig-Adams and Adams, 1996). Furthermore, the extent of the transient fluctuations in EPS was light intensity dependent. These trends were mimicked during greening of both the wild type and the chlorina *f2* mutant of barley at 5 °C and moderate irradiance (250  $\mu\text{mol m}^{-2} \text{s}^{-1}$ ). These transients in EPS reflected transient accumulations of zeaxanthin and a 14 kDa ELIP in both the wild type and the chlorina *f2* mutant (Krol et al., 1999). These patterns of accumulation for zeaxanthin and the 14 kDa ELIP are consistent with the notion that ELIPs may be zeaxanthin-binding proteins which protect the developing photosynthetic apparatus from over-excitation (Krol et al., 1995). However, in a recent study it was shown that the distribution of antheraxanthin and zeaxanthin along the length of barley leaves did not follow the same patterns of distribution as ELIPs. Thus, it was concluded that xanthophyll accumulation is not correlated with the accumulation of ELIPs (Montane et al., 1999). Clearly, further work is required to elucidate unequivocally the role of ELIPs in carotenoid-binding.

Assuming that the transient fluctuations in EPS during greening are due, primarily, to the modulation of the xanthophyll cycle the signal which induces the observed fluctuation in EPS cannot be due to either light or temperature per se. We suggest that the fluctuations in EPS and ELIP levels reflect a response to changes in 'excitation pressure' as a result of transient imbalances between energy absorbed by the developing photochemical apparatus versus energy utilized by metabolism due to limitations in photosynthetic capacity during various stages of chloroplast biogenesis.

## V. Sensing Mechanisms Involved in Photostasis

What is the molecular mechanism underlying photoacclimation responses involved in the maintenance of photostasis in photoautotrophs? Sensing and signaling events involved in photomorphogenesis and plant development are typically associated with photoreceptors such as the red-far red photoreceptor, phytochrome, the blue light photoreceptor, cryptochrome, as well as UV-light photoreceptors (Chory, 1997; Ballaré, 1999). We are unaware of any unequivocal evidence to indicate that phytochrome regulates gene expression during steady-state vegetative growth. Stimulation of physiological processes through phytochrome are usually dependent upon changes in the ratio of red to far red light and are photoperiod dependent. However, the photoacclimation responses described above for terrestrial plants, green algae and cyanobacteria are not regulated by a photoreceptor such as phytochrome for the following reasons: (1) the reductions in Chl content and composition and Lhcb levels can be induced simply by changing the temperature with no change in either irradiance, light quality or photoperiod (Huner et al., 1998) and (2) photoacclimation is sensitive to inhibitors of photosynthetic electron transport (Beale and Appleman, 1971; Koenig, 1990; Naus and Melis, 1992; Escoubas et al., 1995). The most definitive experiments regarding the role of photoreceptors in photoacclimation have been performed by Walters et al. (1999) who exploited the availability of photoreceptor mutants in *Arabidopsis*. They showed that the photoreceptor mutants of *Arabidopsis* are still capable of photoacclimation even though these mutants are impaired in photomorphogenesis. Thus, photoacclimation in fully developed *Arabidopsis* tissue is not photoreceptor dependent.

Based on the differential sensitivity of the photoacclimation response to either DCMU (3-(3,4-dichlorophenyl)-1,2-dimethyl urea) or DBMIB (2,5-dibromo-3-methyl-6-isopropyl-*p*-benzoquinone), it has been proposed that the redox state of the plastoquinone pool may act as the sensor that regulates the photoacclimation response in algae (Escoubas et al., 1995; Wilson and Huner, 2000) as well as cyanobacteria, as first shown by Fujita and co-workers (Fujita et al., 1994). This redox signal can be modulated by either light or temperature and may initiate a transduction pathway that coordinates not

only photosynthesis-related gene expression but also the expression of genes involved in cold acclimation and freezing tolerance as well as plant morphogenesis (Gray et al., 1997; Huner et al., 1998), systemic acclimation to excess irradiance (Karpinski et al., 1999) and cyanobacterial differentiation (Campbell et al., 1993). An intrachloroplastic redox signaling pathway has recently been shown to include the ferredoxin-thioredoxin system as a critical component of redox regulation of chloroplast translation (Bruick and Mayfield, 1999). Although signaling between the chloroplast and the nucleus has been investigated for some time (Taylor, 1989), the nature of the chloroplastic signal and the retrograde signal transduction pathway have yet to be completely elucidated. However, Mg-protoporphyrin IX has been shown to act as a 'plastid factor' in the signal transduction pathway regulating nuclear encoded heat-shock genes (Kropat et al., 1997; 2000).

It appears that the mechanism of photostasis through modulation of  $\sigma_{PSII}$  may involve not one but at least two distinct but related processes: (1) regulation of xanthophyll cycle activity and nonphotochemical quenching and (2) regulation of *Lhcb* gene expression (Wilson and Huner, 2000). In both cases, the PQ pool may act as the sensor. Changes in the transthylakoid pH may regulate xanthophyll cycle activity whereas the redox state of the PQ pool may regulate nuclear gene expression (Escoubas et al., 1995; Maxwell et al., 1995b). Thus, the maintenance of photostasis in terrestrial plants, green algae and cyanobacteria appears to exert a broad influence on diverse molecular, physiological and developmental process which is consistent with the concept of a 'grand design of photosynthesis' initially proposed by Daniel Arnon (Arnon, 1982; Anderson et al., 1995).

## Acknowledgments

NPAH is grateful for the financial support from the Natural Sciences and Engineering Research Council of Canada. Research in the laboratory of GÖ was supported by the Swedish Natural Science Research Council. GÖ and NPAH acknowledge financial support by the Swedish Foundation for International Cooperation in Research and Higher Education. AM acknowledges support by the USDA NRI Competitive Grants Program (Plant Responses to the Environment) and by the US DOE Hydrogen R & D Program.

## References

- Abadía J, Morales F and Abadía A (2000) Photosystem II efficiency in low chlorophyll, iron deficient leaves. *Plant and Soil* 215: 183–192
- Adamska I (1997) ELIPs- light -induced stress proteins. *Physiol Plant* 100: 794–805
- Akoyunoglou G (1984) Thylakoid biogenesis in higher plants: Assembly and reorganization. In: Sybesma C (ed) *Advances in Photosynthesis Research*, Vol 4, pp 595–602. Martinus Nijhoff/ Dr W Junk Publishers, The Hague
- Allen JF and Pfannschmidt T (2000) Balancing the two photosystems: Photosynthetic electron transfer governs transcription of reaction center genes in chloroplasts. *Phil Trans R Soc Lond B* 355: 1351–1359
- Allen JF, Bennett J, Steinback KE and Arntzen CJ (1981) Chloroplast protein phosphorylation couples plastoquinone redox state to distribution of excitation energy between photosystems. *Nature* 291: 21–25
- Anderson JM (1986) Photoregulation of the composition, function and structure of thylakoid membranes. *Annu Rev Plant Physiol* 37: 93–136
- Anderson JM, Chow WS and Park Y-I (1995) The grand design of photosynthesis: Acclimation of the photosynthetic apparatus to environmental cues. *Photosynth Res* 46: 129–139
- Anderson JM, Park Y-I and Chow WS (1998) Unifying model for the inactivation of Photosystem II in vivo under steady-state photosynthesis. *Photosynth Res* 56: 1–13
- Armond PA and Staehelin A (1979) Lateral and vertical displacement of integral membrane proteins during lipid phase transitions in *Anacystis nidulans*. *Proc Natl Acad Sci USA* 76: 1901–1905
- Armond PA, Schreiber U and Björkman O (1978) Photosynthetic acclimation to temperature in the desert shrub, *Larrea divaricata*. II. Light harvesting efficiency and electron transport. *Plant Physiol* 61: 411–415
- Arnon DI (1982) Sunlight, earth life: The grand design of photosynthesis. *The Sciences* 22: 22–27
- Aro E-M, Virgin I and Andersson B (1993) Photoinhibition of Photosystem II. Inactivation, protein damage and turnover. *Biochim Biophys Acta* 1143: 113–134
- Asada K (1996) Radical production and scavenging in the chloroplasts. In: Baker NR (ed) *Photosynthesis and the Environment*, 123–150. Kluwer, Dordrecht
- Baker NR (1991) A possible role for Photosystem II in environmental perturbations of photosynthesis. *Physiol Plant* 81: 563–570
- Ballaré CL (1999) Keeping up with neighbours: Phytochrome sensing and other signalling mechanisms. *Trends Plant Sci* 4: 97–102
- Banet G, Pick U and Zamir A (2000) Light-harvesting complex II pigments and proteins in association with Cbr, a homolog of higher-plant early light-inducible proteins in the unicellular green alga *Dunaliella*. *Planta* 210: 947–955
- Baroli I and Melis A (1996) Photoinhibition and repair in *Dunaliella salina* acclimated to different growth irradiances. *Planta* 198: 640–646
- Baroli I and Melis A (1998) Photoinhibitory damage is modulated by the rate of and by the Photosystem II light-harvesting chlorophyll antenna. *Planta* 205: 288–296
- Beale SI and Appleman D (1971) Chlorophyll synthesis in *Chlorella*. *Plant Physiol* 47: 230–235
- Berry J and Björkman O (1980) Photosynthetic response and adaptation to temperature in higher plants. *Annu Rev Plant Physiol* 31: 491–543
- Bibby TS, Nield J and Barber J (2001) Iron deficiency induces the formation of an antenna ring around trimeric Photosystem I in cyanobacteria. *Nature* 412: 743–745
- Björkman O and Ludlow MM (1972) Characterization of the light climate on the floor of a Queensland rainforest. *Carnegie Inst Washington Year Book* 71: 85–94
- Boekema EJ, Hifney A, Yakushevskaya AE, Piotrowski M, Keegstra W, Berry S, Michel K-P, Pistorius EK and Kruij J (2002) A giant chlorophyll-protein complex induced by iron deficiency in cyanobacteria. *Nature* 412: 745–748
- Bruce D, Brimble S and Bryant DA (1989) State transitions in a phycobilisome-less mutant of the cyanobacterium *Synechococcus* sp. PCC 7002. *Biochim Biophys Acta* 974: 66–73
- Brugnoli E and Björkman O (1992) Chloroplast movements in leaves: Influence on chlorophyll fluorescence and measurements of light induced absorbance changes related to pH and zeaxanthin formation. *Photosynth Res* 32: 23–35
- Bruick RK and Mayfield SP (1999) Light-activated translation of chloroplast mRNAs. *Trends Plant Sci* 4: 190–195
- Burnap RL, Troyan T and Sherman LA (1993) The highly abundant chlorophyll-protein complex of iron-deficient *Synechococcus* sp PCC7942 (CP43') is encoded by the isiA gene. *Plant Physiol* 103: 893–902
- Campbell D, Houmard J and Tandeau de Marsac N (1993) Electron transport regulates cellular differentiation in the filamentous cyanobacterium *Calothrix*. *Plant Cell* 5: 451–463
- Campbell D, Zhou G, Gustafsson P, Öquist G and Clarke AK (1995) Electron transport regulates exchange of two forms of Photosystem II D1 protein in the cyanobacterium *Synechococcus*. *EMBO J* 14: 5457–5466
- Cheniae GM, and Martin IF (1970) Site of manganese within Photosystem II. Roles in O<sub>2</sub> evolution. *Biochim Biophys Acta* 197: 219–239
- Chory J (1997) Light modulation of vegetative development. *Plant Cell* 9: 1225–1234
- Cleland R and Melis A (1987) Probing the events of photoinhibition by altering electron transport activity and light-harvesting capacity in chloroplast thylakoids. *Plant Cell Environ* 10: 747–752
- Cornic G (2000) Drought stress inhibits photosynthesis by decreasing stomatal aperture—not by affecting ATP synthesis. *Trends Plant Sci* 5: 187–188
- Demmig-Adams B and Adams III WW (1996) The role of xanthophyll cycle carotenoids in the protection of photosynthesis. *Trends Plant Sci* 1: 21–26
- Demmig-Adams B, Adams III WW, Ebbert V and Logan BA (1999) Ecophysiology of the xanthophyll cycle. In: Frank HA, Young AJ, Britton G and Cogdell RJ (eds) *The Photochemistry of Carotenoids*, pp 245–269. Kluwer Academic Publishers, Dordrecht
- Drzymalla C, Schroda M and Beck CF (1996) Light-inducible gene *HSP70B* encodes a chloroplast-localized heat shock protein in *Chlamydomonas reinhardtii*. *Plant Mol Biol* 31: 1185–1194
- Durnford DG and Falkowski PG (1997) Chloroplast redox regulation of nuclear gene transcription during photo-



- acclimation. *Photosynth Res* 53: 229–241
- Escoubas J-M, Lomas M, LaRoche J and Falkowski PG (1995) Light intensity regulates cab gene transcription via the redox state of the plastoquinone pool in the green alga, *Dunaliella tertiolecta*. *Proc Nat Acad Sci USA* 92: 10237–10241
- Falk S, Krol M, Maxwell DP, Rezansoff DA, Gray GR and Huner NPA (1994) Changes in in vivo fluorescence quenching in rye and barley as a function of reduced PS II light-harvesting antenna size. *Physiol Plant* 91: 551–558
- Falk S, Samson G, Bruce D, Huner NPA and Laudenbach DE (1995) Functional analysis of the iron-stress induced CP43' polypeptide of PS II in the cyanobacterium *Synechococcus* sp. PCCC 7942. *Photosynth Res* 45: 51–60
- Falk S, Maxwell DP, Laudenbach DE and Huner NPA (1996) Photosynthetic adjustment to temperature. In: Baker NR (ed) *Photosynthesis and the Environment*, pp 367–385. Kluwer Academic Publishers, Dordrecht
- Falkowski PG (1983) Light-shade adaptation and vertical mixing of marine phytoplankton: A comparative field study. *J Mar Res* 41: 215–237
- Falkowski PG and LaRoche J (1991) Acclimation to spectral irradiance in algae. *J Phycol* 27: 8–14
- Fujita Y, Murakami A, Aizawa K and Ohki K (1994) Short-term and long-term adaptation of the photosynthetic apparatus: homeostatic properties of thylakoids. In: Bryant DA (ed) *The molecular biology of cyanobacteria*, pp 677–692. Kluwer Academic Publishers, Dordrecht
- Funk C, Schröder WP, Green BR, Renger G and Andersson B (1995) The PS II-S protein of higher plants: a new type of pigment-binding protein. *Biochemistry* 34: 11133–11141
- Gantt E (1994) Supramolecular membrane organization. In: Bryant DA (ed) *Molecular Biology of Cyanobacteria*, pp 119–138. Kluwer Academic Publishers, Dordrecht
- Ghirardi M, McCauley S and Melis A (1986) Photochemical apparatus organization in the thylakoid membrane of *Hordeum vulgare* wild type and chlorophyll *b*-less chlorina *f2* mutant. *Biochim Biophys Acta* 851: 331–339
- Gilmore AM (1997) Mechanistic aspects of xanthophyll cycle-dependent photoprotection in higher plant chloroplasts and leaves. *Physiol Plant* 99: 197–209
- Gilmore AM and Ball MC (2000) Photoprotection and storage of chlorophyll in overwintering evergreens. *Proc Natl Acad Sci USA* 97: 11098–11101
- Gilmore AM and Govindjee (1999) How higher plants respond to excess light: Energy dissipation in Photosystem II. In: Singhal GS, Renger G, Irrgang K-D, Sapory S and Govindjee (eds) *Concepts in Photobiology: Photosynthesis and Photomorphogenesis*, pp 513–548. Kluwer Academic Publishers, Dordrecht
- Gilmore AM, Shinkarev VP, Hazlett TL and Govindjee (1998) Quantitative analysis of the effects of intrathylakoid pH and xanthophyll cycle pigments on chlorophyll *a* fluorescence lifetime distributions and intensity in thylakoids. *Biochemistry* 37: 13582–13593
- Golbeck JH (1994) Photosystem I in cyanobacteria. In: Bryant DA (ed) *Molecular Biology of Cyanobacteria*, pp 319–360. Kluwer Academic Publishers, Dordrecht
- Gray GR, Chauvin L-P, Sarhan F and Huner NPA (1997) Cold acclimation and freezing tolerance. A complex interaction of light and temperature. *Plant Physiol* 114: 467–474
- Gray GR, Ivanov AG, Krol M and Huner NPA (1998) Adjustment of thylakoid plastoquinone content and electron donor pool size in response to growth temperature and growth irradiance in winter rye (*Secale cereale* L.). *Photosynth Res* 56: 209–221
- Gray JC (1996) Regulation of expression of nuclear genes encoding polypeptides required for the light reactions of photosynthesis. In: Ort DR, Yocum CF (eds) *Oxygenic Photosynthesis: The Light Reactions*, pp 621–641. Kluwer Academic Publishers, Dordrecht
- Green BR and Durnford DG (1996) The chlorophyll-carotenoid proteins of oxygenic photosynthesis. *Annu Rev Plant Physiol Plant Mol Biol* 47: 685–714
- Grossman AR, Schaefer MR, Chiang GG and Collier JL (1994) The responses of cyanobacteria to environmental conditions: Light and nutrients. In: Bryant DA (ed) *The Molecular Biology of Cyanobacteria*, pp 641–675. Kluwer Academic Publishers, Dordrecht
- Guikema JA and Sherman LA (1983) Organization and function of chlorophyll in membranes of cyanobacteria during iron starvation. *Plant Physiol* 73: 250–256
- Haehnel W (1984) Photosynthetic electron transport in higher plants. *Annu Rev Plant Physiol* 35: 659–693
- Harwood JL (1980) Plant acyl lipids: Structure, function, distribution and analysis. In: PK Stumpf and EE Conn (eds) *The Biochemistry of Plants*, pp 1–55. Academic Press, New York
- Havaux M (1998) Carotenoids as membrane stabilizers in chloroplasts. *Trends Plant Sci* 3: 147–151
- Havaux M and Davaud A (1994) Photoinhibition of photosynthesis in chilled potato leaves is not correlated with a loss of Photosystem II activity. *Photosynth Res* 40: 75–92
- Havaux M, Tardy F and Lemoine Y (1998) Photosynthetic light-harvesting function of carotenoids in higher-plant leaves exposed to high light and irradiances. *Planta* 205: 242–250
- Heckathorn SA, Downs CA, Sharkey TD and Coleman JS (1998) The small, methionine-rich chloroplast heat-shock protein protects Photosystem II electron transport during heat stress. *Plant Physiol* 116: 439–444
- Hedddad M and Adamska I (2000) Light stress-regulated two-helix proteins in *Arabidopsis thaliana* related to the chlorophyll *a/b*-binding gene family. *Proc Natl Acad Sci USA* 97: 3741–3746
- Hobe S, Forster R, Klingler J and Paulsen H (1995) N-Proximal sequence motif in light-harvesting chlorophyll *a/b*-binding protein is essential for the trimerization of light-harvesting chlorophyll *a/b* complex. *Biochemistry* 34: 10224–10228
- Horton P, Oxborough K, Rees D and Scholes JD (1988) Regulation of the photochemical efficiency of Photosystem II; consequences for the light response of field photosynthesis. *Plant Physiol Biochem* 26: 453–460
- Horton P, Ruban Av and Walters RG (1996) Regulation of light-harvesting in green plants. *Annu Rev Plant Physiol Plant Mol Biol* 47: 655–684
- Huner NPA, Öquist G, Hurry V, Krol M, Falk S and Griffith M (1993) Photosynthesis, photoinhibition and low temperature acclimation in cold tolerant plants. *Photosynth Res* 37: 19–39
- Huner NPA, Öquist G and Sarhan F (1998) Energy balance and acclimation to light and cold. *Trends Plant Sci* 3: 224–230
- Huner NPA, Krol M, Ivanov AG, Sveshnikov D and Öquist G (2001) CP43' induced under Fe-stress in *Synechococcus* sp. PCC 7942 is associated with PS I. In: PS2001: Proceedings 12th International Congress on Photosynthesis, S3-061. CSIRO Publishing, Melbourne. [CD-ROM]
- Hurry VM and Huner NPA (1992) Effects of cold hardening on

- sensitivity of winter and spring wheat leaves to short-term photoinhibition and recovery of photosynthesis. *Plant Physiol* 100: 1283–1290
- Hurry VM, Krol M, Öquist G and Huner NPA (1992) Effect of long-term photoinhibition on growth and photosynthesis of cold hardened spring and winter wheat. *Planta* 188: 369–375
- Hurry V, Huner N, Selstam E, Gardestrom P and Öquist G (1996a) Photosynthesis at low temperatures. In: Raghavendra AS (ed) *Photosynthesis: A Comprehensive Treatise*, pp 238–249. Cambridge University Press, Cambridge
- Hurry V, Anderson JM, Badger MR and Price GD (1996b) Reduced levels of cytochrome *b6/f* in transgenic tobacco the excitation pressure on Photosystem II without increasing sensitivity to photoinhibition in vivo. *Photosynth Res* 50: 159–169
- Hurry VM, Anderson JM, Chow WS and Osmond CB (1997) Accumulation of zeaxanthin in abscisic acid-deficient mutants of *Arabidopsis* does not affect chlorophyll fluorescence quenching or sensitivity to photoinhibition in vivo. *Plant Physiol* 113: 639–648
- Ivanov AG, Morgan RM, Gray GR, Velitchkova MY and Huner NPA (1998) Temperature/light dependent development of selective resistance to photoinhibition of Photosystem I. *FEBS Lett* 430: 288–292
- Jahns P and Krause GH (1994) Xanthophyll cycle and energy-dependent fluorescence quenching in leaves from pea plants grown under intermittent light. *Planta* 192: 176–182
- Jang J-C and Sheen J (1994) Sugar sensing in higher plants. *Plant Cell* 6: 1665–1679
- Jansson S (1994) The light-harvesting chlorophyll *a/b*-binding proteins. *Biochim Biophys Acta* 1184: 1–19
- Karpinski S, Reynolds H, Karpinska B, Wingsle G, Creissen G and Mullineaux P (1999) Systemic signaling and acclimation in response to excess excitation energy in *Arabidopsis*. *Science* 284: 654–657
- Keck RW and Boyer JS (1974) Chloroplast response to low leaf water potentials. III. Differing inhibition of electron transport and photophosphorylation. *Plant Physiol* 53: 474–479
- Koenig F (1990) Shade adaptation in cyanobacteria. *Photosynth Res* 26: 29–37
- Kozaki A and Takeba G (1996) Photorespiration protects C3 plants from photoinhibition. *Nature* 384: 557–560
- Krause GH (1994) Photoinhibition induced by low temperatures. In: Baker NR and Bowyer JR (eds) *Photoinhibition of Photosynthesis: From Molecular Mechanisms to the Field*, pp 331–348. Bios Scientific, Oxford
- Krause GH and Weis E (1991) Chlorophyll fluorescence and photosynthesis: The basics. *Annu Rev Plant Physiol Plant Mol Biol* 42: 313–349
- Krause GH, Carouge N and Garden H (1999) Long-term effects of temperature shifts on xanthophyll cycle and photoinhibition in spinach (*Spinacia oleracea*). *Aust J Plant Physiol* 26: 125–134
- Krol M, Huner NPA, Williams JP and Maissan E (1988) Chloroplast biogenesis at cold hardening temperatures. Kinetics of trans-3-hexadecenoic acid accumulation and the assembly of LHCII. *Photosynth Res* 15: 115–132
- Krol M, Spangfort MD, Huner NPA, Öquist G, Gustafsson P and Jansson S (1995) Chlorophyll *a/b*-binding proteins, pigment conversions and early light-induced proteins in a Chl *b*-less barley mutant. *Plant Physiol* 107: 873–883
- Krol M, Maxwell DP and Huner NPA (1997) Exposure of *Dunaliella salina* to low temperature mimics the high light-induced accumulation of carotenoids and the carotenoid binding protein (Cbr). *Plant Cell Physiol* 38: 213–216
- Krol M, Ivanov AG, Jansson S, Kloppstech K and Huner NPA (1999) Greening under high light or cold temperature affects the level of xanthophyll-cycle pigments, early light-inducible proteins, and light-harvesting polypeptides in wild-type barley and the *chlorina f2* mutant. *Plant Physiol* 120: 193–203
- Kropat J, Oster U, Rüdiger W and Beck CF (1997) Chlorophyll precursors are signals of chloroplast origin involved in light induction of nuclear heat-shock genes. *Proc Nat Acad Sci (USA)* 94: 14168–14172
- Kropat J, Oster U, Rüdiger W and Beck CF (2000) Chloroplast signalling in the light induction of nuclear *HSP70* genes requires the accumulation of chlorophyll precursors and their accessibility to cytoplasm / nucleus. *Plant J* 24: 523–531
- Krupa Z, Williams JP and Huner N (1992) The role of acyl lipids in reconstitution of lipid-depleted light-harvesting complex II from cold hardened and nonhardened rye. *Plant Physiol* 100: 931–938
- Kühlbrandt W, Wang DN and Fujiyoshi Y (1994) Atomic model of plant light-harvesting determined by electron crystallography. *Nature* 367: 614–621
- Leech RM (1984) Chloroplast development in angiosperms: current knowledge and future prospects. In: Baker NR, Barber J (eds) *Topics in Photosynthesis, Vol 5, Chloroplast Biogenesis*, pp 1–21. Elsevier Science, Amsterdam
- Leonhardt KG and Straus NA (1994) Photosystem II genes *isiA*, *psbD1* and *psbC* in *Anabaena* sp. PCC 7120: Cloning, sequencing and transcriptional regulation in iron-stressed and iron-replete cells. *Plant Mol Biol* 24: 63–73
- Leverenz JW, Öquist G and Wingsle G (1992) Photosynthesis and photoinhibition in leaves of chlorophyll *b*-less barley in relation to absorbed light. *Plant Physiol* 85: 495–502
- Levy H, Tal T, Shaish A and Zamir A (1993) Cbr, an algal homolog of plant early light inducible proteins, is a putative zeaxanthin binding protein. *J Biol Chem* 268: 20892–20896
- Li X-P, Björkman O, Shih C, Grossman AR, Rosenquist M, Jansson S and Niyogi KK (2000) A pigment-binding protein essential for regulation of photosynthetic light-harvesting. *Nature* 403: 391–395
- Logan BA, Demmig-Adams B and Adams WW (1998a) Antioxidants and xanthophyll cycle-dependent energy in *Cucurbita pepo* L. and *Vinca major* L. upon a sudden increase in growth PPFD in the field. *J Exp Bot* 49: 1881–1888
- Logan BA, Grace SC, Adams WW and Demmig-Adams B (1998b) Seasonal differences in xanthophyll cycle characteristics and antioxidants in *Mahonia repens* growing in different light environments. *Oecologia* 116: 9–17
- Long SP, Humphries S and Falkowski PG (1994) Photoinhibition of photosynthesis in nature. *Annu Rev Plant Physiol Plant Mol Biol* 45: 633–662
- Lunde C, Jensen PE, Haldrup A, Knoetzel J and Scheller HV (2000) The PS I-H subunit of Photosystem I is essential for state transitions in plant photosynthesis. *Nature* 408: 613–615
- Machalek KM, Davison IR and Falkowski PG (1996) Thermal acclimation and photoacclimation of photosynthesis in the brown alga *Laminaria saccharina*. *Plant Cell Environ* 19: 1005–1016
- Maxwell DP, Falk S and Huner NPA (1995a) Photosystem II excitation pressure and development of resistance to photoinhibition I. LHCII abundance and zeaxanthin content in



- Chlorella vulgaris*. Plant Physiol 107: 687–694
- Maxwell DP, Laudenbach DE and Huner NPA (1995b) Redox regulation of light-harvesting complex II and *cab* mRNA abundance in *Dunaliella salina*. Plant Physiol 109: 787–795
- Melis A (1991) Dynamics of photosynthetic membrane composition and function. Biochim Biophys Acta 1058: 87–106
- Melis A (1998) Photostasis in plants. In: Williams TP and Thistle AB (eds) Photostasis and Related Phenomena, pp 207–220. Plenum Press, New York
- Melis A (1999) Photosystem-II damage and repair cycle in chloroplasts: What modulates the rate of photodamage in vivo? Trends Plant Sci 4: 130–135
- Melis A, Manodori A, Glick RE, Ghirardi ML, McCauley SW and Neale PJ (1985) The mechanism of photosynthetic membrane adaptation to environmental stress conditions: A hypothesis on the role of electron-transport capacity and of ATP/NADPH pool in the regulation of thylakoid membrane organization and function. Physiol Vég 23: 757–765
- Meyer G and Kloppstech K (1984) A rapidly light-induced chloroplast protein with high turnover coded for by pea nuclear DNA. Eur J Biochem 138: 201–207
- Miskiewicz E, Ivanov AG, Williams JP, Khan MU, Falk S and Huner NPA (2000) Photosynthetic acclimation of the filamentous cyanobacterium, *Plectonema boryanum* UTEX 485, to temperature and light. Plant Cell Physiol 41: 767–775
- Montane M-H, Petzold B and Kloppstech K (1999) Formation of early-light-inducible-protein complexes and status of xanthophyll levels under high light and cold stress in barley (*Hordeum vulgare* L.). Planta 208: 519–527
- Murata N and Los DA (1997) Membrane fluidity and temperature perception. Plant Physiol 115: 875–879
- Nakajima Y, Tsuzuki M and Ueda R (1998) Reduced photoinhibition of a phycocyanin-deficient mutant of *Synechocystis* PCC 6714. J Appl Phycol 10: 447–452
- Naus J and Melis A (1992) Response of the photosynthetic apparatus in *Dunaliella salina* to sublethal concentrations of the herbicide 3-(3',4'-dichlorophenyl)-1,1-dimethyl urea. Photosynthetica 26: 67–78
- Nield J, Funk C and Barber J (2000) Supermolecular structure of Photosystem II and location of the PsbS protein. Phil Trans R Soc Lond B 355: 1337–1344
- Nishida I and Murata N (1996) Chilling sensitivity in plants and cyanobacteria: The crucial contribution of membrane lipids. Annu Rev Plant Physiol Plant Mol Biol 47: 541–568
- Niyogi KK, Grossman AR and Björkman O (1998) *Arabidopsis* mutants define a central role for the xanthophyll in the regulation of photosynthetic energy conversion. Plant Cell 10: 1121–1134
- Nußberger S, Dorr K, Wang DN and Kühlbrandt W (1993) Lipid-protein interactions in crystals of plant light-harvesting complex. J Mol Biol 234: 347–356
- Ohad I, Keren N, Hagit Z, Gong H, Mor TS, Gal A, Tal S and Domovich Y (1994) Light-induced degradation of the Photosystem II reaction centre D1 protein in vivo: An integrative approach. In: Baker NR, Bowyer JR (eds) Photoinhibition of Photosynthesis: From Molecular Mechanisms to the Field, pp 161–177. Bios Scientific, Oxford
- Öquist G and Huner NPA (1992) Cold-hardening induced resistance to photoinhibition in winter rye is dependent upon an increased capacity for photosynthesis. Planta 189: 150–156
- Öquist G and Huner NPA (1993) The temperature dependence of the redox state of  $Q_A$  and the susceptibility of photosynthesis to photoinhibition. Plant Physiol Biochem 31: 683–691
- Öquist G and Martin B (1986) Cold Climates. In: Baker NR, Long SP (eds) Photosynthesis in Contrasting Environments, Vol 7, pp 237–293. Elsevier, New York
- Öquist G, Chow WS and Anderson JM (1992a) Photoinhibition of photosynthesis represents a mechanism for long term regulation of Photosystem II. Planta 186: 450–460
- Öquist G, Chow WS, McCaffery S and Anderson J (1992b) Mechanistic differences in photoinhibition in sun and shade plants. Planta 188: 422–431
- Öquist G, Hurry VM and Huner NPA (1993) Low temperature effects on photosynthesis and correlation with freezing tolerance in spring and winter cultivars of wheat and rye. Plant Physiol 101: 245–250
- Osmond CB (1994) What is photoinhibition? Some insights from comparison of shade and sun plants. In: Baker NR, Bowyer JR (eds) Photoinhibition of Photosynthesis—From Molecular Mechanisms to the Field, pp 1–24. Bios Scientific Publishers, Oxford
- Ottander C, Campbell D and Öquist G (1995) Seasonal changes in Photosystem II organization and pigment composition in *Pinus sylvestris*. Planta 197: 176–183
- Park Y-I, Anderson JM and Chow WS (1995) Photoinactivation of functional Photosystem II and D1-protein synthesis in vivo are independent of the modulation of the photosynthetic apparatus by growth irradiance. Planta 198: 300–309
- Park Y-I, Chow WS, Anderson JM and Hurry VM (1996a) Differential susceptibility of Photosystem II to light stress in light-acclimated pea leaves depends on the capacity for photochemical and non-radiative dissipation of light. Plant Sci 115: 137–149
- Park Y-I, Chow WS, Osmond CB and Anderson JM (1996b) Electron transport to oxygen mitigates against the photoinactivation of Photosystem II in vivo. Photosynth Res 50: 23–32
- Park Y-I, Chow WS and Anderson JM (1997) Antenna size dependency of photoinactivation of Photosystem II light-acclimated pea leaves. Plant Physiol 115: 151–157
- Park Y-I, Sandström S, Gustafsson P and Öquist G (1999) Expression of the *isiA* gene is essential for the survival of the cyanobacterium *Synechococcus* sp. PCC 7942 by protecting Photosystem II from excess light under iron limitation. Mol Microbiol 32: 123–129
- Pfannschmidt T, Nilsson A and Allen JF (1999) Photosynthetic control of chloroplast gene expression. Nature 397: 625–628
- Rezanoff DA (1993) The Photoinhibitory Response of Periwinkle (*Vinca minor* L.). MSc Thesis, The University of Western Ontario, London, Canada
- Reddy KJ, Masamoto K, Sherman DM and Sherman LA (1989) DNA sequence and regulation of the gene (*cbpA*) encoding the 42-kilodalton cytoplasmic membrane carotenoprotein of the cyanobacterium *Synechococcus* sp. strain PCC7942. J Bacteriol 171: 3486–3493
- Sakamoto T and Bryant DA (1998) Growth at low temperature causes nitrogen limitation in the cyanobacterium *Synechococcus* sp. PCC 7002. Arch Microbiol 169: 10–19
- Savitch LV, Maxwell DP and Huner NPA (1996) Photosystem II excitation pressure and photosynthetic carbon metabolism in *Chlorella vulgaris*. Plant Physiol 111: 127–136

- Savitch LV, Massacci A, Gray GR and Huner NPA (2000) Acclimation to low temperature or high light mitigates sensitivity to photoinhibition: Roles of the Calvin cycle and the Mehler reaction. *Aust J Plant Physiol* 27: 253–264
- Schroda M, Vallon O, Wollman F-A, and Beck CF (1999) A chloroplast-targeted heat shock protein 70 (HSP70) contributes to the repair of Photosystem II during and after photoinhibition. *Plant Cell* 11: 1165–1178
- Sharkey TD and Singas EL (1995) Why plants emit isoprene. *Nature* 374: 769
- Somersalo S and Krause GH (1990) Photoinhibition at chilling temperatures and effects of freezing stress on cold acclimated spinach leaves in the field. A fluorescence study. *Physiol Plant* 79: 617–622
- Somerville CR and Ogren WL (1982) Genetic modification of photorespiration. *Trends Biol Sci* 7: 171–174
- Sonoike K (1998) Various aspects of inhibition of photosynthesis under stress - photoinhibition at chilling temperatures versus chilling damage in the light. *J Plant Res* 111: 121–129
- Spiller S and Terry N (1990) Limiting factors in photosynthesis. II. Iron stress diminishes photochemical capacity by reducing the number of photosynthetic units. *Plant Physiol* 65: 121–125
- Straus NA (1994) Iron deprivation: Physiology and gene regulation. In: Bryant DA (ed) *The Molecular Biology of Cyanobacteria*, pp 731–750. Kluwer Academic Publishers, Dordrecht
- Sukenik A, Wyman KD, Bennett J and Falkowski PG (1987) A novel mechanism for regulating the excitation of Photosystem II in a green alga. *Nature* 327: 704–707
- Tanaka A and Melis A (1997) Irradiance dependent changes in the size and composition of the chlorophyll *a-b* light-harvesting complex in the green alga *Dunaliella salina*. *Plant Cell Physiol* 38: 17–24
- Taylor SE and Terry N (1986) Variation in photosynthetic electron transport capacity and its effect on the light modulation of ribulose biphosphate carboxylase. *Photosynth Res* 8: 249–256
- Taylor WC (1989) Regulatory interactions between nuclear and plastid genomes. *Ann Rev Plant Physiol Plant Mol Biol* 40: 211–233
- ten Lohuis MR and Miller DJ (1998) Light-regulated transcription of genes encoding peridinin chlorophyll *a* proteins and the major intrinsic light-harvesting complex proteins in the dinoflagellate *Amphidinium carterae* Hulburt (Dinophyceae). *Plant Physiol* 117: 189–196
- Terashima I, Noguchi K, Itohnemoto T, Park YM, Kubo A and Tanaka K (1998) The cause of PS I photoinhibition at low temperatures in leaves of *Cucumis sativus*, a chilling-sensitive plant. *Physiol Plant* 103: 295–303
- Terry N (1983) Limiting factors in photosynthesis. IV. Iron stress mediated changes in light-harvesting and electron transport capacity and its effects on photosynthesis in vivo. *Plant Physiol* 71: 855–860
- Tezara W, Mitchell VJ, Driscoll SD and Lawlor DW (1999) Water stress inhibits plant photosynthesis by decreasing coupling factor and ATP. *Nature* 401: 914–917
- Thayer SS and Björkman O (1992) Carotenoid distribution and deepoxidation in thylakoid pigment-protein complexes from cotton leaves and bundle-sheath cells of maize. *Photosynth Res* 33: 213–225
- Turpin DH and Bruce D (1990) Regulation of photosynthetic light-harvesting by nitrogen assimilation in the green alga *Selenastrum minutum*. *FEBS Lett* 263: 99–103
- Tyystjarvi E and Aro E-M (1996) The rate constant of photoinhibition, measured in lincomycin-treated leaves, is directly proportional to light intensity. *Proc Nat Acad Sci USA* 93: 2213–2218
- Tyystjarvi E, Kettunen R and Aro E-M (1994) The rate constant of photoinhibition in vitro is independent of the antenna size of Photosystem II but depends on temperature. *Biochim Biophys Acta* 1186: 177–185
- Verhoeven AS, Adams WW and Demmig-Adams B (1998) Two forms of sustained xanthophyll cycle-dependent energy dissipation in overwintering *Euonymus kiautschovicus*. *Plant Cell Environ* 21: 893–903
- Verhoeven AS, Adams WW and Demmig-Adams B (1999) The xanthophyll cycle and acclimation of *Pinus ponderosa* and *Malva neglecta* to winter stress. *Oecologia* 118: 277–287
- Vogelmann TC, Nishio JN and Smith WK (1996) Leaves and light capture: Light propagation and gradients of carbon fixation within leaves. *Trends Plant Sci* 1: 65–70
- Walters RG, Rogers JJM, Shephard F and Horton P (1999) Acclimation of *Arabidopsis thaliana* to the light environment: The role of photoreceptors. *Planta* 209: 517–527
- Weis E (1985) Light and temperature induced changes in the distribution of excitation energy between PS I and PS II in spinach leaves. *Biochim Biophys Acta* 807: 118–126
- Wilson KE and Huner NPA (2000) The role of growth rate, redox-state of the plastoquinone pool and the trans-thylakoid  $\Delta pH$  in photoacclimation of *Chlorella vulgaris* to growth irradiance and temperature. *Planta* 212: 93–102.
- Winder TL and Nishio J (1995) Early iron deficiency stress response in leaves of sugar beet. *Plant Physiol* 108: 1487–1494
- Wingler A, Quick WP, Bungard RA, Bailey KJ, Lea PJ and Leegood RC (1999) The role of photorespiration during drought stress: An analysis utilizing barley mutants with reduced activities of photorespiratory enzymes. *Plant Cell Environ* 22: 361–373
- Wingler A, Lea PJ, Quick WP and Leegood RC (2000) Photorespiration: Metabolic pathways and their role in stress protection. *Phil Trans R Soc Lond B* 355: 1517–1529
- Wykoff DD, Davies JP, Melis A and Grossman AR (1998) The regulation of photosynthetic electron transport during deprivation in *Chlamydomonas reinhardtii*. *Plant Physiol* 117: 129–139
- Yamaguchi K and Nishimura M (2000) Reduction to below threshold levels of glycolate oxidase activities in transgenic tobacco enhances photoinhibition during irradiation. *Plant Cell Physiol* 41: 1397–1406
- Yamamoto HY and Bassi R (1996) Carotenoids: Localization and function. In: Ort DR and Yocum CF (eds) *Oxygenic Photosynthesis: The Light Reactions*, pp 539–563. Kluwer Academic Publishers, Dordrecht
- Yamamoto HY, Bugos RC and Heiber AD (1999) Biochemistry and molecular biology of the xanthophyll cycle. In: Frank HA, Young AJ, Britton G and Cogdell RJ (eds) *The Photochemistry of Carotenoids*, pp 293–303. Kluwer Academic Publishers, Dordrecht

# Chapter 15

## Photoacclimation of Light Harvesting Systems in Eukaryotic Algae

Paul G. Falkowski\* and Yi-Bu Chen

*Environmental Biophysics and Molecular Ecology Program, Institute of Marine and Coastal Science, Rutgers, The State University of New Jersey, New Brunswick, New Jersey 08901, U.S.A.*

Summary .....	424
I. Introduction .....	424
II. Photoacclimation .....	425
III. Light in aquatic environments .....	425
A. Remote Sensing of Phytoplankton Pigments .....	426
B. The Variance Spectrum of Spectral Irradiance in Aquatic Ecosystems .....	427
1. The Wave Flicker Effect .....	428
2. Clouds .....	428
3. Diel Cycles .....	428
4. Vertical Mixing .....	428
IV. Physiological Responses to Changes in Spectral Irradiance .....	429
A. The Photosynthesis-Irradiance Response .....	429
B. Cross Sections .....	429
1. The Optical Cross Section .....	429
2. Application of the $a^*$ Concept to the Calculation of Quantum Yields .....	430
3. The Effective Absorption Cross Section .....	431
4. The Effective Cross Section and the Photosynthesis-Irradiance Relationship .....	432
V. Light Harvesting Systems and the Effective Absorption Cross Section of Photosystem II .....	432
A. Dynamical Alteration of Light Harvesting .....	432
B. Measuring Changes in $\sigma_{PSII}$ .....	432
1. The Pump and Probe Fluorescence .....	433
2. The Fast Repetition Rate Fluorescence (FRRF) Approach .....	433
C. How Does $\sigma_{PSII}$ Change? .....	434
1. State Transitions .....	434
2. The Xanthophyll Cycle .....	436
VII. Light Harvesting Complexes .....	438
A. Alterations in the Pigment Composition of Antenna Complexes .....	438
B. Changes in the Level of Expression of <i>Lhcb</i> Genes .....	439
C. Changes in the Numbers of Reaction Centers, $n$ .....	440
D. The Relationship Between the Optical and Effective Absorption Cross Sections .....	442
VIII. The 'Nested Signal' Hypothesis .....	442
Acknowledgments .....	443
References .....	443

---

\* Author for correspondence, email: falko@imcs.rutgers.edu

## Summary

Photoacclimation is a suite of phenotypically expressed, developmentally independent, reversible physiological feedback responses to short-term (minutes to days) variations in spectral irradiance. These responses are observed in all eukaryotic algal taxa and involve alterations in the optical absorption cross section, the effective absorption cross section, and the rate of electron transfer from water to a terminal acceptor (e.g., carbon dioxide or nitrate). In this chapter, we review the primary physical processes in aquatic ecosystems that provided selection pressure for photoacclimation responses. These processes include the passage of clouds across the sky, vertical mixing, and diel variability in incident solar irradiance. The physiological responses to variations in the spectral irradiance are transduced via the redox state of intersystem electron transport components, especially plastoquinone. In a 'nested' series, responses include state transitions, alterations in the xanthophylls, and net synthesis/degradation of light harvesting complexes. The three processes have different time constants and dynamic ranges, but all result in alterations of the effective absorption cross section of photochemistry, such that light absorption and electron transport are balanced. The balance between light absorption and electron transport optimizes (not maximizes) photosynthesis under a very wide range of light conditions found in natural aquatic ecosystems.

## I. Introduction

Solar radiation is both one of the most predictable yet most stochastic physical variables on Earth. The path of the sun as it crosses the sky is governed by highly deterministic processes, such that at each moment in time the exact amount of incoming solar radiation can be calculated at every point on the Earth's surface. On geological time scales, the orbital variations and changes in solar luminosity can also be calculated, such that the solar spectral irradiance can be inferred for millions of years in the past. The orbital cycles also determine the number of hours of solar radiation for each latitude. Superimposed on such highly deterministic processes are variations in irradiance due to the passage of clouds across the sky,

atmospheric aerosol burdens, and, in the case of aquatic photosynthetic organisms, the vertical position and motions associated with turbulent mixing, tidal variations, and seasonal convection.

To accommodate the high frequency variations in solar irradiance, photosynthetic organisms have developed physiological acclimation strategies that optimize (not maximize) light harvesting and photosynthetic electron transport in response to changes in irradiance. Optimizing light harvesting means dynamically balancing the rate of production of photochemically derived reductants and ATP to the rate of their consumption, primarily (but not solely) by the dark reactions in carbon fixation. Dynamical balance is frequently achieved by adjusting the energy input via regulation of light harvesting systems and the reaction centers that they serve. Several mechanisms have evolved in photosynthetic organisms to accommodate variations in spectral irradiance. These acclimation processes operate on various time scales and include state transitions, thermal dissipation via the xanthophyll cycle, differential expression of carotenoids within pigment protein complexes, and developmentally independent changes in the production of light harvesting pigment protein complexes (Chapter 14, Huner et al.). The ensemble of these processes is called 'photoacclimation' (Falkowski and LaRoche, 1991a). In this chapter we explain that these processes are a nested set of response functions to a single stimulus, namely the redox poise of the photosynthetic electron transport system. As the dynamics of photoacclimation of light harvesting systems are

---

*Abbreviations:*  $\alpha$ ,  $\alpha^B$  – the initial slope of the photosynthesis + irradiance curve. The superscript B denotes that the parameter is normalized to chlorophyll  $a$ ;  $\phi_{\max}$  – the maximum quantum yield of photosynthesis;  $\sigma_{\text{PSII}}$  – the effective photon capture cross section of Photosystem II;  $\tau$  – turnover time for whole chain photosynthetic electron transport;  $a^*$  – the spectrally averaged optical absorption cross section normalized to chlorophyll  $a$ ; DBMIB – dibromothymoquinone; DCMU – 3,4-dichlorophenyl-1,1-dimethylurea;  $E_0$  – irradiance at the air/water interface;  $E_k$  – saturation irradiance for photosynthesis ( $E_k = \alpha^B / P_{\max}^B$ );  $F_m$  – maximum fluorescence;  $F_0$  – initial fluorescence; FRRF – fast repetition rate fluorescence; IR – infrared light; *Lhcb* – gene encoding the major light harvesting protein serving Photosystem II;  $n$  – ratio of Photosystem II reaction centers to total chlorophyll  $a$ ;  $P_{700}$  – reaction center of Photosystem I;  $P_{\max}$ ,  $P_{\max}^B$  – light saturated photosynthesis. The superscript B denotes that the parameter is normalized to chlorophyll  $a$ ;  $Q_A$  – primary quinone in Photosystem II;  $Q_B$  – secondary quinone in Photosystem II; UV – ultra violet light

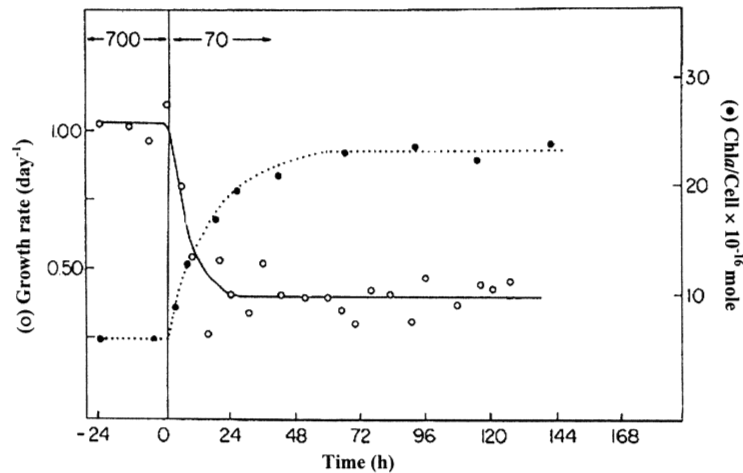


Fig. 1. Changes in the cellular chlorophyll content and growth rate following the transition from 700 to 70  $\mu\text{mol quanta m}^{-2} \text{s}^{-1}$  in the marine chlorophyte *Dunaliella tertiolecta*. Note the five-fold increase in chlorophyll content within 60 h following the light shift. This photoacclimation response has a half time of about 24 h at 20 °C. (Original data from Sukenik et al. 1990)

highly developed in eukaryotic algae, especially the microalgae (phytoplankton), we have used these organisms as models for specific processes. Here we examine what photoacclimation is, how it works, and how it evolved.

## II. Photoacclimation

Photoacclimation is a suite of phenotypically expressed, developmentally independent, reversible, physiological feedback responses to short-term (minutes to days) variations in spectral irradiance (Falkowski and LaRoche, 1991b). These responses are most readily observed in unicellular algae (both eukaryotic and prokaryotic), in which changes in the quality and quantity of pigmentation can be rapidly and reversibly induced by changes in irradiance (Fig. 1). Photoacclimation should not be confused with photoadaptation; in the latter, organisms are genetically selected by environmental constraints to grow under a range of irradiance levels. Hence, many higher plants are 'sun' or 'shade' adapted, and have a limited capacity to acclimate to the converse irradiance regime (Boardman, 1977). For example, corn cannot normally grow under low irradiance levels; it is a genetically selected 'sun' plant (Bennett et al., 1987). Within this constraint, there are acclimation strategies, however these are relatively limited in facilitating acclimation over large changes in irradiance. While some genetic selection to irradiance

(i.e., ecotypes) can be identified in unicellular algae (Falkowski and Owens, 1980; Partensky et al., 1993), the physiological plasticity generally permits a large, reversible acclimation response (Falkowski, 1980). The unicellular algae maintain a high degree of acclimation responses because of the light environment in which they evolved.

## III. Light in aquatic environments

Before discussing photoacclimation and light harvesting per se, let us first consider the environmental forcing function that elicits the responses, namely spectral irradiance and its variance in the environment. Photons entering any environment have only two possible fates: to be absorbed or to be scattered. In aquatic ecosystems, water itself both absorbs and scatters light, and hence, photosynthetic organisms must compete with the bulk medium for energy. The absorption bands of water, resulting from the primary O-H stretching frequencies and its harmonics, are strong in the red and (especially) far-red wavelengths, but not blue or blue-green. These absorption bands are not markedly affected by dissolved salts (i.e., as in seawater), but are affected by dissolved organic matter and gases, especially  $\text{O}_2$ . Dissolved organic matter in aquatic ecosystems contains hundreds (if not thousands) of different molecules, only a few of which have been characterized. On average, the absorption of the ensemble

of these molecules is in the blue and ultra-violet, primarily due to the presence of heterogeneous aromatic carbon molecules and conjugated double bonds in aliphatic hydrocarbon backbones (Aluwihare et al., 1997). Dissolved organic carbon concentrations are highest in coastal waters, rivers, and eutrophic lakes.  $O_2$  attenuates light in the UV, and is, in fact, the strongest absorber of UV-B radiation in the ocean.

Superimposed on these absorption bands is the attenuation of radiation by scattering. The primary scattering process is a consequence of vanishingly small discontinuities in density, sometimes called the 'fluctuation density scattering' process (Smoluchowski, 1908; Einstein, 1910). Briefly, at any moment in time, two adjacent, but equal volumes of water will statistically contain slightly different numbers of water molecules, such that (by definition) the two parcels will have slightly differing densities. From a kinetic viewpoint, the fluctuations in density lead to stochastic fluctuations in refractive indices within the water column. Consequently, photons (even from a coherent source, such as a laser) entering the medium invariably become scattered (Kirk, 1994). The scattering function is inversely proportional to the 4.3<sup>rd</sup> power of the wavelength (Morel, 1974); i.e., blue light is scattered much more than red light. In the portion of the water column, scattering is further enhanced by bubble injection, which can penetrate up to approximately 50 m. Bubbles do not spectrally alter the upwelling radiance, however they tend to make the ocean appear optically 'brighter' (Zhang et al., 1998). Hence, to an observer looking down at the ocean from above, the combination of efficient absorption of long wavelengths of light and the efficient scattering of short wavelengths, leads to an upward flux of light heavily enriched in the blue (Fig. 2). In coastal waters or eutrophic lakes, where the blue light is often attenuated by dissolved organic matter, the resulting water appears darker, and the peak region of light penetration is shifted towards the blue-green. In summary, the selection pressure on pigment protein complexes in aquatic photoautotrophs is dictated by the optical physics of water itself.

In water, the blue (Soret) absorption bands of chlorophylls serve as primary conduits for energy absorption. The red (Q) bands have little ecological relevance; they are manifestations of the lowest singlet excited state and may serve in energy transfer processes, but only rarely serve to absorb light directly (Falkowski and Raven, 1997). It should be noted that

this is not the case for terrestrial plants, where the red bands function in light harvesting directly. Carotenoids and phycobilipigments extend the range of light harvesting of the Soret bands into the green wavelengths. The evolutionary selection of specific carotenoids and phycobilipigments forms one basis for taxonomic classification of phytoplankton at the division level (Green and Durnford, 1996).

Outside of regions directly affected by dissolved organic matter, photosynthetic pigments of phytoplankton are the major constituents that modify color of aquatic ecosystems. Specifically, the blue and blue-green downwelling and upwelling photons are absorbed by chlorophylls and carotenoids (Morel and Prieur, 1977; Morel, 1988; Falkowski and Raven, 1997). With the exception of some cells that produce intracellular gas bubbles or calcium carbonate shells, the back-scattering cross section of phytoplankton is rather low. Hence, the major effect of phytoplankton is on absorption rather than scattering of light (Ahn et al., 1992; Ackleson et al., 1993). As photosynthetic pigments deplete both the upwelling and downwelling irradiance stream of blue and blue-green light, in effect the water becomes 'darker.' The depletion of light in these wavelengths is, in the open ocean, quantitatively proportional to the concentration of photosynthetic pigments in the optical path (i.e., the upper portion of the euphotic zone). Using the ratio of two wavelengths of light, it is possible to determine empirically the water-leaving radiances, i.e., the photons scattered by the ocean back to the atmosphere, to estimate phytoplankton pigment concentrations. This phenomenon forms the basis for the remote sensing of phytoplankton pigments from satellite imagery.

#### *A. Remote Sensing of Phytoplankton Pigments*

The pigment (approximately, the chlorophyll) concentration of the global ocean can be assessed from determining the quantitative changes in ocean color. The basis for this model is that in regions far removed from continental sources of non-biological particles (e.g., the central ocean basins), deviations in ocean color from pure seawater are influenced primarily by biologically derived materials, of which the most important are pigmented phytoplankton. Empirically, the ratio of blue to blue-green upwelling radiances are measured by sensitive narrow band-pass detectors on a satellite. However, only about 5% of the photons reaching the satellite originates from

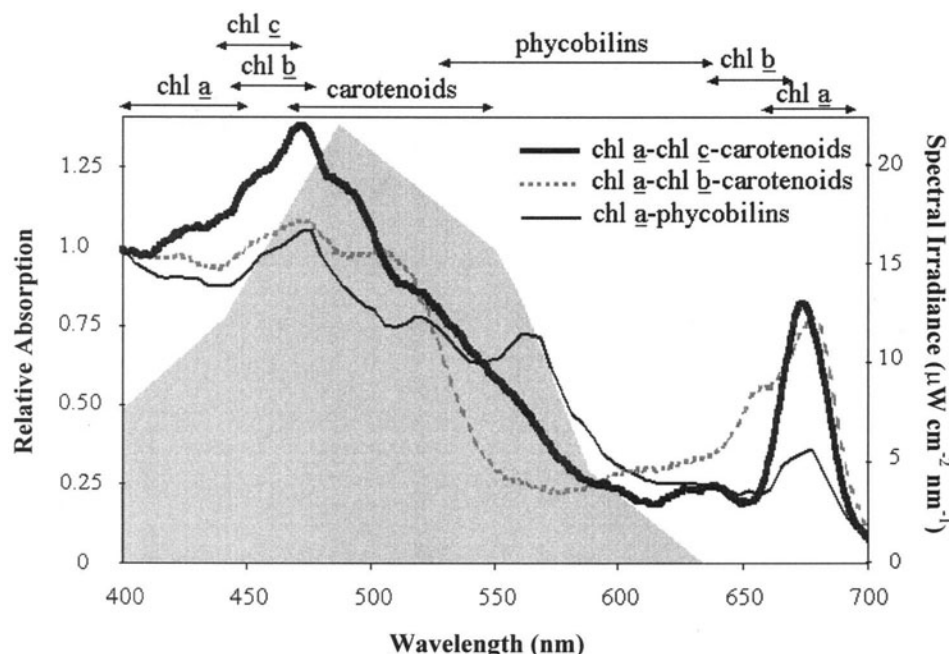


Fig. 2. The relative absorption capabilities for marine phytoplankton that contain chlorophyll *c*, chlorophyll *b*, and phycobilins in the spectrally-skewed light fields found at depth in aquatic ecosystems. The spectral bands absorbed by the major light-harvesting pigments in the marine phytoplankton are denoted by arrows. Spectral irradiance (gray shaded area) from 20 meters depth in the Santa Barbara Channel is presented to illustrate the spectral irradiance found at depth. Note that the red absorption bands of chlorophylls do not harvest light, as the attenuation of red light by water is so strong as to effectively remove those wavelengths from the spectrum of available radiation.

light scattered from the ocean, the remaining photons are scattered from Earth's atmosphere. Empirical corrections are made for the atmospheric signal (using extended red channels in the near-IR, which are spectrally silent for the ocean), and the corrected images are mapped at  $1 \times 1^\circ$  resolution to derive images of ocean color. The images are calibrated with sophisticated in-water optical sensors and optical models to derive pigment concentrations for the first optical depth. The ensemble of remotely sensed images of the variations in ocean color is derived on a daily basis for the global ocean and permits continuous estimation of phytoplankton pigment concentrations over cloud-free regions (Color Plate 1). It should be noted that the derived pigment concentration is linearly dependent on the optical absorption cross section for phytoplankton (see below), and consequently is directly influenced by photoacclimation processes. In practice, average optical absorption cross sections are derived from numerous (hundreds) of spectral measurements. This process can underestimate pigments at high latitudes, where cellular concentrations of pigments are higher

than the global average, or in blooms of highly packaged cells (e.g., surface blooms of filamentous cyanobacteria). Correction for these regional anomalies is done on a case-by-case basis through field-based bio-optical programs.

### *B. The Variance Spectrum of Spectral Irradiance in Aquatic Ecosystems*

In all natural processes that are continuous in time with multiple, overlapping frequency distributions, it is convenient to derive a 'variance spectrum.' The variance spectrum describes the variance about a mean as a function of frequency. Typically, variance spectra cascade from lower to higher frequencies, such that a greater fraction of the variance is contained at lower frequencies. The variance spectrum of spectral irradiance has major components on annual and diel frequencies, and minor components on shorter time scales. To be acclimative, physiological responses to changes in irradiance must match the frequency of the underlying forcing function. In photoacclimation in algae we can ignore seasonal



and annual variations in irradiance, as these frequencies are much longer than cell division cycles or the physiological memory of the light environment. Rather the time scales of interest are a few days and less. Let us consider some of the major forcing functions in a descending order of frequency.

### 1. The Wave Flicker Effect

While the water column in all aquatic ecosystems acts as a band pass filter for solar radiation, the variance spectrum in radiance is generally determined by interactions at the air-water interface or in the atmosphere. Waves at the air-water interface constantly focus and defocus radiation, giving a 'flicker effect' in the upper portion of the water column (Dera and Gordon, 1968). This process can lead to over a 100-fold change in submarine irradiance under clear sky conditions at high latitudes, but is rapidly attenuated with depth because of scattering. The variance spectrum of the wave 'flicker effect' is constrained to high frequencies, on the order of seconds to tenths of seconds. The flicker effect may be important in the photosynthetic responses of fixed benthic organisms (such as seagrasses or symbiotic corals (Falkowski et al., 1990; Greene and Gerard, 1990)). The importance of this effect to phytoplanktonic organisms is unclear. In natural aquatic ecosystems, the flicker effect potentially reduces the duration of exposure (i.e., the product of irradiance and time) to supraoptimal irradiance levels in the upper portion of the water column, thereby reducing photodamage to reaction centers. An analogous situation occurs in higher plant canopies, where leaf flicker can reduce photoinhibition and potentially enhance photosynthetic electron transport (Percy, 1990), however, controlled experiments have not clearly demonstrated a similar response in phytoplankton (Flameling and Kromkamp, 1997). We will revisit this issue later, in the context of the coupling of light harvesting to electron transport.

### 2. Clouds

Among the stochastic processes that result in changes in spectral irradiance, clouds are perhaps the most important. Clouds can attenuate incident solar radiation by over 40-fold within minutes. Climatologically, clouds are a quasi-persistent weather feature; that is, cloud cover is likely to persist for several days in a region, followed by clear sky

conditions. On time scales of minutes to days, phytoplankton can display the full suite of physiological acclimation strategies to changes in irradiance (Falkowski, 1984a). Indeed, there is ample evidence, as we will shortly show, that short-term changes in fluorescence quenching can be observed with the passage of clouds across the sky, and between cloudy and sunny days. The changes in cloud cover, from day-to-day is probably the most critical environmental factor determining the photoadaptive state of phytoplankton in nature.

### 3. Diel Cycles

On most of the Earth's surface, the diel cycle in solar radiation dominates photosynthetic processes. The diel cycle is however, highly predictable, and hence, it is critical to distinguish between circadian rhythms and true photoacclimation processes. In the former, changes in such properties as total chlorophyll per cell display a diel pattern, but the period of the cycle (not the amplitude of the signal) is independent of irradiance. In the latter, the amplitude of the signal, not the period of the cycle, dominates. Simply put, cells photoacclimate to changes in irradiance, not to day-night patterns (Post et al., 1984, 1985).

### 4. Vertical Mixing

Unlike terrestrial plants or benthic photoautotrophs, phytoplankton are not fixed in space. They are vertically transported by turbulent kinetic energy in the upper portion of the water column; in some cases they are capable of vertical migration (Kamykowski, 1981; Villareal and Lipshultz, 1995). Vertical velocities are on the order of 0.1 to 1.0 cm/min. Hence if the upper mixed layer of the water column is approximately 20 m, a cell would be transported from the base to the surface in 3.5 to around 35 h. These vertical motions are sufficiently slow that cells can acclimate to light within the water column (Falkowski, 1983). Indeed, changes in the ratio of light harvesting complexes to reaction centers (i.e., the 'size' of a photosynthetic unit) have been used to follow photoacclimation processes in the water column. Briefly, in most chromophytic, eukaryotic algae (diatoms, coccolithophorids, etc.) photoacclimation can be empirically assessed by following changes in the ratio of chlorophyll *a* to  $P_{700}$ . This ratio can be determined spectrophotometrically (Thornber, 1969; Falkowski and Owens, 1980). From knowledge

of this ratio at various depths in the water column, and from estimates of the first order rate constant for changes in the ratio, one can actually estimate the rate of vertical mixing in the water column (Falkowski, 1983). The results of this, and similar approaches (Lewis et al., 1984) indicate that changes in antenna protein complex expression are concordant with the rates of turbulent mixing in the ocean.

#### IV. Physiological Responses to Changes in Spectral Irradiance

##### A. The Photosynthesis-Irradiance Response

The photosynthesis-irradiance (P-E) response curve is an empirical, experimental manifestation of the light saturation profile for photosynthetic electron transport (Fig. 3). In aquatic ecosystems, P-E responses are usually obtained by following the incorporation of radioactively labeled inorganic carbon (i.e.,  $\text{H}^{14}[\text{C}] \text{O}_3^-$ ) into acid stable organic matter. This technique, introduced by Steemann-Nielsen in 1952 (Steemann-Nielsen, 1952) is extremely sensitive, and consequently, literally hundreds of thousands of P vs. E curves have been obtained since the method was introduced (Falkowski and Woodhead, 1992; Geider and Osborne, 1992). Measurements based on oxygen are also feasible, but the data density is lower. Since the mid 1980s, variable fluorescence has been used (Falkowski et al., 1986; Kolber et al., 1990), and the convenience and sensitivity of this method, coupled with the accessibility of instrumentation, have supplemented if not supplanted the radiocarbon method. Regardless of the method used, the fundamental responses observed are the same.

At low irradiance levels, the initial slope of the P vs. E curve is directly proportional to light. The initial slope, normalized to chlorophyll, is denoted  $\alpha^B$  and has units of  $\text{CO}_2$  fixed (or  $\text{O}_2$  produced)  $\text{chlorophyll}^{-1} \text{ quanta}^{-1} \text{ m}^{-2}$  (Fig. 3). As irradiance increases, photosynthetic rates begin to plateau, ultimately reaching a saturation value. Light saturated rates, normalized to chlorophyll, are denoted  $P_{\text{max}}^B$  and have units of  $\text{CO}_2$  fixed (or  $\text{O}_2$  produced) per chlorophyll per unit time. The intercept between  $\alpha^B$  and  $P_{\text{max}}^B$  (i.e.,  $\alpha^B/P_{\text{max}}^B$ ), extrapolated to the ordinate defines a saturation irradiance,  $E_k$  (Talling, 1957).

The fundamental strategy in photoacclimation is to optimize light harvesting by the cell to optimize

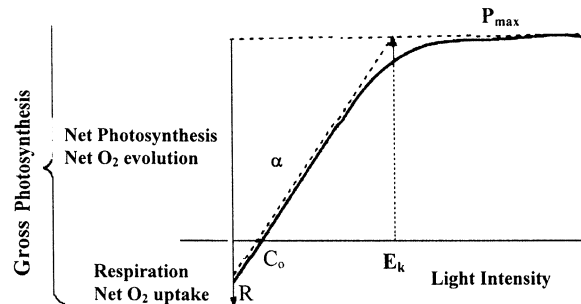


Fig. 3. An example of a typical photosynthesis vs. irradiance curve. This curve could be derived from measurements of net oxygen exchange between the organism and the bulk fluid. In the dark, there is a net consumption of oxygen as a consequence of respiration. Dark respiration,  $R$ , is generally assumed to remain constant in the light. At low irradiance levels, the evolution of oxygen is approximately a linear function of irradiance, and the ratio between photosynthesis and irradiance in this portion of the photosynthesis-irradiance profile is often denoted by the symbol  $\alpha$ . At some irradiance level, photosynthetic rates reach a plateau. The light-saturated rate is denoted  $P_{\text{max}}$ . The saturation irradiance,  $E_k$ , is given as the intercept between  $\alpha$  and  $P_{\text{max}}$ .  $C_0$ , compensation point. At supra-optimal irradiance levels, photosynthetic rates frequently decline from the light-saturated value.

the photosynthetic rate at a given irradiance; the optimal photosynthetic rate is achieved at  $E_k$ . Hence, photosynthesis-irradiance response functions are dynamic. That is, as irradiance changes, cells track the irradiance on time scales of minutes to days and adjust photosynthetic electron transport accordingly. Let us examine what processes are adjustable within the cell and how they are dynamically altered.

##### B. Cross Sections

###### 1. The Optical Cross Section

In terrestrial plants, between 85 to 90% of the photosynthetically available radiation incident on a leaf is absorbed; i.e., to first order a leaf is optically black. The high absorptivity of leaves permits a direct extrapolation of photosynthetic rate normalized to the incident irradiance to be interpreted in the context of quantum yields. This is not to say that higher plants do not photoacclimate; on the contrary, photoacclimation occurs within a leaf (from the upper to the lower surface), within a canopy, and within an ecosystem (Nishio et al., 1994). However, in terrestrial plants, measurements of *spectral* optical absorption cross sections are not required to infer the quantum yield of photosynthesis. In contrast,

unicellular algae are optically thin on a macroscopic scale, and the determination of the spectral absorption of light is required for the calculation of quantum yields (Kirk, 1994).

The precise measurement of the optical absorption cross section of unicellular algae is non-trivial and is complicated by both scattering and the package effect. The optical absorption cross section is a function of cell size, the number and size of the plastids in relation to the cell, the density of thylakoid membranes within the plastid, and the type and concentration of chromophores within the thylakoids (Dubinsky et al., 1986; Berner et al., 1989; Perry and Porter, 1989; Lazzara et al., 1996). From a practical standpoint, cells are generally concentrated on glass fiber filters and their spectral absorption is determined in a spectrophotometer equipped with an integrating sphere or some similar optical system for correcting for scattering. The pigments on the filter are subsequently extracted with a solvent and chlorophyll *a* concentration is determined. The spectral absorptivity is then normalized at each wavelength to chlorophyll *a*, and integrated over the entire spectral irradiance at any moment in time anywhere in the water column to determine the spectral overlap between incident irradiance and light harvesting. The resulting product is the spectrally integrated optical absorption cross section  $a^*$  with units of  $\text{m}^2 \text{mg}^{-1} \text{Chl } a$ .

$a^*$  is critically dependent upon the pigment composition of the cell as well as the package effect. As pigments that absorb at wavelengths other than chlorophyll *a* are added to the cell, the spectrally integrated optical cross section increases. However, if cells add more and more pigment protein complexes to plastids, the thylakoids begin to self shade, and the cross section decreases. Hence, there is a cost to producing more pigments; as a cell increases its concentration of light harvesting complexes, absorptivity per molecule of pigment decreases. To double absorptivity, the cell needs to add approximately four-fold more pigment. In practical terms, the photoacclimation via changes in pigmentation operates between approximately 10 to 1000  $\mu\text{mol quanta m}^{-2} \text{sec}^{-1}$ . Below about 10  $\mu\text{mol quanta m}^{-2} \text{sec}^{-1}$  cells tend to reduce the chlorophyll content (Fig. 4). Between 10 and 1000  $\mu\text{mol quanta m}^{-2} \text{sec}^{-1}$  the response function to irradiance is approximately log normal. Above approximately 1000  $\mu\text{mol quanta m}^{-2} \text{sec}^{-1}$  there is limited reduction in pigment content; other processes, including alteration in composition

of the light harvesting complexes (Sukenik et al., 1987), begin to operate. We will return to this issue later in the discussion of gene expression and photoacclimation in algae.

The product of  $a^*$  and the incident spectral irradiance,  $E_0$ , is the light absorbed per unit chlorophyll *a*. This product gives the total absorption but does not contain any information about how the absorbed radiation is used or partitioned within the organism. For example, if a cell has a high content of non-photosynthetic pigments such as astaxanthin or  $\beta$  carotene, their absorptivity is included in  $a^*$ , and is counted in the calculation of quantum yield. It should be noted moreover, that the calculation of  $a^*$  is not dependent upon spectral intensity, but is dependent upon spectral quality. Hence, the optical cross section will change as the irradiance spectrum changes, regardless of the intensity of the light. For example, as a cell is transported by turbulent mixing into shallower and deeper parts of the water column, both the intensity and spectral composition of the solar radiation will change. Necessarily, as no alga is optically black, the spectral overlap between irradiance and light harvesting pigments will change within the cell at every point in the water column. Hence, the calculation of light absorbed by cells requires detailed knowledge of both the spectral irradiance distribution in the water column as well as the optical absorption cross section of the cells.

## 2. Application of the $a^*$ Concept to the Calculation of Quantum Yields

Let us now consider the application of  $a^*$  to the calculation of the maximum quantum yield of photosynthesis. The application of a simple model through the initial portion of the photosynthesis irradiance curve, in which photosynthesis is normalized to chlorophyll yields  $\alpha$ , which can be formally defined as:

$$\alpha = a^* \phi_{\text{max}} \quad (1)$$

That is, the initial slope of the photosynthesis irradiance curve is related to the maximum quantum yield by the optical absorption cross section. This relationship, which is fundamentally true for all photosynthetic organisms, is critical for algae because  $a^*$  is highly variable, and ranges over a factor of 5 between species and by over a factor of 2 within species, depending upon the physiological state. This

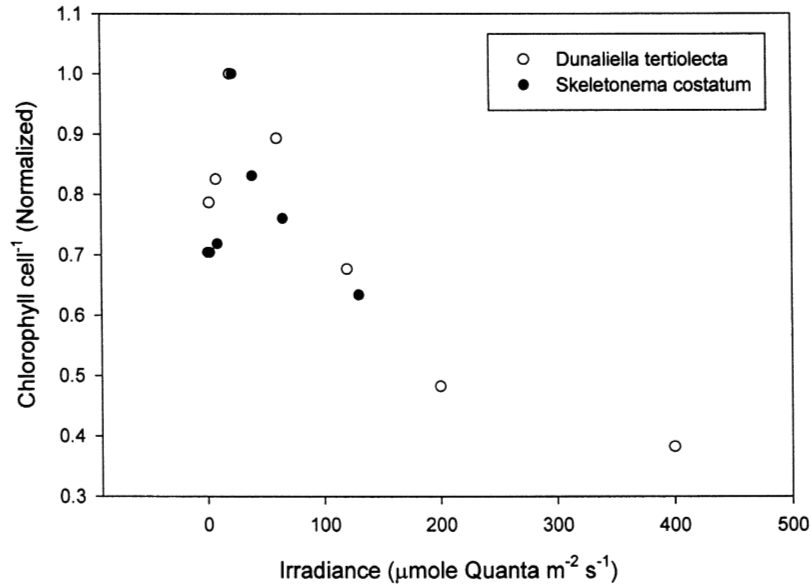


Fig. 4. Changes in the cellular chlorophyll content of two species of unicellular algae: a diatom, *Skeletonema costatum*, and a chlorophyte, *Dunaliella tertiolecta*. Note that the acclimation to low light peaks in both species at about  $30 \mu\text{mol quanta m}^{-2} \text{s}^{-1}$ . The acclimation to higher irradiances is proportional to the log of light intensity.

basic approach has been used to determine the maximum quantum yield of natural phytoplankton communities (Dubinsky and Berman, 1976; Dubinsky, 1980; Bannister and Weidemann, 1984; Babin et al., 1995; 1996). Interestingly, the maximum quantum yields obtained from such measurements are between three- and ten-fold lower than a generally accepted maximum for the Z scheme (0.125). Hence, under most circumstances, factors other than light limit photosynthetic efficiency (Falkowski and Kolber, 1995).

### 3. The Effective Absorption Cross Section

Let us consider the phenomenon of light harvesting for a specific reaction center. Each reaction center receives excitation energy from an ensemble of pigments that have absorbed specific wavelengths of light, and have transferred the light energy from pigment molecule to pigment molecule within the antenna system. If, upon reaching the red-shifted reaction center chlorophyll *a* dimer, the excitation energy is used to generate a stable redox couple (i.e., photochemistry), there is a biochemical or biophysical manifestation of that reaction in either energy storage, chlorophyll fluorescence, oxygen evolution, transient absorption, etc. If excitation energy is delivered in

discrete, short pulses such that it generates only a single photochemical reaction, or if second and subsequent electron transfer reactions are chemically inhibited (for example, with DCMU), the relationship between the rate of excitation delivered and the photochemical reaction defines an 'effective' or 'functional' absorption cross section. In the simplest case, where each reaction center undergoes a single turnover for each excitation absorbed (i.e., a 'single hit'), and there is no energy transfer between reaction centers (i.e., a pure 'puddle' model), the relationship between the excitation energy delivered and photochemistry will follow a cumulative one-hit Poisson distribution (Ley and Mauzerall, 1982):

$$Y/Y_{\max} = (1 - e^{-\sigma I}); \quad (2)$$

where  $Y$  is the yield of the reaction (e.g.,  $\text{O}_2$  evolved) at irradiance  $I$ ;  $Y_{\max}$  is the maximum (irradiance saturated) yield;  $\sigma$  is the effective cross section (with units of  $\text{A}^2/\text{quanta}$ );  $I$  is the excitation energy for a single turnover flash (with units of  $\text{quanta}/\text{A}^2$ ; note that units of time are not required as the reaction is determined for a single electron turnover).

$\sigma_{\text{PSII}}$  describes the efficiency by which absorbed photons can be used to drive a photochemical reaction. Unlike  $a^*$ ,  $\sigma$  incorporates a quantum yield for charge

separation. Like  $a^*$ ,  $\sigma$  is spectrally dependent; that is, different wavelengths of light will have different efficiencies for photochemistry. In the context of PS II,  $\sigma$  can be determined for a single wavelength and extrapolated to other wavelengths from knowledge of the PS II fluorescence excitation spectra.

#### 4. The Effective Cross Section and the Photosynthesis-Irradiance Relationship

Earlier we examined how the optical absorption cross section is related to the maximum quantum yield of photosynthesis. Now let us look at an alternative way of describing that relationship and the rest of the photosynthesis-irradiance curve.

We consider two other parameters:  $n$ , and  $\tau$ .  $n$  is the reciprocal of the Emerson-Arnold number, or the 'size' of the photosynthetic unit; i.e., the ratio of PS II reaction centers to total chlorophyll  $a$  with units of mol  $O_2$  (mol Chl  $a$ )<sup>-1</sup>, or mol PS II (mol Chl  $a$ )<sup>-1</sup>.  $n$  has no biochemical meaning; rather, it is a biophysical contrivance used to calculate electron transport (Herron and Mauzerall, 1971).  $\tau$  is the time required for a single electron to transit from water through the entire photosynthetic electron transport chain to the terminal electron acceptor (e.g.,  $CO_2$ ) at light saturation.  $1/\tau$  has units of s<sup>-1</sup>. Both parameters can be calculated from single turnover, light saturated oxygen flash yields and from light saturated measurements of oxygen evolution in the steady state.

The initial slope of a photosynthesis-irradiance curve,  $\alpha$ , can be related to  $\sigma_{PSII}$  and  $n$  through the equation:

$$\alpha^B = \sigma_{PSII} n, \quad (3)$$

where  $\sigma_{PSII}$  is the spectrally averaged effective absorption cross section for PS II (see Eq. (2)). Equation (3) is dimensionally identical to Eq. (1).

At light saturation, the maximum photosynthetic rate normalized to chlorophyll  $a$  is given by:

$$P_{max}^B = n/\tau. \quad (4)$$

The intercept between the initial slope and the maximum photosynthetic rate gives  $E_k$ . Substitution of Eqs. 3 and 4 into Eq. (1) reveals that:

$$E_k = 1/\sigma_{PSII} \tau. \quad (5)$$

Which can be simply rearranged to give

$$\sigma_{PSII} E_k = 1/\tau. \quad (6)$$

The left hand side of Eq. (6) represents the rate at which photons are effectively harvested by PS II and electrons are injected into the photosynthetic electron transport chain. This is sometimes called 'excitation pressure' (Maxwell et al., 1995; Chapter 13, Huner et al.). The right hand side of Eq. (6) gives the maximum rate at which the electrons are consumed. This is sometimes called 'photosynthetic capacity' (Krause et al., 1989).  $E_k$  is the only irradiance at which these two processes are balanced. Thus, while the maximum quantum yield of photosynthesis will always be greater at irradiance levels  $<E_k$ , the rate of photosynthetic electron transport will inevitably be lower. At irradiance levels  $>E_k$ , there is little or no increase in the overall rate of photosynthetic electron transport, and potentially much damage could be done from over excitation of the reaction centers. Hence, a balanced photosynthetic system is one that tracks changes in irradiance to maintain, as far as possible, a photosynthetic performance that is as close to  $E_k$  as can be achieved. As  $E_0$  is constantly changing, and its changes are totally outside of the control of the organism, how is a balance achieved?

### V. Light Harvesting Systems and the Effective Absorption Cross Section of Photosystem II

#### A. Dynamical Alteration of Light Harvesting

Based on the forgoing discussion, it is clear that cells have several specific, and not mutually exclusive options for dynamically balancing light harvesting with photosynthetic capacity. They can alter  $\sigma_{PSII}$ ,  $n$ , and/or  $\tau$ . Generally one or another 'strategy' predominates (Falkowski and Owens, 1980), but as several 'strategies' persist, even within different species of the same basic taxa, it is not clear that a priori there is any selective advantage of one or another. Let us first examine how changes are brought about to  $\sigma_{PSII}$ .

#### B. Measuring Changes in $\sigma_{PSII}$

Several methods have been developed to measure changes in  $\sigma_{PSII}$ . The first measurements were based

on following the fluorescence induction curve in the presence of DCMU (Malkin and Kok, 1966; Joliot et al., 1973). By comparing such curves with and without the inhibitor, one could get an idea of the ratio of PQ/Qa (Diner and Mauzerall, 1973) and the effective rate of reduction of both quinones. Those measurements were extremely useful in helping to elucidate the kinetics of electron transfer on the acceptor side of PS II, and in the derivation of models of light harvesting in relation to intersystem electron transport capacity (Crofts and Wright, 1983). The measurements facilitated the concept of energy transfer between reaction centers (Joliot et al., 1973; Paillotin, 1976; Lavergne and Trissl, 1995), but the approach suffers from the inherent irreversibility of PS II upon addition of the inhibitor. Moreover, the application of DCMU prevents dynamical analysis of  $\sigma_{\text{PSII}}$ , as, for example, might be induced by changes in background light. Hence, other methods were sought that did not require the application of chemical inhibitors.

The first attempts to measure  $\sigma_{\text{PSII}}$  without inhibitors were based on the flash intensity saturation function of  $\text{O}_2$  evolution using single turnover flashes derived from a laser (Ley and Mauzerall, 1982). That method can be absolutely calibrated and lead to experimental verification of the fundamental concepts of  $\sigma_{\text{PSII}}$  in relation to the absolute quantum yield of photosynthesis (Ley and Mauzerall, 1982). An alternative approach is based on following the flash intensity saturation profile of PS II variable fluorescence using a pump-and-probe technique (Falkowski et al., 1986). Quantitative analyses of simultaneous measurements of  $\text{O}_2$  and variable fluorescence using a pump and probe technique revealed that the two cross sections are statistically indistinguishable (Falkowski et al., 1988) and opened the door for a rapid, sensitive non-destructive approach based on fluorescence techniques. The first of these is a 'pump and probe' approach (Mauzerall, 1972; Falkowski et al., 1986), which subsequently was supplanted by a fast repetition rate fluorescence method.

### 1. The Pump and Probe Fluorescence

Formally, when a cell is placed in darkness and exposed to a weak flash of light, the fluorescence yield obtained is at a minimum, or  $F_0$  level. Following exposure to an actinic 'pump' flash, the fluorescence yield induced by a weak probe flash is obtained. If the fluorescence of the probe flash following the pump flash is determined within a short enough time

such that the reaction centers closed by the pump flash remain closed, the fluorescence yield will record the fraction of reaction centers closed. In practice, this requires that the second probe flash be triggered within 75  $\mu\text{s}$  of the pump flash. The difference between the fluorescence yields prior to and following the pump flash is the variable component of fluorescence ( $F_v$ ). When normalized to  $F_m$ ,  $F_v$  is quantitatively related to the photochemical efficiency of photosynthesis (Butler, 1972).

By changing the intensity of the pump flash, one can saturate the fluorescence profile to obtain the cross section of PS II (Falkowski et al., 1986; Genty et al., 1990). The technique is non-destructive, but time consuming; it can take several minutes to obtain a precise measurement of the effective cross section of PS II (Fig. 5). While tedious, the measurement can be used to follow changes in the cross section of PSII on time scales of minutes (Falkowski, 1992), however the fast repetition rate approach is much more efficient.

### 2. The Fast Repetition Rate Fluorescence (FRRF) Approach

The fast repetition rate fluorescence technique relies on the application of highly controlled sub-saturating pulses of light that cumulatively saturate PS II within a single turnover (Kolber et al., 1998). The individual pulses are approximately 1 ns in duration, and are separated in time by about 3–5 ns (Fig. 6). By cumulatively 'pumping' PS II with a set of such pulses of light energy, the reaction center can be saturated within approximately 60 to 120  $\mu\text{s}$ , depending upon the cross section of PS II. The saturation level gives the variable fluorescence yield corresponding to the reduction of  $Q_A$ . The rate of change in the saturation profile can be used to determine the effective cross section of PS II. The FRRF approach is extremely convenient, and extraordinarily sensitive. It can be used to follow the changes in  $\sigma_{\text{PSII}}$  as a function of background spectral irradiance, temperature, nutrient additions, etc. Moreover, because the cross sections are generated from a single saturation profile, the statistical precision of a single measurement is high, permitting one to follow the dynamics of the effective absorption cross section of PS II on time scales of seconds.

Using an FRRF approach, the excitation pulses can be further manipulated to follow electron transfer kinetics on the acceptor side of PS II, as well as the

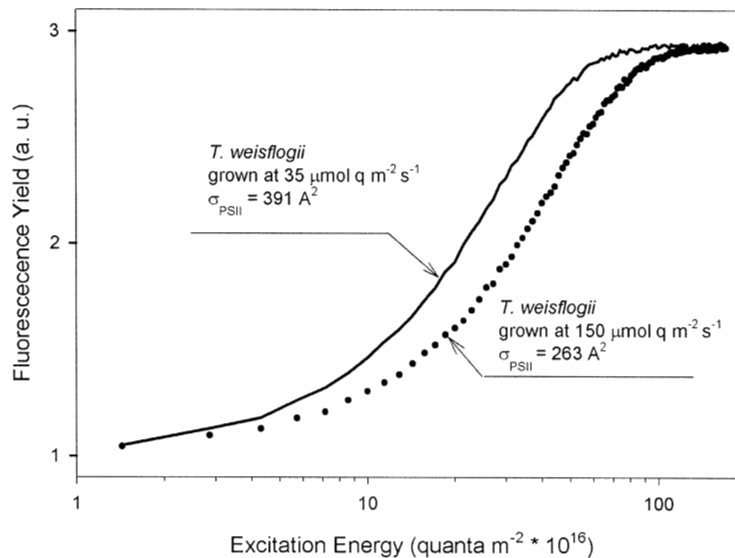


Fig. 5. An example of how the functional absorption cross section of PS II ( $\sigma_{\text{PSII}}$ ) changes as cells photoadapt. The changes in cross sections were measured by following the flash-intensity saturation profiles with a 'pump and probe' fluorometer. The marine diatom, *Thalassiosira weissflogii*, was grown at 150 and 35  $\mu\text{mol quanta m}^{-2} \text{s}^{-1}$ . The cross section for the high light grown cells is 33% lower than that of the low light grown cells.

redox state of the plastoquinone pool (Kolber et al., 1998). Following the initial single-turnover saturation profile, the kinetics of the oxidation of the quinones on the acceptor side of PS II can be assessed by measuring the rate of fluorescence decay with weak probe flashes spaced approximately 5  $\mu\text{s}$  apart. The FRRF can then be employed in a multiple turnover flash sequence (similar to a pulse amplitude modulated measurement, Chapter 13, Krause and Jahns). The multiple turnover flash sequence leads to a reduction of the plastoquinone pool; the difference in the amplitude of the single turnover flash and the multiple turnover flash provides an estimate of the level of reduction of the pool (Kolber et al., 1998).

### C. How Does $\sigma_{\text{PSII}}$ Change?

There are four basic strategies for altering  $\sigma_{\text{PSII}}$ , and we consider them in turn.

#### 1. State Transitions

State transitions, first described by Bonaventura and Myers for *Chlorella* (Bonaventura and Myers, 1969), were subsequently shown to be correlated with a reversible phosphorylation of a fraction of the light harvesting complexes (Allen et al., 1981). In their original analysis, Bonaventura and Myers demon-

strated that upon exposure to a subsaturating spectral irradiance that was preferentially absorbed by PS II the fluorescence yield declined while oxygen evolution remained relatively constant. This process was reversed with light that is primarily absorbed by PS I. The overall transition was induced within about 5 min at 20 °C, and they inferred that the changes in spectral composition were associated with reciprocal changes in the effective absorption cross sections (which they denoted with the symbol  $\alpha$ ) of the two reaction centers. In parallel experiments with a red (phycobililin-containing) alga, Murata (1970), suggested that the spectrally induced changes in energy distributions were associated with 'spillover', that is direct competition for excitations from a common antenna to the other reaction center (see review by Fujita et al., 1994). In chlorophyll *b*-containing organisms, these two models have been resolved by fluorescence analysis that clearly suggests that the state transitions are primarily a consequence of alterations in PS II cross sections (Malkin et al., 1986); whether these changes correspond quantitatively to reciprocal changes in PS I cross sections remains to be conclusively demonstrated (Bruce et al., 1989; Delosme et al., 1996). However there is evidence that a fraction of the light harvesting complex physically migrates from one photosystem to the other during a state transition (Mullineaux et



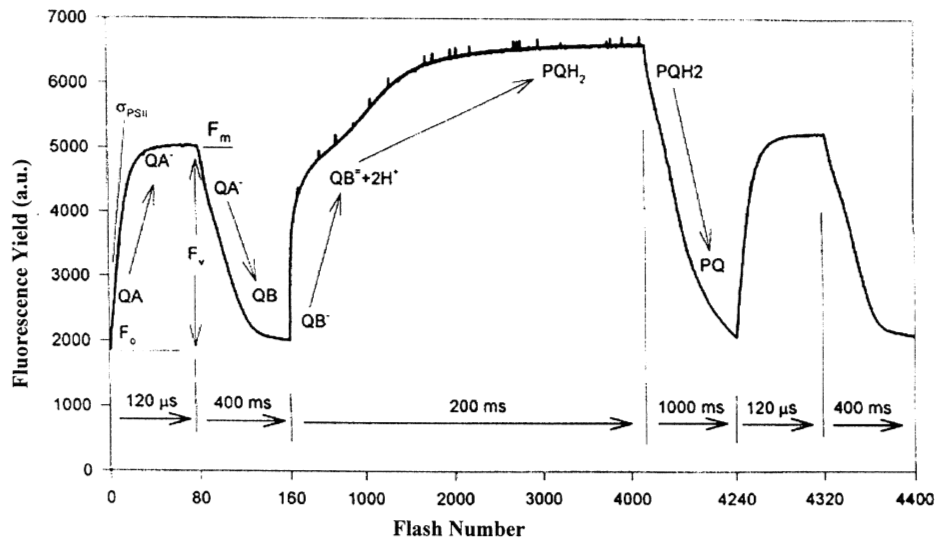


Fig. 6. The kinetic information that can be derived from Fast Repetition Rate Fluorometry (FRRF). In the initial 120  $\mu$ s the effective absorption cross-section and the extent of reduction of the primary electron acceptor in PS II ( $Q_A$ ) can be inferred from the kinetics profile of the fluorescence saturation curve. Following the saturation profile, a weak series of pulses are applied and the electron transfer from  $Q_A$  to  $Q_B$  is measured. This protocol is then followed by long term pumping with subsaturating flashes to reduce the PQ pool. The oxidation rate of  $PQH_2$  is measured over the next 1000 ms with very weak pulses, and the cycle is repeated.

al., 1997). Additionally, there is evidence that a migratory fraction of the light harvesting complex becomes energetically coupled to the reaction center to which it migrates (Wollman and Delepelaire, 1984).

The search for mechanisms for state transitions was stimulated by the observation that upon exposure to DBMIB, radioactively labeled phosphate, supplied as exogenous  $\gamma$   $^{32}$ P-ATP, could phosphorylate a fraction of the light harvesting complex (later to be denoted Lhcb), while DCMU prevented the phosphorylation (Allen et al., 1981). As these two inhibitors lead to the reduction and oxidation, respectively, of the plastoquinone pool, the experimental results suggested that the pool was coupled to a redox regulated kinase (Allen et al., 1981; Bennett, 1984; Allen, 1992). Subsequent experiments clearly suggested that the phosphorylated state was a high fluorescent yield state while the dephosphorylated state corresponded to a low fluorescence yield; i.e., that the phosphorylation and the state transitions were phenomenologically related.

The demonstration of reversible Lhcb phosphorylation in chlorophyll *b*-containing cells (Bennett, 1983) leads to searches for the responsible protein kinases and phosphatases. It was clearly shown that the phosphorylated residue was a threonine (Bennett, 1991). Several putative protein kinases were described, however, most turned out not to be

the responsible enzyme(s) (Hind et al., 1995; Gal et al., 1997), and subsequent biochemical characterization of a thylakoid associated kinase immediately provided information about its sequence (Race and Hind, 1996). Working with *Chlamydomonas* and later with *Arabidopsis*, Kohorn and co-workers identified two thylakoid associated kinases, Tak1 and Tak2b (Snyders and Kohorn, 1999), and using a molecular genetic approach, showed that the loss of Tak1 abolished state transitions (Snyders and Kohorn, 2001). These results provided, for the first time, conclusive evidence that the state transitions are related to a specific thylakoid kinase, and that the kinase is regulated by the redox state and the plastoquinone pool.

It is not likely that the plastoquinone pool per se is the signaling molecule for a protein kinase. Plastoquinone is highly hydrophobic, and is thought to be embedded or sandwiched in the lipid bilayer that forms the thylakoid membranes. Essentially, there is little or no contact between the pool and surface associated thylakoid proteins. One suspected candidate for the signal is the cytochrome  $b_6f$  complex, especially subunit IV, the plastoquinol docking protein associated with that complex (Verner et al., 1997).

In brief, the redox poise of the plastoquinone pool can produce changes in the effective absorption cross

section of PS II by altering the energetic coupling of a fraction of Lhcb to the reaction center of that photosystem. The process appears to be mediated by a redox sensitive protein kinase associated with the outer thylakoid membrane. The changes in absorption cross section afforded by the state transitions are approximately 20%, and are rapidly reversible. The time scale for change in the cross section in *Chlorella* is about 3 min. at 24 °C; the  $Q_{10}$  for the change is about 1.8 (P. Falkowski, unpublished). The change in cross section is directly proportional to the change in  $E_k$ . It remains to be demonstrated to what extent state transitions occur in eukaryotic taxa other than chlorophyte algae. There is some evidence that a similar phenomenon occurs in diatoms (Owens, 1986; Ting and Owens, 1993). However, it is not clear that fucoxanthin or peridinin light harvesting protein complexes undergo reversible protein phosphorylation.

Finally, it should be noted that the state transitions are induced in the laboratory by changes in spectral quality—in fact, the terms ‘State I’ and ‘State II’ arise from the original work of Bonaventura and Myers (1969) in which red light was used to preferentially excite chlorophyll *b* and hence PS II, while far red light was used to excite PS I. As we mentioned earlier, effectively there is no far red light in aquatic ecosystems. The experimentally contrived transitory changes in light quality have no real analogues in natural aquatic ecosystems. Rather, state transitions must be elicited by a change in irradiance—that is, under relatively low irradiance levels, high PS II cross sections are favored (State II), and under relatively high irradiance levels, low PS II cross sections are favored (State I). The changes in the cross sections are triggered by the redox poise of the plastoquinone pool, however, light quantity rather than quality is the primary environmental driver of the response.

## 2. The Xanthophyll Cycle

In 1963, Yamamoto demonstrated a reversible epoxidation of hydrophilic carotenoids in higher plant leaves (Yamamoto et al., 1963). This class of reactions was subsequently demonstrated in all non-phyticobilisome containing oxygenic photoautotrophs, including chromophyte algae. In chlorophyll *b*-containing organisms the reaction sequence is from zeaxanthin through asteroxanthin to violaxanthin, while in chlorophyll *c*-containing organisms it is

generally mediated via diatoxanthin and diadinoxanthin (Hagar and Stransky, 1970), although some of the latter use both (Lohr and Wilhelm, 2001).

The xanthophyll cycle was an interesting curiosity until Demmig-Adams showed a remarkable correlation between the de-epoxidation reaction and chlorophyll fluorescence quenching. In higher plants, the quenching could be as high as 80%, and was induced by exposure to high irradiance. While there are several quenching processes, the xanthophyll cycle appears to correspond to a very large fraction of the total quenching, and unlike many other quenching processes, is generally reversible on the time scale of several minutes to tens of minutes (Demmig et al., 1988).

The exact biophysical mechanism by which fluorescence is quenched via the xanthophyll cycle is unclear. One possibility is that physical aggregation of chlorophyll molecules, induced by the de-epoxidation of the xanthophylls, leads to a reduction in the optical absorption cross section (i.e.,  $a^*$ ) of the entire antenna system, and an associated quenching of the fluorescence (Horton, 1996; Horton et al., 1999). The mechanism of the quenching in this scenario is unclear; however, if this scenario is valid, it should lead to a change in *both* the optical and effective cross sections. An alternative hypothesis is based on direct competition for excitation energy within the light harvesting complex between the reaction center and the xanthophylls, the latter of which, upon de-epoxidation form a singlet state that can be populated with excitations emanating from the lowest singlet excited states of chlorophyll *a* (Owens, 1994; Frank et al., 1996). In effect, the latter hypothesis suggests that the xanthophylls become reversibly activated quenchers within the pigment bed. Upon activation they increase the probability that absorbed photons will be dissipated as heat through non-radioactive energy transfer to carotenoids. Should that occur, the process should lead to a change in the *effective* cross section of one or both reaction centers (depending upon which antenna system the xanthophyll cycle is associated with), but not a change in the *optical* absorption cross section.

The xanthophyll cycle appears to be ubiquitous in all eukaryotic algal lineages, with the possible exception of the cryptophytes and rhodophytes which contain phycobiliproteins. The cycle operates in diatoms (Arsalane et al., 1994; Olaizola and Yamamoto, 1994; Olaizola et al., 1994; Lohr and Wilhelm, 1999), dinoflagellates, coccolithophorids

(P. Falkowski, unpublished), and prymnesiophytes (Frommolt et al., 2001). Using the symbiotic dinoflagellate, *Symbiodinium microadriaticum*, as a model, simultaneous measurements of the effective absorption cross section and changes in the xanthophylls (in this case, diatoxanthin and diadinoxanthin) show a linear correspondence (Fig. 7), with simultaneous quenching of both  $F_o$  and  $F_m$ . These results are consistent with the direct excitation quenching hypothesis, and suggest that the xanthophyll cycle leads to a direct alteration in the effective cross section, not a change in  $a^*$ .

The dynamics and effect of the xanthophyll cycle have been elucidated by following changes in the  $\sigma_{PSII}$  as a function of irradiance in mutants of *Chlamydomonas reinhardtii*. The mutants (Niyogi et al., 1997), deficient in either the ability to form a quencher (DE1, a mutation in the de-epoxidase), or in the ability to relax quenching (DE6, a mutation in the epoxidase), are locked in either a high or low effective cross section status (Fig. 8). In contrast, a wild-type cell with an identical genetic background (DE5) displays approximately a 50% decrease in  $\sigma_{PSII}$  as the cell is brought from low to high irradiance. The corresponding changes in  $E_k$  illustrate how the changes in  $\sigma_{PSII}$  are directly related to the light saturation function for photosynthetic electron transport. The changes in  $\sigma_{PSII}$  are accompanied by small changes in the maximum quantum yield of PS II photochemistry (i.e.,  $F_v/F_m$ ), suggesting an excitation transfer between pigment beds or a small component of reaction center quenching that accompanies the quenching within the light harvesting complex. Because variable fluorescence is the primary signal used to assess the correlation between the changes in the xanthophylls and the effective cross sections, we have limited information on the effect of the xanthophyll cycle on PS I cross sections. A comprehensive discussion of the mechanisms related to fluorescence quenching is given in Chapter 13 (Krause and Jahns)

Both the xanthophyll cycle and the state transitions are manifested in changes in  $\sigma_{PSII}$ . Because the kinetics of the two processes are similar, it is difficult to distinguish between these two phenomena in the field. There is no question however, that these processes are engaged in the natural aquatic ecosystems. Changes in chlorophyll fluorescence quenching associated with the passage of clouds crossing the sky have been observed since the early 1980s (Abbott et al., 1982; Gorbunov et al., 2001),

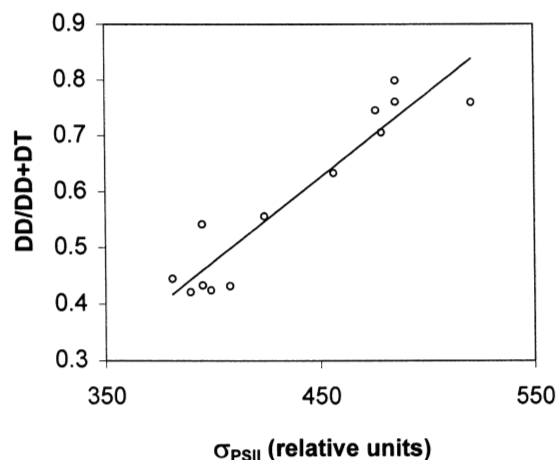


Fig. 7. The correlation between the ratio of diadinoxanthin (DD) to the sum of DD and diatoxanthin (DT), and the effective absorption cross-section of Photosystem II in a dinoflagellate, *Symbiodinium microadriaticum*. Note that as diadinoxanthin is deepoxidized to diatoxanthin, the cross section decreases.

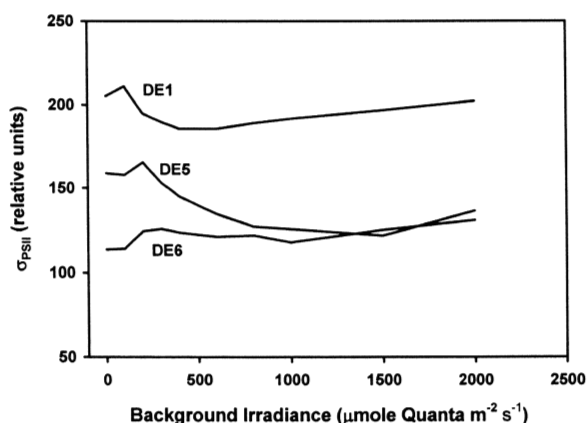


Fig. 8. The effect of background irradiance on the effective cross section of PS II in two mutants and the wild type of *Chlamydomonas*. One mutant (DE1) is locked in a non-quenching state for the xanthophyll cycle, while its complement (DE6) is locked in a quenching state. The wild type (DE5) shows a 50% change in the effective cross section as background irradiance changes. Neither mutant has significant ability to change its functional cross-section. Note that at irradiances less than about 200  $\mu\text{mol quanta m}^{-2} \text{s}^{-1}$ , the small changes in cross section are related to state transitions.

and reversible, non-photochemical quenching of fluorescence associated with enhanced solar radiation has long been observed in the aquatic sciences (Slovacek and Hannan, 1977; Owens et al., 1980; Falkowski and Kiefer, 1985). The quenching process

is clearly discernable in vertical profiles of fluorescence yields taken at mid day compared with those at night (Falkowski and Kolber, 1995).

The xanthophyll cycle has a higher dynamic range (larger 'band-width') than state transitions, but appears to be fundamentally activated by the same process, in this case the reduction of the plastoquinone pool. The de-epoxidation reaction is keyed to the  $\Delta pH$  gradient across the thylakoid membrane (Horton and Ruban, 1992; Rees et al., 1992; Noctor et al., 1993). The  $\Delta pH$  gradient is, in turn, generated by the deposition of protons onto the lumenal side of the thylakoid membrane by plastoquinol (the so-called 'Q' cycle) (Rich 1985). Hence, as the intersystem electron acceptor pool becomes increasingly reduced, both the state transitions (which can redistribute excitation energy between the two reaction centers) and the de-epoxidation of xanthophylls (which reduces the effective absorption cross section of PS II), become engaged. These two processes can alter the PS II cross section by about 50%. What happens when the product of spectral irradiance and the effective absorption cross section (i.e., excitation pressure) increases (or decreases) beyond this dynamic range?

## VII. Light Harvesting Complexes

### A. Alterations in the Pigment Composition of Antenna Complexes

On time scales of hours to days, cells can photoacclimate to changes in irradiance by differential gene expression of light harvesting complex genes and post-translational control of pigments within pre-existing pigment protein complexes. This phenomenon has been most clearly identified in cyanobacteria (Chapter 17, Grossman et al.).

One example of differential gene expression in response to changes in irradiance is found in *Prochlorococcus*. This genus is a group of marine cyanobacteria that contain a chlorophyll *a/b* light harvesting complex. There are two basic strains of *Prochlorococcus*: one contains a relatively low concentration of pigments and appears to be permanently adapted to high light, while the other is a low light strain with relatively high pigment contents (Partensky et al., 1993; Partensky et al., 1997). The Chl *b*-binding proteins in these organisms (Prochloro-

phyte chlorophyll *b*-binding proteins, *pcb*'s) are derived from a separate protein family than that of the Chl *a/b*-binding proteins in chlorophyte algae and higher plants (LaRoche et al., 1996, Garczarek et al., 2000; Chapter 1, Green and Anderson). In the low-light-adapted strain, the *Pcb* gene family is comprised of seven genes encoding different Pcb's. In the high-light-adapted strain, there is a single *pcb* gene (Garczarek et al., 2000). Photoacclimation in the low light strain appears to be associated with differential expression of some of the *pcb* genes (Partensky et al., 1997, Garczarek et al., 2000). The differential expression of the external antenna (*pcbA*) and core (*psbC*) genes has been hypothesized as a mechanism of regulation of the antenna size used by *Prochlorococcus* cells to cope with excess light energy (Garczarek et al., 2001).

Light induced changes in antenna pigment composition in eukaryotic algae is less well understood. In eukaryotic algae, nuclear encoded light harvesting proteins comprise gene families (Grossman et al., 1990; LaRoche et al., 1990, 1994; Green and Durnford, 1996). Changes in light intensity and/or quality may lead to differential expression of one or more of the *Lhcb* genes, which can, in turn, lead to altered pigment composition in the antenna complex. This process can be post-translationally controlled (Mortain-Bertrand et al., 1990), but is also transcriptionally regulated. For example, in the unicellular chlorophyte alga, *Dunaliella tertiolecta*, there are four *Lhcb* genes (Suknik et al., 1988; LaRoche et al., 1990). Under low to moderate light, two of these genes are highly expressed, giving a phenotype relatively rich in chlorophyll *b* (Suknik et al., 1988). If chlorophyll *a* synthesis is blocked with gabaculene and the cells are placed in low light, chlorophyll *a* within the existing light harvesting complexes can be converted to chlorophyll *b* (Mortain-Bertrand et al., 1990). However, when the cells are exposed to high light (approximately 2000  $\mu\text{mol quanta m}^{-2} \text{s}^{-1}$ ), a second set of genes, that preferentially bind lutein, are expressed (Suknik et al., 1987b). The lutein-containing light harvesting protein complex transfers excitation energy to PS II with far lower efficiency than the chlorophyll *b*-containing light harvesting complex. Hence, the differential gene expression, induced solely by changes in light intensity, can lead to antenna systems that have differing effective absorption cross sections.

### B. Changes in the Level of Expression of *Lhcb* Genes

In both prokaryotic and eukaryotic algae, changes in irradiance level lead to changes in the total pigment content of the cells. This phenomenon has been well studied in many algal taxa, and appears to be universal (Myers and Burr, 1940; Myers, 1946; Steemann-Nielsen and Hansen, 1959; Yentsch and Ryther, 1967; Jorgensen, 1969; Falkowski, 1980; Falkowski and Owens, 1980; Perry et al., 1981). In the chlorophyte, *Dunaliella tertiolecta*, changes in cell pigmentation for the light harvesting complexes are transcriptionally mediated (Escoubas et al., 1995) and follow first-order kinetics (Sukenic et al., 1990). Changes in light harvesting complexes often are accompanied by changes in reaction center proteins (Falkowski and Owens, 1980). In some cases, the changes in the level of expression lead to post-translational modification of excess carotenoids, which act as 'sun-screens,' competing with light harvesting complexes for excitation energy (Ben-Amotz and Avron, 1983; Lee and Ding, 1991; Olaizola and Yamamoto, 1994b). In the case of cyanobacteria, changes in chlorophyll content are correlated with changes in reaction centers (Raps et al., 1983; Fujita et al., 1990), however, this does not necessarily occur in eukaryotic algae (Falkowski and Owens, 1980; Falkowski et al., 1981). We will examine the implications of the two photoacclimation strategies in the next section. Regarding the changes in the light harvesting complexes per se, we are faced with the question of how does a cell perceive the changes in irradiance levels and how is that signal transduced to regulate expression of the light harvesting complex genes?

In 1971, Beale and Appleman reported that sub-lethal concentrations of DCMU could upregulate cellular chlorophyll levels in *Chlorella* (Beale and Appleman, 1971). Following on that observation, Escoubas et al. (1995) investigated the effects of numerous photosynthetic electron transport inhibitors on chlorophyll and *Lhcb* mRNA levels in *Dunaliella tertiolecta*. This genus of unicellular chlorophytes displays a particularly wide dynamic range of cellular chlorophyll content and is a convenient model organism for studies of photoacclimation (Falkowski and Owens, 1980; Baroli and Melis, 1996). When 0.5  $\mu\text{M}$  DCMU is added to cultures grown under high light conditions, there is a two fold increase in *Lhcb* mRNA levels (Fig. 9). In contrast, in cells grown with sub-lethal concentrations of DBMIB there was a 75% decrease in the steady state of *lhcb* mRNA levels and cellular chlorophyll content declines. Inhibitors on the donor side of PS II or the acceptor side of PS I have minor effects. Based on these experimental results, Escoubas et al. (1995) concluded that the redox-state of the plastoquinone pool acts as a sensor for photosynthetic acclimation. This conclusion is consistent with the observations by Fujita et al. (1994). Simultaneously, Maxwell et al. (1995) provided evidence that lower temperatures could lead to a reduction of the quinone pool at low light in *Dunaliella salina*. The role of the plastoquinone pool in regulating the acclimation of light-harvesting proteins and other photosynthetic genes was subsequently demonstrated in *Chlorella vulgaris* (Wilson and Huner, 2000) and higher plants (Pfannschmidt et al., 1999).

Perhaps the most compelling evidence that the redox state of the plastoquinone pool is a light sensor

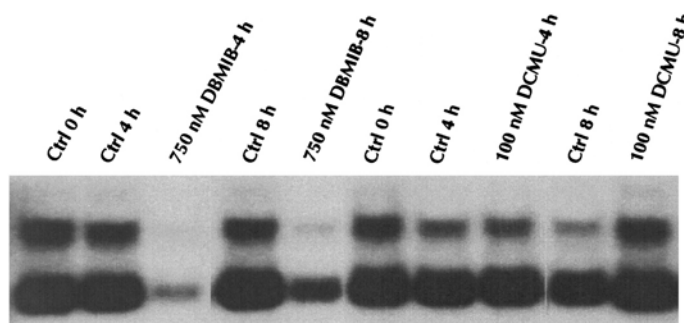


Fig. 9. RNA blot showing how redox poise affects *cab1* (*Lhcb*) transcript abundance in *Dunaliella tertiolecta*. Cultures were grown in the presence of sublethal concentrations of the photosynthesis inhibitors DBMIB and DCMU. In the DBMIB experiment, cultures were illuminated at  $700 \mu\text{E} \cdot \text{l}^{-1} \cdot \text{s}^{-1} \cdot \text{m}^{-2}$ ; in the DCMU experiment, at  $1500 \mu\text{E} \cdot \text{l}^{-1} \cdot \text{s}^{-1} \cdot \text{m}^{-2}$ . The lower bands represent the mature transcript, the upper bands the unprocessed transcript. The same amount of total RNA was loaded for each sample. (Data from Escoubas et al., 1995.)

is based on site directed mutants of *Chlamydomonas reinhardtii* in which Ala251 in the D1 protein of Photosystem II was changed to Leu or Ile (Lardans et al., 1998). This position is at the border of the  $Q_B$  binding site. The Leu and Ile mutants were photosynthetically competent, but the rate of electron transfer from  $Q_A$  to  $Q_B$  was reduced by almost an order of magnitude; i.e., the cell behaves as if it were growing continuously with sub-lethal concentrations of DCMU. The phenotype of these cells is low light adapted (Lardans et al., 1998). Fast repetition rate fluorescence transients on A251L confirm that the plastoquinone pool is oxidized, even under high excitation pressure (Fig. 10). Conversely, a mutation of subunit IV in cytochrome  $b_6f$  in *Chlamydomonas*, which results in a photosynthetically competent cell but with a reduced affinity of plastoquinol in the oxidizing site, is phenotypically a low light adapted cell; the quinone pool in this organism is highly reduced under moderate excitation pressure (Fig. 10).

Several putative regulatory motifs, related to those of higher plants (Terzaghi and Cashmore, 1995) were detected in the *Lhcb* promoter region in *D. tertiolecta*. These were hypothesized to be involved in irradiance mediated transcriptional control of *Lhcb* gene expression (Escoubas et al., 1995). Electrophoretic mobility shift assays were used to identify several DNA-binding complexes whose binding activities are regulated by redox control through the quinone pool. The binding activities of these complexes appear to be enhanced in the presence of DCMU, but decreased with DBMIB. These binding activities occur within a 166 bp long region on the 5' strand upstream of the *Lhc* promoter. Among three tentative binding motifs, all duplicated in that region, a TCTAA box (consensus core sequence: TCTAAHGT) is also found in the similar upstream promoter regions of *cab* genes from *Chlamydomonas reinhardtii* (*cab1*) and *Arabidopsis thaliana* (*cab2* and *cab3*). The correlation between binding kinetics of the DNA-binding complexes and the *Lhc* mRNA levels suggests a regulatory role for those DNA binding proteins during photoacclimation. The signal transduction pathway between chloroplast and nucleus is unknown although the phosphatases inhibitor experiments suggest the involvement of a phosphorylation cascade that could be triggered by a reduced redox state of plastoquinone pool (Escoubas et al., 1995).

### C. Changes in the Numbers of Reaction Centers, $n$

Changes in  $n$  can affect both  $P_{max}^B$  and  $\alpha^B$ , however, the actual affects are counterintuitive. We consider two phenomena: downregulation of PS II reaction centers at high irradiance levels, and net synthesis or degradation of reaction centers resulting from acclimation to a new irradiance.

On time scales of tens of minutes to hours, the cellular content of functional reaction centers can be altered. We will not discuss here the mechanisms that lead to the dynamical 'downregulation' of PS II (Baker and Bowyer, 1992; Osmond, 1994), suffice to say that there are some processes that can temporarily reduce electron transport through PS II reaction centers without an accompanying loss of reaction center proteins. This type of down regulation occurs in natural phytoplankton communities (Falkowski, 1992) and in zooxanthellate corals (Gorbunov et al., 2001) in mid day, and should not be confused with photodamage. In the former, inhibition of plastid encoded protein synthesis (with, for example, lincomycin) does not impact the recovery of the reaction center function at low light, while in the latter it does. Recovery from downregulation obeys first order kinetics with a half-time of about 15 to 60 min, depending upon temperature. The down-regulation phenomenon can be induced by high irradiance levels (or low temperature), and is manifested primarily as a reversible reduction in the quantum yield of PS II (e.g., in variable fluorescence). It should be noted that down regulation (or photodamage to PS II reaction centers, for that matter) does not necessarily affect the overall photosynthetic electron transport rate. Under nutrient replete conditions, there is often excess photosynthetic electron transport capacity; light saturated photosynthesis is limited by consumption of reductants in the dark reactions (Stitt, 1986; Sukenik et al., 1987). Hence, a loss of up to 50% of the reaction centers can have little or no effect on  $P_{max}^B$ , but does affect  $\alpha^B$  (Behrenfeld et al., 1998).

On time scales of hours to days, the accumulation or loss of cellular chlorophyll (during the acclimation to lower or higher irradiance levels, respectively) is often accompanied by changes in the number of reaction centers. As cells acclimate to lower irradiance levels, the increase in density of PS II and PS I reaction centers can be significant (Falkowski et al., 1981; Falkowski, 1984b; Sukenik et al., 1987), however, perhaps paradoxically,  $P_{max}^B$  almost always

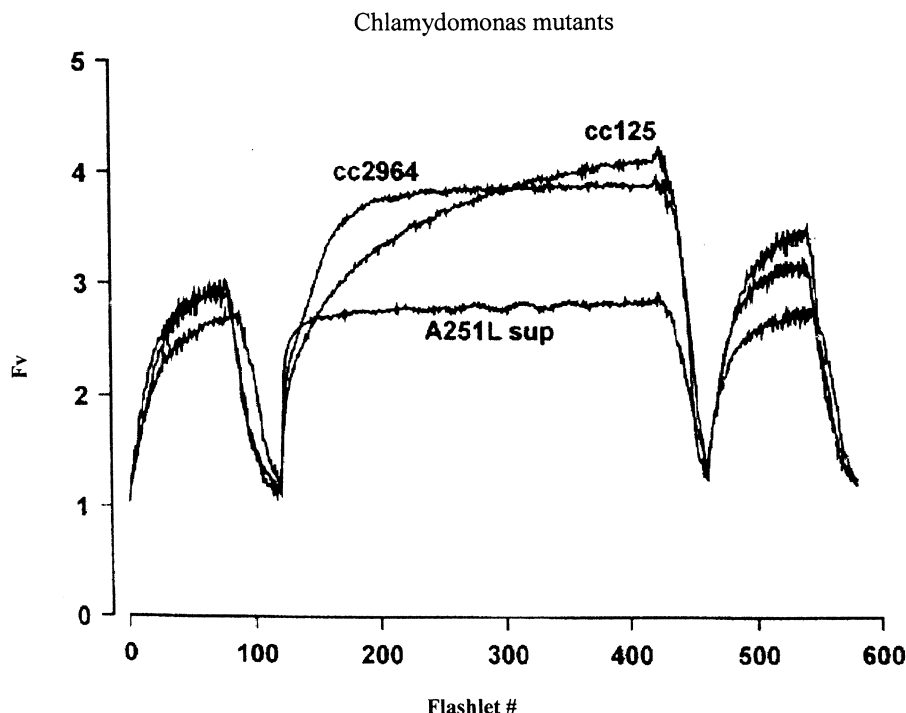


Fig. 10. FRRF profiles (see Fig. 6) of two mutants and a wild type *Chlamydomonas*. In mutant A251L sup, amino acid 251 in the D1 protein was altered by site directed mutagenesis from alanine to leucine, leading to a ten-fold decline in the rate of electron transfer from  $Q_A$  to  $Q_B$ . Note that in this mutant the PQ pool is oxidized under conditions of high excitation pumping. In mutant cc2964, there is a defect in subunit IV of the cytochrome  $b_6f$  complex which slows down the oxidation of  $PQH_2$ . cc125 is the wild type. Relative to the wild type, A251L sup has high chlorophyll content at high light, while cc2964 has low chlorophyll content when the cells are grown at low light. (Data from Lardans et al., 1998)

decreases. Hence, the more reaction centers the cell has, the slower the rate of electron throughput per reaction center. The changes in  $n$  compensate for changes in low irradiance by increasing light harvesting and lowering  $E_k$  but not increasing the maximum quantum yield. Because of self-shading within the cell, increases in cellular chlorophyll (i.e., either through increased synthesis of light harvesting systems and/or by increases in  $n$ ) do not lead to increases in the maximum quantum yield of photosynthesis. Actually, the opposite usually occurs. The higher the cellular content of chlorophyll, the lower the optical absorption cross section per chlorophyll molecule (i.e.,  $a^*$  decreases). Inspection of Eq. (1) reveals that this phenomenon must lead to a decrease in the maximum quantum yield.

It should be noted that to change the level of light harvesting complexes or photosynthetic electron transport components, the cell must differentially synthesize more of the desired component than required for steady state growth (if the component is

to increase), or conversely dilute the component through cell division or via active degradation (if the component is to decrease). These processes are not simply mirror images of each other. An increase in a pool of a component requires resources, such as nitrogen. Under nutrient (especially nitrogen and iron) limitation, cells cannot fully acclimate to low irradiance levels (Greene et al., 1992). When a cell needs to reduce the pool size of a component, such as a light harvesting complex, it can actively degrade as well as dilute the pools (Falkowski, 1984b).

The inverse relationship between  $n$  and  $P_{max}^B$ , first observed in nutrient replete, continuous cultures of *Chlorella* as they acclimated to different light intensities (Myers and Graham, 1971), is associated with changes in  $\tau$ . Essentially, the fundamental observation is that the more reaction centers a cell produces in response to a decrease in light, the slower is the maximum rate of electron transport from water to the terminal acceptor (usually  $CO_2$ ). In examining what may cause this limitation, Sukenik



et al. (1987a) showed that in *Dunaliella*, the changes in  $n$  (and cellular chlorophyll) were not accompanied by changes in Rubisco. Hence, while all the components of the photosynthetic electron transport chain changed in concert, the ratio of the electron transport components to the Calvin cycle capacity changed inversely with irradiance. The ratio of ETC/Rubisco was linearly correlated with the maximum rate of electron transport ( $1/\tau$ ). The effect of this acclimation strategy is that  $E_k$  decreases markedly as cells acclimate to lower irradiance levels, but light saturated photosynthesis declines. As light is increased for a low light acclimated cell, the potential to reduce the plastoquinone pool is higher (because  $E_k$  is lower), hence the cell can use the redox state to decrease the rate of synthesis of light harvesting and electron transport components. How these signals are coordinated amongst all the components involved is unknown.

#### *D. The Relationship Between the Optical and Effective Absorption Cross Sections*

The maximum quantum yield of photosynthesis can be obtained from Eq. (1), however, if we consider both Eqs. 1 and 3, we find:

$$\phi_{\max} = (n \sigma_{\text{PSII}}) / a^* \quad (7)$$

where  $(n \sigma_{\text{PSII}})$  is the effective absorption cross section for a photosynthetic unit (i.e., for  $\text{O}_2$ ) evolution. Hence, the maximum quantum yield of photosynthesis can be related to the ratio of two cross sections: the effective absorption cross section for  $\text{O}_2$  evolution to that of spectrally integrated optical absorption cross section (Falkowski and Raven, 1997; Ley and Mauzerall, 1982). Both cross sections are normalized to chlorophyll.

Equation (7) reveals that changes in  $n$  or  $\sigma_{\text{PSII}}$  can result in changes in the maximum quantum yield of  $\text{O}_2$  evolution without necessarily invoking any change in the quantum yield of photochemistry in PS II. Hence, if a cell decreases  $\sigma_{\text{PSII}}$  by engaging a xanthophyll cycle (for example), as long as  $a^*$  does not change, the maximum quantum yield of photosynthesis will decrease. This conclusion applies to any non-photochemical quenching mechanism in the antenna (i.e., any process that influences  $\sigma_{\text{PSII}}$  but not  $a^*$ ).

### VIII. The 'Nested Signal' Hypothesis

The forgoing discussion of photoacclimation responses suggests that redox signaling involves the plastoquinone pool and perhaps other electron transport carriers (Durnford and Falkowski, 1997; Pfannschmidt et al., 2001). All the primary photoacclimation response functions, regardless of the time scale, suggest that transduction of the primary signal (e.g., spectral irradiance) is mediated by a nested set of responses (Durnford and Falkowski, 1997). This 'nested signal' hypothesis suggests that as irradiance levels increase, the initial reduction of the plastoquinone pool induces a state transition and/or non-photochemical quenching associated with de-epoxidation of xanthophylls. This response, occurring within a few seconds and achieved within minutes, is the first level of feedback within the nested series. As the resulting effective absorption cross section changes, the plastoquinone pool becomes increasingly oxidized. However, if irradiance increases further, and the dynamic range of these short-term alterations in  $\sigma_{\text{PSII}}$  is not sufficient to keep the pool partially oxidized, the continued excitation pressure will lead to a downregulation of *Lhcb* gene expression. This process, once engaged, reduces both the effective and optical cross sections of the cell, and is a second line of response. The cell commitment to this response function is considerable; cessation of steady-state protein synthesis potentially reduces the fitness of the next generation of daughter cells. Cells do not commit to either up- or down-regulation of protein synthesis with the passage of each cloud across the sky. The excitation pressure must be sustained for approximately 10% of the cell division cycle. Finally, at very high irradiance levels, differential expression and/or the accumulation of non-photosynthetically active carotenoids become the last line of response. The signals for these responses remain to be elucidated, however, mutant analysis with *Chlamydomonas reinhardtii* suggests that the redox state of the plastoquinone pool is involved (Forster et al., 2001). The nested response sequence is maintained as cells acclimate to low irradiances, however the sign of the change is reversed.

The natural variance in spectral irradiance has provided a strong selection mechanism for photoacclimation. That these processes appear to be so widely distributed in all algal taxa, and are found to varying degrees in vascular plants (which evolved

from one class of green algae (Bhattacharya and Medlin, 1998)), suggests that the basic mechanisms of the acclimation processes are highly conserved. Fundamentally, the responses facilitate changes in the photosynthesis-irradiance relationship on time scales of minutes to days. Such responses are critical to the evolutionary persistence of each extant algal species, many lineages of which predate terrestrial plants by over 2 billion years of Earth's history (Knoll, 1992). The evolution of the processes themselves presently lies in the realm of speculation, however, we propose that light-induced changes in gene expression were the first strategy to emerge, followed by protein phosphorylation (state-transition), followed by differential gene expression and finally, the xanthophyll cycle. That all of these work in concert to give a flexible set of feedback responses for the photosynthetic machinery is one of the miracles of the evolutionary design of photosynthetic light harvesting systems.

## Acknowledgments

The authors are supported for research on this topic by the U.S. Department of Energy, Office of Energy Biosciences. We thank Bruce Kohorn, Michal Koblizek, and Dion Durnford for discussions.

## References

- Abbott MR, Richerson P J and Powel TM (1982) In situ response of phytoplankton fluorescence to rapid variations in light. *Limnol Oceanogr* 27: 218–225
- Ackleson SG, Cullen JJ, Brown J and Lesser M (1993) Irradiance-induced variability in light scatter from marine phytoplankton in culture. *J Plankton Res* 15: 737–759
- Ahn YH, Bricaud A and Morel A (1992) Light backscattering efficiency and related properties of some phytoplanktons. *Deep Sea Res* 39: 1835–1855
- Allen JF (1992) Protein phosphorylation in regulation of photosynthesis. *Biochim Biophys Acta* 1098: 275–335
- Allen J, Bennett J, Steinback K E and Arntzen CJ (1981) Chloroplast protein phosphorylation couples plastoquinone redox state to distribution of excitation energy between photosystems. *Nature* 291: 25–29
- Aluwihare LI, Repeta DJ and Chen RF (1997) A major biopolymeric component to dissolved organic carbon in seawater. *Nature* 387: 166–169
- Arsalane W, Rousseau B and Duval JC (1994) Influence of the pool size of the xanthophyll cycle on the effects of light stress in a diatom: Competition between photoprotection and photoinhibition. *Photochem and Photobiol* 60: 237–243
- Babin M, Theriault J C, Legendre L, Nieke B, Reuter R and Condal A (1995) Relationship between the maximum quantum yield of carbon fixation and the Gulf of St Lawrence. *Limnol Oceanogr* 40: 956–968
- Babin M, Morel A, Claustre H, Bricaud A, Kolber Z and Falkowski PG (1996) Nitrogen- and irradiance-dependent variations of the maximum quantum yield of carbon fixation in eutrophic, mesotrophic and oligotrophic marine systems. *Deep-Sea Res* 43: 1241–1272
- Baker NR and Bowyer JR (eds) (1992) *Photoinhibition of Photosynthesis: From Molecular Mechanisms to the Field*. Bios, Oxford
- Bannister TT and Weidemann AD (1984) The maximum quantum yield of phytoplankton photosynthesis in situ. *J Plankton Res* 6: 275–294
- Baroli I and Melis A (1996) Photoinhibition and repair in *Dunaliella salina* acclimated to different growth irradiances. *Planta* 198: 640–646.
- Beale SI and Appelman D (1971) Chlorophyll synthesis in *Chlorella*. Regulation by degree of light limitation of growth. *Plant Physiol* 47: 230–235
- Behrenfeld MJ, Prasil O, Kolber ZS, Babin M and Falkowski PG (1999) Compensatory changes in Photosystem II electron turnover rates protect photosynthesis from photoinhibition. *Photosynth Res* 58: 259–268
- Ben-Amotz A and Avron M (1983) On the factors which determine massive  $\beta$ -carotene accumulation in the halotolerant alga *Dunaliella bardawil*. *Plant Physiol* 72: 593–597
- Bennett J (1983) Regulation of photosynthesis by reversible phosphorylation of the light-harvesting chlorophyll *a/b* protein. *Biochem J* 212: 1–13
- Bennett J (1984) Chloroplast protein phosphorylation and the regulation of photosynthesis. *Physiol Plant* 60: 583–590
- Bennett J (1991) Protein phosphorylation in green plant chloroplasts. *Annu Rev Plant Physiol* 42: 281–311
- Bennett J, Schwender JR, Shaw EK, Tempel N, Ledbetter M and Williams RS (1987) Failure of corn leaves to acclimate to low irradiance. Role of protochlorophyllide reductase in regulating levels of five chlorophyll-binding proteins. *Biochim Biophys Acta* 892: 118–129
- Berner T, Dubinsky Z, Wyman K and Falkowski PG (1989) Photoadaptation and the 'package' effect in *Dunaliella tertiolecta* (Chlorophyceae). *J Phycol* 25: 70–78
- Bhattacharya D and Medlin L (1998) Algal phylogeny and the origin of land plants. *Plant Physiol* 116: 9–15
- Boardman NK (1977) Comparative photosynthesis of sun and shade plants. *Annu Rev Plant Physiol* 28: 355–377
- Bonaventura C and Myers J (1969) Fluorescence and oxygen evolution from *Chlorella pyrenoidosa*. *Biochim Biophys Acta* 189: 366–383
- Bruce D, Brimble S and Bryant DA (1989) State transitions in a phycobilisome-less mutant of the cyanobacterium *Synechococcus* sp. PCC 7002. *Biochim Biophys Acta* 974: 66–73
- Butler WL (1972) On the primary nature of fluorescence yield changes associated with photosynthesis. *Proc Nat Acad Sci USA* 69: 3420–3422
- Crofts A R and Wraight CA (1983) The electrochemical domain of photosynthesis. *Biochim Biophys Acta* 726: 149–185
- Delosme R, Olive J and Wollman FA (1996) Changes in light energy-distribution upon state transitions—an in vivo photoacoustic study of the wild-type and photosynthesis

- mutants from *Chlamydomonas-reinhardtii*. Biochim Biophys Acta 1273: 150–158
- Demmig B, Winter K, Krüger A and Czygan F-C (1988) Zeaxanthin and the heat dissipation of excess light energy in *Nerium oleander* exposed to a combination of high light and water stress. Plant Physiol 87: 17–24
- Dera J and Gordon HR (1968) Light field fluctuations in the photic zone. Limnol Oceanogr 13: 697–699
- Diner B and Mauzerall D (1973) The turnover times of photosynthesis and redox properties of the pool of electrons carriers between the photosystem. Biochim Biophys Acta 305: 353–363
- Dubinsky Z (1980) Light utilization efficiency in natural marine phytoplankton communities. In: Falkowski PG (ed) Primary Productivity in the Sea, pp 83–98. Plenum Press, New York.
- Dubinsky Z and Berman T (1976) Light utilization efficiencies of phytoplankton on Lake Kinneret (Sea of Galilee). Limnol Oceanogr 21: 226–230
- Dubinsky Z, Falkowski PG and Wyman K (1986) Light harvesting and utilization in phytoplankton. Plant Cell Physiol 27: 1335–1349
- Durnford DG and Falkowski PG (1997) Chloroplast redox regulation of nuclear gene transcription during photo-acclimation. Photosynth Res 53: 229–241
- Einstein A (1910) Theorie der Opaleszenz von homogenen Flüssigkeiten und Flüssigkeitsgemischen in der Nähe des kritischen Zustandes. Ann Physik 33: 1275
- Escoubas J-M, Lomas M, LaRoche J and Falkowski PG (1995) Light intensity regulation of *cab* gene transcription is signaled by the redox state of the plastoquinone pool. Proc Nat Acad Sci USA 92: 10237–10241
- Falkowski PG (1980) Light-shade adaptation in marine phytoplankton. In: Falkowski PG (ed) Primary Productivity in the Sea, pp 99–117. Plenum Press, New York
- Falkowski PG (1983) Light-shade adaptation and vertical mixing of marine phytoplankton: A comparative field study. J Mar Res 41: 215–237
- Falkowski PG (1984a) Kinetics of adaptation to irradiance in *Dunaliella tertiolecta*. Photosynthetica 18: 62–68
- Falkowski PG (1984b) Physiological responses of phytoplankton to natural light regimes. J Plankton Res 6: 295–307
- Falkowski PG (1992) Molecular ecology of phytoplankton photosynthesis. In: Falkowski PG and Woodhead A (eds) Primary Productivity and Biogeochemical Cycles in the Sea., pp. 47–67. Plenum Press, New York
- Falkowski PG and Kiefer DA (1985) Chlorophyll *a* fluorescence in phytoplankton: Relationship to photosynthesis and biomass. J Plankton Res 7: 715–731
- Falkowski PG and Kolber Z (1995) Variations in chlorophyll fluorescence yields in phytoplankton in the world oceans. Aust J Plant Physiol 22: 341–355
- Falkowski PG and LaRoche J (1991a) Acclimation to spectral irradiance in algae (minireview). J Phycol 27: 8–14
- Falkowski PG and LaRoche J (1991b) Adaptation to spectral irradiance in unicellular algae. J Phycol 27: 8–14
- Falkowski PG and Owens TG (1980) Light shade adaptation: Two strategies in marine phytoplankton. Plant Physiol 66: 632–635
- Falkowski PG and Raven JA (1997) Aquatic Photosynthesis. Oxford, Blackwell Scientific Publishers
- Falkowski PG and Woodhead AD (eds) (1992) Primary Productivity and Biogeochemical Cycles in the Sea. Plenum Press, New York
- Falkowski PG, Owens TG, Ley AC and Mauzerall DC (1981) Effects of growth irradiance levels on the ratio of reaction centers in two species of marine phytoplankton. Plant Physiol 68: 969–973
- Falkowski PG, Wyman K, Ley AC and Mauzerall D (1986) Relationship of steady state photosynthesis to fluorescence in eucaryotic algae. Biochim Biophys Acta 849: 183–192
- Falkowski PG, Kolber Z and Fujita Y (1988) Effect of redox state on the dynamics of Photosystem II during steady-state photosynthesis in eucaryotic algae. Biochim Biophys Acta 933: 432–443
- Falkowski PG, Jokiel PL and Kinzie RA (1990) Irradiance and Corals. In: Dubinsky Z (ed) Coral Reefs, pp 89–107. Elsevier, Amsterdam
- Flameling IA and Kromkamp J (1998) Light dependence of quantum yields for PS II charge separation and oxygen evolution in eucaryotic algae. Limnol Oceanogr. 43: 284–297
- Forster B, Osmond C and Boynton J (2001) Very high light resistant mutants of *Chlamydomonas reinhardtii*: Responses of Photosystem II, nonphotochemical quenching and xanthophyll pigments to light and CO<sub>2</sub>. Photosynth Res 67: 5–15
- Frank HA, Chua A, Chynwat V, Young A, Gosztola D and Wasielewski MR (1996) The lifetimes and energies of the first excited singlet states of diadinoxanthin and diatoxanthin: The role of these molecules in excess energy dissipation in algae. Biochim Biophys Acta 1277: 243–252
- Frommolt R, Reimund G and Wilhelm C (2001) The de-epoxidase and epoxidase reactions of *Mantoniella squamata* (Prasinophyceae) exhibit different substrate-specific reaction kinetics compared to spinach. Planta 213: 446–456
- Fujita Y, Murakami A and Ohki K (1990) Regulation of the stoichiometry of thylakoid components in the photosynthetic system of cyanophytes: Model experiments showing that control of the synthesis or supply of Chl *a* can change the stoichiometric relationship between the two photosystems. Plant Cell Physiol 31: 145–153
- Fujita Y, Murakami A and Aizawa K (1994) Short-term and long-term adaptation of the photosynthetic apparatus: Homeostatic properties of thylakoids. In: Bryant DA (ed) The Molecular Biology of Cyanobacteria, pp 677–692. Kluwer Academic Publisher, Dordrecht
- Gal A, Zer H and Ohad I (1997) Redox-controlled thylakoid protein-phosphorylation—news and views. Physiologia Plantarum 100: 869–885
- Garczarek L, Hess WR, Holtzendorff J, van der Staay GWM, and Partensky F (2000) Multiplication of antenna genes as a major adaptation to low light in a marine prokaryote. Proc Natl Acad Sci USA 97: 4048–4101
- Garczarek L, Partensky F, Irlbacher H, Holtzendorff J, Babin M, Mary I, Thomas JC and Hess WR (2001) Differential expression of antenna and core genes in *Prochlorococcus* PCC 9511 grown under a modulated light-dark cycle. Environ Microbiol 3: 168–175
- Geider RJ and Osborne BA (1992) Algal Photosynthesis: The Measurement of Algal Gas Exchange. Chapman and Hall, New York
- Genty B, Harbison J, Briantais J-M and Baker NR (1990) The relationship between nonphotochemical quenching of

- chlorophyll fluorescence and the rate of Photosystem II photochemistry in leaves. *Photosynth Res* 25: 1772–1782
- Gorbunov MY, Kolber ZS, Lesser MP, and Falkowski PG (2001) Photosynthesis and photoprotection in symbiotic corals. *Limnol Oceanogr* 46: 75–85
- Green BR and Durnford DG (1996) The chlorophyll-carotenoid proteins of oxygenic photosynthesis. *Annu Rev Plant Physiol Plant Mol Biol* 47: 685–714
- Greene RM and Gerard VA (1990) Effects of high-frequency light fluctuations on growth and photoacclimation of the red alga *Chondrus crispus*. *Mar Biol* 105: 337–344
- Greene RM, Geider RJ, Kolber Z and Falkowski PG (1992) Iron-induced changes in light harvesting and photochemical energy conversion processes in eukaryotic marine algae. *Plant Physiol* 100: 565–575
- Grossman A, Manodori A and Snyder D (1990) Light-harvesting proteins of diatoms: Their relationship to the chlorophyll *a/b* binding proteins of higher plants and their mode of transport into plastids. *Mol Gen Genet* 224: 91–100
- Hagar A and Stransky H (1970) The carotenoid pattern and occurrence of the light induced xanthophyll cycle in various classes of algae. V. A few members of the *Cryptophyceae*, *Euglenophyceae*, *Bacillariophyceae*, *Crysophyceae* and *Phaeophyceae*. *Arch Mikrobiol* 73: 77–89
- Herron HA and Mauzerall D (1971) The development of photosynthesis in a greening mutant of *Chlorella* and an analysis of the light saturation curve. *Plant Physiol* 50: 141–148.
- Hind G, Marshak DR and Coughlan SJ (1995) Spinach thylakoid polyphenol oxidase—cloning, characterization, and relation to a putative protein-kinase. *Biochemistry* 34: 8157–8164
- Horton P (1996) Nonphotochemical quenching of chlorophyll fluorescence. *Plant Physiol*: 99–111.
- Horton P and Ruban AV (1992) Regulation of Photosystem II. *Photosynth Res* 34: 375–385
- Horton P, Ruban AV and Young AJ (1999) Regulation of the structure, function of the light-harvesting complexes of Photosystem II by the xanthophyll cycle. In: Frank HA, Young AJ, Britton G and Cogdell RJ (eds) *The Photochemistry of Carotenoids*. Kluwer Academic Publishers, Dordrecht
- Hughes J and Lamparter T (1999) Prokaryotes and phytochrome: The connection to chromophores and signaling. *Plant Physiol* 121: 1059–1068
- Joliot P, Bennoun P and Joliot A (1973) New evidence supporting energy transfer photosynthetic units. *Biochim Biophys Acta* 305: 317–328
- Jorgensen EG (1969) The adaptation of plankton algae IV. Light adaptation in different algal species. *Physiol Plant* 22: 1307–1315
- Kamykowski D (1981) Laboratory experiments on the diurnal vertical migration of marine dinoflagellates through temperature gradient. *Mar Biol* 62: 57–64
- Kirk JTO (1994) *Light and Photosynthesis in Aquatic Ecosystems*. Cambridge University Press, Cambridge
- Knoll AH (1992) The early evolution of eukaryotes: A geological perspective. *Science* 256: 622–627
- Kolber Z, Wyman KD and Falkowski PG (1990) Natural variability in photosynthetic energy conversion efficiency: A field study in the Gulf of Maine. *Limnol Oceanogr* 35: 72–79
- Kolber ZS, Prasil O and Falkowski P (1998) Measurements of variable chlorophyll fluorescence using fast repetition rate techniques: Defining methodology and experimental protocols. *Biochim Biophys Acta* 1376: 88–106
- Krause GH, Kirk M, Heber U and Osmond CB (1989) O<sub>2</sub>-dependent inhibition of photosynthetic capacity in intact isolated chloroplasts and isolated cells from spinach leaves illuminated in the absence of CO<sub>2</sub>. *Planta* 142: 229–233
- Lardans A, Forster B, Prasil O, Falkowski PG, Sobolev V, Edelman M, Osmond CB, Gillham NW and Boynton JE (1998) Biophysical, biochemical, and physiological characterization of *Chlamydomonas reinhardtii* mutants with amino acid substitutions at the Ala 251 residue in the D1 protein that result in varying levels of photosynthetic competence. *J Biol Chem* 273: 11082–11091
- LaRoche J, Bennett J and Falkowski PG (1990a) Characterization of a cDNA encoding for the 28.5 kDa LHCII apoprotein from the unicellular marine chlorophyte, *Dunaliella tertiolecta*. *Gene* 95: 165–171
- LaRoche J, Mortain-Bertrand A and Falkowski PG (1990b) Light-intensity changes in mRNA and LHC II apoproteins from the unicellular marine chlorophyte *Dunaliella tertiolecta*. *Plant Phys* 97: 147–153
- LaRoche J, Henry D, Wyman K, Sukenik A and Falkowski P (1994) Cloning and nucleotide sequence of a cDNA encoding a major fucoxanthin-, chlorophyll *a/c*-containing protein from the chrysophyte *Isochrysis galbana*: Implications for evolution of the cab gene family. *Plant Mol Biol* 25: 355–368
- LaRoche J, van der Staay GW, Partensky F, Ducret A, Aebersold R, Li R, Golden SS, Hiller RG, Wrench PM, Larkum AWD and Green BR (1996) Independent evolution of the prochlorophyte and green plant chlorophyll *a/b* light-harvesting proteins. *Proc Natl Acad Sci USA* 93: 15244–15248
- Lavergne J and Trissl HW (1995) Theory of fluorescence induction in Photosystem-II: Derivation of analytical expressions in a model including exciton-radical-pair equilibrium and restricted energy-transfer between photosynthetic units. *Biophys J* 68: 2474–2492
- Lazzara L, Bricaud A and Claustre H (1996) Spectral absorption and fluorescence excitation properties of phytoplanktonic populations at a mesotrophic and an oligotrophic site in the tropical North-Atlantic (Eumeli Program). *Deep-Sea Res Part I-Oceanogr Res Papers* 43: 1215–1240
- Lee Y-K and Ding S-Y (1991) Accumulation of astaxanthin in *Haematococcus lacustris* (Chlorophyta). *J Phycol* 27: 575–577
- Lewis MR, Horne EPW, Cullen JJ, Oakey NS and Platt T (1984) Turbulent motions may control phytoplankton photosynthesis in the upper ocean. *Nature* 311: 49–50
- Ley AC and Mauzerall D (1982) Absolute absorption cross sections for Photosystem II and the minimum quantum requirement for photosynthesis in *Chlorella vulgaris*. *Biochim Biophys Acta* 680: 95–106
- Lohr M and Wilhelm C (2001) Algae displaying the diadinoxanthin cycle also possess the violaxanthin cycle. *Proc Nat Acad Sci USA* 96: 8784–8789.
- Malkin S and Kok B (1966) Fluorescence induction studies in isolated chloroplasts I. Number of components involved in the reaction and quantum yields. *Biochim Biophys Acta* 126: 413–432
- Malkin S, Telfer A and Barber J (1986) Quantitative analysis of State 1–State 2 transitions in intact leaves using modulated fluorometry—evidence for changes in the absorption cross-

- section of the two photosystems during the transitions. *Biochim Biophys Acta* 848: 48–57
- Mauzerall D (1972) Light-induced changes in *Chlorella*, and the primary photoreaction for the production of oxygen. *Proc Natl Acad Sci USA* 69: 1358–1362
- Maxwell DP, Falk S, Trick CG and Huner NPA (1995) Growth at low temperature mimics high-light acclimation in *Chlorella vulgaris*. *Plant Physiol* 105: 535–543
- Morel A (1974) Optical properties of pure water and pure seawater. In: Jerlov NG and Nielsen ES (eds) *Optical Aspects of Oceanography*, pp 1–24. Academic Press, London
- Morel A (1988) Optical modeling of the upper ocean in relation to its biogenous matter content (case one waters). *J Geophys Res* 93: 10, 749–10, 768
- Morel A and Prieur L (1977) Analysis of variations in ocean color. *Limnol Oceanogr* 22: 709–722
- Mortain-Bertrand A, Bennett J and Falkowski PG (1990) Photoregulation of the light-harvesting chlorophyll protein complex associated with Photosystem II in *Dunaliella tertiolecta*. *Plant Physiol* 94: 304–311
- Mullineaux CW, Tobin MJ and Jones GR (1997) Mobility of photosynthetic complexes in thylakoid membranes. *Nature* 390: 421–424
- Murata N (1970) Control of excitation transfer in photosynthesis. IV. Kinetics of chlorophyll *a* fluorescence in *Porphyra yezoensis*. *Biochim Biophys Acta* 205: 379–389
- Myers J (1946) Culture conditions and the development of the photosynthetic mechanism. IV. Influence of light intensity on photosynthetic characteristics of *Chlorella*. *J Gen Physiol* 30: 429–41
- Myers J and Burr G (1940) Studies on photosynthesis. Some effects of light of high intensity on *Chlorella*. *J Gen Physiol* 24: 45–67
- Myers J and Graham J-R (1971) The photosynthetic unit in *Chlorella* measured by repetitive short flashes. *Plant Physiol* 48: 282–286
- Nishio JN, Sun J and Vogelmann TC (1994) Photoinhibition and the light environment within leaves. In: Baker NR and Bowyer JR (eds) *Photoinhibition of Photosynthesis*, pp. 221–237. Bios Scientific Publishers, New York
- Niyogi KK, Björkman O and Grossman AR (1997) *Chlamydomonas* xanthophyll cycle mutants identified by video imaging of chlorophyll fluorescence quenching. *Plant Cell* 9:1369–1380
- Noctor G, Ruban AV and Horton P (1993) Modulation of delta pH-dependent nonphotochemical quenching of chlorophyll fluorescence in spinach chloroplasts. *Biochim Biophys Acta* 1183: 339–344
- Olaizola M and Yamamoto H (1994) Short-term response of the didinoxanthin cycle and fluorescence yield to high irradiance in *Chaetoceros muelleri* (Bacillariophyceae). *J Phycol* 30: 606–612
- Olaizola M, LaRoche J, Kolber Z and Falkowski PG (1994) Non-photochemical fluorescence quenching and the diadinoxanthin cycle in a marine diatom. *Photosynth Res* 41: 357–370
- Osmond CB (1994) What is photoinhibition? Some insights from comparisons of shade and sun plants. In: Baker NR and Bowyer JR (eds) *Photoinhibition of Photosynthesis: From Molecular Mechanisms to the Field*, pp 1–24. Bios Scientific, Oxford
- Owens TG (1986) Light-harvesting in the diatom *Phaeodactylum tricornutum* II. Distribution of excitation energy between the photosystems. *Plant Physiol* 80: 739–746
- Owens TG (1994) Excitation energy transfer between chlorophylls and carotenoids. A proposed molecular mechanism for non-photochemical quenching. In: Baker N and Bowyer J (eds) *Photoinhibition of Photosynthesis: From Molecular Mechanisms to the Field*, pp 95–109. Bios Scientific, Oxford
- Owens TG, Falkowski PG and Whitley TE (1980) Diel periodicity in cellular chlorophyll content in marine diatoms. *Mar Biol* 59: 71–77
- Paillotin G (1976) Movement of excitations in the photosynthetic domains of Photosystem II. *J Theor Biol* 58: 237–252
- Partensky F, Hoepffner N, Li WKW, Ulloa O and Vaultot D (1993) Photoacclimation of *Prochlorococcus* sp. (Prochlorophyta) strains isolated from the North Atlantic and the Mediterranean Sea. *Plant Physiol* 101: 285–296
- Partensky F, LaRoche J, Wyman K and Falkowski PG (1997) The divinyl-chlorophyll *a/b* protein complexes of two strains of the oxyphototrophic marine prokaryote *Prochlorococcus*-characterization and response to changes in growth irradiance. *Photosynth Res* 51: 209–222
- Pearcy RW (1990) Sunflecks and photosynthesis in plant canopies. *Annu Rev Plant Physiol Plant Mol Biol* 41: 421–453
- Perry MJ and Porter SM (1989) Determination of the cross-section absorption coefficient of individual phytoplankton cells by analytical flow cytometry. *Limnol Oceanogr* 34: 1727–1738
- Perry MJ, Talbot MC and Alberte RS (1981) Photoadaptation in marine phytoplankton: Response of the photosynthetic unit. *Mar Biol* 62: 91–101
- Pfannschmidt T, Nilsson A and Allen J (1999) Photosynthetic control of chloroplast gene expression. *Nature* 397: 625–628
- Pfannschmidt T, Allen J and Oelmüller R (2001) Principles of redox control in photosynthetic gene expression. *Physiologia Plantarum* 112: 1–9
- Post AF, Dubinsky Z and Falkowski PG (1984) Kinetics of light-intensity adaptation in a marine planktonic diatom. *Marine Biology* 83: 231–238
- Post AF, Dubinsky Z, Wyman K and Falkowski PG (1985) Physiological responses of a marine planktonic diatom to transitions in growth irradiance. *Mar Ecol Prog Ser* 25: 161–169
- Race HL and Hind G (1996) A protein kinase in the core of Photosystem II. *Biochemistry* 35: 13006–13010
- Raps S, Wyman K, Siegelman HW and Falkowski PG (1983) Adaptation of the cyanobacterium *Microcystis aeruginosa* to light intensity. *Plant Physiol* 72: 829–832
- Rees D, Noctor G, Ruban A, Crofts J, Young A and Horton P (1992) pH-dependent chlorophyll fluorescence quenching in spinach thylakoids from light treated or dark adapted leaves. *Photosynth Res* 31: 11–19
- Rich PR (1985) Mechanisms of quinol oxidation in photosynthesis. *Photosynth Res* 6: 335–348
- Slovacek RE and Hannan PJ (1977) In vivo fluorescence determination of phytoplankton chlorophyll *a*. *Limnol Oceanogr* 22: 919–925
- Smoluchowski M (1908) Molekular-kinetische Theorie der Opaleszenz von Gasen im kritischen Zustande, sowie einiger verwandter Erscheinungen. *Ann Physik* 25: 205

- Snyders S and Kohorn B (1999) TAK's, Thylakoid Membrane Kinases associated with energy transduction. *J Biol Chem* 274: 9137–9140
- Snyders S and Kohorn B (2001) Disruption of thylakoid kinase TAK1 leads to alteration of light energy transduction in *Arabidopsis*. *J Biol Chem* 276: 32169–32176
- Steemann-Nielsen E (1952) The use of radio-active carbon ( $C^{14}$ ) for measuring organic production in the sea. *J Cons Int Explor Mer* 18: 117–140
- Steemann-Nielsen E and Hansen VK (1959) Light adaptation in marine phytoplankton populations and its interrelation with temperature. *Physiol Plant* 12: 353–370
- Stitt M (1986) Limitation of photosynthesis by carbon metabolism. Evidence for excess electron transport capacity in leaves carrying out photosynthesis in saturating light and  $CO_2$ . *Plant Physiol* 81: 1115–1122
- Sukenik A, Wyman KD, Bennett J and Falkowski PG (1987a) Light-saturated photosynthesis-limitation by electron transport or carbon fixation? *Biochim Biophys Acta* 891: 205–215
- Sukenik A, Wyman KD, Bennett J and Falkowski PG (1987b) A novel mechanism for regulating the excitation of Photosystem II in a green alga. *Nature* 327: 704–707
- Sukenik A, Bennett J and Falkowski PG (1988) Changes in the abundance of individual apoproteins of light-harvesting chlorophyll *a/b*-protein complexes of Photosystem I and II with growth irradiance in the marine chlorophyte *Dunaliella tertiolecta*. *Biochim Biophys Acta* 932: 206–215
- Sukenik A, Bennett J, Mortain-Bertrand A and Falkowski PG (1990) Adaptation of the photosynthetic apparatus to irradiance in *Dunaliella tertiolecta*. *Plant Physiol* 92: 891–898
- Talling JF (1957) Photosynthetic characteristics of some freshwater plankton dynamics in relation to underwater radiation. *New Phytol* 56: 29–50
- Terzaghi WB and Cashmore AR (1995) Light-regulated transcription. *Annu Rev Plant Physiol Plant Mol Biol* 46: 445–474
- Thornber JP (1969) Comparison of a chlorophyll *a* protein complex isolated from a blue green alga with chlorophyll-protein complexes obtained from green bacteria and higher plants. *Biochim Biophys Acta* 172: 230–241
- Ting CS and Owens TG (1993) Photochemical and nonphotochemical fluorescence quenching processes in the diatom *Phaeodactylum tricornutum*. *Plant Physiol* 101: 1323–1330
- Verner A, van Kan PJM, Rich PR, Ohad I and Anderson B (1997) Plastoquinol at the quinol oxidation site of cytochrome *b<sub>f</sub>* mediates signal transduction between light and protein phosphorylation: Thylakoid kinase deactivation by a single-turnover flash. *Proc Nat Acad Sci USA* 94: 1585–1590
- Villareal TA and Lipshultz F (1995) Internal nitrate concentrations in single cells of large phytoplankton from the Sargasso Sea. *J Phycol* 31: 689–696
- Wilson KE and Huner NP (2000) The role of growth rate, redox-state of the plastoquinone pool and the trans-thylakoid [ $\Delta\psi$ ]pH in photoacclimation of *Chlorella vulgaris* to growth irradiance and temperature. *Planta* 212: 93–102
- Wollman FA and Delepelaire P (1984) Correlation between changes in light energy distribution and changes in thylakoid membrane polypeptide phosphorylation on *Chlamydomonas reinhardtii*. *Cell Biol* 98: 1–7
- Yamamoto HY, Nakayama TOM and Chichester CO (1963) Studies on the light and dark interconversions of leaf xanthophylls. *Arch Biochem Biophys* 97: 168–173
- Yentsch CS and Ryther JH (1967) Short-term variation in phytoplankton chlorophyll and their significance. *Limnol Oceanogr* 2: 140–142
- Zhang X, Lewis MR and Johnson B (1998) The role of bubbles in the scattering of light in the ocean. *Applied Optics* 37: 6525–6536

# Chapter 16

## Multi-level Regulation of Purple Bacterial Light-harvesting Complexes

Conan S. Young

*Department of Biomineralization and Department of Cytokine Biology,  
The Forsyth Institute, Boston, MA, U.S.A.*

J. Thomas Beatty\*

*Department of Microbiology and Immunology, University of British Columbia,  
Vancouver, British Columbia, Canada*

Summary .....	450
I. Introduction .....	450
A. Overview of Functions .....	450
B. Overview of Structures .....	450
C. Overview of Light Harvesting Complex Regulation .....	451
II. Gene Organization and Expression .....	452
A. <i>puf</i> (LHI) Operons .....	452
1. Genes and Transcripts .....	452
2. Regulation of Transcription Initiation .....	453
3. Regulation of mRNA Processing .....	455
4. Posttranslational Processes .....	456
B. <i>puc</i> (LHII) Operons .....	456
1. Genes and Transcripts .....	456
2. Regulation of Transcription Initiation .....	456
3. mRNA Processing .....	458
4. Posttranslational Processes .....	458
C. 'Extra' or Unusual LH Structural Genes or Complexes .....	458
III. Assembly of LH Complexes .....	459
A. Reconstitution of LHI Subunits and Complexes In Vitro .....	459
B. Effects of Mutations on In Vivo Assembly of LHI .....	460
C. Effects of Mutations on Assembly of LHII In Vivo .....	461
D. LH Complex Assembly Factors .....	461
1. The LhaA and PucC Proteins .....	461
2. DnaK and GroEL .....	462
IV. Other genes and proteins relevant to LH complex assembly or structure .....	462
A. The PufX Protein .....	462
B. The PufQ Protein .....	463
C. The <i>orf214</i> and <i>orf162b</i> Genes .....	463
D. <i>pucD</i> and <i>pucE</i> Genes .....	464
E. <i>orf428</i> .....	464
F. The $\Omega$ Protein .....	464
V. Concluding Remarks and Future Prospects .....	464
Acknowledgments .....	465
References .....	465

---

\*Author for correspondence, email: jbeatty@interchange.ubc.ca



## Summary

The regulation of purple bacterial photosynthetic light-harvesting complex gene expression is reviewed in the context of the available structure data. Although purple bacterial light-harvesting complexes are relatively simple pigment-protein structures, the amounts (and, in some species, the types) of these structures depend on environmental factors such as oxygen concentration and light intensity. Multiple regulatory mechanisms, which are incompletely understood, modulate the formation of these complexes. This Chapter covers topics ranging from the regulation of gene transcription initiation, through mRNA processing, post-translational enzyme activities and protein modification, to assembly of complexes.

## I. Introduction

### A. Overview of Functions

Purple photosynthetic bacteria contain integral membrane, pigment-protein light-harvesting (LH) complexes that are commonly referred to as LHI or LHII. The LHII complex functions in photosynthesis to absorb and transfer light energy to the LHI complex, which transfers energy to the photochemical reaction center (RC) where a cyclic series of electron and proton transfer reactions initiates. This series of energy transfers and oxidation-reduction reactions, which involve the cytochrome *bc*<sub>1</sub> complex, culminates in the formation of a proton gradient across the cytoplasmic membrane (for reviews see Prince, 1990; Sundstrom and van Grondelle, 1995; Okamura et al., 2000).

### B. Overview of Structures

Although a detailed description of the structures of LH complexes is given in Chapter 5 (Robert et al.), we summarize some key points. A conserved feature of purple bacterial LH complexes is the association of one each of two small proteins (designated  $\alpha$  and  $\beta$ ), two or three bacteriochlorophyll (BChl) molecules, and one or two carotenoid molecules to form a fundamental  $\alpha/\beta$  subunit. It is thought that from eight (LHII) to sixteen (LHI) subunits form the LH complexes. The BChl pigments, and complexes, may be described according to the positions of their main absorption bands in the near-infrared region of the spectrum. For example, the LHI complex is sometimes known as the B870 (or B875, B890, etc.)

complex since the BChl molecules absorb light at 870 nm or other similarly long wavelength when fully oligomerized as part of a complex. Likewise, in some species the LHII complex is designated as the B800-850 complex since the environment around some BChl molecules in this complex causes them to absorb light of 800 nm, whereas other LHII BChl molecules, which interact more closely, absorb at 850 nm. LHI, the RC-associated complex, contains two BChl molecules per subunit, whereas the relatively RC-peripheral LHII contains three BChl molecules per subunit. Various carotenoids exist and some purple bacterial species contain BChl *b* as opposed to BChl *a*, but we do not distinguish between these pigments.

X-ray crystallography of purified LHII complexes from *Rhodopseudomonas acidophila* and *Rhodospirillum rubrum* revealed that the complexes in these crystals have the shape of a torus ('doughnut'). These complexes are composed of concentric rings of eight or nine identical subunits of  $\alpha$  and  $\beta$  proteins (each of which contain an alpha helix that spans the membrane), with three BChl molecules and a carotenoid bound to each subunit (McDermott et al., 1995; Koepke et al., 1996; Chap. 5, Robert et al. and Color Plates 2 and 3). The  $\alpha$  polypeptides form the inner wall of the torus, the  $\beta$  polypeptides form the outer surface, and the BChl and carotenoid pigments are mainly sandwiched between these two proteins. Two-dimensional crystals of the *Rhodobacter capsulatus* LHII complex evaluated by electron microscopy suggested a nonameric arrangement of subunits, similar to the *Rps. acidophila* structure (Oling et al., 1996).

Electron microscopy of two-dimensional crystals of LHI and LHI/RC co-complexes from *Rhodospirillum rubrum* were interpreted as an LHI ring of 16  $\alpha/\beta$  subunits surrounding the RC (Walz and Ghosh, 1997). The LHI complex recently was proposed to be a square structure rather than a circle,

*Abbreviations:* BChl – bacteriochlorophyll; bp – base pairs; LH – light-harvesting; nt – nucleotide; orf – open reading frame; Rb. – *Rhodobacter*; RC – reaction center; Ro. – *Roseobacter*; Rps. – *Rhodopseudomonas*; Rsp. – *Rhodospirillum*; Ru. – *Rubrivax*; Rv. – *Rhodovulum*

and it was speculated that an additional factor might influence the interaction of the RC and LHI complexes to form a square shape (see Section IV.F for a discussion of the *Rsp. rubrum*  $\Omega$  protein) (Stahlberg et al., 1998a; Stahlberg et al., 1998b). A projection map of two-dimensional crystals of the *Rhodopseudomonas viridis* LHI/RC core complex indicated an electron-dense center (thought to be the RC) surrounded by areas of electron density that were interpreted as concentric rings of LHI  $\alpha$  and  $\beta$  polypeptides (Ikeda-Yamasaki et al., 1998). Electron microscopy of two dimensional crystals of LHII, LHI, and LHI/RC co-complexes from *Rhodobacter sphaeroides* revealed structures resembling those observed in *Rps. acidophila*, *Rsp. rubrum*, *Rb. capsulatus* and *Rps. viridis* (Walz et al., 1998).

Electron micrographs of membranes from a mutant strain of *Rb. sphaeroides* lacking the LHII suggested an alternative model, in which two LHI complexes were organized in C-shaped structures, each partially enclosing a RC complex and linked by a single cytochrome  $bc_1$  complex (Jungas et al., 1999). In this

interpretation, the two LHI/RC core complexes have a pseudo two-fold symmetry centered on a single cytochrome  $bc_1$  complex, and it was estimated that each C-shaped LHI structure was composed of 12  $\alpha\beta$  subunits. The organization of LHI as a C-shaped as opposed to a ring structure might not affect light absorption and energy transfer, so long as at least four to six interactive BChls (two to three  $\alpha\beta$  subunits) are present in LHI (Monshouwer et al., 1997).

It is conceivable that there is a degree of heterogeneity in vivo such that LHI complexes contain variable numbers of subunits, and that this variability results in both ring- and C-shaped LHI structures (Pugh et al., 1998).

### C. Overview of Light Harvesting Complex Regulation

A scheme representing some of the factors and the processes involved in LH complex formation is given in Fig. 1, with details available in subsequent pages. In general, cells of purple bacteria exposed to high

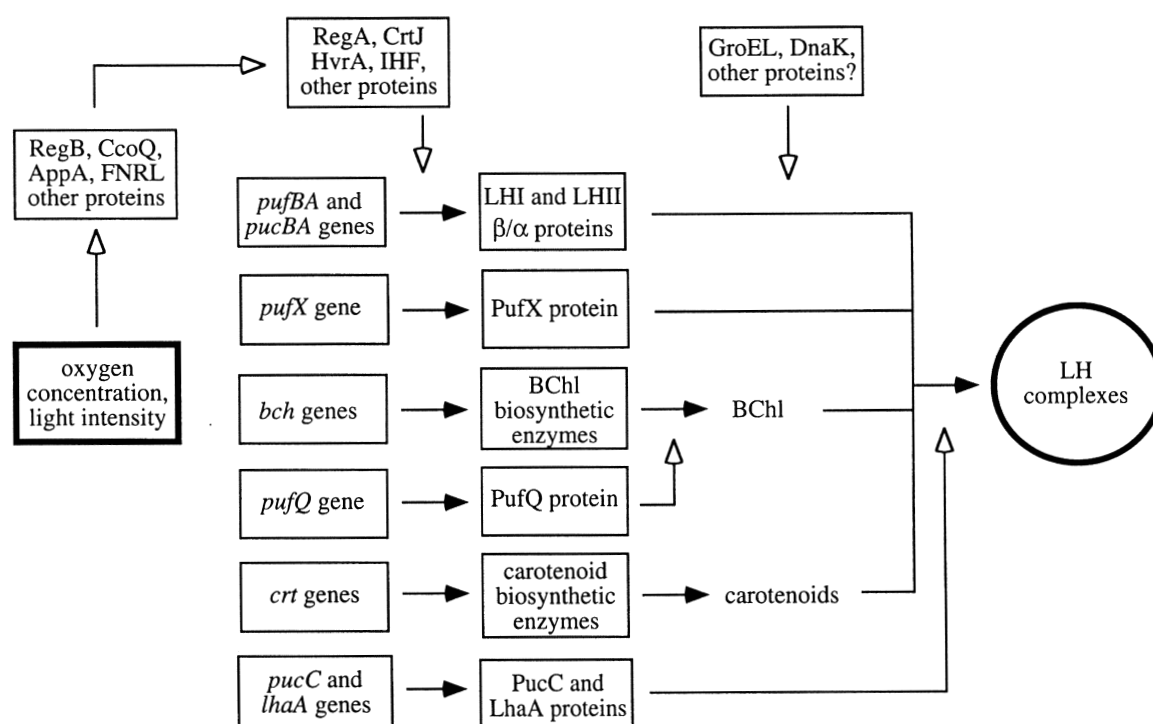


Fig. 1. Abbreviated flow diagram indicating the variety of elements implicated in the regulation of LH complexes in purple bacteria. White arrowheads indicate potential regulatory controls, whereas black arrowheads indicate progressive stages in transcription, translation and assembly. This scheme is a minimal synthesis of the results of experiments on *Rb. capsulatus* and *Rb. sphaeroides*, and lacks some proposed processes and factors. Please see the text for details.

concentrations of oxygen contain few or no LH complexes, and high light intensities reduce LH complex amounts in anaerobic cultures. This regulation occurs during transcription initiation, and post-transcriptionally due to differential rates of mRNA decay and modulation of the activity of pigment synthesis enzymes. The assembly of the LH polypeptides and pigment molecules into pigment-protein complexes adds another potential component of regulation.

Transcription of *bch* (BChl biosynthesis) genes is weakly repressed under aerobic conditions of growth (Bauer and Bird, 1996), and so it seems that significant amounts of BChl biosynthesis enzymes are present in cells that produce little or no BChl. Thus, oxygen regulation of BChl synthesis (and LH complex formation) is to a large extent due to posttranslational modulation of Bchl enzyme activities. Excess (LH- or RC-free) BChl is not detectable in cells, BChl synthesis is reduced in mutants that lack one or more LH complex proteins, and no BChl is produced by mutants that lack all of the pigment-binding proteins of the RC and LH complexes. However, mutants blocked at any of the steps in the BChl biosynthetic pathway accumulate massive amounts of a precursor (the substrate of the enzyme inactivated by mutation), and BChl is overproduced in the presence of inhibitors of heme biosynthesis (Houghton et al., 1982). It seems that free BChl, a precursor or a BChl degradation product) and the production of heme (or a cytochrome) feed-back inhibit the activity of the enzyme that catalyzes the first step (or all enzymes) of the BChl biosynthetic pathway. There is analogous regulation of carotenoid biosynthesis but, although transcription of carotenoid biosynthetic genes varies in response to oxygen concentration, little is known about the regulation of enzyme activity. Recent reviews and other papers describe much of what is summarized in Fig. 1 (Klug, 1993; Bauer, 1995; Biel, 1995; Drews and Golecki, 1995; Wong et al., 1996; Young et al., 1998; Zeilstra-Ryalls et al., 1998; Oh and Kaplan, 2001), yet there is a great need for careful experiments to evaluate the details of these transcriptional and post-transcriptional processes in LH complex regulation.

To summarize this introduction, incompletely understood mechanisms coordinate the synthesis of pigments and pigment-binding proteins of LH complexes in response to environmental conditions. Oxygen inhibits transcription of LH structural protein genes and to a lesser extent pigment biosynthesis

genes, and the activity of pigment biosynthetic enzymes seems to be inhibited by oxygen. High light intensities reduce transcription of LH structural genes and increase BChl degradation. In the following pages we expand on these previously reviewed regulatory processes and include new information on LH complex assembly.

## II. Gene Organization and Expression

Several species of purple photosynthetic bacteria contain a large (ca. 46 kb in *Rb. capsulatus*) chromosomal gene cluster that encodes enzymes for pigment biosynthesis, the protein components of LHI and RC complexes, and an LHI complex assembly factor. The *bch* genes encode BChl biosynthetic enzymes, *crt* genes encode carotenoid biosynthetic enzymes, *puf* genes encode LHI and two (L and M) RC proteins, and the *puhA* gene encodes the third (H) RC protein. In *Rb. capsulatus*, *Rb. sphaeroides*, *Rps. palustris* and *Rubrivivax gelatinosus* the LHII complex genes are not located within this gene cluster (Igarishi et al., 1998; Haselkorn et al. 2001; Mackenzie et al., 2001; <http://genome.ornl.gov/microbial/rpal/>).

Since the greatest number of genetic experiments have been done on *Rb. capsulatus* and *Rb. sphaeroides*, the following text is focussed on these two species.

### A. *puf* (LHI) Operons

#### 1. Genes and Transcripts

The *puf* operons of *Rb. capsulatus* and *Rb. sphaeroides* consist of the genes *pufQBALMX*, but several other species appear to lack *pufQ* and *pufX* genes, at least as part of a *puf* operon (Fig. 2). The *pufB* and *pufA* genes encode, respectively, the LHI  $\beta$  and  $\alpha$  proteins. The *pufQ* gene encodes a protein required for BChl biosynthesis (Section IV.B), and *pufLM* encode the L and M proteins of the RC. In *Rhodobacter* species, *pufX* encodes a protein required to facilitate quinone/quinol exchange between the  $Q_B$  site of the RC and the cytochrome  $bc_1$  complex and, perhaps, for dimerization of LHI/RC core complexes (Youvan et al., 1984; Bauer and Marrs, 1988; Barz and Oesterheldt, 1994; Lilburn et al., 1995; Francia et al., 1999). *Rhodovulum sulfidophilum* contains a *pufQBALMC* gene sequence in which the *pufC* gene encodes a

multi-heme cytochrome similar to (yet interestingly different from) other purple photosynthetic bacteria that contain a *pufC* gene located 3' of *pufM* (Masuda et al., 1999). *Rps. viridis*, *Rsp. molischianum*, *Roseospirillum parvum*, *Amoebobacter purpureus* and the obligately aerobic bacterium *Roseobacter denitrificans* possess a *pufBALMC* operon (Beatty, 1995; Tuschak, Overmann and Beatty, unpublished). The purple sulfur bacterium *Chromatium vinosum* contains a *pufBALMC* operon that is followed by an additional copy of the *pufBA* genes (Corson et al., 1999).

Transcription of the *Rb. capsulatus puf* operon is initiated from three promoters that give rise to overlapping mRNA transcripts (Fig. 2). These promoters consist of the strongly oxygen-regulated *puf* promoter within the *bchZ* gene (located immediately 5' of the *pufQ* gene) and, in order of increasing 5' distance from the *puf* genes, the *bchCXYZ* and *crtEF* pigment biosynthesis gene

promoters (Wellington and Beatty, 1991; Wellington et al., 1991; Bauer, 1995). This transcriptional arrangement couples the transcription of LHI and RC genes to pigment biosynthetic genes, which facilitates rapid transitions from aerobic respiratory to anaerobic photosynthetic growth modes (Wellington et al., 1992).

## 2. Regulation of Transcription Initiation

Although it seems that as much as 60 to 80% of *Rb. capsulatus puf* gene transcription initiates at the *bchCXYZ* and *crtEF* promoters (Fig. 2), we focus on the *puf* promoter region because little research has been done on the regulatory effects of 5' transcription read-through into the *puf* operon (Wellington et al., 1991; Bauer, 1995). Early experiments indicated that the expression of LHI complex (and RC) genes is coordinated with the expression of pigment biosynthetic enzyme genes in response to changes in

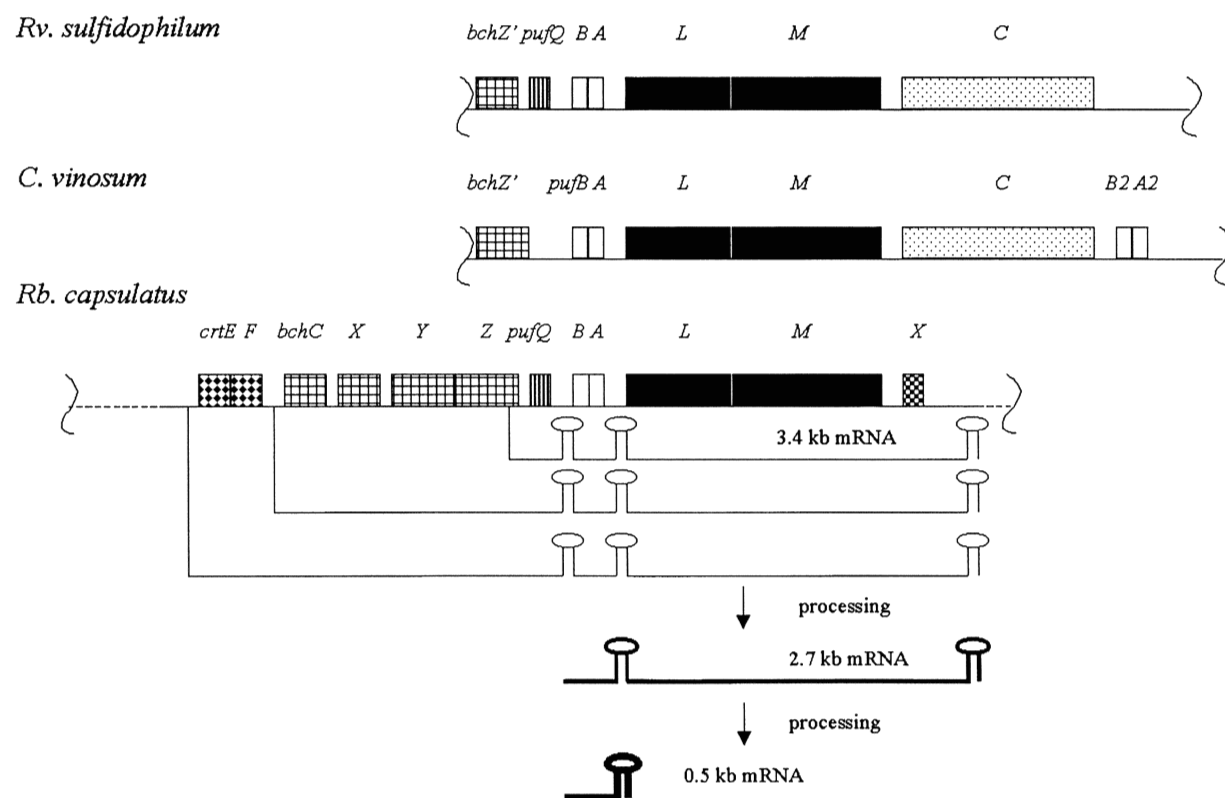


Fig. 2. Comparison of *puf* operon gene organization in three species, and *Rb. capsulatus puf* messages. Carotenoid biosynthesis (*crt*) genes are represented by diamond-filled boxes, BChl biosynthesis (*bch*) genes by grid-filled boxes, RC genes by black boxes, and LHI genes by empty boxes. B2 and A2 designate LHII gene homologs. The positions of RNA stem-loop structures are indicated. Primary transcripts are represented by lines with vertical connections to sites of initiation. The approximate amounts of processing products are represented by lines with thickness indicative of the relative steady-state amounts of each segment.

oxygen tension and light intensity (Clark et al., 1984; Zhu et al., 1986; Zhu and Hearst, 1986). It was reported that inverted repeat DNA sequences located immediately 5' of the *Rb. capsulatus puf* promoter form two distinct protein-DNA complexes under conditions of high oxygen tension, and that a single base pair mutation in this region reduced oxygen- and light-dependent repression of *puf* operon transcription (Narro et al., 1990; Klug, 1991a; Klug and Jock, 1991). An analogous region of dyad symmetry exists upstream of the *puf* promoter in *Rb. sphaeroides*, which was shown to bind a protein under growth conditions of high oxygen tension or high light intensity (Shimada et al., 1993).

Some of the *trans*-active genes that control transcription initiation at the *puf* promoter have been

identified and the signal transduction mechanisms that, in turn, regulate this activity are becoming more clear. Table 1 lists genes that encode *trans*-active proteins or 'downstream' signal transduction components.

A cluster of *Rb. capsulatus* regulatory genes that includes *regA*, *regB*, *hvrA* and *senC* was identified by Bauer and coworkers (Bauer, 1995). The *Rb. capsulatus regA* gene product was the first *trans*-active factor identified in the induction of photosynthesis gene expression at reduced oxygen tensions, as evaluated by the expression of *lacZ* fusions to photosynthesis genes in *regA*<sup>+</sup> and *regA*<sup>-</sup> strains. The RegA derived amino acid sequence is similar to response regulator proteins but not to subclasses of these proteins that bind DNA (Sganga and Bauer,

Table 1. Known or proposed genes that regulate the amounts of LH complexes in response to oxygen concentration or light intensity in purple bacterial species<sup>1</sup>

Gene Designation	Known or Proposed Activity of Gene Product	Species Known to Contain Gene	Representative References
<i>regB</i> <i>prpB</i>	sensor kinase (phosphorylates RegA)	<i>Rb. capsulatus</i> <i>Rv. sulfidophilum</i> <i>Ro. denitrificans</i> <i>Rb. sphaeroides</i>	(Bauer and Bird, 1996) (Masuda et al., 1999) (Masuda et al., 1999) (Eraso and Kaplan, 1996)
<i>regA</i> <i>prpA</i>	response regulator (transcription regulator)	<i>Rb. capsulatus</i> <i>Rv. sulfidophilum</i> <i>Ro. denitrificans</i> <i>Rb. sphaeroides</i>	(Bauer and Bird, 1996) (Masuda et al., 1999) (Masuda et al., 1999) (Eraso and Kaplan, 1994)
<i>crtJ</i> <i>ppsR</i>	transcription regulator	<i>Rb. capsulatus</i> <i>Rb. sphaeroides</i>	(Nickens and Bauer, 1998) (Gomelsky and Kaplan, 1995)
<i>hvrA</i> <i>spbC</i>	light-sensitive transcription regulator	<i>Rb. capsulatus</i> <i>Rb. sphaeroides</i>	(Buggy et al., 1994) (Zeilstra-Ryalls et al., 1998)
<i>fnrL</i>	oxygen/redox-sensitive transcription regulator	<i>Rb. sphaeroides</i>	(Zeilstra-Ryalls and Kaplan, 1998)
<i>ccoQ</i>	transmitters of <i>cytbb<sub>3</sub></i> redox state	<i>Rb. sphaeroides</i>	(Oh and Kaplan, 2001)
<i>himA</i> and <i>hip</i> ( <i>himD</i> )	subunits of IHF (DNA- bending protein)	<i>Rb. sphaeroides</i> <i>Rb. capsulatus</i>	(Zeilstra-Ryalls et al., 1998) (Nickens and Bauer, 1998)
<i>appA</i>	Unknown	<i>Rb. sphaeroides</i>	(Gomelsky and Kaplan, 1998)
<i>mgsS</i>	Unknown	<i>Rb. sphaeroides</i>	(Zeilstra-Ryalls et al., 1998)
<i>orf798</i>	Unknown	<i>Rb. capsulatus</i>	(Pollich and Klug, 1995)

<sup>1</sup> Includes only sequences thought to encode proteins that act near or at the termini of *puf*, *puc* and/or *bch* gene regulatory cascades in the species listed. Some equivalent genes have different names in *Rb. sphaeroides*; for example, *Rb. capsulatus regB* = *prpB* of *Rb. sphaeroides*, etc.

1992). However, DNase I footprinting experiments using a mutant version of the RegA protein (RegA\*) demonstrated binding of RegA\* to *puf* promoter DNA, and it was proposed that RegA directly activates *puf* gene expression by binding to DNA (Du et al., 1998).

The *Rb. capsulatus regB* gene encodes a membrane-bound sensor kinase protein capable of autophosphorylation and transfer of a phosphate group to the RegA protein (Mosley et al., 1994; Inoue et al., 1995). The RegA and RegB proteins appear to be part of a two-component oxygen-sensing regulatory system, which includes the phosphorylation of RegA by RegB followed by RegA activation of gene transcription in response to reduced levels of molecular oxygen (Mosley et al., 1994; Bauer, 1995).

Oxygen-dependent regulation of transcription initiating at the *Rb. capsulatus puf* promoter was proposed to rely on the presence of a late intermediate of BChl synthesis or the BChl molecule itself (Rodig et al., 1999). An additional factor in the activation of *puf* expression in response to oxygen levels is SenC, although the mechanism by which this protein regulates expression is unknown (Buggy and Bauer, 1995).

Homologues of the *Rb. capsulatus regA* and *regB* genes exist in *Rb. sphaeroides* (in which they are known as *prrA* and *prrB*, respectively), as does a *senC* homologue named *prrC*, and disruptions in these genes affect transcription in the same manner in *Rb. capsulatus* (Zeilstra-Ryalls et al., 1998). The *ccoNOQP* genes encode the *cbb<sub>3</sub>* cytochrome *c* oxidase of *Rb. sphaeroides* and the *rdxB* gene encodes a putative membrane-bound protein that is likely to be involved in redox processes. Evidence obtained by mutations of the *cco* and *rdxB* genes led to a model in which the *cbb<sub>3</sub>* oxidase 'senses' high oxygen levels and, in concert with the RdxB protein, generates an inhibitory signal through CcoQ to PrrB which represses *puf* operon expression (Zeilstra-Ryalls et al., 1998; Oh and Kaplan, 1999). Two other loci involved in the regulation of *puf* operon expression in *Rb. sphaeroides* are *appA* and *mgsS*: the *appA* gene seems to encode a redox-sensing protein, and the *mgsS* gene product was proposed to activate *puf* gene expression under anaerobic conditions (Gomelsky and Kaplan, 1998; Zeilstra-Ryalls et al., 1998).

In dim light anaerobic conditions, transcription of the *puf* operon is enhanced in *Rb. capsulatus* and contributes to an increase in the number of RC and

LH complexes (Bauer, 1995). The HvrA protein was shown to bind to the *puf* operon promoter by DNA footprinting analysis and to *trans*-activate *puf* operon transcription under a reduced light intensity (Buggy et al., 1994). The *Rb. sphaeroides* 'SPB' *trans*-active repressor protein that binds to the *puf* promoter region under aerobic or high-light growth conditions has 53% sequence identity to the HvrA protein of *Rb. capsulatus* (Nishimura et al., 1998; Zeilstra-Ryalls et al., 1998). In *Rb. sphaeroides*, blue light of 450 nm has a particularly strong inhibitory effect on the expression of the *puf* operon (Shimada et al., 1992), which might be mediated by the 'SPB' (the *Rb. capsulatus* HvrA) protein (Bauer, 1995).

### 3. Regulation of mRNA Processing

Transcription initiated at the *Rb. capsulatus puf* promoter results in a 3.4 kb mRNA molecule encoding the *pufQBALMX* genes, but this transcript is rapidly degraded to a 2.7 kb *pufBALMX* molecule that in turn is processed to a 0.5 kb message segment encoding only the *pufBA* genes (Fig. 2). There is an increase in stability after each processing step (Adams et al., 1989). The differential stability of *puf* transcript segments is largely responsible for the ~15:1 ratio of LHI:RC polypeptides in cells, and thus constitutes a second level of regulation of *puf* gene expression (Belasco et al., 1985). An RNA stem-loop structure in the intercistronic region between *pufBA* and *pufLMX* message segments inhibits 3'-exoribonucleolytic decay of *pufBA* mRNA and helps stabilize the *pufBA* segment following degradation of the *pufLMX* segment (Klug et al., 1987; Chen et al., 1988). It is possible that a small amount (<25%) of transcription attenuates at this stem-loop (Chen et al., 1988). Recent evidence suggests that RNA stem-loop structures located between *pufQ* and *pufB* message regions stabilize the *pufBA* and *pufBALMX* molecules and enhance degradation of the *pufQ* segment of the *pufQBALMX* transcript (Heck et al., 1996). This surprising finding raises questions about mechanisms of mRNA degradation. The *pufLMX* RNA sequences contain at least three sites where endoribonucleolytic cleavage may be the rate-limiting step in *pufBALMX* message degradation, although it is clear that the degradation of *puf* mRNA depends on a combination of endoribonucleases, exoribonucleases, and several mRNA hairpin structures (Klug and Cohen, 1990; Heck et al., 1996). Degradation of the *pufBALMX* mRNA is accelerated in cells grown

under high oxygen tension, adding an additional level of complexity to the oxygen-dependent regulation of the *puf* operon (Klug, 1991b). Studies of *puf* mRNA decay in *E. coli* suggested that an RNase E-like activity in *Rb. capsulatus* is responsible for the endonucleolytic cleavages both within the *pufLM* region and between *pufQ* and *pufB* (Klug et al., 1992; Heck et al., 1996).

#### 4. Posttranslational Processes

Although the insertion of LH proteins and pigment molecules into the intracytoplasmic membrane and assembly of complexes must result at least in part from the innate properties of the several LH components, various cytoplasmic and membrane-bound proteins seem to be involved in these processes (Drews, 1996). A model for LHI subunit assembly in *Rb. capsulatus* has the translation of the  $\alpha$  and  $\beta$  polypeptides assisted by the chaperonin DnaK, followed by interaction of the  $\alpha$  and  $\beta$  proteins with GroEL, such that stable insertion of the  $\alpha$  and  $\beta$  proteins into the membrane is assisted by GroEL and membrane-bound translocation factors (Drews, 1996) (perhaps LhaA and, in the case of LHII, PucC; Section IV). Thus the activities of chaperonins or membrane-bound translocation/assembly factors could affect the levels of the LHI holocomplex in vivo as part of a posttranslational regulation process.

Phosphorylation of the *Rb. capsulatus*  $\alpha$  polypeptide at the Ser2 may influence oligomerization of the subunits to form the LHI holocomplex (Brand et al., 1995). Pulse-labeling of LHI $\alpha$  and LHII $\alpha$  with [<sup>32</sup>P] indicated that phosphorylation of these polypeptides was greater under aerobic growth conditions than under anaerobic conditions. Although protein phosphorylation could be involved in posttranslational regulation of LH complex formation, its role in this process is unclear (Kerber et al., 1998). Phosphorylation of the chloroplast LHCII complex was proposed to cause a change in its three-dimensional structure, which appears to increase the affinity of this complex for Photosystem I over PS II and thus to regulate the distribution of energy between the two complexes (Allen and Nilsson, 1997). Perhaps phosphorylation of the purple bacterial LH complexes results in conformational changes that modulate energy transfer by affecting the association of these complexes with each other and the RC complex. Other aspects of potential posttranslational regulation are mentioned in Sections III and IV.

### B. *puc* (LHII) Operons

#### 1. Genes and Transcripts

A summary of the organization of the *Rb. capsulatus* *puc* genes and transcripts is given in Fig. 3. The *pucBA* genes encode the protein components of the LHII complex, and have been cloned from several organisms and sequenced (Drews and Golecki, 1995; Germeroth et al., 1996; Hagemann et al., 1997). A LHII complex is not found in all purple photosynthetic bacteria. Although there are several copies of *pucB* ( $\beta$  protein) and *pucA* ( $\alpha$  protein) genes in some species (Section II.C), in *Rb. capsulatus* and *Rb. sphaeroides* a single *puc* operon contains single copies of the *pucBA* genes, followed by the *pucC* gene. In *Rb. capsulatus* the *pucC* gene is followed by the *pucD* and *pucE* genes, yielding the *pucBACDE* operon (Fig. 3) (Gibson et al., 1992; Drews and Golecki, 1995). In *Ru. gelatinosus*, a *pucC* homologue was found 5' of *pucBA* but, interestingly, in the opposite orientation (Simmons et al., 1999; Genbank Accession No. AJ245615). In *Rb. capsulatus*, the *pucC* gene product was proposed to encode a protein that enhances LHII assembly, and the *pucD* gene product (if one exists) appears to be dispensable. The *pucE* gene encodes a 14 kDa  $\gamma$  protein of uncertain function that co-purifies with the LHII complex (however the LHII complex in membranes purified from a *Rb. capsulatus* *pucE* deletion mutant was relatively unstable) (Tichy et al., 1991; LeBlanc and Beatty, 1993; Drews and Golecki, 1995).

Transcription of the *puc* operon in *Rb. capsulatus* and *Rb. sphaeroides* initiates from a light- and oxygen-regulated strong promoter upstream of the *pucB* gene (Zucconi and Beatty, 1988; Lee and Kaplan, 1992; LeBlanc and Beatty, 1993; Nickens and Bauer, 1998). RNA 5'-end mapping and *pucE'*-*lac'*Z gene fusion experiments on *Rb. capsulatus* suggested that a minor promoter within the *pucD* gene drives low-level synthesis of a 0.6 kb *pucE*-encoding transcript (Leblanc et al., 1999).

#### 2. Regulation of Transcription Initiation

The reader is directed to Table 1 for a list of genes that are mentioned in the following text. Oxygen regulation of transcription of the *Rb. capsulatus* *puc* operon is controlled by the RegB/RegA sensor kinase/response regulator proteins (Mosley et al., 1994; Bauer and Bird, 1996). Additionally, the *crtJ* gene



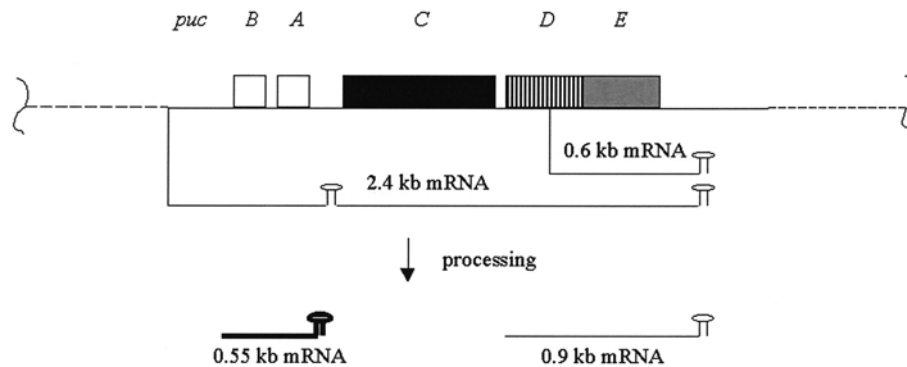


Fig. 3. *Rb. capsulatus puc* operon genes and transcripts. Genes encoding LHII  $\alpha$  and  $\beta$  structural proteins are represented by empty boxes. Transcripts are represented by horizontal lines with vertical connections to sites of initiation, and ribonucleolytic processing products are shown as lines, with thicknesses that indicate the relative steady-state amounts. RNA stem-loop structures are depicted.

product appears to repress transcription under highly aerated conditions (Ponnampalam et al., 1998). DNase I protection and gel mobility shift experiments indicated that CrtJ proteins bind in a cooperative manner to two palindromic sequences spaced approximately 240 bp apart in the *puc* promoter region of *Rb. capsulatus* (Elsen et al., 1998).

Light-mediated regulation of *puc* operon gene expression in *Rb. capsulatus* appears to be controlled in part at the level of transcription initiation (Nickens and Bauer, 1998).

An additional gene in *Rb. capsulatus*, named *orf798*, was identified on the basis of a transposon insertion and DNA sequencing. The *orf798* was required for induction of both the *puc* and *puf* operons anaerobically, and this sequence lacks significant similarity to known genes. Supplementation of *orf798* cultures with vitamin B<sub>12</sub> restored photo-complexes to the wild type level (Pollich et al., 1993; Pollich and Klug, 1995). It is not clear how vitamin B<sub>12</sub> synthesis relates to formation of the photosynthetic apparatus, although a shared biosynthetic pathway leads to a precursor of heme, cobalamin and BChl (Beale, 1995).

Transcription of the *puc* operon in *Rb. sphaeroides* is controlled by the proteins PrrB and PrrA, which seem to function as part of a sensor kinase/response regulator system (Zeilstra-Ryalls et al., 1998), as do the homologous *Rb. capsulatus* RegB/A proteins. In *Rb. sphaeroides*, the *appA* gene was found to encode a *trans*-active factor involved in activation of *puc* gene expression. Recently, a deletion analysis and production of the AppA protein in *E. coli* indicated that AppA is a flavoprotein, and it was proposed that

AppA is a redox-sensing regulator of photosynthesis gene expression (Gomelsky and Kaplan, 1998). The *mgsS* gene was found to be involved in activation of *puc* operon expression under anaerobic growth conditions in *Rb. sphaeroides* (Zeilstra-Ryalls et al., 1998).

The *pucBA* promoter region in *Rb. sphaeroides* and *Rb. capsulatus* was analyzed and several *cis*- and additional *trans*-active factors and regulatory sequences were proposed (Nickens and Bauer, 1998; Zeilstra-Ryalls et al., 1998). In *Rb. sphaeroides*, *cis*-active sequences include an upstream regulatory region (URS) located 629 to 150 nucleotides 5' of the transcriptional start site, which enhances *puc* operon transcription (Lee and Kaplan, 1992). A site required for activation of *puc* operon transcription was found approximately 70 nucleotides 5' of the transcriptional initiation site, and point mutations in one of two regions of dyad symmetry (OR1) reduced aerobic repression of transcription (Lee and Kaplan, 1995). Sequences located about 100 nucleotides 5' of the transcriptional start site show similarity to the recognition sites for the *E. coli* integration host factor (IHF) and fumarate-nitrate regulator (FNR), and the IHF from *E. coli* was reported to bind to the *puc* promoter region (Zeilstra-Ryalls et al., 1998). Similarly, the *Rb. capsulatus* IHF was demonstrated to bind to the *puc* promoter region in gel mobility shift experiments and proposed to stabilize binding of RegA during anaerobic activation of *puc* gene expression (Nickens and Bauer, 1998). A *Rb. sphaeroides* homologue of the *E. coli* FNR protein, FnrL, appears to be required for both photosynthetic and DMSO-dependent (dark) growth under anaerobic

conditions, and a putative FnrL site located 5' of the *puc* operon led to the suggestion that the FnrL protein activates *puc* gene expression in response to reduced oxygen levels (Zeilstra-Ryalls et al., 1998). In *Rb. capsulatus*, dark anaerobic growth was impaired by mutation of a *fnrL* homologue but photosynthetic growth was unaffected (Zeilstra-Ryalls et al., 1997).

Mutations in the *oxyA* (now called *tspO*) and *oxyB* (renamed *ppsR* and a homolog of the *Rb. capsulatus crtJ* gene, see above) loci were found to impair aerobic repression of *Rb. sphaeroides puc* transcription (Lee and Kaplan, 1992; Penfold and Pemberton, 1994). The repressive effect of PpsR on *puc* gene expression seems to be modulated by the 17 kDa outer membrane TspO protein (Yeliseev et al., 1997). It was speculated that TspO regulates the movement of certain small molecules (perhaps a tetrapyrrole) across the outer membrane in response to oxygen concentration and light intensity, and that this activity affects PpsR repressor function (Zeilstra-Ryalls et al., 1998; Oh and Kaplan, 2001). Mutational analyses of the *appA* and *ppsR* genes led to the proposal that the AppA protein senses the redox state and activates PpsR protein repressor function under aerobic growth conditions (Zeilstra-Ryalls et al., 1998). Finally, a 26 kDa protein that binds the *Rb. sphaeroides puc* promoter region 120 nucleotides 5' of the transcriptional start site was identified in gel mobility shift and DNase I protection assays (McGlynn and Hunter, 1992).

### 3. mRNA Processing

In *Rb. capsulatus* two highly abundant *pucBA* RNA species of approximately 550 nt were discovered (Zucconi and Beatty, 1988). Lesser quantities of 0.6 to 0.7 kb, 0.9 to 1.0 kb, 2.4 kb and longer *puc* probe-hybridizing RNA molecules were detected, the latter of which is long enough to encode all of the *puc* operon genes (LeBlanc and Beatty, 1993; Nickens and Bauer, 1998; Leblanc et al., 1999). The *pucC* segment of the 2.4 kb *pucBACDE* transcripts was proposed to undergo endo- and exoribonucleolytic degradation, slowed by an RNA stem-loop structure located between *pucA* and *pucC*, to yield 0.55 kb *pucBA* mRNA molecules (Fig. 3). Thus, although a small amount of transcription attenuation at this putative RNA stem-loop structure was detected, the differential stability of *puc* transcript segments appears to be the main factor that determines PucB

and PucA protein levels relative to PucC (Leblanc et al., 1999).

Large (2.3 and 1.3 kb), low abundance *puc*-complementary RNA molecules were detected in *Rb. sphaeroides*, as was a 0.5 kb high abundance *pucBA* molecule. The longer *puc* transcripts could be the result of weak transcription attenuation at *rho*-independent terminator-like (stem-loop) structures, but the genesis of these transcripts is unclear (Zeilstra-Ryalls et al., 1998). A very small (120 nt) RNA also was detected, but the significance of this molecule is unknown (Lee et al., 1989).

### 4. Posttranslational Processes

The concentration of oxygen was reported to affect the rate at which the PucB protein was incorporated into membranes of *Rb. capsulatus* cells and this seemed to depend on the presence of BChl (Hebermehl and Klug, 1998). Other experiments suggested the possibility of posttranslational regulation in response to different light intensities, because when *puc* mRNA levels were normalized to account for the different rRNA levels present in high and low light-grown cells, the levels of the LHII complex varied inversely with *pucBA* message levels (Zucconi and Beatty, 1988). Although the mechanisms of these regulatory processes are obscure, factors such as the availability of BChl, the rate of incorporation of apoproteins into the membrane, assembly of LHII subunits, and oligomerization of subunits to form a complex could be operative (Section IV). Carotenoid biosynthesis seems to be essential for the formation of the LHII complex in *Rhodobacter* species, whereas the LHI complex is formed in the absence of carotenoid pigments (Feick et al., 1980; Lang and Hunter, 1994; Zeilstra-Ryalls et al., 1998). Additional posttranslational factors are described in Sections III and IV.

#### C. 'Extra' or Unusual LH Structural Genes or Complexes

*Rhodopseudomonas palustris* contains several different forms of the LHII complex and five copies of *pucBA* genes. There is differential regulation of transcription of the five operons dependent upon light intensity, such that all five are transcribed under high light anaerobic growth conditions but only three are transcribed at a low light intensity (Tadros et al.,

1993). One of the *pucBA* gene pairs that is expressed only under high light was heterologously expressed in *Rb. sphaeroides* and gave rise to an LHII complex that transferred energy to the *Rb. sphaeroides* LHI complex, whereas one of the low-light pairs was produced at a low level in *Rb. sphaeroides* but did not transfer energy to LHI (Fowler and Hunter, 1996). Since there are differences in the predicted amino acid sequences of the  $\beta$  and  $\alpha$  subunits of the high-light and low-light LHII complexes of *Rps. palustris*, the heterologous expression system in *Rb. sphaeroides* could be exploited to explore energy transfer between these LHII and LHI complexes in vivo. The ability of *Rps. palustris* to assemble a variety of different peripheral antenna complexes could possibly help it to survive under different light intensities or wavelengths in nature.

The nearly complete genome sequence of *Rb. sphaeroides* (Mackenzie et al., 2001) has revealed a second set of *pucBA* genes. Although these genes do not appear to be expressed in wild type cells, their expression seems to be activated by mutation in a strain from which the first (normally expressed) set was deleted, during prolonged incubation under low light intensity (Tehrani and Beatty, unpublished).

*Rps. acidophila* forms two different types of LHII complex, B800-820 and B800-850, and four variants of *pucBA* genes have been cloned and sequenced. Larger amounts of the B800-850 complex ( $\alpha$  and  $\beta$  polypeptides encoded by the *puc<sup>A</sup>BA* genes, the fourth *pucBA* pair) are present under high-light growth conditions, and only the B800-820 complex(es) under low light. Since a 0.53 kb mRNA transcript encoding the B800-850 genes is present under both high and low light, a post-transcriptional control mechanism evidently operates to reduce expression of these genes under low light intensity (Gardiner et al., 1996). The *Rps. acidophila*  $\alpha$  polypeptides appear to undergo C-terminal processing prior to or during assembly into the mature LHII complex, in contrast to other species (Gardiner et al., 1996).

The purple sulfur bacterium *Chromatium vinosum* contains sequences immediately 3' of the *pufC* gene that encode a second set of LHI  $\alpha$  and  $\beta$  homologs (Corson et al., 1999) (see Fig. 2).

The aerobic anoxygenic phototrophic bacterium *Ro. denitrificans* contains an unusual LH complex absorbing at 806 nm, which is composed of two small polypeptides having apparent molecular masses of 5.0 and 7.0 kDa, in addition to a LHI/RC core

complex. This B806 complex was proposed to be a LHII-like complex, based on its spectroscopic properties (Shimada et al., 1990; Yurkov and Beatty, 1998). Unusual absorption spectra have been obtained from intact cells of or partially purified complexes from several aerobic anoxygenic bacterial species, suggesting the presence of a variety of LH complexes unlike those found in the 'classical' purple photosynthetic bacteria (Yurkov and Beatty, 1998). For example, *Roseococcus thiosulfatophilus* (previously known as *Erythrobacter* Och114) possesses a LHI complex that absorbs maximally at 856 nm and seems to contain four different polypeptides (Gall et al., 1995). The most striking and puzzling differences between aerobic phototrophic bacteria and 'classical' purple bacteria are that the former species are incapable of growth with light as the sole source of energy, and the repressive effect of light on BChl synthesis is so pronounced that prolonged growth of cells in the presence of light results in the absence of detectable amounts of BChl (Yurkov and Beatty, 1998). The recent discovery in *Bradyrhizobium* of a gene that encodes a phytochrome-like protein that controls the formation of the photosynthetic apparatus may lead to an understanding of this curious phenotype (Giraud et al., 2002).

### III. Assembly of LH Complexes

#### A. Reconstitution of LHI Subunits and Complexes In Vitro

We give a brief summary here because a recent review is available (Loach and Parkes-Loach, 1995). The LHI complex can be separated from the RC complex in detergent purification procedures and converted to a subunit form (herein referred to as B820, although preparations from different bacterial species have different absorption maxima), which has a blue-shifted absorption peak compared to the intact complex. Under appropriate conditions the subunit forms an oligomer spectrally identical to the native complex. Despite a high degree of amino acid sequence identity between LHI polypeptides, the *Rb. capsulatus* subunit is less stable than those of *Rb. sphaeroides* or *Rsp. rubrum* (Heller and Loach, 1990; Loach et al., 1994). Site-directed mutagenesis of the *Rb. sphaeroides*  $\beta$  polypeptide suggested that the

difference in stability results from the presence of Met in *Rb. capsulatus* instead of the +4 Tyr residue in *Rb. sphaeroides* (numbers refer to the distance from the His that binds the BChl  $Mg^{2+}$  cation; e.g., +4 means four residues C-terminal from this His). In *Rb. sphaeroides* this +4 Tyr seems to provide a hydrogen bond to the acetyl group of the bound BChl (Davis et al., 1997).

Reconstitution experiments with BChl analogues indicated that the binding site for BChl is specific in that some analogues were not tolerated and no subunits were observed, whereas other alterations to the BChl molecule yielded subunits of reduced stability. These experiments led to proposals for BChl-protein specific interactions (Parkes-Loach et al., 1990; Loach and Parkes-Loach, 1995; Davis et al., 1996) (see Chapter 2, Scheer).

Subunit and oligomeric (e.g., B870) forms of the LHI complex can also be obtained in vitro by combining isolated  $\alpha$  and  $\beta$  polypeptides with BChl in detergent solutions, followed by dialysis to reduce the detergent concentration (Parkes-Loach et al., 1988). Reconstitution experiments using chemically synthesized  $\alpha$  or  $\beta$  peptides truncated or with single amino acid substitutions at conserved residues indicated that a central region of about 40 amino acids in each of these polypeptides contains information sufficient to form a B820 subunit in vitro. However, the B820 subunit has not been observed in vivo, and truncations and amino acid substitutions of LHI polypeptides produced in vivo resulted in reduced levels of complexes (see below). It seems that, although reconstitution experiments reveal fundamental protein-protein and protein-pigment interactions that are sufficient to form the LHI complex in vitro, efficient assembly of complexes in vivo requires structural information and other factors that are not essential for in vitro reconstitution.

To our knowledge, reconstitution of the LHII complex starting from purified subunit polypeptides and pigments has not been accomplished. However, it is possible to remove the B800 BChl molecule reversibly from the *Rb. sphaeroides* LHII complex, by using the detergent Triton BG-10 under acidic conditions. BChl *a* or analogues were added to this B850 preparation, and the resultant bound 'B800' pigment transferred energy to the B850 molecules, as indicated by fluorescence excitation (Bandilla et al., 1998).

### *B. Effects of Mutations on In Vivo Assembly of LHI*

On the basis of site-directed mutations in *Rb. capsulatus*, a consensus sequence for the binding site of BChl in the LHI  $\alpha$  protein was proposed to be Ala-X-X-X-His (Bylina et al., 1988). Replacement of His  $\alpha 32$  (in these and following experiments, the residue numbers refer to the distance from the N terminus) by Thr, Asn, Gln, Pro, Asp or Arg resulted in the absence of the LHI complex as indicated by absorption spectroscopy, as did changing Ala  $\alpha 28$  to Asp, Glu, Phe or His. In contrast, the LHI complex was formed when Ala  $\alpha 28$  was substituted by Gly, Ser, Cys, or Val. These studies suggested that the His  $\alpha 32$  of the *Rb. capsulatus* LHI  $\alpha$  polypeptide acts as a ligand to the  $Mg^{2+}$  ion of BChl, and that Ala  $\alpha 28$  is in van der Waals contact with the BChl (Bylina et al., 1988). Most (but not all) LH proteins contain the sequence Ala/Gly-X-X-X-His, in which His is believed to be a critical BChl ligand (Zuber and Cogdell, 1995).

Site-directed mutagenesis of other *Rb. capsulatus* LHI residues resulted in several effects, depending on the position and nature of the amino acid substitution. Amongst the effects reported were increases or decreases in the amounts of LHI carotenoid and BChl pigments, as well as the complete loss of the LHI and RC complexes. In general, the data implicated several (especially N-terminal) residues in LHI assembly or stability, and indicated that loss of the LHI complex may affect the structure of the RC (Babst et al., 1991). Other experiments, employing  $^{35}S$ -methionine pulse-labeling of mutant LHI proteins followed by SDS-PAGE and autoradiography, yielded additional information regarding the  $\alpha$  sequences that are required for assembly of the LHI complex (Richter et al., 1991). In particular, Trp  $\alpha 8$  was proposed to play a role in insertion of the  $\alpha$  polypeptide into the membrane, whereas mutation of Pro  $\alpha 13$  interfered with stable insertion of the  $\beta$  polypeptide into the membrane. On the basis of the effects of changes of charged amino acids in the N-terminal segments of the LHI proteins, a model was proposed in which electrostatic interaction between negatively charged N-terminal  $\beta$  polypeptide and positively charged N-terminal  $\alpha$  polypeptide residues is a prerequisite for assembly of the LHI complex (Tadros et al., 1984; Tadros et al., 1985; Stiehle et al., 1990; Richter et al., 1992; Drews, 1996). Although

the  $\beta$  polypeptide became associated with the membrane in the absence of the  $\alpha$  polypeptide with the same kinetics as when the  $\alpha$  protein was present, the  $\beta$  subunit appeared to be degraded rapidly when the  $\alpha$  protein was absent. In contrast, only trace quantities of the  $\alpha$  protein were detected in the membrane in the absence of the  $\beta$  protein (Richter et al., 1991).

Site-directed mutations of the *Rb. sphaeroides* LHI His  $\alpha$ 32 and His  $\beta$ 31 residues resulted in the failure of LHI complex formation as indicated by absorption spectroscopy. On the basis of changes made to these His residues (His  $\alpha \rightarrow$  Asn, Leu or Tyr; His  $\beta \rightarrow$  Asn, Gln, Leu or Tyr), it was concluded that the only change compatible with formation of a LHI complex was His  $\beta \rightarrow$  Asn. It was suggested that the absence of complex formation when Asn or Gln replaced His  $\alpha$  was due to greater structural constraints placed upon the  $\alpha$  polypeptide and the BChls that form the inner ring of the LHI holocomplex (Olsen et al., 1997). These observations support the view that, as had been suggested for the *Rb. capsulatus* LHI complex, the His residues  $\alpha$ 32 and  $\beta$ 31 act as ligands to BChls (Olsen et al., 1997). Raman spectroscopic studies of mutants with amino acid substitutions at LHI Trp  $\alpha$ 43 and Trp  $\beta$ 47 suggested that these residues form hydrogen bonds with the acetyl group of the corresponding BChl (Sturgis et al., 1997).

### C. Effects of Mutations on Assembly of LHII In Vivo

Site-directed mutagenesis studies on *Rb. sphaeroides* LHII  $\alpha$  and  $\beta$  polypeptides indicated that the LHII complex did not form when His  $\alpha$ 20 or His  $\beta$ 21 was substituted with Asn, suggesting that these His residues are ligands to the B850 BChl  $\text{Mg}^{2+}$  (Olsen et al., 1997). Probing of the B800 binding site by changing Arg  $\beta$ 31 to His, Asn, Leu, Lys, or Glu generally resulted in blue-shifting of the 800 nm absorption peak, and thus, a reduction in spectral overlap with B850. The reduced spectral overlap was proposed to be partially responsible for a slower rate of energy transfer from B800 to B850 in these mutant complexes (Fowler et al., 1997). This study was followed by a Raman spectroscopic analysis of these mutant complexes, which indicated that Arg  $\beta$ 31 hydrogen bonds to the acetyl moiety of the B800 molecule (Gall et al., 1997). Interestingly, elimination

of the B800 BChl binding site in N-terminal truncations of the LHII  $\alpha$  polypeptide resulted in a 'B850-only' LHII complex (Koolhaas et al., 1998).

### D. LH Complex Assembly Factors

#### 1. The LhaA and PucC Proteins

In *Rb. capsulatus*, the LhaA and PucC proteins are required to obtain normal levels of the LHI and LHII complexes, respectively (Tichy et al., 1989; Bauer et al., 1991; LeBlanc and Beatty, 1993; Young et al., 1998). The deduced amino acid sequence of the PucC protein is 462 amino acids in length and that of the LhaA protein is 477 amino acids, and these sequences exhibit 47% identity in an alignment (Bauer et al., 1991; Young and Beatty, 1999). LhaA and PucC were found to be integral membrane proteins consisting of twelve transmembrane segments, with N- and C-termini located in the cytoplasm (LeBlanc and Beatty, 1996; Young and Beatty, 1998).

The *pucC* gene of *Rb. capsulatus* is transcribed as part of the *pucBACDE* operon (see Fig. 3) and mutations in *pucC* resulted in the complete loss of the LHII complex from *Rb. capsulatus* cells (Tichy et al., 1989; LeBlanc and Beatty, 1993). An investigation into whether *trans* expression of the *pucC* gene in a *lhaA/pucBACDE* double deletion mutant increased the level of the LHI complex yielded negative results. However, when a *puc* operon deletion strain containing a *pucBA $\Delta$ CDE* (*pucC* deletion) expression plasmid was supplemented with other plasmids expressing short *pucC'*::*pho*'A fusions, there were reduced amounts of LHI (LeBlanc, 1995).

The deduced PucC polypeptide from *Rps. acidophila* has 469 amino acids with 58% sequence identity to the *Rb. capsulatus* protein. Overexpression of the *Rps. acidophila pucC* gene from a plasmid in a wild type background increased the levels of LHI and LHII complexes in semiaerobically grown cells (Barrett and Cogdell, 1998).

The *lhaA* gene (previously known as F1696 or *orf1696*) was first detected by DNA sequencing of the *Rb. capsulatus* photosynthesis gene cluster (Youvan et al., 1984). RNA blot and *lacZ* gene fusion analyses demonstrated that *lhaA* is part of the *bchFNBHLM-lhaA-puhA* superoperon, and that its expression is regulated by oxygen due to transcription initiated at the *bchF* promoter. A second oxygen-

regulated promoter (*PpuhA*) located within the coding sequence of *lhaA* contributes to transcription of the *puhA* gene (Bauer et al., 1991). Transposon and interposon mutagenesis of *lhaA* resulted in reductions of the levels of LHI and RC complexes, indicating that *lhaA* plays a role in maintaining steady state levels of these complexes in *Rb. capsulatus* cells (Zsebo and Hearst, 1984; Bauer et al., 1991). The LhaA protein was proposed to function as an assembly factor for the LHI complex on the basis of kinetic studies of the formation and decay of LHI (Young et al., 1998). Possible functions of the LhaA protein include membrane insertion of the LHI  $\alpha$  and  $\beta$  polypeptides, BChl delivery to these apoproteins to form subunits, and oligomerization of subunits to form the holocomplex (Young et al., 1998; Young and Beatty, 1999). However, the exact role of LhaA in LHI assembly is unknown.

Homologues of *lhaA* have been discovered in *Rb. sphaeroides*, *Rps. viridis*, *Ru. gelatinosus* and *Rsp. rubrum* (Donohue et al., 1986; Wiessner, 1990; Berard and Gingras, 1991; Igarishi et al., 1998). In each case the *lhaA* gene is located immediately 5' of the *puhA* gene, as in *Rb. capsulatus*, but no information on the function or expression of *lhaA* in these bacteria has been published.

The cyanobacterium *Synechocystis* sp. PCC6803 (Kaneko et al., 1996) and the prochlorophyte *Prochlorococcus marinus* (personal communication, W. Hess) contain orfs encoding LhaA/PucC homologues with 24% to 25% amino acid sequence identity and similar hydropathy profiles (Young and Beatty, 1999). Cyanobacteria and prochlorophytes do not contain LH complexes similar to those of purple bacteria, yet the presence of *lhaA* homologues in these organisms could provide clues about the activity of this class of proteins. There are great differences in the amino acid sequences of purple bacterial and cyanobacterial or prochlorophyte LH proteins (La Roche et al., 1996; Chapter 4, Green; Chapter 5, Robert et al.). In contrast, the chlorophyll *a* (Chl *a*) and BChl *a* molecules differ only in that Chl *a* has a vinyl group on pyrrole ring I whereas BChl *a* has an acetyl group at this position, and pyrrole ring II of Chl *a* is unsaturated while the same ring of BChl *a* is saturated (Lawlor, 1993; Chapter 2, Scheer). Thus, the amino acid sequence conservation in LhaA/PucC-like proteins could reflect a function in common of BChl (Chl) binding and translocation for LH complex assembly in these otherwise diverse photosynthetic organisms. This speculation led to

the proposed inclusion of the LhaA and PucC proteins in a subset of the 'major facilitator superfamily' of membrane permeases called the BChl delivery family (BCD) (Saier et al., 1999).

## 2. DnaK and GroEL

The DnaK (Hsp 70) and GroEL (Hsp 60) proteins are chaperonins that catalyze the proper folding and assembly of nascent polypeptides into their functional, three-dimensional conformations in the cytoplasm of diverse organisms (Ellis and van der Vies, 1991). The DnaK and GroEL proteins of *Rb. capsulatus* were partially purified, and a cell-free transcription-translation system was used to evaluate their involvement in the synthesis and membrane insertion of the LHI  $\alpha$  and  $\beta$  polypeptides (Meryandini and Drews, 1996). The addition of a DnaK-enriched fraction enhanced translation of both of the LHI polypeptides, whereas GroEL appeared to be required for stable insertion of the  $\alpha$  and  $\beta$  proteins into membranes added to this in vitro translation system. A model was proposed in which DnaK and GroEL comprise part of a *Rb. capsulatus* chaperonin-mediated pathway, which delivers LHI polypeptides to the membrane for insertion by a hypothetical membrane-bound import protein(s) (Langer et al., 1992; Drews, 1996; Meryandini and Drews, 1996).

## IV. Other genes and proteins relevant to LH complex assembly or structure

### A. The PufX Protein

Spectroscopic analyses of *Rb. capsulatus* and *Rb. sphaeroides* *pufX* (Fig. 2) deletion strains indicated that the PufX protein is required for efficient exchange of ubiquinone/ubiquinol molecules between the  $Q_B$  site of the RC and the cytochrome  $bc_1$  complex (Lilburn et al., 1992; Barz and Oesterheld, 1994). It was postulated that the PufX protein associates with the LHI complex to create a gap in the LHI 'ring' which would allow exchange of ubiquinone and ubiquinol at the RC  $Q_B$  site (Barz et al., 1995; Lilburn et al., 1995; Lilburn et al., 1999).

In vitro reconstitution experiments using purified PufX proteins from *Rb. capsulatus* or *Rb. sphaeroides* and LHI  $\alpha$  and  $\beta$  polypeptides suggested that PufX inhibits LHI subunit formation and oligomerization, and that PufX has an affinity for the  $\alpha$  polypeptide



(Recchia et al., 1998; Parkes-Loach et al., 2001). In other experiments, the *Rb. sphaeroides* PufX protein appeared to bind more stably to the LHI/RC core complex than to the LHI or RC complexes alone, as determined by detergent solubilization of complexes from mutants followed by separation of these complexes by sucrose density gradient centrifugation (Pugh et al., 1998). These results confirmed that the PufX protein is part of the LHI/RC core complex, and proteolytic digestion of PufX in membrane vesicles indicated that it is an integral membrane protein with its N-terminus facing the cytoplasm, the same topological arrangement as of the LHI  $\alpha$  and  $\beta$  polypeptides (Drews, 1996; Pugh et al., 1998). Experiments on purified core complexes from *Rb. sphaeroides* PufX<sup>+</sup> and PufX<sup>-</sup> strains suggested that the PufX protein is required for the formation of dimeric LHI/RC core complexes and that there is one PufX molecule per RC complex (Francia et al., 1999). This is consistent with the notion that the PufX protein induces formation of C-shaped LHI structures around the RC (Francia et al., 1999; Jungas et al., 1999).

Linear dichroism spectra of membranes from PufX<sup>+</sup> and PufX<sup>-</sup> (both in an LHII<sup>-</sup> background) *Rb. sphaeroides* cells were interpreted as showing a PufX-dependent, inter-complex organization of LHI/RC core complexes (Frese et al., 2000). These results are consistent with the quasi-crystalline arrays of core complexes in membranes from LHII<sup>-</sup> cells that were evaluated by electron microscopy (Jungas et al., 1999), and additionally indicate that the PufX protein is required to obtain a higher order of organization of the RC and intimately associate LHI complexes in vivo, at least in the absence of the LHII complex.

### B. The PufQ Protein

The *pufQ* gene (Fig. 2) is present in *Rb. capsulatus*, *Rb. sphaeroides* and *Rv. sulfidophilum*. Expression of the *Rb. capsulatus pufQ* gene is required for LH complex formation, presumably because the PufQ protein enhances the synthesis of BChl (or intermediates in *bch* mutant cells) (Bauer and Marrs, 1988; Forrest et al., 1989; Masuda et al., 1999). It was suggested that the PufQ protein carries BChl intermediates at all steps of the BChl biosynthetic pathway (Bauer and Marrs, 1988). The *Rb. capsulatus* PufQ protein is 74 amino acids in length, hydrophobic, and associates with membranes (Fidai et al., 1993, 1994a). In support of the idea that PufQ is involved

in BChl synthesis, a purified recombinant PufQ protein appeared to bind the BChl precursor protochlorophyllide in liposomes composed of soybean phospholipid (Fidai et al., 1994). Furthermore, *trans*-complementation of a *pufQ* deletion strain of *Rb. capsulatus* with the *pufQ* gene on a plasmid increased levels of the BChl precursor uroporphyrinogen III 2-fold compared to a strain lacking *pufQ* gene expression (Fidai et al., 1995). Thus these data indicate that the PufQ protein is involved in BChl biosynthesis at the posttranslational level. However, mutations in the *pufQ* gene of *Rb. sphaeroides* led to changes in the levels of both the LHI and LHII complexes (Gong et al., 1994) and it was proposed that the PufQ protein, in association with BChl, assists the assembly of LH complexes (Zeilstra-Ryalls et al., 1998).

### C. The *orf214* and *orf162b* Genes

The genes *orf214* and *orf162b* are located immediately 3' of the *puhA* gene on the *Rb. capsulatus* chromosome, and *puhA* is located 3' of several *bch* genes and *lhaA* (Haselkorn et al., 2001). All of these genes appear to be co-transcribed (Bauer et al., 1991; Wong et al., 1996; Aklujkar et al., 2000). Homologues of *orfs 214* and *162b* exist 3' of the *puhA* gene in *Rsp. rubrum*, *Rb. sphaeroides*, *Rps. palustris* and *Ru. gelatinosus* (Berard and Gingras, 1991; Igarishi et al., 1998; Aklujkar et al., 2000).

The *Rb. capsulatus* deduced ORF214 protein consists of 214 amino acids and hydropathy analyses indicate an integral membrane location. A translationally in-frame deletion of *orf214* resulted in reduced levels of both RC and LHI, and this phenotype was complemented in *trans* by expressing the *orf214* gene from a plasmid (Wong et al., 1996). It is possible that the ORF214 protein enhances RC assembly, and that in the absence of ORF214 a reduction in the amount of the RC results in a decrease in LHI. It was found that deletions of RC genes in *Rb. capsulatus* and *Rb. sphaeroides* resulted in significant decreases in the levels of LHI, and that deletions of the LHI genes in *Rb. capsulatus* reduced the amounts of the RC (Klug and Cohen, 1988; A. Tehrani and J. T. Beatty, unpublished).

The *Rb. capsulatus* ORF162b protein consists of 162 amino acids, as deduced from the nucleotide sequence of the gene, and hydropathy analysis predicts a single transmembrane segment near the N-terminus. Mutation of the *orf162b* gene reduced LHI



and RC complex levels, and impaired photosynthetic growth (Aklujkar et al. 2000). Thus, like the ORF214 protein, ORF162b appears to play a role in maintaining levels of the LHI and RC complexes. Because interactions between these two complexes appear to be required for mutual stabilization or assembly, it is difficult to ascribe a specific function of ORF214 or ORF162b with regard to either LHI or RC complexes.

#### D. *pucD* and *pucE* Genes

The *pucD* and *pucE* genes are located within the *Rb. capsulatus* *puc* operon (Fig. 3). Mutations of *pucD* did not affect the levels of photocomplexes or the rate of photosynthetic growth of *Rb. capsulatus* cells (Tichy et al., 1989; LeBlanc and Beatty, 1993). A small amount of transcription initiated from a minor promoter embedded within the *pucD* gene sequence contributes to expression of *pucE* (Leblanc et al., 1999). However the function of a PucD protein, if it exists, is unknown and a *pucD* homologue has not been found in other species.

The *pucE* gene encodes a 14 kDa protein, known as the  $\gamma$  subunit, which co-purifies with the LHII complex of *Rb. capsulatus* (Tichy et al., 1989). Mutation of the *pucE* gene resulted in decreased levels of the LHII complex and slower rates of photosynthetic growth of *Rb. capsulatus* at low light intensities. The PucE protein may affect the binding site for the B800 BChl molecule, since greater decreases in the LHII 800 nm peak compared to the 850 nm peak were observed in *pucE* deletion mutants (LeBlanc and Beatty, 1993). Although it seems that in *Rb. capsulatus* the PucE protein interacts with the LHII complex in some way, its exact function is obscure, especially since a *pucE* gene has not been described in other species.

#### E. *orf428*

The *orf428* is thought to be part of the *bchEJG-orf428-bchP-orf176* operon located within the photosynthesis gene cluster of *Rb. capsulatus* (Beatty, 1995). The putative ORF428 protein has 24% amino acid sequence identity with LhaA and PucC. However, disruption of the chromosomal copy of *orf428* did not directly result in a reduction of a photosynthetic complex (Bollivar et al., 1994), and disruption of the *orf428* in a *lhaA/pucC* double mutant background did not clearly suggest a role for *orf428* in LH

complex assembly (Young, 1997). Thus, it seems that *orf428* plays no major role in LH complex assembly or stabilization, and if a protein is produced from *orf428* its function is dispensable.

#### F. The $\Omega$ Protein

The  $\Omega$  protein was reported to be a hydrophobic 4 kDa polypeptide that co-purifies with the LHI complex of *Rsp. rubrum*, and to be present at a 0.1 stoichiometry relative to the  $\alpha$  and  $\beta$  polypeptides. The  $\Omega$  protein appeared to be phosphorylated (as were the LHI  $\alpha$  and  $\beta$  proteins) and this modification was suggested to play a role in regulating energy transfer between LHI complexes (Ghosh et al., 1994). It was speculated that the  $\Omega$  protein may influence the structure of the LHI/RC core complex (Stahlberg et al., 1998b), although the amino acid sequence and function of this polypeptide are unknown.

### V. Concluding Remarks and Future Prospects

This is an exciting time for those of us interested in the regulation of LH complexes in purple photosynthetic bacteria. The observation of dimeric (C-shaped) LHI/RC core complexes in an LHII<sup>-</sup> mutant strain of *Rb. sphaeroides* begs for efforts to determine if this structural organization is present in purple bacteria that naturally lack the LHII complex. A modification of the LH ring paradigm may be required to include the possibility of incompletely circularized, but oligomerized LH complexes in vivo. A high-resolution crystal structure of a LHI/RC core complex would help to elucidate the specific interactions between RC and LHI complexes, and perhaps would indicate if putative components such as the PufX protein, the  $\Omega$  protein and the cytochrome *bc<sub>1</sub>* complex contribute to structure, function and assembly.

The regulation of expression of LH genes is extraordinarily complicated and a variety of transcriptional, translational and posttranslational processes exist, apparently to fine-tune the amounts of LH complexes to allow cells to grow optimally at varying oxygen concentrations and light intensities. Although much has been learned about the control of *puf* and *puc* operon transcription initiation, an outstanding question is the nature of the signal(s) sensed during oxygen and light modulation of gene transcription. Oxygen- or light-driven oxidation/

reduction reactions could be operative (Bauer, 1995; Zeilstra-Ryalls et al., 1998; Oh and Kaplan, 2001), and it was suggested that BChl biosynthetic enzyme activities could be required for light sensing (Rodrig et al., 1999).

The posttranscriptional and posttranslational regulation of LH complex assembly *in vivo* is mediated by an intricate machinery, which includes proteins that function to synthesize and assemble the pigments and polypeptides that comprise these complexes. We look forward to the elucidation of all the factors and processes involved in LH gene transcription and pigment-protein assembly into complexes. Such an understanding of how the regulation of LH complex levels and properties relates to optimal photosynthetic metabolism in response to a changing environment is of fundamental interest, and could be exploited in applications of the biological capture of light energy. The genome sequences of *Rb. capsulatus* (Haselkorn et al., 2001), *Rb. sphaeroides* (Mackenzie et al., 2001) and *Rps. palustris* (<http://genome.ornl.gov/microbial/rpal/>) are a valuable resource for the design and interpretation of experiments to achieve such an understanding.

## Acknowledgments

We thank our colleagues who provided reprints, preprints or other information, and the editors for helpful comments.

## References

- Adams CW, Forrest ME, Cohen SN and Beatty JT (1989) Structural and functional analysis of transcriptional control of the *Rhodobacter capsulatus* *puf* operon. *J Bacteriol* 171: 473–482
- Aklujkar M, Harmer AL, Prince RC and Beatty JT (2000) The *orf162b* sequence of *Rhodobacter capsulatus* encodes a protein that affects the organization of the photosynthetic apparatus. *J Bacteriol* 182: 5440–5447
- Allen JF and Nilsson A (1997) Redox signalling and the structural basis of regulation of photosynthesis by protein phosphorylation. *Physiol Plant* 100: 863–868
- Babst M, Albrecht H, Wegmann I, Brunisholz R and Zuber H (1991) Single amino acid substitutions in the B870  $\alpha$  and  $\beta$  light-harvesting polypeptides of *Rhodobacter capsulatus*: Structural and spectral effects. *Eur J Biochem* 202: 277–284
- Bandilla M, Ucker B, Ram M, Simonin I, Gelhaye E, McDermott G, Cogdell RJ and Scheer H (1998) Reconstitution of the B800 bacteriochlorophylls in the peripheral light harvesting complex B800-850 of *Rhodobacter sphaeroides* 2.4.1 with BChl *a* and modified (bacterio-)chlorophylls. *Biochim Biophys Acta* 1364: 390–402
- Barrett SJ and Cogdell RJ (1998) Investigation of the PucC protein from *Rhodopseudomonas acidophila*. In: Garab G (ed) *Photosynthesis: Mechanisms and Effects*, pp 3091–3094. Kluwer Academic Publishers, Dordrecht
- Barz WP and Oesterhelt D (1994) Photosynthetic deficiency of a *pufX* deletion mutant of *Rhodobacter sphaeroides* is suppressed by point mutations in the light-harvesting complex genes *pufB* and *pufA*. *Biochemistry* 33: 9741–9752
- Barz WP, Vermeglio A, Francia F, Venturoli G, Melandri BA and Oesterhelt D (1995) Role of PufX protein in photosynthetic growth of *Rhodobacter sphaeroides*. 2. PufX is required for efficient ubiquinone/ubiquinol exchange between the reaction center Q<sub>B</sub> site and the cytochrome *bc*<sub>1</sub> complex. *Biochemistry* 34: 15248–15258
- Bauer CE (1995) Regulation of photosynthesis gene expression. In: Blankenship RE, Madigan MT and Bauer CE (eds) *Anoxygenic Photosynthetic Bacteria*, pp 1221–1234. Kluwer Academic Publishers, Dordrecht
- Bauer CE and Bird TH (1996) Regulatory circuits controlling photosynthesis gene expression. *Cell* 85: 5–8
- Bauer CE and Marrs BL (1988) *Rhodobacter capsulatus* *puf* operon encodes a regulatory protein (PufQ) for bacteriochlorophyll biosynthesis. *Proc Natl Acad Sci USA* 85: 7074–7078
- Bauer CE, Buggy J, Yang Z and Marrs BL (1991) The superoperon organization of genes for pigment biosynthesis and reaction center proteins is a conserved feature in *R. capsulatus*: Analysis of overlapping *bcbB* and *pufA* transcripts. *Mol Gen Genet* 228: 433–444
- Beale SI (1995) Biosynthesis and structures of porphyrins and hemes. In: Blankenship RE, Madigan MT and Bauer CE (eds) *Anoxygenic Photosynthetic Bacteria*, pp 153–177. Kluwer Academic Publishers, Dordrecht
- Beatty JT (1995) Organization of photosynthesis gene transcripts. In: Blankenship RE, Madigan MT and Bauer CE (eds) *Anoxygenic Photosynthetic Bacteria*, pp 1209–1219. Kluwer Academic Publishers, Dordrecht
- Belasco JG, Beatty JT, Adams CW, von Gabain A and Cohen SN (1985) Differential expression of photosynthesis genes in *R. capsulatus* results from segmental differences in stability within the polycistronic *rxcA* transcript. *Cell* 40: 171–181
- Berard J and Gingras G (1991) The *puf* structural gene coding for the H subunit of the *Rhodospirillum rubrum* photoreaction center. *Biochem Cell Biol* 69: 122–131
- Biel AJ (1995) Genetic analysis and regulation of bacteriochlorophyll biosynthesis. In: Blankenship RE, Madigan MT and Bauer CE (eds) *Anoxygenic Photosynthetic Bacteria*, pp 1125–1134. Kluwer Academic Publishers, Dordrecht
- Bollivar DW, Suzuki JY, Beatty JT, Dobrowski JM and Bauer CE (1994) Directed mutational analysis of bacteriochlorophyll *a* biosynthesis in *Rhodobacter capsulatus*. *J Mol Biol* 237: 622–640
- Brand M, Garcia AF, Pucheu N, Meryandini A, Kerber N, Tadros MH and Drews G (1995) Phosphorylation of the light-harvesting polypeptide LH1 $\alpha$  of *Rhodobacter capsulatus* at serine after membrane insertion under chemotrophic and phototrophic growth conditions. *Biochim Biophys Acta* 1231: 169–175
- Buggy JJ and Bauer CE (1995) Cloning and characterization of

- senC*, a gene involved in both aerobic respiration and photosynthesis gene expression in *Rhodobacter capsulatus*. J Bacteriol 177: 6958–6965
- Buggy JJ, Sganga MW and Bauer CE (1994) Characterization of a light-responding *trans*-activator responsible for differentially controlling reaction center and light-harvesting I gene expression in *Rhodobacter capsulatus*. J Bacteriol 176: 6936–6943
- Bylina EJ, Robles SJ and Youvan DC (1988) Directed mutations affecting the putative bacteriochlorophyll-binding sites in the light-harvesting I antenna of *Rhodobacter capsulatus*. Israel J Chem 28: 73–78
- Chen C-YA, Beatty JT, Cohen SN and Belasco JG (1988) An intercistronic stem-loop structure functions as an mRNA decay terminator necessary but insufficient for *puf* mRNA stability. Cell 52: 609–619
- Clark WG, Davidson E and Marrs BL (1984) Variation of levels of mRNA coding for antenna and reaction center polypeptides in *Rhodospseudomonas capsulata* in response to changes in oxygen concentration. J Bacteriol 157: 945–948
- Corson GE, Nagashima KVP, Matsuura K, Sakuragi Y, Wettasinghe R, Qin H, Allen R and Knaff DB (1999) Genes encoding light-harvesting and reaction center proteins from *Chromatium vinosum*. Photosyn Res 59: 39–52
- Davis CM, Parkes-Loach PS, Cook CK, Meadows KA, Bandilla M, Scheer H and Loach PA (1996) Comparison of the structural requirements for bacteriochlorophyll binding in the core light-harvesting complexes of *Rhodospirillum rubrum* and *Rhodobacter sphaeroides* using reconstitution methodology with bacteriochlorophyll analogs. Biochemistry 35: 3072–3084
- Davis CM, Bustamante PL, Todd JB, Parkes-Loach PS, McGlynn P, Olsen JD, McMaster L, Hunter CN and Loach PA (1997) Evaluation of structure-function relationships in the core light-harvesting complex of photosynthetic bacteria by reconstitution with mutant polypeptides. Biochemistry 36: 3671–3679
- Donohue TJ, Hoyer JH and Kaplan S (1986) Cloning and expression of the *Rhodobacter sphaeroides* reaction center H gene. J Bacteriol 168: 953–961
- Drews G (1996) Formation of the light-harvesting I (B870) of anoxygenic phototrophic purple bacteria. Arch Microbiol 166: 151–159
- Drews G and Golecki JR (1995) Structure, molecular organization, and biosynthesis of membranes of purple bacteria. In: Blankenship RE, Madigan MT and Bauer CE (eds) Anoxygenic Photosynthetic Bacteria, pp 231–257. Kluwer Academic Publishers, Dordrecht
- Du S, Bird TH and Bauer CE (1998) DNA binding characteristics of RegA\*. J Biol Chem 273: 18509–18513
- Ellis RJ and van der Vies SM (1991) Molecular chaperones. Annu Rev Biochem 60: 321–347
- Elsen S, Ponnampalam SN and Bauer CE (1998) CrtJ bound to distant binding sites interacts cooperatively to aerobically repress photopigment biosynthesis and light harvesting II gene expression in *Rhodobacter capsulatus*. J Biol Chem 273: 30762–30769
- Eraso JM and Kaplan S (1994) *prfA*, a putative response regulator involved in oxygen regulation of photosynthesis gene expression in *Rhodobacter sphaeroides*. J Bacteriol 176: 32–43
- Eraso JM and Kaplan S (1996) Complex regulatory activities associated with the histidine kinase PrrB in expression of photosynthesis genes in *Rhodobacter sphaeroides* 2.4.1. J Bacteriol 178: 7037–7046
- Feick R, van Grondelle R, Rijgersberg CP and Drews G (1980) Fluorescence emission by wild-type- and mutant-strains of *Rhodospseudomonas capsulata*. Biochim Biophys Acta 593: 241–253
- Fidai S, Kalmar GB, Richards WR and Borgford TJ (1993) Recombinant expression of the *pufQ* gene of *Rhodobacter capsulatus*. J Bacteriol 175: 4834–4842
- Fidai S, Hinchigeri SB, Borgford TJ and Richards WR (1994a) Identification of the PufQ protein in membranes of *Rhodobacter capsulatus*. J Bacteriol 176: 7244–7251
- Fidai S, Hinchigeri SB and Richards WR (1994b) Association of protochlorophyllide with the PufQ protein of *Rhodobacter capsulatus*. Biochem Biophys Res Comm 200: 1679–1684
- Fidai S, Dahl JA and Richards WR (1995) Effect of the PufQ protein on early steps in the pathway of bacteriochlorophyll biosynthesis in *Rhodobacter capsulatus*. FEBS Lett 372: 264–268
- Forrest ME, Zucconi AP and Beatty JT (1989) The *pufQ* gene product of *Rhodobacter capsulatus* is essential for formation of B800-850 light-harvesting complexes. Curr Microbiol 19: 123–127
- Fowler GJS and Hunter CN (1996) The synthesis and assembly of functional high and low light LH2 antenna complexes from *Rhodospseudomonas palustris* in *Rhodobacter sphaeroides*. J Biol Chem 271: 13356–13361
- Fowler GJS, Hess S, Pullerits T, Sundstrom V and Hunter CN (1997) The role of  $\beta$ Arg<sub>10</sub> in the B800 bacteriochlorophyll and carotenoid pigment environment within the light-harvesting LH2 complex of *Rhodobacter sphaeroides*. Biochemistry 36: 11282–11291
- Francia F, Wang J, Venturoli G, Melandri BA, Barz WP and Oesterhelt D (1999) The reaction center-LH1 antenna complex of *Rhodobacter sphaeroides* contains one PufX molecule which is involved in dimerization of this complex. Biochemistry 38: 6834–6845
- Frese RN, Olsen JD, Branvall R, Westerhuis WHJ, Hunter CN and van Grondelle R (2000) The long-range supraorganization of the bacterial photosynthetic unit: A key role for PufX. Proc Natl Acad Sci USA 97: 5197–5202
- Gall A, Yurkov V, Cogdell R, Vermeglio A and Robert B (1995) The pigment-protein interactions of some unusual light-harvesting antennae: a Raman study. In: Mathis P (ed) Photosynthesis from Light to Biosphere, pp 251–254. Kluwer Academic Publishers, Dordrecht
- Gall A, Fowler GJS, Hunter CN and Robert B (1997) Influence of the protein binding site on the absorption properties of the monomeric bacteriochlorophyll in *Rhodobacter sphaeroides* LH2 complex. Biochemistry 36: 16282–16287
- Gardiner AT, MacKenzie RC, Barrett SJ, Kaiser K and Cogdell RJ (1996) The purple photosynthetic bacterium *Rhodospseudomonas acidophila* contains multiple puc peripheral antenna complex (LH2) genes: Cloning and initial characterisation of four  $\beta/\alpha$  pairs. Photosynth Res 49: 223–235
- Germeroth L, Reilander H and Michel H (1996) Molecular cloning, DNA sequence and transcriptional analysis of the *Rhodospirillum molischianum* B800/850 light-harvesting genes. Biochim Biophys Acta 1275: 145–150
- Ghosh R, Ghosh-Eicher S, DiBerardino M and Bachofen R

- (1994) Protein phosphorylation in *Rhodospirillum rubrum*: Purification and characterization of a water-soluble B873 protein kinase and a new component of the B873 complex,  $\Omega$ , which can be phosphorylated. *Biochim Biophys Acta* 1184: 28–36
- Gibson LCD, McGlynn P, Chaudhri M and Hunter CN (1992) A putative coproporphyrinogen III oxidase in *Rhodobacter sphaeroides*. II. Analysis of a region of the genome encoding *hemF* and the *puc* operon. *Mol Microbiol* 6: 3171–3186
- Giraud E, Fardoux L, Fourrier N, Hannibal L, Genty B, Bouyer P, Dreyfus B and Vermeglio A (2002) Bacteriophytochrome controls photosystem synthesis in anoxygenic bacteria. *Nature* 417: 202–205
- Gomelsky M and Kaplan S (1995) Genetic evidence that PpsR from *Rhodobacter sphaeroides* 2.4.1 functions as a repressor of *puc* and *bchF* expression. *J Bacteriol* 177: 1634–1637
- Gomelsky M and Kaplan S (1998) AppA, a redox regulator of photosystem formation in *Rhodobacter sphaeroides* 2.4.1, is a flavoprotein. *J Biol Chem* 273: 35319–35325
- Gong L, Lee JK and Kaplan S (1994) The *Q* gene of *Rhodobacter sphaeroides*: Its role in *puf* operon expression and spectral complex assembly. *J Bacteriol* 176: 2946–2961
- Hagemann GE, Katsiou E, Forkl H, Steindorf ACJ and Tadros MH (1997) Gene cloning and regulation of gene expression of the *puc* operon from *Rhodovulum sulfidophilum*. *Biochim Biophys Acta* 1351: 341–358
- Haselkorn R, Lapidus A, Kogan Y, Vlcek C, Paces J, Paces V, Ulbrich P, Pecenkova T, Rebekov D, Milgram A, Mazur M, Cox R, Kyrpides N, Ivanova N, Kapatral M, Los T, Lykidis A, Mikhailova N, Reznik G, Vasieva O and Fonstein M (2001) The *Rhodobacter capsulatus* genome. *Photosynth Res* 70: 43–52
- Hebermehl M and Klug G (1998) Effect of oxygen on translation and posttranslational steps in expression of photosynthesis genes in *Rhodobacter capsulatus*. *J Bacteriol* 180: 3983–3987
- Heck C, Rothfuchs R, Jager A, Rauhut R and Klug G (1996) Effect of the *pufQ-pufB* intercistronic region on *puf* mRNA stability in *Rhodobacter capsulatus*. *Mol Microbiol* 20: 1165–1178
- Heller BA and Loach PA (1990) Isolation and characterization of a subunit form of the B875 light-harvesting complex from *Rhodobacter capsulatus*. *Photochem Photobiol* 51: 621–627
- Houghton JD, Honeybourne CL, Smith KM, Tabba HD and Jones OTG (1982) The use of N-methylprotoporphyrin dimethyl ester to inhibit ferrochelatase in *Rhodopseudomonas sphaeroides* and its effect in promoting biosynthesis of magnesium tetrapyrroles. *Biochem J* 208: 479–486
- Igarishi N, Shimada K, Matsuura K and Nagashima KVP (1998) Photosynthetic gene cluster in purple bacterium, *Rubrivivax gelatinosus*. In: Garab G (ed) *Photosynthesis: Mechanisms and Effects*, pp 2889–2892. Kluwer Academic Publishers, Dordrecht
- Ikeda-Yamasaki I, Odahara T, Mitsuoka K, Fujiyoshi Y and Murata K (1998) Projection map of the reaction center-light harvesting I complex from *Rhodopseudomonas viridis* at 10 Å resolution. *FEBS Lett* 425: 505–508
- Inoue K, Kouadio JK, Mosley CS and Bauer CE (1995) Isolation and in vitro phosphorylation of sensory transduction components controlling anaerobic induction of light harvesting and reaction center gene expression in *Rhodobacter capsulatus*. *Biochemistry* 34: 391–396
- Jungas C, Ranck JL, Rigaud JL, Joliot P and Vermeglio A (1999) Supramolecular organization of the photosynthetic apparatus of *Rhodobacter sphaeroides*. *EMBO J* 18: 534–542
- Kaneko T, Sato S, Kotani H, Tanaka A, Asamizu E, Nakamura Y, Miyajima N, Hirosawa M, Sugiura M, Sasamoto S, Kimura T, Hosouchi T, Matsuno A, Muraki A, Nakazaki N, Naruo K, Okumura S, Shimpo S, Takeuchi C, Wada T, Watanabe A, Yamada M, Yasuda M and Tabata S (1996) Sequence analysis of the genome of the unicellular cyanobacterium *Synechocystis* sp. strain PCC6803. II. Sequence determination of the entire genome and assignment of potential protein-coding regions (supplement). *DNA Res* 3: 185–209
- Kerber N, Pucheu N, Tadros M, Drews G and Garcia A (1998) The phosphorylation of light-harvesting polypeptides LH1 $\alpha$  (B870) and LHII $\alpha$  (B800-850) of *Rhodobacter capsulatus* B10 was higher under chemotrophic oxic than under phototrophic anoxic growth conditions. *Curr Microbiol* 37: 32–38
- Klug G (1991a) A DNA sequence upstream of the *puf* operon of *Rhodobacter capsulatus* is involved in its oxygen-dependent regulation and functions as a protein binding site. *Mol Gen Genet* 226: 167–176
- Klug G (1991b) Endonucleolytic degradation of *puf* mRNA in *Rhodobacter capsulatus* is influenced by oxygen. *Proc Natl Acad Sci USA* 88: 1765–1769
- Klug G (1993) The role of mRNA degradation in the regulated expression of bacterial photosynthesis genes. *Mol Microbiol* 9: 1–7
- Klug G and Cohen SN (1988) Pleiotropic effects of localized *Rhodobacter capsulatus puf* operon deletions on production of light-absorbing pigment-protein complexes. *J Bacteriol* 170: 5814–5821
- Klug G and Cohen SN (1990) Combined actions of multiple hairpin loop structures and sites of rate-limiting endonucleolytic cleavage determine differential degradation rates of individual segments within polycistronic *puf* operon mRNA. *J Bacteriol* 172: 5140–5146
- Klug G and Jock S (1991) A base pair transition in a DNA sequence with dyad symmetry upstream of the *puf* promoter affects transcription of the *puc* operon in *Rhodobacter capsulatus*. *J Bacteriol* 173: 6038–6045
- Klug G, Adams CW, Belasco J, Doerge B and Cohen SN (1987) Biological effects of segmental alterations in mRNA stability: Effects of deletion of the intercistronic hairpin loop region of the *Rhodobacter capsulatus puf* operon. *EMBO J* 6: 3515–3520
- Klug G, Jock S and Rothfuchs R (1992) The rate of decay of *Rhodobacter capsulatus*-specific *puf* mRNA segments is differentially affected by RNase E activity in *Escherichia coli*. *Gene* 121: 95–102
- Koepeke J, Hu X, Muenke C, Schulten K and Michel H (1996) The crystal structure of the light-harvesting complex II (B800-850) from *Rhodospirillum rubrum*. *Structure* 4: 581–597
- Koolhaas MHC, Frese RN, Fowler GJS, Bibby TS, Georgakopoulou S, van der Zwan G, Hunter CN and van Grondelle R (1998) Identification of the upper exciton component of the B850 bacteriochlorophylls of the LH2 antenna complex, using a B800-free mutant of *Rhodobacter sphaeroides*. *Biochemistry* 37: 4693–4698
- La Roche J, van der Staay GW, Partensky F, Ducret A, Aebersold

- R, Li R, Golden SS, Hiller RG, Wrench PM, Larkum AW and Green BR (1996) Independent evolution of the prochlorophyte and green plant chlorophyll *a/b* light-harvesting proteins. *Proc Natl Acad Sci USA* 93: 15244–15248
- Lang HP and Hunter CN (1994) The relationship between carotenoid biosynthesis and the assembly of the light-harvesting LH2 complex in *Rhodobacter sphaeroides*. *Biochem J* 298: 197–205
- Langer T, Lu C, Echols H, Flanagan H, Hayer MK and Hartl FU (1992) Successive action of DnaK, DnaJ, and GroEL along the pathway of chaperone-mediated protein folding. *Nature* 356: 683–689
- LeBlanc H (1995) Directed mutagenesis and gene fusion analysis of the *Rhodobacter capsulatus* *puc* operon. Ph.D. thesis, Vancouver, University of British Columbia
- LeBlanc HN and Beatty JT (1993) *Rhodobacter capsulatus* *puc* operon: Promoter location, transcript sizes and effects of deletions on photosynthetic growth. *J Gen Microbiol* 139: 101–109
- LeBlanc HN and Beatty JT (1996) Topological analysis of the *Rhodobacter capsulatus* PucC protein and effects of C-terminal deletions on light-harvesting complex II. *J Bacteriol* 178: 4801–4806
- Leblanc H, Lang AS and Beatty JT (1999) Transcript cleavage, attenuation and an internal promoter in the *Rhodobacter capsulatus* *puc* operon. *J Bacteriol* 181: 4955–4960
- Lee JK and Kaplan S (1992) *cis*-acting regulatory elements involved in oxygen and light control of *puc* operon transcription in *Rhodobacter sphaeroides*. *J Bacteriol* 174: 1146–1157
- Lee JK and Kaplan S (1995) Transcriptional regulation of *puc* operon expression in *Rhodobacter sphaeroides*: Analysis of the *cis*-acting downstream regulatory sequence. *J Biol Chem* 270: 20453–20458
- Lee JK, Kiley PJ and Kaplan S (1989) Posttranscriptional control of *puc* operon expression of B800-850 light-harvesting complex formation in *Rhodobacter sphaeroides*. *J Bacteriol* 171: 3391–3405
- Lilburn TG, Haith CE, Prince RC and Beatty JT (1992) Pleiotropic effects of *pufX* gene deletion on the structure and function of the photosynthetic apparatus of *Rhodobacter capsulatus*. *Biochim Biophys Acta* 1100: 160–170
- Lilburn TG, Prince RC and Beatty JT (1995) Mutation of the Ser2 codon of the light-harvesting B870  $\alpha$  polypeptide of *Rhodobacter capsulatus* partially suppresses the *pufX* phenotype. *J Bacteriol* 177: 4593–4600
- Lilburn TG, Recchia PS, Parkes-Loach PA, Loach PA, Prince RC and Beatty JT (1999) Functional and structural analyses of the *Rhodobacter capsulatus* PufX protein. In: Garab G (ed) *Current Research in Photosynthesis*, pp 2841–2845. Kluwer Academic Publishers, Dordrecht
- Loach PA and Parkes-Loach PS (1995) Structure-function relationships in core light-harvesting complexes (LHI) as determined by characterization of the structural subunit and by reconstitution experiments. In: Blankenship RE, Madigan MT and Bauer CE (eds) *Anoxygenic Photosynthetic Bacteria*, pp 437–471. Kluwer Academic Publishers, Dordrecht
- Loach PA, Parkes-Loach PS, Davis CM and Heller BA (1994) Probing protein structural requirements for formation of the core light-harvesting complex of photosynthetic bacteria using hybrid reconstitution methodology. *Photosynth Res* 40: 231–245
- Mackenzie C, Choudhary M, Larimer FW, Predki PF, Stilwagen S, Armitage JP, Barber RD, Donohue TJ, Hosler JP, Newman JE, Shapleigh JP, Sockett RE, Zeilstra-Ryalls J and Kaplan S (2001) The home stretch, a first analysis of the nearly completed genome of *Rhodobacter sphaeroides* 2.4.1. *Photosynth Res* 70: 19–41
- Masuda S, Yoshida M, Nagashima KVP, Shimada K and Matsuura K (1999) A new cytochrome subunit bound to the photosynthetic reaction center in the purple bacterium, *Rhodovulum sulfidophilum*. *J Biol Chem* 274: 10795–10801
- McDermott G, Prince SM, Freer AA, Hawthornthwaite-Lawless AM, Papiz MZ, Cogdell RJ and Isaacs NW (1995) Crystal structure of an integral membrane light-harvesting complex from photosynthetic bacteria. *Nature* 374: 517–521
- McGlynn P and Hunter CN (1992) Isolation and characterization of a putative transcription factor involved in the regulation of the *Rhodobacter sphaeroides* *pucBA* operon. *J Biol Chem* 267: 11098–11103
- Meryandini A and Drews G (1996) Import and assembly of the  $\alpha$  and  $\beta$ -polypeptides of the light-harvesting complex I (B870) in the membrane system of *Rhodobacter capsulatus* investigated in an *in vitro* translation system. *Photosynth Res* 47: 21–31
- Monshouwer R, Abrahamsson M, van Mourik F and van Grondelle R (1997) Superradiance and exciton delocalization in bacterial photosynthetic light-harvesting systems. *J Phys Chem B* 101: 7241–7248
- Mosley CS, Suzuki JY and Bauer CE (1994) Identification and molecular genetic characterization of a sensor kinase responsible for coordinately regulating light harvesting and reaction center gene expression in response to anaerobiosis. *J Bacteriol* 176: 7566–7573
- Narro ML, Adams CW, and Cohen SN (1990) Isolation and characterization of *Rhodobacter capsulatus* mutants defective in oxygen regulation of the *puf* operon. *J Bacteriol* 172: 4549–4554
- Nickens DG and Bauer CE (1998) Analysis of the *puc* operon promoter from *Rhodobacter capsulatus*. *J Bacteriol* 180: 4270–4277
- Nishimura K, Shimada H, Hatanaka S, Mizoguchi H, Ohta H, Masuda T and Takamiya K-I (1998) Growth, pigmentation, and expression of the *puf* and *puc* operons in a light-responding-repressor (SPB)-disrupted *Rhodobacter sphaeroides*. *Plant Cell Physiol* 39: 411–417
- Oh JI and Kaplan S (1999) The cbb(3) terminal oxidase of *Rhodobacter sphaeroides* 2.4.1: Structural and functional implications for the regulation of spectral complex formation. *Biochemistry* 38: 2688–2696
- Oh JI and Kaplan S (2001) Generalized approach to the regulation and integration of gene expression. *Molec Microbiol* 39: 1116–1123
- Okamura MY, Paddock ML, Graige MS and Feher G (2000) Proton and electron transfer in bacterial reaction centers. *Biochim Biophys Acta* 1458: 148–163
- Oling F, Boekema EJ, de Zarate IO, Visschers R, van Grondelle R, Keegstra W, Brisson A, and Picorel R (1996) Two-dimensional crystals of LH2 light-harvesting complexes from *Ectothiorhodospira* sp. and *Rhodobacter capsulatus* investigated by electron microscopy. *Biochim Biophys Acta* 1273: 44–50
- Olsen JD, Sturgis JN, Westerhuis WHJ, Fowler GJS, Hunter CN and Robert B (1997) Site-directed modification of the ligands

- to the bacteriochlorophylls of the light-harvesting LH1 and LH2 complexes of *Rhodobacter sphaeroides*. *Biochemistry* 36: 12625–12632
- Parkes-Loach PS, Sprinkle JR and Loach PA (1988) Reconstitution of the B873 light-harvesting complex of *Rhodospirillum rubrum* from the separately isolated  $\alpha$ - and  $\beta$ -polypeptides and bacteriochlorophyll *a*. *Biochemistry* 27: 2718–2727
- Parkes-Loach PS, Michalski TJ, Bass WJ, Smith U and Loach PA (1990) Probing the bacteriochlorophyll binding site by reconstitution of the light-harvesting complex of *Rhodospirillum rubrum* with bacteriochlorophyll *a* analogues. *Biochemistry* 29: 2951–2960
- Parkes-Loach PS, Law CJ, Recchia PA, Kehoe J, Nehrlisch S, Chen J and Loach PA (2001) Role of the core region of the PufX protein in inhibition of reconstitution of the core light-harvesting complexes of *Rhodobacter sphaeroides* and *Rhodobacter capsulatus*. *Biochemistry* 40: 5593–5601
- Penfold RJ and Pemberton JM (1994) Sequencing, chromosomal inactivation, and functional expression of *ppsR*, a gene which represses carotenoid and bacteriochlorophyll synthesis in *Rhodobacter sphaeroides*. *J Bacteriol* 176: 2869–2876
- Pollich M and Klug G (1995) Identification and sequence analysis of genes involved in late steps in cobalamin (vitamin B<sub>12</sub>) synthesis in *Rhodobacter capsulatus*. *J Bacteriol* 177: 4481–4487
- Pollich M, Jock S and Klug G (1993) Identification of a gene required for the oxygen-regulated formation of the photosynthetic apparatus of *Rhodobacter capsulatus*. *Mol Microbiol* 10: 749–757
- Ponnampalam SN, Elsen S and Bauer CE (1998) Aerobic repression of the *Rhodobacter capsulatus bchC* promoter involves cooperative interactions between CrtJ bound to neighboring palindromes. *J Biol Chem* 273: 30757–30761
- Prince RC (1990) Bacterial photosynthesis: From photons to  $\Delta p$ . *Bacteria* 12: 111–149
- Pugh RJ, McGlynn P, Jones MR and Hunter CN (1998) The LHI-RC core complex of *Rhodobacter sphaeroides*: Interaction between components, time-dependent assembly, and topology of the PufX protein. *Biochim Biophys Acta* 1366: 301–316
- Recchia PA, Davis CM, Lilburn TG, Beatty JT, Parkes-Loach PS, Hunter CN and Loach PA (1998) Isolation of the PufX protein from *Rhodobacter capsulatus* and *Rhodobacter sphaeroides*: Evidence of its interaction with the  $\alpha$ -polypeptide of the core light-harvesting complex. *Biochemistry* 37: 11055–11063
- Richter P and Drews G (1991) Incorporation of light-harvesting complex I  $\alpha$  and  $\beta$  polypeptides into the intracytoplasmic membrane of *Rhodobacter capsulatus*. *J Bacteriol* 173: 5336–5345
- Richter P, Cortez N and Drews G (1991) Possible role of the highly conserved amino acids Trp-8 and Pro-13 in the N-terminal segment of the pigment-binding polypeptide LHI  $\alpha$  of *Rhodobacter capsulatus*. *FEBS Lett* 285: 80–84
- Richter P, Brand M and Drews G (1992) Characterization of LHI<sup>−</sup> and LHI<sup>+</sup> *Rhodobacter capsulatus pufA* mutants. *J Bacteriol* 174: 3030–3041
- Rodig J, Jock S and Klug G (1999) Coregulation of the syntheses of bacteriochlorophyll and pigment-binding proteins in *Rhodobacter capsulatus*. *Arch Microbiol* 171: 198–204
- Saier JM, Beatty JT, Goffeau A, Harley KT, Heijne WHM, Huang S-C, Jack DL, Jahn PS, Lew K, Liu J, Pao SS, Paulsen IT, Tseng T-T and Virk PS (1999) The major facilitator superfamily. *J Molec Microbiol Biotech* 1: 257–279
- Sganga MW and Bauer CE (1992) Regulatory factors controlling photosynthetic reaction center and light-harvesting gene expression in *Rhodobacter capsulatus*. *Cell* 68: 945–954
- Shimada H, Iba K and Takamiya K-I (1992) Blue-light irradiation reduces the expression of *puf* and *puc* operons of *Rhodobacter sphaeroides* under semi-aerobic conditions. *Plant Cell Physiol* 33: 471–475
- Shimada H, Ohta H, Masuda T, Shioi Y and Takamiya K (1993) A putative transcription factor binding to the upstream region of the *puf* operon in *Rhodobacter sphaeroides*. *FEBS Lett* 328: 41–44
- Shimada K, Yamazaki I, Tamai N and Mimuro M (1990) Excitation energy flow in a photosynthetic bacterium lacking B850. Fast energy transfer from B806 to B870 in *Erythrobacter* sp. strain OCh114. *Biochem Biophys Acta* 1016: 266–271
- Simmons AE, Mackenzie RC and Cogdell RJ (1999) Cloning and sequencing of the *pucBA* genes from two strains of *Rubrivivax gelatinosus*. *Photosynth Res* 62: 99–106
- Stahlberg H, Dubochet J, Vogel H and Ghosh R (1998a) Are the light-harvesting I complexes from *Rhodospirillum rubrum* arranged around the reaction centre in a square geometry? *J Mol Biol* 282: 819–831
- Stahlberg H, Dubochet J, Vogel H and Ghosh R (1998b) The reaction centre of the photounit of *Rhodospirillum rubrum* is anchored to the light-harvesting complex with four-fold rotational disorder. *Photosynth Res* 55: 363–368
- Stiehle H, Cortez N, Klug G and Drews G (1990) A negatively charged N terminus in the  $\alpha$  polypeptide inhibits formation of light-harvesting complex I in *Rhodobacter capsulatus*. *J Bacteriol* 172: 7131–7137
- Sturgis JN, Olsen JD, Robert B and Hunter CN (1997) Functions of conserved tryptophan residues of the core light-harvesting complex of *Rhodobacter sphaeroides*. *Biochemistry* 36: 2772–2778
- Sundstrom V and van Grondelle R (1995) Kinetics of excitation transfer and trapping in purple bacteria. In: Blankenship RE, Madigan MT and Bauer CE (eds) *Anoxygenic Photosynthetic Bacteria*, pp 349–372. Kluwer Academic Publishers, Dordrecht
- Tadros MH, Suter F, Drews G and Zuber H (1984) Isolation and complete amino acid sequence of the small polypeptide from light-harvesting pigment protein complex I (B870) of *Rhodopseudomonas capsulata*. *Eur J Biochem* 138: 209–212
- Tadros MH, Frank G, Zuber H and Drews G (1985) The complete amino acid sequence of the large bacteriochlorophyll-binding polypeptide B870 $\alpha$  from the light-harvesting complex B870 of *Rhodopseudomonas capsulata*. *FEBS Lett*, 190: 41–44
- Tadros MH, Katsiou E, Hoon MA, Yurkova N and Ramji DP (1993) Cloning of a new antenna gene cluster and expression analysis of the antenna gene family of *Rhodopseudomonas palustris*. *Eur J Biochem* 217: 867–875
- Tichy HV, Oberlé B, Stiehle H, Schiltz E and Drews G (1989) Genes downstream from *pucB* and *pucA* are essential for formation of the B800–850 complex of *Rhodobacter capsulatus*. *J Bacteriol* 171: 4914–4922
- Tichy HV, Albien KU, Gadon N and Drews G (1991) Analysis of the *Rhodobacter capsulatus puc* operon—the *pucC* gene plays a central role in the regulation of LHII (B800–850 complex) expression. *EMBO J* 10: 2949–2955



- Walz T and Ghosh R (1997) Two-dimensional crystallization of the light-harvesting I-reaction centre photounit from *Rhodospirillum rubrum*. *J Mol Biol* 265: 107–111
- Walz T, Jamieson SJ, Bowers CM, Bullough PA and Hunter CN (1998) Projection structures of three photosynthetic complexes from *Rhodobacter sphaeroides*: LH2 at 6 Å, LH1 and RC-LH1 at 25 Å. *J Mol Biol* 282: 833–845
- Wellington CL and Beatty JT (1991) Overlapping mRNA transcripts of photosynthesis gene operons in *Rhodobacter capsulatus*. *J Bacteriol* 173: 1432–1443
- Wellington CL, Taggart AKP and Beatty JT (1991) Functional significance of overlapping transcripts of *crtEF*, *bchCA*, and *puf* photosynthesis gene operons in *Rhodobacter capsulatus*. *J Bacteriol* 173: 2954–2961
- Wellington CL, Bauer CE and Beatty JT (1992) Photosynthesis gene superoperons in purple nonsulfur bacteria: The tip of the iceberg? *Can J Microbiol* 38: 20–27
- Wiessner C (1990) Molekularbiologische analyse der gene des photosynthetischen apparates von *Rhodopseudomonas viridis*. Ph.D thesis, Frankfurt, Johann Wolfgang Goethe-Universität
- Wong DK-H, Collins WJ, Harmer A, Lilburn TG and Beatty JT (1996) Directed mutagenesis of the *Rhodobacter capsulatus* *puhA* gene and orf214: pleiotropic effects on photosynthesis reaction center and light-harvesting 1 complexes. *J Bacteriol* 178: 2334–2342
- Yeliseev AA, Krueger K and Kaplan S (1997) A mammalian mitochondrial drug receptor functions as a bacterial 'oxygen' sensor. *Proc Natl Acad Sci USA* 94: 5101–5106
- Young CS (1997) The role of the *Rhodobacter capsulatus* integral membrane protein, ORF1696, in LHI complex assembly. Ph.D. thesis, Vancouver., University of British Columbia
- Young CS and Beatty JT (1998) Topological model of the *Rhodobacter capsulatus* light-harvesting complex I assembly protein LhaA (previously known as ORF1696). *J Bacteriol* 180: 4742–4745
- Young CS and Beatty JT (1999) Structural and functional analysis of the ORF1696/PucC family of light-harvesting complex assembly proteins. In: Peschek et al. (eds) *The Phototrophic Prokaryotes*, pp 113–126. Kluwer Academic/Plenum Publishers, New York
- Young CS, Reyes RC and Beatty JT (1998) Genetic complementation and kinetic analyses of *Rhodobacter capsulatus* ORF1696 mutants indicate that the ORF1696 protein enhances assembly of the light-harvesting I complex. *J Bacteriol* 180: 1759–1765
- Youvan DC, Bylina EJ, Alberti M, Begusch H and Hearst JE (1984) Nucleotide and deduced polypeptide sequences of the photosynthetic reaction-center, B870 antenna and flanking polypeptides from *R. capsulata*. *Cell* 37: 949–957
- Yurkov VV and Beatty JT (1998) Aerobic anoxygenic phototrophic bacteria. *Microbiol Mol Biol Rev* 62: 695–724
- Zeilstra-Ryalls JH and Kaplan S (1998) Role of the *fmrL* gene in photosystem gene expression and photosynthetic growth of *Rhodobacter sphaeroides* 2.4.1. *J Bacteriol* 180: 1496–1503
- Zeilstra-Ryalls JH, Gabbert K, Mouncey NJ, Kaplan S and Kranz RG (1997) Analysis of the *fmrL* gene and its function in *Rhodobacter capsulatus*. *J Bacteriol* 179: 7264–7273
- Zeilstra-Ryalls J, Gomelsky M, Eraso JM, Yeliseev A, O'Gara J and Kaplan S (1998) Control of photosystem formation in *Rhodobacter sphaeroides*. *J Bacteriol* 180: 2801–2809
- Zhu YS and Hearst JE (1986) Regulation of expression of genes for light-harvesting antenna proteins LH-I and LH-II; reaction center polypeptides RC-L, RC-M, biosynthesis in *Rhodobacter capsulatus* by light and oxygen. *Proc Natl Acad Sci USA* 83: 7613–7617
- Zhu YS, Cook DN, Leach F, Armstrong GA, Alberti M and Hearst JE (1986) Oxygen-regulated mRNAs for light-harvesting and reaction center complexes and for bacteriochlorophyll and carotenoid biosynthesis in *Rhodobacter capsulatus* during the shift from anaerobic to aerobic growth. *J Bacteriol* 168: 1180–1188
- Zsebo KM and Hearst JE (1984) Genetic-physical mapping of a photosynthetic gene cluster from *Rhodopseudomonas capsulata*. *Cell* 37: 937–947
- Zuber H and Cogdell RJ (1995) Structure and organization of purple bacterial antenna complexes. In: Blankenship RE, Madigan MT and Bauer CE (eds) *Anoxygenic Photosynthetic Bacteria*, pp 315–348. Kluwer Academic Publishers, Dordrecht
- Zucconi AP and Beatty JT (1988) Posttranscriptional regulation by light of the steady-state levels of mature B800-850 light-harvesting complexes in *Rhodobacter capsulatus*. *J Bacteriol* 170: 877–882



# Chapter 17

## Environmental Regulation of Phycobilisome Biosynthesis

Arthur R. Grossman\*

*Department of Plant Biology, The Carnegie Institution of Washington,  
260 Panama Street, Stanford, CA 94305, U.S.A.*

Lorraine G. van Waasbergen

*Department of Biology, Box 19498, University of Texas at Arlington,  
Arlington, TX 76019, U.S.A.*

David Kehoe

*Department of Biological Sciences, Jordan Hall, Indiana University,  
Bloomington, IN 47401, U.S.A.*

Summary .....	471
I. Introduction .....	472
II. Phycobilisome Structure .....	472
III. Complementary Chromatic Adaptation .....	473
A. History .....	473
B. Organization and Expression of Genes Encoding PBS Components .....	473
C. The Photobiology of Complementary Chromatic Adaptation .....	476
D. In vivo and In vitro Promoter Analysis .....	476
E. Use of Mutants and Genetic Techniques to Dissect Complementary Chromatic Adaptation .....	477
IV. Model for the Control of Complementary Chromatic Adaptation .....	481
V. Control of Phycobilisome Biosynthesis During Nutrient Limitation .....	482
A. Specific Responses to Nutrient Limitation .....	482
B. General Responses to Nutrient Stress .....	483
C. Model for Control by Nutrient Deprivation .....	486
VI. Concluding Remarks .....	488
Acknowledgments .....	488
References .....	488

### Summary

Photosynthetic activity and the composition of the photosynthetic apparatus are strongly regulated by environmental conditions. Some of the most visually dramatic changes in pigmentation of cyanobacteria during changing nutrient and light conditions reflect marked alterations in components of the major light-harvesting complex in these organisms, the phycobilisome. In some cyanobacteria the composition of the phycobilisome is very sensitive to the wavelengths of light in the environment. The populations of the different pigmented polypeptides or phycobiliproteins, phycocyanin and phycoerythrin, of the phycobilisome are adjusted to optimize absorption of excitation energy present in the environment. This process, called complementary chromatic adaptation, is controlled by a photoreceptor that binds a bilin chromophore and has some similarity to phytochrome of vascular plants. This photoreceptor is thought to represent the first element of a phosphorelay system that regulates genes encoding the phycobiliprotein subunits and linker polypeptides. Phycobilisomes

---

\*Author for correspondence, email: arthur@andrew2.stanford.edu

are also sensitive to nutrient levels and during starvation conditions there is both reduced synthesis and elevated breakdown of phycobilisomes. The degradation of phycobilisomes during nutrient-limited growth results in cells that lose their brilliant blue-green color and appear yellow green or bleached. This bleaching response is controlled by a 'global' regulatory system that may sense the redox state of the cell, the generation of reactive oxygen species and the quality of light in the environment. Some of the regulatory elements critical for controlling nutrient stress responses are also involved in modulating photosynthetic activity when cyanobacteria experience high light conditions. The analyses of these systems highlight the molecular flexibility incorporated into the biosynthetic processes required for construction and maintenance of a light harvesting complex and the nature of the key control elements that interface with environmental cues. At a more basic level, these studies suggest the robustly dynamic nature of the entire photosynthetic apparatus.

## I. Introduction

The colors of plants and algae reflect the pigment-protein complexes that enable these organisms to gather and utilize light energy. Abundant pigment-protein complexes function as light harvesting complexes (LHC) that gather light energy and funnel that energy into the photosynthetic reaction centers. Several different LHC types have evolved with specific chromophores and spectral characteristics (Grossman et al., 1995); most LHC diversity is found amongst members of the different algal groups. LHC types include the chlorophyll *a*, *b* binding proteins of vascular plants and green algae (Jansson, 1994; Green and Durnford, 1996; Durnford et al., 1999), the chlorophyll *a*, *b* binding proteins of the prochlorophytes (LaRoche et al., 1996; van der Staay et al., 1998), the fucoxanthin chlorophyll *a*, *c* proteins of the diatoms and brown algae (Hiller et al., 1991), the peridinin chlorophyll *a* proteins of dinoflagellates (Hofmann et al., 1996) and the phycobilisomes (PBS) of red algae and cyanobacteria (Glazer, 1985; Tandeau de Marsac and Houmard, 1993; Grossman et al., 1995).

---

*Abbreviations:* AP – allophycocyanin;  $\alpha$  PC – the alpha subunit of phycocyanin;  $\beta$  PC – the beta subunit of phycocyanin; CCA – complementary chromatic adaptation; DBMIB – 2,5-bromo-3-methyl-6-isopropyl-*p*-benzoquinone; DCMU – 3-(3,4-dichlorophenyl)-1,1-dimethylurea; GL – green light; FAD – flavin adenine dinucleotide; FMN – flavin mononucleotide; GUS –  $\beta$ -glucuronidase; L – linker polypeptides; LHC – light harvesting complex; PAS – from the PER, ARNT and SIM proteins, in which the domain was first identified; it is often involved in sensing light, redox potential, oxygen and overall energy metabolism in cells; PBS – phycobilisomes; PC – phycocyanin; PC<sub>c</sub> – constitutively expressed PC subunits; PC<sub>i</sub> – red light inducible PC subunits; PC<sub>s</sub> – PC subunits expressed during sulfur limited growth; PE – phycoerythrin; PEC – phycoerythrocyanin; Q<sub>A</sub> – the primary quinone acceptor of Photosystem II; RL – red light

## II. Phycobilisome Structure

PBS are macromolecular complexes present in cyanobacteria and red algae that may constitute 40% of total cellular protein. These peripheral membrane complexes are attached to the outer surface of the thylakoids where they absorb photons and efficiently transfer excitation energy to the photosynthetic reaction centers (Porter et al., 1978; Searle et al., 1978).

The PBS is organized into two structural domains, the core and the rods (Fig. 1), each containing both pigmented and nonpigmented polypeptides. All cyanobacterial and red algal PBS have the chromoproteins (phycobiliproteins) allophycocyanin (AP) and phycocyanin (PC), while many also contain phycoerythrin (PE) or phycoerythrocyanin (PEC). In a number of cases the phycobiliprotein composition of the PBS is altered by light quality (see below). Characteristic phycobiliprotein colors are a consequence of light absorption by linear tetrapyrrole chromophores that are associated with the apoproteins through thioether linkages (Glazer, 1982, 1985). Specific lyases catalyze the attachment of the chromophore to the apoprotein (Fairchild et al., 1992; Fairchild and Glazer, 1994). The phycobiliproteins associate as heterodimers (termed a monomer in the literature) composed of  $\alpha$  and  $\beta$  subunits, that aggregate into trimers ( $\alpha\beta$ )<sub>3</sub> and hexamers ( $\alpha\beta$ )<sub>6</sub>. Nonchromophorylated linker polypeptides (L) facilitate assembly of phycobiliprotein aggregates, stabilize the structure (Glazer, 1982, 1985), and modulate the absorption characteristics of the phycobiliproteins to promote unidirectional flow of excitation energy into the photosynthetic reaction centers.

The PBS core is composed of AP trimers and both pigmented and nonpigmented L polypeptides (Table 1). A high molecular mass core polypeptide,

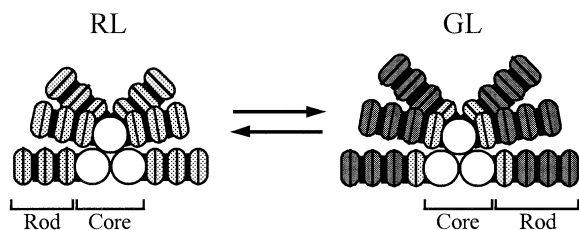


Fig. 1. Architecture of the PBS of the filamentous cyanobacterium *Fremyella diplosiphon* in red light (RL) and green light (GL). The lower portion of the PBS core (AP, white circles) is associated with thylakoid membranes and the rods contain PC (light gray) and/or PE (dark gray). Non-chromophorylated linker polypeptides (blackened areas) serve as scaffolds in the overall structure.

$L_{CM}$  (also called anchor protein), has homology to both phycobiliproteins and L polypeptides (Capuano et al., 1991). The phycobiliprotein-like domain binds a tetrapyrrole chromophore and can serve as a PBS terminal energy acceptor, facilitating excitation energy transfer to photosynthetic reaction centers. The ApcD and ApcF proteins of the phycobilisome core are also critical for transfer of excitation energy to reaction centers (Ashby and Mullineaux, 1999). Generally, six rods, each composed of stacks of PC and PE hexamers, radiate from the core and give the PBS a fan-like appearance. A more detailed description of PBS structure can be found in a number of reviews (Gantt, 1981; Glazer et al., 1983; Glazer, 1985; Sidler, 1994) and is included in Chapter 9 of this volume.

### III. Complementary Chromatic Adaptation

PBS biosynthesis and degradation are dynamic processes that are finely tuned to environmental conditions. Nutrient levels (Yamanaka and Glazer, 1980; Collier and Grossman, 1992, 1994), light quality and light quantity can all dramatically alter the level and composition of the PBS (Bogorad, 1975; Tandeau de Marsac, 1983; Grossman, 1990; Grossman et al., 1993; Tandeau de Marsac and Houmard, 1993). The phenomenon in which the PBS composition changes in response to specific wavelengths of light is linked at both functional and evolutionary levels to photoperception in vascular plants.

#### A. History

Reports that some cyanobacteria have different

pigmentation depending on the wavelengths of light in the environment appeared as early as the 1880s (Engelmann, 1883a; 1883b; 1884). The control of pigmentation in cyanobacteria by light was termed complementary chromatic adaptation (CCA) (Gaidukov, 1903). Following the initial observation of CCA, 90 years passed before Bennett and Bogorad (1971, 1973) demonstrated that the phenomenon of CCA was a consequence of changes in the PBS pigment-protein composition. Action spectra of CCA for the filamentous cyanobacteria *F. diplosiphon* (similar to *Calothrix* PCC 7601) (Haury and Bogorad, 1977; Vogelmann and Scheibe, 1978) and *Tolypothrix tenuis* (Diakoff and Scheibe, 1973) were also measured. The development of molecular tools in the 1970s created new opportunities for elucidating the regulation of PBS biosynthesis. By the latter part of the 1980s, most genes encoding PBS structural polypeptides were cloned, sequenced and their expression characterized (Tandeau de Marsac and Houmard, 1993; Grossman et al., 1994). Furthermore, the isolation and analysis of numerous mutants in CCA (Cobley and Miranda, 1983; Tandeau de Marsac, 1983; Bruns et al., 1989; Chiang et al., 1992) promoted the identification of regulatory elements critical for its control.

#### B. Organization and Expression of Genes Encoding PBS Components

In *F. diplosiphon* the PE:PC ratios reflect the spectral distribution of light in the environment (Tandeau de Marsac, 1977; Bryant, 1981; Bryant and Cohen-Bazire, 1981). Specifically, RL-grown *F. diplosiphon* contains almost no PE and each of the PBS rods has as many as three PC hexamers (associated with specific L polypeptides) (see Fig. 1). If the organism is moved to GL, new PBS are synthesized that contain rods with single PC hexamers (core proximal hexamer) and up to three PE hexamers (and their specific L polypeptides). As the cells grow and replicate, the blue-pigmented PBS of RL-grown cells are gradually diluted and the cells appear more and more red in color. This process is reversible and if the cells are moved back into RL they will once again synthesize PC and stop producing PE. Since PC absorbs light in the red (abs  $\lambda_{max}$  = 620nm) and PE in the green (abs  $\lambda_{max}$  = 560nm), these light-responsive changes in PBS composition facilitate the efficient harvesting of the prevalent wavelengths of light in the environment.

Table 1. Phycobilisome Structural, Biosynthetic and Regulatory Polypeptides<sup>1</sup>

		Expression <sup>2</sup>		
	Gene	RL	GL	Reference
<b>I. Phycobilisome Core</b>				
APC ( $\alpha\beta$ ) <sup>AP</sup>	<i>apcAB</i>	++	++	Houmard et al. (1988a)
Core Linker (L <sub>C</sub> <sup>7,8</sup> )	<i>apcC</i>	++	++	Houmard et al. (1988a)
Core Membrane Linker (L <sub>CM</sub> <sup>120</sup> )	<i>apcE</i>	++	++	Houmard et al. (1988a); Houmard et al. (1990)
Specialized APC subunits				
$\alpha$ <sup>APB</sup>	<i>apcD</i>	++	++	Houmard et al. (1988b)
$\alpha$ <sup>AP2</sup>				
$\beta$ <sup>AP18</sup>	<i>apcF</i>	++	++	
<b>II. Phycobilisome Rods</b>				
Constitutive PC	<i>cpcB1A1</i>	++	++	Conley et al. (1985); Mazel et al. (1988)
Red Light-Inducible PC	<i>cpcB2A2</i>	++	–	Conley et al. (1985)
Sulfur-Stress Inducible PC	<i>cpcB3A3</i>	–	–	Mazel et al. (1988)
Green Light-Inducible PE	<i>cpeBA</i>	–	++	Mazel et al. (1986)
Rod-Core Linker	<i>cpcG</i>	++	++	
Rod Linker				
L <sub>R</sub> <sup>30.5</sup>	<i>cpcH</i>	++	–	Lomax et al. (1987)
L <sub>R</sub> <sup>32.5</sup>	<i>cpcI</i>	++	–	Lomax et al. (1987)
L <sub>R</sub> <sup>9.7</sup>	<i>cpcD</i>	++	–	Lomax et al. (1987)
L <sub>R</sub> <sup>31.8</sup>	<i>cpeC</i>	–	++	Federspiel and Grossman (1990)
L <sub>R</sub> <sup>27.9</sup>	<i>cpcD</i>	–	++	Federspiel and Grossman (1990)
L <sub>R</sub> <sup>27.6</sup>	<i>cpcE</i>	–	++	Federspiel and Scott (1992)
<b>III. Proteins involved in biosynthesis</b>				
CpcEF	<i>cpcEF</i>	+	+	Mazel et al. (1988) Tandeau de Marsac et al. (1988)
CpeYZ	<i>cpeYZ</i>			Tandeau de Marsac et al. (1988)
NblA <sup>3</sup>	<i>nblA</i>			Collier and Grossman (1994)
NblB <sup>4</sup>	<i>nblB</i>			Dolganov and Grossman (1999)
<b>IV. Proteins involved in regulation<sup>5</sup></b>				
RcaA (protein not isolated)	<i>rcaA</i>			Sobczyk et al. (1993)
RcaB (PEPB) (protein not isolated)	<i>rcaB</i>			Sobczyk et al. (1993)
RcaC (complex response regulator)	<i>rcaC</i>			Chiang et al. (1992)
RcaD (protein not isolated)	<i>rcaD</i>			Sobczyk et al. (1994)
RcaE (phytochrome-like photoreceptor)	<i>rcaE</i>			Kehoe and Grossman (1996)
RcaF (response regulator)	<i>rcaF</i>			Kehoe and Grossman (1997)
RpbA (putative <i>cpcB1A1</i> repressor)	<i>rpbA</i>			Kahn and Schaefer (1997)
NblR (response regulator)	<i>nblR</i>			Schwarz and Grossman (1998)
NblS (sensor histidine kinase)	<i>nblS</i>			van Waasbergen et al. (2002)
CpeR (putative ser/thr phosphatase)	<i>cpeR</i>			Seib and Kehoe (2002)

<sup>1</sup> Most of the proteins and genes listed in this table are from *Freymella diplosiphon* or *Calothrix* PCC 7601. Homologous proteins are present in other cyanobacteria. Where no reference is given, there is no report of the isolation and characterization of the gene in either *F. diplosiphon* or *Calothrix* PCC 7601.

<sup>2</sup> High expression is indicated as ++ while very low or no expression as –. If the column under RL or GL is not filled in then expression was not tested in red and green light.

<sup>3</sup> The *nblA* gene is expressed primarily during nutrient stress conditions in *Synechococcus* PCC 7942 (Collier and Grossman, 1994).

<sup>4</sup> The *nblB* gene is constitutively expressed in *Synechococcus* PCC 7942 (Dolganov and Grossman, 1999).

<sup>5</sup> Some of the genes in this category (*rcaA*, *rcaB*, *rcaD*) have not been isolated but instead have been studied biochemically.

The cloning and characterization of a number of genes encoding structural components of the PBS provided the foundation necessary for elucidating regulatory events that control CCA (summarized in Grossman et al., 1995; Grossman and Kehoe, 1997). Genes encoding  $\alpha$  and  $\beta$  subunits of each of the

phycobiliproteins are contiguous on the genome and are cotranscribed. In many cases, polycistronic transcripts, in addition to encoding phycobiliprotein subunits, also encode their associated L polypeptides. Furthermore, in a number of organisms there is more than one gene for the same phycobiliprotein subunit

(see below). A number of proteins that control the biogenesis of PBS have also been partially characterized, and in some cases the genes encoding these polypeptides have been cloned (Kehoe and Grossman, 1996, 1997; Kahn and Schaefer, 1997; Manna et al., 2000). Features of the structural components of the PBS and the regulatory factors involved in PBS biosynthesis are presented in Table 1. Figure 2 depicts the clustering of the genes encoding PBS polypeptides into operons.

In *F. diplosiphon* and *Calothrix* PCC 7601,  $\alpha$  and  $\beta$ AP subunits (designated  $\alpha^{AP}$  and  $\beta^{AP}$ , respectively), encoded by the *apcA1B1* genes, are in an operon that also contains the *apcC1* and *apcE1* genes. The latter two genes encode the core linker polypeptide and the  $L_{CM}$  protein (or anchor protein), respectively (Houmard et al., 1988a,b). This gene cluster is unlinked to two other genes encoding core polypeptides; the *apcD* gene encodes a modified  $\beta$  subunit of AP that serves, along with the  $L_{CM}$ , as a terminal energy acceptor within the PBS and the *apcA2* gene encodes a specialized  $\alpha$ -like AP subunit. The genes encoding core polypeptides (*apcEABC*) are not differentially regulated during CCA.

There are three distinct operons encoding  $\alpha^{PC}$  and  $\beta^{PC}$  subunits (*cpcBA* genes) in *F. diplosiphon* (Conley et al., 1985, 1986, 1988; Mazel et al., 1988; Mazel and Marliere, 1989). The *cpcB1A1* operon is constitutively transcribed and encodes  $PC_c$  subunits

(the subscript indicating that it is constitutive). These genes are regulated by a repressor that is designated RpbA; mutants in the *rpbA* appear bluer than wild type cells and exhibit elevated levels of the *cpcB1A1* transcripts (Kahn et al., 1997). Furthermore the RpbA protein was shown to bind to the *cpcB1A1* promoter (Manna et al., 2000). The operon containing *cpcB1A1* also contains the *cpcE* and *cpcF* genes, which encode a lyase involved in attaching the tetrapyrrole chromophores to the  $\alpha$  subunit of PC (Fairchild et al., 1992; Fairchild and Glazer, 1994). The  $PC_c$  hexamers are located immediately proximal to the PBS core.

The *cpcB2A2* operon is specifically active in RL (inactive in GL) and encodes  $PC_i$  (the subscript indicating that it is inducible), which is critical for CCA. Hexamers of  $PC_i$  represent the major component of PBS rods when cyanobacterial cells are grown in RL. Three genes, designated *cpcH2*, *cpcI2* and *cpcD2* (Lomax et al., 1987), encoding the L proteins that associate with  $PC_i$ , are cotranscribed with *cpcB2A2*. Furthermore, the *cpcB2A2H2I2D2* operon is clustered on the *F. diplosiphon* genome along with *cpcB1A1* and *apcE1A1B1C1* (Conley et al., 1986).

A third PC operon contains *cpcB3A3* plus the genes encoding associated L polypeptides. This operon is only active during sulfur-limited growth (Mazel and Marliere, 1989) and the PC encoded by this operon has been designated  $PC_s$  (the subscript

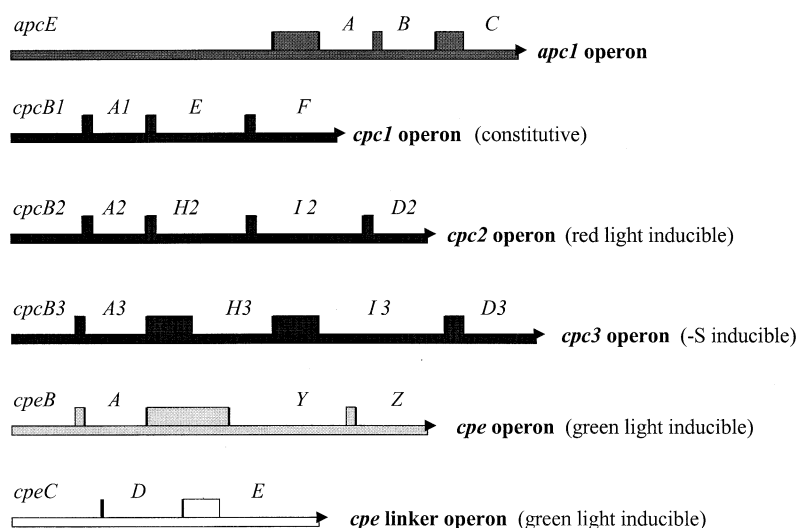


Fig. 2. Diagram of operons encoding phycobiliprotein and linker polypeptides in *Fremyella diplosiphon* and *Calothrix* PCC 7601. The thickened segments of the lines represent intergenic regions. The functions of the different genes in each of the operons and regulatory features of the operons (indicated in Table 1 and to the right of the operon in this figure) are discussed in the text. All of the operons are transcribed from left to right.

indicating activation during sulfur-limitation). The only sulfur-containing amino acids in the  $\alpha$  and  $\beta$  subunits of PC<sub>s</sub> are the cysteines essential for the attachment of the phycobilin chromophores. Hence, when starved for sulfur, *F. diplosiphon* can conserve this nutrient by substituting PC<sub>i</sub> and perhaps PC<sub>c</sub> with PC<sub>s</sub>.

The *cpeBA* operon encodes  $\alpha$  and  $\beta$  subunits of PE (Mazel et al., 1986). In contrast to the situation for the *cpc* and the *apc* operons, the genes encoding the L polypeptides that associate with PE are not contiguous on the genome; they are encoded by the *cpeCDE* operon (Federspiel and Grossman, 1990; Federspiel and Scott, 1992). However, activation and suppression of *cpeBA* and *cpeCDE* are coordinated. Furthermore, the *cpeBA* genes are linked to *cpeY* and *cpeZ*, which are thought to encode the lyase that catalyzes the attachment of the chromophore to the PE apoprotein (Kahn et al., 1997).

### C. The Photobiology of Complementary Chromatic Adaptation

Action spectra for PC and PE synthesis have been measured for both *T. tenuis* and *F. diplosiphon* by quantifying the PE to PC ratios after exposure of the cyanobacteria to narrow bands of light of defined wavelengths (Haury and Bogorad, 1977; Vogelmann and Scheibe, 1978). Maximal PE synthesis and minimal PC synthesis occurred following exposure to 550 nm GL, while maximal PC synthesis and minimal PE synthesis occurred following exposure to 640 nm RL. Synthesis of PC is also stimulated by UV irradiation of 340–360 nm light.

These data suggested that the photoreceptor(s) controlling CCA absorbed GL and RL (either through one or multiple chromophores), but elicited different responses in the two light qualities. PC synthesis and assembly into PBS dominates in RL while PE synthesis and assembly into PBS dominates in GL. In natural sunlight the mixture of RL and GL results in a PBS with intermediate levels of PC and PE.

Fluence response characteristics of *cpcBA* and *cpeBA* expression in *F. diplosiphon* have been measured (Oelmüller et al., 1988a,b). Twice as many photons of light were needed to increase and decrease the abundance of the *cpeBA* mRNAs as were needed to increase and decrease the abundance of the *cpcB2A2* mRNAs. Since there is little change in the half-lives of the mRNAs encoding the phycobili-proteins in RL and GL, the levels of PE and PC<sub>i</sub>

appear to be primarily regulated by changes in the rates of transcription of the *cpeBA* and *cpcB2A2* operons, respectively. These findings raise the possibilities that two separate photoreceptors are involved in controlling the activities of *cpeBA* and *cpcB2A2*, or that signals generated by a single photoreceptor have different efficiencies in modulating *cpeBA* and *cpcB2A2* transcription. Genetic evidence suggests that the latter may be the case (see below).

### D. In vivo and In vitro Promoter Analysis

Proteins in extracts from GL- and RL-grown *F. diplosiphon* that bind to the promoter regions of genes encoding phycobiliproteins and potentially control their expression have been examined in vitro. Three polypeptides appeared to interact with the *cpeBA* promoter in the region positioned –110 to +81 relative to the transcription start site (Sobczyk et al., 1993). One binding protein was identified as RNA polymerase; in vitro DNase I footprinting suggested that RNA polymerase binds to sequences from –40 to +15. Two other polypeptides, designated RcaA and RcaB, also interacted with the *cpeBA* promoter and were only detected in cells maintained in GL. RcaA bound the sequence between –67 and –45; this sequence contains a tandem 5' TTGTTA3' repeat (the two repeat sequences are separated by 4 bp). The exact position of the binding site for RcaB is not clear. While phosphatase treatment did not inhibit the binding of RcaB or RNA polymerase, it did abolish the binding activity of RcaA.

Protein-DNA interactions with the –67 to –44 sequence of *cpeBA* operon were also observed by Schmidt-Goff and Federspiel (1993) using in vivo footprinting, in vitro electrophoretic mobility shift assays, and DMS and DNase I in vitro footprinting. A protein, designated PepB (PE promoter-binding protein), bound to and protected the 5' TTGTTA3' direct repeat located upstream of the transcription start site. Since RcaA and PepB appear to bind the same sequences, it is likely that they are identical proteins. However, there is a major difference between the binding activities observed by Sobczyk et al. (1993) and Schmidt-Goff and Federspiel (1993). In the former study RcaA binding activity was not detected in protein extracts from RL-grown cells, while in the latter study protein extracts from both RL- and GL-grown cells contained PepB binding activity. These contradictory findings remain to be

resolved, although they may reflect different physiological states of the cells used in the two studies.

It is also uncertain if the 5'TTGTTA3' tandem repeat, which is located upstream of the transcription start site of the *cpeBA* operon, plays a major role in controlling expression of phycobiliprotein genes. The sequence is present in *cpeBA* promoters from other cyanobacteria in which PE synthesis is modulated by the wavelength of light. However, it is not present in the *cpeCDE* operon, in spite of the fact that this operon is controlled identically to *cpeBA*. Therefore, if the 5'TTGTTA3' motif is important for CCA, additional elements must be involved in coordinating the transcriptional responses of *cpeBA* and *cpeCDE*.

Interactions of the *cpcB2A2* promoter with soluble *F. diplosiphon* protein have also been examined. Proteins from RL- and GL-grown *F. diplosiphon* cells bind to the -298 to +25 region of the *cpcB2A2* operon (Casey and Grossman, 1994). Based on DNase I footprinting, the major binding was to the sequence extending from -162 to -126. To determine if this region of the promoter was critical for CCA, a chimeric reporter gene was constructed in which the various regions of the *cpcB2A2* promoter were fused to the  $\beta$ -glucuronidase gene (*GUS*). These promoter constructs were reintroduced into *F. diplosiphon*, and the transformants were assayed for light-responsive *GUS* activity. This study demonstrated that the footprinted region was not critical for CCA. In fact, a sequence extending from -76 to +25 relative to the *cpcB2A2* transcription start site was all that was required to confer RL/GL responsiveness to *GUS* expression. When the promoter region was truncated to -37, RL was no longer effective in activating *GUS* and *GUS* activity remained low in both RL and GL. Hence, sequences between -76 and -37 are essential for the activity of the *cpcB2A2* promoter.

Electrophoretic mobility shift assays were used to demonstrate that there was a protein that could bind to the -76 to +25 region of the *cpcB2A2* operon. The binding activity was present in extracts from RL-grown but not GL-grown cells. Furthermore, a DNA fragment from -37 to +25 was able to specifically compete for this binding activity (Casey and Grossman, 1994), suggesting that the sequence from -37 to +25 interacts with a protein that is either only present or only binds in RL-grown cells. This region contains a direct repeat of 5'AAATTGACAAA3'.

Together, the results suggest that the -76 to -37 region of *cpcB2A2* operon contains an element(s) required for overall promoter activity while the -37 to +25 sequence binds a regulatory element that can promote RL-specific transcription from *cpcB2A2*.

### *E. Use of Mutants and Genetic Techniques to Dissect Complementary Chromatic Adaptation*

The studies most effective in revealing factors that control CCA involved mutant generation, characterization and complementation. The isolation of a variety of mutants in CCA (Cobley and Miranda, 1983; Tandeau de Marsac, 1983; Bruns et al., 1989; Chiang et al., 1992; Kehoe and Grossman, 1996) established several mutant classes; these classes included the red (FdR), blue (FdB), green (FdG) and black (FdBk) mutants. At least one of these mutant phenotypes can result from lesions in any of a number of different loci (see below). The FdR mutants appear red under all conditions of illumination; they constitutively synthesize PE while  $PC_i$  is never synthesized. The FdB strains are bluer than wild-type cells in RL and require more GL to suppress  $PC_i$  synthesis than wild-type cells (Casey et al., 1997). The FdG strains exhibit normal  $PC_i$  expression, but the PE genes never become active. In the FdBk mutants there are moderate levels of both PE and  $PC_i$ , however, these levels remain the same in RL and GL (Grossman and Kehoe, 1996, 1997).

Initially, the FdR mutants were most extensively characterized. These strains are fixed in a response normally exhibited only in GL. The patterns of transcript accumulation in the FdR mutants reflect the altered patterns of PE and  $PC_i$  accumulation, suggesting aberrant transcriptional regulation of both the *cpeBA* and *cpcB2A2* operons (Bruns et al., 1989).

The first successful complementation was of the FdR strains with a wild-type recombinant library of *F. diplosiphon* genomic DNA in a plasmid (kanamycin resistance marker gene) originally constructed by John Cobley (Chiang et al., 1992; Schaefer et al., 1993). When the selection pressure was removed from the complemented strain, the wild-type phenotype reverted to that of the mutant. This suggests that elimination of the selective pressure allows the cells to grow at a rate that exceeds the replication rate of the recombinant plasmid. The complementing gene, designated *rcaC*, in the original red mutant was interrupted by an insertion; this insertion probably resulted from transposition of an endogenous, mobile



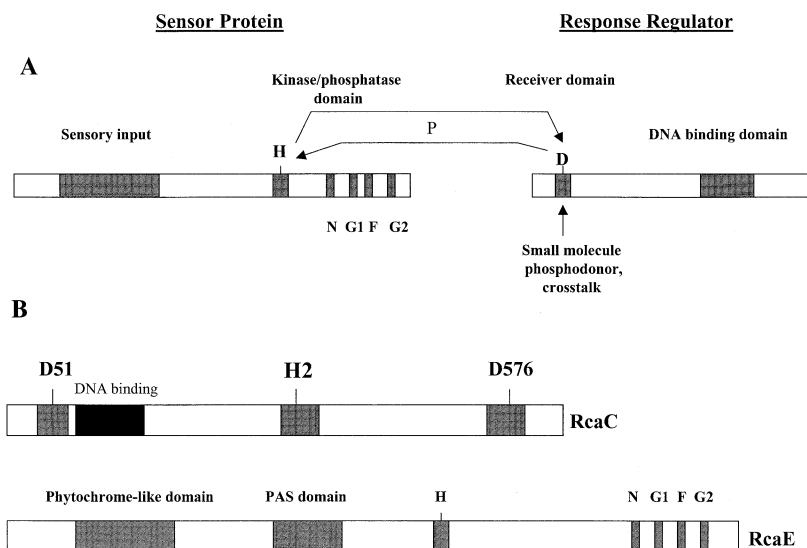


Fig. 3. Two component regulators (A) and the specific regulatory proteins associated with chromatic adaptation (B). Each of the functional domains within the proteins are indicated. A) The sensor protein can catalyze autophosphorylation of the histidine (H) of the H block. The motifs required for phosphorylation are designated N, G1, F and G2. The phosphate associated with the histidine can be transferred to an aspartate residue (D) in the receiver domain of the response regulator. This aspartate can be phosphorylated to some extent by cross-talk with other sensors in the cell or by small molecule phosphodonors. The sensor can also act as a phosphatase and maintain the response regulator in a dephosphorylated state. Phosphorylation of the response regulator can alter the affinity of the DNA binding domain for specific promoters. B) RcaC is an atypical response regulator that is critical for CCA. This protein has two receiver domains with the characteristic aspartates at positions 51 (D51) and 576 (D576), an H2 or histidine phosphotransfer domain that is potentially phosphorylated, and a DNA binding domain. RcaE is the putative sensor that controls CCA. This polypeptide has motifs that are associated with histidine kinase activity (N, G1, F, G2), an H block with a histidine (H) that is potentially phosphorylated, a sequence similar to the chromophore binding domain of vascular plant phytochromes (Phytochrome-like domain) and a PAS domain.

genetic element (Chiang et al., 1992; Kahn and Schaefer, 1998).

The *rcaC* gene encodes a polypeptide of 651 amino acids with sequence similarities to response regulators of two component regulatory systems (for a review see Parkinson and Kofoed, 1992; Appleby et al., 1996). The most simple type of two component regulatory system is depicted in Fig. 3A. These systems have both sensor and response regulator polypeptides. The sensor polypeptides are histidine kinases; upon sensing a specific environmental stimulus they undergo autophosphorylation. N, G1, F and G2 domains contain the information required for kinase activity and the H block contains the phospho-accepting histidine. Following autophosphorylation, the phosphoryl group is passed to an aspartate residue in the conserved receiver domain of a response regulator. Sensor proteins also exhibit phosphatase activity and, under certain conditions, may promote dephosphorylation of their partner response regulator. Often, the response regulator is a transcription factor that binds specific promoter sequences and alters the transcriptional activity of

genes; promoter-binding activity may be regulated by the reversible phosphorylation of the aspartate residue. Also, more than one sensor or response regulator may exist within any given pathway. Typically the perception of an environmental signal (such as light) would trigger a phosphorelay that results in the activation of a number of genes via the phosphorylation of a response regulator (Parkinson and Kofoed, 1992).

RcaC is an unusual response regulator. It is approximately twice as large (73 kDa) as most response regulators and has two, instead of one, conserved, aspartate-containing receiver domains; one is at the amino terminus (D51) and the other at the carboxy terminus (D576) (Fig. 3B). Contiguous to the amino terminal receiver domain is a sequence predicted to bind DNA and between this region and the carboxy terminal receiver domain is a histidine-containing motif that resembles an H block found in some unorthodox sensor proteins (Ishige et al., 1994; Appleby et al., 1996; Kehoe and Grossman, 1997). A variety of unique sensor-response regulator systems termed 'four step phosphorelays' have been

discovered that contain more than two phosphoreceiver domains (Appleby et al., 1996).

We have begun to explore the role of the aspartate phosphorylation domains of RcaC in CCA. Site-directed mutagenesis of *rcaC* was used to convert the D51 and D576 residues to glutamate or asparagine (Kehoe and Grossman, 1995) and the altered *rcaC* genes were transformed into a *rcaC* null mutant. Strains in which D51 was changed to asparagine had constitutive, high level synthesis of PE and essentially no synthesis of PC<sub>2</sub>, which is the same phenotype observed in the original FdR mutant. However, when D51 was changed to a glutamate, CCA became insensitive to light quality with moderate accumulation of both PC and PE. In similar studies with the response regulator NtrC, conversion of the conserved aspartate to a glutamate caused the cells to behave as if the regulatory aspartate residue had been phosphorylated to some extent (Klose et al., 1993). When the aspartate was converted to an asparagine the NtrC behaved as if it were not phosphorylated. The results described for the site-directed mutagenesis of NtrC and RcaC suggest that the D51 residue of the latter is phosphorylated in RL-grown cells and that the phosphorylation results in high level PC and little PE synthesis. Phosphorylation of the protein is mimicked to some extent when D51 is changed to a glutamate (as it is for NtrC). Hence, wild-type cells would dephosphorylate D51 in GL, which would trigger elevated PE synthesis and cause depression of PC synthesis; this phenotype becomes constitutive when the aspartate is changed to asparagine. At this stage it is not clear if RcaC directly interacts with the promoters of the phycobiliprotein operons or if its effect on CCA is indirect. Furthermore, the effects of altering the carboxy-terminal aspartate, D576, or the H block histidine residue of RcaC have not been established.

The FdBk class of mutants was also complemented. The complementing DNA encodes a protein, designated RcaE, with a molecular mass of 74 kDa (Kehoe and Grossman, 1996) (Figure 3B). The carboxy-terminal region of RcaE has the four motifs typical of sensor polypeptides that are required for histidine kinase activity (N, G1, F and G2) as well as an H block. Surprisingly, the amino-terminal half of the protein has a domain of approximately 140 amino acids that is similar to the tetrapyrrole chromophore attachment domain of phytochromes (Kendrick and Kronenberg, 1994); it appears to contain the cysteine residue that covalently binds to the tetrapyrrole chromophore. Recent biochemical studies have

demonstrated that RcaE covalently binds a linear tetrapyrrole chromophore and that the cysteine is required for the covalent attachment of the chromophore to the protein (Kehoe and Grossman, unpublished data). Furthermore, several eukaryotic and prokaryotic (Cph1) phytochromes have been shown to have protein kinase activity in vitro (Yeh et al., 1997; Yeh and Lagarias, 1998), once again supporting an evolutionary relationship between chromophore bearing sensor kinases such as RcaE and the eukaryotic phytochrome photoreceptor family.

Interestingly, RcaE also has sequence similarity to vascular plant ethylene receptors (Chang et al., 1993; Hua et al., 1995; Wilkinson et al., 1995), which are similar to sensor kinases of bacterial two component regulatory systems; they contain the motifs required for histidine kinase activity. In addition, the amino-terminal sequences of ethylene receptors contain two motifs, designated T2L and R2L (Kehoe and Grossman, 1996), that are also present in the amino-terminal half of RcaE. These motifs are similar with respect to both their amino acid sequences and their positions relative to each other; they also overlap the regions of RcaE that are similar to the phytochromes. The significance of these similarities is not yet clear.

The phenotype of the FdBk mutant and the similarity of RcaE to sensor histidine kinases and eukaryotic phytochrome photoreceptors are consistent with a photoreceptor role for RcaE. In the FdBk mutant both the *cpcB2A2* and *cpeBA* operons are partially active (the mixture of PC and PE is responsible for the black-green color of these strains), but their expression is not sensitive to light quality. The finding that mutants null for RcaC synthesize high levels of PE and low levels of PC in either RL or GL combined with the results from the site-directed mutagenesis studies, described above, suggest that activation of *cpcB2A2* and repression of *cpeBA* in RL require phosphorylation of RcaC (Chiang et al., 1992). The critical phosphorylation is at an aspartate residue (D51) in the amino terminal receiver domain (Kehoe and Grossman, 1995). Therefore, the FdBk mutants must have partial and constitutive phosphorylation of the RcaC regulator (and perhaps other regulatory proteins involved in signal transduction; see below). Since the FdBk mutant appears to be null for *rcaE*, this phosphorylation must occur as a consequence of promiscuous phosphorylation by other sensor proteins in the cell (Wanner and Wilmes-Riesenberg, 1992) or by small phosphodonor molecules (Wanner and Wilmes-Riesenberg, 1992;

Wanner, 1994).

The sequence of the entire *Synechocystis* PCC 6803 genome (Cyanobase) revealed at least eight deduced polypeptides related to both RcaE and eukaryotic phytochromes. One of the gene encoding a phytochrome-like protein, designated *cph1*, has been expressed in vitro and is capable of binding a chromophore and undergoing a photochromic shift in absorbance (Yeh et al., 1997). These results suggest that the phytochrome-related polypeptides in cyanobacteria act as photoreceptors. The finding that these proteins also contain domains typical of histidine kinases, has led to renewed efforts to determine whether or not phytochrome exerts its physiological effects by triggering a phosphorylation cascade. Recently Lagarias and colleagues have demonstrated that phytochrome that is synthesized in yeast can undergo autophosphorylation, although it appears to have serine/threonine kinase rather than histidine kinase activity (Yeh and Lagarias, 1998). Defining the signal transduction processes that are triggered by phytochrome-like photoreceptors in prokaryotes is providing us with new insights into mechanisms involved in light-regulated gene expression in plants.

A number of the FdR mutants could not be complemented by *rcaC* (Kehoe and Grossman, 1997). Some of these were complemented by the putative photoreceptor gene *rcaE*, and the rest were complemented by *rcaF*, the gene immediately downstream of *rcaE* on the cyanobacterial genome. Translation of the RcaF protein, which is homologous to response regulators, initiates 12 bp downstream of the translation termination site of *rcaE*. However, like CheY and Spo0F, response regulators involved in flagellar movement in *E. coli* and sporulation in *Bacillus subtilis*, respectively (Clegg and Koshland, 1984; Ravid et al., 1986; Yamaguchi et al., 1986; Wolfe et al., 1987; Parkinson and Kofoed, 1992; Perego and Hoch, 1996), RcaF is very small (124 amino acids) and does not contain an identifiable output domain. RcaF may act as an intermediate in the phosphorelay pathway controlling CCA and transfer phosphate groups from its cognate sensor (presumably RcaE) to other response regulators such as RcaC (see below and Fig. 4).

Since *rcaE* is sufficient for complementing both FdBk (Kehoe and Grossman, 1996) and FdR mutants, different lesions in *rcaE* can generate different pigment phenotypes. Furthermore, a FdR phenotype can result from lesions in at least three distinct genes (*rcaC*, *rcaE*, and *rcaF*). To elucidate the molecular

basis for the above observations, genomic DNA from the FdBk (*rcaE*-FdBk) and FdR (*rcaE*-FdR, *rcaF*-FdR) mutants were analyzed. All of the strains had inserts in the region of the genome containing the *rcaE/rcaF* operon. The insertions appear to be the consequence of transpositions that were triggered during the chemical mutagenesis procedure (Chiang et al., 1992); there is some evidence for stress-induced mobilization of transposable elements in *F. diplosiphon* (Bruns et al., 1989). In the *rcaE*-FdBk mutants the inserts were located within 200 bp of the putative translation start site; the location of these insertions and the lack of detectable RcaE in these mutants, based on Western blot analyses (Kehoe and Grossman, unpublished data), make these mutants likely to be null for *rcaE*. The *rcaE*-FdR mutants also contained insertions, however, they were positioned between the H block and the four conserved motifs critical for histidine kinase activity; this strain appears to make a truncated form of RcaE. The *rcaF*-FdR mutants contained DNA insertions located approximately 200 bp downstream of the *rcaF* translation initiation codon.

The constitutive levels of PE and PC in the *rcaE*-FdBk mutants reflects an intermediate activation state of the system, resulting from low level phosphorylation of the response regulator that is not regulated by CCA (Feng et al., 1992; Lukat et al., 1992; Parkinson and Kofoed, 1992; Wanner and Wilmes-Riesenberg, 1992). Hence, it is likely that RcaF can be phosphorylated to some extent in the absence of RcaE; this phosphorylation is not controlled by light quality and probably results from crosstalk between RcaF and other sensors in the cell or phosphoryl transfer from small molecule phosphodonors. It is not unusual that creating a null mutation in a sensor kinase leads to an intermediate, constitutive activation of the phosphorelay system. In the *rcaE*-FdR mutants, although the truncated RcaE cannot undergo autophosphorylation, it may still be able to bind to RcaF and block its phosphorylation by other molecules and/or retain phosphatase activity, which would maintain RcaF in a dephosphorylated state. A deletion of the same region of the sensor NarQ leads to a loss of the kinase but retention of phosphatase activity (Cavicchioli et al., 1995).

The relationships between RcaE, RcaF and RcaC can also be inferred by examining the effects of overexpression of these regulatory elements in both wild-type and mutant strains during growth in white light (Grossman and Kehoe, 1997; Kehoe and

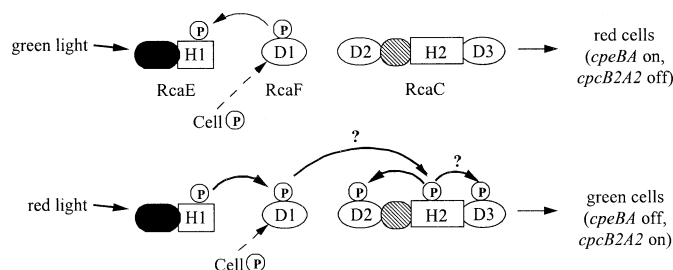


Fig. 4. Current model for the early steps in the signal transduction pathway controlling CCA. In GL, RcaE acts as a phosphatase, dephosphorylating RcaF and maintaining the signal transduction elements in a dephosphorylated state. In RL, RcaE acts as a kinase, phosphorylating RcaF, which in turn can phosphorylate RcaC. The details of the phosphorelay are discussed in the text.

Grossman, 1997). Overexpressing RcaF or RcaC in white light-grown, wild-type cells leads to an increase in PC and a decrease in PE (elevated PC:PE ratio). Increased response regulator levels have been shown to cause phenotypic effects in many systems (Shattuck-Eidens and Kadner, 1983; Clegg and Koshland, 1984; Rogowsky et al., 1987; Hertig et al., 1989; Perego and Hoch, 1991; Eraso and Kaplan, 1994; Cavicchioli et al., 1995; Boyd and Lory, 1996). These effects may reflect an increase in the absolute number of phosphorylated response regulators that result from legitimate interactions with cognate sensor molecules, crosstalk with other cellular sensors, or by transfer of phosphoryl groups from small molecule phosphodonors. The altered phenotype in strains expressing high levels of a response regulator may also result from concentration-mediated activation of non-phosphorylated response regulators; some response regulators are active in higher order aggregates (Fiedler and Weiss, 1995; Mettke et al., 1995). When additional copies of *rcaC* are introduced into the *rcaE*-FdR and *rcaF*-FdR mutants, or when *rcaF* is introduced into the *rcaE* mutant (but not when introduced into the *rcaC* mutant), there is also an increase in PC:PE ratio. These results support the idea of a linear signal transduction pathway in which RcaE is the molecule that senses the light quality followed by transmission of the signal to RcaF and then RcaC.

#### IV. Model for the Control of Complementary Chromatic Adaptation

The three proteins identified as critical for control of CCA are RcaE, RcaF and RcaC. These proteins are members of bacterial two component regulatory systems. However, the phosphorelay system

controlling CCA is unique since it includes, among these three proteins, at least five potential phospho-acceptor domains. Some systems have been studied that have four phosphoacceptor domains; these include phosphorelay systems that control sporulation in *B. subtilis* (Burbulys et al., 1991), transcriptional regulation of virulence factors in *Bordetella pertussis* (Ishige et al., 1994; Uhl and Miller, 1996) and osmoregulation in *Saccharomyces cerevisiae* (Posas et al., 1996).

As shown in the model of Fig. 4, RL stimulates and GL inhibits the transfer of phosphoryl groups along the phosphorelay pathway. RcaE, the phytochrome-related protein, is the sensor that perceives the light signal. We propose that RL causes RcaE to undergo an autophosphorylation followed by transfer of the phosphoryl group to the response regulator RcaF. RcaF may also serve as an entrance point for phosphoryl donors other than RcaE. Phosphorylated RcaF may transfer the phosphoryl group to an H block or histidine phosphotransfer domain within RcaC, which can then pass it to either the amino or (perhaps) the carboxy terminal receiver domain. The amino terminal receiver domain of RcaC is critical for CCA, while the role of the carboxy terminal receiver domain is unclear, although it may function to fine tune the system with respect to other environmental conditions.

But the CCA phosphorelay story does not end with RcaC. There are likely other regulatory factors that are involved in the specific control of either *cpcB2A2* or *cpeBA*. All of the mutants discussed to this point control both *cpcB2A2* and *cpeBA*. Mutants that only affect *cpeBA* expression have been identified and designated turquoise (FdTq) mutants. These mutants exhibit normal regulation of *cpcB2A2* but fail to accumulate *cpeBA* mRNA in GL. Furthermore, FdTq strains show normal control of *cpeCDE*,

suggesting that there are unique features of light regulation that distinguish the *cpeBA* and *cpeCDE* operons. Complementation of the **FdTq** strains resulted in the isolation of two genes designated *trqA* and *trqB*. These genes encode proteins that are most closely related to different classes of protein phosphatases (Seib and Kehoe, 2002). Although the role of TrqA and TrqB in the regulation of the *cpeBA* operon during CCA remains to be precisely established, the similarity of these polypeptides to protein phosphatases is interesting, especially since RcaA binding to the *cpeBA* promoter is modulated by its phosphorylation state (Sobczyk et al 1993). Furthermore, Seib and Kehoe (2002) also demonstrated that some light regulation of the *cpeBA* and *cpeCDE* operons remained in the *rcaE* null mutant. This suggests that there is a second system for RL/GL photoperception that influences the activity of the phycobiliprotein and linker polypeptide genes.

There are still many questions concerning CCA that remain unresolved. We do not know if RcaC binds to the promoters of the phycobiliprotein genes directly and alters their activity or if it binds in conjunction with other phosphorylated components. It is also unclear whether or not a second polypeptide is a component of the RcaE photoreceptor. Also, it is likely that at least one additional photoreceptor system, still undefined, influences the activity of genes encoding the phycobiliproteins and linker polypeptides.

## V. Control of Phycobilisome Biosynthesis During Nutrient Limitation

The PBS can represent 30–40% of the cellular protein, which is a very large commitment for the biosynthetic machinery of the cell. Therefore, as expected, PBS synthesis is highly regulated; it is linked to an array of different environmental conditions in addition to light quality. These conditions would include light intensity, osmolarity, nutrient availability and temperature. As an example, in some cyanobacterial strains high light rapidly depresses phycobiliprotein synthesis. In the case of *Synechococcus* PCC 7942, phycobiliprotein transcript levels decline more gradually than does the synthesis of the polypeptides (Dolganov and Grossman, unpublished). These observations suggest that phycobiliprotein synthesis is controlled by both transcriptional and post-

transcriptional processes. The exact intracellular conditions that are critical for controlling PBS synthesis are not known, however, the cells have probably evolved to balance the utilization of absorbed excitation energy for the production of NADPH and ATP with the cellular requirements (growth and maintenance) for these metabolites. This balance is critical since excess excitation of the photosynthetic reaction centers could result in the production of highly reactive oxygen species that can destroy the cell (Asada, 1994). Changes in extracellular conditions such as nutrient availability, will often result in a change in the redox state of the cell as well as changes in intracellular metabolite pools which, in turn, might modulate both the synthesis and degradation of PBS.

### A. Specific Responses to Nutrient Limitation

The responses of organisms to nutrient availability may be classified as those that are specific to the limiting nutrient and those that are more general and occur during any of a number of different nutrient limitation conditions. The specific acclimation responses include metabolic changes that enable organisms to efficiently scavenge the limiting nutrient from their surroundings. This increased scavenging efficiency is a consequence of elevated synthesis of high affinity transport systems (Grillo and Gibson, 1979; Green and Grossman, 1988; Omata et al., 1993) and the production of hydrolytic enzymes that allow the cells to utilize alternate forms of the limiting nutrient (de Hostos et al., 1988; Ray et al., 1991; Quisel et al., 1996). Both the synthesis of extracellular phosphatases and an increase in the cells capacity for phosphate transport have been reported to occur during phosphorus limitation (Grillo and Gibson, 1979; Ray et al., 1991). Limiting *Synechococcus* PCC 7942 for ammonia leads to the activation of genes encoding transport systems for nitrate and nitrite (Omata et al., 1993). During sulfur-limited growth, *Synechococcus* PCC 7942 has elevated transport of sulfate into the cell, which is dependent upon light and varies with both temperature and pH (Utkilen et al., 1976; Jeanjean and Broda, 1977). A cluster of genes on the *Synechococcus* genome was isolated that encodes the high affinity sulfate transport system and other genes regulated by sulfate availability (Green et al., 1989; Laudenbach and Grossman, 1991; Laudenbach et al., 1991). Interestingly, one gene in this cluster (*cysR*) encodes a

regulatory protein that activates the transcription of a number of genes on the large plasmid in *Synechococcus* PCC 7942; the plasmid-encoded genes appear to be involved in the utilization of various sulfur-containing compounds, including thiocyanate (Nicholson and Laudenbach, 1995; Nicholson et al., 1995).

### *B. General Responses to Nutrient Stress*

General responses to nutrient-limited growth have been sporadically examined over the last 25 years. Dramatic alterations in the ultrastructure of cyanobacterial cells grown under adverse nutrient conditions have been observed via electron microscopy. Sherman and Sherman (Sherman and Sherman, 1983) and Wanner et al. (Wanner et al., 1986) demonstrated that iron-, nitrogen-, and sulfur-deficient *Synechococcus* cells had less than half of the normal complement of thylakoid membranes. The remaining membranes were disorganized and interspersed with large deposits of glycogen. There was also a decrease in the number of carboxysomes and increased formation of polyphosphate granules. Temporal studies of nitrogen-deficient *Synechococcus* PCC 7002 demonstrated that removal of the nutrient caused a loss of PBS followed by a reduction in ribosomes and thylakoid membranes (Stevens and Poane, 1981). Furthermore, there is a rapid loss of oxygen evolving activity in cells deprived of either nitrogen or sulfur; 48 h of starvation leads to a depression in oxygen evolution by over 90%. Cells that have experienced 48 h of phosphorus limitation maintain oxygen evolution at a level of approximately 40% of that observed in unstarved cells. The decline in oxygen evolution is correlated with a loss of fluorescence emission at 685 nm and 695 nm, which is associated with the chlorophyll *a* antennas of Photosystem II and the Photosystem II reaction centers. Measurements of the energy storage capacity of photosynthesis using photoacoustic techniques (Herbert et al., 1990) also suggested that Photosystem II activity was severely diminished in nitrogen- and sulfur-deprived cells (Collier et al., 1994); Photosystem II may be degraded during macronutrient deprivation. In contrast, energy storage by Photosystem I remains approximately the same in starved and unstarved cells. Sustained energy storage by Photosystem I under nutrient stress conditions would help the cells maintain essential metabolic processes and allow for the uptake of the limiting

nutrient once it becomes available.

A visually dramatic, general response of cyanobacteria to nutrient-limited growth is the decrease in pigment molecules in the cell. The first quantification of pigment levels during nutrient deprivation was performed by Allen and Smith (1969). In this and other studies (Yamanaka and Glazer, 1980; Collier and Grossman, 1992), it was shown that exposure of cyanobacteria to nitrogen- and sulfur-starvation conditions caused rapid and almost complete loss of the PBS. Degradation of this abundant light-harvesting complex could provide amino acids or carbon skeletons for the production of other cellular constituents required during nutrient deprivation. It would also reduce the absorption of excess excitation energy; excess absorbed light energy could result in photodamage and cell death. Degradation of the PBS in sulfur-deprived *Synechococcus* PCC 7942 suggests that recycling of phycobiliproteins may also provide the cell with some sulfur in the form of cysteine and methionine. Finally, the 'general' losses of pigmentation in response to macronutrient limitations are not all the same. Cells limited for phosphorus do not degrade the PBS. Reduced pigmentation in phosphorus-starved cells is mostly the result of dilution of the pigment molecules upon cell division; four to six divisions occur after *Synechococcus* cells are diluted into phosphorus-free medium (Collier and Grossman, 1992).

The degradation of the PBS during nutrient stress is an ordered process. Eliminating nitrogen or sulfur from the growth medium provokes a rapid loss of the terminal PC hexamer of the PBS rods and its associated 30 kDa linker polypeptide (Yamanaka and Glazer, 1980; Collier and Grossman, 1992). This is followed by some loss of the second PC hexamer and its associated 33 kDa linker polypeptide, along with a decrease in the number of rods per PBS (Yamanaka and Glazer, 1980); sustained deprivation results in the complete degradation of the PBS.

In early studies with *Anabaena*, PBS degradation was attributed to a specific protease that increased four- to six-fold during nitrogen limitation (Wood and Haselkorn, 1979; Wood and Haselkorn, 1980). The PBS of *Synechococcus* is extremely stable in nutrient-sufficient medium and is rapidly degraded upon transfer of cells to medium lacking in either nitrogen or sulfur, making it unlikely (although not impossible) that the complete loss of the light-harvesting complex is the consequence of a four- to six-fold increase in a specific protease. In our

laboratory, mutants of *Synechococcus* were isolated that could not degrade their PBS during nutrient deprivation. A number of these mutants exhibited no PBS degradation during either sulfur- or nitrogen-deprivation. Some mutants grew at a similar rate, and exhibited a similar susceptibility to high light during the acclimation process as wild-type cells. Hence, even though the mutant cells had a considerable number of PBS that could absorb potentially damaging excitation energy, the mutants appeared to be no more photosensitive than normally acclimating wild-type cells. Additional experiments suggested that the PBS present in the mutant organisms were not able to efficiently transfer harvested light energy to the reaction centers of Photosystem II (Collier and Grossman, unpublished). This uncoupling of the light-harvesting complex from the primary photochemical reactions of Photosystem II (excess excitation of Photosystem II might be the primary cause of photodamage), which also occurs in wild-type cells during nutrient limitation, may explain the lack of increased photosensitivity in these strains. Other nonbleaching mutants died more rapidly than wild-type cells during nutrient limitation.

Complementation of one of the nonbleaching mutants led to the isolation of the *nblA* (nonbleaching) gene, which contains an open reading frame of 59 amino acids. Sequences homologous to NblA are present both in cyanobacteria (Cyanobase) and on the plastid genome of red algae (Apt and Grossman, 1993). The *Synechococcus nblA* transcript only accumulates to high levels in cells starved for nitrogen or sulfur; low levels of the *nblA* transcript are observed in cells maintained in phosphorous-free or in complete medium. Under all conditions tested, the level of expression of *nblA* correlated with decreased PBS levels. When the wild-type *nblA* gene was placed on the autonomously replicating plasmid pPLAN (a shuttle vector constructed by David Laudenbach) and transformed into *Synechococcus*, the level of PBS on a per cell basis declined by 20–30% in nutrient-replete medium. This suggests that multiple copies of *nblA* may result in increased, although still low level expression, and consequently an elevated rate of degradation of the PBS. Furthermore, the cells will degrade the PBS during phosphate stress if *nblA* is placed under the control of the alkaline phosphatase promoter, which is only active during phosphate-limited growth (Ray et al., 1991), and introduced into the cell on the pPLAN vector (Collier and Grossman, 1994).

The studies of *nblA* have raised a number of interesting ideas. Since increased expression of *nblA* can cause PBS degradation, even under conditions in which the PBS is not normally degraded, it is likely to be the primary (only) gene whose activity must be elevated to provoke bleaching during sulfur- or nitrogen-limited growth. The small deduced size of the NblA polypeptide and its lack of similarity to known proteases, suggest that it is not a protease itself. It may function to activate or alter the specificity of a protease, or somehow tag the PBS for degradation. Tagging proteins for degradation may involve covalent attachment of the NblA polypeptide to the PBS, similar to the binding of ubiquitin to proteins in eukaryotes (Hershko, 1988), or the disruption of hydrophobic and/or ionic interactions among various constituents of the PBS, making the proteins of the PBS more susceptible to general proteases in the cell. Finally, although NblA is the only gene product initially needed to provoke PBS degradation, it may be involved in the activation or derepression of other genes in the cell (however, the NblA polypeptide does not resemble any transcriptional regulator characterized to date). Recent experiments have demonstrated the presence of two *nblA* genes in *Synechocystis* PCC 6803. Similar to the case in *Synechococcus*, these genes are strongly expressed and essential for PBS degradation during nitrogen deprivation (Baier et al., 2001; Richaud et al., 2001).

The phenotype of a second nonbleaching mutant was complemented by the *nblB* gene. The NblB protein has homology to a subunit (CpcE) of the lyases that catalyze the covalent attachment of phycocyanobilin and phycoerythrobilin chromophores to apophycobiliproteins subunits (Fairchild et al., 1992; Swanson et al., 1992; Zhou et al., 1992; Fairchild and Glazer, 1994; Jung et al., 1995; Kahn et al., 1997; Dolganov and Grossman, 1999). Mutations in the lyase genes (*cpcE* and *cpcF*) involved in attaching phycocyanobilin to the  $\alpha$  subunit of PC resulted in strains that accumulated very low levels of PC (Swanson et al., 1992; Zhou et al., 1992; Bhalarao et al., 1994). Furthermore, while the  $\beta$  subunit of PC in these strains appeared to be normal, approximately 80% of the  $\alpha$  subunits that were present were not associated with the normal chromophore (Zhou et al., 1992). In vitro experiments using the CpcE and CpcF polypeptides over-expressed in *E. coli* demonstrated that these polypeptides formed heterodimers that were capable of catalyzing the addition of phycocyanobilin to the cysteine (Cys-84)



of the chromophore binding site of the  $\alpha$  subunits of PC (Fairchild et al., 1992; Fairchild and Glazer, 1994). These results strongly suggest that CpcE and CpcF are required for the attachment of the phycocyanobilin chromophore to the  $\alpha$  subunits of PC. Since the initial discovery of the PC  $\alpha$  subunit phycocyanobilin lyase, some of the genes encoding analogous lyases thought to play a role in attachment of bilin tetrapyrroles to phycoerythrin (Wilbanks and Glazer, 1993; Kahn et al., 1997) and phycoerythrocyanin (Jung et al., 1995) subunits have been identified. In all cases, the lyase genes are part of operons encoding phycobiliproteins. In *Synechococcus*, *cpcE* and *cpcF* are located downstream of the *cpcB2A2* gene cluster. The *cpcE* and *cpcF* genes are also located downstream of the *cpcBA* genes in *Pseudanabaena* (Dubbs and Bryant, 1993), *Anabaena* PCC 7120 (Belknap and Haselkorn, 1987), *Fremyella diplosiphon* (Conley et al., 1988) and *Calothrix* PCC 7601 (Mazel et al., 1988; Tandeau de Marsac et al., 1988).

The similarity of NblB with apophycobiliprotein-phycochromobilin lyase subunits suggests that NblB interacts directly with the tetrapyrrole chromophore that is attached to phycobiliprotein subunits. Since a *nblB* mutant does not degrade its PBS during nutrient limitation, it is reasonable to propose that NblB catalyzes the removal of chromophores from the holophycobiliprotein subunits and that only after the chromophore is removed can phycobiliprotein subunits be degraded. Furthermore, *nblB* mutants exhibit higher PC levels than wild-type cells grown in nutrient-replete conditions. Hence, it is likely that NblB is part of the machinery that coordinates degradation of the PBS with changes in ambient environmental conditions. The similarity between NblB and CpcE (and CpeZ and PecE) may reflect the ability of these polypeptides to bind tetrapyrrole chromophores of phycobiliprotein subunits. However, the former may also facilitate cleavage of the tetrapyrrole from PBS subunits.

The phenotype of a third nonbleaching mutant was complemented by the *nblR* gene. This gene encodes a response regulator of two component regulatory systems similar to CopR from *Pseudomonas syringae* (Mills et al., 1993), PhoB from *Escherichia coli* (Makino et al., 1986), SphR from *Synechococcus* (Aiba et al., 1993; Nagaya et al., 1994) and OmpR from *Escherichia coli* (Hall and Silhavy, 1981; Forst et al., 1989). Such response regulators often activate the transcription of genes

involved in the acclimation of bacterial cells to various stress conditions. For example, PhoB activates transcription of the *pho* regulon, which is comprised of several operons that are important for scavenging phosphorus from the environment (Wanner, 1993). CopR is involved in the acclimation of cells to elevated levels of copper (Makino et al., 1986) and OmpR regulates transcription of genes encoding the major outer membrane porin proteins in response to changes in osmolarity (Vega-Palas et al., 1992).

Cyanobacterial strains made null for NblR are defective in a number of different processes. They a) have approximately 150% the level of PBS relative to wild-type cells during nutrient-replete growth in moderate light ( $80 \mu\text{mol photons m}^{-2} \text{ s}^{-1}$ ), b) fail to degrade PBS during sulfur or nitrogen limitation and c) cannot properly modulate PBS levels during exposure to high light. The a), b) and c) phenotypes probably reflect the fact that the *nblR* mutant d) cannot activate *nblA* during nutrient limitation; the mutant also e) dies rapidly when starved for either sulfur or nitrogen, or when exposed to high light (Schwarz and Grossman, 1998). Hence, in addition to controlling PBS degradation, NblR modulates functions critical for cell survival during nutrient-limited and high light conditions. The presence of the photosynthetic electron transport inhibitor DCMU slows the death of the *nblR* mutant during both sulfur and nitrogen starvation, suggesting that the death of this mutant is due to its inability to properly down-regulate photosynthesis upon exposure to stress conditions. NblR does not appear to be involved in controlling the specific responses to nutrient limitation; the activation of genes encoding components of the sulfate transport systems are normally induced in the *nblR* mutant. The nitrogen-specific responses are also likely to be normal in the *nblR* mutant, based on the following reasoning. In *Synechococcus*, most of the genes that respond to levels of nitrogen-containing metabolites become active upon ammonium deprivation in the presence of nitrate (Luque et al., 1994). The *nblR* mutant grows normally in medium that contains nitrate as the sole nitrogen source. Hence, NblR does not prevent the activation of genes encoding nitrate transport and assimilation functions. In sum, NblR appears to play a pivotal role in regulating some of the general stress responses. It is critical for integrating different environmental signals with the metabolism of the cell (including the activity of the photosynthetic apparatus) and is required for viability

during starvation and growth in high light.

Recent experiments demonstrate that in addition to NblR, nitrogen metabolites and the regulatory element NtcA (the global regulator of nitrogen metabolism) influence bleaching and the transcriptional activity of *nblA* (Sauer et al., 1999; Luque et al., 2001). Both NblR and NtcA bind to DNA fragments containing the *nblA* promoter, and an *ntcA* mutant of *Synechococcus* does not accumulate the *nblA* transcript to the same extent as wild-type cells (Luque et al., 2001). These results suggest that both nutrient-specific and more general regulatory elements may work in conjunction to modulate responses of cyanobacteria to nutrient limitation.

The most recent nonbleaching mutant that we have isolated is designated *nblS* (van Waasbergen et al., 2002). Like *nblR*, the *nblS* mutant is sensitive to high light and nutrient limitation and cannot properly activate *nblA*. The *nblS* mutant is also unable to activate *hliA* (a gene that encodes a protein of unknown function with similarity to the chlorophyll-a/b binding proteins of vascular plants), *psbA2* and *psbA3* (genes encoding a D1 subunit of PSII that functions under high light conditions) during exposure of *Synechococcus* cells to high light or blue/UV-A light. Finally, the *nblS* mutant cannot downregulate *psbA1* and *cpcBA* during exposure to high light and blue/UV-A light.

The *nblS* gene encodes a sensor histidine kinase that is typical of bacterial two component regulatory systems. Since NblS controls nutrient stress responses, like NblR, we assume that NblS and NblR constitute a sensor-response regulator pair, although this has not been proven. Interestingly, the expression of *hliA* and other genes controlled by light intensity is not under the control of *nblR*, demonstrating that NblS also controls regulatory pathways that are distinct from those controlled by NblR. These results suggest that NblS may interact with multiple response regulators and that it may serve as a global regulator of cellular processes when the cells experience conditions that severely retard cell growth.

The NblS protein has two predicted amino-terminal membrane spanning domains followed by a region bearing a PAS domain. The PAS domain often binds a prosthetic group and may be involved in controlling the responses of cells to redox, reactive oxygen species or light. The PAS domain of NblS is most similar to the PAS domain of FixL of *Rhizobium*. The FixL PAS domain binds a heme prosthetic group, which is involved in sensing the oxygen status of the

environment (Gilles-Gonzalez et al., 1991, 1994). However, PAS domains of other proteins may bind to prosthetic groups such as FMN, FAD or hydroxycinnamic acid and respond to both light conditions and the redox state of the cell (Taylor and Zhulin, 1999). Experiments using inhibitors of photosynthetic electron transport suggest that NblS may be sensing the extent of reduction of specific electron carriers (perhaps through a redox active cofactor bound to the PAS domain). This postulated mode of action of NblS could explain how a single sensor protein could integrate a number of different environmental conditions. It also suggests that NblS may have a global regulatory role that tunes the metabolic processes in the cell with the utilization of products generated by the photosynthetic electron transport system (van Waasbergen et al., 2002). Other regulators that respond to redox conditions (Alfonso et al 1999; Li and Sherman, 2000) and/or the generation of oxygen radicals are likely to serve in the overall tailoring of cellular metabolism to the potential for cell growth.

### C. Model for Control by Nutrient Deprivation

A model that describes the control of PBS levels during nutrient limitation is presented in Fig. 5. In this model the NblS protein integrates nutrient stress conditions and high light to activate acclimation responses, which includes the degradation of the PBS, activation of the *nblA*, *hliA*, *psbA2* and *psbA3* genes, and depression of activity of the *psbA1* and *cpcBA* genes. We do not yet know whether NblS is critical for regulating transcript levels of other genes that rapidly respond to changes in light conditions. The signal that NblS senses may be the redox state of the cell. Recently, it has been suggested that both the *psbA* and *psaE* genes in cyanobacteria are controlled by the redox state of components of the photosynthetic apparatus (Bissati and Kirilovsky, 2001). During nutrient limitation, as cells tend to generate reduced photosynthetic electron carriers such as the cytochrome  $b_6f$  complex (Fujita et al., 1987, 1994; Durnford and Falkowski, 1997), NblS initiates a phosphorylation cascade in which NblR is activated. NblR turns on the *nblA* gene, and the NblA polypeptide works in conjunction with NblB (which is constitutively expressed) to degrade the PBS. NblR must also activate other processes in the cell (e.g. modification of the photosynthetic apparatus) that favor survival during nutrient stress (and high light

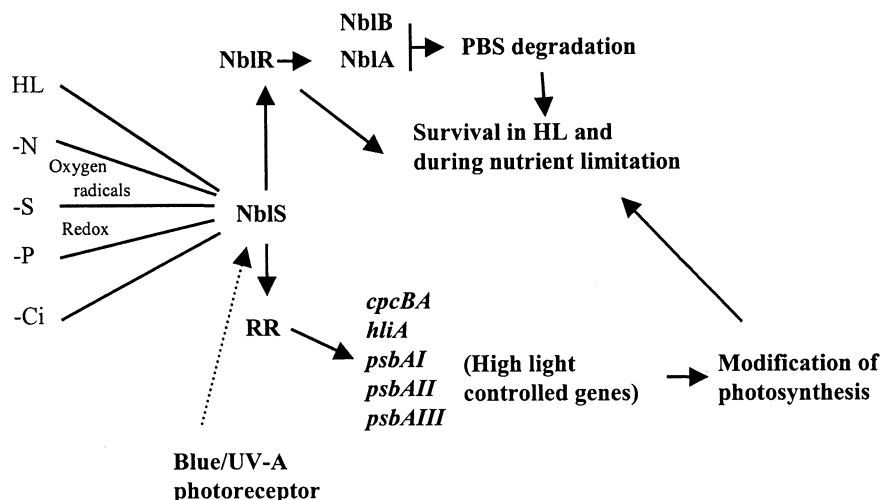


Fig. 5. NblS and regulatory networks that control nutrient stress and high light responses. NblS appears to integrate diverse environmental conditions, possibly through sensing the redox state of the cell. NblS probably interacts with NblR to control nutrient stress responses while the control of the genes activated in high light are likely controlled by a second response regulator (RR) that is signaled by NblS. NblS also mediates the blue/UV-A light response; this may be the result of the direct absorption of light by NblS (via a chromophore bound to the PAS domain) or may be indirect and require a specific blue light photoreceptor.

conditions). NblS appears also to be involved in providing the cell with an advantage during high light exposure by modulating the activity of various genes. The finding that the activation of *hliA*, *psbA2* and *psbA3* does not require NblR suggests that NblS interacts with at least one additional response regulator that has not yet been identified.

One of the major questions remaining is how may NblS be sensing the redox state of the cell. During nutrient limitation, when the anabolism of the cell is slowed down or completely arrested, NADPH, the reductant generated by photosynthetic electron transport, is not recycled as fast as under nutrient-replete conditions and the photosynthetic electron carriers are maintained in a relatively reduced state. Similarly, under high light conditions the electron carriers may be reduced faster than they are re-oxidized. Thus, both nutrient limitation and high light conditions would result in the absorption of excess light energy by the photosynthetic pigments of the cells and the overall environment of the cell would become more reduced. The redox state of the photosynthetic electron carriers is known to modulate cellular transcription (Escoubas et al., 1995), translation (Kim and Mayfield, 1997), state transitions and changes in the stoichiometry of the photosystems (Fujita et al., 1994; Keren and Ohad, 1998). The possibility that NblS/NblR control is linked to the

redox state of photosynthetic electron carriers is supported by the finding that light is required for degradation of the PBS during nutrient limitation. Furthermore both DCMU, which prevents photosynthetic electron flow beyond  $Q_A$ , and DBMIB, which inhibits electron flow through the cytochrome  $b_6f$  complex, alter PBS degradation and the accumulation of *nblA* mRNA during sulfur and nitrogen stress (van Waasbergen and Grossman, unpublished). Interestingly, upon treatment of *Synechococcus* with cyanide (which inhibits both respiration and photosynthetic electron flow at plastocyanin), *hliA* is activated in low light. Similarly, in a PSI mutant of *Synechocystis* PCC 6803, there is elevated expression of the *hliA* genes, even in moderate light (Vermaas, personal communication). These results suggest that hyper-reduction of an electron transport carrier prior to Photosystem I is required for proper acclimation during high light and nutrient limitation responses. Additional experimentation is required to precisely define redox elements that directly interact with NblS.

Factors in addition to the redox state of the photosynthetic apparatus may also be important for tuning the activity of NblS. For example, NblS control favors the pathway that leads to PBS degradation during nutrient limitation, while in high light the system is biased toward the activation of *hliA*, *psbA2*

and *psbA3*. These genes can also be activated by low level blue/UV-A light; this blue/UV-A response is under the control of NblS (van Waasbergen et al., 2002). If NblS binds a flavin, as preliminary data suggests (van Waasbergen, Christie, Briggs and Grossman, unpublished), it may act as a blue/UV-A photoreceptor as well as a redox sensor. At this point there are a number of aspects of this model that are speculative, however it represents an attractive unifying theory that predicts global metabolic effects in response to the redox status of the photosynthetic electron transport chain and the specific light environment in which the cells are growing.

## VI. Concluding Remarks

The structure and functions of LHCs in a number of the different photosynthetic prokaryotes and eukaryotes are being elucidated. As structural aspects of the LHCs become more defined, investigators are devoting some of their efforts to understanding the dynamics of the LHCs with respect to environmental conditions and the way in which these dynamics are regulated. Nutrient levels, light levels and the specific wavelengths of light can all modulate the composition and function of the LHC to maximize efficient utilization of light energy during limited or wavelength-biased irradiance and minimize damage when the absorption of light energy exceeds its utilization. Our current model integrates the biosynthesis of PBS with light quality, light intensity and redox conditions. As our understanding of the dynamics and control of the LHC and photosynthetic function increases, there are possibilities for using molecular technologies to engineer the photosynthetic apparatus for better performance under specific environmental conditions, which can have significant social and economic impact.

## Acknowledgments

We would like to thank both NSF (MCB 9727836) and USDA (97-35301-4575 and 98-35301-6445) for their continued support of our work on the acclimation of cyanobacteria to light conditions and nutrient levels. We also thank Winslow Briggs, John Christie and Devaki Bhaya for helpful discussions. This is a Carnegie Institution of Washington Publication, number 1460.

## References

- Aiba H, Nagaya M and Mizuno T (1993) Sensor and regulator proteins from the cyanobacterium *Synechococcus* species PCC 7942 that belong to the bacterial signal-transduction protein families: implication in the adaptive response to phosphate limitation. *Mol Microbiol* 8: 81–91
- Alfonso M, Perewoska I, Constant S and Kirilovsky D (1999) Redox control of *psbA* expression in cyanobacteria *Synechocystis* strains. *J Photochem Photobiol* 48: 104–113
- Allen MM and Smith AJ (1969) Nitrogen chlorosis in blue-green algae. *Arch Microbiol* 69: 114–120
- Appleby JL, Parkinson, JS and Bourret, RB (1996) The multi-step phosphorelay: Not necessarily a road less traveled. *Cell* 86: 845–848
- Apt KE, and Grossman AR (1993) Characterization and transcript analysis of the major phycobiliprotein subunit genes from *Aglaothamnion neglectum* (*Rhodophyta*). *Plant Mol. Biol* 21: 27–38
- Asada K (1994) Production and action of active oxygen species in photosynthetic tissues. In: Foyer CH and Mullineaux PM (eds) *Causes of Photooxidative Stress and Amelioration of Defense Systems in Plants*, pp 77–104. CRC Press, Boca Raton
- Ashby MK and Mullineaux CW (1999) The role of ApcD and ApcF in energy transfer from phycobilisomes to PSI and PSII in a cyanobacterium. *Photosynth Res* 61: 169–179
- Baier K, Nicklisch S, Grundner C, Reinecke J and Locknau W (2001) Expression of two *nblA*-homologous genes is required for phycobilisome degradation in nitrogen-starved *Synechocystis* sp. PCC 6803. *FEMS Microbiol Lett* 195: 35–39
- Belknap WR and Haselkorn R (1987) Cloning and light regulation of expression of the phycocyanin operon of the cyanobacterium *Anabaena*. *EMBO J* 6: 871–884
- Bennett A and Bogorad L (1971) Properties of subunits and aggregates of blue-green algal biliproteins. *Biochemistry* 10: 3625–3634
- Bennett A and Bogorad L (1973) Complementary chromatic adaptation in a filamentous blue-green alga. *J Cell Biol* 58: 419–435
- Bhalerao RP, Lind LK and Gustafsson P (1994) Cloning of the *cpcE* and *cpcF* genes from *Synechococcus* sp. PCC 6301 and their inactivation in *Synechococcus* sp. PCC 7942. *Plant Mol Biol* 26: 313–326
- Bogorad L (1975) Phycobiliproteins and complementary chromatic adaptation. *Annu Rev Plant Physiol* 26: 369–401
- Boyd JM and Lory S (1996) Dual function of PilS during transcriptional activation of the *Pseudomonas aeruginosa* pilin subunit gene. *J Bacteriol* 178: 831–839
- Bruns B, Briggs WR and Grossman AR (1989) Molecular characterization of phycobilisome regulatory mutants in *Fremyella diplosiphon*. *J Bacteriol* 171: 901–908
- Bryant DA (1981) The photoregulated expression of multiple phycocyanin species: General mechanism for control of phycocyanin synthesis in chromatically adapting cyanobacteria. *Eur J Biochem* 119: 425–429
- Bryant DA and Cohen-Bazire G (1981). Effects of chromatic illumination on cyanobacterial phycobilisomes: Evidence for the specific induction of a second pair of phycocyanin subunits in *Pseudanabaena* 7409 grown in red light. *Eur J Biochem* 119: 415–424

- Burbulys D, Trach K and Hoch JA (1991) Initiation of sporulation in *B. subtilis* is controlled by a multicomponent phosphorelay. *Cell* 64: 545–552
- Capuano V, Braux A-S, Tandeau de Marsac N and Houmard J (1991) The 'anchor polypeptide' of cyanobacterial phycobilisomes. Molecular characterization of the *Synechococcus* sp. PCC 6301 *apcE* gene. *J Biol Chem* 266: 7239–7247
- Casey, ES and Grossman AR (1994) In vivo and in vitro characterization of the light-regulated *cpcB2A2* promoter of *Fremyella diplosiphon*. *J Bacteriol* 176: 6362–6374
- Casey ES, Kehoe DM and Grossman AR (1997) Suppression of mutants aberrant in light intensity responses of complementary chromatic adaptation. *J Bacteriol* 179: 4599–4606
- Cavicchioli R, Schroder I, Constanti M and Gunsalus RP (1995) The NarX and NarQ sensor-transmitter proteins of *Escherichia coli* each require two conserved histidines for nitrate-dependent signal transduction to NarL. *J Bacteriol* 177: 2416–2424
- Chang C, Kwok SF, Bleecker AB and Meyerowitz, EM (1993) *Arabidopsis* ethylene-response gene *ETR1*: Similarity of product to two-component regulators. *Science* 262: 539–544
- Chiang GG, Schaefer MR and Grossman AR (1992) Complementation of a red-light indifferent cyanobacterial mutant. *Proc Natl Acad Sci USA* 89: 9415–9419
- Clegg, D and Koshland, D (1984) The role of a signaling protein in bacterial sensing: Behavioral effects of increased gene expression. *Proc Natl Acad Sci USA* 81: 5056–5060
- Cobley JG and Miranda RD (1983) Mutations affecting chromatic adaptation in the cyanobacterium *Fremyella diplosiphon*. *J Bacteriol* 153: 1486–1492
- Collier JL and Grossman AR (1992) Chlorosis induced by nutrient deprivation in *Synechococcus* sp. Strain PCC 7942: Not all bleaching is the same. *J Bacteriol* 174: 4718–4726
- Collier JL and Grossman AR (1994) A small polypeptide triggers complete degradation of light-harvesting phycobiliproteins in nutrient-deprived cyanobacteria. *EMBO J* 13: 1039–1047
- Collier JL, Herbert SK, Fork DC and Grossman AR (1994) Changes in the cyanobacterial photosynthetic apparatus in response to macronutrient deprivation. *Photosynth Res* 42: 173–183
- Conley PB, Lemaux PG and Grossman AR (1985) Cyanobacterial light-harvesting complex subunits encoded in two red light-induced transcripts. *Science* 230: 550–553
- Conley PB, Lemaux PG, Lomax TL and Grossman AR (1986) Genes encoding major light-harvesting polypeptides are clustered on the genome of the cyanobacterium *Fremyella diplosiphon*. *Proc Natl Acad Sci USA* 83: 3924–3928
- Conley PB, Lemaux PG and Grossman AR (1988) Molecular characterization and evolution of sequences encoding light harvesting components in the chromatically adapting cyanobacterium *Fremyella diplosiphon*. *J Mol Biol* 199: 447–465
- de Hostos EL, Togasaki RK and Grossman AR (1988) Purification and biosynthesis of a derepressible periplasmic arylsulfatase from *Chlamydomonas reinhardtii*. *J Cell Biol* 106: 29–37
- Diakoff S and Scheibe S (1973) Action spectra for chromatic adaptation in *Tolypothrix tenuis*. *Plant Physiol* 51: 382–385
- Dolganov N and Grossman AR (1999) A polypeptide with similarity to phycocyanin  $\alpha$  subunit phycocyanobilin lyase involved in degradation of phycobilisomes. *J Bacteriol* 181: 610–617
- Dubbs JM and Bryant DA (1993) Organization and transcription of the genes encoding two differentially expressed phycocyanins in the cyanobacterium *Pseudoanabaena* sp. PCC 7409. *Photosynth Res* 36: 169–183
- Durnford DG and Falkowski PG (1997) Chloroplast redox regulation of nuclear gene transcription during photo-acclimation. *Photosynth Res* 53: 229–241
- Durnford DG, Deane JA, Tan S, McFadden GI, Gantt E and Green BR (1999) A phylogenetic assessment of the eukaryotic light-harvesting antenna proteins with implications for plastid evolution. *J Mol Evol* 48: 59–68
- El Bissati K and Kirilovsky D (2001) Regulation of *psbA* and *psaE* expression by light quality in *Synechocystis* species PCC 6803. A redox control mechanism. *Plant Physiol* 125: 1988–2000
- Engelmann TW (1883a) Farbe und Assimilation. Assimilation findet nur in den farbstoffhaltigen Plasmathielchen statt. II. Näherer Zusammenhang Zwischen Lichtabsorption und Assimilation. *Botanische Zeitung* 41: 1–13
- Engelmann TW (1883b) Farbe und Assimilation. III. Weitere Folgerungen. *Botanische Zeitung* 41: 17–29
- Engelmann TW (1884) Untersuchungen über die qualitativen Beziehungen Zwischen Absorption des Lichtes und Assimilation in Pflanzenzellen. I. Das Mikrospectrophotometer ein Apparat zur quantitativen Mikrospectralanalyse. II. Experimentelle Grundlagen zur Ermittlung der quantitativen Beziehungen zwischen Assimilationsenergie und Absorptionsgrösse. *Botanische Zeitung* 42: 97–105
- Eraso JM and Kaplan S (1994) *prpA*, a putative response regulator involved in oxygen regulation of photosynthesis gene expression in *Rhodobacter sphaeroides*. *J Bacteriol* 176: 32–43
- Escoubas J-M, Lomas M, LaRoche J and Falkowski PG (1995) Light intensity regulation of *cab* gene transcription is signaled by the redox state of the plastoquinone pool. *Proc Natl Acad Sci USA* 92: 10237–10241
- Fairchild CD and Glazer AN (1994) Oligomeric structure, enzyme kinetics, and substrate specificity of the phycocyanin  $\alpha$  subunit phycocyanobilin lyase. *J Biol Chem* 269: 8686–8694
- Fairchild CD, Zhao J, Zhou J, Colson SE, Bryant DA and Glazer AN (1992) Phycocyanin  $\alpha$ -subunit phycocyanobilin lyase. *Proc Natl Acad Sci USA* 89: 7017–7021
- Federspiel NA and Grossman AR (1990) Characterization of the light-regulated operon encoding the phycoerythrin-associated linker proteins from the cyanobacterium *Fremyella diplosiphon*. *J Bacteriol* 172: 4072–4081
- Federspiel NA and Scott L (1992) Characterization of a light-regulated gene encoding a new phycoerythrin-associated linker protein from the cyanobacterium *Fremyella diplosiphon*. *J Bacteriol* 179: 5994–5998
- Feng J, Atkinson MR, McCleary W, Stock JB, Wanner BL and Ninfa AJ (1992) Role of phosphorylated metabolic intermediates in the regulation of glutamine synthetase synthesis in *Escherichia coli*. *J Bacteriol* 174: 6061–6070
- Fiedler U and Weiss V (1995) A common switch in activation of the response regulators NtrC and PhoB: Phosphorylation induces dimerization of the receiver modules. *EMBO J* 14: 3696–3705
- Forst SA, Delgado J and Inouye M. (1989) Phosphorylation of OmpR by the osmosensor EnvZ modulates expression of the *ompF* and *ompC* genes in *Escherichia coli*. *Proc Natl Acad Sci USA* 86: 6052–6056

- Fujita Y, Murakami A and Ohki K (1987) Regulation of photosystem composition in the cyanobacterial photosynthetic system: The regulation occurs in response to the redox state of the electron pool located between the two photosystems. *Plant Cell Physiol* 28: 283–292
- Fujita Y, Murakami A, Aizawa K and Ohki K (1994) Short-term and long-term adaptation of the photosynthetic apparatus: Homeostatic properties of thylakoids. In: Bryant DA (ed) *The Molecular Biology of Cyanobacteria*, pp 677–692. Bryant DA (ed) Kluwer Academic Publishers, Dordrecht
- Gaidukov N (1903) Die Farbveränderung bei den Prozessen der Komplementären chromatischen Adaptation. *Berichte der Deutschen Botanischen Gesellschaft* 21: 517–522
- Gantt E (1981) Phycobilisomes. *Annu Rev Plant Physiol* 32: 327–347
- Gilles-Gonzalez MA, Ditta GS and Helinski DR (1991) A haemoprotein with kinase activity encoded by the oxygen sensor of *Rhizobium meliloti*. *Nature* 350: 170–172
- Gilles-Gonzalez MA, Gonzalez G, Perutz MF, Kiger L, Marden MC and Poyart C (1994) Heme-based sensors, exemplified by the kinase FixL, are a new class of heme protein with distinctive ligand binding and autoxidation. *Biochem* 33: 8067–8073
- Glazer AN (1982) Phycobilisomes: structure and dynamics. *Ann Rev Microbiol* 36: 173–198
- Glazer AN (1985) Light harvesting by phycobilisomes. *Annu Rev Biophys Biophys Chem* 14: 47–77
- Glazer AN, Lundell DJ, Yamanaka G and Williams RC (1983) The structure of a 'simple' phycobilisome. *Annals Institut Pasteur/Microbiol* 134B: 159–180
- Green BR and Durnford DG (1996) The chlorophyll-carotenoid proteins of oxygenic photosynthesis. *Annu Rev Plant Physiol Plant Mol Biol* 47: 685–714
- Green LS and Grossman AR (1988) Changes in sulfate transport characteristics and protein composition of *Anacystis nidulans* R2 during sulfur deprivation. *J Bacteriol* 170: 583–587
- Green LS, Laudenbach DE and Grossman AR (1989) A region of a cyanobacterial genome required for sulfate transport. *Proc Natl Acad Sci USA* 86: 1949–1953
- Grillo JF and Gibson J (1979) Regulation of phosphate accumulation in the cyanobacterium *Synechococcus*. *J Bacteriol* 140: 508–517
- Grossman AR (1990) Chromatic adaptation and the events involved in phycobilisome biosynthesis. *Plant Cell Environ* 13: 651–666
- Grossman AR and Kehoe DM (1997) Phosphorelay control of phycobilisome biogenesis during complementary chromatic adaptation. *Photosynth Res* 53: 95–108
- Grossman AR, Schaefer MR, Chiang GG and Collier JL (1993) The phycobilisome: A light harvesting complex responsive to environmental conditions. *Microbiol Rev* 57: 725–749
- Grossman AR, Schaefer M, Chiang G and Collier J (1994) The responses of cyanobacteria to environmental conditions: Light and nutrients. In: Bryant D (ed) *The Molecular Biology of Cyanobacteria*, pp 641–675. Kluwer Academic Publishers, Dordrecht
- Grossman AR, Bhaya D, Apt KE and Kehoe DM (1995) Light-harvesting complexes in oxygenic photosynthesis: Diversity, control and evolution. *Annu Rev Genet* 29: 231–287
- Hall MN and Silhavy TJ (1981) The *ompB* locus and the regulation of the major outer membrane porin proteins of *Escherichia coli* K12. *J Mol Biol* 146: 23–43
- Haury JF and Bogorad L (1977) Action spectra for phycobiliprotein synthesis in a chromatically adapting cyanophyte, *Fremyella diplosiphon*. *Plant Physiol* 60: 835–839
- Herbert SK, Fork DC and Malkin S (1990) Photoacoustic measurements in vivo of energy storage by cyclic electron flow in algae and higher plants. *Plant Physiol* 94: 926–934
- Hershko A (1988) Ubiquitin-mediated protein degradation. *J Biol Chem* 263: 15237–15240
- Hertig C, Li RY, Louarn A-M, Garnerone A-M, David M, Batut J, Kahn D and Boistard P (1989) *Rhizobium meliloti* regulatory gene *fixJ* activates transcription of *R. meliloti nifA* and *fixK* genes in *Escherichia coli*. *J Bacteriol* 171: 1736–1738
- Hiller RG, Anderson JM and Larkum AWD (1991) The chlorophyll-protein complexes of algae. In: Scheer H (ed) *Chlorophylls*, pp 529–547. CRC Press, Boca Raton
- Hofmann E, Wrench PM, Sharples FP, Hiller RG, Welte W and Diederichs K (1996) Structural basis of light harvesting by carotenoids: Peridinin-chlorophyll-protein from *Amphidinium carterae*. *Science* 272: 1788–1791
- Houmard J, Capuano V, Cousin T and Tandeau de Marsac N (1988a) Genes encoding core components of the phycobilisome in the cyanobacterium *Calothrix* sp. strain 7601. Occurrence of a multigene family. *J Bacteriol* 170: 5512–5521
- Houmard J, Capuano V, Cousin T and Tandeau de Marsac N (1988b) Isolation and molecular characterization of the gene encoding allophycocyanin B, a terminal energy acceptor in cyanobacterial phycobilisomes. *Mol Microbiol* 2: 101–107
- Houmard J, Capuano V, Columbano, Coursin T and Tandeau de Marsac N (1990) Molecular characterization of the terminal energy acceptor of cyanobacterial phycobilisomes. *Proc Natl Acad Sci USA* 87: 2152–2156
- Hua J, Chang C, Sun Q and Meyerowitz EM (1995) Ethylene insensitivity conferred by *Arabidopsis ERS* gene. *Science* 269: 1712–1714
- Ishige K, Nagasawa S, Tokishita S-I and Mizuno T (1994) A novel device of bacterial signal transducers. *EMBO J* 13: 5195–5202
- Jansson S (1994) The light-harvesting chlorophyll *a/b*-binding proteins. *Biochim Biophys Acta* 1184: 1–19
- Jeanjean R and Broda E (1977) Dependence of sulfate uptake by *Anacystis nidulans* on energy, osmotic shock, and on sulfate starvation. *Arch Microbiol* 114: 19–23
- Jung LJ, Chan CF and Glazer AN (1995) Candidate genes for the phycoerythrocyanin  $\alpha$  subunit lyase. *J Biol Chem* 270: 12877–12884
- Kahn K and Schaefer MR (1997) *rpbA* controls transcription of the constitutive phycocyanin gene set in *Fremyella diplosiphon*. *J Bacteriol* 179: 7695–7704
- Kahn K and Schaefer MR (1998) Cyanobacterial transposons TN5469 and TN5541 represent a novel noncomposite transposon family. *J Bacteriol* 180: 6059–6063
- Kahn K, Mazel D, Houmard J, Tandeau de Marsac N and Schaefer MR (1997) A role for CpeYZ in cyanobacterial phycoerythrin biosynthesis. *J Bacteriol* 179: 998–1006
- Kehoe DM and Grossman AR (1995) The use of site directed mutagenesis in the analysis of complementary chromatic adaptation. In: Mathis P (ed) *Photosynthesis: From Light to Biosphere*, pp 501–504. Kluwer Academic Publishers, Dordrecht
- Kehoe DM and Grossman AR (1996) Similarity of a chromatic adaptation sensor to phytochrome and ethylene receptors.



- Science 273: 1409–1412
- Kehoe DM and Grossman AR (1997) New classes of mutants in complementary chromatic adaptation provide evidence for a novel four-step phosphorelay system. *J Bacteriol* 179: 3914–3921
- Kendrick RE and Kronenberg GHM (eds) (1994). *Photomorphogenesis in Plants*, Kluwer Academic Publishers, Dordrecht
- Keren N and Ohad I (1998) State transition and photoinhibition. In: Rochaix J-D, Goldschmidt-Clermont M and Merchant S (eds) *The Molecular Biology of Chloroplasts and Mitochondria in Chlamydomonas*, pp 569–596. Kluwer Academic Publishers, Dordrecht
- Kim J and Mayfield SP (1997) Protein disulfide isomerase as a regulator of chloroplast translational activation. *Science* 278: 1954–1957
- Klose KE, Weiss DS, and Kustu S (1993) Glutamate at the site of phosphorylation of nitrogen-regulatory protein NTRC mimics aspartyl-phosphate and activates the protein. *J Mol Biol* 232: 67–78
- LaRoche J, Van der Staay GWM, Partensky F, Ducret A, Aebersold R, Li R, Golden SS, Hiller RG, Wrench PM, Larkum AWD and Green BR (1996) Independent evolution of the prochlorophyte and green plant chlorophyll *a/b* light-harvesting proteins. *Proc Natl Acad Sci USA* 93: 15244–15248
- Laudenbach DE and Grossman AR (1991) Characterization and mutagenesis of sulfur-regulated genes in a cyanobacterium: Evidence for function in sulfate transport. *J Bacteriol* 173: 2739–2750
- Laudenbach DE, Ehrhardt D, Green L, and Grossman AR (1991) Isolation and characterization of a sulfur-regulated gene encoding a periplasmically-localized protein with sequence similarity to rhodanese. *J Bacteriol* 173: 2751–2760
- Li H and Sherman LA (2000) A redox-responsive regulator of photosynthesis gene expression in the cyanobacterium *Synechocystis* sp strain PCC 6803. *J Bacteriol* 182: 4268–4277
- Lomax TL, Conley PB, Schilling J and Grossman AR (1987) Isolation and characterization of light-regulated phycobilisome linker polypeptide genes and their transcription as a polycistronic mRNA. *J Bacteriol* 169: 2675–2684
- Lukat GS, McCleary WR, Stock AM and Stock JB (1992) Phosphorylation of bacterial response regulator proteins by low molecular weight phospho-donors. *Proc Natl Acad Sci USA* 89: 718–722
- Luque I, Flores E and Herrero A (1994) Molecular mechanism for the operation of nitrogen control in cyanobacteria. *EMBO J* 13: 2862–2869
- Luque I, Zabulon G, Contreras A and Houmard J (2001) Convergence of two global transcriptional regulators on nitrogen induction of the stress-acclimation gene *nblA* in the cyanobacterium *Synechococcus* sp. PCC 7942. *Mol Microbiol* 41: 937–947
- Makino K, Shinagawa H, Amemura M and Nakata A (1986) Nucleotide sequence of the *phoB* gene, the positive regulatory gene for the phosphate regulon of *Escherichia coli* K-12. *J Mol Biol* 190: 37–44
- Manna P, Nieder RP, Schaefer MR (2000) DNA-binding properties of the *Fremyella diplosiphon* RpbA repressor. *J Bacteriol* 182: 51–56
- Mazel D and Marliere P (1989) Adaptive eradication of methionine and cysteine from cyanobacterial light-harvesting proteins. *Nature* 341: 245–248
- Mazel D, Guglielmi G, Houmard H, Sidler W, Bryant DA and Tandeau de Marsac N (1986) Green light induces transcription of the phycoerythrin operon in the cyanobacterium *Calothrix* 7601. *Nucleic Acids Res* 14: 8279–8290
- Mazel D, Houmard J and Tandeau de Marsac N (1988) A multigene family in *Calothrix* sp. PCC 7601 encodes phycocyanin, the major component of the cyanobacterial light-harvesting antenna. *Mol Gen Genet* 211: 296–304
- Mettke I, Fiedler U and Weiss V (1995) Mechanism of activation of a response regulator: Interaction of NtrC-P dimers induces ATPase activity. *J Bacteriol* 177: 5056–5061
- Mills SD, Jasalavich CA and Cooksey DA (1993) A two-component regulatory system required for copper-inducible expression of the copper resistance operon of *Pseudomonas syringae*. *J Bacteriol* 175: 1656–1664
- Nagaya M, Aiba H and Mizuno T (1994) The *sphR* product, a two-component system response regulator protein, regulates phosphate assimilation in *Synechococcus* sp. strain PCC 7942 by binding to two sites upstream from the *phoA* promoter. *J Bacteriol* 176: 2210–2215
- Nicholson ML and Laudenbach DE (1995) Genes encoded on a cyanobacterial plasmid are transcriptionally regulated by sulfur availability and CysR. *J Bacteriol* 177: 2143–2150
- Nicholson ML, Gaasenbeek M and Laudenbach DE (1995) Two enzymes together capable of cysteine biosynthesis are encoded on a cyanobacterial plasmid. *Mol Gen Genet* 247: 623–632
- Oelmüller R, Conley PB, Federspiel N, Briggs WR and Grossman AR (1988a) Changes in accumulation and synthesis of transcripts encoding phycobilisome components during acclimation of *Fremyella diplosiphon* to different light qualities. *Plant Physiol* 88: 1077–1083
- Oelmüller R, Grossman AR and Briggs WR (1988b) Photo-reversibility of the effect of red and green light pulses on the accumulation in darkness of mRNAs coding for phycocyanin and phycoerythrin in *Fremyella diplosiphon*. *Plant Physiol* 88: 1084–1091
- Omata T, Andriesse X and Hirano A (1993) Identification and characterization of a gene cluster involved in nitrate transport of the cyanobacterium *Synechococcus* sp. PCC 7942. *Mol. Gen Genet* 236: 193–202
- Parkinson JS and Kofoid EC (1992) Communication modules in bacterial signaling proteins. *Annu Rev Genet* 26: 71–112
- Perego M and Hoch JA (1991) Negative regulation of *Bacillus subtilis* sporulation by *spo0E* gene product. *J Bacteriol* 173: 2514–2520
- Perego M and Hoch JA (1996) Protein aspartate phosphatases control the output of two-component signal transduction systems. *Trends Genet* 12: 97–101
- Porter G, Tredwell CJ, Searle GFW and Barber J (1978) Picosecond time-resolved energy transfer in *Porphyridium cruentum*. Part I. In the intact alga. *Biochim Biophys Acta* 501: 232–245
- Posas R, Wurgler-Murphy SM, Maeda T, Witten EA, Tha TC and Saito H (1996) Yeast HOG1 MAP kinase cascade is regulated by a multistep phosphorelay mechanism in the SLN1-YPD1-SSK1 ‘two-component’ osmosensor. *Cell* 86: 865–875
- Quisel J, Wykoff D and Grossman AR (1996) Biochemical characterization of the extracellular phosphatases produced by phosphorus-deprived *Chlamydomonas reinhardtii*. *Plant*



- Physiol 11: 839–848
- Ravid S, Matsumura P and Eisenbach, M (1986) Restoration of flagellar clockwise rotation in bacterial envelopes by insertion of the chemotaxis protein CheY. *Proc Natl Acad Sci USA* 83: 7157–7161
- Ray JM, Bhaya D, Block MA and Grossman, AR (1991) Translation, transcription, and inactivation of the gene for an atypical alkaline phosphatase of *Synechococcus* sp. Strain PCC 7942. *J Bacteriol* 173: 4297–4309
- Richaud C, Zabulon G, Joder A, and Thomas J-C (2001) Nitrogen and sulfur starvation differentially affect phycobilisome degradation and expression of the *nblA* gene in *Synechocystis* Strain PCC6803. *J Bacteriol* 183: 2989–2994
- Rogowsky PM, Close TJ, Chimera JA, Shaw JJ and Kado CI (1987) Regulation of the *vir* genes of *Agrobacterium tumefaciens* plasmid pTiC58. *J Bacteriol* 169: 5101–5112
- Sauer J, Görl M and Forchhammer K (1999) Nitrogen starvation in *Synechococcus* PCC 7942: Involvement of glutamine synthetase and NtcA in phycobilisome degradation and survival. *Arch Microbiol* 172: 247–255
- Schaefer MR, Chiang GG, Cogley JG and Grossman AR (1993) Plasmids from two morphologically distinct cyanobacterial strains share a novel replication origin. *J Bacteriol* 175: 5701–5705
- Schmitt-Goff CM and Federspiel NA (1993) In vivo and in vitro footprinting of a light-regulated promoter in the cyanobacterium *Fremyella diplosiphon*. *J Bacteriol* 175: 1806–1813
- Schwarz R and Grossman AR (1998) A response regulator of cyanobacteria integrates diverse environmental signals and is critical for survival under extreme conditions. *Proc Natl Acad Sci USA* 95: 11008–11013
- Searle GFW, Barber J, Porter G and Tredwell CJ (1978) Picosecond time-resolved energy transfer in *Porphyridium cruentum*. Part II. In the isolated light-harvesting complex (phycobilisomes). *Biochim Biophys Acta* 501: 246–256
- Seib LO and Kehoe DM (2002) A turquoise mutant genetically separates expression of genes encoding phycoerythrin and its associated linker peptides. *J Bacteriol* 184: 962–970
- Shattuck-Eidens DM, and Kadner RJ (1983) Molecular cloning of the *uhp* region and evidence for a positive activator for expression of the hexose phosphate transport system of *Escherichia coli*. *J Bacteriol* 155: 1062–1070
- Sherman DM and Sherman LA (1983) Effect of iron deficiency and iron restoration on ultrastructure of *Anacystis nidulans*. *J Bacteriol* 156: 393–401
- Sidler WA (1994) Phycobilisome and phycobiliprotein structures. In: Bryant D (ed) *The Molecular Biology of Cyanobacteria*, pp 139–216. Kluwer Academic Publishers, Dordrecht
- Sobczyk A, Schyns G, Tandeau de Marsac N and Houmard J (1993) Transduction of the light signal during complementary chromatic adaptation in the cyanobacterium *Calothrix* sp. PCC 7601: DNA-binding proteins and modulation by phosphorylation. *EMBO J* 12: 997–1004
- Sobczyk A, Bely A, Tandeau de Marsac N and Houmard J (1994) A phosphorylated DNA binding protein is specific for the red light signal during complementary chromatic adaptation in cyanobacteria. *Mol Microbiol* 13: 875–885
- Stevens SE and Poane DAM (1981) Accumulation of cyanophycin granules as a result of phosphate limitation in *Agmenellum quadruplicatum*. *Plant Physiol* 67: 716–719
- Swanson RV, Zhou J, Leary JA, Williams T, de Lorimier R, Bryant DA and Glazer AN (1992) Characterization of phycocyanin produced by *cpcE* and *cpcF* mutants and identification of an intergenic suppressor of the defect in bilin attachment. *J Biol Chem* 267: 16146–16154
- Tandeau de Marsac N (1977) Occurrence and nature of chromatic adaptation in cyanobacteria. *J Bacteriol* 130: 82–91
- Tandeau de Marsac N (1983) Phycobilisomes and complementary adaptation in cyanobacteria. *Bulletin de L'Institut Pasteur* 81: 201–254
- Tandeau de Marsac N and Houmard J (1993) Adaptation of cyanobacteria to environmental stimuli: New steps towards molecular mechanisms. *FEMS Microbiology Reviews* 104: 119–190
- Tandeau de Marsac D, Mazel D, Damerval T, Guglielmi G, Capuano V and Houmard J (1988) Photoregulation of gene expression in the filamentous cyanobacterium *Calothrix* sp. PCC7601. *Photosyn. Res* 18: 99–132
- Taylor BL and Zhulin IB (1999) PAS Domains: Internal sensors of oxygen, redox potential, and light. *Microbiol Molec Biol Rev* 63: 479–506
- Uhl MA and Miller JF (1996) Integration of multiple domains in a two-component sensor protein: The *Bordetella pertussis* BvgAS phosphorelay. *EMBO J* 15: 1028–1036
- Utkilen HC, Heldal M and Knutsen G (1976) Characterization of sulfate uptake in *Anacystis nidulans* *Physiol Plant* 38: 217–220
- van der Staay GWM, Moon-van der Staay SY, Garczarek L and Partensky F (1998) Characterization of the Photosystem-I subunits PsaI and PsaL from 2 strains of the marine oxyphototrophic prokaryote *Prochlorococcus*. *Photosynth Res* 57: 183–191
- van Waasbergen LG, Dolganov N and Grossman AR (2002) Environmental control depends on PAS domain-bearing sensor protein. *J Bacteriol* 184: 2481–2490
- Vega-Palas MA, Flores E and Herrero A (1992) NtcA, a global nitrogen regulator from the cyanobacterium *Synechococcus* that belongs to the Crp family of bacterial regulators. *Mol Microbiol* 6: 1853–1859
- Vogelmann TC and Scheibe J (1978) Action spectrum for chromatic adaptation in the blue-green alga *Fremyella diplosiphon*. *Planta* 143: 233–239
- Wanner BL (1993) Gene regulation by phosphate in enteric bacteria. *J Cell Biochem* 51: 47–54
- Wanner BL (1994) Phosphate-regulated genes for the utilization of phosphonates in members of the family *Enterobacteriaceae*. In: Torriani-Gorini A, Yagil E and Silver S (eds) *Phosphate in Microorganisms. Cellular and Molecular Biology*, pp 215–222. ASM Press, Washington, DC
- Wanner BL and Wilmes-Riesenberg MR (1992) Involvement of phosphotransacetylase, acetate kinase, and acetyl phosphate synthesis in the control of the phosphate regulation in an *Escherichia coli*. *J Bacteriol* 174: 2124–2130
- Wanner G, Henkelmann G, Schmidt A and Kost H-P (1986) Nitrogen and sulfur starvation of the cyanobacterium *Synechococcus* 6301. An ultrastructural, morphometrical, and biochemical comparison. *Z Naturforsch* 41c: 741–750
- Wilbanks SM and Glazer AN (1993) Rod Structure of a phycoerythrin-II-containing phycobilisome. 1. Organization and sequence of the gene-cluster encoding the major phycobiliprotein rod components in the genome of marine *Synechococcus* WH 8020. *J Biol Chem* 268: 1226–1235

- Wilkinson JQ, Lanahan MB, Yen H-C, Giovannoni JJ and Klee HJ (1995) An ethylene-inducible component of signal transduction encoded by *Never-ripe*. *Science* 270: 1807–1809
- Wolfe AJ, Conley P, Kramer TJ and Berg HC (1987) Reconstitution of signaling in bacterial chemotaxis. *J Bacteriol* 169: 1878–1885
- Wood NB and Haselkorn R (1979) Proteinase activity during heterocyst differentiation in nitrogen-fixing cyanobacteria. In: Cohen GN and Holzer H (eds) *Limited Proteolysis in Microorganisms*, pp 159–166. US DHEW Publication No. (NIH) 79-1591, Bethesda
- Wood NB and Haselkorn R (1980) Control of phycobiliprotein proteolysis and heterocyst differentiation in *Anabaena*. *J Bacteriol* 141: 1375–1385
- Yamaguchi S, Aizawa S-I, Kihara M, Isomura M, Jones CJ and Macnab RM (1986) Genetic evidence for a switching and energy-transducing complex in the flagellar motor of *Salmonella typhimurium*. *J Bacteriol* 168: 1172–1179
- Yamanaka G and Glazer AN (1980) Dynamic aspects of phycobilisome structure. Phycobilisome turnover during nitrogen starvation in *Synechococcus* sp. *Arch Microbiol* 124: 39–47
- Yeh KC and Lagarias JC (1998) Eukaryotic phytochromes: Light-regulated serine/threonine protein-kinases with histidine kinase ancestry. *Proc Natl Acad Sci* 95: 13976–13981
- Yeh KC, Wu S-H, Murphy JT and Lagarias JC (1997) A cyanobacterial phytochrome two-component light sensory system. *Science* 277: 1505–1508
- Zhou J, Gasparich GE, Stirewalt VL deLorimier R and Bryant DA (1992) The *cpcE* and *cpcF* genes of *Synechococcus* sp. PCC 7002. Construction and phenotypic characterization of interposon mutants. *J Biol Chem* 267: 16138–16145

# Index

## A

- $\alpha$ -carotene 39, 56, 61, 313
- $\alpha,\epsilon$ -carotene 61
- $\alpha_B$  429
- $A_0$  255, 259–260, 262, 265, 274
- $A_1$  255, 259–260, 265, 271, 273–275
- abscisic acid 145
- absorbance
  - time-resolved 119–120
  - P700 390, 392
- absorbance detected magnetic resonance (ADMR) 228
- absorption 30, 69, 85, 92–93, 95, 99, 426, 429 *See also*
  - spectroscopy
  - anisotropy 104
  - bands 3–5
  - coefficient 85–86, 104
  - cross section 23, 30, 85, 429–432, 442
  - Soret 426
  - water 30, 425–429
- absorption maxima
  - carotenoids 57–59
  - length of conjugation system 3–4, 61–63
  - tuning 54
- absorption spectra 3–5, 63, 115, 177, 287, 311
  - carotenoids 63–67
  - tetrapyrroles 4, 47, 54, 55
- absorption spectroscopy
  - transient 274
- Acaryochloris marina* 12, 13, 35, 38, 42, 48, 144, 150, 313
- acclimation 19, 22, 387–388, 402–416,
  - cyanobacteria 410, 414, 473–488
  - eukaryotic algae 424–245, 429–442
  - plants 409–415
  - red algae 315–318,
- Achrochaetium* 313
- Acidiphilium rubrum* 37
- acrylic side-chain
  - chlorophylls and phycobilins 35, 50
- activated decay 274
- activation energy 274
- adaptation 19, 22, 403
- aggregation
  - chlorophyll 33
  - LHCII 227, 230
- Aglaothamnion* 308, 312, 313
- Aiptasia pallida* 347
- ALA *See* 5-aminolevulinic acid
- albino3* 358, 362
- Alexandrium* 326, 340, 341, 346
- algae
  - blue-green *See* cyanobacteria
  - cryptophyte (Cryptophyta) 17–21, 150–154, 297, 333–339
  - dinoflagellates (Dinophyta) 17–21, 339–347, 437
  - glaucophyte (Glaucophyta) 17–21, 38, 48, 148, 151–152, 282–283, 290, 308, 310, 313,
  - green (Chlorophyta) 17–21, 151–153, 155
  - haptophyte (Haptophyta) 17–21, 153, 328–333
  - heterokont (Heterokonta) 17–21, 151, 153–154, 328–333
  - red (Rhodophyta) 17–21, 148–149, 151, 153–154, 282–302, 308–319
- alignment
  - sequence 139, 172
- allophycocyanin (APC) 12, 38, 52, 54–55, 148–149, 284, 293, 309, 335
  - APC-B 311, 312
  - apcA1B1* 475
  - apcA2* 475
  - apcC1* 475
  - ApcD 473
  - ApcE 339
  - ApcF 473
- alloxanthin 39, 57, 325, 326
- alpha-crustacyanin 65
- 5-aminolevulinic acid (ALA) 42–44
  - ALA dehydratase 44
  - ALA synthesis 42–44
- Amoebobacter purpureus* 453
- Amphidinium* 35, 326, 340, 341–342, 345–346, 409
- Anabaena* 147, 414
- Anabaena variabilis* (M-3) 291
- Anacystis nidulans* 292
- analysis
  - photosynthetic pigments 67–69
- anchor polypeptide 288, 291–292, 473 *See also* phycobilisome
- anoxygenic bacteria 8, 34, 35, 169–188, 196–211, 450–465
- antenna systems
  - assembly 459–462
  - cyanobacteria 282–3–2, 472–474
  - evolution 130–160
  - green bacteria 196–211
  - overview 2–23
  - Photosystem I 254–275, 282–284, 291–292, 309, 311–315
  - Photosystem II 220–245, 282–284
  - prochlorophyte 8, 13, 146–147
  - purple bacteria 170–188, 450–451
- antheraxanthin 39, 57, 61, 384, 402
- Anthopleura elegantissima* 340
- antisense plants 269
- APC, Apc, *apc* *See* allophycocyanin
- apicomplexans 17
- Arabidopsis thaliana* 63, 136, 138, 385, 391, 402, 404, 406, 440
  - mutant *nqp4-1* 402
- archebacteria (Archaea) 133–134
- astaxanthin 32, 39, 57, 65, 430 *See also* carotenoids
- atmosphere 132, 160
- atomic force microscopy 10
- ATP synthase 413

## B

$\beta$ -carotene 39, 56, 204, 234–235, 265, 268, 274, 311, 313, 316, 430  
 $\beta,\beta$ -carotene 33, 57, 65  
     S1-energy 66  
     triplet state 67  
 $\beta,\beta'$ -carotene-2R-ol 39, 57  
 $\beta,\epsilon$ -carotene 57  
 $\beta,\psi$ -carotene 57, 61  
 $\beta$ -isorenieratene 39  
 $\beta$ -phycoerythrocyanin 52  
 $\beta$ -cyclization 61  
 $\beta$ -oxygenase 63  
 B-band 47  
 B800 170, 171, 176, 182–184  
 B800-820 459  
 B800-850 34, 450, 459  
 B808-865 199  
 B830 182  
 B850 170–171, 183, 184  
 B870 450  
 Bacillariophyceae (diatoms) 38, 60  
 bacteriorubixanthin 57  
 bacteria  
     aerobic 7, 32, 60  
     anoxygenic 6–11, 34, 35, 169–188, 196–211, 450–465  
     Gram-positive 134  
     green filamentous 6–11, 155, 196–211  
     green nonsulfur. *See* green filamentous  
     green sulfur 6–11, 134, 157, 159, 196–211  
     purple 6–11, 134, 155–157, 170–188, 450–465  
     reaction centers 134, 237  
     Tat pathway 357  
 bacteriochlorin 34, 37  
 bacteriochlorophyll (BChl) 34–48, 188  
     analysis 67–69  
     absorption bands 3, 41, 47  
     BChl/BChl interaction 180  
     delivery 462  
     occurrence 38  
     methylation 36  
     oxidation 188  
     structures 3, 36–37  
     synthesis 42–46, 142  
     transmetalated 37–40, 42  
 bacteriochlorophyll *a* 35, 37–38, 41, 47  
     absorption spectrum 4, 47  
     fluorescence emission spectra 4  
 bacteriochlorophyll *b* 32, 35, 37–38, 41, 46  
 bacteriochlorophyll *c* 36, 38, 41, 46, 199, 202  
 bacteriochlorophyll *d* 36, 38, 41, 46, 199, 202  
 bacteriochlorophyll *e* 36, 38, 41, 46, 199, 202  
 bacteriochlorophyll *f* 36, 38  
 bacteriochlorophyll *g* 37–38, 41, 46  
     BChl *g'* 42  
     BChl *gF* 35  
 bacteriopheophytin *a* (Bphe *a*) 42  
 bacteriorhodopsin 67

bacteriorubixanthinal 39  
*Bangia* 313  
 bangiophycean PE 310  
 barley 415  
     *chlorina* f2 mutant 415  
 baseplate *See* chlorosome  
 basis states 96  
*Batrachospermum* 313  
 BChl *See* bacteriochlorophyll  
 Beer-Lambert law 85  
*Beta vulgaris* 390  
 bilin pigments 48–54 *See also* phycobilins  
     biosynthesis 50–53, 142, 145  
     extinction coefficient 41, 57–59  
     spectroscopy 50, 53–59, 69  
     structures 48–50  
 bilin reductase  
     gene family 145  
 biliprotein *See* phycobiliprotein  
 bilirubin 52  
 biliverdin 50  
 biomarkers 132  
 biosynthesis  
     carotenoids 60–63, 144–145  
     chlorophylls 42–44, 142–144  
     phycobilin chromophores 50–53, 145  
     tetrapyrroles 42–44, 142–144  
*Blastochloris viridis* (*Rhodopseudomonas viridis*) 11, 31, 156, 171, 187, 451  
 blue light photoreceptor 416  
 Boltzmann equilibrium 31  
 Born-Oppenheimer approximation 113  
 BPhe *a* *See* bacteriopheophytin *a*  
 bra-ket notation 106, 123  
 $B_x$  47  
 $B_y$  47

## C

C-1 hydroxylase (CrtC) 62–63  
 C-2 oxygenase (CrtA) 62–63  
 C-PC 301, 311 *See also* phycocyanin  
*c*-type cytochromes 7, 53  
 $C_4$  species  
     NADP-malic enzyme type 376, 378  
 $C_5$ -pathway 42  
 $Ca^{2+}$  ions  
     binding 231  
*Callithamnion* 313  
*Calothrix* PCC7601 52  
 caloxanthin 39, 57  
*Camellia japonica* 376  
 canthaxanthin 39, 57  
 carbon assimilation 404  
 carbon reduction cycle 205  
 carotene  
      $\alpha$ -carotene 39, 56, 61, 313  
      $\alpha,\epsilon$ -carotene 61  
     all-*trans*- $\beta,\beta'$ -carotenes 32, 67, 235

- $\beta$ -carotene 39, 56, 204, 234–235, 265, 268, 274, 311, 313, 316, 430  
 $\beta,\beta$ -carotene 33, 57, 65  
     9-*cis*- $\beta,\beta$ - 67  
 $\beta,\epsilon$ -carotene 57  
 $\beta,\psi$ -carotene 57, 61  
 $\epsilon$ -carotene 39  
 $\zeta$ -carotene 39  
 carotenoid 30, 31, 56–67, 144, 181–182, 184, 200, 265–266, 406, 439  
     absorption 181  
     allenic 60, 65  
     all-*trans* 32, 67, 235  
     analysis 63  
     biosynthesis 60–63, 142, 145, 200  
     *cis/trans* isomerizations 67  
     conformational flexibility 66, 67  
     end groups 56  
     epoxides 33, 68  
     excited states 32, 61, 66  
     glycosylation 63  
     green bacteria 60  
     HPLC 69  
     internal conversion 65  
     isomerization 67  
     modification 61, 63  
     nomenclature 60  
     occurrence 39–40  
     oxygenated 33  
     photoprotection 31–33  
     photosystem I 265–269, 274  
     purple bacterial LH2 181–184  
     radiationless deexcitation 66  
     solubility 63  
     spectroscopy 63–67  
          $S_0$  to  $S_2$  transition 65–67  
          $S_1$  fluorescence 66  
          $S_1$ -state 61  
         substituent effects 65  
     stereochemistry 56, 63  
     structures 56–59  
     triplet state 31, 61, 65, 67  
 carotenoid glucoside 200  
 Cbr 410  
 CD *See* circular dichroism  
 Cd chlorophyll 40  
 cell-sorting 71  
*Ceramium tenuicorne* 318  
*chaos* 358  
 charge separation 69, 236, 239, 242, 273  
     rate of 242, 243  
     transfer-to-the-trap-limited 239  
 charge stabilization 236, 239  
 charge-coupled device (CCD) cameras 392  
 charge-transfer transitions 86, 115  
 chemolithotrophs 132  
 Chl *See* chlorophyll  
 Chl  $a_2$ . *See* divinyl Chl a (Chl  $a_2$ )  
 Chl  $b_2$ . *See* divinyl Chl b (Chl  $b_2$ )  
*Chlamydomonas* 20, 22, 151, 314, 385, 387, 391–392, 407, 414, 435, 437, 440, 442  
     mutants 387, 440  
*Chlorarachnion* 16, 155  
 chlorarachniophytes 14, 17, 38  
*Chlorella* 410, 436, 439  
*chlorina* f2 barley mutant 415  
 chlorins 34, 36  
 chlorobactene 39  
 chlorobactene, 1'-hydroxy, acyl-glucosyl 57  
 Chlorobiaceae 6, 7, 10, 38, 60, 61, 134, 156, 157, 159, 196–217  
*Chlorobium* 10, 137, 143, 156, 196–197, 199–200  
     chlorophyll 199–200  
*Chlorobium limicola* 200  
*Chlorobium phaeobacteroides* 200, 205  
*Chlorobium tepidum* 197–200, 205, 208, 209  
 chlorobiumquinone 205, 207  
 Chloroflexaceae 6, 7, 10, 38, 61, 131, 134, 156–157, 159, 196  
*Chloroflexus* 10, 134, 143, 156, 196–197, 199–200, 202, 205  
 Chlorophyceae (Chlorophyta) 38 *See also* algae, chlorophyte  
     algae  
 chlorophyll (Chl) 30, 34–48, 70, 223  
     absorption spectrum 47, 236, 271  
     accessory 143–144, 236–237  
     aggregation 33  
     analysis 67–69  
     connecting 239  
     double-bond isomerization 46  
     electronic structure 3  
     13<sup>2</sup> (S)-epimers 42  
     esterifying alcohols 35  
     fluorescence 42, 100  
         PAM fluorimetry 373–399  
         photosystem I 269–275  
         photosystem II 236, 238–240, 432–434  
         video imaging 392  
     Hg chlorophyll 40  
     ligation 365  
     long-wavelength 262–263, 269–270, 271, 272, 275  
     metal exchange 38–39, 41–42  
     occurrence 34, 40–41  
     Pb chlorophyll 40  
     peripheral 236  
     porphyrin-type 37  
     propionic acid side-chain 35  
     red 262–263, 269–271, 275  
     structure 36–37  
     synthesis 42–46, 142–144, 364–367  
     triplet states 274  
 chlorophyll *a* 34, 38, 41, 47, 144, 231, 311–312, 315  
     absorption bands 3  
     binding sites 314  
     Chl  $a'$  42  
     dimers 264–265  
     oxygenase 45, 143  
 chlorophyll *a* oxygenase/dehydratase 45  
 chlorophyll *a* to  $P_{700}$  ratio 428  
 chlorophyll *a/b* antenna 8, 20, 222–233, 438–440  
     prochlorophyte 8, 13, 146–147

- proteins 150–154
- chlorophyll *a/c* antenna 9, 20, 150–154, 328–333, 339–347
- cryptophyte 150–154, 330–339
- dinoflagellate 153, 339–347
- haptophyte 151–153, 328–333
- heterokont 151–154, 328–333
- proteins 20, 150–154
- chlorophyll *b* 35, 38, 41, 143, 144, 231
- chlorophyll biosynthesis 42–46
  - evolution of 142–144
  - feedback regulation 43
- chlorophyll *c* 35, 37, 45, 142, 144, 315, 324–348
  - Chl *c*<sub>1</sub> 38, 41
  - Chl *c*<sub>2</sub> 38
  - Chl *c*<sub>3</sub> 38, 41
  - cryptophytes 144
  - galactolipid 35
- chlorophyll *d* 12, 13, 35, 38, 41, 283, 312
  - Chl *d'* 42
- chlorophyll synthase 45, 366
- chlorophyll-chlorophyll interactions 33
- chlorophyllide *a* 13, 16, 37, 142, 365
- chlorophyte (green) alga 17–21, 151–155, 436–442
- chloroplast 14–23
  - development 354–367, 415
  - envelope 14–16, 19
  - evolution of 14, 17, 130, 143–144
  - genome 14–15
  - higher plant 19, 21
  - Sec pathway 357
  - SRP pathway 357
  - TatC 358
  - ultrastructure 18–21
- chloroplastic signal 416
- chloroquinone 30
- chlorosome 6, 8–10, 33, 36, 54, 156, 159, 195–196, 201
  - baseplate 10, 198, 202–204
  - proteins 202
- chloroxanthin dehydrogenase 63
- chloroxanthin synthase 63
- Chromatiaceae 61
- Chromatium* 43
- Chromatium minutissimum* 174
- Chromatium purpuratum* 173
- Chromatium tepidum* 171
- Chromatium vinosum* 5, 171, 173
- chromatography
  - Cu<sup>2+</sup>-affinity 235
  - pigment 69
- chromophore 11, 86, 298–300. *See also* bacteriochlorophyll,
  - carotenoids, chlorophyll, phycobilins
  - binding pocket, site-directed mutagenesis 70
  - binding site 485
  - biosynthetic cost 53–54
  - chemical modification 70
  - configurations 298
  - exchange 70
- chromophytes 35. *See also* algae
- chromoplasts 60
- Chrysophyceae 38
- circular dichroism 86–90, 95, 99, 177–178, 180, 208, 228,
  - 273, 329, 332, 336
  - spectra 337, 342–343
- circularly polarized light 86, 93, 95
- 9-*cis*- $\beta,\beta$ -carotene 67
- cis*-band, carotenoid 65
- cis*-carotenoids 65, 67
- cis*-neoxanthin 67
- cis*-phytoene 67
- 13-*cis*-rhodopinal 61
- cis/trans* isomerizations
  - carotenoid 67
- clouds 428
- Co-tetrapyrrole 43
- CO<sub>2</sub> assimilation
  - quantum yield 389
- coherence 105
- coherent nuclear motions 185
- cold acclimation 416
- common ancestor
  - photosystems 157
- complementary chromatic adaptation 316, 473–481, 476
  - model 481–482
  - mutants 477–481
  - phycobiliprotein gene promoters 476–477
- complex function 106
- configuration interaction 67, 89, 90–91, 104
- confocal microscopy 21
- conformation
  - bilin 54, 55
  - carotenoid 66–67
  - LHCII 384
  - mobility 54
- conjugation system length
  - absorption maximum 3–4, 61, 65–66
  - protective functions 61
- connecting chlorophyll 239
- conservative sorting 356
- convergent evolution 149
- conversion
  - internal 103
- coproporphyrinogen III oxidative decarboxylase 44
- core antenna 8–9, 35
  - 3-D structures of 145
  - evolution of 157–159
- core complex 145
  - family 8, 137, 145–146
  - PS II 238, 240, 243
- Coulomb interaction 301
- Coulombic coupling 344
- coupling strength 96
- CP24 22, 233, 240
  - reconstituted 233
- CP26 22–23, 151, 221, 232, 240
  - reconstituted 232
- CP29 22–23, 63, 151, 231, 240
- CP43 6, 8, 13, 146–147, 159, 234, 283, 309, 414
- CP43' 13, 147, 414
- CP47 6, 8, 13, 146, 159, 234, 283, 309
- cpcB1A1* 475

- cpcB2A2* 475  
*cpcB3A3* 475  
*cpcD2* 475  
*CpcE* 484  
*cpcE* 475, 485  
*CpcF* 484  
*cpcF* 475, 485  
*cpcH2* 475  
*cpcI2* 475  
*cpeBA* 476  
*cpeCDE* 476  
*cpeY* 476  
*cpeZ* 476  
*cpFtsY* 362  
*cpOxa1p* 358, 362  
*cpSecA* 358  
*cpSecE* 358  
*cpSecY* 358  
*cpSRP* pathway 361  
*cpSRP43* 358, 362  
*cpSRP54* 358, 362  
*cpTatC* 358, 361  
*crocoxanthin* 39, 57  
*Chroomonas* sp. *See* *Rhodomonas* sp.  
*cross section* 270, 429–432  
   absorption 23, 30, 85, 429  
   back-scattering 426, 429–432, 442  
*cryptochrome* 416  
*Cryptomonas* 326  
*Cryptomonas*  $\Phi$  ( $\phi$ ) *See* *Guillardia theta*  
*Cryptomonas maculata* 337  
*Cryptomonas rufescens* 337, 339  
*cryptophycean phycoerythrin* 297  
*cryptophyte* (Cryptophyta) 14, 17, 18, 20, 38, 48–50, 144, 151, 282–283, 297, 326  
   nucleomorph 14, 17, 151  
*cryptoviolin* 284  
*cryptoxanthin* 39  
*crystal structure*  
   LH2 174, 175  
   LHCII 151–152, 221, 223–224  
   phycobiliprotein 293  
   PSI 255–266  
   PS II 234–236  
*CsmA* 202–203  
*CsmB* 202  
*CsmC* 202  
*CsmD* 202  
*CsmE* 202  
*CsmF* 202  
*CsmH* 202  
*CsmI* 202  
*CsmJ* 202  
*CsmM* 202  
*CsmN* 202  
*CsmX* 202, 203  
*Cu*  
   chlorophyll 40  
   prospecting 42  
*Cu<sup>2+</sup>* -affinity chromatography 235  
*Cucurbita pepo* L. 406  
*Cyanelles* 38  
*Cyanidium* *See also* *Galdieria*  
*Cyanidium caldarium* 39, 50, 295, 308–309  
*cyanobacteria* 6–9, 11–14, 34, 46, 48, 50, 131, 134, 143–145, 148–149, 282–302, 408, 410, 439  
   2-methylhopanoids 132  
   antenna systems 282–302  
   carotenoids 39–40, 57–560  
   chromophores 38–41  
   evolution of 157–159  
   light harvesting regulation 472–488  
   phycobilins 38, 48–56  
   phycobilisomes 12, 309–310  
*Cyanobacteriaceae* *See* *cyanobacteria*  
*Cyanophora* 308, 313, 318  
*Cyanophora paradoxa* 48, 310, 314  
*Cyanophyta* *See also* *cyanobacteria*  
   Cyanophyta I 38  
   Cyanophyta II 38  
*cyclic electron transport* 405  
*cyclization*  
   carotenoids 60–62  
   Chl or Bchl precursors 43–45  
*Cyclotella* 154, 326, 330, 331  
*Cylindrotheca* 326  
*cysteine*  
   phycobilin-protein ligation 49, 50  
*cytochrome* 86  
*cytochrome b-559* 235, 236  
*cytochrome b<sub>6</sub>f* 21, 70, 405, 435, 440  
*cytochrome c* oxidation 206  
*cytochrome c<sub>6</sub>* 254, 258
- ## D
- $\Delta$ pH  
   across the thylakoid membrane 384  
   persistent 388  
 $\Delta$ pH gradient 438  
 $\Delta$ pH-dependent/Tat pathway 357, 361  
 $\Delta$ 2,6-phytyadienol 42  
*D1* protein 9, 235, 309, 379, 387  
   integration 363  
*D1/D2* 407  
*D2* protein 9, 235, 309, 407  
*dark-decay of variable fluorescence* 377  
*DBMIB* 416, 435, 439  
*DCCD* 231  
*DCMU* 416, 433, 439  
*de-epoxidase*  
   violaxanthin 384, 406, 437  
*decay kinetics* 274  
*decay-associated spectra* 272  
*7',8'-dehydro-spheroidene* (12 cdb) 65  
*Deinococcus/Thermus* 134  
*deletions* 139  
*delivery term* 243  
*deoxyxylulose 5-phosphate (DOXP) pathway* 60, 62, 144–145



depolarization  
 fluorescence 182  
 Dexter mechanism 31–32, 66, 110–111, 274, 301  
 diadinoxanthin 57  
 diadinoxanthin 32, 39, 57, 63, 316, 325–326, 332, 346, 437  
 diapo-carotene-dioate, di-(acyl-glucosyl) 57  
 diapo-carotenes 60  
 diapo-neurosporene 39, 57  
 diapocarotenoate 39  
 diapophytoene 60  
 diatoms 38  
 diatoxanthin 32, 39, 58, 437  
 2,6-dichlorophenolindophenol 338  
*Dictyota* 326, 329  
 diel cycle 428  
 dielectric screening 109  
 differential gene expression 438  
 digitonin 327  
 1',2'-dihydro-3',4'-dehydro-spheroidene (13 cdb) 65  
 5',6'-dihydro-7',8'-dehydro-spheroidene 65  
 15,16-dihydrobiliverdin 49–51, 53, 334–336  
 15,6-dihydrobiliverdin 50  
 1,2-dihydroneurosporene 32, 58  
 dimethylallyl-pyrophosphate 60, 63  
 dinoflagellates (Dinophyta) 14, 17–18, 20, 38, 48, 56, 156, 326  
 dinoxanthin 58  
 diode-array  
 HPLC 69  
 dipolar coupling 66  
 dipole strength 92, 98, 104, 116–117, 121  
 dipole-dipole coupling 108–110, 301, 302, 337, 344  
 disorder 176–177, 184  
 intrinsic 236  
 dissipation of excess energy 69, 224  
 distal antennas 6–12  
 diterpenes 60  
 divinyl Chl *a* (Chl  $a_2$ ) 13  
 divinyl Chl *b* (Chl  $b_2$ ) 13  
 divinyl pigments. *See* 8-vinyl pigments  
 DnaK 462  
 dodecyl- $\beta$ ,D-maltoside 235  
 dot product 106  
 DOXP pathway. *See* deoxyxylulose 5-phosphate 144  
 drought 406  
*Dunaliella* 67, 409  
*Dunaliella bardawil* 32  
*Dunaliella salina* 409–410  
*Dunaliella tertiolecta* 410, 425, 438–439

## E

$\epsilon$ -carotene 39  
 $\epsilon,\epsilon'$ -carotene 57  
 $\epsilon$ -cyclase 61, 63  
 $\epsilon$ -oxygenase 63  
 early light-inducible proteins (ELIPs) 150–152, 155, 221, 233,  
 363, 410, 415  
 echinenone 39, 58  
*Ectothiorhodospira halochloris* 156

eigenfunction 106, 124  
 eigenvalue 106  
 electric field 92  
 electrochromic shift 66  
 electromagnetic radiation 92–95, 103, 107, 116–117  
 electron carrier 254, 258  
 electron crystallography 151, 172, 221, 223  
 electron exchange 31–32, 274  
 energy transfer 66  
 interaction 301  
 electron microscopy  
 freeze-fracture 11, 13  
 immuno-gold labeling 202  
 transmission 19  
 electron transfer 33, 41, 69, 71, 254–255, 257–260  
 rate 441  
 electron transport  
 bacteria 6–8  
 cyclic 405  
 PS II-driven 391  
 electron transport chain 6–8, 255, 257, 259–260, 262  
 electrostatic fields 298  
 ELIPs. *See* early light-induced proteins  
 Emerson-Arnold number 432  
*Emiliania* 37, 326  
 endoplasmic reticulum (ER) 14, 16  
 endosymbiosis 11, 155, 353  
 primary 14–15, 137  
 secondary 14, 16, 138  
 energy. *See also* absorption, fluorescence, spectroscopy  
 absorption 403  
 density 94  
 dissipation 63, 69, 224  
 distribution 318–319, 386  
 quenching 402, 406  
 utilization 403  
 energy transfer 5, 18, 30, 42, 47, 66–67, 69, 71, 207, 209–210,  
 236, 262, 265, 270–275, 291, 301–302  
 carotenoid to BChl 210  
 Chl *b* to Chl *a* 229  
 diffusion-limited 243  
 dynamics 235  
 electron exchange 31–32, 66  
 Förster 108–110, 242, 302, 344  
 kinetics 271  
 resonance 100, 101, 108–111, 119  
 triplet-triplet 274  
 xanthophyll to Chl 228  
 energy-dependent quenching 382, 383, 406  
 energy-gap law 103  
 envelope  
 chloroplast 14, 16, 364  
 chlorosome proteins 202  
 epimers  
 BChl 36  
 epoxidase  
 zeaxanthin 384, 406, 437  
 epoxidation  
 zeaxanthin 63

epoxidation state 415  
 epoxidation-deepoxidation cycles 32  
 epoxide  
   carotenoid 33, 68  
 EPS *See* epoxidation state  
 equilibration 230, 242  
*Erwinia herbicola* 63  
*Erythrobacter* sp. 63  
 erythroxanthin 39, 63  
 erythroxanthin-sulfate 58  
*Escherichia coli* 137, 231  
   TatC 358  
 3-ethylidene bilins 48  
 etiolated seedlings 415  
 eubacteria 6–13, 133–134 *See also* bacteria, prokaryotes  
*Euglena* 155  
 euglenoids (Euglenophyta) 14, 17, 38  
 eukaryotic algae 14–20, 150–154, 297, 308–319, 328–339, 437–442  
   photoacclimation 424–443  
*Euonymus kiautschovicus* 411  
 Eustigmatophyceae 38, 144, 328  
 evolution 132–160  
   atmosphere 132  
   chloroplast 14–22  
   convergent 149  
   heterodimerization of RC proteins 159  
   light-harvesting 14–22, 130–160  
   PsaC 257  
   rate variation 140  
   very early 131  
 evolutionary distances 140  
 exchange coupling 31–32, 66, 110–111, 274, 301  
 excitation energy 270  
   acceptor 272  
   dissipation of excess 69, 224  
   distribution of 272, 386  
   thermal dissipation 383  
   transfer 65, 274  
   trapping of 242–245  
 excitation pressure 404, 408, 432  
 excited state 61, 66, 71, 242, 271  
   carotenoid 32, 66  
   dynamics 61, 66, 71, 242, 271  
   energy 71  
 exciton 88, 90, 95–100, 302  
   calculation 177  
   coupling 30, 48, 71, 95, 208, 262, 263, 265, 271, 273  
     carotenoid 66  
   delocalization 42  
   hopping 187  
   interactions 95, 104, 271  
   short-circuit 242  
   theory 176  
 exciton/radical pair equilibrium model 242  
 expectation value 107, 123–124  
 extended dipole approximation 271  
 extinction coefficient 53, 85, 295, 301  
   bilins 41, 69  
   carotenoids 57–59

Chl and BChl 41  
 extraction  
   of pigments 68  
 extrinsic antenna 6, 9

## F

F430 43, 55  
 F685 238  
 F695 235, 238  
 F<sub>A</sub> 255–257, 260  
 farnesol ester 42  
 farnesyl pyrophosphate 60  
 fast repetition rate fluorescence (FRRF) technique 432–434  
 F<sub>B</sub> 255–257, 260  
 FCP *See* fucoxanthin-Chl *a/c* protein  
 Fe  
   deficiency 413  
   limitation 132, 147, 160  
   porphyrins 4, 50  
 femtosecond transient absorption 229  
 Fenna-Mathews-Olson protein (FMO) 6, 9–10, 156, 196, 198, 204, 207–209  
 ferredoxin 46, 50, 205, 254, 256–257, 260, 416  
 ferredoxin-NADP reductase (FNR) 257  
 ferrochelatase 43, 44  
 FeS centers 203, 255–257, 259–260  
*ffc* 358  
*Fischerella* 147  
 first passage time 244  
 flavodoxin 254, 257  
 flicker effect 428  
 fluctuation density scattering 426  
 fluorescence 95, 100–101, 109, 116–117, 119, 242, 405  
   77K 378, 386, 387  
   anisotropy 103–105, 105, 120  
   bilin 56  
   depolarization 182, 202, 337  
   emission 5, 93  
   excitation 344, 346, 348  
   fast repetition rate (FRRF) 432–434  
   induction effect 272  
   initial 375  
   lifetime 100–101, 103, 109, 116, 117, 272  
   line-narrowing 232  
   non-modulated 374, 376  
   polarization 182, 202, 292, 337  
   PS I 269–275, 376  
   PS II 236, 238–240  
   Pulse amplitude modulated (PAM) 373–392  
   quenching 206, 379–388, 436  
   recovery  
     photobleaching 13  
   single-cell 67  
   spectra 4, 338  
   spectroscopy 4, 66, 100–101, 291  
   spontaneous 116, 119  
   time-resolved 118–119, 229, 344  
   upconversion 119, 229, 344

variable 376–378  
     dark-decay of 377  
     rise of 377  
     yield 56, 100–101, 103, 109, 117, 272  
 fluorometer  
     pulse amplitude modulation 374  
 $F_m$  379, 433  
 FMO. *See* Fenna-Mathews-Olson protein  
 FNR. *See* ferredoxin-NADP reductase; fumarate-nitrate regulator  
 food dyes 61  
 forbidden transition 54, 63, 66, 122  
 7-formyl reductase 45  
 Förster radius 110  
 Förster theory 30, 176, 108–110, 242, 301, 302, 337, 344  
 fossil  
     microorganisms 131  
 four-orbital model 46  
 Franck-Condon factor 109, 114  
 freeze-fracture electron microscopy 11, 13  
 freezing tolerance 413, 416  
*Fremyella diplosiphon* 295, 473–481  
 FRRF *See* fast repetition rate fluorescence technique  
 FtsY 362  
 fucoxanthin 20, 39, 56, 58, 61, 66, 314–316, 324–326, 330–331, 348  
 fucoxanthin, 19'-butanoyloxy 58  
 fucoxanthin, 4-keto-19'-hexanoyloxy 58  
 fucoxanthin Chl a/c protein (FCP) 326–332  
     spectroscopy 329–330  
     protein sequences 330–332  
*Fucus* 326  
 fumarate-nitrate regulator (FNR) 457  
 functional absorption cross-sectional area 403  
 functional groups 71  
 funneling 209  
 $F_v$  379, 433  
 $F_x$  255–257, 260

## G

$\gamma$ -carotene 39, 56  
     1'-hydroxy, acyl-glucosyl 57  
     4-keto 57  
 $\gamma$ -subunit 286  
*Galdieria monilis* 297  
*Galdieria pacifica* 310  
*Galdieria sulphuraria* 39, 50, 154, 308–310, 313, 315  
     gene clusters 141  
     duplication 136–137, 143, 148, 156  
     expression 331  
     family 137  
         bilin reductase 145  
         globin 288  
     loss 136  
     paralogous 141  
     purple photosynthetic bacteria 452–459  
     relocation 138  
     transfer in endosymbiosis 14–16

general protein import apparatus 357  
 genetic variation 136  
 genome 134  
     *Arabidopsis* 138  
 genomics 130  
 geranylgeraniol 36  
     hydrogenation 46  
 geranylgeranyl-pyrophosphate 60, 63  
*Giraudyopsis* 326, 331  
*Glaucocystis* 308  
 glaucocystophyte algae (Glaucophyta) 16, 38, 48, 148, 151–152, 282–283, 290, 308, 310, 313  
 globin family 288  
*Gloeobacter* 12, 290  
 glucoside  
     carotenoid 60, 63, 200  
 glutamate synthase 406  
 glutamate-l-semialdehyde aminotransferase 44  
 glutamic acid 44, 331  
 glutamine 331  
 glutamyl-tRNA 44  
 glycine 44  
 glycolate oxidase 406  
 gold labeling *See* electron microscopy 202  
*Gonyaulax* 326, 340, 341  
 Gram-positive bacteria 134  
 grana 20–22, 224  
     membrane 240  
 green algae 16–21, 151–153, 155, 434, 437–443  
 green gap 30, 35, 53 Falko chap  
 green photosynthetic bacteria 196–211  
     filamentous (nonsulfur, gliding) 6–8, 134, 155, 196  
     sulfur 6–9, 134, 157, 159, 196  
 green plant  
     chloroplast pigments 38–40  
     chloroplast structure 19, 21–23  
     chlorophyll synthesis 43–46  
 greening 233  
 GroEL 462  
 growth irradiance 409  
*Guillardia theta* 138, 155, 326, 338, 339

## H

H-bonds 178–179  
 Hamiltonian 95–96, 107, 114, 121–122, 124  
 haptophytes (Haptophyta) 14, 17–18, 20, 38, 153–154, 326  
 harmonic oscillator 101, 114  
 Hcf106 protein 358, 361  
*hcf106* mutant 358, 359  
 heat stress 377  
 heat-shock gene 416  
 heavy metal incorporation  
     chlorophyll 69  
 heavy metals  
     stressed 42  
*Heliobacillus* 143, 157  
 Heliobacteriaceae 6, 7, 8, 9, 38, 60, 134, 157, 159

*Helio bacterium chlorum* 10, 42  
*Heliothrix* 134, 196  
*Hematococcus pluvialis* 32  
heme 3, 4, 43–44, 51, 53  
  electronic structure 3  
  excited states 4  
  oxygenases 50  
hemoglobin 4–5, 50  
herbaceous winter annuals 412  
herbicides 60, 61  
*Heterocapsa* 326, 339, 341–342, 345–346  
heterokont algae (Heterokonta) 14, 17–21, 56, 153, 154, 326, 328–333  
*Heterosigma akashiwo* 19, 154, 326, 330  
heteroxanthin 39, 58, 326, 332  
hexapyrrole 43  
Hg chlorophyll 40  
high Chl fluorescence  
  mutants 391  
high hydrostatic pressure 180  
high light 405, 487–488  
high temperature 407  
high light-induced proteins (Hlips) 151, 155, 283  
high-resolution spectroscopy 70  
higher plant *See* green plant  
Hlips. *See* high light-induced proteins  
hole burning 115–116  
homogeneous broadening 115  
hopping 271  
*Hordeum vulgare* 382, 391  
horizontal gene transfer. *See* lateral gene transfer  
HPLC 69  
hydrogen peroxide 159  
hydrostatic pressure  
  high 180  
hydroxyl radical 33  
hydroxymethylbilane 43, 44

## I

I-P phase 377  
IHF. *See* integration host factor (IHF)  
illumination  
  intermittent 383, 385, 415  
in vitro protein import 354  
incident spectral irradiance 430  
indels 136, 139  
induced dichroism 104  
infrared spectroscopy 94, 101–102, 108, 114  
inhomogeneous broadening 115, 187, 235  
inhomogeneous distribution 238  
initial fluorescence 375  
  quenching of 385  
initial slope  
  photosynthesis-irradiance curve 432  
integration host factor (IHF) 457  
interaction  
  pigment-pigment 71

intermittent light grown plants 385, 415  
  pea 383  
internal conversion 31, 42, 100, 103, 242  
  carotenoid 65  
intersystem crossing 32, 100, 103, 112, 242, 274  
intersystem electron carriers 7, 405  
intracytoplasmic membrane  
  cyanobacteria 196  
  purple bacteria 11  
invariant sites 143  
iron-sulfur (FeS) cluster 203, 255–257, 259–260  
irradiance 85, 94, 116, 316, 410 *See also* light  
  effects 316  
  response 410  
IsiA 13, 146, 147, 254, 255, 258, 259, 265  
*Isochrysis* 326, 330, 346  
isocyclic ring 34, 46  
isomerization 296  
  carotenoid 67  
  phycoviolobin 296  
isopentenyl pyrophosphate 60, 63  
isoprenoid quinones 205  
isoprenoids 144  
isorenieratene 39, 58, 61  
isotope labeling 71

## J

J-I phase 377  
Jablonski diagram 100

## K

Kasha's rule 103  
Kautsky effect 376  
kinetics  
  trap-limited 243  
Kronecker delta 242

## L

L18 362  
La-chlorophyll 40  
labeling  
  isotope 71  
*Laminaria* 326, 329, 330, 410  
lateral gene transfer 16, 130, 134, 137, 144, 157–159, 196  
lateral heterogeneity 20, 330, 342  
lateral segregation 20–22  
 $L_{CM}$  309–312  
LD. *See* linear dichroism  
LH1 4, 6, 8, 11, 170–188, 450–464 *See also* LHI  
  cost 54  
  green bacteria (B808-866) 198–199  
  modified pigments 70, 155  
  size 67  
LH2 4, 6, 8, 11, 170–188, 450–464 *See also* LHII  
  cost 54  
  crystal structure 174–175  
  modified pigments 70, 155

- LH3 6, 8, 11, 155, 170–188  
 LhaA 461  
 LHC superfamily 4–5, 16, 18–22, 137  
   conserved sequence motifs 152  
   evolution 150–155  
   phylogenetic trees 153, 327  
 LHC I 20, 22, 54, 70, 254–255, 259, 266–270, 283, 309, 311–315, 274–275  
   cryptophyte 337–339  
   energy transfer 274–275  
   LHCI-680 269, 270  
   LHCI-730 270  
   polypeptides 311, 314  
   reconstituted 70, 154  
   red algae 19, 309, 311, 313–315  
 LHC II 18–23, 51, 221–230, 270, 309, 384  
   acclimation 409–410, 412–414  
   connectivity 22  
   chromophore cost 54  
   crystal structure 18, 223–227  
   energy-dependent quenching 384, 436  
   energy transfer 225–226, 228–230, 242–245  
   minor complexes 230–233, 384 *See also* CP24, CP26, CP29  
   oligomerization 225  
   phosphorylation 23, 386, 404–405, 435  
   polypeptides 266, 268–270, 318  
   PS II supercomplexes 240–242  
   reconstituted 70, 226–228  
   spectroscopy 228–233  
   trimers 22, 230, 409  
*Lhc* promoter 440  
*Lhca* polypeptides 266–270, 274  
   Lhca1 255, 266, 268–270, 274  
   Lhca2 255, 268–270  
   Lhca3 255, 268–270  
   Lhca4 255, 266, 268–270, 274  
   Lhca5 268  
   Lhca6 268  
*Lhcb* genes 240  
   transcriptional control 438–440  
*Lhcb* polypeptides 151–154, 240, 403  
   genes 222  
   Lhcb1 22, 222, 240, 409  
   Lhcb2 22, 222, 240, 409  
   Lhcb3 22, 222, 240, 409  
   Lhcb4 22, 268, 409  
   Lhcb5 22, 409  
   Lhcb6 22, 403, 409  
*Lhcc* polypeptides 337–339  
*Lhcd* polypeptides 339–340, 345–347  
*Lhcf* polypeptides 326–332 *See also* fucoxanthin Chl *a/c* protein  
 LHI *See also* LH1  
   multilevel regulation 450–464  
   mutants 460–461  
   reconstitution 459–460  
 LHII *See also* LH2  
   multilevel regulation 450–464  
   mutants 461  
   reconstitution 459–460 450–464  
 lifetime broadening 114  
 ligation  
   autocatalytic 52  
   chlorophyll 365  
 light  
   absorption 3, 23, 30, 85–86, 69, 93, 95, 99, 104, 426, 431, 442  
   circularly polarized 86, 93, 95  
   intensity 94  
   plane polarized 93, 94  
   scattering 426  
 light-harvesting antenna 38, 41 *See also* light-harvesting complex  
   acclimation 409–414  
   algae with Chl *c* 324–246  
   cyanobacteria 282–302, 472–488  
   dynamic alteration 438–440  
   evolution 130–160  
   green bacteria 196–210  
   overview 2–23  
   Photosystem I 254–255, 266–270  
   Photosystem II 220–233  
   purple bacteria 170–188, 451–465  
 light harvesting complex  
   bacterial (anoxygenic) *See* LH1, LH2, LH3, LHI, LHII  
   assembly factors 461–464  
   green bacteria (B808-866) 198–199  
   purple bacteria 170–188, 451–465  
   reconstitution 70, 156, 459–460  
   eukaryotic (chloroplast) 18–22 *See also* LHCI, LHCII  
   minor complexes *See* CP24, CP26, CP29  
   algae *See also* fucoxanthin Chl *a/c* protein (FCP), violaxanthin Chl *a* protein (VCP)  
 light harvesting regulation 451. *See also* acclimation, photoacclimation  
   cyanobacteria 472–488  
 light protection 30, 63  
 light scattering 93, 384  
 light stress 233  
 light-dependent phosphorylation 318  
 linear dichroism (LD) 97, 103–105, 120, 202, 208, 225, 329, 332, 337, 339  
   spectra 342  
 linear polyenes 63  
 linker polypeptide 149, 290, 294, 297, 298, 311–312, 472 *See also* phycobilisome  
 lipid 35, 256  
   peroxidation 33  
 local dielectric constant 179  
 local-field correction 92  
 long-wavelength chlorophylls 269–270, 271, 272, 275  
 low-frequency oscillation 185, 187  
 low-temperature fluorescence 269  
 lumen targeting domain 356  
 lutein 39, 58, 61, 223, 226, 311, 313, 316  
 lyase 34  
   phycocyanobilin 52  
 lycopene 39, 58, 60, 65, 67  
 lycopene  $\epsilon$ -cyclase 145

## M

*Macrocystis* 326, 330, 331  
 macrodomain 242  
 magnetic transition dipole 87, 89  
*Mahonia repens* 411  
*Malva neglecta* 411  
*Mantoniella* 328  
 marker  
     cell-sorting 71  
     pigments 67  
     surface mapping 71  
 Master equation 242  
*Mastigocladus* 290, 294–296, 302, 335  
 matrix  
     substitution 139, 140  
 maximum likelihood 140, 143  
 maximum parsimony 139  
 Mehler reaction 413  
 Membrane *See also* photosynthetic membrane  
     insertion 460, 462  
     potential 66  
     protein integration 362  
     topography 319  
     vesicles 364  
 mesobiliverdin 49, 50, 52, 334  
*Mesotaenium caldariorum* 52  
 metal  
     in porphyrins 33, 38–43, 46, 50, 69  
     lifetime of excited state 4  
 2-methylhopanoids  
     cyanobacteria 132  
 mevalonate pathway 144  
 Mg  
     In chlorophylls 33  
     lifetime of excited state 4  
 Mg protoporphyrin IX methyltransferase 45  
 Mg-[8-vinyl]-protochlorophyllide *a* 38  
 Mg-2,4-divinylpheoporphyrin  $a_5$ -monomethyl ester 142  
 Mg-chelatase 43, 44, 365  
 Mg-protoporphyrin IX 43, 416  
 Mg<sup>2+</sup> transfer 384  
 microbial mat 157  
 microfossils 131  
 microscopy  
     atomic force 10  
     confocal 21  
     immuno-gold labeling 202  
     scanning transmission electron 10  
     transmission electron 19, 202  
 mixed binding sites 227  
 modified chromophores 70  
 module structures 300  
 molar absorption coefficient 87, 92  
 molar ellipticity 87  
 molar extinction coefficients 87, 92  
 molecular opportunism 137, 154  
 monadoxanthin 40, 58  
*Monodus* 326, 328, 333

monogalactosyldiglyceride (MGDG) 201, 326  
 mRNA  
     processing 455, 458  
 multimer model 236  
 multipole expansion 98  
 mutant  
     *Chlamydomonas reinhardtii* 440  
     complementary chromatic adaptation 477  
     high Chl fluorescence 391  
 mutational saturation 140  
 myxobactone 40, 58  
 myxoxanthophyll 40, 58

## N

*n*-dodecyl  $\beta$ -D-maltoside 327, 332  
 N-methyl asparagine 334  
 NAD(P)H:plastoquinone oxidoreductase 376, 392  
 NADH-ring B oxidoreductase 45  
 NADP-malic enzyme type  
     C<sub>4</sub> plants 378  
     C<sub>4</sub> species 376  
 NADPH-geranylgeranyl oxidoreductase 45  
*Nannochloropsis* 326, 328, 333  
*nblA* 484  
*nblB* 484–485  
*nblR* 485  
*nblS* 486  
 neighbor-joining 140, 143  
 neoxanthin 40, 61, 63, 67, 224, 226, 268, 316  
     9-*cis* 58  
 neurosporene 40, 60, 67  
 neutron scattering 71  
 Ni-bacteriochlorophyll 42  
 Ni-chlorophyll 40  
 Ni-tetrapyrrole 43  
 nitrogen assimilation 404, 405  
 nitrogen limitation 483  
 nitrogenase 46  
 nomenclature  
     biliprotein 50  
     carotenoid 60  
 non-modulated fluorescence 374, 376  
 non-photochemical quenching (NPQ) 23, 32, 63, 233, 379–  
     388, 437, 442 *See also* quenching  
     energy-dependent (qE) 382–387, 406  
     photoinhibitory (qI) 382–383, 386–388, 405, 407–408  
     state transition (qT) 382–383, 386–387, 404  
 non-photosynthetic pigments 430  
 nonphotochemical hole burning 115  
 norflurazon 313  
 normal modes 102  
 Northern blotting 331  
 nostoxanthin 40, 58  
*npq4-1* 402  
 nuclear overlap integral 114  
 nuclear wavefunctions 113  
 nuclear-encoded thylakoid proteins 354  
 nucleomorph 14, 16  
     cryptophyte 151

nutrient deprivation responses 486–488  
 nutrient limitation 482

## O

$\Omega$  protein 464  
 O-J phase 377  
 O-K phase 377  
*Ochromonas* 326  
*Odontella* 326, 330  
 okenone 40, 61  
 oleosome 32  
 oligomerization  
   LHCII 20, 225, 413  
 open-chain tetrapyrroles *See* bilins, phycobilins  
   absorption spectra 53–56  
   structures 48–50  
 operator 106, 123–124  
 optical absorption cross section 442, 427, 429  
 orbital overlap 31  
*orf162b* 463  
*orf214* 463  
*orf428* 464  
 orientation factor 301  
 origin *See* evolution  
   chloroplasts 130  
 oscillator strength 92  
 oscillatoxanthin 40  
 oscillaxanthin 58  
*Ostreobium* 31  
 outgroup 141, 143  
 overwintering 411  
 $17^2$  oxidase  
   hypothetical 144  
 oxidative damage 33, 205  
 oxygen 111, 113  
   light effects 452, 454, 456–457  
   reactive species 33  
   quenching 67  
 oxygenase 43, 46, 365  
 oxygenic photosynthesis 6, 7, 12, 404  
   origin of 157–160

## P

$\pi$ -electron systems 3  
 P-457 40, 59  
 $P_{680}$  42, 220, 236  
 $P_{700}$  255–256, 258–260, 262, 265, 271–274, 309  
   absorbance change 390, 392  
 PAM fluorometry. *See* pulse amplitude modulation  
   fluorometry  
 paralogous genes 141  
 parsimony 139, 143  
 PAS domain 486  
*Pavlova* 326, 329, 330  
 Pb-chlorophyll 40  
 PC *See* phycocyanin  
 PC612 334, 337

PC645 334, 337  
 Pcb protein (prochlorophyte Chl *a/b* protein) *See*  
   prochlorophyte  
   *Pcb* gene family 13, 147–148, 438  
 PCB *See* phycocyanobilin  
   3E-PCB 51  
   3Z-PCB 51  
 PChlide *a*. *See* protochlorophyllide *a*  
 PCP. *See* peridinin-chlorophyll *a* protein  
 PE *See* phycoerythrin  
   PE545 334, 336  
   PE555 337  
   PE566 338  
 PE-lyase 52  
 PEB *See* phycoerythrobilin  
   3E-PEB 51  
   3Z-PEB 51  
 peptide  
   signal 356  
 peridinin 40, 59–61, 64–65, 67, 315, 324–326, 339–340, 343,  
   345–346, 348, 409  
 peridinin-chlorophyll *a* protein (PCP) 12, 20, 35, 56, 66, 70,  
   156, 325, 339–340, 344–345  
 peripheral chlorophylls 236  
 periplastid membrane 14, 16  
 periplastid space 14  
 peroxidation  
   lipid 33  
 pH  
   thylakoid 406  
*Phaeodactylum* 326, 330  
 Pheophyceae 38  
 pheophytin *a* 34, 36, 42  
 phonon-induced relaxation 176  
 phosphatase 440  
 phosphatidylglycerol 413  
 phosphoglycerate 406  
 phosphoglycolate 406  
 phosphorelay  
   control 481  
 phosphorus limitation 482, 483  
 phosphorylation 23, 223, 318, 386, 455–456, 464  
   LHCII 23, 386  
   light-dependent 318  
 photo-oxidative damage 405  
 photoacclimation *See also* acclimation  
   cyanobacteria 473–482  
   eukaryotic algae 315–318, 424–443  
   plants 387–388, 402–416  
 photoadaptation 425  
 photobleaching 13  
   fluorescence recovery 13  
 photochemical hole burning 115  
 photochemical quenching (qP) 379–381, 388–389  
 photoconversion 415  
 photodamage 270, 405, 408  
 photoinhibition 318, 378, 382, 386, 405  
 photoisomerization  
   open-chain tetrapyrroles 54  
 photon 95



- counter 408
- echo 184, 185, 229
- echo peak shift
  - three-pulse 229
- photoprotection 60, 18, 31–33, 63, 226, 266, 406
- photoreceptor 416
- photorespiration 389, 391, 404
- photosselection 48, 104
- photostasis 402–417
- photosynthesis
  - capacity 42, 414, 432
  - efficiency of 31, 404
  - evolution of 157–160
  - optimal quantum yield 379
  - oxygenic 6, 7, 12 404
  - quantum yield 382, 442
  - redox control 386
- photosynthesis-irradiance curve 429
  - initial slope 432
- photosynthetic membrane 6
  - bacteria 10–12
  - chloroplast 18–22
- photosynthetic rate
  - maximum 432
- photosynthetic unit size 409
- photosystem densities 317
- photosystem
  - common ancestor 157
  - FeS-type 7–8
  - Q-type 7–8
- Photosystem I (PS I) 42, 254–275, 308–309, 313–315, 317–318
  - fluorescence 376
  - origin 159
  - PS I-200 268
  - PS I-like
    - reaction centers 135
  - quantum efficiency 390
- Photosystem I / Photosystem II stoichiometry 316
- Photosystem II (PS II) 220–242, 282, 317, 378, 432–438
  - core complex 231, 234, 237–241, 243
  - cross-section 429–432
  - electron transport 7, 391
  - energy trapping 242–245
  - LHC II 222–230
  - membrane 243
  - origin 157–160
  - photoinhibition 386
  - potential quantum efficiency 378
  - proteins and genes 221–222
  - PSII-L 238
  - PSII-LHCII complexes 233
  - PS II-LHCII supercomplexes 22, 240–241, 243
  - PS II-like
    - reaction centers 135
  - PSII-S protein 233
  - quantum efficiency 388
  - reaction center 235–243, 440
  - repair cycle 377
- photosynthetic unit size 42, 409
- phototoxicity 43, 56
- photovoltage experiment 242
- phycobilins 6, 12, 30, 44, 48–56, 283, 286–287 *See also* bilin chromophores
  - analysis 68–70
  - biosynthesis 50–53, 142, 145
  - conformation 49, 54, 55
  - covalent linkage 49, 50
  - doubly linked 52
  - extinction coefficient 41, 57–59
  - spectroscopy 50, 53–59, 69
- phycobiliprotein 17, 48–56, 137, 148–150, 282–284, 287–288, 292, 297, 324, 333, 472
  - absorption spectra 287
  - $\alpha$  and  $\beta$  subunits 310
  - biosynthesis 482–488
  - chromophore lyase 485
  - cryptophyte 150, 333
  - crystal structure 150, 288, 293–297
  - denatured 53–54
  - folding energy 34
  - fluorescence 287
  - gene promoters 476
  - nomenclature 50
  - phylogenetic tree 149
- phycobilisome 6, 12, 17, 18, 33–34, 48–50, 52, 143, 148–149, 254, 258, 274, 282, 290, 403, 472–488
  - anchor polypeptide 288, 291–292, 473
  - biosynthesis 482–488
  - degradation 482, 483–484
  - high light responses 487–488
  - linkers 311
  - nutrient deprivation 486–488
  - regulatory components 474
  - structure 309, 472–474
- phycobiliviolin 284
- phycocyanin (PC) 12, 38, 54, 148–149, 284, 295, 308–309, 312, 333–337
- phycocyanobilin 41, 48–49, 54–55, 284, 310, 334, 485
- phycoerythrin (PE) 12, 38, 54, 148, 149, 284, 296, 308–310, 312, 333, 336, 485
  - Prochlorococcus 150
- phycoerythrobilin (PEB) 41, 48–49, 284, 310, 334, 336
- phycoerythrocyanin (PEC) 148–149, 284, 296
- phycoerythrobilin 54
- phycourobilin 41, 48–49, 54, 284, 310
- phycoviolobilin 41, 49–50, 53–54, 284
- phylloquinone 254, 255, 259, 260, 265
- phylogenetic markers
  - carotenoids 60
- phylogenetic tree 138, 139, 150, 288
  - branching order 141
  - LHC superfamily 18–19, 21–23, 150–155, 327
  - outgroup 141, 143
  - phycobiliproteins 149
- phytadienol 42
- phytatetraenol 42
- phytatrienol 42
- phytochrome 48, 50, 52, 416, 479, 480
- phytochromobilin 49, 50

- phytoene 40, 59, 65
  - cis*- 67
  - desaturase 60, 63
  - synthase 60
- phytofluene 40, 59–60
- phytol 35–36
- phytoplankton 60, 63, 68, 426, 428
- pigments 30–71 *See also* chromophores
  - chromatography 69
  - non-photosynthetic 430
  - oligomers 200
  - protective 56
  - quantitation 67, 68
  - spectroscopic analysis 68
  - substitution 69
- pigment-lipid aggregates 202
- pigment-pigment
  - interaction 71, 176, 232, 271
- pigment-protein
  - interaction 71, 232
- Pinus ponderosa* 411
- Pinus sylvestris* 410
- Pisum sativum* 383
- plane polarized light 93, 94
- plant morphogenesis 416
- plants
  - antisense 269
- Plasmodium* 17
- plastid factor 403
- plastocyanin 7, 258, 405
- plastoquinone 405
  - pool 63, 404, 434, 435, 439
- Plectonema boryanum* 410
- Pleurochloris meiringensis* 326, 328, 332
- $P_{\max}$  404
- point-dipole approximation 98, 99, 110, 271
- point-monopole 271
- polarization 47, 87
- polyethylene
  - chromatography columns 69
- polypeptide 309
  - anchor 291–292
  - LHC I 311, 314
  - LHC II 318
  - phycobilisome linker 149, 290, 294, 297, 298, 311–312, 472
- polyprenyl transferase 45
- Polysiphonia urceolata* 296–297, 313
- Polysiphonia sordidum* 297
- POR. *See* protochlorophyllide oxidoreductase
- porphobilinogen
  - deaminase 43, 44
  - synthase 44
- Porphyra umbilicalis* 308, 310
- Porphyra yezoensis* 295
  - ESTs 154
- Porphyridium* 19, 144, 290, 292, 295, 308–314, 316–318
- porphyrin
  - biosynthesis genes 142
  - macrocycle reduction 47
  - phototoxic 43
- post-translational import 354, 356, 456, 458
- PQ. *See* plastoquinone
- Prasinophyceae 38
- prasinoxanthin 40, 59
- precursor proteins 355, 356
- prenyl transferase 60, 63
- primary acceptor 42
- primary electron donor 242, 274
  - triplet state 32
- Prochlorococcus* 13, 42–43, 147–148, 438
  - phycoerythrin subunits 150
- Prochloron* 13, 142, 147
- prochlorophyte 6, 13, 35, 48, 142–144, 147, 150
  - Chl *a/b* polypeptides (Pcbs) 13, 147
- Prochlorothrix* 13, 147
- prokaryotes *See also* bacteria, cyanobacteria
  - photosynthetic 6–14, 134, 157–160
  - symbiotic 35
- proplastid development 354
- Prorocentrum micans* 315
- prospecting
  - Cu 42
- Prosthecochloris* 43, 208
- protease susceptibility mapping 202
- protective pigments 56
  - length of the conjugation system 61
- protein *See also* polypeptide
  - anchor 288, 291–292
  - chlorosomal 202
  - export mechanisms 356
  - high-light-induced 151
  - hydrophobic transmembrane domains 356
  - in vitro import 354
  - membrane integration 362
  - kinase 404, 435
  - membrane insertion 460, 462
  - nuclear-encoded thylakoid 354
  - precursors 355, 356
  - recruitment 137
  - transport
    - folded 361
    - targeting phase 362
- protein-BChl interactions 178
- Proteobacteria *See* purple photosynthetic bacteria
- Proterozoic 160
- protochlorophyllides 37, 43, 46–47
- protochlorophyllide oxidoreductase (POR) 45, 366
- Protogonyaulax tamarensis* 346
- protonation 299
  - bilin 50, 54–56
- protoporphyrin IX 34, 44
- protoporphyrinogen IX 43, 44
- protoporphyrinogen oxidase 44, 365
- PS I. *See* Photosystem I
- PS II. *See* Photosystem II
- PsaA 9, 254–257, 259–262, 264–266, 402
- PsaB 9, 254–257, 259–262, 264–266, 402
- PsaC 255–257, 260
  - psaC* gene 256

PsaD 255–257, 260, 266, 270  
 PsaE 255–258, 260  
 PsaF 255, 257–258, 265–266  
 PsaG 255, 266  
 PsaH 255, 266, 268, 270  
 PsaI 255, 257–258, 266, 270  
 PsaJ 255, 257–259, 261, 266  
 PsaK 255, 257, 259, 261, 266, 270  
 PsaL 255, 257–258, 261, 265–266, 270  
 PsaM 255, 257–258, 261  
 PsaN 255, 266  
 PsaO 255, 266  
 PsaX 255, 257–259, 261, 265  
 PsbA 402  
     *psbAI* 408  
     *psbAIII* 408  
 PsbB 9, 221–222  
 PsbC 9, 221–222  
     *psbC* gene 222, 414  
 PsbD 221–222, 402  
 PsbI 222, 235  
 PsbO 221–222, 238  
 PsbS 23, 151, 152, 363, 403  
     *PsbS* gene 233  
 PsbW 235  
 PsbZ 23, 221  
 pseudo LH1 180–181  
*puc* genes 456  
     *pucD* 464  
     *pucE* 464  
 PucC 461  
*puf* operons 452  
*puf* promoter 454  
*pufQ* 463  
*pufX* 172, 462  
 pulse amplitude modulation fluorometry 374–399  
 pulse-labeling 460  
 pump-probe 119, 228, 433  
 purple bacteria 6–8, 38, 43, 134, 143, 155–160, 170–188  
     aerobic 60  
     gene organization 452–459  
     intracellular membranes 11  
     light harvesting complex  
         assembly 459–464  
         regulation 450–465  
     transcription initiation 453

## Q

Q bands 46, 47, 426  
 Q cycle 438  
 $Q_A$  309, 316, 440  
 $Q_B$  377, 440  
 qE 379–387, 406 *See also* non-photochemical quenching  
     activation energy 384  
     zeaxanthin-dependent 385  
     zeaxanthin-independent 385  
 qI 382–383, 386–388 *See also* non-photochemical quenching  
 qN 379–387, 405 *See also* non-photochemical quenching

qP 380–381, 388–389  
 quantum efficiency 31, 388–391, 404  
     optimal 379  
     potential 378–379  
     PS I 390  
     PS II electron transport 388  
 quantum mechanical calculations 184  
 quantum yield 101, 430  
     CO<sub>2</sub> assimilation 389  
     maximum 430–431  
     photosynthesis 382, 442  
 quenching 101, 272 *See also* non-photochemical quenching  
     coefficient 381–382  
     energy-dependent 382–383, 406  
     fluorescence 379–388  
         initial fluorescence ( $F_0$ ) 385–386  
     non-photochemical 23, 32, 63, 233, 379–388, 405–406, 437, 442  
     photochemical (qP) 380–381, 388–389  
     photoinhibitory (qI) 382, 386  
     singlet state 32  
     state-transition 382, 386  
 quinone 205–207  
     isoprenoid 205  
 $Q_x$  47, 89, 91  
 $Q_y$  47, 89, 91, 104, 176, 178, 271  
     absorption band 35, 46

## R

R-PC 310, 311 *See also* phycocyanin  
 R-PE 310, 311 *See also* phycocyanin  
 radiation  
     field 92  
     UV-B 426  
 radiationless decay 66, 272  
 radiationless transition 56  
     T<sub>1</sub> to S<sub>0</sub> transition 67  
 radiative lifetime 53, 116  
 radical pairs 33  
 Raleigh scattering 107  
 Raman scattering 66, 107–108, 178  
 Raphidophyceae 38  
 RC. *See* reaction center  
 RcaA 476  
 RcaB 476  
 RcaC 478–480  
 RcaE 480  
 RcaF 480  
 reaction center 70, 135, 187, 199, 254–256, 259–262, 270, 431, 440  
     3-D structures of 11, 145, 235  
     bacterial 237  
     efficiency 2  
     evolution 145, 157–160  
     FeS-type 6–9, 145  
     Photosystem I 255–256, 259–260  
     Photosystem II 235–243, 309, 312, 440  
     Q-type 6–8, 145

recombination 32, 136  
 reconstitution 38, 70, 154, 231, 459  
     CP24 32, 136  
     CP26 232  
     LHCII 226  
 recruitment  
     protein 137  
 red algae (Rhodophyta) 17–21, 48, 148–149, 151, 154, 282,  
     297 See also rhodophyte algae  
     antenna systems 308–319, 313  
 red beds 132  
 red chlorophyll 262–263, 269–272, 235, 275  
     catabolite reductases 145  
 redox 416  
     poise 424  
     potential 42, 71, 220  
     regulation 203–207, 386  
     sensing 455  
     signaling 442  
     state 405, 442  
 redox-dependent regulation 204–207  
 refractive index 66, 93, 98, 301  
 regulatory system  
     two component 478  
 relaxation 236  
 remote sensing 68, 426  
 repair 405  
 resonance energy transfer 100–101, 105, 108–111, 119  
 resonance Raman spectroscopy 108, 225, 329  
 respiratory complexes 12  
 response regulator 478  
 retrograde signal 416  
*Rhodella reticulata* 149  
*Rhodella violacea* 308, 311–312, 316, 319  
*Rhodobacter capsulatus* 63, 177, 180, 450  
*Rhodobacter sphaeroides* 43, 45–46, 63, 172, 177–179, 181–  
     183, 187, 451  
 rhodochlorins  
     conversion to 68  
*Rhodomonas* 326, 337, 339  
*Rhodomonas CS24* 297  
*Rhodomonas lens* 336  
*Rhodomonas salina* 337, 338  
 rhodophycean PE 310  
 Rhodophyta 38 See rhodophyte algae  
 rhodophyte algae 16–19, 19, 38, 50, 70,  
     antenna systems 282–302, 290–291, 308–319  
 rhodopin- $\beta$ -D-glucoside 40, 59  
 rhodopin-1'-hydroxy 40, 59  
 rhodopinal, 13-cis 40, 59  
*Rhodopseudomonas acidophila* 36, 173, 174, 175, 176, 177,  
     178, 181, 182, 183, 450  
*Rhodopseudomonas marina* 182  
*Rhodopseudomonas palustris* 173, 458  
*Rhodopseudomonas viridis* 11, 31, 171, 187, 451  
 rhodopsins 67  
*Rhodospirillum molischianum* 174–176, 182–183, 187, 450  
*Rhodospirillum rubrum* 5, 36, 171–172, 180, 182, 450  
 rhodovibrin 40

*Rhodovulum sulfidophilum* 143, 452  
*Roseiflexus castenholzii* 196  
*Roseobacter denitrificans* 453  
*Roseococcus thiosulfatophilus* 179  
*Roseospirillum parvum* 453  
 rotational strength 87, 88, 90  
*rpbA* 475  
 rRNA  
     phylogenetic tree 132–133  
 Rubisco 406, 413–414, 442  
*Rubrivivax gelatinosus* 172

## S

$\sigma_{\text{PSII}}$  431, 432 See cross-section, PS II  
 S assimilation 404  
 S-adenosylmethionine 43, 46  
 $S_0$  to  $S_2$  transition  
     carotenoid 65–66  
 $S_1$ -state  
     carotenoid 61, 66  
 Schrödinger equation 124  
 Scots pine 411  
 Sec pathway 359–361  
 secondary endosymbiosis 16–17, 48, 155  
 SecYEG 360  
 seedling development 226  
 selection rules 66, 102  
*Selenastrum minutum* 405  
 self-aggregation 200  
 sensing 41, 416  
 Sep1 415  
 Sep2 415  
 sequence alignment 139  
 Shemin pathway 42  
 signal peptides 356  
 signal transduction 454  
 signaling events 416  
 signature sequences 139  
 single-photon  
     counting 118, 272  
     timing 235  
 singlet energy transfer 225  
 singlet oxygen 31, 33, 61, 65, 67, 406, 407  
 singlet state 111–113  
     quencher 32  
 singlet-singlet annihilation 111, 229, 230  
 singlet-triplet mixing 274  
 siphonaxanthin 40, 59  
 siphonein 40, 59  
 siroheme 43  
 site-directed mutagenesis 460–461  
     chromophore binding pocket 70  
 site-energy differences 271  
*Skeletonema* 326, 330  
 solvent  
     extraction 68  
     shift 66  
 Soret  
     absorption band 35, 36, 89, 426

spatial equilibration 230  
 special pair 42, 236, 237  
 spectral bandshapes 113–116  
 spectral density 94  
 spectral equilibration 230  
 spectral heterogeneity 271, 273  
 spectral irradiance 425  
 spectroscopy 53  
   0–0 transition 114  
   absorption 85–86  
   bilins 53  
   carotenoid 63–67  
   fluorescence 291  
   fluorescence polarization 292  
   high-resolution 70  
   infrared 94, 101–102, 108, 114  
   resonance Raman 178, 225, 329  
   Stark 180  
   time-resolved 70, 118–120  
 spectrum  
   photosynthetically useful 30  
*Spermothamnion* 313  
 spheroidene 40, 59, 64, 65, 67  
   pathway 61  
 spheroidenone 40, 59  
 spin-orbit coupling 112  
 315  
 spinach (*Spinacea oleracea*) 315–316  
 spirilloxanthin 40, 59, 65, 182  
   synthesis 61–62  
*Spirulina platensis* 293  
 spontaneous pathway 363  
 SRP54s 362  
 stabilization  
   pigments 33–34  
 Stark effect 86, 180  
 state 1 404  
 state 2 319, 404  
 state transition 13, 19, 22, 266, 268, 318, 404, 434–436  
   quenching 382, 386  
 steady-state fluorescence 271, 273  
 stereochemistry 37, 52  
   bilin 50  
   carotenoid 63  
 Stern-Volmer equation 101, 381, 382  
 stimulated emission 93  
 stoichiometry 409  
   PS I/PS II 316  
 Stokes shift 117, 269  
 streak camera 118  
 streptophytes 17  
 stress 403  
   heat 377  
   light 233  
   PS II 378  
 Strickler-Berg equation 117  
 stroma targeting domains 356  
 stroma thylakoids 21  
 stromal and cytosolic fructose biphosphatase 413  
 stromal intermediates 356

substituent effects  
   carotenoid 65  
   chlorophyll 36  
 substitution  
   matrix 139, 140  
   pigment 69  
 succinic acid 44  
 sucrose 413  
 sucrose phosphate synthase 413  
 sulfur limitation 482, 483  
 supercomplex  
   PSII-LHCII 240, 243  
 superfamily  
   globin 288  
   LHCII 18–19, 21–23, 150–155, 327  
 superoxide 33, 205  
   anion radical 407  
 supramolecular organization 48  
 surface mapping  
   marker 71  
*Symbiodinium* 326, 340–342, 347  
   *Symbiodinium microadriaticum* 347, 437  
   *Symbiodinium muscatinei* 341  
*Synechococcus* 147–148  
   *Synechococcus* sp. PCC 6301 290, 292  
   *Synechococcus* sp. PCC 7942 408, 414, 482–487  
*Synechocystis* 147, 414  
   *Synechocystis* sp. PCC 6701 297  
   *Synechocystis* sp. PCC 6803 12, 137, 144, 155, 318, 480, 487  
 synthesis  
   bacteriochlorophyll 43–46, 142  
   bilins 50–53  
   carotenoids 60–63  
   chlorophyll 43–46, 142, 364–367  
   tetrapyrroles 42–46  
 synthetase  
   chlorophyll 366  
 systemic acclimation 416

## T

t-RNA<sup>Glu</sup> 42  
 target analysis 344  
 targeting phase  
   protein transport 362  
 TatC  
   chloroplast 358  
   *E. coli* 358  
 tertiary endosymbionts 48  
 3,4,3',4'-tetrahydrolycopene 65  
 tetrapyrrole 34, 283  
   absorption spectra 47  
   biosynthesis 42–46  
   open-chain 54  
   absorption spectra 54, 55  
*Tetraselmis subcordiformis* 20  
*thai* 358  
 Tha4 358, 361  
    mutant 358

*Thalassiosira* 315, 326, 330–31  
 thermal energy dissipation 383, 384  
 thermo-optic effect 224  
 thioether-bond 50  
 thiol  
   addition to bilins 52  
 thioredoxin 416  
 thioester 460 40, 59  
 three-pulse photon echo peak shift 229  
 thylakoid membrane  
   chloroplast 18–23  
   cyanobacterial 12–13  
    $\Delta$ pH 384  
   kinases 435  
   targeting pathways 358  
 Tic polypeptides 357  
 time-resolved absorbance 70, 119–120, 184, 187, 271  
 time-resolved anisotropy decay 182  
 time-resolved fluorescence 100–101, 103, 109, 116–119, 272  
   spectra 292, 301  
 Toc polypeptides 357  
*Tolypothrix tenuis* 473  
*Toxoplasma* 17  
*trans*- $\Delta^3$ -hexadecenoic acid 413  
*trans*-active genes 454  
 transcription initiation 456  
   purple photosynthetic bacteria 453  
 transcriptional control  
   *Lhcb* 440  
 transduction 30  
 transfer-to-the-trap-limited 243  
   charge separation 239  
 transient absorption  
   changes 301  
   depolarization 229  
   spectroscopy 274  
 transit peptides 356  
 transition dipole 87–88, 92, 97–98, 102–103, 105, 112, 120–  
   123, 122–123, 264, 265  
   magnetic 87, 89  
   moments 47, 48  
 transition energies 273  
 translocation  
   apparatus 353  
   channel 360  
 translocon 361  
 transposition 136  
 trap-limited kinetics 243  
 trapping 262, 271–275  
   excitation energy 242–245  
 Tree of Life 132–133, 141  
 trimerization 223, 318, 409, 413  
 triplet state 32, 100, 103, 110, 111–113, 210, 274, 406  
   carotenoid 65, 67  
   chlorophyll 274  
   excitation transfer 31, 228, 274  
   quenching 225

triplet-minus-singlet 228  
 Triton X-100 235, 329  
 twin arginine motif 358  
 two component regulatory system 478  
 two-photon excitation 66, 337

## U

UDP-glucose 63  
 urogen III *See* uroporphyrinogen III  
   cosynthase 44  
 uroporphyrinogen III 43, 44  
   branch point 43  
   decarboxylase, 43, 44  
   synthase 43, 44  
 UV-B radiation 426  
 UV-light photoreceptors 416

## V

Van der Waals contact 325–226  
 variable fluorescence 376–377  
   rise of 377  
 variance spectrum 427  
 vaucherixanthin 40, 59, 326, 332  
 VCP. *See* violaxanthin-chlorophyll *a*-protein  
 vector 106  
 vegetative growth 416  
 vertical mixing 429  
 vesicles  
   membrane transport 364  
 vibrational mode 101, 103  
 vibronic coupling 66  
 vibronic level 113  
 vibronic transitions 63, 113–115  
 Chl fluorescence  
   video imaging 392  
*Vinca major* L. 406, 411  
*Vinca minor* L. 412  
 [8-vinyl]-chlorophyll *a* 13, 38, 42  
 [8-vinyl]-chlorophyll *b* 13, 38, 42  
 [8-vinyl]-protochlorophyllide *a* 41, 43, 46, 142–143  
 8-vinyl pigments 35  
 8-vinyl reductase 45  
 violaxanthin 32–33, 40, 59, 61, 223, 226, 268–269, 316, 326,  
   329, 384, 402  
   de-epoxidase 63, 384  
   cycle 32, 63  
 violaxanthin chlorophyll *a*-protein 333  
 vitamin B<sub>12</sub> 43, 457

## W

water  
   absorption of 30  
 water-leaving radiances 426  
 wave flicker 428

wavefunction 95, 98, 112–114, 121–125  
   nuclear 113  
 wavenumber 93  
 Web of Life 135  
 wheat 413  
 winter rye 413

## X

X-ray diffraction 221  
 Xanthophyceae 38  
 xanthophyll 56, 265, 268, 437  
   xanthophyll cycle 20, 22, 33, 225, 384, 406, 415, 436–438,  
     442  
     mutants 385  
     PSII 223

## Z

$\zeta$ -carotene 39, 57  
   desaturase 63  
   dihydroxy 57  
 Z-configuration 52  
 Z-scheme 7  
*Zea mays* 389, 391  
 zeaxanthin 32, 40, 59, 61, 63, 268, 311, 313, 315, 384, 402  
   -dependent qE 385  
   -dependent qI 387  
   epoxidation 63, 384  
   -independent qE 385  
 Zn-bacteriochlorophyll 37–40  
 Zn-Proto IX 39



## Advances in Photosynthesis

---

Series editor: Govindjee, University of Illinois, Urbana, Illinois, U.S.A.

---

1. D.A. Bryant (ed.): *The Molecular Biology of Cyanobacteria*. 1994  
ISBN Hb: 0-7923-3222-9; Pb: 0-7923-3273-3
2. R.E. Blankenship, M.T. Madigan and C.E. Bauer (eds.): *Anoxygenic Photosynthetic Bacteria*. 1995  
ISBN Hb: 0-7923-3681-X; Pb: 0-7923-3682-8
3. J. Amesz and A.J. Hoff (eds.): *Biophysical Techniques in Photosynthesis*. 1996  
ISBN 0-7923-3642-9
4. D.R. Ort and C.F. Yocum (eds.): *Oxygenic Photosynthesis: The Light Reactions*. 1996  
ISBN Hb: 0-7923-3683-6; Pb: 0-7923-3684-4
5. N.R. Baker (ed.): *Photosynthesis and the Environment*. 1996  
ISBN 0-7923-4316-6
6. P.-A. Siegenthaler and N. Murata (eds.): *Lipids in Photosynthesis: Structure, Function and Genetics*. 1998  
ISBN 0-7923-5173-8
7. J.-D. Rochaix, M. Goldschmidt-Clermont and S. Merchant (eds.): *The Molecular Biology of Chloroplasts and Mitochondria in Chlamydomonas*. 1998  
ISBN 0-7923-5174-6
8. H.A. Frank, A.J. Young, G. Britton and R.J. Cogdell (eds.): *The Photochemistry of Carotenoids*. 1999  
ISBN 0-7923-5942-9
9. R.C. Leegood, T.D. Sharkey and S. von Caemmerer (eds.): *Photosynthesis: Physiology and Metabolism*. 2000  
ISBN 0-7923-6143-1
10. B. Ke: *Photosynthesis: Photobiochemistry and Photobiophysics*. 2001  
ISBN 0-7923-6334-5
11. E.-M. Aro and B. Andersson (eds.): *Regulation of Photosynthesis*. 2001  
ISBN 0-7923-6332-9
12. C.H. Foyer and G. Noctor (eds.): *Photosynthetic Nitrogen Assimilation and Associated Carbon and Respiratory Metabolism*. 2002  
ISBN 0-7923-6336-1
13. B.R. Green and W.W. Parson (eds.): *Light-Harvesting Antennas in Photosynthesis*. 2003  
ISBN 0-7923-6335-3

For further information about the series and how to order please visit our Website  
<http://www.wkap.nl/series.htm/AIPH>

---

KLUWER ACADEMIC PUBLISHERS – DORDRECHT / BOSTON / LONDON